VOLUME 28 / NUMBER 6
MARCH 23, 1990
ACC. NOS. N90-14184 TO N90-15040

STAR

AN ABSTRACT JOURNAL

Scientific and Technical Aerospace Reports

PRODUCED BY THE
SCIENTIFIC AND TECHNICAL
INFORMATION
DIVISION

NASA

NATIONAL AERONAUTICS AND SPACE ADMINISTRATION

WHAT YOU CAN DO FOR *STAR*

All users of this abstract service are urged to forward reports to be considered for announcement in *STAR*. This will aid NASA in its efforts to provide the fullest possible coverage of all scientific and technical publications that might support aeronautics and space research and development. If you have prepared relevant reports (other than those that you will transmit to NASA, DOD, or DOE through the usual contract- or grant-reporting channels), please send them for consideration to the NASA Scientific and Technical Information Facility, P.O. Box 8757, BWI Airport, MD 21240.

Reprints of journal articles, book chapters, and conference papers are also welcome. These will be considered for announcement in *STAR*'s companion journal, *International Aerospace Abstracts*.

You may specify a particular source to be included in a report announcement if you wish; otherwise the report will be placed on public sale at the National Technical Information Service. Copyrighted publications will be announced but not distributed or sold.

PURCHASE OF *STAR*

The semimonthly issues are available to registered users on annual subscription from the NASA Scientific and Technical Information Facility, ATTN: Registration Services, P.O. Box 8757, BWI Airport, MD 21240. *STAR* is publicly available on annual subscription from the Superintendent of Documents, U.S. Government Printing Office, Washington, DC 20402.

PUBLISHED BY:

UNITED STATES GOVERNMENT
NATIONAL AERONAUTICS AND SPACE ADMINISTRATION
SCIENTIFIC AND TECHNICAL INFORMATION DIVISION
Scientific and Technical Aerospace Reports, Volume 28, is prepared by the NASA Scientific and Technical Information Facility operated for the National Aeronautics and Space Administration by RMS Associates.

The Administrator of the National Aeronautics and Space Administration has determined that the publication of this periodical is necessary in the transaction of the public business required by law of this agency. Use of funds for printing this periodical has been approved by the Director of the Office of Management and Budget through March 22, 1991.

US ISSN 0036-8741

Scientific and Technical Aerospace Reports (STAR) is issued twice a month and contains abstracts and indexes of meeting papers, conference proceedings, and unlimited distribution reports that have been added to the NASA Scientific and Technical Information Database during the preceding period. These citations may also be accessed online via NASA/RECON or via AIAA's Aerospace Database (File 108) through Dialog Information Services, Inc.

STAR subject coverage includes all aerospace-related areas that will help NASA achieve its mission. Material is gathered from all over the world and includes significant input from many countries under exchange and access agreements.

Consult the indexes at the back of this volume to help zero in on what you are looking for. These include:

Subject Index
Personal Author Index
Corporate Source Index
Contract Number Index
Report/Accession Number Index

STAR's companion abstract journal *International Aerospace Abstracts* should be used if you are looking for references to periodicals, books, and published meeting papers or conference proceedings.

Questions and comments should be addressed to:

NASA Scientific and Technical Information Facility
User Services
P.O. Box 8757
BWI Airport, MD 21240
301-621-0150

VOLUME 28 NUMBER 6 / MARCH 23, 1990

TABLE OF CONTENTS

AERONAUTICS

Includes aeronautics (general); aerodynamics; air transportation and safety; aircraft communications and navigation; aircraft design, testing and performance; aircraft instrumentation; aircraft propulsion and power; aircraft stability and control; and research and support facilities (air).

For related information see also *Astronautics.*

01 AERONAUTICS (GENERAL) 717

02 AERODYNAMICS 717

Includes aerodynamics of bodies, combinations, wings, rotors, and control surfaces; and internal flow in ducts and turbomachinery.

For related information see also *34 Fluid Mechanics and Heat Transfer.*

03 AIR TRANSPORTATION AND SAFETY 721

Includes passenger and cargo air transport operations; and aircraft accidents.

For related information see also *16 Space Transportation* and *85 Urban Technology and Transportation.*

04 AIRCRAFT COMMUNICATIONS AND NAVIGATION 722

Includes digital and voice communication with aircraft; air navigation systems (satellite and ground based); and air traffic control.

For related information see also *17 Space Communications, Spacecraft Communications, Command and Tracking* and *32 Communications and Radar.*

05 AIRCRAFT DESIGN, TESTING AND PERFORMANCE 722

Includes aircraft simulation technology.

For related information see also *18 Spacecraft Design, Testing and Performance* and *39 Structural Mechanics.* For land transportation vehicles see *85 Urban Technology and Transportation.*

06 AIRCRAFT INSTRUMENTATION 725

Includes cockpit and cabin display devices; and flight instruments.

For related information see also *19 Spacecraft Instrumentation* and *35 Instrumentation and Photography.*

07 AIRCRAFT PROPULSION AND POWER 725

Includes prime propulsion systems and systems components, e.g., gas turbine engines and compressors; and onboard auxiliary power plants for aircraft.

For related information see also *20 Spacecraft Propulsion and Power, 28 Propellants and Fuels,* and *44 Energy Production and Conversion.*

08 AIRCRAFT STABILITY AND CONTROL 726

Includes aircraft handling qualities; piloting; flight controls; and autopilots.

For related information see also *05 Aircraft Design, Testing and Performance.*

09 RESEARCH AND SUPPORT FACILITIES (AIR) 727

Includes airports, hangars and runways; aircraft repair and overhaul facilities; wind tunnels; shock tubes; and aircraft engine test stands.

For related information see also *14 Ground Support Systems and Facilities (Space).*

ASTRONAUTICS

Includes astronautics (general); astrodynamics; ground support systems and facilities (space); launch vehicles and space vehicles; space transportation; space communications, spacecraft communications, command and tracking; spacecraft design, testing and performance; spacecraft instrumentation; and spacecraft propulsion and power.

For related information see also *Aeronautics.*

12 ASTRONAUTICS (GENERAL) 728

For extraterrestrial exploration see *91 Lunar and Planetary Exploration.*

13 ASTRODYNAMICS 729

Includes powered and free-flight trajectories; and orbital and launching dynamics.

14 GROUND SUPPORT SYSTEMS AND FACILITIES (SPACE) 729

Includes launch complexes, research and production facilities; ground support equipment, e.g., mobile transporters; and simulators.

For related information see also *09 Research and Support Facilities (Air).*

15 LAUNCH VEHICLES AND SPACE VEHICLES 730

Includes boosters; operating problems of launch/space vehicle systems; and reusable vehicles.

For related information see also *20 Spacecraft Propulsion and Power.*

16 SPACE TRANSPORTATION 730

Includes passenger and cargo space transportation, e.g., shuttle operations; and space rescue techniques.

For related information see also *03 Air Transportation and Safety* and *18 Spacecraft Design, Testing and Performance.* For space suits see *54 Man/System Technology and Life Support.*

17 SPACE COMMUNICATIONS, SPACECRAFT COMMUNICATIONS, COMMAND AND TRACKING 730

Includes telemetry; space communications networks; astronavigation and guidance; and radio blackout.

For related information see also *04 Aircraft Communications and Navigation* and *32 Communications and Radar.*

18 SPACECRAFT DESIGN, TESTING AND PERFORMANCE 731

Includes satellites; space platforms; space stations; spacecraft systems and components such as thermal and environmental controls; and attitude controls.

For life support systems see *54 Man/System Technology and Life Support.* For related information see also *05 Aircraft Design, Testing and Performance, 39 Structural Mechanics,* and *16 Space Transportation.*

19 SPACECRAFT INSTRUMENTATION 734

For related information see also *06 Aircraft Instrumentation* and *35 Instrumentation and Photography.*

20 SPACECRAFT PROPULSION AND POWER 734

Includes main propulsion systems and components, e.g. rocket engines; and spacecraft auxiliary power sources.

For related information see also *07 Aircraft Propulsion and Power, 28 Propellants and Fuels, 44 Energy Production and Conversion,* and *15 Launch Vehicles and Space Vehicles.*

CHEMISTRY AND MATERIALS

Includes chemistry and materials (general); composite materials; inorganic and physical chemistry; metallic materials; nonmetallic materials; propellants and fuels; and materials processing.

23 CHEMISTRY AND MATERIALS (GENERAL) N.A.

24 COMPOSITE MATERIALS 736

Includes physical, chemical, and mechanical properties of laminates and other composite materials.

For ceramic materials see *27 Nonmetallic Materials.*

25 INORGANIC AND PHYSICAL CHEMISTRY 738

Includes chemical analysis, e.g., chromatography; combustion theory; electrochemistry; and photochemistry.

For related information see also *77 Thermodynamics and Statistical Physics.*

26 METALLIC MATERIALS 743

Includes physical, chemical, and mechanical properties of metals, e.g., corrosion; and metallurgy.

27 NONMETALLIC MATERIALS 749

Includes physical, chemical, and mechanical properties of plastics, elastomers, lubricants, polymers, textiles, adhesives, and ceramic materials.

For composite materials see *24 Composite Materials.*

28 PROPELLANTS AND FUELS 753

Includes rocket propellants, igniters and oxidizers; their storage and handling procedures; and aircraft fuels.

For related information see also *07 Aircraft Propulsion and Power, 20 Spacecraft Propulsion and Power,* and *44 Energy Production and Conversion.*

29 MATERIALS PROCESSING 755

Includes space-based development of products and processes for commercial application.

For biological materials see *55 Space Biology.*

ENGINEERING

Includes engineering (general); communications and radar; electronics and electrical engineering; fluid mechanics and heat transfer; instrumentation and photography; lasers and masers; mechanical engineering; quality assurance and reliability; and structural mechanics.

For related information see also *Physics.*

31 ENGINEERING (GENERAL) 756

Includes vacuum technology; control engineering; display engineering; cryogenics; and fire prevention.

32 COMMUNICATIONS AND RADAR 757

Includes radar; land and global communications; communications theory; and optical communications.

For related information see also *04 Aircraft Communications and Navigation* and *17 Space Communications, Spacecraft Communications, Command and Tracking.* For search and rescue see *03 Air Transportation and Safety,* and *16 Space Transportation.*

33 ELECTRONICS AND ELECTRICAL ENGINEERING 767

Includes test equipment and maintainability; components, e.g., tunnel diodes and transistors; microminiaturization; and integrated circuitry.

For related information see also *60 Computer Operations and Hardware* and *76 Solid-State Physics.*

34 FLUID MECHANICS AND HEAT TRANSFER 772

Includes boundary layers; hydrodynamics; fluidics; mass transfer and ablation cooling.

For related information see also *02 Aerodynamics* and *77 Thermodynamics and Statistical Physics.*

35 INSTRUMENTATION AND PHOTOGRAPHY 779

Includes remote sensors; measuring instruments and gauges; detectors; cameras and photographic supplies; and holography.

For aerial photography see *43 Earth Resources and Remote Sensing.* For related information see also *06 Aircraft Instrumentation* and *19 Spacecraft Instrumentation.*

36 LASERS AND MASERS 781

Includes parametric amplifiers.

For related information see also *76 Solid-State Physics.*

37 MECHANICAL ENGINEERING 791

Includes auxiliary systems (nonpower); machine elements and processes; and mechanical equipment.

38 QUALITY ASSURANCE AND RELIABILITY 795

Includes product sampling procedures and techniques; and quality control.

39 STRUCTURAL MECHANICS 796

Includes structural element design and weight analysis; fatigue; and thermal stress.

For applications see *05 Aircraft Design, Testing and Performance* and *18 Spacecraft Design, Testing and Performance.*

GEOSCIENCES

Includes geosciences (general); earth resources and remote sensing; energy production and conversion; environment pollution; geophysics; meteorology and climatology; and oceanography.

For related information see also *Space Sciences.*

42 GEOSCIENCES (GENERAL) **801**

43 EARTH RESOURCES AND REMOTE SENSING **801**

Includes remote sensing of earth resources by aircraft and spacecraft; photogrammetry; and aerial photography.

For instrumentation see *35 Instrumentation and Photography.*

44 ENERGY PRODUCTION AND CONVERSION **803**

Includes specific energy conversion systems, e.g., fuel cells; global sources of energy; geophysical conversion; and windpower.

For related information see also *07 Aircraft Propulsion and Power, 20 Spacecraft Propulsion and Power,* and *28 Propellants and Fuels.*

45 ENVIRONMENT POLLUTION **808**

Includes atmospheric, noise, thermal, and water pollution.

46 GEOPHYSICS **813**

Includes aeronomy; upper and lower atmosphere studies; ionospheric and magnetospheric physics; and geomagnetism.

For space radiation see *93 Space Radiation.*

47 METEOROLOGY AND CLIMATOLOGY **815**

Includes weather forecasting and modification.

48 OCEANOGRAPHY **818**

Includes biological, dynamic, and physical oceanography; and marine resources.

For related information see also *43 Earth Resources and Remote Sensing.*

LIFE SCIENCES

Includes life sciences (general); aerospace medicine; behavioral sciences; man/system technology and life support; and space biology.

51 LIFE SCIENCES (GENERAL) **819**

52 AEROSPACE MEDICINE **820**

Includes physiological factors; biological effects of radiation; and effects of weightlessness on man and animals.

53 BEHAVIORAL SCIENCES **820**

Includes psychological factors; individual and group behavior; crew training and evaluation; and psychiatric research.

54 MAN/SYSTEM TECHNOLOGY AND LIFE SUPPORT **821**

Includes human engineering; biotechnology; and space suits and protective clothing.

For related information see also *16 Space Transportation.*

55 SPACE BIOLOGY **822**

Includes exobiology; planetary biology; and extraterrestrial life.

MATHEMATICAL AND COMPUTER SCIENCES

Includes mathematical and computer sciences (general); computer operations and hardware; computer programming and software; computer systems; cybernetics; numerical analysis; statistics and probability; systems analysis; and theoretical mathematics.

59 MATHEMATICAL AND COMPUTER SCIENCES (GENERAL) **822**

60 COMPUTER OPERATIONS AND HARDWARE **823**

Includes hardware for computer graphics, firmware, and data processing.

For components see *33 Electronics and Electrical Engineering.*

61 COMPUTER PROGRAMMING AND SOFTWARE **823**

Includes computer programs, routines, algorithms, and specific applications, e.g., CAD/CAM.

62 COMPUTER SYSTEMS **831**

Includes computer networks and special application computer systems.

63 CYBERNETICS **832**

Includes feedback and control theory, artificial intelligence, robotics and expert systems.

For related information see also *54 Man/System Technology and Life Support.*

64 NUMERICAL ANALYSIS **833**

Includes iteration, difference equations, and numerical approximation.

65 STATISTICS AND PROBABILITY **N.A.**

Includes data sampling and smoothing; Monte Carlo method; and stochastic processes.

66 SYSTEMS ANALYSIS **835**

Includes mathematical modeling; network analysis; and operations research.

67 THEORETICAL MATHEMATICS **836**

Includes topology and number theory.

PHYSICS

Includes physics (general); acoustics; atomic and molecular physics; nuclear and high-energy physics; optics; plasma physics; solid-state physics; and thermodynamics and statistical physics.

For related information see also *Engineering.*

70 PHYSICS (GENERAL) **836**

For precision time and time interval (PTTI) see *35 Instrumentation and Photography;* for geophysics, astrophysics or solar physics see *46 Geophysics, 90 Astrophysics,* or *92 Solar Physics.*

71 ACOUSTICS 837
Includes sound generation, transmission, and attenuation.
For noise pollution see *45 Environment Pollution.*

72 ATOMIC AND MOLECULAR PHYSICS 838
Includes atomic structure, electron properties, and molecular spectra.

73 NUCLEAR AND HIGH-ENERGY PHYSICS 841
Includes elementary and nuclear particles; and reactor theory.
For space radiation see *93 Space Radiation.*

74 OPTICS 842
Includes light phenomena and optical devices.
For lasers see *36 Lasers and Masers.*

75 PLASMA PHYSICS 844
Includes magnetohydrodynamics and plasma fusion.
For ionospheric plasmas see *46 Geophysics.* For space plasmas see *90 Astrophysics.*

76 SOLID-STATE PHYSICS 849
Includes superconductivity.
For related information see also *33 Electronics and Electrical Engineering* and *36 Lasers and Masers.*

77 THERMODYNAMICS AND STATISTICAL PHYSICS 857
Includes quantum mechanics; theoretical physics; and Bose and Fermi statistics.
For related information see also *25 Inorganic and Physical Chemistry* and *34 Fluid Mechanics and Heat Transfer.*

SOCIAL SCIENCES

Includes social sciences (general); administration and management; documentation and information science; economics and cost analysis; law, political science, and space policy; and urban technology and transportation.

80 SOCIAL SCIENCES (GENERAL) N.A.
Includes educational matters.

81 ADMINISTRATION AND MANAGEMENT 857
Includes management planning and research.

82 DOCUMENTATION AND INFORMATION SCIENCE 858
Includes information management; information storage and retrieval technology; technical writing; graphic arts; and micrography.
For computer documentation see *61 Computer Programming and Software.*

83 ECONOMICS AND COST ANALYSIS N.A.
Includes cost effectiveness studies.

84 LAW, POLITICAL SCIENCE AND SPACE POLICY N.A.
Includes NASA appropriation hearings; aviation law; space law and policy; international law; international cooperation; and patent policy.

85 URBAN TECHNOLOGY AND TRANSPORTATION N.A.
Includes applications of space technology to urban problems; technology transfer; technology assessment; and surface and mass transportation.
For related information see *03 Air Transportation and Safety, 16 Space Transportation,* and *44 Energy Production and Conversion.*

SPACE SCIENCES

Includes space sciences (general); astronomy; astrophysics; lunar and planetary exploration; solar physics; and space radiation.
For related information see also *Geosciences.*

88 SPACE SCIENCES (GENERAL) 859

89 ASTRONOMY 860
Includes radio, gamma-ray, and infrared astronomy; and astrometry.

90 ASTROPHYSICS 861
Includes cosmology; celestial mechanics; space plasmas; and interstellar and interplanetary gases and dust.
For related information see also *75 Plasma Physics.*

91 LUNAR AND PLANETARY EXPLORATION 865
Includes planetology; and manned and unmanned flights.
For spacecraft design or space stations see *18 Spacecraft Design, Testing and Performance.*

92 SOLAR PHYSICS 866
Includes solar activity, solar flares, solar radiation and sunspots.
For related information see *93 Space Radiation.*

93 SPACE RADIATION 867
Includes cosmic radiation; and inner and outer earth's radiation belts.
For biological effects of radiation see *52 Aerospace Medicine.* For theory see *73 Nuclear and High-Energy Physics.*

GENERAL

Includes aeronautical, astronautical, and space science related histories, biographies, and pertinent reports too broad for categorization; histories or broad overviews of NASA programs.

99 GENERAL 867

Note: N.A. means that no abstracts were assigned to this category for this issue.

SUBJECT INDEX I-1
PERSONAL AUTHOR INDEX I-55
CORPORATE SOURCE INDEX I-63
CONTRACT NUMBER INDEX I-75
REPORT/ACCESSION NUMBER INDEX .. I-79
APPENDIX—ABOUT STAR A-1

TYPICAL CITATION AND ABSTRACT

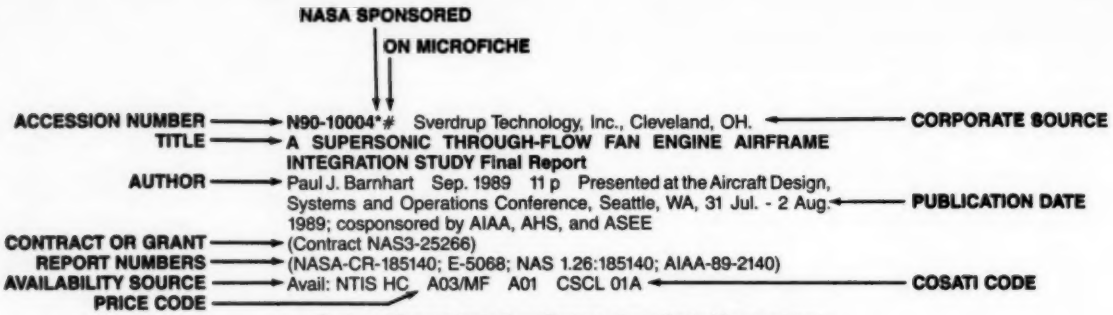
NASA SPONSORED
ON MICROFICHE
ACCESSION NUMBER
N90-10004*# Sverdrup Technology, Inc., Cleveland, OH.
CORPORATE SOURCE
TITLE
A SUPERSONIC THROUGH-FLOW FAN ENGINE AIRFRAME INTEGRATION STUDY Final Report
AUTHOR
Paul J. Barnhart Sep. 1989 11 p Presented at the Aircraft Design, Systems and Operations Conference, Seattle, WA, 31 Jul. - 2 Aug.
PUBLICATION DATE
1989; cosponsored by AIAA, AHS, and ASEE
CONTRACT OR GRANT
(Contract NAS3-25266)
REPORT NUMBERS
(NASA-CR-185140; E-5068; NAS 1.26:185140; AIAA-89-2140)
AVAILABILITY SOURCE
Avail: NTIS HC A03/MF A01 CSCL 01A
COSATI CODE
PRICE CODE

Engine airframe integration effects are investigated for superonsic through-flow fan engines installed on a Mach 3.20 supersonic cruise vehicle. Six different supersonic through-flow fan engine installations covering the effects of engine size, nacelle contour, nacelle placement, and approximate bypass plume effects are presented. The different supersonic through-flow fan installations are compared with a conventional turbine bypass engine configuration on the same basic airframe. The supersonic through-flow fan engine integrations are shown to be comparable to the turbine bypass engine configuration on the basis of installed nacelle wave drag. The supersonic through-flow fan engine airframe integrated vehicles have superior aerodynamic performance on the basis of maximum lift-to-drag ratio than the turbine bypass engine installation over the entire operating Mach number range from 1.10 to 3.20. When approximate bypass plume modeling is included, the supersonic through-flow fan engine configuration shows even larger improvements over the turbine bypass engine configuration. Author

VOLUME 28 NUMBER 6 / MARCH 23, 1990

Scientific and Technical Aerospace Reports

A Semimonthly Publication of the National Aeronautics and Space Administration

01 AERONAUTICS (GENERAL)

N90-14184# Advisory Group for Aerospace Research and Development, Neuilly-Sur-Seine (France).
AGARD HIGHLIGHTS 89/2
Sep. 1989 37 p In FRENCH and ENGLISH
Avail: NTIS HC A03/MF A01

The accomplishments of AGARD are examined and its purposes. AGARD is described as a crucible for knowledge and a springboard for cooperative research which in the years to come will contribute to the building of a stronger Europe within a stronger alliance. An over view is provided of the state of propulsion technologies related to the Propulsion and Energetics Panel (PEP) with comments on associated international activities. A quantum leap in capability is forecast. Hypersonic vehicles and combined cycle engines are of interest but will require more research. In-service support and continuous development cycle of aero gas turbines will benefit from expected technological advancements. The importance of propulsion was stressed and the AGARD Chairman concluded with a recommendation for continued work on reliability of aircraft engines. J.P.S.

02 AERODYNAMICS

Includes aerodynamics of bodies, combinations, wings, rotors, and control surfaces; and internal flow in ducts and turbomachinery.

For related information see also *34 Fluid Mechanics and Heat Transfer.*

N90-14185*# National Aeronautics and Space Administration. Langley Research Center, Hampton, VA.
MEASURED AND PREDICTED AERODYNAMIC COEFFICIENTS AND SHOCK SHAPES FOR AEROASSIST FLIGHT EXPERIMENT (AFE) CONFIGURATION
William L. Wells 1989 52 p
(NASA-TP-2956; L-16644; NAS 1.60:2956) Avail: NTIS HC A04/MF A01 CSCL 01A

Two scaled models of the Aeroassist Flight Experiment (AFE) vehicle were tested in two air wind tunnels and one CF4 tunnel. The tests were to determine the static longitudinal aerodynamic characteristics, and shock shapes for the configuration in hypersonic continuum flow. The tests were conducted with a range of angle of attack to evaluate the effects of Mach number, Reynolds numbers, and normal shock density ratio. Author

N90-14186*# National Aeronautics and Space Administration. Langley Research Center, Hampton, VA.
EFFECT OF BLADE PLANFORM VARIATION ON A SMALL-SCALE HOVERING ROTOR
Susan L. Althoff and Kevin W. Noonan Washington Jan. 1990 26 p Prepared in cooperation with Army Aerostructures Directorate, Hampton, VA
(DA Proj. 1L1-61102-AH-45-A)
(NASA-TM-4146; L-16608; NAS 1.15:4146; AVSCOM-TM-89-B-009) Avail: NTIS HC A03/MF A01 CSCL 01A

A hover test was conducted on a small-scale rotor model for three sets of tapered rotor blades and a baseline rectangular planform rotor blade. All configurations had the same airfoils, twist, and thrust-weighted solidity. The tapered blade planforms had taper initiating at 50, 75, and 94 percent of the blade radius with a taper ratio of 3 to 1 for each blade set. The experiment was conducted for a range of thrust coefficients, and the data were compared to the predictions of three hover analysis methods. The data show the 94 percent tapered blade was slightly more efficient at the higher rotor thrust levels. The other tapered planform rotors did not show the expected improvement over the baseline rotor, and all configurations had similar performance for low thrust coefficients. None of the analysis methods correlated well with the experimental data. Author

N90-14187*# National Aeronautics and Space Administration. Langley Research Center, Hampton, VA.
VALIDATION OF A COMPUTER CODE FOR ANALYSIS OF SUBSONIC AERODYNAMIC PERFORMANCE OF WINGS WITH FLAPS IN COMBINATION WITH A CANARD OR HORIZONTAL TAIL AND AN APPLICATION TO OPTIMIZATION
Harry W. Carlson (PRC Systems Services Co., Hampton, VA.), Christine M. Darden, and Michael J. Mann Jan. 1990 125 p
(NASA-TP-2961; L-16611; NAS 1.60:2961) Avail: NTIS HC A06/MF A01 CSCL 01A

Extensive correlations of computer code results with experimental data are employed to illustrate the use of a linearized theory, attached flow method for the estimation and optimization of the longitudinal aerodynamic performance of wing-canard and wing-horizontal tail configurations which may employ simple hinged flap systems. Use of an attached flow method is based on the premise that high levels of aerodynamic efficiency require a flow that is as nearly attached as circumstances permit. The results indicate that linearized theory, attached flow, computer code methods (modified to include estimated attainable leading-edge thrust and an approximate representation of vortex forces) provide a rational basis for the estimation and optimization of aerodynamic performance at subsonic speeds below the drag rise Mach number. Generally, good prediction of aerodynamic performance, as measured by the suction parameter, can be expected for near optimum combinations of canard or horizontal tail incidence and leading- and trailing-edge flap deflections at a given lift coefficient (conditions which tend to produce a predominantly attached flow). Author

N90-14188*# National Aeronautics and Space Administration. Ames Research Center, Moffett Field, CA.
UNSTEADY AERODYNAMIC SIMULATION OF MULTIPLE BODIES IN RELATIVE MOTION: A PROTOTYPE METHOD
Robert L. Meakin (Sterling Federal Systems, Inc., Moffett Field, CA.) Jul. 1989 19 p Presented at the 9th AIAA Computational Fluid Dynamics Conference, Buffalo, NY, 14-16 Jun. 1989 Previously announced in IAA as A89-41839
(NASA-TM-102181; A-89095; NAS 1.15:102181) Avail: NTIS HC A03/MF A01 CSCL 01A

A prototype method for time-accurate simulation of multiple aerodynamic bodies in relative motion is presented. The method is general and features unsteady chimera domain decomposition techniques and an implicit approximately factored finite-difference procedure to solve the time-dependent thin-layer Navier-Stokes

equations. The method is applied to a set of two- and three-dimensional test problems to establish spatial and temporal accuracy, quantify computational efficiency, and begin to test overall code robustness. Author

N90-14189*# Nevada Univ., Reno. Engineering Research and Development Center.
NUMERICAL INVESTIGATIONS IN THREE-DIMENSIONAL INTERNAL FLOWS Semiannual Status Report, 1 Jan. - 30 Jun. 1989
William C. Rose Dec. 1988 30 p Presented at the 6th National Aero-Space Technical Symposium, Monterey, CA, 24-28 Apr. 1989
(Contract NCC2-507)
(NASA-CR-186068; NAS 1.26:186068) Avail: NTIS HC A03/MF A01 CSCL 01A

In order to develop an understanding of flow fields that exist in sidewall compression inlet models, an explicit, time-accurate full Navier-Stokes code was used to model them. Both laminar and turbulent boundary layers were numerically simulated. These simulations were examined as they were influenced by Mach number, changes in sidewall compression angle, hypersonic viscous interaction effects, and thick entering boundary layers. Cause and effect relationships were established. The numerical simulations were compared with the limited data available to aid in understanding both the simulations and the experiments. J.P.S.

N90-14190*# National Aeronautics and Space Administration. Langley Research Center, Hampton, VA.
EFFECT OF PYLON WAKE WITH AND WITHOUT PYLON BLOWING ON PROPELLER THRUST
Garl L. Gentry, Jr., Earl R. Booth, Jr., and M. A. Takallu (PRC Kentron, Inc., Hampton, VA.) Washington Feb. 1990 26 p
(NASA-TM-4162; L-16645; NAS 1.15:4162) Avail: NTIS HC A03/MF A01 CSCL 01A

Pylon trailing edge blowing was investigated as a means of alleviating the effects of the pylon wake on a pusher arrangement of an advanced single-rotation turboprop. Measurements were made of steady-state propeller thrust and pylon wake pressures and turbulence levels with and without blowing. Results show that the pylon trailing edge blowing practically eliminated the pylon wake, significantly reduced the pylon wake turbulence, and had a relatively small effect on the steady-state propeller thrust. The data are presented with a minimum of analysis. Author

N90-14191 California Inst. of Tech., Pasadena.
AN INVESTIGATION OF THE BURSTING OF TRAILING VORTICES USING NUMERICAL SIMULATION Ph.D. Thesis
Philip Stewart Beran 1989 187 p
Avail: Univ. Microfilms Order No. DA8915375

Solutions of the Navier-Stokes equations are obtained for the flow of an isolated, trailing vortex, and for the swirling flow through a frictionless pipe. In both cases, the flow is assumed to be steady, incompressible and rotationally symmetric. Solutions are computed using Newton's method and Gaussian elimination for a wide range of values of two parameters: Reynolds number, and vortex strength. Pseudo-arclength continuation is employed to facilitate the computation of solution points in the parameter space. The numerical procedure is validated through comparison of solutions obtained in previous investigations for the case of a trailing vortex. Solutions are also compared with results reported by Brown and Lopez (1988) for the case of flow through a pipe. Solutions of the quasi-cylindrical equations are obtained for the flow of a trailing vortex. Solutions are computed using an explicit, space-marching scheme, and are compared with solutions of the Navier-Stokes equations. Dissert. Abstr.

N90-14192 ESDU International Ltd., London (England).
NORMAL FORCE, PITCHING MOMENT, AND SIDE FORCE OF FOREBODY-CYLINDER COMBINATIONS FOR ANGLES OF ATTACK UP TO 90 DEGREES AND MACH NUMBERS UP TO 5
Aug. 1989 20 p Supersedes ESDU-83039; ESDU-85025; and ESDU-86009
(ESDU-89014; ESDU-83039; ESDU-85025; ESDU-86009; ISBN-0-85679-686-7; ISSN-0141-397X) Avail: ESDU

This Data Item 89014, an addition to the Aerodynamic Subseries, provides a simple empirical method for estimating normal forces and pitching moment. Although developed using wind-tunnel data for blunted and pointed tangent-ogive and cone cylinders, and secant-ogive and ellipsoid-nosed cylinders, the method is applicable to any axisymmetric smooth forebody-cylinder combination. It requires as inputs the normal-force-curve and pitching-moment-curve slopes at zero angle of attack, which may be obtained from ESDU 89008, and simple geometric parameters which may be obtained from ESDU 77028. The method predicts normal force within 15 percent at subsonic speeds but within 5 percent at supersonic speeds, and predicts the center of pressure to within 5 percent of body length. The range of data used in the correlation covered forebody fineness ratio of 0.75 to 6.28, overall body fineness ratio of 6 to 22.3 and Mach numbers from 0.27 to 4.5. The use of the method is illustrated by a worked example. The effect of boat-tailing on normal force and pitching moment may be found from ESDU 87033. At high angles of attack, at subsonic and transonic Mach numbers, asymmetric vortex flow may occur on the leeward side of the body, creating an out-of-plane force distribution that may result in large side force and yawing moments and can also affect the normal force. The flow phenomena are considered and the local force distribution is illustrated. The influence of Reynolds number and nose blunting is considered and a discussion of Mach number effects is also given together with an envelope of maximum side force. The existence of various types of flow instability, depending on the Reynolds number/angle of attack combination, can affect the normal force and pitching moment predictions, and the region of applicability is illustrated and found to apply to the majority of the flight cases. ESDU

N90-14193*# Institute for Computer Applications in Science and Engineering, Hampton, VA.
A NOTE CONCERNING THE ONSET OF THREE DIMENSIONALITY AND TIME DEPENDENCE IN GOERTLER VORTICES Final Report
Andrew P. Bassom (Exeter Univ., England) and Sharon O. Seddougui Oct. 1989 29 p Submitted for publication
(Contract NAS1-18605)
(NASA-CR-181956; NAS 1.26:181956; ICASE-89-77) Avail: NTIS HC A03/MF A01 CSCL 01A

Recently Hall and Seddougui (1989) considered the secondary instability of large amplitude Goertler vortices in a growing boundary layer evolving into a three-dimensional flow with wavy vortex boundaries. They obtained a pair of coupled, linear ordinary differential equations for this instability which constituted an eigenproblem for the wavelength and frequency of this wavy mode. Investigations into the nonlinear version of this problem by Seddougui and Bassom have revealed several omissions in the numerical work of Hall and Seddougui. These issues are addressed in this note. In particular, it is found that many neutrally stable modes are possible. The properties of such modes are derived in a high wavenumber limit and it is shown that the combination of the results of Hall and Seddougui and the modifications made here lead to conclusions which are consistent with the available experimental observations. Author

N90-14194 Oklahoma Univ., Norman.
A COMPUTATIONAL ANALYSIS OF THE TRANSONIC FLOW FIELD OF TWO-DIMENSIONAL MINIMUM LENGTH NOZZLES Ph.D. Thesis
Brian Maurice Argrow 1989 142 p
Avail: Univ. Microfilms Order No. DA8921078

The method of characteristics is used to generate supersonic contours for two-dimensional straight sonic line (SSL) and curved sonic line (CSL) minimum length nozzles (MLNs) for exit Mach numbers of two, four and six. These contours are combined with subsonic inlets to determine the influence of the inlet geometry on the sonic-line shape and location, and on the supersonic flow

field. This is accomplished by computing the inviscid and viscous laminar flow fields for Reynolds number of 1,170, 11,700, and 23,400. The flow fields are computed using a modified version of the code VNAP2 which solves the Euler and full Navier-Stokes equations. The results indicate that the inlet geometry directly determines the sonic-line shape and location. Both are almost totally independent of the MLN type, Reynolds number and exit Mach number. Supersonic flow field phenomena including boundary-layer separation and oblique shock waves are also observed to be a direct result of the inlet geometry. The sonic line assumptions made for the SSL prove to be superior to the CSL assumptions for the cases examined. Dissert. Abstr.

N90-14195 Iowa State Univ. of Science and Technology, Ames.
NAVIER-STOKES SOLUTIONS OF 2-D TRANSONIC FLOW OVER UNCONVENTIONAL AIRFOILS Ph.D. Thesis
R. A. Cox 1989 112 p
Avail: Univ. Microfilms Order No. DA8920119

A finite-volume code was written to solve the complete, Reynolds-averaged Navier-Stokes equations around unconventional airfoils. The numerical algorithm is based on a flux-difference splitting form of a total variation diminishing (TVD) scheme. Various modifications to the scheme were incorporated to provide a spatially second-order-accurate scheme in physical space. The scheme is conservative at steady state but employs nonconservative differencing during the integration to steady state to allow incorporation of implicit boundary conditions in the farfield. A zero-equation eddy viscosity model was employed to represent the effects of turbulence. The code was validated by comparisons with flat plate and NACA 0012 data. Excellent results were obtained for both attached flow and shock induced separation cases. Numerical results are also presented for transonic flow over an unconventional airfoil and show good agreement. Dissert. Abstr.

N90-14196 Akron Univ., OH.
NAVIER-STOKES ANALYSIS OF AIRFOILS WITH LEADING EDGE ICE ACCRETIONS Ph.D. Thesis
Mark Gregory Potapczuk 1989 215 p
Avail: Univ. Microfilms Order No. DA8922320

A numerical analysis of the flow field characteristics and the performance degradation of an airfoil with leading edge ice accretions was performed. The important fluid dynamic processes were identified and calculated. Among these were the leading edge separation bubble at low angles of attack, complete separation on the low pressure surface resulting in premature stall, drag rise due to the ice shape, and the effects of angle of attack on the separated flow field. Comparisons to experimental results were conducted to confirm these calculations. A computer code which solves the Navier-Stokes equations in two dimensions, ARC2D, was used to perform the calculations. A Modified Mixing Length turbulence model was developed to improve capabilities in calculating the separated flow phenomena. A grid generation code, GRAPE, was used to produce grids for several ice shape and airfoil combinations. Results indicate that the ability to predict overall performance characteristics, such as lift and drag, at low angles of attack is excellent. Transition location is important for accurately determining separation bubble shape. Details of the flow field in and downstream of the separated regions requires some modifications. Calculations for the stalled airfoil indicate periodic shedding of vorticity that was generated aft of the ice accretion. Time averaged pressure values produce results which compare favorably with experimental information. A turbulence model which accounts for the history effects in the flow may be justified. Dissert. Abstr.

N90-14197 North Carolina State Univ., Raleigh.
NUMERICAL MODELING OF SUPERSONIC TURBULENT REACTING FREE SHEAR LAYERS Ph.D. Thesis
Dean Robert Eklund 1989 112 p
Avail: Univ. Microfilms Order No. DA8918087

To increase the fundamental understanding of the physical processes present within scramjet combustors, an experimental effort is underway at the NASA Langley Research Center to examine the turbulent combustion within supersonic H2 - air coaxial streams. The objective of this study is to numerically model the turbulent mixing and combustion process within these free shear layers and to examine the effects of different turbulence models, of different chemistry models, and of grid refinement upon the numerical solutions. To conduct this study, a computer program was written to solve the axisymmetric Reynolds-averaged Navier-Stokes equations. The numerical method integrates the governing equations using a central-difference finite volume approach while advancing the solution in time using a Runge-Kutta scheme. Turbulence is modeled using three algebraic eddy viscosity models while two finite-rate chemistry models are employed for modeling the H2 - air chemical kinetics. Three turbulent coaxial jet flowfields are calculated. Adjustments to the algebraic turbulence models are found necessary between bases, and hence, these turbulence models do not provide a true predictive capability. The effect of turbulent mixing upon the extent of combustion is demonstrated and the effect of grid refinement is found to be especially important for reacting flows. Dissert. Abstr.

N90-14198# Kansas Univ., Lawrence.
COMPUTATION OF UNSTEADY TRANSONIC FLOW ABOUT AIRFOILS IN FREQUENCY DOMAIN USING THE FULL-POTENTIAL EQUATION Ph.D. Thesis
Horng-Ren Hwang 1988 141 p
Avail: Univ. Microfilms Order No. DA8918375

A new method based on considerations in frequency domain is developed for calculating the nonlinear unsteady aerodynamic flow field about oscillating airfoils using the 2-D, full potential equation. The method employs an averaging technique to separate the governing nonlinear steady equation into its Fourier components for the in-phase and the out-of-phase solutions without time linearization. These two equations are then solved simultaneously with a finite difference scheme which is adopted directly from the one for solving the steady full potential equation. Computed results are compared with results from wind tunnel data and existing computational methods with time-domain integration for NACA 64A010A, NACA 64A006, and MBB-A3 airfoils in pitching, flapping, and plunging oscillations, respectively. It is shown that the present method predicts the unsteady aerodynamic characteristics in good agreement in most cases with experimental data and/or results from other theoretical methods. Effects of Mach number, the motion amplitude, the reduced frequency, and the steady angle of attack on unsteady characteristics are discussed. It is concluded that the method of harmonic averaging is applicable to directly solving unsteady nonlinear transonic aerodynamic problems in frquency domain. Dissert. Abstr.

N90-14199 North Carolina State Univ., Raleigh.
A ONE EQUATION TURBULENCE MODEL FOR TRANSONIC AIRFOILS Ph.D. Thesis
Robert Alan Mitcheltree 1989 108 p
Avail: Univ. Microfilms Order No. DA8918118

A one equation turbulence model based on the turbulent kinetic energy equation is presented. The model is motivated by the success of the Johnson-King model and is developed from the available experimental observations on both attached and separated turbulent flows. The model consists of three elements: an attached flow formulation, a separated flow formulation and an automatic blending function which smoothly switches between the two formulations. A central difference finite volume Navier Stokes code based on a Runge-Kutta time marching scheme is modified to facilitate numerical solution of the resulting set of equations. Results for both attached and separated flow about the NACA 0012 and RAE 2822 airfoils are compared with the Baldwin-Lomax algebraic turbulence model, the q - omega two equation model, the Johnson-King model and available experimental pressure and skin friction data. Based on the results obtained, the model duplicates the success of algebraic models in attached flow cases. For separated flow cases, it predicts shock location and strength closer to the experimentally observed values than both the algebraic and two equation models. However, the model suffers

some limitation in predicting shock location for transonic cases with large shock induced separation. Dissert. Abstr.

N90-14200*# Analytical Methods, Inc., Redmond, WA.
PROGRAM VSAERO THEORY DOCUMENT: A COMPUTER PROGRAM FOR CALCULATING NONLINEAR AERODYNAMIC CHARACTERISTICS OF ARBITRARY CONFIGURATIONS Final Report, Jul. 1984 - May 1987
Brian Maskew Washington NASA Sep. 1987 111 p
(Contract NAS2-11945)
(NASA-CR-4023; NAS 1.26:4023; AMI-8416) Avail: NTIS HC A06/MF A01 CSCL 01A

The VSAERO low order panel method formulation is described for the calculation of subsonic aerodynamic characteristics of general configurations. The method is based on piecewise constant doublet and source singularities. Two forms of the internal Dirichlet boundary condition are discussed and the source distribution is determined by the external Neumann boundary condition. A number of basic test cases are examined. Calculations are compared with higher order solutions for a number of cases. It is demonstrated that for comparable density of control points where the boundary conditions are satisfied, the low order method gives comparable accuracy to the higher order solutions. It is also shown that problems associated with some earlier low order panel methods, e.g., leakage in internal flows and junctions and also poor trailing edge solutions, do not appear for the present method. Further, the application of the Kutta conditions is extremely simple; no extra equation or trailing edge velocity point is required. The method has very low computing costs and this has made it practical for application to nonlinear problems requiring iterative solutions for wake shape and surface boundary layer effects. Author

N90-14201# Naval Postgraduate School, Monterey, CA.
COMPUTATIONAL INVESTIGATION OF INCOMPRESSIBLE AIRFOIL FLOWS AT HIGH ANGLES OF ATTACK M.S. Thesis
John Mark Mathre Dec. 1988 157 p
(AD-A205885) Avail: NTIS HC A08/MF A01 CSCL 01/1

Cebeci's viscous/inviscid interaction program was applied to the analysis of steady, two dimensional, incompressible flow past the NACA 663-018 0010 (Modified), 4412 and the Wortmann FX 63-137 airfoils. Detailed comparisons with the available experimental results show that the essential features are correctly modelled, but that significant discrepancies are found in regions of flow separations. Author

N90-14202*# National Aeronautics and Space Administration. Hugh L. Dryden Flight Research Facility, Edwards, CA.
AN IN-FLIGHT INVESTIGATION OF GROUND EFFECT ON A FORWARD-SWEPT WING AIRPLANE
Robert E. Curry, Bryan J. Moulton, and John Kresse Sep. 1989 14 p Presented at the AGARD Symposium on Aerodynamics of Combat Aircraft, Controls, and of Ground Effect, Madrid, Spain, 2-5 Oct. 1989
(NASA-TM-101708; H-1573; NAS 1.15:101708) Avail: NTIS HC A03/MF A01 CSCL 01A

A limited flight experiment was conducted to document the ground-effect characteristics of the X-29A research airplane. This vehicle has an aerodynamic platform which includes a forward-swept wing and close-coupled, variable incidence canard. The flight-test program obtained results for errors in the airdata measurement and for incremental normal force and pitching moment caused by ground effect. Correlations with wind-tunnel and computational analyses were made. The results are discussed with respect to the dynamic nature of the flight measurements, similar data from other configurations, and pilot comments. The ground-effect results are necessary to obtain an accurate interpretation of the vehicle's landing characteristics. The flight data can also be used in the development of many modern aircraft systems such as autoland and piloted simulations. Author

N90-14203*# National Aeronautics and Space Administration. Lewis Research Center, Cleveland, OH.
EFFICIENT REAL GAS NAVIER-STOKES COMPUTATIONS OF HIGH SPEED FLOWS USING AN LU SCHEME
William J. Coirier 1990 20 p Presented at the 28th Aerospace Sciences Meeting, Reno, NV, 8-11 Jan. 1990; sponsored by AIAA
(NASA-TM-102429; E-5197; NAS 1.15:102429; AIAA-90-0391)
Avail: NTIS HC A03/MF A01 CSCL 01A

An efficient method to account for the chemically frozen thermodynamic and transport properties of air in three dimensional Navier-Stokes calculations was demonstrated. This approach uses an explicitly specified equation of state (EOS) so that the fluid pressure, temperature and transport properties are directly related to the flow variables. Since the pressure is explicitly known as a general function of the flow variables no assumptions are made regarding the pressure derivatives in the construction of the flux Jacobians. The method is efficient since no sub-iterations are required to deduce the pressure and temperature from the flux variables and allows different equations of state to be easily supplied to the code. The flexibility of the EOS approach is demonstrated by implementing a high order TVD upwinding scheme based upon flux differencing and Van Leer's flux vector splitting. The EOS approach is demonstrated by computing the hypersonic flow through the corner region of two mutually perpendicular flat plates and through a simplified model of a scramjet module gap-seal configuration. Author

N90-14204*# Old Dominion Univ., Norfolk, VA. Dept. of Mechanical Engineering and Mechanics.
SUBSONIC STING INTERFERENCE ON THE AERODYNAMIC CHARACTERISTICS OF A FAMILY OF SLANTED-BASE OGIVE-CYLINDERS Final Report, period ending 30 Nov. 1989
Colin P. Britcher, Charles W. Alcorn, and W. Allen Kilgore Jan. 1990 74 p
(Grant NAG1-716)
(NASA-CR-186193; NAS 1.26:186193) Avail: NTIS HC A04/MF A01 CSCL 01A

Support interference free drag, lift, and pitching moment measurements on a range of slanted-base ogive-cylinders were made using the NASA Langley 13 inch Magnetic Suspension and Balance System. Typical test Mach numbers were in the range 0.04 to 0.2. Drag results are shown to be in broad agreement with previous tests with this configuration. Measurements were repeated with a dummy sting support installed in the wind tunnel. Significant support interferences were found at all test conditions and are quantified. Further comparison is made between interference free base pressures, obtained using remote telemetry, and sting cavity pressures. Author

N90-14205*# National Aeronautics and Space Administration. Langley Research Center, Hampton, VA.
EXPERIMENTAL TRANSONIC FLUTTER CHARACTERISTICS OF TWO 72 DEG-SWEEP DELTA-WING MODELS
Robert V. Doggett, Jr., David L. Soistmann, Charles V. Spain, Ellen C. Parker, and Walter A. Silva (Planning Research Corp., Hampton, VA.) Nov. 1989 20 p
(NASA-TM-101659; NAS 1.15:101659) Avail: NTIS HC A03/MF A01 CSCL 01A

Transonic flutter boundaries are presented for two simple, 72 deg. sweep, low-aspect-ratio wing models. One model was an aspect-ratio 0.65 delta wing; the other model was an aspect-ratio 0.54 clipped-delta wing. Flutter boundaries for the delta wing are presented for the Mach number range of 0.56 to 1.22. Flutter boundaries for the clipped-delta wing are presented for the Mach number range of 0.72 to 0.95. Selected vibration characteristics of the models are also presented. Author

N90-14206*# National Aeronautics and Space Administration. Lewis Research Center, Cleveland, OH.
AN ANALYSIS OF THE VISCOUS FLOW THROUGH A COMPACT RADIAL TURBINE BY THE AVERAGE PASSAGE APPROACH
James D. Heidmann and Timothy A. Beach (Sverdrup Technology,

Inc., Cleveland, OH.) 1990 13 p Prepared for presentation at the 35th International Gas Turbine Aeroengine Congress and Exposition, Brussels, Belgium, 11-14 Jun. 1990; sponsored by ASME
(NASA-TM-102471; E-5258; NAS 1.15:102471) Avail: NTIS HC A03/MF A01 CSCL 01A

A steady, three-dimensional viscous average passage computer code is used to analyze the flow through a compact radial turbine rotor. The code models the flow as spatially periodic from blade passage to blade passage. Results from the code using varying computational models are compared with each other and with experimental data. These results include blade surface velocities and pressures, exit vorticity and entropy contour plots, shroud pressures, and spanwise exit total temperature, total pressure, and swirl distributions. The three computational models used are inviscid, viscous with no blade clearance, and viscous with blade clearance. It is found that modeling viscous effects improves correlation with experimental data, while modeling hub and tip clearances further improves some comparisons. Experimental results such as a local maximum of exit swirl, reduced exit total pressures at the walls, and exit total temperature magnitudes are explained by interpretation of the flow physics and computed secondary flows. Trends in the computed blade loading diagrams are similarly explained. Author

N90-14207# George Washington Univ., Washington, DC. School of Engineering and Applied Science.
A COMPOSITE NUMERICAL PROCEDURE FOR CALCULATING THE MOTION OF VORTEX FILAMENTS M.S. Thesis
Craig Miller Kuhne Jan. 1990 84 p
Avail: NTIS HC A05/MF A01 CSCL 01A

A numerical procedure is presented for the solution of the motion of viscous vortex filaments. For the efficient computation of the motion of these vortices, including merging, the numerical procedure combines the asymptotic analysis of Callegari and Ting with a finite-difference method for the solution of the Navier-Stokes equations. The computationally inexpensive asymptotic analysis is used in regions where it is applicable. The finite-difference method is used in the limited regions where vortex merging occurs and the asymptotic analysis cannot be applied. A composite numerical procedure was developed based on this concept. This procedure links previously developed and tested modules that independently employ the asymptotic analysis and finite-difference method. For the current research, the existing codes were modified and numerous support modules written to allow for the development of the final composite computer code. The support modules were designed to provide two-way communication between the asymptotic and the finite-difference modules. The communication involves the supplementing of the boundary conditions on the surfaces of the finite difference computational domains using the asymptotic analysis as well as locating the filaments within the finite difference computational domains to be used by the asymptotic method. The numerical procedure was evaluated through the examination of two test cases: a single vortex ring and two off-center colliding vortex rings. The test cases show that the communication between the asymptotic analysis module and the finite-difference module are correct and demonstrate that the numerical procedure is a viable means by which to calculate the interaction and merging of multiple vortex filaments. Author

N90-14208# Argonne National Lab., IL. Chemical Dynamics Group.
CORRECTIONS FOR NON-IDEAL EFFECTS IN REFLECTED SHOCK WAVES AT LOW MACH NUMBERS
J. V. Michael and J. R. Fisher 1989 7 p Presented at the 17th International Symposium on Shock Waves and Shock Tubes (STS-17), Bethlehem, PA, 17-21 Jul. 1989
(Contract W-31-109-eng-38)
(DE90-002192; CONF-890756-3) Avail: NTIS HC A02/MF A01

Recent and new Flash Photolysis-Shock Tube results are reviewed and are compared to lower temperature results on the same reactions using a recently described procedure for boundary layer corrections in the reflected shock regime. A comparison is also made to the lower temperature results when the data bases are alternatively analyzed by ideal shock wave theory. DOE

N90-14209# Lawrence Livermore National Lab., CA.
KESTREL 3 PROGRAM Final Report
C. Chocol, W. Massey, R. Hoard, J. Hendricks, and M. Newman
17 Apr. 1989 123 p
(Contract W-7405-eng-48)
(DE90-001796; UCID-21674) Avail: NTIS HC A06/MF A01

Information on the major subsystems of the Kestrel balloon system is provided. Detailed data are provided in areas where major design and subsystem testing have taken place. Data are also provided on test support equipment, data acquisition, test conditions, assembly, and procedures within the Pacific Missile Test Center range, where testing occurred. DOE

N90-14210# Sandia National Labs., Albuquerque, NM.
VISUALIZATION OF BOUNDARY LAYER TRANSITION ZONE MOVEMENT ON OSCILLATING AIRFOILS WITH SHEAR-SENSITIVE LIQUID-CRYSTAL COATINGS
Daniel Reda and C. P. Butterfield (Midwest Research Inst., Golden, CO.) 1989 14 p Presented at the Winter Annual Meeting of the American Society of Mechanical Engineers, San Francisco, CA, 10-15 Dec. 1989
(Contract DE-AC04-76DP-00789)
(DE89-009570; SAND-88-3231C; CONF-891208-2) Avail: NTIS HC A03/MF A01

Oscillating and post-stall static airfoil experiments were conducted to test the frequency response of shear-stress-sensitive, temperature-insensitive liquid crystal coatings. The airfoil was a natural-laminar-flow profile designed specifically for vertical axis wind turbine applications (the SAND 0018/50). A full-span model of this contour was exposed to incompressible flows at a freestream Reynolds number (based on chord) of 1.0 x 10(exp 6). Angle-of-attack forcing function was a sine wave of amplitude + or - 10 degrees about a mean angle of 0 degree. Frequencies of oscillation were 0.2, 0.6 and 1.2 hertz, corresponding to reduced frequencies of 0.006, 0.018 and 0.037. Post-stall static experiments were conducted at a fixed angle of attack of 14 degrees, a condition that yielded unsteady leading-edge separation phenomena. Data acquisition was accomplished by video recording. Observations of boundary layer transition zone movement and unsteady leading-edge separation showed the liquid crystal technique capable of visualizing transient surface shear stress events over the stated dynamic range in a continuous and reversible manner, with a color-change response time of less than 0.03 seconds (the framing rate of standard video equipment). DOE

03 AIR TRANSPORTATION AND SAFETY

Includes passenger and cargo air transport operations; and aircraft accidents.

For related information see also *16 Space Transportation* and *85 Urban Technology and Transportation.*

N90-14211# Royal Aircraft Establishment, Farnborough (England).
EVALUATION OF THE INDIRECT EFFECTS OF LIGHTNING ON A SYSTEM: DOUBLE TRANSFER FUNCTION METHOD
G. Chambert and Y. Guillemot (Aerospatiale, Les Mureaux, France) Jan. 1989 16 p Transl. into ENGLISH of Evaluation des Effets Indirects de la Foudre sur un Systeme Methode la Double Fonction de Transfert (Les Mureaux, France, Aerospatiale)
(RAE-Trans-2172; BR111413) Avail: NTIS HC A03/MF A01

A program of evaluation and research into methods of testing on aircraft for the indirect effects of lightning is presented. After a statement of the principles, the validation of the method is undertaken by means of impulsive tests performed on a wing of an A300 and its application to a type AEHP lightning pulse is finally considered. Author

N90-14212*# California Polytechnic State Univ., San Luis Obispo. Dept. of Aeronautical Engineering.
CALIFORNIA AIR TRANSPORTATION STUDY: A TRANSPORTATION SYSTEM FOR THE CALIFORNIA CORRIDOR OF THE YEAR 2010
22 May 1989 195 p
(Contract NASw-4435)
(NASA-CR-186219; NAS 1.26:186219) Avail: NTIS HC A09/MF A02 CSCL 01C

To define and solve the problems of transportation in the California Corridor in the year 2010, the 1989 California Polytechnic State University Aeronautical Engineering Senior Design class determined future corridor transportation needs and developed a system to meet the requirements. A market study, which included interpreting travel demand and gauging the future of regional and national air travel in and out of the corridor, allowed the goals of the project to be accurately refined. Comprehensive trade-off studies of several proposed transporation systems were conducted to determine which components would form the final proposed system. Preliminary design and further analysis were performed for each resulting component. The proposed system consists of three vehicles and a special hub or mode mixer, the Corridor Access Port (CAP). The vehicles are: (1) an electric powered aircraft to serve secondary airports and the CAP; (2) a high speed magnetic levitation train running through the CAP and the high population density areas of the corridor; and (3) a vertical takeoff and landing tilt rotor aircraft to serve both intercity and intrametropolitan travelers from the CAP and city vertiports. The CAP is a combination and an extension of the hub, mode mixer, and Wayport concepts. The CAP is an integrated part of the system which meets the travel demands in the corridor, and interfaces with interstate and international travel. Author

N90-14213# Committee on Science, Space and Technology (U.S. House).
REVIEW OF THE AEROSPACE SAFETY ADVISORY PANEL REPORT FOR NASA FISCAL YEAR 1990 AUTHORIZATION
1989 113 p Hearing before the Subcommittee on Space Science and Applications of the Committee on Science, Space, and Technology, 101st Congress, 1st Session, no. 69, 28 Sep. 1989
(GPO-24-234) Avail: Subcommittee on Space Science and Applications, Washington, D.C. 20510 HC free; SOD HC $3.50 as 552-070-07499-6

The Panel identified five main categories of findings under the National Space Transportation System (NSTS), including management structure, safety enhancements, advanced solid rocket motor, logistics and support, and space shuttle elements. The Panel found that the NSTS management structure has been clarified and strengthened, and that the safety, reliability, maintainability, and quality assurance function is now stronger, more visible, better staffed, and better funded. It was recommended that these funds be protected to maintain safety. It was also recommended that lists of safety enhancements that are maintained be kept current and prioritized. NASA's decision to develop an advanced solid rocket motor was questioned. Implementation should be deferred until other alternatives have been evaluated. The NSTS logistics and support systems showed a satisfactory trend, but an improvement in overhaul and repair turnaround time was recommended. A program to improve solid rocket motors and boosters was also recommended, as well as tests to determine design corrections to meet original requirements for the booster aft skirt. The Panel recommended continued emphasis on developing and using strong risk assessment and management procedures. The Space Station Freedom Program is ungoing a complete review to accommodate anticipated reduced funding levels. Flight safety procedures for all NASA Centers are to be reviewed to determine their adequacy. J.P.S.

04 AIRCRAFT COMMUNICATIONS AND NAVIGATION

Includes digital and voice communication with aircraft; air navigation systems (satellite and ground based); and air traffic control.

For related information see also *17 Space Communications, Spacecraft Communications, Command and Tracking* and *Communications and Radar.*

N90-14214# Computer Resource Management, Inc., Vienna, VA.
NATIONAL AIRSPACE SYSTEM MONITORING OPERATIONAL CONCEPT
William Trent, Rodney Kuhn, and Thomas Pickerell Nov. 1989 44 p
(Contract DTFA01-88-Y-01073)
(NAS-SR-1330; DOT/FAA/DS-89/31) Avail: NTIS HC A03/MF A01

A requirement for the National Airspace System (NAS) is to provide a variety of monitoring services to its users, as identified in the NAS System Requirement Specification, NAS-SR-1000. A concept of operations for monitoring is presented. Monitoring capabilities are described, and the relationships between subsystems, facilities, information, and operators/users are shown. Here the intent is to provide a common perspective for personnel involved in monitoring services, assist in determining whether monitoring procedures meet formal requirements, and support coordination among the organizations involved. Author

N90-14215# Systems Technology, Inc., Hawthorne, CA.
FIELD EVALUATION OF A NISSAN LASER COLLISION AVOIDANCE SYSTEM Final Report
Anthony C. Stein, David Ziedman, and Zareh Parseghian Jan. 1989 32 p
(Contract DTNH22-87-D-07174)
(PB90-105602; STI-TR-1256-1-1; DOT-HS-807-417) Avail: NTIS HC A03/MF A01 CSCL 01C

A laser based anti-collision system developed by Nissan Motor Co. is evaluated. The system is intended to provide a warning to the driver when the equipped vehicle is approaching another vehicle or object at a rate which, if maintained, will result in a collision. Task 1 of these tests was a qualitative evaluation of the anti-collision system under normal driving conditions. The task 2 evaluation was quantitative, and included verification of the range, speed, and closing rate data obtained from the system, as well as testing the interference capability of the unit itself, and possible system malfunctions due to various atmospheric phenomena. It should also be noted that the system used in these tests is several years old. The system, as well as others developed by other manufacturers, have most likely been improved during the intervening years. Author

05 AIRCRAFT DESIGN, TESTING AND PERFORMANCE

Includes aircraft simulation technology.

For related information see also *18 Spacecraft Design, Testing and Performance* and *39 Structural Mechanics.* For land transportation vehicles see *85 Urban Technology and Transportation.*

N90-14216*# Purdue Univ., West Lafayette, IN. School of Aeronautics and Astronautics.
DESIGN OF A SPANLOADER CARGO AIRCRAFT Final Report, 1988-1989
Terrence A. Weisshaar 12 Jun. 1989 25 p
(Contract NASw-4435)
(NASA-CR-186046; NAS 1.26:186046) Avail: NTIS HC A03/MF A01 CSCL 01C

The design features of an aircraft capable of fulfilling a long haul, high capacity cargo mission are described. This span-loading

aircraft, or flying wing, is capable of carrying extremely large payloads and is expected to be in demand to replace the slow-moving cargo ships currently in use. The spanloader seeks to reduce empty weight by eliminating the aircraft fuselage. Disadvantages are the thickness of the cargo-containing wing, and resulting stability and control problems. The spanloader presented here has a small fuselage, low-aspect ratio wings, winglets, and uses six turbofan engines for propulsion. It will have a payload capacity of 300,000 pounds plus 30 first class passengers and 6 crew members. Its projected market is transportation of freight from Europe and the U.S.A. to countries in the Pacific Basin. Cost estimates support its economic feasibility. J.P.S.

N90-14217# Aeronautical Research Labs., Melbourne (Australia). Aircraft Systems.
AcSim: AIRCRAFT SIMULATION PROGRAM WITH APPLICATION TO FLIGHT PROFILE GENERATION
A. G. Page Jun. 1989 38 p
(AD-A212466; ARL-SYS-TM-106; DODA-AR-005-512) Avail: NTIS HC A03/MF A01 CSCL 01/3

Program AcSim was designed to be used in conjunction with a flight profile generator program (FPG2) which is used with an Inertial Navigation System simulator. Both AcSim and FPG2 were written in FORTRAN-77 on an ELXSI System 6400. AcSim is implemented as a subroutine of FPG2 and is called if the user selects a dynamic maneuver segment to be performed. AcSim calculates the dynamic state of an aircraft for a sequence of user specified control surface deflections. The aircrafts linear accelerations and angular velocities are sent back to FPG2 for subsequent processing. A six-degree-of-freedom model is used to simulate the user-defined aircraft. AcSim implements a State Vector approach to solve the non-linear equations of motion simultaneously using a 4th order Runge-Kutta scheme. An optional Eigen Analysis can be performed which provides the user with longitudinal and lateral characteristic equation, their roots (eigen values), transfer functions and unit impulse response functions for the given flight condition. GRA

N90-14218# Advisory Group for Aerospace Research and Development, Neuilly-Sur-Seine (France). Flight Mechanics Panel.
FLIGHT IN ADVERSE ENVIRONMENTAL CONDITIONS
J. F. Renaudie Oct. 1989 29 p Presented at the Flight Mechanics Panel Symposium in Gol, Norway, 8-11 May 1989
(AGARD-AR-277; ISBN-92-835-0531-X) Copyright Avail: NTIS HC A03/MF A01

Four aspects of adverse environmental conditions of interest to the flight mechanics specialists were addressed by this symposium: atmospheric disturbances, reduced visibility, icing and electromagnetic disturbances. All four of these can seriously affect flight safety, comfort and operational capability. The topic was and still is considered to be particularly relevant to the needs of the military community which is putting increased emphasis on the ability of today's and tomorrow's aircraft to fly safely and effectively in the adverse conditions dealt with in this symposium. Author

N90-14219 Georgia Inst. of Tech., Atlanta.
AN EXPERIMENTAL INVESTIGATION OF THE INTERACTION BETWEEN A MODEL ROTOR AND AIRFRAME IN FORWARD FLIGHT Ph.D. Thesis
Albert Gerard Brand 1989 235 p
Avail: Univ. Microfilms Order No. DA8919733

A series of experiments were conducted in the John J. Harper 7 x 9-foot wind tunnel to measure the interaction effects for an idealized rotor-airframe configuration. Detailed pressure measurements on the airframe surface were correlated with quantitative flow visualization data. Correlations allowed for specific structures in the wake flow to be identified with the corresponding effect measured on the airframe. Impingement of the rotor tip vortex on the airframe surface was found to create a low (instantaneous) pressure region on the surface. The interaction of the vortex sheet structure with the airframe also created a low instantaneous pressure on the surface. The effects of the rotor blade on the airframe were significant. A large positive pressure pulsation occurred on the airframe each time a blade passed over the airframe. Suitable theoretical models for explaining these interaction effects were developed, and a comprehensive data base was generated to allow future analytical efforts for predicting these interactions to be tested. Dissert. Abstr.

N90-14220*# National Aeronautics and Space Administration. Ames Research Center, Moffett Field, CA.
GLOBAL STRATOSPHERIC CHANGE: REQUIREMENTS FOR A VERY-HIGH-ALTITUDE AIRCRAFT FOR ATMOSPHERIC RESEARCH
1989 41 p Workshop held in Truckee, CA, 15-16 Jul. 1989
(NASA-CP-10041; A-89243; NAS 1.55:10041) Avail: NTIS HC A03/MF A01 CSCL 01C

The workshop on Requirements for a Very-High-Altitude Aircraft for Atmospheric Research, sponsored by NASA Ames Research Center, was held July 15 to 16, 1989, at Truckee, CA. The workshop had two purposes: to assess the scientific justification for a new aircraft that will support stratospheric research beyond the altitudes accessible to the NASA ER-2; and to determine the aircraft characteristics (e.g., ceiling altitude, payload accommodations, range, flight duration, operational capabilities) required to perform the stratospheric research referred to in the justification. To accomplish these purposes, the workshop brought together a cross-section of stratospheric scientists with several aircraft design and operations experts. The stratospheric scientists included theoreticians as well as experimenters with experience in remote and in situ measurements from satellites, rockets, balloons, aircraft, and the ground. Discussions of required aircraft characteristics focused on the needs of stratospheric research. It was recognized that an aircraft optimal for stratospheric science would also be useful for other applications, including remote measurements of Earth's surface. A brief description of these other applications was given at the workshop. Author

N90-14221 ESDU International Ltd., London (England).
INTRODUCTION TO DATA ITEMS ON FLIGHT PATH OPTIMISATION
Aug. 1989 11 p
(ESDU-89015; ISBN-0-85679-687-5; ISSN-0141-4054) Avail: ESDU

This Data Item 89015, an addition to the Aircraft Performance Subseries, starts by setting out the completely general problem in terms of the equations of motion of the aircraft, the constraints on the state and control variables due to physical or operational limitations, and a performance index which is the quantity to be optimized (for example, time to height). It discusses various simplifications that can then be applied to bring the problem into a solvable form, treating the aircraft as a point mass and ignoring both the rotational motion and airframe flexibility. Although the problem is then reduced to one solvable, it still contains some fourteen equations and some care is needed to justify the use of such complexity; in some cases the performance index will vary quite slowly near the optimum and a trajectory, more easily flow or controlled, a little removed from the true optimum may be acceptable. Finally, the introduction of further simplifications such as assuming lift equals weight, drag is constant at the level-flight value, or small flight path angle, is considered and the value of results obtained is assessed. ESDU

N90-14222# Wichita State Univ., KS. Inst. for Aviation Research.
STALL/SPIN AERODYNAMIC DATA PROJECT Final Report, 1 Oct. 1986 - 30 Sep. 1988
Melvin H. Snyder Sep. 1989 123 p
(DOT/FAA/CT-88/29) Avail: NTIS HC A06/MF A01

The purpose was to develop a bank of aerodynamic data including high angle-of-attack aerodynamic characteristics of 2-D airfoils and characteristics of 3-D wings and of complete airplanes beyond the stall. To fill gaps in available literature, flow visualization studies and wind tunnel tests were to be conducted. Also, a flow

visualization laboratory was to be established to study wing stall and anti-stall devices. The flow visualization laboratory is in operation. A bank of 2-D high angle-of-attack airfoil data was compiled. The 3-D data were acquired; water tunnel and wind tunnel reflection plane tests were performed and continue. Data obtained indicated that movable leading-edge control surfaces show promise toward the goal of controlled flight beyond the stall. Author

N90-14223 Georgia Inst. of Tech., Atlanta.
AN ANALYTICAL METHOD FOR THE PREDICTION OF UNSTEADY ROTOR/AIRFRAME INTERACTIONS IN FORWARD FLIGHT Ph.D. Thesis
Dimitris N. Mavris 1988 314 p
Avail: Univ. Microfilms Order No. DA8916164

A prediction code has been developed at Georgia Tech for the prediction of unsteady aerodynamic rotor-airframe interactions in forward flight. This method is based on the extension and coupling of a lifting line/free-wake rotor analysis (Scully free-wake code) and a source/doublet panel fuselage analysis (VSAERO). Coupling is achieved by iterating on the disturbance velocities induced by the airframe at the rotor inflow plane, and on the effect of the rotor and wake on the airframe. Physical flow features such as the energy addition in the wake and the blade passage effect have been modeled and included in the analysis. Provisions have been made to allow the rotor wake to distort freely in the presence of the airframe. In addition, the code has been extended to account for rotor wake/lifting surface interactions. Preliminary results (both time averaged and unsteady) from this study are presented along with a discussion on possible ways to improve correlations with experimental results. Results from this new code, called GTRAIC (Georgia Tech Rotor Airframe Interaction Code), have been validated against data obtained in the Georgia Tech 2.13 x 2.74 meter wind tunnel for a two bladed teetering rotor mounted over a cylindrical body with a hemispherical nose.
Dissert. Abstr.

N90-14224*# National Aeronautics and Space Administration. Hugh L. Dryden Flight Research Facility, Edwards, CA.
AN IN-FLIGHT TECHNIQUE FOR WIND MEASUREMENT IN SUPPORT OF THE SPACE SHUTTLE PROGRAM
Lisa J. Bjarke and L. J. Ehernberger Washington Nov. 1989 25 p Presented at the Society of Flight Test Engineers 20th Annual Symposium, Reno, NV, 18-21 Sep. 1989
(NASA-TM-4154; H-1566; NAS 1.15:4154) Avail: NTIS HC A03/MF A01 CSCL 01C

A technique to use an aircraft to measure wind profiles in the altitude range of 1,500 to 18,200 m was demonstrated at NASA Ames-Dryden. This demonstration was initiated to determine if an aircraft could measure wind profiles in support of space shuttle launches. The Jimsphere balloon is currently the device used to measure pre-launch wind profiles for the space shuttle. However, it takes approximately an hour for the Jimsphere to travel through the altitudes of interest. If these wind instruments could be taken with an aircraft closer to launch in a more timely manner and with the same accuracy as a Jimsphere balloon, some uncertainties in the measurements could be removed. The aircraft used for this investigation was an F-104G which is capable of flight above 18,000 m. It had conventional research instrumentation to provide air data and flow angles along with a ring laser gyro inertial navigation system (INS) to provide inertial and Euler angle data. During the course of 17 flights, wind profiles were measured in 21 climbs and 18 descents. Preliminary comparisons between aircraft measured wind profiles and Jimsphere measured profiles show reasonable agreement (within 3 m/sec). Most large differences between the profiles can usually be explained by large spatial or time differences between the Jimsphere and aircraft measurements, the fact that the aircraft is not in a wings-level attitude, or INS shifts caused by aircraft maneuvering. Author

N90-14225*# National Aeronautics and Space Administration. Hugh L. Dryden Flight Research Facility, Edwards, CA.
FLIGHT EVALUATION OF A PNEUMATIC SYSTEM FOR UNSTEADY PRESSURE MEASUREMENTS USING CONVENTIONAL SENSORS
Robert E. Curry and Glenn B. Gilyard Washington Aug. 1989 20 p Presented at the 4th AIAA Flight Test Conference, San Diego, CA, 18-20 May 1988
(NASA-TM-4131; H-1508; NAS 1.15:4131) Avail: NTIS HC A03/MF A01 CSCL 01C

A flight experiment was conducted to evaluate a pressure measurement system which uses pneumatic tubing and remotely located electronically scanned pressure transducer modules for in-flight unsteady aerodynamic studies. A parametric study of tubing length and diameter on the attenuation and lag of the measured signals was conducted. The hardware was found to operate satisfactorily at rates of up to 500 samples/sec per port in flight. The signal attenuation and lag due to tubing were shown to increase with tubing length, decrease with tubing diameter, and increase with altitude over the ranges tested. Measurable signal levels were obtained for even the longest tubing length tested, 4 ft, at frequencies up to 100 Hz. This instrumentation system approach provides a practical means of conducting detailed unsteady pressure surveys in flight. Author

N90-14226*# California Polytechnic State Univ., San Luis Obispo. Dept. of Aeronautical Engineering.
PRELIMINARY DESIGN OF FOUR AIRCRAFT TO SERVICE THE CALIFORNIA CORRIDOR IN THE YEAR 2010: THE CALIFORNIA CONDOR, CALIFORNIA SKY-HOPPER, HIGH CAPACITY SHORT RANGE TRANSPORT TILT ROTOR AIRCRAFT NEEDED TO SIMPLIFY INTERCITY TRANSPORTATION
22 May 1989 267 p
(Contract NASw-4435)
(NASA-CR-186232; NAS 1.26:186232) Avail: NTIS HC A12/MF A02 CSCL 01C

The major objective of this project was to design an aircraft for use in the California Corridor in the year 2010. The design process, completed by students in a senior design class at California Polytechnic State University, San Luis Obispo, used a Class 1 airplane design analysis from Jan Roskam's Airplane Design. The California Condor (CC-38), a 38 passenger, 400 mph aircraft, was designed to meet the needs of tomorrow's passengers while conforming to the California Corridor's restrictions. Assumptions were made using today's technology with forecasts into 21st Century technology. Doubling today's commuter aircraft passenger capacity, travelling at Mach .57 with improved cruise efficiencies of over 10 percent, with the ability to land within field lengths of 4000 feet, are the CC-38's strongest points. The California Condor has a very promising future in helping to relieve the air traffic and airport congestion in the 21st Century. Author

N90-14227# Los Alamos National Lab., NM.
DESIGN AND DEMONSTRATION OF HEAT PIPE COOLING FOR NASP AND EVALUATION OF HEATING METHODS AT HIGH HEATING RATES
Michael A. Merrigan and J. Tom Sena 1989 12 p Presented at the 7th National Aero-Space Plane Technology Symposium, Cleveland, OH, 23-27 Oct. 1989
(Contract W-7405-eng-36)
(DE89-016995; LA-UR-89-2876; CONF-8910203-1) Avail: NTIS HC A03/MF A01

An evaluation of two heating methods for demonstration of NASP leading edge heat pipe technology was conducted. The heating methods were and RF induction heated plasma jet and direct RF induction. Tests were conducted to determine coupling from the argon plasma jet on a surface physically similar to a heat pipe. A molybdenum tipped calorimeter was fabricated and installed in an RF induction heated plasma jet for the test. The calorimetric measurements indicated a maximum power coupling of approximately 500 W/sq cm with the RF plasma jet. The effect of change in gas composition on the heating rate was investigated

using helium. An alternative to the plasma heating of a heat pipe tip, an RF concentrator was evaluated for coupling to the hemispherical tip of a heat pipe. A refractory metal heat pipe was designed, fabricated, and tested for the evaluation. The heat pipe was designed for operation at 1400 to 1900 K with power input to 1000 W/sq cm over a hemispherical nose tip. Power input of 800 W/sq cm was demonstrated using the RF concentrator.
DOE

N90-14228*# National Aeronautics and Space Administration. Ames Research Center, Moffett Field, CA.
AIRDATA CALIBRATION OF A HIGH-PERFORMANCE AIRCRAFT FOR MEASURING ATMOSPHERIC WIND PROFILES
Edward A. Haering, Jr. Jan. 1990 27 p Presented at the AIAA 28th Aerospace Sciences meeting, Reno, NV, 8-11 Jan. 1990
(NASA-TM-101714; H-1580; NAS 1.15:101714; AIAA-90-0320)
Avail: NTIS HC A03/MF A01 CSCL 01C

The research airdata system of an instrumented F-104 aircraft has been calibrated to measure winds aloft in support of the space shuttle wind measurement investigation at the National Aeronautics and Space Administration Ames Research Center Dryden Flight Research Facility. For this investigation, wind measurement accuracies comparable to those obtained from Jimsphere balloons were desired. This required an airdata calibration more accurate than needed for most aircraft research programs. The F-104 aircraft was equipped with a research pilot-static noseboom with integral angle-of-attack and flank angle-of-attack vanes and a ring-laser-gyro inertial reference unit. Tower fly-bys and radar acceleration-decelerations were used to calibrate Mach number and total temperature. Angle of attack and angle of sideslip were calibrated with a trajectory reconstruction technique using a multiple-state linear Kalman filter. The F-104 aircraft and instrumentation configuration, flight test maneuvers, data corrections, calibration techniques, and resulting calibrations and data repeatability are presented. Recommendations for future airdata systems on aircraft used to measure winds aloft are also given. Author

06 AIRCRAFT INSTRUMENTATION

Includes cockpit and cabin display devices; and flight instruments.

For related information see also *19 Spacecraft Instrumentation* and *35 Instrumentation and Photography.*

N90-14229*# General Dynamics Corp., San Diego, CA. Space Systems Div.
DEFINITION OF AVIONICS CONCEPTS FOR A HEAVY LIFT CARGO VEHICLE. VOLUME 1: EXECUTIVE SUMMARY Final Report
Sep. 1989 45 p
(Contract NAS8-37578)
(NASA-CR-183818; NAS 1.26:183818) Avail: NTIS HC A03/MF A01 CSCL 01D

A cost effective, multiuser simulation, test, and demonstration facility to support the development of avionics systems for future space vehicles is examined. The technology needs and requirements of future Heavy Lift Cargo Vehicles (HLCVs) are analyzed and serve as the basis for sizing of the avionics facility, although the lab is not limited in use to support of HLCVs. Volume 1 provides a summary of the vehicle avionics trade studies, the avionics lab objectives, a summary of the lab's functional requirements and design, physical facility considerations, and cost estimates. Author

N90-14230*# General Dynamics Corp., San Diego, CA. Space Systems Div.
DEFINITION OF AVIONICS CONCEPTS FOR A HEAVY LIFT CARGO VEHICLE, VOLUME 2 Final Report
Sep. 1989 93 p
(Contract NAS8-37578)
(NASA-CR-183819; NAS 1.26:183819) Avail: NTIS HC A05/MF A01 CSCL 01D

A cost effective, multiuser simulation, test, and demonstration facility to support the development of avionics systems for future space vehicles is defined. The technology needs and requirements of future Heavy Lift Cargo Vehicles (HLCVs) are analyzed and serve as the basis for sizing of the avionics facility although the lab is not limited in use to support of HLCVs. Volume 2 is the technical volume and provides the results of the vehicle avionics trade studies, the avionics lab objectives, the lab's functional requirements and design, physical facility considerations, and a summary cost estimate. Author

N90-14231*# General Dynamics Corp., San Diego, CA. Space Systems Div.
PRELIMINARY DESIGN DOCUMENT: GROUND BASED TESTBED FOR AVIONICS SYSTEMS
Feb. 1989 72 p
(Contract NAS8-37578)
(NASA-CR-183821; NAS 1.26:183821) Avail: NTIS HC A04/MF A01 CSCL 01D

The design and interface requirements for an avionics Ground Based Test bed (GBT) to support Heavy Lift Cargo Vehicles (HLCV) is presented. It also contains data on the vehicle subsystem configurations that are to be supported during their early, pre-PDR developmental phases. Several emerging technologies are also identified for support. A Preliminary Specification Tree is also presented. Author

N90-14232*# National Aeronautics and Space Administration. Langley Research Center, Hampton, VA.
A CANDIDATE CONCEPT FOR DISPLAY OF FORWARD-LOOKING WIND SHEAR INFORMATION
David A. Hinton Oct. 1989 92 p
(NASA-TM-101585; NAS 1.15:101585; DOT/FAA/DS-89/23)
Avail: NTIS HC A05/MF A01 CSCL 01D

A concept is proposed which integrates forward-look wind shear information with airplane performance capabilities to predict future airplane energy state as a function of range. The information could be displayed to a crew either in terms of energy height or airspeed deviations. The anticipated benefits of the proposed display information concept are: (1) a wind shear hazard product that scales directly to the performance impact on the airplane and that has intuitive meaning to flight crews; (2) a reduction in flight crew workload by automatic processing of relevant hazard parameters; and (3) a continuous display of predicted airplane energy state if the approach is continued. Such a display may be used to improve pilot situational awareness or improve pilot confidence in wind shear alerts generated by other systems. The display is described and the algorithms necessary for implementation in a simulation system are provided. Author

07 AIRCRAFT PROPULSION AND POWER

Includes prime propulsion systems and systems components, e.g., gas turbine engines and compressors; and onboard auxilliary power plants for aircraft.

For related information see also *20 Spacecraft Propulsion and Power, 28 Propellants and Fuels,* and *44 Energy Production and Conversion.*

N90-14233 Mississippi State Univ., State College.
ADVANCED 3-D CFD ALGORITHM FOR TURBOMACHINERY Ph.D. Thesis
J. Mark Janus 1989 157 p
Avail: Univ. Microfilms Order No. DA8917069

The building blocks of a computer algorithm are developed for the time-accurate flow analysis of rotating machines. The flow model is a finite volume method utilizing a high resolution approximate Riemann solver for interface flux definitions. The

numerical scheme is a block LU implicit iterative-refinement method which possesses apparent unconditional stability. Multiblock composite gridding is used to orderly partition the field into a specified arrangement of blocks which exhibit varying degrees of similarity. Block-block interfaces, including dynamic interfaces, are treated such as to mimic interior block communication, thus introducing no additional spatial differencing error. Special attention is given to the reduction of in-core memory requirements by placing the burden of secondary storage media. Broad applicability is implied, providing for the means to investigate several configurations. Included within the collection of configurations analyzed is that of the GE UDF counterrotating unducted fan. Comparisons with UDF8-8 experiments are included. Also included are comparisons between UDF8-8 and its uneven-blade-count derivative, the UDF11-9, which has eleven fore and nine aft blades per blade row. Dissert. Abstr.

N90-14234 Georgia Inst. of Tech., Atlanta.
ACOUSTIC-VORTICAL-COMBUSTION INTERACTION IN A SOLID FUEL RAMJET SIMULATOR Ph.D. Thesis
James Arthur Davis 1989 190 p
Avail: Univ. Microfilms Order No. DA8919740

The interaction between vortical structures and an externally applied acoustic field in a complex turbulent flow field was investigated. The flow field was produced by a flow of air over a backward facing step in a rectangular section duct. The purposes of this investigation were: (1) to demonstrate the existence of somewhat organized vortical structures in the shear layer; (2) to demonstrate that the vortical structures are influenced (organized) by an applied acoustic field; (3) to determine if the vortical structures in turn affect the applied acoustic field; and (4) to determine if combustion affects the applied acoustic field. By anemometry and acoustic pressure measurement, together with aeroacoustic theory, the first demonstrations were made. However, in the flow field used, without strong downstream constrictions, there was discernible feedback into the acoustic field only in the presence of combustion. The results obtained have application to ramjet type flow fields. Dissert. Abstr.

N90-14235*# National Aeronautics and Space Administration. Lewis Research Center, Cleveland, OH.
RAMSCRAM: A FLEXIBLE RAMJET/SCRAMJET ENGINE SIMULATION PROGRAM
Leo A. Burkardt and Leo C. Franciscus 1990 6 p Prepared for presentation at the 35th International Gas Turbine Aeroengine Congress and Exposition, Brussels, Belgium, 11-14 Jun. 1990; sponsored by ASME
(NASA-TM-102451; E-5236; NAS 1.15:102451) Avail: NTIS HC A02/MF A01 CSCL 21E

With the resurgence of interest in high supersonic and hypersonic flight there is a need to simulate airbreathing engines which may be used in this flight regime. To meet this requirement the RAMSCRAM code was developed. The code calculates 1-D flow properties at each component interface and the overall performance of the engine. It uses equilibrium thermodynamics which accounts for dissociation and allows for any fuel or combination of fuels. The program can simulate ramjet, scramjet, rocket, and ducted rocket engines. Author

N90-14236*# National Aeronautics and Space Administration. Ames Research Center, Moffett Field, CA.
TEMPORALLY AND SPATIALLY RESOLVED FLOW IN A TWO-STAGE AXIAL COMPRESSOR. PART 2: COMPUTATIONAL ASSESSMENT
Karen L. Gundy-Burlet, Man Mohan Rai, R. Charles Stauter, and Robert P. Dring (United Technologies Research Center, East Hartford, CT.) Jan. 1990 11 p Proposed for presentation at the 35th ASME International Gas Turbine and Aerospace Congress and Exhibition, Brussels, Belgium, 11-14 Jun. 1990
(NASA-TM-102273; A-90048; NAS 1.15:102273) Avail: NTIS HC A03/MF A01 CSCL 21E

Fluid dynamics of turbomachines are complicated due to aerodynamic interactions between rotors and stators. It is necessary to understand the aerodynamics associated with these interactions in order to design turbomachines that are both light and compact as well as reliable and efficient. The current study uses an unsteady, thin-layer Navier-Stokes zonal approach to investigate the unsteady aerodynamics of a multi-stage compressor. Relative motion between rotors and stators is made possible by use of systems of patched and overlaid grids. Results have been computed for a 2 1/2-stage compressor configuration. The numerical data compares well with experimental data for surface pressures and wake data. In addition, the effect of grid refinement on the solution is studied. Author

08 AIRCRAFT STABILITY AND CONTROL

Includes aircraft handling qualities; piloting; flight controls; and autopilots.

For related information see also *05 Aircraft Design, Testing and Performance.*

N90-14237# Calspan Corp., Arnold AFS, TN.
DEVELOPMENT OF A THREE-AXIS TRIM PROGRAM Final Report, Jun. 1988 - May 1989
R. L. Arterbury Sep. 1989 86 p Prepared in cooperation with AEDC, Arnold AFS, TN
(AD-A212883; AEDC-TR-89-10) Avail: NTIS HC A05/MF A01 CSCL 12/5

This report describes the development and validation of a three-axis trim capability computer program which has been added to the Aerodynamic Data Analysis Program currently in use at the Arnold Engineering Development Center. Appendixes provided with the report describe the information requested by the prompting program, show prompting session lists, plots, and files, and include a description and listing of example case output. GRA

N90-14238 ESDU International Ltd., London (England).
EFFECT OF UNSHIELDED AND SHIELDED HORN BALANCES ON HINGE MOMENT COEFFICIENTS FOR CONTROLS AT LOW SPEEDS
Aug. 1989 12 p Supersedes ESDU-87032 and ESDU-Aero-C.04.01.07
(ESDU-89003-A; ESDU-87032; ESDU-Aero-C.04.01.07; ISBN-0-85679-635-2; ISSN-0141-397X) Avail: ESDU

This Data Item 88003, an addition to the Aerodynamic Subseries, gives an semi-empirical method for predicting the increments in the rates of change of hinge moment with incidence and with control deflection for controls fitted with horns at their tips. The increments are functions of control and horn planform geometry and airfoil thickness/chord ratio over the horn span for unswept or moderately swept (up to 30 degrees) hinge lines. However, it was found that the increment with control deflection also depended on the nose shape, being larger for round-nosed horns than for elliptically-nosed horns, and on trailing-edge angle for the unshielded horns only. The range of geometries for which experimental results were available in the literature with which to develop the method is specified; airfoil thickness/chord ratio varies from 0.05 to 0.15. Sketches compare predictions with the experimental results. For unshielded horns the increment with incidence is predicted within 0.05 per radian (for a coefficient based on control area and chord measured aft of the hinge line) and with control deflection to within 0.03 radian. For shielded horns both increments are predicted within 0.025 per radian. ESDU

N90-14239 ESDU International Ltd., London (England).
HINGE MOMENT COEFFICIENT DERIVATIVES FOR TRAILING-EDGE CONTROLS ON WINGS AT SUBSONIC SPEEDS
Jul. 1989 20 p Supersedes ESDU-Aero-C.04.01.05 and ESDU-Aero-C.04.01.00
(ESDU-89009; ESDU-Aero-C.04.01.05; ESDU-Aero-C.04.01.00; ISBN-0-85679-680-8; ISSN-0141-397X) Avail: ESDU

This Data Item 89009, an addition to the Aerodynamic Subseries, provides a prediction method for full span and part span sealed controls that can also be used for elevators and rudders. Data for two-dimensional flow, assumed constant over the span of the control, are corrected for induced angle of attack and induced camber on the basis of lifting surface theory, and Prandtl-Glauert laws similarity are used to correct for compressibility. The part span correction for controls extending spanwise from any station to near the tip is empirical. Sketches compare predictions by the method with experimental data extracted from the literature and show the derivative with deflection within 0.05 per radian. The range of geometrics used in developing the method included wing aspect ratios of 2 to 8, half chord sweeps up to 50 degrees and thickness/chord ratio of 0.06 to 0.14. The two-dimensional data, including if required the effect of either nose or Irving internal balance, are available in other ESDU documents in the Subseries. A worked example illustrates the use of the method. ESDU

N90-14240 ESDU International Ltd., London (England).
EXAMPLE OF PROCEDURE IN CALCULATION OF CONTROL HINGE MOMENTS
Aug. 1989 19 p Supersedes ESDU-Aero-C.04.01.09
(ESDU-89010; ESDU-Aero-C.04.01.09; ISBN-0-85679-681-6; ISSN-0141-397X) Avail: ESDU

This Data Item 89010, an addition to the Aerodynamic Subseries, gives calculation sheets for estimating hinge moment coefficients for trailing-edge controls on a wing, tailplane, or fin. Values to be entered on the sheets can be extracted from other ESDU documents in the Subseries, and the calculation is divided into four steps. The first sheet gives the routine for the two-dimensional characteristics, which may include the effect of a nose or an Irving internal balance. The next sheet deals with establishing the three-dimensional values of the derivatives using the values from the first sheet. The third sheet calculates the increment to the derivatives from a horn balance and the last sheet provides the procedure for treating the effect of a tab. A worked example illustrates the use of the calculation procedures. ESDU

N90-14241 Georgia Inst. of Tech., Atlanta.
OPTIMAL CONTROL OF AERO-ASSISTED ORBIT TRANSFER VEHICLES Ph.D. Thesis
Gyoung Hyun Bae 1989 163 p
Avail: Univ. Microfilms Order No. DA8919731

The problem of real time guidance and optimal control of Aeroassisted Orbit Transfer Vehicles (AOTV's) is discussed. An outline of the research is as follows. The application of Singular Perturbation Theory (SPT) to various types of aircraft problems has produced results that are very useful in designing on-board optimal controllers. Given this fact, the optimal control problem of AOTV's with the capability of large orbit plane change has been addressed using SPT as an underlying method of analysis. Trajectories have been optimized with the view point of minimum energy expenditure. Research was also focused on the derivation of analytic optimal control solutions which can be implemented on-board, and in real time. This research is composed of two major problem areas: optimal reentry, and synergetic plane change with aeroglide. Additionally, synergetic plane change with constrained aeroglide is discussed. Dissert. Abstr.

N90-14242 Georgia Inst. of Tech., Atlanta.
A HELICOPTER FLIGHT PATH CONTROLLER DESIGN VIA A NONLINEAR TRANSFORMATION TECHNIQUE Ph.D. Thesis
Michael William Heiges 1989 248 p
Avail: Univ. Microfilms Order No. DA8919742

Helicopters are highly nonlinear systems to control. They require significant pilot effort in elaborate stability augmentation systems. Current generation flight control systems are synthesized based on approximate linearized models of the aircraft. As a result, gain scheduling must be used to accommodate changes in the dynamic behavior as a flight regime changes. To overcome this difficulty, nonlinear transformation theory is used to develop a controller that gives the desired response in all flight modes. Additionally, singular perturbation theory is employed to simplify the transformation process. Simulations are conducted to evaluate the performance of the controller and its sensitivity to plant parameter uncertainty. Dissert. Abstr.

N90-14243*# Old Dominion Univ., Norfolk, VA. Dept. of Electrical and Computer Engineering.
GUIDANCE AND CONTROL STRATEGIES FOR AEROSPACE VEHICLES Progress Report, 1 Jul. - 31 Dec. 1989
J. L. Hibey, D. S. Naidu, and C. D. Charalambous Dec. 1989 100 p
(Grant NAG1-736)
(NASA-CR-186195; NAS 1.26:186195) Avail: NTIS HC A05/MF A01 CSCL 01C

A neighboring optimal guidance scheme was devised for a nonlinear dynamic system with stochastic inputs and perfect measurements as applicable to fuel optimal control of an aeroassisted orbital transfer vehicle. For the deterministic nonlinear dynamic system describing the atmospheric maneuver, a nominal trajectory was determined. Then, a neighboring, optimal guidance scheme was obtained for open loop and closed loop control configurations. Taking modelling uncertainties into account, a linear, stochastic, neighboring optimal guidance scheme was devised. Finally, the optimal trajectory was approximated as the sum of the deterministic nominal trajectory and the stochastic neighboring optimal solution. Numerical results are presented for a typical vehicle. A fuel-optimal control problem in aeroassisted noncoplanar orbital transfer is also addressed. The equations of motion for the atmospheric maneuver are nonlinear and the optimal (nominal) trajectory and control are obtained. In order to follow the nominal trajectory under actual conditions, a neighboring optimum guidance scheme is designed using linear quadratic regulator theory for onboard real-time implementation. One of the state variables is used as the independent variable in reference to the time. The weighting matrices in the performance index are chosen by a combination of a heuristic method and an optimal modal approach. The necessary feedback control law is obtained in order to minimize the deviations from the nominal conditions. Author

09 RESEARCH AND SUPPORT FACILITIES (AIR)

Includes airports, hangars and runways; aircraft repair and overhaul facilities; wind tunnels; shock tubes; and aircraft engine test stands.

For related information see also *14 Ground Support Systems and Facilities (Space).*

N90-14244*# National Aeronautics and Space Administration. Langley Research Center, Hampton, VA.
CRYOGENIC TEMPERATURE EFFECTS ON STING-BALANCE DEFLECTIONS IN THE NATIONAL TRANSONIC FACILITY
Thomas G. Popernack, Jr. and Jerry B. Adcock Jan. 1990 12 p
(NASA-TM-4157; L-16626; NAS 1.15:4157) Avail: NTIS HC A03/MF A01 CSCL 14B

An investigation was conducted at the National Transonic Facility (NTF) to document the change in sting-balance deflections from ambient to cryogenic temperatures. Space limitations in some NTF models do not allow the use of on-board angle of attack instrumentation. In order to obtain angle of attack data, pre-determined sting-balance bending data must be combined with arc sector angle measurements. Presently, obtaining pretest sting-balance data requires several cryogenic cycles and cold loadings over a period of several days. A method of reducing the calibration time required is to obtain only ambient temperature sting-balance bending data and correct for changes in material properties at cryogenic temperatures. To validate this method, two typical NTF sting-balance combinations were tested. The test results show excellent agreement with the predicted values and the repeatability of the data was 0.01 degree. Author

N90-14245*# Southampton Univ. (England).
TECHNIQUES FOR EXTREME ATTITUDE SUSPENSION OF A WIND TUNNEL MODEL IN A MAGNETIC SUSPENSION AND BALANCE SYSTEM Ph.D. Thesis
David Huw Parker Oct. 1989 274 p
(Grant NsG-7523)
(NASA-CR-181895; NAS 1.26:181895) Avail: NTIS HC A12/MF A02 CSCL 14B

Although small scale magnetic suspension and balance systems (MSBSs) for wind tunnel use have been in existence for many years, they have not found general application in the production testing of flight vehicles. One reason for this is thought to lie in the relatively limited range of attitudes over which a wind tunnel model may be suspended. Modifications to a small MSBS to permit the suspension and control of axisymmetric models over angles of attack from less than zero to over ninety degrees are reported. Previous work has shown that existing arrangement of ten electromagnets was unable to generate one of the force components needed for control at extreme attitudes. Examination of possible solutions resulted in a simple alteration to rectify this deficiency. To generate the feedback signals to control the suspended model, an optical position sensing system using collimated laser beams and photodiode arrays was installed and tested. An analytical basis was developed for distributing the demands for force and moment needed for model stabilization amonge the electromagnets over the full attitude range. This was implemented by an MSBS control program able to continually adjust the distribution for the instantaneous incidence in accordance with prescheduled data. Results presented demonstrate rotations of models from zero to ninety degrees at rates up to ninety degrees per second, with pitching rates rising to several hundred degrees per second in response to step-change demands. A study of a design for a large MSBS suggests that such a system could be given the capability to control a model in six degrees of freedom over an unlimited angle of attack range. Author

N90-14246# Sandia National Labs., Albuquerque, NM. Thermomechanical and Physical Div.
SOLVING THE BLOW-BY PROBLEM IN A TWO-STAGE GUN
Lynn M. Barker and G. W. Wellman Sep. 1989 24 p Presented at the Aeroballistic Range Association Meeting, Paris, France, 24-28 Sep. 1989 Submitted for publication
(Contract DE-AC04-76DP-00789)
(DE90-000842; SAND-89-2034C; CONF-8909229-1) Avail: NTIS HC A03/MF A01

Blow-by is a common occurrence in two stage light gas guns. Although the blow-by is often inconsequential, it can sometimes present a serious problem. Various projectile designs were tried to prevent blow-by, and a successful design is described. Computer calculations which clarify the dynamic performance of the design are presented, along with a parameter variation study to indicate the sensitivity of the design to certain geometric parameters. DOE

12 ASTRONAUTICS (GENERAL)

For extraterrestrial exploration see *91 Lunar and Planetary Exploration.*

N90-14247*# Georgia Inst. of Tech., Atlanta. School of Mechanical Engineering.
MANIPULATION STRATEGIES FOR MASSIVE SPACE PAYLOADS Semiannual Progress Report, 16 May - 15 Nov. 1989
Wayne J. Book 1989 138 p
(Grant NAG1-623)
(NASA-CR-186081; NAS 1.26:186081) Avail: NTIS HC A07/MF A01 CSCL 22A

Control for the bracing strategy is being examined. It was concluded earlier that trajectory planning must be improved to best achieve the bracing motion. Very interesting results were achieved which enable the inverse dynamics of flexible arms to be calculated for linearized motion in a more efficient manner than previously published. The desired motion of the end point beginning at t=0 and ending at t=t sub f is used to calculate the required torque at the joint. The solution is separated into a causal function that is zero for t is less than 0 and an accusal function which is zero for t is greater than t sub f. A number of alternative end point trajectories were explored in terms of the peak torque required, the amount of anticipatory action, and other issues. The single link case is the immediate subject and an experimental verification of that case is being performed. Modeling with experimental verification of closed chain dynamics continues. Modeling effort has pointed out inaccuracies that result from the choice of numerical techniques used to incorporate the closed chain constraints when modeling our experimental prototype RALF (Robotic Arm Large and Flexible). Results were compared to TREETOPS, a multi body code. The experimental verification work is suggesting new ways to make comparisons with systems having structural linearity and joint and geometric nonlinearity. The generation of inertial forces was studied with a small arm that will damp the large arm's vibration. Author

N90-14248# Joint Publications Research Service, Arlington, VA.
JPRS REPORT: SCIENCE AND TECHNOLOGY. USSR: SPACE. SOVIET SPACE PROGRAM TO THE YEAR 2000
Yuriy Ivanovich Zaytsev 30 Aug. 1989 28 p Transl. into ENGLISH of Kosmicheskaya Programma SSSR do 2000 Goda (Moscow, USSR), p 3-64
(JPRS-USP-89-008) Avail: NTIS HC A03/MF A01

The principal space research projects planned by the Soviet Union for the period up to the year 2000 are presented. The range of tasks can be divided into several major fields. One of them is the space nearest earth. This field includes studies of the upper atmosphere, the radiation belts, the earth's magnetosphere, the interplanetary medium, and variations in their parameters as a function of solar activity. In addition to near space, studies will be conducted of the solar system including the moon, Venus, Mars, its moon Phobos, and other celestial objects. In this area, the advantages of international cooperation are pointed out with the study of Halley's Comet cited as an example. Deep space and the development of extra-atmospheric telescopes and astronomical instruments are also of interest to the Soviets. Studies will include X-radiation, gamma astronomy, and radio astronomy. Finally, the Soviet Union plans to continue its study of how to make man at home in space. This will include new materials, new modules, and further expansion of the Mir space station. J.P.S.

N90-14249# Sandia National Labs., Albuquerque, NM.
SANDIA SATELLITE PROGRAM SUMMARY OF OPERATIONAL PROCEDURES
Aug. 1989 59 p
(Contract DE-AC04-76DP-00789)
(DE90-000892; SAND-89-0397) Avail: NTIS HC A04/MF A01

Operational procedures for the Space Systems Department and Space Sensors Department are described. Departmental policies and procedures from design of systems for space applications through qualification for spaceflight are summarized. DOE

N90-14417# National Defence Academy, Yokosuka (Japan). Dept. of Electrical Engineering.
HYBRID PE-RAY-MODE FORMULATION OF HIGH FREQUENCY PROPAGATION IN A BILINEAR TROPOSPHERIC SURFACE DUCT
T. Ishihara and L. B. Felsen (Polytechnic Univ., Farmingdale, NY.) *In* AGARD, Operational Decision Aids for Exploiting or Mitigating Electromagnetic Propagation Effects Sep. 1989 15 p Sponsored by Naval Ocean Systems Center, San Diego, CA (For primary document see N90-14405 06-32)
Copyright Avail: NTIS HC A20/MF A03

13 ASTRODYNAMICS

Includes powered and free-flight trajectories; and orbital and launching dynamics.

N90-14250*# Rice Univ., Houston, TX.
OPTIMAL TRAJECTORIES FOR THE AEROASSISTED FLIGHT EXPERIMENT
A. Miele, T. Wang, W. Y. Lee, and Z. G. Zhao 1989 25 p Presented at the 40th Congress of the International Astronautical Federation, Malaga, Spain, 7-13 Oct. 1989 Sponsored by JPL and Texas Advanced Technology Program
(Grant NAG8-755)
(NASA-CR-186133; NAS 1.26:186133; IAF-89-361) Avail: NTIS HC A03/MF A01 CSCL 22A

The determination of optimal trajectories for the aeroassisted flight experiment (AFE) is discussed. The intent of this experiment is to simulate a GEO-to-LEO transfer, where GEO denotes a geosynchronous earth orbit and LEO denotes a low earth orbit. The trajectories of an AFE spacecraft are analyzed in a 3D-space, employing the full system of 6 ordinary differential equations (ODEs) describing the atmospheric pass. The atmospheric entry conditions are given, and the atmospheric exit conditions are adjusted. Two possible transfers are considered: (1) indirect ascent to a 178 NM perigee via a 197 NM apogee; and (2) direct ascent to a 178 NM apogee. Author

N90-14432# Centre National d'Etudes des Telecommunications, Lannion (France).
CORRECTION OF IONOSPHERIC EFFECTS FOR THE PRECISE ORBIT DETERMINATION OF SATELLITES
F. Foucher, R. Fleury, and P. Lassudrie-Duchesne *In* AGARD, Operational Decision Aids for Exploiting or Mitigating Electromagnetic Propagation Effects Sep. 1989 12 p (For primary document see N90-14405 06-32)
Copyright Avail: NTIS HC A20/MF A03

14 GROUND SUPPORT SYSTEMS AND FACILITIES (SPACE)

Includes launch complexes, research and production facilities; ground support equipment, e.g., mobile transporters; and simulators.

For related information see also *09 Research and Support Facilities (Air).*

N90-14251# Sandia National Labs., Albuquerque, NM. Fluid Mechanics and Heat Transfer Div.
THERMAL ENVIRONMENTAL TESTS ON SPACE SIMULATION CHAMBER
Ronald L. Akau, J. Paul Freshour, and Steve L. Wilde Sep. 1989 40 p
(Contract DE-AC04-76DP-00789)
(DE90-000927; SAND-89-0640) Avail: NTIS HC A03/MF A01

Thermal testing of space payloads at Sandia National Laboratories is conducted in a large cylindrical (7.0 feet in diameter) vacuum chamber with temperature controlled walls. The payload is generally attached to a baseplate with independent temperature controls. To establish well-defined boundary conditions during the tests, uniform wall temperatures are desired in the test chamber. Thermal-vacuum tests were conducted on this space simulation chamber to determine if temperature gradients existed on the chamber shroud and end-bells. Recorded temperature measurements indicated large temperature gradients on the chamber shroud and end-bells. Furthermore, it was difficult to manually control the flow of liquid to the end-bells in order to achieve equal end-bell temperatures. However, results from these tests were used in a computer program developed to predict locations on the shroud and end-balls where a thermocouple would measure the best area-weighted average temperature. These measurements provide necessary boundary temperatures that can be used in a thermal model of a satellite payload. Results were obtained for different shroud and baseplate temperature settings. DOE

N90-14252# Oak Ridge National Lab., TN.
CHARACTERISTICS OF AN ELECTRON-BEAM ROCKET PELLET ACCELERATOR
C. C. Tsai, C. A. Foster, and D. E. Schechter 1989 6 p Presented at the 13th International Symposium on Fusion Engineering, Knoxville, TN, 2-6 Oct. 1989
(Contract DE-AC05-84OR-21400)
(DE90-001595; CONF-891007-17) Avail: NTIS HC A02/MF A01

An electron-beam rocket pellet accelerator has been designed, built, assembled, and tested as a proof-of-principle (POP) apparatus. The main goal of accelerators based on this concept is to use intense electron-beam heating and ablation of a hydrogen propellant stick to accelerate deuterium and/or tritium pellets to ultrahigh speeds (10 to 20 km/s) for plasma fueling of next-generation fusion devices such as the International Thermonuclear Engineering Reactor (ITER). The POP apparatus is described and initial results of pellet acceleration experiments are presented. Conceptual ultrahigh-speed pellet accelerators are discussed. DOE

N90-14253# Oak Ridge National Lab., TN.
ACCELERATION OF SMALL, LIGHT PROJECTILES (INCLUDING HYDROGEN ISOTOPES) TO HIGH SPEEDS USING A TWO-STAGE LIGHT GAS GUN
S. K. Combs, C. R. Foust, M. J. Gouge, and S. L. Milora 1989 23 p Presented at the 36th American Vacuum Society National Vacuum Symposium, Boston, MA, 23-27 Oct. 1989
(Contract DE-AC05-84OR-21400)
(DE90-002479; CONF-891093-9) Avail: NTIS HC A03/MF A01

Small, light projectiles have been accelerated to high speeds using a two-stage light gas gun at Oak Ridge National Laboratory. With 35-mg plastic projectiles (4 mm in diameter), speeds of up to 4.5 km/s have been recorded. The pipe gun technique for freezing hydrogen isotopes in situ in the gun barrel has been used to accelerate deuterium pellets (nominal diameter of 4 mm) to velocities of up to 2.85 km/s. The primary application of this technology is for plasma fueling of fusion devices via pellet injection of hydrogen isotopes. Conventional pellet injectors are limited to pellet speeds in the range 1 to 2 km/s. Higher velocities are desirable for plasma fueling applications, and the two-stage pneumatic technique offers performance in a higher velocity regime. However, experimental results indicate that the use of sabots to encase the cryogenic pellets and protect them for the high peak pressures will be required to reliably attain intact pellets at speeds of approx. 3 km/s or greater. In some limited tests, lithium hydride pellets were accelerated to speeds of up to 4.2 km/s. Also, repetitive operation of the two-stage gun (four plastic pellets fired at approx. 0.5 Hz) was demonstrated for the first time in preliminary tests. The equipment and operation are described, and experimental results and some comparisons with a theoretical model are presented. DOE

N90-14254# Sandia National Labs., Albuquerque, NM.
PERFORMANCE CHARACTERISTICS OF A THREE-STAGE RAILGUN
J. R. Asay and R. S. Hawke 1989 18 p Presented at the Aeroballistic Range Association Meeting, Paris, France, 24-28 Sep. 1989 Prepared in cooperation with Lawrence Livermore National Lab., CA
(Contract DE-AC04-76DP-00789)
(DE90-002533; SAND-89-2198C; CONF-8909229-2) Avail: NTIS HC A03/MF A01

Hypervelocity launchers are used to study the high-pressure equation of state of materials in regimes inaccessible by other methods. Two-stage light gas guns have been extremely useful for these applications, but have a practical velocity limit of about 8 to 9 km/s for impact studies. In this paper, we describe a three-stage launcher consisting of a two-stage light gas gun

combined with a third-stage railgun, which overcomes previous velocity limitations pertaining to two-stage guns. This launcher is being developed for operation to 15 km/s and has achieved projectile velocities of 7.2 km/s to date. DOE

15 LAUNCH VEHICLES AND SPACE VEHICLES

Includes boosters; operating problems of launch/space vehicle systems; and reusable vehicles.

For related information see also *20 Spacecraft Propulsion and Power.*

N90-14255 Department of the Navy, Washington, DC.
ELASTOMERIC IMPULSE ENERGY STORAGE AND TRANSFER SYSTEM Patent
Laurent C. Bissonnette, inventor (to Navy) 18 Jul. 1989 4 p
Filed 1 Jul. 1987
(AD-D014223; US-Patent-4,848,210; US-Patent-Appl-SN-070841; US-Patent-Class-89-1.810) Avail: US Patent and Trademark Office CSCL 19/8

The present invention relates to projectile launching devices and more particularly to an energy storage and low-noise launch system using an elastomeric bladder as the energy storage medium. It is a general purpose and object of the present invention to provide an improved, impulse energy storage and transfer system. Further objects are that this system exhibit a relatively high mechanical efficiency, be simple, reliable and low in cost. These objects are accomplished with the present invention by providing, in combination, a device for storing potential energy in the form of a distended, fluid medium filled, elastomeric bladder and rapidly converting that stored energy into kinetic energy of the working fluid for quietly ejecting a projectile along with the stored fluid from the device and into the surrounding fluid medium. The stored working fluid flows through a tubular launch tube enclosing a projectile. The moving fluid acts to expel the projectile entrained therein. Such an energy storage and transfer system is particularly well suited for, but not limited to, submarine launcher system applications. The present invention can provide the energy required to quietly launch a projectile, such as a torpedo from a submarine. GRA

N90-14256*# National Aeronautics and Space Administration. Marshall Space Flight Center, Huntsville, AL.
PAYLOAD CREW UTILIZATION FOR SPACELAB MISSIONS
K. Y. Ibrahim and J. D. Weiler Jan. 1990 55 p
(NASA-TP-2976; NAS 1.60:2976) Avail: NTIS HC A04/MF A01 CSCL 22A

Planned payload crew utilization on Spacelab mission are analyzed to establish trends and guidelines. The study included missions that have flow to date as well as those in planning. Available data were analyzed on the basis of four major timeline iterations that occur during mission design. Data were categorized and assessed by crewmember, flight day, and mission. Based on the results of this analysis, it was recommended that for the Requirements Review and Preliminary Design Review iterations the maximum utilization per shift should be 75 percent for the Payload Specialist (PS) and 65 percent for the Mission Specialist (MS); and for the basic and final iterations, the maximum utilization shift should be 85 percent for the PS and 75 percent for the MS. Additional recommendations include limiting the amount of activity during the first two shifts whenever possible and establishing a common set of guidelines for the calculations of crew utilization. Author

N90-14257*# Draper (Charles Stark) Lab., Inc., Cambridge, MA.
GUIDANCE, STEERING, LOAD RELIEF AND CONTROL OF AN ASYMMETRIC LAUNCH VEHICLE M.S. Thesis - MIT
Frederick W. Boelitz Aug. 1989 232 p
(Contract NAS9-18147)
(NASA-CR-185598; NAS 1.26:185598; CSDL-T-1036) Avail: NTIS HC A11/MF A02 CSCL 22B

A new guidance, steering, and control concept is described and evaluated for the Third Phase of an asymmetrical configuration of the Advanced Launch System (ALS). The study also includes the consideration of trajectory shaping issues and trajectory design as well as the development of angular rate, angular acceleration, angle of attack, and dynamic pressure estimators. The Third Phase guidance, steering and control system is based on controlling the acceleration-direction of the vehicle after an initial launch maneuver. Unlike traditional concepts, the alignment of the estimated and commanded acceleration-directions is unimpaired by an add-on load relief. Instead, the acceleration-direction steering-control system features a control override that limits the product of estimated dynamic pressure and estimated angle of attack. When this product is not being limited, control is based exclusively on the commanded acceleration-direction without load relief. During limiting, control is based on nulling the error between the limited angle of attack and the estimated angle of attack. This limiting feature provides full freedom to the acceleration-direction steering and control to shape the trajectory within the limit, and also gives full priority to the limiting of angle of attack when necessary. The flight software concepts were analyzed on the basis of their effects on pitch plane motion. Author

16 SPACE TRANSPORTATION

Includes passenger and cargo space transportation, e.g., shuttle operations; and space rescue techniques.

For related information see also *03 Air Transportation and Safety* and *18 Spacecraft Design, Testing and Performance.* For space suits see *54 Man/System Technology and Life Support.*

N90-14258*# Auburn Univ., AL. Dept. of Aerospace Engineering.
PRELIMINARY DESIGN OF THE SHUTTLE-C AVIONICS RECOVERY SYSTEM Final Report
Morgan Brookfield, Deron Decker, Harold Gilbert, David Moore, and Mark Rist Jun. 1989 115 p
(Contract NASw-4435)
(NASA-CR-186230; NAS 1.26:186230) Avail: NTIS HC A06/MF A01 CSCL 22B

The analysis done in developing a recovery system for the Shuttle-C cargo vehicle is presented. This recovery system is comprised of a reentry capsule which houses the vehicles avionics. The avionics are contained in a single package which is extracted from the capsule by the parachute recovery system. The Shuttle-C will be able to satisfy NASA's design and mission requirements. Included, is an analysis of the structural, thermal protection, and parachute recovery systems. A discussion of the merits of the proposed system is also included. Author

17 SPACE COMM., SPACECRAFT COMM., COMMAND & TRACKING

Includes telemetry; space communications networks; astronavigation and guidance; and radio blackout.

For related information see also *04 Aircraft Communications and Navigation* and *32 Communications and Radar.*

N90-14259# Sandia National Labs., Livermore, CA. Telemetry Systems Div.
SAND DEVIL: A DIGITAL VIDEO LINK FOR TELEMETRY APPLICATIONS
James A. Meacham, Cory W. Ottesen, and R. Michael Bell Oct. 1989 110 p
(Contract DE-AC04-76DR-00789)
(DE90-001879; SAND-89-8251) Avail: NTIS HC A05/MF A01

A digital video encoder/decoder was built which is suitable for airborne telemetry. The system allows the use of multiple black and white or a single RGB camera. The spatial resolution, frame rate, and pixel compression algorithm can be tailored to specific

mission requirements. The output bit rate of the encoder can be varied from 0.89 to 7.16 Mbit/sec, depending on test range capability and RF data link considerations. The digital output of the encoder can be encrypted for data security. The system architecture is flexible, yet very simple, leading to a compact design. Also, the entire system is implemented with off-the-shelf components, thus reducing development time and cost. The size of the encoder and decoder can be reduced substantially by using surface mount devices. DOE

N90-14260*# National Aeronautics and Space Administration. Goddard Space Flight Center, Greenbelt, MD.
SHUTTLE LASER TECHNOLOGY EXPERIMENT FACILITY (LTEF)-TO-AIRPLANE LASERCOM EXPERIMENT: AIRPLANE CONSIDERATIONS
Ford Kalil Washington Jan. 1990 82 p
(NASA-TM-100749; NAS 1.15:100749; Rept-90B00014) Avail: NTIS HC A05/MF A01 CSCL 17B

NASA is considering the use of various airplanes for a Shuttle Laser Technology Experiment Facility (LTEF)-to-Airplane laser communications experiment. As supporting documentation, pertinent technical details are included about the potential use of airplanes located at Ames Research Center and Wallops Flight Facility. The effects and application of orbital mechanics considerations are also presented, including slant range, azimuth, elevation, and time. The pros and cons of an airplane equipped with a side port with a bubble window versus a top port with a dome are discussed. Author

18 SPACECRAFT DESIGN, TESTING AND PERFORMANCE

Includes satellites; space platforms; space stations; spacecraft systems and components such as thermal and environmental controls; and attitude controls.

For life support systems see *54 Man/System Technology and Life Support.* For related information see also *05 Aircraft Design, Testing and Performance, 39 Structural Mechanics,* and *16 Space Transportation.*

N90-14261*# National Academy of Sciences - National Research Council, Washington, DC.
LONG-LIVED SPACE OBSERVATORIES FOR ASTRONOMY AND ASTROPHYSICS
Blair D. Savage, Eric E. Becklin, Steven V. W. Beckwith, Lennox L. Cowie, Andrea K. Dupree, James L. Elliot, John S. Gallagher, David J. Helfand, Edward F. Jenkins, and Kenneth J. Johnston (Naval Research Lab., Washington, DC.) et al 1987 60 p
(Contract NASw-3482)
(NASA-CR-185373; NAS 1.26:185373) Avail: NTIS HC A04/MF A01 CSCL 22B

NASA's plan to build and launch a fleet of long-lived space observatories that include the Hubble Space Telescope (HST), the Gamma Ray Observatory (GRO), the Advanced X Ray Astrophysics Observatory (AXAF), and the Space Infrared Telescope Facility (SIRTF) are discussed. These facilities are expected to have a profound impact on the sciences of astronomy and astrophysics. The long-lived observatories will provide new insights about astronomical and astrophysical problems that range from the presence of planets orbiting nearby stars to the large-scale distribution and evolution of matter in the universe. An important concern to NASA and the scientific community is the operation and maintenance cost of the four observatories described above. The HST cost about $1.3 billion (1984 dollars) to build and is estimated to require $160 million (1986 dollars) a year to operate and maintain. If HST is operated for 20 years, the accumulated costs will be considerably more than those required for its construction. Therefore, it is essential to plan carefully for observatory operations and maintenance before a long-lived facility is constructed. The primary goal of this report is to help NASA develop guidelines for the operations and management of these future observatories so as to achieve the best possible scientific results for the resources available. Eight recommendations are given. K.C.D.

N90-14262*# California Univ., Los Angeles. Dept. of Mechanical, Aerospace, and Nuclear Engineering.
RISK-BASED FIRE SAFETY EXPERIMENT DEFINITION FOR MANNED SPACECRAFT Final Report
G. E. Apostolakis, V. S. Ho, E. Marcus, A. T. Perry (American Space Technology, Inc., Santa Monica, CA.), and S. L. Thompson Oct. 1989 191 p
(Contract NAS8-37750)
(NASA-CR-183835; NAS 1.26:183835; UCLA-ENG-90-11) Avail: NTIS HC A09/MF A02 CSCL 22B

Risk methodology is used to define experiments to be conducted in space which will help to construct and test the models required for accident sequence identification. The development of accident scenarios is based on the realization that whether damage occurs depends on the time competition of two processes: the ignition and creation of an adverse environment, and the detection and suppression activities. If the fire grows and causes damage faster than it is detected and suppressed, then an accident occurred. The proposed integrated experiments will provide information on individual models that apply to each of the above processes, as well as previously unidentified interactions and processes, if any. Initially, models that are used in terrestrial fire risk assessments are considered. These include heat and smoke release models, detection and suppression models, as well as damage models. In cases where the absence of gravity substantially invalidates a model, alternate models will be developed. Models that depend on buoyancy effects, such as the multizone compartment fire models, are included in these cases. The experiments will be performed in a variety of geometries simulating habitable areas, racks, and other spaces. These simulations will necessitate theoretical studies of scaling effects. Sensitivity studies will also be carried out including the effects of varying oxygen concentrations, pressures, fuel orientation and geometry, and air flow rates. The experimental apparatus described herein includes three major modules: the combustion, the fluids, and the command and power modules. Author

N90-14263*# Illinois Univ., Urbana-Champaign. Dept. of Aeronautical and Astronautical Engineering.
AEROSPACE VEHICLE DESIGN, SPACECRAFT SECTION. VOLUME 1: PROJECT GROUPS 3 THROUGH 5 Final Project Reports
May 1989 288 p
(Contract NASw-4435)
(NASA-CR-186053; NAS 1.26:186053; AAE-241-Vol-1) Avail: NTIS HC A13/MF A02 CSCL 22B

Three groups of student engineers in an aerospace vehicle design course present their designs for a vehicle that can be used to resupply the Space Station Freedom and provide an emergency crew return to earth capability. The vehicle's requirements include a lifetime that exceeds six years, low cost, the capability for withstanding pressurization, launch, orbit, and reentry hazards, and reliability. The vehicle's subsystems are analyzed. These subsystems are structures, communication and command data systems, attitude and articulation control, life support and crew systems, power and propulsion, reentry and recovery systems, and mission management, planning, and costing. J.P.S.

N90-14264*# Illinois Univ., Urbana-Champaign. Dept. of Aeronautical and Astronautical Engineering.
AEROSPACE VEHICLE DESIGN, SPACECRAFT SECTION. VOLUME 2: PROJECT GROUPS 6 THROUGH 8 Final Project Reports
May 1989 272 p
(Contract NASw-4435)
(NASA-CR-186054; NAS 1.26:186054; AAE-241-Vol-2) Avail: NTIS HC A12/MF A02 CSCL 22B

Three groups of student engineers in an aerospace vehicle

design course present their designs for a vehicle that can be used to resupply the Space Station Freedam and provide emergency crew return to earth capability. The vehicle's requirements include a lifetime that exceeds six years, low cost, the capability for withstanding pressurization, launch, orbit, and reentry hazards, and reliability. The vehicle's subsystems are structures, communication and command data systems, attitude and articulation control, life support and crew systems, power and propulsion, reentry and recovery systems, and mission management, planning, and costing. Special attention is given to spacecraft communications. J.P.S.

N90-14265*# University of Central Florida, Orlando.
THE SPACE STATION TETHERED ELEVATOR SYSTEM
Loren A. Anderson 15 May 1989 346 p
(Contract NASw-4435)
(NASA-CR-186051; NAS 1.26:186051) Avail: NTIS HC A15/MF A02 CSCL 22B

The optimized conceptual engineering design of a space station tethered elevator is presented. The elevator is an unmanned mobile structure which operates on a ten kilometer tether spanning the distance between the Space Station and a tethered platform. Elevator capabilities include providing access to residual gravity levels, remote servicing, and transportation to any point along a tether. The potential uses, parameters, and evolution of the spacecraft design are discussed. Engineering development of the tethered elevator is the result of work conducted in the following areas: structural configurations; robotics, drive mechanisms; and power generation and transmission systems. The structural configuration of the elevator is presented. The structure supports, houses, and protects all systems on board the elevator. The implementation of robotics on board the elevator is discussed. Elevator robotics allow for the deployment, retrieval, and manipulation of tethered objects. Robotic manipulators also aid in hooking the elevator on a tether. Critical to the operation of the tethered elevator is the design of its drive mechanisms, which are discussed. Two drivers, located internal to the elevator, propel the vehicle along a tether. These modular components consist of endless toothed belts, shunt-wound motors, regenerative power braking, and computer controlled linear actuators. The designs of self-sufficient power generation and transmission systems are reviewed. Thorough research indicates all components of the elevator will operate under power provided by fuel cells. The fuel cell systems will power the vehicle at seven kilowatts continuously and twelve kilowatts maximally. A set of secondary fuel cells provides redundancy in the unlikely event of a primary system failure. Power storage exists in the form of Nickel-Hydrogen batteries capable of powering the elevator under maximum loads. Author

N90-14266*# Michigan Univ., Ann Arbor. Aerospace System Design.
PROJECT ARGO: THE DESIGN AND ANALYSIS OF AN ALL-PROPULSIVE AND AN AEROASSISTED VERSION OF A MANNED SPACE TRANSPORTATION VEHICLE Final Report
Apr. 1989 212 p
(Contract NASw-4435)
(NASA-CR-186047; NAS 1.26:186047; Aero-483) Avail: NTIS HC A10/MF A02 CSCL 22B

Project Argo is the design of a manned Space Transportation Vehicle (STV) that would transport payloads between LEO (altitude lying between 278 to 500 km above the Earth) and GEO (altitude is approximately 35,800 km above the Earth) and would be refueled and refurbished at the Space Station Freedom. Argo would be man's first space-based manned vehicle and would provide a crucial link to geosynchronous orbit where the vast majority of satellites are located. The vehicle could be built and launched shortly after the space station and give invaluable space experience while serving as a workhorse to deliver and repair satellites. Eventually, if a manned space station is established in GEO, then Argo could serve as the transport between the Space Station Freedom and a Geostation. If necessary, modifications could be made to allow the vehicle to reach the moon or possibly Mars. Project Argo is unique in that it consists of the design and comparison of two different concepts to accomplish the same mission. The first is an all-propulsive vehicle which uses chemical propulsion for all of its major maneuvers between LEO and GEO. The second is a vehicle that uses aeroassisted braking during its return from GEO to LEO by passing through the upper portions of the atmosphere. K.C.D.

N90-14267*# Houston Univ., TX. Coll. of Architecture.
PARTIAL GRAVITY HABITAT STUDY: WITH APPLICATION TO LUNAR BASE DESIGN
Stephen Capps, Jason Lorandos, Eval Akhidime, Michael Bunch, Denise Lund, Nathan Moore, Kio Murakawa, Larry Bell, Guillermo Trotti, and Deb Neubek et al 1989 138 p
(Contract NASw-4435)
(NASA-CR-186048; NAS 1.26:186048) Avail: NTIS HC A07/MF A01 CSCL 22B

Comprehensive design requirements associated with designing habitats for humans in a partial gravity environment were investigated and then applied to a lunar base design. Other potential sites for application include planetary surfaces such as Mars, variable gravity research facilities, or a rotating spacecraft. Design requirements for partial gravity environments include: (1) locomotion changes in less than normal Earth gravity; (2) facility design issues, such as interior configuration, module diameter and geometry; and (3) volumetric requirements based on the previous as well as psychological issues involved in prolonged isolation. For application to a Lunar Base, it was necessary to study the exterior architecture and configuration to insure optimum circulation patterns while providing dual egress. Radiation protection issues were addressed to provide a safe and healthy environment for the crew, and finally, the overall site was studied to locate all associated facilities in context with the habitat. Mission planning was not the purpose of this study; therefore, a Lockheed scenario was used as an outline for the Lunar Base application, which was then modified to meet the project needs. Author

N90-14268*# National Aeronautics and Space Administration. Lewis Research Center, Cleveland, OH.
SLUSH HYDROGEN (SLH2) TECHNOLOGY DEVELOPMENT FOR APPLICATION TO THE NATIONAL AEROSPACE PLANE (NASP)
Richard L. DeWitt, Terry L. Hardy, Margaret V. Whalen, and G. Paul Richter Jul. 1989 19 p Presented at the Cryogenic Engineering Conference, Los Angeles, CA, 24-28 Jul. 1989; sponsored by the California Univ. at Los Angeles
(NASA-TM-102315; E-5001; NAS 1.15:102315) Avail: NTIS HC A03/MF A01 CSCL 22B

The National Aerospace Plane (NASP) program is giving us the opportunity to reach new unique answers in a number of engineering categories. The answers are considered enhancing technology or enabling technology. Airframe materials and densified propellants are examples of enabling technology. The National Aeronautics and Space Administration's Lewis Research Center has the task of providing the technology data which will be used as the basis to decide if slush hydrogen (SLH2) will be the fuel of choice for the NASP. The objectives of this NASA Lewis program are: (1) to provide, where possible, verified numerical models of fluid production, storage, transfer, and feed systems, and (2) to provide verified design criteria for other engineered aspects of SLH2 systems germane to a NASP. This program is a multiyear multimillion dollar effort. The present pursuit of the above listed objectives is multidimensional, covers a range of problem areas, works these to different levels of depth, and takes advantage of the resources available in private industry, academia, and the U.S. Government. The NASA Lewis overall program plan is summarized. The initial implementation of the plan will be unfolded and the present level of efforts in each of the resource areas will be discussed. Results already in hand will be pointed out. A description of additionally planned near-term experimental and analytical work is described. Author

N90-14269# Hydraulic Research Textron, Valencia, CA. Servocontrols Div.

OPTIMAL STOCHASTIC MODELING AND CONTROL OF FLEXIBLE STRUCTURES Final Report, Sep. 1986 - Sep. 1988

Hagop V. Panossian Sep. 1988 321 p

(Contract F33615-85-C-3220)

(AD-A212347; AFWAL-TR-88-3066) Avail: NTIS HC A14/MF A01 CSCL 01/3

Modeling and control design of large flexible space structures under high uncertainty is considered. Linear stochastic system models with multiplicative and additive noises that are state -, control -, and measurement - dependent are treated extensively. Controllability, observability, and robustness issues are also discussed under various optimality considerations. An optimal stochastic controller is derived under perfect information and a sub-optimal compensator is formulated under partial and noisy information. The intent is to treat the modeling of uncertainties and to develop the appropriate stochastic control that is robust. GRA

N90-14270*# North Carolina Univ., Charlotte. Dept. of Electrical Engineering.

DYNAMICS AND CONTROL OF FLEXIBLE SPACECRAFT DURING AND AFTER SLEWING MANEUVERS Annual Report, 1 May - 31 Oct. 1989

Yogendra P. Kakad 1989 40 p

(Grant NAG1-535)

(NASA-CR-186123; NAS 1.26:186123) Avail: NTIS HC A03/MF A01 CSCL 22B

The dynamics and control of slewing maneuvers of NASA Spacecraft COntrol Laboratory Experiment (SCOLE) are analyzed. The control problem of slewing maneuvers of SCOLE is formulated in terms of an arbitrary maneuver about any given axis. The control system is developed for the combined problem of rigid-body slew maneuver and vibration suppression of the flexible appendage. The control problem formulation incorporates the nonlinear dynamical equations derived previously, and is expressed in terms of a two-point boundary value problem utilizing a quadratic type of performance index. The two-point boundary value problem is solved as a hierarchical control problem with the overall system being split in terms of two subsystems, namely the slewing of the entire assembly and the vibration suppression of the flexible antenna. The coupling variables between the two dynamical subsystems are identified and these two subsystems for control purposes are treated independently in parallel at the first level. Then the state-space trajectory of the combined problem is optimized at the second level. Author

N90-14271*# Teledyne Ryan Electronics, San Diego, CA.

VEHICLE ANTENNA FOR THE MOBILE SATELLITE EXPERIMENT Final Report

Sheng Y. Peng, H. H. Chung, D. Leggiere, W. Foy, G. Schaffner, J. Nelson, W. Pagels, M. Vayner, H. L. Faller, and L. Messer 17 Mar. 1988 332 p

(NASA-CR-186109; NAS 1.26:186109; TRE/SD105665-3B)

Avail: NTIS HC A15/MF A02 CSCL 22B

A low profile, low cost, printed circuit, electronically steered, right hand circularly polarized phase array antenna system has been developed for the Mobile Satellite Experiment (MSAT-X) Program. The success of this antenna is based upon the development of a crossed-slot element array and detailed trade-off analyses for both the phased array and pointing system design. The optimized system provides higher gain at low elevation angles (20 degrees above the horizon) and broader frequency coverage (approximately 8 1/2 percent bandwidth) than is possible with a patch array. Detailed analysis showed that optimum performance could be achieved with a 19 element array of a triangular lattice geometry of 3.9 inch element spacing. This configuration has the effect of minimizing grating lobes at large scan angles plus it improves the intersatellite isolation. The array has an aperture 20 inches in diameter and is 0.75 inch thick overall, exclusive of the RF and power connector. The pointing system employs a hybrid approach that operates with both an external rate sensor and an internal error signal as a means of fine tuning the beam acquisition and track. Steering the beam is done electronically via 18, 3-bit diode phase shifters. A nineteenth phase shifter is not required as the center element serves as a reference only. Measured patterns and gain show that the array meets the stipulated performance specifications everywhere except at some low elevation angles. Author

N90-14272*# National Aeronautics and Space Administration. Langley Research Center, Hampton, VA.

AEROBRAKING CHARACTERISTICS FOR SEVERAL POTENTIAL MANNED MARS ENTRY VEHICLES

Paul V. Tartabini and William T. Suit Nov. 1989 29 p

(NASA-TM-101669; NAS 1.15:101669) Avail: NTIS HC A03/MF A01 CSCL 22B

While a reduction in weight is always desirable for any space vehicle, it is crucial for vehicles to be used in the proposed Manned Mars Mission (MMM). One such way to reduce a spacecraft's weight is through aeroassist braking which is an alternative to retro-rockets, the traditional method of slowing a craft approaching from a high energy orbit. In this paper aeroassist braking was examined for two blunt vehicle configurations and one streamlined configuration. For each vehicle type, a range of lift-to-drag ratios was examined and the entry angle windows, bank profiles, and trajectory parameters were recorded here. In addition, the sensitivities of velocity and acceleration with respect to the entry angle and bank angles were included. Also, the effect of using different atmosphere models was tested by incorporating several models into the simulation program. Author

N90-14273*# National Aeronautics and Space Administration. Lewis Research Center, Cleveland, OH.

CHARACTERIZATION OF TWO MMIC GaAs SWITCH MATRICES AT MICROWAVE FREQUENCIES

Gene Fujikawa 1990 12 p Prepared for presentation at the 13th International Communication Satellite Systems Conference, Los Angeles, CA, 11-15 Mar. 1990; sponsored by AIAA

(NASA-TM-102449; E-5234; NAS 1.15:102449) Avail: NTIS HC A03/MF A01 CSCL 22B

Monolithic GaAs microwave switch matrices for use in satellite switched, time division multiple access communication systems were developed. Two monolithic GaAs MESFET switch matrices were fabricated; one for switching operation at intermediate frequencies, 3.5 to 6.0 GHz, and another for switching at radio frequencies, 17.7 to 20.2 GHz. Key switch parameters were measured for both switch matrices. Author

N90-14274*# Universities Space Research Association, Huntsville, AL.

SPACE STATION ATTACHED PAYLOAD PROGRAM SUPPORT Final Report, 4 Oct. 1988 - 30 Sep. 1989

Maurice G. Estes, Jr. and Bardle D. Brown 27 Oct. 1989 11 p

(Contract NAS8-37583)

(NASA-CR-183838; NAS 1.26:183838; Rept-4) Avail: NTIS HC A03/MF A01 CSCL 22B

The USRA is providing management and technical support for the peer review of the Space Station Freedom Attached Payload proposals. USRA is arranging for consultants to evaluate proposals, arranging meeting facilities for the reviewers to meet in Huntsville, Alabama and management of the actual review meetings. Assistance in developing an Experiment Requirements Data Base and Engineering/Technical Assessment support for the MSFC Technical Evaluation Team is also being provided. The results of the project will be coordinated into a consistent set of reviews and reports by USRA. The strengths and weaknesses analysis provided by the peer panel reviewers will by used NASA personnel in the selection of experiments for implementation on the Space Station Freedom. Author

19 SPACECRAFT INSTRUMENTATION

For related information see also *06 Aircraft Instrumentation* and *35 Instrumentation and Photography.*

N90-14275*# National Aeronautics and Space Administration. Lewis Research Center, Cleveland, OH.
DESIGN CONSIDERATIONS FOR SPACE FLIGHT HARDWARE
Daniel Glover Jan. 1990 23 p
(NASA-TM-102300; E-4979; NAS 1.15:102300) Avail: NTIS HC A03/MF A01 CSCL 22A

The environmental and design constraints are reviewed along with some insight into the established design and quality assurance practices that apply to low earth orbit (LEO) space flight hardware. It is intended as an introduction for people unfamiliar with space flight considerations. Some basic data and a bibliography are included. Author

20 SPACECRAFT PROPULSION AND POWER

Includes main propulsion systems and components, e.g., rocket engines; and spacecraft auxilliary power sources.

For related information see also *07 Aircraft Propulsion and Power, 28 Propellants and Fuels, 44 Energy Production and Conversion,* and *15 Launch Vehicles and Space Vehicles.*

N90-14276*# Remtech, Inc., Huntsville, AL.
SRB THERMAL ENVIRONMENTS Final Report
W. K. Crain, E. C. Knox, C. L. Frost, and C. D. Engel Jun. 1989 62 p
(Contract NAS8-36476)
(NASA-CR-183801; NAS 1.26:183801; RTR-142-03) Avail: NTIS HC A04/MF A01 CSCL 21H

The objective was to utilize and expand the Solid Rocket Booster (SRB) orbital flight test data base for better predictions of future flight environments. There were five tasks associated with this effort: analyze the internal aft skirt wind tunnel data and incorporate it into a data base for generating design and preflight reeentry thermal environments; generate reentry design thermal environments for the SRB steel case with the nozzle extension off; generate reentry design thermal environments for the SRB Filament Wound Case with the nozzle extension off; develop an engineering tool to analyze the 3-D flowfield around the SRB aft skirt during reentry for the purpose of obtaining the frequency and severity of the belching gas intrusion internal to the aft skirt; and perform SRM transient joint flow analysis for subscale and full scale motor firing as well as determine the effects of debonds of the insulation on the fill time and heating within the field joint insulation. In addition, this work was extended to provide support for the 51L Shuttle SRB failure analysis. Author

N90-14277*# Lockheed Missiles and Space Co., Huntsville, AL. Engineering Center.
FLUID FLOW ANALYSIS OF THE SSME HIGH PRESSURE FUEL AND OXIDIZER TURBINE COOLANT SYSTEMS
G. A. Teal Jul. 1989 67 p
(Contract NAS8-36284)
(NASA-CR-183736; NAS 1.26:183736; LMSC-HEC-TR-F268780) Avail: NTIS HC A04/MF A01 CSCL 21H

The objective is to provide improved analysis capability for the Space Shuttle Main Engine (SSME) high pressure fuel and oxidizer turbine coolant systems. Each of the systems was analyzed to determine fluid flow rate and thermodynamic and transport properties at all key points in the systems. Existing computer codes were used as a baseline for these analyses. These codes were modified to provide improved analysis capability. The major areas of improvement are listed. A review of the drawings was performed, and pertinent geometry changes were included in the models. Improvements were made in the calculation of thermodynamic and transport properties for a mixture of hydrogen and steam. A one-dimensional turbine model for each system is included as a subroutine to each code. This provides a closed loop analysis with a minimum of required boundary conditions as input. An improved labyrinth seal model is included in the high pressure fuel turbine coolant model. The modifications and the analysis results are presented in detail. Author

N90-14278* Rocket Research Corp., Redmond, WA.
ARCJET THRUSTER RESEARCH AND TECHNOLOGY. PHASE 1: EXECUTIVE SUMMARY
10 Aug. 1987 31 p
(Contract NAS3-24631)
(NASA-CR-182106; NAS 1.26:182106) Avail: NTIS HC A03/MF A01 CSCL 21H

The principal objective of this two phase program is to conduct the development research required to make the low power arcjet a flight ready technology. Many important results were obtained during Phase 1 to move closer to this objective. Fundamental analyses were performed of the arcjet nozzle, the gas kinetic reaction effects, the thermal environment, and the arc stabilizing vortex. These aided the conceptual understanding of the arcjet and guided design work. A hydrazine (N2H4) arcjet was designed that combined a flight qualified catalyst bed with a modular arcjet. Extensive testing was performed which demonstrated the feasibility of using this propellant in an arcjet for the first time. Startup techniques were developed, stability maintained, material compatibility tests conducted, and performance mapping tests performed. Specific impulse values from 400 to 730 seconds were produced with a non-optimized design. These levels are higher than were originally thought possible and proved that extremely high enthalpy values can be obtained with constricted arc technology. Erosion rate data are promising for lifetime extensions to meet flight application requirements. Power control unit (PCU) development was started with the design and fabrication of a laboratory high switching frequency supply. Valuable data were obtained on PCU operation and on the interaction with the dynamic arc. Phase 2 efforts presently underway are resolving key issues for multi-hundred hour lifetimes, are continuing to investigate arcjet/PCU interactions, and will demonstrate duty cycle N2H4 arcjet/PCU operation in a simulated flight mode for lifetimes consistent with initial applications. Author

N90-14279*# Toledo Univ., OH. Dept. of Electrical Engineering.
ELECTRICAL PERFORMANCE CHARACTERISTICS OF HIGH POWER CONVERTERS FOR SPACE POWER APPLICATIONS Final Report, 1 Jan. 1988 - 30 Sep. 1989
Thomas A. Stuart and Roger J. King Sep. 1989 149 p
(Grant NAG3-708)
(NASA-CR-185947; NAS 1.26:185947) Avail: NTIS HC A07/MF A01 CSCL 10B

The first goal of this project was to investigate various converters that would be suitable for processing electric power derived from a nuclear reactor. The implementation is indicated of a 20 kHz system that includes a source converter, a ballast converter, and a fixed frequency converter for generating the 20 kHz output. This system can be converted to dc simply by removing the fixed frequency converter. This present study emphasized the design and testing of the source and ballast converters. A push-pull current-fed (PPCF) design was selected for the source converter, and a 2.7 kW version of this was implemented using three 900 watt modules in parallel. The characteristic equation for two converters in parallel was derived, but this analysis did not yield any experimental methods for measuring relative stability. The three source modules were first tested individually and then in parallel as a 2.7 kW system. All tests proved to be satisfactory; the system was stable; efficiency and regulation were acceptable; and the system was fault tolerant. The design of a ballast-load converter, which was operated as a shunt regulator, was investigated. The proposed power circuit is suitable for use with BJTs because proportional base drive is easily implemented. A control circuit which minimizes switching frequency ripple and automatically bypasses a faulty shunt section was developed. A nonlinear

state-space-averaged model of the shunt regulator was developed and shown to produce an accurate incremental (small-signal) dynamic model, even though the usual state-space-averaging assumptions were not met. The nonlinear model was also shown to be useful for large-signal dynamic simulation using PSpice.
Author

N90-14280*# Thiokol Corp., Brigham City, UT. Space Operations.
FLIGHT SET 360T004 (STS-30) FIELD JOINT PROTECTION SYSTEM, VOLUME 7 Final Report
Elgie Hale 20 Sep. 1989 65 p
(Contract NAS8-30490)
(NASA-CR-183829; NAS 1.26:183829; TWR-17543-Vol-7; ECS-1012-Vol-7) Avail: NTIS HC A04/MF A01 CSCL 21H

The Redesigned Solid Rocket Motors (RSRM) of the Space Transportation System have three field joints that are protected by the Joint Protection Systems (JPS). The igniter heater was mounted on the igniter flange. This report documents the performance of the JPS and igniter heaters on the pad and the post-flight condition of the JPS components. All observations that were written up as Squawks and/or Problem Reports are also discussed. The primary heaters performed satisfactorily and maintained the field joint temperatures within the required temperature range. A secondary heater failed Dielectric Withstanding Voltage (DWV) test during the joint closeout prior to launch. This heater was not used, however, since the primary heater functioned properly. Post-test inspection revealed that pin A of the heater power cable was shorted to the connector shell. Design changes have been implemented to resolve the heater power cable problem. All field joint assemblies met all of the performance requirements. J.P.S.

N90-14281*# ENTECH Corp., Dallas-Fort Worth Airport, TX.
CONCEPTUAL DESIGN STUDY OF A 5 KILOWATT SOLAR DYNAMIC BRAYTON POWER SYSTEM USING A DOME FRESNEL LENS SOLAR CONCENTRATOR Final Report
Mark J. ONeill, A. J. McDanal, and Don H. Spears Dec. 1989 48 p
(Contract NAS3-24877)
(NASA-CR-185134; NAS 1.26:185134) Avail: NTIS HC A03/MF A01 CSCL 10B

The primary project objective was to generate a conceptual design for a nominal 5 kW solar dynamic space power system, which uses a unique, patented, transmittance-optimized, dome-shaped, point-focus Fresnel lens as the optical concentrator. Compared to reflective concentrators, the dome lens allows 200 times larger slope errors for the same image displacement. Additionally, the dome lens allows the energy receiver, the power conversion unit (PCU), and the heat rejection radiator to be independently optimized in configuration and orientation, since none of these elements causes any aperture blockage. Based on optical and thermal trade studies, a 6.6 m diameter lens with a focal length of 7.2 m was selected. This lens should provide 87 percent net optical efficienty at 800X geometric concentration ratio. The large lens is comprised of 24 gores, which compactly stow together during launch, and automatically deploy on orbit. The total mass of the microglass lens panels, the graphite/epoxy support structure, and miscellaneous hardware is about 1.2 kg per square meter of aperture. The key problem for the dome lens approach relates to the selection of a space-durable lens material. For the first time, all-glass Fresnel lens samples were successfully made by a sol-gel casting process. Author

N90-14282*# National Aeronautics and Space Administration. Marshall Space Flight Center, Huntsville, AL.
MAIN PROPULSION SYSTEM TEST REQUIREMENTS FOR THE TWO-ENGINE SHUTTLE-C
E. E. Lynn and G. K. Platt Dec. 1989 24 p
(NASA-TM-100382; NAS 1.15:100382) Avail: NTIS HC A03/MF A01 CSCL 21H

The Shuttle-C is an unmanned cargo carrying derivative of the space shuttle with optional two or three space shuttle main engines (SSME's), whereas the shuttle has three SSME's. Design and operational differences between the Shuttle-C and shuttle were assessed to determine requirements for additional main propulsion system (MPS) verification testing. Also, reviews were made of the shuttle main propulsion test program objectives and test results and shuttle flight experience. It was concluded that, if significant MPS modifications are not made beyond those currently planned, then main propulsion system verification can be concluded with an on-pad flight readiness firing. Author

N90-14283*# National Aeronautics and Space Administration. Lewis Research Center, Cleveland, OH.
A HEAT RECEIVER DESIGN FOR SOLAR DYNAMIC SPACE POWER SYSTEMS
Karl W. Baker, Miles O. Dustin, and Roger Crane (University of South Florida, Tampa.) 1990 7 p Prepared for presentation at the 1990 International Solar Energy Conference, Miami, FL, 1-4 Apr. 1990; sponsored by ASME
(NASA-TM-102473; E-5253; NAS 1.15:102473) Avail: NTIS HC A02/MF A01 CSCL 10B

An advanced heat pipe receiver designed for a solar dynamic space power system is described. The power system consists of a solar concentrator, solar heat receiver, Stirling heat engine, linear alternator and waste heat radiator. The solar concentrator focuses the sun's energy into a heat receiver. The engine and alternator convert a portion of this energy to electric power and the remaining heat is rejected by a waste heat radiator. Primary liquid metal heat pipes transport heat energy to the Stirling engine. Thermal energy storage allows this power system to operate during the shade portion of an orbit. Lithium fluoride/calcium fluoride eutectic is the thermal energy storage material. Thermal energy storage canisters are attached to the midsection of each heat pipe. The primary heat pipes pass through a secondary vapor cavity heat pipe near the engine and receiver interface. The secondary vapor cavity heat pipe serves three important functions. First, it smooths out hot spots in the solar cavity and provides even distribution of heat to the engine. Second, the event of a heat pipe failure, the secondary heat pipe cavity can efficiently transfer heat from other operating primary heat pipes to the engine heat exchanger of the defunct heat pipe. Third, the secondary heat pipe vapor cavity reduces temperature drops caused by heat flow into the engine. This unique design provides a high level of reliability and performance. Author

N90-14284*# National Aeronautics and Space Administration. Lewis Research Center, Cleveland, OH.
ATOMIC HYDROGEN AS A LAUNCH VEHICLE PROPELLANT
Bryan A. Palaszewski 1990 12 p Presented at the 28th Aerospace Sciences Meeting, Reno, NV, 8-11 Jan. 1990; sponsored by AIAA
(NASA-TM-102459; E-5246; NAS 1.15:102459; AIAA-90-0715) Avail: NTIS HC A03/MF A01 CSCL 21I

An analysis of several atomic hydrogen launch vehicles was conducted. A discussion of the facilities and the technologies that would be needed for these vehicles is also presented. The Gross Liftoff Weights (GLOW) for two systems were estimated; their specific impulses (I sub sp) were 750 and 1500 lb(sub f)/s/lb(sub m). The atomic hydrogen launch vehicles were also compared to the currently planned Advanced Launch System design concepts. Very significant GLOW reductions of 52 to 58 percent are possible over the Advanced Launch System designs. Applying atomic hydrogen propellants to upper stages was also considered. Very high I(sub sp) (greater than 750 lb(sub f)/s/lb(sub m)) is needed to enable a mass savings over advanced oxygen/hydrogen propulsion. Associated with the potential benefits of high I(sub sp) atomic hydrogen are several challenging problems. Very high magnetic fields are required to maintain the atomic hydrogen in a solid hydrogen matrix. The magnetic field strength was estimated to be 30 kilogauss (3 Tesla). Also the storage temperature of the propellant is 4 K. This very low temperature will require a large refrigeration facility for the launch vehicle. The design considerations for a very high recombination rate for the propellant are also discussed. A recombination rate of 210 cm/s is predicted

for atomic hydrogen. This high recombination rate can produce very high acceleration for the launch vehicle. Unique insulation or segmentation to inhibit the propellant may be needed to reduce its recombination rate. Author

N90-14285*# National Aeronautics and Space Administration. Lewis Research Center, Cleveland, OH.
ON PROTECTION OF FREEDOM'S SOLAR DYNAMIC RADIATOR FROM THE ORBITAL DEBRIS ENVIRONMENT. PART 1: PRELIMINARY ANALYSES AND TESTING
Jennifer L. Rhatigan, Eric L. Christiansen, and Michael L. Fleming (LTV Missiles and Electronics Group, Dallas, TX.) 1990 10 p Prepared for presentation at the International Solar Energy Conference, Miami, FL, 1-4 Apr. 1990; sponsored by ASME
(NASA-TM-102458; E-5245; NAS 1.15:102458) Avail: NTIS HC A02/MF A01 CSCL 10B

A great deal of experimentation and analysis was performed to quantify penetration thresholds of components which will experience orbital debris impacts. Penetration was found to depend upon mission specific parameters such as orbital altitude, inclination, and orientation of the component; and upon component specific parameters such as material, density and the geometry particular to its shielding. Experimental results are highly dependent upon shield configuration and cannot be extrapolated with confidence to alternate shield configurations. Also, current experimental capabilities are limited to velocities which only approach the lower limit of predicted orbital debris velocities. Therefore, prediction of the penetrating particle size for a particular component having a complex geometry remains highly uncertain. An approach is described which was developed to assess on-orbit survivability of the solar dynamic radiator due to micrometeoroid and space debris impacts. Preliminary analyses are presented to quantify the solar dynamic radiator survivability, and include the type of particle and particle population expected to defeat the radiator bumpering (i.e., penetrate a fluid flow tube). Results of preliminary hypervelocity impact testing performed on radiator panel samples (in the 6 to 7 km/sec velocity range) are also presented. Plans for further analyses and testing are discussed. These efforts are expected to lead to a radiator design which will perform to requirements over the expected lifetime. Author

23 CHEMISTRY AND MATERIALS (GENERAL)

No abstracts in this category.

24 COMPOSITE MATERIALS

Includes physical, chemical, and mechanical properties of laminates and other composite materials.
For ceramic materials see *27 Nonmetallic Materials.*

N90-14286*# Auburn Univ., AL. Dept. of Mechanical Engineering.
MEASUREMENT OF DAMPING OF GRAPHITE EPOXY COMPOSITE MATERIALS AND STRUCTURAL JOINTS Final Report, Oct. 1984 - Jun. 1989
Malcolm J. Crocker, Mohan D. Rao, P. K. Raju, and Xinche Yan Aug. 1989 205 p
(Contract NAS8-36146)
(NASA-CR-183802; NAS 1.26:183802) Avail: NTIS HC A10/MF A02 CSCL 11D

The damping capacity of graphite epoxy materials and structural joints was evaluated. The damping ratio of different composite specimens and bonded joints were systematically evaluated under normal atmospheric conditions and in a vacuum environment. Free and forced vibration test methods were employed for measuring the damping ratios. The effect of edge support conditions on the damping value of a composite tube specimen was studied by using a series of experiments performed on the specimen with different edge supports. It was found that simulating a free-free boundary conditions by having no constraints at the ends gives the lowest value of the material damping of the composite. The accuracy of the estimation of the damping ratio value was improved by using a curve-fitting technique on the response data obtained through measurement. The effect of outgassing (moisture desorption) on the damping capacity was determined by measuring the damping ratio of the tube specimen in a vacuum environment before and after outgassing had occurred. The effects of high and low temperatures on the damping was also investigated by using a series of experiments on tube and beam specimens. An analytical model to study the vibrations of a bonded lap joint system was formulated. Numerical results were generated for different overlap ratios of the system. These were compared with experimental results. In order to determine the influence of bonded joints on the material damping capacity, experiments were conducted on bonded lap-jointed and double-butt-jointed specimens. These experimental results were compared with simple beam specimens with no joints. K.C.D.

N90-14287*# National Aeronautics and Space Administration. Lewis Research Center, Cleveland, OH.
OXIDATION EFFECTS ON THE MECHANICAL PROPERTIES OF SiC FIBER-REINFORCED REACTION-BONDED SILICON NITRIDE MATRIX COMPOSITES
Ramakrishna T. Bhatt Nov. 1989 38 p Prepared in cooperation with Army Propulsion Lab., Cleveland, OH
(NASA-TM-102360; E-5074; NAS 1.15:102360; AVSCOM-TR-89-C-018) Avail: NTIS HC A03/MF A01 CSCL 11D

The room temperature mechanical properties of SiC fiber reinforced reaction bonded silicon nitride composites were measured after 100 hrs exposure at temperatures to 1400 C in nitrogen and oxygen environments. The composites consisted of approx. 30 vol percent uniaxially aligned 142 micron diameter SiC fibers in a reaction bonded Si3N4 matrix. The results indicate that composites heat treated in a nitrogen environment at temperatures to 1400 C showed deformation and fracture behavior equivalent to that of the as-fabricated composites. Also, the composites heat treated in an oxidizing environment beyond 400 C yielded significantly lower tensile strength values. Specifically in the temperature range from 600 to 1000 C, composites retained approx. 40 percent of their as-fabricated strength, and those heat treated in the temperatures from 1200 to 1400 C retained 70 percent. Nonetheless, for all oxygen heat treatment conditions, composite specimens displayed strain capability beyond the matrix fracture stress; a typical behavior of a tough composite. Author

N90-14288# Department of the Navy, Washington, DC.
METHOD FOR STABILIZATION OF PAN-BASED CARBON FIBERS Patent Application
Leighton H. Peebles, inventor (to Navy) 30 Jun. 1989 11 p
(AD-D014228; US-Patent-Appl-SN-373980) Avail: NTIS HC A03/MF A01 CSCL 11/2

This invention relates to carbon fibers, and more particularly, to an improved process for stabilizing polyacrylonitrile (PAN) based fibers prior to carbonization and high temperature heat treatment. There has been an increasing demand for construction materials of high strength-to-weight ratio and high Young's modulus for use in civilian and military applications, particularly for materials that have good thermal stability. Accordingly, there has been a demand for improved reinforcing fibers to be embodied in structural composites which are exposed to conditions of high temperature and high mechanical stress. Carbon fibers are produced in five manufacturing steps: polymerization of monomers, such as acrylonitrile; orientation of the linear polymer molecules by spinning them into fibers; stabilization by heating the fibers to 150 to 350 C. GRA

N90-14289 Department of the Navy, Washington, DC.
CARBON FIBER REINFORCED METAL MATRIX COMPOSITES Patent
Richard K. Everett, inventor (to Navy) and William F. Henshaw, inventor (to Navy) 1 Aug. 1989 5 p Filed 28 Jun. 1988 (AD-D014245; US-Patent-4,853,294; US-Patent-Appl-SN-212553; US-Patent-Class-428-614) Avail: US Patent and Trademark Office CSCL 11/4

An improved metal, alloy, or intermetallic matrix composite containing carbon reinforcing fibers is formed. The carbon reinforcing fibers are protected from interaction with the matrix material by an inner and on outer barrier layer. The outer layer is any one of the group of stable, non-reactive ceramic materials used to protect fibers, and the inner layer is a ductile, low density, oxygen desorbing rare earth metal. The carbon fibers are particularly useful in forming composites with a titanium aluminide matrix. GRA

N90-14290 Virginia Polytechnic Inst. and State Univ., Blacksburg.
ANALYSIS OF METAL MATRIX COMPOSITE STRUCTURES USING A MICROCHEMICAL CONSTITUTIVE THEORY Ph.D. Thesis
Robert Thomas Arenburg 1989 190 p
Avail: Univ. Microfilms Order No. DA8913738

The nonlinear behavior of continuous fiber reinforced metal matrix composite structures is examined using a micromechanical constitutive theory. Effective lamina and laminate constitutive relations based on the Aboudi micromechanics theory are presented. The inelastic matrix behavior is modeled by the unified viscoplasticity theory of Bodner and Partom. The laminate constitutive relations are incorporated into a first order shear deformation plate theory. The resulting boundary value problem is solved by utilizing the finite element method. Computational aspects of the numerical solution, such as the temporal integration of the inelastic strains and the spatial integration of bending moments are addressed. Numerical results are presented which illustrate the nonlinear response of metal matrix composites subjected to extensional and bending loads. Experimental data from available literature are in good agreement with the numerical results. Dissert. Abstr.

N90-14291 Missouri Univ., Rolla.
FINITE ELEMENT ANALYSIS OF LAMINATED COMPOSITE PLATES Ph.D. Thesis
Virat Chomkway 1989 129 p
Avail: Univ. Microfilms Order No. DA8920394

Higher order theories for laminated composite plates with small and large deflections using the Lagrange multiplier technique are presented. The formulations of the theories are based on the minimization of the total potential energy by using a displacement field containing up to third-order transverse coordinates. The Lagrange multipliers are employed to constrain the displacement functions to satisfy the stress boundary conditions. Some examples using the finite rectangular plates subjected to uniformly distributed and sinusoidal loads and a concentrated load are solved by the finite element method and the results are compared with those in existing literature. The solutions agree well with those presented in earlier investigations for thin plates. Under more relaxed boundary conditions, this study predicts about 10 percent higher values on nondimensional stresses in thick plates leading to the conclusion that the in-plane displacment modes should be included in the expressions of the displacement fields. Experiments on clamped square laminated composite plates were conducted under low and intermediate velocity impact. The transverse deflections of the plates were recorded by a non-contact light-sensitive transducer and a microcomputer. Results of low velocity impact tests are compared with those obtained by static analysis using static-equivalent load. Good agreement is established. Dissert. Abstr.

N90-14292 California Univ., Los Angeles.
ELASTO-PLASTIC ANALYSIS OF UNIDIRECTIONAL FIBER-REINFORCED COMPOSITES SUBJECTED TO TRANSVERSE NORMAL LOADING USING THE FINITE ELEMENT METHOD Ph.D. Thesis
Pascalis K. Gotsis 1989 406 p
Avail: Univ. Microfilms Order No. DA8922219

Elasto-plastic behavior of unidirectional fiber reinforced composites subjected to transverse and normal loading was performed using the finite element method (FEM). The FEM was applied using the computer program CALSAP (an updated version of NONSAP). Pre and post-processor graphic programs (FEGRID, GENERATE1 and PLOTXY) were developed in conjunction with CALSAP to perform the finite element analysis and plot the results. The finite element analysis was based upon the total Lagrangian formulation, the incremental Prandl-Reuss stress-strain equations for the theory of plasticity, and the von Mises yield criterion. The objective of the composites was fourfold: (1) to compute the stress-strain distribution; (2) to examine the incipient plastic yielding and the propagation of the plastic flow within the matrix; (3) to predict where failure of the material will occur; and (4) to compare the numerical results with available solutions in the literature. The finite element method was applied first to examine the elastoplastic behavior of plates reinforced with a single rigid or elastic fiber. A square plate with a hole was also examined for the purpose of comparison with the reinforced plates. The analysis was then applied to the general case of a composite reinforced with many fibers packed in a square or hexagonal array. The solutions of the finite element analysis were compared with available solutions in the literature and with results obtained from application of the finite element computer program MARC. The results were found to be in close agreement. Dissert. Abstr.

N90-14293 Texas A&M Univ., College Station.
A GENERALIZED THERMOMECHANICAL CONSTITUTIVE MODEL FOR METAL MATRIX COMPOSITES WITH PLASTIC STRAIN AND DAMAGE Ph.D. Thesis
Sheryl Kay Bryan 1988 141 p
Avail: Univ. Microfilms Order No. DA8913333

A generalized model for materials with inelastic strain and damage which is applicable to metal matrix composites is developed. The constitutive framework is based on a continuum mechanics approach with constraints on the relationships provided by the laws of thermodynamics. The result is a derivation of the Helmholtz free energy function which is a sum of the free energies for elastic strain, plastic strain, and damage, and a constitutive equation where all coefficients are equal to those for the initial elastic material. In addition, the model is applicable for all material types from orthotropic to isotropic and for a specific material system, requiring only the development of the material dependent damage growth laws to complete the model. Although the resulting equations are similar to those assumed in previous damage mechanics research, this study lends credence via derived information to those previously assumed. Dissert. Abstr.

N90-14294*# National Aeronautics and Space Administration. Lewis Research Center, Cleveland, OH.
PARAMETRIC STUDIES TO DETERMINE THE EFFECT OF COMPLIANT LAYERS ON METAL MATRIX COMPOSITE SYSTEMS
J. J. Caruso, C. C. Chamis, and H. C. Brown (Sverdrup Technology, Inc., Cleveland, OH.) 1990 13 p Prepared for presentation at the 35th Symposium and Exhibition, Anaheim, CA, 2-5 Apr. 1990; sponsored by Society for the Advancement of Material and Process Engineering
(NASA-TM-102465; E-5252; NAS 1.15:102465) Avail: NTIS HC A03/MF A01 CSCL 11D

Computational simulation studies are conducted to identify compliant layers to reduce matrix stresses which result from the coefficient of thermal expansion mismatch and the large temperature range over which the current metal matrix composites will be used. The present study includes variations of compliant layers and their properties to determine their influence on

unidirectional composite and constituent response. Two simulation methods are used for these studies. The first approach is based on a three-dimensional linear finite element analysis of a 9 fiber unidirectional composite system. The second approach is a micromechanics based nonlinear computer code developed to determine the behavior of metal matrix composite system for thermal and mechanical loads. The results show that an effective compliant layer for the SCS 6 (SiC)/Ti-24Al-11Nb (Ti3Al + Nb) and SCS 6 (SiC)/Ti-15V-3Cr-3Sn-3Al (Ti-15-3) composite systems should have modulus 15 percent that of the matrix and a coefficient of thermal expansion of the compliant layer roughly equal to that of the composite system without the CL. The matrix stress in the longitudinal and the transverse tangent (loop) direction are tensile for the Ti3Al + Nb and Ti-15-3 composite systems upon cool down from fabrication. The fiber longitudinal stress is compressive from fabrication cool down. Addition of a recommended compliant layer will result in a reduction in the composite modulus. Author

N90-14295# Argonne National Lab., IL. Materials and Components Technology Div.
APPLICATION OF NEUTRON DIFFRACTION NDE TO HIGH-TEMPERATURE SUPERCONDUCTING COMPOSITES
D. S. Kupperman, J. P. Singh, S. Majumdar, A. C. Raptis, and R. L. Hitterman Aug. 1989 8 p Presented at the 16th Annual Review of Progress in Quantitative NDE, Brunswick, ME, 23-28 Jul. 1989; sponsored in part by Iowa State Univ., Ames Lab., and Bowdoin College
(Contract W-31-109-eng-38)
(DE90-002184; CONF-890770-3) Avail: NTIS HC A02/MF A01

The Argonne Intense Pulsed Neutron Source and General Purpose Powder Diffractometer have been used to study high-(Tc) metal oxide composites composed of yttrium, barium, copper, oxygen, and silver. Neutron diffraction techniques were applied to composites with 15, 20, and 30 pct silver content by volume. We have observed that after sintering, the 30 pct-silver specimens contained both orthorhombic high-(Tc) and tetragonal, non-superconducting phases near the center of the specimens but only the orthorhombic phase near the surface. We have also observed residual tensile strains in Ag as a function of crystallographic direction; three strains range from as high as 0.085 pct in 15 pct Ag samples to as low as about 0.02 pct in a 30 pct Ag sample. Compressive strains in the YBCO (111) crystallographic direction were approximated by correcting for the diffraction peak shift due to changes in stoichiometry with varying Ag content. The estimated compressive-strain values vary from 0.04 pct (15 pct Ag) to 0.09 pct (20 pct Ag) to 0.01 pct (30 pct Ag), with an uncertainty of about 0.03 pct. The decrease in strain in YBCO for the 30 pct Ag composite is consistent with the decrease in Ag strain and may be due to additional creep of the composite.
DOE

N90-14296# Oak Ridge National Lab., TN. Applied Technology Div.
FIBER-OPTIC SENSORS FOR COMPOSITE CURE ANALYSIS AND LIFETIME NONDESTRUCTIVE EVALUATION
J. D. Muhs, M. R. Cates, K. W. Tobin, G. J. Capps, and D. L. Beshears 1989 10 p Presented at the 8th International Congress on Applications of Lasers and Electro-Optics, Orlando, FL, 15-20 Oct. 1989
(Contract DE-AC05-84OR-21400)
(DE90-001739; CONF-891091-2) Avail: NTIS HC A02/MF A01

A proposed multiplexed fiber-optic sensor system capable of analyzing a composite material during its curing cycle and over its service lifetime is presented. The sensor is composed of two independent sensing schemes that will ultimately be multicomplexed onto a specialized single-mode/multimode optical fiber. The first sensing scheme is a fiber-optic viscosity and temperature sensor used for composite cure analyses. This sensor is based on: (1) the laser-induced viscosity-dependent fluorescence phenomena observed in epoxy-based composite materials, and (2) the temperature-dependent decay-time fluorescence phenomena observed in thermographic phosphors. The second sensor is based on a low-finesse, single-mode fiber-optic Fabry-Perot interferometer and is used as a strain/vibration sensor for lifetime nondestructive evaluations on composites. Experimental results have determined that these sensor concepts are feasible alternatives to cure-analysis monitors and conventional strain-analysis techniques.
DOE

25 INORGANIC AND PHYSICAL CHEMISTRY

Includes chemical analysis, e.g., chromatography; combustion theory; electrochemistry; and photochemistry.

For related information see also *77 Thermodynamics and Statistical Physics.*.

N90-14297 ESDU International Ltd., London (England).
THERMOPHYSICAL PROPERTIES OF ISOPROPYL ALCOHOL. PART 1: THE IDEAL GAS AND THE SATURATED LIQUID AND VAPOUR
Oct. 1989 16 p
(ESDU-89017-Pt-1; ISBN-0-85679-689-1; ISSN-0141-4062) Avail: ESDU

This Data Item 89017, an addition to the Physical Data Subseries, gives equations obtained from a critical evaluation of experimental data in the literature for the variation along the saturation line with temperature, for both the liquid and the vapor, of: density, enthalpy, heat capacity at constant pressure, dynamic viscosity, and thermal conductivity. Also given are equations for the variation with temperature along the saturation line of vapor pressure, latent heat of vaporization, and surface tension, together with equations for the variation with temperature for the ideal gas of specific heat capacity at constant pressure, enthalpy, dynamic viscosity, and thermal conductivity. Results on the saturation line evaluated in SI units using the equations are tabulated at 5 K intervals from the melting point to the critical point, or as close to it as possible for some properties. Results for the ideal gas evaluates also in SI units using the equations are tabulated at 10 K intervals from the melting point to 1000 K. In the absence of experimental values some of these results involve extrapolation and they are indicated in the tables. Conversion factors to facilitate use of the data in British units are included. ESDU 89020 provides thermodynamic data for the vapor at elevated pressures. ESDU

N90-14298 ESDU International Ltd., London (England).
ORTHOBARIC DENSITIES AND MOLAR VOLUMES OF LIQUIDS. INTRODUCTION TO DATA ITEMS ISSUED AFTER JULY 1989
Aug. 1989 3 p
(ESDU-89018; ISBN-0-85679-690-5; ISSN-0141-4062) Avail: ESDU

This Data Item 89018, an addition to the Physical Data Subseries, discussed the likely accuracy of measurements of liquid density to be found in the literature and explains how the values of uncertainty given against each predicted value of density in the ESDU documents providing numerical values was derived.
ESDU

N90-14299 ESDU International Ltd., London (England).
ORTHOBARIC DENSITIES AND MOLAR VOLUMES OF LIQUIDS. AROMATIC HYDROCARBONS
Aug. 1989 82 p
(ESDU-89019; ISBN-0-85679-691-3; ISSN-0141-4062) Avail: ESDU

This Data Item 89019, an addition to the Physical Data Subseries, tabulates density and molar volume for 36 aromatic hydrocarbons in the range C6 to C10 (in units of kg/cu m and cu cm/mol respectively) from near the melting point to within a few degrees of the critical point. The temperature interval chosen is varied from 10 K to 1 K to keep the increments in density reasonably small. The data were obtained by fitting an equation to experimental data for density for each compound taken from a wide range of sources in the literature; values established for the constants in the equation for each compound are also tabulated. An estimation

of the accuracy of the prediction is included for each value tabulated, the sources of the data are listed for each compound, and values of the critical point are provided together with normal boiling and melting points. ESDU

N90-14300 ESDU International Ltd., London (England).
THERMOPHYSICAL PROPERTIES OF ISOPROPYL ALCOHOL. PART 2: THERMODYNAMIC PROPERTIES AT ELEVATED PRESSURES
Aug. 1989 42 p Supersedes ESDU-76012
(ESDU-89020-Pt-2; ESDU-76012; ISBN-0-85679-692-3; ISSN-0141-4062) Avail: ESDU

This Data Item 89020, an addition to the Physical Data Subseries, tabulates in SI units from the melting point to the critical point along the saturation line at fixed pressures data for: saturation temperature, liquid density, vapor specific volume, liquid and vapor enthalpy and entropy, latent heat of vaporization, and specific heat capacity. In addition, tables give specific isobars for pressures up to 50 MN/sq m, the variation with temperature for the vapor of specific volume, compression factor, enthalpy, entropy, and specific heat capacities at constant pressure and volume. The data were generated from a single correlating function fitting selected experimental data drawn from the literature, and are therefore self-consistent. An estimate of the error in linear interpolation within the tables is included, and a computer-generated temperature-entropy chart representing the data is provided. To facilitate use of the data in British units, conversion factors are given. No equations for the values are included. ESDU

N90-14301 Northwestern Univ., Evanston, IL.
EFFECTS OF FLAME STRETCH ON THE PROPAGATION, EXTINCTION, AND STABILITY OF PREMIXED FLAMES Ph.D. Thesis
Yeongdae Kim 1989 164 p
Avail: Univ. Microfilms Order No. DA8913984

The effects of flame stretch on the propagation, extinction, and stability of premixed flames were examined theoretically. Specifically, a premixed flame held in the front stangation-point flow of a body was considered. In this configuration, the flame experiences a constant stretch directly proportional to the strain rate. The geometry is not only relatively simple to permit analytical treatment, but was widely used in experiments as well. In particular the thermal expansion, which was neglected in previous work, was taken into account. Moderate values of stretch were considered so that the flame stands outside the viscous boundary layer, well away from the body. A complete solution of the flow field is provided, including the flame stand-off distance in terms of the thermal expansion, the Lewis number Le, and the strain rate. The explicit dependence of the stand-off distance at extinction is provided in terms of all other parameters. The overall effect of the combustion on the fluid flow is in displacing the upcoming flow away from the body. This displacement is more pronounced than that produced by the viscous boundary layer. The role of flame stretch on the stability of premixed flames was also examined. The stability analysis shows that flame stretch may suppress the hydrodynamic instability, observed for long wavelength disturbances. The short wavelength disturbances are known to be stabilized by diffusional transport when Le is greater than 1. Thus, a sufficiently large stretch can make the flame absolutely stable when Le is greater than 1. The critical value of the flame stretch was determined for absolute stability and the neutral stability boundary provided. For small values of stretch, the cellular instability may occur in the form of longitudinal cells.
Dissert. Abstr.

N90-14302 Georgia Inst. of Tech., Atlanta.
A SURFACE COUPLED FLAMELET APPROACH TO DYNAMIC RESPONSE IN HETEROGENEOUS PROPELLANT COMBUSTION Ph.D. Thesis
John Mark Deur 1988 179 p Previously announced in IAA as A88-48754
Avail: Univ. Microfilms Order No. DA8912536

The combustion response of heterogeneous solid propellants, a quantity needed in combustion instability calculations of solid propellant rocket motors, is studied through development of a response model for analogous oxidizer-binder laminate propellants. Two key features of this analysis are incorporation of current experimental knowledge concerning the structure of the laminate combustion zone, resulting in a more detailed and physically realistic description of the phenomena, and development of a modular approach to the analysis, allowing a significant reduction in the complexity of the solution by isolating and then analyzing in a quasi-one-dimensional manner closely coupled flame-surface regions. Results show that there can be significant differences between the responses calculated via the current model and those obtained from classical one-dimensional treatments.
Dissert. Abstr.

N90-14303 Georgia Inst. of Tech., Atlanta.
INVESTIGATION OF COMBUSTION INSTABILITY IN RAMJET COMBUSTORS Ph.D. Thesis
Dierk Martin Reuter 1988 162 p
Avail: Univ. Microfilms Order No. DA8916170

The mechanisms responsible for the driving of longitudinal instabilities in dump-type ramjet combustors are investigated. In particular, the coupling between the core flame which is stabilized at the entrance of the combustor and the longitudinal acoustic field was studied. The time dependent structure of premixed V-shaped flames was experimentally examined using pressure measurements, space and time resolved C-U radical radiation measurements, high speed shadow cine photography, and laser-Doppler velocimetry. It was revealed that the acoustic energy to sustain the instability is mainly supplied by the oscillatory heat release from the flame. Based on this finding, a model was developed which is capable of predicting the acoustic pressure spectrum from measured heat release rates. Furthermore, it was shown that the periodic heat release rates largely result from periodic changes in the flame surface area which are caused by acoustically triggered symmetric vortex shedding in the wake of the flame holders. Lastly, experiments were conducted which used this mechanism to show the suppression of instabilities at the fundamental acoustic mode by staggering multiple flames so that the unsteady heat release fields destructively interfere with one another. Dissert. Abstr.

N90-14304 Virginia Polytechnic Inst. and State Univ., Blacksburg.
FATIGUE ANALYSIS AND RECONSTRUCTION OF HELICOPTER LOAD SPECTRA Ph.D. Thesis
Abolhassan Khosrow Khosrovaneh 1989 163 p
Avail: Univ. Microfilms Order No. DA8913748

Helicopter load histories applied to notched metal samples were taken as examples, and their fatigue lives were predicted by using a simplified version of the local strain approach. This simplified method requires an input load history in the form of the rain-flow matrix and places bounds on the fatigue life. A peak-valley reconstructed history was generated based on the standard spectrum Helix. A second history studied was a more irregular one based on actual flight data. It was used to generate three reconstructed histories based on three principles: peak-valley, to-from, and rain-flow. Emphasis is given to the rain-flow reconstruction method, and different reconstruction methods based on rain-flow cycle counting are presented. Life predictions are presented for all of the above cases, and the comparison with test data and other considerations suggest that the most promising reconstruction approach is one based on rain-flow cycle counting. Finally, a method is presented which reconstructs a history with the same rain-flow cycles and also the same distribution of relative time increments between adjacent peaks and valleys. This reconstructed history gives the same fatigue life as the original history. Dissert. Abstr.

N90-14305*# Pennsylvania State Univ., University Park. Fuel Science Program.
KINETICS AND MECHANISM OF SOOT FORMATION IN HYDROCARBON COMBUSTION Final Technical Report, 25 Oct. 1985 - 28 Feb. 1989
Michael Frenklach 5 Jan. 1990 10 p
(Grant NAG3-668)
(NASA-CR-186162; NAS 1.26:186162) Avail: NTIS HC A02/MF A01 CSCL 21B

The focus of this work was on kinetic modeling. The specific objectives were: detailed modeling of soot formation in premixed flames, elucidation of the effects of fuel structure on the pathway to soot, and the development of a numerical technique for accurate modeling of soot particle coagulation and surface growth. Those tasks were successfully completed and are briefly summarized. J.P.S.

N90-14306# SRI International Corp., Menlo Park, CA.
HIGH TEMPERATURE CHEMISTRY OF COMPLEX VAPORIZATION/DECOMPOSITION PROCESSES Final Report, Sep. 1977 - Aug. 1988
D. L. Hildenbrand 9 Dec. 1988 11 p
(Contracts DE-FG03-86ER-13541; PA-129; EY-76-C-03-0115)
(DE89-016559; DOE/ER-13541/T1) Avail: NTIS HC A03/MF A01

A series of systematic studies were generated of the high temperature vaporization/decomposition behavior of a number of metal sulfates and chromates. A clearer picture is now beginning to emerge regarding the kinetic features of sulfate decompositions, and of the many ways that retardation of the SO3 yields SO2 conversion step affects these processes. The degree to which this step is coupled to the initial lattice SO4(sup =) decomposition is a critical feature, and the action of certain metal and oxide catalysts for the SO3 conversion gave varied results that appear to be strongly temperature dependent. For the alkali sulfates and chromates, which undergo both decomposition and molecular vaporization, these studies yield the first quantitative measure of the relative contributions of these two processes, as well as accurate thermodynamic data for the M2SO4 and M2CrO4 gaseous species. Derived vapor entropies were especially useful in checking the validity of various spectroscopic and molecular constant assignments for the M2SO4 and M2CrO4 species. Overall, the results yield a self consistent base of information that significantly improves the understanding of the high temperature chemistry of these complex and interesting inorganic compounds. DOE

N90-14307# Delaware Univ., Newark. Dept. of Chemical Engineering.
THE GENERALIZED VAN DER WAALS THEORY OF PURE FLUIDS AND MIXTURES Annual Report
Stanley I. Sandler Sep. 1989 31 p
(Contract DE-FG02-85ER-13436)
(DE90-000504; DOE/ER-13436/4) Avail: NTIS HC A03/MF A01

One important goal of our current work is to extend our successful equations of state derived for simple model fluids such as the square well and exponential-six atomic fluids, which are based on theory and computer simulation, to more realistic and complex fluids. We have been concentrating our efforts on small, rigid molecular fluids such as nitrogen, ethane, carbon disulfide, and propane, and trying to understand what important features of these fluids must be accounted for in their thermodynamic description. That is, we are trying to understand why empirical equations, such as the Peng-Robinson equation of state, are useful for spherical and nonspherical molecules (provided the molecules are not too large) even though they contain no structural information other than the critical properties. Our principal tools for gaining insight into the thermodynamic and structural behavior of molecular fluids has been the generalized van der Waals partition function and Monte Carlo computer simulation. DOE

N90-14308# Brigham Young Univ., Provo, UT. Dept. of Chemistry.
SUPERCRITICAL FLUID CHROMATOGRAPHY/SUPERSONIC JET SPECTROSCOPY Progress Report, 1 Jun. - 15 Sep. 1989
Steven R. Goates and Milton L. Lee 1989 7 p
(Contract DE-FG22-86PC-90534)
(DE90-001378; DOE/PC-90534/13) Avail: NTIS HC A02/MF A01

Recent accomplishments have included construction and testing of a new design of pulsed supersonic jet nozzle and characterization of the sheath flow nozzle. Good spectroscopic results were obtained with the pulsed nozzle, and it shows promise for capillary chromatography, but the design must still be improved. Study of the sheath-flow nozzle has illuminated some of the factors governing its behavior, and should help to further optimize its performance with capillary SFC/SJS. Swirl flow patterns may be the cause of the current high pressure limit in its use. Changes in the design of the collection optics were also studied to see if sensitivity could be enhanced for dispersed fluorescence detection with a photodiode array. A major overhaul and upgrade of the excimer laser have aided the work and resulted in improved signal-to-noise in the measurements. DOE

N90-14309# Stanford Univ., CA. Petroleum Research Inst.
DEVICES AND METHODS FOR IN-SITU COMBUSTION IGNITION
David C. Shallcross Oct. 1989 34 p
(Contract DE-FG22-87BC-14126)
(DE89-000766; DOE/BC-14126/12; SUPRI-TR-69) Avail: NTIS HC A03/MF A01

One of the most important tasks during a fireflood is to ensure the ignition of the oil-bearing stratum efficiently and safely. Many different devices have been developed and employed to achieve this aim. The target zone may ignite spontaneously upon injection of an oxygen containing gas without the aid of special equipment. Alternatively, ignition may be hastened or enhanced by the use of gas fired downhole burners, catalytic heaters, electric downhole heaters, or other, chemical means. Other methods involve increasing the reactivity of the formation contents by doping the stratum with compounds that ignite and burn more readily than the reservoir oil. The range of ignition methods and devices that have been developed and applied in the field are surveyed. Not only are successful ignition systems discussed, but also those designs that failed to ignite a formation. In discussing the various techniques, factors considered include reliability, specialized equipment and material requirements, and safety. Another consideration is whether a system or device may be easily reused if ignition is not successful on the first attempt. The use of oxidizing gases than other air is also discussed. DOE

N90-14310# Sandia National Labs., Albuquerque, NM.
FLAME ACCELERATION STUDIES IN THE MINIFLAME FACILITY
S. R. Tieszen, M. P. Sherman, and W. B. Benedick Jul. 1989 33 p
(Contract DE-AC04-76DP-00789)
(DE90-000041; SAND-89-0859) Avail: NTIS HC A03/MF A01

Flame acceleration and deflagration-to-detonation transition (DDT) studies were conducted in a 19.4 cm high, 14.5 cm wide, and 2.242 m long channel (MINIFLAME) that is a 1:12.6 scale model of the 136 cu m FLAME facility. Tests were conducted with two levels of hydrogen concentration (20 and 30 percent), with and without obstacles in the channel, and with three levels of transverse top venting (0, 13, and 50 percent). The flame acceleration results in MINIFLAME are qualitatively similar to those in FLAME; however, the small-scale results are more benign quantitatively. The results show that insufficient venting, 13 percent venting in this case, can promote flame acceleration due to turbulence produced by the flow through the vents in smooth channels. However, with obstacle-generated turbulence in the channel, 13 percent top venting was found to be beneficial. Flame acceleration resulting in DDT was shown to occur in as little as 35 liters of mixture. Comparison of the DDT data with obstacles

in MINIFLAME and FLAME supports d/lambda scaling of DDT, where lambda is the detonation cell width of the mixture and d is the characteristic open diameter of the channel. In the MINIFLAME and FLAME tests, DDT occurred for d/lambda greater than approximately three. Comparison with other experiments shows that the value of d/lambda for DDT is not constant but depends on the obstacle type, spacing, and channel geometry. The comparison of MINIFLAME and FLAME experiments extends the use of d/lambda scaling to different geometries and larger scales than previous studies. Small-scale-model testing of flame acceleration and DDT with the same combustible mixture as the full-scale prototype underpredicts flame speeds, overpressures, and the possibility of DDT. DOE

N90-14311# Argonne National Lab., IL. Materials Science and Chemical Technology Div.
LASER RAMAN SPECTROSCOPY IN STUDIES OF CORROSION AND ELECTROCATALYSIS
C. A. Melendres 1988 43 p Presented at the Spectroscopic and Diffraction Techniques in Interfacial Electrochemistry, Puerto de la Cruz, Spain, 3-15 Jul. 1988
(Contract W-31-109-eng-38)
(DE90-001414; CONF-880732-3) Avail: NTIS HC A03/MF A01

Laser Raman Spectroscopy (LRS) has become an important tool for the in situ structural study of electrochemical systems and processes in recent years. Following a brief introduction of the experimental techniques involved in applying LRS to electrochemical systems, we survey the literature for examples of studies in the inhibition of electrode reactions by surface films (e.g., corrosion and passivation phenomena) as well as the acceleration of reactions by electro-sorbates (electrocatalysis). We deal mostly with both normal and resonance Raman effects on fairly thick surface films in contrast to surface-enhanced Raman investigations of monolayer adsorbates, which is covered in another lecture. Laser Raman spectroelectrochemical studies of corrosion and film formation on such metals as Pb, Ag, Fe, Ni, Co, Cr, Au, stainless steel, etc. in various solution conditions are discussed. Further extension of the technique to studies in high-temperature and high-pressure aqueous environments is demonstrated. Results of studies of the structure of corrosion inhibitors are also presented. As applications of the LRS technique in the area of electrocatalysis, we cite studies of the structure of transition metal macrocyclic compounds, i.e., phthalocyanines and porphyrins, used for catalysis of the oxygen reduction reaction. DOE

N90-14312# California Univ., Berkeley. Dept. of Physics.
NON-LINEAR OPTICAL STUDIES OF ADSORBATES: SPECTROSCOPY AND DYNAMICS Ph.D. Thesis
Xiangdong Zhu (California Univ., Berkeley. Lawrence Berkeley Lab.) Aug. 1989 178 p
(Contract DE-AC03-76SF-00098)
(DE90-001543; LBL-27694) Avail: NTIS HC A09/MF A01

In the first part of this thesis, we have established a systematic procedure to apply the surface optical second-harmonic generation (SHG) technique to study surface dynamics of adsorbates. In particular, we have developed a novel technique for studies of molecular surface diffusions. In this technique, the laser-induced desorption with two interfering laser beams is used to produce a monolayer grating of adsorbates. The monolayer grating is detected with diffractions of optical SHG. By monitoring the first-order second-harmonic diffraction, we can follow the time evolution of the grating modulation from which we are able to deduce the diffusion constant of the adsorbates on the surface. We have successfully applied this technique to investigate the surface diffusion of CO on Ni(111). The unique advantages of this novel technique will enable us to readily study anisotropy of a surface diffusion with variable grating orientation, and to investigate diffusion processes of a large dynamic range with variable grating spacings. In the second part of this work, we demonstrate that optical infrared-visible sum-frequency generation (SFG) from surfaces can be used as a viable surface vibrational spectroscopic technique. We have successfully recorded the first vibrational spectrum of a monolayer of adsorbates using optical infrared-visible SFG. DOE

N90-14313# Lawrence Livermore National Lab., CA.
A NUMERICAL STUDY OF THIN FLAME REPRESENTATIONS
D. A. Rotman and M. Z. Pindera 11 Aug. 1989 24 p Presented at the 12th International Colloquium on the Dynamics of Explosions and Reactive Systems, Ann Arbor, MI, 23-28 Jul. 1989
(Contract W-7405-eng-48)
(DE89-017889; UCRL-100261; CONF-890739-5) Avail: NTIS HC A03/MF A01

In studies of reacting flows, the flame may be viewed as a moving discontinuity endowed with certain properties; notably, it acts as a source of velocity and vorticity. Asymptotic analysis shows this to be justified provided that the flame curvature is small compared to the flame thickness. Such an approach is useful when one is interested in the hydrodynamic effects of the flame on the surrounding flowfield. In numerical models of this kind it is customary to treat the discontinuity as a collection of discrete velocity blobs. It is shown that the velocities associated with such a representation can be very non-smooth, particularly very near to the flame surface. As an alternative, the use is proposed of a finite line source as the basic flame element. Comparisons of the two flame representations are made for several simple test cases as well as for a flame propagating through an enclosure forming the tulip shape. The results show that the use of line sources eliminates spurious fluctuations in nearfield velocities thus allowing for a more accurate calculation of flame propagation and flame flow field interactions. DOE

N90-14314# California Univ., Berkeley. Lawrence Berkeley Lab. Chemical Biodynamics Div.
MAPPING OF UPPER ELECTRONIC REACTION SURFACES BY TUNED LASER PHOTOLYSIS AND BY ABSORPTION AND EMISSION SPECTROSCOPIES Ph.D. Thesis
Meredith Ann Morgan Jul. 1989 183 p
(Contract DE-AC03-76SF-00098)
(DE90-000125; LBL-27632) Avail: NTIS HC A09/MF A02

Potential energy surfaces for photorotamerization of two intramolecularly hydrogen-bonded molecules, o-hydroxybenzaldehyde (OHBA) and methyl salicylate (MS), isolated in cryogenic matrices were spectroscopically mapped. In addition, the external heavy atom effect of krypton and xenon matrices on the coupling between the S(sub 1) and T(sub 1) surfaces of 4-(dimethylamino) benzonitrile was examined. Heavy atom matrices are known to increase rates of spin forbidden processes. The phosphorescence intensity of DMABN increases in krypton and xenon matrices, while the fluorescence intensity, and phosphorescence and fluorescence lifetimes, decrease. These effects are interpreted in terms of a model in which the phosphorescence rate constant increases 300-fold in xenon compared to argon, while the rate constants for intersystem crossing and nonradiative relaxation from the triplet state increase by factors of less than 5. Lifetime measurements in argon matrices doped with heavy atoms indicate that even one heavy atom neighbor has a significant effect on both singlet and triplet lifetimes. DOE

N90-14315# Sandia National Labs., Albuquerque, NM.
SHOCK-INDUCED SOLID STATE REACTIONS AND PHASE TRANSITIONS: X RAY PROFILE STUDIES ON SHOCK-MODIFIED Fe3O4 AND ZrO2 POWDERS
Y. Zhang, B. Morosin, R. A. Graham, C. R. Hubbard, and J. M. Stewart (Maryland Univ., College Park.) 1989 4 p Presented at the American Physical Society Topical Conference on Shock Compression of Condensed Matter, Albuquerque, NM, 14-17 Aug. 1989
(Contract DE-AC04-76DP-00789)
(DE90-000669; SAND-89-0991C; CONF-890812-50) Avail: NTIS HC A01/MF A01

Powder compacts of magnetite and zirconia were subjected to controlled, quantitative high pressure shock loading at peak pressures from 5 to 27 GPa. X ray diffraction lines are broadened,

indicating considerable reduction of the crystallite size and introduction of residual microstrain. At higher pressures, different shock induced reactions are observed in these two materials. DOE

N90-14316# Oak Ridge National Lab., TN. Chemical Technology Div.
ASYMPTOTIC ANALYSIS OF PERFORMANCE OF MEMBRANE MODULES FOR GAS SEPARATIONS
Osman A. Basaran and Michael T. Harris 1989 23 p Presented at the 6th Symposium on Separation Science and Technology for Energy Applications, Knoxville, TN, 22-27 Oct. 1989
(Contract DE-AC05-84OR-21400)
(DE90-000699; CONF-891013-1) Avail: NTIS HC A03/MF A01

The nonlinear equations that govern the variation of molar flow rates and mole fractions in membrane modules for separating binary gas mixtures are solved analytically by asymptotic analysis in (alpha), the selectivity of the fast gas with respect to the slow gas. The results are explicit analytical expressions that show the effect of process parameters and idealized flow patterns (cross flow, CF, co-current flow, CO, and counter-current flow, CC) on system performance. When the selectivity is low, a regular perturbation analysis shows that the CC module is the most efficient, followed by CF and CO modules, except when p(sub r), the permeate to feed pressure ratio, is zero in which case the performance of all three is the same. When the selectivity is large, the nature of the problem changes whether the mole fraction of the fast gas on the feed side at the entrance to the module, (chi)(sub in), is less than or greater than p(sub r). When (chi)(sub in) is greater than p(sub r), a singular perturbation analysis of the equations shows that performance is independent of the type of idealized flow pattern in the module. However, when (chi)(sub in) is less than or equal to p(sub r), a regular perturbation analysis shows that the CC module is the most efficient, followed by CF and CO modules. The results presented enable one to gain a quantitative understanding of membrane-based separations without resorting to extensive numerical calculations. DOE

N90-14317# Lawrence Livermore National Lab., CA.
THE THERMALLY INDUCED GAS-PHASE REACTIONS OF METHANE AND OXYGEN: A COMPARISON OF EXPERIMENTAL AND COMPUTATIONAL RESULTS
Michael W. Droege, Lucy M. Hair, William J. Pitz, and Charles K. Westbrook Apr. 1989 30 p Presented at the American Institute of Chemical Engineers Spring National Meeting, Houston, TX, 2-6 Apr. 1989
(Contract W-7405-eng-48)
(DE90-000785; UCRL-100568; CONF-890430-6) Avail: NTIS HC A03/MF A01

As part of the effort to discover technologies that directly convert methane to higher value chemicals, the development of catalysts that facilitate a partial oxidation or oxidative coupling reaction between methane and oxygen is an area of current active research. In considering the typical experimental conditions used for catalyst studies, it is clear that significant potential exists for the appearance of noncatalyzed, thermally activated gas phase reactions of methane and oxygen. Experimentally, in a quartz reactor at 800 C with a 3:1 methane-to-oxygen ratio and residence times of the order of 5 to 10 sec, significant conversion was observed of methane (30 percent) to light hydrocarbons and CO(x) with appreciable selectivity (25 percent) to C2(sup +) components due solely to these background reactions. In order to better understand and describe the contribution of these background reactions during catalyzed reactions, we have employed a chemical kinetic model (HCT) developed at this Laboratory to describe these homogeneous gas phase reactions. This model was developed over a number of years primarily for the study of methane and natural gas combustion. This model is being used to describe homogenous reactions that lead to the partial oxidation of methane. The model was tested against a series of experimental reactions comparing the effects of various reaction parameters. DOE

N90-14318# Lawrence Livermore National Lab., CA.
THERMODYNAMIC PROPERTIES AND HYDRODYNAMIC RESPONSE OF HIGH-DENSITY HIGH-TEMPERATURE C H N O MIXTURES
Mathias vanThiel Aug. 1989 9 p Presented at the American Physical Society Topical Conference on Shock Compression of Condensed Matter, Albuquerque, NM, 14-17 Aug. 1989
(Contract W-7405-eng-48)
(DE90-000836; UCRL-100832; CONF-890812-56) Avail: NTIS HC A02/MF A01

The development of practical state equations for explosive products has proceeded from the simple ideal gas to an exponential form. This was an adequate representation for the expanding gases behind the detonation front. Overdriven shock states showed deviations from this form, that could be related to phase changes observed in Chemical Equilibrium Calculations with the CHEQ code. These calculations show that the interactions of nitrogen and CO2 with water are of special significance for accurate representation of HMX based explosives. The equilibrium phase line for the separation of a nitrogen rich phase is not known above 700 K but several analyses show that the graphite to diamond line is raised significantly above its equilibrium location. This may be interpreted as a small carbon-cluster effect. Preliminary analysis shows small but significant effects due to carbon cluster EOS. CO dissociation kinetics needs further study. DOE

N90-14319# Lawrence Livermore National Lab., CA.
THE PERIODIC LAW AT HIGH PRESSURES
David A. Young Aug. 1989 8 p Presented at the American Physical Society Topical Conference on Shock Compression of Condensed Matter, Albuquerque, NM, 14-17 Aug. 1989
(Contract W-7405-eng-48)
(DE90-000837; UCRL-100927; CONF-890812-54) Avail: NTIS HC A02/MF A01

The observed periodicity in the properties of the chemical elements at 1 bar was the basis of the Periodic Table in the 19th century. Modern research on the solid and liquid elements at high pressures and temperatures has revealed new patterns of behavior which provide a deeper understanding of periodicity. These patterns include the rapid convergence of atomic volume with compression to a smooth function of atomic number, the inverse relation between volume and bulk modulus, the waves of crystal structure change which traverse the Periodic Table with increasing pressure, the strong correlation of cohesive energy with melting and critical temperature, and the unusual reordering of melting curves at high pressure. The principle of corresponding states is also related to periodicity and may be generalized. DOE

N90-14320# Florida Univ., Gainesville. Dept. of Chemistry.
DEVELOPMENT OF LASER EXCITED ATOMIC FLUORESCENCE AND IONIZATION SPECTROMETRIC METHODS Progress Report, 1 Jan. - 1 Oct. 1989
J. D. Winefordner 1989 23 p
(Contract DE-FG05-88ER-13881)
(DE90-001567; DOE/ER-13881/2) Avail: NTIS HC A03/MF A01

During the past nine months, four exciting research topics were investigated: (1) theoretical considerations and estimations concerning the ultimate detection power of laser fluorescence and laser ionization techniques; (2) experimental evaluation of laser excited atomic fluorescence spectrometry with electrochemical atomization; (3) the development of the theory for resonance ionization detection of weak fluorescence radiation; and (4) evaluation of the analytical capabilities of laser excited fluorescence of atoms in glow discharges. The progress os briefly discussed, in each of the afore mentioned topics. DOE

N90-14321# Wisconsin Univ., Madison. Dept. of Mechanical Engineering.
TEST AND EVALUATION OF POLYMERIC MEMBRANES FOR OXYGEN ENRICHMENT OF AIR Final Report
Kenneth W. Ragland and John G. Whipple Jul. 1989 83 p

(Contract DE-FG07-88ID-12701)
(DE90-000555; DOE/ID-12701/1) Avail: NTIS HC A05/MF A01

Two A/G Technology hollow fiber polymeric membrane separation modules to produce oxygen enriched air were evaluated. In one module the inlet air was pressurized, and in the other a vacuum was pumped on the permeate side of the membrane. The pressurized module contained three cartridges each 3 in. o.d. by 54 in. long, while the vacuum module contained seven cartridges each 3 in. o.d. by 48 in. long. Laboratory performance tests of the modules were conducted, and an economic analysis of the membrane systems for industrial applications was done. The measured performance data were used along with vendor supplied compressor, vacuum pump and turbo-compressor data to analyses industrial air enrichment systems producing 1 ton equivalent pure O2/day and 10 ton equivalent pure O2/day enriched air at 35 percent oxygen. Both the pressurized and vacuum systems are economically attractive and provide a simple payback of less the two years when compared to the use of liquid oxygen. The vacuum system provides greater energy savings, while the pressurized system requires less capital investment. New A/G membranes are undergoing further development. DOE

N90-14322# Pacific Northwest Lab., Richland, WA. Chemical Methods and Separation Group.
COMBINED CAPILLARY ELECTROPHORESIS AND ELECTROSPRAY IONIZATION MASS SPECTROMETRY
Richard D. Smith, Joseph A. Loo, Charles J. Barinaga, Charles G. Edmonds, and Harold R. Udseth Sep. 1989 9 p Presented at the 14th Annual Japanese Society for Biomedical Mass Speculation Meeting, Nagoya, Japan, 28-30 Sep. 1989
(Contract DE-AC06-76RL-01830)
(DE90-001903; PNL-SA-17257; CONF-8909252-1) Avail: NTIS HC A02/MF A01

The special capabilities of the capillary electrophoresis electrospray ionization-mass spectrometer interface for the analysis of peptides and proteins with molecular weights extending to in excess of 100 kilodalton are demonstrated. The dynamic combinations of both capillary zone electrophoresis and capillary isotachophoresis with electrospray ionization are illustrated for mixtures of peptides and proteins. The potential extension of these methods for determination of the primary structure (sequence) of proteins using tandem mass spectrometry is shown to be facilitated by the high charge state of ions produced by the electrospray interface. The relevance of these results for advances in analytical biochemistry is discussed. DOE

N90-14323# Brookhaven National Lab., Upton, NY. Dept. of Physics.
THE FORMATION OF METAL-OXYGEN SPECIES AT LOW TEMPERATURES
S. L. Qiu, C. L. Lin, Jie Chen, and Myron Strongin 1989 16 p Presented at the 36th American Vacuum Society National Vacuum Symposium, Boston, MA, 23-27 Oct. 1989
(Contract DE-AC02-76CH-00016)
(DE90-002298; BNL-43372; CONF-891093-7) Avail: NTIS HC A03/MF A01

The interaction of solid molecular oxygen Li, Cs, K, La, Ag, Cu, and Ba has been studied at 35 K or below using photoemission. A feature near 535 eV in the O 1s core level spectra was observed when Li, Cs, K and La were deposited on solid oxygen. This feature was identified with one electron being donated to an oxygen molecule, i.e., the superoxide species, which as far as we know has not been previously reported for La and Li. A feature at about 531.5 to 533 eV was identified as a peroxide species where two electrons were donated to an oxygen molecule. Finally features at about 528 to 530.5 eV were identified as oxide phases where the molecular oxygen was dissociated into atomic oxygen with formal valence of minus 2. These identifications are crucial in the determinations of the exotic features in the XPS O 1s spectra of the high T sub c superconductors. DOE

N90-14324# Yale Univ., New Haven, CT.
ENERGIES OF ORGANIC COMPOUNDS
K. B. Wiberg 1989 8 p
(Contract DE-FG02-86ER-13460)
(DE90-003174; DOE/ER-13460/T2) Avail: NTIS HC A02/MF A01

The first part of our study of the enthalpy of reduction of carbonyl compounds has been completed and includes four aldehydes, acetone, a series of cyclic ketones and ethyl acetate. The results suggest that some of the literature data for these compounds are significantly in error. Equilibrium constants have been measured for the reaction of carbonyl compounds with water to give hydrates as well as with methanol to give either hemiacetals or acetals. They cover a wide range, and studies are underway to determine the reasons for the differences. Studies of the enthalpies of hydration of some alkenes which yield tertiary alcohols have been completed, as well as a study of the hydrolysis of lactones. The gauche effect has been studied, and has been shown to result from the formation of bent bonds when atoms of much different electronegativity are joined. DOE

26 METALLIC MATERIALS

Includes physical, chemical, and mechanical properties of metals, e.g., corrosion; and metallurgy.

N90-14325# Advisory Group for Aerospace Research and Development, Neuilly-Sur-Seine (France). Structures and Materials Panel.
SUPERPLASTICITY
Sep. 1989 248 p Lecture series held in Rome, Italy, 5-6 Oct. 1989, in Madrid, Spain, 9-10 Oct. 1989, and in Toulouse, France, 12-13 Oct. 1989 Revised version of AGARD lecture series 154
(AGARD-LS-168; AGARD-LS-154-Rev; ISBN-92-835-0525-5)
Copyright Avail: NTIS HC A11/MF A02

Superplasticity was transformed from a metallurgical curiosity to an important production process, particularly for low-to-medium production runs of components for the aerospace industry. The whole spectrum of superplasticity was originally covered in Lecture Series 154 in the autumn of 1987, but such are the rapid advances in this technology, that the series is re-presented, with the same speakers updating their lectures to give the latest information on this most relevant technology and its impact upon the manufacture methods employed for components for aerospace applications. For individual titles, see N90-14326 through N90-14333.

N90-14326# Cranfield Inst. of Tech., Bedford (England). School of Industrial Science.
SUPERPLASTICITY: AN OVERVIEW
Roger Pearce *In* AGARD, Superplasticity Sep. 1989 24 p
(For primary document see N90-14325 06-26)
Copyright Avail: NTIS HC A11/MF A02

Certain alloys, when deformed in tension at particular temperatures and strain rates, show very high elongations. This phenomenon is termed superplasticity. Importantly, the flow stresses at which this phenomenon occurs are extremely low. There are two types of superplasticity: isothermal superplasticity (ISP); and cycling superplasticity (CSP). For ISP, the alloy must possess an ultra-fine grain size which is relatively stable at greater than or equal to 0.5 T(sub m), where T(sub m) is the melting point of the lowest-melting constituent in the alloy, in absolute units, while for CSP the alloy must be capable of being cycled through a phase change. The mechanical properties, manufacturing, and surface properties are reviewed. Author

N90-14327# Washington State Univ., Pullman.
SUPERPLASTIC SHEET FORMING
C. H. Hamilton *In* AGARD, Superplasticity Sep. 1989 23 p
(For primary document see N90-14325 06-26)
Copyright Avail: NTIS HC A11/MF A02

The exceptional ductility of superplastic alloys can be utilized in the shaping and forming of parts, components, and structures

which could not be easily or economically produced by materials of more limited ductility. A number of methods for forming these materials were studied on a laboratory scale, and several of these are being utilized to produce full scale parts on a production basis, with benefits being achieved in cost as well as in design efficiency. The forming of superplastic alloys, however, involves consideration of a number of factors which are interactive and lead to a relatively complex process, especially if maximum capability and minimum cost are to be achieved. These considerations include the superplastic properties of the alloy, effect of temperature, effect of strain rate, microstructural changes during forming and their effect on superplastic properties, effect of die configuration on forming capability, and forming parameters. The forming methods which were demonstrated for superplastic alloys include: blow forming, vacuum forming, thermo-forming, die-less drawing, deep drawing, forging, and superplastic forming with combined diffusion bonding (SPF/DB). With the exception of the forging, these processes utilize the high elongation capability and related resistance to localized necking. Therefore, the thinning gradients which can develop during forming are of primary concern, and relate directly to the material characteristics and the mechanics of stretch forming into a given die configuration. The technology of SPF was found to benefit from modelling of the process, the results of which can guide the selection of pressurization parameters as well as predict the thinning characteristics and tendency to rupture. These concepts are reviewed. Many alloys tend to cavitate, or form internal voids. During SPF processing and mechanical design properties can suffer if this cavitation is severe. Concepts for minimizing or eliminating cavitation are discussed. Author

N90-14328# Stanford Univ., CA. Dept. of Materials Science and Engineering.

ADVANCES AND FUTURE DIRECTIONS IN SUPERPLASTIC MATERIALS

Oleg D. Sherby and Jeffrey Wadsworth (Lockheed Missiles and Space Co., Palo Alto, CA.) *In* AGARD, Superplasticity Sep. 1989 24 p Sponsored by ONR, Washington, DC; ARO, Washington, DC and Lockheed Independent Research and Development Program (For primary document see N90-14325 06-26)

Copyright Avail: NTIS HC A11/MF A02

New events are reviewed in the development and modeling of superplastic materials. Over the last several years, superplasticity was developed in fine microstructures in microduplex stainless steels, aluminum-lithium alloys, mechanically alloyed aluminum, silicon carbide whisker-reinforced aluminum alloys, aluminum-magnesium alloys, and nickel alloys. In the latter three cases, the phenomenon is observed at high strain rates by comparison with most superplastic alloys. In a major breakthrough, a ceramic (yttria stabilized zirconia) and a ceramic composite (yttria stabilized zirconia containing alumina) were shown to be superplastic in tension tests. Superplastic behavior in iron carbide was also observed. Superplastic studies are also underway in intermetallics such as nickel silicides, nickel aluminides, and titanium aluminides. New insights are becoming apparent in the area of modeling superplastic behavior by the integration, into existing models, of new concepts based on grain boundary sliding accommodated by slip and the influence of threshold stresses associated with grain boundary sliding. Newtonian-viscous flow can be approached in fine-grained Class 1 solid solution alloys. Significant advances were also made in understanding internal stress superplasticity; recent examples include zinc, alpha-uranium, zinc-alumina composites and silicon carbide whisker reinforced aluminum alloys. A new model has been proposed for internal stress superplasticity. In other major developments, the mechanisms of superplasticity were successfully applied to consolidation of powders and superplastic behavior was developed in ferrous-based laminated composites. Finally, some neglected areas offering the potential for superplastic flow are reviewed. Author

N90-14329# Manchester Univ. (England). Dept. of Metallurgy and Materials Science.

CAVITATION AND SUPERPLASTICITY

Norman Ridley *In* AGARD, Superplasticity Sep. 1989 14 p (For primary document see N90-14325 06-26)

Copyright Avail: NTIS HC A11/MF A02

Cavitation occurs in many alloy systems during superplastic flow. Cavities either pre-exist or nucleate on grain boundaries and their subsequent growth, coalescence, and interlinkage leads to premature failure. The presence of cavities in superplastically formed components to be used for load bearing applications is clearly undesirable. It is apparent from studies on a wide range of materials that cavity growth is dominated by matrix plastic flow and that coalescence plays an important role in the development of large cavities. Hence, if cavitation damage is to be prevented, it is necessary to inhibit the nucleation event and to avoid the presence of pre-existing defects by careful control of the processing required to produce the superplastic microstructure. The influence that microstructural features and deformation conditions have on cavity nucleation is examined for a number of alloy systems, and it is clear that it is difficult to control these parameters so as to totally avoid cavitation. However, cavitation can be eliminated by the application of a hydrostatic pressure during forming. This reverses the sense of the driving force for cavity growth and the conditions for zero growth, which depend on the geometry of deformation, were identified. Cavitation damage can be prevented by superimposed pressures of 0.5 to 0.75 of the uniaxial flow stress, although lower levels of pressure can substantially reduce the extent of cavitation. Author

N90-14330# Royal Aircraft Establishment, Farnborough (England). Materials and Structures Dept.

DIFFUSION BONDING OF METALS

P. G. Partridge *In* AGARD, Superplasticity Sep. 1989 29 p (For primary document see N90-14325 06-26)

Copyright Avail: NTIS HC A11/MF A02

The need to reduce the cost and weight of aerospace metallic structures has led to increased interest in solid state and liquid phase diffusion bonding processes, especially in combination with superplastic forming. The bonding mechanisms and bonding techniques are reviewed and the process variables that affect metals. The importance of quality control and the limitations of current NDE techniques for diffusion bonding are emphasized. Finally some trends and priorities in diffusion bonding technology are indicated. Author

N90-14331# Royal Aircraft Establishment, Farnborough (England).

THE MECHANICAL PROPERTIES OF SUPERPLASTICALLY FORMED TITANIUM AND ALUMINIUM ALLOYS

P. G. Partridge, D. S. McDarmaid, I. Bottomley, and D. Common (British Aerospace Public Ltd. Co., Bristol, England) *In* AGARD, Superplasticity Sep. 1989 33 p (For primary document see N90-14325 06-26)

Copyright Avail: NTIS HC A11/MF A02

The behavior of aluminum and titanium alloys under superplastic forming conditions is well documented but there is much less published data on the effect of the superplastic forming process on the mechanical properties; these data are essential for the design of structures. The effect of superplastic forming parameters such as temperature, strain and post forming heat treatments upon the tensile, fatigue and fatigue crack growth performance of these alloys are reviewed and the property variation to change in the microstructure are related. During superplastic forming of aluminum alloys intergranular cavities are formed with increasing strain which degrade the material and reduce the mechanical properties. Ways to prevent cavitation both during and after superplastic forming were developed and the effect of these treatments on the mechanical properties will be discussed. Author

N90-14332# British Aerospace Public Ltd. Co., Bristol (England). Civil Aircraft Div.

DESIGNING FOR SUPERPLASTIC ALLOYS

D. Stephen *In* AGARD, Superplasticity Sep. 1989 37 p
(For primary document see N90-14325 06-26)
Copyright Avail: NTIS HC A11/MF A02

Twelve years of development have brought the processes of superplastic forming and diffusion bonding to a state of maturity. These processes provide the opportunity to design components on new projects which are both cost and weight efficient. However, to achieve optimum performance, the designer needs to have an in-depth understanding of the freedoms and limitations provided by these processes. Substantial evidence exists to support the claim that titanium alloys, when processed by the superplastically formed (SPF) diffusion bonded (DB) route, can compete in weight and more particularly cost, with conventional aluminum fabrication. This is likely to be a major factor in the future exploitation of these processes and clearly requires a revision to the designers traditional views of the areas of application for titanium alloys. The more recent developments in the processing of high strength superplastic aluminum alloys will clearly add to the further use of the superplastic forming process on future aerospace products, but the development of a combined SPF/DB process for aluminum alloys, with the full range of capabilities provided currently by titanium alloys, remains to be established. Author

N90-14333# Alcan International Ltd., Banbury (England).
THE MANUFACTURE OF SUPERPLASTIC ALLOYS
R. Grimes *In* AGARD, Superplasticity Sep. 1989 16 p
(For primary document see N90-14325 06-26)
Copyright Avail: NTIS HC A11/MF A02

The requirements in a superplastic sheet material are either to possess a fine uniform grain size or to be capable of developing such a grain structure during the course of superplastic deformation. Alloys that are currently being commercially exploited fall into both categories and the manufacturing routes to produce material with good superplastic behavior using commercial scale processing are considered. Most of the paper is devoted to aluminum alloys since their manufacture in a superplastic form embodies most of the general principles. Since the aluminum alloys do not involve allotropic transformations limited consideration is also given to titanium alloys. Amongst aluminum alloys, the Al-6 percent Cu-0.4 percent Zr system that typifies the supral alloys, requires a specifically developed casting system in order to achieve a very high level of supersaturation with zirconium. Subsequent manufacturing is fairly conventional, the sheet product recrystallizing dynamically during superplastic forming. The higher strength aluminum alloys are conventionally cast but achieve a very fine grain size at the sheet stage by careful thermal mechanical-treatment during the latter stages of semi-fabrication. With titanium the standard production route for the Ti-6Al-4V alloy results in a product with superplastic capabilities perfectly adequate for most applications. Author

N90-14334 Rochester Univ., NY.
EFFECTS OF DISLOCATION SUBSTRUCTURE AND PRESTRAIN ON FRACTURE BEHAVIOR IN ALUMINUM AND STEEL ALLOYS Ph.D. Thesis
Ralph W. Bush 1989 379 p
Avail: Univ. Microfilms Order No. DA8913566

The short rod fracture specimen is used to examine the effects of prestrain, in the form of low cyclic fatigue and tensile predeformation, on the fracture behavior of plain carbon steels, of approximately 0.18 percent carbon content, and a series of tempers of 2024 aluminum alloy. In the case of cyclic predeformation, it is found that all materials used in this study cyclically harden, and this results in a decrease in fracture toughness. Tensile predeformations of 2 percent, in the case of the aluminum alloys, and 10 percent, in the case of a 0.15 percent C mild steel, result in no change in the measured fracture toughness. A dynamic computer simulation utilizing dislocations configured in a dislocation cell wall substructure segment near a sharp crack tip is used to model the effects of the dislocation substructure produced by large amounts of plastic deformation on the fracture behavior of a model material. Plastic zone formation and fracture behavior are monitored under a wide range of experimental conditions. Numerical computations are performed to explore the effects of experimental noise on crack growth stability during a short rod fracture test. Dissert. Abstr.

N90-14335*# National Aeronautics and Space Administration. Lewis Research Center, Cleveland, OH.
CALIBRATION APPROACH TO ELECTRON PROBE MICROANALYSIS: A STUDY WITH PWA-1480, A NICKEL BASE SUPERALLOY
F. M. Terepka, M. Vijayakumar, and S. N. Tewari (Cleveland State Univ., OH.) Dec. 1989 18 p
(Grant NAG8-091)
(NASA-TM-102393; E-5138; NAS 1.15:102393) Avail: NTIS HC A03/MF A01 CSCL 11F

The utility of an indirect calibration approach in electron probe microanalysis is explored. The methodology developed is based on establishing a functional relationship between the uncorrected k-ratios and the corresponding concentrations obtained using one of the ZAF correction schemes, for all the desired elements in the concentration range of interest. In cases where a very large number of analyses are desired, such a technique significantly reduces the total time required for the microprobe analysis without any significant loss of precision in the data. A typical application of the method in the concentration mapping of the transverse cross-section of a dendrite in directionally solidified PWA-1480, a nickel-based superalloy, is described. Author

N90-14336# Aeronautical Research Labs., Melbourne (Australia).
INFLUENCE OF HOLE SURFACE FINISH, CYCLIC FREQUENCY AND SPECTRUM SEVERITY ON THE FATIGUE BEHAVIOR OF THICK SECTION ALUMINUM ALLOY PIN JOINTS Aircraft Structures Report
J. Y. Mann, G. W. Revill, and R. A. Pell Dec. 1989 71 p
(ARL-STRUC-R-430; AR-004-570) Copyright Avail: NTIS HC A04/MF A01

An extensive series of tests was performed on thick (29 mm) clearance-fit pin joints of 2L.65 aluminum alloy. It was found that lug holes having a fine surface finish (1.9 microns) did not have fatigue lives greater than those with a coarse finish (27 microns), under either constant-amplitude or multi-load-level fatigue loading sequences. Thus, unless needed for other functional reasons, it may not be necessary to specify fine circumferential surface finishes in situations where fretting fatigue is likely to be a problem. Within the range 1 Hz to 16 Hz, frequency of cycling had no significant effect on the lives to failure under constant-amplitude and multi-load-level sequences. For each of two severities of spectrum adopted there were essentially no significant differences in fatigue lives under program and pseudo-random loading sequences. Truncation of the once-per-block peak load resulted in significant reductions in life under both spectra. Detailed fractographic studies suggested that the size of the plastic zone caused by the peak load was greater than the extent of fatigue crack propagation within a block. Fractographic examination of small fatigue cracks initiated either at intermetallics or by fretting showed no evidence of early rapid crack growth associated with the short-crack effect. Author

N90-14337# Sandia National Labs., Livermore, CA. Materials Technology Div.
AN ELECTROFORMED NICKEL-SULFUR ALLOY FOR A NOSE CONE
W. D. Bonivert, J. T. Hachman, and H. A. Johnsen Sep. 1989 22 p
(Contract DE-AC04-76DR-00789)
(DE90-000866; SAND-89-8646) Avail: NTIS HC A03/MF A01

A two-component projectile nose cone was required whose outer envelope would provide a stable aerodynamic shape during launch and flight and be frangible upon water impact. Full-scale components with specific mechanical properties were fabricated using electroforming technology. Compressive strengths between 175 to 210 kg/mm(sup 2) with minimum ductility were obtained with a nickel deposit containing 0.08 percent sulfur. DOE

N90-14338# California Univ., Berkeley. Dept. of Materials Science and Mineral Engineering.
THE STRENGTH-TOUGHNESS COMBINATION OF THE ALUMINUM-LITHIUM ALLOYS 2090 AND 2091 AT CRYOGENIC TEMPERATURES Ph.D. Thesis
Judith Glazer (California Univ., Berkeley. Lawrence Berkeley Lab.) Jul. 1989 168 p Sponsored in part by Aluminum Co. of America and Lockheed Missiles and Space Co.
(Contract DE-AC03-76SF-00098)
(DE90-001425; LBL-27607) Avail: NTIS HC A08/MF A01

The strength-toughness combination of the aluminum lithium alloys 2090 (nominal composition Al(2.7)Cu(2.2)Li(0.1)Zr in wt percent) and 2091 (Al(2.2)Cu(2.0)Li(1.5)Mg(0.1)Zr) plate at cryogenic temperatures was investigated. Aluminum lithium alloys have lower density and higher stiffness than conventional aluminum alloys and were developed for aircraft applications. This study was motivated by the possibility of using aluminum-lithium alloys for cryogenic tankage of spacecraft, an application in which light weight, weldability and good cryogenic mechanical properties are at a premium. Alloy 2090-T81 has a strength-toughness combination that improves with decreasing temperature between 300 and 4 K under some conditions. This improvement is accompanied by an increase in the tensile elongation and strain hardening rate, but the large increase in fracture toughness is not reflected in the primary fracture mode. The goal was to develop an understanding of the mechanisms responsible for the increase in fracture toughness at cryogenic temperatures. The mechanical properties of alloy 2090 in other metallurgical conditions and a second alloy, 2091, were also considered. Several mechanisms for interpreting the increased toughness in in-plane orientations at low temperatures were considered. DOE

N90-14339# Oak Ridge National Lab., TN. Metals and Ceramics Div.
SEM (SCANNING ELECTRON MICROSCOPE) IMAGE ANALYSIS OF GRAIN GROWTH IN MICROWAVE-ANNEALED ALUMINA
Monica A. Schmidt, Mark A. Janney, and Jackie R. Mayotte 1989 27 p Presented at the 22nd Annual International Metallographic Society Meeting, Charlotte, NC, 23 Jul. 1989
(Contract DE-AC05-84OR-21400)
(DE90-001606; CONF-8907116-5) Avail: NTIS HC A03/MF A01

An image analysis technique using a scanning electron microscope was developed for accurately reconstructing grain boundaries to measure small changes in grain size and shape. The technique measures individual grain perimeters, areas, Feret's diameters, lengths, and widths, from which other parameters such as interface area per unit volume (S sub v), spherical grain diameter (D), aspect ratio, and shape factor, can be calculated. This technique was applied to study grain growth in microwave versus conventionally annealed alumina. The results demonstrate that the kinetics of grain growth in microwave annealing are significantly faster than those in conventional annealing. This supports the hypothesis that microwaves accelerate either bulk or grain boundary diffusion during the process of grain growth. The microstructural changes resulting from microwave and conventional annealing are similar in terms of grain shape, indicating that the grain growth processes are similar although the kinetics are significantly different. DOE

N90-14340# Westinghouse Savannah River Co., Aiken, SC.
AN EVALUATION OF ELECTROCHEMICAL POTENTIOKINETIC REACTIVATION TECHNIQUES FOR IN-SERVICE MEASUREMENTS ON TYPE 304 STAINLESS STEEL
Karen J. Stoner 1989 18 p Presented at the 22nd Annual International Metallographic Society Meeting, Charlotte, NC, 25-26 Jul. 1989
(Contract DE-AC09-89SR-18035)
(DE89-017859; WSRC-RP-89-333; CONF-8907116-4) Avail: NTIS HC A03/MF A01

Electrochemical potentiokinetic reactivation (EPR) tests can be used to measure quantitatively the sensitization of Type 304 stainless steel. The single loop (SL) and double loop (DL) EPR techniques were compared as non-destructive methods for determining sensitization under both laboratory and simulated field environments. Measurements were performed on specimens heat-treated to produce levels of sensitization from no sensitization to heavy sensitization. At temperatures of 22 C and 30 C testing with standard laboratory and portable field apparatus, both EPR techniques were capable of distinguishing sensitization levels at the range spanning those characterized as being non-susceptible and susceptible to intergranular stress corrosion cracking (IGSCC). Through correlations developed for the test data, it is possible to translate field results to the standard laboratory test conditions. This was demonstrated for the SL test through measurements performed on a pipe specimen containing IGSCC. DOE

N90-14341# California Univ., Berkeley. Lawrence Berkeley Lab. Center for Advanced Materials.
THE EFFECT OF HYDROGEN CHARGING ON THE MECHANICAL PROPERTIES OF ALUMINUM ALLOY 2090
D. Chu and J. W. Morris, Jr. Jul. 1989 12 p Presented at the International Cryogenic Materials Conference, Los Angeles, CA, 24-28 Jul. 1989
(Contract DE-AC03-76SF-00098)
(DE90-000129; LBL-27379; CONF-890701-8) Avail: NTIS HC A03/MF A01

The effect of hydrogen charging on the mechanical properties of peakaged 2090 Al-Cu-Li sheet material was studied. Flat tensile and notched tensile specimens of longitudinal orientation were tested at 77 and 300 K in both the hydrogen charged and uncharged conditions. The results suggest a hydrogen effect appearing as a loss in the ability of the material to withstand stress triaxiality. Macroscopic analysis of the fracture surfaces reveal a greater amount of shear type fracture morphology in charged specimens which may be interpreted as a decrease in the material's ability to resist planar slip. Though differences in the microscopic fracture morphology are found between specimens tested at different temperatures and orientations, no observable difference is found between those that are charged and uncharged. Results establish that the effects of hydrogen charging on the material tested do not appear to be of significant engineering importance. DOE

N90-14342# Westinghouse Savannah River Co., Aiken, SC.
RAPID HEATING TENSILE TESTS OF HYDROGEN-CHARGED HIGH-ENERGY-RATE-FORGED 316L STAINLESS STEEL
W. C. Mosley 19 May 1989 16 p
(Contract DE-AC09-89SR-18035)
(DE90-000591; WSRC-RP-89-268; SRL-HTS-89-0022) Avail: NTIS HC A03/MF A01

The 316L stainless steel is a candidate material for construction of equipment that will be exposed to tritium. Proper design of the equipment will require an understanding of how tritium and its decay product, helium, affect mechanical properties. This memorandum describes results of rapid heating tensile testing of hydrogen-charged specimens of high-energy-rate-forged (HERF) 316L stainless steel. These results provide a data base for comparison with uncharged and tritium-charged-and-aged specimens to distinguish the effects of hydrogen and helium. Details of the experimental equipment and procedures and results for uncharged specimens were reported previously. DOE

N90-14343# Westinghouse Savannah River Co., Aiken, SC.
PHASES IN LANTHANUM-NICKEL-ALUMINUM INTERMETALLIC ALLOYS
W. C. Mosley 1989 42 p Presented at the Electron Microscopy Conference, Miamisburg, OH, 17-19 Oct. 1989
(Contract DE-AC09-89SR-18035)
(DE90-000651; WSRC-RP-89-517; CONF-8910215-1) Avail: NTIS HC A03/MF A01

Lanthanum-nickel-aluminum (LANA) alloys will be used to pump, store and separate hydrogen isotopes in the Replacement Tritium Facility (RTF). The aluminum content (y) of the primary LaNi sub 5 phase is controlled to produce the desired

pressure-temperature behavior for adsorption and desorption of hydrogen. However, secondary phases cause decreased capacity and some may cause undesirable retention of tritium. Twenty-three alloys purchased from Ergenics, Inc., for development of RTF processes have been characterized by scanning electron microscopy (SEM) and by electron microprobe analysis (EMPA) to determine the distributions and compositions of constituent phases. This memorandum reports the results of these characterization studies. Knowledge of the structural characteristics of these alloys is a useful first step in selecting materials for specific process development tests and in interpreting results of those tests. Once this information is coupled with data on hydrogen plateau pressures, retention and capacity, secondary phase limits for RTF alloys can be specified. DOE

N90-14344# Sandia National Labs., Albuquerque, NM.
INTERACTION OF HYDROGEN ISOTOPES WITH METALS: DEUTERIUM TRAPPED AT LATTICE DEFECTS IN PALLADIUM
F. Besenbacher, B. Bech Nielsen, J. K. Noerskov, S. M. Myers, and P. Nordlander (Rutgers - The State Univ., Piscataway, NJ.) 1989 19 p Presented at the Workshop on Cold Fusion Phenomena, Santa Fe, NM, 23-25 May 1989
(Contract DE-AC04-76DP-00789) .
(DE90-000811; SAND-89-2232C; CONF-8905126-5) Avail: NTIS HC A03/MF A01

From an interplay between theory based on the effective-medium scheme and experiments, an extremely simple picture has evolved which is capable of describing a vast number of experimental quantities related to interaction of hydrogen with metals, especially the trapping of hydrogen at defects. It is shown that the trap strengths are determined mainly by the interstitial electron density, and any open structures in the lattice leads to a trap, with the vacancies and voids being the strongest traps. It is also found theoretically and experimentally that up to six hydrogen atoms can be accommodated in a vacancy, and the change in trap strengths with occupancy has been determined. Recent results for the trapping of deuterium to defects in Pd are discussed. DOE

N90-14345# Sandia National Labs., Albuquerque, NM. Thermomechanical and Physical Research Div.
SPALL STRENGTH MEASUREMENTS ON SHOCKLOADED REFRACTORY METALS
Lalit C. Chhabildas, Lynn M. Barker, James R. Asay, and Timothy G. Trucano 1989 5 p Presented at the American Physical Society Topical Conference on Shock Compression of Condensed Matter, Albuquerque, NM, 14-17 Aug. 1989
(Contract DE-AC04-76DP-00789)
(DE90-000839; SAND-89-0836C; CONF-890812-53) Avail: NTIS HC A01/MF A01

Spall strength measurements were performed on molybdenum, tantalum, a tungsten alloy, and a titanium alloy that were shocked initially to stresses of 10 to 20 GPa. There is a correlation of normalized spall strength, i.e., the spall strength divided by its density, with fracture toughness for these materials. Results of these experiments were used to explain the fragment size distribution observed in a series of well-controlled high-pressure gas-driven plate-drive experiments. The mean fragment size obtained for each flier plate is also observed to be related to its normalized spall strength. DOE

N90-14346# Los Alamos National Lab., NM. Center for Materials Science.
MARTENSITE TRANSFORMATION IN NiTi ALLOYS INDUCED BY TENSILE STRESS PULSES
A. M. Thakur, N. N. Thadhani (New Mexico Inst. of Mining and Technology, Socorro.), and R. B. Schwarz 1989 5 p Presented at the American Physical Society Topical Conference on Shock Compression of Condensed Matter, Albuquerque, NM, 14-17 Aug. 1989
(Contract W-7405-eng-36)
(DE90-001832; LA-UR-89-3105; CONF-890812-51) Avail: NTIS HC A01/MF A01

It is shown that tensile stress pulses generated by the reflection of compressive shock waves at a free surface induce martensitic transformation (from B2-CsCl to monoclinic structure), in equiatomic NiTi alloys. The transformation products are in the form of acicular needles with a micro-twined or dislocation substructure. DOE

N90-14347# California Univ., Berkeley. Lawrence Berkeley Lab. Center for Advanced Materials.
THE 4.2 K FRACTURE TOUGHNESS OF 304 STAINLESS STEEL IN A MAGNETIC FIELD
J. W. Chan, Judith Glazer, Z. Mei, and J. W. Morris, Jr. Jul. 1989 14 p Presented at the International Cryogenic Materials Conference, Los Angeles, CA, 24-28 Jul. 1989 Prepared in cooperation with California Univ., Berkeley
(Contract DE-AC03-76SF-00098)
(DE90-002083; LBL-27378; CONF-890701-14) Avail: NTIS HC A03/MF A01

Metastable austenitic steels are used in the structure of high field of superconducting magnets. In this application the alloys sustain high stresses in high magnetic fields at 4.2 K. Safe and effective design demands complete characterization of tensile, fatigue, and fracture toughness behavior of these alloys under the anticipated operating conditions. The characterization problem is complex because these metastable austenitic steels can undergo strain-induced martensitic transformation at cryogenic temperatures. The available data on the behavior of metastable austenitic steels in magnetic fields at 4.2 K is somewhat confusing. It is known that the presence of a high magnetic field during deformation can enhance martensitic transformation in Ni, Ni-Cr, and Mn steels. The tensile behavior and the fatigue behavior of 304L and 304LN, which are, respectively, less stable and more stable than 304, were also investigated in some detail in higher strength fields. Yield strength and fatigue property changes between tests performed in a magnetic field and without a magnetic field were not significant while the ultimate strength increased only slightly. The present work was undertaken to determine the extent and nature of the fracture toughness change of 304 stainless steel at 4.2 K in an 8 T magnetic field. DOE

N90-14348# Edgerton, Germeshausen and Grier, Inc., Idaho Falls, ID.
THE BIOCORROSION OF COPPER BY BIOPOLYMERS AS EXAMINED IN SITU, IN REAL TIME FT-IR/CIR/ATR IN CONJUNCTION WITH PRE AND POST XPS/AES
Anita K. Gianotto, Paul L. Wichlacz, John G. Jolley, Michael R. Hankins, Gill G. Geesey, and Randy B. Wright 1989 7 p Presented at the Annual Meeting and Exhibit of the Society of Mining Engineers, Inc., Las Vegas, NV, 27 Feb. - 2 Mar. 1989
(Contract DE-AC07-76ID-01570)
(DE90-002086; EGG-M-88357; CONF-890238-5) Avail: NTIS HC A02/MF A01

Thin films of copper (2.0 nm on germanium internal reflection elements (IREs) and 3.4 nm on germanium discs) were exposed to 10 percent gum arabic (aqueous solution), 2 percent alginic acid (aqueous solution), 1 percent bacterial culture supernatant (BCS, simulated seawater solution) and 0.5 percent Pseudomonas atlantica exopolymer (simulated seawater solution). The IREs were monitored in-situ, in real time using fourier transform infrared/cylindrical internal reflection/attenuated total reflection spectroscopy as a function of time at ambient conditions. The discs were characterized (pre- and post-exposure) by x ray photoelectron and Auger electron spectroscopies. Ancillary graphite furnace atomic absorption spectroscopy was used to monitor the removal process of the copper thin film from the germanium substrates. Results indicate that Cu was oxidized by gum arabic, alginic acid and BCS. Furthermore, Cu was removed from the Cu/Ge interface by all four polymers. The Cu was found associated with the polymer solutions. DOE

N90-14349# California Univ., Berkeley. Lawrence Berkeley Lab. Materials and Chemical Sciences Div.
EFFECTS OF PRECIPITATE DISTRIBUTION ON 293 K AND 77 K PROPERTIES OF 2090-T81 WELDMENTS

A. J. Sunwoo, S. Miyasato, and J. W. Morris, Jr. Jun. 1989 10 p Presented at the International Cryogenic Materials Conference, Los Angeles, CA, 24-28 Jul. 1989 Prepared in cooperation with California Univ., Berkeley Sponsored in part by ALCOA Labs
(Contract DE-AC03-76SF-00098)
(DE90-002332; LBL-27380; CONF-890701-16) Avail: NTIS HC A02/MF A01

Although 2090-T81 precipitation behavior has been well documented, the weld precipitation behavior has not been as-well characterized. The purpose of this study is to characterize the EB and GTA fusion zone precipitates and their distribution and to correlate the microstructure to 293 K and 77 K properties. The base metal strengths are greatly enhanced by a homogeneous distribution of T(sub 1) precipitates at 293 K and 77 K, but the presence of T(sub 1) and T(sub 2) at the boundaries has an adverse effect on the elongation at 77 K. The weld strengths are limited by a lack of strengthening precipitates. Fusion zone embrittlement is caused by the formation of Cu-Fe containing film and strain localization at the dendrite boundaries. DOE

N90-14350# Los Alamos National Lab., NM.
MULTIPLE MARTENSITIC TRANSFORMATIONS, INCOMMENSURATE/COMMENSURATE PHASES, AND CHARGE-DENSITY-WAVE STATES IN PLUTONIUM METAL: THEIR CONSEQUENCES
T. A. Sandenaw and J. F. Andrew 1989 7 p Presented at the Actinides 1989, Tashkent, USSR, 24-29 Sep. 1989
(Contract W-7405-eng-36)
(DE90-001235; LA-UR-89-3135; CONF-8909225-2) Avail: NTIS HC A02/MF A01

Simultaneous measurements of electrical resistivity, elongation and temperature were made on a Pu metal specimen between approx. 80 and 733 K. This temperature range covers part of the (alpha)-phase range and up through a major portion of the (delta)-phase range. Results are discussed. DOE

N90-14351# California Univ., Berkeley. Lawrence Berkeley Lab. Materials and Chemical Sciences Div.
THE METALLURGICAL DETERMINANTS OF TOUGHNESS AS CRYOGENIC TEMPERATURE
J. W. Morris, Jr., Judith Glazer, and J. W. Chan Jul. 1989 14 p Presented at the International Cryogenic Materials Conference, Los Angeles, CA, 24-28 Jul. 1989 Prepared in cooperation with California Univ., Berkeley
(Contract DE-AC03-76SF-00098)
(DE90-002331; LBL-27377; CONF-890701-15) Avail: NTIS HC A03/MF A01

Cryogenic structural materials can be roughly divided into three classes on the basis of the behavior that determines the strength-toughness characteristic at low temperature. The first class includes materials that undergo a ductile-brittle transition that dominates low temperature behavior. The second includes materials that remain ductile at all temperatures, whose low temperature toughness is governed by the interplay of strength and ductility. The third class includes metastable alloys whose ductility and toughness are largely determined by a low temperature phase transformation. Current models of fracture give some mechanistic insight into the behavior of each class. DOE

N90-14352# Oak Ridge National Lab., TN.
HIGH-TEMPERATURE CORROSION OF HEAT EXCHANGER MATERIALS
J. I. Federer 1989 29 p Presented at the 1st International Ceramic Science and Technology Congress, Anaheim, CA, 31 Oct. - 3 Nov. 1989 Sponsored in part by Aerojet Energy Conversion Co.; Babcock and Wilcox Co.; and Tecogen, Incorporated
(Contract DE-AC05-84OR-21400)
(DE90-001963; CONF-8910120-1) Avail: NTIS HC A03/MF A01

Silicon-based and oxide ceramics are candidate matrix materials for ceramic composites for heat exchanger tubes and other critical applications. The corrosion behavior of matrix materials was investigated by exposure tests in industrial furnaces, and composites containing the most corrosion-resistant matrix materials were tested in laboratory furnaces. SiC and Si sub 3 N sub 4 ceramics corroded severely in industrial furnace atmospheres containing alkali compounds. Oxide ceramics, such as Al sub 2 O sub 3 and ZrO sub 2, corroded relatively little in the same atmospheres, but their corrosion increased with increasing SiO sub 2 content. Most ceramic composites containing hoop-wrapped continuous fiber in Al sub 2 O sub 3 and stabilized ZrO sub 2 matrices exhibited dimensional instability during a laboratory corrosion test, but composites containing helical-wrapped fiber were stable. DOE

N90-14353# Lawrence Livermore National Lab., CA.
FIRST-PRINCIPLES INTERATOMIC POTENTIALS IN TRANSITION METALS: MULTI-ION INTERACTIONS AND THEIR ANALYTIC REPRESENTATION
John A. Moriarty Aug. 1989 11 p Presented at the Conference on Many-Atom Interactions in Solids, Pajulahti, Finland, 5-9 Jun. 1989 Submitted for publication
(Contract W-7405-eng-48)
(DE90-001990; UCRL-100752; CONF-8906238-1) Avail: NTIS HC A03/MF A01

The first-principles, density-functional version of the generalized pseudopotential theory, previously developed for empty- and filled-d-band metals, has now been extended to pure transition metals with partially-filled d-bands. Within this formalism, a rigorous real-space expansion of the bulk total energy has been obtained in terms of widely transferable, structure-independent interatomic potentials, including both central-force pair interactions and angular-force triplet and quadruplet interactions. In the central transition metals, the three-ion and four-ion potentials are essential to a proper description of materials properties, but are necessarily multi-dimensional functions which cannot be easily tabulated. We have, therefore, also developed a simplified version of the theory in which these potentials can be expressed analytically while retaining the most important physics of the full first-principles treatment. The analytic potentials are suitable for wide-scaled applications, including molecular-dynamics and Monte Carlo simulation. The first-principles and analytic theories are here reviewed together with selected applications to the prediction of high-pressure structural phase transitions; phonon anomalies and their close correlation with the present multi-ion potentials; and the vacancy-formation energy. DOE

N90-14354# Argonne National Lab., IL. Materials and Components Technology Div.
EMBRITTLEMENT OF LABORATORY- AND REACTOR-AGED CF-3, CF-8, AND CF-8M DUPLEX STAINLESS STEELS
H. M. Chung and T. R. Leax (Westinghouse Electric Corp., Pittsburgh, PA.) Oct. 1989 30 p Presented at the International Workshop on Intermediate-Temperature Embrittlement Processes in Duplex Stainless Steels, Oxford, England, 1-2 Aug. 1989
(Contract W-31-109-eng-38)
(DE90-002777; CONF-8908175-1) Avail: NTIS HC A04/MF A01

Cast duplex stainless steels of CF-3, CF-8, and CF-8M grades, containing a wide range of chemical composition and ferrite content, were aged in the laboratory at 270 to 450 C to evaluate the kinetics and mechanisms of thermal aging embrittlement. CF-8 and CF-8A steels were also obtained from components of BWRs and PWRs after service of 12 to 22 yr. After mechanical property (i.e., Charpy impact, tensile, and J-R curve) and microhardness tests, the aged specimens were examined by transmission electron microscopy and field-ion atom-probe techniques to elucidate the aging mechanisms and identify critical factors that control the embrittlement kinetics. From the results of microstructural characterization, the primary and secondary embrittlement mechanisms were identified. A mechanistic correlation was obtained between the microstructural characteristics and the activation energy of aging (i.e., the temperature dependence of the aging kinetics) for steels with a range of chemical compositions and subjected to different fabrication and thermal treatment

conditions. The unified correlation, based on spinodal decomposition influenced by G-phase nucleation and growth in ferrite and M23C6 precipitation on ferrite austenite boundaries, provides a good explanation of the complex behavior of the activation energy (18 to 55 kcal/mole) regardless of grade, chemical composition, or fabrication process. DOE

N90-14355# Pacific Northwest Lab., Richland, WA.
ACOUSTIC EMISSION DURING INTERGRANULAR STRESS CORROSION CRACKING
Mark A. Freisel and Russel H. Jones Sep. 1989 15 p Presented at the Conference on Review of Progress in Quantitative NDE, Brunswick, ME, 23-28 Jul. 1989
(Contract DE-AC06-76RL-01830)
(DE90-002894; PNL-SA-17443; CONF-890770-6) Avail: NTIS HC A03/MF A01

The physical and chemical processes taking place during intergranular stress corrosion cracking (IGSCC), in particular the effects of impurities on cracking mechanisms, have been the subjects of a research program sponsored by the Division of Materials Science, Office of Basic Energy Science, U.S. Department of Energy at Pacific Northwest Laboratory (PNL), operated by Battelle Memorial Institute. Acoustic emission (AE) was brought into the program because of the unique ability of AE methods to detect dynamic microscopic fracture processes. The results of these tests are presented. DOE

27 NONMETALLIC MATERIALS

Includes physical, chemical, and mechanical properties of plastics, elastomers, lubricants, polymers, textiles, adhesives, and ceramic materials.

For composite materials see *24 Composite Materials.*

N90-14356 Leeds Univ. (England).
THE STRUCTURE AND PROPERTIES OF LIQUID CRYSTAL POLYMERS Ph.D. Thesis
Michael John Troughton 1988 193 p
Avail: Univ. Microfilms Order No. BRD-84840

Materials studied were thermotropic liquid crystal polymers formed by the copolymerization of p-hydroxybenzoic acid (HBA) and 2,6-hydroxynaphthoic acid (HNA). The dynamic mechanical behavior of HBA/HNA, in both tension and shear, was investigated and results reveal three relaxation transitions over the temperature range -80 C to +120 C. Using results from dielectric and NMR studies, the effect of annealing and varying the monomer ratios of the material on the intensity and position in temperature space of these relaxations was discussed in terms of the motions of specific molecular groups in the polymer chain. The tensile modulus of the HBA/HNA molecular chain was determined at various temperatures by measuring the shift of the meridional x ray diffraction peak at 20 to 43 C with applied stress. The variation of the dynamic mechnical tensile and shear properties of HBA/HNA, together with that of the observed chain modulus, with temperature was successfully interpreted using an approximation to the single phase aggregate model. The results suggest that the tensile modulus of the sample is determined by a combination of the shear of highly aligned, rod-like molecules and the modulus of these molecules which varies with temperature. Dissert. Abstr.

N90-14357# Naval Ocean Systems Center, San Diego, CA.
CRAZING AND DEGRADATION OF FLEXURE STRENGTH IN ACRYLIC PLATES AS A FUNCTION OF TIME Final Report
J. D. Stachiw and J. L. Stachiw (San Diego School System, CA.) Jun. 1989 60 p
(AD-A212835; NOSC/TR-1303) Avail: NTIS HC A04/MF A01 CSCL 11/9

Thick acrylic plates in stressed and unstressed condition were subjected to outdoor weathering for 10 years. The stressed specimens developed surface crazing whose extent and depth were a function of flexure stress to which they were continuously subjected. Continuously applied flexure stress of 2240 psi generated very deep crazing, which resulted in catastrophic failure of the test specimen after 9 years. On the other hand, the specimen subjected to only 810-psi flexure stress displayed no crazing. Based on the study, it is concluded that for continuously stressed structural acrylic plastic components exposed to outdoor environment with 110 F maximum summer temperature, the maximum flexure design stress for a 10 year service life should not exceed 1000 psi; otherwise at the end of the service period, the remaining flexural strength of the weathered material will not provide the minimum required safety factor of 4. It is recommended that stressed acrylic plastic structures only be cleaned safely with water-based cleaners. GRA

N90-14358# Department of the Navy, Washington, DC.
TEMPERATURE STABLE CERAMIC DIELECTRIC COMPOSITIONS Patent Application
Relva C. Buchanan, inventor (to Navy) and Alena K. Maurice, inventor (to Navy) 12 Jun. 1989 16 p
(AD-D014209; US-Patent-Appl-SN-364416) Avail: NTIS HC A03/MF A01 CSCL 11/2

This invention relates to ceramic dielectric insulating materials. More specifically, it relates to a ceramic material having a high dielectric constant with low temperature dependence and low energy loss, for use in the manufacture of compact ceramic capacitors. It further relates to a method of making such ceramic material. A high dielectric constant is essential for the manufacture of compact ceramic capacitors. For a given desired capacitance, other properties being equal, the size of a capacitor is inversely proportional to the dielectric constant. A high dielectric constant thus allows a given capacitance to be provided in a small component. GRA

N90-14359# NATO Advanced Study Inst., Lucca (Italy).
STRUCTURE-PROPERTY RELATIONSHIPS IN SURFACE-MODIFIED CERAMICS. NATO ADVANCED SCIENCE INSTITUTES, SERIES E: APPLIED SCIENCES, VOLUME 170
Carl J. McHargue, ed., Ram Kossowsky, ed., and Wolfgang O. Hofer, ed. (Kernforschungsanlage, Juelich, Germany, F.R.) 1989 531 p Proceedings of the Nato Advanced Study Inst. on Structure-Property Relationships in Surface-Modified Ceramics, Castelvecchio Pascoli, Italy, 28 Aug. - 9 Sep. 1988
(AD-A212939) Avail: NTIS HC A23/MF A03 CSCL 11/2

The use of ion beams for the modification of the structure and properties of the near-surface region of ceramics began in earnest in the early 1980s. Since the mechanical properties of such materials are dominated by surface flaws and the surface stress state, the use of surface modification techniques would appear to be an obvious application. As is often the case in research and development, most of the initial studies can be characterized as cataloging the response of various ceramic materials to a range of ion beam treatments. The systematic study of material and ion beam parameters is well underway and experiments are now being designed to provide specific information about the processing parameter/property relationships. The first group of lectures dealt structure-property with the fundamentals of ion-solid interactions and the defect structure of compounds. Chemical and thermodynamic factors appear to be significantly more important than for simple metallic systems. The second group of lectures concerned the experimentally observed microstructural features and phase structures that develop during ion-beam processing of ceramics. The properties of ion-implanted and ion-beam-mixed ceramics were treated in Part 3, and included discussions on mechanical, tribological, chemical, electrical, and optical properties. The final section was concerned with thin films and coatings prepared by ion-beam-assisted processes. GRA

N90-14360 Michigan Univ., Ann Arbor.
MECHANISMS OF WEAR IN STRUCTURAL CERAMIC MATERIALS Ph.D. Thesis
Oyelayo Oladimeji Ajayi 1989 212 p
Avail: Univ. Microfilms Order No. DA8920490

Engineering ceramic materials were designed for structural applications under severe conditions of high temperature and

chemically aggressive environments. They are, however, good prospects for tribological applications as well. In spite of the great amount of work being done in evaluating the friction and wear behavior of structural ceramics, no satisfactory guidelines exist for the selection of these materials for wear applications. In order to formulate a good predictive wear equation for these materials, the fundamental mechanism of material removal during wear must be adequately understood. In the present work, the wear mechanisms of four commercial structural ceramics (Si3N4, SiC, Al2O3, ZrO2) were investigated under different contact conditions spanning static indentation by a sharp indenter to smooth sliding of a ceramic cylinder on a ceramic flat. Material removal during the wear of ceramics occurs by fracture and fragmentation at the contact interface rather than by the widely assumed subsurface crack linkage. The contact interface damage is different for each of the materials studied. For SiC, wear occurs by grain boundary failure during both static and sliding contact. The other three materials showed some plastic deformation and some cracking at the contact interface during static contact, and wear in sliding occurs by surface fatigue. Dissert. Abstr.

N90-14361 Leeds Univ. (England).
MECHANICAL PROPERTIES AND MORPHOLOGY OF ORIENTED POLYMER BLENDS Ph.D. Thesis
Gabriel Aloysius Gallagher 1988 173 p
Avail: Univ. Microfilms Order No. BRD-85677

A mechanical and morphological analysis of oriented 50/50 blends of PVdF with PMMA and PE with PP is reported; both blends being melt-mixed in a single screw extruder. Analysis of the quench-cooled isotropic blends revealed that the PE/PP blend was incompatible while the PVdB/PMMA was found to be amorphous and hence compatible. Subsequent annealing of this blend caused significant phase 2 PVdF crystallization. Samples of both blends were drawn at a number of temperatures, 110 C proving to be the optimum temperature for drawing PE/PP. From SAXS photographs the highly drawn PVdF/PMMA blend samples were found to possess long-range periodic order both parallel and normal to the draw direction. Measurement of the average longitudinal and lateral crystallite size was performed and a crystallinity estimated on the basis of a three dimensional structural model composed of a crystallite parallelopiped embedded in the amorphous blend. However, the apparent crystal modulus of the highly oriented blend was bound to be very much lower than the theoretical crystal modulus, this discrepancy surviving to temperatures as low as -145 C. This information, in conjection with the proposed three dimensional microstructural unit, was used to adapt the existing parallel-series mechanical model providing reasonable agreement between the predicted and the observed results. Dissert. Abstr.

N90-14362*# National Aeronautics and Space Administration. Lewis Research Center, Cleveland, OH.
DENSITY OF INTERCALATED GRAPHITE FIBERS
James R. Gaier and Melissa E. Slabe (Cleveland State Univ., OH.) Dec. 1989 15 p
(NASA-TM-102411; E-5167; NAS 1.15:102411) Avail: NTIS HC A03/MF A01 CSCL 11C

The density of Amoco P-55, P-75, P-100, and P-120 pitch-based graphite fibers and their intercalation compounds with bromine, iodine monochloride, and copper (II) chloride have been measured using a density gradient column. The distribution of densities within a fiber type is found to be a sensitive indicator of the quality of the intercalation reaction. In all cases the density was found to increase, indicating that the mass added to the graphite is dominant over fiber expansion. Density increases are small (less than 10 percent) giving credence to a model of the intercalated graphite fibers which have regions which are intercalated and regions which are not. Author

N90-14363*# National Aeronautics and Space Administration. Lewis Research Center, Cleveland, OH.
THE 3F CONDENSATION POLYIMIDES: REVIEW AND UPDATE
William B. Alston and Roy F. Gratz (Mary Washington Coll., Fredricksburg, VA.) 1989 6 p Presented at the 1st Pacific Polymer Conference, Maui, HI, 12-15 Dec. 1989; sponsored by Pacific Polymer Federation, Inc. Prepared in cooperation with Army Aviation Systems Command, Cleveland, OH
(NASA-TM-102353; E-5062; NAS 1.15:102353; AVSCOM-TR-89-C-017) Avail: NTIS HC A02/MF A01 CSCL 11C

Nine new condensation polyimides containing the phenyltrifluoroethylidene (3F) linkage were synthesized by the amic-acid route. Several other polyimides, including some with hexafluoroisopropylidene (6F) linkage, were also prepared as controls. Amic-acid solutions were characterized by determining their inherent viscosities prior to thermal conversion into polyimide films. Glass transition temperatures (T sub g), thermogravimetric analysis (TGA), and isothermal weight loss data (at 316, 371, and 371 C under 0.5 MPa air pressure) were obtained for the films. The films were pulverized into molding powders which, in turn, were thermally processed under pressure into neat resin disks. The disks were also characterized by T sub g's and 316 and 371 C isothermal weight losses. The film study identified two new polyimides with T sub g's greater than 371 C and two new polyimides with low rates of weight loss. The resin disks exhibited the same overall trends in T sub g and weight loss as the respective films, however the weight loss per unit surface area was always greater, presumably due to molecular degradation induced during preparation of the molding powders. The overall results indicate that polyimides containing the 3F linkage have T sub g's and thermo-oxidative stability comparable to polyimides containing the 6F group. Alternate technology was also shown by the synthesis of two new polyalkyl substituted 3F diamines and five more new 3F polymers. Their potential as photoresists was demonstrated by T sub g advancement after ultraviolet exposure. Last, four U.S. patents on 3F monomers and polymers were issued and up to eight more are pending. Author

N90-14364# Wisconsin Univ., Madison.
ORDERED CERAMIC MEMBRANES Annual Progress Report, May 1988 - May 1989
Marc A. Anderson, Charles G. Hill, Jr., Walter Z. Zeltner, Michal Bursa, Jonathan Patlak, Qunyin Xu, Mary Gieselmann, and Reid Peterson Jun. 1989 37 p
(Contract DE-AS07-86ID-12626)
(DE89-017426; DOE/ID-12626/4) Avail: NTIS HC A03/MF A01

As in the first two years, research during the third year covered three major areas: preparation and characterization of supports for the membranes; preparation and characterization of the membranes themselves; and determination of the behavior of systems in which the membranes are attached to supports. The primary interest in supports was to develop formulations which would provide more reproducible permeabilities (flux of water through the support). Several different clay formulations were shown to give quite reproducible permeabilities, with the actual permeability varying by nearly an order of magnitude among the different formulations. Supports with smoother surfaces were also fabricated, but rejection studies which compared membranes coated on these supports to membranes coated on rougher supports did not show any significant differences. Ceramic membranes were prepared which are composed of three different materials: alumina, titania and silica. DOE

N90-14365# Burton Technologies, Inc., Raleigh, NC.
FRICTION AND WEAR OF GLASSY CARBON IN SLIDING CONTACT, REVISION 1 Final Report, 30 Sep. 1988 - 30 Jun. 1989
Ralph A. Burton and R. Gaines Burton 1 Sep. 1989 43 p
(Contract DE-AC02-88CE-90027)
(DE90-000743; DOE/CE-90027/1-Rev-1) Avail: NTIS HC A03/MF A01

The goal of this project is evaluate a new family of self lubricated materials, and to define problem areas for further research. Specifically it is to obtain an understanding of the friction and wear behavior of a promising form of vitreous or glassy carbon in

monolithic and reinforced bodies, when run against a representative group of metals and ceramics. This effort serves to evaluate the potential of glassy carbon materials for use in friction and wear applications, through conducting a series of pin-on-disk sliding tests on these materials, and on metals and ceramics which are candidates for similar applications. DOE

N90-14366# Sandia National Labs., Albuquerque, NM. Fuel Science Div.
CHEMISTRY OF LARGE MOLECULES
G. A. Carlson 1989 13 p Presented at the Direct Liquefaction Contractors Review Meeting, Pittsburgh, PA, 2-5 Oct. 1989
(Contract DE-AC04-76DP-00789)
(DE90-000813; SAND-89-2401C; CONF-891081-3) Avail: NTIS HC A03/MF A01

Knowledge of coal molecular structure is important in the understanding of coal reactivity. Computer aided Molecular Design (CAMD) was used to create and study 3-D models of several postulated coal structures (Given, Wiser, Solomon, and Shinn). Using molecular dynamics calculations, the minimum-energy conformations for each structural model were compared. The physical densities of the minimum energy conformations were calculated, and are in agreement with experimental evidence. The frequencies of crosslinking hydrogen bonds were evaluated for these structures. Finally, CAMD was used to study model polymeric compounds, whose structure and reactivity may give new insights into coal conversion processes. DOE

N90-14367# Sandia National Labs., Albuquerque, NM. Surface Science.
AUTOMATED GLASS FIBER DRAWING
William L. Smith Sep. 1989 15 p
(Contract DE-AC04-76DP-00789)
(DE90-000894; SAND-89-1674) Avail: NTIS HC A03/MF A01

The formation of pristine silica fiber sections in an ultra high vacuum environment requires the critical control of production parameters. Glass temperature and fiber draw force must be precisely controlled to produce favorable results. Process control is achieved by automating the operation of a high power CO2 laser and the acquisition of data with a dedicated microprocessor. This combination, with the integration of ocular control through the application of digital image processing techniques, has subsequently led to a consistent and reproducible means of forming high quality pristine glass fiber test sections on the order of 25 to 50 microns in diameter. Fibers formed in this manner are tested to failure (in situ) by applying loads at various rates in controlled environments. This report presents the techniques and devices used to develop this automated fabrication and testing system. DOE

N90-14368*# National Aeronautics and Space Administration. Lewis Research Center, Cleveland, OH.
STRENGTH AND TOUGHNESS OF MONOLITHIC AND COMPOSITE SILICON NITRIDES
Jonathan A. Salem Jan. 1990 20 p
(Contract DE-AI05-87OR-21749)
(NASA-TM-102423; E-5188; NAS 1.15:102423) Avail: NTIS HC A03/MF A01 CSCL 11C

The strength and toughness of two composite and two monolithic silicon nitrides were measured from 25 to 1400 C. The monolithic and composite materials were made from similar starting powders. Both of the composite materials contained 30 vol percent silicon carbide whiskers. All measurements were made by four point flexure in surrounding air and humidity. The composite and monolithic materials exhibited similar fast fracture properties as a function of temperature. Author

N90-14369# Oregon State Univ., Corvallis. Dept. of Physics.
PERTURBED ANGULAR CORRELATIONS IN ZIRCONIA CERAMICS Progress Report No. 6
1989 15 p
(Contract DE-FG06-85ER-45191)
(DE89-017272; DOE/ER-45191/6) Avail: NTIS HC A03/MF A01

This report discusses the recent progress in perturbed angular correlations (PAC) in zirconia ceramics. Topics covered are: (1) zirconia PAC using 181 Ta as probe, (2) zirconia PAC research using 111-Cd as probe, (3) NMR equipment development and initial experiments, and (4) theoretical research. DOE

N90-14370# Lawrence Livermore National Lab., CA.
COMPUTER SYNTHESIS OF CERAMIC PREFORMS FOR MOLTEN-METAL INFILTRATION
Danny C. Halverson, Zuhair A. Munir, and Beverly Y. Lum 19 Dec. 1988 24 p Presented at the International Symposium on Combustion and Plasma Synthesis of High Temperature Materials, San Francisco, CA, 23-26 Oct. 1988
(Contract W-7405-eng-48)
(DE90-000826; UCRL-98854; CONF-8810203-3) Avail: NTIS HC A03/MF A01

Capillarity-thermodynamic studies were conducted to obtain contact-angle data of molten aluminum on boride (B4C, TiB2, AlB12) and carbide (TiC, SiC) substrates to illustrate the feasibility of infiltrating preforms containing these phases with aluminum. Techniques for increasing the exothermic potential of self-propagating high-temperature synthesis (SHS) reactions (exothermic boosting) are suggested for the fabrication of B4C-rich and SiC-rich composite-ceramic preforms for subsequent infiltration with molten aluminum. EXOBOOST, a computer program, was developed to rapidly screen hundreds of ceramic preform combinations based on SHS thermodynamics and exothermic boosting. Preliminary studies on the SHS of TiC indicate that reactant-greenbody properties strongly influence uniformity in the preform microstructure. DOE

N90-14371# Sandia National Labs., Albuquerque, NM.
BULK AND SHEAR MODULI OF EPOXY ENCAPSULANTS
Douglas Adolf, Carolyn Childress, and David Hannum Aug. 1989 10 p
(Contract DE-AC04-76DP-00789)
(DE90-000899; SAND-89-0748) Avail: NTIS HC A02/MF A01

The bulk moduli of common epoxy-based electronic encapsulating polymers were measured directly at room temperature. The dynamic shear moduli of these polymers were measured as a function of temperature and, for some, as a function of frequency. The temperature-frequency data were combined to calculate WLF shift parameters, and room temperature moduli were compared to historical values. Analytical procedures were documented in detail so users may fully understand the accuracy and limitations of the results. DOE

N90-14372# Sandia National Labs., Albuquerque, NM.
PREDICTIVE AGING OF ELASTOMERS IN AIR: THE IMPORTANCE OF UNDERSTANDING DIFFUSION-LIMITED OXIDATION EFFECTS
Kenneth T. Gillen and Roger L. Clough 1989 25 p Presented at the American Chemical Society Rubber Division National Meeting, Detroit, MI, 17-20 Oct. 1989
(Contract DE-AC04-76DP-00789)
(DE90-001385; SAND-89-2441C; CONF-8910267-1) Avail: NTIS HC A03/MF A01

Whenever a new elastomer is formulated or an old formulation is modified, it is important to estimate the material's anticipated lifetime in various use environments. For extended lifetimes (years) this often requires the application of accelerated aging techniques which typically involve the modelling of results obtained at higher-than-ambient environmental stress levels. For many practical applications of elastomers, air is present during environmental exposures -- this usually implies that important oxidation effects underly the degradation of the material. Unfortunately, exposure of elastomers to air during aging often results in inhomogeneously oxidized samples, a complication which impacts attempts both to understand the oxidation process and to extrapolate accelerated exposures to long-term conditions. As was clear for many years, in order to confidently extrapolate shorter-term accelerated

simulations to long-term, air-aging conditions, one must be able to monitor and quantitatively understand diffusion-limited oxidation effects. In this review some of the recent developments in both experimental techniques and theoretical modeling of relevance to this goal are highlighted. DOE

N90-14373# Pennsylvania Univ., Philadelphia.
SYNTHESIS AND PROPERTIES OF NEW PRECERAMIC MATERIALS Research Progress Report, 1 Dec. 1988 - 30 Nov. 1989
Larry G. Sneddon Sep. 1989 9 p
(Contract DE-FG02-87ER-13732)
(DE90-002562; DOE/ER-13732/2) Avail: NTIS HC A02/MF A01

The development of new methods for the production of complex materials is one of the most important problems in modern solid state chemistry and materials science. This project is attempting to apply the synthetic principles which have evolved in inorganic and organometallic chemistry to the production of important non-oxide ceramics, such as boron nitride, boron carbide and metal borides. Our recent work has now resulted in the production of several new polymer systems, including poly(vinylborazine), poly(vinylpentaborane) and poly(borazylene), that have proven to be high yield precursors to boron nitride and/or boron carbide. Current work is now directed toward the synthesis of new types of molecular and polymeric boron-containing species and an exploration of the solid state properties of the ceramics that have been produced in these studies. DOE

N90-14374# Oak Ridge National Lab., TN.
THE 7TH INTERNATIONAL CONFERENCE ON CERAMICS Foreign Trip Report, 12-18 Dec. 1988
P. F. Becher 3 Jan. 1989 7 p
(Contract DE-AC05-84OR-21400)
(DE90-002144; ORNL/FTR-3156) Avail: NTIS HC A02/MF A01

The 7th International Conference on Ceramics addressed current research in the fields of ceramic composites, electronic and superconducting ceramics, and ceramic processing. Technical papers by researchers from western and eastern Europe, Asia (including Japan and China), Australia, and the United States were presented. The traveler presented an invited lecture on the analysis of the toughening behavior in whisker reinforced ceramics and their mechanical properties. DOE

N90-14375# Oak Ridge National Lab., TN. Metals and Ceramics Div.
NUMERICAL AND EMPIRICAL VERIFICATION OF THE STRESS STATE IN A CERAMIC, BUTTON-HEAD, TENSILE SPECIMEN
M. G. Jenkins, M. K. Ferber, R. L. Martin, R. M. Poteat, and V. J. Tennery 1989 34 p Presented at the Annual Automotive Technology Development Contractors Coordination Meeting, Dearborn, MI, 23-26 Oct. 1989
(Contract DE-AC05-84OR-21400)
(DE90-001645; CONF-8910248-1) Avail: NTIS HC A03/MF A01

Characterization of the mechanical properties of ceramics in uniform, uniaxial stress fields is of paramount importance to the successful implementation of sophisticated life prediction methodologies proposed for use in advanced ceramic designs. Recent increases in the use of tensile tests for structural ceramics, coupled with increasing ultimate strengths in these materials have revealed anomalies in the locations and circumstances of failures in the commonly-used button-head, tensile specimen (e.g., non-gage section fractures especially in the button-head area). The objective was to numerically and empirically verify the stress-state in the ceramic, button-head tensile specimen as tested in conjunction with hydraulic couplers in the load train which were reported to consistently hold bending strain errors to less than 1 percent at specimen failure. DOE

N90-14376# Lawrence Livermore National Lab., CA. Dept. of Chemistry and Materials Science.
CHALLENGES IN PROCESSING FOR POLYMER COMPOSITES
Leroy Chiao and T. T. Chiao 13 Sep. 1989 23 p Presented at the 36th Sagamore Conference on Thick Section Composites, Plymouth, MA, 23-26 Oct. 1989
(Contract W-7405-eng-48)
(DE90-002224; UCRL-102028; CONF-8910290-1) Avail: NTIS HC A03/MF A01

Processing technology is considered to be the key for future cost and performance improvement in fiber composite structures. The challenges are discussed in two broad areas: engineering and research. In engineering, the challenge is to reduce cost while maintaining the state-of-the-art quality of composite structures. This can be done through innovative process development work. In research, the challenge is to concentrate on processing science. We need to reexamine and focus on basic issues such as voids, fiber wetting and filament/tow collimation, fiber/resin ratio, uniform fiber distribution and cure effects. These issues, combined and interactive in a laminate, have created many confusing topics such as composite toughness, low transverse failure strain and poor compression properties. To date, processing technology is considered the weak link in the chain of a fiber composite system, which also includes good design practices and proper material selections. This is because process studies in composites have traditionally been considered mundane by many researchers; furthermore, this type of work is very difficult to do in universities. We strongly believe, however, that the highest potential for cost reduction for composites is clearly in processing technology. DOE

N90-14377# Argonne National Lab., IL. Materials Science Div.
ELASTIC SOFTENING IN NANOCRYSTALLINE SILICON
S. R. Phillpot, D. Wolf, and J. F. Lutsko May 1989 7 p Presented at the Materials Research Society Spring Meeting, San Diego, CA, 24-29 Apr. 1989
(Contracts W-31-109-eng-38; N00014-88-F-0019)
(DE90-002268; CONF-8904290-1) Avail: NTIS HC A02/MF A01

It is pointed out that some of the generic physical properties of a nanocrystalline material are similar to those of a grain-boundary superlattice. The structure and elastic properties of a superlattice of twist boundaries on the (110) plane of silicon are calculated as a function of modulation wavelength using a three-body potential. All elastic moduli are found to be softened. This softening is attributed to the relatively small amount of structural disorder at the interfaces. DOE

N90-14378# Argonne National Lab., IL. Materials Science Div.
CHARACTERIZATION OF NANOPHASE MATERIALS BY X RAY DIFFRACTION AND COMPUTER SIMULATION
J. A. Eastman and L. J. Thompson Jun. 1989 7 p Presented at the Materials Research Society Spring Meeting, San Diego, CA, 24-29 Apr. 1989
(Contract W-31-109-eng-38)
(DE90-002270; CONF-8904290-2) Avail: NTIS HC A02/MF A01

The x ray diffraction experiments on nanophase Pd were performed with the primary goal of determining the nature of grain boundary structures in nanophase materials. A kinematical diffraction analysis was developed to interpret x ray (theta)--2(theta) data by comparing actual scans with scans produced by computer simulation. This simulation program has been used to explore the effects on diffracted intensity of a variety of microstructural and grain boundary structural parameters such as void concentration, grain size, grain boundary width, and changes in interplanar spacing and density in grain boundary regions. It has been found that a reasonable match to experimental data is produced by at least two model structures; in one, the material contains randomly positioned voids or vacancies, while in the other, the interplanar spacings in grain boundary regions are varied with respect to the spacings found in the grain interiors. DOE

28 PROPELLANTS AND FUELS

Includes rocket propellants, igniters, and oxidizers; their storage and handling procedures; and aircraft fuels.

For related information see also *07 Aircraft Propulsion and Power, 20 Spacecraft Propulsion and Power,* and *44 Energy Production and Conversion.*

N90-14379# TDA Research, Inc., Wheat Ridge, CO.
PHOTOCONVERSION OF INORGANICS TO METHANE Final Topical Report, Oct. 1987 - Feb. 1989
Robert J. Copeland, Daniel Feinberg, Michael Karpuk, and John Wright May 1989 70 p
(Contract GRI-5087-260-1543)
(PB89-230643; TDA-89-GRI-002; GRI-89/0145) Avail: NTIS HC A04/MF A01 CSCL 21D

The cost of producing gaseous fuels from carbon dioxide, water, and solar energy is evaluated. Such a process must have high conversion efficiency and low capital costs per unit of collection area to be economically attractive. A pond reactor is designed that has a cost which is must lower than other conversion facilities but still higher than is needed to produce economically competitive fuels at projected efficiencies. Due to a change in supply strategy away from long-term synthetic routes to gaseous fuels. FRI has redirected this contract to evaluate other inorganic chemistry related projects. GRA

N90-14380# IRT Corp., San Diego, CA.
STICK PROPELLANT X RAY INSPECTION Report, Sep. 1986 - May 1988
Ron Akre and Harry Chu (Army Armament Munitions and Chemical Command, Dover, NJ.) Sep. 1989 26 p
(Contract DAAA21-86-C-0336)
(AD-A212601; ARPAD-CR-89002) Avail: NTIS HC A03/MF A01 CSCL 19/1

A line scan x ray transmission technique was developed for the stick propellant automated inspection. The system has high reliability and is cost effective. The results are documented of testing the stick propellant x ray inspection system to measure the outer diameter, perforation diameter, web thickness, and density of M31A1E1 propellant sticks. GRA

N90-14381# Fraunhofer-Inst. fuer Chemische Technologie, Berghausen (Germany, F.R.).
INVESTIGATION OF THE PHASE STABILIZING EFFECT OF POTASSIUM FLUORIDE ON AMMONIUM NITRATE Final Report, Dec. 1987 - Feb. 1989
Walter Engel Jul. 1989 149 p
(Contract DAJA45-88-M-0051)
(AD-A213042; R/D-5955-CH-01) Avail: NTIS HC A07/MF A01 CSCL 07/4

Ammonium nitrate is an interesting oxidizer in the field of propellants and explosives. The substance is cheap and readily available. The drawbacks of the substance are caused by its polymorphic properties. It crystallizes at ambient pressure in 5 modifications. Some phase transitions take place at temperatures, which occur under normal storage conditions. These transitions are connected with volume changes that influence severely the properties of products containing ammonium nitrate. Many attempts were made to overcome these difficulties. One of the approaches consist of incorporating different ions into the lattice to change the phase properties. In this context potassium fluoride was used. The doped ammonium nitrate material must be checked to make sure that no undesired phase transitions and volume changes occur in the interesting temperature interval. A measuring system was built up in the past, which allows automatic measurements of series of diffraction patterns while cycling a sample stepwise through the interesting temperature ranges. The series contain information about phase transition temperatures and the participating phases. The system was used to investigate the phase properties of ammonium nitrate samples, which were melted with 2 weight percent of potassium fluoride. GRA

N90-14382 Department of the Navy, Washington, DC.
MEANS FOR PROTECTING ELECTROEXPLOSIVE DEVICES WHICH ARE SUBJECT TO A WIDE VARIETY OF RADIO FREQUENCY Patent
Robert L. Dow, inventor (to Navy) and Paul W. Proctor, inventor (to Navy) 18 Jul. 1989 6 p Filed 1 Oct. 1985
(AD-D014219; US-Patent-4,848,233; US-Patent-Appl-SN-782325)
Avail: US Patent and Trademark Office CSCL 13/12

An RF attenuator for attenuating RF signals in a lead particularly for protecting against unintentional detonation of electrically initiated ammunition is presented. A firing lead is embedded in a body of ferrite material. The firing lead is formed in a planar spiral configuration with reversals of direction. GRA

N90-14383 Department of the Navy, Washington, DC.
PENTAFLUOROTHIO POLYNITROALIPHATIC EXPLOSIVES Patent
Michael E. Sitzmann and William H. Gilligan, inventors (to Navy) 18 Jul. 1989 7 p Filed 24 Jun. 1988 Supersedes AD-D013384
(AD-D014221; US-Patent-4,849,540; US-Patent-Appl-SN-213039; US-Patent-Class-560-156) Avail: US Patent and Trademark Office CSCL 19/1

An object of this invention is to provide new energetic explosive compounds. Other objects of this invention are to provide new pentafluorothio polyaliphatic explosives; to provide new high melting pentafluorothio polyaliphatic explosives; to provide new high energy, high density explosives; and to provide new high energy explosives having good thermal stabilities. This invention provides new high energy, high density, high melting explosives which contain both pentafluorothioethyl, -CH2CH2SF5, groups and polynitroaliphatic groups. These compounds are prepared by the reaction of pentafluoro thioethanol, F5SCH2OH, with selected polynitro aliphatic reactants. The pentafluoro thioethanol can be prepared by the reduction of pentafluoro thioacetyl chloride with lithium aluminum hydride. GRA

N90-14384# Lawrence Livermore National Lab., CA.
DETONATION PRODUCT EQUATION OF STATE FOR BARATOL
John W. Kury and R. Don Breithaupt 18 Aug. 1989 5 p Presented at the 9th International Symposium on Detonation, Portland, OR, 28 Aug. - 1 Sep. 1989
(Contract W-7405-eng-48)
(DE90-001050; UCRL-101761; CONF-890811-38) Avail: NTIS HC A01/MF A01

The metal acceleration ability of the composite explosive Baratol was experimentally determined using a Fabry Perot velocimeter. The Baratol reaction zone has a von Neuman spike pressure of 23.5 GPa. The performance of Baratol was found to be geometry dependent which is attributed to the slow reaction of barium nitrate's oxygen with the TNT detonation products. About 35 percent of the oxygen reacted in the 7 (mu)sec available for metal acceleration. The experimental results were used to generate an equation of state recipe for use in hydrodynamic calculations of the wedge test. DOE

N90-14385# Pennsylvania State Univ., University Park. Coll. of Earth and Mineral Sciences.
THERMAL STABILITY OF JET FUEL Quarterly Report No. 3, Apr. - Jun. 1989
S. Eser, J. Perison, R. M. Copenhaver, and H. H. Schobert 1989 23 p
(Contract DE-AC22-88PC-88827)
(DE90-001160; DOE/PC-88827/T3) Avail: NTIS HC A03/MF A01

The overall objective of this program is to investigate the effect of chemical components on the thermal stability of jet fuel. Specific objectives include the determination of the high temperature thermal stability of a suite of model compounds typical of those present as trace contaminants in the fuel, investigation of the thermal stability of various fractions of a coal-derived and a petroleum-derived JP-8 jet fuel, the determination of the thermal

stability of the unfractionated fuels, and the development of the relationship between the stability of the whole material and the behavior of model compounds of fuel fractions. DOE

N90-14386# EG and G Mound Applied Technologies, Miamisburg, OH.
DEVELOPMENT OF A TITANIUM/BORON BLENDING PROCESS
C. M. Love 1989 9 p Presented at the 14th International Pyrotechnics Seminar, Jersey, England, 18-22 Sep. 1989
(Contract DE-AC04-88DP-43495)
(DE90-001450; MLM-3606(OP); CONF-8909113-6) Avail: NTIS HC A02/MF A01

Efforts to develop a titanium-boron pyrotechnic mixture for a heat source component are described. After a supposedly good blending procedure had been specified, a problem developed. Allegedly identical Ti/B blends exhibited differences in behavior. Extensive analytical characterization of the two blends and experiments designed to determine whether the differences could be related to moisture failed to solve the problem. However, mild grinding was found to activate Ti/B. A stereomicroscope examination revealed the existence of micro-inhomogeneities, which were different in the two blends. A laboratory experiment showed that differences in humidity at the time of blending explains how the two identical blends became different. The extent to which ball milling removes the inhomogeneities is shown. Problems associated with the scale-up of ball milling to production quantities are identified. The effectiveness of a twin shell blender with a pin intensifier is described. Another problem that developed in the latter stages of the program was that the Ti/2B mole ratio blend was judged to be too hot for the component application. The success of tailoring blend output by addition of Al2O3 as a diluent is described. DOE

N90-14387# Brookhaven National Lab., Upton, NY. Process Sciences Div.
THE CONVERSION OF CARBONACEOUS MATERIALS TO CLEAN CARBON AND CO-PRODUCT GASEOUS FUEL
Meyer Steinberg Aug. 1989 12 p Presented at the 5th European Conference on Biomass for Energy and Industry, Lisbon, Portugal, 9-13 Oct. 1989
(Contract DE-AC02-76CH-00016)
(DE90-001561; BNL-42124; CONF-891034-1) Avail: NTIS HC A03/MF A01

A new process has been developed for converting raw carbonaceous materials to clean carbon fuels and coproduct clean gaseous fuel. The process is unique and universal in terms of dealing with all carbon containing raw materials. The process, called HYDROCARB, consists of two basic steps. The raw carbonaceous material is first hydropyrolyzed in an atmosphere of an excess of hydrogen so as to form methane. Any solid ash remains behind in the hydropyrolyzer. This step is then followed by the thermal decomposition of the methane by pyrolysis to carbon black and hydrogen. The hydrogen is then recycled to the first step to repeat the cycle. The excess hydrogen then becomes a coproduct fuel. Using a downflow dense phase media in a moving bed reactor, the exothermic heat in the hydrogenation reaction is used for providing the endothermic heat in the methane pyrolysis step. Thus, the energy and mass efficiency of the process can be very high (approximately 90 percent). The feedstock from the process can be any carbonaceous material including coal, biomass (wood) and agricultural and municipal solid waste. Depending on the scale of the process economic estimates indicate that as a fuel, the clean carbon produced by the HYDROCARB Process can compete with today's price for oil. DOE

N90-14388# Los Alamos National Lab., NM.
STUDY OF NEW MATERIALS FOR GUN PROPELLANT FORMULATIONS
Kien-Yin Lee and Mary M. Stinecipher 1989 5 p Presented at the ADPA International Joint Symposium on Compatibility of Plastics and other Materials with Explosives, Propellants, Pyrotechnics and Processing Propellants, Explosives and Ingredients
(Contract W-7405-eng-36)
(DE89-015285; LA-UR-89-2550; CONF-8910157-1) Avail: NTIS HC A01/MF A01

A search is being conducted for new energetic materials to improve gun-propellant formulations. Theoretical calculations indicate that certain types of high nitrogen compounds produce lower average-molecular-weight gases than those with more carbon, and low average-molecular-weight by-products contribute to higher impetus. Therefore, our target compounds were chosen to contain only the elements C, H, N, and O, with a high percentage of nitrogen, be thermally stable and moderately insensitive to impact. The chemical preparations, impetus, flame temperatures, and heats of formation for the compounds are described. DOE

N90-14389# Los Alamos National Lab., NM.
CALIBRATION CURVES FOR SOME STANDARD GAP TESTS
Allen L. Bowman and Stanley C. Sommer 1989 4 p Presented at the DEA-A-76-G-1218 Meeting, Picatinny Arsenal, NJ, 22-24 Aug. 1989
(Contract W-7405-eng-36)
(DE89-016599; LA-UR-89-2622; CONF-8908139-1) Avail: NTIS HC A01/MF A01

The relative shock sensitivities of explosive compositions are commonly assessed using a family of experiments that can be described by the generic term Gap Test. Gap tests include a donor charge, a test sample, and a spacer, or gap, between two explosive charges. The donor charge, gap material, and test dimensions are held constant within each different version of the gap test. The thickness of the gap is then varied to find the value at which 50 percent of the test samples will detonate. The gap tests measure the ease with a high-order detonation can be established in the test explosive, or the detonability, of the explosive. Test results are best reported in terms of the gap thickness at the 50 percent point. It is also useful to define the shock pressure transmitted into the test sample at the detonation threshold. This requires calibrating the gap test in terms of shock pressure in the gap as a function of the gap thickness. It also requires a knowledge of the shock Hugoniot of the sample explosive. The 2DE reactive hydrodynamic code with Forest Fire burn rates was used for the donor explosives to calculate calibration curves for several gap tests. The model calculations give pressure and particle velocity on the centerline of the experimental set-up and provide information about the curvature and pulse width of the shock wave. DOE

N90-14390# Lawrence Livermore National Lab., CA. Chemistry and Materials Science Dept.
PARTICLE SIZE EFFECTS IN THE INITIATION OF EXPLOSIVES CONTAINING REACTIVE AND NONREACTIVE CONTINUOUS PHASES
Randall L. Simpson, F. H. Helm, P. C. Crawford, and John W. Kury 22 Aug. 1989 11 p Presented at the 9th International Symposium on Detonation, Portland, OR, 28 Aug. - 1 Sep. 1989
(Contract W-7405-eng-48)
(DE90-000786; UCRL-101689; CONF-890811-33) Avail: NTIS HC A03/MF A01

The shock sensitivity of HMX formulations was determined using gun-driven wedge tests and multiple manganin pressure gauge tests. Mean HMX particle size was varied from 5 to 1700 microns. Formulations with inert and reactive continuous fluid phases as well as extrusion cast formulations were tested. Both the HMX particle size and nature of the continuous phases were shown to affect the shock sensitivity. Radiometric experiments were also done to help verify the conclusions about reactivity drawn from the wedge and gauge experiments. DOE

N90-14391# Lawrence Livermore National Lab., CA.
NON-EQUILIBRIUM EFFECTS OF SLOW DIFFUSION CONTROLLED REACTIONS ON THE PROPERTIES OF EXPLOSIVES
Mathias vanThiel and Francis H. Ree Aug. 1989 9 p Presented at the 9th International Symposium on Detonation, Portland, OR,

28 Aug. - 1 Sep. 1989
(Contract W-7405-eng-48)
(DE90-000822; UCRL-99565; CONF-890811-37) Avail: NTIS HC A02/MF A01

The effect of the growth of several phases on the calculated equilibrium properties of explosive product mixtures, is described. Calculations made with a statistical-mechanical multi-phase chemical-equilibrium (CHEQ) code are compared with experiment. Such comparisons show that the equations of state (EOS) of two condensed carbon phases deviate from equilibrium and indicate the appearance of a nitrogen rich phase at high pressure. A cluster structure is discussed in terms of recent theory and experiment, and preliminary calculations, replacing diamond with an estimated cluster EOS indicate small but, for some design work, significant changes of 0.3 percent in density and 2 percent in energy at constant P and T. DOE

N90-14392# Lawrence Livermore National Lab., CA.
PHASE CHANGES IN CARBON AND NITROGEN SYSTEMS: THEIR EFFECTS ON THE DETONATION PROPERTIES OF HIGH EXPLOSIVES
Francis H. Ree and Mathias vanThiel Aug. 1989 8 p Presented at the 9th International Symposium on Detonation, Portland, OR, 28 Aug. - 1 Sep. 1989
(Contract W-7405-eng-48)
(DE90-000829; UCRL-101902; CONF-890811-36) Avail: NTIS HC A02/MF A01

The first part of this paper describes a new three-phase equation of state of condensed carbon and effective intermolecular potentials of N2-N2, N2-N, and N-N pairs in fluid phase. We then examine a supercritical phase change in N2-H2O mixtures using computer simulations and a chemical equilibrium model. The second part deals with applications to two explosives, RX-23-AB and LX-14. The calculation shows that the detonation behavior of these explosives is relatively insensitive to the dissociation of nitrogen (to 90 GPa) but sensitive to the predicted N2-H2O phase separation. For LX-14 we predict that diamond in detonation products will melt near 70 GPa along the Hugoniot and will transform to graphite near 8.5 GPa along the Chapman-Jouguet adiabat. DOE

N90-14393# Lawrence Livermore National Lab., CA.
REACTIVE FLOW MEASUREMENTS AND CALCULATIONS FOR ZrH2-BASED COMPOSITE EXPLOSIVES
Michael J. Murphy, Randall L. Simpson, R. Don Breithaupt, and Craig M. Tarver 18 Aug. 1989 9 p Presented at the 9th International Symposium on Detonation, Portland, OR, 28 Aug. - 1 Sep. 1989
(Contract W-7405-eng-48)
(DE90-000831; UCRL-101861; CONF-890811-35) Avail: NTIS HC A02/MF A01

Cylinder test, Fabry-Perot laser interferometric, and detonation velocity-charge diameter experiments were done to determine the detonation reaction zone structures and reaction product equations of state of a family of HMX/AP/ZrH2/estane explosives. This experimental data base is used to develop ignition and growth reactive flow models of the detonations waves in these composite explosives. The experiments and calculations clearly demonstrate the Zeldovich-von Neumann-Doering (ZND) structure of the detonation reaction zones which are several millimeters long. The inferred reaction rates imply that the HMX in these formulations reacts first at rates comparable to those measured in other HMX-based explosives and propellants. The remaining components of these explosives then decompose at much slower rates. However, this decomposition is rapid enough to contribute to the propagation of the detonation wave and to the total energy delivered in metal acceleration applications. DOE

N90-14394# Lawrence Livermore National Lab., CA.
REACTION ZONE STRUCTURE IN SUPRACOMPRESSED DETONATING EXPLOSIVES
LeRoy G. Green, Craig M. Tarver, and David J. Erskine 18 Aug. 1989 12 p Presented at the 9th International Symposium on Detonation, Portland, OR, 28 Aug. - 1 Sep. 1989
(Contract W-7405-eng-48)
(DE90-000832; UCRL-101862; CONF-890811-34) Avail: NTIS HC A03/MF A01

Nanosecond time resolved particle velocity histories of supracompressed detonation waves in TNT-, TATB-, and HMX-based explosives are measured using a VISAR laser velocimeter and calculated using the ignition and growth reactive flow hydrodynamic computer code model. The Zeldovich-von Neumann-Doering (ZND) detonation wave structure is observed at pressures more than twice the self-sustaining detonation wave pressure. TNT and TATB exhibited a fast reaction which liberates approximately 80 percent of the total available exothermicity within 50 ns, followed by a slower reaction which lasts another 100 to 200 ns. These reaction rates are not strongly dependent on the initial shock pressure. The slower reaction is attributed to diffusion controlled solid carbon coagulation. The ignition and growth model using a ZND type model with a fast reaction preceding a slower reaction to the fully reacted product state accurately calculates the VISAR experimental data for TNT, LX-17, PBX 9404 and RX-26-AF. DOE

N90-14395# Sandia National Labs., Albuquerque, NM.
FAST TRANSIT GAS- AND CONDENSED-PHASE CHEMISTRY OF ENERGETIC MATERIALS
R. D. Skocypec, K. L. Erickson, A. M. Renlund, and W. M. Trott 1989 18 p Presented at the JANNAF Combustion Subcommittee Meeting, Pasadena, CA, 23-27 Oct. 1989
(Contract DE-AC04-76DP-00789)
(DE90-001656; SAND-89-1437C; CONF-8910263-1) Avail: NTIS HC A03/MF A01

An experimental system is being developed to study the fast transient kinetics governing solid phase decomposition and subsequent interaction with decomposition products. The first phase addresses the decomposition step. The experimental system integrates a thin film sample configuration with two chemical diagnostic techniques, time-of-flight mass spectrometry and time resolved infrared spectral photography, and a pulsed laser heat source. This system is designed to examine both condensed phase mechanisms and concurrent gas phase species evolution from samples at temperatures up to 1000 C with microsecond temporal resolution. Tests are underway to demonstrate and assess the use of thin film samples with the experimental system. Results of these tests, the diagnostic capabilities of the experimental system, and the advantages, preparation and characterization of thin film samples are presented. DOE

N90-14396# Department of Energy, Washington, DC. Office of Policy Integration.
ASSESSMENT OF COSTS AND BENEFITS OF FLEXIBLE AND ALTERNATIVE FUEL USE IN THE US TRANSPORTATION SECTOR. TECHNICAL REPORT THREE: METHANOL PRODUCTION AND TRANSPORTATION COSTS
Nov. 1989 46 p
(DE90-002625; DOE/PE-0093) Avail: NTIS HC A04/MF A01

The Department of Energy (DOE) in 1988 undertook a comprehensive technical analysis of a flexible-fuel transportation system in the United States. To keep interested parties informed about the progress of the DOE Alternative Fuels Assessment, the Department periodically publishes reports dealing with particular aspects of this complex study. An analysis of the expected costs to produce methanol and of several related issues are provided. DOE

29 MATERIALS PROCESSING

Includes space-based development of products and processes for commercial applications.

For biological materials see *55 Space Biology.*

N90-14397*# Alabama Univ., Huntsville.
MATERIALS PROCESSING IN LOW GRAVITY Final Report

Gary L. Workman 10 Jul. 1989 26 p
(Contract NAS8-36620)
(NASA-CR-183733; NAS 1.26:183733) Avail: NTIS HC A03/MF A01 CSCL 22A

Work is reported on the Materials Processing Low Gravity Program in which the University of Alabama worked with scientists and engineers at Marshall Space Flight Center to design, implement and perform low gravity experiments with various scientific investigators in materials processing science through March 15, 1989. The facilities used in these short duration low gravity experiments include the Drop Tube and Drop Tower at MSFC, and the KC-135 aircraft at Ellington Field. The utilization of these ground-based low gravity facilities for materials processing was instrumental in determining the feasibility of either performing a particular experiment in the microgravity of Space or continuing on-going activities which may have been delayed due to the absence of shuttle flights during this contractual effort. K.C.D.

N90-14398*# Cleveland State Univ., OH. Dept. of Chemical Engineering.
PRIMARY ARM SPACING IN DIRECTIONALLY SOLIDIFIED Pb-10 WT PERCENT Sn ALLOYS Final Report
M. A. Chopra and S. N. Tewari Jan. 1990 19 p Presented at the 28th Aerospace Sciences Meeting, Reno, NV, 8-11 Jan. 1990; sponsored by AIAA
(Contract NCC3-95)
(NASA-CR-185190; E-5141; NAS 1.26:185190; AIAA-90-0740) Avail: NTIS HC A03/MF A01 CSCL 11F

The dependence of primary arm spacings on growth speed was investigated for cellular and dendritic arrays in Pb-10 wt percent Sn samples directionally solidified under a constant positive thermal gradient in the melt. The gradient of constitutional supercooling was varied from almost zero (near the break-down of the planar liquid-solid interface at small growth speeds, cellular morphology) to near unity (large growth speeds, dendritic morphology). The spatial arrangements of cells and dendrites, as given by their coordination number, are not very different from each other. It appears that primary arm spacing maxima and the cell to dendrite transition are strongly influenced by the magnitude of the solute partition coefficient. The planar to cellular bifurcation is supercritical in Pb-Sn which has a high partition coefficient, as compared to the subcritical behavior reported in Al-Cu and succinonitrile-acetone, both of which have low partition coefficients. The primary arm spacing model due to Hunt agrees with the experimentally observed trend for the whole growth regime. There is a good quantitative agreement at higher gradients of supercooling. However, the model overpredicts the primary arm spacings at low gradients of constitutional supercooling. Author

31 ENGINEERING (GENERAL)

Includes vacuum technology; control engineering; display engineering; cryogenics; and fire prevention.

N90-14399# Rolls-Royce Ltd., Derby (England).
SAS GRAPHICS IN DCF
Jeff Gribbin and Phil Davies 23 Sep. 1988 16 p Presented at the SAS User Group Meeting, 21 Sep. 1988
(PNR90563; ETN-89-95550) Copyright Avail: NTIS HC A03/MF A01

Some get-you-started hints, tips, and examples on creating and inserting pictures into DCF documents, particularly with respect to pictures from SAS and IBM 3800 family printers are provided. Processing of this type is possible using the products SAS version 5, DCF version 3, GDDM version 1. On MVS/TSO it is possible to run in foreground interfacing to DCF through IBM's ISPF/PDF option 4.9. On VM/CMS it is possible either through DCF or PROFS version 2. Difficulties involved in putting rotating pictures in the same orientation as the text are outlined. Solutions to this problem are described. ESA

N90-14400# Commerce Dept., Washington, DC. Office of Metric Programs.
METRIC HANDBOOK FOR FEDERAL OFFICIALS: RECOMMENDATIONS OF THE INTERAGENCY COMMITTEE ON METRIC POLICY
Aug. 1989 51 p
(PB89-226922) Avail: NTIS HC A04/MF A01 CSCL 13B

Recommendations for introduction of metric units in proposed legislation, regulations, data requests and other Government use of measurement units are presented. These recommendations were developed for the Interagency Committee on Metric Policy by its working arm, the Metrication Operating Committee, and its Metric Practice and Preferred Units Subcommittee. Assistance in editing of the documents, coordination and publication in the Federal Register was provided by the U.S. Department of Commerce, Office of Metric Programs, which serves as the secretariat for the ICMP and its subordinate committees. Other Federal documents are provided for convenient reference as appendices. GRA

N90-14401# National Science Foundation, Washington, DC. Div. of Science Resources Studies.
SCIENCE AND TECHNOLOGY RESOURCES IN US INDUSTRY: SURVEYS OF SCIENCE RESOURCES SERIES, 1975-1986
Dec. 1988 111 p
(PB90-107194; NSF-88-321) Avail: NTIS HC A06/MF A01 CSCL 13B

American industrial scientific and technological (ST) resources are explored and summarized in terms of two of the most important parameters of innovation: research and development (R and D) activities, and employment and utilization of scientists, engineers, and technicians. Industry has the predominant role in setting current and future demand for science and engineering personnel. In 1986, industry employed 1.2 million scientists and 1.9 million engineers, representing 55 and 80 percent, respectively, of all personnel in the fields. Between 1976 and 1986, employment of scientists in industry increased 10.7 percent/year, and of engineers, 6.6 percent/year. Industrial firms spend 3/4 of the funds financing R and D performed in the U.S. Author

N90-14402# Sandia National Labs., Albuquerque, NM.
A DISCUSSION OF FIRE SUPPRESSION INDUCED EQUIPMENT DAMAGE AND SYSTEMS IMPACT THROUGH AN EXAMINATION OF SPURIOUS FIRE SUPPRESSION ACTUATION INCIDENTS
Steven P. Nowlen, John A. Lambright, James C. Romig, M. P. Bohn, and Vernon F. Nicolette 1989 10 p Presented at the Post-SMIRT Conference No. 2, Monterey, CA, 21-22 Aug. 1989
(Contract DE-AC04-76DP-00789)
(DE90-000792; SAND-89-1956C; CONF-8908125-6) Avail: NTIS HC A02/MF A01

Current work associated with the investigation of equipment damage induced by the application of fire suppressants is discussed. This discussion will be presented through an examination of several nuclear power plant incidents in which the spurious actuation of one or more fire suppression systems has occurred. The effects of these actuations on plant equipment, systems, and operation will be described. Also presented are the results of scoping calculations of the risk significance of spurious suppression system actuation. Finally, a description of the efforts recommended to further investigate the impact of such incidents on plant operations and plant risks are provided. DOE

N90-14403# Japan Atomic Energy Research Inst., Tokai.
THERMAL DESIGN OF A 10-kW HELIUM REFRIGERATOR
Hidemasa Yamamura, Takashi Kato, Eisuke Tada, Tadao Hiyama, Katsumi Kawano, Masahiko Sato, and Susumu Shimamoto Mar. 1989 41 p
(DE90-701785; JAERI-M-89-040) Avail: NTIS (US Sales Only) HC A03/MF A01

The Proto Toloidal Coil program, which is to develop the large superconducting toloidal coil for the Fusion Experimental Reactor (FER), is being investigated. In this program, construction of the 10-kW helium refrigeration system is indispensable. The optimized

system design of 10-kW helium refrigerator based on the thermal analysis is described. In addition, the key items to be developed for the large scale helium refrigerator (30 kW x 4 units) of the FER are described. DOE

32 COMMUNICATIONS AND RADAR

Includes radar; land and global communications; communications theory; and optical communications.

For related information see also *04 Aircraft Communications and Navigation* and *17 Space Communications, Spacecraft Communications, Command and Tracking.* For search and rescue see *03 Air Transportation and Safety,* and *16 Space Transportation.*

N90-14404# Federal Aviation Administration, Atlantic City, NJ.
DATA LINK PROCESSOR (DLP) OPERATIONAL TEST AND EVALUATION/INTEGRATION TEST PLAN
Norman W. Watts and Noel A. Doucett (System Engineering and Integration, Atlantic City, NJ.) Dec. 1989 64 p
(DOT/FAA/CT-TN89/32) Avail: NTIS HC A04/MF A01

The provision for two way communication with aircraft, via a digital data link, has long been considered a means of providing significant enhancements for safe and efficient flight operations. The Data Link Processor (DLP) being tested will initially perform the ground based data link processing functions necessary to provide appropriately equipped aircraft with pilot requested aviation weather data from a National Weather Data Base via the Mode Select Beacon System (Mode S). The weather data base will contain six products: Surface Observations (SA), Terminal Forecasts (FT), Pilot Reports (UA), Wind and Temperature Aloft Forecasts (FD), Radar Summaries (SD), and Hazardous Weather Advisories. The DLP Operational Test and Evaluation and/or Integration Test Plan depicts all systems that interface with the DLP, and identifies the data that will be communicated between them. This plan sets forth and defines the philosophy, approach, methods, organization, and schedules for the verification of the DLP requirements. This plan provides sufficient detail to define and direct the development of detailed test procedures and to identify the allocation of resources required to support those tests. Author

N90-14405# Advisory Group for Aerospace Research and Development, Neuilly-Sur-Seine (France). Electromagnetic Wave Propagation Panel.
OPERATIONAL DECISION AIDS FOR EXPLOITING OR MITIGATING ELECTROMAGNETIC PROPAGATION EFFECTS
Sep. 1989 475 p In ENGLISH and FRENCH Symposium held in San Diego, CA, 15-19 May 1989
(AGARD-CP-453; ISBN-92-835-0524-7) Copyright Avail: NTIS HC A20/MF A03

Exploitation of mitigation of environmental effects rank equal in importance with weapons systems. The rapidly changing propagation environment throughout NATO's area of concern requires a rapid operational assessment capability. Since operational decision aids require appropriate propagation models and accurate environmental inputs, attention must be paid to propagation modelling, direct and remote sensing techniques and environmental forecasting. To this end, the following topics were covered: General aspects; propagation modeling and validation; decision aids for tropospheric radio progation; decision aids for electro-optical propagation; remote and direct sensing techniques; and forecasting of environmental parameters and operational systems impact. For individual titles, see N90-14406 through N90-14448.

N90-14406# Naval Research Advisory Committee, Washington, DC.
THE IMPORTANCE OF ENVIRONMENTAL DATA **c42**
Gerald Cann and Robert P. Porter *In* AGARD, Operational Decision Aids for Exploiting or Mitigating Electromagnetic Propagation Effects Sep. 1989 6 p (For primary document see N90-14405 06-32)
Copyright Avail: NTIS HC A20/MF A03

A top level analysis of the significance of quantitative knowledge of environmental parameters to naval weapons and naval warfare was conducted. It was concluded that the impact of the environment needs to be considered more thoroughly during the research, development, and acquisition process. This requires a central environmental top level requirement or master plan and a more formalized connection between the organizations involved in various aspects of environmental science. Author

N90-14407# Naval Ocean Systems Center, San Diego, CA. Ocean and Atmospheric Sciences Div.
PROPAGATION ASSESSMENT AND TACTICAL DECISION AIDS
Juergen H. Richter *In* AGARD, Operational Decision Aids for Exploiting or Mitigating Electromagnetic Propagation Effects Sep. 1989 8 p (For primary document see N90-14405 06-32)
Copyright Avail: NTIS HC A20/MF A03

The evolution of real time electromagnetic/electro optic propagation assessment systems for the U.S. Navy is reviewed and applications of such systems to the development of Tacitcal Decision Aids (TDAs) are described. Author

N90-14408# Forschungsinstitut fuer Anthropotechnik, Wachtberg (Germany, F.R.).
HUMAN FACTORS ASPECTS OF DECISION SUPPORT SYSTEMS **c54**
K. F. Kraiss *In* AGARD, Operational Decision Aids for Exploiting or Mitigating Electromagnetic Propagation Effects Sep. 1989 14 p (For primary document see N90-14405 06-32)
Copyright Avail: NTIS HC A20/MF A03

Human factors aspects of decision support system (DSS) design and various relevant dimensions are identified in decision making and problems solving, followed by a discussion of characteristics and constraints in human information processing. On this basis, design goals and guidelines are identified. The implementation of DSS concerns the layout of the human computer interface, the degree of automation, as well as the selection of suitable decision aiding algorithms. It is shown that a novel systems architecture is needed to ensure cooperative task performance of the man computer team. Finally various problems of interacting with DSS and a compilation of available operational experience are addressed. Author

N90-14409# Space and Naval Warfare System, Washington, DC. Environmental Systems Program Office.
THE TACTICAL ENVIRONMENTAL SUPPORT SYSTEM (TESS(3)) **c43**
Jack J. Jensen *In* AGARD, Operational Decision Aids for Exploiting or Mitigating Electromagnetic Propagation Effects Sep. 1989 3 p (For primary document see N90-14405 06-32)
Copyright Avail: NTIS HC A20/MF A03

The U.S. Navy has taken an aggressive step toward the analysis and prediction of the performance of tactical sensors and systems at sea. The TESS(3) is one of three key components now under development which will form the basis for state of the art on-scene tactical support. Along with a high resolution satellite receiver/recorder and the automated Shipboard Meteorological and Oceanographic Observing System (SMOOS), TESS(3) is expected to significantly improve the ability of the tactical commander to exploit potential advantages which accrue from a quantitative knowledge of the surrounding environment. Author

N90-14410# Naval Ocean Systems Center, San Diego, CA. Ocean and Atmospheric Sciences Div.
PROPAGATION-BASED DECISION AIDS IN THE U.S. NAVY
Richard A. Paulus *In* AGARD, Operational Decision Aids for Exploiting or Mitigating Electromagnetic Propagation Effects Sep. 1989 9 p (For primary document see N90-14405 06-32)
Copyright Avail: NTIS HC A20/MF A03

The U.S. Navy was using a shipboard radar propagation

assessment system for the past decade. This system was conceived as the Integrated Refractive Effects Prediction System (IREPS) in 1973; tested at sea in 1976; and installed on most capital ships beginning in 1978. IREPS provided two types of products: displays of refractivity data and sensor performance displays. The workhorse display was the radar coverage diagram used by the air wing to determine penetration or jamming altitudes against hostile radars. This initial capability to exploit propagation effects was received so enthusiastically and proved so successful that the development of Tactical Decision Aids (TDAs) became part of an ongoing program to enhance this capability in the fleet. These TDAs structure the propagation information for the decision maker and perform functions that would otherwise overwhelm him. The decision maker is not directed to a specific course of action but rather is provided a framework within which tradeoff decisions can be made with respect to propagation in conjunction with other essential factors of the mission. This approach to the development of an aircraft stationing aid is discussed along with an overview of several TDAs applicable to various warfare areas. Efforts to incorporate these tactical decisions aids into Navy sea-based command and control systems are explored. Author

N90-14411# Naval Ocean Systems Center, San Diego, CA. Ocean and Atmospheric Sciences Div.

ENGINEER'S REFRACTIVE EFFECTS PREDICTION SYSTEM (EREPS)

Herbert V. Hitney *In* AGARD, Operational Decision Aids for Exploiting or Mitigating Electromagnetic Propagation Effects Sep. 1989 10 p (For primary document see N90-14405 06-32)

Copyright Avail: NTIS HC A20/MF A03

In recent years, electromagnetic tactical decision aids were developed to assess environmental effects on the performance of operational systems such as shipboard radars. In general, these systems have performed well and are now routinely used by operational forces to optimize their use of sensors and deployment of forces. In many cases, the existing tactical decision aid software was taken and used to assess the performance of proposed new sensors. Since the original software was not designed for this purpose, many deficiencies in such a use were soon identified. For example, most engineers prefer to graphically compare performance results as a single design parameter, such as radar pulse length, is varied over a range of possible values. Also, in designing a new system, one is usually more interested in the long-term statistical performance than in single-event performance that the tactical decision aids are normally designed to assess. The Engineer's Refractive Effects Prediction System (EREPS) is a recent development effort tailored to engineering uses and based on the propagation models of the Integrated Refractive Effects Prediction System (IREPS). EREPS is hosted on IBM PC computers for maximum availability to the engineering community, and was developed using interactive graphics displays for optimum comparison studies. The models are designed in such a way as to give results within a few seconds to allow multiple design trade-off studies to be easily performed. EREPS Revision 1.00 was distributed to interested users in the summer of 1988 and is currently being revised for a summer 1989 distribution. Existing and planned capabilities will be presented along with some examples of applications. Author

N90-14412# Naval Ocean Systems Center, San Diego, CA. Signals Warfare Div.

PROPHET AND FUTURE SIGNAL WARFARE DECISION AIDS

Robert B. Rose *In* AGARD, Operational Decision Aids for Exploiting or Mitigating Electromagnetic Propagation Effects Sep. 1989 4 p (For primary document see N90-14405 06-32)

Copyright Avail: NTIS HC A20/MF A03

Decision aids, even well designed ones, have demonstrated a wide range of utility and effectiveness when employed in the operational environment. The development and employment of the PROPHET HF propagation assessment system was observed for over a decade. Recent studies indicate that some of the early assumptions on how the module was to be employed were invalid. Although it uniquely fills a real need and its models and products were extensively tested in operational environments by its users, which include most military and civilian branches of the U.S. Department of Defense, PROPHET faces an uncertain future as a stand-alone system. Its main strength is to provide mission oriented and scenario products to perform HF signal coverage, signal vulnerability and radio circuit connectivity in near real time. While technically sound in meeting these objectives, PROPHET's effectivenss is limited by variations in user training, experience, motivation and the lack of operationally convenient access. These problems appear to apply in some degree to the employment of most decision aids. Based on the PROPHET experience, the fallacies that are common in decision aid development and employment, how they affect the decision aid effectiveness, a recommendation for the next generation propagation assessment decision aid results from an initial demonstration prototyping effort to check out some of the new concepts are described. Author

N90-14413# Naval Research Lab., Washington, DC.

DECISION-AID DESIGN FACTORS IN CONNECTION WITH HF COMMUNICATION AND EMITTER LOCATION DISCIPLINES

John M. Goodman *In* AGARD, Operational Decision Aids for Exploiting or Mitigating Electromagnetic Propagation Effects Sep. 1989 9 p (For primary document see N90-14405 06-32)

Copyright Avail: NTIS HC A20/MF A03

The advance of microcomputer technology, the growing sophistication of specified propagation models, and the expanding ability to sense the medium and apply that knowledge in real time is leading to an improvement in the prediction of system performance for tactical users. The maturation of artificial intelligence disciplines should provide the user of advanced C3I decision aids an ability to manage the plethora of information more effectively. Critical aspects of the process of developing useful and cost-effective decision aids are identified with emphasis upon the HF medium which is strongly propagation-limited and controlled by variable and often unpredictable phenomena. A major factor in this field of activity is the evolution of self-adaptive system architecture incorporating imbedded Real Time Channel Evaluation (RTCE). In this context, the decision aid is a process which is operationally transparent to the the user but could be user-defined. A key to the development of an adaptive resource management capability is the integration of a set of tools or decision aids which direct the system to compensate for pathological effects by adjustment of system parameters. The approach is ultimately limited by the accuracy with which the ionosphere or the HF channel may be specified. The accepted specification accuracy will determine the design approaches to be followed. Author

N90-14414# Naval Ocean Systems Center, San Diego, CA. Ocean and Atmospheric Sciences Div.

LONG WAVE PROPAGATION ASSESSMENT

Jerry A. Ferguson and F. Perry Snyder *In* AGARD, Operational Decision Aids for Exploiting or Mitigating Electromagnetic Propagation Effects Sep. 1989 8 p (For primary document see N90-14405 06-32)

Copyright Avail: NTIS HC A20/MF A03

The long wavelength propagation capability of the Naval Ocean Systems Center is described. This capability applies the concept of the earth-ionosphere waveguide to very low frequency (vlf: 10 kHz to 30 kHz) and low frequency (lf: 30 kHz to 100 kHz) radio propagation. It is used to perform assessment of communications coverage at long wavelengths via graphical displays of signal strength and signal to noise over individual propagation paths and over large geographical areas. The propagation assessment capability is a collection of computer programs which are exercised separately or in sequence depending on the application. The execution of these individual programs for purposes of obtaining coverage maps can be set up by a driver program which automates the process. At the present time, this driver program implements the sequencing of the programs via Digital Equipment's VAX VMS control language. The automation of the calculations depends on accurate specification of the parameters of the earth-ionosphere waveguide. The driver program contains models for these parameters which were developed over a number of years. The

model of the ionsphere is an approximate one which characterizes the conductivity as an exponentially increasing function of height. Some allowance for the nighttime differences between temperate and polar latitudes is made. The lower boundary of the waveguide is defined by a detailed ground conductivity map based on geological formations. Author

N90-14415# Hull Univ. (England). Dept. of Electronic Engineering.
A COMMUNICATIONS SYSTEM WITH AN ADAPTIVE MULTI-FUNCTIONAL ARCHITECTURE
A. H. Kemp *In* AGARD, Operational Decision Aids for Exploiting or Mitigating Electromagnetic Propagation Effects Sep. 1989 10 p Sponsored by British Science and Engineering Research Council (For primary document see N90-14405 06-32)
Copyright Avail: NTIS HC A20/MF A03

Within NATO's area of operations, high frequency (HF) channels exhibit an inherently variable capacity. Furthermore there is also a wide geographical variety of noise sources; in North America atmospheric noise is significant while, in Western Europe, a dominant noise source is co-channel interference. A communications system which can operate across this whole region needs to be both highly adaptive and have a real-time channel evaluation (RTCE) capability. To allow a system to manage multiple adaptive components in an optimum manner while the system configuration and RTCE data vary, a multi-functional regime is proposed. The design and implementation of such an adaptive, multi-functional communications system are described. Author

N90-14416# Naval Ocean Systems Center, San Diego, CA. Ocean and Atmospheric Sciences Div.
AIRBORNE FLIR DETECTION OF SURFACE TARGETS c43
Herbert G. Hughes *In* AGARD, Operational Decision Aids for Exploiting or Mitigating Electromagnetic Propagation Effects Sep. 1989 12 p Sponsored by Office of Navy Technology (For primary document see N90-14405 06-32)
Copyright Avail: NTIS HC A20/MF A03

An algorithm is presented for predicting the detection ranges of a surface target by an airborne Forward Looking Infrared (FLIR) system. The total infrared background radiance scene under cloud-free skies is modeled to include the atmospheric path emissions between the target and sensor and the effects of a wind ruffled sea on the surface emissions and sky radiance reflections. A model is also introduced of the average temperature of a ship based upon the solar heating effects throughout a specified course, the ambient meteorological conditions, and the viewing angle. Together, these two models allow the range to be determined where the difference between the apparent ship's temperature (i.e., the actual ship temperature degraded by the atmospheric trasmittance) and the effective background temperature of the sea surface as viewed from the sensor altitude is equal to the minimum detectable temperature difference of the FLIR. A case study is presented to demonstrate the vulnerability of a Frigate class ship to detection by an airborne common module FLIR during a five hour period where the ship's course changed allowing solar heating of different sides of the ship. The results show considerable increases in predicted detection ranges with altitude using the present algorithm over those based on a fixed temperature difference between a target and its background. Author

N90-14417# National Defence Academy, Yokosuka (Japan). Dept. of Electrical Engineering.
HYBRID PE-RAY-MODE FORMULATION OF HIGH FREQUENCY PROPAGATION IN A BILINEAR TROPOSPHERIC SURFACE DUCT c12
T. Ishihara and L. B. Felsen (Polytechnic Univ., Farmingdale, NY.) *In* AGARD, Operational Decision Aids for Exploiting or Mitigating Electromagnetic Propagation Effects Sep. 1989 15 p Sponsored by Naval Ocean Systems Center, San Diego, CA (For primary document see N90-14405 06-32)
Copyright Avail: NTIS HC A20/MF A03

Prediction of signal strengths due to high frequency sources in the presence of a tropospheric surface or elevated duct poses a problem of substantial complexity because the propagation environment is generally heterogeneous in height as well as in the lateral domain. A prediction algorithm should not only furnish adequate accuracy but also incorporate a parameterization in terms of physical observables so that the output can be properly interpreted. Relevant physical observables include ray fields, normal (trapped) and leaky mode fields, and beam-like (parabolic) propagators. These observables are employed here in self-consistent hybrid combination to model propagation in a laterally homogeneous surface duct with bilinear refractive index profile in height. A reference solution, which was generated by normal and leaky mode summation, is interpreted qualitatively in terms of the corresponding ray field plot. Work is in progress on a quantitative reconstruction of the reference data via the hybrid algorithm. Author

N90-14418# Johns Hopkins Univ., Laurel, MD. Applied Physics Lab.
THE PARABOLIC EQUATION APPROACH TO PREDICTING TROPOSPHERIC PROPAGATION EFFECTS IN OPERATIONAL ENVIRONMENTS
G. Daniel Dockery and Eric R. Thews *In* AGARD, Operational Decision Aids for Exploiting or Mitigating Electromagnetic Propagation Effects Sep. 1989 9 p Sponsored by Naval Sea Systems Command (For primary document see N90-14405 06-32)
Copyright Avail: NTIS HC A20/MF A03

The Electromagnetic Parabolic Equation (EMPE) propagation program was demonstrated to predict accurately the propagation of electromagnetic energy in environments with complicated refractivity characteristics. The validation and application of EMPE have also necessitated the development of new atmospheric measurement techniques as well as methods for representing realistically the range variations of refractivity structures. A brief description of the parabolic equation approach and solution technique is first presented; comparisons with other propagation models are included. The measurement techniques that were used to obtain accurate, high-resolution refractivity data are then discussed. Examples of how such refractivity data, in conjunction with a refractivity range-interpolation algorithm, were used in EMPE to obtain good agreement with measured signal levels are also presented. The problem of developing a useful decision aid for operational systems based on the EMPE program is then addressed. The issues that are discussed include vertical and horizontal resolution of atmospheric data, timeliness of measurements, speed of propagation calculations, use of refractivity models, and automation of the environmental assessment process. An approach that is being pursued at APL for AEGIS shipboard applications, involving the use of expendable rocketborne radiosondes, is described. Author

N90-14419# Naval Ocean Systems Center, San Diego, CA. Ocean and Atmospheric Sciences Div.
RPE: A PARABOLIC EQUATION RADIO ASSESSMENT MODEL
F. J. Ryan *In* AGARD, Operational Decision Aids for Exploiting or Mitigating Electromagnetic Propagation Effects Sep. 1989 10 p Sponsored in part by Office of Naval Technology (For primary document see N90-14405 06-32)
Copyright Avail: NTIS HC A20/MF A03

The use of parabolic wave equation codes to model tropospheric radio propagation is rapidly gaining popularity. To properly implement these powerful techniques into radar performance assessment models, requires a detailed understanding of the inherent errors in the parabolic approximation. Three major sources of errors in split-step parabolic equation solvers are examined: approximation of the elliptic wave operator by a parabolic operator, truncation error in the formal parabolic solution and truncation error in the split-step operator. These errors are discussed in the context of operational codes. Author

N90-14420# Science Research Council, Chilton (England). Radio Communications Research Unit.
A FORECASTING SYSTEM USING THE PARABOLIC EQUATION: APPLICATION TO SURFACE-TO-AIR PROPAGATION IN THE PRESENCE OF ELEVATED LAYERS
K. H. Craig and M. F. Levy *In* AGARD, Operational Decision Aids for Exploiting or Mitigating Electromagnetic Propagation Effects Sep. 1989 13 p Sponsored in part by Procurement Executive, Min istry of Defence (For primary document see N90-14405 06-32)
Copyright Avail: NTIS HC A20/MF A03

The parabolic equation approach to clear-air propagation modeling overcomes many of the difficulties associated with ray and mode theory methods. A parabolic equation model was implemented on a PC based system using a transputer to carry out the computationally intensive numerical integrations. The model was used from VHF to millimetric frequencies and applied to evaporation duct and elevated duct problems. The latter are important for surface-to-air propagation and were difficult to solve because of the complicated structure of the layers. A case study of an elevated duct caused by anticyclonic subsidence shows the importance of up-to-date meteorological data from a wide geographical area. A full-wave calculation of the wideband properties of the propagation channel illustrates the possibilities opened up by the new model. The frequency selective effects can be large, and are sensitive to the small-scale structure of the ducting layers. Author

N90-14421# Thomson-CSF, Velizy (France). Centre d'Applications Radars.
ANALYSIS OF PROPAGATION IN AN INHOMOGENEOUS ATMOSPHERE IN THE HORIZONTAL AND VERTICAL DIRECTION USING THE PARABOLIC EQUATION METHOD
Michel Fournier *In* AGARD, Operational Decision Aids for Exploiting or Mitigating Electromagnetic Propagation Effects Sep. 1989 13 p In FRENCH; ENGLISH summary (For primary document see N90-14405 06-32)
Copyright Avail: NTIS HC A20/MF A03

Operational programs calculating radar coverage are now available on ships having a meteorological capability. A fundamental assumption of these programs is that only vertical variations of refraction index are known and consequently that the atmosphere is homogeneous along the propagation path in the horizontal direction. Measurements made by the French Meteorological Office and by other countries established that this hypothesis may be inconsistent during significal laps of time. Consequently it seems necessary to develop a tool to compare of existing operational programs and those given by more sophisticated programs which are able to take into account variations of refractive index in vertical and horizontal directions. A resolution method of this problem, using the parabolic equation is described. This tool was used for exploitation of index of refraction map from in situ measurements obtained during tests made over the Atlantic Ocean and the Mediterranean Sea. Exploitation of these data allows a study of the effect of horizontal index inhomogeneities of the atmosphere in horizontal direction. Author

N90-14422# Naval Ocean Systems Center, San Diego, CA. Ocean and Atmospheric Sciences Div.
PROPAGATION MODELING FOR SOME HORIZONTALLY VARYING TROPOSPHERIC DUCTS
Richard A. Pappert *In* AGARD, Operational Decision Aids for Exploiting or Mitigating Electromagnetic Propagation Effects Sep. 1989 15 p (For primary document see N90-14405 06-32)
Copyright Avail: NTIS HC A20/MF A03

For propagation assessment in a maritime environment, the assumption of horizontal homogeneity (i.e., invariance of the refractivity structure along the path of propagation) is generally adequate (Hitney et al., 1985). Nevertheless, theoretical methods are available to handle special cases when the assumption fails. For example, horizontal inhomogeneity can in principle be treated by mode conversion methods or by parabolic equation solvers. The theory for a slab mode conversion model is discussed within the context of modified refractive index formalism and applied to several hypothetical laterally inhomogeneous problems including elevated layers as well as shallow evaporative layers. Results of the mode conversion calculations are compared with parabolic equation results generated concurrently by Ko and Burkom (1987). Most of the comparisons, along with the ease of implementation and speed of the parabolic equation calculations relative to the mode conversion analysis, strongly supports the superiority of the parabolic equation method for systems studies involving laterally inhomogeneous tropospheric layering. Author

N90-14423# Dornier System G.m.b.H., Friedrichshafen (Germany, F.R.). Management Consulting.
PROPAGATION PREDICTION FOR THE NORTH SEA ENVIRONMENT
R. Vieth *In* AGARD, Operational Decision Aids for Exploiting or Mitigating Electromagnetic Propagation Effects Sep. 1989 7 p (For primary document see N90-14405 06-32)
Copyright Avail: NTIS HC A20/MF A03

Evaporation ducting can have an important influence on the propagation of electromagnetic waves. The dependence of those ducting conditions on geographic location requires an estimate of occurrence and effects of ducting in various areas. Duct height statistics using long term statistical meteorological data in combination with propagation models are used for this purpose. Jeske's propagation measurements during 1961 at the German coast of the North Sea were taken and compared with the calculated results from the combination of the statistical weather data base and the propagation models, as well as another measurement program performed in Greece. A brief description of the models is followed by an example of the results of the Greek measurements. The German experimental data and duct height distributions for that region are described. Finally the results of measurements and calculations are discussed. A good agreement was found between measured propagation data and predictions based on climatological averages. Author

N90-14424# Science Research Council, Chilton (England). Radio Communications Research Unit.
ASSESSMENT OF ANOMALOUS PROPAGATION PREDICTIONS USING MINISONDE REFRACTIVITY DATA AND THE PARABOLIC EQUATION METHOD
M. F. Levy and K. H. Craig *In* AGARD, Operational Decision Aids for Exploiting or Mitigating Electromagnetic Propagation Effects Sep. 1989 12 p Sponsored in part by Procurement Executive, Ministry of Defence (For primary document see N90-14405 06-32)
Copyright Avail: NTIS HC A20/MF A03

Accurate and easy-to-use systems are now available to measure the refractive index structure in the troposphere. Combined with an efficient package for solving Maxwell's equations for radiowave propagation based on the Parabolic Equation Method, they provide a powerful tool for real time forecasts of anomalous propagation. Quantitative field-strength predictions can be obtained in a few minutes from measured meteorological profiles, on a desk-top computer. However, measurement errors inevitably lead to variability in the predictions, which should be seen in a stochastic light. Some examples based on experimental data are presented, at X-band and in the millimetre wave part of the spectrum, as well as a sensitivity analysis using statistical simulations. The Parabolic Equation Method copes well with noisy refractivity data, and the predictions are fairly insensitive to radiosonde errors. Author

N90-14425# Mitre Corp., Eatontown, NJ.
FORWARD SCATTER PROPAGATION PATH LOSS TESTING USING SURROGATE TERRAIN IN THE 100 TO 1500 MHz REGION
Louis L. Taylor *In* AGARD, Operational Decision Aids for Exploiting or Mitigating Electromagnetic Propagation Effects Sep. 1989 12 p (For primary document see N90-14405 06-32)
Copyright Avail: NTIS HC A20/MF A03

Numerous path loss calculation models were developed for

links employing forward scatter propagation. Variances in propagation loss prediction between these models and the loss experienced when a link is actually established arise because of the manner in which the models represent the large variety of absorbers and reflectors present in the actual terrain. A method to enrich a model with actual measurements that produce a more accurate method of predicting propagation loss is described. The method is based upon selecting a surrogate section of terrain for the actual terrain over which a propagation loss determination is desired, then measuring the forward scatter loss variation through this surrogate terrain. The loss value is then used as a factor in the simplified mathematical model used for the desired prediction. Examples are given of the use of this technique to assist in the design and implementation of a wide area VHF/UHF radio network serving a large fleet of mobile units. Through use of this method, one learns to judge when existing models may be used and when measurements are indicated, how to estimate the effects of different types of terrain and foliage upon propagation, and how these effects change in different seasons of the year. Author

N90-14426# Institut National des Sciences Appliquees, Rennes (France). Laboratoire Composants et Systemes pour Telecommunications.

IMPROVING THE QUALITY OF A SPREAD-SPECTRUM RADIOMOBILE LINK

A. Daniel, G. ElZein, M. Salehudin, and J. Citerne *In* AGARD, Operational Decision Aids for Exploiting or Mitigating Electromagnetic Propagation Effects Sep. 1989 9 p In FRENCH (For primary document see N90-14405 06-32)

Copyright Avail: NTIS HC A20/MF A03

A means for improving the quality of a digital spread-spectrum mobile radio link with the aid of a multipath diversity system is described. The novelty of the system lies in the use of a transverse filter designed using a surface acoustic wave (SAW) multiconnector delay line and adapted to the pulse response of the channel (obtained through a convoluter). The adaptation of the receiver to the channel transmission parameters is accomplished with an instantaneous coefficient of balance. The multipaths are then combined in order to eliminate, as well as possible, the selective fading occurring with a mobile radio link. Transl. by M.G.

N90-14427# Centre National d'Etudes des Telecommunications, Lannion (France).

NEW PERSPECTIVES FOR THE INVERSION OF BACKSCATTER IONOGRAMS

N. Ruelle, J. Y. LeSaout, and L. Bertel (Rennes Univ., France) *In* AGARD, Operational Decision Aids for Exploiting or Mitigating Electromagnetic Propagation Effects Sep. 1989 9 p (For primary document see N90-14405 06-32)

Copyright Avail: NTIS HC A20/MF A03

High frequency (HF) backscatter sounders offer the perspective of real-time sensing of ionospheric radio propagation conditions in an extended area. However, to this date, difficulties are experienced with the interpretation of sounding data, which places a severe limit on the operational use of these sounders. The French National Telecommunications Research Centre is constructing a sounder of original design. The new possibilities for data interpretation offered by this system are evaluated and possible operational implications discussed. Author

N90-14428# Illinois Univ., Urbana-Champaign.

DESIGN OF A COMPENSATION FILTER FOR A QUADRATIC PHASE COMMUNICATION CHANNEL

K. C. Yeh and R. L. Mickelson *In* AGARD, Operational Decision Aids for Exploiting or Mitigating Electromagnetic Propagation Effects Sep. 1989 14 p (For primary document see N90-14405 06-32)

(Contract DAAB07-87-K-A0006)

Copyright Avail: NTIS HC A20/MF A03

There was always great interest in understanding and describing the dispersive effects that occur in many types of communication channels. An analysis of a general dispersive channel is performed by a set of weighted delay lines. This model clearly illustrates that mitigation of dispersive effects can be achieved via an inverse filtering procedure. Specifically, a compensation filter is designed using a conjugate delay line. Ideally, complete compensation can be achieved and a replica of the transmitted signal can be restored. In practical implementation and application, these idealized conditions can never be met. Nevertheless, this channel simulator and compensation filter are implemented for a quadratic phase transfer function. The system is tested for three basic signals: Gaussian pulse, rectangular pulse, and sudden phase-switched signal. In addition, the case of transmitting multiple pulses is considered. The simulation yields good results for moderate dispersion. As dispersiveness increases, the number of taps in the compensation filter must be increased in order to restore the received signal to a reasonable approximation of its original shape. Author

N90-14429# Signatron, Inc., Lexington, MA.

IMPROVED RELIABILITY PREDICTION FOR HF DIGITAL VOICE TRANSMISSION

Alfonso Malaga *In* AGARD, Operational Decision Aids for Exploiting or Mitigating Electromagnetic Propagation Effects Sep. 1989 10 p (For primary document see N90-14405 06-32)

Copyright Avail: NTIS HC A20/MF A03

A method for predicting the performance of High Frequency (HF) digital voice transmission is described. The method takes into account the effects of multipath propagation and signal processing techniques which exploit the multipath to achieve improved performance. A propagation prediction model which provides the necessary multipath and signal-to-noise ratio statistics is also described. Author

N90-14430# Air Force Systems Command, Hanscom AFB, MA. Ionospheric Physics Lab.

A MODERN TRANS-IONOSPHERIC PROPAGATION SENSING SYSTEM

G. J. Bishop, J. A. Klobuchar, A. E. Ronn, and M. G. Bedard (Air Weather Service, Scott AFB, IL.) *In* AGARD, Operational Decision Aids for Exploiting or Mitigating Electromagnetic Propagation Effects Sep. 1989 11 p (For primary document see N90-14405 06-32)

Copyright Avail: NTIS HC A20/MF A03

One of the most important potential problems with modern military systems which utilize spacecraft is the effect of the ionosphere on the radio signals which pass to and from the spacecraft. Such systems include active communications and navigation satellites as well as both ground-based and potential space-based ranging systems. The major effects the ionosphere can have on such systems are the additional time delay the electrons in the earth's ionosphere add to the free space path delay, the short term rate of change of this additional delay, amplitude scintillation or fading effects the signal encounters due to irregularities in the ionosphere, and Faraday rotation of linearly polarized radio waves transmitted through the ionosphere. While some of these effects were studied adequate models of these effects on military systems still do not exist. A modern trans-ionospheric sensing system, called TISS, is being procured which will consist of a number of stations located throughout the world, making real time measurements of the time delay of the ionosphere, and its rate of change, as well as amplitude scintillation, along several different viewing directions from each station. These trans-ionospheric measurements will be used to allow models, which currently provide only monthly propagation parameters. The real-time specifications of these parameters can then be used as decision aids in both the tactical and the strategic military environments. The TISS will include first order artificial intelligence design to aid in gathering the most appropriate sets of available real-time trans-ionospheric propagation data, and will communicate these data sets to the Air Weather Service Forecasting Center where they will be tailored to specific military customers. Author

N90-14431# Lowell Univ., MA. Center for Atmospheric Research.
A PORTABLE IONOSONDE IN SUPPORT OF RELIABLE COMMUNICATIONS
D. Mark Haines, D. F. Kitrosser, B. W. Reinisch, and F. J. Gorman (Army Communications-Electronics Command, Fort Monmouth, NJ.) *In* AGARD, Operational Decision Aids for Exploiting or Mitigating Electromagnetic Propagation Effects Sep. 1989 8 p (For primary document see N90-14405 06-32)
Copyright Avail: NTIS HC A20/MF A03

The temporal and spatial variations in ionospheric structure have frustrated the efforts of communications and radar system operators who base their frequency management decisions on monthly mean predictions or computer based models. A low power miniature version of the Digisonde sounders capable of making real-time on-site measurements to support communications or surveillance operations was produced. The system compensates for a low power transmitter by employing intrapulse phase coding, digital pulse compression and Doppler integration. The data acquisition, control, signal processing, display, storage and automatic data analysis functions were all condensed into a single multi-tasking, multiple processor computer system while the analog circuitry was condensed and simplified by use of reduced transmitter power, wide bandwidth devices, and commercially available PC expansion boards. Noteworthy new technology involved in this system includes: an electronically switched active crossed dipole receiving antenna; a TMS 320C25 digital signal processor; compact DC-DC converters allowing full operation on a single 24 VDC battery; a high speed data acquisition board interfaced via an IBM-AT expansion bus; a proprietary multi-tasking operating system; reprogrammable PROM based coherent oscillators; use of complementary codes which virtually eliminate the time domain pulse compression sidelobes typical of pulse compression systems; and automatic mode identification and parameter scaling by an embedded expert system. Author

N90-14432# Centre National d'Etudes des Telecommunications, Lannion (France).
CORRECTION OF IONOSPHERIC EFFECTS FOR THE PRECISE ORBIT DETERMINATION OF SATELLITES **c13**
F. Foucher, R. Fleury, and P. Lassudrie-Duchesne *In* AGARD, Operational Decision Aids for Exploiting or Mitigating Electromagnetic Propagation Effects Sep. 1989 12 p (For primary document see N90-14405 06-32)
Copyright Avail: NTIS HC A20/MF A03

In the near future, space missions in altimetry, geodesy, or precise positioning will often require satellite orbits to be determined with subdecimetric accuracies. In orbit determination systems extensive use is made of Doppler measurements performed on radio signals propagating between the satellite and ground stations. Such systems, however, are highly sensitive to propagation errors brought about by the atmosphere. The effects of the ionosphere on Doppler measurements is assessed and a model of the ionospheric error is described. A correction scheme is examined for orbit determination systems based on Doppler data. Particular emphasis is placed on the post-processing of the Doppler data from the DORIS system, a precise orbit determination system designed for remote sensing satellites of the new generation. Simulation results show that the major part of the ionospheric error can be removed by model correction. Author

N90-14433# Hull Univ. (England). Communications Research Group.
THE USE OF BROADCAST SIGNALS FOR PASSIVE SENSING IN AUTOMATED HF COMMUNICATION SYSTEMS
N. G. Riley *In* AGARD, Operational Decision Aids for Exploiting or Mitigating Electromagnetic Propagation Effects Sep. 1989 8 p (For primary document see N90-14405 06-32)
Copyright Avail: NTIS HC A20/MF A03

The use of passive sensing for derivation of HF system control data has advantages over active techniques from both tactical and spectrum conservation points of view. Methods are described by which ionospheric data may be derived from passive sensing of the HF spectrum. Data derived using these techniques may be used in the operational decision process to control automated HF communication systems. The techniques described are facilitated by the availability of powerful, low-cost signal processors and fast tuning receivers allowing a high level of signal processing to be performed in real time. Author

N90-14434# Paris-Sud Univ., Cachan (France).
THE USE OF BACKSCATTER FOR MODELLING IONOSPHERE AND JAMMING IN VERY SHORT TERM FORECASTS
J. Caratori and C. Goutelard *In* AGARD, Operational Decision Aids for Exploiting or Mitigating Electromagnetic Propagation Effects Sep. 1989 16 p In FRENCH; ENGLISH summary (For primary document see N90-14405 06-32)
Copyright Avail: NTIS HC A20/MF A03

High frequency (HF) radio links involving reflection from the ionosphere are mainly long-range communications. The setting up of an optimum link, requires the knowledge of the real propagation and interference data. Several types of ionospheric predictions, based on different ionospheric soundings, are necessary in order to take account of the medium variability. A centralized backscatter sounding station is well adapted to provide short-term predictions. However, the interpretation of the data, and the inversion of the ionogram are difficult. A method of inversion, taking account of horizontal gradients is proposed. Experiments carried out at the station studio of the Letti showed its validity. Interferences are very important in the HF band, and represent the second factor to deal with. The spatial decorrelation of interferences is highlighted, and the derivation of predictions for the Western Europe zone is discussed. These predictions are then used to compute the signal to noise ratio of a link. Author

N90-14435# Massachusetts Technological Lab., Inc., Bethesda, MD.
COMMUNICATION OVERVIEW PROGRAM (COP)
D. J. Fang, I. Benoliel, and H. Soicher (Army Communications-Electronics Command, Fort Monmouth, NJ.) *In* AGARD, Operational Decision Aids for Exploiting or Mitigating Electromagnetic Propagation Effects Sep. 1989 8 p (For primary document see N90-14405 06-32)
Copyright Avail: NTIS HC A20/MF A03

In establishing a communications system for fulfilling a given mission requirement, multiple levels of decision-making processes are encountered. The decision making process at the lowest level, such as subsystem design and component specification can be accomplished by known routines and procedures, or even by computer packages known as CAD. The middle level of decision-making involves professional articulation as the processes generally involve trade-off's and optimization. As such, engineering prejudice, preference and experience play a significant role. The highest level of decision making, because of its nature, generally is more policy oriented rather than technically oriented. In this level, a broad view including the background, the finance, priority and other administrative concerns are included for decision. The unfortunate part of this is that the decision makers often do not have the necessary insight in making a proper technical decision which has a profound and unequivocal impact on the implementation at lower levels. The Communication Overview Program (COP) is being developed for applications at the highest level of decision-making. The program is not a design tool but is intended to provide the necessary scenarios and technical insights to assure a correct decision can be made for the establishment of a communications system to carry out a given mission. Author

N90-14436# German Military Geophysical Office, Traben-Trarbach (Germany, F.R.).
THE THERMAL BEHAVIOR OF NATURAL BACKGROUNDS AND ITS PREDICTION BY MEANS OF NUMERICAL MODELS **c43**
Fritz G. Wollenweber *In* AGARD, Operational Decision Aids for Exploiting or Mitigating Electromagnetic Propagation Effects Sep.

1989 12 p (For primary document see N90-14405 06-32)
Copyright Avail: NTIS HC A20/MF A03

The Federal Office for Military Technology and Procurement together with the German Military Geophysical Office (GMGO) are conducting a research effort to establish procedures to describe and to predict thermal behavior of natural backgrounds under varying meteorological conditions. The experimental phase of this effort started in 1988 with measurements of surface temperatures of different backgrounds like trees, crops, pasture, roads and buildings together with meteorological measurements. These measurements are conducted in two geographical locations, the Meppen proving ground in Northern Germany and Oberjettenberg proving ground in the Alps. The measurement campaign has a time frame of at least one year with measurements taking place during three days each month. It is anticipated to gather a data set that reflects the full range of thermal backgrounds for tactically important locations in Central Europe. One objective of this effort is to compare and evaluate thermal background models that are under development as a companion task. The results of the Meppen '85 experiment, a pilot study to this campaign, are presented. The results are compared with predictions of the current version of the U.S. Air Force Tactical Decision Aid (USAF TDA) and with the thermal background model CANOPY developed by GMGO. The GMGO model determines energy exchange within canopies with a multi-layer approach for energy, moisture, and momentum fluxes. In comparison with measurements the GMGO model performs much better than the USAF IR-TDA model. Differences between model results can be explained by the neglect of latent heat flux in the USAF TDA model for vegetation backgrounds and its semi-statistical approach. Author

N90-14437# Defence Research Establishment Valcartier (Quebec).

REMOTE SENSING OF THE AEROSOL SCATTERING COEFFICIENT WITH A MULTI-FIELD-OF VIEW LIDAR **c43**

Luc R. Bissonnette and Daniel L. Hutt *In* AGARD, Operational Decision Aids for Exploiting or Mitigating Electromagnetic Propagation Effects Sep. 1989 13 p (For primary document see N90-14405 06-32)
Copyright Avail: NTIS HC A20/MF A03

A new lidar technique is proposed for the remote determination of the obscuration effects of natural and man-made aerosols. It is based on the simultaneous measurement of the lidar returns at different fields of view. By ratioing these returns, the need is eliminated for a backscatter-to-extinction relation which makes the inversion of the single-scattering lidar-measurements subject to uncertainties. A system operating at 1.054 micrometers and fields of view of 5, 25, 50, and 75 mrad is described. Preliminary results are discussed. Author

N90-14438# Naval Postgraduate School, Monterey, CA. Dept. of Meteorology.

PHYSICAL MODELS FOR AEROSOL IN THE MARINE MIXED-LAYER

Gerrit deLeeuw, Kenneth L. Davidson, Stuart G. Gathman, and R. V. Noonkester (Naval Ocean Systems Center, San Diego, CA.) *In* AGARD, Operational Decision Aids for Exploiting or Mitigating Electromagnetic Propagation Effects Sep. 1989 8 p (For primary document see N90-14405 06-32)
Copyright Avail: NTIS HC A20/MF A03

A model is presented to calculate the vertical variation of aerosol extinction coefficients throughout the marine atmospheric boundary layer. It is referred to as the Naval Oceanic Vertical Aerosol Model (NOVAM). NOVAM is a combination of empirical and physical models, formulated to describe the often observed non-uniform, but also non-logarithmic, profiles. The physical model is based on the dynamical processes affecting the production, mixing, deposition and size of the aerosol within the marine atmosphere. A status report is presented including a critical evaluation.

Author

N90-14439# Forschungsinstitut fuer Hochfrequenzphysik, Werthhoven (Germany, F.R.).

LOW LEVEL RANGE COVERAGE PERFORMANCE PREDICTION FOR VHF RADAR

H. Kuschel *In* AGARD, Operational Decision Aids for Exploiting or Mitigating Electromagnetic Propagation Effects Sep. 1989 13 p (For primary document see N90-14405 06-32)
Copyright Avail: NTIS HC A20/MF A03

A VHF radar frequencies the range coverage is not strictly limited by the quasi-optical horizon like at microwave radar frequencies but is extended due to diffraction propagation. This effect, here called beyond-the-horizon (BTH) detection capability is strongly dependent on the propagation path and thus on the terrain structure. The availability of digital terrain maps gives way to the use of computerized methods for the prediction of radar range coverage in real environment. In combination with wave propagation models suitable for diffraction at terrain structures, digital terrain data can even be used for the prediction of BTH target detectability at VHF radar. Here the digital landmass system (DLSS) terrain database was used in combination with a multiple-knife-edge diffraction model to predict the diffraction attenuation between the radar and the potential target positions, especially beyond the optical horizon. The propagation paths extracted from the database are modeled as a sequence of diffraction screens suited for the application of a Fresnel-Kirchhoff algorithm yielding the knife-edge-diffraction attenuation. This terrain related propagation model was verified by a large number of measurements at different frequencies. Implemented in a fast computer system, this prediction model can be used for mission planning of air operations. Considering hostile VHF radar coverage and terrain condition for flight path optimization or, on the other hand it can assist in siting mobile radars for gap filling according to the actual threat situation. Calculations of the diffraction propagation using the prediction model, yield range coverage patterns in real terrain situations, allowing to quantify the BTH detection advantage of VHF radar compared to microwave radar. An experimental large wavelength radar LARA (VHF) built flying targets beyond the close horizon. Here, especially the detection of hiding helicopters by exploiting diffractive wave propagation was examined. Measurements at different VHF frequencies were carried out, to validate the results obtained by simulation. Author

N90-14440# Organisatie voor Toegepast Natuurwetenschappelijk Onderzoek, The Hague (Netherlands). Physics and Electronics Lab.

THE EFFECT OF OBLATE SPHEROIDAL DROPS ON RAIN ATTENUATION AT 94 GHz: COMPARISON BETWEEN THEORY AND EXPERIMENT

W. P. M. N. Keizer *In* AGARD, Operational Decision Aids for Exploiting or Mitigating Electromagnetic Propagation Effects Sep. 1989 10 p (For primary document see N90-14405 06-32)
Copyright Avail: NTIS HC A20/MF A03

Rain induced attenuations for horizontally and vertically polarized waves at 94 GHz were measured on a 935 m link and compared with theoretical predictions. During the experiment which covered a period of two years the raindrop size distribution along the propagation was also recorded. The theoretical predictions were based on the actually measured raindrop size distributions and assumed both spherical and spheroidal shapes for the raindrops. The calculations for oblate spheroidal raindrops showed that horizontally polarized waves are more attenuated by rain than vertically polarized waves. It was also found that the Mie scattering theory for spherical raindrops underestimates the rain attenuation for both polarizations. The comparison of the measured rain attenuation results with the predictions confirmed completely the outcome of the theoretical calculations. A remarkable improvement in the accuracy of rain attenuation modeling for horizontal and vertical polarization was noted when a spheroidal drop shape was taken into account instead of the spherical shape. Author

N90-14441# Hava Ikmal Bakim Merkezi Komutanligi, Ankara (Turkey).
MITIGATING DOPPLER SHIFT EFFECT IN HF MULTITONE DATA MODEM
Yasar Sonlu *In* AGARD, Operational Decision Aids for Exploiting or Mitigating Electromagnetic Propagation Effects Sep. 1989 8 p (For primary document see N90-14405 06-32)
Copyright Avail: NTIS HC A20/MF A03

Digital communications over High Frequency (HF) radio channels are getting important in recent years. Current HF requirements are for data transmission at rates 2.4 kbps or more to accomodate computer data links and digital secure voice. HF modems which were produced to meet these speeds are, serial modems and parallel modems. On the other hand, the HF sky-wave communication medium, the ionosphere, has some propagation problems such as multipath and Doppler shift. The effect of Doppler shift in a parallel modem which employs Differential Quadrature Phase Shift Keying (DQPSK) modulation is considered and a correction method to mitigate the Doppler Shift effect is introduced. Author

N90-14442# Naval Environmental Prediction Research Facility, Monterey, CA.
A ONE-DIMENSIONAL SHIPBOARD MODEL FOR FORECASTING REFRACTIVE EFFECTS IN THE PLANETARY BOUNDARY LAYER
Paul M. Tag *In* AGARD, Operational Decision Aids for Exploiting or Mitigating Electromagnetic Propagation Effects Sep. 1989 4 p (For primary document see N90-14405 06-32)
Copyright Avail: NTIS HC A20/MF A03

In order to forecast the refractivity structure in the atmosphere, the accompanying temperature and moisture structures must be forecast. As a means of providing shipboard-generated forecasts of low-level temperature and moisture structures in the planetary boundary layer, the Navy has converted a sophisticated, turbulence model to a micro-computer. This model, called the Navy Over-Water Local Atmospheric Prediction System (NOWLAPS), is part of the Tactical Environmental Support System (TESS), a shipboard, automated, environmental diagnosis/prediction system. NOWLAPS is a one-dimensional, second order closure model that can provide forecasts over water for temperature, moisture, and winds up to heights of 2 km, and out to 24 hrs. From these temperature and moisture distributions, the refractivity profile can be generated. Author

N90-14443# Pacific Missile Test Center, Point Mugu, CA. Geophysics Div.
WEATHER SATELLITE AND COMPUTER MODELING APPROACHES TO ASSESSING PROPAGATION OVER MARINE ENVIRONMENTS
Jay S. Rosenthal, Roger A. Helvey, Steven W. Lyons (Texas A&M Univ., College Station.), Alan D. Fox, Richard Szymber, and Lee Eddington *In* AGARD, Operational Decision Aids for Exploiting or Mitigating Electromagnetic Propagation Effects Sep. 1989 15 p (For primary document see N90-14405 06-32)
Copyright Avail: NTIS HC A20/MF A03

Exploiting electromagnetic propagation in the Navy's marine environment requires an ability to assess and predict atmospheric refractive structure over the ocean. Efforts are underway to develop such capabilities by correlating duct existence, height and intensity to synoptic and mesoscale weather features. In addition to the latter conventional parameters, meteorological satellite data, through pattern recognition was valuable in inferring important aspects of ducting conditions. More recently, a technique was developed to derive duct height information directly from computer-processed infrared (IR) satellite data over ocean regions capped by stratified low clouds. This approach, still in development, also provides a means of measuring the horizontal variability of duct height which is crucial to determining the appropriateness and useability of various propagation models for predicting systems performance. Inferring the impact of horizontal variability over the ocean was facilitated by use of range-dependent raytrace techniques which allow inputs from such diverse sources as local radiosonde observations; predicted marine layer depth (from a mixed-layer mesoscale model); and duct heights derived from the satellite-IR duct technique. Author

N90-14444# Signatron, Inc., Lexington, MA.
TROPO: A TECHNIQUE FOR PREDICTING PROPAGATION AND MODEM PERFORMANCE OF DIGITAL TROPOSCATTER SYSTEMS
Steen A. Parl *In* AGARD, Operational Decision Aids for Exploiting or Mitigating Electromagnetic Propagation Effects Sep. 1989 9 p (For primary document see N90-14405 06-32)
Copyright Avail: NTIS HC A20/MF A03

The capabilities of a PC-based decision aid for digital troposcatter link engineering are presented. The program includes propagation effects such as multipath and spatial diversity, as well as adaptive modem performance, transmitter emission control filtering. The model uses the existing NBS method for predicting long term effects and for short-term effect below 1 GHz. Above 1 GHz it uses a turbulent volume scattering model. It uses numerical integration whenever possible to avoid coarse analytical approximations. A key function is its ability to evaluate advanced diversity receiver and modem techniques. A predecessor of this program was used by the USAF to evaluate and engineer current and planned digital troposcatter links. Author

N90-14445# Organisatie voor Toegepast Natuurwetenschappelijk Onderzoek, The Hague (Netherlands). Physics and Electronics Lab.
MODELLING UHF PROPAGATION FOR FREQUENCY ASSIGNMENT IN RADIO RELAY NETWORKS
Jean-Paul M. G. Linnartz (Technische Hogeschool, Delft, Netherlands) *In* AGARD, Operational Decision Aids for Exploiting or Mitigating Electromagnetic Propagation Effects Sep. 1989 10 p (For primary document see N90-14405 06-32)
Copyright Avail: NTIS HC A20/MF A03

An account is given of experiences in developing UHF-propagation models for the terrain of the North German plain which is characterized by woods and farmland. A few empirical results on the relevance of modeling the interaction between diffraction and groundwave propagation are discussed. However, the focus is mainly on (statistical) methods used to select appropriate models, rather than going into the (physical) details of propagation mechanisms. Since local variability of the field strength prohibits prediction of the feasibility of radio relay links with absolute reliability, (static) diversity tests are recommended to avoid antenna positioning in local multipath nulls. It is shown that such antenna position tests are only worthwhile if the propagation model forecasts local mean signal powers with sufficient reliability. Author

N90-14446# National Telecommunications and Information Administration, Boulder, CO. Inst. for Telecommunications Sciences.
PATTERN RECOGNITION TECHNIQUES APPLIED TO THE NASA-ACTS ORDER-WIRE PROBLEM
Kenneth C. Allen *In* AGARD, Operational Decision Aids for Exploiting or Mitigating Electromagnetic Propagation Effects Sep. 1989 11 p (For primary document see N90-14405 06-32)
Copyright Avail: NTIS HC A20/MF A03

The National Aeronautics and Space Administration (NASA) is planning to launch an Advanced Communication Technology Satellite (ACTS). This satellite will use several methods to adaptively mitigate the effects of fading due to rain in its 20- and 30-GHz links. A decision algorithm is needed to control the implementation of these mitigating techniques. The use of a learning pattern recognition algorithm as the solution to this problem is explored. The algorithm is applied to data simulating fading on a slant path through the atmosphere at 20 and 28.8 GHz. The data were scaled from data measured on a 1-km path at 28.8 GHz in Hilo, Hawaii. The sole cause of fading in the data was attenuation due to rainfall on the path. The results indicate, at least for the test data, that the use of the most recently measured value of the received signal level (RSL) is adequate for predicting the future RSL and can be used to decide when the mitigating

techniques should be used. More complicated algorithms based on linear combinations of previous RSL samples do not perform significantly better than the simple previous value approach.
Author

N90-14447# Forschungsinstitut der Deutschen Bundespost, Darmstadt (Germany, F.R.).
THE FTZ HF PROPAGATION MODEL FOR USE ON SMALL COMPUTERS AND ITS ACCURACY
Th. Damboldt and P. Suessmann *In* AGARD, Operational Decision Aids for Exploiting or Mitigating Electromagnetic Propagation Effects Sep. 1989 10 p (For primary document see N90-14405 06-32)
Copyright Avail: NTIS HC A20/MF A03

A self-contained method of estimating the critical frequency and the height of the ionosphere is described. This method was implemented in the computer program FTZMUF2. The accuracy of the method tested against the CCIR-Atlas (Report 340) yielded an average difference of less than 0.1 MHz and a standard deviation of 2.3 MHz. The FTZ HF field-strength prediction method is described which is based on the systematics found in previously measured field-strength data and implemented in a field-strength formula based thereon. The accuracy of the method -when compared with about 16,000 measured monthly medians contained in CCIR data bank D- equals that of main-frame computer predictions. The average difference is about 0 dB and the standard deviation is about 11 dB. Author

N90-14448# Allgemeine Elektrizitaets-Gesellschaft, Ulm (Germany, F.R.). Radio and Radar Systems Group.
THE CHARACTERISTICS OF THE HF RADIO CHANNEL AND ITS INFLUENCE ON MODERN HF DATA COMMUNICATION SYSTEM DESIGN
Detlev Borgmann and Juegen Lindner *In* AGARD, Operational Decision Aids for Exploiting or Mitigating Electromagnetic Propagation Effects Sep. 1989 12 p (For primary document see N90-14405 06-32)
Copyright Avail: NTIS HC A20/MF A03

A basic requirement for the design and realization of modern HF data communication systems is the detailed analysis and modeling of the transmission medium. How this analysis and modeling of the HF radio channel influences the design of such data communication systems are described. The characteristics of the HF radio channel by parameters like multipath and Doppler spread and its variation with time, short and long term statistics, variation of useful frequencies with time are described and a short introduction into modeling is given. A modern system design coping with the unwanted characteristics of the transmission medium is examined. As an example a system is presented, which is realized according to the open systems interconnection architecture proposed by ISO and in which the protocols of layers 1 to 3 are adapted to the medium HF radio. Details are described of an adaptive frequency management system with its operational requirements, the basic functions and the position within the communications system. The frequency management system is implemented as a functional module or a radio link processor, which is a part of the data communication system. The frequency management system comprises the following features: long term prediction and analysis; short term analysis with link statistics; and channel monitoring with measurement of noise and interference. Some results of field test with this frequency management system are presented. Author

N90-14449# Department of the Navy, Washington, DC.
FREQUENCY INDEPENDENT CONSTANT BEAMWIDTH DIRECTIONAL LENS ANTENNA FOR VERY WIDEBAND AND MULTI-CHANNEL ELECTROMAGNETIC COMMUNICATIONS Patent
Robert L. Sternberg, inventor (to Navy) 11 Jul. 1989 5 p Filed 7 Jul. 1988
(AD-D014214; US-Patent-4,847,628; US-Patent-Appl-SN-216056)
Avail: US Patent and Trademark Office CSCL 09/1

A frequency independent constant beamwidth lens antenna concept is described utilizing a point source to point focus nonspherical lens. The essential feature is that a twisted planar or hyperbolic paraboloidal phase or wave front is formed by the antenna which then in turn produces a frequency independent constant beamwidth beam in the far field of the antenna for radiation or reception of planar or nearly planar spherical waves. Moreover, the frequency independent constant beamwidth beam may be steered or scanned in azimuth without moving the lens antenna or a plurality of fixed beams in different directions may be formed simultaneously by the lens antenna. GRA

N90-14450# RJO Enterprises, Inc., Lexington, MA.
CONFIGURATION DEVELOPMENT FOR ROMENET Final Report, Oct. 1987 - Jan. 1988
Lawrence Rhue Oct. 1989 31 p
(Contract F09603-87-G-0659)
(AD-A213367; RADC-TR-89-170) Avail: NTIS HC A03/MF A01 CSCL 25/5

A plan prepared by RJO Enterprises and BBN Communications Corporation (BBNCC) for the design of ROMENET, a DDN-like testbed for the Rome Air Development Center (RADC) Wide Area Networks (WAN) laboratory is presented. The ROMENET is intended to provide RADC with the ability to test and evaluate the performance and vulnerability of the Defense Data Network (DDN) technologies in support of specific Major Command programs and activities at RADC. It will also support experimentation with packet switched network technologies and includes facilities to analytically evaluate the performance of the network and its associated equipment and media. In addition, ROMENET will provide a simulation vehicle for controlled interference or jamming into the media for vulnerability assessment. Through interfaces with the RADC Battle Management Laboratory (BML), ROMENET will allow the Air Force to assess the restorative and performance characteristics of the network under stressed conditions. The closed environment of ROMENET makes it ideal for creating and testing routing algorithms and network control protocols. GRA

N90-14451 Department of the Navy, Washington, DC.
FREQUENCY AGILE SYNTHETIC APERTURE RADAR Patent
Donald R. Wehner, inventor (to Navy) 25 Jul. 1989 24 p Filed 1 Feb. 1988
(AD-D014235; US-Patent-4,851,848; US-Patent-Appl-SN-151042)
Avail: US Patent and Trademark Office CSCL 17/9

A radar transmission, reception and signal processing system generates high resolution synthetic aperture radar ground maps from air or space platforms using waveforms in which frequency is changed pulse-to-pulse. The transmitted radar signal is comprised of a series N bursts with n pulses per burst wherein each of the pulsed is a fixed frequency step, delta f either above or below one or the other of the n pulses, i.e., the n pulses comprises an ordered set and further, preferably, wherein the set of n pulses is arranged in time as a random permutation of the ordered set. In each of the k sample gates for each burst the n complex samples of reflectivity are inverse Fourier transformed from frequency domain samples of reflectivity to synthetic range domain profiles to result in an array of aligned range profiles in each of k coarse range delay positions. Azimuth or cross-range processing is accomplished by thetic range cell with a suitable azimuth reference to result in a set of complex numbers that represent complex reflectivity maps of the earth's surface in that coarse range bin.
GRA

N90-14452*# Analex Corp., Cleveland, OH.
DATA COMPRESSION TECHNIQUES APPLIED TO HIGH RESOLUTION HIGH FRAME RATE VIDEO TECHNOLOGY Final Report
William G. Hartz, Robert E. Alexovich, and Marc S. Neustadter Washington NASA Dec. 1989 139 p
(Contract NAS3-24564)
(NASA-CR-4263; E-5126; NAS 1.26:4263) Avail: NTIS HC A07/MF A01 CSCL 17B

An investigation is presented of video data compression applied to microgravity space experiments using High Resolution High

Frame Rate Video Technology (HHVT). An extensive survey of methods of video data compression, described in the open literature, was conducted. The survey examines compression methods employing digital computing. The results of the survey are presented. They include a description of each method and assessment of image degradation and video data parameters. An assessment is made of present and near term future technology for implementation of video data compression in high speed imaging system. Results of the assessment are discussed and summarized. The results of a study of a baseline HHVT video system, and approaches for implementation of video data compression, are presented. Case studies of three microgravity experiments are presented and specific compression techniques and implementations are recommended. Author

N90-14453*# Clemson Univ., SC. Radar Systems Lab.
ADAPTIVE CLUTTER REJECTION FILTERS FOR AIRBORNE DOPPLER WEATHER RADAR APPLIED TO THE DETECTION OF LOW ALTITUDE WINDSHEAR
Byron M. Keel 4 Dec. 1989 190 p
(Grant NAG1-928)
(NASA-CR-186211; NAS 1.26:186211; TR-11) Avail: NTIS HC A09/MF A01 CSCL 17I

An optimum adaptive clutter rejection filter for use with airborne Doppler weather radar is presented. The radar system is being designed to operate at low-altitudes for the detection of windshear in an airport terminal area where ground clutter returns may mask the weather return. The coefficients of the adaptive clutter rejection filter are obtained using a complex form of a square root normalized recursive least squares lattice estimation algorithm which models the clutter return data as an autoregressive process. The normalized lattice structure implementation of the adaptive modeling process for determining the filter coefficients assures that the resulting coefficients will yield a stable filter and offers possible fixed point implementation. A 10th order FIR clutter rejection filter indexed by geographical location is designed through autoregressive modeling of simulated clutter data. Filtered data, containing simulated dry microburst and clutter return, are analyzed using pulse-pair estimation techniques. To measure the ability of the clutter rejection filters to remove the clutter, results are compared to pulse-pair estimates of windspeed within a simulated dry microburst without clutter. In the filter evaluation process, post-filtered pulse-pair width estimates and power levels are also used to measure the effectiveness of the filters. The results support the use of an adaptive clutter rejection filter for reducing the clutter induced bias in pulse-pair estimates of windspeed. Author

N90-14454# Gosudarstvennyi Komitet po Ispolzovaniyu Atomnoi Energii, Serpukhov (USSR). Inst. Fiziki Vysokikh Ehnergij.
FAST SERIAL COMMUNICATION MODULE
A. A. Lebedev, S. A. Medved, and Yu. V. Mikhajlov 1988 3 p In RUSSIAN; ENGLISH summary
(DE89-633753; IFVE-ONF-88-28) Avail: NTIS (US Sales Only) HC A01/MF A01

A module for communication between two heterogeneous data acquisition systems in the SUMMA system is described. The data are stored in a buffer with 2 Kbyte capacity and are transmitted by serial code with 1.8 Mbit/s rate. DOE

N90-14455# Sandia National Labs., Albuquerque, NM.
A RADAR SIMULATION PROGRAM FOR A 1024-PROCESSOR HYPERCUBE
John L. Gustafson, Robert E. Benner, Mark P. Sears, and Thomas D. Sullivan 1989 16 p Presented at the Supercomputing '89 Conference, Reno, NV, 13-17 Nov. 1989
(Contract DE-AC04-76DP-00789)
(DE89-014494; SAND-89-1423C; CONF-891149-3) Avail: NTIS HC A03/MF A01

A fast parallel version of existing synthetic aperture radar (SAR) simulation program, SRIM, was developed. On a 1024-processor NCUBE hypercube it runs an order of magnitude faster than on a CRAY X-MP or CRAY Y-MP processor. This speed advantage is coupled with an order of magnitude advantage in machine acquisition cost. SRIM is a somewhat large (30,000 lines of FORTRAN 77) program designed for uniprocessors; its restructuring for hypercube provides new lessons in the task of altering older serial programs to run well on modern parallel architectures. The techniques used for parallelization, and the performance obtained are described. Several novel parallel approaches to problems of task distribution, and direct output were required. These techniques increase performance and appear to have general applicability for massive parallelism. The hierarchy necessary to dynamically manage (i.e., load balance) a large ensemble is described. The ensemble is used in a heterogeneous manner, with different programs on different parts of the hypercube. The heterogeneous approach takes advantage of the independent instruction streams possible on MIMD machines. DOE

N90-14456# Oak Ridge National Lab., TN.
ELECTRON HEATING AND STATIC SHEATH ENHANCEMENT IN FRONT OF ENERGIZED RF ANTENNAS
M. D. Carter, D. B. Batchelor, and E. F. Jaeger 1989 18 p Presented at the IAEA Technical Committee Meeting on ICRF/Edge Physics, Munich, Federal Rep. of Germany, 2-5 Oct. 1989
(Contract DE-AC05-84OR-21400)
(DE90-001334; CONF-8910225-5) Avail: NTIS HC A03/MF A01

An analytic model was developed to describe the increased plasma potential and acceleration of ions in the vicinity of an ICRF Faraday shield. This model gives an estimate for the electron distribution function using a heating model with decorrelation caused by reflection of the electrons from the static sheath at the point where a magnetic field line intersects a grounded wall. The loss rate of the electrons from the system can be calculated from this distribution function. The expected static potential is then estimated by equating electron and ion loss rates, assuming either that the ion loss satisfies the Bohm sheath criterion or that ion gyro-orbits strike a nearby wall. The analytic model for the electrons is in good agreement with a Monte Carlo model using realistic values of the RF electric fields. These RF near-field values were calculated, including the linear near-field plasma response and the Faraday shield. Results include the findings that a linear model for the RF plasma response is valid for typical experimental parameters and that plasma currents must be included in the RF near-field calculation. It is also found that the static potential is sufficiently increased by electron heating so that it could easily cause impurities to be generated from the antenna structure. Results of the expected static potential are given for various ion species. DOE

N90-14457# Sandia National Labs., Albuquerque, NM.
DETECTION OF A CHIRPING ELECTROMAGNETIC SIGNAL
Samuel D. Stearns 1989 13 p Presented at the Asilomar Conference on Signals, Systems and Computers, Monterey, CA, 31 Oct. 1989
(Contract DE-AC04-76DP-00789)
(DE90-002105; SAND-89-2525C; CONF-8910264-1) Avail: NTIS HC A03/MF A01

A matched chirp transform (MCT) method for detecting a dispersive electromagnetic pulse is described. The unique feature of this transform is that it gives a distribution of signal amplitude over time rather than frequency, and thereby simplifies signal detection and identification in the case described here. In the MCT method, the incoming signal is matched to a set of signal segments that chirp in accordance with an expected model of the dispersive medium. The performance of the MCT method is compared with that of a standard periodogram method of frequency measurement. DOE

33 ELECTRONICS AND ELECTRICAL ENGINEERING

Includes test equipment and maintainability; components, e.g., tunnel diodes and transistors; microminiaturization; and integrated circuitry.

For related information see also *60 Computer Operations and Hardware* and *76 Solid-State Physics*.

N90-14458# Knudson Engineering, Inc., Portland, OR.
POWER FACTOR CONTROLLER STUDY
Aug. 1989 91 p Prepared for Bonneville Power Administration, Portland, OR
(Contract DE-AM79-86BP-64849)
(DE89-017655; DOE/BP-64849/1) Avail: NTIS HC A05/MF A01

The complete report is divided into three parts as follows: (1) This report combines a historical perspective with a current assessment of the use of power factor controllers for three-phase ac motor energy savings. The power factor controller (PFC) is a power electronics device that reduces voltage to a motor during periods of reduced motor torque requirements. (2) A power factor controller (PFC) is a power electronics device that reduces voltage to a motor during periods of reduced motor torque requirements. This report is the DEMONSTRATION phase of the PFC study. The phase report consists of three task reports -- Site Selection, Demonstration Preparation, and Demonstration. The reports explain how three sites were selected for demonstration, describe what was measured at each site and the method of measurement, and compare measured energy savings with calculated predictions of energy savings. The report concludes that PFCs can save energy on carefully selected motor applications. (3) The results of the demonstration task are described in this report. A power factor controller (PFC) is a power electronics device that reduces voltage to a motor during periods of reduced motor torque requirements. The demonstration phase of this study calculates projected energy savings with the use of a PFC and compares measured performance with the calculations. The effect of the PFC on motor power requirements, power factor and energy consumption shall be measured. DOE

N90-14459 Department of the Navy, Washington, DC.
METHOD AND APPARATUS TO ENHANCE THE SENSITIVITY OF CYLINDRICAL MAGNETOSTRICTIVE TRANSDUCER TO MAGNETIC FIELDS Patent
Aileen M. Yurek, inventor (to Navy) 25 Jul. 1989 5 p Filed 15 Apr. 1988 Supersedes AD-D013818
(AD-D014218; US-Patent-4,850,098; US-Patent-Appl-SN-181996; US-Patent-Class-29-527.2) Avail: US Patent and Trademark Office CSCL 14/2

This patent discloses a fiber optic sensor using the treated coil of optical fiber as a structural support system for the sensor, and a method for making such a sensor. GRA

N90-14460# Department of the Navy, Washington, DC.
ELECTROCHEMICAL PREPARATION OF SILVER OXIDE ELECTRODES HAVING HIGH THERMAL STABILITY Patent Application
Daniel R. Glen, inventor (to Navy), Azzam N. Mansour, inventor (to Navy), Kathleen M. ONeill, inventor (to Navy), Steven Dallek, inventor (to Navy), and Benjamin F. Larrick, inventor (to Navy) 2 Aug. 1989 15 p
(AD-D014224; US-Patent-Appl-SN-674254) Avail: NTIS HC A03/MF A01 CSCL 09/1

This invention relates to electrochemical cells and more particularly to silver oxide electrodes. Accordingly an object of this invention is to provide a new method of electrochemically preparing AgO electrodes. Another object of this invention is to provide a method of increasing the shelf life of electrochemically prepared silver oxide electrodes. A further object of this invention is to increase the energy capacity of electrochemically prepared AgO electrodes. These and other objects of this invention are achieved by improvements in the process for preparing AgO cathodes by anodizing silver plaques in basic electrolytes and in the performance of the anodizing process at a temperature in the range of from about 70 C to just under the reflux temperature of the electrolyte. GRA

N90-14461# Department of the Navy, Washington, DC.
HIGH POWER TRANSDUCERS Patent Application
Arthur E. Clark, inventor (to Navy) 29 Jun. 1989 12 p
(AD-D014225; US-Patent-Appl-SN-374119) Avail: NTIS HC A03/MF A01 CSCL 20/3

Magnetic energy is converted into mechanical energy by applying a changing magnetic field to a rare earth alloy of the formula Tb(x)Dy(l-x) at a temperature in the range of about K to 170K, wherein x and the operating temperature are selected to minimize the basal plane anisotropy. GRA

N90-14462# Department of the Navy, Washington, DC.
SILVER COMPOSITE CATHODES FOR ALKALINE SECONDARY BATTERIES Patent Application
William A. Ferrando, inventor (to Navy) 2 Aug. 1989 13 p
(AD-D014227; US-Patent-Appl-SN-389218) Avail: NTIS HC A03/MF A01 CSCL 09/1

This invention relates to electrochemical cells and more particularly to silver electrodes for electrochemical cells. Accordingly, an object of this invention is to provide a new, lighter weight silver electrode for secondary cells. Another object of this invention is to provide an electrode which requires less silver to operate. A further object of this invention is to provide a silver electrode which uses the silver more efficiently. Yet another object of the invention is to provide an easier, less expensive method of manufacturing silver electrodes for secondary cells. GRA

N90-14463# Department of the Navy, Washington, DC.
FABRICATION OF NBN BASED ELECTRONIC DEVICES WITH SILICON BARRIERS Patent Application
Edward Cukauskas, inventor (to Navy) and William Carter, inventor (to Navy) 30 Jun. 1989 12 p
(AD-D014230; US-Patent-Appl-SN-374035) Avail: NTIS HC A03/MF A01 CSCL 09/1

A method of making a Josephson Junction is disclosed which includes the steps of depositing a base electrode layer of a refractory superconducting material on a substrate, depositing first a passivation layer on the base electrode, depositing a barrier layer of refractory insulating semiconducting material on the passivation layer, depositing a second passivation layer on the barrier layer, and depositing a counter electrode on the second passivation layer. The layers are deposited at a substrate temperature of from about 5 to about 7 C in an Ultra High Vacuum sputtering system at a base pressure of less than or equal to 5 x 10(exp 8) Torr. In the preferred embodiment a base electrode and counter electrode of NbN are separated by a barrier layer of hydrogenated silicon. When exposed to high post processing temperatures this structure maintains a chemically stable interface with the substrate. GRA

N90-14464# Department of the Navy, Washington, DC.
SILVER-NICKEL COMPOSITE CATHODES FOR ALKALINE SECONDARY BATTERIES Patent Application
William A. Ferrando, inventor (to Navy) 16 Aug. 1989 13 p
(AD-D014231; US-Patent-Appl-SN-395547) Avail: NTIS HC A03/MF A01 CSCL 07/2

A method for producing lightweight silver-nickel composite electrodes by infiltrating a graphite fiber plaque with a suspension of finely divided nickel powder in an aqueous solution of AgNO3 is presented. A method for drying the graphite fiber plaque to produce a coating of AgNO3 crystals and nickel particles on the surfaces of the graphite fibers is also presented. A procedure is described for heating the coated graphite fiber plaque at a temperature about the melting point of AgNO3 until the AgNO3 melts and wets the nickel particles and the surfaces of the graphite fibers. A procedure is also presented for heating the molten AgNO3 coated graphite fiber plaque at a temperature from the decomposition temperature of AgNO3 to about 600 C until the

AgNO3 decomposes to form a thin uniform silver metal coating over the nickel particles and the surfaces of the graphite fibers. The silver-nickel particle coated graphite plaques are electrochemically treated to convert the silver to silver active material (Ag2O2) and the nickel to nickel active material (Ni(OH)2). GRA

N90-14465# Department of the Army, Washington, DC.
HIGH RESOLUTION, WIDE BAND CHIRP-Z SIGNAL ANALYZER Patent Application
William J. Skudera, Jr., inventor (to Army) and Charles E. Konig, inventor (to Army) 25 Sep. 1989 14 p
(AD-D014240; US-Patent-Appl-SN-411752) Avail: NTIS HC A03/MF A01 CSCL 09/1

Wide band and narrow band Chirp-Z channels are interfaced to enhance signal analysis resolution for the signal's individual component wave forms over a wide signal bandwidth. The frequency characteristic of a selected component wave form is matched to the sweeping local oscillator and filter frequency parameters of the narrow band channel in accordance with the relative position occupied by the frequency characteristic of the selected component wave form in the frequency segregated time domain of said wide band channel. In one preferred embodiment, a mixer and a voltage controlled oscillator are utilized to accomplish the frequency matching and in another embodiment, a band-pass filter precisely defines the bandwidth of the selected component wave form. For still another embodiment, the voltage input to the voltage control oscillator is controlled in accordance with the difference in frequency between the selected component wave form and said narrow band channel. GRA

N90-14466 Department of the Navy, Washington, DC.
SYMMETRIC WAVEGUIDE JUNCTION COMBINER Patent
Donald R. Bowling and Charles F. Smith, inventors (to Navy) 1 Aug. 1989 16 p Filed 4 Oct. 1988
(AD-D014243; US-Patent-4,853,650; US-Patent-Appl-SN-254554) Avail: US Patent and Trademark Office CSCL 09/1

A microwave power combiner having a spherical region from which six rectangular waveguides extend oppositely along mutually orthogonal diameters. The long dimension of each waveguide cross section extends along a diagonal of a cube circumscribing the region and extends orthogonally to this long dimension of the opposite waveguide. One waveguide is an input for an injection locking signal, and four waveguides are an inputs for power to be combined in the region from oscillators controlled by the signal. No circulator is required, and the combined power may be output through the remaining waveguide or through the injection locking input waveguide. A number of the combiners may be connected with the output of one combiner serving as an injection locking input or as one power input to another of the combiners. GRA

N90-14467*# Wisconsin Univ., Madison. Dept. of Electrical and Computer Engineering.
HIGH POWER DENSITY dc/dc CONVERTER: SELECTION OF CONVERTER TOPOLOGY Interim Report, Jul. 1987 - Jun. 1988
Deepakraj M. Divan 3 Jan. 1990 92 p
(Grant NAG3-804)
(NASA-CR-186129; NAS 1.26:186129) Avail: NTIS HC A05/MF A01 CSCL 09C

The work involved in the identification and selection of a suitable converter topology is described. Three new dc/dc converter topologies are proposed: Phase-Shifted Single Active Bridge DC/DC Converter; Single Phase Dual Active Bridges DC/DC Converter; and Three Phase Dual Active Bridges DC/DC Converter (Topology C). The salient features of these topologies are: (1) All are minimal in structure, i.e., each consists of an input and output bridge, input and output filter and a transformer, all components essential for a high power dc/dc conversion process; (2) All devices of both the bridges can operate under near zero-voltage conditions, making possible a reduction of device switching losses and hence, an increase in switching frequency; (3) All circuits operate at a constant frequency, thus simplifying the task of the magnetic and filter elements; (4) Since, the leakage inductance of the transformer is used as the main current transfer element, problems associated with the diode reverse recovery are eliminated. Also, this mode of operation allows easy paralleling of multiple modules for extending the power capacity of the system; (5) All circuits are least sensitive to parasitic impedances, infact the parasitics are efficently utilized; and (6) The soft switching transitions, result in low electromagnetic interference. A detailed analysis of each topology was carried out. Based on the analysis, the various device and component ratings for each topology operating at an optimum point, and under the given specifications, are tabulated and discussed. Author

N90-14468*# Georgia Tech Research Inst., Atlanta. Microelectronics Research Center.
THEORETICAL AND MATERIAL STUDIES OF THIN-FILM ELECTROLUMINESCENT DEVICES Final Report
C. J. Summers Mar. 1989 72 p
(Grant NAG1-586; Proj. A-4168)
(NASA-CR-186104; NAS 1.26:186104) Avail: NTIS HC A04/MF A01 CSCL 09A

Thin-film electroluminescent (TFEL) devices are studied for a possible means of achieving a high resolution, light weight, compact video display panel for computer terminals or television screens. The performance of TFEL devices depends upon the probability of an electron impact exciting a luminescent center which in turn depends upon the density of centers present in the semiconductor layer, the possibility of an electron achieving the impact excitation threshold energy, and the collision cross section itself. Efficiency of such a device is presently very poor. It can best be improved by increasing the number of hot electrons capable of impact exciting a center. Hot electron distributions and a method for increasing the efficiency and brightness of TFEL devices (with the additional advantage of low voltage direct current operation) are investigated. J.P.S.

N90-14469# Sandia National Labs., Albuquerque, NM.
REVIEW OF SURFACE FLASHOVER THEORY
R. A. Anderson 1989 15 p Presented at the Large Area Electron Beam Diode Workshop, Monterey, CA, 7 Jun. 1989
(Contract DE-AC04-76DP-00789)
(DE90-000806; SAND-89-1276C; CONF-8906200-2) Avail: NTIS HC A03/MF A01

Over the past several decades, many researchers have contributed to the understanding of the flashover of electrically stressed insulators in vacuum, and a wealth of theories have been proposed to explain the many surprising attributes of this complex breakdown mechanism. Surface flashover appears to comprise at least two distinct phenomena which can be distinguished as being cathode-initiated or anode-initiated, with the former having received by far the most attention. Several models describing cathode-initiated flashover have been built on the pioneering work of Boersch and coworkers, published in 1963, and credit the breakdown mechanism to the action of an intense secondary-electron-emission avalanche on the insulator surface. Other researchers consider the electron avalanche to be only partially, if at all, responsible, and invoke various hot-carrier effects in the insulator bulk, the surface interfacial region, or in a layer of gas adsorbed on the insulator surface. Anode-initiated flashover, which contends with the cathode-initiated variety for the breakdown of insulators of conventional design, is thought to involve bulk breakdown in a way related to treeing failure. In spite of the considerable effort applied to understanding vacuum surface flashover, no single theory appears capable of explaining all the data, and new and often unexpected observations continue to be made. DOE

N90-14470# Lawrence Livermore National Lab., CA.
ELECTRIC-GUN STUDIES OF CONDUCTORS IN HIGH MAGNETIC FIELDS AND EXPERIMENTS IN DYNAMIC FLUX COMPRESSION
J. E. Osher, H. H. Chau, R. S. Lee, R. E. Tipton, and R. C. Weingart 21 Jul. 1989 9 p Presented at the 5th International Conference on Megagauss Magnetic Field Generation and Related

Topics, Novosibirsk, USSR, 3-7 Jul. 1989
(Contract W-7405-eng-48)
(DE90-000815; UCRL-100323; CONF-890710-20) Avail: NTIS HC A02/MF A01

The devices we call electric guns operate by discharging a fast capacitor bank through a thin, metallic bridge-foil load. The explosion of the foil and the accompanying magnetic forces acting on the bridge-foil plasma accelerate a thin flyer plate of dielectric material initially placed on top of the bridge foil. In hypervelocity impact studies with the linear electric gun, a thin, flat flyer is punched out of a cover sheet of dielectric (or dielectric/metallic composite) material by the explosion of the bridge foil and accelerated down a short barrel to impact on a target. In the coaxial gun, a cylindrical bridge foil is used to implode a cylindrical dielectric or dielectric/metallic composite (liner) flyer to produce a high peak compression through axial convergence. In this paper we discuss the range of currents, their rate of rise, and the magnetic fields attained by our fast capacitor banks, which supply power to the electric gun to explode the bridge foil. Also included is a brief study of the change of resistance of the bridge-foil element as a function of time for various flyer mass loadings for the linear geometry of the gun. The change in resistance can be viewed as a type of opening switch for pulsed-power applications. DOE

N90-14471# Sandia National Labs., Albuquerque, NM. Advanced Battery Business Unit.
TERRESTRIAL NICKEL/HYDROGEN BATTERY DEVELOPMENT AT JOHNSON CONTROLS, INC.
R. L. Beauchamp and J. P. Zagrodnik 1989 7 p Presented at the 9th Battery and Electrochemical Contractors' Conference, Alexandria, VA, 13-17 Nov. 1989
(Contract DE-AC04-76DP-00789)
(DE89-015843; SAND-89-7103C; CONF-891132-2) Avail: NTIS HC A02

This paper is a very brief summary of the life cycle cost and efficiency of the nickel-hydrogen battery to be used with photovoltaic charging. DOE

N90-14472# Sandia National Labs., Albuquerque, NM.
SODIUM/SULFUR EVALUATION AT SNL
J. M. Freese 1989 7 p Presented at the 9th Battery and Electrochemical Contractors' Conference, Alexandria, VA, 13-17 Nov. 1989
(Contract DE-AC04-76DP-00789)
(DE89-015846; SAND-89-1886C; CONF-891132-3) Avail: NTIS HC A02/MF A01

Sandia National Laboratories (SNL) has been involved in the evaluation of the sodium/sulfur technology for several years. Until recently, the effort concentrated on the performance of single cells. Recently, the evaluation of 4-cell string was initiated. The majority of the activity during the past two years has focused on cells from Chloride Silent Power, Limited (CSPL). To date, four groups of PB cells and 4-cell strings, which consisted of PB cells, have been evaluated. The first group of ten cells delivered to Sandia were on test for approximately one year. The majority of these cells failed due to corrosion problems in the sulfur seal. However, two cells completed over 800 cycles, and one of these cells completed nearly 1600 cycles. DOE

N90-14473# Sandia National Labs., Albuquerque, NM.
ZINC/BROMINE BATTERY EVALUATION AT SNL (SANDIA NATIONAL LABORATORY)
S. L. Lott, P. C. Butler, and J. M. Freese 1989 6 p Presented at the 9th Battery and Electrochemical Contractors' Conference, Alexandria, VA, 13-17 Nov. 1989
(Contract DE-AC04-76DP-00789)
(DE89-015847; SAND-89-1852C; CONF-891132-1) Avail: NTIS HC A02/MF A01

Three prototype zinc/bromine batteries were evaluated at Sandia during the last year. The objectives of these tests were to determine performance, cycle life, durability of the auxiliary components, and failure mechanisms. All three were deliverables from a Sandia development contract with Energy Research Corporation (ERC). The test results were communicated to ERC along with suggestions for improving battery design and reliability. DOE

N90-14474# Texas A&M Univ., College Station. Dept. of Physics.
RECENT DEVELOPMENTS OF GIGATRON TECHNOLOGY
Peter M. McIntyre, Stephen M. Elliott, Henry Gray (Naval Research Lab., Washington, DC.), Bo Lee, Yaoqi Pang, and Milorad B. Popovic 1989 8 p Presented at the International Conference on High Energy Accelerators, Tsukuba, Japan, 20-26 Aug. 1989
(Contract DE-AC02-85ER-40236)
(DE90-001067; CONF-890803-28) Avail: NTIS HC A02/MF A01

Gigatron is a new design concept for microwave power devices. A gated field emitter array is employed as a directly modulated cathode. A ribbon beam configuration is used to mitigate space charge effects and provide for efficient output coupling. A traveling wave output coupler is used to obtain optimum coupling to a wide beam. Recent cathode tests are reported. Modeling of the bunched emission process has led to an improved cathode fabrication procedure. A new application of a similar structure has led to a design for a new technology for precision tracking chambers for SSC detectors. DOE

N90-14475# Oak Ridge National Lab., TN. Instrumentation and Controls Div.
INTEGRATING AND ENHANCING TOOLS FOR ASIC (APPLICATION-SPECIFIC INTEGRATED CIRCUITS) DESIGN USING MOSIS (METAL OXIDE SEMICONDUCTOR IMPLEMENTATION SERVICE) FABRICATION
D. F. Newport, C. L. Britton, Jr., G. T. Alley, W. L. Bryan, M. S. Emery, M. N. Ericson, H. R. Brashear, and D. W. Bouldin (Tennessee Univ., Knoxville.) 1989 5 p Presented at the IEEE Nuclear Science Symposium and Exhibits, San Francisco, CA, 25-27 Oct. 1989
(Contract DE-AC05-84OR-21400)
(DE90-001601; CONF-891087-4) Avail: NTIS HC A01/MF A01

Application-specific integrated circuits (ASICs), which have traditionally been cost-effective only for high volume applications, can now be designed using high quality, inexpensive tools and can be fabricated in small quantities using MOSIS (Metal Oxide Semiconductor Implementation Service). Numerous computer-aided design tools developed under government sponsorship are available to organizations within the United States for just a media handling fee (typically about $200 each). The tool integration and enhancement activities described in this paper have resulted in a proven set of high quality aids that permit the design of custom and semicustom analog and digital ASICs. Examples of projects implemented using this tool set are given along with the support activities that are being conducted to transfer this technology to other federal agencies and universities. DOE

N90-14476# Sandia National Labs., Albuquerque, NM.
EFFECTS OF COMPOSITION AND AGE HARDENING ON PRECIOUS METAL ELECTRICAL CONTACTS
L. E. Pope and D. E. Peebles 1988 20 p Presented at the 34th Annual IEEE Holm Conference on Electrical Contacts, San Francisco, CA, 26 Sep. 1988
(Contract DE-AC04-76DP-00789)
(DE88-008791; SAND-88-1004C; CONF-880946-1) Avail: NTIS HC A03/MF A01

Precious metal alloys are commonly used for wiper electrical contacts in electromechanical devices which operate in dry and inert atmospheres. A pin-on-plate experimental configuration was used to evaluate two different palladium alloy pins (ASTM B540 and ASTM B563) sliding on a gold alloy plate (ASTM B541) age hardened at two temperatures. For all combinations of test conditions, except the higher palladium content alloy (ASTM B563), two stages of wear were observed: a prow of Au alloy was formed on the palladium alloy pin and work hardening and roughening of the wear track occurred with transfer and backtransfer of Au alloy material. With the higher palladium alloy pin (ASTM B563) a friction

polymer was formed for laboratory air testing. The prow formed on the pin was a mechanical mixture of gold alloy plate and palladium alloy pin materials; palladium was found in the wear track for this experimental condition, while no palladium was found in wear tracks for the other test conditions. Segregation of zinc, silver and copper in wear tracks occurred for all test conditions, but the extent of segregation was dependent on contact couple combination and heat treatment of the gold alloy plate. The least amount of segregation was observed when the gold alloy plate was age hardened at 426 C. More segregation occurred for testing in helium than for testing in vacuum with a low partial pressure of oxygen. The largest segregation of metallic elements occurred for laboratory air testing, but the total metallic content of wear tracks was low; the wear tracks consisted primarily of carbon. Segregation was slightly larger with the higher palladium alloy (ASTM B563) pin. DOE

N90-14477# Sandia National Labs., Albuquerque, NM. Combustion Research Facility.
A SOFTWARE-BASED CONTROLLER FOR GENERATION OF SYNCHRONIZED PULSES FOR USE WITH ROTATING MACHINERY
Axel O. zurLoye Aug. 1989 20 p
(Contract DE-AC04-76DR-00789)
(DE89-016672; SAND-89-8247) Avail: NTIS HC A03/MF A01

An IBM PC/AT based software package was developed to synchrotronize test equipment with rotating machinery. Up to eight outputs can be controlled independently. The pulse sequences can be as long as 254 shaft encoder revolutions and repeat until terminated. Unlike most purpose-built controllers, this software package is highly flexible. Complicated pulse sequences are easily generated and can quickly be modified using the built-in editor or a standard text editor. While the software requires a dedicated computer, implementation is easier and more cost effective than construction of a purpose-built controller. DOE

N90-14478# Argonne National Lab., IL. Chemical Technology Div.
MODELING OF SODIUM/METAL CHLORIDE BATTERIES
P. A. Nelson 1989 8 p Presented at the 24th Intersociety Energy Conversion Engineering Conference, Arlington, VA, 6-11 Aug. 1989
(Contract W-31-109-eng-38)
(DE89-017685; CONF-890815-29) Avail: NTIS HC A02/MF A01

The performance of sodium/iron chloride cells was modeled to determine the effect of a high ratio of solid electrolyte surface area to cell capacity. Preliminary studies showed that electrolyte configurations of either multiple tubes joined to a header or compartmented flat structures would result in high performance cells. A detailed calculation of performance of 215 Ah cells of the latter configuration resulted in cell specific energy of 187 Wh/kg and a specific power of 293 W/kg. A 61.6 kWh battery of these cells designed for the GM-G Van would weigh only 416 kg and have a volume of only 283 L. These calculated performances greatly exceed the experimental accomplishments of conventional cells having a single tubular electrolyte. DOE

N90-14479# Lawrence Livermore National Lab., CA.
EXPERIMENTAL INVESTIGATION OF A FAST-ACTING EXPLODING METALLIC FOIL OPENING SWITCH
N. E. Molau, J. E. Vernazza, R. A. Anderson, D. A. Goerz, and R. R. Heritsch 1989 6 p Presented at the 7th Institute of Electrical and Electronics Engineers Pulsed Power Conference, Monterey, CA, 12-14 Jun. 1989
(Contract W-7405-eng-48)
(DE90-001051; UCRL-100362; CONF-890665-51) Avail: NTIS HC A02/MF A01

Experiments were conducted to investigate the use of thin radially spoked metallic foils as fast-acting opening switches operating on nanosecond timescales. Such devices could be useful in special applications requiring a tailored output from a pulsed power source. The advantage of this concept is that the device is inexpensive, simple, rugged, and reliable for single shot applications. Experimental results are presented and discussed. The effects of varying several fuse parameters are summarized and some limitations of the design are discussed. DOE

N90-14480# Los Alamos National Lab., NM.
ENERGY RATINGS FOR METAL OXIDE VARISTORS UNDER REPETITIVELY PULSED OPERATION
J. G. Melton 1989 6 p Presented at the 13th International Symposium on Fusion Engineering, Knoxville, TN, 2-6 Oct. 1989
(Contract W-7405-eng-36)
(DE90-002353; LA-UR-89-3271; CONF-891007-54) Avail: NTIS HC A02/MF A01

Nonlinear resistors can be used to improve the energy transfer efficiency of inductive energy storage systems that use resistive transfer elements. Improved energy transfer efficiency can result in significant cost savings in some large systems if the cost of the nonlinear resistor is less than the cost of the energy storage and charging hardware that the resistor replaces. Experimental tests are described that were done to determine appropriate energy ratings for ZnO Metal Oxide Varistors (MOVs) for pulsed conditions from 10 to 20 ms long. Tests were performed first on single MOV units which were forced to failure in a small number of shots. Then several sets of matched pairs were operated under identical conditions to investigate current sharing and the statistics of failure. Test results show that the standard rating method used by manufacturers relating peak current, pulse length, and expected lifetime are adequate, but somewhat conservative. The manufacturers' energy ratings project to a very economical nonlinear transfer resistor. DOE

N90-14481# Los Alamos National Lab., NM.
HIGH SPEED TRANSFER SWITCH WITH 50 kA AND 50 kV RATINGS
W. A. Reass, R. J. Kasik, and W. A. Wilds 1989 5 p Presented at the 13th International Symposium on Fusion Engineering, Knoxville, TN, 2-6 Oct. 1989; sponsored by IEEE
(Contract W-7405-eng-36)
(DE90-002448; LA-UR-89-3291; CONF-891007-61) Avail: NTIS HC A02/MF A01

This paper gives the mechanical design and electrical parameters of a pneumatically operated transfer switch. This design is used to switch 3-second 50-kA current pulses, and is easily capable of 75 kA operation, with water-cooled versions capable of 20 kA continuously. Although the switch is not specifically designed to make or break 50 kA, it is provided with auxiliary Elkonite arcing contacts that have proven their value in protecting the main electrodes even under repetitive (50 kA) fault conditions. Included in this presentation will be the results of extensive life testing and associated criteria. DOE

N90-14482# Lawrence Livermore National Lab., CA.
INDUCTIVE STORE OPENING SWITCH AND TESTS FOR ENERGY TRANSFER TO A LOAD
P. Poulsen, J. L. Cutting, R. S. Hawke, A. J. McAlice, P. A. Pincosy, and J. B. Chase 12 Oct. 1989 8 p Presented at the 5th International Conference on Megagauss Magnetic Field Generation and Related Topics, Novosibirsk, USSR, 3-7 Jul. 1989
(Contract W-7405-eng-48)
(DE90-002818; UCRL-100641; CONF-890710-24) Avail: NTIS HC A02/MF A01

Power from the output of an explosive generator can be quickly and efficiently switched by transformer-coupled circuits with a fuse as the switching element. Numerical studies indicate that this technique should be able to switch 2 MA of current into a resistive load of 20 Ohms in 100 ns or less, producing in the load a near steady-state pulse with a duration of 1 microsecond about 100 ns after the switching begins. We report in this paper the results of ongoing experiments to create a fuse with a short switching time (about 100 ns), a high resistance ratio (approximately 300), and adequate voltage holding characteristics. We found that a tamper consisting of both Mylar and SiO grease substantially increases

both the resistance ratio of a fuse, and the length of time a high resistance ratio is maintained, relative to what is observed in fuses tamped with Mylar alone. DOE

N90-14483# Texas A&M Univ., College Station. Dept. of Physics.
GIGATRON: A NEW TECHNOLOGY FOR MICROWAVE POWER DEVICES
Peter M. McIntyre, Stephen M. Elliott, Henry Gray (Naval Research Lab., Washington, DC.), Bo Lee, Yaoqi Pang, and Milorad B. Popovic 1988 8 p Presented at the SPIE Symposium of High Power Microwave Devices, Los Angeles, CA, Oct. 1988
(Contract DE-AC02-85ER-40236)
(DE90-001066; CONF-8810432-1) Avail: NTIS HC A02/MF A01

The gigatron is a new design concept for microwave power devices. A gated field emitter array is employed to produce microwave modulated electron beam directly from the cathode. A ribbon beam configuration is used to mitigate space change effects and provide efficient output coupling. A traveling wave output coupler is used to obtain optimum coupling to a wide beam. RF conversion efficiency is estimated at approx. 75 percent. Gigatron family devices were designed for applications from 3 GHz to 60 GHz frequency, from 30 W microtubes for phased array antenna drivers to 500 MW drivers for linac colliders. DOE

N90-14484# Lawrence Livermore National Lab., CA.
FURTHER STUDIES OF TRANSVERSE STRESS EFFECTS IN CABLE-IN-CONDUIT CONDUCTORS
L. T. Summers and J. R. Miller 14 Aug. 1989 9 p Presented at the International Cryogenic Materials Conference, Los Angeles, CA, 24-25 Jul. 1989 Submitted for publication
(Contract W-7405-eng-48)
(DE90-001517; UCRL-100272; CONF-890701-11) Avail: NTIS HC A02/MF A01

The effect of transverse stress on critical current has been examined for Cable-In-Conduit Conductors (CICC's) containing three active superconducting composite strands in cables containing a total of 21 strands. In measurements of this type reported previously, only soft copper was used for the inactive strands, allowing the possibility that peaking of stresses at strand cross-over points were avoided by deformation of the copper strands during CICC fabrication and testing. In the present experiments, the degree of critical current degradation was measured as a function of applied load for various void fractions for cable patterns using stainless steel wires as the inactive strands. The reduction of critical current, expressed as a function of load divided by the projected area of the core of the superconducting composite strand, was found to be similar to that observed in cables containing copper inactive strands. All the CICC's tested show a higher sensitivity to transverse stress as compared to single wires. At compressive loads of 50 MPa or less, the region of interest to magnet designers, the critical current is, at worse, 79 percent of the critical current in unloaded samples. The sensitivity to transverse load is a function of CICC void fraction, lower void fractions having less susceptibility to degradation. The results of this investigation indicate that the performance of large magnets employing CICC designs need not be seriously degraded due to transmitted or self-induced Lorentz loads. DOE

N90-14485# Sandia National Labs., Albuquerque, NM.
ELECTRICAL BREAKDOWN IN VACUUM Working Group Report
Robert Anderson, Lynn Hatfield, Garry Allen, Malcolm Buttram, George Erickson, Rod Latham, George Vogtlin, Lon Enloe, Art Guenther, and Charles Mansfield (Los Alamos National Lab., NM.) et al 1989 17 p Presented at the Large Area Electron Beam Diode Workshop, Monterey, CA, 7 Jun. 1989
(Contract DE-AC04-76DP-00789)
(DE90-001623; SAND-89-2216C; CONF-8906200-3) Avail: NTIS HC A03/MF A01

The working group on electrical breakdown in vacuum was charged with considering all possible mechanisms by which electrical breakdown might occur either through the vacuum or along insulator bushings in large area electron beam emitter assemblies. It was understood that present systems need to be scaled up, by an order of magnitude or more in both beam area and total energy, to meet demands for higher power and larger size machines, and that increases in the e-beam current density and transport efficiency are also sought. A consideration of the consequences of such a scale-up was pertinent to many of the topics listed in the working-group agenda. Our group attempted to address each of these topics. DOE

N90-14486# Edgerton, Germeshausen and Grier, Inc., Idaho Falls, ID.
LABORATORY TESTING OF SONNENSCHEIN DF6V180 6 VOLT TRACTION BATTERY
J. E. Hardin Jul. 1989 23 p
(Contract DE-AC07-76ID-01570)
(DE90-002080; EGG-EP-8656) Avail: NTIS HC A03/MF A01

The purpose of this report is to describe the testing performed on the Sonnenschein DF6V180 sealed lead-acid 6 volt traction battery by the INEL Electric Vehicle Battery Laboratory, to present the results and conclusions of this testing, and to make appropriate recommendations. DOE

N90-14487# Argonne National Lab., IL. Materials and Components Technology Div.
PRACTICAL SUPERCONDUCTOR DEVELOPMENT FOR ELECTRICAL POWER APPLICATIONS Annual Report, FY 1988
Roger B. Poeppel, Uthamalingam Balachandran, I. D. Bloom, Stephen E. Dorris, J. T. Dusek, J. E. Emerson, K. C. Goretta, K. E. Gray, J. R. Hull, and R. T. Kampwirth et al Feb. 1989 54 p
(Contract W-31-109-eng-38)
(DE90-001804; ANL-88-37) Avail: NTIS HC A04/MF A01

Development of useful high-temperature superconductors (HTSCs) requires synthesis of the various superconducting oxide compounds; fabrication of wires, tapes, and thin films from these compounds; capability of forming composite structures that incorporate integral insulators or stabilizers; and design of efficient components and systems. This report documents research efforts aimed at producing superconducting components based on the oxide systems Y-Ba-Cu-O, Bi-Sr-Ca-Cu-O, and Tl-Ca-Ba-Cu-O. Topics discussed are synthesis of compounds from each system; fabrication of monolithic tapes, wires, and castings; effects of silver additions on mechanical and electrical properties; fabrication of composite tapes that incorporate silver or ceramic substrates; use of pressure or electrochemical bonding to connect the superconductors to high-conductivity metals; fabrication of thin films for electronic devices; optimization of heat treatment schedules; the microstructural, mechanical, and electrical properties of the forms produced; and studies on the thermomagnetic stabilities of HTSCs and the implications for system design. Collaborations in this research between Argonne National Laboratory, universities, industrial partners, and other national laboratories are identified and results from the collaborations are presented. The report closes with an assessment of the status of the research efforts as of September 1988. DOE

N90-14488# Argonne National Lab., IL. Electrochemical Technology Program.
SODIUM/SULFUR POST-TEST ANALYSIS AT ANL
John A. Smaga 1989 6 p Presented at the 9th Battery and Electrochemical Contractors' Conference, Washington, DC, 13-17 Nov. 1989
(Contract W-31-109-eng-38)
(DE90-001911; CONF-891132-7) Avail: NTIS HC A02/MF A01

One activity of Argonne's Analysis and Diagnostics Laboratory has been the examination of selected sodium/sulfur cells that were built and tested by Chloride Silent Power Ltd. (CSPL) as part of the Exploratory Battery Technology Development Program at Sandia National Laboratories. The more recent examinations have involved long-lived (greater than 400 cycles) cells of both basic cell designs (PB and XPB). The examined cells can be

further differentiated according to the different designs used for the seal assembly and the sodium electrode. The detailed examinations conducted with the specialized facilities maintained at ANL have led to some significant findings stemming from these design variations. Some of the results for case corrosion, electrolyte contamination, and seal degradation are presented, and the effect of the design changes on these conditions is discussed. DOE

N90-14489# Idaho National Engineering Lab., Idaho Falls.
BATTERY TECHNOLOGY ASSESSMENT AND R AND D PLAN
Gary L. Henriksen 1989 11 p Presented at the Electric and Hybrid Vehicle Contractors' Meeting, Idaho Falls, ID, 6-8 Sep. 1989
(Contract DE-AC07-76ID-01570)
(DE90-002007; EGG-M-89361; CONF-8909181-6) Avail: NTIS HC A03/MF A01

To guide future EV battery R and D programs, the U.S. Department of Energy (DOE) commissioned a comprehensive assessment of secondary battery technologies. A total of 67 battery developers -- from the United States, Canada, Europe, Asia, and Africa -- were solicited to submit battery design concepts for an Improved Dual-Shaft Electric Propulsion (IDSEP) van. A team of 10 consultants and 7 representatives from DOE laboratories evaluated 42 developer responses and consultant-prepared designs. Using six criteria -- five technical/economic criteria and a maturity/technical barriers criterion -- the assessment identified 12 most-promising batteries. Employing a generic EV-battery development-process framework, the assessment results were used to formulate multi-year R and D plans and schedules for the most-promising developmental batteries. DOE

N90-14490# Los Alamos National Lab., NM.
A COST EFFECTIVE BATTERY BANK FOR I(SUP 2)T TESTING AND EVALUATION OF ELECTRICAL SWITCHGEAR
W. A. Reass 1989 4 p Presented at the 13th International Symposium on Fusion Engineering, Knoxville, TN, 2-6 Oct. 1989
(Contract W-7405-eng-36)
(DE90-002350; LA-UR-89-3277; CONF-891007-58) Avail: NTIS HC A02/MF A01

The electrical design and mechanical construction of a 50 kA step switched battery bank. Individual fuses protect each of the forty parallel isolated strings of three series (12 V) batteries. Step current waveforms of 12.5 kA, 25 kA, 37.5 kA, and 50 kA are produced by 8 sets of pneumatically driven 20 pole step switches and current limiting stainless steel trombone resistors. Inexpensive, yet conservatively designed, Group 65 Motorcraft car batteries are used to give an I(sup 2)t capability of better than 5 x 10(exp 9). The battery bank has well over 1500 shots, with testing of commercial switchgear continuing. In addition to the battery bank engineering data, results of repetitive testing of vacuum interrupters at their I(sup 2)t limit will be provided. DOE

N90-14491# Pinnacle Research Inst., Cupertino, CA.
THE SECONDARY SLURRY-ZINC/AIR BATTERY Final Report
H. B. SierraAlcazar, P. D. Nguyen, G. E. Mason, and A. A. Pinoli Jul. 1989 47 p Prepared in cooperation with California Univ., Berkeley, Lawrence Berkeley Lab.
(Contract DE-AC03-76SF-00098)
(DE90-002600; LBL-27466) Avail: NTIS HC A04/MF A01

The rechargeability of the slurry-Zn/air battery was demonstrated with a practical recharge cell that requires minimal hydraulic and mechanical energy for operation. A dendritic Zn was deposited on a Mg plate substrate from which it was easily, periodically and automatically scraped to regenerate dendritic Zn slurries. Excellent discharge results were obtained with the regenerated dendritic Zn slurry, comparable to those obtained with slurries made with mixtures of Zn powder. The dendritic Zn slurry allowed, however, twice the utilization of Zn. DOE

N90-14492# Lawrence Livermore National Lab., CA.
TESTING AND PERFORMANCE OF A HIGH-GAIN FLUX-COMPRESSION GENERATOR
P. A. Pincosy, J. L. Cutting, and J. B. Chase 30 Aug. 1989 7 p Presented at the 5th International Conference on Megagauss Magnetic Field Generation and Related Topics, Novosibirsk, USSR, 3-7 Jul. 1989
(Contract W-7405-eng-48)
(DE90-002808; UCRL-100585; CONF-890710-23) Avail: NTIS HC A02/MF A01

A workable high-grain high-explosive helical magnetic-flux-compression generator (HEG) must be fabricated with the required tolerances, and the expanding high explosive and armature must be centered and radically uniform. The tolerance and expansion issues were tested with a mini-HEG having a constant density of stator turns that would simulate the first part of a full-scale generator, which also has a constant turns density. The mini size was scaled on the basis of parameter changes that respected the tolerance requirements for alignment and thickness of the armature wall. A precision initiator was tested separately on the high explosive to be used in the armature. Uniformity and smoothness of the armature's expansion were tested separately. The mini-HEG was tested for turn-skipping and to evaluate the predictions of our circuit analysis simulation program, CIRC. The turn-to-turn voltage stress was also measured. DOE

34 FLUID MECHANICS AND HEAT TRANSFER

Includes boundary layers; hydrodynamics; fluidics; mass transfer; and ablation cooling.

For related information see also *02 Aerodynamics* and *77 Thermodynamics and Statistical Physics.*

N90-14493*# National Aeronautics and Space Administration. Langley Research Center, Hampton, VA.
SURFACE FLOW AND HEATING DISTRIBUTIONS ON A CYLINDER IN NEAR WAKE OF AEROASSIST FLIGHT EXPERIMENT (AFE) CONFIGURATION AT INCIDENCE IN MACH 10 AIR
William L. Wells Jan. 1990 58 p
(NASA-TP-2954; L-16623; NAS 1.60:2954) Avail: NTIS HC A04/MF A01 CSCL 20D

Experimental heat transfer distributions and surface streamline directions are presented for a cylinder in the near wake of the Aeroassist Flight Experiment forebody configuration. Tests were conducted in air at a nominal free stream Mach number of 10, with post shock Reynolds numbers based on model base height of 6,450 to 50,770, and angles of attack of 5, 0, -5, and -10 degrees. Heat transfer data were obtained with thin film resistance gage and surface streamline directions by the oil flow technique. Comparisons between measured values and predicted values were made by using a Navier-Stokes computer code. Author

N90-14494*# United Technologies Research Center, East Hartford, CT.
LASER VELOCIMETER AND TOTAL PRESSURE MEASUREMENTS IN CIRCULAR-TO-RECTANGULAR TRANSITION DUCTS Final Report
William P. Patrick and Duane C. McCormick Jun. 1988 121 p
(Contract NAS3-24616)
(NASA-CR-182286; NAS 1.26:182286; UTRC-87-41) Avail: NTIS HC A06/MF A01 CSCL 20D

A comprehensive set of total pressure and three-component laser velocimetry (LV) data were obtained within two circular-to-rectangular transition ducts at low subsonic speeds. This set of reference data was acquired for use in identifying secondary flow mechanisms and for assessing the accuracy of computational procedures for calculating such flows. Data were obtained at the inlet and exit planes of an aspect ratio three duct having a length-to-diameter ratio of one (AR310) and an aspect ratio six duct having a length-to-diameter ratio of three (AR630). Each duct was unseparated throughout its transition section. It is therefore concluded that secondary flows can play an important part in the fluid dynamics of transition ducts and needs to be addressed in

computational analysis. The strength of the secondary flows depends on both the aspect ratio and relative axial duct length.
Author

N90-14495 Exeter Univ. (England).
AN EXPERIMENTAL AND THEORETICAL STUDY OF THE AEROACOUSTICS OF EXTERNAL-COANDA GAS FLARES Ph.D. Thesis
Caroline Parsons 1988 331 p
Avail: Univ. Microfilms Order No. BRDX85421

Experimental and theoretical means have been used to investigate the fluid dynamics and aeroacoustics of both stepped and unstepped external Coanda flares. Flow visualization techniques have been used to observe the one-eight scale model flare flow fields whilst simultaneously carrying out various sound measurements in the hope of being able to relate observed flow features to specific types of aerodynamic noise. Particular attention has been paid to the stepped model flare in the present work, for comparison with previous work on the unstepped model flare. Test have been carried out on two full-scale flares of different sizes which confirm that the previously assumed inverse-length scaling law does indeed hold in the case of flare noise frequency. Comparisons can therefore be made between the results of model and full-size flare tests, and these indicate that although the full-size flare also emits discrete tones, the nature of these tones are very different from those emitted by the model flares. Several possible reasons for the differences in the two sets of results are discussed. A theoretical study of the high-frequency turbulent mixing noise associated with a model Indair flare jet has been carried out. Because of the complicated nature of such a curved radial wall-jet, the theory has first been developed for a plane two-dimensional wall-jet. Dissert. Abstr.

N90-14496 Houston Univ., TX.
FLUID-PARTICLE INTERACTION IN SOLID-LIQUID TWO-PHASE GRID TURBULENCE Ph.D. Thesis
Stefan Georg Schreck 1988 196 p
Avail: Univ. Microfilms Order No. DA8912672

The interaction between solid spheres and a fluid in the nearly isotropic flow field downstream of a grid was studied experimentally. Also neutrally buoyant plastic particles and heavier glass particles of the size of 600 to 710 microns and of concentrations of 0.2 to 1.5 percent were considered. Velocity measurements of both phases were conducted with a laser Doppler velocimeter. It was found that the relationship between the motion of the particles and the motion of the fluid is not affected by particle concentration of up to 1.5 percent. Estimates of particle-particle interaction based on measured velocity cross-correlations between the phases indicate that particle-particle interaction does not play a role in the suspensions studied. The decay rate of turbulence kinetic energy is monotonically increased with increasing particle concentration. The particles increase the isotropy of the flow field. A new random-walk model was developed to predict the diffusion of a passive scalar in isotropic turbulence. The predicted scalar diffusion coefficient is constant in the initial period of decay for the single-phase flow, however, it decreases downstream for suspensions of particles. Dissert. Abstr.

N90-14497 Mississippi State Univ., State College.
A DYNAMIC MULTIBLOCK APPROACH TO SOLVING THE UNSTEADY EULER EQUATIONS ABOUT COMPLEX CONFIGURATIONS Ph.D. Thesis
Abdollah Arabshahi 1989 126 p
Avail: Univ. Microfilms Order No. DA8917049

The objective is the development of a numerical method which can accurately and economically solve the unsteady Euler equations for three-dimensional flow fields around complex configurations, particularly a generic aircraft with a store in the captive and vertical launch position. A cell centered finite volume spatial discretization is applied to the three-dimensional, time-dependent, Euler equations written in general time-dependent curvilinear coordinates. Two algorithms are presented for solving the system of Euler equations. The first algorithm is based on flux-vector splitting while the second algorithm is based on flux-difference splitting using Roe averaged variables. For both algorithms, an implicit upwind biased approach is employed to integrate the spatially discretized equations in time. The multiblock technique utilizes the concept of decomposing the flow field between the surfaces of the configuration and some outer far field boundary into a set of blocks. Calculated results compared with experimental data indicate that the present Euler solver can calculate transonic flow fields efficiently and accurately over complex geometries. Furthermore, the results demonstrate how computational fluid dynamics (CFD) can be used to accurately simulate steady and, for the first time, unsteady fluid flow over a complete wing-pylon-store configuration with the store in the captive and vertical launch positions. Dissert. Abstr.

N90-14498*# Lehigh Univ., Bethlehem, PA.
EMBEDDED FUNCTION METHODS FOR COMPRESSIBLE HIGH SPEED TURBULENT FLOW Progress Report
J. D. A. Walker 1989 19 p
(Grant NAG1-8321)
(NASA-CR-186131; NAS 1.26:186131) Avail: NTIS HC A03/MF A01 CSCL 20D

Fundamental issues relating to compressible turbulent flow are addressed. The focus has been on developing methods and testing concepts for attached flows rather than trying to force a conventional law of the wall into a zone of backflow. Although the dynamics of the near-wall flow in an attached turbulent boundary layer are relatively well documented, the dynamical features of a zone of reversed turbulent flow are not, nor are they well understood. Incompressibility introduces effects and issues that have been dealt with only marginally in the literature, therefore, the present work has been focussed on attached high-speed flows. The wall function method has been extended up through the supersonic to hypersonic speeds. Algorithms have been successfully introduced into the code that calculates the flow all the way to the wall, and testing is being carried out for progressively more complex flow situations. J.P.S.

N90-14499 Leeds Univ. (England).
THE FLUID MECHANICS OF FILTERS Ph.D. Thesis
Michael Lewis Hildyard 1988 228 p
Avail: Univ. Microfilms Order No. BRD-86244

The use of fibrous filters to remove unwanted suspended particles from a carrier fluid has increased substantially in recent years, partly due to the increase awareness of damage (both to health and machinery) these particles can cause. The design of analytical and empirical approaches with the former method using suitable models to explain the latter method and also to suggest possible improvements. A largely numerical approach is made by modeling a filter as an array of cylinders and finding a detailed description of both the fluid and the particle flows through such a model. As a first attempt at this, the enormous complexity of a general flow is simplified by assuming that the Reynolds number of the flow is either very large (potential flow approximation) or very small (creeping flow) and by the adoption of a regular array of cylinders. The fluid flow pattern and the particle collection efficiency are calculated, together with the pressure gradient, for several arrays and are shown to be in good agreement with existing theoretical and experimental results. The flow in the interior of the arrays is found and shown to be affected (more than hitherto realized) by conditions at the upstream boundary. The determination of the particle concentration in a carrier fluid is also very important and an examination of a simple sampler is made in order to demonstrate under what conditions a sampler should operate so as to enable meaningful measures of concentration to be determined. Dissert. Abstr.

N90-14500 Stanford Univ., CA.
AN ENTROPY BASED APPROACH TO NONLINEAR STABILITY Ph.D. Thesis
Marshal Lockhart Merriam 1989 214 p
Avail: Univ. Microfilms Order No. DA8919450

Many numerical methods used in Computational Fluid Dynamics

(CFD) incorporate an artificial dissipation term to suppress spurious oscillations and control nonlinear instabilities. The same effect can be accomplished by using upwind techniques, sometimes augmented with limiters to form Total Variation Diminishing (TVD) schemes. An analysis based on numerical satisfaction of the second law of thermodynamics allows many such methods to be compared and improved upon. For example, certain TVD schemes tend to square a smooth pulse. These can be detected a priori by their negative entropy production rates. A nonlinear stability proof is given for discrete scalar equations arising from a conservation law. Solutions to such equations are bounded in the L2 norm if the second law of thermodynamics is satisfied in a global sense over a periodic domain. It is conjectured that an analogous statement is true for discrete equations arising from systems of conservation laws. Stability in the L2 norm is not sufficient to exclude expansion shocks, oscillations, and other unphysical phenomena. Numerical experiments suggest that a more restrictive condition, a positive entropy production rate in each cell, is both necessary and sufficient to exclude such phenomena. Dissert. Abstr.

N90-14501 Stanford Univ., CA.
NUMERICAL SOLUTION OF THE INCOMPRESSIBLE NAVIER-STOKES EQUATIONS Ph.D. Thesis
Stuart Eames Rogers 1989 110 p
Avail: Univ. Microfilms Order No. DA8919466

An efficient, accurate, and robust algorithm was obtained for the numerical solution of the incompressible Navier-Stokes equations in 2-D and 3-D generalized curvilinear coordinates for both steady state and time dependent flow problems. This is accomplished with the use of the method of artificial compressibility and high order flux difference splitting technique for the differencing of the convective terms. Time accuracy is obtained in the numerical solutions by subiterating the equations in pseudo-time for each physical time step. The system of equations is solved with a line relaxation scheme which allows the use of very large pseudo-time steps leading to fast convergence for steady state problems as well as for the subiterations of time dependent problems. Numerous laminar test flow problems are computed and presented with a comparison against analytically known solutions or experimental results. These include the flow in a driven cavity, the flow over a backward-facing step, the steady and unsteady flow over a circular cylinder, flow over an oscillating plate, flow through a 1-D inviscid channel with oscillating back pressure, the steady state flow through a square duct with a 90 degree bend, and the flow through an artificial heart configuration with moving boundaries. An adequate comparison with the analytical or experimental results is obtained in all cases. Numerical comparisons of the upwind differencing with central differencing plus artificial dissipation indicates that the upwind differencing provides a much more robust algorithm, which requires significantly less computing time. The time dependent problems require on the order of 10 to 20 subiterations, indicating that the elliptical nature of the problem does require a substantial amount of computing effort. Dissert. Abstr.

N90-14502 Colorado Univ., Boulder.
THE STABILITY OF TAYLOR-COUETTE FLOW WITH RADIAL HEATING Ph.D. Thesis
Mohamed El-Sayed Ali 1988 215 p
Avail: Univ. Microfilms Order No. DA8912169

The stability of circular Couette flow with radial heating across vertically oriented coaxial cylinders is investigated using linearized stability theory. The physical problem is governed by five parameters: the Taylor number Ta, the Groshof number G, the Prandtl number Pr, the cylinder aspect ration A, and the radius ratio eta. In the model infinite aspect ratio is assumed and critical stability boundaries are calculated for a conduction regime base flow. A rational analysis is made to derive the full governing perturbation equations and test flow stability subject to both axisymmetric and nonaxisymmetric disturbances. The flow may be driven to instability by competition between centrifugal, buoyancy, and shear force mechanisms. In spite of this complexity, the existence of solution symmetries of the perturbation equations with respect to the sense of radial heating and the sense of cylinder rotation are proven. The linear boundary-value problem defined by 16 first-order differential equations is solved using the software package SUPORT in combination with the nonlinear equation solver SNSQE. Critical stability boundaries at fixed Pr and eta were determined by searching for the minimum value of either Ta or G over all wavelengths K and mode numbers n. Dissert. Abstr.

N90-14503 Iowa State Univ. of Science and Technology, Ames.
HEAT TRANSFER TO A STATIONARY AND MOVING SPHERE IMMERSED IN A FLUIDIZED BED Ph.D. Thesis
Chetan Jitendra Desai 1989 392 p
Avail: Univ. Microfilms Order No. DA8920123

The motion of submerged objects in fluidized beds and the corresponding improvement in the heat transfer rate has been largely unexplored. This improvement in heat transfer rate is significant in the design and operating cost of industrial fluidized beds that are used for heat treatment of metal objects, solid waste to be burned, gasification of coal particles, freezing of food grains, and coating operation. The heat transfer to a stationary sphere, a vertically downward moving sphere, and an oscillating copper sphere submerged in an air fluidized bed of glass particles was studied with the bed at standard pressure and temperature conditions. Several of the important variables known to influence the heat transfer rate to a stationary sphere in an air fluidized bed were determined as well as the effect of forced linearly downward motion and oscillating motion of the sphere on heat transfer rate. Dissert. Abstr.

N90-14504 Liverpool Univ. (England).
APPLICATIONS OF A NEW EXACT SOLUTION OF THE NAVIER-STOKES EQUATIONS TO FLOW IN PIPES OF VARYING WIDTH Ph.D. Thesis
Tracy Colgan 1987 166 p
Avail: Univ. Microfilms Order No. BRDX86166

Applications of a new, exact solution to the axisymmetric Navier-Stokes equations were studied. The important feature of this solution is that it is valid for all Reynolds numbers. All recent research in this field has needed to make a variety of assumptions regarding the physical properties of the flow. Consequently, this new solution has provoked a great deal of interest and has widespread implications in further research. A significant feature of this new solution is the non-zero radial velocity on surfaces equidistant from the axis of the pipe, and as such, applications to tubes with impremeable boundaries requires pipes to have varying radius. The first case to be considered was that of peristaltic transport, that is the movement of fluid by travelling, sinusoidal waves of contraction along a tube. This problem is of considerable relevance in biomechanics and in the pumping of corrosive fluids. Previous research into peristalsis has tackled specific approximated cases of small and large Reynolds number and good agreement was found between flow features of these and those of this solution. Subsequent research has concentrated on flow through pipes of slowly varying cross sectional area, with both porous and impermeable boundaries. Industry has expressed interest in transport of fluids along such pipes. However, the majority of the work done was either numerical or experimental and deals only with the particular flow characteristics. The solution for the impermeable case is found as a series in the axial parameter and use a number of computational tools, algebraic computing, and numerical software packages to obtain the coefficients. The work was completed by a study of a combination of variable width and suction. Families of boundaries are obtained for the necessary streamline distributions and the corresponding mass transfer profiles are presented. Dissert. Abstr.

N90-14505 Leeds Univ. (England).
HEAT TRANSFER IN CONVECTIVE BOUNDARY LAYER AND CHANNEL FLOWS Ph.D. Thesis
Tahir Mahmood 1988 237 p
Avail: Univ. Microfilms Order No. BRD-86151

Discussed here are five separate problems, each linked through the general area of heat transfer and fluid flow. In the first chapter

the effect of a moving wall on a wall jet is treated. In the second and third chapters axisymmetric flows are discussed, the second chapter dealing with the mixed convection flow on a vertical cylinder in a uniform stream, and in the third the similarity solutions for axisymmetric mixed convection flow are analyzed in detail. The final chapters deal with the mixed convection flow in a duct and the flow generated by an indentation in the duct wall under the basic assumption that the duct is narrow. This enables the governing equations to be simplified and these are treated in some detail. Dissert. Abstr.

N90-14506 Toledo Univ., OH.
A NUMERICAL TECHNIQUE FOR ANALYSIS OF RESISTOJET NOZZLE FLOW Ph.D. Thesis
Paul Frank Penko 1989 115 p
Avail: Univ. Microfilms Order No. DA8917584

A numerical technique is presented for computation of compressible, viscous flow in small converging-diverging rocket nozzles typical of resistojets. The computational scheme is implicit and uses Gauss-Siedel line relaxation to solve the thin-layer approximation to the Navier-Stokes equations. The equations are written in conservative form for 2-dimensional planar or axisymmetric coordinates. The scheme is finite volume and splitting of the inviscid flux vectors is employed. The resulting matrix of equations, that is solved for the conservation variables, is in block-tridiagonal form. Computational grids and computed results, including numerical convergence rate and plots of constant Mach Number contours, are presented to various conical nozzle geometries, gases, and Reynolds Numbers. The strong viscous structure of the flow in resistojet nozzles is clearly illustrated.
Dissert. Abstr.

N90-14507 Leeds Univ. (England).
MULTIGRID SOLUTIONS OF ELLIPTIC FLUID FLOW PROBLEMS Ph.D. Thesis
Nigel George Wright 1988 186 p
Avail: Univ. Microfilms Order No. BRD-86095

An efficient FAS multigrid solution strategy is presented for the accurate and economic simulation of convection dominated flows. The use of a high-order approximation to the convective transport terms found in the governing equations of motion was investigated in conjunction with an unsegregated smoothing technique. Results are presented for a sequence of problems of increasing complexity requiring that careful attention be directed toward the proper treatment of different types of boundary condition. The classical two-dimensional problem of flow in a lid-driven cavity is investigated in depth for flows at Reynolds number of 100, 400 and 1000. This gives an extremely good indication of the power of a multigrid approach. Next, the solution methodology is applied to flow in a three-dimensional lid-driven cavity at different Reynolds numbers, with cross-reference being made to predictions obtained in the corresponding two-dimensional simulations, and to the flow over a step discontinuity in the case of an abruptly expanding channel. Although, at first sight, these problems appear to require only minor extensions to the existing approach, it is found that they are rather more idiosyncratic. Finally, the governing equations and numerical algorithm are extended to encompass the treatment of thermally driven flows. The solution to two such problems is presented and compared with corresponding results obtained by traditional methods.
Dissert. Abstr.

N90-14508 Maryland Univ., College Park.
AN EXPERIMENTAL INVESTIGATION OF SHEAR LAYER MIXING IN SUPERSONIC FLOWS Ph.D. Thesis
Gary Alan Sullins 1988 133 p
Avail: Univ Microfilms Order No. DA8912355

In the design of a combustor, information is necessary for the mixing of the fuel and air in order to determine the optimum combustor length. In scramjet combustors the mixing often takes place in a shear layer that is formed between the fuel and air. An experimenatl study was made of shear layers in supersonic flows aimed at determining what mechanisms affect the shear layer so that the mixing could be better predicted. Sufficient instream information was provided for use in checking existing Computational Fluid Dynamics (CFD) codes. The shear layer between a supersonic 2-D air stream (M = 2 or M = 3) was mixed with a near sonic 2-D air stream (M approx. = 1.2). Instream measurements of pitot pressure and cone static pressure were used to determine mean velocity profiles at various axial locations. These velocity profiles were used to determine the shear layer spreading rate and are compared with various predictions. Wall measurements of static pressure, temperature, and skin friction were also taken and are presented. The instream measurements were also used for comparison with an existing CFD code. Reasonable agreement between the measured and calculated results was obtained.
Dissert. Abstr.

N90-14509 Mississippi State Univ., State College.
THREE-DIMENSIONAL SOLUTION-ADAPTIVE GRID GENERATION OF COMPOSITE CONFIGURATIONS Ph.D. Thesis
Yen Tu 1989 113 p
Avail: Univ. Microfilms Order No. DA8917084

A solution adaptive grid generation procedure is developed and applied to 3-D inviscid transonic fluid flow around complex geometries using a composite block grid structure. The adaptation is based upon control functions in an elliptic grid generation system. The control function is constructed in a manner such that a proper grid network can be generated as a fluid flow solution is evolving. The grid network is boundary conforming for accurate representation of boundary conditions. The procedure implemented allows orthodonality at boundaries for more accurate computations, while smoothness is implicit in the elliptic equations. The approach allows multiple block grid systems to be constructed to treat complex configurations as well. The solution adaptive computational procedure was accomplished by coupling the elliptic grid generation technique with an implicit, finite volume, upwind Euler flow solver. In simulating trasonic fluid flow around finned body of revolution and a multiple store configuration, the grid systems adapt to pressure gradients in the flow field. Results obtained show that the technique is capable of generating grid networks proper for the simulations of complex aerodynamic configurations.
Dissert. Abstr.

N90-14510 Oklahoma Univ., Norman.
STABILITY OF A SUPERSONIC BOUNDARY LAYER ON A SHARP CONE AT A SMALL ANGLE OF ATTACK Ph.D. Thesis
Deifallah Ali Dajeh 1988 139 p
Avail: Univ. Microfilms Order No. DA8914152

The stability of the supersonic laminar boundary layer on a sharp, 10-degree half angle cone at a zero angle of attack and at a small angle of attack was investigated. A small angle of attack was found to make significant changes, compared to a zero angle of attack, in the stability characteristics of the boundary layer. Neutral-stability curves for both cases were presented. For an angle of attack of 2.5-degrees, the critical Reynolds number increased on the windward side and decreased on the leeward side. The windward boundary layer profiles were more stable than the boundary layer profiles of the axisymmetric case as well as the leeward side. Some important issues were not resolved within the present study. However, recommendations on how to tackle them are suggested. Dissert. Abstr.

N90-14511*# National Aeronautics and Space Administration. Lewis Research Center, Cleveland, OH.
THERMAL/STRUCTURAL ANALYSES OF SEVERAL HYDROGEN-COOLED LEADING-EDGE CONCEPTS FOR HYPERSONIC FLIGHT VEHICLES
Herbert J. Gladden, Matthew E. Melis, Theodore T. Mockler, and Mike Tong (Sverdrup Technology, Inc., Cleveland, OH.) 1990 16 p Presented at the 28th Aerospace Sciences Meeting, Reno, NV, 8-11 Jan. 1990; sponsored by AIAA Original contains color illustrations
(NASA-TM-102391; E-4788; NAS 1.15:102391; AIAA-90-0053)
Avail: NTIS HC A03/MF A01 CSCL 20D

The aerodynamic heating at high flight Mach numbers, when shock interference heating is included, can be extremely high and can exceed the capability of most conventional metallic and potential ceramic materials available. Numerical analyses of the heat transfer and thermal stresses are performed on three actively cooled leading-edge geometries (models) made of three different materials to address the issue of survivability in a hostile environment. These analyses show a mixture of results from one configuration to the next. Results for each configuration are presented and discussed. Combinations of enhanced internal film coefficients and high material thermal conductivity of copper and tungsten are predicted to maintain the maximum wall temperature for each concept within acceptable operating limits. The exception is the TD nickel material which is predicted to melt for most cases. The wide range of internal impingement film coefficients (based on correlations) for these conditions can lead to a significant uncertainty in expected leading-edge wall temperatures. The equivalent plastic strain, inherent in each configuration which results from the high thermal gradients, indicates a need for further cyclic analysis to determine component life. Author

N90-14512*# Sverdrup Technology, Inc., Cleveland, OH.
THERMOCAPILLARY MIGRATION OF LIQUID DROPLETS IN A TEMPERATURE GRADIENT IN A DENSITY MATCHED SYSTEM Final Report
N. Rashidnia and R. Balasubramaniam (Case Western Reserve Univ., Cleveland, OH.) Dec. 1989 28 p
(Contracts NAS3-25266; NCC3-140)
(NASA-CR-185178; E-5192; NAS 1.26:185178) Avail: NTIS HC A03/MF A01 CSCL 20D

An experimental investigation of thermocapillary flow in droplets of a vegetable oil (partially hydrogenated soybean oil) immersed in silicone oil was conducted in a test cell with a heated top wall and a cooled bottom wall. The liquids are nearly immiscible and have equal densities at a temperature below the room temperature, thus providing a simulation of low-gravity conditions by reducing the buoyancy forces. The interfacial tension between the two oils was measured in the temperature range 20 to 50 C using a capillary tube and (d sigma)/(d T) was determined to be negative. Droplets ranging in sizes from 3 mm to 1 cm diameter were injected into the silicone oil. The vertical temperature profile in the bulk liquid (silicone oil) produces temperature variations along the interface which induce variations in the interfacial tension. The flow inside the droplet driven by the resulting interfacial shear stresses was observed using a laser light-sheet flow visualization technique. The flow direction is consistent with the sign of (d sigma)/(d T). The observed maximum surface velocities are compared to the theoretical predictions of Young et al. (1959). Author

N90-14513*# Institute for Computer Applications in Science and Engineering, Hampton, VA.
THE ANALYSIS AND MODELING OF DILATATIONAL TERMS IN COMPRESSIBLE TURBULENCE Final Report
S. Sarkar, G. Erlebacher, M. Y. Hussaini, and H. O. Kreiss (California Univ., Los Angeles.) Dec. 1989 34 p Submitted for publication
(Contract NAS1-18605)
(NASA-CR-181959; NAS 1.26:181959; ICASE-89-79) Avail: NTIS HC A03/MF A01 CSCL 20D

It is shown that the dilatational terms that need to be modeled in compressible turbulence include not only the pressure-dilatation term but also another term - the compressible dissipation. The nature of these dilatational terms in homogeneous turbulence is explored by asymptotic analysis of the compressible Navier-Stokes equations. A non-dimensional parameter which characterizes some compressible effects in moderate Mach number, homogeneous turbulence is identified. Direct numerical simulations (DNS) of isotropic, compressible turbulence are performed, and their results are found to be in agreement with the theoretical analysis. A model for the compressible dissipation is proposed; the model is based on the asymptotic analysis and the direct numerical simulations. This model is calibrated with reference to the DNS results regarding the influence of compressibility on the decay rate of isotropic turbulence. An application of the proposed model to the compressible mixing layer has shown that the model is able to predict the dramatically reduced growth rate of the compressible mixing layer. Author

N90-14514# Centro Brasileiro de Pesquisas Fisicas, Rio de Janeiro.
GENERAL EXACT SOLUTION FOR HOMOGENEOUS TIME-DEPENDENT SELF-GRAVITATING PERFECT FLUIDS
Patricio Gaete and Roberto Hojman (Chile Univ., Santiago.) 1988 17 p Submitted for publication
(Grants N-0622/88; N-020/87)
(DE89-618425; CBPF-NF-063/88; ISSN-0029-3865) Avail: NTIS (US Sales Only) HC A03/MF A01

A procedure to obtain the general exact solution of Einstein equations for a self-gravitating spherically symmetric static perfect fluid obeying an arbitrary equation of state, is applied to time dependent Kantowsky-Sachs line elements (with spherical, planar and hyperbolic symmetry). As in the static case, the solution is generated by an arbitrary function of the independent variable and its first derivative. To illustrate the results, the whole family of (plane-symmetric) solutions with a gamma-law equation of state is explicity obtained in terms of simple known functions. It is also shown that, while in the static plane-symmetric line elements, every metric is in one to one correspondence with a partner-metric (both originated from the same generatrix function), in this case every generatrix function univocally determines one metric. DOE

N90-14515# Lawrence Livermore National Lab., CA.
PROPAGATION OF DETONATION WAVES FROM AN IMPACT REGION
R. S. Lee, W. C. Tao, and L. D. Crouch 1989 10 p Presented at the 9th International Symposium on Detonation, Portland, OR, 28 Aug. - 1 Sep. 1989
(Contract W-7405-eng-48)
(DE90-001184; UCRL-99559; CONF-890811-40) Avail: NTIS HC A02/MF A01

An experimental system was developed to study the propagation of a detonation wave away from a region that is initiated by the impact of a thin flyer plate. The propagation of detonation waves away from this region in pressed pellets of TATB and in RX-26-AF, a TATB/HMX formulation is studied. The system permits measurements at elevated, ambient, and low temperatures. The the distance-time trajectory and arrival time of the detonation front at the downstream face of the explosive pellets is measured for pellets with thicknesses of 1 to 16 mm over the temperature range -80 to +80 C. DOE

N90-14516# Houston Univ., TX. Dept. of Mechanical Engineering.
COMPARATIVE STUDY OF THE VORTICITY FIELD IN TURBULENT FLOWS: THEORY, EXPERIMENTS, AND COMPUTATIONS Progress Report
Fazle Hussain 10 Oct. 1989 20 p
(Contract DE-FG05-88ER-13839)
(DE90-001399; DOE/ER-13839/2) Avail: NTIS HC A03/MF A01

The coherent structures approach was used to understand, analyze and model turbulent flows. Vorticity was considered as the defining property of coherent structures. Turbulent flows are characterized by vortical structures undergoing deformation and interaction due to self- and mutual inductions. One of the primary objectives was to obtain a detailed understanding of these interactions. The concepts of vortex dynamics, when applied to coherent structures, help in understanding many of the peculiarities of noncircular jets, especially elliptic jets. The structures in these jets have nonplanar advections, thus having the simplicity allowing their evolution, yet retaining the 3-D features generic of all coherent structures in turbulent shear flows. DOE

N90-14517*# National Aeronautics and Space Administration. Lewis Research Center, Cleveland, OH.
SPATIAL EVOLUTION OF NONLINEAR ACOUSTIC MODE INSTABILITIES ON HYPERSONIC BOUNDARY LAYERS
M. E. Goldstein and D. W. Wundrow (State Univ. of New York, Buffalo.) Dec. 1989 30 p
(Contract NAS3-25266; NGT-50085; NASA Order C-99066-G)
(NASA-TM-102431; E-5075-1; ICOMP-89-30; NAS 1.15:102431)
Avail: NTIS HC A03/MF A01 CSCL 20D

The effects are considered of strong critical layer nonlinearity on the spatial evolution of an initially linear acoustic mode instability wave on a hypersonic flat plate boundary layer. The analysis shows that nonlinearity, which is initially confined to a thin critical layer, first becomes important when the amplitude of the pressure fluctuations become 0(1/M exp 4 ln M exp 2), where M is the free stream Mach number. The flow outside the critical layer is still determined by linear dynamics and therefore takes the form of a linear instability wave, but with its amplitude completely determined by the flow within the critical layer. The latter flow is determined by a coupled set of nonlinear equations, which were solved numerically. Author

N90-14518# Lawrence Livermore National Lab., CA.
GRANULAR FLOW: NUMERICAL SIMULATION OF DRY GRANULAR FLOWS AND CALCULATION OF HYDRODYNAMIC INTERACTIONS IN SUSPENSIONS Report, 1 Oct. 1988 - 30 May 1989
Anthony J. C. Ladd and Otis R. Walton Jul. 1989 12 p Presented at the Joint DOE/NSF Workshop on Fluid-Solids Transport, Pleasanton, CA, 15-17 May 1989
(Contract W-7405-eng-48)
(DE89-017544; UCRL-101605; CONF-8905209-1) Avail: NTIS HC A03/MF A01

Research emphasized two major topics: determination of the flow behavior of rapidly shearing dry granular solids and calculation of hydrodynamics forces in creeping flows of suspensions of spherical particles. Discrete particle computer models that calculate the motion of each inelastic, frictional particle in large assemblies were applied to the simulation of dry granular flows. A hard sphere model, employing instantaneous collisions and straight line trajectories between collisions, was used to perform binary mixture calculations with size ratios from 1 to 4. These simulations showed a stronger sample size dependence than previously recognized and qualitatively confirmed earlier results that stresses in shearing mixtures with large size ratios are lower than predicted by current theories. As part of the study of dry granular flows we also added new boundary conditions to the models, translated them to standard FORTRAN 77 for portability and continued existing collaborative efforts and established new collaborative research agreements with various University researchers. The suspension modeling portion of this research emphasized development of new accurate and efficient numerical schemes for calculating hydrodynamic interactions in suspensions of spherical particles. The method is based on a multipole moment expansion of the induced force density acting on the fluid at the surface of each particle. The convergence of the multipole expansion was improved by including the short-range lubrication forces explicitly. Numerical results for the viscosity, diffusion constant, sedimentation velocity, and permeability were obtained and serve to illustrate the various stages of development of the method and to assess their effectiveness in representing the hydrodynamic interactions. DOE

N90-14519# Argonne National Lab., IL. Energy and Environmental Systems Div.
SELECTION OF THE ENERGY-EFFICIENT ENHANCEMENT GEOMETRY FOR SINGLE-PHASE TURBULENT FLOW INSIDE TUBES
T. J. Rabas 1989 13 p Presented at the ASME/AIChE National Heat Transfer Conference, Philadelphia, PA, 6-9 Aug. 1989
(Contract W-31-109-eng-38)
(DE89-017690; CONF-890819-25) Avail: NTIS HC A03/MF A01

Heat transfer enhancements inside tubes such as ribs, fins, and flutes are a proven technique for increasing the thermal performance of heat transfer equipment. Unfortunately, there is always an increased pressure drop that accompanies the improved thermal performance. Enhancement geometries that maximize the efficiency index (the ratio of the heat transfer to the friction factor enhancement values) are addressed. It is demonstrated that energy efficient enhancement geometries are not always selected; the disruption heights are usually too high, and very little attention is given to the disruption shape. An enhancement mechanism map is first presented. With this map, energy efficient geometry sets can be identified and others discarded. Tube types that should receive more consideration are those that rely on the swirl and boundary layer thinning (3-D roughness) mechanisms. It is also demonstrated that the most energy efficient geometries are those that permit operation in the transition region. The roughness Reynolds number appears to adequately characterize these conditions; however, the magnitude depends on the disruption shape and mechanism type for a given Prandtl number fluid. DOE

N90-14520# Los Alamos National Lab., NM.
PERTURBATIONS IN HIGH-VELOCITY GAS FLOW
W. B. Harvey and R. G. McQueen 1989 5 p Presented at the American Physical Society Topical Conference on Shock Compression of Condensed Matter, Albuquerque, NM, 14-17 Aug. 1989
(Contract W-7405-eng-36)
(DE90-000539; LA-UR-89-3017; CONF-890812-48) Avail: NTIS HC A01/MF A01

High velocity explosive products or other low-density gases are often used to accelerate metal plates to high velocities. Perturbations in otherwise uniform flow configurations are sometimes sufficient to cause interactions that can rapidly destroy the integrity of the plates. In this study perturbations were introduced in uniform gas flows of detonated HE products and strongly shocked polyethylene, CH2. The primary diagnostics were smear-camera records obtained when these gases impinged on layers of plexiglas separated by small argon-filled gaps. These records show shock-arrival times at various levels and thus determine not only the size of the perturbation but also its strength. Perturbations in HE gases running into H2 and in CH2 into H2 were studied. Two-dimensional hydrodynamic calculations are in excellent agreement with the experiments, and enable one to study details of the flow not possible from experimental results. DOE

N90-14521# New York Univ., New York. Inst. of Mathematical Sciences.
THE LAMINAR TO SLUG FLOW TRANSITION IN HELE-SHAW FLOW
James Glimm, Wei Guo (State Univ. of New York, Stony Brook.), and Qiang Zhang Sep. 1989 29 p
(Contract DE-FG02-88ER-25053; NSF DMS-86-19856)
(DE90-000636; DOE/ER-25053/2) Avail: NTIS HC A03/MF A01

Foam generation is a promising method to increase the efficiency of enhanced oil recovery processes. The present study began with the observation that the pinch off of bubbles upstream of an obstacle (pore throat) is a mechanism for bubble (i.e., foam) generation. We find support for this mechanism through a study of the laminar to slug flow transition in an idealized physical and geometrical setting. Transitions between multiphase flow regimes are of basic interest. A surprising conclusion of our study is the reversal of fingering stability caused by a strong transverse flow field. DOE

N90-14522# Los Alamos National Lab., NM.
A NEW SIMULATION METHOD FOR THE EFFICIENT CALCULATION OF BENCHMARKS FOR DETONATION PRODUCTS EQUATIONS OF STATE
M. S. Shaw 1989 26 p Presented at the 9th International Symposium on Detonation, Portland, OR, 28 Aug. - 1 Sep. 1989

(Contract W-7405-eng-36)
(DE90-001837; LA-UR-89-3060; CONF-890811-32) Avail: NTIS HC A03/MF A01

A new variation on the Monte Carlo method is presented here in the context of its potential impact on the development of detonation products equations of state (EOS). The configurational density of states and other quantities are determined for a nonstandard reference simulation. Then the EOS for a linear combination of potentials is evaluated through a density of states transformation at arbitrary densities and temperatures in the fluid range. The computer time required for the EOS calculation (including free energies) is negligible once the reference simulation is made. The EOS over the entire fluid regime for a Lennard-Jones fluid (including the location of the gas/liquid equilibrium phase line) is calculated. Preliminary results on the extension of the method to the exponential-six potential are presented. The efficient calculation of benchmarks over the very large parameter space of relevance to detonation products EOS may now be possible. DOE

N90-14523# Edgerton, Germeshausen and Grier, Inc., Idaho Falls, ID.
FIELD TESTING OF A CERAMIC HEAT EXCHANGER FOR HEAT RECOVERY APPLICATION
M. S. Sohal 1988 29 p Presented at the 25th American Society of Mechanical Engineers/American Inst. of Chemical Engineers/American Nuclear Society National Heat Transfer Conference, Houston, TX, 24-27 Jul. 1988
(Contracts DE-AC07-76ID-01570; DE-FC07-81ID-12170)
(DE90-002082; EGG-M-36387; CONF-880724-29) Avail: NTIS HC A03/MF A01

AiResearch Company, Torrance, California, developed a 5 MMBtu/hr ceramic-metallic hybrid High Temperature Burner-Duct-Recuperator (HTBDR) system to recover energy from hot (up to 2500 F), dirty, and corrosive glue gas streams and preheat combustion air up to 2000 F. To reduce the cost and size of the ceramic recuperator, ceramic tubes with internal cruciform baffles were developed. The HTBDR system was tested on a 20 MMBtu/hr rotary forging furnace for about 2000 hours. To facilitate tube replacements, final design configuration uses horizontally mounted tubes. A maximum air preheat temperature of about 1916 F was achieved with a flue gas temperature of 2122 F. This represents fuel savings of about 30 to 50 percent (depending upon the amount of excess air) compared with an unrecuperated furnace. The overall design and operation of the recuperator proved to be successful up to the time of material failure. X ray diffraction of some failed components indicated that there was some residual Silicon in the interior regions and complete nitriding did not occur during the fabrication process. Degradation of failed components was probably caused by oxidation of residual silicon and by the stresses caused due to different coefficient of thermal expansion of various compounds during thermal cycling. A combination of severe and numerous thermal cycling coupled with incomplete nitriding was the most likely cause of material failure. DOE

N90-14524# Pittsburgh Univ., PA. Dept. of Chemical and Petroleum Engineering.
PIPE AND BEND EROSION BY PNEUMATIC TRANSPORT OF SOLIDS AT HIGH TEMPERATURE Final Report
George E. Klinzing, Luis A. Borzone, and Wen-Ching Yang (Westinghouse Research and Development Center, Pittsburgh, PA.) Jun. 1989 217 p
(Contract DE-FG22-85PC-80524)
(DE89-015741; DOE/PC-80524/T15) Avail: NTIS HC A10/MF A02

The erosion of various components of a pneumatic transport line was studied through basic experiments, commercial scale test runs and computer simulation. The main objective was to study the effect of the operating variables on the erosion rates of refractory lined straight sections and bends. Temperatures ranging from 22 to 830 C, gas velocities from 12.9 to 34 m/s and solid flow rates from 48 to 225 kg/h were tested in a High Temperature Pneumatic Transport Test Facility. Four kinds of refractory concretes were used as targets. The erodent materials were river sand, coal slag and alumina. The effect of gas velocity and solids slow rate on the erosion rate was correlated in terms of power laws, while temperature effects proved to be more complex, since mechanical properties of both erodent and target materials change with temperature. The erosion of circular bends was evaluated using a computer model that combines computational particle dynamics and experimental data to predict the erosion pattern inside the bend. Experiments on the erosion of wedge samples, performed in the erosion test facility, and data on particle-wall collisions, obtained with the help of high speed photographic techniques, were the basic set of data used in the simulation. As an alternative to circular radius bends, and experimental study of wear and flow patterns in blinded T-bends was performed. The internal geometry in this kind of bends was determined by the solids deposition, and complex erosion patterns appeared as the operating variables were manipulated. DOE

N90-14525# International Centre for Theoretical Physics, Trieste (Italy).
UNSTEADY HYDROMAGNETIC FLOW OF A RADIATING GAS IN A VERTICAL CHANNEL WITH AXIAL TEMPERATURE VARIATION
A. R. Bestman May 1989 12 p
(DE90-600934; IC-89/94) Avail: NTIS (US Sales Only) HC A03/MF A01

The effect of transience on the hydromagnetic flow of a thermally radiating gas in a vertical channel is investigated under the assumption that the gas is optically thin, non-grey and non equilibrium; and the induced magnetic field may be neglected. Analytical solutions are obtained for thermal tooth pulses via Fourier series expansion. The effect of the variation of free convection, magnetic and radiation parameters on the shear stress and heat transfer at the walls are discussed quantitively. DOE

N90-14526# Idaho National Engineering Lab., Idaho Falls.
COURSE A: NUMERICAL MODELING OF TWO-PHASE FLOWS FOR PRESENTATION AT ECOLE D'ETE D'ANALYSE NUMERIQUE
Victor Ransom May 1989 376 p Presented at the Summer School on Numerical Analysis, Saclay, France, 12-23 Jun. 1989 Sponsored in part by Commissariat a l'Energie Atomique and Institut National de Recherche en Informatique et d'Automatique
(Contract DE-AC07-76ID-01570)
(DE90-002074; EGG-EAST-8546; CONF-8906249-1) Avail: NTIS HC A17/MF A03

This course is designed to provide an introduction to the application of two-fluid modeling techniques to two-phase or, more generally, multiphase flows, and to the numerical methods that were developed for solution of such problems. The methods that are presented have evolved to a large extent as a result of international efforts to improve the understanding of light-water-reactor transient response to postulated loss of coolant accidents. Transient simulation codes that are based on these methods are now in routine use throughout the international light-water-reactor safety research and regulatory organizations. DOE

N90-14527# Purdue Univ., West Lafayette, IN. Dept. of Nuclear Engineering.
INTERFACIAL AREA IN TWO-PHASE FLOW
M. Ishii and M. J. Tan (Argonne National Lab., IL.) 1989 11 p Presented at the 7th Symposium on Energy Engineering Sciences, Argonne, IL, 19-21 Jun. 1989
(Contract W-31-109-eng-38)
(DE90-002210; CONF-8906112-2) Avail: NTIS HC A03/MF A01

Knowledge of interfacial area is required for analysis and prediction of transient and steady characteristics of two-phase flow systems using the two-fluid models. Based on a survey of published work on the subject of interfacial area, it is recognized that there is virtually no data base for local interfacial area. The ongoing

development of interfacial area models and experimental techniques for measurement of local interfacial area concentration in gas-liquid and liquid-liquid two-phase systems is described. Mathematical relations between local interfacial area concentration and measurable quantities are derived based on kinematics and geometry. Two methods for determining local interfacial area are identified; both entail detection of passage of interfaces through fixed locations in the flow field. A multiple-sensor electrical-resistivity probe technique is being developed for determination of local interfacial area in vertical gas-liquid bubbly flows. The technique consists of simultaneous measurements at two or four locations in the two-phase flow field of the local electrical resistivity of the two-phase mixture. Methods for data analysis are described. Limitations of the technique are briefly discussed. DOE

N90-14528# Sandia National Labs., Albuquerque, NM.
CTH: A THREE-DIMENSIONAL SHOCK WAVE PHYSICS CODE
J. Michael McGlaun, S. L. Thompson, and M. G. Elrick (Kaman Sciences Corp., Albuquerque, NM.) 1989 13 p Presented at the Hypervelocity Impact Symposium, San Antonio, TX, 12-14 Dec. 1989
(Contract DE-AC04-76DP-00789)
(DE89-016529; SAND-89-0607C; CONF-891214-6) Avail: NTIS HC A03/MF A01

CTH is a software system under development at Sandia National Laboratories, Albuquerque, to model multidimensional, multi-material, large deformation, strong shock wave physics. One-dimensional rectilinear, cylindrical, and spherical meshes; 2-D rectangular, and cylindrical meshes; and 3-D rectangular meshes are currently available. A two-step Eulerian solution scheme is used with these meshes. The first step is a Lagrangian step in which the cells distort to follow the material motion. The second step is a remesh step where the distorted cells are mapped back to the Eulerian mesh. CTH has several models that are useful for simulating strong shock, large deformation events. Both tabular and analytic equations of state are available. CTH can model elastic-plastic behavior, high explosive detonation, fracture, and motion of fragments smaller than a computational cell. The elastic-plastic model is elastic-perfectly plastic with thermal softening. A programmed burn model is available for modelling high explosive detonation. The Jones-Wilkins-Lee equation of state is available for modelling high explosive reaction products. Fracture can be initiated based on pressure or principle stress. A special model is available for moving fragments smaller than a computational cell with statistically the correct velocity. This model is very useful for analyzing fragmentation experiments and experiments with witness plates. The models, and novel features of CTH are described. Special emphasis is placed on the features that are novel to CTH or are not direct generalizations of 2-D models. Another paper by Trucano and McGlaun describes several hypervelocity impact calculations using CTH. DOE

35 INSTRUMENTATION AND PHOTOGRAPHY

Includes remote sensors; measuring instruments and gages; detectors; cameras and photographic supplies; and holography.

For aerial photography see *43 Earth Resources and Remote Sensing.* For related information see also *06 Aircraft Instrumentation,* and *19 Spacecraft Instrumentation.*

N90-14529 Department of the Navy, Washington, DC.
METHOD FOR FABRICATING THIN FILM METALLIC MESHES FOR USE AS FABRY-PEROT INTERFEROMETER ELEMENTS, FILTERS AND OTHER DEVICES Patent
Charles J. Taylor, inventor (to Navy), Julius Grossman, inventor (to Navy), Jacqueline Fischer, inventor (to Navy), Howard A. Smith, inventor (to Navy), and Martin C. Peckerar, inventor (to Navy) 4 Apr. 1989 11 p Filed 21 Jul. 1987 Supersedes AD-013460 (AD-D014236; US-Patent-4,818,661; US-Patent-Appl-SN-079962)
Avail: US Patent and Trademark Office CSCL 09/1

A method of fabricating a free-standing wire mesh grid pattern having a smooth, flat surface is disclosed. A thermal oxide is selectively applied to front and back sides of a silicon substrate. A central portion of the oxide on the back side is removed. A resist layer is applied onto the oxide on the front side of the substrate. A resist mesh pattern with a border encompassing that resist mesh pattern is lithographically developed on the resist layer. Chrome and gold layers are sequentially deposited onto the border and into the resist mesh pattern to create a wire mesh pattern within the resist mesh pattern. The resist layer, including the developed resist mesh pattern, is removed to expose the wire mesh pattern from the front side of the substrate. A nickel layer is deposited over the gold layer to developed a wider wire mesh pattern. A second gold layer is then deposited over the nickel layer to form a wire mesh grid pattern composed of chrome, gold, nickel and gold layer. GRA

N90-14530*# Thiokol Corp., Brigham City, UT. Space Operations.
JPS HEATER AND SENSOR LIGHTNING QUALIFICATION Final Test Report
M. Cook 4 Oct. 1989 152 p Revised
(Contract NAS8-30490)
(NASA-CR-183830; NAS 1.26:183830; TWR-16389A-Rev-A)
Avail: NTIS HC A08/MF A01 CSCL 14B

Simulated lightning strike testing of the Redesigned Solid Rocket Motor (RSRM) field joint protection system heater assembly was performed at Thiokol Corp., Wendover Lightning Facility. Testing consisted of subjecting the lightning evaluation test article to simulated lightning strikes and evaluating the effects of heater cable transients on cables within the systems tunnel. The maximum short circuit current coupled onto a United Space Boosters, Inc. operational flight cable within the systems tunnel, induced by transients from all cables external to the systems tunnel, was 92 amperes. The maximum open-circuit voltage coupled was 316 volts. The maximum short circuit current coupled onto a United Space Boosters, Inc. operational flight cable within the systems tunnel, induced by heater power cable transients only, was 2.7 amperes; the maximum open-circuit voltage coupled was 39 volts. All heater power cable induced coupling was due to simulated lightning discharges only, no heater operating power was applied during the test. The results showed that, for a worst-case lightning discharge, the heater power cable is responsible for a 3.9 decibel increase in voltage coupling to operational flight cables within the systems tunnel. Testing also showed that current and voltage levels coupled onto cables within the systems tunnel are partially dependant on the relative locations of the cables within the systems tunnel. Author

N90-14531# Transportation Systems Center, Cambridge, MA. Office of Technology Applications.
METHODOLOGY FOR THE CALIBRATION OF AND DATA ACQUISITION WITH A SIX-DEGREE-OF-FREEDOM ACCELERATION MEASUREMENT DEVICE Final Report, Jul. 1983 - Feb. 1988
Harvey Lee, Gordon Plank, Herbert Weinstock, and Michael Coltman Jun. 1989 275 p Sponsored by National Highway Traffic Safety Administration, Washington, DC
(PB89-233597; DTS-74; DOT-TSC-NHTSA-88-3; DOT-HS-807-370) Avail: NTIS HC A12/MF A02 CSCL 14B

Described here is a methodology for calibrating and gathering data with a six-degree-of-freedom acceleration measurement device that is intended to measure head acceleration of anthropomorphic dummies and human volunteers in automotive crash testing and head impact trauma studies. Error models (system equations) were developed for systems using six accelerometers in a coplanar (3-2-1) configuration, nine accelerometers in a coplanar (3-3-3) configuration and nine accelerometers in a non-coplanar (3-2-2-2) configuration and the accuracy and stability of these systems were compared. The model was verified under various input and computational conditions. Results of parametric

sensitivity analyses which included parameters such as system geometry, coordinate system location, data sample rate and accelerometer cross axis sensitivities are presented. Recommendations to optimize data collection and reduction are given. Complete source listings of all of the software developed are presented.

N90-14532*# DePaul Univ., Chicago, IL. Dept. of Computer Science.
AN IMAGE COMPRESSION ALGORITHM FOR A HIGH-RESOLUTION DIGITAL STILL CAMERA Final Technical Report, 15 Sep. 1988 - 31 Dec. 1989
Rosalee Nerheim 1989 9 p
(Grant NAG9-313)
(NASA-CR-185079; NAS 1.26:185079) Avail: NTIS HC A02/MF A01 CSCL 14B

The Electronic Still Camera (ESC) project will provide for the capture and transmission of high-quality images without the use of film. The image quality will be superior to video and will approach the quality of 35mm film. The camera, which will have the same general shape and handling as a 35mm camera, will be able to send images to earth in near real-time. Images will be stored in computer memory (RAM) in removable cartridges readable by a computer. To save storage space, the image will be compressed and reconstructed at the time of viewing. Both lossless and loss-y image compression algorithms are studied, described, and compared. J.P.S.

N90-14533*# National Aeronautics and Space Administration. Langley Research Center, Hampton, VA.
A CAPACITIVE TECHNIQUE FOR REAL-TIME MONITORING POLYMER COATING THICKNESS ON CARBON FILAMENTS DURING PREPREGGING PROCESS
Abe Eftekhari (Analytical Services and Materials, Inc., Hampton, VA.) and John J. Chapman Dec. 1989 8 p
(NASA-TM-101682; NAS 1.15:101682) Avail: NTIS HC A02/MF A01 CSCL 14B

A technique for gauging the coating thickness during prepreg processing of carbon fibers was developed. It is based on the concept of measuring the capacitance of a cylindrical condenser through which a bundle of prepregged fibers is passed axially. Empirical results indicate the capacitance of this condenser element is linearly related to the polymer coating thickness on the fibers in the bundle. The capacitive transducer was successfully used to measure the polymer thickness on several test fiber bundles under static conditions. Author

N90-14534*# Northwestern Univ., Evanston, IL. Dept. of Materials Science and Engineering.
ELECTRICAL PROPERTIES OF MATERIALS FOR HIGH TEMPERATURE STRAIN GAGE APPLICATIONS Final Report
John O. Brittain 28 Feb. 1989 26 p
(Grant NAG3-501)
(NASA-CR-186192; NAS 1.26:186192) Avail: NTIS HC A03/MF A01 CSCL 14B

A study was done on the electrical resistance of materials that are potentially useful as resistance strain gages at high temperatures under static strain conditions. Initially a number of binary alloys were investigated. Later, third elements were added to these alloys, all of which were prepared by arc melting. Several transition metals were selected for experimentation, most prepared as thin films. Difficulties with electrical contacts thwarted efforts to extend measurements to the targeted 1000 C, but results obtained did suggest ways of improving the electrical resistance characteristics of certain materials. J.P.S.

N90-14535# Sandia National Labs., Albuquerque, NM. Experimental Mechanics Dept.
EVALUATION OF SHOCK ISOLATION TECHNIQUES FOR A PIEZORESISTIVE ACCELEROMETER
Vesta I. Bateman, R. Glenn Bell, and Neil T. Davie Jun. 1989 7 p Presented at the 60th Shock and Vibration Symposium, Virginia Beach, VA, 14-16 Nov. 1989
(Contract DE-AC04-76DP-00789)
(DE89-014496; SAND-89-1641C; CONF-891152-1) Avail: NTIS HC A02/MF A01

Sandia conducts impact testing for a variety of structures. In this slapdown test, one end of the cask impacts the hard concrete target, then the structure rotates so that the other end of the cask impacts the target. During an impact test, metal to metal contact may occur within the structure and produce high frequency, high amplitude shock inputs. The high frequency portion of this transient vibration was observed to excite the accelerometer resonance even though this resonance exceeds 350 kHz. The amplitude of the resonating accelerometer response can be so large that the data are clipped and are rendered useless. If the data are not clipped, a digital filter must be applied to eliminate the undesired accelerometer resonant response. If possible, it is more desirable to prevent excitation of the accelerometer resonance. This may be accomplished by mechanically isolating the accelerometer from the high frequency excitation without degrading the transducer response in the bandwidth of interest which is usually 10 kHz or less. To achieve this desirable isolation, two mounting configurations were designed and characterized. The objective is to describe the evaluation technique and to discuss the shock isolation properties of each mounting configuration. One configuration was actually used in a field test of bomb impacting a target. DOE

N90-14536# EG and G Mound Applied Technologies, Miamisburg, OH.
ELECTROTHERMAL RESPONSE TESTING MORE THAN A QUALITY ASSURANCE TOOL
A. C. Munger 1989 11 p Presented at the 14th International Pyrotechnics Seminar, Jersey, England, 18-22 Sep. 1989
(Contract DE-AC04-88DP-43495)
(DE90-001449; MLM-3607(OP); CONF-8909113-5) Avail: NTIS HC A03/MF A01

A simple engineering model of hot wire behavior was constructed based on the electrothermal parameters that can be obtained by the application of that nondestructive test technique. The model uses the data taken before the pyrotechnic charge is loaded on the wire as background data. The data taken as a loaded component is modified by the before loading data. The ETR data is combined with the auto-ignition temperature for the pyrotechnic and the restive heating capacity for the bridgewire to predict an approximate ignition time for the device. A modification of the procedure can be used to predict the no-fire level of the device. A reasonable estimate of the spread in ignition threshold currents at constant current can be obtained by applying the data spread in the ETR gamma values to the no-fire estimate. One of the major benefits of the model is that the temperature of the pyrotechnic mix and the bridgewire can be calculated and presented graphically. This visualization brings together many of the known facts about the electrically ignited system. The relationship between hot and cold firings, high and low current inputs, and the thermal properties of the ignition interface are easily seen. DOE

N90-14537# State Univ. of New York, Stony Brook. Dept. of Physics.
A SCANNING PHOTOELECTRON MICROSCOPE (SPEM) AT THE NATIONAL SYNCHROTRON LIGHT SOURCE (NSLS)
Harold Ade, Janos Kirz, Steve Hulbert, Erik Johnson, Erik Anderson, and Dieter Kern (International Business Machines Corp., Yorktown Heights, NY.) 1989 11 p Presented at the 9th International Conference on Vacuum Ultraviolet Radiation Physics, Honolulu, HI, 14-18 Aug. 1989
(Contracts DE-AC02-76CH-00016; DE-AC03-76SF-00078; NSF DMR-88-15043)
(DE90-001551; BNL-43327; CONF-890809-2) Avail: NTIS HC A03/MF A01

A scanning photoelectron microscope (SPEM) at the X1A beamline of the National Synchrotron Light Source (NSLS) is being developed and commissioned. It is designed to make use of the Soft X ray Undulator (SXU) at the NSLS. This high brightness source illuminates a Fresnel zone plate, which forms a focused

probe, is less than or equal to 0.2 micrometer in size, on the specimen surface. A grating monochromator selects the photon energy in the 400 to 800 eV range with an energy resolution of better than 1 eV. The expected flux in the focus is in the 5 x 10(exp 7) - 10(exp 9) photons/s range. A single pass Cylindrical Mirror Analyzer (CMA) is used to record photoemission spectra, or to form an image within a fixed electron energy bandwidth as the specimen is mechanically scanned. As a first test, a 1000 mesh Au grid was successfully imaged with a resolution of about 1 micrometer and the CMA tuned to the Au 4 f photoelectron peak. Once it is commissioned, a program is planned which will utilize the microscope to study beam sensitive systems, such as thin oxide/sub-oxide films of alumina and silica, and ultimately various adsorbates on these films. DOE

N90-14538# Lawrence Livermore National Lab., CA. Physics Dept.
A FIBER-FED IMAGING SPECTROMETER
K. P. Ziock and C. J. Hailey 25 Aug. 1989 7 p Presented at the 33rd SPIE Annual International Technical Symposium on Optical and Optoelectronic Applied Science and Engineering, San Diego, CA, 6-11 Aug. 1989
(Contract W-7405-eng-48)
(DE90-001008; UCRL-101800; CONF-890836-16) Avail: NTIS HC A02/MF A01

A novel, low-energy (0.1 to 10 MeV), imaging, gamma-ray spectrometer is reported. This device has excellent position resolution (approximately 2 mm at 350 KeV), near unity quantum efficiency, and alkali halide-type energy resolution at an extremely low cost per unit area. This is possible through the separation of the energy and position sensing functions in an alkali halide-based gamma-ray detector. DOE

N90-14539# Brookhaven National Lab., Upton, NY. National Synchrotron Light Source.
SOFT X RAY MICROSCOPE USING FOURIER TRANSFORM HOLOGRAPHY
I. McNulty, Janos Kirz, C. Jacobsen, Erik Anderson, M. R. Howells (California Univ., Berkeley. Lawrence Berkeley Lab.), and H. Rarback 1989 10 p Presented at the 7th Synchrotron Radiation Instrumentation (SRI) National Conference, Berkeley, CA, 6-10 Aug. 1989
(Contract DE-AC02-76CH-00016)
(DE90-002291; BNL-43374; CONF-890802-14) Avail: NTIS HC A02/MF A01

A Fourier transform holographic microscope with an anticipated resolution of better than 100 nm has been built. Extensive testing of the apparatus has begun. Preliminary results include the recording of interference fringes using 3.6 nm x rays. The microscope employs a charge-coupled device (CCD) detector array of 576 (times) 384 elements. The system is illuminated by soft x rays from a high brightness undulator. The reference point source is formed by a Fresnel zone plate with a finest outer zone width of 50 nm. Sufficient temporal coherence for hologram formation is obtained by a spherical grating monochromator. The x ray hologram intensities at the recording plane are to be collected, digitized and reconstructed by computer. Data acquisition is under CAMAC control, while image display and off-line processing takes place on a VAX graphics workstation. Computational models of Fourier transform hologram synthesis, and reconstruction in the presence of noise, have demonstrated the feasibility of numerical methods in two dimensions, and that three-dimensional information is potentially recoverable. DOE

N90-14540# Lawrence Livermore National Lab., CA.
RADIATION DAMAGE AND ITS INFLUENCE ON SOURCE REQUIREMENTS FOR HIGH RESOLUTION X RAY HOLOGRAPHY
Richard A. London 1989 8 p Presented at the Conference on X ray Microimaging for the Life Sciences, Berkeley, CA, 24-26 May 1989 Submitted for publication
(Contract W-7405-eng-48)
(DE90-002508; UCRL-100702; CONF-8905192-2) Avail: NTIS HC A02/MF A01

Soft x ray holography offers the possibility of obtaining high resolution, 3-D images of living cells and organelles therein. To achieve a specified resolution, a certain number of photons must be scattered by the smallest features of interest within the sample. This requires a certain irradiating fluence, the magnitude of which depends on the wavelength of the x rays and the scattering cross-sections of the features. Unfortunately, irradiation of the sample will be accompanied by the absorption of x rays. If the dose is large, the sample will be damaged, possibly compromising the quality of the image. A theoretical study of the scattering and absorption of x rays during the creation of a hologram is described. Using a new prescription for scattering by condensed biological materials (e.g., protein and/or DNA) within the aqueous environment of a cell, we estimate the irradiating fluence required for a certain resolution and the associated sample dose. The relative merits of different x ray wavelengths are discussed. A wavelength of about 44 angstrom, just outside the water window (23.2 to 43.7 angstrom), appears to be optimal in that the required fluence and dose are minimized, while reasonable x ray penetrability is maintained. Estimates are given for the minimum source energy required and the maximum duration of an exposure to capture an image before blurring due heat induced motion. The use of colloidal gold tagging can enhance image contrast and reduce the required irradiating fluence and sample damage. DOE

N90-14541# Brookhaven National Lab., Upton, NY. Dept. of Applied Science.
AMPEROMETRIC BIOSENSORS FOR GLUCOSE, LACTATE, AND GLYCOLATE BASED ON OXIDASES AND REDOX-MODIFIED SILOXANE POLYMERS
Paul D. Hale, Toru Inagaki, Hung Sui Lee, Terje A. Skotheim, Hiroko I. Karan, and Yoshi Okamoto (Polytechnic Univ., Brooklyn, NY.) 1989 7 p Presented at the Symposium on Biosensors, Chapel Hill, NC, 7-9 Sep. 1989 Submitted for publication
(Contract DE-AC02-76CH-00016)
(DE90-002301; BNL-43112; CONF-8909256-1) Avail: NTIS HC A02/MF A01

Amperometric biosensors based on flavin-containing oxidases undergo several steps which produce a measurable current that is related to the concentration of substrate. In the initial step, the substrate converts the oxidized flavin adenine dinucleotide (FAD) or flavin mononucleotide (FMN) into the reduced form FADH sub 2 or FMNH sub 2. Because these cofactors are located well within the enzyme molecule, direct electron transfer to the surface of a conventional electrode does not occur to a measurable degree. A common method of facilitating this electron transfer is to introduce oxygen into the system because it is the natural acceptor for the oxidases; the oxygen is reduced by the FADH sub 2 or FMNH sub 2 to hydrogen peroxide, which can then be detected electrochemically. The major drawback to this approach is the fact that oxidation of hydrogen peroxide requires a large overpotential, thus making these sensors susceptible to interference from electroactive species. To lower the necessary applied potential, several non-physiological redox couples have been employed to shuttle electrons between the flavin moieties and the electrode. The present paper describes the development of amperometric biosensors based on flavin-containing enzymes and a family of polymeric mediators. DOE

36 LASERS AND MASERS

Includes parametric amplifiers.
For related information see also *76 Solid-State Physics.*

N90-14542*# Michigan Univ., Ann Arbor. Space Physics Research Lab.
HIGH RESOLUTION DOPPLER LIDAR Final Report
Vincent J. Abreu, Paul B. Hays, and John E. Barnes Oct. 1989 32 p

(Grant NAG1-817)
(NASA-CR-183288; NAS 1.26:183288) Avail: NTIS HC A03/MF A01 CSCL 20E

A high resolution lidar system was implemented to measure winds in the lower atmosphere. The wind speed along the line of sight was determined by measuring the Doppler shift of the aerosol backscattered laser signal. The system in its present configuration is stable, and behaves as indicated by theoretical simulations. This system was built to demonstrate the capabilities of the detector system as a prototype for a spaceborne lidar. The detector system investigated consisted of a plane Fabry-Perot etalon, and a 12-ring anode detector. This system is generically similar to the Fabry-Perot interferometer developed for passive wind measurements on board the Dynamics Explorer satellite. That this detector system performs well in a lidar configuration was demonstrated. Author

N90-14543# Department of the Navy, Washington, DC.
MONOLITHIC LASER DIODE STRUCTURE FOR MICROWAVE GENERATION Patent Application
Lew Goldberg, inventor (to Navy) and Joseph F. Weller, inventor (to Navy) 4 May 1989 20 p
(AD-D014210; US-Patent-Appl-SN-347132) Avail: NTIS HC A03/MF A01 CSCL 09/3

A semiconductor laser structure for generating high frequency modulation of light intensity is disclosed. The apparatus comprises a semiconductor substrate, a semiconductor master laser and first and second semiconductor slave lasers fabricated adjacent to each other on the semiconductor substrate. Bias current applied to the master oscillator is modulated at a preselected frequency to cause the master laser to generate a plurality of optical frequency modulation sidebands. The first and second slave lasers, which are tuned to be close to the preselected first and second sidebands of the master laser, are injection-locked to the first and second preselected sidebands of the master laser. GRA

N90-14544# Groupement de Recherches Coordonnees Interaction Laser Matiere, Palaiseau (France).
[ACTIVITIES REPORT IN LASER MATTER INTERACTIONS] Annual Report, 1987 [RAPPORT D'ACTIVITE 1987 DU GROUPEMENT DE RECHERCHES COORDONNEES INTERACTION LASER-MATIERE]
Christine Labaune, ed., Danielle Smadja, ed., and Francoise Angibault, ed. Jun. 1988 277 p Partly in ENGLISH and FRENCH Original contains color illustrations
(ETN-90-95515) Avail: NTIS HC A13/MF A02

The main subjects developed in the conference include transport-compression interactions, plasma generation, plasma composition, Langmuir waves, radiative transfer, x ray lasers, microstructure modifications after laser impact, population inversions, simulation studies and instrumentation. For individual titles, see N90-14545 through N90-14580.

N90-14545# Ecole Polytechnique, Palaiseau (France). Lab. pour l'Utilisation des Lasers Intenses.
FAST ELECTRONS IN A LASER GENERATED PLASMA [ELECTRONS RAPIDES DANS UN PLASMA CREE PAR LASER]
Christophe Rousseaux, Francois Amiranoff, Christine Labaune, Bertrand Mabille, and Gilles Matthieussent (Paris XI Univ., Orsay, France) *In* Groupment de Recherches Coordonnees Interaction Laser Matiere, Activities Report in Laser Matter Interactions Jun. 1988 p 1-6 In FRENCH (For primary document see N90-14544 06-36)
Avail: NTIS HC A13/MF A02

A Neodymium laser beam is focused on a terphane film (C8H10O4, 1.5 microns) on a 50 microns target area. Silicon detectors collect the electrons deviated by a magnetic film. Hot electrons are counted for six energy levels. It is shown that the hot electrons produced in the explosion of the film are characterized by a temperature of some tenths of KeV. The angular diagram is oriented more or less parallel to the laser beam. ESA

N90-14546# Ecole Polytechnique, Palaiseau (France). Lab. pour l'Utilisation des Lasers Intenses.
PRODUCTION OF HOMOGENEOUS PLASMAS FOR LASER-PLASMA INTERACTION EXPERIMENTS [PRODUCTION DE PLASMAS HOMOGENES POUR LES EXPERIENCES D'INTERACTION LASER-PLASMA]
Christine Labaune, Francois Amiranoff, Gilles Matthieussent (Paris XI Univ., Orsay, France), Christophe Rousseaux, Jean-Baptiste Paire, Jean-Marc Verdiell, and P. Zeitoun *In* Groupement de Recherches Coordonnees Interaction Laser Matiere, Activities Report in Laser Matter Interactions Jun. 1988 p 7-11 (For primary document see N90-14544 06-36)
Avail: NTIS HC A13/MF A02

The plasma is created either by impact on solid targets, or by explosion of a thin polystyrene film using a neodymium laser. In the case of the thin film the plasma has an electronic density profile more or less parabolic in the laser axis sense and uniform in the perpendicular sense. A Mach Zehnder interferometer allowed optimization of the beam focusing conditions, as well as the targets. The resulting plasmas have the required uniformity. ESA

N90-14547# Toulouse Univ. (France). Centre de Physique Atomique.
EXPERIMENTAL STUDY ON THE FILAMENTARY INSTABILITY IN LASER-MATTER INTERACTIONS AT SHORT WAVE LENGTHS [ETUDE EXPERIMENTALE DE L'INSTABILITE DE FILAMENTATION DANS L'INTERACTION LASER MATIERE A COURTE LONGUEUR D'ONDE]
Jacques Briand, Cecile Arnas, Jean-Claude Kieffer, Alain Gomes, Yves Quemener, J.-P. Dinguirard, and Michel Armengaud *In* Groupement de Recherches Coordonnees Interaction Laser Matiere, Activities Report in Laser Matter Interactions Jun. 1988 p 12-19 In FRENCH (For primary document see N90-14544 06-36)
Avail: NTIS HC A13/MF A02

A neodymium laser beam is focused on solid targets, carbon and aluminum in particular. Pinhole cameras with berilium windows are used to characterize the plasma structure. It is observed that the plasma jets are produced by hydrodynamic effects and that the periodic structures are related to filamentary instability. ESA

N90-14548# Toulouse Univ. (France). Centre de Physique Atomique.
STRONG LANGMUIR TURBULENCE AND SECOND HARMONICS IN LASER-MATTER INTERACTIONS [TURBULENCE FORTE DE LANGMUIR ET HARMONIQUE DEUX DANS L'INTERACTION LASER-MATIERE]
Jacques Briand, Jean-Claude Kieffer, Luc Berge, Alain Gomes, Yves Quemener, J.-P. Dinguirard, Cecile Arnas, and Denis Pesme (Ecole Polytechnique, Palaiseau, France) *In* Groupement de Recherches Coordonnees Interaction Laser Matiere, Activities Report in Laser Matter Interactions Jun. 1988 p 20-26 In FRENCH (For primary document see N90-14544 06-36)
Avail: NTIS HC A13/MF A02

Parametric instabilities are studied at high (10 exp 15 w/sq cm) energy flux using a neodymium laser. A separator allows the spectral image on an electronic fast camera and on a scanning slot camera with a temporal resolution of 5 ps. The lateral observation of the second harmonics allows the attribution to Langmuir turbulences, of the widening of the spectra towards the red. The Zakharov theories on the Langmuir collapse are confirmed. ESA

N90-14549# Ecole Polytechnique, Palaiseau (France). Centre de Physique Theorique.
EFFECTS OF TEMPORAL AND INDUCED SPATIAL INCOHERENCE ON PARAMETRIC INSTABILITIES IN LASER PLASMA INTERACTIONS
Denis Pesme *In* Groupement de Recherches Coordonnees Interaction Laser Matiere, Activities Report in Laser Matter Interactions Jun. 1988 p 27-42 (For primary document see N90-14544 06-36)

(Contract W-7405-eng-48)
Avail: NTIS HC A13/MF A02

The effects of induced spatial incoherence, or of a temporal laser incoherence, or both, upon the parametric instabilities in the corona are studied. The results are used to give some order of magnitude in the case of a Mylar target. It is found that the efficiency of a spatial incoherence for reducing the parametric instabilities is rather low compared with the efficiency of a temporal incoherence, except in the case of forward scattering. ESA

N90-14550# Toulouse Univ. (France). Centre de Physique Atomique.
THE SUPERSONIC ANISOTROPIC COLLAPSE OF LANGMUIR WAVES [LE COLLAPSE SUPERSONIQUE ANISOTROPE DES ONDES DE LANGMUIR]
Luc Berge, G. Pelletier, and Denis Pesme (Ecole Polytechnique, Palaiseau, France) *In* Groupement de Recherches Coordonnees Interaction Laser Matiere, Activities Report in Laser Matter Interactions Jun. 1988 p 43-47 In FRENCH (For primary document see N90-14544 06-36)
Avail: NTIS HC A13/MF A02

The investigation of the strong nonlinear effects leading to the collaspe of Langmuir waves is based on the analysis of solutions of a system coupling a Schroedinger equation with an ionic equation. A quasi invariant method is applied to two types of transformations and a scaling law is obtained. The stability of the partial differential equations solution is proved. ESA

N90-14551# Toulouse Univ. (France). Centre de Physique Atomique.
ASPECTS OF FIELD THEORY RELATED TO THE ZAKHAROV PROBLEM [ASPECTS DE THEORIE DES CHAMPS RELATIFS AU PROBLEME DE ZAKHAROV]
Luc Berge *In* Groupement de Recherches Coordonnees Interaction Laser Matiere, Activities Report in Laser Matter Interactions Jun. 1988 p 48-51 In FRENCH (For primary document see N90-14544 06-36)
Avail: NTIS HC A13/MF A02

The approach of the strong Langmuir turbulence proposed by Zakharov is discussed. The nonlinear system is described by partial differential equations coupling the electric field envelope to matter density variations. It is shown that a Langmuir wave collapses in finite time because of the influence of nonlinear effects on dispersion. The three fields capable of interactions are scalars, either complex or real. The power corresponding to acoustic emission during supersonic collapse is evaluated. ESA

N90-14552# Ecole Polytechnique, Palaiseau (France). Centre de Physique Theorique.
LIMITATIONS IN THE GROWING OF A PLASMA WAVE PRODUCED BY HETERODYNING TWO LASERS DUE TO MODULATIONS AND DECAY INSTABILITIES [LIMITATION DE LA CROISSANCE D'UNE ONDE PLASMA GENEREE PAR LE BATTEMENT DE DEUX LASERS DUE A L'EXISTENCE DES INSTABILITES MODULATIONNELLES ET DE DECAY]
Denis Pesme, G. Laval, and Nicolas Sylvestre *In* Groupement de Recherches Coordonnees Interaction Laser Matiere, Activities Report in Laser Matter Interactions Jun. 1988 p 52-62 In FRENCH (For primary document see N90-14544 06-36)
Avail: NTIS HC A13/MF A02

The stability of a Langmuir wave coupled to ion movement is studied. The growing rate of instable oscillations is calculated as a function of the plasma wave intensity. It is shown that this plasma wave amplitude is lower than the prediction from the saturation theory due to relativistic effects. ESA

N90-14553# Ecole Polytechnique, Palaiseau (France). Centre de Physique Theorique.
USE OF PLASMAS FOR THE ACCELERATION OF PARTICLES TO VERY HIGH ENERGY [UTILISATION DES PLASMAS POUR L'ACCELERATION DES PARTICULES A TRES HAUTE ENERGIE]
Patrick Mora *In* Groupement de Recherches Coordonnees Interaction Laser Matiere, Activities Report in Laser Matter Interactions Jun. 1988 p 63-72 In FRENCH (For primary document see N90-14544 06-36)
Avail: NTIS HC A13/MF A02

Plasma waves excited by heterodyning two laser beams are studied. The saturation level of the plasma wave assuming several mechanisms is analyzed. The destruction of the wave coherence due to the modulation instability effect is discussed. A synthesis of the conclusions is presented by giving the amplitude of the plasma wave as a function of the incident laser flux, for a set of typical experimental parameters. ESA

N90-14554# Toulouse Univ. (France). Centre de Physique Atomique.
INTERACTION OF A LOW FLUX LASER BEAM WITH A SOLID TARGET [INTERACTION D'UN FAISCEAU LASER AVEC UNE CIBLE SOLIDE A BAS FLUX]
Jean-Claude Kieffer, Jacques Briand, Alain Gomes, Yves Quemener, J.-P. Dinguirard, and Michel Armengaud *In* Groupement de Recherches Coordonnees Interaction Laser Matiere, Activities Report in Laser Matter Interactions Jun. 1988 p 73-78 In FRENCH (For primary document see N90-14544 06-36)
Avail: NTIS HC A13/MF A02

The interaction of a neodymium laser beam with a carbon or aluminum target is studied. The flux used is below 10 exp 11 w/sq cm. The plasma characteristics are studied by interferometry and spectroscopy. The results show that plasma phenomena are dominated by a detonation wave propagating at a velocity of about 1 cm/microsec. The temperatures are between 1 and 3 eV. ESA

N90-14555# Paris XI Univ., Orsay (France). Lab. de Physique des Gaz et des Plasmas.
BOX EXPERIMENTS. NONLINEAR EFFECTS AT PLASMA RESONANCE [EXPERIENCES EN CAISSON. EFFETS NON LINEAIRES A LA RESONANCE DE PLASMA]
Brigitte Cros, Pierre Fischer, Jacques Godiot, Philippe Louarn, and Gilles Matthieussent *In* Groupement de Recherches Coordonnees Interaction Laser Matiere, Activities Report in Laser Matter Interactions Jun. 1988 p 79-84 In FRENCH (For primary document see N90-14544 06-36)
Avail: NTIS HC A13/MF A02

The experiment made in an argon plasma box is related to the resonant absorption of an electromagnetic wave with frequency near the plasma resonance. The electromagnetic wave is fed by a horn hyperfrequency antenna. When adjusting to nonlinear conditions, the spatial and temporal evolutions of the plasma wave amplitude depend strongly on the L characteristics value of the density gradient. ESA

N90-14556# Observatoire du Mont-Gros, Nice (France). Lab. de Physique de la Matiere Condensee.
SIMULATED BRILLOUIN BACKSCATTERING IN OPTICAL FIBERS: A RING RESONATOR [RETRODIFFUSION BRILLOUIN STIMULEE DANS LES FIBRES OPTIQUES: RESONATEUR EN ANNEAU]
Jean Botineau, Olivier Legrand, Claude Leycuras, Carlos Montes, and Eric Picholle *In* Groupement de Recherches Coordonnees Interaction Laser Matiere, Activities Report in Laser Matter Interactions Jun. 1988 p 85-96 In FRENCH (For primary document see N90-14544 06-36)
Avail: NTIS HC A13/MF A02

The space-time behavior of the nonlinear interaction between a long laser pulse and a nonlinear optical media was studied using an 83 m optical fiber stimulated by an ionized argon laser. The numerical models of the coherent stimulated Brillouin backscatter allowed a better interpretation of the coupling efficiency. An oscillator is implemented where the coupling is assured, by the diffraction of an optical-acoustical modulator, resulting in better oscillator stability. ESA

N90-14557# Citroen Industrie, Paris (France). DRAS.
EXPERIMENTAL STUDY OF THE SHOCK WAVES GENERATED BY HIGH ENERGY LASER PULSES [ETUDE EXPERIMENTALE DES ONDES DE CHOC ENGENDREES PAR LASER PULSE DE FORTE ENERGIE]
Jean Fournier, Patrick Ballard, Remy Fabbro, and Edouard Fabre (Ecole Polytechnique, Palaiseau, France) *In* Groupement de Recherches Coordonnees Interaction Laser Matiere, Activities Report in Laser Matter Interactions Jun. 1988 p 97-106 In FRENCH (For primary document see N90-14544 06-36)
Avail: NTIS HC A13/MF A02

The mechanical and metallurgical effects produced by the focusing of a high energy laser on a metallic target are investigated. A ballistic method was employed to study high velocity rotating metallic targets. Data for 3 ns pulses at 1.06 m wavelength are presented. For the same energy density, the plasma confinement increases the studied mechanical impulse effect by two orders of magnitude. ESA

N90-14558# Ecole Nationale Superieure de Mecanique et d'Aerotechnique, Poitiers (France). Lab. d'Energetique et de Detonique.
MICROSTRUCTURE INDUCED BY LASER SHOCK IN AN AUSTENITIC STEEL [MICROSTRUCTURE INDUITE PAR CHOC LASER DANS UN ACIER AUSTENITIQUE]
Martine Hallouin, Francis Cottet, Jean-Pierre Romain, Patrick Darquey, and M. Gerland *In* Groupement de Recherches Coordonnees Interaction Laser Matiere, Activities Report in Laser Matter Interactions Jun. 1988 p 107-111 In FRENCH (For primary document see N90-14544 06-36)
Avail: NTIS HC A13/MF A02

The residual microstructure after laser shock, with impact holding time largely inferior to conventional impacts is studied. The laser flux are 10 exp 12 W/sq cm for 3 to 30 ns pulse duration. The induced shock is from 200 to 500 kbar. The hardness of the surface increases from 190 HV to 450. The results from electron microscopy show a microstructure similar to that obtained with conventional impact. ESA

N90-14559# Ecole Nationale Superieure de Mecanique et d'Aerotechnique, Poitiers (France). Lab. d'Energetique et de Detonique.
DYNAMIC SINTERING OF METALLIC POWDERS BY LASER SHOCK [COMPACTION DYNAMIQUE DE POUDRES METALLIQUES PAR CHOC LASER]
Patrick Darquey, Jean-Pierre Romain, Martine Hallouin, and Francis Cottet *In* Groupement de Recherches Coordonnees Interaction Laser Matiere, Activities Report in Laser Matter Interactions Jun. 1988 p 112-118 In FRENCH (For primary document see N90-14544 06-36)
Avail: NTIS HC A13/MF A02

Experimental sintering of metallic powders is carried out using a 0.53 micrometer laser beam of 2 (10 to the 9th power) W/sq cm, with 25 ns pulses focused over 2 mm diameter. The experimental target is aluminum powder presintered statically at 60 percent density. The tests show that the method is feasible. ESA

N90-14560# Ecole Polytechnique, Palaiseau (France). Lab. de Physique des Milieux Ionises.
MEASUREMENT OF THE HIGH DENSITY ZONE OF A PLASMA TARGET BY ABSORPTION SPECTROSCOPY [MESURE DE LA ZONE DENSE D'UNE CIBLE PAR SPECTROSCOPIE D'ABSORPTION]
Claude Chenais-Popovics, Christian Fievet, Jean-Paul Geindre, Jean-Claude Gauthier, and Nathalie Tragin *In* Groupement de Recherches Coordonnees Interaction Laser Matiere, Activities Report in Laser Matter Interactions Jun. 1988 p 119-124 In FRENCH (For primary document see N90-14544 06-36)
Avail: NTIS HC A13/MF A02

The absorption of x rays from a continuous source is studied using the k alpha lines of chlorine ions originally belonging to the laser target. The spectra are solved and integrated to determine the electron temperatures and the absorption lengths in the absorption zone. It is shown that the study of the absorption of the n=1 and n=2 quantum levels allow the analysis of the plasma as well as of the mechanisms creating the absorption. ESA

N90-14561# Ecole Polytechnique, Palaiseau (France). Lab. pour l'Utilisation des Lasers Intenses.
TIME INTEGRATED STUDY OF SPECTRAL EMISSION IN THE X-UV DOMAIN AT THE OUTLET OF A LASER SHOCK, AT THE BACK OF SINGLE OR DOUBLE FOIL TARGETS [ETUDE DE L'EMISSION SPECTRALE RESOLUE TEMPORELLEMENT DANS LE DOMAINE X-UV DU DEBOUCHE D'UN CHOC A L'ARRIERE DE FEUILLES SIMPLES ET DOUBLES FEUILLES]
Remy Fabbro, Bernard Faral, Jean-Claude Gauthier, Claude Chenais-Popovics, Jean-Paul Geindre, and H. Pepin (Quebec Univ., Montreal.) *In* Groupement de Recherches Coordonnees Interaction Laser Matiere, Activities Report in Laser Matter Interactions Jun. 1988 p 125-129 In FRENCH (For primary document see N90-14544 06-36)
Avail: NTIS HC A13/MF A02

The influence of target configuration and residual heating on the laser shock induced pressure is studied using thin aluminum foils irradiated at 0.26 micrometers wavelength at 5 x 10(exp 14) W/sq cm. A multi diode X detector and integrating film cameras are located ahead and behind the targets. The results show that the X-UV spectroscopy is a convenient method to study high intensity laser shock. ESA

N90-14562# Ecole Polytechnique, Palaiseau (France). Lab. pour l'Utilisation des Lasers Intenses.
MEASUREMENT OF THE X-UV EMISSION FROM THE BACK FACE OF THIN FOILS ILLUMINATED BY AN A4 OMEGA LASER [MESURE DE L'EMISSION XUV DE FACES ARRIERES DE FEUILLES MINCES ILLUMINEES PAR LASER A 4 OMEGA]
Rene Benattar, J. L. Godart, and Victor Malka *In* Groupement de Recherches Coordonnees Interaction Laser Matiere, Activities Report in Laser Matter Interactions Jun. 1988 p 130-133 In FRENCH (For primary document see N90-14544 06-36)
Avail: NTIS HC A13/MF A02

The emission from back faces of thin aluminum or gold targets illuminated with 0.26 micrometers wavelength was studied. A Schwarzschild microscope was used for 80 eV measurements, and another microscope for 40 eV analysis. It was found that at the back of the target appear two x ray emissions, the first 200 ps after irradiation and related to preheating of the plasma, and the second 1 ns after irradiation, related to the shock wave. ESA

N90-14563# Ecole Polytechnique, Palaiseau (France). Lab. pour l'Utilisation des Lasers Intenses.
X RAY SHADOWSCOPY IN IMPLOSION EXPERIMENTS [OMBROSCOPIE EN RAYONS X DANS LES EXPERIENCES D'IMPLOSION]
Rene Benattar, Jean-Michel Boudene, Edouard Fabre, Victor Malka, Alain Michard, Henri Timsit, and Anne-Marie Tournade *In* Groupement de Recherches Coordonnees Interaction Laser Matiere, Activities Report in Laser Matter Interactions Jun. 1988 p 134-137 In FRENCH (For primary document see N90-14544 06-36)
Avail: NTIS HC A13/MF A02

An experiment was carried out concerning the illumination with an x ray beam of a microballoon being imploded, to deduce from the measured absorption the density of the matter compressed in the implosion. The space resolution and imagery problems were solved, but the energy available on the exploring beam was not large enough to obtain adequate contrast. ESA

N90-14564# Toulouse Univ. (France). Centre de Physique Atomique.
NUMERICAL SIMULATION OF THE PREHEATING BY X RAYS IN SPHERICAL PLASMAS [SIMULATION NUMERIQUE DU PRECHAUFFAGE PAR RAYONNEMENT X DANS LES PLASMAS SPHERIQUES]

J.-P. Dinguirard, Dominiaziano Mostacci, Jacques Briand, Alain Gomes, Jean-Claude Kieffer, Yves Quemener, Luc Berge, and Cecile Arnas *In* Groupement de Recherches Coordonnees Interaction Laser Matiere, Activities Report in Laser Matter Interactions Jun. 1988 p 138-141 In FRENCH Original contains color illustrations (For primary document see N90-14544 06-36)
Avail: NTIS HC A13/MF A02

Numerical simulations were carried out of microspherical glass targets filled with neon illuminated by a 0.26 micrometer laser at 80 Joules and 500 psec pulses. The main absorption process was assumed to be the inverse Bremsstrahlung. A comparison with experimental results shows that an emissivity following Planck's law is a good approximation. It is shown that the preheating effect is important for the materials with high Z coefficient and for thicker wall targets. ESA

N90-14565# Lawrence Livermore National Lab., CA.
MODIFICATION OF IONIC POPULATION BY NON-MAXWELLIAN EFFECTS [MODIFICATION DES POPULATIONS IONIQUES PAR LES EFFETS NON-MAXWELLIENS]
Yim Lee and Michele Lamoureux (Paris-Sud Univ., Orsay, France) *In* Groupement de Recherches Coordonnees Interaction Laser Matiere, Activities Report in Laser Matter Interactions Jun. 1988 p 142-144 In FRENCH (For primary document see N90-14544 06-36)
Avail: NTIS HC A13/MF A02

The ion composition of plasmas is studied, with particular attention to non-Maxwellian effects and Ne, Na and Se ions. The Lasnex software for hydrodynamic computations is adapted to include non-Maxwellian ionization rates. The time evolution of the ion populations after a 0.54 microns laser pulse on a thin selenium foil is described. It is found that the non-Maxwellian character is a handicap for the most charged ions (F- and O-). ESA

N90-14566# Paris-Sud Univ., Orsay (France). Lab. de Spectroscopie Atomique et Ionique.
ANISOTROPY OF ELECTRON DISTRIBUTIONS RELATED TO THE ANISOTROPY AND POLARIZATION OF THE CONTINUOUS EMITTED X RAYS [ANISOTROPIE DES DISTRIBUTIONS D'ELECTRONS EN RELATION AVEC L'ANISOTROPIE ET LA POLARISATION DU RAYONNEMENT X CONTINU EMIS]
Michele Lamoureux *In* Groupement de Recherches Coordonnees Interaction Laser Matiere, Activities Report in Laser Matter Interactions Jun. 1988 p 145-146 In FRENCH (For primary document see N90-14544 06-36)
Avail: NTIS HC A13/MF A02

The radiation recombination and the braking radiation are studied using analytical and parametric cross sections. Relatively simple expressions for the emmissivity coefficients are obtained from the distribution functions of a toroidal symmetry plasma. Within the approximations adopted, the emission and its polarization are maximum in the direction perpendicular to the toroidal symmetry. A polarization rate of over 40 percent is predicted for Tokamak plasmas. ESA

N90-14567# Paris VI Univ. (France). Lab. de Spectroscopie Atomique des Plasmas.
ATOMIC STRUCTURE AND SPECTRAL PERTURBATIONS IN HOT DENSE PLASMAS [STRUCTURE ATOMIQUE ET PERTURBATIONS SPECTRALES DANS LES PLASMAS DENSES ET CHAUDS] **c75**
Hoe Nguyen, Jose Banon, Gerard Coulaud, Brigitte Detat, Jeanne Grumberg, Michel Koenig, Elisabeth Leboucher, Philippe Malnoult, and Laurent Terray *In* Groupement de Recherches Coordonnees Interaction Laser Matiere, Activities Report in Laser Matter Interactions Jun. 1988 p 147-159 In FRENCH (For primary document see N90-14544 06-36)
Avail: NTIS HC A13/MF A02

The stationary electronic states of multiple centers immersed in dense plasmas are studied resolving simultaneously the Schroedinger equation related to the electron and the Poisson equation related to the set of electrons existing in a confined volume. The numerical solution of the nonlinear Poisson equation is based on the finite difference method. Each iteration leads to a linear system solved using an implicit method. The Shroedinger equation is solved by a variational method. The spectral perturbations and the radiative transfer in dense plasmas are also discussed. ESA

N90-14568# Paris VI Univ. (France). Lab. de Spectroscopie Atomique des Plasmas.
TRANSVERSAL INHOMOGENEITY AND RADIATIVE TRANSFER IN PLASMAS OBTAINED BY LASER IMPACT [INHOMOGENEITE TRANSVERSE ET TRANSFERT RADIATIF DANS LES PLASMAS OBTENUS PAR IMPACT LASER] **c75**
Claire Bousquet, Jeanne Grumberg, Elisabeth Leboucher, Hoe Nguyen, and Alain Poquerusse (Ecole Polytechnique, Palaiseau, France) *In* Groupement de Recherches Coordonnees Interaction Laser Matiere, Activities Report in Laser Matter Interactions Jun. 1988 p 160-166 In FRENCH (For primary document see N90-14544 06-36)
Avail: NTIS HC A13/MF A02

A theoretical and experimental study on the characterization of dense plasmas obtained by laser impact is presented. The evolution of spectral lines as a function of the target geometry and composition is analyzed. A neodymium laser beam is used with pulses of 500 ps and wavelength of 0.256 microns. The observations are made perpendicular to the laser axis with a Paburce spectrometer. The study of the measurements of spectral line integrated intensity as a function of large thickness shows that the plasmas with radius larger than 30 microns are strongly nonhomogeneous and autoabsorbents. ESA

N90-14569# Ecole Polytechnique, Palaiseau (France). Lab. de Physique des Milieux Ionises.
THE AVERAGE ION MODEL. COMPUTATION OF THE ABSORPTION AND EMISSION COEFFICIENTS IN HOT PLASMAS [LE MODELE DE L'ION MOYEN. CALCUL DES COEFFICIENTS D'ABSORPTION ET D'EMISSION DANS LES PLASMAS CHAUDS EN ETL ET HORS ETL] **c75**
Jean-Claude Gauthier and Jean-Paul Geindre *In* Groupement de Recherches Coordonnees Interaction Laser Matiere, Activities Report in Laser Matter Interactions Jun. 1988 p 167-175 In FRENCH (For primary document see N90-14544 06-36)
Avail: NTIS HC A13/MF A02

A program was developed to evaluate the emission and absorption plasma coefficient variations as a function of the density, temperature and the atomic number of the specimen. The treatment is simplified because of the reduced number of characteristic frequencies which are necessary for the hydrodynamic code. The approach is less efficient when applied to high Z atoms. ESA

N90-14570# Ecole Polytechnique, Palaiseau (France). Lab. de Physique des Milieux Ionises.
XRAD: A ONE DIMENSIONAL LAGRANGIAN CODE WITH RADIATIVE TRANSPORT [XRAD: UN CODE 1D LAGRANGIEN AVEC TRANSPORT RADIATIF] **c75**
Jean-Claude Gauthier and Jean-Paul Geindre *In* Groupement de Recherches Coordonnees Interaction Laser Matiere, Activities Report in Laser Matter Interactions Jun. 1988 p 176-188 In FRENCH (For primary document see N90-14544 06-36)
Avail: NTIS HC A13/MF A02

A radiative transfer model is developed and implemented on a vector computer. The method is applied to one temperature, two dimensional geometry, and uses an entirely implicit solution of matter density conservation, velocities and cell energy equations. The emission properties are calculated by the average ion method. The results are in good agreement with the simulations and spectroscopic experimental data. ESA

N90-14571# Paris-Sud Univ., Orsay (France). Lab. de Spectroscopie Atomique et Ionique.
POPULATION INVERSIONS CALCULATED FOR LITHIUM-LIKE IONS IN A PLASMA [INVERSIONS DE POPULATION CALCULEES DANS DES IONS LITHIUMOIDES AU SEIN D'UN PLASMA] **c75**
Helene Guennou, Annie Klisnick, Clary Moeller, and Alain Sureau *In* Groupement de Recherches Coordonnees Interaction Laser Matiere, Activities Report in Laser Matter Interactions Jun. 1988 p 189-192 In FRENCH (For primary document see N90-14544 06-36)
Avail: NTIS HC A13/MF A02

Lithium-like ions are studied in order to improve the soft x ray emission in shorter wavelengths. These ions present real advantages in a plasma in active recombination. Previous work investigating Ca, Ti and Cu ions is continued. A table is presented with data on the evolution of efficiency gains for different transmissions of the studied ions. It is shown that if a much shorter wavelength is not required, an important gain may be obtained by means of the 4 to 5 transitions. ESA

N90-14572# Paris-Sud Univ., Orsay (France). Lab. de Spectroscopie Atomique et Ionises.
STUDY OF LITHIUM-LIKE IONS FOR AMPLIFYING RADIATION BELOW 100 ANGSTROMS. EXPERIMENT AT THE RUTHERFORD APPLETON LABORATORY [ETUDES DES IONS LITHIUMOIDES POUR L'AMPLIFICATION DE RAYONNEMENT AU DESSOUS DE 100 ANGSTROMS. EXPERIENCE AU RUTHERFORD APPLETON LABORATORY] **c75**
Annie Klisnick, Gerard Jamelot, Antoine Carillon, Pierre Jaegle, M. H. Key, M. Grande, O. Willi, G. Kiehn, J. Edwards, and C. L. S. Lewis (Queens Univ., Belfast, Northern Ireland) et al *In* Groupement de Recherches Coordonnees Interaction Laser Matiere, Activities Report in Laser Matter Interactions Jun. 1988 p 193-196 In FRENCH (For primary document see N90-14544 06-36)
Avail: NTIS HC A13/MF A02

The generation of x ray laser radiation is studied through experiments carried out with ions of lithium-like electronic structure. The work with C-14+ ions is done using carbon fiber targets covered with an NaCl film. The focusing setup is described. The spectra obtained at the recombination are presented. The best gain is obtained with 3d-4f transition at 58.6 angstroms. ESA

N90-14573# Paris-Sud Univ., Orsay (France). Lab. de Spectroscopie Atomique et Ionique.
SINGLE BEAM INTERACTIONS FOR THE STUDY OF X RAY LASERS [INTERACTIONS MONOFAISCEAU POUR L'ETUDE DU LASER EN RAYONS X] **c75**
Pierre Jaegle, Antoine Carillon, Fouard Gadi, Bernard Gauthe, Gerard Jamelot, and Annie Klisnick *In* Groupement de Recherches Coordonnees Interaction Laser Matiere, Activities Report in Laser Matter Interactions Jun. 1988 p 197-201 In FRENCH (For primary document see N90-14544 06-36)
Avail: NTIS HC A13/MF A02

Several flat targets were tried in order to find the best geometry for the amplification in the x ray region for plasmas several centimeters long. Massive targets lead to decreasing gain with increasing plasma length. An amplification is searched using the lithium-like sulphur ion in the 3d-5f transition at 65.2 angstroms. The absorption spectra show the existence of population inversions of this kind, but the amplification is not demonstrated. ESA

N90-14574# Paris-Sud Univ., Orsay (France). Lab. de Spectroscopie Atomique et Ionique.
X-UV AMPLIFICATION IN A PLASMA COLUMN OF FIVE CENTIMETERS. FIVE BEAMS EXPERIMENT [AMPLIFICATION X-UV DANS UNE COLONNE DE PLASMA DE 6 CM DE LONGUEUR. EXPERIENCE A CINQ FAISCEAUX] **c75**
Pierre Jaegle, Antoine Carillon, Michel Cousy, P. Dhez, Fouard Gadi, Bernard Gauthe, M. Grande (Rutherford High Energy Lab., Chilton, England), Gerard Jamelot, Annie Klisnick, and J. C. Lagron et al *In* Groupement de Recherches Coordonnees Interaction Laser Matiere, Activities Report in Laser Matter Interactions Jun. 1988 p 202-204 In FRENCH (For primary document see N90-14544 06-36)
Avail: NTIS HC A13/MF A02

The X-UV radiation emitted in the axis of the plasma is analyzed by means of a grazing spectrometer. Targets are massive aluminum and 1000 angstrom aluminum foils on polyethylene supports. The emission of 105.7 line corresponding to the 3d-5f transition of A110+ is the most intense while the 3d-4f has a probability 10 times higher. The use of multilayer mirrors allows increase of the detected intensity by a factor of 1.5 to 2. ESA

N90-14575# Ecole Polytechnique, Palaiseau (France). Lab. pour l'Utilisation des Lasers Intenses.
CHARACTERISTICS OF AN X RAY SOURCE CREATED BY A LASER PLASMA [CARACTERISTIQUES D'UNE SOURCE DE RAYONS X CREEE PAR PLASMA LASER] **c75**
Isabelle Toubhans, Remy Fabbro, H. Pepin, and M. Chaker (Quebec Univ., Montreal.) *In* Groupement de Recherches Coordonnees Interaction Laser Matiere, Activities Report in Laser Matter Interactions Jun. 1988 p 205-211 In FRENCH (For primary document see N90-14544 06-36)
Avail: NTIS HC A13/MF A02

A neodymium laser at 1.06 microns is used to create a plasma by impact on a metallic target. The x ray emission is measured by a set of diodes and pin-diodes and a network spectrometer. A computer program calculates the x ray spectrum from the diode signal analysis. Another computer program is used to derive the x ray spectra from the network spectrometer data and for numerical simulations. It is shown that this x ray source is applicable to microlithography. ESA

N90-14576# Ecole Polytechnique, Palaiseau (France). Lab. Pour l'Utilisation des Lasers Intenses.
LASER ACTIVITIES [ACTIVITES LASER]
Didier Bruneau, Michel Hartmann, and Anne-Marie Tournade *In* Groupement de Recherches Coordonnees Interaction Laser Matiere, Activities Report in Laser Matter Interactions Jun. 1988 p 213-214 In FRENCH (For primary document see N90-14544 06-36)
Avail: NTIS HC A13/MF A02

The activities of a laser development laboratory in 1987 are summarized. The research subjects include synchronous oscillators for 1 ns pulses at 100 ps commutation, development of an alignment bench and the study of a pulse generator for the laser acceleration of particles by heterodyning two beams with 100 to 150 wavelength difference. ESA

N90-14577# Groupement de Recherches Coordonnees Interaction Laser Matiere, Palaiseau (France).
TRAPEZOIDAL CRYSTAL IN THE SIX BEAM IMPLOSION [CRISTAL TRAPEZOIDAL SUR L'IMPLOSION A SIX FAISCEAUX]
Alain Poquerusse *In its* Activities Report in Laser Matter Interactions Jun. 1988 p 215-219 In FRENCH (For primary document see N90-14544 06-36)
Avail: NTIS HC A13/MF A02

The Pabutec spectrograph is equipped with a Bragg trapezoidal crystal flexed by elasticity. The optical aspects of this setup are described. It is shown that for the first order of diffraction, the main limitation is the own crystal resolution power, while for the second order it is the Doppler widening or the source lines. ESA

N90-14578# Groupement de Recherches Coordonnees Interaction Laser Matiere, Palaiseau (France).
DEVELOPMENT OF X DIAGNOSTICS WITH 1 Gw LASER PULSES [UN MODELE DE REPONSE AUX RAYONS X POUR LE FILM SB]
Alain Poquerusse *In its* Activities Report in Laser Matter Interactions Jun. 1988 p 220-225 In FRENCH (For primary document see N90-14544 06-36)
Avail: NTIS HC A13/MF A02

A laser pulse is used to generate a metallic ion plasma emitting

x rays with a wide spectrum. This x ray source is intended to carry on diagnostics in laser-matter interactions. The experimental setup described includes a 1 Gw 4 ns pulses YLF infrared laser with a short cavity oscillator and a Pockels cell. The x ray emissions produced by plasmas created by impact on copper and aluminum targets are described. Spectra and energy distribution are given.
ESA

N90-14579# Institut d'Optique Theorique et Appliquee, Paris (France).
TOMOGRAPHIC IMAGERY BY MULTISLOT CODING APPLIED TO X RAY DIAGNOSTICS OF LASER PLASMAS: IMPLEMENTATION OF A DIRECT ELECTRONIC DETECTION CAMERA [IMAGERIE TOMOGRAPHIQUE PAR CODAGE MULTIFENTES POUR LE DIAGNOSTIC X DES PLASMAS LASER: REALISATION D'UNE CAMERA A DETECTION ELECTRONIQUE DIRECTE] **c74**
N. deBeaucoudrey, A. Bellemain, P. Fournet, D. Phalippou, L. Garnero, and J. P. Hugonin *In* Groupement de Recherches Coordonnees Interaction Laser Matiere, Activities Report in Laser Matter Interactions Jun. 1988 p 226-231 In FRENCH (For primary document see N90-14544 06-36)
Avail: NTIS HC A13/MF A02

A micro-imagery system is developed to visualize x emission from plasma lasers. The resulting images may be two or three dimensional. The multislot coding principle is explained. The camera is equipped with charge coupled devices. The first experimental results including five sections of a plasma x source are described.
ESA

N90-14580# Ecole Polytechnique, Palaiseau (France). Lab. pour l'Utilisation des Lasers Intenses.
DEVELOPMENT OF X DIAGNOSTICS AROUND THE PULSE 1 LASER [DEVELOPPEMENT DE DIAGNOSTICS X AUTOUR DU LASER PULSE 1] **c74**
Rene Benattar and Bertrand Paris *In* Groupement de Recherches Coordonnees Interaction Laser Matiere, Activities Report in Laser Matter Interactions Jun. 1988 p 232-237 In FRENCH Original contains color illustrations (For primary document see N90-14544 06-36)
Avail: NTIS HC A13/MF A02

The single layer Kodak SB film which is frequently used in x ray spectrography for laser-matter interaction studies is studied. Precise sensitivity measurements are used to characterize the physical structure of the film in order to define an accurate theoretical interpretation. The model allows a precision of about 20 percent to predict responses in the 0.1 to 10 KeV domain.
ESA

N90-14581# National Oceanic and Atmospheric Administration, Boulder, CO. Wave Propagation Lab.
STATISTICS OF TWO-COLOR LASER BEAM PROPAGATION IN THE TURBULENT ATMOSPHERE (SPECTRAL CORRELATION)
Richard J. Lataitis and James H. Churnside Jun. 1989 23 p
(PB89-236699; NOAA-TM-ERL-WPL-167) Avail: NTIS HC A03/MF A01 CSCL 20E

Expressions were developed for the statistics of the angle-of-arrival fluctuations and of the irradiance fluctuations for a two-color laser beam after propagation through refractive turbulence in the atmosphere. The correlation, the cospectrum, and the coherence are included. The fluctuations in the angle-of-arrival and irradiance at two wavelengths were found to be highly correlated for most conditions of interest.
Author

N90-14582# Fortuna-Werke, Stuttgart (Germany, F.R.).
EUROLASER CO2 LASER Final Report
Richard Jesinger Mar. 1989 15 p In GERMAN; ENGLISH summary
(Contract BMFT-13-EU-0035)
(ETN-90-95907) Avail: NTIS HC A03/MF A01

The developmental phases of a CO2 laser are summarized. The building of a small pump according to data collected in early investigations is described. This pump is designed for a CO2 laser of one to two kW. Vast numbers of these lasers are being built. They are almost exclusively equipped with Roots pumps. These pumps are recommended due to their small size, availability, and low price.
ESA

N90-14583*# Old Dominion Univ., Norfolk, VA. Dept. of Mathematical Sciences.
THEORETICAL STUDIES OF SOLAR LASERS AND CONVERTERS Progress Report, 15 May - 31 Dec. 1989
John H. Heinbockel Jan. 1990 47 p
(Grant NAG1-757)
(NASA-CR-186194; NAS 1.26:186194) Avail: NTIS HC A03/MF A01 CSCL 20E

The research described consisted of developing and refining the continuous flow laser model program including the creation of a working model. The mathematical development of a two pass amplifier for an iodine laser is summarized. A computer program for the amplifier's simulation is included with output from the simulation model.
J.P.S.

N90-14584# Sao Paulo Univ. (Brazil). Inst. de Fisica.
NONLINEAR QUANTUM EFFECTS IN THE MASER MODEL: A LARGE N SCALING BEHAVIOUR
J. N. Maki, M. C. Nemes, and M. P. Pato Dec. 1988 23 p
(DE89-631631; IFUSP-P-763) Avail: NTIS (US Sales Only) HC A03/MF A01

The time evolution of the mean photon number is numerically studied for different initial conditions. We find an approximate scaling of the curves for the various values of N when they are plotted against tau = t/N/sup (alpha) and the coefficient (alpha), empirically determined, is found to be directly related to the spectral distribution of the initial condition over the exact states. Its value can be obtained from the N-dependence of the relevant eigenvalues. The approximate periodicity of the curves can also be understood in terms of the spectral distribution of the initial condition.
DOE

N90-14585# Gosudarstvennyi Komitet po Ispolzovaniyu Atomnoi Energii, Moscow (USSR). Inst. Atomnoj Ehnergii.
NUMERICAL SIMULATION OF LASER RADIATION PROPAGATION IN NON-UNIFORM ABSORBING MEDIUM. GEOMETRICAL OPTICS APPROXIMATION
L. A. Bolshov, V. A. Vorobev, M. F. Kanevskij, V. D. Kanyukova, and A. I. Yudin 1988 23 p In RUSSIAN; ENGLISH summary
(DE89-632014; IAE-4732/16) Avail: NTIS (US Sales Only) HC A03/MF A01

The algorithm of numerical study of coherent radiation propagation in the approximation of geometrical optics in the inhomogeneous absorbing medium is suggested and developed. The results of test calculations are given. The results of model calculations of powerful laser radiation with plasma are presented.
DOE

N90-14586# Lawrence Livermore National Lab., CA.
PROOF-OF-PRINCIPLE EXPERIMENT FOR A HOT ELECTRON PUMPED XUV AMPLIFIER
W. Goldstein, D. Price, M. Rosen, A. Clark, C. Cerjan, D. Fields, and V. Slivinsky Aug. 1989 22 p Presented at the 9th Vacuum Ultraviolet Radiation Conference, Honolulu, HI, 17-21 Jul. 1989
(Contract W-7405-eng-48)
(DE90-000820; UCRL-100906; CONF-8907130-4) Avail: NTIS HC A03/MF A01

An x ray laser scheme was recently proposed based on the pumping of neonlike 3s-3p transitions using inner-shell ionization of sodium-like ions by suprathermal electrons. Since this laser operates in principle with no population in the neonlike charge-state, power requirements can be reduced from the standard collisionally driven amplifier, and the problem of line-trapping can be ameliorated. Model calculations using a quasi-steady state collisional-radiative model indicated that measurable gains could be obtained in practical experiments. We propose a

proof-of-principle experiment to demonstrate the pumping of neonlike excited states by hot electrons. An (approximately) 1 ns long, 0.53 (mu) laser beam, will be focused on a solid dot target of dilute bromine, to create a cool, dense plasma. The pulse and target will be optimized to produce as much sodiumlike population as possible in the corona. This low-fluence green pulse does not produce suprathermals. A second, (approximately) 100 ps, 1.06 m pulse of 10(sup 15) W/cm(sup 2) will be piggybacked on the first, to create hot electrons. The timing of the red beam will be optimized with respect to the sodiumlike fraction of the cool plasma. The hot electrons create a transient population of neonlike ions, coincident with the red beam, that are detected by their characteristic n=3 to n=2 resonant x ray emission. DOE

N90-14587# Consultec Scientific, Inc., Knoxville, TN.
ASSESSMENT OF RESEARCH NEEDS FOR LASER TECHNOLOGIES APPLIED TO ADVANCED SPECTROGRAPHIC METHODS
Nov. 1989 128 p
(Contract DE-AC01-88ER-30131)
(DE90-001154; DOE/ER-30131/T8) Avail: NTIS HC A07/MF A01

The Department of Energy (DOE) recognizes that new developments in laser technology and laser spectroscopy can substantially improve the ability to carry out the mission of its Office of Health and Environmental Research (OHER). In brief, the mission of OHER is to support programs of research which provide the knowledge necessary for DOE to protect the human health and the environment from potentially adverse effects associated with the production and utilization of energy resources. For some years, the OHER program has included some support for the development of laser technology, and especially laser spectroscopy. This support has provided the bases for the demonstration of remarkably sensitive laser systems for the detection of chemical substances at the atomic and the molecular levels. At the present time, both laser technology and laser spectroscopy are surging ahead at an unprecedented rate. Thus, DOE requested that its Office of Program Analysis conduct a study to identify the opportunities in this laser revolution to further enhance the role of laser spectroscopy in the OHER mission. This DOE study was managed by Consultec Scientific, inc., who furnished from its staff the Principal Investigator, who, in turn, coordinated the enthusiastic efforts of a group of consultants consisting of some of the world's best scientists in the development and use of laser technology for spectroscopic purposes. This expert panel, during the course of its study, took a global view of laser science and from this perspective identified a number of recent developments which could substantially improve the ability of OHER to perform its increasingly important mission. DOE

N90-14588# Los Alamos National Lab., NM.
NUMERICAL SIMULATIONS OF FREE-ELECTRON LASER OSCILLATORS
Brian D. McVey, John C. Goldstein, R. L. Tokar, C. James Elliott, S. J. Gitomer, Mark J. Schmitt (Mission Research Corp., Los Alamos, NM.), and L. E. Thode 1988 16 p Presented at the 10th International Free-Electron Laser Conference, Jerusalem, Israel, 19 Aug. - 2 Sep. 1988
(Contract W-7405-eng-36)
(DE89-003488; LA-UR-88-3758; CONF-8808146-6) Avail: NTIS HC A03/MF A01

A numerical simulation capability was developed to model the physics and realistic design constraints of free electron laser oscillators driven by RF linear accelerators. Two computer codes were written, FELEX and FELP. The code FELP is a one spatial dimension code with essentially unlimited time or spectral resolution. The codes are complementary and their use is dependent upon the problem being addressed. The code FELP is used to model optical and electron micropulse structure, broadband noise, and the sideband instability. The code FELEX models accelerator generated electron beam distributions, the transport of these distributions through wigglers with misalignments and field errors, self-consistent interaction with the optical field, and propagation of the optical field through resonators with realistically modelled components. FELEX is routinely used to match resonator designs to the optical parameters of the electron beam, and used to investigate the physics of 3-D micropulse effects. Some details of the codes are presented along with various examples of simulation results. DOE

N90-14589# Los Alamos National Lab., NM.
CHAOTIC BEHAVIOR IN NONLINEAR POLARIZATION DYNAMICS
Daniel David, D. D. Holm, and Michael V. Tratnik 1989 24 p Presented at the Nearly Integrable Systems and Applications, Minneapolis, MN, 7-11 Nov. 1989
(Contract W-7405-eng-36)
(DE89-013453; LA-UR-89-1664; CONF-891151-1) Avail: NTIS HC A03/MF A01

The problem of two counterpropagating optical laser beams was analyzed in a slightly nonlinear medium from the point of view of Hamiltonian systems; the one-beam subproblem is also investigated as a special case. These systems are studied as integrable dynamical systems which undergo chaotic behavior under various types of perturbations. The phase space for the two-beam problem is C squared x C squared when restricted to the regime of travelling-wave solutions. The method of reduction is used for Hamiltonian systems invariant under one-parameter symmetry groups to demonstrate that the phase space reduces to the two-sphere S squared and is therefore completely integrable. The phase portraits of the system are classified and the bifurcations that modify these portraits are also determined; some new degenerate bifurcations are presented in this context. Finally, various physically relevant perturbations are introduced and the Melnikov method is used to prove that horseshoe chaos and Arnold diffusion occur as consequences of these perturbations. DOE

N90-14590# Lawrence Livermore National Lab., CA.
LABORATORY X RAY LASERS
D. L. Matthews Aug. 1989 6 p
(Contract W-7405-eng-48)
(DE90-000879; UCID-21803) Avail: NTIS HC A02/MF A01

One of the most innovative spinoffs of ICF technology and physics was the development of the x ray wavelength laser. The first incontrovertible demonstration of this type of laser came from LLNL in 1984 using the Novette laser to pump a selenium foil target. The power and energy of Novette were then needed to produce a column of plasma of sufficient length to achieve a sufficient gainlength product (approximately 5.5, this corresponds to an amplification of approximately 250X) that could unquestionably illustrate the lasing effect. LLNL ICF expertise was also required to develop time-resolved spectrometers used to view the lasing transitions at approximately 20 nm, a region of the XUV spectrum normally dominated by high backgrounds. The design of the x ray laser amplifier, which required maintaining nonequilibrium level populations in a tailored plasma having the proper conditions for gain and x ray laser beam propagation, was accomplished with modified versions of ICF kinetics and hydrodynamics codes. Since the first demonstration, progress in the development of the x ray laser was rapid. New achievements include production of megawatt power levels at 20 nm, amplified spontaneous emission levels approaching saturation intensity GL of approximately 17 at 20 nm, efficiency (x ray laser energy/pump energy) approximately 10(exp 6), the demonstration of double and triple pass amplification (hinting at the possibility of producing x ray wavelength resonators), the focusing of x ray lasers to pump other types of lasers and the first demonstration of an x ray hologram produced by an x ray laser. The generation of amplification at ever shorter wavelength is possible using various types of inversion schemes. We depict below this progress benchmarked against production of gain in the water window (2.2 to 4.4 nm,), where applications to biological imaging may be facilitated. DOE

N90-14591# Lawrence Livermore National Lab., CA.
THE CURRENT STATUS OF X RAY CONVERSION EFFICIENCY MODELING
Steven Langer Aug. 1989 12 p
(Contract W-7405-eng-48)
(DE90-000931; UCID-21801) Avail: NTIS HC A03/MF A01

Conversion efficiency (CE) experiments measure the fraction of the energy in a laser beam illuminating a (gold) disk which is converted into x rays. In the summer of 1987 a series of experiments using gold disks made of a mixture of gold and beryllium was performed. These experiments produced high quality data on the spatial, temporal, and spectral properties of the x rays emitted by laser illuminated disks, as well as measuring the CE. The new and more detailed results have prompted several revisions in modeling of the conversion process. A summary is provided of the status of conversion efficiency modeling and shows that the models accurately reproduce many features of the data. DOE

N90-14592# Oak Ridge National Lab., TN. Solid State Div.
PROSPECTS FOR WAVELENGTH TUNABLE LASERS BASED ON VACANCY DEFECTS IN ALKALINE-EARTH OXIDES
Y. Chen, V. M. Orera, and R. Gonzalez Sep. 1989 8 p Presented at the 5th International Tunable Laser Conference, Irkutsk, USSR, 20-23 Sep. 1989
(Contract DE-AC05-84OR-21400)
(DE90-001078; CONF-8909211-1) Avail: NTIS HC A02/MF A01

Research on color centers in the alkali halides has proven fruitful in that the recent development of tunable lasers was a direct outgrowth of the studies. It is expected that research on the alkaline-earth oxides will also bear fruit in this area. In this article we discuss the merits and problems of using defects for tunable lasers. The discussions are confined to CaO and MgO crystals. Vacancies such as the F(sup +) center (an anion vacancy with one electron which is therefore positively charged with respect to the lattice) constitute a four-level system. Vacancies can provide higher gain than transition metal or rare-earth ions. DOE

N90-14593# Los Alamos National Lab., NM.
QUALIFICATION OF DIODE FOIL MATERIALS FOR EXCIMER LASERS
R. G. Anderson, R. P. Shurter, and E. A. Rose 1989 5 p Presented at the IEEE Pulsed Power Conference, Albuquerque, NM, 11-14 Jun. 1989
(Contract W-7405-eng-36)
(DE90-000602; LA-UR-89-3041; CONF-8906218-1) Avail: NTIS HC A01/MF A01

The Aurora facility at Los Alamos National Laboratory uses KrF excimer lasers to produce 248 nm light for inertial confinement fusion applications. Diodes in each amplifier produce relativistic electron beams to pump a Kr-F-Ar gas mixture. A foil is necessary to separate the vacuum diode from the laser gas. High tensile strength, high electron transmission, low ultraviolet reflectivity, and chemical compatibility with fluorine have been identified as requisite foil properties. Several different materials were acquired and tested for use as diode foils. Transmission and fluorine compatibility tests were performed using the Electron Gun Test Facility (EGTF) at Los Alamos. Off-line tests of tensile strength and reflectivity were performed. Titanium foil, which is commonly used as a diode foil, was found to generate solid and gaseous fluoride compounds, some of which are highly reactive in contact with water vapor. DOE

N90-14594# Oak Ridge National Lab., TN. Applied Technology Div.
SOLID-STATE FLUORESCENCE ABOVE 1000 C: APPLICATION TO HIGH-TEMPERATURE LASER THERMOMETRY
M. R. Cates, S. W. Allison, G. J. Pogatshnik, and A. R. Bugos (Tennessee Univ., Knoxville.) 1989 9 p Presented at the 8th International Congress on Applications of Lasers and Electro-Optics (ICALEO 8), Orlando, FL, 15-20 Oct. 1989
(Contract DE-AC05-84OR-21400)
(DE90-000728; CONF-891091-1) Avail: NTIS HC A02/MF A01

Rare-earth doped phosphors are discussed here which exhibit intense fluorescence well above 1000 C. This is a rare characteristic for solid-state materials. One immediate application for them is thermometry. For example, surface temperatures of rotating components, systems in hostile or restricted environments, and systems in environments with very high temperature backgrounds are measurable with phosphor thermographic methods. The subject phosphors, Y2O3:Eu, LuPO4:Eu, YPO4:Eu, and LuPO4:Dy, provide the capability to extend these methods to very high temperatures. The use of pulsed ultraviolet (UV) laser activation of these phosphors leads to numerous practical application possibilities. The phosphor characteristics plus various fluorescence decay times vs temperature are shown, along with discussion of their high-temperature applications. DOE

N90-14595# Lawrence Livermore National Lab., CA.
THE DEVELOPMENT OF COHERENT X RAY LASERS FOR X RAY HOLOGRAPHY
D. L. Matthews, J. Trebes, Richard A. London, and M. Rosen Aug. 1989 15 p Presented at the Conference on X Ray Microimaging for the Life Sciences, Berkeley, CA, 24-26 May 1989
(Contract W-7405-eng-48)
(DE90-000784; UCRL-100920; CONF-8905192-1) Avail: NTIS HC A03/MF A01

Several of the research paths to develop an x ray laser capable of producing the flux required to obtain x ray holograms of biological structures in live cells are described. These paths include optimization of the current Ni-like Yb laser which operates at 5.02 nm as well as the introduction of a new Ni-like Ta laser which operates at 4.48 nm, i.e., is the near optimum wavelength for holographic imaging of biological objects. Current predictions indicate that at least 20 microJ of spatially-coherent radiation needs to be produced in a pulselength of 50 psec and focussed at the sample to a beam of 10 micrometer diameter. A detailed description is provided which should meet these requirements. In addition, some comments will be given on future trends in x ray laser development, namely toward more efficient table top systems. DOE

N90-14596# Lawrence Livermore National Lab., CA.
ULTRAHIGH-BRIGHTNESS LASERS AND THEIR APPLICATIONS
M. D. Perry Aug. 1989 10 p
(Contract W-7405-eng-48)
(DE90-000877; UCID-21805) Avail: NTIS HC A02/MF A01

New short-pulse laser technology has made possible the production of extremely strong laser fields (I greater than 10(exp 17) W/sq cm) from small scale systems. The use of these new techniques on intermediate to large scale Nd:glass based laser systems makes possible, in principle, the production of 1000 TW (Petawatt) pulses. Such pulses yield focused intensities exceeding 10(exp 21) W/sq cm, corresponding to an electric field in excess of 100 e/a(sub o)(sup 2) and an energy density equivalent to that of a 10 KeV blackbody (3 x 10(exp 10) J/cu cm). Such a source would have important applications in x ray laser research and lead to a fundamentally new class of experiments in atomic, nuclear, plasma and high-energy density physics. Some of the advances which make such laser sources possible have grown naturally out of our laser research in support of the ICF Program. This paper introduces these new techniques and examines some of the specific applications both of Petawatt pulses requiring large systems and more modest 10 TW pulses now achievable with table-top systems. DOE

N90-14597# Connecticut Coll., New London.
A COMPACT, HIGH-POWERED FAR-INFRARED (FIR) LASER Technical Progress Report, 22 Jan. - 18 Aug. 1989
18 Aug. 1989 20 p

(Contract DE-AC03-87SF-17128)
(DE89-016786; DOE/SF-17128/T1) Avail: NTIS HC A03/MF A01

A compact CO2(13)CH3F laser system where the FIR laser cavity is inserted in a pump, three mirror CO2 laser cavity, with optically switched semiconductor cavity dumping, will be designed and tested. The 1.207 mm cavity dumped oscillator is expected to be characterized by predominantly single longitudinal mode, narrow linewidth operation and to produce peak powers of order 100 kW in pulses of order 10 ns duration. The 1.2mm wavelength lies in an atmospheric transmission window (1 dB/km at sea level), which opens up the possibility of millimeter wave space or ground based radar and communications systems. The laser can also be used as a FIR spectroscopic source to investigate dynamic properties of elementary excitations of the solid state. Although much progress was made, the project is behind schedule due to a malfunctioning pump CO2 laser. An extension has been requested and it is anticipated that testing of the laser system can begin shortly. DOE

N90-14598# Massachusetts Inst. of Tech., Cambridge. Plasma Fusion Center.
SELF-FIELD-INDUCED CHAOTIC ELECTRON MOTION IN FREE ELECTRON LASERS
Chiping Chen and Ronald C. Davidson Sep. 1989 17 p Presented at the 11th International Free Electron Laser Conference, Naples, FL, 28 Aug. - 1 Sep. 1989
(Contract DE-AC02-78ET-51013)
(DE90-001710; PFC/JA-89-43; CONF-8908134-14) Avail: NTIS HC A03/MF A01

It is shown that the inclusion of the equilibrium self fields of the electron beam results in chaotic electron motion in the field configuration consisting of a constant-amplitude helical wiggler magnetic field and a uniform axial guide field. The threshold value of the self-field parameter epsilon = omega(sub pb)(sup 2)/4 Omega(sub c)(sup 2) is determined for the onset of chaoticity in the Group-1 and Group-2 orbits for the parameter regime corresponding to moderately high beam current (and density). The time scale for self-field-induced changes in the particle orbits is found to be of the order of beam-transit time through one wiggler period. DOE

N90-14599# Los Alamos National Lab., NM.
OPTICAL DESIGN AND PERFORMANCE OF AN XUV FEL (FREE-ELECTRON LASER) OSCILLATOR
John C. Goldstein, Brian D. McVey, and Brian E. Newnam 1989 9 p Presented at the 11th International Free Electron Laser Conference, Naples, FL, 28 Aug. - 1 Sep. 1989
(Contract W-7405-eng-36)
(DE90-002381; LA-UR-89-3438; CONF-8908134-8) Avail: NTIS HC A02/MF A01

A study of numerical simulation of the performance of a multifacet metal mirror ring resonator FEL is presented for several extreme ultraviolet radiation wavelengths. Laser performance in the presence of mirror aberrations and thermal distortion is calculated for two different output coupling methods, a scraper mirror and a hole. DOE

N90-14600# Los Alamos National Lab., NM.
COMPACT RF-LINAC FREE-ELECTRON LASERS
John C. Goldstein, Richard L. Sheffield, Bruce E. Carlsten, and Roger W. Warren 1989 14 p Presented at the 11th International Free Electron Laser Conference, Naples, FL, 28 Aug. - 1 Sep. 1989; sponsored by SPIE Submitted for publication
(Contract W-7405-eng-36)
(DE90-002386; LA-UR-89-3406; CONF-8908134-9) Avail: NTIS HC A03/MF A01

Design studies using the INEX simulation methods are presented for an infrared compact RF-linac driven FEL. The possibility of such a device relies upon two technological advances: a very bright electron beam from a linac with a photocathode injector, and a short period, high field wiggler. DOE

N90-14601# Los Alamos National Lab., NM.
INEX (INTEGRATED NUMERICAL EXPERIMENT) SIMULATIONS OF THE LOS ALAMOS HIBAF (HIGH-BRIGHTNESS ACCELERATOR FREE-ELECTRON LASER) FREE-ELECTRON LASER MOPA (MASTER OSCILLATOR POWER AMPLIFIER) EXPERIMENT
John C. Goldstein, Bruce E. Carlsten, and Brian D. McVey 1989 17 p Presented at the 11th International Free Electron Laser Conference, Naples, FL, 28 Aug. - 1 Sep. 1989 Submitted for publication Sponsored in part by Army Ballistic Missile Defense Organization
(Contract W-7405-eng-36)
(DE90-002387; LA-UR-89-3397; CONF-8908134-10) Avail: NTIS HC A03/MF A01

Results are presented of Integrated Numerical Experiment (INEX) simulations of the performance of a 1-m untapered wiggler FEL oscillator driving a 2-m wiggler FEL amplifier for the new HIBAF (High-Brightness Accelerator Free-Electron Laser) facility at Los Alamos. INEX simulations utilize a numerically-generated electron micropulse, from ISIS/PARMELA calculations of the photoinjector linac/beam transport system, in the 3-D FEL simulation code FELEX. DOE

N90-14602# Los Alamos National Lab., NM.
LASING ON THE THIRD HARMONIC
Roger W. Warren, L. C. Haynes, D. W. Feldman, W. E. Stein, and S. J. Gitomer 1989 12 p Presented at the 11th International Free Electron Laser Conference, Naples, FL, 28 Aug. - 1 Sep. 1989
(Contract W-7405-eng-36)
(DE90-002389; LA-UR-89-3394; CONF-8908134-12) Avail: NTIS HC A03/MF A01

The Los Alamos Free-Electron Laser has recently lased near 4 (mu)m on the third harmonic of the fundamental frequency of about 12 (mu)m. By choice of intercavity apertures and cavity length, lasing can be forced to occur on both frequencies simultaneously or on either one alone. DOE

N90-14603# Los Alamos National Lab., NM.
ANALYTICAL TREATMENT OF ELECTRON TRAJECTORY STRAIGHTENER ISSUES IN FREE-ELECTRON LASERS
C. James Elliott and D. C. Quimby (Spectra Technology, Inc., Bellevue, WA.) 1989 23 p Presented at the 11th International Free Electron Laser Conference, Naples, FL, 28 Aug. - 1 Sep. 1989
(Contract W-7405-eng-36)
(DE90-002405; LA-UR-89-3486; CONF-8908134-13) Avail: NTIS HC A03/MF A01

The poincare orbit of the electron's journey must be straight and narrow through a many period free electron laser (FEL). To utilize an available technology level, the straightest wiggler orbit operating point (SWOOP) is chosen by adjusting the spacing parameter of an orbit correction scheme. This eases the requirements for achieving the full potential of FEL wigglers. One quality index, one cost index, two quality factors, two measures of field noise, an improvement index, and a straightener classification scheme are concepts that facilitate the analysis. Only when the field noise is large is this analysis of direct use. A reader-friendly description culminates in the comparison of two schemes to illustrate the methods. Two coupled first order langevin equations have solutions that are proven to be Gaussian variables. The solutions are used to give the required cross correlations. These results are coupled with a simple graphical technique and give an expression for the angular variance in the correction corridor. The two components of this variance are compared to a fiducial scheme and yield the two quality factors from which the quality, improvement and cost indices are computed. DOE

N90-14604# Oak Ridge National Lab., TN. Solid State Div.
STUDIES OF NEUTRAL AND ION TRANSPORT DURING LASER ABLATION OF 1:2:3 SUPERCONDUCTORS BY OPTICAL ABSORPTION SPECTROSCOPY
D. B. Geohegan and D. N. Mashburn 1989 10 p Presented

at the Conference on Superconductivity and Applications, Buffalo, NY, 19-21 Sep. 1989
(Contract DE-AC05-84OR-21400)
(DE90-001968; CONF-890971-5) Avail: NTIS HC A02/MF A01

Transient optical absorption spectroscopy, a new diagnostic technique for examining the density of ground state neutrals and ions following laser ablation, has been utilized for the first time to study the transport of ground state Y, Ba, Cu, Y(+), and Ba(+) following laser ablation of Y1Ba2Cu3O(x) pellets under film deposition conditions. The technique reveals significantly broadened velocity distributions with a low velocity component which is absent from velocity distributions inferred from monitoring excited state plume fluorescence. Ion probe measurements confirm this low velocity component. High resolution emission spectroscopy is also utilized to examine the spectral broadening arising from collision processes in the laser plasma as well as obtain estimates of plasma densities. DOE

N90-14605# Idaho National Engineering Lab., Idaho Falls.
NONCONTACTING LASER ULTRASONIC GENERATION AND DETECTION AT THE SURFACE OF MOLTEN METAL
G. V. Garcia, N. M. Carlson, K. L. Telschow, and J. A. Johnson 1989 7 p Presented at the Conference on Review of Progress in Quantitative NDE, Brunswick, ME, 24-28 Jul. 1989 Submitted for publication
(Contract DE-AC07-76ID-01570)
(DE90-002020; EGG-M-89209; CONF-890770-4) Avail: NTIS HC A02/MF A01

Proof of principle for using lasers to generate and detect ultrasound for the measurement of molten pool depth is described. Tin was chosen for these experiments because it has a low melting point and does not require any special equipment to produce a molten metal pool. To keep initial experiments simple, the depth of the molten pool was determined using a noncontacting sensor without any solid/liquid interfaces present. The results are compared to data available from experiments that used buffer rods to determine properties of molten tin. DOE

N90-14606# Los Alamos National Lab., NM.
THEORY OF HARMONIC RADIATION USING A SINGLE-ELECTRON SOURCE MODEL
Mark J. Schmitt and C. James Elliott 1989 20 p Presented at the 11th International Free Electron Laser Conference, Naples, FL, 28 Aug. - 1 Sep. 1989 Sponsored in part by the Army Strategic Defense Command
(Contract W-7405-eng-36)
(DE90-002412; LA-UR-89-3581; CONF-8908134-16) Avail: NTIS HC A03/MF A01

Significant progress was recently made toward the understanding of the various mechanisms that generate harmonic radiation in plane-polarized free electron lasers. Within the context of a single frequency coherent-spontaneous emission model, a distributed transverse source function for a single electron was derived. This source is multiply peaked, with the number of peaks being equal to the harmonic number. The peaks and nulls in the radiation source are analogous to the radiation peaks seen in the spontaneous radiation pattern of a single electron. When the distributed source function is averaged over transverse space, the simplified 1-D results are recovered. The distributed source function model predicts the generation of even harmonic radiation with odd-symmetry in the electron wiggle plane (for electrons traveling along the wiggler axis) and odd harmonic radiation patterns with even transverse symmetry. A method for modeling the multi-pole nature of the harmonic radiation on a discrete grid is described. When the transverse electron beam distribution is slowly varying, all the harmonics can be adequately modeled with multi-poles having only a few peaks. This model was incorporated into the 3-D FEL simulation code FELEX. Simulations of the Los Alamos and Stanford FEL oscillators were performed. How the harmonic transverse spatial electric field profiles change for different operating conditions is examined. DOE

N90-14607# Oak Ridge National Lab., TN.
NONRESONANT AND RESONANT MULTIPHOTON IONIZATION OF (NO)(SUB n) AND Ar(SUB n)NO CLUSTERS WITH PICOSECOND LASER PULSES
D. Barton Smith and John C. Miller 1989 24 p Presented at the Faraday Symposium: The Royal Society of Chemistry, London, England, 12-14 Dec. 1989
(Contract DE-AC05-84OR-21400)
(DE89-016853; CONF-891252-1) Avail: NTIS HC A03/MF A01

High peak power laser pulses were used to effect multiphoton ionization (MPI) in supersonic nozzle expansions of nitric oxide in argon. The NO(sub n less than or = 5) clusters were detected for the first time by a multiphoton laser technique. The Ar2 and Ar(sub n less than or = 7)NO complexes were also observed. Results from a number of different visible and ultraviolet wavelengths are compared and interpreted with reference to the known electronic states of NO(sub n) and NO(sub n)(+). When resonant with the dissociative B1 state of NO2 at approx. 217 nm, cluster ions are observed with picosecond but not with nanosecond laser pulses. In contrast, nonresonant MPI at certain wavelengths results in parent cluster ions with either nanosecond or picosecond lasers. The use of such high-peak power lasers for the characterization of cluster beams is discussed and compared with more conventional electron impact techniques. DOE

37 MECHANICAL ENGINEERING

Includes auxiliary systems (nonpower); machine elements and processes; and mechanical equipment.

N90-14608*# Rockwell International Corp., Canoga Park, CA. Rocketdyne Div.
EXTRAVEHICULAR ACTIVITY WELDING EXPERIMENT Final Report
J. Kevin Watson 21 Aug. 1989 158 p Original contains color illustrations
(Contract NAS8-37753)
(NASA-CR-183848; NAS 1.26:183848; RI/RD89-216) Avail: NTIS HC A08/MF A01 CSCL 13I

The In-Space Technology Experiments Program (INSTEP) provides an opportunity to explore the many critical questions which can only be answered by experimentation in space. The objective of the Extravehicular Activity Welding Experiment definition project was to define the requirements for a spaceflight experiment to evaluate the feasibility of performing manual welding tasks during EVA. Consideration was given to experiment design, work station design, welding hardware design, payload integration requirements, and human factors (including safety). The results of this effort are presented. Included are the specific objectives of the flight test, details of the tasks which will generate the required data, and a description of the equipment which will be needed to support the tasks. Work station requirements are addressed as are human factors, STS integration procedures and, most importantly, safety considerations. A preliminary estimate of the cost and the schedule for completion of the experiment through flight and postflight analysis are given. Author

N90-14609 Illinois Univ., Chicago.
STABILITY AND DYNAMICS OF CONSTRAINED FLEXIBLE MULTIBODY SYSTEMS Ph.D. Thesis
Sitki Kemal Ider 1988 163 p
Avail: Univ. Microfilms Order No. DA8909052

Development of a new method for the reduction of the equations of motion subjected to kinematical and geometrical constraints is explored, and a new procedure for handling the singularity occurrence when the Jacobian changes rank is also examined. The concepts are applied to both rigid and highly flexible systems. This includes the geometric nonlinearities and the coupling between the rigid and elastic motion. First the equations of motion for general constrained multibody systems are developed using Kane's equations, finite element method and modal analysis techniques. A recursive formulation of the equations is used

together with an extended form of the partial velocity vectors. A nonlinear strain energy formulation is used for the structural geometric coupling between the axial and transverse deformations in 3-D beams. The corresponding geometrical stiffness matrix is derived. Closed loops and kinematical constraints are included into the system via constraint equations obtained using the partial velocity vectors. A new matrix theorem for determining the orthogonal complement of the Jacobian matrix is developed. For singular configurations that occur when the constraint equations become linearly dependent, a methodology for obtaining a full rank constraint matrix and hence a full rank reduction by using higher derivatives is developed. Examples illustrated include a spatial robotic manipulator in deployment and spin-up maneuvers, and rigid and flexible manipulators at singular configurations.
Dissert. Abstr.

N90-14610 Department of the Navy, Washington, DC.
PRESSURE SENSITIVE RELEASE DEVICE Patent
Willie B. Freeman, inventor (to Navy) 18 Jul. 1989 6 p Filed 25 Aug. 1988 Supersedes AD-D013938
(AD-D014220; US-Patent-4,848,262; US-Patent-Appl-SN-236696)
Avail: US Patent and Trademark Office CSCL 13/9

A release mechanism is triggered when the pressure differential on the sidewall of a sealed container reaches a predetermined threshold level at which the container either implodes or explodes to sufficiently decrease the spacing between the ends of the container and thereby achieve the release. False triggering due to percussion or shock waves may be precluded by disposing a shield about the sidewall.
GRA

N90-14611# Department of the Navy, Washington, DC.
A METHOD OF SOLDERING ALUMINUM Patent Application
A. P. Divecha, inventor (to Navy), William A. Ferrando, inventor (to Navy), P. Hesse, inventor (to Navy), and S. Karmarkar, inventor (to Navy) 29 Aug. 1989 6 p
(AD-D014226; US-Patent-Appl-SN-401197) Avail: NTIS HC A02/MF A01 CSCL 11/6

This invention relates to methods of joining metal parts and more particularly to methods of soldering aluminum. Accordingly an object of this invention is to provide a new method of soldering aluminum and its alloy. Another object of this invention is to provide treated aluminum surfaces which can easily be soldered. These and other objects of this invention are accomplished by providing a process comprising: wetting an aluminum or aluminum alloy surface with molten silver nitrate; heating the AgNO3 coated aluminum surface at a temperature of from the decomposition temperature of AgNO3 to about 550 C to decompose the AgNO3 and form a Ag metal film.
GRA

N90-14612 Ohio State Univ., Columbus.
FINITE ELEMENT ANALYSIS OF FRICTIONAL CONTACT PROBLEMS Ph.D. Thesis
Moon Hyuk Im 1989 212 p
Avail: Univ. Microfilms Order No. DA8913654

A brief review of friction phenomena and friction models is made. Finite element formulations and solution algorithms are discussed in conjunction with Coulomb's and power friction law. Efficient numerical techniques for the finite element analysis of frictional contact problems are developed. Adaptation of successive over-relaxation method is studied and a modified partial flexibility method is proposed. The accuracy and convergence characteristics of the presented numerical algorithms are demonstrated and tested for various selected examples. Solution accuracy and computing time requirements are studied by comparing with other solution methods. Numerical results obtained by applying the power law and Coulomb's friction law are also compared. Unlike other approximate solution methods, the modified flexibility method gives the most accurate solutions for a wide range of friction coefficients. Also the computing time associated with the modified flexibility method is much less than that for other methods. The modified partial flexibility method is applied to elastoplastic contact problems with incremental loading by incorporating the tangential stiffness technique. The obtained solutions are shown to be physically acceptable. Overall, the modified partial flexibility method is shown to be a very effective and accurate method for solving complex contact problems involving elastic-to-elastic or rigid-to-elastoplastic contact.
Dissert. Abstr.

N90-14613# Environmental Protection Agency, Ann Arbor, MI. Control Technology and Applications Branch.
COLD STARTING A NEAT METHANOL (M100) VEHICLE WITH LONG DURATION SPARK IGNITION
Robert I. Bruetsch Jun. 1989 24 p
(PB89-230692; EPA/AA/CTAB-89/05) Avail: NTIS HC A03/MF A01 CSCL 21B

A test program was devised at EPA's Motor Vehicle Emission Laboratory to evaluate the Nissan long duration spark ignition (LDSI) system on an M100 test vehicle to determine whether cold starting neat methanol at low ambient temperatures can be improved. Modifications were made to the vehicle's ignition system and stock cold start injectors were utilized. Successful cold starts were obtained down to 20 F.
Author

N90-14614 Texas Univ., Austin.
TIRE MODELING BY FINITE ELEMENTS Ph.D. Thesis
Luis Oliveira Faria 1989 165 p
Avail: Univ. Microfilms Order No. DA8920698

The rolling contact of three dimensional bodies was studied and applied to tire modeling. First, the kinematics of steady state motion in general axisymmetric bodies is discussed. Stress measures and the equations of motion are established together with general requirements on constitutive equations to ensure that a steady state is maintained. Specific constitutive equations to model tire components are then presented. Boundary conditions that model the interaction of the body with its surroundings are discussed, which concludes the formulation of the boundary value problem for rolling contact. This boundary value problem is then given a variational formulation, which is the first step for finite element discretization. Shell finite elements and three dimensional brick finite elements are presented and numerical examples obtained for rolling friction, stress concentrations in composites, and modeling of tires are discussed. The phenomenon of standing waves in tires is discussed based on solutions to a model problem in elasticity, which presents some of the observed phenomena.
Dissert. Abstr.

N90-14615 Iowa Univ., Iowa City.
CONTROLLER DESIGN FOR A ROBOTIC MANIPULATOR Ph.D. Thesis
Dong-Jin Lim 1988 336 p
Avail: Univ. Microfilms Order No. DA8913200

A method for designing a controller for a robotic manipulator is investigated. The objective is to synthesize a controller using only the observable state variables such that the system response follows a given ramp reference input with zero steady state error under a ramp disturbance. The main difficulties are caused by the Coulomb frictions, the spring effect of the link between the drive motor and the manipulator arm, and the unmeasurable state variables. The proposed is based on augmenting the system by additional integrators and feeding back the delayed values of the observable variables. When the closed loop system exhibits a limit cycle, the feedback parameters are readjusted by employing the describing function method so that either the limit cycle is completely eliminated or the magnitude of the limit cycle is reduced to an acceptably small level.
Dissert. Abstr.

N90-14616 Council for National Academic Awards (England).
TRANSIENT RESPONSE OF FLEXIBLE ROTOR-BEARING SYSTEMS SUBJECTED TO COMBINED UNBALANCE AND GROUND EXCITATIONS Ph.D. Thesis
J. O. Cheung 1988 320 p
Avail: Univ. Microfilms Order No. BRDX85799

There already exists, in literature, a number of solutions to the problem of the dynamic response of rotor-bearing systems subjected to base excitations. Unfortunately, most researchers have concentrated on modeling the hydrodynamic journal bearing using

the so-called linear oil film force coefficients. However, when large perturbations within the bearings are experienced, the oil film behavior is nonlinear. Therefore, it is essential that the model must be capable of predicting the nonlinear characteristics of the fluid film in the journal bearing. The transient shock analysis of flexible rotor-bearing systems, was investigated using the Newmark combined with the force iterative time marching scheme. Two criteria, namely the relative displacement error and relative hydrodynamic force error, were used to examine the accuracy of the results at each time step in the numerical integration process. The flexible rotor is represented by a series of 2 noded finite rotor elements by employing the finite element approach, based upon the variational calculus. The characteristics of the ground shock excitation is theoretically modeled using the properties of the decaying sinusoidal wave. The discrete Fourier transform technique was used to identify the frequency contents in the non-synchronous response of the rotor-bearing system, obtained from the theoretical shock simulation. The main emphasis was placed upon the investigation into the effects of various ground shock excitations on the displacement response of rotor-bearing systems. Dissert. Abstr.

N90-14617*# National Aeronautics and Space Administration. Lewis Research Center, Cleveland, OH.

COMPARISON OF TWO DROPLET SIZING SYSTEMS IN AN ICING WIND TUNNEL

J. R. Oldenburg and R. F. Ide (Army Aviation Systems Command, Cleveland, OH.) 1990 19 p Presented at the 28th Aerospace Sciences Meeting, Reno, NV, 8-11 Jan. 1990; sponsored by AIAA
(DA Proj. 1L1-62209-A4-7A)
(NASA-TM-102456; E-5240; NAS 1.15:102456; AVSCOM-TM-89-C-015; AIAA-90-0668) Avail: NTIS HC A03/MF A01 CSCL 13B

A comparison between the Phase Doppler Analyzer and the combined measurements from the Particle Measuring Systems Forward Scattering Spectrometer Probe and the Optical Array Probe was conducted in an icing wind tunnel using NASA Icing Research Tunnel spray nozzles to produce the icing cloud. Clouds with a range of volume median diameters from 10 to greater than 50 microns were used for the instrument comparisons. A comparison of the volume median diameter from the Phase Doppler Particle Analyzer and only the Forward Scattering Spectrometer Probe indicated agreement up to 18 microns. A combined volume median diameter was calculated from the droplet distribution of the Optical Array Probe and the Forward Scattering Spectrometer Probe. A comparison of the combined volume median diameters and the Phase Doppler Particle Analyzer volume median diameters showed agreement up to 30 microns with the agreement deteriorating rapidly above 30 microns. Droplet distributions from the Phase Doppler Particle Analyzer, the Forward Scattering Spectrometer Probe, and Optical Array Probe are presented. Author

N90-14618# Sandia National Labs., Albuquerque, NM. Explosive Subsystems Div.

PROJECTILE IMPACT HUGONIOT PARAMETERS FOR SELECTED MATERIALS

Manuel G. Vigil Aug. 1989 58 p
(Contract DE-AC04-76DP-00789)
(DE90-000891; SAND-89-1571) Avail: NTIS HC A04/MF A01

The Rankine Hugoniot equation relating the conversion of momentum across a shock front and the empirical relationship for shock velocity as a function of particle velocity are used to calculate the impact pressures for selected materials. The shock velocity and particle velocities are then calculated as a function of impact pressures. The calculated data are graphically presented sets of three figures for the selected materials as follows: impact pressure as a function of impact velocity, impact pressure as a function of particle velocity, impact pressure as a function of shock velocity. Given the projectile impact velocity and material Hugoniot information, this graphical representation of the data allows for a fast approximation of the impact pressure particle velocity, and shock velocity in the target material. DOE

N90-14619# Oak Ridge National Lab., TN.

BES WELDING SCIENCE CONTRACTORS SUMMARY REPORT, 1988 TO 1989

S. A. David, comp., J. M. Vitek, T. Zacharia, T. DebRoy, J. Szekely, D. K. Matlock, D. L. Olson, J. W. Morris, and A. J. Sunwoo (California Univ., Berkeley.) 1989 35 p
(Contract DE-AC05-84OR-21400)
(DE90-001004; ORNL/M-939) Avail: NTIS HC A03/MF A01

The progress made in welding science by ORNL, Penn State University, MIT, Colorado School of Mines, and the University of California is reviewed. ORNL is investigating the physical metallurgy of weldments and to develop the capability to predict weld metal microstructure and properties. Mass transfer during laser welding is being studied by Penn State University. MIT is studying the modelling of transport phenomena in weldpools. The role of composition and microstructure gradients on weld metal properties and behavior is covered by the Colorado School of Mines. The University of California has worked with the welding of 2090 Al-Cu-Li Alloy for cryogenic use. DOE

N90-14620# Edgerton, Germeshausen and Grier, Inc., Idaho Falls, ID.

DERIVATION OF SYNTHETIC MISSION PROFILES FROM ELECTRIC VEHICLE FIELD DATA

Raymond K. Fink 1989 5 p Presented at the 9th Electric Vehicle Symposium, Toronto, Ontario, 13-16 Nov. 1989
(Contract DE-AC07-76ID-01570)
(DE89-011125; EGG-M-88114; CONF-891133-1) Avail: NTIS HC A01/MF A01

A method using Monte Carlo sampling was developed for synthesizing prototypical time histories of velocity and power from mission summary data gathered with the on-board Versatile Data Acquisition Systems (VDAS). The basic approach is to construct a set of probability distributions for mechanical power in each velocity range of the VDAS data, from which power values are randomly sampled at each time step. The corresponding velocity changes are then calculated from the equations of motion, resulting in a time history of the desired length which should produce the same effects on vehicle systems as the (unknown) original vehicle operation. Some results are presented, and limitations of the process are discussed. DOE

N90-14621# Imatran Voima Oy, Helsinki (Finland).

EXPERT SYSTEM FOR FAULT DIAGNOSTICS OF ROTATING MACHINES

A. Korteniemi Dec. 1988 64 p
(DE89-766980; IVO-A-06/88) Avail: NTIS (US Sales Only) HC A04/MF A01

In this report the fault diagnostics based on vibration caused by a turbogenerator rotating with constant speed was modelled and an off-line expert system prototype was carried out in a research environment. This work acquaints the reader with the fundamental principles of the diagnostics of rotating machines and with the essential concepts relating to the expert system. Especially the development process of the expert system as well as the surface and deep knowledge in the architecture of an expert system are presented. The study surveys different kinds of techniques to reason with inexact or uncertain information, because the expressing of them was one of the main concerns when building the prototype system. The software development environment is also described. In the modelled prototype, the knowledge is presented by dividing it into several levels according to the role it has in the reasoning process. The domain theories are described by a structural and a behavioural model of the machine to be diagnosted. The diagnosis strategy is modelled by dividing it into several separate strategies. Finally, the prototype is validated by letting it solve three randomly selected problems with known results. DOE

N90-14622# Surrey Univ., Guildford (England). Dept. of Chemical and Process Engineering.

SINGLE PARTICLE FRICTION TESTS WITH CELLULOSE ACETATE SPHERE SAMPLES

U. Tuzun 31 May 1989 75 p Prepared for Lawrence Livermore National Lab., CA
(Contract W-7405-eng-48)
(DE89-017537; UCRL-21228) Avail: NTIS HC A04/MF A01

A detailed account of all the experimental work carried out for LLNL using the single particle shear cell in the department of Chemical and Process Engineering of Surrey University, Guildford, United Kingdom is presented. Experimental work with two spheres in contact was performed. Particles were positioned into the specially made sample holders by the micro screws. The contact centers were lined up under the magnifying glass. The behavior of the interparticle contact region between the two spheres was examined by performing the following series of tests: (1) normal force versus normal displacement test, (2) tangential force limit at gross sliding with increased normal load and decreasing normal load, and (3) tangential force versus micro displacement during initial loading to friction limit and during unloading from friction limit. Work was also performed on single sphere against a flat wall surface. Results are discussed. DOE

N90-14623# Argonne National Lab., IL. Center for Transportation Research.
MARKETS FOR HIGH-SPEED INTERCITY MAGLEV TECHNOLOGY: A SYSTEMS ANALYSIS APPROACH
Howard T. Coffey and Larry R. Johnson Jun. 1989 18 p Presented at the SAE Conference and Expo on Future Transportation Technology, Vancouver, British Columbia, 6-10 Aug. 1989
(Contract W-31-109-eng-38)
(DE89-017683; CONF-8908144-2) Avail: NTIS HC A03/MF A01

The technical feasibility of constructing and operating maglev vehicles at speeds of 250 to 300 mph has been amply demonstrated and is accepted here as a reality. Herein, the markets into which passenger or freight carrying systems based on this technology can be introduced with economic reasonableness are evaluated. The characteristics and capabilities (particularly the capacity and comparative costs) of the system are enumerated and discussed from the points of view of the passengers, the airlines (as potential operators), and the traveling public. It is shown that if the system is integrated into the existing transportation system as a supplement to the airline system, it meets the criteria required for the introduction of any new product or service into a market. The financial enhancement of the maglev system resulting from the use of trunk routes with feeder lines diverging to various ultimate destinations becomes an extremely important consideration. DOE

N90-14624# Allied-Signal Aerospace Co., Kansas City, MO. Kansas City Div.
NEW TOOL-HOLDING CONCEPT Final Report
G. V. Hill Oct. 1989 10 p
(Contract DE-AC04-76DP-00613)
(DE90-000880; KCP-613-4126) Avail: NTIS HC A02/MF A01

A hydraulic holding system and cutting tools to take advantage of the holding system were developed. This system allows the cutting tool to be manufactured, inspected, and used in the same type mounting system. The ability of this system to accurately and repeatedly hold the cutting tools on centerline has resulted in a significant reduction in scrap rate and lost production workforce. It also resulted in an increased quality level for the cutting tools that are now manufactured. DOE

N90-14625# Oak Ridge National Lab., TN. Fuel Recycle Div.
RESULTS OF THE MANIPULATOR TEST TEST STAND STUDY: COMPARISON OF MANIPULATORS AND EVALUATION OF EQUIPMENT ITEMS
C. T. Kring, S. L. Schrock, J. V. Draper, S. Hayashi, H. Kawakami, S. Horii, E. Omori, and Y. Fujita (Power Reactor and Nuclear Fuel Development Corp., Tokyo, Japan) Aug. 1989 36 p
(Contract DE-AC05-84OR-21400)
(DE90-000977; ORNL/TM-11023) Avail: NTIS HC A03/MF A01

The results are discribed of a study jointly conducted by staff members of the Consolidated Fuel Reprocessing Program at the Oak Ridge National Laboratory (ORNL) in the United States and the Power Reactor and Nuclear Fuel Development Corporation (PNC) in Japan. The study was performed to evaluate the performance of servomanipulator systems developed by the respective participants as part of their in-cell maintenance systems for use in future nuclear fuel reprocessing facilities. The following servomanipulators were tested: (1) the Central Research Laboratory's model M-2; (2) the advanced servomanipulator (ASM); and (3) the Meidensha Prototype-2 (P-2). A series of experimental tasks and a test platform called the Manipulator Test Test Stand (MTTS) were jointly designed by ORNL and PNC. An evaluation of the servomanipulator system was based on the time required to complete these tasks. PNC and ORNL consider these tasks to be typical of those required for future reprocessing applications. DOE

N90-14626# Oak Ridge National Lab., TN.
FRENCH TECHNOLOGICAL PROGRESS IN THE FIELD OF ROBOTICS AND TELEOPERATION Foreign Trip Report, 9-30 Sep. 1989
B. S. Richardson 16 Oct. 1989 17 p
(Contract DE-AC05-84OR-21400)
(DE90-001590; ORNL/FTR-3406) Avail: NTIS HC A03/MF A01

A survey of robotics research activity in France was performed for the U.S. Army to obtain a broad perspective on French robotics activities and to identify topics for possible U.S./French cooperation. French government and industrial laboratories were visited in the Paris area, Grenoble, Toulon, and Toulouse. The team was very well received, and there was significant interest in setting up meaningful collaboration. The French have a significant ongoing effort in mobile robotics and, through several joint European research programs, are in the process of increasing this effort. The facilities and resources committed to mobile robotics research were impressive. There is a significant amount of cooperation among government agencies, industry, and universities. Areas for possible collaboration were agreed upon as well as a follow-up visit to the U.S. by the French and a possible exchange of engineers. The details of the collaboration will be addressed following issuance of the Army report summarizing the visit to France. DOE

N90-14627# Argonne National Lab., IL.
OPPORTUNITIES AND PROSPECTS FOR MAGLEV IN NORTH AMERICA
Tony R. Eastham and Howard T. Coffey 1989 5 p Presented at the 5th World Conference on Transport Research, Yokohama, Japan, 10-14 Jul. 1989
(Contract W-31-109-eng-38)
(DE90-002190; CONF-890790-3) Avail: NTIS HC A02/MF A01

As a result of early research in many countries, including the USA and Canada, and developments particularly in the Federal Republic of Germany and in Japan, the technologies of magnetic suspension and linear electric drives have matured to the stage at which low-speed systems are operational and high-speed systems have reached prototype test and demonstration. Maglev is now recognized as a realistic option for the 1990s and is being assessed in parallel with high-speed rail service in many corridor studies. Maglev is becoming available at a time when both road and air congestion is threatening the mobility that North America has come to expect. The fast, clean, energy-efficient characteristics should allow Maglev systems to contribute to the solution of impending transportation problems. This paper reviews the opportunities and prospects for the implementation of Maglev in North America. DOE

N90-14628# Skoda Works, Pilsen (Czechoslovakia). Nuclear Power Construction Div.
MEASURING THE THICKNESS OF AUSTENITIC WELD DEPOSITS ON CARBON STEEL WALLS USING A MAGNETIC METHOD

K. Wagner 1988 17 p
(DE89-635446; ZJE-280) Avail: NTIS (US Sales Only) HC A03/MF A01

The theoretical background is described for a magnetic method characterized by a marked compensation of the undesirable effect of delta-ferrite content in the deposit, on the accuracy of measuring deposit thickness. A description is also given of the basic types of sensors and the results are summarized for comparing measurements performed on weld deposits of VVER-type reactor pressure vessels. DOE

N90-14629# Sandia National Labs., Albuquerque, NM.
A LABORATORY TEST FOR FUEL INJECTOR DEPOSIT STUDIES
1989 31 p Presented at the SAE International Fuels and Lubricants Meeting, Baltimore, MD, 25-28 Sep. 1989
(Contract DE-AC04-76DP-00789)
(DE90-000802; SAND-89-2222C; CONF-8909219-1) Avail: NTIS HC A03/MF A01

A Port Fuel Injector Deposit (PFID) test was developed which provides repeatable results. The test can discriminate gasolines with differing fuel injector fouling tendencies in vehicles. Results confirm previous work that added mono- and diolefins increase deposit growth. The test is also able to evaluate the performance of additives. Other factors found to affect injector deposit formation include: injector soak temperature, injector soak pressure, weeping vs. non-weeping injectors, and the presence of oxygen around the injector pintle. The PFID test can be run in about one quarter the time needed to evaluate fuels in vehicle and dynamometer tests. DOE

N90-14630# Idaho National Engineering Lab., Idaho Falls.
CHARACTERIZATION OF ELECTRIC VEHICLE VELOCITY AND POWER PROFILES USING ROAD TEST DATA
A. F. Burke, R. K. Fink, R. A. Richardson, and E. J. Dowgiallo (Department of Energy, Washington, DC.) 1989 9 p Presented at the SAE Conference and Expo on Future Transportation Technology, Vancouver, Canada, 6-10 Aug. 1989
(Contract DE-AC07-76ID-01570)
(DE90-002085; EGG-M-89258; CONF-8908144-3) Avail: NTIS HC A02/MF A01

The use of electric vehicle road test data to characterize various missions in terms of velocity time-histories and battery power profiles is discussed. The data utilized were taken on the Griffon Van at Detroit Edison using the VDAS on-board data system, which stores the data in several frequency-of-occurrence matrices. Time based data are not available from VDAS. Construction of velocity-time cycles from the mechanical power-velocity matrices has proven to be difficult. A new VDAS, which stores the vehicle/battery data in time based files, was designed and built at the INEL. Bench testing of the unit is near completion and in-vehicle testing began in June 1989. The new VDAS utilizes the same sensors as in the original VDAS and yields essentially the same data variables. The frequency-of-occurrence matrices can be constructed from the time based data using a Vax 2000 workstation and commercially available software. Work is continuing on developing vehicle and battery test cycles from VDAS field data for the various missions. The availability of vehicle and battery data taken with an on-board data system permits the characterization of a variety of missions for different vehicle powertrains and batteries. Vehicle and battery designers will then have the information needed to assess the suitability of particular vehicle and battery designs for particular missions and applications. DOE

N90-14631# Oak Ridge National Lab., TN.
THE FEASIBILITY OF WELDING OF IRRADIATED MATERIALS
H. T. Lin and B. A. Chin 1989 13 p Presented at the 4th International Conference on Fusion Reactor Materials, Kyoto, Japan, 4-8 Dec. 1989
(Contract DE-AC05-84OR-21400)
(DE90-002200; CONF-891204-4) Avail: NTIS HC A03/MF A01

Helium was implanted into solution-annealed (SA) 316 stainless steel, 20 percent cold-worked (CW) 316 stainless steel and titanium-modified Primary Candidate Alloy (PCA) through tritium decay to levels ranging from 0.18 to 256 appm. Full penetration welds were then made on helium-doped materials using gas tungsten arc welding (GTAW) under fully constrained conditions. Intergranular heat-affected zone (HAZ) cracking was observed in all of the materials containing greater than 1 appm He. Electron microscopy showed that the HAZ cracking originated from the growth and coalescence of grain boundary (GB) helium bubbles. Bubble growth kinetics in the HAZ is explained by stress-enhanced diffusive cavity growth. Results suggest that the propensity for HAZ cracking can be reduced by the preexisting cold-worked structure and by finely-distributed MC precipitates that refine the distribution of helium bubbles and minimize the flow of vacancies in grain boundaries. DOE

N90-14632# Sandia National Labs., Albuquerque, NM. Solid Dynamics Dept.
HYPERVELOCITY IMPACT CALCULATIONS USING CTH: CASE STUDIES
Timothy G. Trucano and J. Michael McGlaun 1989 29 p Presented at the Hypervelocity Impact Symposium, San Antonio, TX, 12-14 Dec. 1989
(Contract DE-AC04-76DP-00789)
(DE90-002891; SAND-89-0598C; CONF-891214-9) Avail: NTIS HC A03/MF A01

In this paper, we discuss the application of CTH, a multi-dimensional Eulerian shock wave physics code, by discussing its application to hypervelocity impact problems. CTH is heavily used for this and other types of applications. We will not attempt to provide a broad discussion of examples and capabilities. Rather, we choose to focus on certain features of CTH that are of interest in gaining understanding of some of the more delicate issues of numerical impact simulations. DOE

38 QUALITY ASSURANCE AND RELIABILITY

Includes product sampling procedures and techniques; and quality control.

N90-14633 Northwestern Univ., Evanston, IL.
NONDESTRUCTIVE EVALUATION OF FLAW CLUSTERS AND THIN LAYER INTERFACES Ph.D. Thesis
George Edward Kechter 1989 131 p
Avail: Univ. Microfilms Order No. DA8913983

Two problems of non-destructive evaluation using ultrasonic waves are investigated. First, characterization of individual spherical cavities using ultrasonic fields backscattered from epoxy specimens containing clusters of cavities. Then, obtaining the reflection coefficient of an interface between two elastic layers. Specifically a thin layer bonded to a much thicker one. To characterize the cavities, elastodynamic modeling, experimental investigation, and digital signal processing are employed. A new deconvolution technique that combines linear and bandpass homomorphic deconvolutions using the complex cepstrum is presented and shown to be useful for this problem. After applying this new method to digitized ultrasonic measurements from the epoxy specimens, very satisfactory agreement between the measurements and elastodynamic models is achieved. Using feature analysis of the processed measurements and the ray-theory of wave propagation, the radius of a single spherical cavity in the cluster is determined. To obtain the reflection coefficient of the thin layer bonded to a half-space, another new method is presented. This straightforward technique recovers the desired reflection coefficient using only algebraic manipulation of the linearly deconvolved measurements. Computer synthesized waveforms are used to simulate backscattered ultrasonic measurements from the layer-half-space configuration. After digitally processing these noise-corrupted signals using the new method, very satisfactory agreement between the extracted and actual reflection coefficient is obtained. Both phase and magnitude are in agreement. Dissert. Abstr.

N90-14634# Nauchno-Issledovatelskii Inst. Atomnykh Reaktororov, Dimitrovgrad (USSR).
ASSESSMENT OF THE EFFICIENCY OF NONDESTRUCTIVE TECHNIQUES IN MATERIALS TESTING STUDIES BASED ON THE INFORMATION CRITERION
V. B. Ivanov 1988 13 p In RUSSIAN; ENGLISH summary (DE89-635444; NIIAR-10(721)) Avail: NTIS (US Sales Only) HC A03/MF A01

Problems are considered in applying information theory to the assessment of the efficiency of using nondestructive methods of investigation. Results of measuring an empirical body of information, contained in experimental data files, can serve as an additional criterion for choosing a method, hardware and software, and providing for the method. DOE

N90-14635# Westinghouse Savannah River Co., Aiken, SC.
FAILURE PROBABILITY ESTIMATE OF TYPE 304 STAINLESS STEEL PIPING
W. L. Daugherty, N. G. Awadalla, R. L. Sindelar, H. S. Mehta, and S. Ranganath (General Electric Co., San Jose, CA.) 1989 7 p Presented at the Natural Phenomena Hazards Mitigation Conference, Knoxville, TN, 3-5 Oct. 1989
(Contract DE-AC09-89SR-18035)
(DE90-000659; DP-MS-89-83; CONF-8910192-8) Avail: NTIS HC A02/MF A01

The primary source of in-service degradation of the SRS production reactor process water piping is intergranular stress corrosion cracking (IGSCC). IGSCC has occurred in a limited number of weld heat affected zones, areas known to be susceptible to IGSCC. A model has been developed to combine crack growth rates, crack size distributions, in-service examination reliability estimates and other considerations to estimate the pipe large-break frequency. This frequency estimates the probability that an IGSCC crack will initiate, escape detection by ultrasonic (UT) examination, and grow to instability prior to extending through-wall and being detected by the sensitive leak detection system. These events are combined as the product of four factors: (1) the probability that a given weld heat affected zone contains IGSCC, (2) the conditional probability, given the presence of IGSCC, that the cracking will escape detection during UT examination, (3) the conditional probability, given a crack escapes detection by UT, that it will not grow through-wall and be detected by leakage, and (4) the conditional probability, given a crack is not detected by leakage, that it grows to instability prior to the next UT exam. These four factors estimate the occurrence of several conditions that must coexist in order for a crack to lead to a large break of the process water piping. DOE

N90-14636# Los Alamos National Lab., NM.
QUALITY ASSURANCE AND QUALITY CONTROL FOR THE COMPACT PHYSICS RESEARCH FACILITY (CPRF) AND ZTH EXPERIMENT
R. W. Kewish, Jr. 1989 5 p Presented at the 13th International Symposium on Fusion Engineering, Knoxville, TN, 2-6 Oct. 1989
(Contract W-7405-eng-36)
(DE90-002352; LA-UR-89-3275; CONF-891007-56) Avail: NTIS HC A02/MF A01

In compliance with DOE Order 5700.6B, which establishes policies to assure quality achievement in DOE programs, a quality assurance and quality control program was instituted whose primary goal is to assure that reliable components are available with which to assemble the CPRF/ZTH experiment. The Code of Federal Regulations 10 CFR 50, appendix B, and the ANSI standard N45.2 were used as a primary source of guidance in establishing a plan for the QA program. Accepted codes, such as the National Electric Code (NEC), and standards adopted by organizations such as ANSI, IEEE, ASME, and NEMA were used in the design and production of components in keeping with the primary goal of the CPRF program. In setting up the CPRF/ZTH quality assurance program it was the intention to have these standards apply to all suppliers, both within and outside the Laboratory. DOE

39 STRUCTURAL MECHANICS

Includes structural element design and weight analysis; fatigue; and thermal stress.

For applications see *05 Aircraft Design, Testing and Performance* and *18 Spacecraft Design, Testing and Performance*.

N90-14637 Nottingham Univ. (England).
THE STRESS ANALYSIS OF THIN-WALLED SCREWED TUBULAR JOINTS Ph.D. Thesis
T. P. Broadbent 1988 360 p
Avail: Univ. Microfilms Order No. BRD-85416

The aim was to optimize the thread form to be used in large diameter, thin walled, tubular, screwed joints which may be used as connections in the tethers of Tension-Leg Platforms. Frozen-stress, photoelastic techniques were used to measure the distributions of thread load and peak fillet stresses around the thread spirals of models with different thread shapes and loaded with different loading modes of axial tension, preload only, preload plus tension and eccentric tension. From detailed photoelastic measurements of the distribution of stress around individual thread fillets it was found that the fillet stress at any position in the thread spiral is the sum of those due to the stresses in the model wall plus those due to the shear force carried by the thread. Due to the time and cost involved in manufacturing, analyzing a sufficient number of Araldite models to carry out a full analysis of the effect of thread parameters on fillet stresses it was decided to use axisymmetric, 8 noded, isoparametric, finite elements. Fillet stress distributions obtained using finite elements and 3-D photoelasticity were checked for agreement of results for threads of similar shapes before the range of shapes analyzed was extended using finite elements. Dissert. Abstr.

N90-14638*# Brown Univ., Providence, RI. Div. of Engineering.
GROUP IMPLICIT CONCURRENT ALGORITHMS IN NONLINEAR STRUCTURAL DYNAMICS Final Report
M. Ortiz and E. D. Sotelino Oct. 1989 104 p
(Grant NAG1-634)
(NASA-CR-185950; NAS 1.26:185950) Avail: NTIS HC A06/MF A01 CSCL 20K

During the 70's and 80's, considerable effort was devoted to developing efficient and reliable time stepping procedures for transient structural analysis. Mathematically, the equations governing this type of problems are generally stiff, i.e., they exhibit a wide spectrum in the linear range. The algorithms best suited to this type of applications are those which accurately integrate the low frequency content of the response without necessitating the resolution of the high frequency modes. This means that the algorithms must be unconditionally stable, which in turn rules out explicit integration. The most exciting possibility in the algorithms development area in recent years has been the advent of parallel computers with multiprocessing capabilities. So, this work is mainly concerned with the development of parallel algorithms in the area of structural dynamics. A primary objective is to devise unconditionally stable and accurate time stepping procedures which lend themselves to an efficient implementation in concurrent machines. Some features of the new computer architecture are summarized. A brief survey of current efforts in the area is presented. A new class of concurrent procedures, or Group Implicit algorithms is introduced and analyzed. The numerical simulation shows that GI algorithms hold considerable promise for application in coarse grain as well as medium grain parallel computers.
Author

N90-14639# Virginia Polytechnic Inst. and State Univ., Blacksburg. Dept. of Engineering Science and Mechanics.
NON-LINEAR VIBRATIONS, STABILITY, AND DYNAMICS OF STRUCTURES AND MECHANISMS Final Report, 1 Mar. 1988 - 31 May 1989
A. H. Nayfeh and D. T. Mook Aug. 1989 288 p
(Contract DAAL03-88-G-0013)
(AD-A212152; ARO-25614.1-EG-CF) Avail: NTIS HC A13/MF A02 CSCL 01/2

The topics addressed include: Chaotic Oscillations in Mechanical Systems, On Understanding Chaos in Nonlinear Oscillators Having a Single Equilibrium Position, Bifurcations in a Forced Softening Duffing Oscillator, Suppression of Chaos by Nonlinear Damping, Modal Interaction in the Response of Shells to a Subharmonic Excitation, Response of a Single-Degree-of-Freedom System to a Nonstationary Parametric Excitation Dynamic Snap-Buckling Under Stochastic Loads, A New Approach to Stochastic Flap-Lag Stability of a Rotor Blade in Hover, On the Adaptive Control of Dynamic Systems with Flexible Structures, On the Stabilization of Tethered Satellite Systems, A Mathematical Formulation and Control Expressions for Compliant Control of Constrained Robot Manipulators, Fractals and Chaos in Elastic Systems, Nonlinear Nonlinear Oscillation of a Flexible Cantilever Nonlinear Oscillations in a Rotating Shaft System, Nonlinear Effects in the Static and Dynamic Behavior of Beams and Rotor Blades, Dynamics of Beams with Tip Masses and Attached to a Moving Base, Non-Linear Oscillations of an Inextensible, Air-Inflated, Cylindrical Membrane, A Finite Element Method for Nonlinear Panel Flutter of Composite Laminates, Planar Response of Elastic Cables to a Subharmonic or Superharmonic Excitation, Nonlinear Large Rotational Structural Dynamics, and Joint Damping and Joint Nonlinearity Effects in Dynamics of Space Structures. GRA

N90-14640*# National Aeronautics and Space Administration. Lewis Research Center, Cleveland, OH.

VISCOPLASTICITY: A THERMODYNAMIC FORMULATION

A. D. Freed and J. L. Chaboche (Office National d'Etudes et de Recherches Aerospatiales, Paris, France) Nov. 1989 21 p Submitted for publication

(NASA-TM-102388; E-5129; NAS 1.15:102388) Avail: NTIS HC A03/MF A01 CSCL 20K

A thermodynamic foundation using the concept of internal state variables is given for a general theory of viscoplasticity, as it applies to initially isotropic materials. Three fundamental internal state variables are admitted. They are: a tensor valued back stress for kinematic effects, and the scalar valued drag and yield strengths for isotropic effects. All three are considered to phenomenologically evolve according to competitive processes between strain hardening, strain induced dynamic recovery, and time induced static recovery. Within this phenomenological framework, a thermodynamically admissible set of evolution equations is put forth. This theory allows each of the three fundamental internal variables to be composed as a sum of independently evolving constituents. Author

N90-14641*# National Aeronautics and Space Administration. Lewis Research Center, Cleveland, OH.

THERMAL FATIGUE DURABILITY FOR ADVANCED PROPULSION MATERIALS

Gary R. Halford Oct. 1989 13 p Presented at the Australian Aeronautical Conference, Melbourne, Australia, 9-11 Oct. 1989; sponsored in part by The Inst. of Engineers, Australia; The Royal Aeronautical Society; and The Aeronautical Research Lab.

(NASA-TM-102348; E-5057; NAS 1.15:102348) Avail: NTIS HC A03/MF A01 CSCL 20K

A review is presented of thermal and thermomechanical fatigue (TMF) crack initiation life prediction and cyclic constitutive modeling efforts sponsored recently by the NASA Lewis Research Center in support of advanced aeronautical propulsion research. A brief description is provided of the more significant material durability models that were created to describe TMF fatigue resistance of both isotropic and anisotropic superalloys, with and without oxidation resistant coatings. The two most significant crack initiation models are the cyclic damage accumulation model and the total strain version of strainrange partitioning. Unified viscoplastic cyclic constitutive models are also described. A troika of industry, university, and government research organizations contributed to the generation of these analytic models. Based upon current capabilities and established requirements, an attempt is made to project which TMF research activities most likely will impact future generation propulsion systems. Author

N90-14642*# National Aeronautics and Space Administration. Lewis Research Center, Cleveland, OH.

A NONLINEAR HIGH TEMPERATURE FRACTURE MECHANICS BASIS FOR STRAINRANGE PARTITIONING

Takayuki Kitamura (Kyoto Univ., Japan) and Gary R. Halford Oct. 1989 17 p

(NASA-TM-4133; E-4733; NAS 1.15:4133) Avail: NTIS HC A03/MF A01 CSCL 20K

A direct link was established between Strainrange Partitioning (SRP) and high temperature fracture mechanics by deriving the general SRP inelastic strain range versus cyclic life relationships from high temperature, nonlinear, fracture mechanics considerations. The derived SRP life relationships are in reasonable agreement based on the experience of the SRP behavior of many high temperature alloys. In addition, fracture mechanics has served as a basis for derivation of the Ductility-Normalized SRP life equations, as well as for examination of SRP relations that are applicable to thermal fatigue life prediction. Areas of additional links between nonlinear fracture mechanics and SRP were identified for future exploration. These include effects of multiaxiality as well as low strain, nominally elastic, long life creep fatigue interaction. Author

N90-14643 ESDU International Ltd., London (England).

FLEXURAL AND TORSIONAL-FLEXURAL BUCKLING OF THIN-WALLED OPEN SECTION STRUTS

Mar. 1989 5 p Supersedes ESDU-Struct-01.01.22

(ESDU-89007; ESDU-Struct-01.01.22; ISBN-0-85679-678-6; ISSN-0141-4097) Avail: ESDU

This Data Item 89007, an addition to the Structures Subseries, gives the cubic equation for the buckling stress of a strut of arbitrary open section under the interaction of the flexural and torsional buckling modes. When the section has an axis of symmetry, buckling will occur in either the flexural mode or in the torsional-flexural mode, the buckling stress for which is given by the solution of a quadratic equation. For sections in which the centroid and the shear center coincide (which are those with two axes of symmetry or with point symmetry such as a Z-section with equal flanges) there is no interaction and buckling will occur at the least stress of the two Euler buckling stresses and the torsional buckling stress. A fully worked example illustrates the use of the equations. ESDU

N90-14644 Council for National Academic Awards (England).

FATIGUE FRACTURE IN THE PRESENCE OF SHOT PEENING RESIDUAL STRESSES: INITIATION, PROPAGATION, AND RELAXATION PHENOMENA Ph.D. Thesis

D. W. Hammond 1988 180 p

Avail: Univ. Microfilms Order No. BRDX85805

Both experimental and theoretical work performed in order to analyze fatigue fracture in the presence of shot peening induced residual stresses is described. Four contrasting alloys were examined by fatigue testing and use was made of different test techniques to illustrate some of the phenomena associated with fatigue fracture in shot peened components. The results demonstrate that in order to characterize the process of fatigue in a component bearing residual stresses, it is necessary to consider three groups of variables. These are the applied and residual stress state, the geometry of the component and the flaws it contains and the nature of the alloy itself, including any propensity to work harden, recover or undergo phase changes due to peening or fatigue loading. Dissert. Abstr.

N90-14645# Sydney Univ. (Australia). School of Civil and Mining Engineering.

A THEORETICAL INVESTIGATION OF THE COLUMN BEHAVIOR OF COLD-FORMED SQUARE HOLLOW SECTIONS

P. W. Key and G. J. Hancock Dec. 1988 109 p

(PB89-225981; R-584) Avail: NTIS HC A06/MF A01 CSCL 20K

A large deflection elastic-plastic analysis has been developed and is used to investigate the column behavior of Australian produced cold-formed square hollow sections. The analysis can

account for plate geometric imperfections, the variation of yield stress around a section, the stress-strain characteristics of the material forming the section and the highly complex patterns of residual stress produced by the cold forming process. Stub and pin-ended column tests were performed and detailed measurements of yield stress and residual stress taken. The finite strip analysis including these distributions of yield stress and residual stress is used to investigate the behavior of the stub and pin-ended columns. In particular, the influence of the measured through thickness residual stress components on the ultimate load and behavior of the SHS columns is demonstrated. Author

N90-14646# Sydney Univ. (Australia). School of Civil and Mining Engineering.
A STUDY OF INCREMENTAL-ITERATIVE STRATEGIES FOR NONLINEAR ANALYSES
M. J. Clarke and G. J. Hancock Dec. 1988 54 p
(PB89-226005; R-587) Avail: NTIS HC A04/MF A01 CSCL 20K

A study of incremental-iterative solution techniques for geometrically nonlinear analyses is discussed. The solution methods documented are based on a modified Newton-Raphson approach, meaning that the tangent stiffness matrix is computed at the commencement of each load step but is then held constant throughout the equilibrium iterations. A consistent mathematical notation is employed in the description of the iterative and load incrementation strategies, enabling the simple inclusion of several solution options in a computer program. Criteria for detecting when the applied external load increment should reverse sign are described. A challenging example of a circular arch exhibiting snap-through and snap-back behavior is solved using several different iterative and load incrementation strategies. The performance of the solution schemes is evaluated and conclusions drawn. Author

N90-14647# Sydney Univ. (Australia). School of Civil and Mining Engineering.
A FINITE STRIP METHOD FOR THE ELASTIC-PLASTIC LARGE DISPLACEMENT ANALYSIS OF THIN-WALLED AND COLD-FORMED STEEL SECTIONS
P. W. Key and G. J. Hancock Dec. 1988 109 p
(PB89-226021; R-583) Avail: NTIS HC A06/MF A01 CSCL 20K

A large deflection elastic-plastic analysis was developed using the finite strip method to determine the nonlinear local buckling behavior of cold-formed sections in compression. The analysis accounts for plate geometric imperfections, the variation of yield stress around a section, the stress-strain characteristics of the material forming the section and the highly complex patterns of residual stress produced by the cold forming process. The nonlinear overall buckling behavior of members can also be analyzed with a modification to the displacement functions in the finite strip analysis. The analysis is verified against reliable solutions for the nonlinear local buckling behavior of plates and plate assemblies in axial compression and bending, and the nonlinear overall buckling behavior of a strut. The effect of the high levels of residual stress present in these sections is demonstrated using the finite strip analysis. GRA

N90-14648 Michigan Univ., Ann Arbor.
LOCALIZED VIBRATIONS OF NEARLY PERIODIC STRUCTURES WITH IRREGULARITIES Ph.D. Thesis
Philip Dao Cha 1989 226 p
Avail: Univ. Microfilms Order No. DA8920516

Dynamic analysis of periodic assemblies is typically made under the assumption that the components making up the periodic structure are identical to one another. However, due to the inherent structural irregularities arising from unavoidable manufacturing and material tolerances, no structure can ever be made perfectly periodic. The effects of disorder on the dynamics of nearly periodic assemblies of monocoupled, multi-mode component systems are examined. Both the modal characteristics and the transmission of vibration from a local source of excitation are considered. Slight irregularities among the components of nearly periodic structures are found to have drastic effects on the dynamics of the entire assembly: the free vibration modes become localized to a small geometric region and the vibration energy is confined near the source of excitation. Perturbation schemes are developed to predict the occurrence of localization and to evaluate the systems sensitivity to disorder. A statistical formulation is chosen that provides a comprehensive analytic description of localization effects. Since component mode analysis is used to model the nearly periodic structure, the theoretical results obtained are generic, and thus valid for many engineering periodic structures. The degree of localization is shown to depend on the disorder strength, the modal coupling, the location of the constraint between subsystems, and the excitation frequency. In general, the localization effects increase rapidly with frequency. In fact, for arbitrarily small disorders severe localization is unavoidable if the mode number is large enough. This has important consequences for periodic engineering structures such as mistuned bladed-disk assemblies. Dissert. Abstr.

N90-14649 Missouri Univ., Rolla.
SHEAR STRAIN LOCALIZATION PHENOMENON IN VISCOPLASTIC MATERIALS Ph.D. Thesis
Chang-Ho Kim 1989 89 p
Avail: Univ. Microfilms Order No. DA8920397

The phenomenon is investigated of shear strain localization in elastic-viscoplastic materials which exhibit strain hardening, strain rate hardening, and thermal softening. The simple shearing deformations is studied of a block made of such a material and the material defect, flaw or inhomogeneity by adding a temperature perturbation at the center of the block is modeled. The resulting initial boundary value problem is solved numerically. The effect of modeling the material of the block as a dipolar material in which the strain gradient is also taken as an independent variable is also presented. For a better understanding of the finite element mesh to be used, an adaptive mesh refinement technique was developed based on distributing uniformly the scaled residuals in the balance of linear momentum and the balance of internal energy. Results obtained by using three different integration schemes, namely the Crank-Nicolson method, Adams-Moulton method and the Gear method are also presented. It is found that for simple materials, as the shear stress within the region of localization collapses, an unloading elastic shear wave emanates outwards from the edges of the shear band. For dipolar material the localization of the deformation is considerably delayed as compared to that for nonpolar materials, the shear stress does not collapse suddenly but decreases gradually, there is no unloading wave traveling outwards from the edges of the band, and the region of localized deformation is wider as compared to that for nonpolar materials. Dissert. Abstr.

N90-14650 Tufts Univ., Medford, MA.
MECHANICS OF INTERACTION OF A CRACK WITH MICROCRACKS Ph.D. Thesis
Eric Louis Montagut 1989 88 p
Avail: Univ. Microfilms Order No. DA8920025

In brittle materials such as ceramics or brittle polymers, propagation of a macrocrack is often accompanied by extensive microcracking, resulting in the appearance of a damage zone around the crack tip. This zone interacts with the main crack affecting the mechanics of its propagation. The micromechanics of crack-damage interactions and the resulting macroscopic consequences (changes in effective stress intensity factors, etc...) constitute the topic of this work. It is established, in particular, that contrary to many existing models, there is no correlation between reduction of the effective elastic moduli in the damage zone and the effect of the damage zone on the stress intensity factors. Various other aspects of the micromechanics of the crack-damage system are examined. The analysis is based on a recently developed approach to many cracks problems. Dissert. Abstr.

N90-14651 Ohio State Univ., Columbus.
CRACK PROBLEMS FOR ELASTIC-PLASTIC MATERIALS UNDER ANTIPLANE SHEAR LOADINGS Ph.D. Thesis
I-Min Hsu 1989 178 p
Avail: Univ. Microfilms Order No. DA8913652

Analytic solutions to Mode III crack problems for elastic-plastic materials are investigated. In particular, three problems: (1) a semi-infinite crack in an infinite strip; (2) an edge-crack in a semi-infinite body; and (3) an edge-crack in a semi-infinite strip, are formulated and solved. Linear field equations in the strain plane are obtained by applying the hodograph transformation to the nonlinear field equations in the physical plane. In the elastic region, while a closed-form solution is available for problem 1, solutions to problems 2 and 3 are obtained by solving the Weiner-Hopf problems. The elastic-domain solution and the plastic-domain solution include two sets of undeterminded constants. These constants are determined by the continuity conditions on the elastic-plastic boundary. The matching procedure for the edge-crack problems requires numerical integrations and solving truncated systems of linear equations, which are accomplished by using computer codes. Studying the crack tip fields, including the plastic zone, strains ahead of crack tip, and the crack opening displacements, shows that problems 1 and 2 are limiting cases of problem 3. Dissert. Abstr.

N90-14652*# Ohio Univ., Athens. Dept. of Civil Engineering.
PARALLEL EIGENANALYSIS OF FINITE ELEMENT MODELS IN A COMPLETELY CONNECTED ARCHITECTURE Final Report
F. A. Akl and M. R. Morel Nov. 1989 112 p
(Grant NAG3-762)
(NASA-CR-185166; NAS 1.26:185166) Avail: NTIS HC A06/MF A01 CSCL 20K

A parallel algorithm is presented for the solution of the generalized eigenproblem in linear elastic finite element analysis, (K)(phi) = (M)(phi)(omega), where (K) and (M) are of order N, and (omega) is order of q. The concurrent solution of the eigenproblem is based on the multifrontal/modified subspace method and is achieved in a completely connected parallel architecture in which each processor is allowed to communicate with all other processors. The algorithm was successfully implemented on a tightly coupled multiple-instruction multiple-data parallel processing machine, Cray X-MP. A finite element model is divided into m domains each of which is assumed to process n elements. Each domain is then assigned to a processor or to a logical processor (task) if the number of domains exceeds the number of physical processors. The macrotasking library routines are used in mapping each domain to a user task. Computational speed-up and efficiency are used to determine the effectiveness of the algorithm. The effect of the number of domains, the number of degrees-of-freedom located along the global fronts and the dimension of the subspace on the performance of the algorithm are investigated. A parallel finite element dynamic analysis program, p-feda, is documented and the performance of its subroutines in parallel environment is analyzed. Author

N90-14653# Lawrence Livermore National Lab., CA.
VERIFICATION OF THE NIKE3D STRUCTURAL ANALYSIS CODE BY COMPARISON AGAINST THE ANALYTIC SOLUTION FOR A SPHERICAL CAVITY UNDER A FAR-FIELD UNIAXIAL STRESS
Edward J. Kansa Jan. 1989 116 p
(Contract W-7405-eng-48)
(DE90-000929; UCID-21811) Avail: NTIS HC A06/MF A01

The original scope of this task was to simulate the stresses and displacements of a hard rock tunnel experimental design using a suitable three-dimensional finite element code. NIKE3D was selected as a suitable code for performing these primarily approximate linearly elastic 3-D analyses, but it required modifications to include initial stress, shear traction boundary condition and excavation options. During the summer of 1988, such capabilities were installed in a special version of NIKE3D. Subsequently, we verified both the LLNL's commonly used version of NIKE3D and our private modified version against the analytic solution for a spherical cavity in an elastic material deforming under a far-field uniaxial stress. We find the results produced by the unmodified and modified versions of NIKE3D to be in good agreement with the analytic solutions, except near the cavity, where the errors in the stress field are large. As can be expected from a code based on a displacement finite element formulation, the displacements are much more accurate than the stresses calculated from the 8-noded brick elements. To reduce these errors to acceptable levels, the grid must be refined further near the cavity wall. The level of grid refinement required to simulate accurately tunneling problems that do not have spatial symmetry in three dimensions using the current NIKE3D code is likely to exceed the memory capacity of the largest CRAY 1 computers at LLNL. DOE

N90-14654# Sandia National Labs., Albuquerque, NM. Experimental Mechanics Dept.
COMPARISON OF SHOCK SEVERITY MEASURES
Thomas J. Baca 1989 16 p Presented at the 60th Shock and Vibration Symposium, Virginia Beach, VA, 14-16 Nov. 1989
(Contract DE-AC04-76DP-00789)
(DE90-000790; SAND-89-1678C; CONF-891152-3) Avail: NTIS HC A03/MF A01

In an effort to clarify the issues associated with quantifying shock severity, the merits of two measures of shock severity are compared. The first measure is the widely used absolute acceleration shock response spectrum (SAA). The second measure of shock severity is relatively new and is known as the shock intensity spectrum (SIS). Overall information content of SAA and SIS spectra are compared and discussed in the context of two shock excitations having known amplitude, duration, and frequency content. The first is a burst of band-limited white noise and the second is a classical haversine pulse. After describing both the SAA and SIS shock measures, numerous examples are described which emphasize the strengths and limitations of each shock characterization method. This discussion reveals how the use of different shock measures may alter an engineer's conclusions about relative shock severity between two shock environments. DOE

N90-14655*# National Aeronautics and Space Administration. Lewis Research Center, Cleveland, OH.
A NEW UNIFORMLY VALID ASYMPTOTIC INTEGRATION ALGORITHM FOR ELASTO-PLASTIC-CREEP AND UNIFIED VISCOPLASTIC THEORIES INCLUDING CONTINUUM DAMAGE
A. Chulya and K. P. Walker (Engineering Science Software, Inc., Smithfield, RI.) Dec. 1989 72 p
(NASA Order C-99066-G)
(NASA-TM-102344; E-5052; ICOMP-89-22; NAS 1.15:102344)
Avail: NTIS HC A04/MF A01 CSCL 20K

A new scheme to integrate a system of stiff differential equations for both the elasto-plastic creep and the unified viscoplastic theories is presented. The method has high stability, allows large time increments, and is implicit and iterative. It is suitable for use with continuum damage theories. The scheme was incorporated into MARC, a commercial finite element code through a user subroutine called HYPELA. Results from numerical problems under complex loading histories are presented for both small and large scale analysis. To demonstrate the scheme's accuracy and efficiency, comparisons to a self-adaptive forward Euler method are made. Author

N90-14656*# National Aeronautics and Space Administration. Lewis Research Center, Cleveland, OH.
CONCURRENT PROCESSING ADAPTATION OF AEROPLASTIC ANALYSIS OF PROPFANS
David C. Janetzke and Durbha V. Murthy (Toledo Univ., OH.) Jan. 1990 24 p Prepared for presentation at the 31st Structures, Structural Dynamics, and Materials Conference, Long Beach, CA, 2-4 Apr. 1990; cosponsored by AIAA, ASME, ASCE, AHS, and ASC
(Grant NAG3-742)

(NASA-TM-102455; E-5105; NAS 1.15:102455) Avail: NTIS HC A03/MF A01 CSCL 20K

Discussed here is a study involving the adaptation of an advanced aeroelastic analysis program to run concurrently on a shared memory multiple processor computer. The program uses a three-dimensional compressible unsteady aerodynamic model and blade normal modes to calculate aeroelastic stability and response of propfan blades. The identification of the computational parallelism within the sequential code and the scheduling of the concurrent subtasks to minimize processor idle time are discussed. Processor idle time in the calculation of the unsteady aerodynamic coefficients was reduced by the simple strategy of appropriately ordering the computations. Speedup and efficiency results are presented for the calculation of the matched flutter point of an experimental propfan model. The results show that efficiencies above 70 percent can be obtained using the present implementation with 7 processors. The parallel computational strategy described here is also applicable to other aeroelastic analysis procedures based on panel methods. Author

N90-14657# Oak Ridge National Lab., TN.
FRACTURE MECHANICS OF POROUS MATERIALS Foreign Trip Report, 16 May - 11 Aug. 1989
L. J. Gray 15 Sep. 1989 5 p
(Contract DE-AC05-84OR-21400)
(DE90-000023; ORNL/FTR-3377) Avail: NTIS HC A01/MF A01

The primary subject of this trip was the development of a boundary element/finite element analysis system for computational fracture mechanics. The procedures for merging the ORNL/Cornell University boundary element fracture code with the finite element program SESAM were agreed upon, and are currently being implemented. The adopted algorithm relies on the superelement capabilities of the SESAM code. Discussions were held with scientists at the Bergen Scientific Centre on the modeling of fractured rock. A project to develop realistic computer models of naturally occurring fracture patterns is being carried out by a geologist and a physicist; it is expected that these models can be employed in future environmental modeling work. DOE

N90-14658# Sandia National Labs., Albuquerque, NM. Thermomechanical and Physical Div.
IMPLICATIONS AND ORIGINS OF SHOCK STRUCTURE IN SOLIDS
J. E. Dunn 1989 13 p Presented at the American Physical Society Topical Conference on Shock Compression of Condensed Matter, Albuquerque, NM, 14-17 Aug. 1989
(Contract DE-AC04-76DP-00789)
(DE90-000846; SAND-89-1011C; CONF-890812-52) Avail: NTIS HC A03/MF A01

One dimensional plane shock waves have been widely used to study the mechanical response of solids to high velocity impact. For many materials, under a certain range of impact pressures, there exists a two-wave structure of which the first wave, the so-called elastic precursor, travels at a velocity near to that of sound waves, while the second wave, the so-called plastic shock wave, travels at a slower speed which increases with impact pressure. While the full two-wave structure is thus not steady (i.e., does not propagate without change of form), each component wave may be treated as steady after sufficient propagation distance. While a variety of subtleties can be involved in treating the elastic precursor, just those aspects of a material's constitutive nature that evince themselves in steady, structured, plastic shock waves, are discussed here. DOE

N90-14659# Oak Ridge National Lab., TN.
ENGINEERING APPROACHES TO THE APPLICATION OF FRACTURE TOUGHNESS DATA IN THE NUCLEAR INDUSTRY
J. G. Merkle 1989 11 p Presented at the Materials Properties Council Workshop on Scatter of Fracture Toughness Data in the Transition Temperature Regime, Boulder, CO, 16 Jul. 1987
(Contract DE-AC05-84OR-21400)
(DE90-001596; CONF-8707219-1) Avail: NTIS HC A03/MF A01

The procedures for measuring the plane strain fracture toughness, K(sub Ic), of metals were originally developed for relatively high yield strength materials, the toughnesses of which were not affected by strain rate. The application of these procedures to lower yield strength and higher toughness structural and pressure vessel steels have since revealed a perplexing combination of problems involving the effects of geometry, stable crack growth and strain rate on the measured values of toughness. Only the geometric problems were encountered in the development of the procedures for measuring K(sub Ic). For fracture in the linear elastic range of the load-displacement curve, these problems were overcome by specifying specimen dimensions sufficiently large with respect to the plastic zone size at fracture. However, in the case of structural and pressure vessel steels, it is not always possible to test specimens large enough for fracture to occur prior to general yielding. Therefore, in these cases, the effects of large-scale yielding prior to fracture cannot be avoided, but since they presently have no analytical explanation they are being treated empirically. The problems of geometry and strain rate effects on toughness discussed herein are complex and difficult to solve. However, taking advantage of the improvements that were recently made in the hardware and software available for performing three-dimensional elastic-plastic and viscoplastic stress analysis, it should be possible to significantly improve the analysis of small-specimen, elastic-plastic fracture toughness data. DOE

N90-14660# Argonne National Lab., IL. Materials and Components Technology Div.
APPROXIMATE METHODS FOR DYNAMIC PLASTIC DEFORMATION OF STRUCTURES
Carl K. Youngdahl 1989 12 p Presented at the 7th Symposium on Energy Engineering Sciences, Argonne, IL, 19-21 Jun. 1989
(Contract W-31-109-eng-38)
(DE90-002214; CONF-8906112-3) Avail: NTIS HC A03/MF A01

To illustrate the development of approximation methods and correlation parameters for dynamic plasticity, the problem of a long tube loaded by a time dependent region is considered for a rigid, perfectly plastic material. The final plastic deformation is found to depend on an effective applied force, an effective applied moment, an effective length of the loaded region, and the deformation which would be attained if the loading were applied impulsively. A procedure is developed for approximating the results by closed form solutions for loadings applied to fixed regions. The implications of the solutions with respect to other approximation methods and extension of the method to include strain hardening effects are discussed. DOE

N90-14661# Oak Ridge National Lab., TN. Metals and Ceramics Div.
A COMPUTER-CONTROLLED AUTOMATED TEST SYSTEM FOR FATIGUE AND FRACTURE TESTING
R. K. Nanstad, D. J. Alexander, R. L. Swain, J. T. Hutton, and D. L. Thomas 1989 31 p Presented at the ASTM Symposium on the Applications of Automation Technology to Fatique, Kansas City, MO, 22-23 May 1989
(Contract DE-AC05-84OR-21400)
(DE90-002931; CONF-8905112-3) Avail: NTIS HC A03/MF A01

A computer-controlled system consisting of a servohydraulic test machine, an in-house designed test controller, and a desktop computer was developed for performing automated fracture toughness and fatigue crack growth testing both in the laboratory and in hot cells for remote testing of irradiated specimens. Both unloading compliance and dc-potential drop can be used to monitor crack growth. The test controller includes a dc-current supply programmer, a function generator for driving the servohydraulic test machine to required test outputs, five measurement channels (each consisting of low-pass filter, track/hold amplifier, and 16-bit analog-to-digital converter), and digital logic for various control and data multiplexing functions. The test controller connects to

the computer via a 16-bit wide photo-isolated bidirectional bus. The computer, a Hewlett-Packard series 200/300, inputs specimen and test parameters from the operator, configures the test controller, stores test data from the test controller in memory, does preliminary analysis during the test, and records sensor calibrations, specimen and test parameters, and test data on flexible diskette for later recall and analysis with measured initial and final crack length information. During the test, the operator can change test parameters as necessary. DOE

N90-14662# Argonne National Lab., IL.
CRITICAL TIME STEP ESTIMATION FOR THREE-DIMENSIONAL EXPLICIT IMPACT ANALYSIS
R. F. Kulak 1989 9 p Presented at the Structures Under Shock and Impact Conference, Cambridge, MA, 11-13 Jul. 1989
(Contract W-31-109-eng-38)
(DE90-002187; CONF-8907161-1) Avail: NTIS HC A02/MF A01

A method to obtain a bound on the critical time step of impact problems that employ explicit integration and penalty type contact elements is presented. The method uses a Gerschgorin bound obtained from a partially assembled stiffness matrix for the nodes that belong to elements involved in the contact region. A numerical example is presented to illustrate the method's effectiveness. DOE

42 GEOSCIENCES (GENERAL)

N90-14663# California Univ., Berkeley. Lawrence Berkeley Lab.
EARTH SCIENCES DIVISION ANNUAL REPORT 1988
Aug. 1989 194 p
(Contract DE-AC03-76SF-00098)
(DE90-002617; LBL-26362) Avail: NTIS HC A09/MF A01

Scientists and engineers of the Earth Sciences Division, following the mission of a multipurpose National Laboratory, conduct research on a wide variety of topics relevant to the nation's energy development programs. The activities for 1988 are summarized. The Earth Sciences Division has developed unique expertise in several research areas. Much of the Division's research deals with the physical and chemical properties and processes in the earth's crust, from the partially saturated, low-temperature near-surface environment to the high-temperature environments characteristic of regions where magmatic-hydrothermal processes are active. Strengths in laboratory and field instrumentation, numerical modeling, and in-situ measurement allow study of the transport of mass and heat through geologic media -- studies that now include the appropriate chemical reactions and the hydraulic-mechanical complexities of fractured rock systems. Related and parallel laboratory and field investigations address the effects of temperature, pressure, stresses, pore fluids, and fractures on the elastic and electrical properties of rock masses. These studies are concerned with rock behavior in the brittle and ductile crustal regimes, and they drive the development of improved geomechanical and geophysical tools and techniques for mapping and characterizing heterogeneity in the subsurface. DOE

N90-14406# Naval Research Advisory Committee, Washington, DC.
THE IMPORTANCE OF ENVIRONMENTAL DATA
Gerald Cann and Robert P. Porter *In* AGARD, Operational Decision Aids for Exploiting or Mitigating Electromagnetic Propagation Effects Sep. 1989 6 p (For primary document see N90-14405 06-32)
Copyright Avail: NTIS HC A20/MF A03

43 EARTH RESOURCES AND REMOTE SENSING

Includes remote sensing of earth resources by aircraft and spacecraft; photogrammetry; and aerial photography.

For instrumentation see *35 Instrumentation and Photography.*

N90-14664*# Wisconsin Univ., Madison. Cooperative Inst. for Meteorological Satellite Studies.
AN INVESTIGATION OF SATELLITE SOUNDING PRODUCTS FOR THE REMOTE SENSING OF THE SURFACE ENERGY BALANCE AND SOIL MOISTURE Final Technical Report, 1 Oct. 1986 - 30 Aug. 1989
George R. Diak Nov. 1989 73 p
(Grant NAG5-854)
(NASA-CR-186073; NAS 1.26:186073) Avail: NTIS HC A04/MF A01 CSCL 08M

Improved techniques for the remote sensing of the land surface energy balance (SEB) and soil moisture would greatly improve prediction of climate and weather as well as be of benefit to agriculture, hydrology and many associated fields. Most of the satellite remote sensing methods which were researched to date rely upon satellite-measured infrared surface temperatures or their time changes as a remote sensing signal. Optimistically, only four or five levels of information (wet to dry) in surface heating/evaporation are discernable by surface temperature methods and a good understanding of atmospheric conditions is necessary to bring them to this accuracy level. Skin temperature methods were researched as well as begun work on several new methods for the remote sensing of the SEB, some elements of which are applicable to current and retrospective data sources and some which will rely on instrumentation from the Earth Observing System (EOS) program in the 1990s. Author

N90-14665# Naval Ocean Research and Development Activity, Bay Saint Louis, MS.
NORDA'S PATTERN ANALYSIS LABORATORY: CURRENT CONTRIBUTIONS TO NAVAL MAPPING, CHARTING, AND GEODESY Final Report
Maura C. Lohrenz Apr. 1989 32 p
(AD-A212731; NORDA-221) Avail: NTIS HC A03/MF A01 CSCL 08/2

The Mapping, Charting and Geodesy (MC and G) Division at the Naval Ocean Research and Development Activity (NORDA) is the primary activity within the U.S. Navy for conducting research and development (R and D) in direct support of naval MC and G requirements. Projects include R and D in the general areas of charting, remote sensing, bathymetry, geophysics, photogrammetry, reconnaissance, and ocean surveillance in support of the U.S. Navy, the U.S. Marine Corps, and the Defense Mapping Agency. NORDA's Pattern Analysis Branch, MC and G Division, is concerned with all aspects of digital MC and G data, including hardware, software, and data bases. The primary computing facility of this branch is the Pattern Analysis Laboratory (PAL). The configuration of the PAL, its current and anticipated capabilities, and its role in naval MC and G projects, are described. GRA

N90-14666# Naval Ocean Research and Development Activity, Bay Saint Louis, MS.
A ROUGH TRANSFORM TECHNIQUE FOR EXTRACTING LEAD FEATURES FROM SEA ICE IMAGERY
Florence M. Fetterer and Ronald J. Holyer 11 Jul. 1989 5 p
(AD-A212758; NORDA-PR-89-034-321) Avail: NTIS HC A01/MF A01 CSCL 08/12

Infrared imagery from polar-orbiting satellites provides a synoptic and long-term view of lead patterns in Artic pack ice. The large quantity of satellite data in image form suggests the use of automated methods for compiling lead statistics from imagery. A Hough transform technique for the semi-automated extraction of lead orientation and spacing is described and first results are presented. GRA

N90-14667 Oxford Univ. (England).
REMOTE SENSING OF ATMOSPHERIC WATER VAPOUR BY PRESSURE MODULATION RADIOMETRY Ph.D. Thesis
G. R. Davis 1987 238 p
Avail: Univ. Microfilms Order No. BRD-85924

The Stratospheric and Mesospheric Sounder (SAMS) used the technique of pressure modulation radiometry to measure the temperature and constituent distributions in the middle atmosphere. Two channels in the SAMS were devoted to the detection of water vapor, but the analysis of these data have produced unexpectedly high mixing ratios in the region of the stratopause. An attempt is described to resolve the discrepancy between theory and experiment by a laboratory investigation of the pressure modulation of water vapor. A pressure modulation technique is described and a mathematical formulation is given. The spectroscopy of the H2O rotation band is considered and it is shown that there are large uncertainties in most aspects of the problem. In particular, the shapes of the collision broadened line wings under both self and foreign broadened conditions are poorly determined. The pressure modulation of water vapor is investigated and it is shown by direct measurement of the pressure cycle that a linear model used by previous workers was incorrect. A transmission experiment is described and the results are compared with theory. It was necessary to introduce a continuum absorption to resolve the discrepancy in the wideband channel, and the strength of the excess is shown to be consistent with measurements in other spectral regions. In the pressure modulation channel, the agreement was excellent and no modifications were required. Application of these results to the SAMS data shows that the anomalous retrievals remained unexplained. A number of possible explanations are suggested and a far infrared intercomparison experiment is proposed. Dissert. Abstr.

N90-14668# Indiana State Univ., Terre Haute.
IMAGE PROCESSING OF LANDSAT MSS DATA FOR BURIED VALLEY DETECTION IN NORTHERN INDIANA Ph.D. Thesis
John Leo Hammen, III 1988 167 p
Avail: Univ. Microfilms Order No. DA8921049

The extensive sand and gravel aquifers often found in glacially buried valleys are important sources of potable groundwater. Recent studies indicate that LANDSAT Multispectral Scanner (MSS) data may be useful in delineating readily apparent surficial phenomena which may be associated with underlying glaciofluvial deposits. To date, however, little use has been made of digital image enhancements which may reveal more subtly spectral patterns serving as surrogate indicators of buried valley aquifers. This study investigates the use of computer-enhanced LANDSAT MSS data in the detection of a glacially buried valley in northern Indiana. A multi-temporal MSS data set was used to analyze the spatial distribution of selected surficial features hypothesized to indicate the areal extent of the buried valley. Enhancement techniques ranged from simple image manipulation to complex data transformations previously shown to highlight the occurrence of the selected features. Primary results indicated that soil type, as portrayed on early spring imagery, may be useful for buried valley detection in this locale and that many of the more complex data transformations yielded little or no increase in information extraction than that yielded by the simpler enhancement techniques. Dissert. Abstr.

N90-14669*# Bionetics Corp., Cocoa Beach, FL.
SUMMARY OF 1987 AND 1988 MANATEE AERIAL SURVEYS AT KENNEDY SPACE CENTER
Jane A. Provancha and Mark J. Provancha Feb. 1989 21 p
(Contract NAS10-10285)
(NASA-TM-102783; NAS 1.15:102783) Avail: NTIS HC A03/MF A01 CSCL 13B

Aerial surveys of manatees conducted since 1977 at Kennedy Space Center (KSC) have provided a very useful and cost effective monitoring tool in the assessment of abundance and distribution of manatees in the northern Banana River. Data collected in the mid 1980's as part of the KSC Environmental Monitoring Program indicated that the numbers of manatees utilizing the northern Banana River had increased dramatically from earlier years and that the animals appeared to have changed their distribution patterns within the area as well (Provancha and Provancha 1988). United States Fish and Wildlife Service (USFWS) and Florida Department of Natural Resources (FLDNR) conducted bimonthly aerial surveys in 1986 for the entire Florida east coast. Their data clearly show that the Banana River has the highest concentration of manatees during the non-winter months when compared to all other segments of the east coast surveys (B. Wiegle/FLDNR, unpublished data). They further show that, in spring, an average of 71 percent of the manatees in Brevard county were located in the Banana River. During that period 85 percent of the animals were north of the NASA Causeway (State Road (SR) 402) in the KSC security zone. These data indicate the importance of the KSC waters to the Florida east coast manatee population. We reinitiated KSC surveys in 1987 to document distributions and numbers of manatees during the spring influx. Aerial censuses were continued throughout the year in 1988 and this report provides a summary of our findings for the two years. Author

N90-14670*# Colorado Univ., Boulder. Center for the Study of Earth from Space.
EVALUATION OF THE AIRBORNE VISIBLE-INFRARED IMAGING SPECTROMETER FOR MAPPING SUBTLE LITHOLOGICAL VARIATION Final Report
Fred A. Kruse 1990 59 p Original contains color illustrations
(Grant NAGw-1143)
(NASA-CR-186213; NAS 1.26:186213) Avail: NTIS HC A04/MF A01 CSCL 08B

The Airborne Visible/Infrared Imaging Spectrometer (AVIRIS), flown aboard the NASA ER-2 aircraft in 1987 and 1989, used four linear arrays and four individual spectrometers to collect data simultaneously from the 224 bands in a scanned 614 pixel-wide swath perpendicular to the aircraft direction. The research had two goals. One was to evaluate the AVIRIS data. The other was to look at the subtle lithological variation at the two test sites to develop a better understanding of the regional geology and surficial processes. The geometric characteristics of the data, adequacy of the spatial resolution, and adequacy of the spectral sampling interval are evaluated. Geologic differences at the test sites were mapped. They included lithological variation caused by primary sedimentary layering, facies variation, and weathering; and subtle mineralogical differences caused by hydrothermal alterations of igneous and sedimentary rocks. The investigation used laboratory, field, and aircraft spectral measurements; known properties of geological materials; digital image processing and spectrum processing techniques; and field geologic data to evaluate the selected characteristics of the AVIRIS data. J.P.S.

N90-14671# Oak Ridge National Lab., TN.
GLOBAL NATURAL RESOURCE MONITORING AND ASSESSMENT Foreign Trip Report, 23 Sep. - 7 Oct. 1989
Virginia H. Dale 16 Oct. 1989 12 p
(Contract DE-AC05-84OR-21400)
(DE90-001294; ORNL/FTR-3411) Avail: NTIS HC A03/MF A01

A presentation was given on the need for monitoring forests on a worldwide basis and a strategy to do so. Ways to promote institutional collaboration for global monitoring was examined by a working group. Observations are summarized with focus on issues relating to Oak Ridge National Laboratory's (ORNL's) Center for Global Environmental Studies. The possibility of a joint ORNL-Swiss research program to develop a spatial model of forests was discussed. DOE

N90-14409# Space and Naval Warfare System, Washington, DC. Environmental Systems Program Office.
THE TACTICAL ENVIRONMENTAL SUPPORT SYSTEM (TESS(3))
Jack J. Jensen *In* AGARD, Operational Decision Aids for Exploiting or Mitigating Electromagnetic Propagation Effects Sep. 1989 3 p (For primary document see N90-14405 06-32)
Copyright Avail: NTIS HC A20/MF A03

N90-14416# Naval Ocean Systems Center, San Diego, CA. Ocean and Atmospheric Sciences Div.
AIRBORNE FLIR DETECTION OF SURFACE TARGETS
Herbert G. Hughes *In* AGARD, Operational Decision Aids for Exploiting or Mitigating Electromagnetic Propagation Effects Sep. 1989 12 p Sponsored by Office of Navy Technology (For primary document see N90-14405 06-32)
Copyright Avail: NTIS HC A20/MF A03

N90-14436# German Military Geophysical Office, Traben-Trarbach (Germany, F.R.).
THE THERMAL BEHAVIOR OF NATURAL BACKGROUNDS AND ITS PREDICTION BY MEANS OF NUMERICAL MODELS
Fritz G. Wollenweber *In* AGARD, Operational Decision Aids for Exploiting or Mitigating Electromagnetic Propagation Effects Sep. 1989 12 p (For primary document see N90-14405 06-32)
Copyright Avail: NTIS HC A20/MF A03

N90-14437# Defence Research Establishment Valcartier (Quebec).
REMOTE SENSING OF THE AEROSOL SCATTERING COEFFICIENT WITH A MULTI-FIELD-OF VIEW LIDAR
Luc R. Bissonnette and Daniel L. Hutt *In* AGARD, Operational Decision Aids for Exploiting or Mitigating Electromagnetic Propagation Effects Sep. 1989 13 p (For primary document see N90-14405 06-32)
Copyright Avail: NTIS HC A20/MF A03

44 ENERGY PRODUCTION AND CONVERSION

Includes specific energy conversion systems, e.g., fuel cells; global sources of energy; geophysical conversion; and windpower.

For related information see also *07 Aircraft Propulsion and Power, 20 Spacecraft Propulsion and Power,* and *28 Propellants and Fuels.*

N90-14672*# Jet Propulsion Lab., California Inst. of Tech., Pasadena.
RESULTS OF THE 1989 NASA/JPL BALLOON FLIGHT SOLAR CELL CALIBRATION PROGRAM
B. E. Anspaugh and R. S. Weiss 15 Nov. 1989 40 p
(NASA-CR-186114; JPL-Publ-89-47; NAS 1.26:186114) Avail: NTIS HC A03/MF A01 CSCL 10A

The 1989 solar cell calibration balloon flight was successfully completed on August 9, 1989, meeting all objectives of the program. Forty-two modules were carried to an altitude of 118,000 ft (36.0 km). The calibrated cells can now be used as reference standards in simulator testing of cells and arrays. Author

N90-14673# Energy Conversion Devices, Inc., Troy, MI.
RESEARCH ON HIGH-EFFICIENCY, MULTIPLE-GAP, MULTIJUNCTION, AMORPHOUS-SILICON-BASED ALLOY THIN-FILM SOLAR CELLS Semiannual Subcontract Report, 1 Mar. - 31 Aug. 1988
S. Guha Jun. 1989 63 p
(Contracts DE-AC02-83CH-10093; ZB-7-06003-4)
(DE89-009444; SERI/STR-211-3526) Avail: NTIS HC A04/MF A01

Results are presented of research on advancing the understanding of amorphous silicon based alloys and their use in small area multijunction solar cells. The principal objectives of the program are to develop a broad scientific base for the chemical, structural, optical, and electronic properties of amorphous silicon based alloys; to determine the optimum properties of these alloy materials as they relate to high efficiency cells; to determine the optimum device configuration for multijunction cells; and to demonstrate proof-of-concept, multijunction, a Si alloy-based solar cells with 18 percent efficiency under standard AM1.5 global insolation conditions and with an area of at least 1 sq cm. A major focus of the work was the optimization of a novel, multiple graded structure that enhances cell efficiency through band gap profiling. The principles of the operation of devices incorporating such a structure, computer simulations of those, and experimental results for both single- and multijunction cells prepared by using the novel structure are discussed in detail. DOE

N90-14674# Sandia National Labs., Albuquerque, NM. Wind Energy Research Div.
CONTROL OF THE VARIABLE SPEED GENERATOR ON THE SANDIA 34-METRE VERTICAL AXIS WIND TURBINE
Mark E. Ralph 1989 11 p Presented at Windpower '89, San Francisco, CA, 24-27 Sep. 1989
(Contract DE-AC04-76DP-00789)
(DE90-000803; SAND-89-0986C; CONF-890981-2) Avail: NTIS HC A03/MF A01

The DOE/Sandia 34-meter VAWT Test Bed is a 500kW variable-speed wind turbine. The turbine is operated between 25 and 38 rpm and has been characterized from a structural and aerodynamic standpoint. A preliminary variable speed control algorithm has been implemented on the Test Bed. This paper describes the initial variable-speed control algorithm developed for the Test Bed and the performance of that algorithm to date. Initial performance comparisons between variable-speed and fixed-speed operation are made as well as some thoughts on the expansion of the operating envelope of the Test Bed. DOE

N90-14675# Morgantown Technology Center, WV.
PROCEEDINGS OF THE FIRST ANNUAL FUEL CELLS CONTRACTORS REVIEW MEETING
W. J. Huber, ed. May 1989 386 p Meeting held in Morgantown, WV, 2-4 May 1989
(DE89-011699; DOE/METC-89/6105; CONF-890572) Avail: NTIS HC A17/MF A03

The overall objective of this program is to develop the essential technology for private sector commercialization of the various fuel cell electrical generation systems. The purpose of this meeting was to bring together the research and development (R and D) participants in the DOE/Fossil Energy-sponsored Fuel Cells Program to present key results of their research. Major emphasis was on phosphoric acid, molten carbonate, and solid oxide technology efforts. Research results of the coal gasification and gas stream cleanup R and D activities pertinent to the Fuel Cells Program were also highlighted. Thirty-six papers and poster presentations were given in six formal sessions and one informal poster session: Solid Oxide Fuel Cells R and D (10 papers); Solid Oxide Fuel Cells Systems Studies (1 paper); Molten Carbonate Fuel Cells R and D (9 papers); Molten Carbonate Fuel Cells System Studies (3 papers); METC's On-Site Gasification/Cleanup Program (1 paper); Phosphoric Acid Fuel Cells R and D (8 papers); and Poster Presentations (4 presentations by METC on R and D coal gasification and gas stream cleanup pertinent to the Fuel Cells Program). Individual projects are processed separately for the data bases. DOE

N90-14676# Los Alamos National Lab., NM.
USE OF SUPERCONDUCTING PLATES AND SHELLS TO DEFLECT MAGNETIC NOISE FIELDS: APPLICATION TO MEG
William Calvin Overton, Jr., David B. vanHulsteyn, and Edward R. Flynn 1989 3 p Presented at the 11th Annual International Conference of the IEEE Engineering in Medicine and Biology Society, Seattle, WA, 9-12 Nov. 1989
(Contract W-7405-eng-36)
(DE89-012592; LA-UR-89-1520; CONF-891148-1) Avail: NTIS HC A02/MF A01

Insertion of a superconducting plate or shell in a magnetic field causes a surface current distribution which opposes the applied field. Resultant fields near plate edges are higher while those near centers are much lower than applied fields. Use is made of these principles in magnetoencephalography by placing suitably oriented gradiometers at points where noise fields are smallest. Signals from nearby brain wave sources are enhanced because the net signal is a combination of that from the sources

and that from its image. The principles of noise deflection and source imaging are applied to new concepts of gradiometry. DOE

N90-14677# Los Alamos National Lab., NM. Advanced Engineering Technology.
HEAT AND MASS TRANSFER DESIGN ISSUES IN PEM FUEL CELL HARDWARE
Trung Nguyen, James C. Hedstrom, and Nicholas E. Vanderborgh 1989 12 p Presented at the American Institute of Chemical Engineers Annual Meeting, San Francisco, CA, 5-10 Nov. 1989
(Contract W-7405-eng-36)
(DE89-016779; LA-UR-89-2947; CONF-891113-1) Avail: NTIS HC A03/MF A01

Dynamic moisture transport within polymeric electrolytes influences PEM fuel cell performance. Lowering electrolyte moisture content leads to decreased ionic transport rates, and other long term effects including polymer degradation. Results illustrate anode dehydration, the effect of water transport concurrent with the proton flux, is significant in single cells at current densities exceeding 500 ma/sq cm, and at higher temperatures. Evaporation and condensation to and from the gas phase contribute significantly to the cell thermal flows. Several strategies for successful high current density operation of these devices are presented. DOE

N90-14678*# National Aeronautics and Space Administration. Lewis Research Center, Cleveland, OH.
TECHNOLOGY DEVELOPMENT PROGRAM FOR AN ADVANCED MICROSHEET GLASS CONCENTRATOR
Scott W. Richter (Sverdrup Technology, Inc., Cleveland, OH.) and Dovie E. Lacy 1990 8 p Prepared for presentation at the 1990 International Solar Energy Conference, Miami, FL, 1-4 Apr. 1990; sponsored in part by ASME
(NASA-TM-102406; E-5158; NAS 1.15:102406) Avail: NTIS HC A02/MF A01 CSCL 10A

Solar Dynamic Space Power Systems are candidate electrical power generating systems for future NASA missions. One of the key components in a solar dynamic power system is the concentrator which collects the sun's energy and focuses it into a receiver. In 1985, the NASA Lewis Research Center initiated the Advanced Solar Dynamic Concentrator Program with funding from NASA's Office of Aeronautics and Space Technology (OAST). The objectives of the Advanced Concentrator Program is to develop the technology that will lead to lightweight, highly reflective, accurate, scaleable, and long lived (7 to 10 years) space solar dynamic concentrators. The Advanced Concentrator Program encompasses new and innovative concepts, fabrication techniques, materials selection, and simulated space environmental testing. The Advanced Microsheet Glass Concentrator Program, a reflector concept, that is currently being investigated both in-house and under contract is discussed. Author

N90-14679# Glasstech Solar, Inc., Wheatridge, CO.
PREPARATION AND PROPERTIES OF HIGH DEPOSITION a-Si:H FILMS AND SOLAR CELLS USING DISILANE Final Subcontract Report, 1 May 1988 - 30 Apr. 1989
H. Chatham and P. K. Bhat Sep. 1989 27 p Prepared for Midwest Research Inst., Golden, CO
(Contract DE-AC02-83CH-10093)
(DE89-009467; SERI/STR-211-3562) Avail: NTIS HC A03/MF A01

The focus of research during the second phase of SERI Contract No. ZB-7-06002-1 was the fabrication of high efficiency amorphous silicon p-i-n solar cells using intrinsic layers deposited at high deposition rate (minus 2 nm/s) from disilane discharges. In order to achieve this goal, we utilized higher discharge excitation frequencies (10 to 110 MHz) to improve the intrinsic layer properties. In this report, we discuss the influence of the driving frequency at fixed RF power density on silane and disilane discharges, the properties of materials deposited from these discharges, and the performance of p-i-n devices fabricated using intrinsic layers deposited at a rate of minus 2 nm/s from disilane 110 MHz discharges. The use of higher excitation frequency in disilane discharges increases the deposition rate and results in films with improved properties compared with those deposited at similar deposition rate by increasing the RF power. As a result of these improvements, we have fabricated a p-i-n device at a deposition rate of 2nm/s with an AM1.5 efficiency of 9.7 percent over an area of 1 cm(sup 2). This result exceeds the goals of this contract. DOE

N90-14680# Sandia National Labs., Albuquerque, NM. Exploratory Batteries Div.
POLARIZATION OF Li/SOCl2 CELLS
Frank M. Delnick, Terry R. Guilinger, and Joel O. Stevenson Aug. 1989 10 p
(Contract DE-AC04-76DP-00789)
(DE90-000883; SAND-89-0875) Avail: NTIS HC A02/MF A01

The relationship is described between constant resistive load, constant current, and constant voltage discharges of electrochemical cells using the concept of the polarization curve. This concept is demonstrated under constraints for a prismatic Li/SOCl2 laboratory cell. It is shown that each of these discharges yields the same information about the electrochemical couple which drives the cell. DOE

N90-14681# Midwest Research Inst., Golden, CO. Solar Energy Research Inst.
THIN FILM CADMIUM TELLURIDE, ZINC TELLURIDE, AND MERCURY ZINC TELLURIDE SOLAR CELLS Annual Report, 1 Jul. 1988 - 30 Jun. 1989
T. L. Chu (University of Central Florida, Orlando.) Oct. 1989 31 p
(Contract DE-AC02-83CH-10093)
(DE89-009499; SERI/STR-211-3586) Avail: NTIS HC A03/MF A01

The first year was covered of a program to investigate: (1) the deposition of CdTe films by various techniques; (2) the deposition of transparent conducting semiconductor (TCS) films by various techniques; (3) the preparation and evaluation of thin film CdTe solar cells; and (4) the deposition and characterization of ZnTe films and heterojunctions. CdTe films were deposited on glass and SnO2/glass substrates by metal organic chemical vapor deposition (MOCVD) by reacting dimethylcadmium (DMCd) with diisopropyl tellurium (DITe) in H2. The optical bandgap was 1.50 eV. The conductivity type of the films could be controlled by controlling the DMCd/DITe molar ratio in the reaction mixture. This is a promising technique for the preparation of thin film CdTe homojunction solar cells. CdS films were deposited from aqueous solutions by reacting thiourea and cadmium acetate in an ammonical solution. The films show good optical transmission in the above-bandgap region but are porous and impure. The photovoltaic characteristics of cells employing solution-grown CdS films are therefore inferior to those employing vacuum evaporated CdS films. Films of ZnO, ZnS, and ZnTe were deposited, via MOCVD, on glass and SnO2/glass substrates, and ZnO/ZnTe heterojunctions were produced. Open circuit voltages of 0.6 to 0.7 V were measured for ZnS/ZnTe heterojunctions. DOE

N90-14682# Midwest Research Inst., Golden, CO. Wind Research Branch.
AN INITIAL LOOK AT THE DYNAMICS OF THE MICROSCALE FLOW FIELD WITHIN A LARGE WIND FARM IN RESPONSE TO VARIATIONS IN THE NATURAL INFLOW
N. D. Kelley Oct. 1989 5 p Presented at the Windpower '89 Conference and Exposition, San Francisco, CA, 24-27 Sep. 1989
(Contract DE-AC02-83CH-10093)
(DE89-009501; SERI/TP-257-3591; CONF-890981-3) Avail: NTIS HC A01/MF A01

Some early results from a study to examine the influence of the natural inflow structure on the internal microscale turbulence environment of a large wind farm are discussed. Two fully equipped, high resolution boundary layer measurement systems were employed to document the alteration of the turbulent structure as the flow entered and left a wind park consisting of 41 rows of turbines. These systems collected data continuously for a period

of several weeks during the peak wind season in San Gorgonio Pass. In addition, statistical summaries of the inflow and outflow characteristics from a hub-height elevation were recorded prior to, during and after the detailed measurement period. Results of these hub-height summaries are discussed and interpreted. DOE

N90-14683# Pacific Northwest Lab., Richland, WA.
LOW-TEMPERATURE CONVERSION OF HIGH-MOISTURE BIOMASS: CONTINUOUS REACTOR SYSTEM RESULTS
D. C. Elliott, L. J. Sealock, Jr., R. S. Butner, E. G. Baker, and G. G. Neuenschwander Oct. 1989 56 p
(Contract DE-AC06-76RL-01830)
(DE90-000984; PNL-7126) Avail: NTIS HC A04/MF A01

Pacific Northwest Laboratory (PNL) is developing a low temperature, catalytic process for converting high moisture biomass feedstocks and other wet organic substances to useful gaseous fuels. This system, in which thermocatalytic conversion takes place in an aqueous environment, was designed to overcome the problems usually encountered with high water content feedstocks. The process uses a reduced nickel catalyst at temperatures as low as 350 C and pressures ranging from 2000 to 4000 psig; conditions favoring the formation of gas consisting mostly of methane. The results of numerous batch tests showed that the system could convert feedstocks not readily converted by conventional methods. Fifteen tests were conducted in a continuous reactor system to further evaluate the effectiveness of the process for high moisture biomass gasification and to obtain conversion rate data needed for process scaleup. During the tests, the complex gasification reactions were evaluated by several analytical methods. The results of these tests show that the heating value of the gas ranged from 400 to 500 Btu/scf, and if the carbon dioxide is removed, the product gas is pipeline quality. Conversion of the feedstocks was high. Engineering analysis indicates that, based on these results, a tubular reactor can be designed that should convert greater than 99 percent of the carbon fed as high moisture biomass to a gaseous product in a reaction time of less than 11 min. DOE

N90-14684# Argonne National Lab., IL. Chemical Technology Div.
ELECTRODE DEVELOPMENT IN MONOLITHIC SOLID OXIDE FUEL CELLS
Dennis W. Dees, Uthamalingam Balachandran, Stephen E. Dorris, John J. Heiberger, Charles C. McPheeters, and John J. Picciolo 1989 7 p Presented at the American Institute of Chemical Engineers Annual Meeting, San Francisco, CA, 5-10 Nov. 1989
(Contract W-31-109-eng-38)
(DE90-001910; CONF-891113-5) Avail: NTIS HC A02/MF A01

The interfacial resistance of thin three-layer ceramic solid oxide fuel cell composites was studied at 100 C using ac impedance techniques. The anode interfacial resistance was found to increase dramatically when the H2O content decreased below 0.03 atm in a H2/H2O fuel system. A similar effect was also observed for the CO/CO2 fuel system. Increases in the anode interfacial resistance were also observed in the presence of H2S. Significant decreases in the anode interfacial resistance were accomplished by tailoring the electrode's microstructure. DOE

N90-14685# Argonne National Lab., IL. Chemical Technology Div.
CALORIMETRIC MEASUREMENTS ON ELECTROCHEMICAL CELLS WITH Pd-D CATHODES
L. Redey, K. M. Myles, Dennis W. Dees, M. Krumpelt, and D. R. Vissers 1989 27 p Presented at the Workshop on Cold Fusion Phenomena, Santa Fe, NM, 23-25 May 1989
(Contract W-31-109-eng-38)
(DE90-002198; CONF-8905126-7) Avail: NTIS HC A03/MF A01

Two series of experiments were performed to determine the conditions of cell operation that produce sufficient heat to be useful for the production of energy. In the first series, the results from a differential temperature analysis of identical light- and heavy-water electrochemical cells were too ambiguous and, thus not suitable for evaluating excess heat effects. In the second series, two Pd-D/LiOD-saturated D(sub 2)O/Pt cells were operated at current densities between 15 and 500 mA/cm(sup 2) in a constant-heat-loss-rate twin calorimeter for 460 hours. Water loss measurements during the experiments indicated that the recombination reaction (D(sub 2) + O(sub 2) (yields) D(sub 2)O) did not occur. The D/Pd ratio was determined gravimetrically during the experiments. No excess heat was found within the sensitivity (0.13 W, 0.082 W/cm(sup 3) of Pd, 0.013 W/cm(sup 2) of Pd) and precision ((plus minus)0.3 W) of the calorimeter. DOE

N90-14686# Oak Ridge National Lab., TN. Energy and Economic Analysis Section.
HOW FAR CAN THE WORLD GET ON ENERGY EFFICIENCY ALONE
Martin T. Katzman 1989 14 p Presented at the 11th Annual North American Conference of the International Association for Energy Economists, Los Angeles, CA, 16-18 Oct. 1989
(Contract DE-AC05-84OR-21400)
(DE90-001349; CONF-8910162-4) Avail: NTIS HC A03/MF A01

A recent analysis suggests that by pursuing a path of energy efficiency, the industrial world can maintain and the developing world can achieve a high standard of living with little increase in primary energy consumption over the next 50 years. Moreover, this scenario can be achieved with a reduction of fossil fuel consumption. Three basic issues discussed at a workshop recently held at ORNL are presented to address this thesis. First, is this thesis plausible; to what extent can the scenario be achieved with currently or nearly available technology. Second, why can't a better job be done in reaching the potential; what are the barriers to the deeper penetration of energy-efficient technologies. Third, what policy and technological strategies are necessary to fulfill this scenario. DOE

N90-14687# Midwest Research Inst., Golden, CO. Solar Energy Research Inst.
RESEARCH ON HIGH-EFFICIENCY, SINGLE-JUNCTION, MONOLITHIC, THIN-FILM AMORPHOUS SILICON SOLAR CELLS Final Report, 1 Feb. 1986 - 31 Jan. 1987
D. E. Carlson, R. R. Ayra, M. S. Bennett, J. A. Brewer, A. W. Catalano, R. V. DAiello, C. R. Dickson, C. M. Fortmann, J. L. Newton, and J. G. ODowd et al Sep. 1989 94 p Prepared in cooperation with Solarex Corp., Newtown, PA
(Contract DE-AC02-83CH-10093)
(DE89-000846; SERI/STR-211-3410) Avail: NTIS HC A06/MF A01 CSCL 20A

Results are presented of the third phase of research in high efficiency, single junction, monolithic, thin-film, a-Si solar cells. Six glow discharge deposition systems, including an in-line multichamber system, were used to grow both doped and undoped a-Si films. In single load lock system, a-Si was deposited over 1000 sq cm substrates with less then a 1 pct variation in thickness and low oxygen impurity levels. The system produced 1000 sq cm submodules with active-area efficiencies of 8.7 pct. A model was developed for light scattering in textured tin oxide that predicts scattered transmission through the air/glass/tin oxide/air configuration to within a few percent. Textured tin oxide films were grown by chemical vapor deposition using tin tetrachloride. Solar cell efficiencies of about 11 pct were obtained in small area p-i-n cells with reflective back contacts of Ti/Ag that exhibit external quantum efficiencies as high as 58.7 pct at 700 nm; other cells with ITO/Ag back contacts have had quantum efficiencies as high as 64 pct at 700 nm. High performance cells were fabricated by employing dopant and carbon concentration gradients near the p/i interface. Total-area efficiencies around 8 pct were obtained for submodules in which the patterning was done by laser scribing. DOE

N90-14688# Midwest Research Inst., Golden, CO.
COMPUTER SIMULATION OF WIND/DIESEL SYSTEM OPERATION
Sep. 1989 100 p Prepared in cooperation with AeroVironment,

Inc., Monrovia, CA; Integral Technologies, Inc., Westmont, IL
(Contract DE-AC02-83CH-10093)
(DE89-009445; SERI/STR-257-3479) Avail: NTIS HC A06/MF A01

A computer code, SOLSTOR W/D was examined, that determines (for a site's wind energy resources, load requirements, and economic constraints) the components and sizes for a wind/diesel system that result in the lowest cost of energy. Wind diesel systems are defined as electricity generation stations in the 50-kW to 1-MW range that are not connected to another electricity network, use wind energy as the first source of supply to meet demand, and contain sufficient energy storage and/or backup diesel electric generators to compensate for lapses in wind energy. The computer code also determines, for the same input load, the requirements and economics that are the best number and size for an isolated diesel(s) system so that comparisons for wind/diesel systems and diesel-only systems can be made. SOLSTOR W/D provides a systematic method to show whether wind/diesel systems can be an attractive means of saving fossil fuel without significantly affecting electricity quality or production cost. DOE

N90-14689# Midwest Research Inst., Golden, CO.
HIGH-EFFICIENCY LARGE-AREA CdTe MODULES Annual Report, 1 Jul. 1988 - 30 Jun. 1989
S. P. Albright and B. Ackerman (Photon Energy, Inc., El Paso, TX.) Oct. 1989 32 p
(Contract DE-AC02-83CH-10093)
(DE89-009498; SERI/STR-211-3585) Avail: NTIS HC A03/MF A01

A small solar cell with an efficiency of 12.3 percent was examined. The high efficiency of this device was largely due to improving the window layer. Analyzing the diode characteristics of this cell indicates that the largest potential for fill-factor improvement lies in reducing the diode quality factor. Through outdoor life testing of encapsulated modules and accelerated life testing of laboratory cells, the CdS/CdTe structure has demonstrated the long term stability necessary for photovoltaic products. Also described is a preformed metal backcap, which is fitted with hermetic feed-through tubes and used for encapsulization. Using the results of these studies, PEI produced sample modules with efficiencies very close to the original objectives, including a 1 sq ft module with an output of 6.1 W and an active area of 754 sq cm. For this module, the active area efficiency was 8.1 percent and the aperture efficiency was 7.3 percent. DOE

N90-14690# Argonne National Lab., IL. Chemical Technology Div.
INTERFACIAL EFFECTS IN MONOLITHIC SOLID OXIDE FUEL CELLS
Dennis W. Dees, Uthamalingam Balachandran, Stephen E. Dorris, John J. Heiberger, Charles C. McPheeters, and John J. Picciolo 1989 6 p Presented at the Electrochemical Society Fall Meeting, Hollywood, FL, 15-20 Oct. 1989
(Contract W-31-109-eng-38; ARPA Order 4850)
(DE90-001914; CONF-8910107-2) Avail: NTIS HC A02/MF A01

The interfacial resistance of thin three-layer ceramic solid oxide fuel cell composites was studied at 1000 degrees using ac impedance techniques. The anode interfacial resistance was found to increase dramatically when the H sub 2 O content decreased below 0.03 atm in a H sub 2/H sub 2 O fuel system. Increases in the anode interfacial resistance were also observed in the presence of H sub 2 S. Significant decreases in the anode interfacial resistance were accomplished by tailoring the electrode's microstructure. DOE

N90-14691# Pacific Northwest Lab., Richland, WA. Materials Sciences Dept.
SOLID OXIDE FUEL CELLS ELECTRODES BASED ON In(SUB 2)O(SUB 3)-PrO(SUB 1.83)-ZrO(SUB 2)
J. Lambert Bates, William J. Weber, and Curtis W. Griffin Oct. 1989 17 p Presented at the Electrochemical Society Fall Meeting, Hollywood, FL, 15-20 Oct. 1989
(Contract DE-AC06-76RL-01830)
(DE90-002666; PNL-SA-17036; CONF-8910107-3) Avail: NTIS HC A03/MF A01

Oxides based on In2O3-PrO1.83-ZrO2 and having high electrical conductivity were developed as cathode materials for solid oxide fuel cells. A ternary phase diagram developed at 1823 K relates the electrical, thermal and electrochemical properties to compositions and structures of the material. The bcc In2O3 solid solution containing ZrO2 and PrO2 exhibits the highest electrical conductivity. Two phase fcc-bcc structures provide high electrical conductivity with mixed ion-electron conduction, thermal expansion characteristics and fabricability compatible with other SOFC materials. The oxides are thermally stable in air to 1473 K, but are easily reduced at 1273 K. Electrochemical testing of an fcc-bcc composition with an externally applied current showed some densification of interface and exsolution of In2O3 at the cathode-electrolyte interface. DOE

N90-14692# Pacific Northwest Lab., Richland, WA.
DETAILED ANALYSIS OF THE WAKE AND FREE-FLOW CHARACTERISTICS AT THE GOODNOE HILLS MOD-2 SITE
D. L. Elliott and J. C. Barnard Sep. 1989 8 p Presented at Windpower '89, San Francisco, CA, 24-27 Sep. 1989
(Contract DE-AC06-76RL-01830)
(DE90-002725; PNL-SA-17250; CONF-890981-4) Avail: NTIS HC A02/MF A01

Wind data collected on meteorological towers at the Goodnoe Hills MOD-2 wind turbine site were analyzed to characterize the free wind turbine wakes over the site. Free flow characteristics examined were the variability of wind speed and turbulence intensity across the site as a function of wind direction. Scattered areas of trees upwind of the site caused pronounced variations in the wind flow over the site. A substantial increase in the turbulence, as well as a considerable decrease in the mean wind speed, was observed when a tower was downwind of the trees. Wind turbine wake characteristics analyzed included the average velocity deficits, wake turbulence, and the vertical profile of the wake. Wake behavior downwind of the turbines was analyzed at distances from 2 to 10 rotor diameters. The relationship between velocity deficit and downwind distance was surprisingly linear. Largest deficits were at low wind speeds and low turbulence intensities. Wake turbulence was greatest along the flanks of the wake, and the vertical variation of deficits was greater below hub height than above. DOE

N90-14693# California Univ., Berkeley. Lawrence Berkeley Lab. Applied Science Div.
TECHNOLOGY BASE RESEARCH PROJECT FOR ELECTROCHEMICAL ENERGY STORAGE Annual Report, 1988
Kim Kinoshita, ed. May 1989 28 p
(Contract DE-AC03-76SF-00098)
(DE90-002604; LBL-27037) Avail: NTIS HC A04/MF A01

This report summarizes the progress made by the Technology Base Research (TBR) Project for Electrochemical Energy Storage during calendar year 1988. The primary objective of the TBR Project, which is sponsored by the Department of Energy (DOE) and managed by Lawrence Berkeley Laboratory (LBL), is to identify electrochemical technologies that can satisfy stringent performance and economic requirements for electric vehicles and stationary energy storage applications. The ultimate goal is to transfer the most-promising electrochemical technologies to the private sector or to another DOE project (e.g., SNL's ETD Project) for further development and scale-up. DOE

N90-14694# Midwest Research Inst., Golden, CO. Solar Energy Research Inst.
HYDROGEN RADICAL ENHANCED GROWTH OF SOLAR CELLS Annual Report, 1 Jun. 1987 - 31 Mar. 1989
J. M. Borrego and S. K. Ghandhi (Rensselaer Polytechnic Inst., Troy, NY.) Oct. 1989 31 p
(Contract DE-AC02-83CH-10093)

(DE89-009497; SERI/STR-211-3584) Avail: NTIS HC A03/MF A01

This Phase 1 research involves basic studies of the plasma process and the design and construction of an epitaxial reactor for use with radical species. Experiments were begun on the use of H radicals and He radicals for substrate cleaning prior to epitaxy. Work with the reactor was initiated with a series of experiments in the use of radicals for substrate cleaning prior to epitaxial growth. The H radical was found to be relatively critical, since excessive cleaning resulted in the formation of indium droplets. This was caused by the reaction of InP with H radical to form phosphine gas. Using He radicals eliminated this problem. Moreover, their longer lifetime gives them an additional advantage over H radicals, as far as delivery to the growth environment is concerned. It was noted that the growth rate of InP, at low temperatures, is erratic from run to run. Prior to conventional growth (without radicals), He radical cleaning results in a consistent growth rate at low temperatures. Work with materials grown in a He radical and H radical environment also began. Initial results indicate an increased growth rate at low temperatures, but there is some loss in material quality. Work is in progress to quantify these results. An extensive materials characterization effort is also described. DOE

N90-14695# Midwest Research Inst., Golden, CO. Solar Energy Research Inst.

PHOTOVOLTAIC MEASUREMENTS AND PERFORMANCE BRANCH Annual Report, FY 1988

F. A. Abou-Elfotouh, ed. and P. Dippo, ed. Jan. 1989 153 p
(Contract DE-AC02-83CH-10093)
(DE89-009500; SERI/PR-213-3590) Avail: NTIS HC A08/MF A01

The Photovoltaic (PV) Measurements and Performance Branch of the Solar Energy Research Institute (SERI) provides extensive PV materials, device, and component characterization, measurement, fabrication, and modeling research and support for the international PV research community in the context of the U.S. Department of Energy's PV Research Program goals. This report summarizes the Branch's progress from 1 October 1987 through 1 October 1988. The five technical sections present a succinct overview of the capabilities and accomplishments of the various research groups in the branch, namely, Surface and Interface Analysis, Materials Characterization, Device Modeling and Fabrication, Cell Performance and Electro-Optical Characterization, and Advanced Module Testing and Performance. The report highlights the main research project completed in FY 1988 including measurements in more than 80 branch-originated journal and conference publications, in collaboration with, or in support of, about 130 university, industrial, government, and in-house research groups. DOE

N90-14696# Sunpower, Inc., Athens, OH.

SYSTEM DESIGN AND PERFORMANCE PREDICTION OF A FREE-PISTON STIRLING ENGINE/MAGNETIC COUPLING/COMPRESSOR ASSEMBLY IN A GAS RESIDENTIAL HEAT PUMP

G. Chen and W. T. Beale 1989 18 p Presented at the Winter Annual Meeting of the American Society of Mechanical Engineers, San Francisco, CA, 10-15 Dec. 1989
(Contract DE-AC05-84OR-21400)
(DE89-016070; CONF-891208-14) Avail: NTIS HC A03/MF A01

Based on the previous evaluation of a magnetic coupling and the described system-design targets, a gas fired free piston Stirling engine/magnetic coupling/compressor (FPSE/MC/C) assembly as a power module for a residential heat pump application was designed and analyzed. A porous combustor/FPSE/magnetic coupling/variable gas control spring/reciprocating compressor assembly was the design selected. Based on the system characteristics, design efforts are described on the following issues: (1) design of a combustor allowing low pressure of natural gas supply; (2) the means to achieve engine power-load matching; (3) the method to maintain the assembly as a resonant system tuning over a wide range of operating conditions; (4) the design of an engine/coupling structure to minimize the magnet mass without sacrificing its mechanical properties; and (5) compressor load capacity modulation. The system analysis and the system performance, which is analytically predicted and described, indicate all the system design goals can be met leading to a strong recommendation for further development. DOE

N90-14697# Oak Ridge National Lab., TN. Energy Div.

HEAT TRANSFER OF BURIED PIPE FOR HEAT PUMP APPLICATION

Viung C. Mei Jul. 1989 8 p Presented at the Winter Annual Meeting of the American Society of Mechanical Engineers, San Francisco, CA, 10-15 Dec. 1989
(Contract DE-AC05-84OR-21400)
(DE90-000580; CONF-891208-19) Avail: NTIS HC A02/MF A01

Ground coil heat pump systems are well known for their potential of energy conservation. The majority of the ground coil designs were based on the application of the line source theory. A modified line source method was later derived to calculate the ground temperature distribution by dividing the ground around the coil into blocks. However, the line source approach has some major drawbacks, which often leads to the over-design of the ground coil. It was anticipated that in order for the ground coil heat pump systems to be economically competitive with other residential heating and cooling systems, ground coil over-design had to be kept at a minimum. A new ground coil model was derived, which was based on energy balance rather than the line source theory. It was aimed to accurately predict the operation of ground coils. It is, therefore, interesting to compare different ground coil models by using them to simulate the same field test data. The results indicated that the new model predicted the experimental data better than the other two models. Herein, the above mentioned three ground coil models were selected for study. The results indicated that the model based on energy balance predicted the test data best. DOE

N90-14698# Pacific Northwest Lab., Richland, WA.

TURBULENT WIND AT THE EQUATORIAL SEGMENT OF AN OPERATING DARRIEUS WIND TURBINE BLADE

J. R. Connell (Colorado State Univ., Fort Collins.) and V. R. Morris Sep. 1989 20 p Presented at the 9th Wind Energy Symposium, New Orleans, LA, 14-18 Jan. 1989
(Contract DE-AC06-76RL-01830)
(DE90-002672; PNL-SA-17459; CONF-8901170-1) Avail: NTIS HC A03/MF A01

Six turbulent wind time series, measured at equally spaced equator-height locations on a circle 3 m outside a 34-m Darrieus rotor, are analyzed to approximate the wind fluctuations experienced by the rotor. The flatwise lower root-bending stress of one blade was concurrently recorded. The wind data are analyzed in three ways: wind components that are radial and tangential to the rotation of a blade were rotationally sampled; induction and wake effects of the rotor were estimated from the six Eulerian time series; and turbulence spectra of both the measured wind and the modeled wind from the PNL theory of rotationally sampled turbulence. The wind and the rotor response are related by computing the spectral response function of the flatwise lower root-bending stress. Two bands of resonant response that surround the first and second flatwise modal frequencies shift with the rotor rotation rate. DOE

N90-14699# Department of Energy, Washington, DC.

NEW HEATING AND COOLING TECHNOLOGY: REGENERATIVE HEAT PUMP ACCORDING TO THE VUILLEUMIER PRINCIPLE

Franz X. Eder 1989 19 p Transl. into ENGLISH from Neuartigen Heiz- und Kuhltechnik: Regenerative Waermepumpe nach dem Vuilleumier-Prinzip, Nunich, p 52-68 2-58 Transl. by SCITRAN, Inc., Redwood City, CA.
(DE90-002701; DOE-tr-89-13) Avail: NTIS HC A03/MF A01

The regenerative heat pump which can be heated from outside which has been developed by the firm PETRY, Neumarkt/Opf.

West Germany and was supported by the Bavarian Economic Ministry, is based on a circular process invented by VUILLEUMIER and patented in 1918. During the 60's this principle was used in the construction of thermally propelled cold machines of low power. It was used for temperatures down to -50 C cooling, for example, infrared detectors and similar devices. Its practical use as a heat pump or cold aggregate for higher heat performances was analyzed for the first time in 1981 by the author at the firm ASK-Bayreuth. But it was only in 1984, during collaboration with the firm PETRY, that an operational and high performance design was established. DOE

45 ENVIRONMENT POLLUTION

Includes atmospheric, noise, thermal, and water pollution.

N90-14700*# Jet Propulsion Lab., California Inst. of Tech., Pasadena.
ENVIRONMENTAL PROJECTS. VOLUME 8: MODIFICATIONS OF WASTEWATER EVAPORATION PONDS
15 Oct. 1989 93 p
(Contract NAS7-918)
(NASA-CR-186099; JPL-Publ-87-4-Vol-8; NAS 1.26:186099)
Avail: NTIS HC A05/MF A01 CSCL 13B

The Goldstone Deep Space Communications Complex (GDSCC), located in the Mojave Desert about 45 miles north of Barstow, California, and about 160 miles northeast of Pasadena, is part of NASA's Deep Space Network, one of the world's largest and most sensitive scientific telecommunications and radio navigation networks. The Goldstone Complex is managed, technically directed, and operated for NASA by the Jet Propulsion Laboratory (JPL) of the California Institute of Technology in Pasadena, California. Activities at the GDSCC are carried out in support of seven parabolic dish antennas. These activities may give rise to environmental hazards: use of hazardous chemicals, asbestos, and underground storage tanks as well as the generation of hazardous wastes and the disposal of wastewater. Federal, state, and local laws governing the management of hazardous substances, asbestos, underground storage tanks and wastewater disposal have become so complex there is a need to devise specific programs to comply with the many regulations that implement these laws. In support of the national goal of the preservation of the environment and the protection of human health and safety, NASA, JPL, and the GDSCC have adopted a position that their operating installations shall maintain a high level of compliance with these laws. One of the environmental problems at the GDSCC involved four active, operational, wastewater evaporation ponds designed to receive and evaporate sewage effluent from upstream septic tank systems. One pair of active wastewater evaporation ponds is located at Echo Site, while another operational pair is at Mars Site. Author

N90-14701# United States Man and the Biosphere Program, Washington, DC.
MANAGING MARINE PROTECTED AREAS: AN ACTION PLAN
Nancy Foster, ed. and Michele H. Lemay, ed. Mar. 1989 77 p
Presented at the International Marine Protected Area Management Seminar, FL - CA, 1-2 Jun. 1986
(PB89-158778; PUB-9673) Avail: NTIS HC A05/MF A01 CSCL 13B

The International Marine Protected Area Management Seminar was 1 to 12 June 1986 and was hosted by the U.S. National Marine Sanctuaries Program and the U.S. Man and the Biosphere Program with the support of several international organizations. The Seminar provided a forum for discussing the problems facing marine protected areas and solutions for their effective management in the future. This Action Plan was prepared as a cooperative effort by the participants of the Seminar in an attempt to consolidate current views on marine protected area management. The Action Plan outlines the elements of a fully operational marine protected area program at the national, regional, or local scale. These elements include: planning for sustainable and multiple use; economics; marine interpretation and education; research and monitoring; traditions, customs, and culture; submerged cultural resources; developing an international network. Author

N90-14702# Colorado State Univ., Fort Collins. Dept. of Agricultural and Chemical Engineering.
AN EVALUATION OF TREND DETECTION TECHNIQUES FOR USE IN WATER QUALITY MONITORING PROGRAMS
Jim C. Loftis, Robert C. Ward, Ronald D. Phillips, and Charles H. Taylor Mar. 1989 150 p Sponsored by US Environmental Protection Agency, Corvallis, OR
(PB89-100058; EPA/600/3-89/037) Avail: NTIS HC A07/MF A01 CSCL 13B

Information goals for a long term water quality monitoring program to measure the impacts due to acid precipitation were developed using the Acid Precipitation Act of 1980 (PL 96-294, Title VII) as a basis. These broad information goals were refined to obtain statistical hypotheses for which statistical tests could be employed as part of a data analysis plan. Seven statistical tests were identified as capable of providing the desired information regarding trends in individual systems. The tests were evaluated under various conditions (i.e., distribution shape, seasonality and serial correlation) in order to determine how well they might perform as part of a data analysis plan. A Monte Carlo simulation approach was used to evaluate the tests. For annual sampling, the Kendall-tau (also known as the Mann-Kendall) test is recommended. For seasonal sampling, the Seasonal Kendall or analysis of covariance (ANOCOV) on rank tests are recommended. Author

N90-14703# Nevada Univ. System, Reno. Energy and Environmental Engineering Center.
PROFILE MEASUREMENTS OF SULFUR DIOXIDE, NITROGEN OXIDES, AND NITRIC ACID DEPOSITION VELOCITIES IN CALIFORNIA'S SOUTH COAST AIR BASIN
Alan W. Gertler, Grover Prowell, Norman F. Robinson, David Rogers, Fred Rogers, and John G. Watson Mar. 1989 135 p
(Contract ARB-A4-145-32)
(PB90-104001; DRI-8067.1F1) Avail: NTIS HC A07/MF A01 CSCL 13B

The Desert Research Institute performed a three-week dry deposition measurement field program in the South Coast Air Basin of California to quantify the deposition velocities and their associated uncertainties for sulfur dioxide, sulfate aerosol, nitrogen oxides, and nitric acid. The measurements took place in May and June, 1986 on a flat, grass-covered surface near Carson, CA. Deposition velocities were estimated by the profile method, based on gas concentration gradient measurements and associated wind and temperature data acquired on a 5 meter tower, using a sampling frequency of 1 Hz. GRA

N90-14704# Northeastern Forest Experiment Station, Broomall, PA. Publications Group.
PROCEEDINGS OF THE US/FRG (FED. REPUBLIC OF GERMANY) RESEARCH SYMPOSIUM: EFFECTS OF ATMOSPHERIC POLLUTANTS ON THE SPRUCE-FIR FORESTS OF THE EASTERN UNITED STATES AND THE FED. REPUBLIC OF GERMANY Forest Service General Technical Report
Gerard Hertel 1988 517 p Symposium held in Burlington, VT, 19-23 Oct. 1987 Sponsored by Northeastern Area State and Private Forestry; Green Mountain National Forest; USDA Office of International Cooperation and Development; EPA; Vermont Univ.; Vermont Div. of Forestry; AMAX; Consolidation Coal Co.; and Peabody Coal Co.
(PB90-107160; FSGTR-NE-120; NEFES/89-17) Avail: NTIS HC A22/MF A03 CSCL 13B

Sixty-six papers are included which were presented at the U.S./FRG research symposium: Effects of Atmospheric Pollutants on the Spruce-Fir Forests of the Eastern United States and the

Federal Republic of Germany, which was held October 19 to 23, 1987, in Burlington, Vermont. GRA

N90-14705# Iowa Univ., Iowa City. Dept. of Civil and Environmental Engineering.
STEADY STATE MODEL TO DETERMINE LAKE RESOURCES AT RISK TO ACID DEPOSITION IN THE SIERRA NEVADA, CALIFORNIA Final Report
Andrew I. Nishida and Jerald L. Schnoor Jul. 1989 208 p
(Contract ARB-A7-320-36)
(PB89-103995; ARB-R-89/407) Avail: NTIS HC A10/MF A02 CSCL 13B

A data base was compiled on 198 lakes in the Sierra Nevada, California, along with deposition information collected by the Air Resources Board, the National Acid Deposition Program, and the Department of Water Resources. A simple charge balance model was then devised to predict the acid neutralizing capacity (ANC) of these lakes based on current lake and deposition chemistry. The model was run using deposition scenarios that proposed a doubling and halving of the deposition of sulfuric acid and ammonium nitrate. GRA

N90-14706# Alaska Univ., Fairbanks. School of Agriculture and Land Resource Management.
DECOMPOSITION IN ARCTIC TERRESTRIAL ENVIRONMENTS Summary Report
Gary A. Laursen 1989 3 p
(Contract DE-FG06-84ER-60248)
(DE90-001198; DOE/ER-60248/T1) Avail: NTIS HC A01/MF A01

The principal goal is to further elucidate the rate and quality of microbial decomposition within cold, wet, Arctic tundra peat soils found in water tract systems of Foothills Province terrain (8 to 10 degrees) on the north slope of Alaska. Research objectives include demonstration of four hypotheses. A positive correlation exists between the rate of decomposing litter and the viable microbial (fungal) biomass, as measured by ARP activities and direct counts, associated with that litter. In Arctic tundra peat soil systems, there exists a positive correlation between the presence and abundance of viable mycelial biomass and the enzymatic potential for degradative activity as measured by the presence of cellulase, peroxidase, chitinase and protease enzymes produced by the miocrobial community. Substrate quality, as defined by lignin to cellulose ratios, influences the rate of natural litter decomposition. The lignin to total nitrogen ratio describes an inverse correlation to decomposition rates of litter. DOE

N90-14707# Massachusetts Univ., Amherst.
CLIMATE SYSTEM RESEARCH STUDIES OF GLOBAL AND REGIONAL INSTRUMENTAL DATA Progress Report, 1 Dec. 1988 - 30 Nov. 1989
Raymond S. Bradley, Henry F. Diaz, and Philip D. Jones Sep. 1989 6 p
(Contract DE-FG02-89ER-69017)
(DE90-001205; DOE/ER-69017/1) Avail: NTIS HC A02/MF A01

Further improvements in the DOE temperature and precipitation station data sets were made and a new merged set of temperature data (1851 to 1989) is in preparation. The world-wide precipitation data set is also being improved, and a study of precipitation variations over different continental regions was published. A draft of a joint U.S./U.S.S.R. paper on temperature and precipitation changes over the last 150 years was also prepared. There were 1545 and 656 precipitation stations used in analyzing Northern and Southern Hemisphere precipitation, respectively. All these stations had at least 35 years of data in the period 1921 to 1960. The number of station records available declines dramatically for the 1970s and 1980s, particularly over Africa and Asia. Considerable amounts of additional precipitation data have been located for Africa, Australia and Asia, principally for the post-1970 period, and these are currently being digitized. DOE

N90-14708# Committee on Commerce, Science, and Transportation (U.S. Senate).
CONSUMER OZONE PROTECTION ACT OF 1989
1989 107 p Hearing on S. 870 before the Subcommittee on the Consumer of the Committee on Commerce, Science and Transportation, 101st Congress, 1st Session, 19 Oct. 1989
(S-Hrg-101-377; GPO-24-159) Avail: Subcommittee on the Consumer, Senate, Washington, D.C. 20510 HC free; SOD HC $3.25 as 552-070-07449-0

Hearings before a subcommittee of the Senate Committee on Commerce, Science, and Transportation are presented in regard to the labeling of consumer products containing substances that contribute to the depletion of the ozone layer in the upper atmosphere; regulation of the sale, distribution, and use of such substances in consumer products and services in and affecting interstate commerce; and recapture and recycling of such substances, and for other purposes. B.G.

N90-14709# Pacific Northwest Lab., Richland, WA.
GLOBAL ENERGY AND THE GREENHOUSE ISSUE
Michael J. Scott, James A. Edmonds, Mark A. Kellogg, and Robert W. Schultz Sep. 1989 20 p Presented at the 14th World Energy Conference, Montreal, Quebec, 17-22 Sep. 1989
(Contract DE-AC06-76RL-01830)
(DE90-001394; PNL-SA-16496-1; CONF-890901-1) Avail: NTIS HC A03/MF A01

Global energy production and use results in the release of CO2 and other gases to the atmosphere which affect the atmosphere's radiative character. The accumulation of CO2 and other radiatively important gases (RIGs) is thought to result in higher mean global surface temperatures and other climatic changes, whose character would vary regionally around the globe. Of critical importance to determining the timing and magnitude of global climate change is an understanding of long term global energy systems. DOE

N90-14710# Lawrence Livermore National Lab., CA. Atmospheric and Geophysical Sciences Div.
ON THE MITIGATION OF NON-CO2 GREENHOUSE GASES
Donald J. Wuebbles Jul. 1989 8 p Presented at the Joint Power Generation Conference, Dallas, TX, 22-26 Oct. 1989
(Contract W-7405-eng-48)
(DE89-016659; UCRL-101523; CONF-891002-2) Avail: NTIS HC A02/MF A01

Much of the concern about potential effects of greenhouse gases on the future state of climate have been related to the growing atmospheric concentration of carbon dioxide. Concentrations of a number of other radiatively important atmospheric trace constituents are also changing, many at rates much larger than the current rate of change in CO2 concentrations. For example, methane concentrations are increasing about one percent per year, while concentrations of several chlorofluorocarbons are increasing by more than 4 percent per year. In each case, the increasing concentrations of these gases, which are emitted at the Earth's surface, are thought to be related to human activities. The combined effects of these other greenhouse gases on climate could be cumulatively as large as the effects estimated for CO2. Besides the direct radiative effects that these gases can have on climate, there are also potential indirect effects on climate through their chemical interactions with other greenhouse gases, such as ozone and water vapor. Evidence is mounting that such indirect effects are occurring. What is known regarding these changing greenhouse gas concentrations, in particular their budgets and causes of the changing atmospheric concentrations are described. It also attempts to examine issues affecting the mitigation of their potential effects on future climate. DOE

N90-14711# Oak Ridge National Lab., TN. Environmental Science Div.
CANOPY STOMATAL CONDUCTANCE
Dennis D. Baldocchi, Robert J. Luxmoore, and Jerry L. Hatfield (Agricultural Research Service, Ames, IA.) 14 Jul. 1989 31 p

Presented at the Workshop on Stomatal Conductance, University Park, PA, 11 Apr. 1989 Submitted for publication
(Contract DE-AC05-84OR-21400)
(DE89-016860; CONF-8904269-1) Avail: NTIS HC A03/MF A01

Stomata are major conduits for the diffusion of many trace gas species between leaves and the atmosphere. The role of the stomata in controlling gas exchange between the terrestrial biosphere and the atmosphere at the landscape, meso- and global-scales has only recently been recognized. Further advances in modelling large-scale trace gas exchange will depend on our ability to understand and model stomatal mechanics at the scale of the pertinent sub-unit, which is typically that of the canopy. This paper describes two approaches for estimating canopy stomatal conductance. One approach is based on bottom-up scaling. This approach computes canopy stomatal conductance by integrating detailed leaf-level and environmentally-driven, physiological processes with the use of a detailed canopy micrometeorology model. The other approach is based on top-down scaling. It interprets the integrated canopy stomatal conductance from measured fluxes of trace gas exchange. Frameworks for extending these scaling approaches to non-idea conditions are given. DOE

N90-14712# Oak Ridge National Lab., TN.
THE IMPACT OF GLOBAL WARMING ON THE ENERGY SYSTEM
William Fulkerson 1989 35 p Presented at the 2nd University of California Global Climate Change Workshop, Davis, CA, 6 Sep. 1989
(Contract DE-AC05-84OR-21400)
(DE89-017775; CONF-8909192-1) Avail: NTIS HC A03/MF A01

One of the most important impacts of global warming may be the changes in the energy system which result not from warming per se but from societal reactions to the prospect of warming. Changing the energy system from being 80 percent dependent on fossil fuels will be difficult at best and expensive. In fact, none of the nonfossil energy sources are yet ready to substitute for fossil fuels at the massive scale required or at reasonable costs. So, for the near to mid-term the best strategy for moderating the rate of increase of CO2 in the atmosphere is by much more efficient use and conversion of energy. Nevertheless, sustained reduction of emissions requires better nonfossil sources and expanded RD and D efforts necessary to provide the insurance we need. It is evidenced that a combined public and private sector investment of $1 (times) 10(sup 6)/year is needed. This compares to the current level of energy R and D which is estimated to cost in the range of $3 to 6 billion/year. Thus, our insurance is about a 16 to 33 percent increase. The investment is likely to yield good returns in the form of improved technologies which will be useful whether or not the changing greenhouse effect is as serious as many fear. DOE

N90-14713# Brookhaven National Lab., Upton, NY. Environmental Chemistry Div.
INTERNATIONAL CONFERENCE ON GLOBAL AND REGIONAL ATMOSPHERIC ENVIRONMENTAL CHEMISTRY AND VISIT TO HANGZHOU, CHINA, FOREIGN TRIP REPORT
Yin-Nan Lee 19 Jul. 1989 69 p Conference held in Beijing, China, 1-15 May 1989
(Contract DE-AC02-76CH-00016)
(DE90-000099; DOE/FTR-90000099) Avail: NTIS HC A04/MF A01

This international conference in atmospheric environmental chemistry, which was organized principally by C. S. Kiang of Georgia Institute of Technology and Wang Wenxing of the Chinese Research Academy of Environmental Sciences, was attended by about 80 scientists. The papers presented covered a large spectrum of interest ranging from troposphere to stratosphere and from regional pollution problems to global climate change. The participation of scientists from nearly all continents and the recognition of the cross boundary nature of environmental concerns made this conference an important vehicle to forge a consensus that any environmental consequences arising from human activities can be brought to control only through international collaboration of all countries. Visits to the three institutions afforded an opportunity to familiarize oneself with their research and to exchange views with Chinese scientists on priorities of environmental concerns. DOE

N90-14714# Oak Ridge National Lab., TN. Environmental Sciences Div.
APPLICATION OF SURFACE ANALYSIS METHODS TO STUDIES OF ATMOSPHERIC DEPOSITION IN FORESTS
S. E. Lindberg 1989 16 p Presented at the International Congress on Forest Decline Research: State of Knowledge and Perspectives, Friedrichshafen, Fed. Republic of Germany, 2-6 Oct. 1989
(Contract DE-AC05-84OR-21400)
(DE90-000562; CONF-8910122-1) Avail: NTIS HC A03/MF A01

Various surface analysis methods have been applied to the quantification of dry and total atmospheric deposition in recent years. Several of these methods have proved very useful in studies over large spatial and temporal scales, where application of atmospheric methods are limited. The methodology, assumptions, and applications of some of these methods are reviewed here, and examples provided of recent results. Some of these methods can provide the field data necessary for: (1) testing of regional deposition models, (2) development of process-level models of in-canopy dry deposition, and (3) comparison with results of applications of micrometeorological methods to deposition in complex terrain. These methods involve some assumptions which have not been rigorously tested and require further evaluation. DOE

N90-14715# Lawrence Livermore National Lab., CA. Atmospheric and Geophysical Sciences Div.
CLIMATE PROJECTIONS WITH REGIONAL RESOLUTION
Michael C. MacCracken Aug. 1989 15 p
(Contract W-7405-eng-48)
(DE90-000858; UCID-21769) Avail: NTIS HC A03/MF A01

The increasing atmospheric concentrations of carbon dioxide and other radiatively active gases will enhance the ability of the atmosphere to trap infrared radiation and thereby lead to warming of the climate. Numerical models suggest that the global average surface air temperature can be expected to increase a few degrees during the twenty-first century. This estimate is probably uncertain by a factor of at least two. The uncertainties in estimates of regional changes of temperature and precipitation are even greater. Despite these uncertainties, there is broad agreement that the persistence of such changes would be unprecedented in historical times. DOE

N90-14716# Argonne National Lab., IL. Center for Transportation Research.
ENVIRONMENTAL QUALITY AND THE SHIFT TO ALTERNATIVE FUELS: PROGRESS AND INTERIM FINDINGS OF A DEPARTMENT OF ENERGY STUDY OF TRANSITION IN VEHICULAR POWER SYSTEMS
Christopher L. Saricks, John B. Rajan, and Margaret K. Singh 22 Aug. 1989 32 p Presented at the American Institute of Chemical Engineer's Summer National Meeting, Philadelphia, PA, 20-23 Aug. 1989
(Contract W-31-109-eng-38)
(DE90-002178; CONF-890814-9) Avail: NTIS HC A03/MF A01

The goal of the last component, environmental consideration, is to identify potential environmental, health, and safety constraints and effects that could jeopardize a smooth transition or might render some aspects of transition inadvisable. These effects are not necessarily better or worse, just different. Specific tasks include: (1) developing a quantitative estimate of the relative air emissions due to domestic fuel production and vehicular operation of each fuel penetration scenario identified by the fuel distribution and vehicle supply component, (2) estimating air quality and waste

disposal effects of these scenarios, and (3) defining public and occupational safety and health issues related to domestic fuel and power system production, fuel handling, and vehicular operation. No attempt to quantify or assign a value to net environmental benefits is undertaken as part of the DOE analysis. This report focuses on this third study component, discussing the environmental, health and safety (EH and S) transition issues that have been identified as of July 1, 1989 and describing methodologies to be applied in forthcoming quantitative analyses. As appropriate, findings to date from other components of the study will be cited. The following section, which presents EH and S concerns for each of the three prime candidate alternative fuels, is drawn largely from a forthcoming study progress report. DOE

N90-14717# Pacific Northwest Lab., Richland, WA. Dept. of Computational Sciences.

INTEGRATED COMPUTER-BASED TOOLS TO FACILITATE ENVIRONMENTAL MONITORING, ASSESSMENT, AND RESTORATION

Paula J. Cowley and James C. Brown Oct. 1989 13 p Presented at the 28th Hanford Symposium on Health and the Environment, Richland, WA, 16-19 Oct. 1989

(Contract DE-AC06-76RL-01830)

(DE90-002732; PNL-SA-16875; CONF-891053-8) Avail: NTIS HC A03/MF A01

The vast amounts of scientific and technical data gathered during the process of environmental monitoring, assessment, and restoration make the effective application of computer-based tools essential. This paper describes how an integrated set of automated resources is being applied at the Hanford Site to effectively manage the data gathered during site characterization and monitoring and to provide an environment that facilitates analysis and assessment. The Hanford Environmental Information System (HEIS) has upgraded our previous monitoring and characterization capabilities and represents significant advances in our ability to manage, retrieve, and display data. An integrated data base, a geographic information system (that allows data to be displayed on a map), and support graphics allow the user to generate spatially related visualizations and perform data extractions. This allows the user to gain insight quickly and easily by obtaining a complete picture of the data of interest. HEIS also provides the capability to share the information with other software environments for further analysis and assessment. DOE

N90-14718# Oak Ridge National Lab., TN. Environmental Sciences Div.

DISCUSSIONS OF GLOBAL ENVIRONMENTAL PROBLEMS

Bernhard Krahl-Urban (Kernforschungsanlage, Juelich, Germany, F.R.) 2 Nov. 1989 5 p Meeting held in Oak Ridge, TN, 16-20 Oct. 1989

(Contract DE-AC05-84OR-21400)

(DE90-002747; ORNL/FTR-3452) Avail: NTIS HC A02/MF A01

A West German scientist visited the Oak Ridge National Laboratory (ORNL) at the request of the Environmental Sciences Division to provide programmatic interpretations and technical overviews of research topics addressing international environmental issues. Many of today's environmental problems can no longer be considered as regional-scale impacts. Global warming, acidification, ozone depletion, drought, deforestation, and air pollution effects are global-level processes that can only be effectively approached by international scientific cooperation. The visitor's recommendations for the final planning and coordination of international environmental issues emphasized focusing on international cooperation with research institutions in West Germany and in other countries of the European Community. Several key global environmental issues are addressed by the Juelich Nuclear Research Center (KFA Juelich), West Germany. Scientific cooperation with KFA Juelich should be promising in theoretical ecology, systems analysis, and toxicology. Scientific exchange between ORNL and KFA Juelich in environmental sciences was initiated by the visitor. DOE

N90-14719# International Centre for Theoretical Physics, Trieste (Italy).

A MODEL FOR THE SIMULATION OF THE OZONE BUDGET IN THE ATMOSPHERE UNDER ANTHROPOGENIC PERTURBATION

A. R. Bestman (Port Harcourt Univ., Nigeria) Apr. 1989 10 p Submitted for publication

(DE89-636294; IC-89/34) Avail: NTIS (US Sales Only) HC A02/MF A01

A simple model is proposed for the laboratory simulation of the anthropogenic perturbation of the ozone (O3) in the middle atmosphere. It consists of two vertical plates maintained at very high but nearly equal temperatures, in between which is a binary mixture of a chemically reacting fluid. The plates are rotated about a horizontal axis. Adopting the optically thin non-grey gas approximation for radiative heat transfer, the differential equations governing the velocity components, temperature and mass concentration are integrated in a close form. The solutions show good agreement with the exact integral formalism for the radiative flux under the same assumption of nearly equal wall temperatures. DOE

N90-14720# International Centre for Theoretical Physics, Trieste (Italy).

MODELLING OF THE EFFECTS OF THE EQUATORIAL ELECTROJET ON ITS ENVIRONMENT

A. R. Bestman (Port Harcourt Univ., Nigeria) Mar. 1989 20 p Submitted for publication

(DE89-636298; IC-89/33) Avail: NTIS (US Sales Only) HC A03/MF A01

The effect of the equatorial electrojet on the velocity vector and the temperature of the surrounding environment is modelled by the classical magnetohydrodynamic equations. Under the assumption of small hydrodynamic and magnetic Reynolds numbers and an electrojet magnetic field which oscillates along its axis, z, the nonlinear governing equations are solved by asymptotic approximation. The effect of the intensity of the magnetic field, inter alia, on the flow variables are deduced quantitatively. For example, when the field intensity is small, the temperature distribution is large and vice versa. Also at the higher approximation, there is a component of the flow variables which is completely independent of the axis, z, of the magnetic field variation. Since the classical equation for the temperature is quite similar to the mass diffusion equation, light is shed on the effect of the electrojet on the atmospheric ozone in its vicinity. Indeed the thermal field and the ozone concentration are affected similarly. DOE

N90-14721# Lawrence Livermore National Lab., CA.

QUANTIFYING THE LINK BETWEEN CHANGE IN RADIATIVE BALANCE AND ATMOSPHERIC TEMPERATURE

Michael C. McCracken, ed. Aug. 1989 16 p Presented at the DOE Carbon Dioxide Research Program Workshop, Germantown, MD, 24-25 Apr. 1989

(Contract W-7405-eng-48)

(DE90-000819; UCRL-101736; CONF-8904276-1) Avail: NTIS HC A03/MF A01

There has been a seemingly increasing divergence between the observed warming of about 0.5 C over the past 100 years and the estimates of the most recent climate model simulations that a doubling of the carbon dioxide concentration will lead to an increase in global average temperatures of perhaps 1.5 to 5 C. While there are many factors to consider in attempting to reconcile these different quantities (e.g., ocean thermal lag, atmospheric composition changes, volcanic aerosols, etc.), the level of uncertainty in estimates of future climate change clearly needs to be reduced. The purpose of this workshop was to solicit scientific counsel as part of the process of developing a new research effort to quantify the link between increasing greenhouse gases and climate change. This program of research would stress observations, field experiments and laboratory approaches as a means of resolving the apparent inconsistencies between the climate model predictions of the expected climate change to date and the observed climate system, as well as seeking to reduce

the large uncertainties evident in recent studies of the treatment of cloud feedbacks. The objective of the workshop was to review the state-of-the-art for measuring the radiative balance and to explore possible experiments to link the cause and effect from changes in atmospheric composition to atmospheric temperature and other measures of climate change. DOE

N90-14722# Oak Ridge National Lab., TN. Environmental Sciences Div.
STRATEGY FOR MONITORING THE EFFECTS OF LAND USE CHANGE ON ATMOSPHERIC CO2 CONCENTRATIONS
Virginia H. Dale 1989 11 p Presented at the Global Natural Resource Monitoring and Assessments: Preparing for the 21st Century, Venice, Italy, 24-30 Sep. 1989
(Contract DE-AC05-84OR-21400)
(DE90-001635; CONF-8909243-1) Avail: NTIS HC A03/MF A01

Land use changes may be responsible for as much as 50 percent of the increase in atmospheric CO2 that is thought to be causing climatic warming. The major cause of current land use is tropical deforestation. Estimating the rates of tropical deforestation is difficult, and, thus there is high uncertainty as to its contribution to atmospheric CO2. Remote sensing data can provide an independent, relatively quick, and spatially disaggregated estimate of the amount of clearing that is occurring. DOE

N90-14723# Department of Energy, Washington, DC. Office of Health and Environmental Research.
CARBON DIOXIDE AND CLIMATE: SUMMARIES OF RESEARCH IN FY 1989
Oct. 1989 87 p
(DE90-001791; DOE/ER-0425) Avail: NTIS HC A05/MF A01

Scientific and public interest in greenhouse gases, climate warming, and global change has virtually exploded in 1989. The Department's focused research on CO2 contributed sound and timely scientific information to the myriad of questions produced by the groundswell of interest and concern. Research projects summarized provided the data base that made timely responses possible, and the contributions from participating scientists are genuinely appreciated. The nation's interest has been well served. In the past year, the core CO2 research has continued to improve the scientific knowledge needed to project future atmospheric CO2 concentrations, to estimate climate sensitivity, and to assess the responses of vegetation to rising concentrations of CO2 and climate change. The Carbon Dioxide Research Program's goal is to develop sound scientific information for policy formation and governmental action in response to changes of atmospheric CO2. During this year, the Program was moved into the Office of Health and Environmental Research and was combined with other atmospheric research activities. The work is now administered by the Atmosphere and Climate Research Division (ACRD). In addition to supporting core CO2 research and developing a program around the new initiatives, ACRD is responsible for atmospheric science and climate. Its scope includes atmospheric chemistry, numerical modeling, laboratory studies, and field experiments. This Program Summary describes projects funded by the Carbon Dioxide Research Program during FY 1989 and gives a brief overview of the objectives, organization, and accomplishments of that research. DOE

N90-14724# Argonne National Lab., IL.
US ENERGY USE: NEW TECHNOLOGIES AND POLICIES IN RESPONSE TO GLOBAL WARMING
D. G. Streets, C. N. Bloyd, and D. M. Kenski Jun. 1989 39 p Presented at the Conference on Responding to the Threat of Global Warming: Options for the Pacific and Asia, Honolulu, HI, 21-27 Jun. 1989
(Contract W-31-109-eng-38)
(DE90-002170; CONF-8906244-1) Avail: NTIS HC A03/MF A01

Energy use and production accounts for by far the largest portion of emissions of greenhouse gases in the United States and the world. The US Environmental Protection Agency (EPA) has estimated that, worldwide, these activities were responsible for 57 percent of greenhouse warming in the 1980s. Other activities and their respective contributions include agriculture, 14 percent; land use and modification, 9 percent; chlorofluorocarbon (CFC) use, 17 percent; and other (nonenergy) industry, 3 percent. Given this importance of energy activities, it is appropriate that efforts to forestall global warming have focused on these activities. Because the United States consumes the largest share of world energy and thus produces the largest share of greenhouse gas emissions, it is the target of many such efforts. A number of U.S. government responses to global warming have been proposed or are now under way. For example, the 101st Congress has seen 11 bills dealing with global warming issues; a research program on climate change has been promised $190 million for 1990; and the United States has signed the Montreal Protocol to control CFCs. U.S. energy and related emissions of greenhouse gases is discussed. Energy use in each sector is briefly characterized and several new technologies for energy use in that sector are described. Finally, national and state policies that offer potential to reduce energy use are discussed. This discussion is limited by space considerations to only a sampling of the many technologies under development and policy options that have been proposed. DOE

N90-14725# General Sciences Corp., Laurel, MD.
ANALYSIS OF ACID RAIN AND ASSOCIATED PHENOMENA Final Report
Sep. 1989 14 p
(Contract DE-AC01-85FE-60850)
(DE90-002555; DOE/FE-60850/T1) Avail: NTIS HC A03/MF A01

The Department of Energy, Office of Fossil Energy, Office of Coal Utilization, Advanced Conversion and Gasification (OCUAC and G) is and has been engaged in numerous research and development programs which will greatly increase the use of coal and other abundant fossil energy resources. In combination, these technology programs and energy systems characterize OCUAC and G's approach to accomplishing their strategic objectives of: clean coal, new fuel forms for coal, new coal utilization processes, coal gasification, modular equipment systems, and environmental protection. Under this contract, GSC is to assist OCUAC and G in meeting their strategic objective by providing services related to three task areas: literature surveys, acid rain analysis, and interfacing of energy systems. During this period considerable attention was paid to performing literature surveys, analysis of emissions and deposition data, and the review of energy systems. Notable accomplishments are summarized. DOE

N90-14726# Oak Ridge National Lab., TN.
NITROGEN DEPOSITION TO FOREST TREES Foreign Trip Report, 30 Sep. - 13 Oct. 1989
George E. Taylor, Jr. and Paul J. Hanson Oct. 1989 19 p
(Contract DE-AC05-84OR-21400)
(DE90-003285; ORNL/FTR-3432) Avail: NTIS HC A03/MF A01

Issues discussed at two major international conferences focusing on the interaction between the atmosphere and vegetation in terrestrial ecosystems, are reported. The first conference addressed the issue of forest decline, whereas the second focused on controlled-environment methodologies for characterizing the influence of physical and chemical changes in the atmosphere on crops and forest trees. Visits to research sites in southern Germany are also reported. DOE

N90-14727*# National Aeronautics and Space Administration, Washington, DC.
DRAFT ENVIRONMENTAL IMPACT STATEMENT FOR THE ULYSSES MISSION (TIER 2)
Feb. 1990 186 p
(NASA-TM-102903; NAS 1.15:102903) Avail: NTIS HC A09/MF A01 CSCL 13B

This Draft Environmental Impact Statement (DEIS) addresses the environmental impacts which may be caused by the preparation and operation of the Ulysses spacecraft, including its planned

launch on the Space Transportation System (STS) Shuttle and the alternative of canceling further work on the mission. The launch configuration will use the STS/Inertial Upper Stage (IUS)/Payload Assist Module-Special(PAM-S) combination. The Tier 1 EIS included a delay alternative which considered the Titan 4 launch vehicle as an alternative booster stage for launch in 1991 or later. However, the U.S. Air Force, which procures the Titan 4 for NASA, could not provide a Titan 4 vehicle for the 1991 launch opportunity because of high priority Department of Defense requirements. The only expected environmental effects of the proposed action are associated with normal Shuttle launch operations. These impacts are limited largely to the near-field at the launch pad, except for temporary stratospheric ozone effects during launch and occasional sonic boom effects near the landing site. These effects have been judged insufficient to preclude Shuttle launches. In the event of (1) an accident during launch, or (2) reentry of the spacecraft from earth orbit, there are potential adverse health and environmental effects associated with the possible release of plutonium dioxide from the spacecraft's radioisotope thermoelectric generators (RTG). The potential effects considered in this EIS include risks of air and water quality impacts, local land area contamination, adverse health and safety impacts, the disturbance of biotic resources, impacts on wetland areas or areas containing historical sites, and socioeconomic impacts. Intensive analysis of the possible accidents associated with the proposed action are underway and preliminary results indicate small health or environmental risks. The results of a Final Safety Analysis Report will be available for inclusion into the final EIS. Author

46 GEOPHYSICS

Includes aeronomy; upper and lower atmosphere studies; ionospheric and magnetospheric physics; and geomagnetism.

For space radiation see *93 Space Radiation.*

N90-14728*# Universities Space Research Association, Boulder, CO.

GROUP-KINETIC THEORY AND MODELING OF ATMOSPHERIC TURBULENCE Final Report, 1 Dec. 1984 - 30 Nov. 1987

C. M. Tchen 8 Aug. 1989 77 p

(Contract NAS8-36153)

(NASA-CR-183776; NAS 1.26:183776) Avail: NTIS HC A05/MF A01 CSCL 04A

A group kinetic method is developed for analyzing eddy transport properties and relaxation to equilibrium. The purpose is to derive the spectral structure of turbulence in incompressible and compressible media. Of particular interest are: direct and inverse cascade, boundary layer turbulence, Rossby wave turbulence, two phase turbulence; compressible turbulence, and soliton turbulence. Soliton turbulence can be found in large scale turbulence, turbulence connected with surface gravity waves and nonlinear propagation of acoustical and optical waves. By letting the pressure gradient represent the elementary interaction among fluid elements and by raising the Navier-Stokes equation to higher dimensionality, the master equation was obtained for the description of the microdynamical state of turbulence. Author

N90-14729 Maryland Univ., College Park.

AN OBSERVATIONAL STUDY OF INTRAMONTHLY QUASI-PERIODICITIES IN THE NORTHERN HEMISPHERE, EXTRATROPICAL GEOPOTENTIAL HEIGHT FIELD Ph.D. Thesis

John Robert Lanzante 1988 209 p

Avail: Univ. Microfilms Order No. DA8912315

Intramonthly quasi-periodicities (IQPs) in the extratropical, cold season tropospheric geopotential height data of the Northern Hemisphere were studied through the use of rotated complex principal components (RCPCs). Heights at the 700 mb level, which span 36 years, were preprocessed using a 10 to 30 day bandpass filter prior to the RCPC analysis. Tests of rotation sensitivity and robustness insured the stability of the RCPC analysis. A Monte Carlo procedure was used to objectively identify episodes of occurrence. Composite maps which depict the evolution of the IQPs over a typical lifecycle were found useful in interpreting their behavior. Three classes of IQPs were found. The first class contains several modes which each involve a high latitude transient disturbance and a quasiperiodically oscillating standing wave. The distinction between the modes is mostly in the location of the standing wave pattern. The wavenumber 1 transient is probably the 16-day wave or Rossby normal mode which was identified in the atmosphere by others. The second class consists of only one mode, an oscillating dipole concentrated in the Atlantic sector, which is speculated to be the result of a regional, baroclinic zonal index cycle. The third class contains several distinct regional mid-latitude wave trains which to a large extent are progressive; the two most important are located over Eurasia and North America. Dissert. Abstr.

N90-14730 Harvard Univ., Cambridge, MA.

A LOW-ORDER MODEL OF THE EQUATORIAL OCEAN-ATMOSPHERE SYSTEM Ph.D. Thesis

Roberto Legnani 1989 133 p

Avail: Univ. Microfilms Order No. DA8914689

A low order model of the equatorial ocean-atmosphere coupled system is presented. The model atmosphere includes a hydrological cycle with cloud-radiation interaction. The model ocean is based on mixed layer dynamics with a parameterization of entrainment processes. The coupling takes place via transfer to momentum, sensible heat, latent heat and short wave and long wave radiation through the ocean surface. The dynamical formulation is that of the primitive equations of an equatorial beta-plane, with zonally periodic and meridionally infinite geometry. The system is expanded into the set of normal modes pertinent to the linear problem and severly truncated to a few modes; 54 degrees of freedom are retained. Some nonlinear terms of the equations are evaluated in physical space and then projected onto the functional space; other terms are evaluated directly in the functional space. Sensitivity tests to variations of the parameters are performed, and some results from 10-year initial value simulations are presented. The model is capable of supporting oscillations of different time scales, ranging from a few days to a few years; it prefers a particular zonally asymmetric state, but temporarily switches to a different (opposite) zonally asymmetric state in an event-like fashion. Dissert. Abstr.

N90-14731 Nevada Univ., Reno.

CONVECTIVE BOUNDARY LAYER AND MODELING OF DISPERSION Ph.D. Thesis

Nizam Uddin Ahmed 1989 143 p

Avail: Univ. Microfilms Order No. DA8922229

Looping, bifurcation, and meandering of a plume are generally observed in a convective field. The blobby or puffy concentration patterns associated with these plumes are marked deviations from what is expected from either conventional K-theory or Gaussian distribution formulae. A numerical model was developed for material dispersion in a convective boundary layer from both elevated and ground sources. Mechanistic formulation, rather than parameterization, or statistical behavior of planetary boundary layer (PBL) phenomena, was used as a basis. The dispersion mechanism is considered to be due to mixing between the updraft and the downdraft. This model uses two universal constants, (turbulent entrainment constant, a, and decay constant A) and a mixing scheme directly supported by observations. Researchers examined the dispersion pattern from the elevated and ground sources. For elevated sources, the maximum concentration descends first to the ground level at some distance downwind, and then rises, depending on the inversion height, the mean wind and height at which material is released. The updrafts have a higher velocity than the downdrafts and consequently the downdrafts occupy a larger horizontal area. In some cases the updrafts and downdrafts are comparable and materials are caught equally in the updrafts and downdrafts. The concentration of materials is split into two parts, one moving downward and the other upward. It is shown

using the same mechanistic principles, that different convective situations cause different concentration patterns (for example, looping, bifurcating of a plume, and ascending of center line).
Dissert. Abstr.

N90-14732 Michigan Univ., Ann Arbor.
A MEASUREMENT OF HYDROXYL IN THE DAYTIME MESOSPHERE Ph.D. Thesis
Richard Philip Cageao 1989 277 p
Avail: Univ. Microfilms Order No. DA8920507

Hydroxyl is a very reactive free radical which dominates the odd-hydrogen - odd-oxygen reaction chemistry in the earth's mesosphere. The objective of this thesis was the development of an instrument which would measure the concentration of hydroxyl in the mesosphere and an assessment, based on this data, of the current understanding of mesospheric chemistry. A new instrument, a coupled Ebert-Fastie spectrometer and Fabry-Perot interferometer (UV-FPI), was developed to measure spectroscopically the ultraviolet solar resonance fluorescence emission of hydroxyl. The instrument was designed to observe these emissions in the near-ultraviolet at 3087 A against the bright background of Rayleigh scattered sunlight. The background was suppressed by the high resolution Fabry-Perot interferometer operating over the narrow wavelength region defined by the Ebert-Fastie spectrometer bandpass. The remote measurement of hydroxyl was made from a sounding rocket platform with the instrument viewing the earth's limb for the maximum integrated path length of hydroxyl emission. The sounding rocket payload also carried instruments which made simultaneous in situ and remote sensing measurements of atomic oxygen and temperature, respectively. Dissert. Abstr.

N90-14733 Michigan Univ., Ann Arbor.
THE RETRIEVAL OF THE CONCENTRATIONS OF NITRIC OXIDE AND NITROGEN DIOXIDE FROM SATELLITE SOLAR OCCULTATION MEASUREMENTS AT SUNSET AND SUNRISE Ph.D. Thesis
Constantinos Ioannis Cartalis 1989 220 p
Avail: Univ. Microfilms Order No. DA8920509

HALOE (Halogen Occultation Experiment), scheduled to fly on the Upper Atmosphere Research Satellite (UARS) in 1991, aims to retrieve the vertical concentration profiles of seven minor stratospheric constituents in order to improve the understanding of ozone's photochemistry. The solar occultation method is employed for the measurement of the absorption of solar light for different altitudes. This method can effectively measure minor chemical constituents, due to the long paths solar rays need to follow before they are collected by the satellite. Once the measurements are obtained, an inversion code is applied to retrieve the vertical concentration profiles. Here, the emphasis is the retrieval of the concentrations of nitric oxide and nitrogen dioxide, which both play an active role in the photochemistry of ozone. The investigation is complicated because of their large diurnal changes which are intensified at sunrise and sunset. Consequently, the retrieval of NO and NO2 from solar occultation measurements at twilight needs to take into account the lifetimes and the rapid variations of NO and NO2. If the temporal and spatial variations of NO and NO2 are neglected, the resulting errors for altitudes less than 20 km reach 100 and 5 percent respectively and for both sunset and sunrise. A photochemical scheme is developed and a separate code calculates the photodissociation rates of the species involved in photochemical reactions, as a function of latitude, temperature, altitude and season. Dissert. Abstr.

N90-14734# NSI Technology Services Corp., Corvallis, OR. Environmental Research Lab.
CLIMATE-BIOSPHERE INTERACTIONS SCOPE OF WORK
George A. King Sep. 1989 30 p Sponsored by US Environmental Protection Agency, Corvallis, OR
(PB90-106444; EPA/600/3-89/054) Avail: NTIS HC A03/MF A01 CSCL 04A

Research which will be undertaken over the next 5 years is described. First, the scientific questions that must be addressed in order to answer important public policy needs concerning the potential environmental effects of global climatic change are presented. Next, the general research approaches that will be used to answer the scientific questions are described. An overview is presented of the project, as is a discussion of the relationship of the project's research with other global change research, and a budget summary. Author

N90-14735*# Illinois Univ., Urbana-Champaign. Dept. of Electrical and Computer Engineering.
ROCKET STUDIES OF THE LOWER IONOSPHERE Final Report, 1 Aug. 1971 - 18 Feb. 1989
Sidney A. Bowhill Jan. 1990 32 p
(Grant NGR-14-005-181)
(NASA-CR-186187; NAS 1.26:186187) Avail: NTIS HC A03/MF A01 CSCL 04A

The earth's ionosphere in the altitude range of 50 to 200 km was investigated by rocket-borne sensors, supplemented by ground-based measurement. The rocket payloads included mass spectrometers, energetic particle detectors, Langmuir probes and radio propagation experiments. Where possible, rocket flights were included in studies of specific phenomena, and the availability of data from other experiments greatly increased the significance of the results. The principal ionospheric phenomena studied were: winter anomaly in radiowave absorption, ozone and molecular oxygen densities, mid-latitude sporadic-E layers, energetic particle precipitation at middle and low latitudes, ionospheric instabilities and turbulence, and solar eclipse effects in the D and E regions. This document lists personnel who worked on the project, and provides a bibliography of resultant publications. J.P.S.

N90-14736*# Lunar and Planetary Inst., Houston, TX.
WORKSHOP ON THE ARCHEAN MANTLE
L. D. Ashwal, ed. 1989 105 p Workshop held in Houston, TX, 11-13 Jan. 1989
(Contract NASw-4066)
(NASA-CR-186156; NAS 1.26:186156; LPI-TR-89-05) Avail: NTIS HC A06/MF A01 CSCL 08G

The Workshop on the Archaen mantle considers and discusses evidence for the nature of earth's Archaen mantle, including its composition, age and structure, influence on the origin and evolution of earth's crust, and relationship to mantle and crustal evolution of the other terrestrial planets. The summaries of presentations and discussions are based on recordings made during the workshop and on notes taken by those who agreed to serve as summarizers. Author

N90-14737# Lawrence Livermore National Lab., CA.
A STUDY OF THE DIFFERENCE BETWEEN GRAVIMETRIC AND GAMMA-GAMMA DENSITY NEAR THE SURFACE IN NORTHERN YUCCA FLAT
J. R. Hearst and N. R. Burkhard 1989 50 p Presented at the 5th Symposium on Containment of Underground Nuclear Detonations, Santa Barbara, CA, 19-21 Sep. 1989
(Contract W-7405-eng-48)
(DE89-017886; UCRL-101709; CONF-8909163-2) Avail: NTIS HC A03/MF A01

Although the mean and median of the difference between average density from 50 to 200 m below the surface in 43 holes in northern Yucca Flat computed from a density log and that computed from borehole gravity using the measured free air gradient is very close to zero, the range of values is very large. Many individual values of the difference are significantly different from zero. When the gravimetric density is computed using a free air gradient calculated from the surface gravity on an irregular but approx. 300 m grid, the mean and median of the difference between gravimetric and gamma-gamma density is slightly closer to zero than when the measured free air gradient is used. The range of values is not significantly decreased. Proposed explanations for this large range fall into two categories: anomalies in the gravity field or its horizontal derivative at the sites with large difference range, causing changes in the free air gradient or the near surface gravimetric density, and mechanisms that affect the bulk density

near the borehole, causing changes in the gamma-gamma density. Many proposed explanations were investigated and have found no single mechanism that is consistent with the data. These results indicate that the choice of method of determining free air gradient causes no significant change in the difference between near surface gamma density and gravimetric density, and that there is no obvious method of eliminating the range. Because calculation from surface gravity is much less expensive than tower measurement, and there is no evidence that it is less accurate, it is considered the logical method for routinely obtaining free air gradient until some evidence is found to suggest the contrary. An attempt was made to optimize the calculational procedure. The tradeoff is between the accuracy of the calculated free air gradient and the amount of surface gravity data required. DOE

N90-14738# Brookhaven National Lab., Upton, NY. Dept. of Applied Science.
EXTRATERRESTRIAL HALOGEN AND SULFUR CONTENT OF THE STRATOSPHERE
S. R. Sutton and G. J. Flynn (State Univ. of New York, Plattsburgh.) Jun. 1989 13 p Presented at the Lunar Planetary Science Conference, Houston, TX, 12-18 Mar. 1989 Prepared in cooperation with Chicago Univ., IL
(Contract DE-AC02-76CH-00016)
(DE89-017623; BNL-43096; CONF-8903111-5) Avail: NTIS HC A03/MF A01

Interplanetary dust represents a potential source of environmentally important chemical species in the Earth's atmosphere. The stratospheric content of halogens and sulfur from extraterrestrial sources was estimated. Two computational methods were employed because of the uncertainties in models of atmospheric evolution of meteor debris. One estimate was based on the total stratospheric aerosol load and the relative influxes from interplanetary dust and tropospheric sources. The second, viscous settling method yields a greater stratospheric component. The steady state extraterrestrial influxes of halogens are minor compared to tropospheric sources but the sulfur input may be comparable to the present observed stratospheric content. Temporal enhancements in the meteoroid flux, such as passage through comet debris lanes or impact by large bodies, may produce significant chemical perturbations in the atmosphere. DOE

N90-14739# Pacific Northwest Lab., Richland, WA.
THE IDENTIFICATION OF TERRAIN-INDUCED CIRCULATIONS USING PRINCIPAL COMPONENTS
E. D. Skyllingstad and M. N. Schwartz Jun. 1989 15 p Presented at the 11th Conference of Probability and Statistics, Monterey, CA, 1-5 Oct. 1989
(Contract DE-AC06-76RL-01830)
(DE90-001991; PNL-SA-17164-HEDR; CONF-8910277-1) Avail: NTIS HC A03/MF A01

The application of principal component analysis to regional wind fields can provide an objective method for the identification of synoptic, thermal, and topographical effects. These results can be applied to regional wind forecasting by providing a frequency distribution for various wind-field transitions from the current observed state or used in defining climatological wind fields for air quality studies. In future work, a principal component analysis of large-scale forcing will be combined with the regional wind-field study to provide a more objective link between synoptic and mesoscale patterns. Synoptic-scale situations from operational meteorological models could then be used to predict changes in the local wind field. DOE

N90-14740# Pacific Northwest Lab., Richland, WA.
BEYOND THE IDMY (INTERNATIONAL DAYLIGHTING MEASUREMENTS YEAR): A NETWORK INSTRUMENT FOR LOW-COST DATA ACQUISITION
J. J. Michalsky, R. Perez, L. Harrison (State Univ. of New York, Albany.), and B. A. LeBaron Jul. 1989 12 p Presented at the Symposium on Daylighting and Solar Radiation Measurement, Berlin, Fed. Republic of Germany, 9-11 Oct. 1989
(Contract DE-AC06-76RL-01830)
(DE90-002722; PNL-SA-17311; CONF-8910285-1) Avail: NTIS HC A03/MF A01

The International Daylighting Measurements Year (IDMY) network will acquire a data base to test models that convert solar irradiance data to daylight availability data for all skies and geometries. These models will subsequently be used to convert routine solar irradiance data to the desired daylight quantities. An instrument is described that provides for a substantial reduction in capital and maintenance costs associated with acquiring diffuse and total horizontal and direct normal irradiance. A simple procedure is outlined for correcting the silicon cell sensor to yield root-mean-square errors within 10 watts/sq m of first class thermopile pyranometers and pyrheliometers. DOE

47 METEOROLOGY AND CLIMATOLOGY

Includes weather forecasting and modification.

N90-14741*# National Aeronautics and Space Administration. Langley Research Center, Hampton, VA.
ATLAS OF ALBEDO AND ABSORBED SOLAR RADIATION DERIVED FROM NIMBUS 6 EARTH RADIATION BUDGET DATA SET, JULY 1975 TO MAY 1978
G. Louis Smith, T. Dale Bess, and David Rutan (PRC Kentron, Inc., Hampton, VA.) [1989] 88 p
(NASA-RP-1230; L-16601; NAS 1.61:1230) Avail: NTIS HC A05/MF A01 CSCL 04B

An atlas of monthly mean global contour maps of albedo and absorbed solar radiation is presented. The atlas is based on 35 months of continuous measurements from July 1975 through May 1978. The data were retrieved from measurements made by the shortwave wide field-of-view radiometer of the first Earth Radiation Budget (ERB) instrument, which flew on the Nimbus 6 spacecraft in 1975. Profiles of zonal mean albedos and absorbed solar radiation are tabulated. These geographical distributions are provided as a resource for studying the radiation budget of the earth. This atlas of albedo and absorbed solar radiation complements the atlases of outgoing longwave radiation by Bess and Smith in NASA-RP-1185 and RP-1186, also based on the Nimbus 6 and 7 ERB data. Author

N90-14742 Bristol Univ. (England).
RAINFALL ESTIMATION OVER AFRICA USING SATELLITE DATA Ph.D. Thesis
Giles DSouza 1988 290 p
Avail: Univ. Microfilms Order No. BRDX85251

The empirical development and testing of a new method for satellite-based rainfall estimation over Africa is described. The method was designed to estimate rain/no-rain areas on the basis of bispectral thresholding of three pairs of daytime visible and infrared images and temperature thresholding of three nighttime infrared images from the Meteosat satellite. It was initially tested, at a reduced spatial resolution, over the whole continent of Africa for the months of January and July, 1985. In comparison with available ground station data, satellite-derived maps of rain/no-rain areas were much more spatially continuous and complete. Daily estimates were obtained by the spatial interpolation of reported rainfall at calibration stations within daily satellite-estimated rain areas. These, when aggregated together, formed the best 10-day and 30-day estimates of rainfall. Verification was carried out at three levels: comparison of point estimates, comparison of area-average amounts, and comparison of estimated and observed spatial patterns of rainfall. Dissert. Abstr.

N90-14743# Colorado State Univ., Fort Collins. Dept. of Atmospheric Science.
SUMMARY OF 1989 ATLANTIC TROPICAL CYCLONE ACTIVITY AND SEASONAL FORECAST VERIFICATION
William M. Gray 20 Nov. 1989 37 p Sponsored by NSF, Washington, DC
Avail: NTIS HC A03/MF A01

The tropical cyclone (TC) activity which occurred in the Atlantic Basin during 1989 is summarized. The author's seasonal forecast of TC activity that was issued in late May, and updated in late July is verified. This forecast was based on the author's previous research (Gray, 1983, 1984a, 1984b) and new research which relates seasonal Atlantic hurrican activity to: (1) the El Nino (EN); (2) the Quasi-Biennial Oscillation (QBO) of equatorial 30 mb and 50 mb stratospheric winds; (3) Caribbean Basin-Gulf of Mexico Sea-Level Pressure Anomaly (SLPA) in spring and early summer; and (4) lower latitude Caribbean Basin 200 mb (12 km altitude) zonal wind anomaly in June and July in non El Nino seasons. Information received by the author as of 26 May 1988 indicated that the 1989 hurricane season should have been a below average season with about 4 hurricanes, 7 named storms of hurricanes and tropical storm intensity, 15 hurricane days and 30 named storms days. An updated forecast was issued on 28 July 1989 with the number of named storms increased to 9 and named storm days to 35 and other forecast parameters the same. The actual number of hurricans which occurred in 1989 was 7 (three above the forecast); the number of named storms was 10 (one above forecast); number of hurricane days was 35 and number of named storm days was 66 - both much higher than forecast.

Author

N90-14744 Delaware Univ., Newark.
THE DEVELOPMENT OF A SPATIAL SYNOPTIC CLIMATOLOGICAL INDEX FOR ENVIRONMENTAL ANALYSIS Ph.D. Thesis
Robert Eugene Davis 1988 224 p
Avail: Univ. Microfilms Order No. DA8914327

A spatial synoptic climatological index is developed which is capable of assessing and analyzing the impact of synoptic-scale variations on numerous environmental parameters. Based upon surface weather data for the conterminous U.S. for 1984, daily maps are produced which show those areas under the influence of similar weather conditions. The index is developed by applying principal components analysis to a daily matrix of 141 stations by 24 weather elements (chosen to represent both thermal/moisture and surface flow characteristics). The resulting component scores are grouped using a two-stage clustering technique. This yields a map showing lobes of air having relatively homogeneous weather characteristics. These lobes (clusters) are spatially coherent and correspond closely to surface weather map features.

Dissert. Abstr.

N90-14745 Texas A&M Univ., College Station.
SYNOPTIC SCALE TROPICAL WAVES IN MULTICHANNEL SATELLITE RADIANCE DATA Ph.D. Thesis
James Royal Schaefer 1988 129 p
Avail: Univ. Microfilms Order No. DA8913438

Diagnosis of tropical weather systems on the synoptic scale is limited severely by a near total absence of conventional in-situ observations, particularly over the North Pacific. Analysis procedures are developed to minimize the limitations of satellite sounding data: compositing of numerous events to increase the data coverage and thereby fill in gaps due to cloud contamination and smooth the contamination associated with individual satellite passes; Empirical Orthogonal Function (EOF) decomposition to account for the high vertical correlation within observations; averaging and filtering to isolate and identify weak and poorly observed signals; and, nonlinear regression to quantify previously detected synoptic signals. Three months (January to March 1984) of multichannel radiance data form sounders on NOAA-7 and 8 are analyzed to extract the synoptic scale information content. Two synoptic systems are isolated and investigated: tropical plumes; and, a 2800 km tropospheric thermal wave believed to be a newly observed feature of the tropical atmosphere.

Dissert. Abstr.

N90-14746 State Univ. of New York, Albany.
INVERTED SURFACE TROUGHS ACCOMPANYING ROCKY MOUNTAIN LEE-SIDE CYCLOGENESIS Ph.D. Thesis
Len George Keshishian 1989 292 p
Avail: Univ. Microfilms Order No. DA8919341

A unique type of cyclone developing to the lee of the Rocky Mountains that does not conform to the polar-front cyclone model described by Bjerknes and Solberg (1922) is examined. The distinguishing surface feature occurs in the form of an inverted trough accompanying lee-side cyclogenesis. A climatology based upon an examination of the colder months (October to April) during a twelve year period (1974 to 1986) revealed 42 cases of in situ inverted trough formation accompanying cyclogenesis to the lee of the Rocky Mountains. Using Northern Hemisphere gridded analyses archived on compact disc, composites of 850 mb and 500 mb height and thermal fields, and sea-level pressure and temperature fields were generated. These composites comprised 16 selected cases of inverted trough formation over an arbitrarily chosen geographical domain to the lee of the mountains. Similar composites for cyclogenesis without inverted trough formation were generated to compare the synoptic-scale environment and the quasi-geostrophic forcing associated with each. The comparative study suggests that the large-scale forcing of vertical motion for the IT composite was crucial in producing a synoptic-scale flow regime favorable for focussing a zone of warm air advection over the central and northern Plains to the lee of the Rockies. The inverted trough formed in response to sea-level pressure falls associated with the thermal advection pattern.

Dissert. Abstr.

N90-14747 Oklahoma Univ., Norman.
THE DYNAMICS OF SIMULATED CONVECTIVE STORMS IN HURRICANE ENVIRONMENTS Ph.D. Thesis
Eugene Williamson McCaul, Jr. 1989 194 p
Avail: Univ. Microfilms Order No. DA8921090

Numerical simulations of convection in selected hurricane environments show that supercell storms are possible, even when buoyancy is relatively small. In one simulated supercell, the dynamic pressure force is found to reach a maximum about three times as strong as that of buoyancy in the late stages of the simulation. Updrafts reach peak intensity at low levels, often around 2 to 3 km AGL, and may exceed magnitudes expected from consideration of moist CAPE alone. Interactions between updraft and ambient vertical shear, and, later, growing contributions from vorticity, appear to dominate the development of the dynamic pressure field. Although the weak byoyancy tends to restrict storm intensity, a favorable matching of the vertical distribution of buoyancy with that of the vertical shear allows the pressure forces to become strong enough to take up the slack. Terms in the disturbance kinetic energy budget are correspondingly more strongly influenced by pressure effects than by buoyancy. Although the simulated supercells display the very strong, organized rotation characteristic of tornadic storms, many of the multicell storms which appear in the simulation also contain local concentrations of vorticity intense enough to suggest tornado potential.

Dissert. Abstr.

N90-14748# Illinois State Water Survey, Champaign.
FREQUENCY DISTRIBUTIONS OF HEAVY RAINSTORMS IN ILLINOIS
Floyd A. Huff and James R. Angel 1989 42 p Sponsored in part by Illinois Dept. of Transportation, Div. of Water Resources (PB90-100215; ISWS/CIR-172/89) Avail: NTIS HC A03/MF A01 CSCL 04B

A condensed version is presented of an extensive report on the distribution of heavy rainstorms in Illinois, based on data for 61 precipitation stations operated during 1901 to 1983. Shown are annual frequency distributions of point rainfall for periods ranging from 5 minutes to 10 days and for recurrence intervals varying from 2 months to 100 years. Results are presented in two forms: mean relations for 10 regions of approximately homogeneous precipitation climate, and statewide isohyetal maps based on the 61 station data. Also discussed are the results of an investigation pertaining to Chicago and the surrounding six counties subject to urban influences on the precipitation distribution. Information is provided on the urban influences on the two Illinois counties adjacent to St. Louis.

Author

N90-14749# National Weather Service, Fort Worth, TX. Scientific Services Div.
SUMMARY OF PAPERS, STUDIES, CONFERENCE PRESENTATIONS: 1987-1988 (FROM THE NATIONAL WEATHER SERVICE, SOUTHERN REGION)
Sep. 1989 21 p
(PB90-103896; NOAA-TM-NWS-SR-126) Avail: NTIS HC A03/MF A01 CSCL 04B

This document, the first in a projected annual series, is a summary of information provided by the National Weather Service Southern Region offices. It lists publications, technical presentations, and local studies undertaken or accomplished in the Region during 1987 and 1988. GRA

N90-14750# National Weather Service, Silver Spring, MD. Techniques Development Lab.
USE OF OPERATIONAL 0-6 AND 3-9 h QUANTITATIVE PRECIPITATION FORECASTS FOR PREDICTING HEAVY RAIN EVENTS
Jerome P. Charba and Joel T. Moeller Jun. 1989 41 p
(PB90-103946; NOAA-TM-NWS-TDL-80) Avail: NTIS HC A03/MF A01 CSCL 04B

New 0-6 and 3-9 h objective quantitative precipitation forecasts (OBJ) for the coterminous U.S. were recently implemented in the National Weather Service. The forecasts are issued in the form of isohyets of both the maximum point precipitation amount and the probability of equalling or exceeding specific amounts in the 40 x 40 n mi boxes. After taking into account differences in the event forecast, the performance of the isohyetical maximum amounts were compared with manual and model generated quantitative precipitation forecasts (QPF's) issued 2 to 12 hrs earlier from the National Meteorological Center. Results show the accuracy of the OBJ forecasts was substantially better than the longer range NMC QPF's, particularly for the heavier amounts. Author

N90-14751# National Center for Atmospheric Research, Boulder, CO.
WORKSHOP ON SYNOPTIC METEOROLOGY INSTRUCTION
Robert Gall, George Huffman, and Carlyle Wash Jul. 1989 197 p Workshop held in Boulder, CO, 25-29 Jul. 1989
(Grant NSF ATM-87-09659)
(PB90-109950) Avail: NTIS HC A09/MF A02 CSCL 04B

As hardware and software systems for interactive computer processing of weather data become more affordable, transportable, and powerful, their use in the synoptic meteorology classroom is not only possible but necessary for the training of modern meteorologists. For this reason synoptic meteorology instructors have been evaluating the role these systems will play in the classroom and how to incorporate their capabilities into the curriculum. In addition to the opportunities presented by microcomputers, a number of new observational systems have been developed that will dramatically alter the ability to diagnose the current state of the atmosphere. As with the computer driven display systems, output from these new data sources will have to be incorporated into synoptic meteorology instruction. In light of these new observational and computational capabilities, this was considered to be an excellent time to organize a workshop on synoptic meteorology instruction. The workshop proceedings are presented. Author

N90-14752# National Center for Atmospheric Research, Boulder, CO. Climate and Global Dynamics Div.
A GLOBAL OCEAN WIND STRESS CLIMATOLOGY BASED ON ECMWF (EUROPEAN CENTRE FOR MEDIUM RANGE WEATHER FORECASTS) ANALYSES
Kevin E. Trenberth, Jerry G. Olson, and William G. Large Aug. 1989 98 p
(Grants NSF ATM-87-09659; NA86AA-N-RG0100)
(PB90-109968; NCAR/TN-338+STR) Avail: NTIS HC A05/MF A01 CSCL 04B

Computations of the surface wind stress over the global oceans have been made using surface winds from the ECMWF for 7 years. The drag coefficient is a function of wind speed and atmospheric stability, and the density is computed for each observation. Seven year climatologies of wind stress, wind stress curl and Sverdrup transport are computed and compared with those of other studies. The interannual variability of these quantities over the 7 years is presented. Results of the long term and individual monthly means are archived and available at NCAR. It is anticipated that these fields will be useful for driving ocean general circulation models. The wind stress statistics over the southern oceans are believed to be the most reliable available because of the paucity of direct wind observations. The main shortcomings with the current results are in the tropics. Author

N90-14753# California Inst. of Tech., Pasadena. Environmental Engineering Labs.
CHARACTERIZATION OF CLOUD CHEMISTRY AND FREQUENCY OF CANOPY EXPOSURE TO CLOUDS IN THE SIERRA NEVADA Final Report
Michael R. Hoffmann, Jeffrey L. Collett, Jr., and Bruce C. Daube, Jr. Mar. 1989 344 p
(Contract ARB-A6-185-32)
(PB89-104035; ARB-R-89/408) Avail: NTIS HC A15/MF A02 CSCL 04B

The objectives of the study were to characterize the frequency of cloud intereption in the Sierra Nevada of central California as a function of elevation; to determine the spatial and temporal variation in the chemical composition of the intercepted cloudwater; and to investigate the relationship between cloudwater chemistry and the concentration of precursor aerosol and gases. Cloudwater sampled in Sequoia National Park had pH values ranging from 4.4 to 5.7. The advance of cold fronts into the park appears to lead to higher aerosol and gas phase pollutant concentrations that are seen under normal mountain/valley circulation, producing higher cloudwater concentrations than might otherwise be expected. Estimates of annual deposition rates of NO3, SO4(-2), NH4(+), and H(+) due to cloudwater impaction are comparable to those measured in precipitation. Author

N90-14754*# Clemson Univ., SC. Radar Systems Lab.
THE EFFECTS OF CLUTTER-REJECTION FILTERING ON ESTIMATING WEATHER SPECTRUM PARAMETERS
W. T. Davis 28 Jul. 1989 96 p
(Grants NAG1-928; NGT-70055)
(NASA-CR-186212; NAS 1.26:186212; TR-10) Avail: NTIS HC A05/MF A01 CSCL 04B

The effects of clutter-rejection filtering on estimating the weather parameters from pulse Doppler radar measurement data are investigated. The pulse pair method of estimating the spectrum mean and spectrum width of the weather is emphasized. The loss of sensitivity, a measure of the signal power lost due to filtering, is also considered. A flexible software tool developed to investigate these effects is described. It allows for simulated weather radar data, in which the user specifies an underlying truncated Gaussian spectrum, as well as for externally generated data which may be real or simulated. The filter may be implemented in either the time or the frequency domain. The software tool is validated by comparing unfiltered spectrum mean and width estimates to their true values, and by reproducing previously published results. The effects on the weather parameter estimates using simulated weather-only data are evaluated for five filters: an ideal filter, two infinite impulse response filters, and two finite impulse response filters. Results considering external data, consisting of weather and clutter data, are evaluated on a range cell by range cell basis. Finally, it is shown theoretically and by computer simulation that a linear phase response is not required for a clutter rejection filter preceeding pulse-pair parameter estimation. Author

N90-14755# Brown Univ., Providence, RI. Dept. of Geological Sciences.
EVALUATION OF CLIMATIC MODELS: COMPARISON OF SIMULATED AND OBSERVED PATTERNS FOR PAST CLIMATES Progress Report, 1 Feb. 1989 - 31 Jan. 1990
Warren L. Prell, Thompson Webb, III, and John E. Kutzbach

(Wisconsin Univ., Madison.) Oct. 1989 19 p
(Contract DE-FG02-85ER-60304)
(DE90-001228; DOE/ER-60304/5) Avail: NTIS HC A03/MF A01

Comparison of the general circulation model (GCM) results with paleoclimatic data can yield critical tests of the models that are being used in carbon dioxide research. In particular, the comparison of model results with paleoclimatic data can illustrate the sensitivity of the model's response to variations in the seasonal radiation budget as well as to changes in other boundary conditions. These comparisons also provide the opportunity to check the sensitivity of the climatic response of critical components of the climate system such as sea-ice and soil moisture. During the past several years, paleoclimatic data was used to test NCAR CCM (National Center for Atmospheric Research, Community Climate Model) after changing its boundary conditions to those appropriate for simulating past climates. Regional and global paleoclimatic data sets of pollen, lake level, and marine plankton data were assembled and much of the data was calibrated in climatic terms. Methods were also developed that permit direct quantitative comparisons between the data and model results. These comparisons show some of the strengths and weaknesses of the model. DOE

N90-14756# Lawrence Livermore National Lab., CA.
CLIMATOLOGY OF LAWRENCE LIVERMORE NATIONAL LABORATORY
Frank J. Gouveia and K. Renee Chapman Sep. 1989 208 p
(Contract W-7405-eng-48)
(DE90-000905; UCID-21686) Avail: NTIS HC A10/MF A02

Meteorological data collected from 1979 to 1987 at Lawrence Livermore National Laboratory are analyzed in this report. These data are 15-min averages of wind speed, wind direction, standard deviation of the wind direction, temperature, and relative humidity. Calculated values include crosswind turbulence, absolute humidity, and stability class. Hourly averages were computed and used for most of the analysis. Frequency distributions of wind speed and horizontal wind fluctuations as well as joint frequency distributions of wind speed, wind direction, and stability are presented. The data show a marked seasonal variability and this phenomenon is explored in depth. An example is presented to show how the data set may be queried to find the probability of a specific set of meteorological conditions. In addition, a comparison is made of these data and data from another tower located nearby. The data are very similar despite slight differences, which may be explained by differences between the sampling locations in surface roughness and proximity to buildings. DOE

N90-14757# Pacific Northwest Lab., Richland, WA.
METEOROLOGICAL MONITORING FOR ENVIRONMENTAL/DOSE ASSESSMENT AND EMERGENCY RESPONSE MODELING: HOW MUCH IS ENOUGH
Clifford S. Glantz 1989 10 p Presented at the 28th Hanford Life Sciences Symposium on Environmental Monitoring, Restoration and Assessment: What Have We Learned, Richland, WA, 16-19 Oct. 1989
(Contract DE-AC06-76RL-01830)
(DE90-002726; PNL-SA-17367; CONF-891053-9) Avail: NTIS HC A02/MF A01

In evaluation the effectiveness and appropriateness of meteorological monitoring programs, managers responsible for planning and operating emergency response or environmental/dose assessment systems must routinely question whether enough meteorological data are being obtained to adequately support system applications. There is no simple answer or cookbook procedure that can be followed in generating an appropriate answer to this question. The answer must be developed through detailed consideration of the intended applications for the data, the capabilities of the models that would use the data, pollutant release characteristics, terrain in the modeling region, the size of the modeling domain, and the distribution of human population in the modeling domain. It is recommended that manager consult meteorologists when assessing these factors; the meteorologist's detailed knowledge of, and experience in, studying atmospheric transport and diffusion should assist the manager in determining the appropriate level of meteorological monitoring. DOE

48 OCEANOGRAPHY

Includes biological, dynamic, and physical oceanography; and marine resources.

For related information see also *43 Earth Resources and Remote Sensing.*

N90-14758# National Academy of Sciences - National Research Council, Washington, DC. Ocean Studies Board.
MID-OCEANIC RIDGE: A DYNAMIC GLOBAL SYSTEM
1988 342 p Proceedings of a Workshop held in Gleneden Beach, OR, 6-10 Apr. 1987
(PB89-198691) Avail: NTIS HC A15/MF A02 CSCL 08C

The topics discussed include: Seafloor measurements--future developments; Applications of gravity data in mid-ocean ridge studies; Mid-ocean ridge processes; Magnetic studies; A research perspective for marine multichannel seismic research on mid-ocean ridges; Electromagnetic methods in mid-ocean ridge studies; Seafloor positioning; Seafloor sampling; Two ideas and some comments on remotely-operated vehicles. GRA

N90-14759# National Marine Fisheries Service, Seattle, WA. Resource Ecology and Fisheries Management Div.
TUNING OF THE OSCURS (OCEAN SURFACE CURRENT SIMULATIONS) NUMERICAL MODEL TO OCEAN SURFACE MEASUREMENTS IN THE GULF OF ALASKA
W. James Ingraham, Jr. and Robert K. Miyahara Aug. 1989 74 p
(PB89-103979; NOAA-TM-NMFS-F/NWC-168) Avail: NTIS HC A04/MF A01 CSCL 08C

An empirical model for numerical ocean surface current simulations (OSCURS) that was developed in 1988 to analyze variability in Lagrangian drift in the North Pacific Ocean and Bering Sea (north of lat. 35 N) was assessed. The model, which computes currents from the vector sum of geostrophic current plus wind drift, was tuned with data from the Gulf of Alaska, collected in 1978 with satellite tracked drifters drogued at 20 m. By applying incremented linear tuning coefficients to find the best fit, its sensitivity to several functions was evaluated for computing drift speed and angle of deflection of the current to the right of the wind. Despite limitations due to the computation of winds from Fleet Numerical Oceanography Center gridded sea level pressure data, the 90 km grid size, and the once daily time step, remarkably good visual agreement was obtained between the model's progressive vector tracks and two out of the three drifters available. Author

N90-14760# Indiana Univ., Bloomington. Dept. of Chemistry.
ORGANIC GEOCHEMICAL AND TECTONIC EVOLUTION OF THE MIDCONTINENT RIFT SYSTEM: ORGANIC GEOCHEMISTRY AND MICROPALEONTOLOGY Progress Report
J. M. Hayes, L. M. Pratt, and Andrew H. Knoll (Harvard Univ., Cambridge, MA.) Jun. 1989 33 p
(Contract DE-FG02-88ER-13978)
(DE89-017561; DOE/ER-13978/1) Avail: NTIS HC A03/MF A01

Siltstones and shales of the mid-Proterozoic Nonesuch Formation are widely postulated to be effective petroleum source rocks based on the occurrence of active oil seeps and tarry residues within parts of the Copper Range Mine. Most previous organic geochemical research has focused on mineralized sedimentary strata and associated oils in the lower-most 5 meters of the Nonesuch Formation exposed in mine excavations. Recently, non-mineralized sediments from outcrops along the shore of Lake Michigan and exploration cores drilled along the subsurface trend to the east of White Pine have been studied. Substantial variation in the lateral and vertical distribution of fine-grained facies within

the Nonesuch is apparent from our studies of the non-mineralized suites of samples. Research at Indiana University is focused on the relationship between organic geochemistry and depositional environment in the Nonesuch Formation. Our principal objectives are: (1) to describe the distribution of fine-grained lithofacies; (2) to determine organic-carbon, carbonate-carbon, and total-sulfur contents of these units; (3) to characterize the extractable bitumen and conduct preliminary analyses of selected biomarkers (hopanoids, steroids, and monomethyl-substituted cyclohexyl alkanes); and (4) to infer the depositional environment and biological affinities of organic matter preserved in the Nonesuch. DOE

51 LIFE SCIENCES (GENERAL)

N90-14761*# Florida Univ., Gainesville. Dept. of Aerospace Engineering.
ENGINEERING SCIENCES DESIGN. DESIGN AND IMPLEMENTATION OF COMPONENTS FOR A BIOREGENERATIVE SYSTEM FOR GROWING HIGHER ORDER PLANTS IN SPACE Final Report
Gale E. Nevill, Jr. Apr. 1989 106 p
(Contract NASw-4435)
(NASA-CR-186056; NAS 1.26:186056; EGM-4001) Avail: NTIS HC A06/MF A01 CSCL 06C

The primary goal was to address specific needs in the design of an integrated system to grow higher plants in space. With the needs defined, the emphasis was placed on the design and fabrication of devices to meet these needs. Specific attention was placed on a hand-held harvester, a nutrient concentration sensor, an air-water separator, and a closed-loop biological system simulation. Author

N90-14762# Florida Univ., Gainesville. Dept. of Physiology.
HIGH-FREQUENCY VENTILATION IN DOGS WITH THREE GASES OF DIFFERENT DENSITIES Final Technical Report
Marc L. Jaeger Aug. 1989 75 p
(Contract N00014-85-K-0123)
(AD-A212862) Avail: NTIS HC A04/MF A01 CSCL 23/5

Dogs were ventilated with a high frequency oscillation, HFO, device varying the frequency (2 to 20 Hz), the tidal volume (25 to 100 ml), and the resident gas (He, N2, SF6). Tidal volume was measured with a body plethysmograph. Blood gases were measured after a quasi steady state was established. The kinematic viscosity of the breathing gas mixture, which changed by 1700 pct, was found to have little effect on arterial P(sub O2) and P(sub CO2). The results are consistent with findings in a model which consisted of tubes of different diameters and with the theory of Taylor-type diffusion. In addition, experiments were performed reducing and increasing the equipment dead space. This resulted in changes of P(sub O2) and that were appreciably less than those resulting from variations of tidal volume of the same magnitude. These results suggest that, high frequency ventilation (HFV), at increased and decreased ambient pressure is technically possible. GRA

N90-14763*# Lockheed Engineering and Sciences Co., Washington, DC.
USSR SPACE LIFE SCIENCES DIGEST. INDEX TO ISSUES 21-25
Lydia Razran Hooke, ed. NASA 31 Jan. 1990 100 p
(Contract NASw-4292)
(NASA-CR-3922(30); NAS 1.26:3922(30)) Avail: NTIS HC A08 CSCL 06C

This bibliography provides an index to issues 21 through 25 of the USSR Space Life Sciences Digest. There are two sections. The first section lists bibliographic citations of abstracts in these issues, grouped by topic area categories. The second section provides a key word index for the same abstracts. The topic categories include exobiology, space medicine and psychology, human performance and man-machine systems, various life/body systems, human behavior and adaptation, biospherics, and others. Author

N90-14764# Argonne National Lab., IL. Chemistry Div.
FACTORS AFFECTING ELECTRON SPIN POLARIZATION IN PHOTOSYNTHETIC SYSTEMS
M. C. Thurnauer, L. L. Feezel, A. L. Morris, U. Smith, and J. R. Norris 1989 4 p Presented at the 8th International Congress on Photosynthesis, Stockholm, Sweden, 6-11 Aug. 1989 Submitted for publication
(Contract W-31-109-eng-38)
(DE90-000196; CONF-8908117-6) Avail: NTIS HC A01/MF A01

A model was developed for the electron spin polarized (esp) in P(sub 870)(sup +)Q(sup -) which includes contributions of both P(sub 870)(sup +)I(sup -) and P(sub 870)(sup +)Q(sup -) interactions to the esp of P(sub 870)(sup +)Q(sup -). It was shown how factors such as kinetics, magnetic interactions, and structure affect the esp. This model can then be applied to assess the esp in PSI in terms of primary electron transfer steps. DOE

N90-14765# Northwestern Univ., Evanston, IL. Dept. of Biochemistry, Molecular Biology, and Cell Biology.
COMPARISON OF STRUCTURAL SUBUNITS OF THE CORE LIGHT-HARVESTING COMPLEXES OF PHOTOSYNTHETIC BACTERIA
Paul A. Loach, Pamela S. Parkes-Loach, Mary C. Chang, Barbara A. Heller, Peggy L. Bustamante, and Tomasz Michalski (Argonne National Lab., IL.) 1989 10 p Presented at the Molecular Biology of Photosynthetic Prokaryotea Symposium, Freiburg, Fed. Republic of Germany, 2-5 Aug. 1989 Submitted for publication
(Contract W-31-109-eng-38; GM-11741; NSF DMB-87-17997)
(DE90-001412; CONF-8908164-1) Avail: NTIS HC A03/MF A01

Development of the biochemical methodology for preparation of structural subunits of the core LH complex and their reconstitution from individual components has provided a tool for probing structure-function relationships at three different levels: BCh1 binding, polypeptide interaction within the LH complex, and interaction between the LH complex and the RC. Further cultivation of this experimental approach should provide improved knowledge about how BCh1 is bound and how the LH complex performs its function. DOE

N90-14766# California Univ., Berkeley. Lawrence Berkeley Lab.
X RAY MICROIMAGING FOR THE LIFE SCIENCES
David Attwood, ed. and Bob Barton, ed. Aug. 1989 206 p Presented at the Conference on X ray Microimaging for the Life Sciences, Berkeley, CA, 24-26 May 1989
(Contract DE-AC03-76SF-00098)
(DE90-002613; LBL-27660; CONF-8905192) Avail: NTIS HC A10/MF A02

The workshop brought together the physical and biological science communities to explore the potential for imaging of macromolecular to sub-organelle structures, in their natural state, with spacial resolutions beyond those hitherto demonstrated. Emphasis was on direct imaging techniques applied to biological problems of structure and function, sequencing, and mapping. The requisite high brightness radiation sources, such as short wavelength undulators and x ray lasers, were also addressed. In addition there were overviews of current and projected capabilities utilizing tunneling techniques, electron microscopy, and x ray crystallographic techniques. Individual papers are processed separately for the data base. DOE

52 AEROSPACE MEDICINE

Includes physiological factors; biological effects of radiation; and effects of weightlessness on man and animals.

N90-14767 Temple Univ., Philadelphia, PA.
THE EFFECTS OF NONSELECTIVE AND SELECTIVE BETA BLOCKADE UPON NONSHIVERING THERMOGENESIS DURING AN ACUTE COLD EXPOSURE IN COLD ACCLIMATED MEN Ph.D. Thesis
Kyriakos M. Evrenoglou 1989 131 p
Avail: Univ. Microfilms Order No. DA8920240

The effects of nonselective and selective beta blockage upon nonshivering thermogenesis during an acute cold exposure in acclimated men was determined. Thermoregularity measurements were conducted in both a neutral (25 C) climate and a cold (5 C) climate. The data collected for each subject in each of the six experimental sessions consisted of heart rate (HR), oxygen consumption (VO2), core temperature (Tr), mean skin temperature (Ts), mean body temperture (Tb), shivering (EMG), and forearm blood flow (FBF). The experimental population consisted of four male subjects with a mean age of 18 and 22. All subjects were previously cold acclimated. Three drug treatments were employed in which each drug was given twice, once during the neutral exposure and the other during the cold exposure. Each subject was given either a placebo, propranolol, (1.05 mg/kg.wt), or atenolol (50 mg). Dissert. Abstr.

N90-14768# Food and Drug Administration, Rockville, MD. Center for Devices and Radiological health.
BIOLOGICAL EFFECTS OF HYPERTHERMIA AND POTENTIAL RISK ASSOCIATED WITH ULTRASONIC EXPOSURE
Benjamin R. Fisher Jul. 1989 30 p
(PB89-100702; FDA/CDRH-89/106) Avail: NTIS HC A03/MF A01 CSCL 06S

The high intensities that have been reported in 510(k) applications for some diagnostic ultrasound devices, particularly pulsed Doppler cardiovascular units, cause concern about the safety of these devices. The average intensities of some of these devices approach the intensity levels used for therapeutic heating. This concern is further heightened by reports on the use of pulsed Doppler devices to monitor blood flow in the fetal heart, placenta, and ovarian umbilical vessels. The purpose of the report is to provide an overview of the potential biological consequences that may result from exposure to high temporal average ultrasound intensities. A thermal mechanistic approach is used for the analysis because: (1) thermal effects are the predominant consequence of high temporal average intensitites; (2) heating is the best understood mechanism of action of ultrasound; and (3) a thermal approach is supported by substantial data in the literature.
Author

53 BEHAVIORAL SCIENCES

Includes psychological factors; individual and group behavior; crew training and evaluation; and psychiatric research.

N90-14769# Office of Naval Research, Arlington, VA.
COGNITIVE AND NEURAL SCIENCES DIVISION 1989 PROGRAMS Summary Report, 1 Oct. 1988 - 30 Sep. 1989
Willard S. Vaughan Sep. 1989 244 p
(AD-A212634; OCNR-114289-22) Avail: NTIS HC A11/MF A02 CSCL 05/8

Cognitive and Neural Sciences programs develop fundamental knowledge about human capabilities and performance characteristics which guide Navy and Marine Corps efforts to improve personnel assessments for selection and classification, training, equipment and system designs for human operation and maintenance. One goal is to provide scientific underpinning for more accurate prediction and enhancement of human performance in training and operational environments. A second goal is to understand the neurobiological constraints and computational capabilities of neural information processing systems for future device implementation. The Division has core programs in cognitive, perceptual and neural sciences which seek to understand human behavior at successively deeper levels of analysis. GRA

N90-14770# Lawrence Livermore National Lab., CA.
MIPS AND BIPS ARE MEGAFLOPS: LIMITS OF UNIDIMENSIONAL ASSESSMENTS
William W. Banks and Michael Pihlman Jul. 1989 7 p Presented at the 33rd Annual Meeting of Human Factors Society, Denver, CO, 16-20 Oct. 1989
(Contract W-7405-eng-48)
(DE89-015707; UCRL-101061-Rev-1; CONF-8910155-2-Rev-1)
Avail: NTIS HC A02/MF A01

We believe that a failure to incorporate human performance measures into system test protocols will result in imprecise and incomplete data when attempting to estimate field test performance from a total systems perspective. Traditional methods of evaluating local area network (LAN) performance generally refer to the network's throughput, time delays, data rate (BIPS), or media access protocol efficiency. These measures are quite acceptable when determining point-to-point benchmark network performance but do not take into account the more global man-machine performance issues associated with people using network systems to perform tasks and execute functions concurrently within a total systems context. This paper experimentally compares differences in human productivity and efficiency while using: an existing data gathering system consisting of several geographically distributed, unconnected, and disparate mainframes; and a prototype Intelligent Gateway connecting mainframes and offering the user less complexity in procedure execution and an easy to use interface. Tests were conducted with volunteer users in a repeated measures experimental design. Each test subject was randomly assigned to each of two conditions and required to execute routine tasks with each of two systems. Analysis of variance (ANOVA) results revealed significant differences in task completion times and human error rates between the two systems. An increase in human productivity/efficiency was observed using the gateway LAN. We propose to extend the traditional computer performance measurement boundaries, which now encompass only the network hardware, to include an overall input-to-output LAN performance measure, combining both measures of user productivity and network performance. A discussion of trade-offs between unidimensional assessment methods using large sample sizes and multiple methods with small sample sizes is also presented.
DOE

N90-14771# Los Alamos National Lab., NM.
WORKLOAD INDUCED SPATIO-TEMPORAL DISTORTIONS AND SAFETY OF FLIGHT
Christopher L. Barrett and Scott A. Weisgerber (Naval Weapons Center, China Lake, CA.) 1989 19 p Presented at the Advisory Group for Aerospace Research and Development (AGARD) Meeting, Copenhagen, Denmark, 2-6 Oct. 1989
(Contract W-7405-eng-36)
(DE89-016613; LA-UR-89-2895; CONF-8910208-1) Avail: NTIS HC A03/MF A01

A theoretical analysis of the relationship between cognitive complexity and the perception of time and distance is presented and experimentally verified. Complex tasks produce high rates of mental representation which affect the subjective sense of duration and, through the subjective time scale, the percept of distance derived from dynamic visual cues (i.e., visual cues requiring rate integration). The analysis of the interrelationship of subjective time and subjective distance yields the prediction that, as a function of cognitive complexity, distance estimates derived from dynamic visual cues will be longer than the actual distance whereas estimates based on perceived temporal duration will be shorter than the actual distance. This prediction was confirmed in an experiment in which subjects (both pilots and non-pilots) estimated distances using either temporal cues or dynamic visual cues. The distance estimation task was also combined with secondary loading tasks in order to vary the overall task complexity. The results

indicated that distance estimates based on temporal cues were underestimated while estimates based on visual cues were overestimated. This spatio-temporal distortion effect increased with increases in overall task complexity. DOE

54 MAN/SYSTEM TECHNOLOGY AND LIFE SUPPORT

Includes human engineering; biotechnology; and space suits and protective clothing.

For related information see also *16 Space Transportation.*

N90-14772# Civil Aeromedical Inst., Oklahoma City, OK.
PERFORMANCE EVALUATION OF THE PURITAN-BENNETT CREW-MEMBER PORTABLE PROTECTIVE BREATHING DEVICE AS PRESCRIBED BY PORTIONS OF FAA ACTION NOTICE A-8150.2 Final Report
E. A. Higgins, G. A. McLean, P. J. Lyne, G. E. Funkhouser, and J. W. Young May 1989 101 p
(AD-A211113; DOT/FAA/AM-89-8) Avail: NTIS HC A06/MF A01 CSCL 05/8

This study was undertaken, on request, to evaluate the performance of the Puritan-Bennett portable crew protective breathing device for contaminant leaks. Tests were conducted in the facilities of the FAA Civil Aeromedical Institute (CAMI) in Oklahoma City, OK. The test sequence followed an iterative process in which problems were identified, modifications made to correct deficiencies, and the device retested until problems could be solved. With adequate quality assurance, the final version of the Puritan-Bennett crewmember portable protective breathing device, as tested at CAMI, would meet the requirements of FAA's Action Notice A-8150.2 regarding contaminant leak protection, O2 concentration, CO2 concentration, inhalation/exhalation pressures and inhalation temperature. GRA

N90-14773# Federal Aviation Administration, Oklahoma City, OK. Civil Aeromedical Inst.
COMPARISON OF PROTECTIVE BREATHING EQUIPMENT PERFORMANCE AT GROUND LEVEL AND 8,000 FEET ALTITUDE USING PARAMETERS PRESCRIBED BY PORTIONS OF FAA ACTION NOTICE A-8150.2 Final Report
T. T. Schlegel, E. A. Higgins, G. A. McLean, P. J. Lyne, H. M. England, and P. A. Attocknie Jun. 1989 19 p
(AD-A212852; DOT/FAA/AM-89-10) Avail: NTIS HC A03/MF A01 CSCL 23/5

Two types of crewmember protective breathing equipment (PBE) were performance tested for compliance with Action Notice A-8150.2 at ground level (-1,300 feet) and 8,000 feet altitude. PBE 1 was a hood with oral-nasal mask, which used potassium superoxide to remove carbon dioxide and produce its oxygen supply. PBE 2 was a hood only, which contained lithium hydroxide to absorb carbon dioxide and compressed oxygen cylinders to supply breathable air. The parameters tested were PBE oxygen and carbon dioxide levels, temperature, and breathing resistance-pressure. Five units of each PBE type were subjected to testing; for within-PBE comparisons each type of unit was worn by the same human subjects at both altitudes. Relatively little difference in PBE performance was obtained at the different altitudes for both types of PBE. Oxygen partial pressures were somewhat reduced at the higher altitude for both types of PBE, carbon dioxide partial pressure was slightly greater at ground level for PBE 2, internal temperature was higher for PBE performed adequately for the intended purpose at either altitude , but further testing would be necessary to certify PBE to meet additional requirements, such as use at altitudes above 8,000 feet. GRA

N90-14774# Defence and Civil Inst. of Environmental Medicine, Downsview (Ontario).
INTEGRATED G-SUIT/IMMERSION SUIT
James A. Firth and Jean C. Steffler Jun. 1989 32 p
(AD-A212989; DCIEM-89-TR-22) Avail: NTIS HC A03/MF A01 CSCL 06/8

Canadian Forces (CF) aircrew flying CF18 and CF5 aircraft are required to wear anti-G suits to provide protection against the effects of high G forces experienced during air combat maneuvers (ACM). They are also required to wear immersion suits with the G suits on domestic coastal operations to provide protection against hypothermia in the event of an emergency involving ejection and water landing. The standard CF anti-G suit was worn over the immersion suit, which being bulky, created discomfort and contributed to reduced G protection this combination does not permit proper G suit fit on the wearer. The National Defense Headquarters (NDHQ) tasked the Medical Life Support Division (MLSD) of this Institute (DCIEM) to develop a Canadian anti-G suit incorporating fixtures which would allow the anti-G suit to be worn under the immersion. MLSD identified suitable hardware to suit. In conjunction with MLSD support, a Canadian Aerospace Company manufactured two prototype anti-G suits which were successfully integrated with the immersion suit. Subsequent to favorable comments from initial flights trials, NDHQ directed MLSD to procure 20 modified anti-G suits for user trial by designated CF18 and CF5 aircraft squadrons. As a consequence of user trial acceptance, NDHQ has ordered sufficient quantities of the modified anti-G suit and associated immersion suit interface hardware to meet a foreseeable operational requirement. GRA

N90-14775 Surrey Univ., London (England).
THE DEVELOPMENT OF A MODEL OF THE HUMAN RESPONSES TO LOAD CARRIAGE Ph.D. Thesis
Ian P. M. Randle 1988 351 p
Avail: Univ. Microfilms Order No. BRDX85648

Past research on manual load carriage has had very limited applicability to the type of load carriage which occurs in industry. The majority of studies have investigated steady continuous load carriage on the back, rather than the intermittent shuttle type of carry in the arms which is more common in industry. Furthermore concentration was generally on the central cardiovascular or metabolic responses, and paid little attention to local muscle fatigue. The highly stylized modes of carriage used in some previous studies were also shown to differ significantly from the more realistic freely chosen modes used. This further limits their applicability. Although potentially useful, current prediction models for load carriage tasks were found to be inappropriate for intermittent carrying, and had a poor level of agreement. A need was identified therefore to develop prediction models for industrial load carriage tasks, and to make a systematic study of local muscle fatigue in load carriage. A methodology for investigating local muscle fatigue was also developed. Despite high levels of intra- and inter-subject variability in response, this medthodology proved useful in detecting the task conditions which were most associated with peripheral muscle fatigue. Dissert. Abstr.

N90-14776# Oak Ridge National Lab., TN. Engineering Physics and Mathematics Div.
HUMAN FACTORS SURVEY OF ADVANCED INSTRUMENTATION AND CONTROLS
Richard J. Carter 1989 22 p Presented at the 17th Water Reactor Safety Information Meeting, Rockville, MD, 23-25 Oct. 1989
(Contract DE-AC05-84OR-21400)
(DE90-002477; CONF-8910222-5) Avail: NTIS HC A03/MF A01

A survey oriented towards identifying the human factors issues in regard to the use of advanced instrumentation and controls (I and C) in the nuclear industry was conducted. A number of United States (U.S.) and Canadian nuclear vendors and utilities were participants in the survey. Human factors items, subsumed under the categories of computer-generated displays (CGD), controls, organizational support, training, and related topics, were discussed. The survey found the industry to be concerned about the human factors issues related to the implementation of advanced I and C. Fifteen potential human factors problems were identified. They include: the need for an advanced I and C guideline equivalent to

NUREG-0700; a role change in the control room from operator to supervisor; information overload; adequacy of existing training technology for advanced I and C; and operator acceptance and trust. DOE

N90-14777# Edgerton, Germeshausen and Grier, Inc., Idaho Falls, ID.
HUMAN FACTORS EVALUATION OF ELECTROLUMINESCENT DISPLAY NUMBER 1
Jack L. Auflick Aug. 1989 18 p
(Contract DE-AC07-76ID-01570)
(DE90-002231; EGG-HFRU-8654) Avail: NTIS HC A03/MF A01

This report consists of an an electroluminescent display, done by scientists and researchers in the Human Factors Research Unit at EG&G, Idaho, Inc. The purpose of this evaluation was to examine the 'Sunlight Readability' of one electroluminescent (EL) display; a display which may be incorporated into a new generation of US Army diesel generators. The basic finding of this evaluation is that this particular EL display is not sunlight readable. DOE

N90-14408# Forschungsinstitut fuer Anthropotechnik, Wachtberg (Germany, F.R.).
HUMAN FACTORS ASPECTS OF DECISION SUPPORT SYSTEMS
K. F. Kraiss *In* AGARD, Operational Decision Aids for Exploiting or Mitigating Electromagnetic Propagation Effects Sep. 1989 14 p (For primary document see N90-14405 06-32)
Copyright Avail: NTIS HC A20/MF A03

55 SPACE BIOLOGY

Includes exobiology; planetary biology; and extraterrestrial life.

N90-14778*# National Aeronautics and Space Administration, Washington, DC.
EXPLORING THE LIVING UNIVERSE: A STRATEGY FOR SPACE LIFE SCIENCES
Jun. 1988 231 p Original contains color illustrations
(NASA-TM-101891; NAS 1.15:101891) Avail: NTIS HC A11/MF A02 CSCL 06C

The status and goals of NASA's life sciences programs are examined. Ways and mean for attaining these goals are suggested. The report emphasizes that a stronger life sciences program is imperative if the U.S. space policy is to construct a permanently manned space station and achieve its stated goal of expanding the human presence beyond earth orbit into the solar system. The same considerations apply in regard to the other major goal of life sciences: to study the biological processes and life in the universe. A principal recommendation of the report is for NASA to expand its program of ground- and space-based research contributing to resolving questions about physiological deconditioning, radiation exposure, potential psychological difficulties, and life support requirements that may limit stay times for personnel on the Space Station and complicate missions of more extended duration. Other key recommendations call for strengthening programs of biological systems research in: controlled ecological life support systems for humans in space, earth systems central to understanding the effects on the earth's environment of both natural and human activities, and exobiology. J.P.S.

59 MATHEMATICAL AND COMPUTER SCIENCES (GENERAL)

N90-14779*# Institute for Computer Applications in Science and Engineering, Hampton, VA.
KRYLOV METHODS PRECONDITIONED WITH INCOMPLETELY FACTORED MATRICES ON THE CM-2 Final Report
Harry Berryman, Joel Saltz, William Gropp, and Ravi Mirchandaney (Yale Univ., New Haven, CT.) Dec. 1989 11 p Submitted for publication
(Contract NAS1-18605)
(NASA-CR-181961; ICASE-89-54; NAS 1.26:181961) Avail: NTIS HC A03/MF A01 CSCL 12A

The performance is measured of the components of the key interative kernel of a preconditioned Krylov space interative linear system solver. In some sense, these numbers can be regarded as best case timings for these kernels. Sweeps were timed over meshes, sparse triangular solves, and inner products on a large 3-D model problem over a cube shaped domain discretized with a seven point template. The performance of the CM-2 is highly dependent on the use of very specialized programs. These programs mapped a regular problem domain onto the processor topology in a careful manner and used the optimized local NEWS communications network. The rather dramatic deterioration in performance was documented when these ideal conditions no longer apply. A synthetic workload generator was developed to produce and solve a parameterized family of increasingly irregular problems. Author

N90-14780# Argonne National Lab., IL.
PROCEEDINGS OF THE FOCUSED RESEARCH PROGRAM ON SPECTRAL THEORY AND BOUNDARY VALUE PROBLEMS. VOLUME 4: NONLINEAR DIFFERENTIAL EQUATIONS
Gail W. Pieper, ed. Aug. 1989 234 p Program presented in Argonne, IL, 1986-1987
(Contract W-31-109-eng-38)
(DE90-000920; ANL-87-26-Vol-4) Avail: NTIS HC A11/MF A02

Papers are contained for the following topics: Self-Intersecting Solutions of the Prescribed Mean Curvature Equation; Bounds for Vertical Points of Solutions of Prescribed Mean Curvature Type Equations, 1; Large Solutions of Elliptic Equations Involving Critical Exponents; Non-Negative Solutions for a Class of Radially Symmetric Non-Positone Problems; Quenching for Semilinear Singular Parabolic Problems; Existence Results of Steady States of Semilinear Reaction-Diffusion Equations and Their Applications; Uniqueness Results for Some Nonlinear Initial and Boundary Value Problems; Uniqueness of Non-Negative Solutions of a Class of Semilinear Elliptic Equations; A Non-Oscillation Theorem for the Emden-Fowler Equation; Ground States for Semilinear Elliptic Equations with Critical Exponents; Concavity and Monotonicity Properties of Solutions of Emden-Fowler Equations; Uniqueness for a Class of Non-Linear Initial Value Problems; Oscillation of Emden-Fowler Systems; and Local and Global Properties of Solutions of Quasilinear Elliptic Equations. These papers will be indexed separately. DOE

N90-14781# Argonne National Lab., IL. Mathematics and Computer Science Div.
RESEARCH IN MATHEMATICS AND COMPUTER SCIENCE AT ARGONNE, JULY 1, 1986 TO JANUARY 6, 1988
Gail W. Pieper, ed. 1988 71 p
(Contract W-31-109-eng-38)
(DE88-010343; ANL-88-18) Avail: NTIS HC A05/MF A01

The research activities in the Mathematics and Computer Science Division at Argonne National Laboratory are reviewed. A brief look is given at the MCS staff and the research facilities, and discusses various projects carried out in two major areas of research: analytical and numerical methods and advanced computer systems concepts. Information on division staff, visitors, workshops, and seminars is found in the appendixes. DOE

60 COMPUTER OPERATIONS AND HARDWARE

Includes hardware for computer graphics, firmware, and data processing.

For components see *33 Electronics and Electrical Engineering.*

N90-14782# Lawrence Livermore National Lab., CA. Computer Center.
HIGH PERFORMANCE PARALLEL ARCHITECTURES
Roger E. Anderson Sep. 1989 7 p Presented at the Supercomputing '89 Conference, Reno, NV, 13-17 Nov. 1989
(Contract W-7405-eng-48)
(DE90-001055; UCRL-101911; CONF-891149-7) Avail: NTIS HC A02/MF A01

Current high performance parallel computer architectures are compared. A taxonomy is presented to show computer architecture from the user programmer's point-of-view. The effects of the taxonomy upon the programming model are described. Some current architectures are described with respect to the taxonomy. Finally, some predictions about future systems are presented. DOE

N90-14783*# Sverdrup Technology, Inc., Cleveland, OH.
USER'S GUIDE TO PMESH: A GRID-GENERATION PROGRAM FOR SINGLE-ROTATION AND COUNTERROTATION ADVANCED TURBOPROPS Final Report
Saif A. Warsi Dec. 1989 25 p
(Contract NAS3-24105)
(NASA-CR-185156; E-5152; NAS 1.26:185156) Avail: NTIS HC A03/MF A01 CSCL 09B

A detailed operating manual is presented for a grid generating program that produces 3-D meshes for advanced turboprops. The code uses both algebraic and elliptic partial differential equation methods to generate single rotation and counterrotation, H or C type meshes for the z - r planes and H type for the z - theta planes. The code allows easy specification of geometrical constraints (such as blade angle, location of bounding surfaces, etc.), mesh control parameters (point distribution near blades and nacelle, number of grid points desired, etc.), and it has good runtime diagnostics. An overview is provided of the mesh generation procedure, sample input dataset with detailed explanation of all input, and example meshes. Author

N90-14784*# Southwest Research Inst., San Antonio, TX.
HIGH VOLUME DATA STORAGE ARCHITECTURE ANALYSIS Final Report
James M. Malik 19 Jan. 1990 39 p
(Contract NCC9-16; SwRI Proj. 05-3269)
(NASA-CR-186239; NAS 1.26:186239) Avail: NTIS HC A03/MF A01 CSCL 09B

A High Volume Data Storage Architecture Analysis was conducted. The results, presented in this report, will be applied to problems of high volume data requirements such as those anticipated for the Space Station Control Center. High volume data storage systems at several different sites were analyzed for archive capacity, storage hierarchy and migration philosophy, and retrieval capabilities. Proposed architectures were solicited from the sites selected for in-depth analysis. Model architectures for a hypothetical data archiving system, for a high speed file server, and for high volume data storage are attached. J.P.S.

61 COMPUTER PROGRAMMING AND SOFTWARE

Includes computer programs, routines, alogorithms, and specific applications, e.g., CAD/CAM.

N90-14785*# Colorado Univ., Boulder. Dept. of Electrical and Computer Engineering.
FORCE USER'S MANUAL: A PORTABLE, PARALLEL FORTRAN Final Report
Harry F. Jordan, Muhammad S. Benten, Norbert S. Arenstorf, and Aruna V. Ramanan Washington Jan. 1990 38 p
(Grant NAG1-640)
(NASA-CR-4265; NAS 1.26:4265) Avail: NTIS HC A03/MF A01 CSCL 09B

The use of Force, a parallel, portable FORTRAN on shared memory parallel computers is described. Force simplifies writing code for parallel computers and, once the parallel code is written, it is easily ported to computers on which Force is installed. Although Force is nearly the same for all computers, specific details are included for the Cray-2, Cray-YMP, Convex 220, Flex/32, Encore, Sequent, Alliant computers on which it is installed. Author

N90-14786*# Houston Univ., Clear Lake, TX. Research Inst. for Computing and Information Systems.
TRANSFERRING DATA OBJECTS: A FOCUSED Ada INVESTIGATION
Sue LeGrand (Softech, Inc., Houston, TX.) 30 Apr. 1988 15 p
(Contract NCC9-16)
(NASA-CR-186065; NAS 1.26:186065) Avail: NTIS HC A03/MF A01 CSCL 09B

The use of the Ada language does not guarantee that data objects will be in the same form or have the same value after they have been stored or transferred to another system. There are too many possible variables in such things as the formats used and other protocol conditions. Differences may occur at many different levels of support. These include program level, object level, application level, and system level. A standard language is only one aspect of making a complex system completely homogeneous. Many components must be standardized and the various standards must be integrated. The principal issues in providing for interaction between systems are of exchanging files and data objects between systems which may not be compatible in terms of their host computer, operating system or other factors. A typical resolution of the problem of invalidating data involves at least a common external form, for data objects and for representing the relationships and attributes of data collections. Some of the issues dealing with the transfer of data are listed and consideration is given on how these issues may be handled in the Ada language. Author

N90-14787*# Auburn Univ., AL. Dept. of Computer Science and Engineering.
QUEST/Ada: QUERY UTILITY ENVIRONMENT FOR SOFTWARE TESTING OF Ada
David B. Brown Nov. 1989 100 p
(Contract NCC8-14)
(NASA-CR-186121; NAS 1.26:186121) Avail: NTIS HC A05/MF A01 CSCL 09B

Results of research and development efforts are presented for Task 1, Phase 2 of a general project entitled, The Development of a Program Analysis Environment for Ada. A prototype of the QUEST/Ada system was developed to collect data to determine the effectiveness of the rule-based testing paradigm. The prototype consists of five parts: the test data generator, the parser/scanner, the test coverage analyzer, a symbolic evaluator, and a data management facility, known as the Librarian. These components are discussed at length. Also presented is an experimental design for the evaluations, an overview of the project, and a schedule for its completion. J.P.S.

N90-14788 Carnegie-Mellon Univ., Pittsburgh, PA.
THE PROCESSES OF SCIENTIFIC RESEARCH: THE STRATEGY OF EXPERIMENTATION Ph.D. Thesis
Deepak Kulkarni 1988 177 p
Avail: Univ. Microfilms Order No. DA8913067

A program, KEKADA, was produced that is capable of carrying out intelligent experimental programs on problems similar to those faced by a number of experimental scientists. KEKADA has a set of experimentation strategies, that were detected from the traces of the behaviors of actual scientists. KEKADA strategies include: focusing on a surprising phenomenon, characterizing the surprising phenomenon by general strategies such as magnification, applying divide-and-conquer, determining the scope of phenomenon, factor-analysis, relating to similar phenomena, and domain-specific strategies and hypotheses. The domain-specific heuristics in KEKADA are efficient and practical instantiations of general strategies such as -- controlled experimentation, determination of complexity of a process, testing of a causal chain, componential analysis, differencing and divide-and-conquer. The reasons why KEKADA in its present form would not be a good experimental scientist are analyzed. Dissert. Abstr.

N90-14789*# National Aeronautics and Space Administration. Langley Research Center, Hampton, VA.
SOFTWARE REUSE ISSUES
Susan J. Voigt, ed. and Kathryn A. Smith, ed. Washington Dec. 1989 168 p Workshop held in Melbourne, FL, 17-18 Nov. 1988
(NASA-CP-3057; L-16667; NAS 1.55:3057) Avail: NTIS HC A08/MF A01 CSCL 09B

NASA Langley Research Center sponsored a Workshop on NASA Research in Software Reuse on November 17-18, 1988 in Melbourne, Florida, hosted by Software Productivity Solutions, Inc. Participants came from four NASA centers and headquarters, eight NASA contractor companies, and three research institutes. Presentations were made on software reuse research at the four NASA centers; on Eli, the reusable software synthesis system designed and currently under development by SPS; on Space Station Freedom plans for reuse; and on other reuse research projects. This publication summarizes the presentations made and the issues discussed during the workshop. For individual titles, see N90-14790 through N90-14807.

N90-14790*# Software Productivity Solutions, Inc., Melbourne, FL.
AUTOMATED REUSEABLE COMPONENTS SYSTEM STUDY RESULTS
Kathy Gilroy *In* NASA, Langley Research Center, Software Reuse Issues Dec. 1989 p 5-15 (For primary document see N90-14789 06-61)
Avail: NTIS HC A08/MF A01 CSCL 09B

The Automated Reusable Components System (ARCS) was developed under a Phase 1 Small Business Innovative Research (SBIR) contract for the U.S. Army CECOM. The objectives of the ARCS program were: (1) to investigate issues associated with automated reuse of software components, identify alternative approaches, and select promising technologies, and (2) to develop tools that support component classification and retrieval. The approach followed was to research emerging techniques and experimental applications associated with reusable software libraries, to investigate the more mature information retrieval technologies for applicability, and to investigate the applicability of specialized technologies to improve the effectiveness of a reusable component library. Various classification schemes and retrieval techniques were identified and evaluated for potential application in an automated library system for reusable components. Strategies for library organization and management, component submittal and storage, and component search and retrieval were developed. A prototype ARCS was built to demonstrate the feasibility of automating the reuse process. The prototype was created using a subset of the classification and retrieval techniques that were investigated. The demonstration system was exercised and evaluated using reusable Ada components selected from the public domain. A requirements specification for a production-quality ARCS was also developed. Author

N90-14791*# Software Productivity Solutions, Inc., Melbourne, FL.
KNOWLEDGE-BASED REUSABLE SOFTWARE SYNTHESIS SYSTEM
Cammie Donaldson *In* NASA, Langley Research Center, Software Reuse Issues Dec. 1989 p 17-31 (For primary document see N90-14789 06-61)
Avail: NTIS HC A08/MF A01 CSCL 09B

The Eli system, a knowledge-based reusable software synthesis system, is being developed for NASA Langley under a Phase 2 SBIR contract. Named after Eli Whitney, the inventor of interchangeable parts, Eli assists engineers of large-scale software systems in reusing components while they are composing their software specifications or designs. Eli will identify reuse potential, search for components, select component variants, and synthesize components into the developer's specifications. The Eli project began as a Phase 1 SBIR to define a reusable software synthesis methodology that integrates reusabilityinto the top-down development process and to develop an approach for an expert system to promote and accomplish reuse. The objectives of the Eli Phase 2 work are to integrate advanced technologies to automate the development of reusable components within the context of large system developments, to integrate with user development methodologies without significant changes in method or learning of special languages, and to make reuse the easiest operation to perform. Eli will try to address a number of reuse problems including developing software with reusable components, managing reusable components, identifying reusable components, and transitioning reuse technology. Eli is both a library facility for classifying, storing, and retrieving reusable components and a design environment that emphasizes, encourages, and supports reuse. Author

N90-14792*# Software Productivity Solutions, Inc., Melbourne, FL.
IMPACT OF DOMAIN ANALYSIS ON REUSE METHODS
Kathy Gilroy *In* NASA, Langley Research Center, Software Reuse Issues Dec. 1989 p 33-39 (For primary document see N90-14789 06-61)
Avail: NTIS HC A08/MF A01 CSCL 09B

The SPS is performing a study for the U.S. Army CECOM on the impact of domain analysis on reuse methods. Domain analysis is the first activity that should be performed in the development of reusable software. It identifies the commonalities between systems within a given problem (such as navigation systems or database management). In the software arena these commonalities are implemented as software components that can be reused by new systems within that application domain. The objectives of the study are to develop an approach that makes domain analysis practical and effective for the Army, to reinforce the importance of domain analysis for software reuse programs, and to summarize and coalesce domain analysis information into a single reference source. Existing methods and tools are being analyzed, critical issues identified, and key automation issues addressed. Based on these, a methodology and set of guidelines for domain analysis are being developed. Potential automated tools will be identified for each activity in the methodology. Author

N90-14793*# Software Productivity Solutions, Inc., Melbourne, FL.
CLASSIC-Ada(TM)
Lois Valley *In* NASA, Langley Research Center, Software Reuse Issues Dec. 1989 p 41-48 (For primary document see N90-14789 06-61)
Avail: NTIS HC A08/MF A01 CSCL 09B

The SPS product, Classic-Ada, is a software tool that supports object-oriented Ada programming with powerful inheritance and dynamic binding. Object Oriented Design (OOD) is an easy, natural development paradigm, but it is not supported by Ada. Following

the DOD Ada mandate, SPS developed Classic-Ada to provide a tool which supports OOD and implements code in Ada. It consists of a design language, a code generator and a toolset. As a design language, Classic-Ada supports the object-oriented principles of information hiding, data abstraction, dynamic binding, and inheritance. It also supports natural reuse and incremental development through inheritance, code factoring, and Ada, Classic-Ada, dynamic binding and static binding in the same program. Only nine new constructs were added to Ada to provide object-oriented design capabilities. The Classic-Ada code generator translates user application code into fully compliant, ready-to-run, standard Ada. The Classic-Ada toolset is fully supported by SPS and consists of an object generator, a builder, a dictionary manager, and a reporter. Demonstrations of Classic-Ada and the Classic-Ada Browser were given at the workshop. Author

N90-14794*# National Aeronautics and Space Administration. Goddard Space Flight Center, Greenbelt, MD.
PROTOTYPE SOFTWARE REUSE ENVIRONMENT AT GODDARD SPACE FLIGHT CENTER
Walt Truszkowski *In* NASA, Langley Research Center, Software Reuse Issues Dec. 1989 p 49-54 (For primary document see N90-14789 06-61)
Avail: NTIS HC A08/MF A01 CSCL 09B

The Goddard Space Flight Center (GSFC) work is organized into four phases and includes participation by a contractor, CTA, Inc. The first phase was an automation study, which began with a comprehensive survey of software development automation technologies. Eight technical areas were analyzed for goals, current capabilities, and obstacles. The study documented current software development practice in GSFC Mission Operations and Data Systems Directorate, and presented short- and long-term recommendations that included focus on reuse and object-oriented development. The second phase, which has been completed, developed a prototype reuse environment with tools supporting object-oriented requirements analysis and design. This phase addressed the operational concept of software reuse, i.e., it attempted to understand how software can be reused. This environment has two semantic networks: object and keywords, and includes automated search, interactive browsing and a graphical display of database contents. Phase 3 was a domain analysis of Payload Operations Control Center (POCC) software. The goal in this phase was to create an initial repository of reusable components and techniques. Seven existing Operations Control Centers at GSFC were studied, but the domain analysis proved to be very slow. A lesson learned from this was that senior people who understand the environment and the functionality of the area are needed to perform successful domain analyses. Author

N90-14795*# Jet Propulsion Lab., California Inst. of Tech., Pasadena.
JPL REUSE PROGRAM
James W. Brown *In* NASA, Langley Research Center, Software Reuse Issues Dec. 1989 p 55-60 (For primary document see N90-14789 06-61)
Avail: NTIS HC A08/MF A01 CSCL 09B

The goal of the JPL reuse activity is to develop a quantitative understanding of the factors which encourage or inhibit software reuse, and of productivity improvements achievable through reuse. The primary activity is the measurement of parameters relevant to reuse in the environment of actual projects. The program has three objectives: (1) to develop a model to allow assessment of competing reuse techniques, (2) to extend reuse from the unit to the sub-system level, and (3) to expand from specific applications to a broader application domain. Application domains, which apply to all interplanetary projects, include Mission Operations, Science Information Systems, Flight Software, and Simulations. The program is targeting all phases and activities of the life cycle and a full range of software products. The approach will be both experimental (observe, hypothesize and evaluate) and constructive (introduce new tools and techniques). The primary target projects are Deep Space Network activities - the Ground Facilities facility upgrade, the Network Operations Control Center upgrade, and the Signal Processing Center. This is the first group of closely related projects being done in Ada at JPL. A reuse base will be developed initially by classifying potentially reusable components from one project; it will be used and expanded with additional projects. Author

N90-14796*# National Aeronautics and Space Administration. Lyndon B. Johnson Space Center, Houston, TX.
JOHNSON SPACE CENTER SOFTWARE REUSE ACTIVITY
Steve Gorman *In* NASA, Langley Research Center, Software Reuse Issues Dec. 1989 p 61-63 (For primary document see N90-14789 06-61)
Avail: NTIS HC A08/MF A01 CSCL 09B

There is a strong operational interest in reuse and commonality at the Johnson Space Center (JSC). Although commonality and reuse were not emphasized in the Space Shuttle Orbiter Project, it is a major goal for Space Station Freedom and the Software Support Environment (SSE). Research activities at JSC are generally conducted through the Software Engineering Research Center (SERC) of the University of Houston at Clear Lake. The Life Cycle Model developed by SERC includes reuse at each phase, but reuse is not a principal theme. The SSE is a significant entry point for new reuse technology, and the SERC can provide consultation and possible prototypes. SERC is seen as an interface to other NISE reuse researchers. The AdaNET is managed at JSC through the University of Houston at Clear Lake for the NASA Office of Technology Utilization. It may also be a gateway for reuse research. Author

N90-14797*# National Aeronautics and Space Administration. Langley Research Center, Hampton, VA.
REUSE RESEARCH PLANS AT LANGLEY RESEARCH CENTER
Susan J. Voigt and Carrie Walker *In its* Software Reuse Issues Dec. 1989 p 65-66 (For primary document see N90-14789 06-61)
Avail: NTIS HC A08/MF A01 CSCL 09B

The reuse activities at Langley have centered on the development of the Eli System by SPS. The development of a computer systems design environment at Langley was described as a target application for the future Eli system. This environment combines software development tools with an architecture design and analysis tool. Specifically, a Computer-Aided Software Engineering (CASE) system, under development at Charles Stark Draper Laboratory for Langley, is being used to generate Ada code for use in architecture functional simulations using the Architecture Design and Assessment System (ADAS). The Eli system will be included in this tool set and will be used to organize and promote reuse of the functional simulation code modules. Author

N90-14798*# Software Productivity Consortium, Herndon, VA.
REUSE AT THE SOFTWARE PRODUCTIVITY CONSORTIUM
David M. Weiss *In* NASA, Langley Research Center, Software Reuse Issues Dec. 1989 p 67-88 (For primary document see N90-14789 06-61)
Avail: NTIS HC A08/MF A01 CSCL 09B

The Software Productivity Consortium is sponsored by 14 aerospace companies as a developer of software engineering methods and tools. Software reuse and prototyping are currently the major emphasis areas. The Methodology and Measurement Project in the Software Technology Exploration Division has developed some concepts for reuse which they intend to develop into a synthesis process. They have identified two approaches to software reuse: opportunistic and systematic. The assumptions underlying the systematic approach, phrased as hypotheses, are the following: the redevelopment hypothesis, i.e., software developers solve the same problems repeatedly; the oracle hypothesis, i.e., developers are able to predict variations from one redevelopment to others; and the organizational hypothesis, i.e., software must be organized according to behavior and structure to take advantage of the predictions that the developers make. The conceptual basis for reuse includes: program families, information hiding, abstract interfaces, uses and information hiding

hierarchies, and process structure. The primary reusable software characteristics are black-box descriptions, structural descriptions, and composition and decomposition based on program families. Automated support can be provided for systematic reuse, and the Consortium is developing a prototype reuse library and guidebook. The software synthesis process that the Consortium is aiming toward includes modeling, refinement, prototyping, reuse, assessment, and new construction. Author

N90-14799*# National Aeronautics and Space Administration, Washington, DC.
SSFP APPROACH TO SOFTWARE REUSE
Peg Snyder *In* NASA, Langley Research Center, Software Reuse Issues Dec. 1989 p 89-96 (For primary document see N90-14789 06-61)
Avail: NTIS HC A08/MF A01 CSCL 09B

This talk began by presenting the Space Station Freedom Program (SSFP) definitions of software commonality and software reuse. Software commonality is the use of identical, interchangeable, functionally compatible, or similar software items to satisfy different sets of functionally similar requirements. The Software Support Environment (SSE) and the Data Management System (DMS) of onboard computing facilities are examples of SSFP common software. Software reuse is the use of identical, compatible, or similar software items in either modified or unmodified form to satisfy development activities at any point in the software life cycle; in other words, taking an existing item and applying it to another development activity. Software commonality has been mandated in several critical areas (such as the SSE and DMS) and a policy directive is under review. A software reuse study group was established in May 1988 to gather background information (see Level 2 Software Reuse Study that follows by Scott Herman). The SSFP Program Definition and Requirements Document contains requirements for SSE support in the area of software reuse. The SSE is a collection of tools and rules, and provides the common environment to be used for the life cycle management of all SSFP operational software. Author

N90-14800*# Grumman Technical Services, Inc., Reston, VA.
LEVEL 2 SOFTWARE REUSE STUDY
Scott E. Herman *In* NASA, Langley Research Center, Software Reuse Issues Dec. 1989 p 97-103 (For primary document see N90-14789 06-61)
Avail: NTIS HC A08/MF A01 CSCL 09B

The Space Station Freedom Program (SSFP) Level 2 Software Reuse Study group was formed by Bob Nelson (NASA SSFP) from members of the Information Systems Program Support Contract (PSC) team. The objectives of the study were to identify existing software reuse libraries, to identify existing reusability processes and experiences, to identify reusability analysis tools and users, and to provide recommendations for a software reusability process for the SSFP. To date the following have been delivered: (1) definitions of commonality and reuse, (2) a report on existing software reuse libraries and library management systems, (3) a report on reuse process and methodology gleaned from software reuse experts, and (4) a report on software attributes for measuring commonality and reusability. Three implementation alternatives for a repository of reusable components were identified: centralized at the SSE Development Facility (SSEDF), a distributed approach across the network of Software Production Facilities, and a directory approach. A number of findings from the reuse study and several reuse strategy considerations were presented. Author

N90-14801*# Lockheed Missiles and Space Co., Houston, TX.
AN SSE APPROACH TO REUSABILITY
David L. Badal *In* NASA, Langley Research Center, Software Reuse Issues Dec. 1989 p 105-110 (For primary document see N90-14789 06-61)
Avail: NTIS HC A08/MF A01 CSCL 09B

The SSE project has engineering analysis and design efforts under way for the development of the SSE reusability library management system. An ad hoc committee on reuse has been meeting for several months identifying design considerations and learning about Ruben Prieto-Diaz faceted classification, CAMP domain analysis, SPC activities, SEI activities, and SPS activities. A standard format was developed for the Ada prologue for reusable components (both specification and body). The SSE reusability process can be viewed as a transformation process with minimized losses and difficulties. Author

N90-14802*# Planning Research Corp., Houston, TX.
SUPPORT FOR LIFE-CYCLE PRODUCT REUSE IN NASA'S SSE
Charles Shotton *In* NASA, Langley Research Center, Software Reuse Issues Dec. 1989 p 111-118 (For primary document see N90-14789 06-61)
Avail: NTIS HC A08/MF A01 CSCL 09B

The Software Support Environment (SSE) is a software factory for the production of Space Station Freedom Program operational software. The SSE is to be centrally developed and maintained and used to configure software production facilities in the field. The PRC product TTCQF provides for an automated qualification process and analysis of existing code that can be used for software reuse. The interrogation subsystem permits user queries of the reusable data and components which have been identified by an analyzer and qualified with associated metrics. The concept includes reuse of non-code life-cycle components such as requirements and designs. Possible types of reusable life-cycle components include templates, generics, and as-is items. Qualification of reusable elements requires analysis (separation of candidate components into primitives), qualification (evaluation of primitives for reusability according to reusability criteria) and loading (placing qualified elements into appropriate libraries). There can be different qualifications for different installations, methodologies, applications and components. Identifying reusable software and related components is labor-intensive and is best carried out as an integrated function of an SSE. Author

N90-14803*# Science Applications International Corp., Houston, TX.
INITIAL Ada COMPONENTS EVALUATION
Travis Moebes *In* NASA, Langley Research Center, Software Reuse Issues Dec. 1989 p 119-133 (For primary document see N90-14789 06-61)
Avail: NTIS HC A08/MF A01 CSCL 09B

The SAIC has the responsibility for independent test and validation of the SSE. They have been using a mathematical functions library package implemented in Ada to test the SSE IV and V process. The library package consists of elementary mathematical functions and is both machine and accuracy independent. The SSE Ada components evaluation includes code complexity metrics based on Halstead's software science metrics and McCabe's measure of cyclomatic complexity. Halstead's metrics are based on the number of operators and operands on a logical unit of code and are compiled from the number of distinct operators, distinct operands, and total number of occurrences of operators and operands. These metrics give an indication of the physical size of a program in terms of operators and operands and are used diagnostically to point to potential problems. McCabe's Cyclomatic Complexity Metrics (CCM) are compiled from flow charts transformed to equivalent directed graphs. The CCM is a measure of the total number of linearly independent paths through the code's control structure. These metrics were computed for the Ada mathematical functions library using Software Automated Verification and Validation (SAVVAS), the SSE IV and V tool. A table with selected results was shown, indicating that most of these routines are of good quality. Thresholds for the Halstead measures indicate poor quality if the length metric exceeds 260 or difficulty is greater than 190. The McCabe CCM indicated a high quality of software products. Author

N90-14804*# Carnegie-Mellon Univ., Pittsburgh, PA. Software Engineering Inst.
APPLICATION OF REUSABLE SOFTWARE COMPONENTS AT THE SEI

Robert Holibaugh *In* NASA, Langley Research Center, Software Reuse Issues Dec. 1989 p 135-145 (For primary document see N90-14789 06-61)
Avail: NTIS HC A08/MF A01 CSCL 09B

Robert Holibaugh of the Software Engineering Institute described a project which is studying the application of reusable software components. The primary goals are to gain practical experience with state-of-the-art reusable components, methods, and tools and to capture the lessons learned in the application of reuse technology. In addition the project will assess the impact of reuse on the software development process and products and will identify and validate the information that facilities software reuse during system development. The project includes two tasks - a reuse experiment and a redevelopment effort. The reuse experiment will define a life cycle and a methodology for reuse-based development, and define and implement a data collection mechanism for measuring the development. The redevelopment effort will construct a reuse test bed and will redevelop and realistically test subsystems from an embedded mission-critical real-time application. The reuse experiment will produce several products including a tested real-time application, reuse-based components and tools evaluation, a reuse-based development method, a framework for data collection, a framework for measuring productivity, and lessons learned data. Successful development with reusable components will require a rich set of components and an integrating methodology. The Tomahawk Land Attack Missile system is the application for the redevelopment effort. Author

N90-14805*# Houston Univ., Clear Lake, TX.
TECHNOLOGY TRANSFER IN SOFTWARE ENGINEERING
Peter C. Bishop *In* NASA, Langley Research Center, Software Reuse Issues Dec. 1989 p 149-153 (For primary document see N90-14789 06-61)
Avail: NTIS HC A08/MF A01 CSCL 09B

The University of Houston-Clear Lake is the prime contractor for the AdaNET Research Project under the direction of NASA Johnson Space Center. AdaNET was established to promote the principles of software engineering to the software development industry. AdaNET will contain not only environments and tools, but also concepts, principles, models, standards, guidelines and practices. Initially, AdaNET will serve clients from the U.S. government and private industry who are working in software development. It will seek new clients from those who have not yet adopted the principles and practices of software engineering. Some of the goals of AdaNET are to become known as an objective, authoritative source of new software engineering information and parts, to provide easy access to information and parts, and to keep abreast of innovations in the field. Author

N90-14806*# MountainNet, Dellslow, WV.
AdaNET SERVICES
Michael Digman *In* NASA, Langley Research Center, Software Reuse Issues Dec. 1989 p 155-158 (For primary document see N90-14789 06-61)
Avail: NTIS HC A08/MF A01 CSCL 09B

MountainNet is a small firm which serves as a distribution center for AdaNET Services. These services include providing host systems and telecommunications for AdaNET, developing and supporting AdaNET Information Services, and developing a dynamic software inventory. AdaNET hosts are a Data General MV8000II and DEC VAX. Telecommunications are provided via the MountainNet private network and the Telenet public access dial network. Initially, the AdaNET Information Services will include software repositories, user communications and forums, software engineering information, bibliographic and library services, and an educational directory. The dynamic software inventory, which will become available in January 1990, will contain software engineering code and parts. Author

N90-14807*# Inference Corp., Los Angeles, CA.
ADVANCED SOFTWARE DEVELOPMENT WORKSTATION PROJECT
Daniel Lee *In* NASA, Langley Research Center, Software Reuse Issues Dec. 1989 p 159-163 (For primary document see N90-14789 06-61)
(Contract NAS9-17766)
Avail: NTIS HC A08/MF A01 CSCL 09B

The Advanced Software Development Workstation Project, funded by Johnson Space Center, is investigating knowledge-based techniques for software reuse in NASA software development projects. Two prototypes have been demonstrated and a third is now in development. The approach is to build a foundation that provides passive reuse support, add a layer that uses domain-independent programming knowledge, add a layer that supports the acquisition of domain-specific programming knowledge to provide active support, and enhance maintainability and modifiability through an object-oriented approach. The development of new application software would use specification-by-reformulation, based on a cognitive theory of retrieval from very long-term memory in humans, and using an Ada code library and an object base. Current tasks include enhancements to the knowledge representation of Ada packages and abstract data types, extensions to support Ada package instantiation knowledge acquisition, integration with Ada compilers and relational databases, enhancements to the graphical user interface, and demonstration of the system with a NASA contractor-developed trajectory simulation package. Future work will focus on investigating issues involving scale-up and integration. Author

N90-14808*# Southwest Research Inst., San Antonio, TX.
CONTINUATION OF RESEARCH IN SOFTWARE FOR SPACE OPERATIONS SUPPORT Semiannual Report
Mark D. Collier 4 Jan. 1989 79 p
(Grant NAG9-388; SwRI Proj. 05-2984)
(NASA-CR-186092; NAS 1.26:186092) Avail: NTIS HC A05/MF A01 CSCL 09B

Software technologies relevant to workstation executives are discussed. Evaluations of problems, potential or otherwise, seen with IBM's Workstation Executive (WEX) 2.5 preliminary design and applicable portions of the 2.5 critical design are presented. Diverse graphics requirements of the Johnson Space Center's Mission Control Center Upgrade (MCCU) are also discussed. The key is to use tools that are portable, compatible with the X window system, and best suited to the requirements of the associated application. This will include a User Interface Language (UIL), an interactive display builder, and a graphic plotting/modeling system. Work sheets are provided for POSIX 1003.4 real-time extensions and the requirements for the Center's automated information systems security plan, referred to as POSIX 1003.6, are discussed. J.P.S.

N90-14809# Scientex Corp., Rockville, MD.
GRAFIN: GRAFIX INTERACTIVE MANUAL Report, Jul - Aug. 1989
G. McHale, A. Haghighi, and S. Basu Jul. 1989 161 p
(Contract DTFH61-87-Z-00116)
(PB89-232136; Rept-9100; FHWA/RD-89/176) Avail: NTIS HC A08/MF A01 CSCL 09B

The GRAFIX INteractive (GRAFIN) program has been developed to make the old GRADIX post-processing program easier for the researcher to use. The GRAFIN program allows the user to display graphic output from Federal Highway Administration computer simulation programs. The program queries the user for appropriate vehicle, barrier, and terrain information and gathers and manages all necessary files for graphic output production. The GRAFIN program is structured as two main parts; a front-end portion to manage program files, and a modified version of the old GRAFIX program. The report serves as a stand-alone manual for the GRAFIN program and an addendum to the old GRAFIX manual. Author

N90-14810 State Univ. of New York at Buffalo, Amherst.
SOME EDGE-ENHANCING OPERATORS AND THEIR APPLICATIONS TO IMAGE ENHANCEMENT AND EDGE DETECTION Ph.D. Thesis
Soon Young Park 1989 104 p
Avail: Univ. Microfilms Order No. DA8913540

Some edge-enhanced operators, and their applications to image enhancement and edge detection are investigated. The characteristics of some edge-enhanced operators are analyzed which are based on a modification of the Laplacian, called the order static (OS) Laplacian. In particular, the deterministic and statistical properties of the edge-enhancing operators are analyzed. The deterministic properties are studied by using the two-dimensional convex/concave (C/C) edge model. The statistical properties of the edge-enhancing operators are analyzed for white Gaussian input signals. The performance of the edge-enhancing operators are assessed by applying them to real images. An edge-enhancing operator called the selective average (SA), that can produce step-like edges while reducing noise is then considered and analyze the effect of SA prefiltering on edge detection. One- and two-dimensional edge detectors are considered. In the one-dimensional case, the uni- and bi-variate output density functions for SA filtering are derived, and the error probabilities for a simple 1-D gradient type edge detector following SA prefiltering are obtained theoretically. In the case of two dimension, the error probabilities associated with the Sobel operator are obtained through computer simulation. The error probabilities for SA filtering are compared with those for median filtering.
Dissert. Abstr.

N90-14811*# Houston Univ., Clear Lake, TX. Research Inst. for Computing and Information Systems.
THE DEVELOPMENT OF AN Ada PROGRAMMING SUPPORT ENVIRONMENT DATABASE: SEAD (SOFTWARE ENGINEERING AND Ada DATABASE), USER'S MANUAL
Morris Liaw and Donna Evesson (GHG Corp., Houston, TX.) 1 Nov. 1988 83 p
(Contract NCC9-16)
(NASA-CR-181219; NAS 1.26:181219) Avail: NTIS HC A05/MF A01 CSCL 09B

This is a manual for users of the Software Engineering and Ada Database (SEAD). SEAD was developed to provide an information resource to NASA and NASA contractors with respect to Ada-based resources and activities that are available or underway either in NASA or elsewhere in the worldwide Ada community. The sharing of such information will reduce the duplication of effort while improving quality in the development of future software systems. The manual describes the organization of the data in SEAD, the user interface from logging in to logging out, and concludes with a ten chapter tutorial on how to use the information in SEAD. Two appendices provide quick reference for logging into SEAD and using the keyboard of an IBM 3270 or VT100 computer terminal.
J.P.S.

N90-14812*# Bowie State Coll., MD.
POWER SPECTRAL ESTIMATION ALGORITHMS Final Report
Manjit S. Bhatia Dec. 1989 34 p
(Grant NAG5-499)
(NASA-CR-186189; NAS 1.26:186189) Avail: NTIS HC A03/MF A01 CSCL 09B

Algorithms to estimate the power spectrum using Maximum Entropy Methods were developed. These algorithms were coded in FORTRAN 77 and were implemented on the VAX 780. The important considerations in this analysis are: (1) resolution, i.e., how close in frequency two spectral components can be spaced and still be identified; (2) dynamic range, i.e., how small a spectral peak can be, relative to the largest, and still be observed in the spectra; and (3) variance, i.e., how accurate the estimate of the spectra is to the actual spectra. The application of the algorithms based on Maximum Entropy Methods to a variety of data shows that these criteria are met quite well. Additional work in this direction would help confirm the findings. All of the software developed was turned over to the technical monitor. A copy of a typical program is included. Some of the actual data and graphs used on this data are also included.
Author

N90-14813*# Auburn Univ., AL. Dept. of Computer Science and Engineering.
A GRAPHICALLY ORIENTED SPECIFICATION LANGUAGE FOR AUTOMATIC CODE GENERATION. GRASP/Ada: A GRAPHICAL REPRESENTATION OF ALGORITHMS, STRUCTURE, AND PROCESSES FOR Ada, PHASE 1 Final Report
James H. Cross, II, Kelly I. Morrison, Charles H. May, Jr., and Kathryn C. Waddel Sep. 1989 154 p Prepared for Alabama Univ., Huntsville
(Contract NCC8-13)
(NASA-CR-183212; NAS 1.26:183212) Avail: NTIS HC A08/MF A01 CSCL 09B

The first phase of a three-phase effort to develop a new graphically oriented specification language which will facilitate the reverse engineering of Ada source code into graphical representations (GRs) as well as the automatic generation of Ada source code is described. A simplified view of the three phases of Graphical Representations for Algorithms, Structure, and Processes for Ada (GRASP/Ada) with respect to three basic classes of GRs is presented. Phase 1 concentrated on the derivation of an algorithmic diagram, the control structure diagram (CSD) (CRO88a) from Ada source code or Ada PDL. Phase 2 includes the generation of architectural and system level diagrams such as structure charts and data flow diagrams and should result in a requirements specification for a graphically oriented language able to support automatic code generation. Phase 3 will concentrate on the development of a prototype to demonstrate the feasibility of this new specification language.
K.C.D.

N90-14814# Sandia National Labs., Albuquerque, NM.
THE PHASE GRADIENT AUTOFOCUS ALGORITHM: AN OPTIMAL ESTIMATOR OF THE PHASE DERIVATIVE
P. H. Eichel Sep. 1989 16 p
(Contract DE-AC04-76DP-00789)
(DE90-000895; SAND-89-0761) Avail: NTIS HC A03/MF A01

The phase gradient algorithm represents a powerful new signal processing technique with applications to aperture synthesis imaging. These include, for example, synthetic aperture radar phase correction and stellar image reconstruction. The algorithm combines redundant information present in the data to arrive at an estimate of the phase derivative. In this report, we show that the estimator is in fact a linear, minimum variance estimator of the phase derivative.
DOE

N90-14815# Westinghouse Savannah River Co., Aiken, SC. Computer Systems Engineering Group.
SELECTING AND EFFECTIVELY USING A COMPUTER AIDED SOFTWARE ENGINEERING TOOL
D. L. Kuhn 1989 11 p Presented at the Annual Westinghouse Computer Symposium, Pittsburgh, PA, 6-7 Nov. 1989 Submitted for publication
(Contract DE-AC09-89SR-18035)
(DE89-017876; WSRC-RP-89-483; CONF-891192-7) Avail: NTIS HC A03/MF A01

Software engineering is a science by which user requirements are translated into a quality software product. Computer Aided Software Engineering (CASE) is the scientific application of a set of tools and methods to a software which results in high-quality, defect-free, and maintainable software products. The Computer Systems Engineering (CSE) group of Separations Technology at the Savannah River Site has successfully used CASE tools to produce high-quality, reliable, and maintainable software products. The selection process CSE used to acquire a commonly available CASE product and how the CSE group effectively used this CASE tool to consistently produce quality software are detailed.
DOE

N90-14816# Westinghouse Savannah River Co., Aiken, SC.
PERSONAL COMPUTER PROCESS DATA ACQUISITION

L. O. Dworjanyn 1989 8 p Presented at the Annual Westinghouse Computer Symposium, Pittsburgh, PA, 6-7 Nov. 1989 Submitted for publication
(Contract DE-AC09-89SR-18035)
(DE89-017877; WSRC-RP-89-461; CONF-891192-6) Avail: NTIS HC A02/MF A01

A simple Basic program was written to permit personal computer data collection of process temperatures, pressures, flows, and inline analyzer outputs for a batch-type, unit operation. The field voltage outputs were read on an IEEE programmable digital multimeter using a programmable scanner to select different output lines. The data were stored in ASCII format to allow direct analysis by spreadsheet programs. DOE

N90-14817# California Univ., Berkeley. Lawrence Berkeley Lab.
VERSATILITY OF THE CFR ALGORITHM FOR LIMITED ANGLE RECONSTRUCTION
I. Fujieda, K. Heiskanen, and V. Perez-Mendez Aug. 1989 4 p Presented at the IEEE Nuclear Science Symposium and Exhibits, San Francisco, CA, 25-27 Oct. 1989
(Contract DE-AC03-76SF-00098)
(DE90-001421; LBL-27696; CONF-891087-2) Avail: NTIS HC A01/MF A01

The Constrained Fourier Reconstruction (CFR) algorithm and the Iterative Reconstruction Reprojection (IRR) algorithm are evaluated based on their accuracy for three types of limited angle reconstruction problems. The CFR algorithm performs better for problems such as x ray CT imaging of a nuclear reactor core with one large data gap due to structural blocking of the source and detector pair. For gated heart imaging by x ray CT, radioisotope distribution imaging by PET or SPECT, using a polygonal array of gamma cameras with insensitive gaps between camera boundaries, the IRR algorithm has a slight advantage over the CFR algorithm but the difference is not significant. DOE

N90-14818# Lawrence Livermore National Lab., CA.
PROGRAM CICC FLOW AND HEAT TRANSFER IN CABLE-IN-CONDUIT CONDUCTORS
Robert L. Wong 20 Nov. 1989 6 p Presented at the 13th International Symposium on Fusion Engineering, Knoxville, TN, 2-6 Oct. 1989 Submitted for publication
(Contract W-7405-eng-48)
(DE90-001519; UCRL-101241; CONF-891007-14) Avail: NTIS HC A02/MF A01

Computer program CICC was written for use in the thermo-fluids design of superconducting magnets for tokamak reactors, which use forced flow, helium cooled, cable-in-conduit conductors (CICC). In addition to background heat loads that vary with space and time, these superconductors can develop normal zones that generate electrical resistance heat. Program CICC models the transient thermodynamic and fluid dynamic system response to background heating and normal zone propagation in the superconductor. The computational algorithm described couples a 1-D, compressible pipe flow model (including flow choking) with 2-D, axisymmetric heat conduction models of the superconductor cable, the conduit, and the epoxy conduit insulation. National Institute of Standards and Technology helium properties are used. The model is verified by comparison with measured temperature and pressure profiles from thermal expulsion experiments. DOE

N90-14819# Los Alamos National Lab., NM. Computer Network Engineering.
THE HIGH-SPEED CHANNEL (HSC) AND ULTRA-SPEED NETWORKS
Don E. Tolmie 1989 7 p Presented at BROADBAND (Foc/Lan) '89, San Francisco, CA, 30 Oct. - 3 Nov. 1989
(Contract W-7405-eng-36)
(DE89-015283; LA-UR-89-2560; CONF-8910158-1) Avail: NTIS HC A02/MF A01

Excellent success was made, and user productivity increased, with a research project which provided computer-generated video-type output of physics calculations. Now ways are being investigated to provide this visualization capability to many users in a networked environment. The need is seed for networking with channel speeds in the 800-Mbit/s range for data transfers to graphics displays, to storage systems, and between machines. A basic building block to achieve this capability is the High-Speed Channel (HSC) being worked on in American National Standards Institute (ANSI) Task Group X3T9.3. The HSC provides a point-to-point channel with speeds of 800 and 1600 Mbit/s (100 and 200 MByte/s). Industry interest is very high, and vendors are starting to produce hardware. Los Alamos is also working with some vendors on computer networks built around the HSC, crossbar switches, and intelligent network interfaces. A project is also underway to develop a fiber-optic transport media to support the higher layer protocols of HSC, the Intelligent Peripheral Interface (IPI) and the Small Computer System Interface (SCSI). DOE

N90-14820# California Univ., Berkeley. Lawrence Berkeley Lab.
THE DESIGN OF A COMPUTER SYSTEM FOR IMAGE SIMULATION AND IMAGE PROCESSING OF HIGH RESOLUTION ELECTRON MICROGRAPHS
Roar Kilaas and M. A. OKeefe Jul. 1989 13 p Presented at the Symposium on Computer Simulation of Electron Microscope Diffraction and Images, Las Vegas, NV, 28 Feb. - 3 Mar. 1989
(Contract DE-AC03-76SF-00098)
(DE90-000179; LBL-27444; CONF-8902135-1) Avail: NTIS HC A03/MF A01

The task of assembling a system for simulation and processing of High Resolution Transmission Electron Microscope images is discussed with attention paid to both hardware and software. Two separate systems are presented, one optimized for low cost, the other for performance. In both systems, the emphasis is on compatibility between the separate components making up the system. Finally a third system is presented, adding the functionality of real time data acquisition and processing. DOE

N90-14821# Lawrence Livermore National Lab., CA.
USING OBJECT-ORIENTED DEVELOPMENT TO SUPPORT PROTOTYPING
Lin Zucconi, Gregory Mack, and Lloyd G. Williams Sep. 1989 6 p Presented at the 12th International Conference on Software Engineering, Nice, France, Sep. 1989
(Contract W-7405-eng-48)
(DE90-000547; UCRL-101437; CONF-8909240-1) Avail: NTIS HC A02/MF A01

Prototyping can be a valuable tool in software development, particularly in cases where the requirements are uncertain or where there is a significant amount of risk associated with the implementation (Boeh84), (Boeh88). The use of prototyping can, however, lead to several problems. These include: a less coherent design than would be obtained with a specification-based approach, poor (or nonexistent) documentation, and a tendency to deliver the prototype as the finished product as schedule pressures mount. A project is described in which more formal software development methods were used in parallel with a prototyping effort to develop a real time monitor and control computer system. The prototype was used to define and clarify the requirements for the system. The more formal approach was used to capture and document those requirements. The resulting description of the system was then used to capture and document those requirements. The resulting description of the system was then used to migrate the prototype to a first version production system. This combined approach helped to overcome many of the problems typically associated with prototyping alone. DOE

N90-14822# Virginia Polytechnic Inst. and State Univ., Blacksburg. Dept. of Computer Science.
PARALLEL MATHEMATICAL SOFTWARE Progress Report, 16 Aug. 1988 - 14 Feb. 1990
C. J. Ribbens and L. T. Watson Oct. 1989 5 p
(Contract DE-FG05-88ER-25068)

(DE90-002694; DOE/ER-25068/1) Avail: NTIS HC A02/MF A01

The purpose of this report is to summarize work done during the first 18 months on the project, Parallel Mathematical Software, supported by the U.S. Department of Energy. Since the two major problem domains for this research are elliptic partial differential equations (and the software package ELLPACK) and systems of nonlinear equations (and the software package HOMPACK), we organize this report into two major sections. This paper details aspects of our work that relate to ELLPACK; and discusses progress in connection with HOMPACK. DOE

N90-14823# Los Alamos National Lab., NM. Theoretical Div.
ALGORITHMIC RANDOMNESS, PHYSICAL ENTROPY, MEASUREMENTS, AND THE SECOND LAW
Wojciech H. Zurek 1989 22 p Presented at the 3rd International Symposium on Foundations of Quantum Mechanics, Tokyo, Japan, 27 Aug. - 8 Sep. 1989
(Contract W-7405-eng-36)
(DE90-002413; LA-UR-89-3576; CONF-890875-3) Avail: NTIS HC A03/MF A01

Algorithmic information content is equal to the size -- in the number of bits -- of the shortest program for a universal Turing machine which can reproduce a state of a physical system. In contrast to the statistical Boltzmann Gibbs Shannon entropy, which measures ignorance, the algorithmic information content is a measure of the available information. It is defined without a recourse to probabilities and can be regarded as a measure of randomness of a definite microstate. I suggest that the physical entropy S -- that is, the quantity which determines the amount of the work, delta W, which can be extracted in the cyclic isothermal expansion process through the equation: delta W = k(sub B)T(delta)S -- is a sum of two contributions: the mission information measured by the usual statistical entropy and the known randomness measured by the algorithmic information content. The sum of these two contributions is a constant of motion in the process of a dissipation less measurement on an equilibrium ensemble. This conservation under a measurement, which can be traced back to the noiseless coding theorem of Shannon, is necessary to rule out existence of a successful Maxwell's demon. DOE

N90-14824# Lawrence Livermore National Lab., CA.
INTERACTIVE MULTIDIMENSIONAL DATA ANALYSIS AND UNDERSTANDING
S. G. Azevedo, C. Grant, J. Brase, J. P. Fitch, and M. Miller Aug. 1989 7 p
(Contract W-7405-eng-48)
(DE90-001794; UCID-21796) Avail: NTIS HC A02/MF A01

The goal in FY 88 was to assemble and coordinate the software and hardware required to accurately and quickly process, display, and interpret multidimensional data. These capabilities are of fundamental scientific importance and can directly impact Laboratory and national defense programs. The progress using new interactive display algorithms and novel computer architectures is described. A significant impact on a variety of Laboratory programs and will be continuing this project will be continued under the name of Scientific Visualization in FY 89. DOE

N90-14825# Argonne National Lab., IL.
STRAND: A PRACTICAL PARALLEL PROGRAMMING LANGUAGE
Ian Foster and Stephen Taylor (California Inst. of Tech., Pasadena.) 1989 17 p Presented at the North American Conference on Logic Programming, Cleveland, OH, 16-20 Oct. 1989
(Contract W-31-109-eng-38)
(DE90-002861; CONF-8910288-1) Avail: NTIS HC A03/MF A01

Effective parallel programming requires tools that facilitate the design and implementation of parallel algorithms and provide portability across parallel computers. Strand is the first such tool to be available on a broad range of multiprocessor architectures, including hypercubes, meshes, computing surfaces, banyan networks, shared-memory machines, and local area networks. Strand is a new concurrent logic programming language. Its design is motivated by extensive experience with previous languages of this type. This experience indicated that for most practical parallel programming requirements, these research languages were too complex, inefficient and difficult to implement. Strand applies a broad variety of simplifications to achieve a practical parallel programming tool. This paper describes the issues surrounding the Strand design and reports on initial experiences with the language. DOE

N90-14826*# Cornell Univ., Ithaca, NY. Dept. of Computer Science.
THE ROLE OF ORDER IN DISTRIBUTED PROGRAMS
Kenneth P. Birman and Keith Marzullo May 1989 24 p Sponsored in part by Siemens Corp.
(Contract NAG2-593; N00140-87-C-8904; ARPA Order 6037)
(NASA-CR-186252; NAS 1.26:186252; TR-89-1001) Avail: NTIS HC A03/MF A01 CSCL 09B

The role of order in building distributed systems is discussed. It is the belief that a principle of event ordering underlies the wide range of operating systems mechanisms that were put forward for building robust distributed software. Stated concisely, this principle achieves correct distributed behavior by ordering classes of distributed events that conflict with one another. By focusing on order, simplified descriptions can be obtained and convincingly correct solutions to problems that might otherwise have looked extremely complex. Moreover, it is observed that there are a limited number of ways to obtain order, and that the choice made impacts greatly on performance. Author

N90-14827# Oak Ridge National Lab., TN. Engineering Physics and Mathematics Div.
SOME NUMERICAL EXPERIMENTS CONCERNING THE EQUATION OF STATE ALGORITHM FOR MULTI-MATERIAL CELLS IN HULL
Thomas J. Burns 1989 4 p Presented at the Hypervelocity Impact Symposium, San Antonio, TX, 12-14 Dec. 1989
(Contract DE-AC05-84OR-21400)
(DE89-008240; CONF-891214-1) Avail: NTIS HC A01/MF A01

The solution of the partial differential equations of continuum mechanics as implemented in HULL requires that each mesh cell be well-characterized from a materials standpoint. Based on this viewpoint, the ideal situation is that each mesh cell consist of a single material, well-described by an equation of state (EOS), constitutive relations, etc. On the other hand, an Eulerian formulation is typically required to analyze hypervelocity impacts due to the very large deformations of both the projectile and target. The advection of materials and their associated properties from one mesh cell to another inherent in such a formulation however, inevitably leads to the creation of multi-material cells. Thus, one requirement for the use of the Eulerian formulation is that some provision for characterizing the multi-material cells via a single set of properties be implemented as a bridge between the two calculational modes. This procedure has been termed (for want of a better term) the equation of state algorithm for multi-material cells and is discussed in this paper. DOE

N90-14828# Lawrence Livermore National Lab., CA.
A TUTORIAL ON SOFTWARE RELIABILITY ENGINEERING
J. Dennis Lawrence 12 May 1989 21 p Presented at the Computer Measurement Group Annual Meeting, Reno, NV, 11-15 Dec. 1989
(Contract W-7405-eng-48)
(DE89-012368; UCRL-100671; CONF-891222-1) Avail: NTIS HC A03/MF A01

Computer systems are increasingly being required to operate free from externally-detected failures. This is particularly true in the case of large distributed real-time and transaction-processing systems in application areas such as transportation, medicine, defense, finance, marketing and communications. There are many similarities in approaches and techniques between performance analysis and reliability analysis, so the local performance expert is

a natural person to approach for help with reliability problems. This tutorial will provide an introduction to reliability engineering, primarily as it applies to software development. It consists of four parts. The first part defines some important terms, and describes some ways to classify faults and failures. The second portion describes various kinds of activities that can be carried out during the life cycle of the application system, especially those that will be of interest to the reliability expert. The fourth section discusses various techniques for achieving software fault tolerance. Finally, a few modeling techniques and the problems of accurate data collection are discussed. DOE

62 COMPUTER SYSTEMS

Includes computer networks and special application computer systems.

N90-14829*# National Aeronautics and Space Administration. Hugh L. Dryden Flight Research Facility, Edwards, CA.
THE AEROSPACE ENERGY SYSTEMS LABORATORY: A BITBUS NETWORKING APPLICATION
Richard D. Glover and Nora ONeill-Rood Washington Nov. 1989 15 p Presented at the iRUG 6th International Conference, Bethesda, MD, 13-14 Nov. 1989
(NASA-TM-4149; H-1569; NAS 1.15:4149) Avail: NTIS HC A03/MF A01 CSCL 12A

The NASA Ames-Dryden Flight Research Facility developed a computerized aircraft battery servicing facility called the Aerospace Energy Systems Laboratory (AESL). This system employs distributed processing with communications provided by a 2.4-megabit BITBUS local area network. Customized handlers provide real time status, remote command, and file transfer protocols between a central system running the iRMX-II operating system and ten slave stations running the iRMX-I operating system. The hardware configuration and software components required to implement this BITBUS application are required. Author

N90-14830 British Petroleum Co. Ltd., London (England).
COORDINATION OF PROCESSING ELEMENTS IN A MULTIPROCESSOR COMPUTER Patent Application
Andrew David Cromarty, inventor (to World Intellect and John Norman Harrison, inventor (to World Intellect 6 Feb. 1987 20 p
(WO-Patent-88/04075; WO-Patent-Appl-SN-PCT/GB87/000; Int-Patent-Class-G06F-15/06; ETN-90-95242) Avail: World Intellectual Property Organization, 34 Chemin des Colombettes, CH-1211 Geneva 20, Switzerland

The application of an improved processor element (PE) in a multiprocessor computer is described. The PE synchronization is to be applied in computer operation modes in which either each PE executes the same instruction at the same time, or each PE executes different instructions but operates on a common stream of data. The computer controller has a code/data-ready means to signal to the PEs that data or an instruction is available on the bus. The PEs each have a processor-ready means to signal to the controller that they are ready to read the data or instruction, and a read-enable means actuated by a code/data-ready signal from the controller to allow the PE to read the data or instruction. A processor-ready signal is initiated when there is no code/data-ready signal from the controller. A code/data-ready signal is only indicated when all the PEs give a ready signal and is only terminated when no PE gives a ready signal. ESA

N90-14831# Los Alamos National Lab., NM. Computing and Communications Lab.
MULTIPLE CROSSBAR NETWORK: INTEGRATED SUPERCOMPUTING FRAMEWORK
Randy L. Hoebelheinrich 1989 17 p Presented at the Supercomputing '89 Conference, Reno, NV, 13-17 Nov. 1989
(Contract W-7405-eng-36)
(DE89-012614; LA-UR-89-1627; CONF-891149-2) Avail: NTIS HC A03/MF A01

At Los Alamos National Laboratory, site of one of the world's most powerful scientific supercomputing facilities, a prototype network for an environment that links supercomputers and workstations is being developed. Driven by a need to provide graphics data at movie rates across a network from a Cray supercomputer to a Sun scientific workstation, the network is called the Multiple Crossbar Network (MCN). It is intended to be a coarsely grained, loosely coupled, general purpose interconnection network that will vastly increase the speed at which supercomputers communicate with each other in large networks. The components of the network are described, as well as work done in collaboration with vendors who are interested in providing commercial products. DOE

N90-14832# Lawrence Livermore National Lab., CA.
THE DELTA-t TRANSPORT PROTOCOL: FEATURES AND EXPERIENCE USEFUL FOR HIGH PERFORMANCE NETWORKS
Richard W. Watson 1989 9 p Presented at the 14th Conference on Local Computer Networks, Minneapolis, MN, 10-12 Oct. 1989
(Contract W-7405-eng-48)
(DE89-016542; UCRL-101652; CONF-8910209-1) Avail: NTIS HC A02/MF A01

With the advent of new high performance networks and distributed systems there is renewed interest in transport protocol designs that can support both request/response and stream styles of communication. Delta-t is a transport protocol designed to meet such goals. Delta- t's main contribution is in the area of connection management, where it achieves hazard free connection management without explicit packet exchanges. The Delta-t's features, connection management, and some implementation lessons useful for high performance networks are reviewed. DOE

N90-14833# Los Alamos National Lab., NM. Computer Network Engineering Div.
MULTIPLE CROSSBAR NETWORK: A SWITCHED HIGH-SPEED LOCAL NETWORK
Randy L. Hoebelheinrich and Richard G. Thomsen 1989 16 p Presented at the 14th Conference on Local Computer Networks, Minneapolis, MN, 10-12 Oct. 1989
(Contract W-7405-eng-36)
(DE90-001839; LA-UR-89-3155; CONF-8910209-2) Avail: NTIS HC A03/MF A01

The Multiple Crossbar Network (MCN) is a prototype High-Speed Local Network at the Los Alamos National Laboratory. It will interconnect supercomputers, network servers and workstations from various commercial vendors. The MCN can also serve as a backbone for message traffic between local area networks. The MCN is a switched local network of switching nodes called Cross-Point Stars (CPs). Hosts and CPs are connected by 800-Mbit/s (100-Mbyte/s) point-to-point ANSI High-Speed Channels. The CPs include RISC-based network protocol processors called Crossbar Interfaces and a switching core called the Crossbar Switch. Protocols include physical, data link, intranet, and network access functionality. Various internet and transport protocols are intended to run above the MCN protocol suite. A network management and simple naming service is also included within the Los Alamos Network Architecture. Immediate applications include visualization. The MCN is intended to also serve as a framework for multicomputer applications. DOE

N90-14834# Lawrence Livermore National Lab., CA.
PCP (PARALLEL C PREPROCESSOR): A PARALLEL EXTENSION OF C THAT IS 99 PERCENT FAT FREE
Eugene D. Brooks, III 27 Sep. 1989 15 p Presented at the Supercomputing '89 Conference, Reno, NV, 13-17 Nov. 1989 Revised Submitted for publication
(Contract W-7405-eng-48)
(DE90-002813; UCRL-99673-Rev-1; CONF-891149-10-Rev-1)
Avail: NTIS HC A03/MF A01

The fork-join model for parallel computation requires efficient compiler and hardware support if it is to be used for tightly coupled

applications. Because of deficiencies in compiler and hardware support, most existing implementations of the fork-join model require relatively large grain parallelism if good efficiency is to be obtained. We present an alternative parallel programming paradigm called the split-join model. When nested concurrency is encountered in the split-join model the team of processors is disassociated into subteams which independently handle the separate sections of parallel code. The key advantage of the split-join model is that it can be efficiently implemented with a machine independent preprocessor and a small amount of machine dependent run time support. Extensive compiler and hardware support is not required. We describe the language constructs implemented in PCP and their efficient implementation. DOE

N90-14835# Sandia National Labs., Albuquerque, NM. Exploratory Systems Development.
GENERALIZATION IN BACKPROPAGATION NETWORKS: AN EMPIRICAL STUDY USING IMAGE DATA
Mary M. Moya, R. Joseph Fogler, and Larry D. Hostetler 1989 12 p Presented at the IEEE Conference on Neutral Information Processing Systems, Denver, CO, 27-30 Nov. 1989
(Contract DE-AC04-76DP-00789)
(DE89-012658; SAND-89-1442C; CONF-891150-1) Avail: NTIS HC A03/MF A01

The ability of trained multi-layer, first order feedforward networks to generalize the perspective-invariant classification of image data is reported. The method is introduced of interactive training which is useful when specific types of non-target images are important in the classification. Within interactive training, it is shown that the network can recognize perspective-independent images of one object and reject perspective-independent images of other objects in its training set, as well as reject a significant number of images of other objects on which it was not trained. However, the first order network is still not capable of reliable one-class generalization. Therefore, a method is introduced for training a network with images on the boundary of the target class for one-class generalization. The generalization ability is reported of a second order network trained with this method. Also described is the implementation of the feedforward network in a fixed-point hardware implementation that can process images at more than a billion connections per second. DOE

N90-14836*# University of South Florida, Tampa. Intelligent Systems Lab.
ARCHITECTURES FOR REASONING IN PARALLEL Final Report
Lawrence O. Hall [1989] 37 p
(Grant NAG2-487)
(NASA-CR-186237; NAS 1.26:186237) Avail: NTIS HC A03/MF A01 CSCL 09B

The research conducted has dealt with rule-based expert systems. The algorithms that may lead to effective parallelization of them were investigated. Both the forward and backward chained control paradigms were investigated in the course of this work. The best computer architecture for the developed and investigated algorithms has been researched. Two experimental vehicles were developed to facilitate this research. They are Backpac, a parallel backward chained rule-based reasoning system and Datapac, a parallel forward chained rule-based reasoning system. Both systems have been written in Multilisp, a version of Lisp which contains the parallel construct, future. Applying the future function to a function causes the function to become a task parallel to the spawning task. Additionally, Backpac and Datapac have been run on several disparate parallel processors. The machines are an Encore Multimax with 10 processors, the Concert Multiprocessor with 64 processors, and a 32 processor BBN GP1000. Both the Concert and the GP1000 are switch-based machines. The Multimax has all its processors hung off a common bus. All are shared memory machines, but have different schemes for sharing the memory and different locales for the shared memory. The main results of the investigations come from experiments on the 10 processor Encore and the Concert with partitions of 32 or less processors. Additionally, experiments have been run with a stripped down version of EMYCIN. Author

N90-14837*# Cornell Univ., New York, NY. Dept. of Computer Science.
HOW ROBUST ARE DISTRIBUTED SYSTEMS
Kenneth P. Birman Jun. 1989 15 p
(Contract NAG2-593; N00140-87-C-8904; ARPA Order 6037)
(NASA-CR-186242; NAS 1.26:186242; TR-89-1014) Avail: NTIS HC A03/MF A01 CSCL 09B

A distributed system is made up of large numbers of components operating asynchronously from one another and hence with imcomplete and inaccurate views of one another's state. Load fluctuations are common as new tasks arrive and active tasks terminate. Jointly, these aspects make it nearly impossible to arrive at detailed predictions for a system's behavior. It is important to the successful use of distributed systems in situations in which humans cannot provide the sorts of predictable realtime responsiveness of a computer, that the system be robust. The technology of today can too easily be affected by worn programs or by seemingly trivial mechanisms that, for example, can trigger stock market disasters. Inventors of a technology have an obligation to overcome flaws that can exact a human cost. A set of principles for guiding solutions to distributed computing problems is presented. J.P.S.

63 CYBERNETICS

Includes feedback and control theory, artificial intelligence, robotics and expert systems.

For related information see also *54 Man/System Technology and Life Support.*

N90-14838 Department of the Navy, Washington, DC.
ROBOTIC VISION SYSTEM Patent
Norman M. Witriol, inventor (to Navy), William H. Brumage, inventor (to Navy), and David H. Cowling, inventor (to Navy) 1 Aug. 1989 9 p Filed 8 Apr. 1988
(AD-D014246; US-Patent-4,853,771; US-Patent-Appl-SN-179327)
Avail: US Patent and Trademark Office CSCL 12/9

A robotic vision system for real time operation based on a luminous fiduciary code located upon a robot and an object the robot is to operate on. The luminescent code, when irradiated, locate the position of the object relative to the robot thus allowing placement of the fiduciary codes, on the object and the robot, into a predetermined desired position and orientation. GRA

N90-14839*# Illinois Univ., Urbana-Champaign. Coordinated Science Lab.
NETRA: A PARALLEL ARCHITECTURE FOR INTEGRATED VISION SYSTEMS. 1: ARCHITECTURE AND ORGANIZATION
Alok N. Choudhary, Janak H. Patel, and Narendra Ahuja Dec. 1989 40 p
(Grant NAG1-613)
(NASA-CR-185955; NAS 1.26:185955; UILU-ENG-89-2241; CSG-117) Avail: NTIS HC A03/MF A01 CSCL 09B

Computer vision is regarded as one of the most complex and computationally intensive problems. An integrated vision system (IVS) is considered to be a system that uses vision algorithms from all levels of processing for a high level application (such as object recognition). A model of computation is presented for parallel processing for an IVS. Using the model, desired features and capabilities of a parallel architecture suitable for IVSs are derived. Then a multiprocessor architecture (called NETRA) is presented. This architecture is highly flexible without the use of complex interconnection schemes. The topology of NETRA is recursively defined and hence is easily scalable from small to large systems. Homogeneity of NETRA permits fault tolerance and graceful degradation under faults. It is a recursively defined tree-type hierarchical architecture where each of the leaf nodes consists of a cluster of processors connected with a programmable crossbar with selective broadcast capability to provide for desired flexibility.

A qualitative evaluation of NETRA is presented. Then general schemes are described to map parallel algorithms onto NETRA. Algorithms are classified according to their communication requirements for parallel processing. An extensive analysis of inter-cluster communication strategies in NETRA is presented, and parameters affecting performance of parallel algorithms when mapped on NETRA are discussed. Finally, a methodology to evaluate performance of algorithms on NETRA is described.
Author

N90-14840# Central Research Inst. of Electric Power Industry, Tokyo (Japan). Energy and Environment Lab.
SURVEY OF ADAPTIVE CONTROL THEORY AND ITS APPLICATIONS
Masayoshi Eguchi Dec. 1988 66 p In JAPANESE; ENGLISH summary
(DE89-901270; CRIE-T-87116) Avail: NTIS (US Sales Only) HC A04/MF A01

Present situation of adaptive control theory and its application was studied, and its application possibilities to electric system control and future subjects were clarified with the purpose of improving control effects by altering appropriately the control systems online according to the changes of dynamic responses accompanied with the changes of the operating points of electric systems. On the assumption of ideal conditions, many designing methods were proposed and they are now almost completed. These methods were classified, and their correlations were systematized so that they might be put to use in the future theoretical studies and application. Researches on the case that ideal conditions are not satisfied were active these days. Strong points and weak points of these research methods and the future subjects were also indicated. Some of the research results on the application to unitary plants were put to practical use. Researches on the application to electric system controls are active nowadays; and as far as the control of local phenomena is concerned, the research results are considered applicable in the present status of theory. Application to the control of a whole electric system is a future research subject.
DOE

64 NUMERICAL ANALYSIS

Includes iteration, difference equations, and numerical approximation.

N90-14841# Florida Univ., Gainesville. Center for Mathematical System Theory.
MATHEMATICAL TECHNIQUES FOR SYSTEM REALIZATION AND IDENTIFICATION Final Report, 1 Apr. 1988 - 31 Mar. 1989
Rodolt Emil Kalman Jun. 1989 9 p
(Grant AF-AFOSR-0249-87; AF Proj. 2304)
(AD-A212088; AFOSR-89-1201TR) Avail: NTIS HC A02/MF A01 CSCL 12/1

Research supported by grants AFOSR-87-0429 and AFOSR-87-0249 has emphasized algebraic systems theory and the identification of systems from noisy data. Identification, which is based on mathematical (primarily algebraic) ideas has been the area of our main effort. Much work at the Center has been in preparation of reanalyses of published data and exposition of new methods of analysis of noisy data. Research on basic aspects of algebraic system theory has also been active. This research contributes to the study of identification, because it is concerned with deep results about system properties in the exact, that is, noise-free case.
GRA

N90-14842*# Institute for Computer Applications in Science and Engineering, Hampton, VA.
PARALLEL PROJECTED VARIABLE METRIC ALGORITHMS FOR UNCONSTRAINED OPTIMIZATION Final Report
T. L. Freeman (Liverpool Univ., England) Oct. 1989 14 p Submitted for publication
(Contract NAS1-18605)
(NASA-CR-181930; NAS 1.26:181930; ICASE-89-73) Avail: NTIS HC A03/MF A01 CSCL 12A

The parallel variable metric optimization algorithms of Straeter (1973) and van Laarhoven (1985) are reviewed, and the possible drawbacks of the algorithms are noted. By including Davidon (1975) projections in the variable metric updating, researchers can generalize Straeter's algorithm to a family of parallel projected variable metric algorithms which do not suffer the above drawbacks and which retain quadratic termination. Finally researchers consider the numerical performance of one member of the family on several standard example problems and illustrate how the choice of the displacement vectors affects the performance of the algorithm.
Author

N90-14843*# Hampton Univ., VA. Dept. of Applied Mathematics.
A TWO DIMENSIONAL POWER SPECTRAL ESTIMATE FOR SOME NONSTATIONARY PROCESSES M.S. Thesis
Gregory L. Smith [1989] 73 p
(Grant NAG1-768)
(NASA-CR-186100; NAS 1.26:186100) Avail: NTIS HC A04/MF A01 CSCL 12A

A two dimensional estimate for the power spectral density of a nonstationary process is being developed. The estimate will be applied to helicopter noise data which is clearly nonstationary. The acoustic pressure from the isolated main rotor and isolated tail rotor is known to be periodically correlated (PC) and the combined noise from the main and tail rotors is assumed to be correlation autoregressive (CAR). The results of this nonstationary analysis will be compared with the current method of assuming that the data is stationary and analyzing it as such. Another method of analysis is to introduce a random phase shift into the data as shown by Papoulis to produce a time history which can then be accurately modeled as stationary. This method will also be investigated for the helicopter data. A method used to determine the period of a PC process when the period is not know is discussed. The period of a PC process must be known in order to produce an accurate spectral representation for the process. The spectral estimate is developed. The bias and variability of the estimate are also discussed. Finally, the current method for analyzing nonstationary data is compared to that of using a two dimensional spectral representation. In addition, the method of phase shifting the data is examined.
Author

N90-14844*# National Aeronautics and Space Administration. Lewis Research Center, Cleveland, OH.
ON THE APPLICATION OF SUBCELL RESOLUTION TO CONSERVATION LAWS WITH STIFF SOURCE TERMS
Shih-Hung Chang (Cleveland State Univ., OH.) Nov. 1989 14 p
(NASA Order C-99066-G)
(NASA-TM-102384; E-5123; ICOMP-89-27; NAS 1.15:102384)
Avail: NTIS HC A03/MF A01 CSCL 12A

LeVeque and Yee recently investigated a one-dimensional scalar conservation law with stiff source terms modeling the reacting flow problems and discovered that for the very stiff case most of the current finite difference methods developed for non-reacting flows would produce wrong solutions when there is a propagating discontinuity. A numerical scheme, essentially nonoscillatory/subcell resolution - characteristic direction (ENO/SRCD), is proposed for solving conservation laws with stiff source terms. This scheme is a modification of Harten's ENO scheme with subcell resolution, ENO/SR. The locations of the discontinuities and the characteristic directions are essential in the design. Strang's time-splitting method is used and time evolutions are done by advancing along the characteristics. Numerical experiment using this scheme shows excellent results on the model problem of LeVeque and Yee. Comparisons of the results of ENO, ENO/SR, and ENO/SRCD are also presented.
Author

N90-14845# Grenoble-1 Univ. (France). Lab. des Techniques de l'Informatique, des Mathematiques, de la Microelectronique et de la Microscop

BLOCK PREDICTOR (LOW ORDER) CORRECTOR METHODS TO SOLVE ORDINARY DIFFERENTIAL EQUATIONS ON PARALLEL COMPUTERS

P. S. Rao and D. Trystram (Hyderabad Univ., India) Dec. 1988 41 p

(IMAG-RR-757-M; ETN-90-95692) Avail: NTIS HC A03/MF A01

Families of low order predictors for use with the corrector methods for the integration of Ordinary Differential Equations (ODE) are presented. The corrector methods together with the predictors are analyzed for stability. The free parameter(s) of the predictors are for enhancing the stability characteristics and to reduce the local truncation errors of the BPC (block predictor-corrector) methods. The methods have larger intervals of absolute stability than those of Birta and Abou Rabia's families. The families are implemented on a hypercube parallel computer. The superiority of the method with respect to the larger size(s) of stability intervals is illustrated with numerical examples. The speed-up and efficiency of the families of methods is demonstrated. ESA

N90-14846# Grenoble-1 Univ. (France). Lab. des Tech. de l'Informatique, des Math., de la Microelectronique et de la Microscopie Quant.

ESTIMATING METHODS FOR COUNTING PROCESS INTENSITIES: NON-PARAMETRIC METHODS [ESTIMATION REGULIERE DE LA FONCTION D'INTENSITE D'UN PROCESSUS PONCTUEL. METHODES NON PARAMETRIQUES]

A. Antoniadis and G. Gregoire Apr. 1989 25 p In FRENCH; ENGLISH summary

(IMAG-RR-774-M; ETN-90-95703) Avail: NTIS HC A03/MF A01

An extensive survey of some non-parametric estimation methods for counting process intensities is presented. The methods are based on Aalen's multiplicative intensity models. After introducing the important tools from the theory of counting processes, Aalen's estimator of the integrated intensity function is discussed and some kernel estimators for the intensity itself, obtained by smoothing the increments of the Aalen estimator, are described. Three major approaches for non-parametric estimation are concentrated on: the method of Sieves (A. Karr), the penalized maximum likelihood method (A. Antoniadis and G. Gregoire), and the orthogonal series (least squares) method (I. McKeague). For each of these cases, the method is presented and the important properties of the derived estimators are summarized. The use of these methods for analyzing survival data is emphasized. Several other approaches are briefly presented and discussed. ESA

N90-14847*# Institute for Computer Applications in Science and Engineering, Hampton, VA.

LOCAL ERROR ESTIMATES FOR DISCONTINUOUS SOLUTIONS OF NONLINEAR HYPERBOLIC EQUATIONS Final Report

Eitan Tadmor (Tel-Aviv Univ., Israel) Dec. 1989 22 p Submitted for publication

(Contract NAS1-18605)

(NASA-CR-181960; ICASE-89-80; NAS 1.26:181960) Avail: NTIS HC A03/MF A01 CSCL 12A

Let u(x,t) be the possibly discontinuous entropy solution of a nonlinear scalar conservation law with smooth initial data. Suppose u sub epsilon(x,t) is the solution of an approximate viscosity regularization, where epsilon greater than 0 is the small viscosity amplitude. It is shown that by post-processing the small viscosity approximation u sub epsilon, pointwise values of u and its derivatives can be recovered with an error as close to epsilon as desired. The analysis relies on the adjoint problem of the forward error equation, which in this case amounts to a backward linear transport with discontinuous coefficients. The novelty of this approach is to use a (generalized) E-condition of the forward problem in order to deduce a W(exp 1,infinity) energy estimate for the discontinuous backward transport equation; this, in turn, leads one to an epsilon-uniform estimate on moments of the error u(sub epsilon) - u. This approach does not follow the characteristics and, therefore, applies mutatis mutandis to other approximate solutions such as E-difference schemes. Author

N90-14848*# Institute for Computer Applications in Science and Engineering, Hampton, VA.

MODIFIED CHEBYSHEV PSEUDOSPECTRAL METHOD WITH O(N EXP -1) TIME STEP RESTRICTION Final Report

Dan Kosloff and Hillel Tal-Ezer (Tel-Aviv Univ., Israel) Dec. 1989 29 p Submitted for publication

(Contract NAS1-18605)

(NASA-CR-181958; ICASE-89-71; NAS 1.26:181958) Avail: NTIS HC A03/MF A01 CSCL 12A

The extreme eigenvalues of the Chebyshev pseudospectral differentiation operator are O(N exp 2) where N is the number of grid points. As a result of this, the allowable time step in an explicit time marching algorithm is O(N exp -2) which, in many cases, is much below the time step dictated by the physics of the partial differential equation. A new set of interpolating points is introduced such that the eigenvalues of the differentiation operator are O(N) and the allowable time step is O(N exp -1). The properties of the new algorithm are similar to those of the Fourier method. The new algorithm also provides a highly accurate solution for non-periodic boundary value problems. Author

N90-14849# Los Alamos National Lab., NM. Center for Nonlinear Studies.

NUMERICAL METHODOLOGIES FOR SOLVING PARTIAL DIFFERENTIAL EQUATIONS

James M. Hyman 1989 24 p Presented at the NATO Advanced Research Workshop on the Numerical Modeling of Nonlinear Stellar Pulsation, Les Arcs, France, 20-24 Mar. 1989

(Contract W-7405-eng-36)

(DE90-001842; LA-UR-89-3136; CONF-8903121-2) Avail: NTIS HC A03/MF A01

The numerical methods for solving systems of partial differential equations can be analyzed by decoupling the space and time discretizations and analyzing them independently. First a method is selected to discretize the differential equation in space and incorporate the boundary conditions. The spectrum of this discrete operator is then used as a guide to choose an appropriate method to integrate the equations through time. The dissipative effects of a numerical method are crucial to constructing reliable methods for conservation laws. This is particularly true when the solution is discontinuous as in a shock wave or contact discontinuity. Choosing an accurate method to accomplish each of these tasks, space and time discretization and incorporating artificial dissipation in the numerical solution, determines the success of the calculation. We will describe the methodologies used in each of these choices to construct reliable, accurate and efficient methods. DOE

N90-14850# Argonne National Lab., IL.

A COMPARISON RESULT AND ELLIPTIC EQUATIONS INVOLVING SUBCRITICAL EXPONENTS

Man Kam Kwong 1989 20 p Presented at the International Conference on Nonlinear Diffusion Equations and Their Equilibrium States, Newton, England, 20-29 Aug. 1989

(Contract W-31-109-eng-38)

(DE90-001772; CONF-8908178-1) Avail: NTIS HC A03/MF A01

It is well known that good bounds for solutions of nonlinear differential equations are difficult to obtain. A theorem is established comparing non-negative solutions (having identical initial values) of the equations u(double prime)(t) + q(t)u(sup p)(t) + r(t)u(t) = 0 and v(double prime)(t) + k(t)q(t)v(sup p)(t) + r(t)u(t) = 0, respectively. If q(t), r(t) is greater than or equal to 0, k(t) is greater than or equal to 1, k(t) is nondecreasing, and the first equation satisfies a certain uniqueness criterion, the result asserts that u(t) is greater than or equal to v(t). Both the uniqueness assumption on the equation and the monotonicity requirement on k(t) are necessary. A particular case of this theorem plays a central role

in a recent paper of Atkinson and Peletier in the study of asymptotic behavior of nonlinear elliptic equations involving a critical exponent. A simple corollary of the result provides information on the same type of equations with subcritical exponents. DOE

N90-14851# Argonne National Lab., IL. High Energy Physics Div.
HAMILTONIAN FLOWS, SU(INFINITY), SO(INFINITY), USp(INFINITY), AND STRINGS
Cosmas Zachos 1989 8 p Presented at the 1st International Conference on Radioactive Nuclear Beams, Berkeley, CA, 16-18 Oct. 1989
(Contract W-31-109-eng-38)
(DE90-001987; ANL-HEP-CP-89-55; CONF-891044-1) Avail: NTIS HC A02/MF A01

Based on the infinite-dimensional algebras introduced, SU(infinity) is identified with general Hamiltonian flows in 2-d phase-space, SO(infinity) with flows generated by x-p-odd Hamiltonians, and USp(infinity) with those of Hamiltonians of special symmetry. Gauge theories for SU(infinity), SO(infinity), and USp(infinity) are thus formulated in terms of surface (sheet) coordinates for toroidal phase-space. Spacetime-independent configurations of their gauge fields directly yield the quadratic Schild-Eguchi string action. DOE

N90-14852# International Centre for Theoretical Physics, Trieste (Italy).
ON SOME INTEGRAL RELATIONS INVOLVING A GENERALIZED HYPERGEOMETRIC POLYNOMIAL
I. A. Khan and R. Prasad May 1989 7 p
(DE90-600729; IC-89/93) Avail: NTIS (US Sales Only) HC A02/MF A01

Some integral relations involving a generalized hypergeometric polynomial, have been further extended by employing Mellin's inversion formula. The results obtained here, yield very interesting particular cases. DOE

N90-14853# International Centre for Theoretical Physics, Trieste (Italy).
CLASSIFICATION OF MODULAR INVARIANT PARTITION FUNCTIONS FOR THE TWISTED N=2 SUPERCONFORMAL ALGEBRA, TWISTED SU(2) KAC-MOODY ALGEBRA AND D(SUB 2K) PARAFERMIONS
Vladimir K. Dobrev and Alexander H. Ganchev May 1989 17 p
(DE90-600767; IC-89/98) Avail: NTIS (US Sales Only) HC A03/MF A01

The characters of the twisted n=2 super-Virasoro algebra (or equivalently - the twisted su(2) Kac-Moody algebra) and the closely related characters for the twisted sector of the parafermion algebra are represented in terms of order N (Theta)-constants with characteristics. All modular invariants for order N (Theta)-functions with characteristics are characterized by (delta) N such that either (delta) or N/(delta) is odd. The modular invariant Z(sub 2) orbifold partition functions for theories with $c=3k/(k+2)$ are found and classified in an A-D-E series. DOE

N90-14854# Joint Inst. for Nuclear Research, Dubna (USSR).
ITERATIVE METHODS OF DOMAIN DECOMPOSITION WITH CROSS-POINTS FOR THE SOLUTION OF DISCRETE ELLIPTIC PROBLEMS
E. P. Zhidkov, G. E. Mazurkevich, and B. N. Khoromsky 1989 23 p Presented at the Czechoslovak Conference on Differential Equations and Their Application, Jul. 1989
(DE90-000719; JINR-E-11-89-174) Avail: NTIS (US Sales Only) HC A03/MF A01

A method of domain decomposition with cross-points (box decomposition) is used for the solution of finite-difference elliptic boundary value problems in rectangle and in parallelepiped. Capacitance matrix and preconditioners for iterative solution of arising algebraic problem are constructed by means of Poincare-Steklov operators. The convergence properties of iterative algorithms depend on local characteristics of subdomains on the number N of unknowns in one direction in subdomains, and are independent of the number of subdomains and of jumps of elliptic operator coefficients as long as these jumps only occur across the subdomain boundaries. The dependence of convergence on discretization of the problem is defined by ln N for two-dimensional problems, by (radical)N ln N for three-dimensional problems. The results of numerical experiments illustrating convergence properties are presented. DOE

N90-14855# Los Alamos National Lab., NM. Computer Research and Applications.
SYMPLECTIC NUMERICAL INTEGRATION OF HAMILTONIAN SYSTEMS
Clint Scovel 11 Sep. 1989 38 p Presented at the Mathematical Sciences Research Institute Workshop on Geometry of Hamiltonian Systems, Berkeley, CA, 6-15 Jun. 1989
(Contract W-7405-eng-36)
(DE90-002380; LA-UR-89-3465; CONF-8906248-1) Avail: NTIS HC A03/MF A01

Some general techniques are described which are available for symplectic or Lie-Poisson integration and illustrate the results with some numerical computations. In this spirit, also discussed are reversible integration, equivariant integration, integration of volume preserving flows, and symplectic cellular automata. The intention is not to be exhaustive but to give a representative review. DOE

65 STATISTICS AND PROBABILITY

Includes data sampling and smoothing; Monte Carlo method; and stochastic processes.

No abstracts in this category.

66 SYSTEMS ANALYSIS

Includes mathematical modeling; network analysis; and operations research.

N90-14856*# National Aeronautics and Space Administration. Lewis Research Center, Cleveland, OH.
APPLICATION OF HEURISTIC SATELLITE PLAN SYNTHESIS ALGORITHMS TO REQUIREMENTS OF THE WARC-88 ALLOTMENT PLAN
Ann O. Heyward, Charles H. Reilly, Eric K. Walton, Fernando Mata, and Carl Olen (Ohio State Univ., Columbus.) 1990 13 p Prepared for presentation at the 13th International Communications Satellite Systems Conference, Los Angeles, CA, 11-15 Mar. 1990; sponsored by AIAA
(Grant NAG3-159)
(NASA-TM-102479; E-5266; NAS 1.15:102479; AIAA-90-0815)
Avail: NTIS HC A03/MF A01 CSCL 12B

Creation of an Allotment Plan for the Fixed Satellite Service at the 1988 Space World Administrative Radio Conference (WARC) represented a complex satellite plan synthesis problem, involving a large number of planned and existing systems. Solutions to this problem at WARC-88 required the use of both automated and manual procedures to develop an acceptable set of system positions. Development of an Allotment Plan may also be attempted through solution of an optimization problem, known as the Satellite Location Problem (SLP). Three automated heuristic procedures, developed specifically to solve SLP, are presented. The heuristics are then applied to two specific WARC-88 scenarios. Solutions resulting from the fully automated heuristics are then compared with solutions obtained at WARC-88 through a combination of both automated and manual planning efforts. Author

N90-14857# Lawrence Livermore National Lab., CA. Special Studies Program.
CONCERNING ADVANCED ARCHITECTURES FOR STRATEGIC DEFENSE
Lowell Wood 1988 10 p Presented at the First Strategic Defence Initiative Conference, Washington, DC, 13-15 Mar. 1988
(Contract W-7405-eng-48)
(DE90-001894; UCRL-98434; CONF-8803244-1) Avail: NTIS HC A03/MF A01

A brief history of strategic defense is given, then leads to modern architectures in such programs. DOE

N90-14858# Idaho National Engineering Lab., Idaho Falls.
SOLUTION BIAS IN COMPLEX SYSTEMS MODELING
Bruce Kaplan, Mike Mecherikoff, and Harold Blackman 1988 6 p Presented at the Human Factors Society Annual Meeting, Anaheim, CA, 24-28 Oct. 1988
(Contract DE-AC07-76ID-01570)
(DE90-002001; EGG-M-88277; CONF-881058-6) Avail: NTIS HC A02/MF A01

Each discipline tends to use analytic tools that lead them to solutions within their own discipline, and steer them away from others. Within a discipline, we tend to pose solutions that align with our areas of interest or expertise. Clients can be guided into work which may not be the best solution to their particular set of problems or needs. DOE

67 THEORETICAL MATHEMATICS

Includes topology and number theory.

N90-14859# Washington Univ., Seattle. Dept. of Applied Mathematics.
A TENSOR PRODUCT b-SPLINE METHOD FOR 3D MULTI-BLOCK ELLIPTIC GRID GENERATION
Joseph W. Manke Dec. 1988 24 p
(Contract DE-FG06-88ER-25061; AF-AFOSR-0154-86)
(DE89-017440; DOE/ER-25061/2) Avail: NTIS HC A03/MF A01

A tensor product b-spline method was formulated for multi-block numerical grid generation. The Cartesian coordinate functions for a block are represented as a sum of tensor product b-spline basis functions defined on a parameter space for the block. The tensor product b-spline basis functions are constructed so that the basis functions and their first partials are continuous on the parameter space. The coordinate functions inherit this smoothness: a grid computed by evaluating the coordinate functions along constant parameter lines leads to smooth grid lines with smoothly varying tangents. The expansion coefficients for the coordinate functions are computed by solving the usual elliptic grid generation equations using simple collocation. This assures that the computed grid has the smoothness and resolution expected for an elliptic grid with appropriate control. An important result of the formulation is that the dimension of the collocation equations is the number of distinct knots for the tensor product b-spline basis functions. Combining this results with the smoothness of the b-spline representation makes it possible to reduce the dimension of the tensor product method with respect to the finite difference method, simply by using fewer knots than grid points. The expansion of the Cartesian coordinate functions were formulated as a sum of tensor product b-spline basis functions, and then the collocation and boundary condition equations were derived for the usual elliptic grid generation equations. The structure of the system of equations was investigated for the expansion coefficients and then a solution algorithm formulated to compute the coefficients. Finally, the implementation of the method in a 2D multi-block grid code was described and the performance of the method discussed for several grids. DOE

N90-14860# Institute of Nuclear Physics, Novosibirsk (USSR).
VECTOR FIELDS AND GRAVITY ON THE LATTICE
V. M. Khatsymovsky 1988 15 p Submitted for publication
(DE89-633885; IYF-88-105) Avail: NTIS (US Sales Only) HC A03/MF A01

The problem of discretization of vector field on Regge lattice is considered. The approach is based on geometrical interpretation of the vector field as the field of infinitesimal coordinate transformation. A discrete version of the vector field action is obtained as a particular case of the continuum action, and it is shown to have the true continuum limit. DOE

70 PHYSICS (GENERAL)

For precision time and time interval (PTTI) see *35 Instrumentation and Photography;* for geophysics, astrophysics or solar physics see *46 Geophysics, 90 Astrophysics,* or *92 Solar Physics.*

N90-14861# Gosudarstvennyi Komitet po Ispolzovaniyu Atomnoi Energii, Serpukhov (USSR). Inst. Fiziki Vysokikh Ehnergij.
ON-LINE SYSTEM TO MEASURE MAGNETIC CHARACTERISTICS OF STEEL SAMPLES
G. M. Antonichev, O. V. Afanasev, and Yu. B. Dubasov 1988 8 p In RUSSIAN; ENGLISH summary
(DE89-633443; IFVE-OUNK-88-132) Avail: NTIS (US Sales Only) HC A02/MF A01

Using on-line system, one investigates the effect of low-temperatu re (up to 4.2 K) cooling on magnetic properties of electrotechnical steel samples. Dependence of hysteresis losses in proper cycles of reverse magnetization with values of magnetic induction in a sample, which reach saturation induction, is studied. Application of the system allows one to carry out routine monitoring of magnetic characteristics of different steels and to choose the most fitting one for application as a superconducting-dipole yoke of the IHEP accelerating storage complex. The system includes the 100 W programmable bipolar current source, analogue integrator, programmable timer and reference voltage generator, two-channel programmable amplifier, two bipolar 12-th bit ADC with 4K memory buffer, SUMMA interface and microcomputer CM-4. DOE

N90-14862# Lawrence Livermore National Lab., CA. Dept. of Physics.
PATH INTEGRAL SIMULATIONS OF LIQUID HELIUM
Roy Pollock Aug. 1989 21 p Presented at the Los Alamos Workshop on Quantum Simulations of Condensed Matter Phenomena, Los Alamos, NM, 8-11 Aug. 1989
(Contract W-7405-eng-48)
(DE90-001171; UCRL-101905; CONF-8908106-4) Avail: NTIS HC A03/MF A01

Monte Carlo path integral methods are now used to reproduce most of the non-dynamic properties of normal and superfluid helium in two and three dimensions in good agreement with the experiment. Most of these properties can be related to simple geometric aspects of the paths. The superfluid transition in two and three dimensions will be emphasized. DOE

N90-14863# Oak Ridge National Lab., TN. Metals and Ceramics Div.
X RAY MICROPROBE FOR THE MICROCHARACTERIZATION OF MATERIALS
C. J. Sparks and G. E. Ice 1988 11 p Presented at the Fall Meeting of the Materials Research Society, Boston, MA, 28 Nov. - 3 Dec. 1988
(Contract DE-AC05-84OR-21400)
(DE89-006038; CONF-881155-44) Avail: NTIS HC A03/MF A01

The unique properties of x rays offer many advantages over those of electrons and other charged particles for the microcharacterization of materials. X rays are more efficient in exciting characteristic x ray fluorescence and produce higher fluorescent signal-to-background ratios than obtained with electrons. Such x ray microprobes will also produce

unprecedentedly low levels of detection in diffraction, EXAFS, Auger, and photoelectron spectroscopies for structural and chemical characterization and elemental identification. These major improvements in microcharacterization capabilities will have wide-ranging ramifications not only in materials science but also in physics, chemistry, geochemistry, biology, and medicine. DOE

N90-14864# Australian National Univ. Canberra. Dept. of Theoretical Physics.
SYMMETRY BREAKING BIFURCATIONS OF A CURRENT SHEET
R. D. Parker, R. L. Dewar, and J. L. Johnson Aug. 1988 24 p Submitted for publication
(DE90-601005; ANU/TPP-88/01) Avail: NTIS HC A03/MF A01

Using a time evolution code with periodic boundry conditions, the viscoresistive hydromagnetic equations describing an initially static, planar current sheet with large Lundquist number were evolved for times long enough to reach a steady state. A cosh squared x resistivity model was used. For long periodicity lengths, L(sub p), the resistivity gradient drives flows which cause forced reconnection at x point current sheets. Using L(sub p) as a bifurcation parameter, two new symmetry breaking bifurcations were found - a transition to an asymmetric island chain with nonzero, positive or negative phase velocity, and a transition to a static state with alternating large and small islands. These states are reached after a complex transient behavior which involves a competition between secondary current sheet instability and coalescence. DOE

N90-14865# California Univ., Berkeley. Lawrence Berkeley Lab. Energy Div.
SUPERCONDUCTING MAGNETS IN SPACE
Michael A. Green Aug. 1989 8 p Presented at the Winter Annual Meeting of the American Society of Mechanical Engineers, San Francisco, CA, 10-15 Dec. 1989
(Contract DE-AC03-76SF-00098)
(DE90-002671; LBL-27745; CONF-891208-23) Avail: NTIS HC A02/MF A01

Applications for superconducting magnets in space include particle astrophysics detectors, semiconductor crystal growth, magnetic refrigerators to reach temperatures of a few millikelvin and magnetic energy storage. Superconducting magnets are well suited for use in space because they consume very little power, and superconductors can operate at current densities which are much higher than conventional conductors. The general requirements are presented for superconducting magnets in space. The selection of a cryogenic working fluid and the selection of superconductor for space magnets are discussed. A 260 mm warm bore 3 T solenoid and the ASTROMAG particle astrophysics experiment solenoid for the space station are presented as examples of superconducting magnetic technology for use in space. DOE

71 ACOUSTICS

Includes sound generation, transmission and attenuation. For noise pollution see *45 Environmental Pollution.*

N90-14866*# Boeing Commercial Airplane Co., Seattle, WA.
EVALUATION OF ANALYSIS TECHNIQUES FOR LOW FREQUENCY INTERIOR NOISE AND VIBRATION OF COMMERCIAL AIRCRAFT
A. E. Landmann, H. F. Tillema, and S. E. Marshall Oct. 1989 73 p Prepared in cooperation with Cambridge Collaborative, Inc., MA
(Contract NAS1-18027)
(NASA-CR-181851; NAS 1.26:181851) Avail: NTIS HC A04/MF A01 CSCL 20A

The application of selected analysis techniques to low frequency cabin noise associated with advanced propeller engine installations is evaluated. Three design analysis techniques were chosen for evaluation including finite element analysis, statistical energy analysis (SEA), and a power flow method using element of SEA (computer program Propeller Aircraft Interior Noise). An overview of the three procedures is provided. Data from tests of a 727 airplane (modified to accept a propeller engine) were used to compare with predictions. Comparisons of predicted and measured levels at the end of the first year's effort showed reasonable agreement leading to the conclusion that each technique had value for propeller engine noise predictions on large commercial transports. However, variations in agreement were large enough to remain cautious and to lead to recommendations for further work with each technique. Assessment of the second year's results leads to the conclusion that the selected techniques can accurately predict trends and can be useful to a designer, but that absolute level predictions remain unreliable due to complexity of the aircraft structure and low modal densities. Author

N90-14867 Kentucky Univ., Lexington.
BOUNDARY ELEMENT ANALYSIS OF SINGLE AND MULTIDOMAIN PROBLEMS IN ACOUSTICS Ph.D. Thesis
Chunyuen Raymond Cheng 1988 209 p
Avail: Univ. Microfilms Order No. DA8914898

A numerical technique based on the boundary element method for the solution of single-domain linear interior acoustic boundary value problems governed by the Helmholtz equation for time-harmonic acoustic waves was developed. A boundary element computer code is developed to study the acoustic fields in an enclosed acoustic region. The development of the method is general, but the area of application is broad. The specific applications considered are the prediction of acoustic behavior in an acoustical cavity and transmission loss of various expansion-type mufflers and acoustical silencers. The method is shown to be accurate in studying the acoustic response in an enclosed cavity and is particularly useful in predicting the transmission loss of an acoustical filter in the frequency region where the one-dimensional plane-wave theory is invalid. The validity and the usefulness of the technique is demonstrated using comparisons with experimental, analytical and other numerical results. Both axisymmetric and fully three-dimensional geometries are considered. The analysis capability and applicability of the boundary element method are also extended to multidomain problems in which the interior acoustic region can be divided into a few subdomains. The multidomain boundary element procedure is further extended to include analysis of the coupled interior/exterior acoustic problems. Dissert. Abstr.

N90-14868 Catholic Univ. of America, Washington, DC.
WIDE-ANGLE PROPAGATION IN INHOMOGENEOUS FLUIDS AND ELASTIC SOLIDS USING PERTURBATION METHODS Ph.D. Thesis
Stephen Charles Wales 1989 267 p
Avail: Univ. Microfilms No. DA8913824

The development of propagation models for fluid and elastic media is described. A specific objective is the development of a vector parabolic equation for elastic media corresponding to the scalar parabolic equation for fluids. Beginning from the foundation of factored wave theory for fluid media a strong forward scattering approximation is developed. It is then shown that the approximation may be further reduced to yield the same narrow-angle parabolic equation for fluid media. An analogous strong forward scattering approximation is then developed for elastic media and the appropriate limits taken to arrive at the narrow-angle parabolic equations for elastic media. The narrow-angle parabolic equations derived by this method exhibit all of the physically expected features. The solution is seen to be identical in form to the solution for an inhomogeneous fluid medium with additional coupling terms describing the transfer of energy between the longitudinal and shear waves. The equations are then compared with those of other existing parabolic theories for elastic media and the strong forward scattering approximation for a simple test case to determine the properties of each theory. Two computer programs were written to evaluate the models, one each for fluids and solids. The computer program for the fluid models is capable of handling a

large number of different models. A comparison between the models is presented. The second computer program implements the narrow-angle parabolic equations for elastic solids. The results are evaluated for physical rationality and against an exact model for some of the cases. Dissert. Abstr.

N90-14869# Naval Postgraduate School, Monterey, CA.
CONTROL OF AN EXPERIMENT TO MEASURE ACOUSTIC NOISE IN THE SPACE SHUTTLE M.S. Thesis
Charles B. Cameron Jun. 1989 252 p
(NPS62-89-022) Avail: NTIS HC A12/MF A02

The potential use of a general-purpose controller to measure acoustic vibration autonomously in the Space Shuttle Cargo Bay during launch is described. The experimental package will be housed in a Shuttle Get Away Special (GAS) canister. The control functions were implemented with software written largely in the C programming language. An IBM MS DOS computer and C cross-compiler were used to generate Z-80 assembly language code, assemble and link this code, and then transfer it to EPROM for use in the experiment's controller. The software is written in a modular fashion to permit adapting it easily to other applications. The software combines the experimental control functions with a menu-driven, diagnostic subsystem to ensure that the software will operate in practice as it does in theory and under test. The experiment uses many peripheral devices controlled by the software described here. These devices include: (1) a solid-state data recorder; (2) a bubble memory storage module; (3) a real-time clock; (4) an RS-232C serial interface; (5) a power control subsystem; (6) a matched filter subsystem to detect activation of the Space Shuttle's auxillary power units five minutes prior to launch; (7) a launch detection subsystem based on vibrational and barometric sensors; (8) analog-to-digital converters; and (9) a heater subsystem. The matched filter design is discussed in detail and the results of a computer simulation of the performance of its most critical sub-circuit are presented. Author

N90-14870# Idaho National Engineering Lab., Idaho Falls.
PROCESS MONITORING USING OPTICAL ULTRASONIC WAVE DETECTION
K. L. Telschow, J. B. Walter, G. V. Garcia, and D. C. Kunerth 1989 7 p Presented at the Conference on Review of Progress in Quantitative NDE, Brunswick, ME, 24-28 Jul. 1989 Submitted for publication
(Contract DE-AC07-76ID-01570)
(DE90-002021; EGG-M-89119; CONF-890770-2) Avail: NTIS HC A02/MF A01

Optical ultrasonic wave detection techniques are being developed for process monitoring. An important limitation on optical techniques is that the material surface, in materials processing applications, is usually not a specular reflector and in many cases is totally diffusely reflecting. This severely degrades the light collected by the detection optics, greatly reducing the intensity and randomly scattering the phase of the reflected light. A confocal Fabry-Perot interferometer, which is sensitive to the Doppler frequency shift resulting from the surface motion and not to the phase of the collected light, is well suited to detecting ultrasonic waves in diffusely reflecting materials. This paper describes the application of this detector to the real-time monitoring of the sintering of ceramic materials. DOE

N90-14871# Argonne National Lab., IL. Materials and Components Technology Div.
CAVITATION-CONTROLLED ULTRASONIC AGITATOR
S. H. Sheen, W. P. Lawrence, and A. C. Raptis Oct. 1989 5 p Presented at the IEEE Ultrasonics Symposium and Ferroelectrics and Frequency Control Society Meeting, Montreal, Quebec, 3-6 Oct. 1989
(Contract W-31-109-eng-38)
(DE90-002773; CONF-8910216-3) Avail: NTIS HC A01/MF A01

High intensity ultrasound generally produces nonlinear acoustic cavitation and streaming in liquids. The ultrasonic energy required to cause cavitation and streaming in a liquid depends on the physical properties of the liquid, e.g., surface tension, viscosity, and entrained gases. Both cavitation and streaming generate acoustic noise whose signatures may be used to distinguish the stage of agitation and thus allow the process to be controlled. An ultrasonic agitator was designed for application in a confined area with a high temperature, high pressure, and corrosive environment. Control of this agitator is based on the detection of noise levels and subharmonics produced during cavitation and streaming. Noise signatures of agitation in different liquids and in liquids with particles were determined, and discussed. DOE

N90-14872# Sandia National Labs., Albuquerque, NM.
EFFECTIVE UTILIZATION OF ACOUSTIC WAVE SENSOR RESPONSES: SIMULTANEOUS MEASUREMENT OF VELOCITY AND ATTENUATION
S. J. Martin and A. J. Ricco 1989 21 p Presented at the Ultrasonics Symposium, Montreal, Quebec, 3 Oct. 1989
(Contract DE-AC04-76DP-00789)
(DE90-002580; SAND-89-1472C; CONF-8910216-2) Avail: NTIS HC A03/MF A01

When acoustic wave devices are used as sensors, responses arise from perturbations in wave propagation characteristics (velocity and attenuation) caused by wave interactions with a surface layer. Simultaneous measurement of both velocity and attenuation changes helps elucidate the wave perturbation mechanisms. A number of wave-surface layer interactions have been investigated involving surface acoustic waves (SAWs) in the gas phase and acoustic plate modes (APMs) in liquids. These include: (1) mass loading of a SAW, (2) acoustoelectric interactions between SAWs and a conductive film overlay, (3) mass loading of an APM, and (4) viscous coupling of an APM to an adjacent liquid medium. DOE

72 ATOMIC AND MOLECULAR PHYSICS

Includes atomic structure, electron properties, and molecular spectra.

N90-14873# Lund Univ. (Sweden).
A STUDY OF RECOIL PROTONS IN ULTRA-RELATIVISTIC NUCLEUS-NUCLEUS COLLISIONS
M. I. Adamovich, M. M. Aggarwal, R. Arora, Y. A. Alexandrov, E. Basova, K. B. Bhalla, A. Bhasin, V. S. Bhatia, R. A. Bondarenko, and T. H. Burnett (Washington Univ., Seattle.) et al Jun. 1989 14 p
(LUIP-8907; LUNFD6/(NFFK-7104)1-13(1989); ISSN-0348-9329)
Avail: NTIS HC A03/MF A01

An investigation of the energy dependence of grey prong producing particles in O-16(+) emulsion interactions at energies from 2.1 to 200 A GeV is reported. Many of the features of these particles, known from hadron-induced interactions, are shown to be of importance also in heavy-ion interactions, i.e., multiplicity and angular distributions as well as the impact parameter dependence are energy independent. Furthermore the angular distribution seems to be independent of the projectile and target masses as well as centrality of the interactions. Both the Fritiof and Ranft models fail to reproduce this general angular shape. Author

N90-14874*# National Aeronautics and Space Administration. Ames Research Center, Moffett Field, CA.
A DIAGNOSTIC FOR DETERMINING THE QUALITY OF SINGLE-REFERENCE ELECTRON CORRELATION METHODS
Timothy J. Lee and Peter R. Taylor (Eloret Corp., Sunnyvale, CA.) 1989 15 p
(Contracts NCC2-371; NCC2-552)
(NASA-TM-101929; NAS 1.15:101929) Avail: NTIS HC A03/MF A01 CSCL 20H

It was recently proposed that the Euclidian norm of the t(sub 1) vector of the coupled cluster wave function (normalized by the number of electrons included in the correlation procedure) could be used to determine whether a single-reference-based electron

correlation procedure is appopriate. This diagnostic, T(sub 1) is defined for use with self-consistent-field molecular orbitals and is invariant to the same orbital rotations as the coupled cluster energy. T(sub 1) is investigated for several different chemical systems which exhibit a range of multireference behavior, and is shown to be an excellent measure of the importance of non-dynamical electron correlation and is far superior to C(sub 0) from a singles and doubles configuration interaction wave function. It is further suggested that when the aim is to recover a large fraction of the dynamical electron correlation energy, a large T(sub 1) (i.e., greater than 0.02) probably indicates the need for a multireference electron correlation procedure. Author

N90-14875# Argonne National Lab., IL.
PROCEEDINGS OF THE CONFERENCE ON HIGH-SPIN NUCLEAR STRUCTURE AND NOVEL NUCLEAR SHAPES
1988 317 p Conference held in Argonne, IL, 13-15 Apr. 1988 Sponsored in part by Chicago Univ.
(Contract W-31-109-eng-38)
(DE88-013968; ANL-PHY-88-2; CONF-880496) Avail: NTIS HC A14

The proceedings of the conference on High Spin Nuclear Structure and Novel Nuclear Shapes are presented. The major topic covered are: Superdeformation, Octupole deformation, Quasicontinuum structure, Hot nuclei, and Structure near the yrast line. DOE

N90-14876# Joint Inst. for Nuclear Research, Dubna (USSR). Lab. of High Energy.
NARROW ONE-CHANNEL RESONANCES AND THEIR MANIFESTATION IN THE PURE ELASTIC SCATTERING OF UNPOLARIZED PARTICLES
V. L. Lyuboshits 1988 15 p In RUSSIAN; ENGLISH summary
(DE89-632177; JINR-R-2-88-507) Avail: NTIS (US Sales Only) HC A03/MF A01

An energy dependence of the effective cross section of pure elastic resonance scattering in the presence of a constant background is investigated on the basis of the S-matrix unitarity condition. The relations are obtained which describe the range of changing the pure elastic scattering total cross section for non-identical as well as for identical particles in the passage through a narrow one-channel resonance. A finite width of the energetic resolution is taken into account. The results are applied to the analysis of the influence of narrow two-proton resonances on the elastic pp-scattering behaviour below the threshold of meson production. DOE

N90-14877# Gosudarstvennyi Komitet po Ispolzovaniyu Atomnoi Energii, Moscow (USSR). Inst. Atomnoj Ehnergii.
STRUCTURAL PECULIARITIES AND MOLECULAR PROPERTIES OF CHARGE COMPLEXES FORMED ON POSITIVE ION INJECTION INTO DENSE INERT GAS MEDIA
S. G. Potapov, L. P. Suchanov, and G. L. Gutsev 1988 21 p In RUSSIAN
(DE89-633953; IAE-4623/12) Avail: NTIS (US Sales Only) HC A03/MF A01

The formation of charge complexes resulting from penetration of positive ions into the dense inert gas media is modelled on the basis of Hartree-Fock-Roothaan method calculations of the potential energy surface of proton interaction with n inert gas atoms R. It is shown that molecular ions of the type RH(+), R2H(+) with binding energy D(sub E) is greater than or equal to 0.3 eV are formed at n is less than or equal to 2, and a polarization envelope of atoms R around ion R2H(+) is formed only at n is greater than or equal to 3. Using the results of Hartree-Fock calculations on vibrational spectra and those of discrete variational X(sub alpha)-method calculations on the electronic spectra, the capabilities of experimental optical registration of the predicted ion-molecular compounds in dense inert gas media are analyzed. DOE

N90-14878# Brookhaven National Lab., Upton, NY.
A THEORETICAL PERSPECTIVE ON NEUTRINO PHYSICS
William J. Marciano Sep. 1989 10 p Presented at the Workshop on Physics at the Main Injector, Batavia, IL, 16-18 May 1989
(Contract DE-AC02-76CH-00016)
(DE90-000759; BNL-43292; CONF-8905183-4) Avail: NTIS HC A02/MF A01

A survey of sin(squared) theta(sub W), rho, CKM matrix, and axial-isoscalar neutral current measurements via neutrino scattering is presented. Loop effects due to heavy top or a fourth generation are described. Neutrino oscillations are discussed in a three generation mixing framework and some motivation for nu(sub mu) yields nu(sub tau) oscillation searches is given. DOE

N90-14879# Michigan Univ., Ann Arbor. Dept. of Physics.
STUDIES OF ELEMENTARY PARTICLES: PROPOSAL Progress Report
16 May 1989 90 p
(Contract DE-AC02-76ER-01112)
(DE90-001120; DOE/ER-01112/1989) Avail: NTIS HC A05/MF A01

The following tasks are discussed: Task 1 has completed and successfully operated 8 Michigan muon array patches for the UMC experiment. Data from the detector has already improved the limits on the ratio of gamma rays to hadrons in primary cosmic rays. The Task 2 built luminosity monitor for the Mark 2 detector is functioning well and fulfilling its key role in the determination of the Z mass and width. Major Task 2 contributions to the machine diagnostics, the beamstrahlung monitor and wire scanner, have provided critical tuning information for the SLC. Task 4 has recently reported the detection of 200 GeV (gamma)-rays from the Crab Nebula with a statistical significance of 5.8 sigma. This observation confirms the importance of imaging techniques for VHE gamma ray astronomy. The Michigan theory group (Task 7) has focused on: Working to understand the systematics of gluon dynamics in poorly understood pseudoscalar meson decays; Exploring the consequences of heavy Higgs boson and/or a top quark more massive than the W(sup +(minus)) or Z; Surveying the potentially attractive ways of experimentally searching for the Higgs boson of the minimal Standard Model or the spectrum of Higgs bosons to be expected in extensions of the Standard Model; Calculating the radiative corrections for W(+) + W(-) yields W(+) + W(-) as a precision test of the Standard Model, especially in its sensitivity to the Higgs sector; Investigating the modifications of general relativity arising from quantum fluctuations of matter; Exploring phenomenological test of CP violation dynamics; Developing relations between the strong CP problem and ElectroWeak CP violation; and Investigating 4-Fermi interactions in Technicolor models. DOE

N90-14880# Virginia Polytechnic Inst. and State Univ., Blacksburg. Dept. of Physics.
THE AMY EXPERIMENT Progress Report
1989 9 p
(Contract DE-AS05-80ER-10713)
(DE90-001153; DOE/ER-10713/T2) Avail: NTIS HC A02/MF A01

The AMY experiment is one of three major experiments at TRISTAN which is studying the states of matter produced in electron positron annihilations in the center of mass energy range of 50 to 65 GeV. It provides information between the lower energy facilities such as PEP and PETRA and the new facilities SLC and LEP which are designed to operate in the region of the Z(sup 0) mass near 90 GeV. In the region of the AMY experiment, interaction cross sections are near their minimum of about 100 pb, making it difficult to acquire large data samples during typical running cycles. This last year has seen an accumulation of about 10--(minus)12pb(sup (minus)1) of integrated luminosity in the energy range from 58 to 61.7 GeV. Despite this limited data sample, the AMY experiment has been extremely active in attempting to extract the minimum amount of information from the data. Some of the most significant results are discussed in this paper. DOE

N90-14881# Brookhaven National Lab., Upton, NY.
STRING MODELS FOR ULTRARELATIVISTIC HEAVY ION COLLISIONS: LUND MODEL VERSUS COLOR EXCHANGE MODELS
K. Werner 1988 8 p Presented at the 3rd International Conference on the Intersections Between Particle and Nuclear Physics, Rockport, ME, 14 May 1988
(Contract DE-AC02-76CH-00016)
(DE88-015856; BNL-41502; CONF-8805142-24) Avail: NTIS HC A02/MF A01

Similarities and differences between several string models are discussed for ultrarelativistic nucleus nucleus scattering, being proposed to account for normal collisions (with no quark gluon plasma involved). DOE

N90-14882# Oak Ridge National Lab., TN. Health and Safety Research Div.
INTERACTION OF LOW-ENERGY ELECTRONS AND POSITRONS WITH CONDENSED MATTER: STOPPING POWERS AND INELASTIC MEAN FREE PATHS FROM OPTICAL DATA
J. C. Ashley 1989 19 p Presented at the 12th Werner Brandt International Workshop on Charged Particle Penetration Phenomena, San Sebastian, Spain, 4-7 Sep. 1989
(Contract DE-AC05-84OR-21400)
(DE90-001001; CONF-8909210-2) Avail: NTIS HC A03/MF A01

An optical-data model is described for evaluating energy loss per unit pathlength and inelastic mean free path for low-energy electrons and positrons (approx. less than 10 KeV) from optical data on the medium of interest. Exchange between the incident electron and electrons in the medium is included. Results from the optical-data model are compared with previous theoretical calculations. DOE

N90-14883# Oak Ridge National Lab., TN. Health and Safety Research Div.
DIRECTION-DEPENDENT STOPPING POWER AND BEAM DEFLECTION IN ANISOTROPIC SOLIDS
Oakley H. Crawford 1989 15 p Presented at the 12th Werner Brandt International Workshop on Charged Particle Penetration Phenomena, San Sebastian, Spain, 4-7 Sep. 1989
(Contract DE-AC05-84OR-21400)
(DE90-001076; CONF-8909210-1) Avail: NTIS HC A03/MF A01

Directional effects on the motion of swift ions in anisotropic media are studied. The stopping power is a function of the direction of the velocity relative to the principle axes of the medium, and there is a nonzero lateral force on the ion tending to bend its trajectory. These effects arise from the anisotropy of the dielectric response, and are distinct from channeling. Simple expressions are derived for the stopping power and lateral force in the nonrelativistic high-velocity limit, and calculations are performed for crystalline graphite. DOE

N90-14884# Argonne National Lab., IL.
HEAVY ION INTERACTIONS
John P. Schiffer (Chicago Univ., IL.) 1989 20 p Presented at the International Nuclear Physics Conference, Sao Paulo, Brazil, 20-26 Aug. 1989
(Contract W-31-109-eng-38)
(DE90-001410; CONF-890826-4) Avail: NTIS HC A03/MF A01

Nuclear Physics has come a long way since its inception 70 years ago. We have learned a great deal about nuclear structure and nuclear interactions and we have a lot to learn yet. Our understanding of the substructure of protons and neutrons in terms of their elementary constituents has also evolved to the present level of Quantum Chromodynamics (QCD) and the Standard Model. Early work on nuclear reactions involving light projectiles did a great deal in elucidating the characteristic nuclear symmetries and the dynamic phenomena associated with nuclei. As accelerator and ion source technologies evolve it has become possible to accelerate heavier nuclei in addition to electrons, protons, and the very light nuclear systems. From these developments in the tools of our science we are deriving new knowledge: learning about otherwise inaccessible nuclear properties, of the dynamic characteristics of nuclear matter, and about the production of mesons, antiparticles, and other exotic objects in the collision of complex nuclear systems. The subject cuts across much of nuclear physics and it is difficult to give a cohesive overview. Current areas of the subject are discussed. DOE

N90-14885# California Univ., Berkeley. Lawrence Berkeley Lab. Accelerator and Fusion Research Div.
MULTIPLE ELECTRON CAPTURE IN CLOSE ION-ATOM COLLISIONS
A. S. Schlachter, J. W. Stearns, K. H. Berkner, E. M. Bernstein, M. W. Clark, R. D. DuBois, W. G. Graham, T. J. Morgan, D. W. Mueller, and M. P. Stockli (Kansas State Univ., Manhattan.) et al 24 Jul. 1989 7 p Presented at the 16th International Conference on the Physics of Electronic and Atomic Collisions, New York, NY, 26 Jul. - 1 Aug. 1989 Sponsored in part by Western Michigan Univ. Faculty Research and Creative Activities Support Fund and UKSERC
(Contracts DE-AC03-76SF-00098; DE-AC06-76RL-01830)
(DE90-001541; LBL-27553; CONF-890708-9) Avail: NTIS HC A02/MF A01

Collisions in which a fast highly charged ion passes within the orbit of K electron of a target gas atom are selected by emission of a K x ray from the projectile or target. Measurement of the projectile charge state after the collision, in coincidence with the K x ray, allows measurement of the charge-transfer probability during these close collisions. When the projectile velocity is approximately the same as that of target electrons, a large number of electrons can be transferred to the projectile in a single collision. The electron-capture probability is found to be a linear function of the number of vacancies in the projectile L shell for 47-MeV calcium ions in an Ar target. DOE

N90-14886# Lawrence Livermore National Lab., CA.
BIOMODAL SPONTANEOUS FISSION
E. K. Hulet 26 Sep. 1989 12 p Presented at the 50th Anniversary of Nuclear Fission, Leningrad, USSR, 16-20 Oct. 1989
(Contract W-7405-eng-48)
(DE90-001516; UCRL-101174; CONF-8910227-1) Avail: NTIS HC A03/MF A01

Investigations of mass and kinetic-energy distributions from spontaneous fission were extended in recent years to an isotope of element 104 and, for half-lives, to an isotope of element 108. The results were surprising in that spontaneous fission half-lives have turned out to be much longer than expected and mass and kinetic-energy distributions were found to abruptly shift away from those of the lighter actinides, showing two modes of fission. These new developments have caused a re-evaluation of the understanding of the fission process, bringing an even deeper appreciation of the role played by nuclear shell effects upon spontaneous fission properties. DOE

N90-14887# Department of Energy, Washington, DC.
THE ULTIMATE STRUCTURE OF MATTER: THE US HIGH ENERGY PHYSICS PROGRAM FROM THE 1950S THROUGH THE 1980S
Oct. 1989 43 p
(DE90-001784; DOE/ER-0412) Avail: NTIS HC A03/MF A01

The following topics in high energy physics are discussed: the particle zoo; the strong and the weak; the particle explosion; deep inside the nucleon; the search for unity; physics in collision; the standard model; particles and the cosmos; and practical benefits. DOE

N90-14888# Los Alamos National Lab., NM.
PHYSICS WITH ULTRA-LOW ENERGY ANTIPROTONS
D. B. Holtkamp, M. H. Holzscheiter, and R. J. Hughes 1989 6 p Presented at the Workshop on Physics at Fermilab in the 1990's, Breckenridge, CO, 15-24 Aug. 1989

(Contract W-7405-eng-36)
(DE90-002397; LA-UR-89-3537; CONF-890872-2) Avail: NTIS HC A02/MF A01

The experimental observation that all forms of matter experience the same gravitational acceleration is embodied in the weak equivalence principle of gravitational physics. However, no experiment has tested this principle for particles of antimatter such as the antiproton or the antihydrogen atom. Clearly, the question of whether antimatter is in compliance with weak equivalence is a fundamental experimental issue, which can best be addressed at an ultra-low energy antiproton facility. This paper addresses the issue. DOE

N90-14889# Argonne National Lab., IL. Materials Science Div.
ATOMIC MATCHING ACROSS INTERNAL INTERFACES
Karl L. Merkle May 1989 8 p Presented at the Materials Research Society Spring Meeting, San Diego, CA, 24-29 Apr. 1989
(Contract W-31-109-eng-38)
(DE90-002266; CONF-8904290-3) Avail: NTIS HC A02/MF A01

The atomic structure of internal interfaces in dense-packed systems has been investigated by high-resolution electron microscopy (HREM). Similarities between the atomic relaxations in heterophase interfaces and certain large-angle grain boundaries have been observed. In both types of interfaces localization of misfit leads to regions of good atomic matching within the interface separated by misfit dislocation-like defects. It appears that, whenever possible, the GB structures assume configurations in which the atomic coordination is not too much different from the ideal lattice. It is suggested that these kinds of relaxations primarily occur whenever the translational periods along the GB are large or when the interatomic distances are incommensurate. Incorporation of low index planes into the GB appears to lead to preferred, i.e., low energy structures, that can be quite dense with good atomic matching across a large fraction of the interface. DOE

73 NUCLEAR AND HIGH-ENERGY PHYSICS

Includes elementary and nuclear particles; and reactor theory.

For space radiation see *93 Space Radiation.*

N90-14890*# National Aeronautics and Space Administration. Langley Research Center, Hampton, VA.
CALCULATION OF TWO-NEUTRON MULTIPLICITY IN PHOTONUCLEAR REACTIONS
John W. Norbury (Rider Coll., Lawrenceville, NJ.) and Lawrence W. Townsend Jan. 1990 11 p
(NASA-TP-2968; L-16610; NAS 1.60:2968) Avail: NTIS HC A03/MF A01 CSCL 20H

The most important particle emission processes for electromagnetic excitations in nucleus-nucleus collisions are the ejection of single neutrons and protons and also pairs of neutrons and protons. Methods are presented for calculating two-neutron emission cross sections in photonuclear reactions. The results are in a form suitable for application to nucleus-nucleus reactions. Author

N90-14891# Nationaal Inst. voor Kernfysica en Hoge Energiefysica, Amsterdam (Netherlands).
NIKHEF-K CONTRIBUTIONS TO THE 1989 PARTICLE ACCELERATOR CONFERENCE
1989 17 p Conference held in Chicago, IL, 20-23 Mar. 1989
(NIKHEF/AmPS/89/03; ETN-90-95976) Avail: NTIS HC A03/MF A01

Five papers relating to pulse-stretcher projects which constitute contributions made by NIKHEF-K (Nationaal Instituut voor Kernfysica en Hoge-Energiefysica Sector-K), to the 1989 Particle Accelerator Conference held in Chicago, USA, 20 to 23 Mar. 1989, are presented. They relate specifically to the Amsterdam pulse stretcher project, an energy spectrum compressor system and optics for this project, modification of MEA (medium energy accelerator) modulator-klystron units enabling short pulse injection into a pulse-stretcher ring, and performance and modification of the MEA RF drive system. For individual titles, see N90-14892 through N90-14896.

N90-14892# Nationaal Inst. voor Kernfysica en Hoge Energiefysica, Amsterdam (Netherlands).
THE AMSTERDAM PULSE STRETCHER PROJECT (AMPS)
G. Luijckx, J. H. M. Bijleveld, H. Boer Rookhuizen, P. J. T. Bruinsma, A. P. Kaan, F. B. Kroes, L. H. Kuijer, R. Maas, J. G. Noomen, and J. C. Post et al *In its* NIKHEF-K Contributions to the 1989 Particle Accelerator Conference 1989 p 1-3 Sponsored by the Stichting voor Fundamenteel Onderzoek der Materie and the Netherlands Foundation for Scientific Research (For primary document see N90-14891 06-73)
Avail: NTIS HC A03/MF A01

Modifications to the existing 500 MeV, 1 percent duty factor electron linac facility Medium Energy Accelerator (MEA), which is primarily used for electron scattering experiments, are described. A stretcher and storage ring to be added to the MEA facility is described which will obtain electron beams with a high duty factor. The ring operates at energies between 250 and 900 MeV and with circulating currents up to 200 mA. The storage mode is used for internal target physics. ESA

N90-14893# Nationaal Inst. voor Kernfysica en Hoge Energiefysica, Amsterdam (Netherlands).
OPTICS OF THE AMSTERDAM PULSE STRETCHER (AMPS)
R. Maas and Y. Y. Wu *In its* NIKHEF-K Contributions to the 1989 Particle Accelerator Conference 1989 p 4-6 Sponsored by the Stichting voor Fundamenteel Onderzoek der Materie and the Netherlands Foundation for Scientific Research (For primary document see N90-14891 06-73)
Avail: NTIS HC A03/MF A01

The AmPS (Amsterdam pulse stretcher) machine, designed as a dual purpose machine, as a pulse stretcher and as a storage ring for electrons, is discussed with reference to the operations. In its second mode the stored beam is used in conjunction with an internal (jet) target. The internal target limits the lifetime of the beam to minutes so the storage requirements (e.g., vacuum) are modest. In pulse stretcher mode the energy range is 250 to 800 MeV and this is extended to 900 MeV in storage mode. A current storage of up to 200 mA is anticipated. ESA

N90-14894# Nationaal Inst. voor Kernfysica en Hoge Energiefysica, Amsterdam (Netherlands).
MODIFICATION OF MEA MODULATOR-KLYSTRON UNITS ENABLING SHORT PULSE INJECTION INTO A PULSE-STRETCHER RING
F. B. Kroes and E. Heine *In its* NIKHEF-K Contributions to the 1989 Particle Accelerator Conference 1989 p 7-9 Sponsored by the Stichting voor Fundamenteel Onderzoek der Materie and the Netherlands Foundation for Scientific Research (For primary document see N90-14891 06-73)
Avail: NTIS HC A03/MF A01

Adaptation of the present modulator-Klystron units from 4 MW, 2 percent duty factor, to 10 MW, 0.2 percent duty factor mode of operation, in order to modify the present 500 MeV, 1 percent duty factor MEA (medium energy accelerator) into a 900 MeV, 0.1 percent duty factor injector for a newly built pulse-stretching ring is discussed. Design principles of these modulators are described with attention to the video-pulse shape requirements dictated by performance requirements. The device must deliver low emittance, high duty factor beams for nuclear physics experiments. Prototype tests of the video-pulse forming modifications are presented. ESA

N90-14895# Nationaal Inst. voor Kernfysica en Hoge Energiefysica, Amsterdam (Netherlands).
PERFORMANCE AND MODIFICATION OF THE MEA RF DRIVE SYSTEM
F. B. Kroes, T. G. B. W. Sluyk, and B. Heutenik *In its* NIKHEF-K Contributions to the 1989 Particle Accelerator Conference 1989 p 10-12 Sponsored by the Stitching voor Fundamenteel Onderzoek der Materie and the Netherlands Foundation for Scientific Research (For primary document see N90-14891 06-73)
Avail: NTIS HC A03/MF A01

Modification of the twelve modulator-klystron units serving the 500 MeV linear electron MEA (medium energy accelerator) to convert the accelerator into a 900 MeV, 0.2 percent duty factor injector for the pulse stretcher project is described. The klystrons are to be provided with higher input RF peak power which implies modification to the RF drive system. Design consideration for the modification and initial system tests are presented. ESA

N90-14896# Nationaal Inst. voor Kernfysica en Hoge Energiefysica, Amsterdam (Netherlands).
AN ENERGY SPECTRUM COMPRESSOR SYSTEM (ESC) FOR THE AMSTERDAM PULSE STRETCHER (AMPS)
J. G. Noomen and R. Maas *In its* NIKHEF-K Contributions to the 1989 Particle Accelerator Conference 1989 p 13-15 Sponsored by the Stichting voor Fundamenteel Onderzoek der Materie and the Netherlands Foundation for Scientific Research (For primary document see N90-14891 06-73)
Avail: NTIS HC A03/MF A01

Modification of the present 2 percent duty factor 500 MeV linac MEA (medium energy accelerator) to a low duty factor (0.1 percent) injector for a pulse stretcher ring under construction in order to obtain high duty (90 percent) electron beams is described. Considerations concerning required energy range, beam loading, phase errors, and current ripple which determine the longitudinal dispersion, and the required RF power source are presented. ESA

N90-14897# Westinghouse Hanford Co., Richland, WA.
INTRODUCTORY TESTIMONY: HEARING ON NUCLEAR POWER IN SPACE
John Nolan Sep. 1989 61 p
(Contract DE-AC06-87RL-10930)
(DE90-001137; WHC-SA-0727) Avail: NTIS HC A04/MF A01

The uses of nuclear power in space are examined. Various systems are discussed and an outline of a slide presentation is given. The testing and safety of these programs is also briefly mentioned. DOE

N90-14898# Sandia National Labs., Albuquerque, NM. Independent Evaluation Group.
A REVIEW OF GAS-COOLED REACTOR CONCEPTS FOR SDI (STRATEGIC DEFENSE INITIATIVE)
A. C. Marshall, ed. Aug. 1989 150 p
(Contract DE-AC04-76DP-00789)
(DE89-016962; SAND-87-0558) Avail: NTIS HC A08/MF A01

A review was completed of multimegawatt gas cooled reactor concepts proposed for SDI applications. The study concluded that the principal reason for considering gas cooled reactors for burst mode operation was the potential for significant system mass savings over closed cycle systems if open cycle gas cooled operation (effluent exhausted to space) is acceptable. The principal reason for considering gas cooled reactors for steady state operation is that they may represent a lower technology risk than other approaches. In the review, nine gas cooled reactor concepts were compared to identify the most promising. For burst mode operation, the NERVA (Nuclear Engine for Rocket Vehicle Application) derivative reactor concept emerged as a strong first choice since its performance exceeds the anticipated operational requirements and the technology was demonstrated and is retrievable. Although the NERVA derivative concepts were determined to be the lead candidates for the Multimegawatt Steady State (MMWSS) mode as well, their lead over the other candidates is not as great as for the burst mode. DOE

N90-14899# Los Alamos National Lab., NM. Theoretical Div.
THE CREATION OF HIGH ENERGY DENSITIES WITH ANTIMATTER BEAMS
W. R. Gibbs and J. W. Kruk (Rice Univ., Houston, TX.) 1989 18 p Presented at the International Meeting on Physics at KAON, Bad Honnef, Federal Rep. of Germany, 7-9 Jun. 1989
(Contract W-7405-eng-36)
(DE90-002383; LA-UR-89-3426; CONF-8906194-3) Avail: NTIS HC A03/MF A01

The use of antiprotons (and antideuterons) for the study of the behavior of nuclear matter at high energy density is considered. It is shown that high temperatures and high energy densities can be achieved for small volumes. Also investigated is the strangeness production in antimatter annihilation. It is found that the high rate of Lambda production seen in a recent experiment is easily understood. The Lambda and K-short rapidity distributions are also reproduced by the model considered. DOE

74 OPTICS

Includes light phenomena; and optical devices.
For lasers see *36 Lasers and Masers.*

N90-14900*# Lick Observatory, Santa Cruz, CA.
CCD TV FOCAL PLANE GUIDER DEVELOPMENT AND COMPARISON TO SIRTF APPLICATIONS Final Report
David M. Rank 15 Jan. 1989 25 p
(Contract NCC2-485)
(NASA-CR-185977; NAS 1.26:185977) Avail: NTIS HC A03/MF A01 CSCL 20F

It is expected that the SIRTF payload will use a CCD TV focal plane fine guidance sensor to provide acquisition of sources and tracking stability of the telescope. Work has been done to develop CCD TV cameras and guiders at Lick Observatory for several years and have produced state of the art CCD TV systems for internal use. NASA decided to provide additional support so that the limits of this technology could be established and a comparison between SIRTF requirements and practical systems could be put on a more quantitative basis. The results of work carried out at Lick Observatory which was designed to characterize present CCD autoguiding technology and relate it to SIRTF applications is presented. Two different design types of CCD cameras were constructed using virtual phase and burred channel CCD sensors. A simple autoguider was built and used on the KAO, Mt. Lemon and Mt. Hamilton telescopes. A video image processing system was also constructed in order to characterize the performance of the auto guider and CCD cameras. Author

N90-14901# Department of the Navy, Washington, DC.
INTERFEROMETRIC SURFACE DISTORTION DETECTOR Patent Application
Arthur E. Scotese, inventor (to Navy), Shih L. Huang, inventor (to Navy), and Armando J. Gaetano, inventor (to Navy) 20 Apr. 1989 14 p
(AD-D014211; US-Patent-Appl-SN-342919) Avail: NTIS HC A03/MF A01 CSCL 14/2

Portable shadow moire apparatus is disclosed for indiscriminately manipulating the grid and light source thereof over a specimen surface, with the grid oriented substantially in parallel therewith and in close proximity thereto. Self aligning support is provided on such apparatus, along with height adjustability for that support. Utilization of very high density grids is made possible by such apparatus to enhance the detection sensitivity thereof. Light source direction variability is also provided to control the magnitude of detectable distortion. GRA

N90-14902# Carnegie-Mellon Univ., Pittsburgh, PA. Robotics Inst.
A SAMPLED-GRATING MODEL OF MOIRE PATTERNS FROM DIGITAL IMAGING
John Krumm and Steven A. Shafer Jul. 1989 32 p
(Contract F33615-87-C-1499; ARPA Order 4976)
(AD-A213364; CMU-RI-TR-89-19) Avail: NTIS HC A03/MF A01 CSCL 20/6

Traditional crossed-grating moire, as well as newer sampled-grating (scanning) moire, have proven to be effective methods of shape measurement. There is speculation that the moire patterns of a sampled grating, which are due to aliasing, can be modeled with crossed gratings. The two are compared and it is shown that while crossed gratings can correctly predict the frequencies of a sampled grating, they cannot correctly predict the amplitudes. A new model is formulated which accounts for multiple stages of sampling and transmission, and show how neglecting multiple stages can lead to mistakes in moire analysis. The model is demonstated with an experiment using a digital imaging system. GRA

N90-14903 Department of the Navy, Washington, DC.
PROGRAMMABLE NEAR-INFRARED RANGING SYSTEM Patent
Hobart R. Everett, Jr., inventor (to Navy) 25 Jul. 1989 11 p Filed 26 Feb. 1988
(AD-D014237; US-Patent-4,851,661; US-Patent-Appl-SN-160944)
Avail: US Patent and Trademark Office CSCL 17/11

A high angular resolution ranging system particularly suitable for indoor applications involving mobile robot navigation and collision avoidance uses a programmable array of light emitters that can be sequentially incremented by the microprocessor. A plurality of adjustable level threshold detectors are used in an optical receiver for detecting the threshold level of the light echoes produced when light emitted from one or more of the emitters is reflected by a target or object in the scan path of the ranging system. GRA

N90-14904 Department of the Navy, Washington, DC.
NARROW BAND AND WIDE ANGLE HEMISPHERICAL INTERFERENCE OPTICAL FILTER Patent
Harry Rieger, inventor (to Navy) 25 Jul. 1989 8 p Filed 27 Jun. 1988
(AD-D014238; US-Patent-4,851,664; US-Patent-Appl-SN-213034)
Avail: US Patent and Trademark Office CSCL 20/6

An optical interference filter has narrow linewidth and wide acceptance angle and includes a hemisphere coated to provide a narrow bandpass filter at a desired wavelength at normal incidence while other wavelengths at normal incidence are absorbed or reflected. A photodetector placed at the center of the hemisphere detects the desired wavelength only. Other wavelengths that are shorter than the wavelength of the filter are transmitted through the filter to be absorbed by a black absorbing surface around the photodetector. Thus, only the frequency of interest at normal incidence provides a representative signal at the detector. GRA

N90-14905*# Strainoptic Technologies, Inc., North Wales, PA.
SPECTRAL CONTENTS READOUT OF BIREFRINGENT SENSOR Final Report, 13 Jul. 1987 - 13 Jul. 1989
Alex S. Redner Oct. 1989 63 p
(Contract NAS2-12666)
(NASA-CR-179444; H-1581; NAS 1.26:179444; Rept-87-955)
Avail: NTIS HC A04/MF A01 CSCL 20F

The technical objective of this research program was to develop a birefringent sensor, capable of measuring strain/stress up to 2000 F and a readout system based on Spectral Contents analysis. As a result of the research work, a data acquisition system was developed, capable of measuring strain birefringence in a sensor at 2000 F, with multi-point static and dynamic capabilities. The system uses a dedicated spectral analyzer for evaluation of stress-birefringence and a PC-based readout. Several sensor methods were evaluated. Fused silica was found most satisfactory. In the final evaluation, measurements were performed up to 2000 F and the system performance exceeded expectations. Author

N90-14906# National Oceanic and Atmospheric Administration, Boulder, CO. Wave Propagation Lab.
PROBABILITY DENSITY FUNCTION OF OPTICAL SCINTILLATIONS (SCINTILLATION DISTRIBUTION)
James H. Churnside and Richard J. Lataitis Jul. 1989 46 p
(Contract ASL-87-8013)
(PB89-103912; NOAA-TM-ERL-WPL-169) Avail: NTIS HC A03/MF A01 CSCL 20F

The probability density function of optical scintillation in the turbulent atmosphere is investigated theoretically and experimentally. The lognormally modulated Rician is the best available model for these fluctuations. For large apertures, this model reduces to a simple lognormal density function, which can be used under most practical situations. This information is useful for modeling the performance of many electro-optical systems in the atmosphere. Author

N90-14907*# Technion - Israel Inst. of Tech., Haifa. Dept. of Aeronautical Engineering.
DEFERRED ELECTRONIC HETERODYNE MOIRE DEFLECTOMETRY: A METHOD FOR TRANSIENT DENSITY FIELDS MEASUREMENT Annual Report
Josef Stricker Oct. 1989 27 p
(Grant NAGw-933)
(NASA-CR-182982; NAS 1.26:182982) Avail: NTIS HC A03/MF A01 CSCL 20F

Effects of spherical aberrations of the mirror used in the moire system on the angular resolution of the system are investigated. It is shown that the spherical aberrations may reduce significantly the performance of the conventional moire deflectometer. However, due to the heterodyne procedure, this is not the case with the heterodyne moire system. A moire system with a constant speed moving grating is demonstrated. It is shown that the system readout is linear and the system does not need calibration. In addition, the repeatability of the measurements is improved in this system as compared to the sinusoidally moving grating setup. The problem of the photographic plates alignment is solved by using a mechanical system in which the plate is held firmly throughout the experiment and accurately replaced after removing for photographic processing. The effect of a circular detector's aperture size on readout was tested. It is shown that the spatial phase variations, observed when scanning along a straight moire fringe, may considerably be reduced. At present we may say that both the on-line and the deferred heterodyne moire techniques may reliably be used. The errors of phase readings are 1 deg and 5 deg for the on-line and deferred methods. The total error due to subtraction of two readings at each position is, therefore, 1.4 deg and 7 deg, respectively. Further research for improving the deferred system is suggested. Author

N90-14908# California Univ., Berkeley. Lawrence Berkeley Lab.
REALTIME TRACKING SYSTEM FOR WIDE-FIELD-OF-VIEW TELESCOPE
Hye-Sook Park 21 Aug. 1989 4 p Presented at Electronic Imaging '89, Boston, MA, 2-5 Oct. 1989
(Contract W-7405-eng-48)
(DE90-001147; UCRL-99801; CONF-8910196-2) Avail: NTIS HC A01/MF A01

A wide-field-of-view telescope is being constructed with smart focal plane processors that recognize moving objects in the field-of-view and tracks them with high resolution. The telescope lens is made of concentric blocks of glass viewing a 60 degree field-of-view. Intensified CCD cameras on the focal plane acquire images which are processed by a Datacube image processor. The system views the night sky, extracts the position and intensity of stars, and recognizes and tracks any artificial satellites which move through the field-of-view. DOE

N90-14909# Lawrence Livermore National Lab., CA.
DESIGN OF INCOHERENT IMAGING ARRAYS
J. P. Fitch 13 Aug. 1989 9 p
(Contract W-7405-eng-48)
(DE90-000861; UCID-21751) Avail: NTIS HC A02/MF A01

Two techniques which we have used to design telescope arrays for high resolution imaging applications are described. The first technique is applicable to arrays with a relatively small, O(10), number of apertures and is essentially an exhaustive search with a simple in-line test which allows the search space to be pruned by an order of magnitude. In the second technique, arrays of a large number of apertures are designed using a fractal approach by recursively combining the results from several array patterns with fewer apertures. DOE

N90-14579# Institut d'Optique Theorique et Appliquee, Paris (France).
TOMOGRAPHIC IMAGERY BY MULTISLOT CODING APPLIED TO X RAY DIAGNOSTICS OF LASER PLASMAS: IMPLEMENTATION OF A DIRECT ELECTRONIC DETECTION CAMERA [IMAGERIE TOMOGRAPHIQUE PAR CODAGE MULTIFENTES POUR LE DIAGNOSTIC X DES PLASMAS LASER: REALISATION D'UNE CAMERA A DETECTION ELECTRONIQUE DIRECTE]
N. deBeaucoudrey, A. Bellemain, P. Fournet, D. Phalippou, L. Garnero, and J. P. Hugonin *In* Groupement de Recherches Coordonnees Interaction Laser Matiere, Activities Report in Laser Matter Interactions Jun. 1988 p 226-231 In FRENCH (For primary document see N90-14544 06-36)
Avail: NTIS HC A13/MF A02

N90-14580# Ecole Polytechnique, Palaiseau (France). Lab. pour l'Utilisation des Lasers Intenses.
DEVELOPMENT OF X DIAGNOSTICS AROUND THE PULSE 1 LASER [DEVELOPPEMENT DE DIAGNOSTICS X AUTOUR DU LASER PULSE 1]
Rene Benattar and Bertrand Paris *In* Groupement de Recherches Coordonnees Interaction Laser Matiere, Activities Report in Laser Matter Interactions Jun. 1988 p 232-237 In FRENCH Original contains color illustrations (For primary document see N90-14544 06-36)
Avail: NTIS HC A13/MF A02

75 PLASMA PHYSICS

Includes magnetohydrodynamics and plasma fusion.
For ionospheric plasmas see *46 Geophysics*. For space plasmas see *90 Astrophysics*.

N90-14910*# California Univ., Los Angeles. Dept. of Physics.
HIGH-FREQUENCY INSTABILITY OF THE SHEATH-PLASMA RESONANCE
R. L. Stenzel 1989 43 p
(Grant NAGw-1570)
(NASA-CR-186127; NAS 1.26:186127) Avail: NTIS HC A03/MF A01 CSCL 20I

Coherent high frequency oscillations near the electron plasma frequency (omega approx. less than omega sub p) are generated by electrodes with positive dc bias immersed in a uniform Maxwellian afterglow plasma. The instability occurs at the sheath-plasma resonance and is driven by a negative RF sheath resistance associated with the electron inertia in the diode-like electron-rich sheath. With increasing dc bias, i.e., electron transit time, the instability exhibits a hard threshold, downward frequency pulling, line broadening and copious harmonics. The fundamental instability is a bounded oscillation due to wave evanescence, but the harmonics are radiated as electromagnetic waves from the electrodes acting like antennas. Wavelength and polarization measurements confirm the emission process. Electromagnetic waves are excited by electrodes of various geometries (planes, cylinders, spheres) which excludes other radiation mechanisms such as orbitrons or beam-plasma instabilities. The line broadening mechanism was identified as a frequency modulation via the electron transit time by dynamic ions. Ion oscillations at the sheath edge give rise to burst-like RF emissions. These laboratory observations of a new instability are important for antennas in space plasmas, generation of coherent beams with diodes, and plasma diagnostics. Author

N90-14911 Princeton Univ., NJ.
ENERGY DEPOSITION IN LOW POWER COAXIAL PLASMA THRUSTERS Ph.D. Thesis
Roger Metcalf Myers 1989 201 p
Avail: Univ. Microfilms Order No. DA8920432

The energy deposition in steady-state, low power, coaxial plasma thrusters operated between 10 and 30 kW with argon and nitrogen propellants was studied experimentally and analytically. The major energy sinks were found to be electrode losses (primarily anode), propellant ionization, and thrust. Performance measurements showed the efficiency and specific impulse to vary between two and ten percent and 500 and 1200 seconds, respectively, as functions of thruster current level, propellant flow rate, and thruster geometry. Thrust was found to increase quadratically with current, in agreement with theoretical models of self-field electromagnetic thrusters. Spectroscopic studies of the plasma exhaust with argon propellant showed it to consist primarily of singly and doubly ionized argon, with an electron temperature between 1.2 and 1.7 eV and electron densities between 2 x 10 (exp 13) cu cm and 5 x 10 (exp 13) cu cm. Floating potential measurements showed the anode fall voltage to be between 65 and 95 percent of the total thruster voltage depending on thruster geometry, propellant, and current level. Non-intrusive cathode surface temperature and erosion measurements revealed that the cathode energy balance was governed by electron cooling, surface radiation and conduction through the cathode base. Comparisons of these new results with data from megawatt class, quasi-steady magnetoplasmadynamic thrusters revealed similarities between the plasma properties and acceleration mechanisms of the devices, but showed they have dramatically different anode power fractions. Attempts to increase thruster efficiency by decreasing the chamber radius were not successful, indicating that major changes in thruster design and/or power level will be required to achieve high efficiency, high specific impulse operation. Dissert. Abstr.

N90-14912# Gosudarstvennyi Komitet po Ispolzovaniyu Atomnoi Energii, Moscow (USSR). Inst. Atomnoj Ehnergii.
LASER PROBING NON-CYLINDRICAL Z-PINCH IN NEAR-ISOLATOR REGION OF A DISCHARGED CHAMBER
V. I. Mikhajlov and M. M. Orlov 1988 9 p In RUSSIAN; ENGLISH summary
(DE89-632018; IAE-4672/7) Avail: NTIS (US Sales Only) HC A02/MF A01

Physical processes reducing the effectiveness of radiation characteristics of the non-cylindrical Z-pinch are considered. One of the processes studied is the secondary break-down of discharge space with the formation of a current channel shunting the main current of the discharge circuit and spatially localized along insulator surface. The experiments are performed using the plasma focus type device. Deuterium and xenon mixture with partial pressures ratio is the working gas. The working pressure of the mixture varied within 0.4 to 0.7 Torr. The probing is performed by ruby laser with modulated quality factor included into the circuit of interferometric measurements. The main attention is paid to the processes in the near-insulator discharge chamber region. DOE

N90-14913# Gosudarstvennyi Komitet po Ispolzovaniyu Atomnoi Energii, Moscow (USSR). Inst. Atomnoj Ehnergii.
TOROIDAL ROTATION RETARDATION AND ION ANOMALOUS TRANSPORT BY DRIFT WAVES IN A TOKAMAK
M. V. Osipenko, O. P. Pogutse, and R. V. Shurygin 1988 20 p In RUSSIAN
(DE89-634427; IAE-4663/6) Avail: NTIS (US Sales Only) HC A03/MF A01

A set of equations of anomalous rotating plasma hydrodynamics

in a weak collision mode with allowance for running - away and trapped particles has been obtained in terms of quasilinear theory taking into account spectra close to those measured experimentally. It is shown that in a banana regime the anomalous transport is determined by ions, the viscosity and thermal conductivity coefficients coinciding within the numerical factor. The scaling obtained for the time of a toroidal rotation slowing down due to anomalous viscosity is in reasonable agreement with the experiment. DOE

N90-14914# Sandia National Labs., Albuquerque, NM.
MODELING OF RUNAWAY ELECTRON DAMAGE FOR THE DESIGN OF TOKAMAK PLASMA FACING COMPONENTS
K. A. Niemer, C. D. Croessmann, J. G. Gilligan, and H. H. Bolt (Max-Planck-Inst. fuer Plasmaphysik, Garching, Germany, F.R.) 1989 8 p Presented at the 13th International Symposium on Fusion Engineering, Knoxville, TN, 2-6 Oct. 1989
(Contract DE-AC04-76DP-00789)
(DE90-000847; SAND-89-2405C; CONF-891007-3) Avail: NTIS HC A02/MF A01

Cracking, craters, spotty damage (discoloration), and missing chunks of material have been observed on limiters and along the midplane of tokamak inner walls. This damage is assumed to be due to runaway electron discharges. These runaway electrons have been predicted to range in energy from a few MeV to several hundred MeV. The energy density from the runaway electron discharges range from 10 to 500 MJ/sq m over pulse lengths of 5 to 50 msec. The PTA code package is a 3-D, time dependent, computational code package used to predict energy deposition, temperature rise, and damage on tokamak first wall and limiter materials from runaway electron impact. Two experiments were modeled to validate the PTA code package. The first experiment tested the thermal and structural response from high energy electron impact on different fusion materials, and the second experiment simulated runaway electrons scattering through a plasma facing surface (graphite) into an internal structure (copper). The PTA calculations compared favorably with the experimental results. In particular, the PTA models identified gap conductance, thermal contact, x ray generation in materials, and the placement of high stopping power materials as key factors in the design of plasma facing components, resistant to runaway electron damage. DOE

N90-14915# Lawrence Livermore National Lab., CA.
LAWRENCE LIVERMORE NATIONAL LABORATORY (LLNL) RESEARCH ON COLD FUSION
K. I. Thomassen, ed., J. F. Holzrichter, ed., F. T. Aldridge, B. Balke, J. Bowers, D. B. Bullen, M. D. Cable, M. Caffee, R. B. Campbell, and C. Colmenares et al 14 Sep. 1989 70 p
(Contract W-7405-eng-48)
(DE90-000930; UCID-21809) Avail: NTIS HC A04/MF A01

With the appearance of reports on Cold Fusion, scientists at the Lawrence Livermore National Laboratory (LLNL) began a series of increasingly sophisticated experiments and calculations to explain these phenomena. These experiments can be categorized as follows: (1) simple experiments to replicate the Utah results, (2) more sophisticated experiments to place lower bounds on the generation of heat and production of nuclear products, (3) a collaboration with Texas A and M University to analyze electrodes and electrolytes for fusion by-products in a cell producing 10 pct excess heat (we found no by-products), and (4) attempts to replicate the Frascati experiment that first found neutron bursts when high-pressure deuterium gas in a cylinder with Ti chips was temperature-cycled. We failed in categories (1) and (2) to replicate either the Pons/Fleischmann or the Jones phenomena. We have seen phenomena similar to the Frascati results, (4) but these low-level burst signals may not be coming from neutrons generated in the Ti chips. Summaries of our experiments are described in Section 2, as is a theoretical effort based on cosmic ray muons to describe low-level neutron production. Details of the experimental groups' work are contained in the six appendices. At LLNL, independent teams were spontaneously formed in response to the early announcements on cold fusion. This report's format follows this organization. DOE

N90-14916# Massachusetts Inst. of Tech., Cambridge. Plasma Fusion Center.
ION COLLECTION BY PROBING OBJECTS IN FLOWING MAGNETIZED PLASMAS Ph.D. Thesis
Kyu-Sun Chung Apr. 1989 196 p
(Contract DE-AC02-78ET-51013)
(DE90-001711; DOE/ET-51013/275; PFC/RR-89-13) Avail: NTIS HC A09/MF A02

A new 1-D collisionless kinetic model is developed for the flow of ions to probing structures in drifting plasmas. The cross field flow into the presheath is modelled by accounting consistently for particle exchange between the collection flux tube and the outer plasma. Numerical solutions of the self-consistent plasma/sheath equations are obtained with arbitrary external ion temperature and parallel plasma flow velocity. Results are presented of the spatial dependence of the ion distribution function as well as its moments (density, particle flux, temperature, and power flux). The ion current to the probe is obtained and the ratio of the upstream to downstream currents is found to be well represented. The results agree well with comparable recent fluid calculations but show substantial deviations from other models which ignore particle exchange out of the presheath. No evidence is found of the formation of shocks in the downstream wake, contrary to the implications of some fluid theories. The previous kinetic model is extended by generalizing cross field transport and adding ionization to the source of the Boltzmann equation along the presheath. Ion sheath current density and ratio (R) of upstream to downstream current are obtained as a function of plasma drift velocity, equivalent viscosity, ion temperature, and ionization rate. Constants (K) in the form R = exp(Ku(sub d)) are obtained in terms of viscosity, ion temperature, and ionization rate. The effect of an electrical bias applied to the object on the presheath characteristics is discussed. DOE

N90-14917# Los Alamos National Lab., NM.
PERFORMANCE OF THE 10-kV, 100-kA PULSED-POWER MODULES FOR THE FRX-C MAGNETIC COMPRESSION EXPERIMENT
D. J. Rej and W. J. Waganaar 1989 5 p Presented at the 7th Institute of Electrical and Electronics Engineers Pulsed Power Conference, Monterey, CA, 12-14 Jun. 1989
(Contract W-7405-eng-36)
(DE89-014027; LA-UR-89-1909; CONF-890665-31) Avail: NTIS HC A01/MF A01

Detailed performance data collected from over a year's operation of the 25 and 50-kJoule pulsed-power capacitor-bank modules developed for the Los Alamos magnetic fusion facility FRX-C are presented. These modules supply the 5-MA magnet current needed for the compressional heating of compact toroid plasmoids. To date, 54 modules were built and successfully tested at their full design rating: 100-kA peak output current at 10-kV charge, tau(sub 1/4) = 60 microsec (25-kJ module), or 110 microsec (50-kJ module), crowbar L/R is less than or equal to 1 ms. Modules are compact, cost about $5000 each, and though designed for 25 or 50 kJ, they can be easily modified for other pulsed-power applications. Energy is stored in 25-kJ capacitors. Start and crowbar switching is performed with a pair of water-cooled, size-D ignitrons. As an alternative to an ignitron, crowbar switching by solid-state rectifiers has been successfully demonstrated. Current is conducted between components and to the load by parallel-plate transmission lines and by a parallel array of commercially-available coaxial cable. DOE

N90-14918# Los Alamos National Lab., NM.
TWO-DIMENSIONAL BEHAVIOR OF MEGAGAUSS-FIELD-CONFINED SOLID FIBER Z-PINCHES
Irvin R. Lindemuth 1989 6 p Presented at the 5th International Conference on Megagauss Magnetic Field Generation and Related Topics, Novosibirsk, USSR, 3-7 Jul. 1989

(Contract W-7405-eng-36)
(DE90-000684; LA-UR-89-3250; CONF-890710-19) Avail: NTIS HC A02/MF A01

At Los Alamos, one-dimensional and two-dimensional magnetohydrodynamic (MHD) computations were performed for the formation and evolution of fiber-formed plasmas. The one-dimensional computations show that current in the existing Los Alamos and Naval Research Laboratory experiments is carried by hot plasma which was ablated from the solid fiber. The two-dimensional computations exhibit m = 0 unstable behavior in the hot, exterior plasma prior to complete ablation of the solid fiber; the m = 0 behavior enhances the fiber ablation rate. The MHD model used in the computations accesses the Los Alamos SESAME tabulated atomic data base computer library to determine material properties. The MHD partial differential equations are solved numerically using an alternating-direction implicit finite difference method which does not resort to fractional time steps, or operator splitting. The computations use cold start initial conditions in an attempt to compute the behavior of the pinches from t = 0. The two-dimensional computations begin with a 2 percent random variation superimposed upon the density profile of the solid core to provide perturbations for instability growth. In this paper, the two-dimensional computations are further examined. In the computations reported here, two-different axial lengths, l, are considered, l = 5 mm and l = 300 micrometers to study long- and short-wavelength behavior. The long-wavelength computations show the formation and evolution of hot spots in the hot corona surrounding the cold, solid core of the plasma channel; subsequently, hot spots form on the axis of the discharge. The short-wavelength computations exhibit a periodic re-establishment of a quasi-one-dimensional configuration. DOE

N90-14919# Sandia National Labs., Albuquerque, NM.
THERMAL LOADS ON TOKAMAK PLASMA FACING COMPONENTS DURING NORMAL OPERATION AND DISRUPTIONS
Robert T. McGrath 1989 15 p Presented at the 11th International Vacuum Congress and 7th International Conference on Solid Surfaces, Cologne, Fed. Republic of Germany, 25-29 Sep. 1989
(Contract DE-AC04-76DP-00789)
(DE90-000794; SAND-89-2064C; CONF-890906-4) Avail: NTIS HC A03/MF A01

Power loadings experienced by tokamak plasma facing components during normal operation and during off-normal events are discussed. A model for power and particle flow in the tokamak boundary layer is presented and model predictions are compared to infrared measurements of component heating. The inclusion of the full three-dimensional geometry of the component and of the magnetic flux surface is very important in the modeling. Experimental measurements show that misalignment of component armor tile surfaces by only a millimeter can lead to significant localized heating. An application to the design of plasma facing components for future machines is presented. Finally, thermal loads expected during tokamak disruptions are discussed. The primary problems are surface melting and vaporization due to localized intense heating during the disruption thermal quench and volumetric heating of the component armor and structure due to localized impact of runaway electrons. DOE

N90-14920# Lawrence Livermore National Lab., CA.
MICROWAVE TOKAMAK EXPERIMENT (MTX) FIRST YEAR OF OPERATION AND FUTURE PLANS
M. C. Jackson 20 Sep. 1989 5 p Presented at the 13th International Symposium on Fusion Engineering, Knoxville, TN, 2-6 Oct. 1989
(Contract W-7405-eng-48)
(DE90-000817; UCRL-101132; CONF-891007-7) Avail: NTIS HC A01/MF A01

The Microwave Tokamak Experiment (MTX) at Lawrence Livermore National Laboratory (LLNL) began plasma operations in November 1988, and the main goal is the study of electron-cyclotron heating (ECH) in plasma discharges. The MTX tokamak was relocated from the Massachusetts Institute of Technology (MIT), and plasma parameters were recreated that are similar to those generated while the tokamak was at MIT. After stable ohmic operation was achieved, single pulse FEL heating experiments began. During this phase, the FEL operated at low power levels on the way to its ultimate goal of 2 GW and 140 GHz with a 30-ns pulse length. A number of new diagnostics were developed to measure these fast FEL pulses and the resulting plasma effects. Results are presented that show the correlation of MTX data with MIT data, some of the operational modifications and procedures used, results to date from preliminary tokamak operations with the FEL, and the near-term operational plans. DOE

N90-14921# Lawrence Livermore National Lab., CA.
MICROWAVE TRANSPORT SYSTEMS FOR THE MTX (MICROWAVE TOKAMAK EXPERIMENT)
B. Felker and S. W. Ferguson 27 Sep. 1989 4 p Presented at the 13th International Symposium on Fusion Engineering, Knoxville, TN, 2-6 Oct. 1989
(Contract W-7405-eng-48)
(DE90-000821; UCRL-101184; CONF-891007-9) Avail: NTIS HC A01/MF A01

This paper presents the design and construction, as well as the initial operation, of the Microwave Transmission System. The system consists of containment vessels, mirror boxes, mirrors, an alignment system, two turbo-molecular pump vacuum stations, and a microwave source. Fifty-ns-length pulses of 6-MeV electrons pass through a free electron laser (FEL) wiggler. A 300 W extended interaction oscillator (EIO) of 140 GHz frequency supplies the seed signal for amplification in the wiggler. The electron beam is dumped and the microwave beam is transmitted quasi-optically 90 ft by six aluminum mirrors through an evacuated tube. Three of the mirrors are elliptical paraboloids and the others are flat. A seventh mirror is rotated into the microwave beam to divert it into a load tank. The transport vacuum vessel is 20-in.-diameter stainless steel tube with bellows and mirror boxes at each mirror. Two vacuum systems at each end of the transport tube allow a base pressure of 10(exp -7) Torr to be attained by 7000 L/s of turbo-molecular pumping. Also at each mirror, at the MTX vessel, and at the two ends of the wiggler waveguide are HeNe laser detectors used for vacuum alignment. Descriptions of the major components, their requirements and system requirements are presented, and the initial operation of the system and its performance are described. DOE

N90-14922# Lawrence Livermore National Lab., CA.
MTX (MICROWAVE TOKAMAK EXPERIMENT)/ELF (ELECTRON LASER FACILITY) 2 MICROWAVE POWER MEASUREMENTS AND CALIBRATION FOR THE 2-GW, 140-GHz, ELF 2 FREE ELECTRON LASER (FEL)
S. W. Ferguson, R. Stever, A. Throop, B. Felker, and R. Franklin 27 Sep. 1989 5 p Presented at the 13th International Symposium on Fusion Engineering, Knoxville, TN, 2-6 Oct. 1989
(Contract W-7405-eng-48)
(DE90-000825; UCRL-101104; CONF-891007-8) Avail: NTIS HC A01/MF A01

We have developed techniques for measuring the power and frequency of the Electron Laser Facility (ELF) 2 Free-Electron Laser (FEL) used for plasma heating experiments on the Microwave Tokamak Experiment (MTX). We also have designed a multichannel, 140-GHz receiver capable of measuring FEL power levels from 10 mW to 0.1 (mu)W within an accuracy of + or - 1 dB with a 50-dB dynamic range and a 2-ns response time. By using calibrated attenuators, we can measure power levels from 10 GW to 0.1 (mu)W. We sample the microwave output of the FEL in a microwave load tank by using WR-8 or WR-28 stub waveguide antennas. Microwave turning mirrors are used to guide the microwave beam down an evacuated beam tube to the MTX. Stub, WR-8, fundamental-mode, waveguide antennas are used for beam detection on the microwave turning mirrors. Orthogonal, WR-8, stub waveguides are machined into the surfaces of the mirrors and used as directional couplers to measure forward and

reflected power from the FEL. The microwave power is then transported to the microwave receiver via a low-loss, over-moded, WR-28 waveguide. A movable modes probe in the microwave load tank is used to scan across the microwave beam to determine the modes content of the beam. Frequency stability of the FEL is measured with a Fast, Frequency-Modulation Detector (FFMD) capable of measuring frequency shifts and modulation on a 2- to 4-ns time frame. DOE

N90-14923# Lawrence Livermore National Lab., CA.
PRECISION TIMING AND INTERLOCKS SYSTEMS FOR FEL (FREE-ELECTRON LASER) HEATING EXPERIMENTS ON MTX (MICROWAVE TOKAMAK EXPERIMENT)
D. E. Petersen 20 Sep. 1989 5 p Presented at the 13th International Symposium on Fusion Engineering, Knoxville, TN, 2-6 Oct. 1989
(Contract W-7405-eng-48)
(DE90-000833; UCRL-101130; CONF-891007-4) Avail: NTIS HC A01/MF A01

A new precision timing system has been installed on the Microwave Tokamak Experiment (MTX) at Lawrence Livermore National Laboratory (LLNL). The purpose of the system is to synchronize the tokamak's plasma discharge with a 140-GHz, 2-GW microwave pulse generated by a free-electron laser (FEL). The installation involved modifying the existing sequencer system and adding Digital delay generators, three in-house-designed CAMAC modules and other components. The system controls placement of the 30-ns FEL pulse during the MTX plasma discharge. It also provides precision triggers for the microwave plasma diagnostics. These triggers are distributed over 100-Mbit/s fiber-optic links. The MTX interlock system has been expanded to provide personnel safety during FEL experiments, to protect the FEL and related equipment, and to control the path of the FEL beam starting from the FEL's output, through the beam transport system, and into the tokamak. This paper describes how the existing MTX timing and interlocks systems were upgraded to accommodate these new FEL experiments. DOE

N90-14924# Lawrence Livermore National Lab., CA.
MICROWAVE TOKAMAK EXPERIMENT: AN OVERVIEW OF THE CONSTRUCTION AND CHECKOUT PHASE
L. L. Lang and H. H. Bell 28 Sep. 1989 5 p Presented at the 13th International Symposium on Fusion Engineering, Knoxville, TN, 2-6 Oct. 1989
(Contract W-7405-eng-48)
(DE90-000834; UCRL-101186; CONF-891007-5) Avail: NTIS HC A01/MF A01

At Lawrence Livermore National Laboratory (LLNL), the Microwave Tokamak Experiment (MTX) was constructed to demonstrate the feasibility of using microwave pulses produced from a free electron laser (FEL) to provide electron cyclotron heating (ECH) for use in tokamaks, particularly high field machines. The MTX consists primarily of the ALCATOR C tokamak and power supplies that were documented and disassembled at the Massachusetts Institute of Technology (MIT) and shipped to LLNL in April 1987. Many additions were made, including a new primary power system from the Magnetic Fusion Test Facility (MFTF) substation, a new commutation system, substantially upgraded seismic support system for earthquake loading, a fast controls system for use with the FEL, a new data acquisition system, and a new vault facility. These systems were checked out and put into operation in October 1988; the first plasma was achieved in November 1988. Also constructed and installed was the microwave transmission system and the local microwave system to be used with the FEL. These systems transmit the microwaves to MTX quasi-optically through an evacuated tube. The ongoing plasma operations, both with and without FEL heating, are described in a companion paper. DOE

N90-14925# Pacific Northwest Lab., Richland, WA.
COLD FUSION: ALCHEMIST'S DREAM
E. D. Clayton Sep. 1989 26 p
(Contract DE-AC06-76RL-01830)
(DE90-000865; PNL-6993) Avail: NTIS HC A03/MF A01

In this report the following topics relating to cold fusion are discussed: muon catalyzed cold fusion; piezonuclear fusion; sundry explanations pertaining to cold fusion; cosmic ray muon catalyzed cold fusion; vibrational mechanisms in excited states of D2 molecules; barrier penetration probabilities within the hydrogenated metal lattice/piezonuclear fusion; branching ratios of D2 fusion at low energies; fusion of deuterons into He-4; secondary D+T fusion within the hydrogenated metal lattice; helium-3 to helium-4 ratio within the metal lattice; shock induced fusion; and anomalously high isotopic ratios of helium-3/helium-4. DOE

N90-14926# Lawrence Livermore National Lab., CA. Dept. of Physics.
EQUATION OF STATE AND OPACITY OF DENSE PLASMAS
F. J. Rogers and C. A. Iglesias 28 Sep. 1989 13 p Presented at the 24th Yamada Conference on Strongly Coupled Plasma Physics, Tokyo, Japan, 29 Aug. - 2 Sep. 1989
(Contract W-7405-eng-48)
(DE90-002223; UCRL-101115; CONF-8908133-5) Avail: NTIS HC A03/MF A01

Recent research on the equation of state and opacity of dense plasmas has been strongly driven by discrepancies between calculation and observation of a wide variety of astrophysical quantities such as the solar neutrino flux rate, the period ratio of Cepheid variable stars, and lithium depletion in the Hyades stellar cluster. A summary of some recent work based on a many-body activity expansion of the grand-partition function is given. An integral part of this work involves methods for calculating atomic data and occupation numbers ior excited states in dense plasmas. DOE

N90-14927# Lawrence Livermore National Lab., CA.
STARLIGHT: A STATIONARY INERTIAL-CONFINEMENT-FUSION REACTOR WITH NONVAPORIZING WALLS
John H. Pitts 30 Sep. 1989 6 p Presented at the 13th International Symposium on Fusion Engineering, Knoxville, TN, 2-6 Oct. 1989
(Contract W-7405-eng-48)
(DE90-002315; UCRL-102100; CONF-891007-49) Avail: NTIS HC A02/MF A01

The Starlight concept for an inertial-confinement-fusion (ICF) reactor utilizes a softball-sized solid-lithium x ray and debris shield that surrounds each fuel pellet as it is injected into the reactor. The shield is sacrificial and vaporizes as it absorbs x ray and ion-debris energy emanating from the fusion reactions in the fuel pellets. However, the energy deposition time at the surface if the first wall is lengthened by four orders of magnitude (to greater than 100 microns) which allows the energy to be conducted into the wall fast enough to prevent vaporization. Starlight operates at 5 Hz with 300-MJ-yield fuel pellets. It features a stationary, nonvaporizing first wall that eliminates erosion and shock waves which can destroy the wall; also, it allows arbitrary fuel pellet illumination geometries so that efficient coupling of either laser or heavy ion beam driver energy to the fuel pellet can be achieved. When neutrons penetrate the shield, the wall experiences neutron damage that limits its lifetime. Hence, we must choose wall materials that have ab economic lifetime. We describe the general concept and a specific design for laser drivers using a 6-m-radius, 2 1/4 Cr 1 Mo steel first wall. We include heat transfer calculations used to establish the radius and structural analysis that shows stresses are within allowable limits. A wall lifetime of over six years is predicted. DOE

N90-14928# International Centre for Theoretical Physics, Trieste (Italy).
ON THE THERMAL STABILITY OF FLOW OF A RADIATING TWO-COMPONENT PLASMA IN A POROUS MEDIUM BETWEEN TWO ROTATING CYLINDERS
A. R. Bestman (Port Harcourt Univ., Nigeria) Mar. 1989 14 p

Submitted for publication
(DE89-636426; IC-89/30) Avail: NTIS (US Sales Only) HC A03/MF A01

This paper studies the effect of magnetic field on the convective instability of a radiating fluid in a porous medium confined between two rotating cylinders. The temperature of the walls of the cylinders are large but the temperature difference is small so that the radiative flux equation could be linearized. Only for very small radiation parameter, of order 0(0.01), does instability first set in via adverse temperature gradient. Otherwise rotational instability is more fatal. DOE

N90-14929# Wisconsin Univ., Madison.
THEORETICAL REVERSED FIELD PINCH STUDIES Annual Progress Report, 31 Oct. 1988 - 1 Nov. 1989
1989 10 p
(Contract DE-FG02-85ER-53212)
(DE90-002114; DOE/ER-53212/144) Avail: NTIS HC A02/MF A01

This report discusses the following topics: Nonlinear behavior of the reversed field pinch with non-ideal boundary conditions; Field error effects on 3-D equilibria; and Hall effects. DOE

N90-14930# Texas Univ., Austin. Inst. for Fusion Studies.
STABILITY OF THE GLOBAL ALFVEN EIGENMODE IN THE PRESENCE OF FUSION ALPHA PARTICLES IN AN IGNITED TOKAMAK PLASMA
G. Y. Fu and J. W. VanDam May 1989 25 p
(Contract DE-FG05-80ET-53088)
(DE89-016618; DOE/ET-53088/370; IFSR-370) Avail: NTIS HC A03/MF A01

The stability of the Global Alfven Eigenmodes is investigated in the presence of super-Alfvenic energetic particles, such as the fusion-product alpha particles in an ignited deuterium-tritium tokamak plasma. Alpha particles tend to destabilize these modes when omega (sub * alpha) greather than (omega)(sub A), where omega (sub A) is the shear-Alfven modal frequency and omega (sub * alpha) is the alpha particle diamagnetic drift frequency. This destabilization due to alpha particles is found to be greatly enhanced when the alpha particles are modeled with a slowing-down distribution function rather than with a Maxwellian. However, previously neglected electron damping due to the magnetic curvature drift is found to be comparable in magnitude to the destabilizing alpha particle term. Furthermore, the effects of toroidicity are also found to be stabilizing, since the intrinsic toroidicity induces poloidal mode coupling, which enhances the parallel electron damping from the sideband shear Alfven Landau resonance. In particular, for the parameters of the proposed Compact Ignition Tokamak, the Global Alfven Eigenmodes are found to be completely stabilized by either the electron damping that enters through the magnetic curvature drift or the damping introduced by finite toroidicity. DOE

N90-14931# Argonne National Lab., IL. Fusion Power Program.
COMPUTATION OF ELECTROMAGNETIC EFFECTS IN A TOKAMAK DUE TO A PLASMA DISRUPTION
Larry R. Turner 1989 10 p Presented at the International Symposium and Team Workshop on 3-D Electromagnetic Field Analysis Okayama, Japan, 11-13 Sep. 1989
(Contract W-31-109-eng-38)
(DE90-001764; CONF-8909257-1) Avail: NTIS HC A02/MF A01

To model the consequences of a plasma disruption in a tokamak one must combine a code that computes the detailed MHD behavior of the plasma with one that treats the 3-D features of the conducting toroidal components around the plasma. The Next European Torus Team have undertaken a treatment of electromagnetic effects from plasma disruptions using both open loop and closed loop integration of codes. In America, workers at Oak Ridge National Laboratory, Idaho National Engineering Laboratory, and Argonne National Laboratory have looked at plasma disruption effects on the ITER blanket using the codes TSC and EDDYNET. Results show how the forces on a blanket segment depend on the number and size of the segments and on the gap between them. DOE

N90-14932# Lawrence Livermore National Lab., CA.
PRACTICAL ASPECTS OF A 2-D EDGE-PLASMA MODEL
M. E. Rensink, D. N. Hill, G. D. Porter, and B. J. Braams (Princeton Univ., NJ.) Jul. 1989 6 p Presented at the 13th Conference on the Numerical Simulation of Plasmas, Santa Fe, NM, 17-19 Sep. 1989
(Contract W-7405-eng-48)
(DE90-002995; UCRL-101481; CONF-890931-9) Avail: NTIS HC A02/MF A01

The poloidal divertor configuration is considered the most promising solution to the particle and energy exhaust problem for a tokamak reactor. The scrape-off layer plasma surrounding the core and the high recycling plasma near the divertor plates can be modelled by fluid equations for particle, momentum and energy transport. A numerical code (B2) based on a 2-D multi-fluid model was developed for the study of edge plasmas in tokamaks. Some key features of this model as applied to the DIII-D tokamak are identified. DOE

N90-14933# Lodestar Research Corp., Boulder, CO.
FUNDAMENTAL STUDIES OF FUSION PLASMAS Annual Performance Report
R. E. Aamodt, P. J. Catto, D. A. Dippolito, and J. R. Myra 27 Jun. 1989 17 p
(Contract DE-FG02-88ER-53263)
(DE90-002343; DOE/ER-53263/7; LRC-89-7) Avail: NTIS HC A03/MF A01

In this paper, summary reports are given on significant new results for understanding and controlling tokamak performance under the application of high power ICH; new results on understanding the complicated interaction of plasma, atomic and surface physics in the tokamak edge plasma with intense rf fields; and new results on the neoclassical transport of energetic alpha particles. DOE

N90-14934*# Iowa Univ., Iowa City. Dept. of Physics and Astronomy.
PARTICLE SIMULATIONS IN MAGNETOSPHERIC PLASMAS Final Technical Report, 1 Nov. 1988 - 31 Oct. 1989
Ken-Ichi Nishikawa 26 Jan. 1990 7 p
(Grant NAGw-1239)
(NASA-CR-186238; NAS 1.26:186238) Avail: NTIS HC A02/MF A01 CSCL 20I

In view of the recent remarkable advancement of computer technology and simulation software, simulation studies are one of the most powerful academic tools for establishment of quantitative space physics and modelling of our space environment. The complex nature encountered in space plasma physics has motivated considerable development in computer simulations, which have played an essential role in the development of space plasma theory. This report describes research undertaken to understand physical processes involved in plasma waves observed in the magnetospheric plasmas, and associated nonlinear phenomena such as heating, diffusion, and acceleration of particles due to excited waves. The research explains and clarifies the observational data both qualitatively and quantitatively. Author

N90-14567# Paris VI Univ. (France). Lab. de Spectroscopie Atomique des Plasmas.
ATOMIC STRUCTURE AND SPECTRAL PERTURBATIONS IN HOT DENSE PLASMAS [STRUCTURE ATOMIQUE ET PERTURBATIONS SPECTRALES DANS LES PLASMAS DENSES ET CHAUDS]
Hoe Nguyen, Jose Banon, Gerard Coulaud, Brigitte Detat, Jeanne Grumberg, Michel Koenig, Elisabeth Leboucher, Philippe Malnoult, and Laurent Terray *In* Groupement de Recherches Coordonnees Interaction Laser Matiere, Activities Report in Laser Matter Interactions Jun. 1988 p 147-159 In FRENCH (For primary document see N90-14544 06-36)
Avail: NTIS HC A13/MF A02

N90-14568# Paris VI Univ. (France). Lab. de Spectroscopie Atomique des Plasmas.
TRANSVERSAL INHOMOGENEITY AND RADIATIVE TRANSFER IN PLASMAS OBTAINED BY LASER IMPACT [INHOMOGENEITE TRANSVERSE ET TRANSFERT RADIATIF DANS LES PLASMAS OBTENUS PAR IMPACT LASER]
Claire Bousquet, Jeanne Grumberg, Elisabeth Leboucher, Hoe Nguyen, and Alain Poquerusse (Ecole Polytechnique, Palaiseau, France) *In* Groupement de Recherches Coordonnees Interaction Laser Matiere, Activities Report in Laser Matter Interactions Jun. 1988 p 160-166 In FRENCH (For primary document see N90-14544 06-36)
Avail: NTIS HC A13/MF A02

N90-14569# Ecole Polytechnique, Palaiseau (France). Lab. de Physique des Milieux Ionises.
THE AVERAGE ION MODEL. COMPUTATION OF THE ABSORPTION AND EMISSION COEFFICIENTS IN HOT PLASMAS [LE MODELE DE L'ION MOYEN. CALCUL DES COEFFICIENTS D'ABSORPTION ET D'EMISSION DANS LES PLASMAS CHAUDS EN ETL ET HORS ETL]
Jean-Claude Gauthier and Jean-Paul Geindre *In* Groupement de Recherches Coordonnees Interaction Laser Matiere, Activities Report in Laser Matter Interactions Jun. 1988 p 167-175 In FRENCH (For primary document see N90-14544 06-36)
Avail: NTIS HC A13/MF A02

N90-14570# Ecole Polytechnique, Palaiseau (France). Lab. de Physique des Milieux Ionises.
XRAD: A ONE DIMENSIONAL LAGRANGIAN CODE WITH RADIATIVE TRANSPORT [XRAD: UN CODE 1D LAGRANGIEN AVEC TRANSPORT RADIATIF]
Jean-Claude Gauthier and Jean-Paul Geindre *In* Groupement de Recherches Coordonnees Interaction Laser Matiere, Activities Report in Laser Matter Interactions Jun. 1988 p 176-188 In FRENCH (For primary document see N90-14544 06-36)
Avail: NTIS HC A13/MF A02

N90-14571# Paris-Sud Univ., Orsay (France). Lab. de Spectroscopie Atomique et Ionique.
POPULATION INVERSIONS CALCULATED FOR LITHIUM-LIKE IONS IN A PLASMA [INVERSIONS DE POPULATION CALCULEES DANS DES IONS LITHIUMOIDES AU SEIN D'UN PLASMA]
Helene Guennou, Annie Klisnick, Clary Moeller, and Alain Sureau *In* Groupement de Recherches Coordonnees Interaction Laser Matiere, Activities Report in Laser Matter Interactions Jun. 1988 p 189-192 In FRENCH (For primary document see N90-14544 06-36)
Avail: NTIS HC A13/MF A02

N90-14572# Paris-Sud Univ., Orsay (France). Lab. de Spectroscopie Atomique et Ionises.
STUDY OF LITHIUM-LIKE IONS FOR AMPLIFYING RADIATION BELOW 100 ANGSTROMS. EXPERIMENT AT THE RUTHERFORD APPLETON LABORATORY [ETUDES DES IONS LITHIUMOIDES POUR L'AMPLIFICATION DE RAYONNEMENT AU DESSOUS DE 100 ANGSTROMS. EXPERIENCE AU RUTHERFORD APPLETON LABORATORY]
Annie Klisnick, Gerard Jamelot, Antoine Carillon, Pierre Jaegle, M. H. Key, M. Grande, O. Willi, G. Kiehn, J. Edwards, and C. L. S. Lewis (Queens Univ., Belfast, Northern Ireland) et al *In* Groupement de Recherches Coordonnees Interaction Laser Matiere, Activities Report in Laser Matter Interactions Jun. 1988 p 193-196 In FRENCH (For primary document see N90-14544 06-36)
Avail: NTIS HC A13/MF A02

N90-14573# Paris-Sud Univ., Orsay (France). Lab. de Spectroscopie Atomique et Ionique.
SINGLE BEAM INTERACTIONS FOR THE STUDY OF X RAY LASERS [INTERACTIONS MONOFAISCEAU POUR L'ETUDE DU LASER EN RAYONS X]
Pierre Jaegle, Antoine Carillon, Fouard Gadi, Bernard Gauthe, Gerard Jamelot, and Annie Klisnick *In* Groupement de Recherches Coordonnees Interaction Laser Matiere, Activities Report in Laser Matter Interactions Jun. 1988 p 197-201 In FRENCH (For primary document see N90-14544 06-36)
Avail: NTIS HC A13/MF A02

N90-14574# Paris-Sud Univ., Orsay (France). Lab. de Spectroscopie Atomique et Ionique.
X-UV AMPLIFICATION IN A PLASMA COLUMN OF FIVE CENTIMETERS. FIVE BEAMS EXPERIMENT [AMPLIFICATION X-UV DANS UNE COLONNE DE PLASMA DE 6 CM DE LONGUEUR. EXPERIENCE A CINQ FAISCEAUX]
Pierre Jaegle, Antoine Carillon, Michel Cousy, P. Dhez, Fouard Gadi, Bernard Gauthe, M. Grande (Rutherford High Energy Lab., Chilton, England), Gerard Jamelot, Annie Klisnick, and J. C. Lagron et al *In* Groupement de Recherches Coordonnees Interaction Laser Matiere, Activities Report in Laser Matter Interactions Jun. 1988 p 202-204 In FRENCH (For primary document see N90-14544 06-36)
Avail: NTIS HC A13/MF A02

N90-14575# Ecole Polytechnique, Palaiseau (France). Lab. pour l'Utilisation des Lasers Intenses.
CHARACTERISTICS OF AN X RAY SOURCE CREATED BY A LASER PLASMA [CARACTERISTIQUES D'UNE SOURCE DE RAYONS X CREEE PAR PLASMA LASER]
Isabelle Toubhans, Remy Fabbro, H. Pepin, and M. Chaker (Quebec Univ., Montreal.) *In* Groupement de Recherches Coordonnees Interaction Laser Matiere, Activities Report in Laser Matter Interactions Jun. 1988 p 205-211 In FRENCH (For primary document see N90-14544 06-36)
Avail: NTIS HC A13/MF A02

76 SOLID-STATE PHYSICS

Includes superconductivity.

For related information, see also *33 Electronics and Electrical Engineering* and *36 Lasers and Masers.*

N90-14935# Department of the Navy, Washington, DC.
METHOD OF MAKING SELF-ALIGNED GaAs/AlGaAs FET'S Patent Application
John E. Davey, inventor (to Navy) and A. Christou, inventor (to Navy) 27 Jun. 1989 23 p
(AD-D014229; US-Patent-Appl-SN-371778) Avail: NTIS HC A03/MF A01 CSCL 09/1

A method of making a self-aligned FET includes the following steps. First, a selectively doped heterostructure substrate having a predetermined crystalline structure is obtained having a heavily doped top GaAs layer, having a heavily doped AlGaAs layer under the top layer that is resistant to orientation-dependent etching, and having an undoped underlying AlGaAs layer which is deposited on the top layer. Then, an uppermost GaAs layer is deposited on the top layer. Then, an angular recess is etched through the uppermost GaAs layer and through the top heavily doped GaAs layer of the heterostructure substrate with an orientation-dependent etchant down to the etch resistant AlGaAs layer, whereby the length of the angular recess is wider at the base of the recess than at the top of the recess because of the predetermined crystalline structure and the orientation-dependent etchant. Next, a refractory metal gate of tantalum silicide is deposited in the recess. The length of the refractory metal gate is substantially the same as the length of the top of the recess and is aligned therewith. The refractory metal gate is then covered with an etch resistant polyimide material. GRA

N90-14936# Department of the Navy, Washington, DC.
MULTIBAND PHOTOCONDUCTIVE DETECTOR BASED ON LAYERED SEMICONDUCTOR QUANTUM WELLS Patent Application
Stephen G. Bishop, inventor (to Navy) and Benjamin V.

Shanabrook, inventor (to Navy) 29 Jun. 1989 20 p
(AD-D014232; US-Patent-Appl-SN-372961) Avail: NTIS HC A03/MF A01 CSCL 17/5

A multiband photoconductive detector and method for simultaneously and separately detecting and distinguishing light or radiation from a large number of different wavelength bands is disclosed. The multiband photoconductive detector comprises a plurality of low energy gap semiconductor layers of preselected progressively decreasing thicknesses of a first material, a plurality of high energy gap semiconductor layers of a second material interleaved with the plurality of low energy gap semiconductor layers, and a plurality of pairs of electrical contacts respectively applied to the plurality of low energy gap semiconductor layers and adapted to respectively receive associated bias voltages to enable the plurality of low energy gap semiconductor layers to constitute a corresponding plurality of separate photoconductive detectors with a preselected plurality of different wavelength bands. GRA

N90-14937 Department of the Navy, Washington, DC.
METHOD OF SENSITIZING PB-SALT EPITAXIAL FILMS FOR SCHOTTKY DIODES Patent
Tak-Kin Chu, inventor (to Navy) and Francisco Santiago, inventor (to Navy) 1 Aug. 1989 7 p Filed 27 Jul. 1988
(AD-D014244; US-Patent-4,853,339; US-Patent-Appl-SN-244962) Avail: US Patent and Trademark Office CSCL 20/12

This invention relates to photodetectors and more particularly to infrared-sensitive photodiodes. It is well established that single crystal films of lead chalcogenides, lead tin chalcogenides, and lead cadmium chalcogenides can be epitaxially grown on heated alkali metal halide substrates by vacuum evaporation. The chalcogenides used include the sulfides, selenides, tellurides, and mixtures thereof. The substrates are single crystals of infrared transparent alkali metal halides and alkaline earth halides. Examples include barium fluoride, strontium fluoride, calcium fluoride, lithium fluoride, sodium chloride, potassium chloride, etc. It is also well known that the vacuum deposition of a metal contact of certain materials such as lead or indium, on the surface of an epitaxial layer of a led chalcogenide, lead tin chalcogenide, or lead cadmium chalcogenide creates a non-Ohmic Schottky barrier at the point of contact, resulting in an infrared sensitive photodiode. GRA

N90-14938# Rome Univ. (Italy). Dipt. di Fisica.
SPECTRAL PROPERTIES OF ONE DIMENSIONAL QUASI-CRYSTALS
J. Bellissard, B. Jochum, E. Scoppola, and D. Testard (Aix-Marseilles Univ., France) 6 Mar. 1989 27 p
(Preprint-659; ETN-90-95791) Avail: NTIS HC A03/MF A01

The discrete one dimensional Schroedinger operator with quasi-periodic potential is investigated. Quasi periodic structures, which play an important role in solid state physics, can be described using such operators. The properties of quasi-crystals are described in this manner. The eigenvalue problem from the original model is not completely solved from a rigorous point of view. ESA

N90-14939# Chronar Corp., Princeton, NJ.
STUDY OF MICROCRYSTALLINE, SILICON-CARBON p-LAYERS PREPARED BY PHOTO-CVD AND GLOW DISCHARGE Final Subcontract Report, 1 Dec. 1987 - 30 Nov. 1988
H. Schade Jun. 1989 16 p
(Contracts DE-AC02-83CH-10093; XB-5-04092-1)
(DE89-009438; SERI/STR-211-3527) Avail: NTIS HC A03/MF A01

Preparation conditions were established for microcrystalline silicon (uc-Si:H) p-type films deposited by both mercury sensitized photochemical vapor deposition and RF glow discharge. The degree of microcrystallinity in individual films was evaluated in terms of the dark conductivity and optical absorption. Both deposition methods have produced uc-Si: p-layers with conductivities as high as 0.5 S/cm, and optical band gaps between 2.0 and 2.4 eV. For the deposition of such films on glass, a strong decrease of the conductivity below thicknesses of about 100 nm is observed, which is associated with a percolation threshold for conduction. Based on this observation, relatively thick microcrystalline p-layers were incorporated into p-i-n structures. The effect of microcrystallinity is demonstrated by an improvement in the open circuit voltage, whereas a reduction of the short circuit current is accounted for by a decrease in the blue response, due to the excessive absorbance of the relatively thick microcrystalline p-layer. Efficiency improvements require microcrystalline p-layers of lower absorbance, and/or higher conductivity of thinner layers, provided substantial barrier formation at the conductive-transparent-oxide/p-layer interface can be avoided. DOE

N90-14940# Oak Ridge National Lab., TN. Solid State Div.
STATIC AND DYNAMIC MAGNETIZATION PROPERTIES OF Y1Ba2Cu3O(SUB z) THIN FILMS
S. T. Sekula Aug. 1989 15 p Presented at the European Conference on High-T(sub c) Thin Films and Single Crystals, Ustron, Poland, 30 Sep. - 4 Oct. 1989
(Contract DE-AC05-84OR-21400)
(DE89-017584; CONF-890939-1) Avail: NTIS HC A03/MF A01

Magnetization studies were carried out on Y1Ba2Cu3O(z) (YBCO) thin films that were e-beam evaporated onto circular discs of single crystal SrTiO3 with (001) and (110) faces as well as KTaO3 with (001) faces. The measurements were made using vibrating sample (VSM) and SQUID-based magnetometry with the applied field perpendicular to the substrate surface. Critical current densities J(sub c)(H,T) are deduced from the magnetic hysteresis. Flux creep effects are observed over longer periods with the SQUID magnetometer. Analysis of the results of low frequency response of these films to collinear ac and dc magnetic fields are compared with the dc magnetometry results. J(sub c)(H,T) is observed to be quite sensitive to the type of epitaxial growth on the various substrates. DOE

N90-14941# Los Alamos National Lab., NM.
ION BEAM ANALYSIS AND MODIFICATION OF THIN-FILM, HIGH-TEMPERATURE SUPERCONDUCTORS
Michael Nastasi Oct. 1989 25 p
(Contract W-7405-eng-36)
(DE90-000918; LA-11499-MS) Avail: NTIS HC A03/MF A01

The application of ion beams to ceramic processing is a very powerful technique. In particular, ion beams have been shown to be very effective in producing novel material properties through their rather violent interactions with the component atoms of the ceramics. However, in all these cases ions are used to process and produce changes in ceramics, changes that must be monitored by other techniques. This paper shows that, in addition to modifying materials, ion beams can be used in a more gentle but very powerful way to explore what happens to a ceramic thin film as a result of processing. The following discussions are concerned exclusively with a new and exciting class of ceramic: the high-temperature superconductor (HTS). We will discuss the application of various ion beam backscattering techniques as well as examine the use of ion implantation in the processing of these materials. DOE

N90-14942# Oak Ridge National Lab., TN. Solid State Div.
THEORY OF STRONGLY FLUCTUATING SUPERCONDUCTIVITY
S. H. Liu Sep. 1989 10 p Presented at the Conference on Superconductivity and Applications, Buffalo, NY, 19-21 Sep. 1989
(Contract DE-AC05-84OR-21400)
(DE90-001073; CONF-890971-1) Avail: NTIS HC A02/MF A01

In superconductors with short coherence lengths, such as the copper oxides, the order parameter is prone to phase fluctuations. Josephson showed that phase fluctuations are coupled to the density of Cooper pairs so that they are always accompanied by space and time varying supercurrents. It is shown how the variation of the order parameter, its phase, and the charge density can be mapped onto a magnetic problem by a real space extension of the pseudo-spin representation of Anderson. It is shown that at long wavelengths the charge fluctuation is asymptotically decoupled

from the order parameter fluctuation so that the problem is isomorphic to the XY model. In particular, at low temperatures there exist collective excitations, the so-called phase waves, which are analogous to spin waves in magnetic systems. Two experiments are proposed to test the theoretical predictions. DOE

N90-14943# Brookhaven National Lab., Upton, NY.
X RAY REFLECTIVITY STUDY OF SiO2 ON Si
S. M. Heald, J. K. D. Jayanetti, A. A. Bright, and G. W. Rubloff (IBM Watson Research Center, Yorktown Heights, NY.) 1989 12 p Presented at the 36th American Vacuum Society National Vacuum Symposium, Boston, MA, 23-27 Oct. 1989
(Contracts DE-AC02-76CH-00016; DE-AS05-80ER-10742)
(DE90-001326; BNL-42928; CONF-891093-4) Avail: NTIS HC A03/MF A01

X ray reflectivity is a powerful probe of thin film morphology. It can be used for nondestructive determination of the interface and surface roughness, thickness and density of the layers. The application is presented of the technique to the case of SiO2 on Si. Experimental reflectivity results with a dynamic range of 10(exp 6) were obtained on a number of oxide layers prepared using processing conditions. The reflectivity oscillations caused by oxide layers could be easily observed over this entire range, and significant differences were observed between samples. In particular, a PECVD grown oxide is found to have an interfacial layer of lower density. DOE

N90-14944# Oak Ridge National Lab., TN.
ION BEAM PROCESSING OF ADVANCED ELECTRONIC MATERIALS
N. W. Cheung, ed., A. D. Marwick, ed. (IBM Watson Research Center, Yorktown Heights, NY.), and J. B. Roberto, ed. 1989 393 p Presented at the Symposium on Ion Beam Processing of Advanced Electronic Materials, San Diego, CA, 25-27 Apr. 1989
(Contract DE-AC05-84OR-21400)
(DE89-017342; CONF-8904275) Avail: NTIS HC A17/MF A03

Research programs discussed at the materials research society symposia on ion beam processing of advanced electronic materials are presented. Major topics include: shallow implantation and solid phase epitaxy; damage effects; focused ion beams; MeV implantation; high dose implantation; implantation in III-V materials and multilayers; and implantation in electronic materials. Individual projects are processed separately for the data bases. DOE

N90-14945# Oak Ridge National Lab., TN.
SOLID STATE DIVISION Progress Report, period ending 31 Mar. 1989
P. H. Green, ed. and D. M. Watson, ed. Aug. 1989 248 p
(Contract DE-AC05-84OR-21400)
(DE90-000979; ORNL-6571) Avail: NTIS HC A11/MF A02

This report contains brief discussions on work done in the Solid State Division of Oak Ridge National Laboratory. The topics covered are: theoretical solid state physics; neutron scattering; physical properties of materials; the synthesis and characterization of materials; ion beam and laser processing; and structure of solids and surfaces. DOE

N90-14946# Brookhaven National Lab., Upton, NY. National Synchrotron Light Source.
REFLECT: A COMPUTER PROGRAM FOR THE X RAY REFLECTIVITY OF BENT PERFECT CRYSTALS
V. Etelaeniemi, P. Suortti (Helsinki Univ., Finland), and W. Thomlinson Sep. 1989 19 p
(Contract DE-AC02-76CH-00016)
(DE90-001266; BNL-43247) Avail: NTIS HC A03/MF A01

The design of monochromators for x ray applications, using either standard laboratory sources on synchrotron radiation sources, requires a knowledge of the reflectivity of the crystals. The reflectivity depends on the crystals used, the geometry of the reflection, the energy range of the radiation, and, in the present case, the cylindrical bending radius of the optical device. The reader is allowed to become familiar with, and therefore use, a computer program called REFLECT which was used in the design of a dual beam Laue monochromator for synchrotron angiography. The results of REFLECT were compared to measured reflectivities for both bent Bragg and Laue geometries. The results are excellent and should give full confidence in the use of the program. DOE

N90-14947# State Univ. of New York, Buffalo. Dept. of Physics.
X RAY STUDIES OF STRAIN, INTERFACE, AND IMPURITY IN SEMICONDUCTORS Technical Progress Report, 1 Jul. 1988 - 30 Jun. 1989
Yi-Han Kao 1989 12 p
(Contract DE-FG02-87ER-45283)
(DE90-001525; DOE/ER-45283/4) Avail: NTIS HC A03/MF A01

In the past years, the EXAFS techniques were used to investigate the local structure around various atomic species in different semiconductor and superconductor systems. EXAFS spectra contain information on interatomic distance, coordination number, and disorder, thus are uniquely suited for studying the microstructure in materials where there is a lack of long-range structural order. In the previous studies, EXAFS data were obtained by measuring either x ray fluorescence or transmission near the K absorption edge of As, In, Ga, Co, Zn, Se, Nb, Ge, Cu, Y, Ba, Fe, O, and Ag. Some EXAFS spectra near the oxygen K edge were obtained by measuring the total electron yield. The materials studied in our EXAFS experiments include InAs/AlSb, InAs/GaAs, InGaAs/InP, CoSi2/Si(111) heterostructures, As-doped Si (Si:As) and Bi (Bi:As), NbGeAl compounds, and chemically-doped Y-Ba-Cu-O superconductor systems. In the cases of semiconductor heterostructures grown by epitaxy and single crystals, fluorescence EXAFS measurements were made exclusively in order to preserve the integrity of these special samples. DOE

N90-14948# Brookhaven National Lab., Upton, NY. Materials Science Div.
FLUX PINNING AND MICROSTRUCTURE IN YBa2Cu3O7
M. Suenaga, D. O. Welch, Youwen Xu, Y. Zhu, A. K. Ghosh, and A. R. Moodenbaugh 1989 15 p Presented at Windpower '89, San Francisco, CA, 24-27 Sep. 1989
(Contract DE-AC02-76CH-00016)
(DE90-001562; BNL-43312; CONF-890971-2) Avail: NTIS HC A03/MF A01

Critical current densities J(sub c) of superconductors are one of the most important properties of superconductors in the majority of applications. Unfortunately, in spite of the fact that tremendous efforts have been mounted internationally in studies of the high temperature oxide superconductors, the current values of J(sub c) are disappointingly low except in single crystal bulk specimens and films with the current flowing in the basal planes. When 2 percent of the Cu in YBa2Cu3O7 is replaced by either Al or Fe, it is found that the intragranular critical current densities of these alloyed oxides were reduced. On the other hand, it was also found that substitution for Cu by 2 percent Ni did not show any effect on J(sub c) at 10 K. In order to illustrate what are the primary controlling parameters in reducing the values of J(sub c) when small amounts of Cu were replaced by Fe or Al, some elementary aspects of flux pinning mechanisms are first reviewed. Then it will be shown how those parameters which are pertinent to flux pinning may be estimated for these specimens. Finally, what is probably the most prominent cause for the reduction in J(sub c) is deduced for the specimens discussed. DOE

N90-14949# Los Alamos National Lab., NM.
HIGH-TEMPERATURE/HIGH-PRESSURE X RAY DIFFRACTION: RECENT DEVELOPMENTS
D. Schiferl, S. W. Johnson, and A. S. Zinn 1989 4 p Presented at the AIRAPT and EHPRG International High Pressure Science and Technology Conference, Paderborn, Fed. Republic of Germany, 17-21 Jul. 1989
(Contract W-7405-eng-36)
(DE89-015255; LA-UR-89-2419; CONF-890798-6) Avail: NTIS HC A01/MF A01

Two Merrill-Bassett diamond-anvil cells were developed for

specialized high-temperature uses. The first is constructed largely of rhenium to provide uniform, constant P and T on the order of 20 GPa at 1200 K for extended periods. The second is for single-crystal x ray diffraction, but can be heated to 630 K at 20 GPa to grow single-crystal samples which cannot be produced at room temperature. With this cell, the crystal structure of epsilon-O2 was shown to be monoclinic with a = 3.649 A, b = 5.493 A, c = 7.701 A, and Beta = 116.11 degrees at 19.7 GPa. DOE

N90-14950# Argonne National Lab., IL. Materials Science Div.
HIGH RESOLUTION-ANGLE RESOLVED PHOTOEMISSION STUDIES OF HIGH TEMPERATURE SUPERCONDUCTORS
C. G. Olson, R. Liu, D. W. Lynch, B. W. Veal, Y. C. Chang, P. Z. Jiang, J. Z. Liu, A. P. Paulikas, A. J. Arko, and R. S. List (Los Alamos National Lab., NM.) Aug. 1989 5 p Presented at the International Conference on Materials and Mechanisms of Superconductivity - High-Temperature Superconductors, Stanford, CA, 23-28 Jul. 1989
(Contract W-31-109-eng-38)
(DE89-017691; CONF-890718-29) Avail: NTIS HC A01/MF A01

Recent photoemission studies of YBa2Cu3O(7-delta) and Bi2Sr2CaCu2O8 performed with high energy and angular resolution have provided detailed information on the nature of the states near the Fermi level. Measurements of the superconducting gap, band dispersion, and the density of states near the Fermi level in the normal state all support a Fermi liquid description of these materials. DOE

N90-14951# Argonne National Lab., IL. Materials Science Div.
OXYGEN STOICHIOMETRY, STRUCTURAL TRANSITIONS, AND THERMODYNAMIC BEHAVIOR OF THE YBa2Cu3O(x) SYSTEM
M. Tetenbaum, L. A. Curtiss, B. Tani, B. Czech, and M. Blander 1989 22 p Presented at the NATO Advanced Study Institute on High Temperature Superconductors-Physics and Materials Sciences, Bad Windsheim, Fed. Republic of Germany, 13-26 Aug. 1989
(Contract W-31-109-eng-38)
(DE89-017694; CONF-890806-2) Avail: NTIS HC A03/MF A01

Electromotive force (EMF) measurements of oxygen fugacities as a function of oxygen stoichiometry in the YBa2Cu3O(x) system (1-2-3 superconductor) were carried out over the composition range x (approx. equal) 6.15 to 6.9 and the temperature range 400 to 750 C. A coulometric titration technique with an yttria-doped zirconia electrolyte was used for these measurements. By means of this technique, the oxygen content of the superconductor is varied by well defined small amounts, and the equilibrium oxygen partial pressures can be established from the EMF measurements. The overall objective of these studies is to investigate the phase transformations and thermodynamic behavior of the YBa2Cu3O(x) system as a function of oxygen partial pressure, oxygen stoichiometry, and temperature. DOE

N90-14952# Oak Ridge National Lab., TN. Chemical Physics Section.
DEVELOPMENT OF A REAL TIME MONITOR FOR SUPERCONDUCTIVE THIN FILM PREPARATION
C. H. Chen Sep. 1989 9 p Presented at the Microelectronic Integrated Processing Conference, Santa Clara, CA, 8-13 Oct. 1989
(Contract DE-AC05-84OR-21400)
(DE89-017772; CONF-8910197-2) Avail: NTIS HC A02/MF A01

In general, the preparation of a superconductive thin film involves the vaporization of various chemicals. The species deposited on substrates include neutral atoms or molecules in ground states, atoms and molecules in excited states, ions in ground states and ions in excited states. An instrument which has the capability of the quantitative determination of atoms, molecules, and ions in various electronic states should provide very detailed information on the mechanism of formation of superconductive films. A position sensitive monitor of various oxide compounds relative to the flow and pressure of oxygen should reveal the role of oxygen in superconductive film preparation. An ideal method of monitoring the deposition process is to continuously track the deposition in situ and automatically maintain optimum film growth. With this goal in mind, we have investigated several diagnostic methods. In this work, fluorescence spectra are presented which indicate suitability for monitoring excited atoms, molecules, and ions; mass analysis of laser desorbed ions is described; and the application of resonance ionization spectroscopy (RIS) to monitor desorbed neutral atoms and molecules is discussed. DOE

N90-14953# Brookhaven National Lab., Upton, NY.
GLANCING ANGLE X RAY STUDIES OF OXIDE FILMS
A. J. Davenport and H. S. Isaacs 1989 7 p Presented at the 6th International Symposium on Passivity: Passivation of Metals and Semiconductors, Sapporo, Japan, 24-28 Sep. 1989
(Contracts DE-AC02-76CH-00016; DE-AS05-80ER-10742)
(DE89-017828; BNL-42550; CONF-890960-1) Avail: NTIS HC A02/MF A01

High brightness synchrotron radiation incident at glancing angles has been used to study inhibiting species present in low concentrations in oxide films on aluminum. Glancing incident angle fluorescence measurements give surface-sensitive information on the valence state of elements from the shape of the x ray absorption edge. Angle-resolved measurements show the depth distribution of the species present. DOE

N90-14954# Los Alamos National Lab., NM. Theoretical Div.
SUPERCONDUCTIVITY FROM FINITE-U VALENCE FLUCTUATIONS
B. H. Brandow 1989 7 p Presented at the International Conference on the Physics of Highly Correlated Electron Systems, Santa Fe, NM, 11-15 Sep. 1989
(Contract W-7405-eng-36)
(DE90-000603; LA-UR-89-3037; CONF-890953-6) Avail: NTIS HC A02/MF A01

The finite-U pairing mechanism of Newns is explored by an adaptation of the previous U = infinity variational treatment of the Anderson lattice. This pairing mechanism is found to be opposed by a magnetic tendency arising from Gutzwiller renormalization of the hybridization. This competition restricts superconductivity to the parameter regime delta is approximately U, and this also reproduces the parabolic rise and fall of T(sub c) in La(2-x)Sr(x)CuO(4) with increasing x. Re-analysis of the photoemission and BIS data for CuO reveals that indeed Delta is greater than on approximately U for this compound, contrary to previous work. DOE

N90-14955# Los Alamos National Lab., NM.
A SIMPLE FIGURE OF MERIT FOR HIGH TEMPERATURE SUPERCONDUCTING SWITCHES
E. M. Honig 1989 4 p Presented at the 7th Institute of Electrical and Electronics Engineers Pulsed Power Conference, Monterey, CA, 12-14 Jun. 1989
(Contract W-7405-eng-36)
(DE90-000610; LA-UR-89-2946; CONF-890665-49) Avail: NTIS HC A01/MF A01

The discovery of the new high temperature superconductors has revived interest in many special applications, including superconducting switches. For comparison of switch types, a simple figure of merit based in switch performance is proposed, derived for superconducting switches, and then calculated for thyristors and vacuum switches. The figure of merit is then used to show what critical current density would be needed for superconducting switches to compete with more conventional switches. DOE

N90-14956# Los Alamos National Lab., NM.
MUON SR INVESTIGATION OF MAGNETISM AND SUPERCONDUCTIVITY IN (Y(1-x)Pr(x))Ba2Cu3O7
D. W. Cooke, R. S. Kwok, M. S. Jahan, R. L. Lichti, T. R. Adams, C. Boekema, W. K. Dawson, A. Kebede, J. Schwegler, and J. E. Crow (Temple Univ., Philadelphia, PA.) et al 1989 11 p Presented at the International Conference on the Physics of Highly

Correlated Electron Systems, Santa Fe, NM, 11-15 Sep. 1989
(Contract W-7405-eng-36)
(DE90-000689; LA-UR-89-3221; CONF-890953-4) Avail: NTIS HC A03/MF A01

Muon spin rotation and relaxation techniques were used to study the superconductivity and magnetism in (Y(1-x)Pr(x))Ba2Cu3O7 (0 is less than or equal to x is less than or equal to 1) and PrBa2Cu3O6. Clear evidence for magnetic ordering of the Cu moments within the Cu-O planes is seen. Additionally, a lower magnetic transition is observed which, based upon previous work, has been associated with the ordering of Pr moments on the Y sublattice of the YBa2Cu3O7 structure. For x = 1, the upper Neel temperature T(sub N1) is approximately 270 K and the magnitude of the fully developed local magnetic field is approximately 16 mT. Below the lower Neel temperature T(sub N2) = 17 K, the magnitude of the static field is reduced to approximately 12 mT. For 0.4 is less than or equal to x is less than or equal to 0.54, there appears to be a coexistence region of long-range magnetism and superconductivity. DOE

N90-14957# Oak Ridge National Lab., TN. Metals and Ceramics Div.
PRACTICAL LIMITATIONS OF ALCHEMI MEASUREMENTS ON ORDERED INTERMETALLIC ALLOYS
J. Bentley 11 Sep. 1989 5 p Presented at the EMAG-MICRO 89 Meeting, London, England, 13-15 Sep. 1989 Submitted for publication
(Contract DE-AC05-84OR-21400)
(DE90-000700; CONF-8909207-2) Avail: NTIS HC A01/MF A01

ALCHEMI determinations of sublattice occupancy in Cu50Au(50-x)Pd(x) alloys and Ni3Al-based alloys containing Fe, Co, and Hf illustrate some practical limitations of the technique. The restrictions imposed by domain size, disordered surface layers, illumination conditions, coherent bremsstrahlung peaks, ionization delocalization effects, and the need for axial rather than planar channeling are discussed. DOE

N90-14958# Lawrence Livermore National Lab., CA.
SUPERCONDUCTING AND MICROSTRUCTURAL PROPERTIES OF SHOCK-COMPACTED HIGH-T SUB c OXIDE POWDERS
C. L. Seaman, E. A. Early, M. B. Maple (California Univ., San Diego.), W. J. Nellis, J. B. Holt, M. Kamegai, and G. S. Smith Aug. 1989 5 p Presented at the American Physical Society Topical Conference on Shock Compression of Condensed Matter, Albuquerque, NM, 14-17 Aug. 1989
(Contract W-7405-eng-48)
(DE90-000823; UCRL-101901; CONF-890812-57) Avail: NTIS HC A01/MF A01

Shock compacted specimens of YBa2Cu3O(7-delta) and HoBa2Cu3O(7-delta) high-T(sub c) oxide powder mixed with 30 percent (vol) Ag powder were prepared using the LLNL two-stage light-gas gun in the 30 to 200 kbar range. We report the experimental technique and results of an investigation of the microstructural and superconducting properties of these composite specimens. Measurements of magnetic susceptibility show that bulk superconductivity is retained in this pressure range with T(sub c) onsets unchanged at 91 K. Oxide particle size is reduced with increasing shock pressure. Complete resistive transitions are observed at T(sub c) = 90 K only after subsequent heat treatment in oxygen. A transport critical current density of 320 A/sq cm at 77 K in zero field was measured for a specimen shocked to 167 kbar, suggesting that the shock process might introduce defects which serve to pin magnetic flux vortices and thereby increase J(sub c). DOE

N90-14959# Lawrence Livermore National Lab., CA.
EFFECTS OF SHOCK-INDUCED DEFECTS ON FLUX PINNING IN YBa2Cu3O(7-DELTA)
S. T. Weir, W. J. Nellis, E. A. Early, C. L. Seaman, and M. B. Maple (California Univ., San Diego.) Aug. 1989 3 p Presented at the International Conference on Materials and Mechanisms of Superconductivity - High-Temperature Superconductors, Stanford, CA, 23-28 Jul. 1989
(Contract W-7405-eng-48)
(DE90-000824; UCRL-101900; CONF-890718-30) Avail: NTIS HC A01/MF A01

A composite specimen of YBa2Cu3O(7-delta) and silver was fabricated by shock-compacting to 167 kbar a mixture of YBa2Cu3O(7-delta) and silver powders. The magnetic flux pinning energy of this specimen was then measured as a function of temperature using flux relaxation data obtained with a SQUID magnetometer. Our results show that the pinning energy of the shock-compacted sample is significantly higher than the pinning energy of the YBa2Cu3O(7-delta) before compaction. The increase in flux pinning energy is presumably due to the introduction of shock-induced defects into the YBa2Cu3O(7-delta). This result is significant because higher pinning energies imply higher intragranular critical currents. DOE

N90-14960# Lawrence Livermore National Lab., CA.
SHOCK-INDUCED DEFECTS AND FLUX PINNING IN YBa2Cu3O SUB 7-DELTA + Ag COMPOSITES
S. T. Weir, W. J. Nellis, M. J. Kramer, C. L. Seaman, E. A. Early, and M. B. Maple (California Univ., San Diego.) Aug. 1989 5 p Presented at the American Physical Society Topical Conference on Shock Compression of Condensed Matter, Albuquerque, NM, 14-17 Aug. 1989
(Contract W-7405-eng-48)
(DE90-000827; UCRL-101904; CONF-890812-58) Avail: NTIS HC A01/MF A01

A composite specimen of YBa2Cu3O(7-delta) and silver was fabricated by shock-compacting to 167 kbar a mixture of YBa2Cu3O(7-delta) powder and 30 percent volume silver powder. The recovered sample was then studied with Transmission Electron Microscopy (TEM), and the amount of magnetic flux pinning exhibited by the YBa2Cu3O(7-delta) component was determined with a SQUID magnetometer. We find that the shock process resulted in a large increase in the flux pinning energy of the sample. This result is significant because higher pinning energies imply higher intragranular critical currents. DOE

N90-14961# Argonne National Lab., IL. Energy and Environmental Systems Div.
APPLICATIONS OF SUPERCONDUCTOR TECHNOLOGIES TO TRANSPORTATION
D. M. Rote, J. S. Herring (Idaho National Engineering Lab., Idaho Falls.), and T. P. Sheahen Jun. 1989 92 p
(Contract W-31-109-eng-38)
(DE90-000856; ANL/CNSV-68) Avail: NTIS HC A05/MF A01

This report assesses transportation applications of superconducting devices, such as rotary motors and generators, linear synchronous motors, energy storage devices, and magnets. Among conventional vehicles, ships appear to have the greatest potential for maximizing the technical benefits of superconductivity, such as smaller, lighter, and more-efficient motors and, possibly, more-efficient generators. Smaller-scale applications include motors for pipeline pumps, all-electric and diesel-electric locomotives, self-propelled rail cars, and electric highway vehicles. For diesel-electric locomotives, superconducting units would eliminate space limitations on tractive power. Superconducting magnetic energy storage devices appear most suitable for regenerative braking or power assistance in grade climbing, rather than for long-term energy storage. With toroidal devices (especially for onboard temporary energy storage), external fields would be eliminated. With regard to new vehicle technologies, the use of superconducting devices would only marginally enhance the benefits of inductive-power-coupled vehicles over conventional electric vehicles, but could enable magnetically levitated (maglev) vehicles to obtain speeds of 520 km/h or more. This feature, together with the quiet, smooth ride, might make maglev vehicles an attractive alternative to intercity highway-vehicle or airlane trips in the range of 100 to 600 miles. Electromagnetic airport applications are not yet feasible. DOE

N90-14962# Sandia National Labs., Albuquerque, NM.
THE EFFECTS OF HEAVY PARTICLE RADIATION ON SEMICONDUCTOR DEVICES
James E. Gover 1989 10 p Presented at the Japan Atomic Energy Research Institute Symposium, Takasaki, Japan, 6-10 Nov. 1989
(Contract DE-AC04-76DP-00789)
(DE90-001679; SAND-89-2539C; CONF-8911103-1) Avail: NTIS HC A02/MF A01

Heavy particle radiation can produce upsets in digital circuits as well as trigger burn out or breakdown in power MOSFETs and MNOS nonvolatile memories. Latch-up may also be stimulated by heavy ions. Work done on the effects of heavy particle radiation on PN junctions, CMOS inverters, CMOS latch, MOSFET and non-volatile memories is covered. DOE

N90-14963# Edgerton, Germeshausen and Grier, Inc., Idaho Falls, ID.
DISSIPATION MEASUREMENT IN HIGH T(SUB c) SUPERCONDUCTORS WITH ELECTROMAGNETIC PROBES
K. L. Telschow and T. K. OBrien (Idaho State Univ., Pocatello.) 1989 8 p Presented at the Conference on Review of Progress in Quantitative NDE, Brunswick, ME, 23-28 Jul. 1989
(Contract DE-AC07-76ID-01570)
(DE90-002058; EGG-M-89153; CONF-890770-5) Avail: NTIS HC A02/MF A01

The new ceramic superconducting materials, which have transition temperatures above that of liquid nitrogen, have great potential. However, most fabrication schemes produce consolidated forms with relatively low critical currents; successful application of these materials requires a means of measuring their critical parameters (such as critical current) that can be used to monitor and control fabrication processes. A technique is described for measuring the onset of dissipation in a superconducting coating in a local and noncontacting manner. This work begins the process of developing noncontacting techniques for the measurement of critical currents on a local scale with the capability of providing spatial information. DOE

N90-14964# Argonne National Lab., IL. Materials Science Div.
THEORY OF THE ENERGETICS AND NONCLASSICAL NUCLEATION FOR MARTENSITIC TRANSFORMATIONS FROM PARTIALLY SOFT LATTICE MODES
S.-K. Chan Jul. 1989 8 p Presented at the International Conference on Martensitic Phase Transformations (ICOMAT-89), Sydney, Australia, 3-7 Jul. 1989
(Contract W-31-109-eng-38)
(DE90-002182; CONF-8907114-3) Avail: NTIS HC A02/MF A01

A nonclassical approach to the energetics and nucleation in martensitic transformations has been developed, based on the concept of partial softening of lattice modes and the use of continuum mechanics. It is shown that from an expansion of the free energy density in powers of symmetry-adapted strains, the nature of the instability and the degree of asymmetry of supercooling and superheating can be explained in terms of the temperature dependence of some elastic constants. It is further shown that by including spatial gradients, the critical radius of nucleation as a function of temperature and of compressive and shear stresses can be obtained. DOE

N90-14965# Argonne National Lab., IL. Materials and Components Technology Div.
THE EFFECT OF COMPOSITION AND PROCESSING ON HIGH T(SUB c) SUPERCONDUCTORS CONTAINING BISMUTH
A. S. Nash (Marquette Univ., Milwaukee, WI.), K. C. Goretta, and Roger B. Poeppel Jun. 1989 15 p Presented at the Powder Metallurgy Conference, San Diego, CA, 11-14 Jun. 1989
(Contract W-31-109-eng-38)
(DE90-002203; CONF-8906119-4) Avail: NTIS HC A03/MF A01

The effect of doping and fabrication parameters on the transition temperature and structure of high-T(sub c) Bi-Sr-Ca-Cu oxide superconducting compounds doped with silver and SnO(sub 2) were studied. It was found that SnO(sub 2) lowers the melting point of 4336 producing single-phase high-T(sub c) superconductor at low levels of doping and firing temperatures, 750 to 825 C. The semiconducting behavior observed in samples fired at higher temperatures is attributed to the loss of oxygen in copper-oxide sheets. The effect of level of doping and firing temperature on T(sub c) and structure of Bi-based superconductors beyond the range discussed in this paper are under further investigation. DOE

N90-14966# Argonne National Lab., IL.
CHARGE TRANSFER AND BOND LENGTHS IN YBa2Cu(SUB 3-x)M(SUB x)O(SUB 6+y)
J. D. Jorgensen, J. J. Rhyne, D. A. Neumann, P. F. Miceli, J. M. Tarascon, L. H. Greene, and P. Barboux 1989 8 p Presented at the 13th Particle Accelerator Conference, Chicago, IL, 20-23 Mar. 1989
(Contract W-31-109-eng-38)
(DE90-002241; CONF-890335-269) Avail: NTIS HC A02/MF A01

We discuss the effects of doping on the Cu chain sites in YBa(sub 2)Cu(sub 3-x)M(sub x)O(sub 6+y). The relationship between bond lengths obtained from neutron scattering and charge transfer is evaluated in terms of bond valence. In particular, it is concluded that removing an oxygen from the chains transfers one electron to the planes. DOE

N90-14967# Argonne National Lab., IL. Materials Science Div.
POWDER NEUTRON DIFFRACTION STUDY OF THE STRUCTURAL PHASE DIAGRAM OF THE Ba(SUB 1-x)K(SUB x)BiO3 SYSTEM
S. Y. Pei, J. D. Jorgensen, D. G. Hinks, B. D. Dabrowski, D. R. Richards, A. W. Mitchell, S. K. Sinha, D. Vaknin, J. M. Newsam, and A. J. Jacobson (Exxon Research and Engineering Co., Annandale, NJ.) Jul. 1989 9 p Presented at the Conference on Oxygen Disorder Effects in High T(sub c) Superconductors, Trieste, Italy, 18-21 Apr. 1989
(Contract W-31-109-eng-38)
(DE90-002264; CONF-890480-3) Avail: NTIS HC A02/MF A01

In this article we present a brief report of recent work carried out to elucidate the phase diagram of the Ba(sub 1-x)K(sub x)BiO(sub 3) system. A full account of this investigation will be published shortly. The recently discovered high-T(sub c) superconductor Ba(sub 1-x)K(sub x)BiO(sub 3) is unique in the sense that unlike the other high-T(sub c) superconductors, it does not contain CuO(sub 2) planes and is cubic rather than layered in structure. It does, however, exhibit a series of structural phase transitions as a function of both K concentration x and temperature. Superconductivity occurs only in a cubic phase and disappears abruptly at x (le) 0.4 where the behavior apparently becomes non-metallic. Few details have been available hitherto of the structural phases found as x is decreased, and some of the reported results are not consistent with each other. The present measurements were carried out on the H4S triple axis spectrometer at Brookhaven's High Flux Reactor and on the Special Environment Powder Diffractometer (SEPD) at Argonne's Intense Pulsed Neutron Source. DOE

N90-14968# Los Alamos National Lab., NM.
MICROWAVE CHARACTERIZATION OF HIGH-TEMPERATURE SUPERCONDUCTORS
D. W. Cooke, E. R. Gray, P. N. Arendt, J. G. Beery, B. L. Bennett, D. R. Brown, R. J. Houlton, M. S. Jahan, A. J. Klapetzky, and M. A. Maez et al 1989 12 p Presented at the Conference on Monitoring and Control of Plasma-Enhanced Processing and Multichamber Growth of Semiconductors, Santa Clara, CA, 8-13 Oct. 1989
(Contract W-7405-eng-36)
(DE90-002408; LA-UR-89-3616; CONF-891090-1) Avail: NTIS HC A03/MF A01

Thick (10 to 15 (mu)m) Tl-Ba-Ca-Cu-O films have been deposited onto yttria-stabilized zirconia and Ag substrates by d.c.

magnetron sputtering techniques. Direct deposition onto 1 inch diameter yttria-stabilized zirconia yields films with typical 22 GHz surface resistance (R sub s) values of 5.2 plus or minus 2 m(Omega) and 52 (plus minus) 2 m(Omega) at 10 K and 77 K, respectively. For comparison, R sub s of Cu at this same frequency is 10 m(Omega) at 4 K and 22 m(Omega) at 77 K. Tl-Ba-Ca-Cu-O films have also been deposited onto 1 in diameter Ag substrates using Au/Cu, Cu, and BaF sub 2 buffer layers. The lowest R sub s values were obtained on films with a BaF sub 2 buffer layer, typical values being 7.8 plus or minus 2 m(Omega) and 30.6 (plus minus) 2 m(Omega) (measured at 22 GHz) at 10 K and 77 K, respectively. Larger films (1.5 in diameter) with similar R sub s values were prepared using this same technique, demonstrating that the fabrication process can be scaled to larger surface areas. These films are promising for radiofrequency cavity applications because they are thick (50 to 75 times the London penetration depth), have relatively large surface areas, are fabricated on metallic substrates, and have R sub s values that are competitive with Cu at 77 K and are lower than Cu at 4 K. DOE

N90-14969# Los Alamos National Lab., NM.
RF SUPERCONDUCTIVITY RESEARCH AND DEVELOPMENT AT LOS ALAMOS NATIONAL LABORATORY
D. W. Cooke, E. R. Gray, R. J. Houlton, G. P. Lawrence, J. A. McGill, E. Meyer, C. Morris, B. Rusnak, and T. P. Starke 1989 11 p Presented at the 4th Workshop on RF Superconductivity, Tsukuba, Japan, 14-18 Aug. 1989
(Contract W-7405-eng-36)
(DE90-002440; LA-UR-89-3331; CONF-8908145-4) Avail: NTIS HC A03/MF A01

Los Alamos National Laboratory is engaged in two distinct areas of RF superconductivity research and development. One program is devoted to studying the RF properties of high-temperature superconductors (HTS) and assessing their potential for accelerator-cavity applications. Our best results to date have come from YBa sub 2 Cu sub 3 O sub 7 films (0.8 microns) electron-beam deposited onto LaGaO sub 3 substrates. A typical surface resistance value is 0.2 plus or minus 0.1 m(Omega) measured at 22 GHz and 4 K, which is only a factor of 2 to 4 higher than Nb. A second area of RF superconductivity R and D at Los Alamos involves fabricating and testing conventional Nb superconducting RF cavities. Facilities are being constructed for polishing, cleaning, and testing both small (3-GHz) and large (805-MHz) Nb cavities. Much of our effort is being devoted to understanding the proper techniques for welding, cleaning, and handling Nb cavities, to ensure good high-field performance. Nb cavity applications are foreseen in upgrades to LAMPF, compact free-electron lasers, and high-current CW proton linacs. A single 402.5-MHz Nb cavity (in a beam cryostat) is presently being acquired from industry to provide a momentum compactor for the low-energy pion beam at LAMPF. DOE

N90-14970# Oak Ridge National Lab., TN. Solid State Div.
MAGNETIC EXCITATIONS IN THULIUM METAL
J. A. Fernandez-Baca, R. M. Nicklow, and J. J. Rhyne (National Inst. of Standards and Technology, Gaithersburg, MD.) 1989 9 p Presented at the 34th Conference on Magnetism and Magnetic Materials, Boston, MA, 28 Nov. - 1 Dec. 1989
(Contract DE-AC05-84OR-21400)
(DE90-002475; CONF-891117-9) Avail: NTIS HC A02/MF A01

Inelastic neutron scattering measurements were performed on a single crystal specimen of Tm at wavevectors kappa = (1,1, zeta) and (0,0,2 + zeta) (zeta = 0, ... , 1). Most of the measurements were made at T = 5K, where Tm exhibits a seven layer ferrimagnetic-antiphase-domain structure (four moments up, parallel to the c-axis, followed by three moments down). At this temperature the excitation spectra consist of three peaks. The two lower energy excitations were identified as originating from magneto-vibrational scattering from the TA phonon, while the higher energy excitation is magnetic and exhibits only a weak dispersion (between 8.3 and 9.6 meV). At T = 50K, a temperature at which the system exhibits a c-axis sinusoidally modulated structure, the magnetic mode shows significant softening and broadening. The magneto-vibrational scattering vanishes above the Neel temperature (T(sub N) = 58.5K) while the magnetic mode persists at least up to T = 70K. These results suggest that the Hamiltonian in this system is dominated by the crystal-field-anistropy energy, and that the exchange interaction is relatively weak. DOE

N90-14971# International Centre for Theoretical Physics, Trieste (Italy).
A MODEL OF THE ISOTOPE EFFECT OF THE OXIDE SUPERCONDUCTOR
Li-Yuan Zhang (Peking Univ., China) Mar. 1989 7 p Submitted for publication
(DE89-635907; IC-89/21) Avail: NTIS (US Sales Only) HC A02/MF A01

A possible mechanism of producing negative correlation energy centers is proposed. Combining this electronic attractive potential with phonon mediated attractive potential between carriers, the isotope effect exponent of La-Sr-Cu-O system is quantitatively explained. Generally, the isotope effect exponent is smaller than 1/2 in this mechanism. DOE

N90-14972# Instituto de Pesquisas Energeticas e Nucleares, Sao Paulo (Brazil). Departamento de Metalurgia Nuclear.
Bi-Sr-Ca-Cu-O SUPERCONDUCTING CERAMICS
Reginaldo Muccillo, Eliana N. S. Muccillo, Jose Carlos Bressiani, Laercio Gomes, and Spero Penha Morato Feb. 1989 12 p In PORTUGUESE; ENGLISH summary
(DE89-636225; IPEN-PUB-247; ISSN-0101-3084) Avail: NTIS (US Sales Only) HC A03/MF A01

BiSrCaCu2O(x) ceramic samples with a superconducting phase at 107 K were synthesized. The critical temperature was determined by Meissner effect measurements. That same 107 K phase was also detected in the following compounds: Bi2Sr2Ca2Cu3O(x) and Bi3.6Sr2.7Ca2.7Cu4O(x). DOE

N90-14973# International Centre for Theoretical Physics, Trieste (Italy).
MACROSCOPIC PERSISTENT CURRENTS IN HIGH TEMPERATURE CERAMIC SUPERCONDUCTORS
A. G. Saif (Atomic Energy Establishment, Cairo, Egypt) Mar. 1989 8 p Submitted for publication
(DE89-636232; IC-89/49) Avail: NTIS (US Sales Only) HC A02/MF A01

We study the macroscopic persistent currents (PC) in a thick cylindrical shell of ceramic high temperature superconductors (HTS) in the framework of a generalized Ginzburg-Landau theory (GGL), based on the coexistence of antiferromagnetism and superconductivity. It is shown that, in the absence of the applied magnetic field, the PC differ in nature from the current associated with the Meissner effect. Moreover, we found that the maximum PC is greater than the critical PC. This study may serve for further technological progress with HTS. DOE

N90-14974# Argonne National Lab., IL.
MICROSTRUCTURE AND ELECTRICAL PROPERTIES OF BULK HIGH-T(SUB c) SUPERCONDUCTORS
Uthamalingam Balachandran, M. J. McGuire, K. C. Goretta, C. A. Youngdahl, Donglu Shi, S. Danyluk (Illinois Univ., Chicago.), and Roger B. Poeppel Sep. 1989 8 p Presented at the Conference on Superconductivity and Applications, Buffalo, NY, 19-21 Sep. 1989 Submitted for publication
(Contract W-31-109-eng-38)
(DE90-001762; CONF-890971-3) Avail: NTIS HC A02/MF A01

Bulk forms of the superconductors Y-Ba-Cu-O and Bi-Sr-Ca-Cu-O generally have a low critical current density (J sub c). At 77 K in zero magnetic field, values greater than about 10(3) A cm sup minus 2 have seldom been obtained. The most notable exceptions are for melt-textured rods and filaments, for which J sub c values often exceed 10(4) A cm sup minus 2. Values of J sub c approaching 10(4) A cm sup minus 2 have also been reported for wires and tapes processed in Ag tubes. Little information about the microstructures of these composite conductors has emerged. This work was undertaken to examine

the relationships between processing, microstructure, and electrical properties for high-temperature superconductors processed as pellets or Ag-clad tapes. DOE

N90-14975# Argonne National Lab., IL. Materials Science Div.
MAGNETOTRANSPORT STUDIES OF EPITAXIAL Cr THIN FILMS
J. E. Mattson, B. Brumitt, M. B. Brodsky, and J. B. Ketterson (Northwestern Univ., Evanston, IL.) 1989 15 p Presented at the 34th Conference on Magnetism and Magnetic Materials, Boston, MA, 28 Nov. - 1 Dec. 1989 Submitted for publication
(Contract W-31-109-eng-38)
(DE90-001930; CONF-891117-5) Avail: NTIS HC A03/MF A01

The results of transport measurements on epitaxial Cr thin films were reported. The variation of T(sub N) (the Neel transition) with respect to the film thickness is discussed in terms of the stress in the film. In addition, the temperature dependence of the magnetoresistance (MR) and Hall effect for temperatures from 4 K to 150 K are also discussed, with particular attention to the temperature dependence of the non-linear portion of the Hall data. DOE

N90-14976# Argonne National Lab., IL.
IMPROVED PERFORMANCE OF LOW-T(SUB c) SUPERCONDUCTORS FOR DETECTION OF MINIMUM-IONIZING PARTICLES
Alberto Gabutti, K. E. Gray, and R. G. Wagner 1989 13 p Presented at the 3rd International Workshop on Low Temperature Detectors for Neutrinos and Dark Matter, L'Aquila, Italy, 20-23 Sep. 1989
(Contract W-31-109-eng-38)
(DE90-001985; CONF-8909218-1) Avail: NTIS HC A03/MF A01

Conclusive experimental evidence is presented for granular aluminum films to support the previous conjecture that practical detectors of minimum-ionizing particles (mips) will greatly benefit from, and most probably require, superconducting transition temperatures, T(sub c), closer to a low operating temperature. These measurements have verified the detection of a continuous spectrum of charged particles which deposit energy in a range extending up to a few times larger than mips. The important advantage of low-T(sub c) materials is that the strips can be wider, thus avoiding the inevitable nonuniformities which become particularly bothersome in practical devices requiring lengths of order 1 cm and sub-micron widths. The measurements indicate the same sensitivity in a 2 micrometers wide g-Al strip as a 0.2 micrometer Nb strip, and calculations confirm this. In addition, the effect of normal state resistivity, rho(sub n), of the superconducting material was established using an x ray source. DOE

N90-14977# Argonne National Lab., IL. Materials Science Div.
MAGNETIC AND ELECTRICAL PROPERTIES
M. B. Brodsky and J. E. Mattson Aug. 1989 26 p Presented at the American Crystallographic Association Annual Meeting, Seattle, WA, 23-29 Jul. 1989
(Contract W-31-109-eng-38)
(DE90-002183; CONF-890771-5) Avail: NTIS HC A03/MF A01

The development of controlled growth of monolayers and thin metallic films has led to a number of studies in which the magnetic and electrical properties are modified by interfaces. Cases are considered where the property modifications are caused by structural changes driven by the interfaces. Types of systems to be considered include free surfaces, thin layers, film sandwiches and superlattices. As is shown, there are often observed property changes where the underlying, structural change is not clearly delineated. The literature is extensive and only a sample is given. DOE

N90-14978# Lawrence Livermore National Lab., CA.
MICRO-SCALE SIMULATION OF DYNAMIC COMPACTION OF OXIDE AND METAL POWDER MIXTURE
M. Kamegai, Otis R. Walton, and A. G. Taylor 2 Oct. 1989 11 p Presented at the American Physical Society Topical Conference on Shock Compression of Condensed Matter, Albuquerque, NM, 14-17 Aug. 1989
(Contract W-7405-eng-48)
(DE90-002220; UCRL-100792; CONF-890812-60) Avail: NTIS HC A03/MF A01

Many features of the dynamic compaction of powders are potentially favorable for use in processing high T(sub c) oxide superconductors. Conventional sintering methods tend to produce unwanted impurities, voids, and oxygen-deficient grain boundaries and have, thus, failed to form bulk oxide superconductors with high critical current. One proposed approach for a dynamic process is to compress a mixture of high purity single crystallite particles and fine silver particles. Computer modeling of dynamic compaction has thus far been limited to bulk simulation of the process by continuum mechanics codes. Results of compaction experiments are not reliably predicted with such techniques because the micro-scale dynamics of powder compaction are only modeled by phenomenological approximation. A micro-scale simulation technique was developed and applied to computer models similar to those of molecular dynamics, which were originally designed to simulate the flow behavior of inelastic, frictional particles. In this method, the oxide grain is represented by a nearly elastic sphere while an individual silver grain is modeled by an aggregate of effective inelastic-frictional particles bound by a prescribed interparticle force. The first 2-D simulation results for a simple configuration (a single aggregate silver grain crushed between two nearly elastic ceramic spheres) are compared with the continuum calculations for the same configuration. This micro-scale simulation technique can be extended to study an assembly of dissimilar grains in 3-D space. DOE

N90-14979# Argonne National Lab., IL. Materials Science Div.
ANISOTROPY OF OXYGEN TRACER DIFFUSION IN YBa2Cu3O7-DELTA SINGLE CRYSTALS
S. J. Rothman, J. L. Routbort, J.-Z. Liu, J. W. Downey, L. J. Thompson, Y. Fang, Donglu Shi, J. E. Baker, J. P. Rice, and D. M. Ginsberg (Illinois Univ., Urbana.) et al Sep. 1989 13 p Presented at the Symposium on Atomic Migration and Defects in Materials, Indianapolis, IN, 1-5 Oct. 1989 Submitted for publication
(Contracts W-31-109-eng-38; DE-AC02-76ER-01198)
(DE90-001931; CONF-8910273-1) Avail: NTIS HC A03/MF A01

The crystal structure of YBa sub 2 Cu sub 3 O sub 7- delta strongly suggests that the diffusion of oxygen in this material will be highly anisotropic, with diffusion in the ab plane being much faster than diffusion parallel to the c axis, and this has been assumed in most analyses of diffusion in YBa sub 2 Cu sub 3 O sub 7- delta. The present data confirm this hypothesis; the diffusion coefficient in the ab plane is several orders of magnitude greater than the diffusion coefficient along the c axis. Some interesting artifacts of the measurement, due to this strong anisotropy, are also revealed. Oxygen exchange in polycrystalline samples of YBa sub 2 Cu sub 3 O sub 7- delta is discussed in terms of these results. DOE

N90-14980# Argonne National Lab., IL. Materials Science Div.
SURFACE MAGNETO-OPTICAL STUDIES OF ULTRATHIN FERROMAGNETIC FILMS
C. Liu and S. D. Bader May 1989 14 p Presented at the 2nd International Workshop on the Magnetic Properties of Low-Dimensional Systems, San Luis Potosi, Mexico, 22-26 May 1989 Submitted for publication
(Contract W-31-109-eng-38)
(DE90-002199; CONF-8905188-2) Avail: NTIS HC A03/MF A01

The surface magneto-optic Kerr effect is used to study the existence of monolayer magnetism and the surface magnetic anisotropy of epitaxial films of Fe deposited on Cu(100), Ru(0001), and Pd(100). The critical behavior of Fe/Pd(100) is also characterized and found to be in agreement with 2-D Ising-model results. DOE

N90-14981# Argonne National Lab., IL. Materials Science Div.
QUASICRYSTALS AND GRAIN BOUNDARIES
N. Rivier Jul. 1989 20 p Presented at the 3rd International Meeting on Quasicrystals: Incommensurate Structures in Condensed Matter, Vista Hermosa, Mexico, 29 May - 2 Jun. 1989
(Contract W-31-109-eng-38)
(DE90-002213; CONF-8905239-1) Avail: NTIS HC A03/MF A01

Recent experimental and theoretical evidence suggests that grain boundaries are quasiperodic structures made of inflatable sequences of structural units. A general grain boundary is a grid of dislocations with the same inflation multiplier (a quadratic irrational) in every direction. Structural units are defined topologically as screw or edge dislocation lines on the boundary. Inflation is a geometrical and arithmetic operation expanding a finite sequence of topological units into a longer one. The structure has inflation symmetry if the same operation is repeated. Whereas inflation generalizes translation symmetry of classical crystallography, a direct product of inflatable sequences forms a tiling which realizes rotation symmetry. The two symmetries are compatible for only a few distinct patterns, up to affinities. Bulk quasicrystalline particles can grow on some grain boundaries, suggesting that quasicrystals are structures of minimal free energy under specific, but not common boundary conditions. DOE

N90-14982# Los Alamos National Lab., NM.
DYNAMICAL SIMULATION OF DISLOCATION MICROSTRUCTURE
A. Gulluglo, D. J. Srolovitz (Michigan Univ., Ann Arbor.), R. LeSar, and P. S. Lomdahl 1989 11 p Presented at the TMS Meeting on Simulation and Theory of Evolving Microstructures, Indianapolis, IN, Oct. 1989
(Contract W-7405-eng-36)
(DE90-003192; LA-UR-89-3721; CONF-8910304-1) Avail: NTIS HC A03/MF A01

We report the development of a computer simulation technique to model the motion of a large number of mutually interacting dislocations under the influence of an applied stress. The dislocation motion is simulated using a method akin to molecular dynamics except that dislocation coordinates are employed instead of atomic coordinates. The formation of dislocation substructure is studied as a function of applied stress and density and the resulting spatial distribution of dislocations is analyzed. DOE

N90-14983# Los Alamos National Lab., NM.
THE INFLUENCE OF THE SUBSTRATE SURFACE ON THE NUCLEATION AND GROWTH OF SUPERCONDUCTING THIN FILMS
Soumendra Nath Basu, Nicole Bordes, Anthony D. Rollett, Michael R. Cohen, and Michael Nastasi 1989 5 p Presented at the Materials Research Society Fall Meeting, Boston, MA, 27 Nov. - 2 Dec. 1989
(Contract W-7405-eng-36)
(DE90-003649; LA-UR-89-4010; CONF-891119-14) Avail: NTIS HC A01/MF A01

The quality of epitaxially grown superconducting thin films is dependent on the nature of the substrate surface. In this study, the surface of a group of zone axes (100) oriented SrTiO3 single crystals was modified by mechanical polishing, thermal annealing and chemical etching. A study of the YBa2Cu3O(7-x) thin films grown on these substrates showed that high quality superconducting films were obtained when the substrate surface was highly oriented in the group of zone axes (100) direction and was also microscopically smooth. DOE

77 THERMODYNAMICS AND STATISTICAL PHYSICS

Includes quantum mechanics; theoretical physics; and Bose and Fermi statistics.

For related information see also *25 Inorganic and Physical Chemistry* and *34 Fluid Mechanics and Heat Transfer.*

N90-14984# Gosudarstvennyi Komitet po Ispolzovaniyu Atomnoi Energii, Obninsk (USSR). Fiziko-Ehnergeticheskij Inst.
SEMI-EMPIRICAL THEORY OF HEAT-TRANSFER WHEN BOILING
A. P. Sapankevich 1988 11 p In RUSSIAN
(DE89-635418; FEI-1956) Avail: NTIS (US Sales Only) HC A03/MF A01

A semi-empirical model of heat-transfer when boiling based on simultaneous and indepenent (physically) existence of two mechanisms of heat transfer: convection and evaporation - during boiling is described. Intensity of convective heat exchange is characterized by the heat exchange coefficient and by temperature head wall-liquid, and quantity of heat rate to evaporate is determined by mass flow of evaporated liquid, which depends on the value of mass transfer coefficient and liquid moving head. DOE

80 SOCIAL SCIENCES (GENERAL)

Includes educational matters.

No abstracts in this category.

81 ADMINISTRATION AND MANAGEMENT

Includes management planning and research.

N90-14985*# Howard Univ., Washington, DC. School of Engineering.
A DYNAMIC SYSTEMS ENGINEERING METHODOLOGY RESEARCH STUDY. PHASE 2: EVALUATING METHODOLOGIES, TOOLS, AND TECHNIQUES FOR APPLICABILITY TO NASA'S SYSTEMS PROJECTS
Arthur S. Paul, Tepper L. Gill, and Arlene P. Maclin 10 Oct. 1989 145 p
(Grant NAG5-995)
(NASA-CR-181319; NAS 1.26:181319) Avail: NTIS HC A07/MF A01 CSCL 05A

A study of NASA's Systems Management Policy (SMP) concluded that the primary methodology being used by the Mission Operations and Data Systems Directorate and its subordinate, the Networks Division, is very effective. Still some unmet needs were identified. This study involved evaluating methodologies, tools, and techniques with the potential for resolving the previously identified deficiencies. Six preselected methodologies being used by other organizations with similar development problems were studied. The study revealed a wide range of significant differences in structure. Each system had some strengths but none will satisfy all of the needs of the Networks Division. Areas for improvement of the methodology being used by the Networks Division are listed with recommendations for specific action. J.P.S.

N90-14986*# Houston Univ., Clear Lake, TX. Research Inst. for Computing and Information Systems.
DEVELOPING INTEGRATED PARAMETRIC PLANNING MODELS FOR BUDGETING AND MANAGING COMPLEX PROJECTS
Vance A. Etnyre and Ken U. Black 18 Apr. 1988 13 p

(Contract NCC9-16)
(NASA-CR-186006; NAS 1.26:186006; RICIS-IM-7) Avail: NTIS HC A03/MF A01 CSCL 05A

The applicability of integrated parametric models for the budgeting and management of complex projects is investigated. Methods for building a very flexible, interactive prototype for a project planning system, and software resources available for this purpose, are discussed and evaluated. The prototype is required to be sensitive to changing objectives, changing target dates, changing costs relationships, and changing budget constraints. To achieve the integration of costs and project and task durations, parametric cost functions are defined by a process of trapezoidal segmentation, where the total cost for the project is the sum of the various project cost segments, and each project cost segment is the integral of a linearly segmented cost loading function over a specific interval. The cost can thus be expressed algebraically. The prototype was designed using Lotus-123 as the primary software tool. This prototype implements a methodology for interactive project scheduling that provides a model of a system that meets most of the goals for the first phase of the study and some of the goals for the second phase. J.P.S.

82 DOCUMENTATION AND INFORMATION SCIENCE

Includes information management; information storage and retrieval technology; technical writing; graphic arts; and micrography.

For computer documentation see *61 Computer Programming and Software.*

N90-14987# Lister Hill National Center for Biomedical Communications, Bethesda, MD. Communications Engineering Branch.
DOCUMENT PRESERVATION BY ELECTRONIC IMAGING. VOLUME 1: SYNOPSIS
George R. Thoma, F. L. Walker, Susan E. Hauser, and Michael J. Gill Apr. 1989 32 p
(PB89-226526) Avail: NTIS HC A03/MF A01 CSCL 05B

A research and development program which investigates the applicability of digital electronic imaging (EI) and the storage on digital optical WORM disks to the problem of document preservation is examined. Volume 1 is the synopsis. It consists of a brief history and background of the program; a list of the attributes an EI system for document preservation should possess; a system description; a summary of findings; and major conclusions and recommendations. Author

N90-14988# Lister Hill National Center for Biomedical Communications, Bethesda, MD. Communications Engineering Branch.
DOCUMENT PRESERVATION BY ELECTRONIC IMAGING. VOLUME 2: SYSTEM AND EXPERIMENT DESCRIPTION
George R. Thoma, F. L. Walker, Susan E. Hauser, and Michael J. Gill Apr. 1989 182 p
(PB89-226534) Avail: NTIS HC A09/MF A02 CSCL 05B

A research and development program which investigates the applicability of digital electronic imaging and storage on digital optical WORM disks to the problem of document perservation is examined. Volume 2 consists of technical descriptions of the prototype Document Conversion System (DCS), its constituent workstations, and the experiments using it as a test bed to investigate the role of EI in preservation. The DCS is described as is the preservation experiments and findings related to design, performance, and cost. A discussion is given of the key stages of document conversion: document capture, quality control and archiving (transfer to optical media), along with a description of the workstation, both hardware and software, needed to implement the three stages. Automated access is also discussed. Author

N90-14989# Lister Hill National Center for Biomedical Communications, Bethesda, MD. Communications Engineering Branch.
DOCUMENT PRESERVATION BY ELECTRONIC IMAGING. VOLUME 3: APPENDICES
Susan E. Hauser, F. L. Walker, Michael J. Gill, and George R. Thoma Apr. 1989 54 p In Journal On Selected Areas In Communications (IEEE) v. 7, no. 2, Feb. 1989
(PB89-226542) Avail: NTIS HC A04/MF A01 CSCL 05B

A research and development program which investigates the applicability of digital electronic imaging and storage on digital optical WORM disks to the problem of document preservation is examined. Volume 3 is a collection of appendices describing the image communications systems used, a review of commercially available systems for electronic document storage and retrieval, and other supporting materials. Author

N90-14990# National Agricultural Library, Beltsville, MD.
PROCEEDINGS OF THE CONFERENCE ON APPLICATION OF SCANNING METHODOLOGIES IN LIBRARIES
Donald L. Blamberg, ed., Carol Dowling, ed., and Claudia V. Weston, ed. 1989 143 p Conference held in Beltsville, MD, 17-18 Nov. 1988
(PB89-233415) Avail: NTIS HC A07/MF A01 CSCL 05B

The volume of proceedings contains previously unpublished papers presented during the Conference on Application of Scanning Methodologies in Libraries. The conference, held on 17 and 18 November 1988, at the National Agricultural Library in Beltsville, Maryland, focused on current projects and techniques using scanning and optical character recognition technologies in the library and information community. The aim of the conference was to provide a forum through which librarians and information professionals could learn the advantages and disadvantages of this emerging technology, gaining knowledge which could open the door to potential applications in their own institutions. Author

N90-14991 Massachusetts Univ., Amherst.
THE DESIGN AND IMPLEMENTATION OF AN INTELLIGENT INTERFACE FOR INFORMATION RETRIEVAL Ph.D. Thesis
Roger Howard Thompson 1989 227 p
Avail: Univ. Microfilms Order No. DA8917411

Commercial information (text) retrieval systems have been available since the early 1960's. While they have provided a service allowing individuals to find useful documents out of the millions of documents contained in online databases, there are a number of problems that prevent the user from being more effective. The primary problems are an inadequate means for specifying information needs, a single way of responding to all users and their information needs, and an inadequate user interface. Described here is the design and implementation of I3R, an intelligent interface for information retrieval, the purpose of which is to overcome the limitations of current information retrieval systems by providing multiple ways of assisting the user to precisely specify his information need and to search for information. The system organization is based on a blackboard architecture and consists of a number of experts that work cooperatively to assist the user. The operation of the experts is coordinated by a control expert that makes its decisions based on a plan derived from the analysis of human search intermediaries, end user dialogues, and user model. The experts provide multiple formal search strategies, the use and collection of domain knowledge and browsing assistance. The operation of the system is demonstrated by four scenarios. Author

N90-14992# National Technical Information Service, Springfield, VA. Office of International Affairs.
ACCESSING JAPANESE TECHNICAL INFORMATION: A GROUP OF ESSAYS EXTRACTED FROM THE NTIS (NATIONAL TECHNICAL INFORMATION SERVICE) DIRECTORY OF JAPANESE TECHNICAL RESOURCES IN THE UNITED STATES FOR 1987 AND 1988
1989 70 p
(PB90-100165) Avail: NTIS HC A04/MF A01 CSCL 05B

Each year, NTIS produces a directory of Japanese technical information resources in the U.S. In addition to the actual directory sections of the publication, every annual edition contains a series of essays concerning various aspects of access to Japanese technical information. These essays are presented which originally appeared in the out of print 1987 and 1988 editions of the directory. Topics include: A comparison of infrastructures for technology transfer that exist in Japan and the U.S.; A private sector view on how the U.S. Government can work with industry to make Japanese S and T information more accessible and available in the U.S.; Barriers to accessing Japanese S and T information; Impressions of America's readiness to take advantage of Japan's technology; and The status of machine aided translation projects in the U.S., Japan and Europe. Author

N90-14993# Assistant Secretary of Defense (Public Affairs), Washington, DC.
DOD (DEPARTMENT OF DEFENSE) FREEDOM OF INFORMATION ACT PROGRAM (INCORPORATING CHANGES 1 AND 2)
C. Talbott Jul. 1989 84 p
(PB90-104753; DOD-5400.7-R) Avail: NTIS HC A05/MF A01 CSCL 05B

The regulation provides policies and procedures for the DOD implementation of the Freedom of Information Act, as amended by the Freedom of Information Reform Act of 1986. Due to its size and complexity, there is no central repository for DOD records. Consequently, the military departments and separate defense agencies operate their own Freedom of Information programs under the policy guidance set forth by the Regulation. The addresses of the military departments and separate defense agencies are in Appendix B; requests for their records should be forwarded to the respective department or agency. Author

N90-14994# National Inst. of General Medical Sciences, Bethesda, MD.
NOMENCLATURE FOR PHYSICAL MAPPING OF COMPLEX GENOMES
Aug. 1989 12 p Presented at the Conference on Nomenclature for Physical Mapping of Complex Genomes, Rockville, MD, 13-14 Apr. 1989 Prepared in cooperation with DOE, Washington, DC and California Univ., San Francisco
(DE89-015173; CONF-8904252-Summ) Avail: NTIS HC A03/MF A01

Among these issues, that of establishing nomenclature conventions, was seen to be fundamental to the development of useful data management systems and essential for the orderly and efficient development of such systems. Therefore, the present workshop was convened, as the first in the recommended series, to identify the issues involved in establishing nomenclature standards and to develop a set of recommendations for such standards. This report summarizes the proceedings of the workshop and lays out specific proposals for naming DNA entities for physical mapping. The scientific community should discuss and develop these proposals so that naming conventions can be established. The proposals apply specifically to human DNA entities; however, the relevance to nomenclature in other systems should be part of the broader discussion. DOE

N90-14995*# Jet Propulsion Lab., California Inst. of Tech., Pasadena.
PUBLICATIONS OF THE JET PROPULSION LABORATORY, 1988
15 Dec. 1989 32 p
(NASA-CR-185956; JPL-Bibl-39-30; NAS 1.26:185956) Avail: NTIS HC A03/MF A01 CSCL 05B

This bibliography describes and indexes by primary author the externally distributed technical reporting, released during calendar year 1988, that resulted from scientific and engineering work performed, or managed, by the Jet Propulsion Laboratory. Three classes of publications are included: JPL publications in which the information is complete for a specific accomplishment; articles from the quarterly Telecommunications and Data Acquisition (TDA) Progress Report; and articles published in the open literature. Author

83 ECONOMICS AND COST ANALYSIS

Includes cost effectiveness studies.

No abstracts in this category.

84 LAW, POLITICAL SCIENCE AND SPACE POLICY

Includes NASA appropriation hearings; aviation law; space law and policy; international law; international cooperation; and patent policy.

No abstracts in this category.

85 URBAN TECHNOLOGY AND TRANSPORTATION

Includes applications of space technology to urban problems; technology transfer; technology assessment; and surface and mass transportation.

For related information see also *03 Air Transportation and Safety, 16 Space Transportation,* and *44 Energy Production and Conversion.*

No abstracts in this category.

88 SPACE SCIENCES (GENERAL)

N90-14996# National Academy of Sciences - National Research Council, Washington, DC.
AN INTERNATIONAL DISCUSSION ON RESEARCH IN SOLAR AND SPACE PHYSICS
1983 37 p Presented at the Workshop on Solar and Space Physics, Hilton Head, SC, 20-23 Sep. 1983
Avail: NTIS HC A03/MF A01

This report is the result of a four-day workshop convened jointly by the U.S. National Academy of Sciences/National Research Council and the European Science Foundation (ESF). Fifty scientists from thirteen nations attended, representing the U.S. Space Science Board (SSB) and the ESF's Space Science Committee (SSC), for the purpose of investigating the prospects for more effective cooperation in research in solar and space physics. Discussions during the workshop concerned: (1) the status of solar and space physics as academic subjects, in order to investigate the potential for the future of these research areas in terms of the training of new scientists; (2) the future plans and programs of National Aeronautics and Space Administration (NASA), European Space Agency (ESA), and several European countries, in order to assess the potential for cooperation in expected research opportunities; and (3) U.S./European cooperation in terms of past successes and problems. Much of the discussion concerned the differences between the U.S. and European systems in the planning of space programs, initiating missions, and selecting and developing experiments. It was

recommended that an international solar and space physics program should be established and that it should be constructed from currently planned missions by ESA and NASA. K.C.D.

N90-14997*# National Aeronautics and Space Administration. Ames Research Center, Moffett Field, CA.
SALTATION THRESHOLDS AND ENTRAINMENT OF FINE PARTICLES AT EARTH AND MARTIAN PRESSURES
Rodman Leach, Ronald Greeley (Arizona Univ., Tucson.), and James Pollack Nov. 1989 42 p
(Contract NCC2-346)
(NASA-TM-102193; A-89136; NAS 1.15:102193) Avail: NTIS HC A03/MF A01 CSCL 03B

An open circuit wind tunnel designed to operate in a large vacuum chamber was built at NASA-Ames to investigate saltation threshold, flux, deflation rates, and other aeolian phenomena on the planet Mars. The vacuum chamber will operate at pressures as low as 4 mbar, and the tunnel operates at windspeeds as high as 150 m/sec. Either air or CO2 can be used as a working fluid. It was found that, to a first order approximation, the same dynamic pressure was required at Martian pressure to entrain or saltate particles as was required on Earth, although wind and particle speed are considerably higher at Martian pressure. A 2nd wind tunnel, designed to operate aboard the NASA KC-135 0-g aircraft to obtain information on the effect of gravity on saltation threshold and the interparticle force at 0-g, is also described and test data presented. Some of the experiments are summarized and various aspects of low pressure aeolian entrainment for particles 12 to 100 micron in diameter are discussed, some of them unique to low pressure testing and some common in Earth pressure particle transport testing. The facility, the modes of operation, and the materials used are described. Author

N90-14998*# Lunar and Planetary Inst., Houston, TX. Publications Services Staff.
ABSTRACTS FOR THE 52ND ANNUAL MEETING OF THE METEORITICAL SOCIETY
1989 337 p Meeting held in Vienna, Austria, 31 Jul. - 4 Aug. 1989; sponsored by Vienna Univ., Naturhistorisches Museum, Lunar and Planetary Inst. and Ministry of Science and Research, Vienna
(Contract NASw-4066)
(NASA-CR-186160; NAS 1.26:186160; LPI-CONTRIB-712) Avail: NTIS HC A15/MF A02 CSCL 03A

Various topics in meteorology are discussed. These topics include chondrites, chondrule, iron and other minerals, impact cratering, lunar studies, early earth and early solar system processes, rare gases and cosmic dust. J.P.S.

89 ASTRONOMY

Includes radio, gamma-ray, and infrared astronomy, and astrometry.

N90-14999*# Pennsylvania State Univ., University Park. Dept. of Astronomy.
THEORY OF WIDE-ANGLE PHOTOMETRY FROM STANDARD STARS
Peter D. Usher Oct. 1989 108 p
(Grant NAG5-361)
(NASA-CR-185964; NAS 1.26:185964) Avail: NTIS HC A06/MF A01 CSCL 03A

Wide angle celestial structures, such as bright comet tails and nearby galaxies and clusters of galaxies, rely on photographic methods for quantified morphology and photometry, primarily because electronic devices with comparable resolution and sky coverage are beyond current technological capability. The problem of the photometry of extended structures and of how this problem may be overcome through calibration by photometric standard stars is examined. The perfect properties of the ideal field of view are stated in the guise of a radiometric paraxial approximation, in the hope that fields of view of actual telescopes will conform. Fundamental radiometric concepts are worked through before the issue of atmospheric attenuation is addressed. The independence of observed atmospheric extinction and surface brightness leads off the quest for formal solutions to the problem of surface photometry. Methods and problems of solution are discussed. The spectre is confronted in the spirit of standard stars and shown to be chimerical in that light, provided certain rituals are adopted. After a brief discussion of Baker-Sampson polynomials and the vexing issue of saturation, a pursuit is made of actual numbers to be expected in real cases. While the numbers crunched are gathered ex nihilo, they demonstrate the feasibility of Newton's method in the solution of this overdetermined, nonlinear, least square, multiparametric, photometric problem. Author

N90-15000 Manchester Univ. (England).
RADIO AND OPTICAL OBSERVATIONS OF NEARBY ACTIVE GALAXIES Ph.D. Thesis
Brian A. Harrison 1988 247 p
Avail: Univ. Microfilms Order No. BRD-85581

High resolution radio and optical observations of nearby active galaxies are described. The radio observations were obtained using MERLIN, the VLA and the European VLBI network, while the optical observations were obtained using the Isaac Newton Telescope. Detailed observation of the Seyfert galaxy NGC4151 are presented and show that the kiloparsee-scale extended narrow line optical structure appears to be aligned along the same axis as the parsec-scale radio structure. This provides very strong evidence that collimated ejection is occurring in NGC4151 with the collimation taking place on scales less than 1pc (i.e., within the Broad Line Region). MERLIN 408-Hz and 1666-MHz observations of a selection of Seyfert and radio elliptical galaxies are presented and it is shown that the radio emmision in these two classes of active galaxies are similar. These observations are discussed together with detailed (VLBI and VLA) radio and optical observations of the Seyfert galaxy NGC7674 in the context of the various models that have been proposed to account for the radio and optical emission in the Narrow Line Region of active galaxies. Multi-frequency radio observations of the core dominated galaxy NGC1275 are used to determine how the radio jet from the core interacts with the surrounding inter-galactic medium.
Dissert. Abstr.

N90-15001 Manchester Univ. (England).
MERLIN AND VLBI OBSERVATIONS OF THE RADIO GALAXY VIRGO A Ph.D. Thesis
William Junor 1987 386 p
Avail: Univ. Microfilms Order No. BRD-85592

Earth rotation aperture synthesis observations have been made of the nearby radio galaxy Virgo A using the Multiple Element Radio Linked Interferometer Network (MERLIN) and Very Long Baseline Interferometry (VLBI). These data have been used to investigate the physics of the central radio source in this galaxy over a variety of size scales. VLBI observation and data reduction techniques have been extended to produce a high resolution map of the prominent radio jet at a wavelength of lambda 18 cm. The existence of a well-defined, linear feature roughly perpendicular to the jet axis in knot A is confirmed. The morphology of this feature is consistent with an oblique shock in a supersonic jet. VLBI observations show that the jet is collimated with approximately 1 light-month of the nucleus. MERLIN imaging polarimetry at lambda 18 cm has revealed the possible presence of a large-scale screen between the jet and the observer. This is likely to be associated with the extensive radio/x ray halo. Depolarisation in the individual components of the jet (the knots) is shown to be consistent with such a screen.
Dissert. Abstr.

N90-15002 Brandeis Univ., Waltham, MA.
VLA AND VLBI OBSERVATIONS OF CORE DOMINATED QUASARS Ph.D. Thesis
Ronald Ivan Kollgaard 1989 235 p
Avail: Univ. Microfilms Order No. DA8922193

High dynamic range Very Large Array (VLA) observations of the total intensity and linear polarization of 24 powerful, core dominated quasars were made at 5 GHz, as well as the first

milliarsecond linear polarization observations of 3C 273. For ten quasars the resolution of the VLA was sufficient to reveal details of the compact extended emission surrounding the bright cores. The former all exhibit one sided jets, and most show evidence of diffuse haloes. The luminosity of the extended emission is sufficient for those to be Fanaroff-Riley Class 2 radio sources. This interpretation is confirmed by the linear polarization structure of the jets and terminal hotspots. If these quasars are similar to powerful lobe dominated sources but are oriented with jet axes close to the line of sight, the large degrees of polarization observed in the hotspots suggest that they are travelling at speeds upsilon greater than 0.5c. The superluminal quasar 3C 345 was imaged with a variety of resolutions. In spite of the bending on the milliarsecond scale, it was found that the jet of 3C 345 is very straight for the first two seconds and then has two knots which show an abrupt shift in azimuth. The inferred magnetic field in the jet is offset approximately 30 degrees from a perpendicular orientation with respect to the jet axis. This quasar also appears to have a faint counter jet, with the jet/counter jet luminosity ratio suggesting jet speeds of upsilon is greater than 0.56c. There is also an asymmetric diffuse halo. Milliarsecond polarization observations of 3C 345 show that the core (component D) is very weakly polarized. Appreciable polarized flux was detected from five of the superluminal components in the jet, with the fractional polarization increasing with distance from D. Dissert. Abstr.

90 ASTROPHYSICS

Includes cosmology; celestial mechanics; space plasmas; and interstellar and interplanetary gases and dust.

For related information see also *75 Plasma Physics*.

N90-15003 Colorado Univ., Boulder.
PROPERTIES OF EVOLVED STAR CIRCUMSTELLAR GRAINS Ph.D. Thesis
Richard H. Buss, Jr. 1988 226 p
Avail: Univ. Microfilms Order No. DA8912181

The properties of evolved star circumstellar grains were examined by observing M supergiant binaries, carbon star binaries, and post asymptotic giant (AGB) stars with various astronomical observatories and by relying on results of previous investigators of these stars. Ultraviolet, infrared, and visual data, including spectra and photometry were acquired. The grain compositions and grain spectral extinction of an M supergiant were derived, as well as detecting no extinction around other M supergiants. From the infrared emission, it was inferred that some M supergiant binaries had grains and other did not. The grains had similar compositions and structure to those grains around single M supergiants, though the ultraviolet radiation from the hot star in the binaries appeared to suppress or inhibit the formation of grains. Infrared emission also indicated that most binary carbon stars with hot stars had carbonaceous SiC grains similar in structure and amounts to single carbon stars. Yet the ultraviolet radiation, through the photoexcitation of infrared transistions, did reveal the presence of tiny clusters or molecules reminiscent of aromatic hydrocarbons. These binary carbon star micrograins, however, seemed different from interstellar medium micrograins (PAHs) and seemed to diminish in number as the carbon star temperature decreased. The complex post AGB star grains revealed that some interstellar diffuse bands arise from grains different than PAHs and even perhaps from grains different than amorphous carbon. The post AG grains also indicated that the extinction bump does not arise from PAHs nor from some diffuse-band grains nor even perhaps from large hydrocarbon grains. Dissert. Abstr.

N90-15004*# Boston Univ., MA.
METEORITIC BASALTS Final Report, 1986 - 1989
Allan H. Treiman 26 Oct. 1989 27 p
(Grant NAG9-168)
(NASA-CR-185949; NAS 1.26:185949) Avail: NTIS HC A03/MF A01 CSCL 03B

The objectives were to: explain the abundances of siderophile elements in the SNC meteorite suite, of putative Martian origin; discover the magmatic origins and possibly magma compositions behind the Nakhla meteorite, one of the SNC meteorites; and a re-evaluation of the petrology of Angra dos Reis, a unique meteorite linked to the earliest planetary bodies of the solar nebula. A re-evaluation of its petrography showed that the accepted scenario for its origin, as a cumulate igneous rock, was not consistent with the meteorite's textures (Treiman). More likely is that the meteorite represents a prophyritic igneous rock, originally with magma dominant. Studies of the Nakhla meteorite, of possible Martian origin, although difficult, were successful. It became necessary to reject the basic categorization of Nakhla: that is was a cumulate igneous rock. Detailed studies of the chemical zoning of Nakhlas' minerals, coupled with the failure of experimental studies to yield expected results, forced the conclusion that Nakhla is not a cumulate rock in the usual sense: a rock composed of igneous crystals and intercrystal magma. Study of the siderophile element abundances in the SNC meteorite groups involved trying to find reasonable core formation processes and parameters that would reproduce the observed abundances. Modelling was successful, and delimited a range of models which overlap with those reasonable from geophysical constraints. Author

N90-15005 California Inst. of Tech., Pasadena.
EVIDENCE FOR ANOMALOUS COSMIC RAY HYDROGEN Ph.D. Thesis
Eric Richard Christian 1989 185 p
Avail: Univ. Microfilms Order No. DA8915376

The High Energy Telescopes on the Voyager 1 and Voyager 2 spacecraft are used to measure the differential energy spectra of hydrogen and other elements. During the period of minimum solar modulation in 1987, changes in the shape of the hydrogen energy spectra are observed. It is shown that these changes are difficult to explain in the framework of current modulation theory, and are consistent with the emergence of an anomalous cosmic ray (ACR) hydrogen component. ACR hydrogen is predicted by the current theories of anomalous cosmic rays, but this is the first evidence that ACR hydrogen is actually present. Several different estimates of the contribution of ACR hydrogen are used to obtain peak fluxes of 0.33 + or - 0.12 particles/sq m s sr MeV and 0.67 + or - 0.18 particles/sq m s sr MeV for Voyager 1 and Voyager 2 respectively during the time period 1987/209-313. Using a model developed by Cummings and Stone (1987), researchers relate these fluxes of ACR hydrogen and the peak fluxes of ACR helium to the relative abundance of hydrogen and helium, n(H I)/n(He I), in the neutral gas flowing into the solar system from the local values of 3 + or - 1 and 5 + or - for n(HI/n(HeI), which should be compared to the cosmic relaive abundance of approximately 10. Values are consistent with the previous results obtained from solar ultraviolet backscatter experiments, and support the hypothesis that hydrogen is substantially ionized in the very local interstellar medium. Dissert. Abstr.

N90-15006 Illinois Univ., Urbana-Champaign.
A STUDY OF THE INFRARED EMISSION OF GALACTIC SUPERNOVA REMNANTS Ph.D. Thesis
Richard Giles Arendt 1989 250 p
Avail: Univ. Microfilms Order No. DA8916210

The nature of the infrared (IR) emission of supernova remnants (SNRs) was investigated, and this radiation was used to reveal the physical properties of SNRs and the gas and dust contained. The success of the Infrared Astronomical Satellite (IRAS) in 1983 made possible this project. An attempt was made to find the general characteristics of the IR emission of SNRs. A survey of the known galactic SNRs in the IRAS data base was completed. It is found that only one third of the galactic SNRs show detectable IR emission. Many remnants are confused with other galactic IR sources. The youngest SNRs exhibit spectra of relatively warm dust at approximately 90 K. Older SNRs exhibit spectra that indicate dust grains within the SNRs have temperatures spanning a range from approximately 150 to 30 K. Supernova remnants can not be distinguished from other galactic IR sources on the basis of their IR colors alone. The dust within and the IR emission of a single

SNR, Puppis A, are studied. The IR morphology of Puppis A and its environments reveal that the appearance of the SNR is strongly influenced by its interaction with a nearby molecular cloud. Detailed analysis of the IR emission shows that small grains (approximately 10 A) must be present in the SNR to account for this emission observed at 12 and 25 micrometers. There is some evidence of destruction of grains within the SNR. The temperature and density of the gas in which the dust is embedded, and the geometry of the emitting regions are inferred from the IR emission at specific locations across the SNR. Dissert. Abstr.

N90-15007 Rutgers - The State Univ., New Brunswick, NJ.
ULTRAVIOLET PROPERTIES OF HOT STARS IN GLOBULAR CLUSTERS Ph.D. Thesis
Bruce M. Altner 1988 514 p
Avail: Univ. Microfilms Order No. DA8914193

Most of the interesting and important stages of stellar evolution beyond the horizontal branch (HB) occur in the temperature realms best investigated by ultraviolet (UV) astronomy. Studied here are the UV properties of hot HB and post-HB stars found in a sample of galactic globular clusters, based on spectra obtained with the International Ultraviolet Explorer (IUE). Using techniques developed specifically for the purpose, researchers separate the overlapping spectra of individual hot stars in the crowded central regions of the clusters. Researchers determine the physical properties of the separated core sources by comparing them to model stellar atmospheres, Population I standards, faint blue halo stars and previously known UV-bright cluster stars, from which an attempt is made to better understand their evolutionary status.
Dissert. Abstr.

N90-15008 Kent Univ., Canterbury (England).
HYPERVELOCITY IMPACT STUDIES ON THE GIOTTO COMET HALLEY MISSION Ph.D. Thesis
Suzanne Theresa Evans 1988 214 p
Avail: Univ. Microfilms Order No. BRDX85816

Giotto, one of five spacecraft sent to probe comet Halley, carried on-board ten scientific instruments for the purpose of investigating the cometary nucleus, coma and gas and dust emissions. Of these instruments, the Dust Impact Detection System (DIDSY) and the calibration of two of its subsystems are described. The DIDSY microphone sensors rely for their operation on the transfer of momentum from hypervelocity cometary dust particles to the spacecraft shield resulting in the release of acoustic energy. Hypervelocity impact phenomena are discussed, particularly in relation to the low velocity calibration techniques used, namely low velocity microbeads and particles accelerated by a light gas gun; pulsed laser irradiation is considered as a suitable simulation of hypervelocity particle impacts. Following the successful encounter of Giotto with comet Halley in March 1986, some of the preliminary data analysis is presented with emphasis on the larger, discrete particles. Dissert. Abstr.

N90-15009 California Univ., Berkeley.
COOLING FLOWS IN CLUSTERS OF GALAXIES Ph.D. Thesis
Avery Abraham Meiksin 1988 197 p
Avail: Univ. Microfilms Order No. DA8916790

X ray measurements of many clusters of galaxies reveal a hot Intracluster Medium (ICM) that has a cooling time less than a Hubble time. After a review of past and current literature, two tasks are undertaken. The first is to examine the role heat conduction could play. It is demonstrated that the density and temperature profiles of the cooling flows in Virgo and Perseus are consistent with a steady state model in which heat conduction reduces the accretion rates by an order of magnitude. A study of the global stability, however, suggests that such solutions are unlikely to occur. The second task is to simulate the evolution of a cooling flow, and possible formation of a galaxy from thermal instabilities, in a proper cosmological setting. Two evolutionary stages are found, a dynamical accretion state composed of two competing similarity solutions followed by a quasi-steady state cooling flow. Dissert. Abstr.

N90-15010# Arizona State Univ., Tempe.
MOBILITY OF SULFUR IN THERMALLY ALTERED METEORITES Ph.D. Thesis
Thomas Michael Primus 1989 146 p
Avail: Univ. Microfilms Order No. DA8919640

Sulfur and volatile trace element (bismuth, cadmium, and thallium) mobility were studied in Allende (CV3) and Leedey (L6) chondrite samples heated for 1 to 168 hours, at 100 C increments, from 400 to 1000 C in a low pressure environment of hydrogen and oxygen. A vacuum system was constructed to heat samples in an open and closed environment. Three trace elements were determined by direct analysis of solids using electrothermal atomic absorption spectroscopy. Sulfur was determined by either iodometric titration or infrared absorption of sulfur dioxide expelled during inductive heating of samples in an oxygen environment. The sulfur gases released during the heating experiments were also analyzed by gas chromatography to better understand the mechanism of sulfur mobility. Sulfur is very mobile in a low pressure oxygen environment (10 exp -8 power atm) at 650 C. Sulfur is also mobilized in a low-pressure hydrogen environment (10 exp -5 power atm) at 650 C, but to a lesser extent. Ordinary chondrites have a constant sulfur content. They are depleted in sulfur by a factor of two compared to CI chondrites. The results are compared to earlier heating experiments completed by the Purdue group, J. Cripe and J. W. Larimer (1976) and E. K. Gibson, Jr. (1976). The loss of volatile trace elements from ordinary chondrites by simple open system metamorphism is not supported by the results obtained. Dissert. Abstr.

N90-15011 Texas Univ., Austin.
THE INSTABILITY AND FRAGMENTATION OF THE ENVELOPE OF SUPERNOVA 1987A Ph.D. Thesis
Sean Patrick Clancy 1989 213 p
Avail: Univ. Microfilms Order No. DA8920680

The detection of high energy radiation from the SN1987A was observed much earlier than predicted. One possible interpretation of this discrepancy is that the expanding shock front became unstable due to Rayleigh-Taylor modes, thus allowing the radiation to leak out sooner than unperturbed models suggested. To investigate the stability of the expanding shock front within a stellar model, the general purpose 3-D explicit Eulerian self gravitating hydrodynamics code was developed. The code uses explicit operator splitting hydrodynamical equations in cylindrical coordinates with a moving mesh option. Second order monotonic advection terms are used in the equations. The code was tested extensively in numerical calculations, and in numerical simulations of fluid dynamic problems. Numerical investigations on the fluid dynamic phenomena and on the astrophysical problems were explored. Using analytical and numerical initial presupernova models, the expanding shock front was not found to become unstable and fragment within the hydrodynamical timescale for all models, including the more realistic one, considered herein.
Dissert. Abstr.

N90-15012 Texas Univ., Austin.
AS OBSERVATIONAL AND THEORETICAL INVESTIGATION OF STELLAR FLARES Ph.D. Thesis
Suzanne Louise Hawley 1989 169 p
Avail: Univ. Microfilms Order No. DA8920722

Multi-wavelength observations of a giant flare on the star AD Leo were obtained with the 2.1m and 0.9m telescopes at McDonald Observatory and the International Ultraviolet Explorer satellite. The quality, spectral coverage and time resolution of the data represent a major improvement over any published stellar flare data. A self-consistent theoretical model was developed to investigate the effects of chromospheric heating by thermal conduction and soft x ray irradiation from a flare heated corona. Assuming a one-dimensional coronal loop geometry, atmospheres were produced for overlying coronal temperatures of 8, 10, 15, and 20 million degrees Kelvin. The atmospheres satisfy the equations of hydrostatic equilibrium, steady state energy balance, and statistical equilibrium and radiative transfer in many optically thick transitions of hydrogen, ionized calcium and ionized magnesium. A second

theoretical model was then developed to predict the temporal evolution of the coronal temperature under the influence of a time varying flare heating rate. Combining the models, the chromospheric emission model predictions in the hydrogen Balmer lines, Ca II K, Mg II h + k and the optical continuum were compared to the observations, with the result that much of the gradual phase flare emission could be produced by the x ray and conductive heated atmospheres. Dissert. Abstr.

N90-15013 Kent Univ., Canterbury (England).
VERY HIGH RESOLUTION RADIO OBSERVATIONS OF MOLECULAR CLOUD CORES Ph.D. Thesis
B. D. Heaton 1988 213 p
Avail: Univ. Microfilms Order No. BRDX86263

The environments of three young stellar objects are studied by means of molecular line and continuum observations. For each star forming region the distribution of gas has been traced from interstellar dimensions down to solar system sized condensations. Whilst the signposts of star formation are similar in each case, (i.e., the presence of OH and H2O masers, obscured infrared sources, broad CO lines, etc.), the source morphologies are quite different and exceedingly complex. The first region studied, G35.2 to 0.74N, contains probably the finest example of a rotating disc, seen almost edge on. Orthogonal to the disc, high velocity molecular outflow, observed in CO, appears to lie in the plane of the sky. The outflow seems to be driven by a stellar wind manifested as twin beams from the central exciting source. In contrast, the dominant source of molecular line emission from G34.3 + 0.15 is a dense ultracompact core associated with a highly luminous HII region. Spectra observed towards this core show strong evidence of both self absorption and absorption against the continuum at velocities both red and blue shifted with respect to the cloud LSR velocity. A model is proposed in which cold foreground gas collapsing towards the core, and warm gas close to but expanding away from the core, produce the absorption features.
Dissert. Abstr.

N90-15014 Baylor Univ., Waco, TX.
A MODEL OF THE THERMAL AND ELECTRICAL PROPERTIES OF COSMIC DUST PARTICLES Ph.D. Thesis
Phillip Delbert Anz-Meador 1989 292 p
Avail: Univ. Microfilms Order No. DA8918502

A computer model of the electrical and thermal properties of an interplanetary dust particle (IDP) was developed. The IDP is treated as a spherical grain consisting of a matrix material which may incorporate inclusions of a dissimilar material. Finite difference techniques model the heat energy and charge transport. Bulk electrical charge, potential, and temperature are calculated as a function of time. An ensemble of particles are subjected to environments of varying radiation densities, e.g., the Earth's magnetosphere. Results are examined and discussed. Recommendations for further theoretical and experimental work are given. Dissert. Abstr.

N90-15015 Yale Univ., New Haven, CT.
PERTURBATION METHODS FOR THE CALCULATION OF GRAVITATIONAL WAVES FROM SLIGHTLY NON-SPHERICAL SPACETIMES WITH APPLICATIONS TO STELLAR CORE COLLAPSE Ph.D. Thesis
H. Edward Seidel 1988 206 p
Avail: Univ. Microfilms Order No. DA8917729

A method for the calculation of gravitational radiation from perturbations of spherically symmetric, realistic background stellar models is presented. The numerical background hydrodynamic code is based on a scheme developed by May and White, is fully relativistic, and can be used with any equation of state. Special emphasis will be placed on even-parity perturbations, based on the work of Moore, numerical results are presented for dust collapse to a black hole and for stellar collapse models designed to simulate a type II supernova. In this case, researchers find that odd-parity perturbations of such models are capable of radiating up to 10 to the -7th power stellar masses in gravitational radiation energy. For the even-parity perturbations, preliminary results are presented for dust collapse and for stellar collapse models with a polytropic equation of state. The polytropic models do not well represent current supernova models, but they do provide a basis for comparison of the even- and odd-parity perturbations under relativistic conditions in a collapsing star with a polytropic equation of state. For such polytropic stellar models, researchers find that even-parity perturbations are capable of radiating an order of magnitude more in gravitational wave energy than corresponding odd-parity perturbations. Dissert. Abstr.

N90-15016*# California Univ., Berkeley. Center for Particle Astrophysics.
SUPERSYMMETRIC DARK MATTER ABOVE THE W MASS
Kim Griest, Marc Kamionkowski, and Michael S. Turner (Fermi National Accelerator Lab., Batavia, IL.) Nov. 1989 62 p
(Grant NAGw-1340)
(NASA-CR-186168; NAS 1.26:186168; FERMILAB-Pub-89/239-A; CfPA-TH-89-016) Avail: NTIS HC A04/MF A01 CSCL 03B

The cosmological consequences are studied for the minimal supersymmetric extension of the standard model in the case that the neutralino is heavier than W. The cross section was calculated for annihilation of heavy neutralinos into final states containing gauge and Higgs bosons (XX yields WW, ZZ, HH, HW, HZ), where X is the lightest, nth neutralino and the results are compared with the results with those previously obtained for annihilation into fermions to find the relic cosmological abundance for the most general neutralino. The new channels are particularly important for the Higgsino-like and mixed-state neutralinos, but are sub-dominant (to the fermion-antifermion annihilation channels) in the case that the neutralino is mostly a gaugino. The effect of the top quark mass is also considered. Using these cross sections and the cosmological constraint omega(sub X)h squared is less than or approximately 1, the entire range of cosmologically acceptable supersymmetric parameter space is mapped and a very general bound on the neutralino mass is discovered. For a top quark mass of less than 180 GeV, neutralinos heavier than 3200 GeV are cosmologically inconsistent, and if the top quark mass is less than 120 GeV, the bound is lowered to 2600 GeV. Neutralino states that are mostly gaugino are constrained to be lighter than 550 GeV. It is found that a heavy neutralino that contributes omega(sub X) is approximately 1 arises for a very wide range of model parameters and makes, therefore, a very natural and attractive dark matter candidate. Author

N90-15017# Centro Brasileiro de Pesquisas Fisicas, Rio de Janeiro.
BLACK-HOLE DECAY AND TOPOLOGICAL STABILITY IN QUANTUM GRAVITY
Ligia M. C. S. Rodrigues, Ivano Damiao Soares, and Jorge Zanelli (Chile Univ., Santiago.) 1988 18 p Submitted for publication Sponsored in part by Coordenacao do Aperfeicoamento do Pessoal de Nivel Superior; Fundacao de Amparo a Pesquisa do Rio de Janeiro, Brazil; and FONDECYT, Chile
(DE89-618785; CBPF-NF-060/88; ISSN-0029-3865) Avail: NTIS (US Sales Only) HC A03/MF A01

In the context of Quantum Gravity, the evolution of Schwarzschild black-holes is studied. The superspace of the theory is restricted to a class of geometries that contains the Schwarzschild solution for different masses as well as other geometries with different topologies. It is shown that, black-holes are topologically stable under quantum fluctuations but unstable under quantum processes of emission and absorption of gravitons. It is found that, the probability of emission behaves as exp (-(alpha) M(sub f) - M(sub i)), where M(sub i) and M(sub f) are the masses associated to the initial and final states, respectively and (alpha) is a positive constant of the order of 1. As the black-hole looses mass it evolves towards a state corresponding to a black-hole of very small mass that cannot be distinguished from a pure graviton state. DOE

N90-15018# Centro Brasileiro de Pesquisas Fisicas, Rio de Janeiro.
IS THE NUMBER OF PHOTONS CONSERVED IN AN EXPANDING UNIVERSE
M. Novello, L. A. R. Oliveira, and J. M. Salim 1988 35 p Submitted for publication
(DE89-618836; CBPF-NF-058/88; ISSN-0029-3865) Avail: NTIS (US Sales Only) HC A03/MF A01

A Friedman - like scenario in which, due to gravitational interaction, the total number of photons existing in the Universe changes as the Universe expands, is described. The photon number distribution function, in thermal equilibrium, exhibits an explicit dependence on a non-vanishing chemical potential term. This non-null value for the chemical potential of the photon is due to the presence of tidal effects, arising from the direct coupling of the photons - which, in a gravitational field, should not be treated as idealized point-like objects - to the curvature of space-time. As a result, the ratio n(gamma)/n(sub B) between the numbers of photons and baryons in the Universe is shown to be not a constant, but rather a function of cosmic time, vanishing when the singularity of the standard FRW model is reached. In consequence, some of the supposed fundamental problems of standard Cosmology (e.g., the explanation of the constancy of the ration n(gamma)/n(sub B) and thus of the origin of the total amount of entropy observed today are but apparent ones in the present scenario, and may be ipso facto solved. DOE

N90-15019# Universidade Federal do Rio de Janeiro (Brazil). Inst. de Fisica.
CLASSICAL APPROACH TO HIGHER-DERIVATIVE GRAVITY
A. J. Accioly (Instituto de Fisica Teorica, Sao Paulo, Brazil) 1988 22 p Submitted for publication Sponsored in part by FAPESP, Brazil and Conselno Nacional de Desenvolvimento Cientifico e Teonologico
(DE89-631649; IFT-P-31/88) Avail: NTIS (US Sales Only) HC A03/MF A01

Two classical routes towards higher-derivative gravity theory are described. The first one is a geometrical route, starting from first principles. The second route is a formal one, and is based on a recent theorem by Castagnino et al. A cosmological solution of the higher-derivative field equations is exhibited which in a classical framework singles out this gravitation theory. DOE

N90-15020# Los Alamos National Lab., NM.
THE SOFTEST EINSTEIN AGN (ACTIVE GALACTIC NUCLEI)
F. A. Cordova, J. Kartje, K. O. Mason, and J. P. D. Mittaz (London Univ., England) 1989 10 p Presented at the Einstein to AXAF Conference, Cambridge, MA, Nov. 1989
(Contract W-7405-eng-36)
(DE89-009389; LA-UR-89-863; CONF-891127-1) Avail: NTIS HC A02/MF A01

A coarse spectral study was undertaken to find the softest sources detected with the Imaging Proportional Counter (IPC) on the Einstein Observatory. Of the nearly 7700 IPC sources, 226 have color ratios that make them candidate ultrasoft sources; of these, 83 have small enough errors that it can be said with confidence that they have a spectral component similar to those of the white dwarfs Sirius and HZ 43, nearby stars such as (alpha) Cen and Procyon, and typical polar cataclysmic variables. By means of catalog searches and ground based optical and radio observations, so far 96 of the 226 candidate soft sources were identified; 37 of them are active galactic nuclei (AGN). In the more selective subset of 83 sources, 47 were identified, 12 of them with AGN. The list of 47 identifications is given in Cordova et al. For one QSO in the sample, E0132.8--411, a fit was obtained for the pulse-height data to a power-law model and for the energy spectral index of 2.2(sub -0.4)(sup +0.6). For the remainder of the AGN in the higher confidence sample it was infered on the basis of their x ray colors that they have a similar spectral component. Two-thirds of the AGN are detected below 0.5 KeV only, while the remainder evidence a flatter spectral component in addition to the ultra-soft component. DOE

N90-15021# Fermi National Accelerator Lab., Batavia, IL.
GAMMA RAY LINES FROM DARK MATTER ANNIHILATION
G. F. Giudice Aug. 1989 13 p Presented at the Topical Seminar on Astrophysics and Particle Physics, San Miniato, Italy, 8-12 May 1989
(Contract DE-AC02-76CH-03000)
(DE90-000779; FNAL/C-89/188-T; CONF-8905222-1) Avail: NTIS HC A03/MF A01

If direct annihilation of dark matter particles into a pair of photons occurs in the galactic halo, a narrow gamma-ray line can be discovered at future gamma-ray detectors sensitive to the GeV region. The signals predicted by different dark matter candidates are analyzed. DOE

N90-15022# California Univ., Berkeley. Lawrence Berkeley Lab. Nuclear Science Div.
SUPERNOVAE, COMPACT STARS, AND NUCLEAR PHYSICS
Norman K. Glendenning 25 Aug. 1989 27 p Presented at the International Nuclear Physics Conference, Sao Paulo, Brazil, 20-26 Aug. 1989 Submitted for publication
(Contract DE-AC03-76SF-00098)
(DE90-002682; LBL-27747; CONF-890826-6) Avail: NTIS HC A03/MF A01

We briefly review the current understanding of supernova. We investigate the implications of rapid rotation corresponding to the frequency of the new pulsar reported in the supernovae remnant SN1987A. It places very stringent conditions on the equation of state if the star is assumed to be bound by gravity alone. We find that the central energy density of the star must be greater than 12 times that of nuclear density to be stable against the most optimistic estimate of general relativistic instabilities. This is too high for the matter to plausibly consist of individual hadrons. We conclude that the newly discovered pulsar, if its half-millisecond signals are attributable to rotation, cannot be a neutron star. We show that it can be a strange quark star, and that the entire family of strange stars can sustain high rotation under appropriate conditions. We discuss the conversion of a neutron star to strange star, the possible existence of a crust of heavy ions held in suspension by centrifugal and electric forces, the cooling and other features. DOE

N90-15023# Los Alamos National Lab., NM.
A SOURCE OF OBSERVATIONAL CONSTRAINTS ON THE STRUCTURE OF WOLF-RAYET WINDS
Larry H. Auer and Gloria Koenigsberger (Universidad Nacional Autonoma de Mexico, Mexico City.) 1989 4 p Presented at the Hot Stars Workshop, Boulder, CO, 6-11 Aug. 1989
(Contract W-7405-eng-36)
(DE90-001236; LA-UR-89-3310; CONF-8908167-1) Avail: NTIS HC A01/MF A01

In some WR + O-star binary systems the Wolf-Rayet (WR) wind eclipses the O star. The profile changes as a function of impact are reproduced with a simple model which gives information on both the radial dependence of the velocity and opacity. DOE

N90-15024# Los Alamos National Lab., NM. Theoretical Div.
DARK MATTER AND THE SOLAR NEUTRINO PROBLEM: CAN PARTICLE PHYSICS PROVIDE A SINGLE SOLUTION
Geoffrey B. West 1989 12 p Presented at the 4th Family Symposium, Santa Monica, CA, Mar. 1989 Submitted for publication
(Contract W-7405-eng-36)
(DE90-001827; LA-UR-89-3124) Avail: NTIS HC A03/MF A01

We show how a relatively simple extension of the standard model can give a natural explanation for both the solar neutrino and dark matter problems. What is required is a new stable neutral lepton with a mass in the 4 to 8 GeV range. One possibility is a fourth generation neutrino interacting with matter either electromagnetically or via higgs-exchange (in addition, of course, to Z(degree)-exchange). In the former case, a new charged lepton with mass (approximately) 10 GeV would be required in order to generate a sufficiently large magnetic moment. The present experimental situation makes this possibility rather doubtful. In the

latter case, a light higgs with mass (approximately) 1 GeV is required; this is still not ruled out experimentally. In any case, direct (or indirect) detection of dark matter will, during the next year, seal the fate of this model. DOE

91 LUNAR AND PLANETARY EXPLORATION

Includes planetology; and manned and unmanned flights. For spacecraft design or space stations see *18 Spacecraft Design, Testing and Performance.*

N90-15025*# Georgia Inst. of Tech., Atlanta. School of Electrical Engineering.
LABORATORY EVALUATION AND APPLICATION OF MICROWAVE ABSORPTION PROPERTIES UNDER SIMULATED CONDITIONS FOR PLANETARY ATMOSPHERES Annual Status Report, 1 Feb. - 31 Oct. 1989
Paul G. Steffes Oct. 1989 50 p
(Grant NAGw-533)
(NASA-CR-185916; SA-SR-12; NAS 1.26:185916) Avail: NTIS HC A03/MF A01 CSCL 03B

Radio absorptivity data for planetary atmospheres obtained from spacecraft radio occultation experiments and earth-based radio astronomical observations can be used to infer abundances of microwave absorbing atmospheric constituents in those atmospheres, as long as reliable information regarding the microwave absorbing properties of potential constituents is available. Work performed has shown that laboratory measurements of the millimeter-wave opacity of ammonia between 7.5 mm and 9.3 mm and also at the 3.2 mm wavelength require a different lineshape to be used in the theoretical prediction for millimeter-wave ammonia opacity than was previously used. The recognition of the need to make such laboratory measurements of simulated planetary atmospheres over a range of temperatures and pressures which correspond to the altitudes probed by both radio occultation experiments and radio astronomical observations, and over a range of frequencies which correspond to those used in both radio occultation experiments and radio astronomical observations, has led to the development of a facility at Georgia Tech which is capable of making such measurements. It has been the goal of this investigation to conduct such measurements and to apply the results to a wide range of planetary observations, both spacecraft and earth-based, in order to determine the identity and abundance profiles of constituents in those planetary atmospheres. K.C.D.

N90-15026*# Lunar and Planetary Inst., Houston, TX.
WORKSHOP ON MOON IN TRANSITION: APOLLO 14, KREEP, AND EVOLVED LUNAR ROCKS
G. J. Taylor, ed. and P. H. Warren, ed. [1989] 157 p Workshop held in Houston, TX, 14-16 Nov. 1988
(Contract NASw-4066)
(NASA-CR-186153; NAS 1.26:186153; LPI-TR-89-03) Avail: NTIS HC A08/MF A01 CSCL 03B

Lunar rocks provide material for analyzing lunar history and now new evaluation procedures are available for discovering new information from the Fra Mauro highlands rocks, which are different from any other lunar samples. These and other topics were discussed at this workshop, including a new evaluation of the nature and history of KREEP, granite, and other evolved lunar rock types, and ultimately a fresh evaluation of the transition of the moon from its early anorthosite-forming period to its later stages of KREEPy, granitic, and mare magmatism. The summary of presentations and discussion is based on notes taken by the respective summarizers during the workshop. J.P.S.

N90-15027*# National Aeronautics and Space Administration. Lyndon B. Johnson Space Center, Houston, TX.
THE APOLLO 15 COARSE FINES (4-10 mm)
Graham Ryder and Sarah Bean Sherman (Lunar and Planetary Inst., Houston, TX.) Dec. 1989 218 p
(Contract NASw-4066)
(NASA-TM-101934; JSC-24035; NAS 1.15:101934; PSB-Publ-81) Avail: NTIS HC A10/MF A02 CSCL 03B

A new catalog of the Apollo 15 coarse fines particles is presented. Powell's macroscopic descriptions, resulting from his 1972 particle by particle binocular examination of all of the Apollo 15 4 to 10 mm fines samples, are retained. His groupings are also retained, but petrographic, chemical, and other data from later analyses are incorporated into this catalog to better characterize individual particles and describe the groups. A large number of particles have no characterization beyond that done by Powell. Complete descriptions of the particles and all known references are provided. The catalog is intended for anyone interested in the rock types collected by Dave Scott and Jim Irwin in the Hadley-Appenine region, and particularly for researchers requiring sample allocations. J.P.S.

N90-15028*# Texas Univ., Austin. Dept. of Aerospace Engineering and Engineering Mechanics.
M.I.N.G., MARS INVESTMENT FOR A NEW GENERATION: ROBOTIC CONSTRUCTION OF A PERMANENTLY MANNED MARS BASE Final Report
Jeff Amos, Randy Beeman, Susan Brown, John Calhoun, John Hill, Lark Howorth, Clay McFaden, Paul Nguyen, Philip Reid, and Stuart Rexrode et al 1 May 1989 124 p
(Contract NASw-4435)
(NASA-CR-186224; NAS 1.26:186224) Avail: NTIS HC A06/MF A01 CSCL 03B

A basic procedure for robotically constructing a manned Mars base is outlined. The research procedure was divided into three areas: environment, robotics, and habitat. The base as designed will consist of these components: two power plants, communication facilities, a habitat complex, and a hanger, a garage, recreation and manufacturing facilities. The power plants will be self-contained nuclear fission reactors placed approx. 1 km from the base for safety considerations. The base communication system will use a combination of orbiting satellites and surface relay stations. This system is necessary for robotic contact with Phobos and any future communication requirements. The habitat complex will consist of six self-contained modules: core, biosphere, science, living quarters, galley/storage, and a sick bay which will be brought from Phobos. The complex will be set into an excavated hole and covered with approximately 0.5 m of sandbags to provide radiation protection for the astronauts. The recreation, hangar, garage, and manufacturing facilities will each be transformed from the four one-way landers. The complete complex will be built by autonomous, artificially intelligent robots. Robots incorporated into the design are as follows: Large Modular Construction Robots with detachable arms capable of large scale construction activities; Small Maneuverable Robotic Servicers capable of performing delicate tasks normally requiring a suited astronaut; and a trailer vehicle with modular type attachments to complete specific tasks; and finally, Mobile Autonomous Rechargeable Transporters capable of transferring air and water from the manufacturing facility to the habitat complex. Author

N90-15029*# Colorado Univ., Boulder.
CIS-LUNAR SPACE INFRASTRUCTURE LUNAR TECHNOLOGIES: EXECUTIVE SUMMARY Final Report
W. Faller, A. Hoehn, S. Johnson, P. Moos, and N. Wiltberger 1989 135 p
(Contract NASw-4435)
(NASA-CR-186220; NAS 1.26:186220) Avail: NTIS HC A07/MF A01 CSCL 13B

Technologies necessary for the creation of a cis-Lunar infrastructure, namely: (1) automation and robotics; (2) life support systems; (3) fluid management; (4) propulsion; and (5) rotating technologies, are explored. The technological focal point is on the development of automated and robotic systems for the implementation of a Lunar Oasis produced by Automation and Robotics (LOAR). Under direction from the NASA Office of Exploration, automation and robotics were extensively utilized as an initiating stage in the return to the Moon. A pair of autonomous

rovers, modular in design and built from interchangeable and specialized components, is proposed. Utilizing a buddy system, these rovers will be able to support each other and to enhance their individual capabilities. One rover primarily explores and maps while the second rover tests the feasibility of various materials-processing techniques. The automated missions emphasize availability and potential uses of Lunar resources, and the deployment and operations of the LOAR program. An experimental bio-volume is put into place as the precursor to a Lunar environmentally controlled life support system. The bio-volume will determine the reproduction, growth and production characteristics of various life forms housed on the Lunar surface. Physicochemical regenerative technologies and stored resources will be used to buffer biological disturbances of the bio-volume environment. The in situ Lunar resources will be both tested and used within this bio-volume. Second phase development on the Lunar surface calls for manned operations. Repairs and re-configuration of the initial framework will ensue. An autonomously-initiated manned Lunar oasis can become an essential component of the United States space program.
Author

N90-15030*# National Aeronautics and Space Administration. Lewis Research Center, Cleveland, OH.
SP-100 POWER SYSTEM CONCEPTUAL DESIGN FOR LUNAR BASE APPLICATIONS
Lee S. Mason, Harvey S. Bloomfield, and Donald C. Hainley (Sverdrup Technology, Inc., Cleveland, OH.) 1989 22 p Presented at the 6th Symposium on Space Nuclear Power Systems, Albuquerque, NM, 8-12 Jan. 1989; sponored by Inst. for Space Nuclear Power Studies
(NASA-TM-102090; E-5083; NAS 1.15:102090) Avail: NTIS HC A03/MF A01 CSCL 03B

A conceptual design is presented for a nuclear power system utilizing an SP-100 reactor and multiple Stirling cycle engines for operation on the lunar surface. Based on the results of this study, it was concluded that this power plant could be a viable option for an evolutionary lunar base. The design concept consists of a 2500 kWt (kilowatt thermal) SP-100 reactor coupled to eight free-piston Stirling engines. Two of the engines are held in reserve to provide conversion system redundancy. The remaining engines operate at 91.7 percent of their rated capacity of 150 kWe. The design power level for this system is 825 kWe. Each engine has a pumped heat-rejection loop connected to a heat pipe radiator. Power system performance, sizing, layout configurations, shielding options, and transmission line characteristics are described. System components and integration options are compared for safety, high performance, low mass, and ease of assembly. The power plant was integrated with a proposed human lunar base concept to ensure mission compatibility. This study should be considered a preliminary investigation; further studies are planned to investigate the effect of different technologies on this baseline design.
Author

92 SOLAR PHYSICS

Includes solar activity, solar flares, solar radiation and sunspots.

For related information see *93 Space Radiation.*

N90-15031# National Geophysical Data Center, Boulder, CO.
SOLAR-GEOPHYSICAL DATA NUMBER 538, JUNE 1989. PART 1: (PROMPT REPORTS). DATA FOR MAY, APRIL 1989, AND LATE DATA
Helen E. Coffey, ed. Jun. 1989 147 p
(PB89-223838; SGD-538-Pt-1; LC-79-640375; ISSN-0038-0911)
Avail: NTIS HC A07/MF A01 CSCL 03B

A detailed solar geophysical index for 1988 to 1989 is presented. Data for May 1989 includes: IUWDS (International Ursigram and World Days Service) alert periods (advance and worldwide), solar activity indices, solar flares, solar radio emission, and Stanford mean solar magnetic field. Data for April 1989 includes: solar active regions, sudden ionospheric disturbances, solar radio spectral observations, geomagnetic indices, and radio propagation indices. Other data includes: solar active regions - H-alpha synoptic charts 1813 for March 1989, solar radio emission - Nancay 169 MHz solar interferometric chart for April 1989, cosmic rays climax and Huancayo for March 1989, and geomagnetic indices - sudden commencements/solar flare effects for February 1989. GRA

N90-15032# National Geophysical Data Center, Boulder, CO.
SOLAR-GEOPHYSICAL DATA NUMBER 538, JUNE 1989. PART 2: (COMPREHENSIVE REPORTS). DATA FOR DECEMBER 1988 AND MISCELLANEOUS
Helen E. Coffey, ed. Jun. 1989 117 p
(PB89-223846; SGD-538-Pt-2; LC-79-640375; ISSN-0038-0911)
Avail: NTIS HC A06/MF A01 CSCL 03B

A detailed index of solar geophysical data for 1988 and 1989 is presented. Data for December 1988 includes: solar flares, solar radio bursts at fixed frequencies, solar x ray radiation from GOES satellite, mass ejections from the Sun, and active prominences and filaments. Miscellaneous data includes: Meudon Carte Synoptique Carrington Rotation 1808 for October 1988, solar wind-IMP for December 8, 1988 to February 1989, solar irradiance-ERBE for 1984 to 1988, NOAA 9 data for 1985 to 1988, and NOAA 10 data for 1986 to 1987. GRA

N90-15033# National Geophysical Data Center, Boulder, CO.
SOLAR-GEOPHYSICAL DATA NUMBER 539, JULY 1989. PART 1: (PROMPT REPORTS). DATA FOR JUNE, MAY 1989, AND LATE DATA
Helen E. Coffey, ed. Jul. 1989 159 p
(PB89-235451; SGD-539-Pt-1; ISSN-0038-0911; LC-79-640375)
Avail: NTIS HC A08/MF A01 CSCL 03B

Solar data are presented for June, and May 1989. The data for June 1989 include: solar activity indices, solar flares, solar radio emission, and Stanford mean solar magnetic field. Data for May include: solar active regions, sudden ionospheric disturbances, solar radio spectral observations, cosmic ray measurements by neutron monitor, and geomagnetic indices. Late data include: solar radio emission (Nancay 169 MHz solar interferometric chart May 1989).
Author

N90-15034# National Geophysical Data Center, Boulder, CO.
SOLAR-GEOPHYSICAL DATA NUMBER 539, JULY 1989. PART 2: (COMPREHENSIVE REPORTS). DATA FOR JANUARY 1989, AND MISCELLANEOUS
Helen E. Coffey, ed. Jul. 1989 170 p
(PB89-235469; SGD-539-Pt-2; LC-79-640375; ISSN-0038-0911)
Avail: NTIS HC A08/MF A01 CSCL 03B

A detailed index for 1988 to 1989 of data for January 1989 is given. Information is given concerning solar flares, solar radio bursts at fixed frequencies, interplanetary solar particles and plasma, solar x ray radiation from GOES satellite, mass ejections from the sun, active prominences and filaments; and miscellaneous data -- Meudon carte synoptique -- Carrington rotation.
Author

N90-15035# National Geophysical Data Center, Boulder, CO.
SOLAR-GEOPHYSICAL DATA NUMBER 540, AUGUST 1989. PART 1: (PROMPT REPORTS). DATA FOR JULY, JUNE 1989, AND LATE DATA
Helen E. Coffey, ed. Aug. 1989 159 p
(PB90-108572; SGD-540-Pt-1; LC-79-640375; ISSN-0038-0911)
Avail: NTIS HC A08/MF A01 CSCL 03B

A detailed index of solar geophysical data for 1988 to 1989 is presented. Data for July 1989 includes: IUWDS (International Ursigram and World Days Service) alert periods (advance and worldwide), solar activity indices, solar flares, solar radio emission, and Stanford mean solar magnetic field. Data for June 1989 includes: solar active regions, sudden ionospheric disturbances, solar radio spectral observations, cosmic ray measurements by neutron monitor, and geomagnetic indices. Miscellaneous data includes: cosmic ray measurements by neutron monitors for May 1989, and geomagnetic indices for March to April 1989. GRA

N90-15036*# National Aeronautics and Space Administration. Marshall Space Flight Center, Huntsville, AL.
THE SOLAR ACTIVITY MEASUREMENTS EXPERIMENTS (SAMEX) FOR IMPROVED SCIENTIFIC UNDERSTANDING OF SOLAR ACTIVITY
[1989] 27 p Original contains color illustrations
(NASA-TM-100372; NAS 1.15:100372) Avail: NTIS HC A03/MF A01 CSCL 03B

The Solar Activity Measurements Experiments (SAMEX) mission is described. It is designed to provide a look at the interactions of magnetic fields and plasmas that create flares and other explosive events on the sun in an effort to understand solar activity and the nature of the solar magnetic field. The need for this mission, the instruments to be used, and the expected benefits of SAMEX are discussed. J.P.S.

93 SPACE RADIATION

Includes cosmic radiation; and inner and outer earth's radiation belts.

For biological effects of radiation see *52 Aerospace Medicine*. For theory see *73 Nuclear and High-Energy Physics*.

N90-15037 Bristol Univ. (England).
A LARGE DETECTOR FOR COSMIC RAY ABUNDANCE AND ENERGY MEASUREMENTS Ph.D. Thesis
C. Alsop 1988 182 p
Avail: Univ. Microfilms Order No. BRDX85185

A large aperture, balloon borne cosmic ray detector was designed to measure the energy spectra of individual cosmic ray species with Z greater than 8 in the energy range 0.3GeV/N to 400GeV/N. The energy dependence of the abundance spectrum extending up to such high energies will provide valuable data for determining the nature of the origin and propagation of cosmic rays in the Galaxy. The properties of cosmic ray nuclei and the interpretation of the energy dependence of the abundance spectrum are discussed. The design and response of the BUGS IV cosmic ray detector are described. The measurement techniques used are gas scintillation, gas proportional scintillation and Cerenkov radiation from both gases and solids. The light collection properties of the detector and several experimental investigations of the light collection efficiency of the drift chamber region are described. The expected signals from the gas scintillation and gas Cerenkov emissions are predicted and the choice of a suitable scintillating gas mixture for minimizing the uncertainty in the charge and energy measurements is considered. The theoretical aspects of electron drift and diffusion in gases and several experimental investigations on the electron drift in the BUGS IV drift chamber are given. Also some preliminary results from a uniform field drift chamber are included which demonstrate the sensitivity of the electron drift velocity in inert gas mixtures to water vapor contamination. The expected overall performance of BUGS IV and the results of an experimental simulation of the parachute landing of the detector are given. Dissert. Abstr.

N90-15038 Maryland Univ., College Park.
KILOMETRIC TYPE III RADIO BURSTS AND INTERPLANETARY TRANSIENTS Ph.D. Thesis
Robert John MacDowall 1988 158 p
Avail: Univ. Microfilms Order No. DA8912321

The first detailed observation and analysis of interplanetary (IP) type III bursts which undergo sudden intensity changes are presented. Two major event categories are studied: cutoffs in which type III intensity is abruptly reduced (by a factor of 10 or more) at some frequency and remains at the reduced level for all lower frequencies, and narrow band intensifications which frequently occur on the high frequency edge of a cutoff. Based on their apparent radial velocities as well as their occurrence at the same frequencies as kilometric type II emission, a subset of the sudden intensity change events are demonstrated to be associated with IP shocks. Consequently, they provide a new tool for shock detection in the inner heliosphere. Two causes proposed for the shock associated type III burst cutoffs are enhanced levels of background electrons and pitch angle scattering. In the vicinities of IP shocks, the observed background levels of electrons with energies greater than 2 KeV are frequently enhanced by up to 2 orders of magnitude over ambient levels. The magnetic field fluctuations observed downstream of many shocks are effective in pitch angle scattering type III electrons. Either of these mechanisms may reduce the effective height of the bump-on-tail distribution, and thereby influence the Langmuir wave growth and evolution. Dissert. Abstr.

N90-15039# National Geophysical Data Center, Boulder, CO.
SOLAR-GEOPHYSICAL DATA NUMBER 540, AUGUST 1989. PART 2: (COMPREHENSIVE REPORTS). DATA FOR FEBRUARY 1989
Helen E. Coffey, ed. Aug. 1989 98 p
(PB89-108598; SGD-540-Pt-2; LC-79-640375; ISSN-0038-0911)
Avail: NTIS HC A05/MF A01 CSCL 03B

A detailed index of solar geophysical data for 1988 to 1989 is presented. Data for February 1989 includes: solar flares, solar radio bursts at fixed frequencies, interplanetary solar particles and plasma, solar x ray radiation from GOES satellite, graphs, mass ejections from the sun, and active prominences and filaments. GRA

99 GENERAL

N90-15040*# New World Services, Inc., FL.
CHRONOLOGY OF KSC AND KSC RELATED EVENTS FOR 1988 Annual Report, 1988
Ken Nail, Jr., ed. Mar. 1989 116 p
(Contract NAS10-10600)
(NASA-TM-101915; NAS 1.15:101915; KSC-KHR-13) Avail: NTIS HC A06/MF A01 CSCL 05D

A record of KSC events and a reference source for historians and other researchers is given. Arrangements is by day and month and individual articles are attributed to published sources. An index has been added to this edition. Author

SUBJECT INDEX

Typical Subject Index Listing

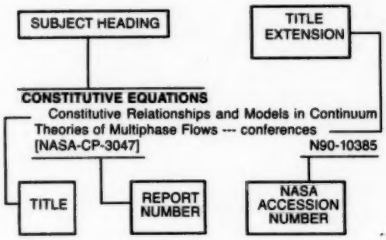

The subject heading is a key to the subject content of the document. Titles, report numbers, and accession numbers of pertinent documents are provided under each subject heading. When the title is insufficiently descriptive of the document content, a title extension has been added, separated from the title by three hyphens. The report number helps to indicate the type of document cited (e.g., NASA report, NASA translation, NASA contractor report). The NASA accession number is the number by which the document abstracts are arranged in this journal and by which the document is sold or requested. The titles, with title extensions if present, are arranged under each subject heading in ascending accession number order. The subject headings have been selected from the latest revision of the *NASA Thesaurus* (NASA SP-7064).

A

A STARS
As observational and theoretical investigation of stellar flares N90-15012
Perturbation methods for the calculation of gravitational waves from slightly non-spherical spacetimes with applications to stellar core collapse N90-15015
ABERRATION
Deferred electronic heterodyne moire deflectometry: A method for transient density fields measurement
[NASA-CR-182982] N90-14907
ABLATION
Studies of neutral and ion transport during laser ablation of 1:2:3 superconductors by optical absorption spectroscopy
[DE90-001968] N90-14604
ABSORPTION
Non-linear optical studies of adsorbates: Spectroscopy and dynamics
[DE90-001543] N90-14312
ABSORPTION SPECTROSCOPY
Mapping of upper electronic reaction surfaces by tuned laser photolysis and by absorption and emission spectroscopies
[DE90-000125] N90-14314
Measurement of the high density zone of a plasma target by absorption spectroscopy N90-14560
Studies of neutral and ion transport during laser ablation of 1:2:3 superconductors by optical absorption spectroscopy
[DE90-001968] N90-14604
ABSORPTIVITY
The average ion model. Computation of the absorption and emission coefficients in hot plasmas N90-14569
Laboratory evaluation and application of microwave absorption properties under simulated conditions for planetary atmospheres
[NASA-CR-185916] N90-15025
ACCELERATION (PHYSICS)
Acceleration of small, light projectiles (including hydrogen isotopes) to high speeds using a two-stage light gas gun
[DE90-002479] N90-14253
Methodology for the calibration of and data acquisition with a six-degree-of-freedom acceleration measurement device
[PB89-233597] N90-14531
Physics with ultra-low energy antiprotons
[DE90-002397] N90-14888
ACCELEROMETERS
Methodology for the calibration of and data acquisition with a six-degree-of-freedom acceleration measurement device
[PB89-233597] N90-14531
Evaluation of shock isolation techniques for a piezoresistive accelerometer
[DE89-014496] N90-14535
ACCIDENT PREVENTION
Field evaluation of a Nissan laser collision avoidance system
[PB90-105602] N90-14215
ACETATES
Single particle friction tests with cellulose acetate sphere samples
[DE89-017537] N90-14622
ACHONDRITES
Meteoritic basalts
[NASA-CR-185949] N90-15004
ACID RAIN
An evaluation of trend detection techniques for use in water quality monitoring programs
[PB89-100058] N90-14702
Steady state model to determine lake resources at risk to acid deposition in the Sierra Nevada, California
[PB89-103995] N90-14705
Application of surface analysis methods to studies of atmospheric deposition in forests
[DE90-000562] N90-14714
Analysis of acid rain and associated phenomena
[DE90-002555] N90-14725
Nitrogen deposition to forest trees
[DE90-003285] N90-14726
ACOUSTIC EMISSION
Acoustic emission during intergranular stress corrosion cracking
[DE90-002894] N90-14355
Cavitation-controlled ultrasonic agitator
[DE90-002773] N90-14871
ACOUSTIC INSTABILITY
Spatial evolution of nonlinear acoustic mode instabilities on hypersonic boundary layers
[NASA-TM-102431] N90-14517
ACOUSTICS
Acoustic-vortical-combustion interaction in a solid fuel ramjet simulator N90-14234
Boundary element analysis of single and multidomain problems in acoustics N90-14867
Effective utilization of acoustic wave sensor responses: Simultaneous measurement of velocity and attenuation
[DE90-002580] N90-14872
ACRYLIC RESINS
Crazing and degradation of flexure strength in acrylic plates as a function of time
[AD-A212835] N90-14357
ACTIVATION ENERGY
Embrittlement of laboratory- and reactor-aged CF-3, CF-8, and CF-8M duplex stainless steels
[DE90-002777] N90-14354
ACTIVE GALACTIC NUCLEI
The softest Einstein AGN (Active Galactic Nuclei)
[DE89-009389] N90-15020
ACTS
Pattern recognition techniques applied to the NASA-ACTS order-wire problem N90-14446
ADA (PROGRAMMING LANGUAGE)
Transferring data objects: A focused Ada investigation
[NASA-CR-186065] N90-14786
QUEST/Ada: Query utility environment for software testing of Ada
[NASA-CR-186121] N90-14787
Classic-Ada(TM) N90-14793
Reuse research plans at Langley Research Center N90-14797
SSFP approach to software reuse N90-14799
An SSE approach to reusability N90-14801
Initial Ada components evaluation N90-14803
Advanced Software Development Workstation Project N90-14807
The development of an Ada programming support environment database: SEAD (Software Engineering and Ada Database), user's manual
[NASA-CR-181219] N90-14811
A graphically oriented specification language for automatic code generation. GRASP/Ada: A Graphical Representation of Algorithms, Structure, and Processes for Ada, phase 1
[NASA-CR-183212] N90-14813
ADAPTIVE CONTROL
Non-linear vibrations, stability, and dynamics of structures and mechanisms
[AD-A212152] N90-14639
Survey of adaptive control theory and its applications
[DE89-901270] N90-14840
ADAPTIVE FILTERS
Improving the quality of a spread-spectrum radiomobile link N90-14426
Adaptive clutter rejection filters for airborne Doppler weather radar applied to the detection of low altitude windshear
[NASA-CR-186211] N90-14453
ADVANCED SOLID ROCKET MOTOR (STS)
Review of the Aerospace Safety Advisory Panel report for NASA fiscal year 1990 authorization
[GPO-24-234] N90-14213
ADVECTION
Inverted surface troughs accompanying Rocky Mountain lee-side cyclogenesis N90-14746
Some numerical experiments concerning the equation of state algorithm for multi-material cells in HULL
[DE89-008240] N90-14827
AEOLIAN TONES
Saltation thresholds and entrainment of fine particles at Earth and Martian pressures
[NASA-TM-102193] N90-14997
AERIAL RECONNAISSANCE
Airborne FLIR detection of surface targets N90-14416
AEROACOUSTICS
An experimental and theoretical study of the aeroacoustics of external-Coanda gas flares N90-14495
AEROASSIST
Measured and predicted aerodynamic coefficients and shock shapes for Aeroassist Flight Experiment (AFE) configuration
[NASA-TP-2956] N90-14185
Optimal control of aero-assisted orbit transfer vehicles N90-14241
Guidance and Control strategies for aerospace vehicles
[NASA-CR-186195] N90-14243
Optimal trajectories for the aeroassisted flight experiment
[NASA-CR-186133] N90-14250
Project Argo: The design and analysis of an all-propulsive and an aeroassisted version of a manned space transportation vehicle
[NASA-CR-186047] N90-14266
Aerobraking characteristics for several potential manned Mars entry vehicles
[NASA-TM-101669] N90-14272
AEROBRAKING
Aerobraking characteristics for several potential manned Mars entry vehicles
[NASA-TM-101669] N90-14272
AERODYNAMIC BALANCE
Development of a three-axis trim program
[AD-A212883] N90-14237

AERODYNAMIC CHARACTERISTICS
Measured and predicted aerodynamic coefficients and shock shapes for Aeroassist Flight Experiment (AFE) configuration
[NASA-TP-2956] N90-14185
An in-flight investigation of ground effect on a forward-swept wing airplane
[NASA-TM-101708] N90-14202
Subsonic sting interference on the aerodynamic characteristics of a family of slanted-base ogive-cylinders
[NASA-CR-186193] N90-14204
Effect of unshielded and shielded horn balances on hinge moment coefficients for controls at low speeds
[ESDU-89003-A] N90-14238
Concurrent processing adaptation of aeroplastic analysis of propfans
[NASA-TM-102455] N90-14656

AERODYNAMIC COEFFICIENTS
Measured and predicted aerodynamic coefficients and shock shapes for Aeroassist Flight Experiment (AFE) configuration
[NASA-TP-2956] N90-14185

AERODYNAMIC CONFIGURATIONS
Measured and predicted aerodynamic coefficients and shock shapes for Aeroassist Flight Experiment (AFE) configuration
[NASA-TP-2956] N90-14185
Program VSAERO theory document: A computer program for calculating nonlinear aerodynamic characteristics of arbitrary configurations
[NASA-CR-4023] N90-14200
Aerobraking characteristics for several potential manned Mars entry vehicles
[NASA-TM-101669] N90-14272

AERODYNAMIC HEATING
Thermal/structural analyses of several hydrogen-cooled leading-edge concepts for hypersonic flight vehicles
[NASA-TM-102391] N90-14511

AERODYNAMIC NOISE
An experimental and theoretical study of the aeroacoustics of external-Coanda gas flares
N90-14495

AERODYNAMIC STABILITY
Stability of a supersonic boundary layer on a sharp cone at a small angle of attack N90-14510

AERODYNAMIC STALLING
Stall/spin aerodynamic data project
[DOT/FAA/CT-88/29] N90-14222

AERODYNAMICS
Control of the variable speed generator on the Sandia 34-metre vertical axis wind turbine
[DE90-000803] N90-14674

AEROELASTICITY
Concurrent processing adaptation of aeroplastic analysis of propfans
[NASA-TM-102455] N90-14656

AERONAUTICAL ENGINEERING
California air transportation study: A transportation system for the California Corridor of the year 2010
[NASA-CR-186219] N90-14212

AEROSOLS
Remote sensing of the aerosol scattering coefficient with a multi-field-of view lidar N90-14437
Physical models for aerosol in the marine mixed-layer N90-14438

AEROSPACE ENGINEERING
The space station tethered elevator system
[NASA-CR-186051] N90-14265
CIS-lunar space infrastructure lunar technologies: Executive summary
[NASA-CR-186220] N90-15029

AEROSPACE ENVIRONMENTS
Particle simulations in magnetospheric plasmas
[NASA-CR-186238] N90-14934

AEROSPACE INDUSTRY
Design and demonstration of heat pipe cooling for NASP and evaluation of heating methods at high heating rates
[DE89-016995] N90-14227
Reuse at the Software Productivity Consortium N90-14798

AEROSPACE MEDICINE
USSR Space Life Sciences Digest. Index to issues 21-25
[NASA-CR-3922(30)] N90-14763
Exploring the living universe: A strategy for space life sciences
[NASA-TM-101891] N90-14778

AEROSPACE PLANES
Slush Hydrogen (SLH2) technology development for application to the National Aerospace Plane (NASP)
[NASA-TM-102315] N90-14268

AEROSPACE VEHICLES
Guidance and Control strategies for aerospace vehicles
[NASA-CR-186195] N90-14243
Aerobraking characteristics for several potential manned Mars entry vehicles
[NASA-TM-101669] N90-14272

AFRICA
Rainfall estimation over Africa using satellite data N90-14742

AGING (METALLURGY)
Embrittlement of laboratory- and reactor-aged CF-3, CF-8, and CF-8M duplex stainless steels
[DE90-002777] N90-14354
BES welding science contractors summary report, 1988 to 1989
[DE90-001004] N90-14619

AIR
Test and evaluation of polymeric membranes for oxygen enrichment of air
[DE90-000555] N90-14321

AIR DEFENSE
Integrated G-suit/immersion suit
[AD-A212989] N90-14774

AIR FLOW
Navier-Stokes solutions of 2-D transonic flow over unconventional airfoils N90-14195
Numerical modeling of supersonic turbulent reacting free shear layers N90-14197
Heat transfer to a stationary and moving sphere immersed in a fluidized bed N90-14503

AIR MASSES
The development of a spatial synoptic climatological index for environmental analysis N90-14744

AIR POLLUTION
Profile measurements of sulfur dioxide, nitrogen oxides, and nitric acid deposition velocities in California's south coast air basin
[PB90-104001] N90-14703
Proceedings of the US/FRG (Fed. Republic of Germany) research symposium: Effects of Atmospheric Pollutants on the Spruce-Fir Forests of the Eastern United States and the Fed. Republic of Germany
[PB90-107160] N90-14704
International Conference on Global and Regional Atmospheric Environmental Chemistry and visit to Hangzhou, China, foreign trip report
[DE90-000099] N90-14713
Strategy for monitoring the effects of land use change on atmospheric CO2 concentrations
[DE90-001635] N90-14722
Nitrogen deposition to forest trees
[DE90-003285] N90-14726
Extraterrestrial halogen and sulfur content of the stratosphere
[DE89-017623] N90-14738

AIR TRAFFIC
Preliminary design of four aircraft to service the California Corridor in the year 2010: The California Condor, California Sky-Hopper, high capacity short range transport tilt rotor aircraft needed to simplify intercity transportation
[NASA-CR-186232] N90-14226

AIR TRAFFIC CONTROL
National airspace system monitoring operational concept
[NAS-SR-1330] N90-14214
Adaptive clutter rejection filters for airborne Doppler weather radar applied to the detection of low altitude windshear
[NASA-CR-186211] N90-14453

AIR TRANSPORTATION
California air transportation study: A transportation system for the California Corridor of the year 2010
[NASA-CR-186219] N90-14212

AIR WATER INTERACTIONS
A forecasting system using the parabolic equation: Application to surface-to-air propagation in the presence of elevated layers N90-14420
Physical models for aerosol in the marine mixed-layer N90-14438
A low-order model of the equatorial ocean-atmosphere system N90-14730

AIRBORNE EQUIPMENT
Evaluation of the airborne visible-infrared imaging spectrometer for mapping subtle lithological variation
[NASA-CR-186213] N90-14670

AIRCRAFT COMMUNICATION
Data Link Processor (DLP) operational test and evaluation/integration test plan
[DOT/FAA/CT-TN89/32] N90-14404

AIRCRAFT CONTROL
Design of a spanloader cargo aircraft
[NASA-CR-186046] N90-14216

AIRCRAFT DESIGN
California air transportation study: A transportation system for the California Corridor of the year 2010
[NASA-CR-186219] N90-14212
Design of a spanloader cargo aircraft
[NASA-CR-186046] N90-14216
Preliminary design of four aircraft to service the California Corridor in the year 2010: The California Condor, California Sky-Hopper, high capacity short range transport tilt rotor aircraft needed to simplify intercity transportation
[NASA-CR-186232] N90-14226

AIRCRAFT ENGINES
AGARD Highlights 89/2 N90-14184

AIRCRAFT HAZARDS
Flight in adverse environmental conditions
[AGARD-AR-277] N90-14218

AIRCRAFT NOISE
A two dimensional power spectral estimate for some nonstationary processes
[NASA-CR-186100] N90-14843
Evaluation of analysis techniques for low frequency interior noise and vibration of commercial aircraft
[NASA-CR-181851] N90-14866

AIRCRAFT PERFORMANCE
Introduction to data items on flight path optimisation
[ESDU-89015] N90-14221

AIRCRAFT SPIN
Stall/spin aerodynamic data project
[DOT/FAA/CT-88/29] N90-14222

AIRCRAFT STABILITY
Design of a spanloader cargo aircraft
[NASA-CR-186046] N90-14216

AIRCRAFT WAKES
Effect of pylon wake with and without pylon blowing on propeller thrust
[NASA-TM-4162] N90-14190

AIRFOIL PROFILES
Computation of unsteady transonic flow about airfoils in frequency domain using the full-potential equation N90-14198

AIRFOILS
Navier-Stokes solutions of 2-D transonic flow over unconventional airfoils N90-14195
A one equation turbulence model for transonic airfoils N90-14199
Computational investigation of incompressible airfoil flows at high angles of attack
[AD-A205865] N90-14201
Visualization of boundary layer transition zone movement on oscillating airfoils with shear-sensitive liquid-crystal coatings
[DE89-009570] N90-14210
Stall/spin aerodynamic data project
[DOT/FAA/CT-88/29] N90-14222
Effect of unshielded and shielded horn balances on hinge moment coefficients for controls at low speeds
[ESDU-89003-A] N90-14238

AIRFRAMES
An experimental investigation of the interaction between a model rotor and airframe in forward flight N90-14219
An analytical method for the prediction of unsteady rotor/airframe interactions in forward flight N90-14223

AIRPORTS
California air transportation study: A transportation system for the California Corridor of the year 2010
[NASA-CR-186219] N90-14212

ALBEDO
Atlas of albedo and absorbed solar radiation derived from Nimbus 6 earth radiation budget data set, July 1975 to May 1978
[NASA-RP-1230] N90-14741

ALCOHOLS
Comparison of structural subunits of the core light-harvesting complexes of photosynthetic bacteria
[DE90-001412] N90-14765

ALGEBRA
Mathematical techniques for system realization and identification
[AD-A212088] N90-14841
Classification of modular invariant partition functions for the twisted N=2 superconformal algebra, twisted SU(2) Kac-Moody algebra and D(sub 2K) parafermions
[DE90-600767] N90-14853

ALGORITHMS
Navier-Stokes solutions of 2-D transonic flow over unconventional airfoils N90-14195
Advanced 3-D CFD algorithm for turbomachinery N90-14233
The parabolic equation approach to predicting tropospheric propagation effects in operational environments N90-14418
Pattern recognition techniques applied to the NASA-ACTS order-wire problem N90-14446
Data compression techniques applied to high resolution high frame rate video technology
[NASA-CR-4263] N90-14452
Numerical solution of the incompressible Navier-Stokes equations N90-14501
An image compression algorithm for a high-resolution digital still camera
[NASA-CR-185079] N90-14532

Numerical simulation of laser radiation propagation in non-uniform absorbing medium. Geometrical optics approximation
[DE89-632014] N90-14585
Group implicit concurrent algorithms in nonlinear structural dynamics
[NASA-CR-185950] N90-14638
A new uniformly valid asymptotic integration algorithm for elasto-plastic-creep and unified viscoplastic theories including continuum damage
[NASA-TM-102344] N90-14655
Power spectral estimation algorithms
[NASA-CR-186189] N90-14812
The phase gradient autofocus algorithm: An optimal estimator of the phase derivative
[DE90-000895] N90-14814
Versatility of the CFR algorithm for limited angle reconstruction
[DE90-001421] N90-14817
Program CICC flow and heat transfer in Cable-In-Conduit Conductors
[DE90-001519] N90-14818
Algorithmic randomness, physical entropy, measurements, and the second law
[DE90-002413] N90-14823
Interactive multidimensional data analysis and understanding
[DE90-001794] N90-14824
Some numerical experiments concerning the equation of state algorithm for multi-material cells in HULL
[DE89-008240] N90-14827
Architectures for reasoning in parallel
[NASA-CR-186237] N90-14836
Parallel projected variable metric algorithms for unconstrained optimization
[NASA-CR-181930] N90-14842
Numerical methodologies for solving partial differential equations
[DE90-001842] N90-14849
Application of heuristic satellite plan synthesis algorithms to requirements of the WARC-88 allotment plan
[NASA-TM-102479] N90-14856

ALIPHATIC COMPOUNDS
Pentafluorothio polynitroaliphatic explosives
[AD-D014221] N90-14383

ALKALINE BATTERIES
Silver composite cathodes for alkaline secondary batteries
[AD-D014227] N90-14462
Silver-nickel composite cathodes for alkaline secondary batteries
[AD-D014231] N90-14464

ALKALINE EARTH OXIDES
Prospects for wavelength tunable lasers based on vacancy defects in alkaline-earth oxides
[DE90-001078] N90-14592

ALL SKY PHOTOGRAPHY
Theory of wide-angle photometry from standard stars
[NASA-CR-185964] N90-14999

ALLOYS
Superplasticity: An overview N90-14326
Electrical properties of materials for high temperature strain gage applications
[NASA-CR-186192] N90-14534

ALPHA PARTICLES
Stability of the Global Alfven Eigenmode in the presence of fusion alpha particles in an ignited tokamak plasma
[DE89-016618] N90-14930

ALTIMETRY
Correction of ionospheric effects for the precise orbit determination of satellites N90-14432

ALUMINUM
A method of soldering aluminum
[AD-D014226] N90-14611
Glancing angle x ray studies of oxide films
[DE89-017828] N90-14953

ALUMINUM ALLOYS
Advances and future directions in superplastic materials N90-14328
The mechanical properties of superplastically formed titanium and aluminium alloys N90-14331
The manufacture of superplastic alloys N90-14333
Influence of hole surface finish, cyclic frequency and spectrum severity on the fatigue behavior of thick section aluminum alloy pin joints
[ARL-STRUC-R-430] N90-14336
The strength-toughness combination of the aluminum-lithium alloys 2090 and 2091 at cryogenic temperatures
[DE90-001425] N90-14338
The effect of hydrogen charging on the mechanical properties of aluminum alloy 2090
[DE90-000129] N90-14341
Phases in lanthanum-nickel-aluminum intermetallic alloys
[DE90-000651] N90-14343
A method of soldering aluminum
[AD-D014226] N90-14611

ALUMINUM GALLIUM ARSENIDES
Method of making self-aligned GaAs/AlGaAs FET's
[AD-D014229] N90-14935

ALUMINUM OXIDES
SEM (Scanning Electron Microscope) image analysis of grain growth in microwave-annealed alumina
[DE90-001606] N90-14339
Ordered ceramic membranes
[DE89-017426] N90-14364

AMMONIUM NITRATES
Investigation of the phase stabilizing effect of potassium fluoride on ammonium nitrate
[AD-A213042] N90-14381
Steady state model to determine lake resources at risk to acid deposition in the Sierra Nevada, California
[PB89-103995] N90-14705

AMORPHOUS SILICON
Research on high-efficiency, single-junction, monolithic, thin-film amorphous silicon solar cells
[DE89-000846] N90-14687

AMPLIFICATION
X-UV amplification in a plasma column of five centimeters. Five beams experiment N90-14574
Proof-of-principle experiment for a hot electron pumped XUV amplifier
[DE90-000820] N90-14588

ANALYSIS (MATHEMATICS)
Mathematical techniques for system realization and identification
[AD-A212088] N90-14841

ANGLE OF ATTACK
Normal force, pitching moment, and side force of forebody-cylinder combinations for angles of attack up to 90 degrees and Mach numbers up to 5
[ESDU-89014] N90-14192
Stability of a supersonic boundary layer on a sharp cone at a small angle of attack N90-14510

ANGULAR CORRELATION
Perturbed angular correlations in zirconia ceramics
[DE89-017272] N90-14369

ANGULAR DISTRIBUTION
A study of recoil protons in ultra-relativistic nucleus-nucleus collisions
[LUIP-8907] N90-14873

ANISOTROPIC FLUIDS
The supersonic anisotropic collapse of Langmuir waves N90-14550

ANISOTROPIC MEDIA
Direction-dependent stopping power and beam deflection in anisotropic solids
[DE90-001076] N90-14883

ANISOTROPY
Anisotropy of electron distributions related to the anisotropy and polarization of the continuous emitted x rays N90-14566
Anisotropy of oxygen tracer diffusion in YBa2Cu3O7-delta single crystals
[DE90-001931] N90-14979

ANNEALING
SEM (Scanning Electron Microscope) image analysis of grain growth in microwave-annealed alumina
[DE90-001606] N90-14339

ANNIHILATION REACTIONS
Gamma ray lines from dark matter annihilation
[DE90-000779] N90-15021

ANNUAL VARIATIONS
An evaluation of trend detection techniques for use in water quality monitoring programs
[PB89-100058] N90-14702
Climatology of Lawrence Livermore National Laboratory
[DE90-000905] N90-14756

ANODES
Interfacial effects in monolithic solid oxide fuel cells
[DE90-001914] N90-14690

ANTENNA ARRAYS
Vehicle antenna for the mobile satellite experiment
[NASA-CR-186109] N90-14271

ANTENNA DESIGN
Vehicle antenna for the mobile satellite experiment
[NASA-CR-186109] N90-14271
Frequency independent constant beamwidth directional lens antenna for very wideband and multi-channel electromagnetic communications
[AD-D014214] N90-14449

ANTICYCLONES
A forecasting system using the parabolic equation: Application to surface-to-air propagation in the presence of elevated layers N90-14420

ANTIFERROMAGNETISM
Macroscopic persistent currents in high temperature ceramic superconductors
[DE89-636232] N90-14973

ANTINUCLEONS
The creation of high energy densities with antimatter beams
[DE90-002383] N90-14899

ANTIPROTONS
Physics with ultra-low energy antiprotons
[DE90-002397] N90-14888
The creation of high energy densities with antimatter beams
[DE90-002383] N90-14899

APOLLO 15 FLIGHT
The Apollo 15 coarse fines (4-10 mm)
[NASA-TM-101934] N90-15027

APPLICATIONS PROGRAMS (COMPUTERS)
A composite numerical procedure for calculating the motion of vortex filaments N90-14207
Guidance, steering, load relief and control of an asymmetric launch vehicle
[NASA-CR-185598] N90-14257
The stability of Taylor-Couette flow with radial heating N90-14502
The average ion model. Computation of the absorption and emission coefficients in hot plasmas N90-14569
XRAD: A one dimensional Lagrangian code with radiative transport N90-14570
Characteristics of an x ray source created by a laser plasma N90-14575
JPL reuse program N90-14795
Advanced Software Development Workstation Project N90-14807
Some numerical experiments concerning the equation of state algorithm for multi-material cells in HULL
[DE89-008240] N90-14827

APPROXIMATION
The fluid mechanics of filters N90-14499
Approximate methods for dynamic plastic deformation of structures
[DE90-002214] N90-14660

AQUIFERS
Image processing of LANDSAT MSS data for buried valley detection in northern Indiana N90-14668

ARC JET ENGINES
Arcjet thruster research and technology. Phase 1: Executive summary
[NASA-CR-182106] N90-14278

ARC WELDING
The feasibility of welding of irradiated materials
[DE90-002200] N90-14631

ARCHES
A study of incremental-iterative strategies for nonlinear analyses
[PB89-226005] N90-14646

ARCHITECTURE (COMPUTERS)
The Tactical Environmental Support System (TESS(3)) N90-14409
The characteristics of the HF radio channel and its influence on modern HF data communication system design N90-14448
A radar simulation program for a 1024-processor hypercube
[DE89-014494] N90-14455
CTH: A three-dimensional shock wave physics code
[DE89-016529] N90-14528
Parallel eigenanalysis of finite element models in a completely connected architecture
[NASA-CR-185166] N90-14652
High performance parallel architectures
[DE90-001055] N90-14782
High volume data storage architecture analysis
[NASA-CR-186239] N90-14784
Selecting and effectively using a computer aided software engineering tool
[DE89-017876] N90-14815
The High-Speed Channel (HSC) and ultra-speed networks
[DE89-015283] N90-14819
The design of a computer system for image simulation and image processing of high resolution electron micrographs
[DE90-000179] N90-14820
Using object-oriented development to support prototyping
[DE90-000547] N90-14821
Interactive multidimensional data analysis and understanding
[DE90-001794] N90-14824
A tutorial on software reliability engineering
[DE89-012368] N90-14828
Multiple crossbar network: Integrated supercomputing framework
[DE89-012614] N90-14831

The Delta-t transport protocol: Features and experience useful for high performance networks [DE89-016542] N90-14832
Generalization in backpropagation networks: An empirical study using image data [DE89-012658] N90-14835
Architectures for reasoning in parallel [NASA-CR-186237] N90-14836
NETRA: A parallel architecture for integrated vision systems. 1: Architecture and organization [NASA-CR-185955] N90-14839

ARCTIC REGIONS
A rough transform technique for extracting lead features from sea ice imagery [AD-A212758] N90-14866
Decomposition in Arctic terrestrial environments [DE90-001198] N90-14706

ARGON PLASMA
Box experiments. Nonlinear effects at plasma resonance N90-14555

ARRAYS
Design of incoherent imaging arrays [DE90-000861] N90-14909

ARTIFICIAL INTELLIGENCE
Decision-aid design factors in connection with HF communication and emitter location disciplines N90-14413
A modern trans-ionospheric propagation sensing system N90-14430

ASTRONOMICAL OBSERVATORIES
Long-lived space observatories for astronomy and astrophysics [NASA-CR-185373] N90-14261
Properties of evolved star circumstellar grains N90-15003

ASTROPHYSICS
The ultimate structure of matter: The US High Energy Physics Program from the 1950s through the 1980s [DE90-001784] N90-14887
An international discussion on research in solar and space physics N90-14996

ASYMPTOTIC GIANT BRANCH STARS
Properties of evolved star circumstellar grains N90-15003

ASYMPTOTIC METHODS
A new uniformly valid asymptotic integration algorithm for elasto-plastic-creep and unified viscoplastic theories including continuum damage [NASA-TM-102344] N90-14655

ASYMPTOTIC SERIES
Asymptotic analysis of performance of membrane modules for gas separations [DE90-000699] N90-14316

ATLANTIC OCEAN
Analysis of propagation in an inhomogeneous atmosphere in the horizontal and vertical direction using the parabolic equation method N90-14421

ATMOSPHERIC CHEMISTRY
Global stratospheric change: Requirements for a Very-High-Altitude Aircraft for Atmospheric Research [NASA-CP-10041] N90-14220
On the mitigation of non-CO2 greenhouse gases [DE89-016659] N90-14710
International Conference on Global and Regional Atmospheric Environmental Chemistry and visit to Hangzhou, China, foreign trip report [DE90-000099] N90-14713
Nitrogen deposition to forest trees [DE90-003285] N90-14726
Characterization of cloud chemistry and frequency of canopy exposure to clouds in the Sierra Nevada [PB89-104035] N90-14753

ATMOSPHERIC CIRCULATION
Airdata calibration of a high-performance aircraft for measuring atmospheric wind profiles [NASA-TM-101714] N90-14228
An observational study of intramonthly quasi-periodicities in the Northern Hemisphere, extratropical geopotential height field N90-14729

ATMOSPHERIC COMPOSITION
The retrieval of the concentrations of nitric oxide and nitrogen dioxide from satellite solar occultation measurements at sunset and sunrise N90-14733
The development of a spatial synoptic climatological index for environmental analysis N90-14744
Evaluation of climatic models: Comparison of simulated and observed patterns for past climates [DE90-001228] N90-14755

ATMOSPHERIC DIFFUSION
Meteorological monitoring for environmental/dose assessment and emergency response modeling: How much is enough [DE90-002726] N90-14757

ATMOSPHERIC EFFECTS
Hybrid PE-ray-mode formulation of high frequency propagation in a bilinear tropospheric surface duct N90-14417
Design of a compensation filter for a quadratic phase communication channel N90-14428
A modern trans-ionospheric propagation sensing system N90-14430
Correction of ionospheric effects for the precise orbit determination of satellites N90-14432
Remote sensing of the aerosol scattering coefficient with a multi-field-of view lidar N90-14437
Physical models for aerosol in the marine mixed-layer N90-14438
The effect of oblate spheroidal drops on rain attenuation at 94 GHz: Comparison between theory and experiment N90-14440
TROPO: A technique for predicting propagation and modern performance of digital troposcatter systems N90-14444
Pattern recognition techniques applied to the NASA-ACTS order-wire problem N90-14446

ATMOSPHERIC ENTRY
Optimal trajectories for the aeroassisted flight experiment [NASA-CR-186133] N90-14250
Aerobraking characteristics for several potential manned Mars entry vehicles [NASA-TM-101669] N90-14272

ATMOSPHERIC GENERAL CIRCULATION MODELS
Climate system research studies of global and regional instrumental data [DE90-001205] N90-14707
Evaluation of climatic models: Comparison of simulated and observed patterns for past climates [DE90-001228] N90-14755

ATMOSPHERIC MODELS
Operational Decision Aids for Exploiting or Mitigating Electromagnetic Propagation Effects [AGARD-CP-453] N90-14405
Hybrid PE-ray-mode formulation of high frequency propagation in a bilinear tropospheric surface duct N90-14417
The use of backscatter for modelling ionosphere and jamming in very short term forecasts N90-14434
Physical models for aerosol in the marine mixed-layer N90-14438
The effect of oblate spheroidal drops on rain attenuation at 94 GHz: Comparison between theory and experiment N90-14440
A one-dimensional shipboard model for forecasting refractive effects in the planetary boundary layer N90-14442
A low-order model of the equatorial ocean-atmosphere system N90-14730
Laboratory evaluation and application of microwave absorption properties under simulated conditions for planetary atmospheres [NASA-CR-185916] N90-15025

ATMOSPHERIC PRESSURE
Saltation thresholds and entrainment of fine particles at Earth and Martian pressures [NASA-TM-102193] N90-14997

ATMOSPHERIC RADIATION
Quantifying the link between change in radiative balance and atmospheric temperature [DE90-000819] N90-14721
A low-order model of the equatorial ocean-atmosphere system N90-14730

ATMOSPHERIC SOUNDING
New perspectives for the inversion of backscatter ionograms N90-14427
The use of backscatter for modelling ionosphere and jamming in very short term forecasts N90-14434
Remote sensing of atmospheric water vapour by pressure modulation radiometry N90-14667

ATMOSPHERIC TEMPERATURE
Quantifying the link between change in radiative balance and atmospheric temperature [DE90-000819] N90-14721

ATMOSPHERIC TURBULENCE
Probability density function of optical scintillations (scintillation distribution) [PB89-103912] N90-14906

ATMOSPHERICS
A communications system with an adaptive multi-functional architecture N90-14415

ATOMIC COLLISIONS
Multiple electron capture in close ion-atom collisions [DE90-001541] N90-14885

ATOMIC MOBILITIES
Mobility of sulfur in thermally altered meteorites N90-15010

ATOMIC STRUCTURE
Multiple martensitic transformations, incommensurate/commensurate phases, and charge-density-wave states in plutonium metal: Their consequences [DE90-001235] N90-14350
Atomic structure and spectral perturbations in hot dense plasmas N90-14567
Structural peculiarities and molecular properties of charge complexes formed on positive ion injection into dense inert gas media [DE89-633953] N90-14877

ATOMS
Development of laser excited atomic fluorescence and ionization spectrometric methods [DE90-001567] N90-14320
Multiple electron capture in close ion-atom collisions [DE90-001541] N90-14885
Atomic matching across internal interfaces [DE90-002266] N90-14889

ATTENUATORS
Means for protecting electroexplosive devices which are subject to a wide variety of radio frequency [AD-D014219] N90-14382

ATTITUDE CONTROL
Development of a three-axis trim program [AD-A212883] N90-14237
Techniques for extreme attitude suspension of a wind tunnel model in a magnetic suspension and balance system [NASA-CR-181895] N90-14245

ATTITUDE STABILITY
Techniques for extreme attitude suspension of a wind tunnel model in a magnetic suspension and balance system [NASA-CR-181895] N90-14245

AUSTENITIC STAINLESS STEELS
The metallurgical determinants of toughness as cryogenic temperature [DE90-002331] N90-14351
Microstructure induced by laser shock in an austenitic steel N90-14558
Measuring the thickness of austenitic weld deposits on carbon steel walls using a magnetic method [DE89-635446] N90-14628

AUTOMATIC CONTROL
Automated glass fiber drawing [DE90-000894] N90-14367
CCD TV focal plane guider development and comparison to SIRTF applications [NASA-CR-185977] N90-14900
CIS-lunar space infrastructure lunar technologies: Executive summary [NASA-CR-186220] N90-15029

AUTOMATIC TEST EQUIPMENT
A computer-controlled automated test system for fatigue and fracture testing [DE90-002931] N90-14661

AUTOMOBILE ACCIDENTS
Field evaluation of a Nissan laser collision avoidance system [PB90-105602] N90-14215

AUTOMOBILES
Methodology for the calibration of and data acquisition with a six-degree-of-freedom acceleration measurement device [PB89-233597] N90-14531

AUTOREGRESSIVE PROCESSES
Adaptive clutter rejection filters for airborne Doppler weather radar applied to the detection of low altitude windshear [NASA-CR-186211] N90-14453

AVIONICS
Definition of avionics concepts for a heavy lift cargo vehicle. Volume 1: Executive summary [NASA-CR-183818] N90-14229
Definition of avionics concepts for a heavy lift cargo vehicle, volume 2 [NASA-CR-183819] N90-14230
Preliminary design document: Ground based testbed for avionics systems [NASA-CR-183821] N90-14231
Preliminary design of the Shuttle-C avionics recovery system [NASA-CR-186230] N90-14258

AWARDS
AGARD Highlights 89/2 N90-14184

AXIAL FLOW
Temporally and spatially resolved flow in a two-stage axial compressor. Part 2: Computational assessment [NASA-TM-102273] N90-14236

AXISYMMETRIC BODIES
Tire modeling by finite elements N90-14614

AXISYMMETRIC FLOW
Applications of a new exact solution of the Navier-Stokes equations to flow in pipes of varying width N90-14504

Heat transfer in convective boundary layer and channel flows N90-14505

B

BACKGROUND RADIATION
The thermal behavior of natural backgrounds and its prediction by means of numerical models N90-14436
BACKSCATTERING
New perspectives for the inversion of backscatter ionograms N90-14427
The use of backscatter for modelling ionosphere and jamming in very short term forecasts N90-14434
Simulated Brillouin backscattering in optical fibers: A ring resonator N90-14556
BACTERIA
Comparison of structural subunits of the core light-harvesting complexes of photosynthetic bacteria [DE90-001412] N90-14765
BALANCE
Cryogenic temperature effects on sting-balance deflections in the National Transonic Facility [NASA-TM-4157] N90-14244
BALLOON-BORNE INSTRUMENTS
Kestrel 3 Program [DE90-001796] N90-14209
A large detector for cosmic ray abundance and energy measurements N90-15037
BANDPASS FILTERS
High resolution, wide band Chirp-Z signal analyzer [AD-D014240] N90-14465
Narrow band and wide angle hemispherical interference optical filter [AD-D014238] N90-14904
BARIUM COMPOUNDS
Muon SR investigation of magnetism and superconductivity in (Y(1-x)Pr(x))Ba2Cu3O7 [DE90-000689] N90-14956
BARIUM OXIDES
High resolution-angle resolved photoemission studies of high temperature superconductors [DE89-017691] N90-14950
Effects of shock-induced defects on flux pinning in YBa2Cu3O(7-delta) [DE90-000824] N90-14959
Anisotropy of oxygen tracer diffusion in YBa2Cu3O7-delta single crystals [DE90-001931] N90-14979
BARRIER LAYERS
Fabrication of NBN based electronic devices with silicon barriers [AD-D014230] N90-14463
Multiband photoconductive detector based on layered semiconductor quantum wells [AD-D014232] N90-14936
BASALT
Meteoritic basalts [NASA-CR-185949] N90-15004
BASE PRESSURE
Subsonic sting interference on the aerodynamic characteristics of a family of slanted-base ogive-cylinders [NASA-CR-186193] N90-14204
BASIC (PROGRAMMING LANGUAGE)
Personal computer process data acquisition [DE89-017877] N90-14816
BAYS (STRUCTURAL UNITS)
Control of an experiment to measure acoustic noise in the space shuttle [NPS62-89-022] N90-14869
BEAM INTERACTIONS
Single beam interactions for the study of x ray lasers N90-14573
BEND TESTS
Strength and toughness of monolithic and composite silicon nitrides [NASA-TM-102423] N90-14368
BERING SEA
Tuning of the OSCURS (Ocean Surface Current Simulations) numerical model to ocean surface measurements in the Gulf of Alaska [PB89-103979] N90-14759
BIBLIOGRAPHIES
Rocket studies of the lower ionosphere [NASA-CR-186187] N90-14735
USSR Space Life Sciences Digest. Index to issues 21-25 [NASA-CR-3922(30)] N90-14763
Publications of the Jet Propulsion Laboratory, 1988 [NASA-CR-185956] N90-14995
BINARY ALLOYS
Electrical properties of materials for high temperature strain gage applications [NASA-CR-186192] N90-14534
BINARY MIXTURES
Asymptotic analysis of performance of membrane modules for gas separations [DE90-000699] N90-14316
BINARY STARS
Properties of evolved star circumstellar grains N90-15003
BIOASSAY
Amperometric biosensors for glucose, lactate, and glycolate based on oxidases and redox-modified siloxane polymers [DE90-002301] N90-14541
BIOASTRONAUTICS
USSR Space Life Sciences Digest. Index to issues 21-25 [NASA-CR-3922(30)] N90-14763
BIOCONVERSION
Low-temperature conversion of high-moisture biomass: Continuous reactor system results [DE90-000984] N90-14683
BIOINSTRUMENTATION
Amperometric biosensors for glucose, lactate, and glycolate based on oxidases and redox-modified siloxane polymers [DE90-002301] N90-14541
The development of coherent x ray lasers for x ray holography [DE90-000784] N90-14595
BIOLOGICAL EFFECTS
Biological effects of hyperthermia and potential risk associated with ultrasonic exposure [PB89-100702] N90-14768
BIOMASS
Low-temperature conversion of high-moisture biomass: Continuous reactor system results [DE90-000984] N90-14683
BIOMASS ENERGY PRODUCTION
Low-temperature conversion of high-moisture biomass: Continuous reactor system results [DE90-000984] N90-14683
BIOPOLYMERS
The biocorrosion of copper by biopolymers as examined in situ, in real time FT-IR/CIR/ATR in conjunction with pre and post XPS/AES [DE90-002086] N90-14348
BIOREACTORS
Low-temperature conversion of high-moisture biomass: Continuous reactor system results [DE90-000984] N90-14683
BIOSPHERE
Managing marine protected areas: An action plan [PB89-158778] N90-14701
Climate-biosphere interactions scope of work [PB90-108444] N90-14734
BIREFRINGENCE
Spectral contents readout of birefringent sensor [NASA-CR-179444] N90-14905
BISMUTH
The effect of composition and processing on high T(sub c) superconductors containing bismuth [DE90-002203] N90-14965
BISMUTH OXIDES
Bi-Sr-Ca-Cu-O superconducting ceramics [DE89-636225] N90-14972
BIT SYNCHRONIZATION
Coordination of processing elements in a multiprocessor computer [WO-PATENT-88/04075] N90-14830
BLACK HOLES (ASTRONOMY)
Perturbation methods for the calculation of gravitational waves from slightly non-spherical spacetimes with applications to stellar core collapse N90-15015
Black-hole decay and topological stability in quantum gravity [DE89-618785] N90-15017
BLOCKING
The effects of nonselective and selective beta blockade upon nonshivering thermogenesis during an acute cold exposure in cold acclimated men N90-14767
BLOOD
High-frequency ventilation in dogs with three gases of different densities [AD-A212862] N90-14762
BLOWING
Effect of pylon wake with and without pylon blowing on propeller thrust [NASA-TM-4162] N90-14190
BLUE STARS
Ultraviolet properties of hot stars in globular clusters N90-15007
BLUNT BODIES
Measured and predicted aerodynamic coefficients and shock shapes for Aeroassist Flight Experiment (AFE) configuration [NASA-TP-2956] N90-14185
BOILING
Semi-empirical theory of heat-transfer when boiling [DE89-635418] N90-14984
BONDING
Superplasticity [AGARD-LS-168] N90-14325
BOOSTER ROCKET ENGINES
Review of the Aerospace Safety Advisory Panel report for NASA fiscal year 1990 authorization [GPO-24-234] N90-14213
BORING MACHINES
New tool-holding concept [DE90-000880] N90-14624
BORON
Development of a titanium/boron blending process [DE90-001450] N90-14386
BORON CARBIDES
Synthesis and properties of new preceramic materials [DE90-002562] N90-14373
BORON NITRIDES
Synthesis and properties of new preceramic materials [DE90-002562] N90-14373
BOSONS
Narrow one-channel resonances and their manifestation in the pure elastic scattering of unpolarized particles [DE89-632177] N90-14876
BOUNDARY ELEMENT METHOD
Boundary element analysis of single and multidomain problems in acoustics N90-14867
BOUNDARY LAYER EQUATIONS
Effects of flame stretch on the propagation, extinction, and stability of premixed flames N90-14301
BOUNDARY LAYER FLOW
Heat transfer in convective boundary layer and channel flows N90-14505
Spatial evolution of nonlinear acoustic mode instabilities on hypersonic boundary layers [NASA-TM-102431] N90-14517
BOUNDARY LAYER PLASMAS
Practical aspects of a 2-D edge-plasma model [DE90-002995] N90-14932
BOUNDARY LAYER SEPARATION
Navier-Stokes solutions of 2-D transonic flow over unconventional airfoils N90-14195
Navier-Stokes analysis of airfoils with leading edge ice accretions N90-14196
Computational investigation of incompressible airfoil flows at high angles of attack [AD-A205885] N90-14201
BOUNDARY LAYER STABILITY
Stability of a supersonic boundary layer on a sharp cone at a small angle of attack N90-14510
Spatial evolution of nonlinear acoustic mode instabilities on hypersonic boundary layers [NASA-TM-102431] N90-14517
BOUNDARY LAYER TRANSITION
Visualization of boundary layer transition zone movement on oscillating airfoils with shear-sensitive liquid-crystal coatings [DE89-009570] N90-14210
BOUNDARY LAYERS
A note concerning the onset of three dimensionality and time dependence in Goertler vortices [NASA-CR-181956] N90-14193
Convective boundary layer and modeling of dispersion N90-14731
BOUNDARY VALUE PROBLEMS
Evaluation of the indirect effects of lightning on a system: Double transfer function method [RAE-TRANS-2172] N90-14211
Dynamics and control of flexible spacecraft during and after slewing maneuvers [NASA-CR-186123] N90-14270
Analysis of metal matrix composite structures using a microchemical constitutive theory N90-14290
The stability of Taylor-Couette flow with radial heating N90-14502
Proceedings of the Focused Research Program on Spectral Theory and Boundary Value Problems. Volume 4: Nonlinear Differential Equations [DE90-000920] N90-14780
A tensor product b-spline method for 3D multi-block elliptic grid generation [DE89-017440] N90-14859
Boundary element analysis of single and multidomain problems in acoustics N90-14867
BRAYTON CYCLE
Conceptual design study of a 5 kilowatt solar dynamic Brayton power system using a dome Fresnel lens solar concentrator [NASA-CR-185134] N90-14281
BREATHING APPARATUS
High-frequency ventilation in dogs with three gases of different densities [AD-A212862] N90-14762

Performance evaluation of the Puritan-Bennett crew-member portable protective breathing device as prescribed by portions of FAA action notice A-8150.2
[AD-A211113] N90-14772
Comparison of protective breathing equipment performance at ground level and 8,000 feet altitude using parameters prescribed by portions of FAA action notice A-8150.2
[AD-A212852] N90-14773

BREMSSTRAHLUNG
Numerical simulation of the preheating by x rays in spherical plasmas N90-14564

BRIGHTNESS
Ultrahigh-brightness lasers and their applications
[DE90-000877] N90-14596
Human factors evaluation of electroluminescent display Number 1
[DE90-002231] N90-14777

BRILLOUIN EFFECT
Simulated Brillouin backscattering in optical fibers: A ring resonator N90-14556

BRITTLE MATERIALS
Mechanics of interaction of a crack with microcracks N90-14650

BRITTLENESS
Mechanics of interaction of a crack with microcracks N90-14650

BROADCASTING
The use of broadcast signals for passive sensing in automated HF communication systems N90-14433

BROKEN SYMMETRY
Symmetry breaking bifurcations of a current sheet
[DE90-601005] N90-14864

BUCKLING
Flexural and torsional-flexural buckling of thin-walled open section struts
[ESDU-89007] N90-14643

BUDGETING
Developing integrated parametric planning models for budgeting and managing complex projects
[NASA-CR-186006] N90-14986

BULK MODULUS
Bulk and shear moduli of epoxy encapsulants
[DE90-000899] N90-14371

C

C (PROGRAMMING LANGUAGE)
PCP (Parallel C Preprocessor): A parallel extension of C that is 99 percent fat free
[DE90-002813] N90-14834

CADMIUM TELLURIDES
Thin film cadmium telluride, zinc telluride, and mercury zinc telluride solar cells
[DE89-009499] N90-14681
High-efficiency large-area CdTe modules
[DE89-009498] N90-14689

CALCIUM OXIDES
Prospects for wavelength tunable lasers based on vacancy defects in alkaline-earth oxides
[DE90-001078] N90-14592
Bi-Sr-Ca-Cu-O superconducting ceramics
[DE89-636225] N90-14972

CALIBRATING
Airdata calibration of a high-performance aircraft for measuring atmospheric wind profiles
[NASA-TM-101714] N90-14228
Calibration approach to electron probe microanalysis: A study with PWA-1480, a nickel base superalloy
[NASA-TM-102393] N90-14335
Calibration curves for some standard Gap Tests
[DE89-016599] N90-14389
Methodology for the calibration of and data acquisition with a six-degree-of-freedom acceleration measurement device
[PB89-233597] N90-14531
Single particle friction tests with cellulose acetate sphere samples
[DE89-017537] N90-14622
Results of the 1989 NASA/JPL balloon flight solar cell calibration program
[NASA-CR-186114] N90-14672
MTX (Microwave Tokamak Experiment)/ELF (Electron Laser Facility) 2 microwave power measurements and calibration for the 2-GW, 140-GHz, ELF 2 Free Electron Laser (FEL)
[DE90-000825] N90-14922

CALORIMETERS
Calorimetric measurements on electrochemical cells with Pd-D cathodes
[DE90-002198] N90-14685

CAMERAS
An image compression algorithm for a high-resolution digital still camera
[NASA-CR-185079] N90-14532
Tomographic imagery by multislot coding applied to x ray diagnostics of laser plasmas: Implementation of a direct electronic detection camera N90-14579

CANARD CONFIGURATIONS
Validation of a computer code for analysis of subsonic aerodynamic performance of wings with flaps in combination with a canard or horizontal tail and an application to optimization
[NASA-TP-2961] N90-14187

CANOPIES (VEGETATION)
Canopy stomatal conductance
[DE89-016860] N90-14711
Characterization of cloud chemistry and frequency of canopy exposure to clouds in the Sierra Nevada
[PB89-104035] N90-14753

CAPACITANCE
A capacitive technique for real-time monitoring polymer coating thickness on carbon filaments during prepregging process
[NASA-TM-101682] N90-14533

CAPACITORS
Temperature stable ceramic dielectric compositions
[AD-D014209] N90-14358

CAPILLARIES
Combined capillary electrophoresis and electrospray ionization mass spectrometry
[DE90-001903] N90-14322

CARBON
The conversion of carbonaceous materials to clean carbon and co-product gaseous fuel
[DE90-001561] N90-14387
Phase changes in carbon and nitrogen systems: Their effects on the detonation properties of high explosives
[DE90-000829] N90-14392

CARBON DIOXIDE
Global energy and the greenhouse issue
[DE90-001394] N90-14709
Canopy stomatal conductance
[DE89-016860] N90-14711
Strategy for monitoring the effects of land use change on atmospheric CO2 concentrations
[DE90-001635] N90-14722

CARBON DIOXIDE CONCENTRATION
Quantifying the link between change in radiative balance and atmospheric temperature
[DE90-000819] N90-14721
Carbon dioxide and climate: Summaries of research in FY 1989
[DE90-001791] N90-14723
US energy use: New technologies and policies in response to global warming
[DE90-002170] N90-14724

CARBON DIOXIDE LASERS
Automated glass fiber drawing
[DE90-000894] N90-14367
Eurolaser CO2 laser
[ETN-90-95907] N90-14582
A compact, high-powered far-infrared (FIR) laser
[DE89-016786] N90-14597

CARBON FIBERS
Method for stabilization of pan-based carbon fibers
[AD-D014228] N90-14288
Carbon fiber reinforced metal matrix composites
[AD-D014245] N90-14289
A capacitive technique for real-time monitoring polymer coating thickness on carbon filaments during prepregging process
[NASA-TM-101682] N90-14533

CARBON MONOXIDE
Strategy for monitoring the effects of land use change on atmospheric CO2 concentrations
[DE90-001635] N90-14722

CARBON STARS
Properties of evolved star circumstellar grains N90-15003

CARBON STEELS
Effects of dislocation substructure and prestrain on fracture behavior in aluminum and steel alloys N90-14334
Measuring the thickness of austenitic weld deposits on carbon steel walls using a magnetic method
[DE89-635446] N90-14628

CARBONACEOUS MATERIALS
The conversion of carbonaceous materials to clean carbon and co-product gaseous fuel
[DE90-001561] N90-14387

CARDIOVASCULAR SYSTEM
The development of a model of the human responses to load carriage N90-14775

CARGO
Control of an experiment to measure acoustic noise in the space shuttle
[NPS62-89-022] N90-14869

CARGO AIRCRAFT
Design of a spanloader cargo aircraft
[NASA-CR-186046] N90-14216

CARIBBEAN REGION
Summary of 1989 Atlantic tropical cyclone activity and seasonal forecast verification N90-14743

CASTING
The manufacture of superplastic alloys N90-14333

CATHODES
Silver-nickel composite cathodes for alkaline secondary batteries
[AD-D014231] N90-14464
Gigatron: A new technology for microwave power devices
[DE90-001066] N90-14483
Calorimetric measurements on electrochemical cells with Pd-D cathodes
[DE90-002198] N90-14685

CAVITATION FLOW
Cavitation and superplasticity N90-14329
Cavitation-controlled ultrasonic agitator
[DE90-002773] N90-14871

CAVITY RESONATORS
Hydrogen radical enhanced growth of solar cells
[DE89-009497] N90-14694
RF superconductivity research and development at Los Alamos National Laboratory
[DE90-002440] N90-14969

CELL CATHODES
Electrochemical preparation of silver oxide electrodes having high thermal stability
[AD-D014224] N90-14460
Silver composite cathodes for alkaline secondary batteries
[AD-D014227] N90-14462

CELLULOSE
Single particle friction tests with cellulose acetate sphere samples
[DE89-017537] N90-14622

CENTRAL PROCESSING UNITS
Concurrent processing adaptation of aeroplastic analysis of propfans
[NASA-TM-102455] N90-14656
Coordination of processing elements in a multiprocessor computer
[WO-PATENT-88/04075] N90-14830
Architectures for reasoning in parallel
[NASA-CR-186237] N90-14836

CERAMIC MATRIX COMPOSITES
Oxidation effects on the mechanical properties of SiC fiber-reinforced reaction-bonded silicon nitride matrix composites
[NASA-TM-102360] N90-14287

CERAMICS
Carbon fiber reinforced metal matrix composites
[AD-D014245] N90-14289
Advances and future directions in superplastic materials N90-14328
Temperature stable ceramic dielectric compositions
[AD-D014209] N90-14358
Structure-property relationships in surface-modified ceramics. NATO Advanced Science Institutes, series E: Applied Sciences, volume 170
[AD-A212939] N90-14359
Mechanisms of wear in structural ceramic materials N90-14360
Ordered ceramic membranes
[DE89-017426] N90-14364
Perturbed angular correlations in zirconia ceramics
[DE89-017272] N90-14369
Computer synthesis of ceramic preforms for molten-metal infiltration
[DE90-000826] N90-14370
Synthesis and properties of new preceramic materials
[DE90-002562] N90-14373
The 7th International Conference on Ceramics
[DE90-002144] N90-14374
Numerical and empirical verification of the stress state in a ceramic, button-head, tensile specimen
[DE90-001645] N90-14375
Thermal/structural analyses of several hydrogen-cooled leading-edge concepts for hypersonic flight vehicles
[NASA-TM-102391] N90-14511
Field testing of a ceramic heat exchanger for heat recovery application
[DE90-002082] N90-14523
Mechanics of interaction of a crack with microcracks N90-14650
Interfacial effects in monolithic solid oxide fuel cells
[DE90-001914] N90-14690
Ion beam analysis and modification of thin-film, high-temperature superconductors
[DE90-000918] N90-14941
Solid State Division
[DE90-000979] N90-14945
Bi-Sr-Ca-Cu-O superconducting ceramics
[DE89-636225] N90-14972

Macroscopic persistent currents in high temperature ceramic superconductors
[DE89-636232] N90-14973

CERENKOV COUNTERS
A large detector for cosmic ray abundance and energy measurements N90-15037

CERENKOV RADIATION
A large detector for cosmic ray abundance and energy measurements N90-15037

CHANNEL FLOW
Heat transfer in convective boundary layer and channel flows N90-14505
Unsteady hydromagnetic flow of a radiating gas in a vertical channel with axial temperature variation
[DE90-600934] N90-14525

CHAOS
Chaotic behavior in nonlinear polarization dynamics
[DE89-013453] N90-14589

CHARACTER RECOGNITION
Proceedings of the Conference on Application of Scanning Methodologies in Libraries
[PB89-233415] N90-14990

CHARACTERIZATION
Nondestructive evaluation of flaw clusters and thin layer interfaces N90-14633
The processes of scientific research: The strategy of experimentation N90-14788
Microwave characterization of high-temperature superconductors
[DE90-002408] N90-14968

CHARGE COUPLED DEVICES
CCD TV focal plane guider development and comparison to SIRTF applications
[NASA-CR-185977] N90-14900

CHARGE EFFICIENCY
Terrestrial nickel/hydrogen battery development at Johnson Controls, Inc.
[DE89-015843] N90-14471
Sodium/sulfur evaluation at SNL
[DE89-015846] N90-14472

CHARGE TRANSFER
Charge transfer and bond lengths in YBa2Cu(sub 3-x)M(sub x)O(sub 6+y)
[DE90-002241] N90-14966

CHARGING
Terrestrial nickel/hydrogen battery development at Johnson Controls, Inc.
[DE89-015843] N90-14471

CHARTS
NORDA's pattern analysis laboratory: Current contributions to naval mapping, charting, and geodesy
[AD-A212731] N90-14665

CHEBYSHEV APPROXIMATION
Modified Chebyshev pseudospectral method with O(N exp -1) time step restriction
[NASA-CR-181958] N90-14848

CHEMICAL ANALYSIS
Laboratory testing of Sonnenschein DF6V180 6 volt traction battery
[DE90-002080] N90-14486

CHEMICAL COMPOSITION
Effects of composition and age hardening on precious metal electrical contacts
[DE88-008791] N90-14476
BES welding science contractors summary report, 1988 to 1989
[DE90-001004] N90-14619
The effect of composition and processing on high T(sub c) superconductors containing bismuth
[DE90-002203] N90-14965

CHEMICAL ELEMENTS
The Periodic Law at high pressures
[DE90-000837] N90-14319

CHEMICAL ENGINEERING
Synthesis and properties of new preceramic materials
[DE90-002562] N90-14373

CHEMICAL EXPLOSIONS
Fast transit gas- and condensed-phase chemistry of energetic materials
[DE90-001656] N90-14395

CHEMICAL REACTIONS
Shock-induced solid state reactions and phase transitions: X ray profile studies on shock-modified Fe3O4 and ZrO2 powders
[DE90-000669] N90-14315
Photoconversion of inorganics to methane
[PB89-230643] N90-14379
Non-equilibrium effects of slow diffusion controlled reactions on the properties of explosives
[DE90-000822] N90-14391

CHEMOTHERAPY
The effects of nonselective and selective beta blockade upon nonshivering thermogenesis during an acute cold exposure in cold acclimated men N90-14767

CHIRP SIGNALS
High resolution, wide band Chirp-Z signal analyzer
[AD-D014240] N90-14465

CHLOROPHYLLS
Comparison of structural subunits of the core light-harvesting complexes of photosynthetic bacteria
[DE90-001412] N90-14765

CHONDRITES
Abstracts for the 52nd Annual Meeting of the Meteoritical Society
[NASA-CR-186160] N90-14998
Mobility of sulfur in thermally altered meteorites N90-15010

CHONDRULE
Abstracts for the 52nd Annual Meeting of the Meteoritical Society
[NASA-CR-186160] N90-14998

CHROMATES
High temperature chemistry of complex vaporization/decomposition processes
[DE89-016559] N90-14306

CHROMIUM
Magnetotransport studies of epitaxial Cr thin films
[DE90-001930] N90-14975

CHRONOLOGY
Chronology of KSC and KSC related events for 1988
[NASA-TM-101915] N90-15040

CIRCUITS
Laser probing non-cylindrical Z-pinch in near-isolator region of a discharged chamber
[DE89-632018] N90-14912

CLASSIFICATIONS
Classification of modular invariant partition functions for the twisted N=2 superconformal algebra, twisted SU(2) Kac-Moody algebra and D(sub 2K) parafermions
[DE90-600767] N90-14853
The Apollo 15 coarse fines (4-10 mm)
[NASA-TM-101934] N90-15027

CLEAN FUELS
The conversion of carbonaceous materials to clean carbon and co-product gaseous fuel
[DE90-001561] N90-14387

CLIMATE CHANGE
Climate system research studies of global and regional instrumental data
[DE90-001205] N90-14707
Global energy and the greenhouse issue
[DE90-001394] N90-14709
International Conference on Global and Regional Atmospheric Environmental Chemistry and visit to Hangzhou, China, foreign trip report
[DE90-000099] N90-14713
Climate projections with regional resolution
[DE90-000858] N90-14715
Quantifying the link between change in radiative balance and atmospheric temperature
[DE90-000819] N90-14721
Carbon dioxide and climate: Summaries of research in FY 1989
[DE90-001791] N90-14723
US energy use: New technologies and policies in response to global warming
[DE90-002170] N90-14724
Climate-biosphere interactions scope of work
[PB90-106444] N90-14734
Evaluation of climatic models: Comparison of simulated and observed patterns for past climates
[DE90-001228] N90-14755

CLIMATOLOGY
A rough transform technique for extracting lead features from sea ice imagery
[AD-A212758] N90-14666
Climate-biosphere interactions scope of work
[PB90-106444] N90-14734
The identification of terrain-induced circulations using principal components
[DE90-001991] N90-14739
The development of a spatial synoptic climatological index for environmental analysis N90-14744
Inverted surface troughs accompanying Rocky Mountain lee-side cyclogenesis N90-14746
Use of operational 0-6 and 3-9 h quantitative precipitation forecasts for predicting heavy rain events
[PB90-103946] N90-14750
Climatology of Lawrence Livermore National Laboratory
[DE90-000905] N90-14756

CLOSED ECOLOGICAL SYSTEMS
Engineering sciences design. Design and implementation of components for a bioregenerative system for growing higher order plants in space
[NASA-CR-186056] N90-14761

CLOUDS (METEOROLOGY)
Characterization of cloud chemistry and frequency of canopy exposure to clouds in the Sierra Nevada
[PB89-104035] N90-14753

CLUTTER
Adaptive clutter rejection filters for airborne Doppler weather radar applied to the detection of low altitude windshear
[NASA-CR-186211] N90-14453
The effects of clutter-rejection filtering on estimating weather spectrum parameters
[NASA-CR-186212] N90-14754

COAL
Chemistry of large molecules
[DE90-000813] N90-14366
Analysis of acid rain and associated phenomena
[DE90-002555] N90-14725

COANDA EFFECT
An experimental and theoretical study of the aeroacoustics of external-Coanda gas flares N90-14495

COATINGS
Visualization of boundary layer transition zone movement on oscillating airfoils with shear-sensitive liquid-crystal coatings
[DE89-009570] N90-14210
An electroformed nickel-sulfur alloy for a nose cone
[DE90-000866] N90-14337
Dissipation measurement in high T(sub c) superconductors with electromagnetic probes
[DE90-002058] N90-14963

COAXIAL FLOW
Numerical modeling of supersonic turbulent reacting free shear layers N90-14197

COAXIAL PLASMA ACCELERATORS
Energy deposition in low power coaxial plasma thrusters N90-14911

CODING
SAND DEVIL: A digital video link for telemetry applications
[DE90-001879] N90-14259

COEFFICIENT OF FRICTION
Finite element analysis of frictional contact problems N90-14612

COGNITION
Cognitive and Neural Sciences Division 1989 programs
[AD-A212634] N90-14789
Workload induced spatio-temporal distortions and safety of flight
[DE89-016613] N90-14771

COHERENT RADIATION
Laser probing non-cylindrical Z-pinch in near-isolator region of a discharged chamber
[DE89-632018] N90-14912

COLD GAS
Very high resolution radio observations of molecular cloud cores N90-15013

COLD WORKING
A theoretical investigation of the column behavior of cold-formed square hollow sections
[PB89-225981] N90-14645
A finite strip method for the elastic-plastic large displacement analysis of thin-walled and cold-formed steel sections
[PB89-226021] N90-14647

COLLISION AVOIDANCE
Field evaluation of a Nissan laser collision avoidance system
[PB90-105602] N90-14215
Programmable near-infrared ranging system
[AD-D014237] N90-14903

COLLISIONLESS PLASMAS
Ion collection by probing objects in flowing magnetized plasmas
[DE90-001711] N90-14916

COLLISIONS
Granular flow: Numerical simulation of dry granular flows and calculation of hydrodynamic interactions in suspensions
[DE89-017544] N90-14518

COLOR CENTERS
Prospects for wavelength tunable lasers based on vacancy defects in alkaline-earth oxides
[DE90-001078] N90-14592

COLUMNS
A theoretical investigation of the column behavior of cold-formed square hollow sections
[PB89-225981] N90-14645

COMBUSTION
Acoustic-vortical-combustion interaction in a solid fuel ramjet simulator N90-14234

COMBUSTION CHAMBERS
Investigation of combustion instability in ramjet combustors N90-14303
System design and performance prediction of a free-piston Stirling engine/magnetic coupling/compressor assembly in a gas residential heat pump
[DE89-016070] N90-14696

COMBUSTION PRODUCTS
A new simulation method for the efficient calculation of benchmarks for detonation products equations of state
[DE90-001837] N90-14522
Environmental quality and the shift to alternative fuels: Progress and interim findings of a Department of Energy study of transition in vehicular power systems
[DE90-002178] N90-14716
Analysis of acid rain and associated phenomena
[DE90-002555] N90-14725
COMBUSTION STABILITY
A surface coupled flamelet approach to dynamic response in heterogeneous propellant combustion N90-14302
Investigation of combustion instability in ramjet combustors N90-14303
COMET NUCLEI
Hypervelocity impact studies on the Giotto comet Halley mission N90-15008
COMMAND AND CONTROL
Propagation-based decision aids in the U.S. Navy N90-14410
COMMUNICATION NETWORKS
Data Link Processor (DLP) operational test and evaluation/integration test plan
[DOT/FAA/CT-TN89/32] N90-14404
Configuration development for ROMENET
[AD-A213367] N90-14450
Multiple crossbar network: A switched high-speed local network
[DE90-001839] N90-14833
COMMUTER AIRCRAFT
Preliminary design of four aircraft to service the California Corridor in the year 2010: The California Condor, California Sky-Hopper, high capacity short range transport tilt rotor aircraft needed to simplify intercity transportation
[NASA-CR-186232] N90-14226
COMPACTING
Superconducting and microstructural properties of shock-compacted high-T sub c oxide powders
[DE90-000823] N90-14958
Effects of shock-induced defects on flux pinning in YBa2Cu3O(7-delta)
[DE90-000824] N90-14959
Shock-induced defects and flux pinning in YBa2Cu3O sub 7-delta + Ag composites
[DE90-000827] N90-14960
Micro-scale simulation of dynamic compaction of oxide and metal powder mixture
[DE90-002220] N90-14978
COMPENSATORS
Optimal stochastic modeling and control of flexible structures
[AD-A212347] N90-14269
COMPLEX SYSTEMS
Solution bias in complex systems modeling
[DE90-002001] N90-14858
COMPOSITE MATERIALS
AGARD Highlights 89/2 N90-14184
Application of neutron diffraction NDE to high-temperature superconducting composites
[DE90-002184] N90-14295
Fiber-optic sensors for composite cure analysis and lifetime nondestructive evaluation
[DE90-001739] N90-14296
High-temperature corrosion of heat exchanger materials
[DE90-001963] N90-14352
Computer synthesis of ceramic preforms for molten-metal infiltration
[DE90-000826] N90-14370
Reactive flow measurements and calculations for ZrH2-based composite explosives
[DE90-000831] N90-14393
Silver-nickel composite cathodes for alkaline secondary batteries
[AD-D014231] N90-14464
COMPOSITE STRUCTURES
Measurement of damping of graphite epoxy composite materials and structural joints
[NASA-CR-183802] N90-14286
Analysis of metal matrix composite structures using a microchemical constitutive theory N90-14290
Strength and toughness of monolithic and composite silicon nitrides
[NASA-TM-102423] N90-14368
COMPOUNDING
Development of a titanium/boron blending process
[DE90-001450] N90-14386
COMPRESSIBLE FLOW
Embedded function methods for compressible high speed turbulent flow
[NASA-CR-186131] N90-14498
COMPRESSING
Electric-gun studies of conductors in high magnetic fields and experiments in dynamic flux compression
[DE90-000815] N90-14470
Comparison of protective breathing equipment performance at ground level and 8,000 feet altitude using parameters prescribed by portions of FAA action notice A-8150.2
[AD-A212852] N90-14773
COMPUTATION
Example of procedure in calculation of control hinge moments
[ESDU-89010] N90-14240
COMPUTATIONAL FLUID DYNAMICS
Numerical investigations in three-dimensional internal flows
[NASA-CR-186068] N90-14189
Efficient real gas Navier-Stokes computations of high speed flows using an LU scheme
[NASA-TM-102429] N90-14203
An analysis of the viscous flow through a compact radial turbine by the average passage approach
[NASA-TM-102471] N90-14206
Advanced 3-D CFD algorithm for turbomachinery N90-14233
Temporally and spatially resolved flow in a two-stage axial compressor. Part 2: Computational assessment
[NASA-TM-102273] N90-14236
A dynamic multiblock approach to solving the unsteady Euler equations about complex configurations N90-14497
An entropy based approach to nonlinear stability N90-14500
Applications of a new exact solution of the Navier-Stokes equations to flow in pipes of varying width N90-14504
A numerical technique for analysis of resistojet nozzle flow N90-14506
An experimental investigation of shear layer mixing in supersonic flows N90-14508
Comparative study of the vorticity field in turbulent flows: Theory, experiments, and computations
[DE90-001399] N90-14516
COMPUTATIONAL GRIDS
A numerical technique for analysis of resistojet nozzle flow N90-14506
CTH: A three-dimensional shock wave physics code
[DE89-016529] N90-14528
Modified Chebyshev pseudospectral method with O(N exp -1) time step restriction
[NASA-CR-181958] N90-14848
COMPUTER AIDED DESIGN
Chemistry of large molecules
[DE90-000813] N90-14366
Communication Overview Program (COP) N90-14435
Integrating and enhancing tools for ASIC (Application-Specific Integrated Circuits) design using MOSIS (Metal Oxide Semiconductor Implementation Service) fabrication
[DE90-001601] N90-14475
Reuse research plans at Langley Research Center N90-14797
Selecting and effectively using a computer aided software engineering tool
[DE89-017876] N90-14815
COMPUTER AIDED MANUFACTURING
Computer synthesis of ceramic preforms for molten-metal infiltration
[DE90-000826] N90-14370
COMPUTER ASSISTED INSTRUCTION
Workshop on synoptic meteorology instruction
[PB90-109950] N90-14751
COMPUTER DESIGN
High volume data storage architecture analysis
[NASA-CR-186239] N90-14784
COMPUTER GRAPHICS
Engineer's Refractive Effects Prediction System (EREPS) N90-14411
GRAFIN: GRAFIX interactive manual
[PB89-232136] N90-14809
A graphically oriented specification language for automatic code generation. GRASP/Ada: A Graphical Representation of Algorithms, Structure, and Processes for Ada, phase 1
[NASA-CR-183212] N90-14813
The High-Speed Channel (HSC) and ultra-speed networks
[DE89-015283] N90-14819
COMPUTER INFORMATION SECURITY
How robust are distributed systems
[NASA-CR-186242] N90-14837
COMPUTER NETWORKS
Configuration development for ROMENET
[AD-A213367] N90-14450
NORDA's pattern analysis laboratory: Current contributions to naval mapping, charting, and geodesy
[AD-A212731] N90-14665
Integrated computer-based tools to facilitate environmental monitoring, assessment, and restoration
[DE90-002732] N90-14717
AdaNET services N90-14806
The High-Speed Channel (HSC) and ultra-speed networks
[DE89-015283] N90-14819
Multiple crossbar network: Integrated supercomputing framework
[DE89-012614] N90-14831
The Delta-t transport protocol: Features and experience useful for high performance networks
[DE89-016542] N90-14832
Generalization in backpropagation networks: An empirical study using image data
[DE89-012658] N90-14835
How robust are distributed systems
[NASA-CR-186242] N90-14837
COMPUTER PROGRAMMING
Force user's manual: A portable, parallel FORTRAN
[NASA-CR-4265] N90-14785
QUEST/Ada: Query utility environment for software testing of Ada
[NASA-CR-186121] N90-14787
Impact of domain analysis on reuse methods N90-14792
Classic-Ada(TM) N90-14793
Prototype software reuse environment at Goddard Space Flight Center N90-14794
Johnson Space Center software reuse activity N90-14796
Reuse research plans at Langley Research Center N90-14797
Reuse at the Software Productivity Consortium N90-14798
SSFP approach to software reuse N90-14799
Level 2 software reuse study N90-14800
Support for life-cycle product reuse in NASA's SSE N90-14802
Application of reusable software components at the SEI N90-14804
Technology transfer in software engineering N90-14805
AdaNET services N90-14806
Advanced Software Development Workstation Project N90-14807
A graphically oriented specification language for automatic code generation. GRASP/Ada: A Graphical Representation of Algorithms, Structure, and Processes for Ada, phase 1
[NASA-CR-183212] N90-14813
Selecting and effectively using a computer aided software engineering tool
[DE89-017876] N90-14815
Programmable near-infrared ranging system
[AD-D014237] N90-14903
COMPUTER PROGRAMS
Validation of a computer code for analysis of subsonic aerodynamic performance of wings with flaps in combination with a canard or horizontal tail and an application to optimization
[NASA-TP-2961] N90-14187
Program VSAERO theory document: A computer program for calculating nonlinear aerodynamic characteristics of arbitrary configurations
[NASA-CR-4023] N90-14200
An analysis of the viscous flow through a compact radial turbine by the average passage approach
[NASA-TM-102471] N90-14206
RAMSCRAM: A flexible ramjet/scramjet engine simulation program
[NASA-TM-102451] N90-14235
Development of a three-axis trim program
[AD-A212883] N90-14237
Fluid flow analysis of the SSME high pressure fuel and oxidizer turbine coolant systems
[NASA-CR-183736] N90-14277
Thermophysical properties of isopropyl alcohol. Part 2: Thermodynamic properties at elevated pressures
[ESDU-89020-PT-2] N90-14300
Data Link Processor (DLP) operational test and evaluation/integration test plan
[DOT/FAA/CT-TN89/32] N90-14404
Long wave propagation assessment N90-14414
TROPO: A technique for predicting propagation and modem performance of digital troposcatter systems N90-14444
The FTZ HF propagation model for use on small computers and its accuracy N90-14447
A software-based controller for generation of synchronized pulses for use with rotating machinery
[DE89-016672] N90-14477
Surface flow and heating distributions on a cylinder in near wake of Aeroassist Flight Experiment (AFE) configuration at incidence in Mach 10 Air
[NASA-TP-2954] N90-14493

An experimental investigation of shear layer mixing in supersonic flows N90-14508
Granular flow: Numerical simulation of dry granular flows and calculation of hydrodynamic interactions in suspensions
[DE89-017544] N90-14518
CTH: A three-dimensional shock wave physics code
[DE89-016529] N90-14528
Numerical simulations of free-electron laser oscillators
[DE89-003488] N90-14588
INEX (Integrated Numerical Experiment) simulations of the Los Alamos HIBAF (High-Brightness Accelerator Free-Electron Laser) free-electron laser MOPA (Master Oscillator Power Amplifier) experiment
[DE90-002387] N90-14601
Verification of the NIKE3D structural analysis code by comparison against the analytic solution for a spherical cavity under a far-field uniaxial stress
[DE90-000929] N90-14653
Critical time step estimation for three-dimensional explicit impact analysis
[DE90-002187] N90-14662
Computer simulation of wind/diesel system operation
[DE89-009445] N90-14688
User's guide to PMESH: A grid-generation program for single-rotation and counterrotation advanced turboprops
[NASA-CR-185156] N90-14783
The processes of scientific research: The strategy of experimentation N90-14788
Software Reuse Issues
[NASA-CP-3057] N90-14789
Automated reuseable components system study results N90-14790
Knowledge-based reusable software synthesis system N90-14791
Impact of domain analysis on reuse methods N90-14792
JPL reuse program N90-14795
Initial Ada components evaluation N90-14803
Application of reusable software components at the SEI N90-14804
AdaNET services N90-14806
Personal computer process data acquisition
[DE89-017877] N90-14816
Program CICC flow and heat transfer in Cable-In-Conduit Conductors
[DE90-001519] N90-14818
Using object-oriented development to support prototyping
[DE90-000547] N90-14821
Parallel mathematical software
[DE90-002694] N90-14822
Interactive multidimensional data analysis and understanding
[DE90-001794] N90-14824
A tutorial on software reliability engineering
[DE89-012368] N90-14828
The Aerospace Energy Systems Laboratory: A BITBUS networking application
[NASA-TM-4149] N90-14829
Boundary element analysis of single and multidomain problems in acoustics N90-14867
REFLECT: A computer program for the x ray reflectivity of bent perfect crystals
[DE90-001266] N90-14946
Micro-scale simulation of dynamic compaction of oxide and metal powder mixture
[DE90-002220] N90-14978
The instability and fragmentation of the envelope of supernova 1987A N90-15011

COMPUTER STORAGE DEVICES
An image compression algorithm for a high-resolution digital still camera
[NASA-CR-185079] N90-14532

COMPUTER SYSTEMS DESIGN
Reuse research plans at Langley Research Center N90-14797
Continuation of research in software for space operations support
[NASA-CR-186092] N90-14808
The design of a computer system for image simulation and image processing of high resolution electron micrographs
[DE90-000179] N90-14820

COMPUTER SYSTEMS PERFORMANCE
MIPs and BIPs are megaflops: Limits of unidimensional assessments
[DE89-015707] N90-14770
High performance parallel architectures
[DE90-001055] N90-14782
Coordination of processing elements in a multiprocessor computer
[WO-PATENT-88/04075] N90-14830
Multiple crossbar network: Integrated supercomputing framework
[DE89-012614] N90-14831

COMPUTER SYSTEMS PROGRAMS
JPL reuse program N90-14795
Control of an experiment to measure acoustic noise in the space shuttle
[NPS62-89-022] N90-14869

COMPUTER VISION
Robotic vision system
[AD-D014246] N90-14838
NETRA: A parallel architecture for integrated vision systems. 1: Architecture and organization
[NASA-CR-185955] N90-14839

COMPUTERIZED SIMULATION
Unsteady aerodynamic simulation of multiple bodies in relative motion: A prototype method
[NASA-TM-102181] N90-14188
An investigation of the bursting of trailing vortices using numerical simulation N90-14191
RAMSCRAM: A flexible ramjet/scramjet engine simulation program
[NASA-TM-102451] N90-14235
Temporally and spatially resolved flow in a two-stage axial compressor. Part 2: Computational assessment
[NASA-TM-102273] N90-14236
Solving the blow-by problem in a two-stage gun
[DE90-000842] N90-14246
Fluid flow analysis of the SSME high pressure fuel and oxidizer turbine coolant systems
[NASA-CR-183736] N90-14277
Effects of dislocation substructure and prestrain on fracture behavior in aluminum and steel alloys N90-14334
Characterization of nanophase materials by x ray diffraction and computer simulation
[DE90-002270] N90-14378
Weather satellite and computer modeling approaches to assessing propagation over marine environments N90-14443
A radar simulation program for a 1024-processor hypercube
[DE89-014494] N90-14455
Testing and performance of a high-gain flux-compression generator
[DE90-002808] N90-14492
Multigrid solutions of elliptic fluid flow problems N90-14507
Perturbations in high-velocity gas flow
[DE90-000539] N90-14520
A new simulation method for the efficient calculation of benchmarks for detonation products equations of state
[DE90-001837] N90-14522
Pipe and bend erosion by pneumatic transport of solids at high temperature
[DE89-015741] N90-14524
CTH: A three-dimensional shock wave physics code
[DE89-016529] N90-14528
Numerical simulation of the preheating by x rays in spherical plasmas N90-14564
Theoretical studies of solar lasers and converters
[NASA-CR-186194] N90-14583
Numerical simulation of laser radiation propagation in non-uniform absorbing medium. Geometrical optics approximation
[DE89-632014] N90-14585
Numerical simulations of free-electron laser oscillators
[DE89-003488] N90-14588
INEX (Integrated Numerical Experiment) simulations of the Los Alamos HIBAF (High-Brightness Accelerator Free-Electron Laser) free-electron laser MOPA (Master Oscillator Power Amplifier) experiment
[DE90-002387] N90-14601
Hypervelocity impact calculations using CTH: Case studies
[DE90-002891] N90-14632
Computer simulation of wind/diesel system operation
[DE89-009445] N90-14688
The effects of clutter-rejection filtering on estimating weather spectrum parameters
[NASA-CR-186212] N90-14754
Evaluation of climatic models: Comparison of simulated and observed patterns for past climates
[DE90-001228] N90-14755
Some edge-enhancing operators and their applications to image enhancement and edge detection N90-14810
The design of a computer system for image simulation and image processing of high resolution electron micrographs
[DE90-000179] N90-14820
Solution bias in complex systems modeling
[DE90-002001] N90-14858
Symmetry breaking bifurcations of a current sheet
[DE90-601005] N90-14864
Computation of electromagnetic effects in a tokamak due to a plasma disruption
[DE90-001764] N90-14931
Particle simulations in magnetospheric plasmas
[NASA-CR-186238] N90-14934
Micro-scale simulation of dynamic compaction of oxide and metal powder mixture
[DE90-002220] N90-14978
Dynamical simulation of dislocation microstructure
[DE90-003192] N90-14982
A model of the thermal and electrical properties of cosmic dust particles N90-15014

CONCENTRATION (COMPOSITION)
Profile measurements of sulfur dioxide, nitrogen oxides, and nitric acid deposition velocities in California's south coast air basin
[PB90-104001] N90-14703

CONCURRENT PROCESSING
The Tactical Environmental Support System (TESS(3)) N90-14409
Group implicit concurrent algorithms in nonlinear structural dynamics
[NASA-CR-185950] N90-14638
Concurrent processing adaptation of aeroplastic analysis of propfans
[NASA-TM-102455] N90-14656
Strand: A practical parallel programming language
[DE90-002861] N90-14825

CONDENSED MATTER PHYSICS
Interaction of low-energy electrons and positrons with condensed matter: Stopping powers and inelastic mean free paths from optical data
[DE90-001001] N90-14882

CONDUCTIVE HEAT TRANSFER
Cooling flows in clusters of galaxies N90-15009

CONDUCTORS
Further studies of transverse stress effects in cable-in-conduit conductors
[DE90-001517] N90-14484

CONFERENCES
Flight in adverse environmental conditions
[AGARD-AR-277] N90-14218
Superplasticity
[AGARD-LS-168] N90-14325
The 7th International Conference on Ceramics
[DE90-002144] N90-14374
Operational Decision Aids for Exploiting or Mitigating Electromagnetic Propagation Effects
[AGARD-CP-453] N90-14405
Proceedings of the First Annual Fuel Cells Contractors Review Meeting
[DE89-011699] N90-14675
International Conference on Global and Regional Atmospheric Environmental Chemistry and visit to Hangzhou, China, foreign trip report
[DE90-000099] N90-14713
Workshop on synoptic meteorology instruction
[PB90-109950] N90-14751
Mid-Oceanic Ridge: A Dynamic Global System
[PB89-198691] N90-14758
Proceedings of the Focused Research Program on Spectral Theory and Boundary Value Problems. Volume 4: Nonlinear Differential Equations
[DE90-000920] N90-14780
Software Reuse Issues
[NASA-CP-3057] N90-14789
Proceedings of the Conference on High-Spin Nuclear Structure and Novel Nuclear Shapes
[DE88-013968] N90-14875
NIKHEF-K contributions to the 1989 Particle Accelerator Conference
[NIKHEF/AMPS/89/03] N90-14891
Proceedings of the Conference on Application of Scanning Methodologies in Libraries
[PB89-233415] N90-14990
Nomenclature for physical mapping of complex genomes
[DE89-015173] N90-14994
Abstracts for the 52nd Annual Meeting of the Meteoritical Society
[NASA-CR-186160] N90-14998

CONFIGURATION INTERACTION
A diagnostic for determining the quality of single-reference electron correlation methods
[NASA-TM-101929] N90-14874

CONGRESSIONAL REPORTS
Consumer Ozone Protection Act of 1989
[S-HRG-101-377] N90-14708

CONIFERS
Proceedings of the US/FRG (Fed. Republic of Germany) research symposium: Effects of Atmospheric Pollutants on the Spruce-Fir Forests of the Eastern United States and the Fed. Republic of Germany
[PB90-107160] N90-14704

CONSERVATION LAWS
On the application of subcell resolution to conservation laws with stiff source terms
[NASA-TM-102384] N90-14844

Local error estimates for discontinuous solutions of nonlinear hyperbolic equations
[NASA-CR-181960] N90-14847

CONSTITUTIVE EQUATIONS
Analysis of metal matrix composite structures using a microchemical constitutive theory N90-14290

CONSTRAINTS
Stability and dynamics of constrained flexible multibody systems N90-14609

CONSTRUCTION
M.I.N.G., Mars Investment for a New Generation: Robotic construction of a permanently manned Mars base
[NASA-CR-186224] N90-15028

CONTAMINANTS
Analysis of acid rain and associated phenomena
[DE90-002555] N90-14725
Characterization of cloud chemistry and frequency of canopy exposure to clouds in the Sierra Nevada
[PB89-104035] N90-14753
Performance evaluation of the Puritan-Bennett crew-member portable protective breathing device as prescribed by portions of FAA action notice A-8150.2
[AD-A211113] N90-14772

CONTINUOUS RADIATION
Anisotropy of electron distributions related to the anisotropy and polarization of the continuous emitted x rays N90-14566

CONTINUOUS WAVE LASERS
Theoretical studies of solar lasers and converters
[NASA-CR-180194] N90-14583

CONTINUUM MECHANICS
A generalized thermomechanical constitutive model for metal matrix composites with plastic strain and damage N90-14293
A new uniformly valid asymptotic integration algorithm for elasto-plastic-creep and unified viscoplastic theories including continuum damage
[NASA-TM-102344] N90-14655

CONTRAROTATING PROPELLERS
User's guide to PMESH: A grid-generation program for single-rotation and counterrotation advanced turboprops
[NASA-CR-185156] N90-14783

CONTROL SURFACES
Stall/spin aerodynamic data project
[DOT/FAA/CT-88/29] N90-14222
Example of procedure in calculation of control hinge moments
[ESDU-89010] N90-14240

CONTROL SYSTEMS DESIGN
Control of an experiment to measure acoustic noise in the space shuttle
[NPS62-89-022] N90-14869

CONTROL THEORY
Survey of adaptive control theory and its applications
[DE89-901270] N90-14840

CONTROLLERS
Optimal control of aero-assisted orbit transfer vehicles N90-14241
A helicopter flight path controller design via a nonlinear transformation technique N90-14242
Controller design for a robotic manipulator N90-14615
Control of an experiment to measure acoustic noise in the space shuttle
[NPS62-89-022] N90-14869

CONVECTION
Heat transfer in convective boundary layer and channel flows N90-14505
Multigrid solutions of elliptic fluid flow problems N90-14507
Convective boundary layer and modeling of dispersion N90-14731
The dynamics of simulated convective storms in hurricane environments N90-14747
Semi-empirical theory of heat-transfer when boiling
[DE89-635418] N90-14984

CONVERGENCE
Parallel projected variable metric algorithms for unconstrained optimization
[NASA-CR-181930] N90-14842

COOLANTS
Fluid flow analysis of the SSME high pressure fuel and oxidizer turbine coolant systems
[NASA-CR-183736] N90-14277

COOLING
Design and demonstration of heat pipe cooling for NASP and evaluation of heating methods at high heating rates
[DE89-016995] N90-14227
Thermal/structural analyses of several hydrogen-cooled leading-edge concepts for hypersonic flight vehicles
[NASA-TM-102391] N90-14511
New heating and cooling technology: Regenerative heat pump according to the Vuilleumier principle
[DE90-002701] N90-14699

COOLING FLOWS (ASTROPHYSICS)
Cooling flows in clusters of galaxies N90-15009

COOLING SYSTEMS
Fluid flow analysis of the SSME high pressure fuel and oxidizer turbine coolant systems
[NASA-CR-183736] N90-14277

COORDINATION
National airspace system monitoring operational concept
[NAS-SR-1330] N90-14214

COPOLYMERIZATION
The structure and properties of liquid crystal polymers N90-14356

COPPER
The biocorrosion of copper by biopolymers as examined in situ, in real time FT-IR/CIR/ATR in conjunction with pre and post XPS/AES
[DE90-002086] N90-14348

COPPER OXIDES
Static and dynamic magnetization properties of Y1Ba2Cu3O(sub z) thin films
[DE89-017584] N90-14940
Muon SR investigation of magnetism and superconductivity in (Y(1-x)Pr(x))Ba2Cu3O7
[DE90-000689] N90-14956
Bi-Sr-Ca-Cu-O superconducting ceramics
[DE89-636225] N90-14972

CORES
Very high resolution radio observations of molecular cloud cores N90-15013

CORONAL LOOPS
As observational and theoretical investigation of stellar flares N90-15012

CORRELATION
Perturbed angular correlations in zirconia ceramics
[DE89-017272] N90-14369
A diagnostic for determining the quality of single-reference electron correlation methods
[NASA-TM-101929] N90-14874

CORROSION
Laser Raman spectroscopy in studies of corrosion and electrocatalysis
[DE90-001414] N90-14311
The biocorrosion of copper by biopolymers as examined in situ, in real time FT-IR/CIR/ATR in conjunction with pre and post XPS/AES
[DE90-002086] N90-14348
High-temperature corrosion of heat exchanger materials
[DE90-001963] N90-14352
Sodium/sulfur post-test analysis at ANL
[DE90-001911] N90-14488

CORROSION PREVENTION
Glancing angle x ray studies of oxide films
[DE89-017828] N90-14953

COSMIC DUST
A model of the thermal and electrical properties of cosmic dust particles N90-15014

COSMIC RAYS
Solar-geophysical data number 538, June 1989. Part 1: (Prompt reports). Data for May, April 1989, and late data
[PB89-223638] N90-15031

COSMOLOGY
The ultimate structure of matter: The US High Energy Physics Program from the 1950s through the 1980s
[DE90-001784] N90-14887
Supersymmetric dark matter above the W mass
[NASA-CR-186168] N90-15016
Is the number of photons conserved in an expanding universe
[DE89-618836] N90-15018
Classical approach to higher-derivative gravity
[DE89-631649] N90-15019

COST ANALYSIS
Assessment of costs and benefits of flexible and alternative fuel use in the US transportation sector. Technical report three: Methanol production and transportation costs
[DE90-002625] N90-14396
A review of gas-cooled reactor concepts for SDI (Strategic Defense Initiative)
[DE89-016962] N90-14898

COST EFFECTIVENESS
Decision-aid design factors in connection with HF communication and emitter location disciplines N90-14413

COST ESTIMATES
Definition of avionics concepts for a heavy lift cargo vehicle. Volume 1: Executive summary
[NASA-CR-183815] N90-14229
Definition of avionics concepts for a heavy lift cargo vehicle, volume 2
[NASA-CR-183819] N90-14230
Developing integrated parametric planning models for budgeting and managing complex projects
[NASA-CR-186006] N90-14986

COSTS
Elastomeric impulse energy storage and transfer system
[AD-D014223] N90-14255

COUETTE FLOW
The stability of Taylor-Couette flow with radial heating N90-14502

COULOMB COLLISIONS
Controller design for a robotic manipulator N90-14615

COUNTING
Estimating methods for counting process intensities: Non-parametric methods
[IMAG-RR-774-M] N90-14846

CRACK INITIATION
Thermal fatigue durability for advanced propulsion materials
[NASA-TM-102348] N90-14641

CRACK OPENING DISPLACEMENT
Crack problems for elastic-plastic materials under antiplane shear loadings N90-14651

CRACK PROPAGATION
Effects of dislocation substructure and prestrain on fracture behavior in aluminum and steel alloys N90-14334
The 4.2 K fracture toughness of 304 stainless steel in a magnetic field
[DE90-002083] N90-14347
Failure probability estimate of Type 304 stainless steel piping
[DE90-000659] N90-14635
A nonlinear high temperature fracture mechanics basis for strainrange partitioning
[NASA-TM-4133] N90-14642
Fracture mechanics of porous materials
[DE90-000023] N90-14657
Engineering approaches to the application of fracture toughness data in the nuclear industry
[DE90-001596] N90-14659

CRACK TIPS
Mechanics of interaction of a crack with microcracks N90-14650
Crack problems for elastic-plastic materials under antiplane shear loadings N90-14651

CRACKING (FRACTURING)
A computer-controlled automated test system for fatigue and fracture testing
[DE90-002931] N90-14661

CRACKS
The feasibility of welding of irradiated materials
[DE90-002200] N90-14631
Crack problems for elastic-plastic materials under antiplane shear loadings N90-14651

CRASHES
Methodology for the calibration of and data acquisition with a six-degree-of-freedom acceleration measurement device
[PB89-233597] N90-14531

CRAY COMPUTERS
Multiple crossbar network: Integrated supercomputing framework
[DE89-012614] N90-14831

CREEP PROPERTIES
Application of neutron diffraction NDE to high-temperature superconducting composites
[DE90-002184] N90-14295
BES welding science contractors summary report, 1988 to 1989
[DE90-001004] N90-14619
A nonlinear high temperature fracture mechanics basis for strainrange partitioning
[NASA-TM-4133] N90-14642

CREW PROCEDURES (INFLIGHT)
Payload crew utilization for spacelab missions
[NASA-TP-2976] N90-14256

CRITICAL POINT
Thermophysical properties of isopropyl alcohol. Part 2: Thermodynamic properties at elevated pressures
[ESDU-89020-PT-2] N90-14300

CRUDE OIL
Devices and methods for in-situ combustion ignition
[DE89-000766] N90-14309
The laminar to slug flow transition in Hele-Shaw flow
[DE90-000636] N90-14521

CRYOGENIC TEMPERATURE
The strength-toughness combination of the aluminum-lithium alloys 2090 and 2091 at cryogenic temperatures
[DE90-001425] N90-14338
The metallurgical determinants of toughness as cryogenic temperature
[DE90-002331] N90-14351

CRYOGENICS
Cryogenic temperature effects on sting-balance deflections in the National Transonic Facility
[NASA-TM-4157] N90-14244
CRYOSTATS
Thermal design of a 10-kW helium refrigerator
[DE90-701785] N90-14403
CRYSTAL DEFECTS
Interaction of hydrogen isotopes with metals: Deuterium trapped at lattice defects in palladium
[DE90-000811] N90-14344
CRYSTAL DISLOCATIONS
Quasicrystals and grain boundaries
[DE90-002213] N90-14981
CRYSTAL GROWTH
SEM (Scanning Electron Microscope) image analysis of grain growth in microwave-annealed alumina
[DE90-001606] N90-14339
Primary arm spacing in directionally solidified Pb-10 wt percent Sn alloys
[NASA-CR-185190] N90-14398
CRYSTAL LATTICES
Interaction of hydrogen isotopes with metals: Deuterium trapped at lattice defects in palladium
[DE90-000811] N90-14344
Solid oxide fuel cells electrodes based on In(sub 2)O(sub 3)-PrO(sub 1.83)-ZrO(sub 2)
[DE90-002666] N90-14691
Atomic matching across internal interfaces
[DE90-002266] N90-14889
Ion beam processing of advanced electronic materials
[DE89-017342] N90-14944
X ray studies of strain, interface, and impurity in semiconductors
[DE90-001525] N90-14947
Practical limitations of ALCHEMI measurements on ordered intermetallic alloys
[DE90-000700] N90-14957
Theory of the energetics and nonclassical nucleation for martensitic transformations from partially soft lattice modes
[DE90-002182] N90-14964
Quasicrystals and grain boundaries
[DE90-002213] N90-14981
CRYSTAL OPTICS
Trapezoidal crystal in the six beam implosion N90-14577
REFLECT: A computer program for the x ray reflectivity of bent perfect crystals
[DE90-001266] N90-14946
CRYSTAL STRUCTURE
The Periodic Law at high pressures
[DE90-000837] N90-14319
Perturbed angular correlations in zirconia ceramics
[DE89-017272] N90-14369
Prospects for wavelength tunable lasers based on vacancy defects in alkaline-earth oxides
[DE90-001078] N90-14592
REFLECT: A computer program for the x ray reflectivity of bent perfect crystals
[DE90-001266] N90-14946
X ray studies of strain, interface, and impurity in semiconductors
[DE90-001525] N90-14947
High-temperature/high-pressure x ray diffraction: Recent developments
[DE89-015255] N90-14949
Oxygen stoichiometry, structural transitions, and thermodynamic behavior of the YBa2Cu3O(x) system
[DE89-017694] N90-14951
Superconductivity from finite-U valence fluctuations
[DE90-000603] N90-14954
Powder neutron diffraction study of the structural phase diagram of the Ba(sub 1-x)K(sub x)BiO3 system
[DE90-002264] N90-14967
Anisotropy of oxygen tracer diffusion in YBa2Cu3O7-delta single crystals
[DE90-001931] N90-14979
Quasicrystals and grain boundaries
[DE90-002213] N90-14981
CRYSTAL SURFACES
Non-linear optical studies of adsorbates: Spectroscopy and dynamics
[DE90-001543] N90-14312
CRYSTALLINITY
Study of microcrystalline, silicon-carbon p-layers prepared by photo-CVD and glow discharge
[DE89-009438] N90-14939
CRYSTALLOGRAPHY
Spectral properties of one dimensional quasi-crystals
[PREPRINT-659] N90-14938
CRYSTALS
Atomic matching across internal interfaces
[DE90-002266] N90-14889
CUES
Workload induced spatio-temporal distortions and safety of flight
[DE89-016613] N90-14771
CURING
Fiber-optic sensors for composite cure analysis and lifetime nondestructive evaluation
[DE90-001739] N90-14296
CURRENT DENSITY
Heat and mass transfer design issues in PEM fuel cell hardware
[DE89-016779] N90-14677
Polarization of Li/SOCl2 cells
[DE90-000883] N90-14680
Calorimetric measurements on electrochemical cells with Pd-D cathodes
[DE90-002198] N90-14685
Static and dynamic magnetization properties of Y1Ba2Cu3O(sub z) thin films
[DE89-017584] N90-14940
Flux pinning and microstructure in YBa2Cu3O7
[DE90-001562] N90-14948
A simple figure of merit for high temperature superconducting switches
[DE90-000610] N90-14955
CURRENT SHEETS
Symmetry breaking bifurcations of a current sheet
[DE90-601005] N90-14864
CUTTERS
New tool-holding concept
[DE90-000880] N90-14624
CYCLOGENESIS
Inverted surface troughs accompanying Rocky Mountain lee-side cyclogenesis N90-14746
CYCLONES
Inverted surface troughs accompanying Rocky Mountain lee-side cyclogenesis N90-14746
CYLINDRICAL BODIES
Method and apparatus to enhance the sensitivity of cylindrical magnetostrictive transducer to magnetic fields
[AD-D014218] N90-14459
Surface flow and heating distributions on a cylinder in near wake of Aeroassist Flight Experiment (AFE) configuration at incidence in Mach 10 Air
[NASA-TP-2954] N90-14493
CYLINDRICAL SHELLS
Subsonic sting interference on the aerodynamic characteristics of a family of slanted-base ogive-cylinders
[NASA-CR-186193] N90-14204

D

DAMAGE
Cavitation and superplasticity N90-14329
Mechanisms of wear in structural ceramic materials N90-14360
Review of surface flashover theory
[DE90-000806] N90-14469
Hypervelocity impact calculations using CTH: Case studies
[DE90-002891] N90-14632
A new uniformly valid asymptotic integration algorithm for elasto-plastic-creep and unified viscoplastic theories including continuum damage
[NASA-TM-102344] N90-14655
DAMAGE ASSESSMENT
Risk-based fire safety experiment definition for manned spacecraft
[NASA-CR-183835] N90-14262
DARK MATTER
Supersymmetric dark matter above the W mass
[NASA-CR-186168] N90-15016
Gamma ray lines from dark matter annihilation
[DE90-000779] N90-15021
Dark matter and the solar neutrino problem: Can particle physics provide a single solution
[DE90-001827] N90-15024
DATA ACQUISITION
Methodology for the calibration of and data acquisition with a six-degree-of-freedom acceleration measurement device
[PB89-233597] N90-14531
Derivation of synthetic mission profiles from electric vehicle field data
[DE89-011125] N90-14620
Beyond the IDMY (International Daylighting Measurements Year): A network instrument for low-cost data acquisition
[DE90-002722] N90-14740
Application of reusable software components at the SEI N90-14804
Personal computer process data acquisition
[DE89-017877] N90-14816
Publications of the Jet Propulsion Laboratory, 1988
[NASA-CR-185956] N90-14995
DATA BASE MANAGEMENT SYSTEMS
Integrated computer-based tools to facilitate environmental monitoring, assessment, and restoration
[DE90-002732] N90-14717
DATA BASES
Stall/spin aerodynamic data project
[DOT/FAA/CT-88/29] N90-14222
SRB thermal environments
[NASA-CR-183801] N90-14276
The importance of environmental data N90-14406
The FTZ HF propagation model for use on small computers and its accuracy N90-14447
Advanced Software Development Workstation Project N90-14807
The development of an Ada programming support environment database: SEAD (Software Engineering and Ada Database), user's manual
[NASA-CR-181219] N90-14811
The design and implementation of an intelligent interface for information retrieval N90-14991
DATA COMPRESSION
Data compression techniques applied to high resolution high frame rate video technology
[NASA-CR-4263] N90-14452
An image compression algorithm for a high-resolution digital still camera
[NASA-CR-185079] N90-14532
DATA LINKS
Data Link Processor (DLP) operational test and evaluation/integration test plan
[DOT/FAA/CT-TN89/32] N90-14404
DATA MANAGEMENT
Transferring data objects: A focused Ada investigation
[NASA-CR-186065] N90-14786
SSFP approach to software reuse N90-14799
DATA PROCESSING
Coordination of processing elements in a multiprocessor computer
[WO-PATENT-88/04075] N90-14830
The AMY Experiment
[DE90-001153] N90-14880
A dynamic systems engineering methodology research study. Phase 2: Evaluating methodologies, tools, and techniques for applicability to NASA's systems projects
[NASA-CR-181319] N90-14985
DATA PROCESSING EQUIPMENT
Data Link Processor (DLP) operational test and evaluation/integration test plan
[DOT/FAA/CT-TN89/32] N90-14404
DATA PROCESSING TERMINALS
Theoretical and material studies of thin-film electroluminescent devices
[NASA-CR-186104] N90-14468
The development of an Ada programming support environment database: SEAD (Software Engineering and Ada Database), user's manual
[NASA-CR-181219] N90-14811
DATA REDUCTION
MERLIN and VLBI observations of the radio galaxy Virgo A N90-15001
DATA RETRIEVAL
High volume data storage architecture analysis
[NASA-CR-186239] N90-14784
Document preservation by electronic imaging. Volume 1: Synopsis
[PB89-226526] N90-14987
Document preservation by electronic imaging. Volume 2: System and experiment description
[PB89-226534] N90-14988
Document preservation by electronic imaging. Volume 3: Appendices
[PB89-226542] N90-14989
DATA SIMULATION
Pattern recognition techniques applied to the NASA-ACTS order-wire problem N90-14446
DATA STORAGE
High volume data storage architecture analysis
[NASA-CR-186239] N90-14784
Document preservation by electronic imaging. Volume 1: Synopsis
[PB89-226526] N90-14987
Document preservation by electronic imaging. Volume 2: System and experiment description
[PB89-226534] N90-14988
Document preservation by electronic imaging. Volume 3: Appendices
[PB89-226542] N90-14989
DATA STRUCTURES
Transferring data objects: A focused Ada investigation
[NASA-CR-186065] N90-14786
DATA SYSTEMS
Prototype software reuse environment at Goddard Space Flight Center N90-14794

DATA TRANSFER (COMPUTERS)
Transferring data objects: A focused Ada investigation
[NASA-CR-186065] N90-14786
Multiple crossbar network: A switched high-speed local network
[DE90-001839] N90-14833
DATA TRANSMISSION
Mitigating Doppler shift effect in HF multitone data modem N90-14441
The characteristics of the HF radio channel and its influence on modern HF data communication system design N90-14448
DAYTIME
Beyond the IDMY (International Daylighting Measurements Year): A network instrument for low-cost data acquisition
[DE90-002722] N90-14740
DECAY
Biomodal spontaneous fission
[DE90-001516] N90-14886
DECISION MAKING
Operational Decision Aids for Exploiting or Mitigating Electromagnetic Propagation Effects
[AGARD-CP-453] N90-14405
Propagation assessment and tactical decision aids N90-14407
Human factors aspects of decision support systems N90-14408
Propagation-based decision aids in the U.S. Navy N90-14410
Engineer's Refractive Effects Prediction System (EREPS) N90-14411
PROPHET and future signal warfare decision aids N90-14412
Decision-aid design factors in connection with HF communication and emitter location disciplines N90-14413
The parabolic equation approach to predicting tropospheric propagation effects in operational environments N90-14416
Communication Overview Program (COP) N90-14435
TROPO: A technique for predicting propagation and modem performance of digital troposcatter systems N90-14444
DECOMPOSITION
High temperature chemistry of complex vaporization/decomposition processes
[DE89-016559] N90-14306
Fast transit gas- and condensed-phase chemistry of energetic materials
[DE90-001656] N90-14395
Iterative methods of domain decomposition with cross-points for the solution of discrete elliptic problems
[DE90-000719] N90-14854
DEEP SPACE
JPRS Report: Science and technology. USSR: Space. Soviet space program to the year 2000
[JPRS-USP-89-008] N90-14248
DEEP SPACE NETWORK
JPL reuse program N90-14795
DEFECTS
Effects of shock-induced defects on flux pinning in YBa2Cu3O(7-delta)
[DE90-000824] N90-14959
Shock-induced defects and flux pinning in YBa2Cu3O sub 7-delta + Ag composites
[DE90-000827] N90-14960
DEFENSE PROGRAM
Concerning advanced architectures for strategic defense
[DE90-001894] N90-14857
DOD (Department of Defense) Freedom of Information Act Program (incorporating changes 1 and 2)
[PB90-104753] N90-14903
DEFLECTION
Cryogenic temperature effects on sting-balance deflections in the National Transonic Facility
[NASA-TM-4157] N90-14244
Finite element analysis of laminated composite plates N90-14291
A theoretical investigation of the column behavior of cold-formed square hollow sections
[PB89-225981] N90-14645
Direction-dependent stopping power and beam deflection in anisotropic solids
[DE90-001076] N90-14883
DEFORESTATION
Strategy for monitoring the effects of land use change on atmospheric CO2 concentrations
[DE90-001635] N90-14722
DEFORMATION
Cavitation and superplasticity N90-14329
Further studies of transverse stress effects in cable-in-conduit conductors
[DE90-001517] N90-14484
CTH: A three-dimensional shock wave physics code
[DE89-016529] N90-14528
Stability and dynamics of constrained flexible multibody systems N90-14609
Dynamical simulation of dislocation microstructure
[DE90-003192] N90-14982
DEGRADATION
Further studies of transverse stress effects in cable-in-conduit conductors
[DE90-001517] N90-14484
Sodium/sulfur post-test analysis at ANL
[DE90-001911] N90-14488
DELAY LINES
Design of a compensation filter for a quadratic phase communication channel N90-14428
DELTA WINGS
Experimental transonic flutter characteristics of two 72 deg-sweep delta-wing models
[NASA-TM-101659] N90-14205
DEMAND (ECONOMICS)
How far can the world get on energy efficiency alone
[DE90-001349] N90-14686
DENDRITIC CRYSTALS
Primary arm spacing in directionally solidified Pb-10 wt percent Sn alloys
[NASA-CR-185190] N90-14398
DENSE PLASMAS
Atomic structure and spectral perturbations in hot dense plasmas N90-14567
Transversal inhomogeneity and radiative transfer in plasmas obtained by laser impact N90-14568
Equation of state and opacity of dense plasmas
[DE90-002223] N90-14926
DENSITY (MASS/VOLUME)
Orthobaric densities and molar volumes of liquids. Aromatic hydrocarbons
[ESDU-89019] N90-14299
Density of intercalated graphite fibers
[NASA-TM-102411] N90-14362
DENSITY MEASUREMENT
Orthobaric densities and molar volumes of liquids. Introduction to data items issued after July 1989
[ESDU-89018] N90-14298
Orthobaric densities and molar volumes of liquids. Aromatic hydrocarbons
[ESDU-89019] N90-14299
DEOXYRIBONUCLEIC ACID
Nomenclature for physical mapping of complex genomes
[DE89-015173] N90-14994
DEPOSITION
Preparation and properties of high deposition a-Si:H films and solar cells using disilane
[DE89-009467] N90-14679
Profile measurements of sulfur dioxide, nitrogen oxides, and nitric acid deposition velocities in California's south coast air basin
[PB90-104001] N90-14703
Steady state model to determine lake resources at risk to acid deposition in the Sierra Nevada, California
[PB89-103995] N90-14705
Application of surface analysis methods to studies of atmospheric deposition in forests
[DE90-000562] N90-14714
DEPOSITS
Measuring the thickness of austenitic weld deposits on carbon steel walls using a magnetic method
[DE89-635446] N90-14628
DESIGN ANALYSIS
The space station tethered elevator system
[NASA-CR-186051] N90-14265
Partial gravity habitat study: With application to lunar base design
[NASA-CR-186048] N90-14267
DETECTION
Detection of a chirping electromagnetic signal
[DE90-002105] N90-14457
Noncontacting laser ultrasonic generation and detection at the surface of molten metal
[DE90-002020] N90-14605
Process monitoring using optical ultrasonic wave detection
[DE90-002021] N90-14870
Interferometric surface distortion detector
[AD-D014211] N90-14901
DETONABLE GAS MIXTURES
Phase changes in carbon and nitrogen systems: Their effects on the detonation properties of high explosives
[DE90-000829] N90-14392
DETONATION
Flame acceleration studies in the MINIFLAME facility
[DE90-000041] N90-14310
Detonation product equation of state for Baratol
[DE90-001050] N90-14384
Calibration curves for some standard Gap Tests
[DE89-016599] N90-14389
Non-equilibrium effects of slow diffusion controlled reactions on the properties of explosives
[DE90-000822] N90-14391
Phase changes in carbon and nitrogen systems: Their effects on the detonation properties of high explosives
[DE90-000829] N90-14392
Reactive flow measurements and calculations for ZrH2-based composite explosives
[DE90-000831] N90-14393
Reaction zone structure in supracompressed detonating explosives
[DE90-000832] N90-14394
A new simulation method for the efficient calculation of benchmarks for detonation products equations of state
[DE90-001837] N90-14522
DETONATION WAVES
Propagation of detonation waves from an impact region
[DE90-001184] N90-14515
DETONATORS
Detonation product equation of state for Baratol
[DE90-001050] N90-14384
Electrothermal response testing more than a quality assurance tool
[DE90-001449] N90-14536
DEUTERIUM
Interaction of hydrogen isotopes with metals: Deuterium trapped at lattice defects in palladium
[DE90-000811] N90-14344
Cold fusion: Alchemist's dream
[DE90-000865] N90-14925
DEUTERONS
Cold fusion: Alchemist's dream
[DE90-000865] N90-14925
DIAMAGNETISM
Dissipation measurement in high T(sub c) superconductors with electromagnetic probes
[DE90-002058] N90-14963
DIELECTRICS
Temperature stable ceramic dielectric compositions
[AD-D014209] N90-14358
DIESEL ENGINES
Computer simulation of wind/diesel system operation
[DE89-009445] N90-14688
DIFFERENCE EQUATIONS
Numerical solution of the incompressible Navier-Stokes equations N90-14501
DIFFERENTIAL EQUATIONS
The stability of Taylor-Couette flow with radial heating N90-14502
Proceedings of the Focused Research Program on Spectral Theory and Boundary Value Problems. Volume 4: Nonlinear Differential Equations
[DE90-000920] N90-14780
Block predictor (low order) corrector methods to solve ordinary differential equations on parallel computers
[IMAG-RR-757-M] N90-14845
A comparison result and elliptic equations involving subcritical exponents
[DE90-001772] N90-14850
DIFFERENTIATION
Modified Chebyshev pseudospectral method with O(N exp -1) time step restriction
[NASA-CR-181958] N90-14548
DIFFRACTION PATTERNS
A sampled-grating model of moire patterns from digital imaging
[AD-A213364] N90-14902
DIFFRACTION PROPAGATION
Low level range coverage performance prediction for VHF radar N90-14439
Modelling UHF propagation for frequency assignment in radio relay networks N90-14445
DIFFUSION
Predictive aging of elastomers in air: The importance of understanding diffusion-limited oxidation effects
[DE90-001385] N90-14372
Non-equilibrium effects of slow diffusion controlled reactions on the properties of explosives
[DE90-000822] N90-14391
Anisotropy of oxygen tracer diffusion in YBa2Cu3O7-delta single crystals
[DE90-001931] N90-14979
DIFFUSION WELDING
Diffusion bonding of metals N90-14330
Designing for superplastic alloys N90-14332
DIGITAL COMPUTERS
Data compression techniques applied to high resolution high frame rate video technology
[NASA-CR-4263] N90-14452
DIGITAL DATA
An image compression algorithm for a high-resolution digital still camera
[NASA-CR-185079] N90-14532

DIGITAL RADAR SYSTEMS
Data Link Processor (DLP) operational test and evaluation/integration test plan
[DOT/FAA/CT-TN89/32] N90-14404
DIGITAL SYSTEMS
SAND DEVIL: A digital video link for telemetry applications
[DE90-001879] N90-14259
A sampled-grating model of moire patterns from digital imaging
[AD-A213364] N90-14902
Document preservation by electronic imaging. Volume 1: Synopsis
[PB89-226526] N90-14987
Document preservation by electronic imaging. Volume 2: System and experiment description
[PB89-226534] N90-14988
Document preservation by electronic imaging. Volume 3: Appendices
[PB89-226542] N90-14989
DIGITAL TECHNIQUES
Data compression techniques applied to high resolution high frame rate video technology
[NASA-CR-4263] N90-14452
DIMENSIONAL ANALYSIS
MIPs and BIPs are megaflops: Limits of unidimensional assessments
[DE89-015707] N90-14770
DIMENSIONAL MEASUREMENT
Algorithmic randomness, physical entropy, measurements, and the second law
[DE90-002413] N90-14823
DIODES
Monolithic laser diode structure for microwave generation
[AD-D014210] N90-14543
DIRECT POWER GENERATORS
Electrical performance characteristics of high power converters for space power applications
[NASA-CR-185947] N90-14279
DIRECTIONAL ANTENNAS
Frequency independent constant beamwidth directional lens antenna for very wideband and multi-channel electromagnetic communications
[AD-D014214] N90-14449
DIRECTIONAL SOLIDIFICATION (CRYSTALS)
Primary arm spacing in directionally solidified Pb-10 wt percent Sn alloys
[NASA-CR-185190] N90-14398
DIRECTORIES
Accessing Japanese technical information: A group of essays extracted from the NTIS (National Technical Information Service) Directory of Japanese Technical Resources in the United States for 1987 and 1988
[PB90-100165] N90-14992
DISCONNECT DEVICES
Pressure sensitive release device
[AD-D014220] N90-14610
DISCONTINUITY
Local error estimates for discontinuous solutions of nonlinear hyperbolic equations
[NASA-CR-181960] N90-14847
DISCRETE FUNCTIONS
Numerical methodologies for solving partial differential equations
[DE90-001842] N90-14849
DISPERSING
Convective boundary layer and modeling of dispersion N90-14731
DISPLACEMENT
Finite element analysis of laminated composite plates N90-14291
A finite strip method for the elastic-plastic large displacement analysis of thin-walled and cold-formed steel sections
[PB89-226021] N90-14647
DISPLAY DEVICES
A candidate concept for display of forward-looking wind shear information
[NASA-TM-101585] N90-14232
Engineer's Refractive Effects Prediction System (EREPS) N90-14411
Theoretical and material studies of thin-film electroluminescent devices
[NASA-CR-186104] N90-14468
Human factors evaluation of electroluminescent display Number 1
[DE90-002231] N90-14777
DISSIPATION
The analysis and modeling of dilatational terms in compressible turbulence
[NASA-CR-181959] N90-14513
Dissipation measurement in high T(sub c) superconductors with electromagnetic probes
[DE90-002058] N90-14963
DISTORTION
Workload induced spatio-temporal distortions and safety of flight
[DE89-016613] N90-14771
DISTRIBUTED PROCESSING
The role of order in distributed programs
[NASA-CR-186252] N90-14826
The Aerospace Energy Systems Laboratory: A BITBUS networking application
[NASA-TM-4149] N90-14829
How robust are distributed systems
[NASA-CR-186242] N90-14837
DISTRIBUTION FUNCTIONS
Is the number of photons conserved in an expanding universe
[DE89-618836] N90-15018
DIURNAL VARIATIONS
The retrieval of the concentrations of nitric oxide and nitrogen dioxide from satellite solar occultation measurements at sunset and sunrise N90-14733
DIVING (UNDERWATER)
High-frequency ventilation in dogs with three gases of different densities
[AD-A212862] N90-14762
DOCUMENTS
Publications of the Jet Propulsion Laboratory, 1988
[NASA-CR-185956] N90-14995
DOPPLER EFFECT
Mitigating Doppler shift effect in HF multitone data modem N90-14441
High resolution Doppler lidar
[NASA-CR-183288] N90-14542
DOPPLER RADAR
Adaptive clutter rejection filters for airborne Doppler weather radar applied to the detection of low altitude windshear
[NASA-CR-186211] N90-14453
DOSAGE
Meteorological monitoring for environmental/dose assessment and emergency response modeling: How much is enough
[DE90-002726] N90-14757
DOSIMETERS
Assessment of research needs for laser technologies applied to advanced spectrographic methods
[DE90-001154] N90-14587
DROP SIZE
Comparison of two droplet sizing systems in an icing wind tunnel
[NASA-TM-102456] N90-14617
DROPS (LIQUIDS)
Thermocapillary migration of liquid droplets in a temperature gradient in a density matched system
[NASA-CR-185178] N90-14512
DRUGS
The effects of nonselective and selective beta blockade upon nonshivering thermogenesis during an acute cold exposure in cold acclimated men N90-14767
DUCTILITY
Superplastic sheet forming N90-14327
DUCTS
A forecasting system using the parabolic equation: Application to surface-to-air propagation in the presence of elevated layers N90-14420
Propagation modeling for some horizontally varying tropospheric ducts N90-14422
Laser velocimeter and total pressure measurements in circular-to-rectangular transition ducts
[NASA-CR-182286] N90-14494
Heat transfer in convective boundary layer and channel flows N90-14505
DUST
A study of the infrared emission of galactic supernova remnants N90-15006
Hypervelocity impact studies on the Giotto comet Halley mission N90-15008
DYNAMIC CHARACTERISTICS
Non-linear vibrations, stability, and dynamics of structures and mechanisms
[AD-A212152] N90-14639
DYNAMIC CONTROL
Optimal stochastic modeling and control of flexible structures
[AD-A212347] N90-14269
DYNAMIC LOADS
Critical time step estimation for three-dimensional explicit impact analysis
[DE90-002187] N90-14662
Survey of adaptive control theory and its applications
[DE89-901270] N90-14840
DYNAMIC MODELS
AcSim: Aircraft simulation program with application to flight profile generation
[AD-A212466] N90-14217
DYNAMIC RESPONSE
Manipulation strategies for massive space payloads
[NASA-CR-186081] N90-14247
A surface coupled flamelet approach to dynamic response in heterogeneous propellant combustion N90-14302
Stability and dynamics of constrained flexible multibody systems N90-14609
DYNAMIC STRUCTURAL ANALYSIS
Manipulation strategies for massive space payloads
[NASA-CR-186081] N90-14247
Measurement of damping of graphite epoxy composite materials and structural joints
[NASA-CR-183802] N90-14286
Stability and dynamics of constrained flexible multibody systems N90-14609
Group implicit concurrent algorithms in nonlinear structural dynamics
[NASA-CR-185950] N90-14638
Non-linear vibrations, stability, and dynamics of structures and mechanisms
[AD-A212152] N90-14639
DYNAMICAL SYSTEMS
Chaotic behavior in nonlinear polarization dynamics
[DE89-013453] N90-14589

E

EARTH CRUST
Workshop on the Archean Mantle
[NASA-CR-186156] N90-14736
EARTH IONOSPHERE
Long wave propagation assessment N90-14414
Correction of ionospheric effects for the precise orbit determination of satellites N90-14432
Rocket studies of the lower ionosphere
[NASA-CR-186187] N90-14735
EARTH MAGNETOSPHERE
Particle simulations in magnetospheric plasmas
[NASA-CR-186238] N90-14934
EARTH MANTLE
Workshop on the Archean Mantle
[NASA-CR-186156] N90-14736
EARTH ORBITS
Design considerations for space flight hardware
[NASA-TM-102300] N90-14275
EARTH RADIATION BUDGET
Atlas of albedo and absorbed solar radiation derived from Nimbus 6 earth radiation budget data set, July 1975 to May 1978
[NASA-RP-1230] N90-14741
Evaluation of climatic models: Comparison of simulated and observed patterns for past climates
[DE90-001228] N90-14755
EARTH RESOURCES
How far can the world get on energy efficiency alone
[DE90-001349] N90-14686
EARTHQUAKES
Comparison of shock severity measures
[DE90-000790] N90-14654
ECLIPSES
A source of observational constraints on the structure of Wolf-Rayet winds
[DE90-001236] N90-15023
ECLIPSING BINARY STARS
A source of observational constraints on the structure of Wolf-Rayet winds
[DE90-001236] N90-15023
ECONOMIC ANALYSIS
California air transportation study: A transportation system for the California Corridor of the year 2010
[NASA-CR-186219] N90-14212
The conversion of carbonaceous materials to clean carbon and co-product gaseous fuel
[DE90-001561] N90-14387
Markets for high-speed intercity Maglev technology: A systems analysis approach
[DE89-017683] N90-14623
EDDY VISCOSITY
Navier-Stokes solutions of 2-D transonic flow over unconventional airfoils N90-14195
Group-kinetic theory and modeling of atmospheric turbulence
[NASA-CR-183776] N90-14728
EDGE DETECTION
Some edge-enhancing operators and their applications to image enhancement and edge detection N90-14810
EDUCATION
Workshop on synoptic meteorology instruction
[PB90-109950] N90-14751
EFFICIENCY
Selection of the energy-efficient enhancement geometry for single-phase turbulent flow inside tubes
[DE89-017690] N90-14519

Assessment of the efficiency of nondestructive techniques in materials testing studies based on the information criterion
[DE89-635444] N90-14634
How far can the world get on energy efficiency alone
[DE90-001349] N90-14686

EIGENVALUES
AcSim: Aircraft simulation program with application to flight profile generation
[AD-A212466] N90-14217
Parallel eigenanalysis of finite element models in a completely connected architecture
[NASA-CR-185166] N90-14652

EIGENVECTORS
AcSim: Aircraft simulation program with application to flight profile generation
[AD-A212466] N90-14217
Parallel eigenanalysis of finite element models in a completely connected architecture
[NASA-CR-185166] N90-14652

EINSTEIN EQUATIONS
General exact solution for homogeneous time-dependent self-gravitating perfect fluids
[DE89-618425] N90-14514

EJECTION
Integrated G-suit/immersion suit
[AD-A212989] N90-14774
Calculation of two-neutron multiplicity in photonuclear reactions
[NASA-TP-2968] N90-14890

ELASTIC MEDIA
Crack problems for elastic-plastic materials under antiplane shear loadings N90-14651

ELASTIC PROPERTIES
Elastic softening in nanocrystalline silicon
[DE90-002268] N90-14377
Wide-angle propagation in inhomogeneous fluids and elastic solids using perturbation methods N90-14868

ELASTIC SCATTERING
Narrow one-channel resonances and their manifestation in the pure elastic scattering of unpolarized particles
[DE89-632177] N90-14876

ELASTOMERS
Elastomeric impulse energy storage and transfer system
[AD-D014223] N90-14255
Predictive aging of elastomers in air: The importance of understanding diffusion-limited oxidation effects
[DE90-001385] N90-14372

ELASTOPLASTICITY
Elasto-plastic analysis of unidirectional fiber-reinforced composites subjected to transverse normal loading using the finite element method N90-14292
Shear strain localization phenomenon in viscoplastic materials N90-14649
A new uniformly valid asymptotic integration algorithm for elasto-plastic-creep and unified viscoplastic theories including continuum damage
[NASA-TM-102344] N90-14655

ELECTRIC BATTERIES
Modeling of sodium/metal chloride batteries
[DE89-017685] N90-14478
Battery technology assessment and R and D plan
[DE90-002007] N90-14489
A cost effective battery bank for I(sup 2)T testing and evaluation of electrical switchgear
[DE90-002350] N90-14490
Characterization of electric vehicle velocity and power profiles using road test data
[DE90-002085] N90-14630
Technology Base Research Project for electrochemical energy storage
[DE90-002604] N90-14693
The Aerospace Energy Systems Laboratory: A BITBUS networking application
[NASA-TM-4149] N90-14829

ELECTRIC BRIDGES
High power density dc/dc converter: Selection of converter topology
[NASA-CR-186129] N90-14467

ELECTRIC CONTACTS
Effects of composition and age hardening on precious metal electrical contacts
[DE88-008791] N90-14476

ELECTRIC DISCHARGES
Electrical breakdown in vacuum
[DE90-001623] N90-14485

ELECTRIC ENERGY STORAGE
Technology Base Research Project for electrochemical energy storage
[DE90-002604] N90-14693

ELECTRIC FIELDS
Review of surface flashover theory
[DE90-000806] N90-14469

ELECTRIC GENERATORS
Control of the variable speed generator on the Sandia 34-metre vertical axis wind turbine
[DE90-000803] N90-14674

ELECTRIC MOTOR VEHICLES
Derivation of synthetic mission profiles from electric vehicle field data
[DE89-011125] N90-14620
Characterization of electric vehicle velocity and power profiles using road test data
[DE90-002085] N90-14630

ELECTRICAL FAULTS
Electrical breakdown in vacuum
[DE90-001623] N90-14485

ELECTRICAL PROPERTIES
Practical superconductor development for electrical power applications
[DE90-001804] N90-14487
Electrical properties of materials for high temperature strain gage applications
[NASA-CR-186192] N90-14534
Microstructure and electrical properties of bulk high-T(sub c) superconductors
[DE90-001762] N90-14974
Magnetic and electrical properties
[DE90-002183] N90-14977
A model of the thermal and electrical properties of cosmic dust particles N90-15014

ELECTRICAL RESISTANCE
Inductive store opening switch and tests for energy transfer to a load
[DE90-002818] N90-14482

ELECTRICAL RESISTIVITY
Solid oxide fuel cells electrodes based on In(sub 2)O(sub 3)-PrO(sub 1.83)-ZrO(sub 2)
[DE90-002686] N90-14691

ELECTRO-OPTICS
Physical models for aerosol in the marine mixed-layer N90-14436
Photovoltaic Measurements and Performance Branch
[DE89-009500] N90-14695

ELECTROCATALYSTS
Laser Raman spectroscopy in studies of corrosion and electrocatalysis
[DE90-001414] N90-14311
Proceedings of the First Annual Fuel Cells Contractors Review Meeting
[DE89-011699] N90-14675

ELECTROCHEMICAL CELLS
Electrochemical preparation of silver oxide electrodes having high thermal stability
[AD-D014224] N90-14460
Calorimetric measurements on electrochemical cells with Pd-D cathodes
[DE90-002198] N90-14685

ELECTROCHEMISTRY
An evaluation of electrochemical potentiokinetic reactivation techniques for in-service measurements on Type 304 stainless steel
[DE89-017859] N90-14340
Proceedings of the First Annual Fuel Cells Contractors Review Meeting
[DE89-011699] N90-14675
Polarization of Li/SOCl2 cells
[DE90-000883] N90-14680
Electrode development in monolithic solid oxide fuel cells
[DE90-001910] N90-14684
Interfacial effects in monolithic solid oxide fuel cells
[DE90-001914] N90-14690

ELECTRODEPOSITION
Technology Base Research Project for electrochemical energy storage
[DE90-002604] N90-14693

ELECTRODES
Electrochemical preparation of silver oxide electrodes having high thermal stability
[AD-D014224] N90-14460
Sodium/sulfur post-test analysis at ANL
[DE90-001911] N90-14488
Interfacial effects in monolithic solid oxide fuel cells
[DE90-001914] N90-14690
Technology Base Research Project for electrochemical energy storage
[DE90-002604] N90-14693

ELECTROENCEPHALOGRAPHY
Use of superconducting plates and shells to deflect magnetic noise fields: Application to MEG
[DE89-012592] N90-14676

ELECTROFORMING
An electroformed nickel-sulfur alloy for a nose cone
[DE90-000866] N90-14337

ELECTROLUMINESCENCE
Theoretical and material studies of thin-film electroluminescent devices
[NASA-CR-186104] N90-14468
Human factors evaluation of electroluminescent display Number 1
[DE90-002231] N90-14777

ELECTROLYTES
Electrochemical preparation of silver oxide electrodes having high thermal stability
[AD-D014224] N90-14460
Sodium/sulfur post-test analysis at ANL
[DE90-001911] N90-14488
Heat and mass transfer design issues in PEM fuel cell hardware
[DE89-016779] N90-14677
Technology Base Research Project for electrochemical energy storage
[DE90-002604] N90-14693

ELECTROMAGNETIC COUPLING
JPS heater and sensor lightning qualification
[NASA-CR-183830] N90-14530

ELECTROMAGNETIC FIELDS
Computation of electromagnetic effects in a tokamak due to a plasma disruption
[DE90-001764] N90-14931

ELECTROMAGNETIC INTERFERENCE
The parabolic equation approach to predicting tropospheric propagation effects in operational environments N90-14418

ELECTROMAGNETIC NOISE
Use of superconducting plates and shells to deflect magnetic noise fields: Application to MEG
[DE89-012592] N90-14676

ELECTROMAGNETIC PULSES
Detection of a chirping electromagnetic signal
[DE90-002105] N90-14457

ELECTROMAGNETIC RADIATION
Operational Decision Aids for Exploiting or Mitigating Electromagnetic Propagation Effects
[AGARD-CP-453] N90-14405
Propagation prediction for the North Sea environment N90-14423
The effect of oblate spheroidal drops on rain attenuation at 94 GHz: Comparison between theory and experiment N90-14440

ELECTROMAGNETIC SHIELDING
JPS heater and sensor lightning qualification
[NASA-CR-183830] N90-14530

ELECTROMAGNETIC WAVE TRANSMISSION
The parabolic equation approach to predicting tropospheric propagation effects in operational environments N90-14418
Weather satellite and computer modeling approaches to assessing propagation over marine environments N90-14443

ELECTRON ACCELERATORS
Characteristics of an electron-beam rocket pellet accelerator
[DE90-001595] N90-14252
Modification of MEA modulator-klystron units enabling short pulse injection into a pulse-stretcher ring N90-14894
Performance and modification of the MEA RF drive system N90-14895
An Energy Spectrum Compressor system (ESC) for the Amsterdam pulse stretcher (AmPS) N90-14896

ELECTRON BEAMS
Characteristics of an electron-beam rocket pellet accelerator
[DE90-001595] N90-14252
Recent developments of gigatron technology
[DE90-001067] N90-14474
Gigatron: A new technology for microwave power devices
[DE90-001066] N90-14483
Electrical breakdown in vacuum
[DE90-001623] N90-14485
Self-field-induced chaotic electron motion in free electron lasers
[DE90-001710] N90-14598
Compact RF-linac free-electron lasers
[DE90-002386] N90-14600
Analytical treatment of electron trajectory straightener issues in free-electron lasers
[DE90-002405] N90-14603
An Energy Spectrum Compressor system (ESC) for the Amsterdam pulse stretcher (AmPS) N90-14896
Microwave Transport Systems for the MTX (Microwave Tokamak Experiment)
[DE90-000821] N90-14921
RF superconductivity research and development at Los Alamos National Laboratory
[DE90-002440] N90-14969

ELECTRON CAPTURE
Multiple electron capture in close ion-atom collisions
[DE90-001541] N90-14885

ELECTRON CYCLOTRON HEATING
Microwave Tokamak Experiment (MTX) first year of operation and future plans
[DE90-000817] N90-14920
Microwave Tokamak Experiment: An overview of the construction and checkout phase
[DE90-000834] N90-14924
ELECTRON DENSITY (CONCENTRATION)
Numerical simulation of laser radiation propagation in non-uniform absorbing medium. Geometrical optics approximation
[DE89-632014] N90-14585
ELECTRON DISTRIBUTION
Electron heating and static sheath enhancement in front of energized RF antennas
[DE90-001334] N90-14456
Anisotropy of electron distributions related to the anisotropy and polarization of the continuous emitted x rays N90-14566
ELECTRON GUNS
Characteristics of an electron-beam rocket pellet accelerator
[DE90-001595] N90-14252
Electric-gun studies of conductors in high magnetic fields and experiments in dynamic flux compression
[DE90-000815] N90-14470
ELECTRON IMPACT
Theoretical and material studies of thin-film electroluminescent devices
[NASA-CR-186104] N90-14468
Modeling of runaway electron damage for the design of tokamak plasma facing components
[DE90-000847] N90-14914
ELECTRON MICROSCOPES
A Scanning Photoelectron Microscope (SPEM) at the National Synchrotron Light Source (NSLS)
[DE90-001551] N90-14537
ELECTRON MICROSCOPY
SEM (Scanning Electron Microscope) image analysis of grain growth in microwave-annealed alumina
[DE90-001606] N90-14339
The design of a computer system for image simulation and image processing of high resolution electron micrographs
[DE90-000179] N90-14820
ELECTRON MOBILITY
Self-field-induced chaotic electron motion in free electron lasers
[DE90-001710] N90-14598
ELECTRON PHONON INTERACTIONS
A model of the isotope effect of the oxide superconductor
[DE89-635907] N90-14971
ELECTRON PLASMA
High-frequency instability of the sheath-plasma resonance
[NASA-CR-186127] N90-14910
Modeling of runaway electron damage for the design of tokamak plasma facing components
[DE90-000847] N90-14914
ELECTRON PROBES
Calibration approach to electron probe microanalysis: A study with PWA-1480, a nickel base superalloy
[NASA-TM-102393] N90-14335
ELECTRON SCATTERING
Interaction of low-energy electrons and positrons with condensed matter: Stopping powers and inelastic mean free paths from optical data
[DE90-001001] N90-14882
NIKHEF-K contributions to the 1989 Particle Accelerator Conference
[NIKHEF/AMPS/89/03] N90-14891
ELECTRON SOURCES
Theory of harmonic radiation using a single-electron source model
[DE90-002412] N90-14606
ELECTRON SPIN
Factors affecting electron spin polarization in photosynthetic systems
[DE90-000196] N90-14764
ELECTRON TRAJECTORIES
Analytical treatment of electron trajectory straightener issues in free-electron lasers
[DE90-002405] N90-14603
ELECTRON TRANSFER
Factors affecting electron spin polarization in photosynthetic systems
[DE90-000196] N90-14764
Multiple electron capture in close ion-atom collisions
[DE90-001541] N90-14885
Charge transfer and bond lengths in YBa2Cu(sub 3-x)M(sub x)O(sub 6+y)
[DE90-002241] N90-14966
ELECTRON TRANSITIONS
Atomic structure and spectral perturbations in hot dense plasmas N90-14567
ELECTRONIC EQUIPMENT
Power factor controller study
[DE89-017655] N90-14458
Fabrication of NBN based electronic devices with silicon barriers
[AD-D014230] N90-14463
Human factors evaluation of electroluminescent display Number 1
[DE90-002231] N90-14777
ELECTRONS
A diagnostic for determining the quality of single-reference electron correlation methods
[NASA-TM-101929] N90-14874
Interaction of low-energy electrons and positrons with condensed matter: Stopping powers and inelastic mean free paths from optical data
[DE90-001001] N90-14882
ELECTROPHORESIS
Combined capillary electrophoresis and electrospray ionization mass spectrometry
[DE90-001903] N90-14322
ELEMENTARY PARTICLES
Studies of elementary particles: Proposal
[DE90-001120] N90-14879
ELEVATORS (CONTROL SURFACES)
Hinge moment coefficient derivatives for trailing-edge controls on wings at subsonic speeds
[ESDU-89009] N90-14239
ELEVATORS (LIFTS)
The space station tethered elevator system
[NASA-CR-186051] N90-14265
ELLIPSES
A tensor product b-spline method for 3D multi-block elliptic grid generation
[DE89-017440] N90-14859
ELLIPTIC DIFFERENTIAL EQUATIONS
Parallel mathematical software
[DE90-002694] N90-14822
A comparison result and elliptic equations involving subcritical exponents
[DE90-001772] N90-14850
Iterative methods of domain decomposition with cross-points for the solution of discrete elliptic problems
[DE90-000719] N90-14854
ELLIPTICAL GALAXIES
Radio and optical observations of nearby active galaxies N90-15000
EMBEDDED COMPUTER SYSTEMS
A portable ionosonde in support of reliable communications N90-14431
EMBEDDING
Embedded function methods for compressible high speed turbulent flow
[NASA-CR-186131] N90-14498
EMBRITTLEMENT
Effects of precipitate distribution on 293 K and 77 K properties of 2090-T81 weldments
[DE90-002332] N90-14349
Embrittlement of laboratory- and reactor-aged CF-3, CF-8, and CF-8M duplex stainless steels
[DE90-002777] N90-14354
EMISSION
Analysis of acid rain and associated phenomena
[DE90-002555] N90-14725
EMISSION SPECTRA
Mapping of upper electronic reaction surfaces by tuned laser photolysis and by absorption and emission spectroscopies
[DE90-000125] N90-14314
The formation of metal-oxygen species at low temperatures
[DE90-002298] N90-14323
Solid-state fluorescence above 1000 C: Application to high-temperature laser thermometry
[DE90-000728] N90-14594
A study of the infrared emission of galactic supernova remnants N90-15006
EMISSIVITY
The average ion model. Computation of the absorption and emission coefficients in hot plasmas N90-14569
EMITTANCE
An experimental and theoretical study of the aeroacoustics of external-Coanda gas flares N90-14495
EMITTERS
Decision-aid design factors in connection with HF communication and emitter location disciplines N90-14413
EMPLOYMENT
Science and technology resources in US industry: Surveys of science resources series, 1975-1986
[PB90-107194] N90-14401
ENCAPSULATING
Bulk and shear moduli of epoxy encapsulants
[DE90-000899] N90-14371
ENERGY BUDGETS
An investigation of satellite sounding products for the remote sensing of the surface energy balance and soil moisture
[NASA-CR-186073] N90-14664
ENERGY CONSERVATION
Power factor controller study
[DE89-017655] N90-14458
How far can the world get on energy efficiency alone
[DE90-001349] N90-14686
Global energy and the greenhouse issue
[DE90-001394] N90-14709
US energy use: New technologies and policies in response to global warming
[DE90-002170] N90-14724
ENERGY CONSUMPTION
Characterization of electric vehicle velocity and power profiles using road test data
[DE90-002085] N90-14630
ENERGY CONVERSION EFFICIENCY
The current status of x ray conversion efficiency modeling
[DE90-000931] N90-14591
Research on high-efficiency, multiple-gap, multijunction, amorphous-silicon-based alloy thin-film solar cells
[DE89-009444] N90-14673
Research on high-efficiency, single-junction, monolithic, thin-film amorphous silicon solar cells
[DE89-000846] N90-14687
High-efficiency large-area CdTe modules
[DE89-009498] N90-14689
Photovoltaic Measurements and Performance Branch
[DE89-009500] N90-14695
The impact of global warming on the energy system
[DE89-017775] N90-14712
ENERGY GAPS (SOLID STATE)
Multiband photoconductive detector based on layered semiconductor quantum wells
[AD-D014232] N90-14936
ENERGY LEVELS
Prospects for wavelength tunable lasers based on vacancy defects in alkaline-earth oxides
[DE90-001078] N90-14592
High resolution-angle resolved photoemission studies of high temperature superconductors
[DE89-017691] N90-14950
ENERGY SPECTRA
Evidence for anomalous cosmic ray hydrogen N90-15005
A large detector for cosmic ray abundance and energy measurements N90-15037
ENERGY STORAGE
Elastomeric impulse energy storage and transfer system
[AD-D014223] N90-14255
A heat receiver design for solar dynamic space power systems
[NASA-TM-102473] N90-14283
Energy ratings for metal oxide varistors under repetitively pulsed operation
[DE90-002353] N90-14480
Performance of the 10-kV, 100-kA pulsed-power modules for the FRX-C magnetic compression experiment
[DE89-014027] N90-14917
ENERGY TECHNOLOGY
How far can the world get on energy efficiency alone
[DE90-001349] N90-14686
The impact of global warming on the energy system
[DE89-017775] N90-14712
ENERGY TRANSFER
Energy ratings for metal oxide varistors under repetitively pulsed operation
[DE90-002353] N90-14480
Inductive store opening switch and tests for energy transfer to a load
[DE90-002818] N90-14482
Energy deposition in low power coaxial plasma thrusters N90-14911
ENGINE DESIGN
SP-100 power system conceptual design for lunar base applications
[NASA-TM-102090] N90-15030
ENGINE NOISE
Evaluation of analysis techniques for low frequency interior noise and vibration of commercial aircraft
[NASA-CR-181851] N90-14866
ENGINE TESTS
AGARD Highlights 89/2 N90-14184
ENRICHMENT
Test and evaluation of polymeric membranes for oxygen enrichment of air
[DE90-000555] N90-14321
ENTHALPY
Energies of organic compounds
[DE90-003174] N90-14324

ENTRAINMENT
Saltation thresholds and entrainment of fine particles at Earth and Martian pressures
[NASA-TM-102193] N90-14997
ENTROPY
An entropy based approach to nonlinear stability N90-14500
Algorithmic randomness, physical entropy, measurements, and the second law
[DE90-002413] N90-14823
ENVIRONMENT EFFECTS
Engineer's Refractive Effects Prediction System (EREPS) N90-14411
Proceedings of the US/FRG (Fed. Republic of Germany) research symposium: Effects of Atmospheric Pollutants on the Spruce-Fir Forests of the Eastern United States and the Fed. Republic of Germany
[PB90-107160] N90-14704
A model for the simulation of the ozone budget in the atmosphere under anthropogenic perturbation
[DE89-636294] N90-14719
Modelling of the effects of the equatorial electrojet on its environment
[DE89-636298] N90-14720
Draft Environmental Impact Statement for the Ulysses Mission (Tier 2)
[NASA-TM-102903] N90-14727
Climate-biosphere interactions scope of work
[PB90-106444] N90-14734
ENVIRONMENT POLLUTION
Discussions of global environmental problems
[DE90-002747] N90-14718
ENVIRONMENT PROTECTION
Environmental Projects. Volume 6: Modifications of wastewater evaporation ponds
[NASA-CR-186099] N90-14700
Managing marine protected areas: An action plan
[PB89-158778] N90-14701
ENVIRONMENTAL CHEMISTRY
International Conference on Global and Regional Atmospheric Environmental Chemistry and visit to Hangzhou, China, foreign trip report
[DE90-000099] N90-14713
ENVIRONMENTAL MONITORING
Summary of 1987 and 1988 manatee aerial surveys at Kennedy Space Center
[NASA-TM-102783] N90-14669
Profile measurements of sulfur dioxide, nitrogen oxides, and nitric acid deposition velocities in California's south coast air basin
[PB90-104001] N90-14703
Integrated computer-based tools to facilitate environmental monitoring, assessment, and restoration
[DE90-002732] N90-14717
ENVIRONMENTAL QUALITY
Environmental quality and the shift to alternative fuels: Progress and interim findings of a Department of Energy study of transition in vehicular power systems
[DE90-002178] N90-14716
ENVIRONMENTAL SURVEYS
Draft Environmental Impact Statement for the Ulysses Mission (Tier 2)
[NASA-TM-102903] N90-14727
ENVIRONMENTAL TESTS
Thermal environmental tests on space simulation chamber
[DE90-000927] N90-14251
ENZYME ACTIVITY
Decomposition in Arctic terrestrial environments
[DE90-001196] N90-14706
EPITAXY
Hydrogen radical enhanced growth of solar cells
[DE89-009497] N90-14694
Method of sensitizing PB-Salt epitaxial films for Schottky diodes
[AD-D014244] N90-14937
The influence of the substrate surface on the nucleation and growth of superconducting thin films
[DE90-003649] N90-14983
EPOXY RESINS
Bulk and shear moduli of epoxy encapsulants
[DE90-000899] N90-14371
EQUATIONS OF MOTION
AcSim: Aircraft simulation program with application to flight profile generation
[AD-A212466] N90-14217
Introduction to data items on flight path optimisation
[ESDU-89015] N90-14221
Multigrid solutions of elliptic fluid flow problems N90-14507
Chaotic behavior in nonlinear polarization dynamics
[DE89-013453] N90-14589
Self-field-induced chaotic electron motion in free electron lasers
[DE90-001710] N90-14598
Stability and dynamics of constrained flexible multibody systems N90-14609
EQUATIONS OF STATE
The generalized van der Waals theory of pure fluids and mixtures
[DE90-000504] N90-14307
Thermodynamic properties and hydrodynamic response of high-density high-temperature C H N O mixtures
[DE90-000836] N90-14318
The Periodic Law at high pressures
[DE90-000837] N90-14319
Detonation product equation of state for Baratol
[DE90-001050] N90-14384
Non-equilibrium effects of slow diffusion controlled reactions on the properties of explosives
[DE90-000822] N90-14391
General exact solution for homogeneous time-dependent self-gravitating perfect fluids
[DE89-618425] N90-14514
Perturbations in high-velocity gas flow
[DE90-000539] N90-14520
A new simulation method for the efficient calculation of benchmarks for detonation products equations of state
[DE90-001837] N90-14522
Some numerical experiments concerning the equation of state algorithm for multi-material cells in HULL
[DE89-008240] N90-14827
Equation of state and opacity of dense plasmas
[DE90-002223] N90-14926
Perturbation methods for the calculation of gravitational waves from slightly non-spherical spacetimes with applications to stellar core collapse N90-15015
EQUATORIAL ATMOSPHERE
A low-order model of the equatorial ocean-atmosphere system N90-14730
EQUATORIAL ELECTROJET
Modelling of the effects of the equatorial electrojet on its environment
[DE89-636298] N90-14720
EROSION
Pipe and bend erosion by pneumatic transport of solids at high temperature
[DE89-015741] N90-14524
ERROR ANALYSIS
Methodology for the calibration of and data acquisition with a six-degree-of-freedom acceleration measurement device
[PB89-233597] N90-14531
Some edge-enhancing operators and their applications to image enhancement and edge detection N90-14810
Local error estimates for discontinuous solutions of nonlinear hyperbolic equations
[NASA-CR-181960] N90-14847
ESTIMATES
Rainfall estimation over Africa using satellite data N90-14742
Local error estimates for discontinuous solutions of nonlinear hyperbolic equations
[NASA-CR-181960] N90-14847
ESTIMATING
Normal force, pitching moment, and side force of forebody-cylinder combinations for angles of attack up to 90 degrees and Mach numbers up to 5
[ESDU-89014] N90-14192
Example of procedure in calculation of control hinge moments
[ESDU-89010] N90-14240
The effects of clutter-rejection filtering on estimating weather spectrum parameters
[NASA-CR-186212] N90-14754
Power spectral estimation algorithms
[NASA-CR-186189] N90-14812
Estimating methods for counting process intensities: Non-parametric methods
[IMAG-RR-774-M] N90-14846
ETCHING
Method of making self-aligned GaAs/AlGaAs FET's
[AD-D014229] N90-14935
EULER EQUATIONS OF MOTION
A dynamic multiblock approach to solving the unsteady Euler equations about complex configurations N90-14497
EUROPEAN SPACE AGENCY
An international discussion on research in solar and space physics N90-14996
EVACUATING (TRANSPORTATION)
Aerospace vehicle design, spacecraft section. Volume 1: Project Groups 3 through 5
[NASA-CR-186053] N90-14263
Aerospace vehicle design, spacecraft section. Volume 2: Project Groups 6 through 8
[NASA-CR-186054] N90-14264
EVAPORATION
High temperature chemistry of complex vaporization/decomposition processes
[DE89-016559] N90-14306
Propagation prediction for the North Sea environment N90-14423
Environmental Projects. Volume 8: Modifications of wastewater evaporation ponds
[NASA-CR-186099] N90-14700
Method of sensitizing PB-Salt epitaxial films for Schottky diodes
[AD-D014244] N90-14937
Semi-empirical theory of heat-transfer when boiling
[DE89-635418] N90-14984
EXCIMER LASERS
Qualification of diode foil materials for excimer lasers
[DE90-000602] N90-14593
EXCITATION
Theoretical and material studies of thin-film electroluminescent devices
[NASA-CR-186104] N90-14468
Transient response of flexible rotor-bearing systems subjected to combined unbalance and ground excitations N90-14816
Calculation of two-neutron multiplicity in photonuclear reactions
[NASA-TP-2968] N90-14890
EXOBIOLOGY
USSR Space Life Sciences Digest. Index to issues 21-25
[NASA-CR-3922(30)] N90-14763
Exploring the living universe: A strategy for space life sciences
[NASA-TM-101891] N90-14778
EXPANSION
Is the number of photons conserved in an expanding universe
[DE89-618836] N90-15018
EXPERIMENT DESIGN
Shuttle Laser Technology Experiment Facility (LTEF)-to-airplane lasercom experiment: Airplane considerations
[NASA-TM-100749] N90-14260
Design considerations for space flight hardware
[NASA-TM-102300] N90-14275
Engineering sciences design. Design and implementation of components for a bioregenerative system for growing higher order plants in space
[NASA-CR-186056] N90-14761
QUEST/Ada: Query utility environment for software testing of Ada
[NASA-CR-186121] N90-14787
EXPERIMENTATION
The processes of scientific research: The strategy of experimentation N90-14788
EXPERT SYSTEMS
A portable ionosonde in support of reliable communications N90-14431
Expert system for fault diagnostics of rotating machines
[DE89-766980] N90-14621
Knowledge-based reusable software synthesis system N90-14791
Architectures for reasoning in parallel
[NASA-CR-186237] N90-14836
The design and implementation of an intelligent interface for information retrieval N90-14991
EXPLODING WIRES
Electrothermal response testing more than a quality assurance tool
[DE90-001449] N90-14536
EXPLOSIONS
Testing and performance of a high-gain flux-compression generator
[DE90-002808] N90-14492
EXPLOSIVES
Thermodynamic properties and hydrodynamic response of high-density high-temperature C H N O mixtures
[DE90-000836] N90-14318
Pentafluorothio polynitroaliphatic explosives
[AD-D014221] N90-14383
Detonation product equation of state for Baratol
[DE90-001050] N90-14384
Calibration curves for some standard Gap Tests
[DE89-016599] N90-14389
Non-equilibrium effects of slow diffusion controlled reactions on the properties of explosives
[DE90-000822] N90-14391
Phase changes in carbon and nitrogen systems: Their effects on the detonation properties of high explosives
[DE90-000829] N90-14392
Reactive flow measurements and calculations for ZrH2-based composite explosives
[DE90-000831] N90-14393

Reaction zone structure in supracompressed detonating explosives
[DE90-000832] N90-14394
Fast transit gas- and condensed-phase chemistry of energetic materials
[DE90-001656] N90-14395

EXPONENTS
A comparison result and elliptic equations involving subcritical exponents
[DE90-001772] N90-14850

EXPOSURE
Radiation damage and its influence on source requirements for high resolution x ray holography
[DE90-002508] N90-14540
Biological effects of hyperthermia and potential risk associated with ultrasonic exposure
[PB89-100702] N90-14768

EXTINCTION
Effects of flame stretch on the propagation, extinction, and stability of premixed flames N90-14301

EXTRAVEHICULAR ACTIVITY
Extravehicular activity welding experiment
[NASA-CR-183848] N90-14608

EXTREME ULTRAVIOLET RADIATION
Proof-of-principle experiment for a hot electron pumped XUV amplifier
[DE90-000820] N90-14586

EXTREMELY LOW FREQUENCIES
MTX (Microwave Tokamak Experiment)/ELF (Electron Laser Facility) 2 microwave power measurements and calibration for the 2-GW, 140-GHz, ELF 2 Free Electron Laser (FEL)
[DE90-000825] N90-14922

F

F-104 AIRCRAFT
Airdata calibration of a high-performance aircraft for measuring atmospheric wind profiles
[NASA-TM-101714] N90-14228

FABRICATION
Sandia Satellite Program summary of operational procedures
[DE90-000892] N90-14249
Designing for superplastic alloys N90-14332
An electroformed nickel-sulfur alloy for a nose cone
[DE90-000866] N90-14337
Automated glass fiber drawing
[DE90-000894] N90-14367
Integrating and enhancing tools for ASIC (Application-Specific Integrated Circuits) design using MOSIS (Metal Oxide Semiconductor Implementation Service) fabrication
[DE90-001601] N90-14475
Practical superconductor development for electrical power applications
[DE90-001804] N90-14487
Method for fabricating thin film metallic meshes for use as Fabry-Perot interferometer elements, filters and other devices
[AD-D014236] N90-14529
Results of the 1989 NASA/JPL balloon flight solar cell calibration program
[NASA-CR-186114] N90-14672
Technology development program for an advanced microsheet glass concentrator
[NASA-TM-102406] N90-14678
Photovoltaic Measurements and Performance Branch
[DE89-009500] N90-14695

FABRY-PEROT INTERFEROMETERS
Method for fabricating thin film metallic meshes for use as Fabry-Perot interferometer elements, filters and other devices
[AD-D014236] N90-14529
High resolution Doppler lidar
[NASA-CR-183288] N90-14542

FACTOR ANALYSIS
The processes of scientific research: The strategy of experimentation N90-14788

FAILURE
Electrical breakdown in vacuum
[DE90-001623] N90-14485
Failure probability estimate of Type 304 stainless steel piping
[DE90-000659] N90-14635

FAILURE ANALYSIS
SRB thermal environments
[NASA-CR-183801] N90-14276
Cavitation and superplasticity N90-14329
Numerical and empirical verification of the stress state in a ceramic, button-head, tensile specimen
[DE90-001645] N90-14375
A laboratory test for fuel injector deposit studies
[DE90-000802] N90-14629

FAILURE MODES
Zinc/bromine battery evaluation at SNL (Sandia National Laboratory)
[DE89-015847] N90-14473

FAR INFRARED RADIATION
A compact, high-powered far-infrared (FIR) laser
[DE89-016786] N90-14597

FATIGUE (BIOLOGY)
The development of a model of the human responses to load carriage N90-14775

FATIGUE (MATERIALS)
A computer-controlled automated test system for fatigue and fracture testing
[DE90-002931] N90-14661

FATIGUE LIFE
Fatigue analysis and reconstruction of helicopter load spectra N90-14304
Thermal fatigue durability for advanced propulsion materials
[NASA-TM-102348] N90-14641

FAULT TOLERANCE
NETRA: A parallel architecture for integrated vision systems. 1: Architecture and organization
[NASA-CR-185955] N90-14839

FEASIBILITY ANALYSIS
Applications of superconductor technologies to transportation
[DE90-000856] N90-14961

FERMI LIQUIDS
High resolution-angle resolved photoemission studies of high temperature superconductors
[DE89-017691] N90-14950

FERRITES
Embrittlement of laboratory- and reactor-aged CF-3, CF-8, and CF-8M duplex stainless steels
[DE90-002777] N90-14354

FERROMAGNETIC FILMS
Surface magneto-optical studies of ultrathin ferromagnetic films
[DE90-002199] N90-14980

FIBER COMPOSITES
Oxidation effects on the mechanical properties of SiC fiber-reinforced reaction-bonded silicon nitride matrix composites
[NASA-TM-102360] N90-14287
Carbon fiber reinforced metal matrix composites
[AD-D014245] N90-14289
Elasto-plastic analysis of unidirectional fiber-reinforced composites subjected to transverse normal loading using the finite element method N90-14292
Parametric studies to determine the effect of compliant layers on metal matrix composite systems
[NASA-TM-102465] N90-14294
Friction and wear of glassy carbon in sliding contact, revision 1
[DE90-000743] N90-14365
Challenges in processing for polymer composites
[DE90-002224] N90-14376

FIBER OPTICS
Fiber-optic sensors for composite cure analysis and lifetime nondestructive evaluation
[DE90-001739] N90-14296
Method and apparatus to enhance the sensitivity of cylindrical magnetostrictive transducer to magnetic fields
[AD-D014218] N90-14459
A fiber-fed imaging spectrometer
[DE90-001008] N90-14538
Simulated Brillouin backscattering in optical fibers: A ring resonator N90-14556
Spectral contents readout of birefringent sensor
[NASA-CR-179444] N90-14905

FIBERS
Density of intercalated graphite fibers
[NASA-TM-102411] N90-14362
Experimental study on the filamentary instability in laser-matter interactions at short wave lengths N90-14547

FIELD EFFECT TRANSISTORS
Method of making self-aligned GaAs/AlGaAs FET's
[AD-D014229] N90-14935
The effects of heavy particle radiation on semiconductor devices
[DE90-001679] N90-14962

FIELD OF VIEW
Remote sensing of the aerosol scattering coefficient with a multi-field-of view lidar N90-14437

FIELD STRENGTH
The FTZ HF propagation model for use on small computers and its accuracy N90-14447
Kilometric type III radio bursts and interplanetary transients N90-15038

FIELD THEORY (PHYSICS)
Aspects of field theory related to the Zakharov problem N90-14551

FILM THICKNESS
A capacitive technique for real-time monitoring polymer coating thickness on carbon filaments during prepregging process
[NASA-TM-101682] N90-14533

FILTRATION
The fluid mechanics of filters N90-14499

FINITE DIFFERENCE THEORY
Computation of unsteady transonic flow about airfoils in frequency domain using the full-potential equation N90-14198
On the application of subcell resolution to conservation laws with stiff source terms
[NASA-TM-102384] N90-14844
Iterative methods of domain decomposition with cross-points for the solution of discrete elliptic problems
[DE90-000719] N90-14854

FINITE ELEMENT METHOD
Finite element analysis of laminated composite plates N90-14291
Elasto-plastic analysis of unidirectional fiber-reinforced composites subjected to transverse normal loading using the finite element method N90-14292
Finite element analysis of frictional contact problems N90-14612
Tire modeling by finite elements N90-14614
Transient response of flexible rotor-bearing systems subjected to combined unbalance and ground excitations N90-14616
Non-linear vibrations, stability, and dynamics of structures and mechanisms
[AD-A212152] N90-14639
Parallel eigenanalysis of finite element models in a completely connected architecture
[NASA-CR-185166] N90-14652

FINITE VOLUME METHOD
Advanced 3-D CFD algorithm for turbomachinery N90-14233

FIR FILTERS
Adaptive clutter rejection filters for airborne Doppler weather radar applied to the detection of low altitude windshear
[NASA-CR-186211] N90-14453
The effects of clutter-rejection filtering on estimating weather spectrum parameters
[NASA-CR-186212] N90-14754

FIRE DAMAGE
Risk-based fire safety experiment definition for manned spacecraft
[NASA-CR-183835] N90-14262
A discussion of fire suppression induced equipment damage and systems impact through an examination of spurious fire suppression actuation incidents
[DE90-000792] N90-14402

FIRE EXTINGUISHERS
A discussion of fire suppression induced equipment damage and systems impact through an examination of spurious fire suppression actuation incidents
[DE90-000792] N90-14402

FIRE FIGHTING
A discussion of fire suppression induced equipment damage and systems impact through an examination of spurious fire suppression actuation incidents
[DE90-000792] N90-14402

FIRE PREVENTION
Risk-based fire safety experiment definition for manned spacecraft
[NASA-CR-183835] N90-14262

FIRES
A discussion of fire suppression induced equipment damage and systems impact through an examination of spurious fire suppression actuation incidents
[DE90-000792] N90-14402

FISSION
Biomodal spontaneous fission
[DE90-001516] N90-14886

FLAME PROPAGATION
Effects of flame stretch on the propagation, extinction, and stability of premixed flames N90-14301
Flame acceleration studies in the MINIFLAME facility
[DE90-000041] N90-14310
A numerical study of thin flame representations
[DE89-017889] N90-14313

FLAMES
Flame acceleration studies in the MINIFLAME facility
[DE90-000041] N90-14310
A numerical study of thin flame representations
[DE89-017889] N90-14313

FLANGES
Flight set 360T004 (STS-30) field joint protection system, volume 7
[NASA-CR-183829] N90-14280

FLAPS (CONTROL SURFACES)
Validation of a computer code for analysis of subsonic aerodynamic performance of wings with flaps in combination with a canard or horizontal tail and an application to optimization
[NASA-TP-2961] N90-14187
FLARE STARS
As observational and theoretical investigation of stellar flares N90-15012
FLASHOVER
Review of surface flashover theory
[DE90-000806] N90-14469
FLEXIBILITY
Crazing and degradation of flexure strength in acrylic plates as a function of time
[AD-A212835] N90-14357
Finite element analysis of frictional contact problems N90-14612
Flexural and torsional-flexural buckling of thin-walled open section struts
[ESDU-89007] N90-14643
FLEXIBLE BODIES
Manipulation strategies for massive space payloads
[NASA-CR-186081] N90-14247
Optimal stochastic modeling and control of flexible structures
[AD-A212347] N90-14269
Stability and dynamics of constrained flexible multibody systems N90-14609
Transient response of flexible rotor-bearing systems subjected to combined unbalance and ground excitations N90-14616
FLEXIBLE SPACECRAFT
Dynamics and control of flexible spacecraft during and after slewing maneuvers
[NASA-CR-186123] N90-14270
FLIGHT CHARACTERISTICS
Global stratospheric change: Requirements for a Very-High-Altitude Aircraft for Atmospheric Research
[NASA-CP-10041] N90-14220
FLIGHT CLOTHING
Integrated G-suit/immersion suit
[AD-A212989] N90-14774
FLIGHT CONDITIONS
Flight in adverse environmental conditions
[AGARD-AR-277] N90-14218
FLIGHT CONTROL
A helicopter flight path controller design via a nonlinear transformation technique N90-14242
Guidance, steering, load relief and control of an asymmetric launch vehicle
[NASA-CR-185598] N90-14257
FLIGHT CREWS
Performance evaluation of the Puritan-Bennett crew-member portable protective breathing device as prescribed by portions of FAA action notice A-8150.2
[AD-A211113] N90-14772
FLIGHT MECHANICS
Flight in adverse environmental conditions
[AGARD-AR-277] N90-14218
FLIGHT PATHS
AcSim: Aircraft simulation program with application to flight profile generation
[AD-A212466] N90-14217
Introduction to data items on flight path optimisation
[ESDU-89015] N90-14221
A helicopter flight path controller design via a nonlinear transformation technique N90-14242
Low level range coverage performance prediction for VHF radar N90-14439
FLIGHT SAFETY
Flight in adverse environmental conditions
[AGARD-AR-277] N90-14218
Workload induced spatio-temporal distortions and safety of flight
[DE89-016613] N90-14771
FLIGHT SIMULATION
AcSim: Aircraft simulation program with application to flight profile generation
[AD-A212466] N90-14217
FLIGHT TESTS
An in-flight investigation of ground effect on a forward-swept wing airplane
[NASA-TM-101708] N90-14202
An in-flight technique for wind measurement in support of the space shuttle program
[NASA-TM-4154] N90-14224
Flight evaluation of a pneumatic system for unsteady pressure measurements using conventional sensors
[NASA-TM-4131] N90-14225
SRB thermal environments
[NASA-CR-183801] N90-14276
FLIR DETECTORS
Airborne FLIR detection of surface targets N90-14416
FLOW DISTRIBUTION
Numerical investigations in three-dimensional internal flows
[NASA-CR-186068] N90-14189
A computational analysis of the transonic flow field of two-dimensional minimum length nozzles N90-14194
Navier-Stokes solutions of 2-D transonic flow over unconventional airfoils N90-14195
Navier-Stokes analysis of airfoils with leading edge ice accretions N90-14196
Computation of unsteady transonic flow about airfoils in frequency domain using the full-potential equation N90-14198
An analysis of the viscous flow through a compact radial turbine by the average passage approach
[NASA-TM-102471] N90-14206
Acoustic-vortical-combustion interaction in a solid fuel ramjet simulator N90-14234
Effects of flame stretch on the propagation, extinction, and stability of premixed flames N90-14301
A numerical study of thin flame representations
[DE89-017689] N90-14313
An experimental and theoretical study of the aeroacoustics of external-Coanda gas flares N90-14495
Fluid-particle interaction in solid-liquid two-phase grid turbulence N90-14496
A dynamic multiblock approach to solving the unsteady Euler equations about complex configurations N90-14497
Numerical solution of the incompressible Navier-Stokes equations N90-14501
Three-dimensional solution-adaptive grid generation of composite configurations N90-14509
Spatial evolution of nonlinear acoustic mode instabilities on hypersonic boundary layers
[NASA-TM-102431] N90-14517
The laminar to slug flow transition in Hele-Shaw flow
[DE90-000636] N90-14521
An initial look at the dynamics of the microscale flow field within a large wind farm in response to variations in the natural inflow
[DE89-009501] N90-14682
FLOW GEOMETRY
A computational analysis of the transonic flow field of two-dimensional minimum length nozzles N90-14194
Selection of the energy-efficient enhancement geometry for single-phase turbulent flow inside tubes
[DE89-017690] N90-14519
FLOW MEASUREMENT
Reactive flow measurements and calculations for ZrH2-based composite explosives
[DE90-000831] N90-14393
FLOW STABILITY
A note concerning the onset of three dimensionality and time dependence in Goertler vortices
[NASA-CR-181956] N90-14193
Effects of flame stretch on the propagation, extinction, and stability of premixed flames N90-14301
An entropy based approach to nonlinear stability N90-14500
The stability of Taylor-Couette flow with radial heating N90-14502
FLOW VELOCITY
Fluid flow analysis of the SSME high pressure fuel and oxidizer turbine coolant systems
[NASA-CR-183736] N90-14277
Fluid-particle interaction in solid-liquid two-phase grid turbulence N90-14496
Embedded function methods for compressible high speed turbulent flow
[NASA-CR-186131] N90-14498
Heat transfer to a stationary and moving sphere immersed in a fluidized bed N90-14503
An experimental investigation of shear layer mixing in supersonic flows N90-14508
Pipe and bend erosion by pneumatic transport of solids at high temperature
[DE89-015741] N90-14524
Ion collection by probing objects in flowing magnetized plasmas
[DE90-001711] N90-14916
FLOW VISUALIZATION
Visualization of boundary layer transition zone movement on oscillating airfoils with shear-sensitive liquid-crystal coatings
[DE89-009570] N90-14210
FLUID DYNAMICS
Laser velocimeter and total pressure measurements in circular-to-rectangular transition ducts
[NASA-CR-182286] N90-14494
An experimental and theoretical study of the aeroacoustics of external-Coanda gas flares N90-14495
On the application of subcell resolution to conservation laws with stiff source terms
[NASA-TM-102384] N90-14844
FLUID FLOW
Fluid flow analysis of the SSME high pressure fuel and oxidizer turbine coolant systems
[NASA-CR-183736] N90-14277
The fluid mechanics of filters N90-14499
On the application of subcell resolution to conservation laws with stiff source terms
[NASA-TM-102384] N90-14844
FLUID JETS
Supercritical fluid chromatography/supersonic jet spectroscopy
[DE90-001378] N90-14308
FLUID MECHANICS
The fluid mechanics of filters N90-14499
Interfacial area in two-phase flow
[DE90-002210] N90-14527
FLUID-SOLID INTERACTIONS
Fluid-particle interaction in solid-liquid two-phase grid turbulence N90-14496
FLUIDIZED BED PROCESSORS
Heat transfer to a stationary and moving sphere immersed in a fluidized bed N90-14503
FLUIDS
The generalized van der Waals theory of pure fluids and mixtures
[DE90-000504] N90-14307
Wide-angle propagation in inhomogeneous fluids and elastic solids using perturbation methods N90-14868
FLUORESCENCE
Development of laser excited atomic fluorescence and ionization spectrometric methods
[DE90-001567] N90-14320
X ray microprobe for the microcharacterization of materials
[DE89-006038] N90-14863
FLUORO COMPOUNDS
Pentafluorothio polynitroaliphatic explosives
[AD-D014221] N90-14383
FLUOROPOLYMERS
The 3F condensation polyimides: Review and update
[NASA-TM-102353] N90-14363
FLUTTER ANALYSIS
Experimental transonic flutter characteristics of two 72 deg-sweep delta-wing models
[NASA-TM-101659] N90-14205
FLUX DENSITY
The creation of high energy densities with antimatter beams
[DE90-002383] N90-14899
FLUX PINNING
Flux pinning and microstructure in YBa2Cu3O7
[DE90-001562] N90-14948
Effects of shock-induced defects on flux pinning in YBa2Cu3O(7-delta)
[DE90-000824] N90-14959
Shock-induced defects and flux pinning in YBa2Cu3O sub 7-delta + Ag composites
[DE90-000827] N90-14960
FLUX VECTOR SPLITTING
A dynamic multiblock approach to solving the unsteady Euler equations about complex configurations N90-14497
FOCAL PLANE DEVICES
CCD TV focal plane guider development and comparison to SIRTF applications
[NASA-CR-185977] N90-14900
FOCUSING
The phase gradient autofocus algorithm: An optimal estimator of the phase derivative
[DE90-000895] N90-14614
FOREBODIES
Normal force, pitching moment, and side force of forebody-cylinder combinations for angles of attack up to 90 degrees and Mach numbers up to 5
[ESDU-89014] N90-14192
FORECASTING
Operational Decision Aids for Exploiting or Mitigating Electromagnetic Propagation Effects
[AGARD-CP-453] N90-14405
A forecasting system using the parabolic equation: Application to surface-to-air propagation in the presence of elevated layers N90-14420
Assessment of anomalous propagation predictions using minisonde refractivity data and the parabolic equation method N90-14424
A modern trans-ionospheric propagation sensing system N90-14430
The use of backscatter for modelling ionosphere and jamming in very short term forecasts N90-14434
A one-dimensional shipboard model for forecasting refractive effects in the planetary boundary layer N90-14442

Modelling UHF propagation for frequency assignment in radio relay networks N90-14445
Testing and performance of a high-gain flux-compression generator [DE90-002808] N90-14492
Comparison of shock severity measures [DE90-000790] N90-14654
Global natural resource monitoring and assessment [DE90-001294] N90-14671
Turbulent wind at the equatorial segment of an operating Darrieus wind turbine blade [DE90-002672] N90-14698
Application of surface analysis methods to studies of atmospheric deposition in forests [DE90-000562] N90-14714
Climate projections with regional resolution [DE90-000858] N90-14715
The identification of terrain-induced circulations using principal components [DE90-001991] N90-14739

FOREST MANAGEMENT
Proceedings of the US/FRG (Fed. Republic of Germany) research symposium: Effects of Atmospheric Pollutants on the Spruce-Fir Forests of the Eastern United States and the Fed. Republic of Germany [PB90-107160] N90-14704

FORESTS
Global natural resource monitoring and assessment [DE90-001294] N90-14671
Proceedings of the US/FRG (Fed. Republic of Germany) research symposium: Effects of Atmospheric Pollutants on the Spruce-Fir Forests of the Eastern United States and the Fed. Republic of Germany [PB90-107160] N90-14704
Application of surface analysis methods to studies of atmospheric deposition in forests [DE90-000562] N90-14714
Nitrogen deposition to forest trees [DE90-003285] N90-14726

FORMING TECHNIQUES
Superplastic sheet forming N90-14327

FOURIER ANALYSIS
Frequency agile synthetic aperture radar [AD-D014235] N90-14451
Comparison of shock severity measures [DE90-000790] N90-14654
Versatility of the CFR algorithm for limited angle reconstruction [DE90-001421] N90-14817

FOURIER TRANSFORMATION
Soft x ray microscope using Fourier transform holography [DE90-002291] N90-14539

FRACTIONATION
Thermal stability of jet fuel [DE90-001160] N90-14385

FRACTURE MECHANICS
Effects of dislocation substructure and prestrain on fracture behavior in aluminum and steel alloys N90-14334
The effect of hydrogen charging on the mechanical properties of aluminum alloy 2090 [DE90-000129] N90-14341
Non-linear vibrations, stability, and dynamics of structures and mechanisms [AD-A212152] N90-14639
A nonlinear high temperature fracture mechanics basis for strainrange partitioning [NASA-TM-4133] N90-14642
Fatigue fracture in the presence of shot peening residual stresses: Initiation, propagation, and relaxation phenomena N90-14644
Mechanics of interaction of a crack with microcracks N90-14650
Fracture mechanics of porous materials [DE90-000023] N90-14657
Engineering approaches to the application of fracture toughness data in the nuclear industry [DE90-001596] N90-14659

FRACTURE STRENGTH
Effects of dislocation substructure and prestrain on fracture behavior in aluminum and steel alloys N90-14334
The strength-toughness combination of the aluminum-lithium alloys 2090 and 2091 at cryogenic temperatures [DE90-001425] N90-14338
The 4.2 K fracture toughness of 304 stainless steel in a magnetic field [DE90-002083] N90-14347
Strength and toughness of monolithic and composite silicon nitrides [NASA-TM-102423] N90-14368
Engineering approaches to the application of fracture toughness data in the nuclear industry [DE90-001596] N90-14659

FRACTURING
Mechanisms of wear in structural ceramic materials N90-14360

FRAGMENTATION
Spall strength measurements on shockloaded refractory metals [DE90-000839] N90-14345
Mechanisms of wear in structural ceramic materials N90-14360
Hypervelocity impact calculations using CTH: Case studies [DE90-002891] N90-14632

FRANCE
French technological progress in the field of robotics and teleoperation [DE90-001590] N90-14626

FREE CONVECTION
Unsteady hydromagnetic flow of a radiating gas in a vertical channel with axial temperature variation [DE90-600934] N90-14525

FREE ELECTRON LASERS
Numerical simulations of free-electron laser oscillators [DE89-003488] N90-14588
Self-field-induced chaotic electron motion in free electron lasers [DE90-001710] N90-14598
Optical design and performance of an XUV FEL (Free-Electron Laser) oscillator [DE90-002381] N90-14599
Compact RF-linac free-electron lasers [DE90-002386] N90-14600
INEX (Integrated Numerical Experiment) simulations of the Los Alamos HIBAF (High-Brightness Accelerator Free-Electron Laser) free-electron laser MOPA (Master Oscillator Power Amplifier) experiment [DE90-002387] N90-14601
Lasing on the third harmonic [DE90-002389] N90-14602
Analytical treatment of electron trajectory straightener issues in free-electron lasers [DE90-002405] N90-14603
Theory of harmonic radiation using a single-electron source model [DE90-002412] N90-14606
Microwave Transport Systems for the MTX (Microwave Tokamak Experiment) [DE90-000821] N90-14921
MTX (Microwave Tokamak Experiment)/ELF (Electron Laser Facility) 2 microwave power measurements and calibration for the 2-GW, 140-GHz, ELF 2 Free Electron Laser (FEL) [DE90-000825] N90-14922
Precision timing and interlocks systems for FEL (Free-Electron Laser) heating experiments on MTX (Microwave Tokamak Experiment) [DE90-000833] N90-14923
Microwave Tokamak Experiment: An overview of the construction and checkout phase [DE90-000834] N90-14924
RF superconductivity research and development at Los Alamos National Laboratory [DE90-002440] N90-14969

FREE FLOW
Surface flow and heating distributions on a cylinder in near wake of Aeroassist Flight Experiment (AFE) configuration at incidence in Mach 10 Air [NASA-TP-2954] N90-14493
Detailed analysis of the wake and free-flow characteristics at the Goodnoe Hills MOD-2 site [DE90-002725] N90-14692

FREE RADICALS
Atomic hydrogen as a launch vehicle propellant [NASA-TM-102459] N90-14284
A measurement of hydroxyl in the daytime mesosphere N90-14732

FREQUENCY ASSIGNMENT
Modelling UHF propagation for frequency assignment in radio relay networks N90-14445
Application of heuristic satellite plan synthesis algorithms to requirements of the WARC-88 allotment plan [NASA-TM-102479] N90-14856

FREQUENCY MEASUREMENT
Detection of a chirping electromagnetic signal [DE90-002105] N90-14457

FREQUENCY MODULATION
Monolithic laser diode structure for microwave generation [AD-D014210] N90-14543

FRESNEL LENSES
Conceptual design study of a 5 kilowatt solar dynamic Brayton power system using a dome Fresnel lens solar concentrator [NASA-CR-185134] N90-14281

FRICTION
Mechanisms of wear in structural ceramic materials N90-14360
Finite element analysis of frictional contact problems N90-14612
Tire modeling by finite elements N90-14614
Single particle friction tests with cellulose acetate sphere samples [DE89-017537] N90-14622

FRICTION FACTOR
Selection of the energy-efficient enhancement geometry for single-phase turbulent flow inside tubes [DE89-017690] N90-14519
Finite element analysis of frictional contact problems N90-14612

FUEL CELLS
Proceedings of the First Annual Fuel Cells Contractors Review Meeting [DE89-011699] N90-14675
Heat and mass transfer design issues in PEM fuel cell hardware [DE89-016779] N90-14677
Electrode development in monolithic solid oxide fuel cells [DE90-001910] N90-14684
Interfacial effects in monolithic solid oxide fuel cells [DE90-001914] N90-14690
Solid oxide fuel cells electrodes based on In(sub 2)O(sub 3)-PrO(sub 1.83)-ZrO(sub 2) [DE90-002666] N90-14691
Technology Base Research Project for electrochemical energy storage [DE90-002604] N90-14693

FUEL CONSUMPTION
Assessment of costs and benefits of flexible and alternative fuel use in the US transportation sector. Technical report three: Methanol production and transportation costs [DE90-002625] N90-14396

FUEL CONTROL
Guidance and Control strategies for aerospace vehicles [NASA-CR-186195] N90-14243

FUEL INJECTION
A laboratory test for fuel injector deposit studies [DE90-000802] N90-14629

FUEL PRODUCTION
Photoconversion of inorganics to methane [PB89-230643] N90-14379
Assessment of costs and benefits of flexible and alternative fuel use in the US transportation sector. Technical report three: Methanol production and transportation costs [DE90-002625] N90-14396

FUELS
A laboratory test for fuel injector deposit studies [DE90-000802] N90-14629

FUNCTIONS (MATHEMATICS)
Parallel projected variable metric algorithms for unconstrained optimization [NASA-CR-181930] N90-14842
Classification of modular invariant partition functions for the twisted N=2 superconformal algebra, twisted SU(2) Kac-Moody algebra and D(sub 2K) parafermions [DE90-600767] N90-14853

FUSELAGES
An analytical method for the prediction of unsteady rotor/airframe interactions in forward flight N90-14223

FUSES
Experimental investigation of a fast-acting exploding metallic foil opening switch [DE90-001051] N90-14479

G

GALACTIC CLUSTERS
Cooling flows in clusters of galaxies N90-15009

GALACTIC COSMIC RAYS
A large detector for cosmic ray abundance and energy measurements N90-15037

GALACTIC EVOLUTION
Cooling flows in clusters of galaxies N90-15009

GALACTIC STRUCTURE
A study of the infrared emission of galactic supernova remnants N90-15006

GALLIUM ARSENIDES
Characterization of two MMIC GaAs switch matrices at microwave frequencies [NASA-TM-102449] N90-14273
Method of making self-aligned GaAs/AlGaAs FET's [AD-D014229] N90-14935

GAMMA RAY ASTRONOMY
JPRS Report: Science and technology. USSR: Space. Soviet space program to the year 2000 [JPRS-USP-89-008] N90-14248

Studies of elementary particles: Proposal
[DE90-001120] N90-14879

GAMMA RAY OBSERVATORY
Long-lived space observatories for astronomy and astrophysics
[NASA-CR-185373] N90-14261

GAMMA RAY SPECTROMETERS
A fiber-fed imaging spectrometer
[DE90-001008] N90-14538

GAMMA RAYS
Gamma ray lines from dark matter annihilation
[DE90-000779] N90-15021

GAS COMPOSITION
Profile measurements of sulfur dioxide, nitrogen oxides, and nitric acid deposition velocities in California's south coast air basin
[PB90-104001] N90-14703

GAS EXCHANGE
Canopy stomatal conductance
[DE89-016860] N90-14711
High-frequency ventilation in dogs with three gases of different densities
[AD-A212862] N90-14762

GAS FLOW
Perturbations in high-velocity gas flow
[DE90-000539] N90-14520
Unsteady hydromagnetic flow of a radiating gas in a vertical channel with axial temperature variation
[DE90-600934] N90-14525

GAS GUNS
Acceleration of small, light projectiles (including hydrogen isotopes) to high speeds using a two-stage light gas gun
[DE90-002479] N90-14253

GAS MIXTURES
Asymptotic analysis of performance of membrane modules for gas separations
[DE90-000699] N90-14316

GAS TEMPERATURE
Unsteady hydromagnetic flow of a radiating gas in a vertical channel with axial temperature variation
[DE90-600934] N90-14525

GAS TUNGSTEN ARC WELDING
Extravehicular activity welding experiment
[NASA-CR-183848] N90-14608
BES welding science contractors summary report, 1988 to 1989
[DE90-001004] N90-14619

GAS TURBINES
AGARD Highlights 89/2 N90-14184

GAS-GAS INTERACTIONS
Canopy stomatal conductance
[DE89-016860] N90-14711

GASEOUS FUELS
Photoconversion of inorganics to methane
[PB89-230643] N90-14379
The conversion of carbonaceous materials to clean carbon and co-product gaseous fuel
[DE90-001561] N90-14387

GASES
High-frequency ventilation in dogs with three gases of different densities
[AD-A212862] N90-14762

GATES (CIRCUITS)
Method of making self-aligned GaAs/AlGaAs FET's
[AD-D014229] N90-14935

GAUGE THEORY
Hamiltonian flows, SU(infinity), SO(infinity), USp(infinity), and strings
[DE90-001987] N90-14851

GENES
Nomenclature for physical mapping of complex genomes
[DE89-015173] N90-14994

GEOCHEMISTRY
Earth Sciences Division annual report 1988
[DE90-002617] N90-14663
Organic geochemical and tectonic evolution of the midcontinent rift system: Organic geochemistry and micropaleontology
[DE89-017561] N90-14760

GEODESY
Correction of ionospheric effects for the precise orbit determination of satellites N90-14432
NORDA's pattern analysis laboratory: Current contributions to naval mapping, charting, and geodesy
[AD-A212731] N90-14665

GEOGRAPHY
Integrated computer-based tools to facilitate environmental monitoring, assessment, and restoration
[DE90-002732] N90-14717

GEOLOGICAL FAULTS
Fracture mechanics of porous materials
[DE90-000023] N90-14657
Organic geochemical and tectonic evolution of the midcontinent rift system: Organic geochemistry and micropaleontology
[DE89-017561] N90-14760

GEOMAGNETISM
Solar-geophysical data number 538, June 1989. Part 1: (Prompt reports). Data for May, April 1989, and late data
[PB89-223838] N90-15031

GEOMETRICAL OPTICS
Numerical simulation of laser radiation propagation in non-uniform absorbing medium. Geometrical optics approximation
[DE89-632014] N90-14585

GEOMETRY
Flame acceleration studies in the MINIFLAME facility
[DE90-000041] N90-14310
Testing and performance of a high-gain flux-compression generator
[DE90-002808] N90-14492

GEOPHYSICS
The thermal behavior of natural backgrounds and its prediction by means of numerical models N90-14436
Earth Sciences Division annual report 1988
[DE90-002617] N90-14663
Solar-geophysical data number 539, July 1989. Part 1: (Prompt reports). Data for June, May 1989, and late data
[PB89-235451] N90-15033
Solar-geophysical data number 539, July 1989. Part 2: (Comprehensive reports). Data for January 1989, and miscellaneous
[PB89-235469] N90-15034

GEOPOTENTIAL HEIGHT
An observational study of intramonthly quasi-periodicities in the Northern Hemisphere, extratropical geopotential height field N90-14729

GEOSTROPHIC WIND
Tuning of the OSCURS (Ocean Surface Current Simulations) numerical model to ocean surface measurements in the Gulf of Alaska
[PB89-103979] N90-14759

GET AWAY SPECIALS (STS)
Control of an experiment to measure acoustic noise in the space shuttle
[NPS62-89-022] N90-14869

GIANT STARS
An observational and theoretical investigation of stellar flares N90-15012

GIOTTO MISSION
Hypervelocity impact studies on the Giotto comet Halley mission N90-15008

GLASS FIBERS
Automated glass fiber drawing
[DE90-000894] N90-14367

GLASS LASERS
Ultrahigh-brightness lasers and their applications
[DE90-000877] N90-14596

GLASS TRANSITION TEMPERATURE
The 3F condensation polyimides: Review and update
[NASA-TM-102353] N90-14363

GLASSY CARBON
Friction and wear of glassy carbon in sliding contact, revision 1
[DE90-000743] N90-14365

GLOBAL WARMING
The impact of global warming on the energy system
[DE89-017775] N90-14712
Climate projections with regional resolution
[DE90-000858] N90-14715
Discussions of global environmental problems
[DE90-002747] N90-14718
Carbon dioxide and climate: Summaries of research in FY 1989
[DE90-001791] N90-14723
US energy use: New technologies and policies in response to global warming
[DE90-002170] N90-14724

GLOBULAR CLUSTERS
Ultraviolet properties of hot stars in globular clusters N90-15007

GLOW DISCHARGES
Development of laser excited atomic fluorescence and ionization spectrometric methods
[DE90-001567] N90-14320
Study of microcrystalline, silicon-carbon p-layers prepared by photo-CVD and glow discharge
[DE89-009438] N90-14939

GLUCOSE
Amperometric biosensors for glucose, lactate, and glycolate based on oxidases and redox-modified siloxane polymers
[DE90-002301] N90-14541

GOVERNMENT/INDUSTRY RELATIONS
Accessing Japanese technical information: A group of essays extracted from the NTIS (National Technical Information Service) Directory of Japanese Technical Resources in the United States for 1987 and 1988
[PB90-100165] N90-14992
DOD (Department of Defense) Freedom of Information Act Program (incorporating changes 1 and 2)
[PB90-104753] N90-14993

GRADIENTS
The phase gradient autofocus algorithm: An optimal estimator of the phase derivative
[DE90-000895] N90-14814

GRAIN BOUNDARIES
SEM (Scanning Electron Microscope) image analysis of grain growth in microwave-annealed alumina
[DE90-001606] N90-14339
Elastic softening in nanocrystalline silicon
[DE90-002268] N90-14377
Characterization of nanophase materials by x ray diffraction and computer simulation
[DE90-002270] N90-14378
The feasibility of welding of irradiated materials
[DE90-002200] N90-14631
Atomic matching across internal interfaces
[DE90-002266] N90-14889
Anisotropy of oxygen tracer diffusion in YBa2Cu3O7-delta single crystals
[DE90-001931] N90-14979
Quasicrystals and grain boundaries
[DE90-002213] N90-14981

GRAPHITE
Density of intercalated graphite fibers
[NASA-TM-102411] N90-14362

GRAPHITE-EPOXY COMPOSITES
Measurement of damping of graphite epoxy composite materials and structural joints
[NASA-CR-183802] N90-14286

GRATINGS (SPECTRA)
Non-linear optical studies of adsorbates: Spectroscopy and dynamics
[DE90-001543] N90-14312
A sampled-grating model of moire patterns from digital imaging
[AD-A213364] N90-14902

GRAVIMETRY
A study of the difference between gravimetric and gamma-gamma density near the surface in northern Yucca Flat
[DE89-017886] N90-14737
Mid-Oceanic Ridge: A Dynamic Global System
[PB89-198691] N90-14758

GRAVITATION
Partial gravity habitat study: With application to lunar base design
[NASA-CR-186048] N90-14267
General exact solution for homogeneous time-dependent self-gravitating perfect fluids
[DE89-618425] N90-14514
Vector fields and gravity on the lattice
[DE89-633885] N90-14860
Black-hole decay and topological stability in quantum gravity
[DE89-618785] N90-15017
Classical approach to higher-derivative gravity
[DE89-631649] N90-15019

GRAVITATIONAL EFFECTS
Mid-Oceanic Ridge: A Dynamic Global System
[PB89-198691] N90-14758

GRAVITATIONAL FIELDS
A study of the difference between gravimetric and gamma-gamma density near the surface in northern Yucca Flat
[DE89-017886] N90-14737
Physics with ultra-low energy antiprotons
[DE90-002397] N90-14868

GRAVITATIONAL WAVES
Perturbation methods for the calculation of gravitational waves from slightly non-spherical spacetimes with applications to stellar core collapse N90-15015

GRAVITY ANOMALIES
A study of the difference between gravimetric and gamma-gamma density near the surface in northern Yucca Flat
[DE89-017886] N90-14737

GRAZING INCIDENCE
Glancing angle x ray studies of oxide films
[DE89-017828] N90-14953

GREENHOUSE EFFECT
Global energy and the greenhouse issue
[DE90-001394] N90-14709
On the mitigation of non-CO2 greenhouse gases
[DE89-016659] N90-14710
The impact of global warming on the energy system
[DE89-017775] N90-14712

Climate projections with regional resolution
[DE90-000858] N90-14715
Discussions of global environmental problems
[DE90-002747] N90-14718
Quantifying the link between change in radiative balance and atmospheric temperature
[DE90-000819] N90-14721
Strategy for monitoring the effects of land use change on atmospheric CO2 concentrations
[DE90-001635] N90-14722
Carbon dioxide and climate: Summaries of research in FY 1989
[DE90-001791] N90-14723
US energy use: New technologies and policies in response to global warming
[DE90-002170] N90-14724

GRID GENERATION (MATHEMATICS)
Three-dimensional solution-adaptive grid generation of composite configurations N90-14509
User's guide to PMESH: A grid-generation program for single-rotation and counterrotation advanced turboprops
[NASA-CR-185156] N90-14783
A tensor product b-spline method for 3D multi-block elliptic grid generation
[DE89-017440] N90-14859

GROUND BASED CONTROL
Program VSAERO theory document: A computer program for calculating nonlinear aerodynamic characteristics of arbitrary configurations
[NASA-CR-4023] N90-14200
Prototype software reuse environment at Goddard Space Flight Center N90-14794

GROUND EFFECT (AERODYNAMICS)
An in-flight investigation of ground effect on a forward-swept wing airplane
[NASA-TM-101708] N90-14202

GROUND SPEED
Characterization of electric vehicle velocity and power profiles using road test data
[DE90-002085] N90-14630

GROUND TESTS
Introductory testimony: Hearing on nuclear power in space
[DE90-001137] N90-14897

GROUND WATER
Image processing of LANDSAT MSS data for buried valley detection in northern Indiana N90-14668

GROUP THEORY
Group-kinetic theory and modeling of atmospheric turbulence
[NASA-CR-183776] N90-14728

GUIDANCE (MOTION)
Optimal control of aero-assisted orbit transfer vehicles N90-14241
Guidance and Control strategies for aerospace vehicles
[NASA-CR-186195] N90-14243
Guidance, steering, load relief and control of an asymmetric launch vehicle
[NASA-CR-185598] N90-14257

GUIDANCE SENSORS
CCD TV focal plane guider development and comparison to SIRTF applications
[NASA-CR-185977] N90-14900

GUN PROPELLANTS
Study of new materials for gun propellant formulations
[DE89-015285] N90-14388

H

HABITATS
Partial gravity habitat study: With application to lunar base design
[NASA-CR-186048] N90-14267

HALF CONES
Stability of a supersonic boundary layer on a sharp cone at a small angle of attack N90-14510

HALL EFFECT
Theoretical reversed field pinch studies
[DE90-002114] N90-14929
Magnetotransport studies of epitaxial Cr thin films
[DE90-001930] N90-14975

HALLEY'S COMET
Hypervelocity impact studies on the Giotto comet Halley mission N90-15008

HALOGEN OCCULTATION EXPERIMENT
The retrieval of the concentrations of nitric oxide and nitrogen dioxide from satellite solar occultation measurements at sunset and sunrise N90-14733

HALOGENS
Extraterrestrial halogen and sulfur content of the stratosphere
[DE89-017623] N90-14738

HAMILTON-JACOBI EQUATION
Symplectic numerical integration of Hamiltonian systems
[DE90-002380] N90-14855

HAMILTONIAN FUNCTIONS
Hamiltonian flows, SU(infinity), SO(infinity), USp(infinity), and strings
[DE90-001987] N90-14851
Symplectic numerical integration of Hamiltonian systems
[DE90-002380] N90-14855
Spectral properties of one dimensional quasi-crystals
[PREPRINT-659] N90-14938

HANDBOOKS
Metric handbook for Federal officials: Recommendations of the Interagency Committee on Metric Policy
[PB89-226922] N90-14400

HARDNESS
Engineering approaches to the application of fracture toughness data in the nuclear industry
[DE90-001596] N90-14659

HARDWARE
High volume data storage architecture analysis
[NASA-CR-186239] N90-14784

HARMONIC GENERATIONS
Theory of harmonic radiation using a single-electron source model
[DE90-002412] N90-14606

HARMONIC RADIATION
Theory of harmonic radiation using a single-electron source model
[DE90-002412] N90-14606

HARMONICS
Strong Langmuir turbulence and second harmonics in laser-matter interactions N90-14548
Lasing on the third harmonic
[DE90-002389] N90-14602

HARTREE APPROXIMATION
Structural peculiarities and molecular properties of charge complexes formed on positive ion injection into dense inert gas media
[DE89-633953] N90-14877

HAZARDS
Environmental Projects. Volume 8: Modifications of wastewater evaporation ponds
[NASA-CR-186099] N90-14700

HEAO
The softest Einstein AGN (Active Galactic Nuclei)
[DE89-009389] N90-15020

HEAT EXCHANGERS
High-temperature corrosion of heat exchanger materials
[DE90-001963] N90-14352
Thermal design of a 10-kW helium refrigerator
[DE90-701785] N90-14403
Field testing of a ceramic heat exchanger for heat recovery application
[DE90-002082] N90-14523

HEAT FLUX
Thermal loads on tokamak plasma facing components during normal operation and disruptions
[DE90-000794] N90-14919

HEAT PIPES
Design and demonstration of heat pipe cooling for NASP and evaluation of heating methods at high heating rates
[DE89-016995] N90-14227
A heat receiver design for solar dynamic space power systems
[NASA-TM-102473] N90-14283

HEAT PUMPS
System design and performance prediction of a free-piston Stirling engine/magnetic coupling/compressor assembly in a gas residential heat pump
[DE89-016070] N90-14696
Heat transfer of buried pipe for heat pump application
[DE90-000580] N90-14697
New heating and cooling technology: Regenerative heat pump according to the Vuilleumier principle
[DE90-002701] N90-14699

HEAT RESISTANT ALLOYS
Calibration approach to electron probe microanalysis: A study with PWA-1480, a nickel base superalloy
[NASA-TM-102393] N90-14335
Thermal fatigue durability for advanced propulsion materials
[NASA-TM-102348] N90-14641

HEAT STORAGE
A heat receiver design for solar dynamic space power systems
[NASA-TM-102473] N90-14283

HEAT TRANSFER
Design and demonstration of heat pipe cooling for NASP and evaluation of heating methods at high heating rates
[DE89-016995] N90-14227
Surface flow and heating distributions on a cylinder in near wake of Aeroassist Flight Experiment (AFE) configuration at incidence in Mach 10 Air
[NASA-TP-2954] N90-14493
Heat transfer to a stationary and moving sphere immersed in a fluidized bed N90-14503
Heat transfer in convective boundary layer and channel flows N90-14505
Selection of the energy-efficient enhancement geometry for single-phase turbulent flow inside tubes
[DE89-017690] N90-14519
Field testing of a ceramic heat exchanger for heat recovery application
[DE90-002082] N90-14523
Course A: Numerical modeling of two-phase flows for presentation at Ecole d'Ete d'Analyse Numerique
[DE90-002074] N90-14526
Interfacial area in two-phase flow
[DE90-002210] N90-14527
Heat and mass transfer design issues in PEM fuel cell hardware
[DE89-016779] N90-14677
Heat transfer of buried pipe for heat pump application
[DE90-000580] N90-14697
New heating and cooling technology: Regenerative heat pump according to the Vuilleumier principle
[DE90-002701] N90-14699
Program CICC flow and heat transfer in Cable-In-Conduit Conductors
[DE90-001519] N90-14818
Starlight: A stationary inertial-confinement-fusion reactor with nonvaporizing walls
[DE90-002315] N90-14927
Semi-empirical theory of heat-transfer when boiling
[DE89-635418] N90-14984

HEAT TRANSFER COEFFICIENTS
Heat transfer to a stationary and moving sphere immersed in a fluidized bed N90-14503

HEAT TREATMENT
Practical superconductor development for electrical power applications
[DE90-001804] N90-14487

HEATERS
Flight set 360T004 (STS-30) field joint protection system, volume 7
[NASA-CR-183829] N90-14280

HEATING
Rapid heating tensile tests of hydrogen-charged high-energy-rate-forged 316L stainless steel
[DE90-000591] N90-14342
The stability of Taylor-Couette flow with radial heating N90-14502
New heating and cooling technology: Regenerative heat pump according to the Vuilleumier principle
[DE90-002701] N90-14699

HEAVY IONS
A study of recoil protons in ultra-relativistic nucleus-nucleus collisions
[LUIP-8907] N90-14873
String models for ultrarelativistic heavy ion collisions: Lund model versus color exchange models
[DE88-015856] N90-14881
Heavy ion interactions
[DE90-001410] N90-14884

HEAVY LIFT LAUNCH VEHICLES
Definition of avionics concepts for a heavy lift cargo vehicle. Volume 1: Executive summary
[NASA-CR-183818] N90-14229
Definition of avionics concepts for a heavy lift cargo vehicle, volume 2
[NASA-CR-183819] N90-14230

HELICOPTER CONTROL
A helicopter flight path controller design via a nonlinear transformation technique N90-14242

HELICOPTERS
Effect of blade planform variation on a small-scale hovering rotor
[NASA-TM-4146] N90-14186
An experimental investigation of the interaction between a model rotor and airframe in forward flight N90-14219
An analytical method for the prediction of unsteady rotor/airframe interactions in forward flight N90-14223
A helicopter flight path controller design via a nonlinear transformation technique N90-14242
Fatigue analysis and reconstruction of helicopter load spectra N90-14304
A two dimensional power spectral estimate for some nonstationary processes
[NASA-CR-186100] N90-14843

HELIUM
Thermal design of a 10-kW helium refrigerator
[DE90-701785] N90-14403
Hydrogen radical enhanced growth of solar cells
[DE89-009497] N90-14694

HELIUM ISOTOPES
Cold fusion: Alchemist's dream
[DE90-000865] N90-14925
HETERODYNING
Limitations in the growing of a plasma wave produced by heterodyning two lasers due to modulations and decay instabilities N90-14552
Deferred electronic heterodyne moire deflectometry: A method for transient density fields measurement
[NASA-CR-182962] N90-14907
HETEROJUNCTIONS
Thin film cadmium telluride, zinc telluride, and mercury zinc telluride solar cells
[DE89-009499] N90-14681
HIERARCHIES
Communication Overview Program (COP) N90-14435
Supersymmetric dark matter above the W mass
[NASA-CR-186168] N90-15016
HIGH ALTITUDE
Comparison of protective breathing equipment performance at ground level and 8,000 feet altitude using parameters prescribed by portions of FAA action notice A-8150.2
[AD-A212852] N90-14773
HIGH ALTITUDE BALLOONS
Kestrel 3 Program
[DE90-001796] N90-14209
HIGH ENERGY INTERACTIONS
A study of recoil protons in ultra-relativistic nucleus-nucleus collisions
[LUIP-8907] N90-14873
The ultimate structure of matter: The US High Energy Physics Program from the 1950s through the 1980s
[DE90-001784] N90-14887
HIGH FREQUENCIES
Hybrid PE-ray-mode formulation of high frequency propagation in a bilinear tropospheric surface duct N90-14417
HIGH GAIN
Testing and performance of a high-gain flux-compression generator
[DE90-002808] N90-14492
HIGH LEVEL LANGUAGES
A graphically oriented specification language for automatic code generation. GRASP/Ada: A Graphical Representation of Algorithms, Structure, and Processes for Ada, phase 1
[NASA-CR-183212] N90-14813
HIGH POWER LASERS
A compact, high-powered far-infrared (FIR) laser
[DE89-016786] N90-14597
HIGH PRESSURE
Thermophysical properties of isopropyl alcohol. Part 2: Thermodynamic properties at elevated pressures
[ESDU-89020-PT-2] N90-14300
The Periodic Law at high pressures
[DE90-000837] N90-14319
High-temperature/high-pressure x ray diffraction: Recent developments
[DE89-015255] N90-14949
HIGH RESOLUTION
High resolution, wide band Chirp-Z signal analyzer
[AD-D014240] N90-14465
An image compression algorithm for a high-resolution digital still camera
[NASA-CR-185079] N90-14532
Radiation damage and its influence on source requirements for high resolution x ray holography
[DE90-002508] N90-14540
Very high resolution radio observations of molecular cloud cores N90-15013
HIGH SPEED
Efficient real gas Navier-Stokes computations of high speed flows using an LU scheme
[NASA-TM-102429] N90-14203
High speed transfer switch with 50 kA and 50 kV ratings
[DE90-002448] N90-14481
Embedded function methods for compressible high speed turbulent flow
[NASA-CR-186131] N90-14498
The High-Speed Channel (HSC) and ultra-speed networks
[DE89-015283] N90-14819
HIGH STRENGTH
The manufacture of superplastic alloys N90-14333
HIGH STRENGTH ALLOYS
Designing for superplastic alloys N90-14332
HIGH TEMPERATURE
Thermodynamic properties and hydrodynamic response of high-density high-temperature C H N O mixtures
[DE90-000836] N90-14318
Pentafluorothio polynitroaliphatic explosives
[AD-D014221] N90-14383
Electrical properties of materials for high temperature strain gage applications
[NASA-CR-186192] N90-14534
High-temperature/high-pressure x ray diffraction: Recent developments
[DE89-015255] N90-14949
HIGH TEMPERATURE GAS COOLED REACTORS
A review of gas-cooled reactor concepts for SDI (Strategic Defense Initiative)
[DE89-016962] N90-14898
HIGH TEMPERATURE PLASMAS
Atomic structure and spectral perturbations in hot dense plasmas N90-14567
The average ion model. Computation of the absorption and emission coefficients in hot plasmas N90-14569
HIGH TEMPERATURE SUPERCONDUCTORS
Application of neutron diffraction NDE to high-temperature superconducting composites
[DE90-002184] N90-14295
Practical superconductor development for electrical power applications
[DE90-001804] N90-14487
Static and dynamic magnetization properties of Y1Ba2Cu3O(sub z) thin films
[DE89-017584] N90-14940
Ion beam analysis and modification of thin-film, high-temperature superconductors
[DE90-000918] N90-14941
Flux pinning and microstructure in YBa2Cu3O7
[DE90-001562] N90-14948
High resolution-angle resolved photoemission studies of high temperature superconductors
[DE89-017691] N90-14950
Oxygen stoichiometry, structural transitions, and thermodynamic behavior of the YBa2Cu3O(x) system
[DE89-017694] N90-14951
A simple figure of merit for high temperature superconducting switches
[DE90-000610] N90-14955
Microwave characterization of high-temperature superconductors
[DE90-002408] N90-14968
RF superconductivity research and development at Los Alamos National Laboratory
[DE90-002440] N90-14969
Macroscopic persistent currents in high temperature ceramic superconductors
[DE89-636232] N90-14973
HIGH VACUUM
Thermal environmental tests on space simulation chamber
[DE90-000927] N90-14251
HIGHWAYS
GRAFIN: GRAFIX interactive manual
[PB89-232136] N90-14809
HINGES
Effect of unshielded and shielded horn balances on hinge moment coefficients for controls at low speeds
[ESDU-89003-A] N90-14238
Hinge moment coefficient derivatives for trailing-edge controls on wings at subsonic speeds
[ESDU-89009] N90-14239
Example of procedure in calculation of control hinge moments
[ESDU-89010] N90-14240
HMX
Particle size effects in the initiation of explosives containing reactive and nonreactive continuous phases
[DE90-000786] N90-14390
HODOGRAPHS
Crack problems for elastic-plastic materials under antiplane shear loadings N90-14651
HOLDERS
New tool-holding concept
[DE90-000880] N90-14624
HOLES (MECHANICS)
Influence of hole surface finish, cyclic frequency and spectrum severity on the fatigue behavior of thick section aluminum alloy pin joints
[ARL-STRUC-R-430] N90-14336
HOLOGRAPHY
Soft x ray microscope using Fourier transform holography
[DE90-002291] N90-14539
Radiation damage and its influence on source requirements for high resolution x ray holography
[DE90-002508] N90-14540
The development of coherent x ray lasers for x ray holography
[DE90-000784] N90-14595
HOMOGENEOUS TURBULENCE
The analysis and modeling of dilatational terms in compressible turbulence
[NASA-CR-181959] N90-14513
HORIZONTAL TAIL SURFACES
Validation of a computer code for analysis of subsonic aerodynamic performance of wings with flaps in combination with a canard or horizontal tail and an application to optimization
[NASA-TP-2961] N90-14187
HOT ELECTRONS
Theoretical and material studies of thin-film electroluminescent devices
[NASA-CR-186104] N90-14468
Fast electrons in a laser generated plasma N90-14545
Proof-of-principle experiment for a hot electron pumped XUV amplifier
[DE90-000820] N90-14586
HOT STARS
Ultraviolet properties of hot stars in globular clusters N90-15007
HOVERING
Effect of blade planform variation on a small-scale hovering rotor
[NASA-TM-4146] N90-14186
HUBBLE SPACE TELESCOPE
Long-lived space observatories for astronomy and astrophysics
[NASA-CR-185373] N90-14261
HUMAN BEHAVIOR
Cognitive and Neural Sciences Division 1989 programs
[AD-A212634] N90-14769
HUMAN BODY
Methodology for the calibration of and data acquisition with a six-degree-of-freedom acceleration measurement device
[PB89-233597] N90-14531
HUMAN FACTORS ENGINEERING
Project Argo: The design and analysis of an all-propulsive and an aeroassisted version of a manned space transportation vehicle
[NASA-CR-186047] N90-14266
Human factors aspects of decision support systems N90-14408
Extravehicular activity welding experiment
[NASA-CR-183848] N90-14608
MIPs and BIPs are megaflops: Limits of unidimensional assessments
[DE89-015707] N90-14770
Human factors survey of advanced instrumentation and controls
[DE90-002477] N90-14776
Human factors evaluation of electroluminescent display Number 1
[DE90-002231] N90-14777
Solution bias in complex systems modeling
[DE90-002001] N90-14858
HUMAN PERFORMANCE
Cognitive and Neural Sciences Division 1989 programs
[AD-A212634] N90-14769
MIPs and BIPs are megaflops: Limits of unidimensional assessments
[DE89-015707] N90-14770
HUMAN RESOURCES
Science and technology resources in US industry: Surveys of science resources series, 1975-1986
[PB90-107194] N90-14401
HUMIDITY
Test and evaluation of polymeric membranes for oxygen enrichment of air
[DE90-000555] N90-14321
Climatology of Lawrence Livermore National Laboratory
[DE90-000905] N90-14756
HURRICANES
Summary of 1989 Atlantic tropical cyclone activity and seasonal forecast verification N90-14743
The dynamics of simulated convective storms in hurricane environments N90-14747
HYDRATION
Energies of organic compounds
[DE90-003174] N90-14324
HYDRAZINES
Arcjet thruster research and technology. Phase 1: Executive summary
[NASA-CR-182106] N90-14278
HYDROCARBON COMBUSTION
Kinetics and mechanism of soot formation in hydrocarbon combustion
[NASA-CR-186162] N90-14305
HYDROCARBONS
Orthobaric densities and molar volumes of liquids. Aromatic hydrocarbons
[ESDU-89019] N90-14239
On the mitigation of non-CO2 greenhouse gases
[DE89-016659] N90-14710

HYDRODYNAMIC EQUATIONS
A numerical study of thin flame representations
[DE89-017889] N90-14313
Modelling of the effects of the equatorial electrojet on its environment
[DE89-636298] N90-14720
HYDRODYNAMICS
Corrections for non-ideal effects in reflected shock waves at low Mach numbers
[DE90-002192] N90-14208
Thermodynamic properties and hydrodynamic response of high-density high-temperature C H N O mixtures
[DE90-000836] N90-14318
Detonation product equation of state for Baratol
[DE90-001050] N90-14384
Reaction zone structure in supracompressed detonating explosives
[DE90-000832] N90-14394
Granular flow: Numerical simulation of dry granular flows and calculation of hydrodynamic interactions in suspensions
[DE89-017544] N90-14518
Hypervelocity impact calculations using CTH: Case studies
[DE90-002891] N90-14632
Perturbation methods for the calculation of gravitational waves from slightly non-spherical spacetimes with applications to stellar core collapse N90-15015
HYDROGEN
The effect of hydrogen charging on the mechanical properties of aluminum alloy 2090
[DE90-000129] N90-14341
Hydrogen radical enhanced growth of solar cells
[DE89-009497] N90-14694
Evidence for anomalous cosmic ray hydrogen N90-15005
HYDROGEN ATOMS
Atomic hydrogen as a launch vehicle propellant
[NASA-TM-102459] N90-14284
HYDROGEN BONDS
Chemistry of large molecules
[DE90-000813] N90-14366
HYDROGEN EMBRITTLEMENT
Rapid heating tensile tests of hydrogen-charged high-energy-rate-forged 316L stainless steel
[DE90-000591] N90-14342
Acoustic emission during intergranular stress corrosion cracking
[DE90-002894] N90-14355
HYDROGEN FUELS
Slush Hydrogen (SLH2) technology development for application to the National Aerospace Plane (NASP)
[NASA-TM-102315] N90-14268
HYDROGEN ISOTOPES
Acceleration of small, light projectiles (including hydrogen isotopes) to high speeds using a two-stage light gas gun
[DE90-002479] N90-14253
Interaction of hydrogen isotopes with metals: Deuterium trapped at lattice defects in palladium
[DE90-000811] N90-14344
HYDROLOGY
Earth Sciences Division annual report 1988
[DE90-002617] N90-14663
HYDROLYSIS
Energies of organic compounds
[DE90-003174] N90-14324
HYDROSTATICS
As observational and theoretical investigation of stellar flares N90-15012
HYDROXYL EMISSION
A measurement of hydroxyl in the daytime mesosphere N90-14732
HYPERBOLIC DIFFERENTIAL EQUATIONS
Local error estimates for discontinuous solutions of nonlinear hyperbolic equations
[NASA-CR-181960] N90-14847
HYPERCUBE MULTIPROCESSORS
A radar simulation program for a 1024-processor hypercube
[DE89-014494] N90-14455
HYPERGEOMETRIC FUNCTIONS
On some integral relations involving a generalized hypergeometric polynomial
[DE90-600729] N90-14852
HYPERSONIC FLIGHT
Thermal/structural analyses of several hydrogen-cooled leading-edge concepts for hypersonic flight vehicles
[NASA-TM-102391] N90-14511
HYPERSONIC FLOW
Measured and predicted aerodynamic coefficients and shock shapes for Aeroassist Flight Experiment (AFE) configuration
[NASA-TP-2956] N90-14185
Efficient real gas Navier-Stokes computations of high speed flows using an LU scheme
[NASA-TM-102429] N90-14203
Spatial evolution of nonlinear acoustic mode instabilities on hypersonic boundary layers
[NASA-TM-102431] N90-14517
HYPERSONIC VEHICLES
Measured and predicted aerodynamic coefficients and shock shapes for Aeroassist Flight Experiment (AFE) configuration
[NASA-TP-2956] N90-14185
Thermal/structural analyses of several hydrogen-cooled leading-edge concepts for hypersonic flight vehicles
[NASA-TM-102391] N90-14511
HYPERTHERMIA
Biological effects of hyperthermia and potential risk associated with ultrasonic exposure
[PB89-100702] N90-14768
HYPERVELOCITY IMPACT
On protection of Freedom's solar dynamic radiator from the orbital debris environment. Part 1: Preliminary analyses and testing
[NASA-TM-102458] N90-14285
Hypervelocity impact calculations using CTH: Case studies
[DE90-002891] N90-14632
Some numerical experiments concerning the equation of state algorithm for multi-material cells in HULL
[DE89-008240] N90-14827
Hypervelocity impact studies on the Giotto comet Halley mission N90-15008
HYPERVELOCITY LAUNCHERS
Performance characteristics of a three-stage railgun
[DE90-002533] N90-14254
HYPOTHERMIA
Integrated G-suit/immersion suit
[AD-A212989] N90-14774
HYSTERESIS
Multiple martensitic transformations, incommensurate/commensurate phases, and charge-density-wave states in plutonium metal: Their consequences
[DE90-001235] N90-14350
On-line system to measure magnetic characteristics of steel samples
[DE89-633443] N90-14861

I

IBM COMPUTERS
The development of an Ada programming support environment database: SEAD (Software Engineering and Ada Database), user's manual
[NASA-CR-181219] N90-14811
ICE ENVIRONMENTS
Decomposition in Arctic terrestrial environments
[DE90-001198] N90-14706
ICE FORMATION
Navier-Stokes analysis of airfoils with leading edge ice accretions N90-14196
Comparison of two droplet sizing systems in an icing wind tunnel
[NASA-TM-102456] N90-14617
IDEAL FLUIDS
General exact solution for homogeneous time-dependent self-gravitating perfect fluids
[DE89-618425] N90-14514
IDEAL GAS
Thermophysical properties of isopropyl alcohol. Part 1: The ideal gas and the saturated liquid and vapour
[ESDU-89017-PT-1] N90-14297
IGNITERS
Flight set 360T004 (STS-30) field joint protection system, volume 7
[NASA-CR-183829] N90-14280
Devices and methods for in-situ combustion ignition
[DE89-000766] N90-14309
IGNITION
Devices and methods for in-situ combustion ignition
[DE89-000766] N90-14309
Flame acceleration studies in the MINIFLAME facility
[DE90-000041] N90-14310
IGNITION SYSTEMS
Cold starting a neat methanol (M100) vehicle with long duration spark ignition
[PB89-230692] N90-14613
IMAGE ANALYSIS
SEM (Scanning Electron Microscope) image analysis of grain growth in microwave-annealed alumina
[DE90-001606] N90-14339
IMAGE ENHANCEMENT
Some edge-enhancing operators and their applications to image enhancement and edge detection N90-14810
IMAGE PROCESSING
Automated glass fiber drawing
[DE90-000894] N90-14367
An image compression algorithm for a high-resolution digital still camera
[NASA-CR-185079] N90-14532
The development of coherent x ray lasers for x ray holography
[DE90-000784] N90-14595
NORDA's pattern analysis laboratory: Current contributions to naval mapping, charting, and geodesy
[AD-A212731] N90-14665
A rough transform technique for extracting lead features from sea ice imagery
[AD-A212758] N90-14666
Image processing of LANDSAT MSS data for buried valley detection in northern Indiana N90-14668
X ray microimaging for the life sciences
[DE90-002613] N90-14766
The phase gradient autofocus algorithm: An optimal estimator of the phase derivative
[DE90-000895] N90-14814
The design of a computer system for image simulation and image processing of high resolution electron micrographs
[DE90-000179] N90-14820
Interactive multidimensional data analysis and understanding
[DE90-001794] N90-14824
Generalization in backpropagation networks: An empirical study using image data
[DE89-012658] N90-14835
Design of incoherent imaging arrays
[DE90-000861] N90-14909
Document preservation by electronic imaging. Volume 2: System and experiment description
[PB89-226534] N90-14988
Document preservation by electronic imaging. Volume 3: Appendices
[PB89-226542] N90-14989
IMAGE RECONSTRUCTION
Versatility of the CFR algorithm for limited angle reconstruction
[DE90-001421] N90-14817
IMAGERY
SAS graphics in DCF
[PNR90563] N90-14399
Image processing of LANDSAT MSS data for buried valley detection in northern Indiana N90-14668
IMAGES
SAND DEVIL: A digital video link for telemetry applications
[DE90-001879] N90-14259
IMAGING SPECTROMETERS
A fiber-fed imaging spectrometer
[DE90-001008] N90-14538
Evaluation of the airborne visible-infrared imaging spectrometer for mapping subtle lithological variation
[NASA-CR-186213] N90-14670
IMAGING TECHNIQUES
Data compression techniques applied to high resolution high frame rate video technology
[NASA-CR-4263] N90-14452
A fiber-fed imaging spectrometer
[DE90-001008] N90-14538
Tomographic imagery by multislot coding applied to x ray diagnostics of laser plasmas: Implementation of a direct electronic detection camera N90-14579
Laboratory x ray lasers
[DE90-000879] N90-14590
X ray microimaging for the life sciences
[DE90-002613] N90-14766
A sampled-grating model of moire patterns from digital imaging
[AD-A213364] N90-14902
Realtime tracking system for wide-field-of-view telescope
[DE90-001147] N90-14908
Design of incoherent imaging arrays
[DE90-000861] N90-14909
MERLIN and VLBI observations of the radio galaxy Virgo A N90-15001
IMPACT DAMAGE
Modeling of runaway electron damage for the design of tokamak plasma facing components
[DE90-000847] N90-14914
IMPACT LOADS
Performance characteristics of a three-stage railgun
[DE90-002533] N90-14254
Propagation of detonation waves from an impact region
[DE90-001184] N90-14515
Microstructure induced by laser shock in an austenitic steel N90-14558
Dynamic sintering of metallic powders by laser shock N90-14559

Projectile impact Hugoniot parameters for selected materials
[DE90-000691] N90-14618
Hypervelocity impact calculations using CTH: Case studies
[DE90-002891] N90-14632
Implications and origins of shock structure in solids
[DE90-000846] N90-14658
Critical time step estimation for three-dimensional explicit impact analysis
[DE90-002187] N90-14662

IMPACT STRENGTH
Hypervelocity impact calculations using CTH: Case studies
[DE90-002891] N90-14632

IMPACT TESTS
On protection of Freedom's solar dynamic radiator from the orbital debris environment. Part 1: Preliminary analyses and testing
[NASA-TM-102458] N90-14285
Evaluation of shock isolation techniques for a piezoresistive accelerometer
[DE89-014496] N90-14535
Some numerical experiments concerning the equation of state algorithm for multi-material cells in HULL
[DE89-008240] N90-14827

IMPINGEMENT
An experimental investigation of the interaction between a model rotor and airframe in forward flight N90-14219

IMPLOSIONS
X ray shadowscopy in implosion experiments N90-14563
Trapezoidal crystal in the six beam implosion N90-14577

IN-FLIGHT MONITORING
An in-flight investigation of ground effect on a forward-swept wing airplane
[NASA-TM-101708] N90-14202
An in-flight technique for wind measurement in support of the space shuttle program
[NASA-TM-4154] N90-14224

INCOHERENCE
Effects of temporal and induced spatial incoherence on parametric instabilities in laser plasma interactions N90-14549
Design of incoherent imaging arrays
[DE90-000861] N90-14909

INCOMPRESSIBLE FLOW
Computational investigation of incompressible airfoil flows at high angles of attack
[AD-A205885] N90-14201
Numerical solution of the incompressible Navier-Stokes equations N90-14501

INDEXES (DOCUMENTATION)
Publications of the Jet Propulsion Laboratory, 1988
[NASA-CR-185956] N90-14995

INDIUM COMPOUNDS
Solid oxide fuel cells electrodes based on In(sub 2)O(sub 3)-PrO(sub 1.83)-ZrO(sub 2)
[DE90-002666] N90-14691

INDIUM PHOSPHIDES
Hydrogen radical enhanced growth of solar cells
[DE89-009497] N90-14894

INELASTIC COLLISIONS
Interaction of low-energy electrons and positrons with condensed matter: Stopping powers and inelastic mean free paths from optical data
[DE90-001001] N90-14882

INELASTIC SCATTERING
A theoretical perspective on neutrino physics
[DE90-000759] N90-14878
Solid State Division
[DE90-000979] N90-14945
Magnetic excitations in thulium metal
[DE90-002475] N90-14970

INERTIAL CONFINEMENT FUSION
Starlight: A stationary inertial-confinement-fusion reactor with nonvaporizing walls
[DE90-002315] N90-14927

INFILTRATION
Computer synthesis of ceramic preforms for molten-metal infiltration
[DE90-000826] N90-14370

INFORMATION MANAGEMENT
Integrated computer-based tools to facilitate environmental monitoring, assessment, and restoration
[DE90-002732] N90-14717
High volume data storage architecture analysis
[NASA-CR-186239] N90-14784

INFORMATION RETRIEVAL
Automated reuseable components system study results N90-14790
The design and implementation of an intelligent interface for information retrieval N90-14991

INFORMATION SYSTEMS
Integrated computer-based tools to facilitate environmental monitoring, assessment, and restoration
[DE90-002732] N90-14717
JPL reuse program N90-14795
Level 2 software reuse study N90-14800
AdaNET services N90-14806

INFORMATION THEORY
Assessment of the efficiency of nondestructive techniques in materials testing studies based on the information criterion
[DE89-635444] N90-14834
Solution bias in complex systems modeling
[DE90-002001] N90-14858

INFRARED IMAGERY
A rough transform technique for extracting lead features from sea ice imagery
[AD-A212758] N90-14666
Rainfall estimation over Africa using satellite data N90-14742

INFRARED LASERS
Development of X diagnostics with 1 Gw laser pulses N90-14578
A compact, high-powered far-infrared (FIR) laser
[DE89-016786] N90-14597

INFRARED RADIATION
Weather satellite and computer modeling approaches to assessing propagation over marine environments N90-14443

INFRARED SPECTRA
A study of the infrared emission of galactic supernova remnants N90-15006

INFRARED SPECTROMETERS
Evaluation of the airborne visible-infrared imaging spectrometer for mapping subtle lithological variation
[NASA-CR-186213] N90-14670

INHOMOGENEITY
Transversal inhomogeneity and radiative transfer in plasmas obtained by laser impact N90-14568

INITIATION
Particle size effects in the initiation of explosives containing reactive and nonreactive continuous phases
[DE90-000786] N90-14390

INITIATORS (EXPLOSIVES)
Means for protecting electroexplosive devices which are subject to a wide variety of radio frequency
[AD-D014219] N90-14382

INJECTION
Acceleration of small, light projectiles (including hydrogen isotopes) to high speeds using a two-stage light gas gun
[DE90-002479] N90-14253

INJECTORS
Cold starting a neat methanol (M100) vehicle with long duration spark ignition
[PB89-230692] N90-14613
A laboratory test for fuel injector deposit studies
[DE90-000802] N90-14629

INLET FLOW
A computational analysis of the transonic flow field of two-dimensional minimum length nozzles N90-14194

INORGANIC COMPOUNDS
Photoconversion of inorganics to methane
[PB89-230643] N90-14379

INSULATION
Temperature stable ceramic dielectric compositions
[AD-D014209] N90-14358

INTEGRAL EQUATIONS
On some integral relations involving a generalized hypergeometric polynomial
[DE90-600729] N90-14852

INTEGRATED CIRCUITS
Characterization of two MMIC GaAs switch matrices at microwave frequencies
[NASA-TM-102449] N90-14273
Integrating and enhancing tools for ASIC (Application-Specific Integrated Circuits) design using MOSIS (Metal Oxide Semiconductor Implementation Service) fabrication
[DE90-001601] N90-14475
The effects of heavy particle radiation on semiconductor devices
[DE90-001679] N90-14962

INTEGRATED MISSION CONTROL CENTER
Prototype software reuse environment at Goddard Space Flight Center N90-14794

INTERATOMIC FORCES
First-principles interatomic potentials in transition metals: Multi-ion interactions and their analytic representation
[DE90-001990] N90-14353

INTERCALATION
Density of intercalated graphite fibers
[NASA-TM-102411] N90-14362

INTERFACE STABILITY
Fabrication of NBN based electronic devices with silicon barriers
[AD-D014230] N90-14463

INTERFACES
SAS graphics in DCF
[PNR90563] N90-14399
Nondestructive evaluation of flaw clusters and thin layer interfaces N90-14633
The development of an Ada programming support environment database: SEAD (Software Engineering and Ada Database), user's manual
[NASA-CR-181219] N90-14811
Atomic matching across internal interfaces
[DE90-002266] N90-14889
Magnetic and electrical properties
[DE90-002183] N90-14977
The design and implementation of an intelligent interface for information retrieval N90-14991

INTERFACIAL TENSION
Thermocapillary migration of liquid droplets in a temperature gradient in a density matched system
[NASA-CR-185178] N90-14512

INTERFEROMETERS
Fiber-optic sensors for composite cure analysis and lifetime nondestructive evaluation
[DE90-001739] N90-14296

INTERGALACTIC MEDIA
Cooling flows in clusters of galaxies N90-15009

INTERMETALLICS
Carbon fiber reinforced metal matrix composites
[AD-D014245] N90-14289
Advances and future directions in superplastic materials N90-14328
Phases in lanthanum-nickel-aluminum intermetallic alloys
[DE90-000651] N90-14343
Practical limitations of ALCHEMI measurements on ordered intermetallic alloys
[DE90-000700] N90-14957

INTERNAL COMPRESSION INLETS
Numerical investigations in three-dimensional internal flows
[NASA-CR-186068] N90-14189

INTERNATIONAL COOPERATION
AGARD Highlights 89/2 N90-14184
Discussions of global environmental problems
[DE90-002747] N90-14718
An international discussion on research in solar and space physics N90-14996

INTERNATIONAL SYSTEM OF UNITS
Metric handbook for Federal officials: Recommendations of the Interagency Committee on Metric Policy
[PB89-226922] N90-14400

INTERPLANETARY DUST
Extraterrestrial halogen and sulfur content of the stratosphere
[DE89-017623] N90-14738
A model of the thermal and electrical properties of cosmic dust particles N90-15014
Solar-geophysical data number 540, August 1989. Part 2: (Comprehensive reports). Data for February 1989
[PB89-108598] N90-15039

INTERPLANETARY MAGNETIC FIELDS
Kilometric type III radio bursts and interplanetary transients N90-15038

INTERPOLATION
Thermophysical properties of isopropyl alcohol. Part 2: Thermodynamic properties at elevated pressures
[ESDU-89020-PT-2] N90-14300
Rainfall estimation over Africa using satellite data N90-14742
Modified Chebyshev pseudospectral method with O(N exp -1) time step restriction
[NASA-CR-181958] N90-14848

INTERPROCESSOR COMMUNICATION
Fast serial communication module
[DE89-633753] N90-14454

INTERSTELLAR MASERS
Very high resolution radio observations of molecular cloud cores N90-15013

INTERSTELLAR MATTER
Properties of evolved star circumstellar grains N90-15003
Evidence for anomalous cosmic ray hydrogen N90-15005

INVARIANCE
Classification of modular invariant partition functions for the twisted N=2 superconformal algebra, twisted SU(2) Kac-Moody algebra and D(sub 2K) parafermions
[DE90-600767] N90-14853

INVESTMENTS
The impact of global warming on the energy system
[DE89-017775] N90-14712

INVISCID FLOW
Three-dimensional solution-adaptive grid generation of composite configurations N90-14509
ION BEAMS
Structure-property relationships in surface-modified ceramics. NATO Advanced Science Institutes, series E: Applied Sciences, volume 170
[AD-A212939] N90-14359
Ion beam analysis and modification of thin-film, high-temperature superconductors
[DE90-000918] N90-14941
Ion beam processing of advanced electronic materials
[DE89-017342] N90-14944
ION DENSITY (CONCENTRATION)
Modification of ionic population by non-Maxwellian effects N90-14565
ION IMPLANTATION
Structure-property relationships in surface-modified ceramics. NATO Advanced Science Institutes, series E: Applied Sciences, volume 170
[AD-A212939] N90-14359
Ion beam analysis and modification of thin-film, high-temperature superconductors
[DE90-000918] N90-14941
Ion beam processing of advanced electronic materials
[DE89-017342] N90-14944
ION INJECTION
Structural peculiarities and molecular properties of charge complexes formed on positive ion injection into dense inert gas media
[DE89-633953] N90-14877
ION MOTION
Direction-dependent stopping power and beam deflection in anisotropic solids
[DE90-001076] N90-14883
ION TEMPERATURE
Ion collection by probing objects in flowing magnetized plasmas
[DE90-001711] N90-14916
IONIC COLLISIONS
String models for ultrarelativistic heavy ion collisions: Lund model versus color exchange models
[DE88-015856] N90-14881
Heavy ion interactions
[DE90-001410] N90-14884
IONIZATION
Development of laser excited atomic fluorescence and ionization spectrometric methods
[DE90-001567] N90-14320
Combined capillary electrophoresis and electrospray ionization mass spectrometry
[DE90-001903] N90-14322
Nonresonant and resonant multiphoton ionization of (NO)(sub n) and Ar(sub n)NO clusters with picosecond laser pulses
[DE89-016853] N90-14607
Improved performance of low-T(sub c) superconductors for detection of minimum-ionizing particles
[DE90-001985] N90-14976
IONOGRAMS
New perspectives for the inversion of backscatter ionograms N90-14427
IONOSONDES
A portable ionosonde in support of reliable communications N90-14431
IONOSPHERIC PROPAGATION
The use of backscatter for modelling ionosphere and jamming in very short term forecasts N90-14434
IONS
Studies of neutral and ion transport during laser ablation of 1:2:3 superconductors by optical absorption spectroscopy
[DE90-001968] N90-14604
Multiple electron capture in close ion-atom collisions
[DE90-001541] N90-14885
Toroidal rotation retardation and ion anomalous transport by drift waves in a tokamak
[DE89-634427] N90-14913
IRON CHLORIDES
Modeling of sodium/metal chloride batteries
[DE89-017685] N90-14478
IRON METEORITES
Meteoritic basalts
[NASA-CR-185949] N90-15004
IRRADIANCE
Solar-geophysical data number 538, June 1989. Part 2: (Comprehensive reports). Data for December 1988 and miscellaneous
[PB89-223846] N90-15032
IRRADIATION
The feasibility of welding of irradiated materials
[DE90-002200] N90-14631
The effects of heavy particle radiation on semiconductor devices
[DE90-001679] N90-14962
IRREGULARITIES
Localized vibrations of nearly periodic structures with irregularities N90-14648
ISING MODEL
Surface magneto-optical studies of ultrathin ferromagnetic films
[DE90-002199] N90-14980
ISOPROPYL ALCOHOL
Thermophysical properties of isopropyl alcohol. Part 2: Thermodynamic properties at elevated pressures
[ESDU-89020-PT-2] N90-14300
ISOTOPE EFFECT
A model of the isotope effect of the oxide superconductor
[DE89-635907] N90-14971
ISOTOPES
Phases in lanthanum-nickel-aluminum intermetallic alloys
[DE90-000651] N90-14343
Heavy ion interactions
[DE90-001410] N90-14884
ISOTROPIC MEDIA
Viscoplasticity: A thermodynamic formulation
[NASA-TM-102388] N90-14640
ISOTROPIC TURBULENCE
The analysis and modeling of dilatational terms in compressible turbulence
[NASA-CR-181959] N90-14513
ISOTROPY
A generalized thermomechanical constitutive model for metal matrix composites with plastic strain and damage N90-14293
Fluid-particle interaction in solid-liquid two-phase grid turbulence N90-14496
ITERATION
A study of incremental-iterative strategies for nonlinear analyses
[PB89-226005] N90-14646
ITERATIVE SOLUTION
Program VSAERO theory document: A computer program for calculating nonlinear aerodynamic characteristics of arbitrary configurations
[NASA-CR-4023] N90-14200
Approximate methods for dynamic plastic deformation of structures
[DE90-002214] N90-14660
Krylov methods preconditioned with incompletely factored matrices on the CM-2
[NASA-CR-181961] N90-14779
Versatility of the CFR algorithm for limited angle reconstruction
[DE90-001421] N90-14817
Iterative methods of domain decomposition with cross-points for the solution of discrete elliptic problems
[DE90-000719] N90-14854

J

JAMMING
The use of backscatter for modelling ionosphere and jamming in very short term forecasts N90-14434
JET ENGINE FUELS
Thermal stability of jet fuel
[DE90-001160] N90-14385
JOINTS (JUNCTIONS)
Measurement of damping of graphite epoxy composite materials and structural joints
[NASA-CR-183802] N90-14286
The stress analysis of thin-walled screwed tubular joints N90-14637
JOSEPHSON JUNCTIONS
Fabrication of NBN based electronic devices with silicon barriers
[AD-D014230] N90-14463
Theory of strongly fluctuating superconductivity
[DE90-001073] N90-14942
JOURNAL BEARINGS
Transient response of flexible rotor-bearing systems subjected to combined unbalance and ground excitations N90-14616

K

KINEMATICS
Tire modeling by finite elements N90-14614
High-frequency ventilation in dogs with three gases of different densities
[AD-A212862] N90-14762
KINETIC ENERGY
Elastomeric impulse energy storage and transfer system
[AD-D014223] N90-14255
Biomodal spontaneous fission
[DE90-001516] N90-14886
KINETIC EQUATIONS
Kinetics and mechanism of soot formation in hydrocarbon combustion
[NASA-CR-186162] N90-14305
Group-kinetic theory and modeling of atmospheric turbulence
[NASA-CR-183776] N90-14728
Ion collection by probing objects in flowing magnetized plasmas
[DE90-001711] N90-14916
KINETIC THEORY
Group-kinetic theory and modeling of atmospheric turbulence
[NASA-CR-183776] N90-14728
KINETICS
Laboratory x ray lasers
[DE90-000879] N90-14590
Hypervelocity impact calculations using CTH: Case studies
[DE90-002891] N90-14632
KLYSTRONS
Modification of MEA modulator-klystron units enabling short pulse injection into a pulse-stretcher ring N90-14894
Performance and modification of the MEA RF drive system N90-14895
KNOWLEDGE
Knowledge-based reusable software synthesis system N90-14791
KNOWLEDGE REPRESENTATION
Advanced Software Development Workstation Project N90-14807

L

LABORATORIES
Lawrence Livermore National Laboratory (LLNL) research on cold fusion
[DE90-000930] N90-14915
LACTATES
Amperometric biosensors for glucose, lactate, and glycolate based on oxidases and redox-modified siloxane polymers
[DE90-002301] N90-14541
LAGRANGE COORDINATES
XRAD: A one dimensional Lagrangian code with radiative transport N90-14570
LAKE MICHIGAN
Organic geochemical and tectonic evolution of the midcontinent rift system: Organic geochemistry and micropaleontology
[DE89-017561] N90-14760
LAKES
Steady state model to determine lake resources at risk to acid deposition in the Sierra Nevada, California
[PB89-103995] N90-14705
LAMINAR BOUNDARY LAYER
Numerical investigations in three-dimensional internal flows
[NASA-CR-186068] N90-14189
Stability of a supersonic boundary layer on a sharp cone at a small angle of attack N90-14510
LAMINAR FLOW
Numerical solution of the incompressible Navier-Stokes equations N90-14501
The laminar to slug flow transition in Hele-Shaw flow
[DE90-000836] N90-14521
LAMINATES
Finite element analysis of laminated composite plates N90-14291
LAND USE
Strategy for monitoring the effects of land use change on atmospheric CO2 concentrations
[DE90-001635] N90-14722
LANDSAT SATELLITES
Image processing of LANDSAT MSS data for buried valley detection in northern Indiana N90-14668
LANTHANUM ALLOYS
Phases in lanthanum-nickel-aluminum intermetallic alloys
[DE90-000651] N90-14343
LARGE SPACE STRUCTURES
Dynamics and control of flexible spacecraft during and after slewing maneuvers
[NASA-CR-186123] N90-14270
LASER APPLICATIONS
Shuttle Laser Technology Experiment Facility (LTEF)-to-airplane lasercom experiment: Airplane considerations
[NASA-TM-100749] N90-14260
Development of laser excited atomic fluorescence and ionization spectrometric methods
[DE90-001567] N90-14320
Laser activities N90-14576

Assessment of research needs for laser technologies applied to advanced spectrographic methods
[DE90-001154] N90-14587
Laboratory x ray lasers
[DE90-000879] N90-14590
Solid-state fluorescence above 1000 C: Application to high-temperature laser thermometry
[DE90-000728] N90-14594
Noncontacting laser ultrasonic generation and detection at the surface of molten metal
[DE90-002020] N90-14605

LASER BEAMS
Field evaluation of a Nissan laser collision avoidance system
[PB90-105602] N90-14215
Statistics of two-color laser beam propagation in the turbulent atmosphere (spectral correlation)
[PB89-236899] N90-14581
Laboratory x ray lasers
[DE90-000879] N90-14590
The current status of x ray conversion efficiency modeling
[DE90-000931] N90-14591

LASER CAVITIES
A compact, high-powered far-infrared (FIR) laser
[DE89-016786] N90-14597

LASER DOPPLER VELOCIMETERS
Reaction zone structure in supracompressed detonating explosives
[DE90-000832] N90-14394
Laser velocimeter and total pressure measurements in circular-to-rectangular transition ducts
[NASA-CR-182286] N90-14494

LASER HEATING
Numerical simulation of the preheating by x rays in spherical plasmas N90-14564

LASER INDUCED FLUORESCENCE
Fiber-optic sensors for composite cure analysis and lifetime nondestructive evaluation
[DE90-001739] N90-14296
Solid-state fluorescence above 1000 C: Application to high-temperature laser thermometry
[DE90-000728] N90-14594

LASER MATERIALS
Qualification of diode foil materials for excimer lasers
[DE90-000602] N90-14593

LASER OUTPUTS
Activities report in laser matter interactions
[ETN-90-95515] N90-14544

LASER PLASMA INTERACTIONS
Activities report in laser matter interactions
[ETN-90-95515] N90-14544
Fast electrons in a laser generated plasma N90-14545
Production of homogeneous plasmas for laser-plasma interaction experiments N90-14546
Experimental study on the filamentary instability in laser-matter interactions at short wave lengths N90-14547
Strong Langmuir turbulence and second harmonics in laser-matter interactions N90-14548
Effects of temporal and induced spatial incoherence on parametric instabilities in laser plasma interactions N90-14549
The supersonic anisotropic collapse of Langmuir waves N90-14550
Aspects of field theory related to the Zakharov problem N90-14551
Limitations in the growing of a plasma wave produced by heterodyning two lasers due to modulations and decay instabilities N90-14552
Interaction of a low flux laser beam with a solid target N90-14554
Box experiments. Nonlinear effects at plasma resonance N90-14555
Experimental study of the shock waves generated by high energy laser pulses N90-14557
Measurement of the high density zone of a plasma target by absorption spectroscopy N90-14560
Time integrated study of spectral emission in the X-UV domain at the outlet of a laser shock, at the back of single or double foil targets N90-14561
Measurement of the X-UV emission from the back face of thin foils illuminated by an A4 omega laser N90-14562
X ray shadowscopy in implosion experiments N90-14563
Modification of ionic population by non-Maxwellian effects N90-14565
Atomic structure and spectral perturbations in hot dense plasmas N90-14567
The average ion model. Computation of the absorption and emission coefficients in hot plasmas N90-14569
XRAD: A one dimensional Lagrangian code with radiative transport N90-14570
Population inversions calculated for lithium-like ions in a plasma N90-14571
Study of lithium-like ions for amplifying radiation below 100 angstroms. Experiment at the Rutherford Appleton Laboratory N90-14572
Single beam interactions for the study of x ray lasers N90-14573
X-UV amplification in a plasma column of five centimeters. Five beams experiment N90-14574
Characteristics of an x ray source created by a laser plasma N90-14575
Laser activities N90-14576
Development of X diagnostics with 1 Gw laser pulses N90-14578
Tomographic imagery by multislot coding applied to x ray diagnostics of laser plasmas: Implementation of a direct electronic detection camera N90-14579

LASER PLASMAS
Activities report in laser matter interactions
[ETN-90-95515] N90-14544
Fast electrons in a laser generated plasma N90-14545
Production of homogeneous plasmas for laser-plasma interaction experiments N90-14546
Experimental study on the filamentary instability in laser-matter interactions at short wave lengths N90-14547
Strong Langmuir turbulence and second harmonics in laser-matter interactions N90-14548
Effects of temporal and induced spatial incoherence on parametric instabilities in laser plasma interactions N90-14549
The supersonic anisotropic collapse of Langmuir waves N90-14550
Aspects of field theory related to the Zakharov problem N90-14551
Limitations in the growing of a plasma wave produced by heterodyning two lasers due to modulations and decay instabilities N90-14552
Use of plasmas for the acceleration of particles to very high energy N90-14553
Interaction of a low flux laser beam with a solid target N90-14554
Box experiments. Nonlinear effects at plasma resonance N90-14555
Measurement of the high density zone of a plasma target by absorption spectroscopy N90-14560
Time integrated study of spectral emission in the X-UV domain at the outlet of a laser shock, at the back of single or double foil targets N90-14561
Measurement of the X-UV emission from the back face of thin foils illuminated by an A4 omega laser N90-14562
X ray shadowscopy in implosion experiments N90-14563
Numerical simulation of the preheating by x rays in spherical plasmas N90-14564
Modification of ionic population by non-Maxwellian effects N90-14565
Anisotropy of electron distributions related to the anisotropy and polarization of the continuous emitted x rays N90-14566
Transversal inhomogeneity and radiative transfer in plasmas obtained by laser impact N90-14568
The average ion model. Computation of the absorption and emission coefficients in hot plasmas N90-14569
XRAD: A one dimensional Lagrangian code with radiative transport N90-14570
Population inversions calculated for lithium-like ions in a plasma N90-14571
Study of lithium-like ions for amplifying radiation below 100 angstroms. Experiment at the Rutherford Appleton Laboratory N90-14572
Single beam interactions for the study of x ray lasers N90-14573
X-UV amplification in a plasma column of five centimeters. Five beams experiment N90-14574
Characteristics of an x ray source created by a laser plasma N90-14575
Laser activities N90-14576
Trapezoidal crystal in the six beam implosion N90-14577
Development of X diagnostics with 1 Gw laser pulses N90-14578
Tomographic imagery by multislot coding applied to x ray diagnostics of laser plasmas: Implementation of a direct electronic detection camera N90-14579
Development of X diagnostics around the pulse 1 laser N90-14580

LASER PUMPING
Eurolaser CO2 laser
[ETN-90-95907] N90-14582

LASER SPECTROSCOPY
Laser Raman spectroscopy in studies of corrosion and electrocatalysis
[DE90-001414] N90-14311
Mapping of upper electronic reaction surfaces by tuned laser photolysis and by absorption and emission spectroscopies
[DE90-000125] N90-14314
Studies of neutral and ion transport during laser ablation of 1:2:3 superconductors by optical absorption spectroscopy
[DE90-001968] N90-14604

LASER TARGET INTERACTIONS
Experimental study of the shock waves generated by high energy laser pulses N90-14557

LASER TARGETS
Activities report in laser matter interactions
[ETN-90-95515] N90-14544
Fast electrons in a laser generated plasma N90-14545
Production of homogeneous plasmas for laser-plasma interaction experiments N90-14546
Experimental study on the filamentary instability in laser-matter interactions at short wave lengths N90-14547
Strong Langmuir turbulence and second harmonics in laser-matter interactions N90-14548
Effects of temporal and induced spatial incoherence on parametric instabilities in laser plasma interactions N90-14549
Interaction of a low flux laser beam with a solid target N90-14554
Experimental study of the shock waves generated by high energy laser pulses N90-14557
Microstructure induced by laser shock in an austenitic steel N90-14558
Dynamic sintering of metallic powders by laser shock N90-14559
Measurement of the high density zone of a plasma target by absorption spectroscopy N90-14560
Time integrated study of spectral emission in the X-UV domain at the outlet of a laser shock, at the back of single or double foil targets N90-14561
Measurement of the X-UV emission from the back face of thin foils illuminated by an A4 omega laser N90-14562
X ray shadowscopy in implosion experiments N90-14563
Modification of ionic population by non-Maxwellian effects N90-14565
Transversal inhomogeneity and radiative transfer in plasmas obtained by laser impact N90-14568
The average ion model. Computation of the absorption and emission coefficients in hot plasmas N90-14569
Population inversions calculated for lithium-like ions in a plasma N90-14571
Study of lithium-like ions for amplifying radiation below 100 angstroms. Experiment at the Rutherford Appleton Laboratory N90-14572
Single beam interactions for the study of x ray lasers N90-14573
X-UV amplification in a plasma column of five centimeters. Five beams experiment N90-14574
Characteristics of an x ray source created by a laser plasma N90-14575
Development of X diagnostics with 1 Gw laser pulses N90-14578

LASERS
Monolithic laser diode structure for microwave generation
[AD-D014210] N90-14543
Numerical simulation of laser radiation propagation in non-uniform absorbing medium. Geometrical optics approximation
[DE89-632014] N90-14585
Laser probing non-cylindrical Z-pinch in near-isolator region of a discharged chamber
[DE89-632018] N90-14912
Starlight: A stationary inertial-confinement-fusion reactor with nonvaporizing walls
[DE90-002315] N90-14927

LASING
Lasing on the third harmonic
[DE90-002389] N90-14602

LATCH-UP
The effects of heavy particle radiation on semiconductor devices
[DE90-001679] N90-14962

LATTICES
Vector fields and gravity on the lattice
[DE89-633885] N90-14860

LAUNCH VEHICLES
Guidance, steering, load relief and control of an asymmetric launch vehicle
[NASA-CR-185598] N90-14257
Atomic hydrogen as a launch vehicle propellant
[NASA-TM-102459] N90-14284

LAUNCHING
Guidance, steering, load relief and control of an asymmetric launch vehicle
[NASA-CR-185598] N90-14257
LEAD (METAL)
Method of sensitizing PB-Salt epitaxial films for Schottky diodes
[AD-D014244] N90-14937
LEAD ACID BATTERIES
Laboratory testing of Sonnenschein DF6V180 6 volt traction battery
[DE90-002080] N90-14486
LEAD ALLOYS
Primary arm spacing in directionally solidified Pb-10 wt percent Sn alloys
[NASA-CR-185190] N90-14398
LEADING EDGE FLAPS
Navier-Stokes analysis of airfoils with leading edge ice accretions N90-14196
LEADING EDGES
Stall/spin aerodynamic data project
[DOT/FAA/CT-88/29] N90-14222
Thermal/structural analyses of several hydrogen-cooled leading-edge concepts for hypersonic flight vehicles
[NASA-TM-102391] N90-14511
LENS ANTENNAS
Frequency independent constant beamwidth directional lens antenna for very wideband and multi-channel electromagnetic communications
[AD-D014214] N90-14449
LENS DESIGN
Conceptual design study of a 5 kilowatt solar dynamic Brayton power system using a dome Fresnel lens solar concentrator
[NASA-CR-185134] N90-14281
LEPTONS
The AMY Experiment
[DE90-001153] N90-14880
LIBRARIES
Automated reuseable components system study results N90-14790
Knowledge-based reusable software synthesis system N90-14791
Reuse at the Software Productivity Consortium N90-14798
Level 2 software reuse study N90-14800
An SSE approach to reusability N90-14801
Support for life-cycle product reuse in NASA's SSE N90-14802
AdaNET services N90-14806
Proceedings of the Conference on Application of Scanning Methodologies in Libraries
[PB89-233415] N90-14990
LIE GROUPS
Hamiltonian flows, SU(infinity), SO(infinity), USp(infinity), and strings
[DE90-001987] N90-14851
LIFE (DURABILITY)
Predictive aging of elastomers in air: The importance of understanding diffusion-limited oxidation effects
[DE90-001385] N90-14372
Sodium/sulfur evaluation at SNL
[DE89-015846] N90-14472
Zinc/bromine battery evaluation at SNL (Sandia National Laboratory)
[DE89-015847] N90-14473
Support for life-cycle product reuse in NASA's SSE N90-14802
LIFE CYCLE COSTS
Terrestrial nickel/hydrogen battery development at Johnson Controls, Inc.
[DE89-015843] N90-14471
LIFE SCIENCES
USSR Space Life Sciences Digest. Index to issues 21-25
[NASA-CR-3922(30)] N90-14763
X ray microimaging for the life sciences
[DE90-002613] N90-14766
Exploring the living universe: A strategy for space life sciences
[NASA-TM-101891] N90-14778
LIFE SUPPORT SYSTEMS
CIS-lunar space infrastructure lunar technologies: Executive summary
[NASA-CR-186220] N90-15029
LIFTING ROTORS
An analytical method for the prediction of unsteady rotor/airframe interactions in forward flight N90-14223
LIGHT EMISSION
VLA and VLBI observations of core dominated quasars N90-15002
LIGHT GAS GUNS
Solving the blow-by problem in a two-stage gun
[DE90-000842] N90-14246
Acceleration of small, light projectiles (including hydrogen isotopes) to high speeds using a two-stage light gas gun
[DE90-002479] N90-14253
LIGHT SCATTERING
Simulated Brillouin backscattering in optical fibers: A ring resonator N90-14556
LIGHT SOURCES
A Scanning Photoelectron Microscope (SPEM) at the National Synchrotron Light Source (NSLS)
[DE90-001551] N90-14537
Interferometric surface distortion detector
[AD-D014211] N90-14901
LIGHT TRANSMISSION
Probability density function of optical scintillations (scintillation distribution)
[PB89-103912] N90-14906
LIGHTNING
Evaluation of the indirect effects of lightning on a system: Double transfer function method
[RAE-TRANS-2172] N90-14211
JPS heater and sensor lightning qualification
[NASA-CR-183830] N90-14530
LIMESTONE
Organic geochemical and tectonic evolution of the midcontinent rift system: Organic geochemistry and micropaleontology
[DE89-017561] N90-14760
LIMITERS (FUSION REACTORS)
Thermal loads on tokamak plasma facing components during normal operation and disruptions
[DE90-000794] N90-14919
LINE SPECTRA
Gamma ray lines from dark matter annihilation
[DE90-000779] N90-15021
LINEAR ACCELERATORS
Compact RF-linac free-electron lasers
[DE90-002386] N90-14600
An Energy Spectrum Compressor system (ESC) for the Amsterdam pulse stretcher (AmPS) N90-14896
LINEAR EQUATIONS
Group implicit concurrent algorithms in nonlinear structural dynamics
[NASA-CR-185950] N90-14638
Krylov methods preconditioned with incompletely factored matrices on the CM-2
[NASA-CR-181961] N90-14779
LINEAR POLARIZATION
VLA and VLBI observations of core dominated quasars N90-15002
LINEAR SYSTEMS
Optimal stochastic modeling and control of flexible structures
[AD-A212347] N90-14269
LIQUID CHROMATOGRAPHY
Supercritical fluid chromatography/supersonic jet spectroscopy
[DE90-001378] N90-14308
LIQUID CRYSTALS
Visualization of boundary layer transition zone movement on oscillating airfoils with shear-sensitive liquid-crystal coatings
[DE89-009570] N90-14210
The structure and properties of liquid crystal polymers N90-14356
LIQUID HELIUM
Path integral simulations of liquid helium
[DE90-001171] N90-14862
LIQUID METALS
Computer synthesis of ceramic preforms for molten-metal infiltration
[DE90-000826] N90-14370
LIQUID-LIQUID INTERFACES
Interfacial area in two-phase flow
[DE90-002210] N90-14527
LIQUID-VAPOR INTERFACES
Interfacial area in two-phase flow
[DE90-002210] N90-14527
LIQUIDS
Thermophysical properties of isopropyl alcohol. Part 1: The ideal gas and the saturated liquid and vapour
[ESDU-89017-PT-1] N90-14297
Orthobaric densities and molar volumes of liquids. Introduction to data items issued after July 1989
[ESDU-89018] N90-14298
Orthobaric densities and molar volumes of liquids. Aromatic hydrocarbons
[ESDU-89019] N90-14299
LITHIUM
Population inversions calculated for lithium-like ions in a plasma N90-14571
LITHIUM ALLOYS
Advances and future directions in superplastic materials N90-14328
The strength-toughness combination of the aluminum-lithium alloys 2090 and 2091 at cryogenic temperatures
[DE90-001425] N90-14338
LITHIUM SULFUR BATTERIES
Polarization of Li/SOCl2 cells
[DE90-000883] N90-14680
LITHOLOGY
Evaluation of the airborne visible-infrared imaging spectrometer for mapping subtle lithological variation
[NASA-CR-186213] N90-14670
LOAD TESTS
Elasto-plastic analysis of unidirectional fiber-reinforced composites subjected to transverse normal loading using the finite element method N90-14292
LOADS (FORCES)
Normal force, pitching moment, and side force of forebody-cylinder combinations for angles of attack up to 90 degrees and Mach numbers up to 5
[ESDU-89014] N90-14192
Fatigue analysis and reconstruction of helicopter load spectra N90-14304
Influence of hole surface finish, cyclic frequency and spectrum severity on the fatigue behavior of thick section aluminum alloy pin joints
[ARL-STRUC-R-430] N90-14336
Inductive store opening switch and tests for energy transfer to a load
[DE90-002818] N90-14482
The stress analysis of thin-walled screwed tubular joints N90-14637
A theoretical investigation of the column behavior of cold-formed square hollow sections
[PB89-225981] N90-14645
A study of incremental-iterative strategies for nonlinear analyses
[PB89-226005] N90-14648
The development of a model of the human responses to load carriage N90-14775
Thermal loads on tokamak plasma facing components during normal operation and disruptions
[DE90-000794] N90-14919
LOCAL AREA NETWORKS
MIPs and BIPs are megaflops: Limits of unidimensional assessments
[DE89-015707] N90-14770
The Aerospace Energy Systems Laboratory: A BITBUS networking application
[NASA-TM-4149] N90-14829
Multiple crossbar network: A switched high-speed local network
[DE90-001839] N90-14833
LOGIC PROGRAMMING
Strand: A practical parallel programming language
[DE90-002861] N90-14825
LONG DURATION SPACE FLIGHT
JPRS Report: Science and technology. USSR: Space. Soviet space program to the year 2000
[JPRS-USP-89-008] N90-14248
LOSSES
Forward scatter propagation path loss testing using surrogate terrain in the 100 to 1500 MHz region N90-14425
LOW ASPECT RATIO WINGS
Experimental transonic flutter characteristics of two 72 deg-sweep delta-wing models
[NASA-TM-101659] N90-14205
LOW GRAVITY MANUFACTURING
Materials processing in low gravity
[NASA-CR-183733] N90-14397
LOW TEMPERATURE
The formation of metal-oxygen species at low temperatures
[DE90-002298] N90-14323
Cold starting a neat methanol (M100) vehicle with long duration spark ignition
[PB89-230692] N90-14613
LUGS
Influence of hole surface finish, cyclic frequency and spectrum severity on the fatigue behavior of thick section aluminum alloy pin joints
[ARL-STRUC-R-430] N90-14336
LUNAR BASES
Partial gravity habitat study: With application to lunar base design
[NASA-CR-186048] N90-14267
SP-100 power system conceptual design for lunar base applications
[NASA-TM-102090] N90-15030
LUNAR EXPLORATION
Workshop on Moon in Transition: Apollo 14, KREEP, and Evolved Lunar Rocks
[NASA-CR-186153] N90-15026
CIS-lunar space infrastructure lunar technologies: Executive summary
[NASA-CR-186220] N90-15029

LUNAR GEOLOGY
Workshop on Moon in Transition: Apollo 14, KREEP, and Evolved Lunar Rocks
[NASA-CR-186153] N90-15026
The Apollo 15 coarse fines (4-10 mm)
[NASA-TM-101934] N90-15027
LUNAR ROCKS
Workshop on Moon in Transition: Apollo 14, KREEP, and Evolved Lunar Rocks
[NASA-CR-186153] N90-15026
The Apollo 15 coarse fines (4-10 mm)
[NASA-TM-101934] N90-15027
LUNAR ROVING VEHICLES
CIS-lunar space infrastructure lunar technologies: Executive summary
[NASA-CR-186220] N90-15029

M

M STARS
Properties of evolved star circumstellar grains
N90-15003
MACH NUMBER
Normal force, pitching moment, and side force of forebody-cylinder combinations for angles of attack up to 90 degrees and Mach numbers up to 5
[ESDU-89014] N90-14192
Corrections for non-ideal effects in reflected shock waves at low Mach numbers
[DE90-002192] N90-14208
MACHINING
New tool-holding concept
[DE90-000880] N90-14624
MAGNESIUM OXIDES
Prospects for wavelength tunable lasers based on vacancy defects in alkaline-earth oxides
[DE90-001078] N90-14592
MAGNETIC COMPRESSION
Performance of the 10-kV, 100-kA pulsed-power modules for the FRX-C magnetic compression experiment
[DE89-014027] N90-14917
MAGNETIC FIELDS
High power transducers
[AD-D014225] N90-14461
Electric-gun studies of conductors in high magnetic fields and experiments in dynamic flux compression
[DE90-000815] N90-14470
Use of superconducting plates and shells to deflect magnetic noise fields: Application to MEG
[DE89-012592] N90-14676
Two-dimensional behavior of Megagauss-field-confined solid fiber Z-pinches
[DE90-000684] N90-14918
Theoretical reversed field pinch studies
[DE90-002114] N90-14929
Macroscopic persistent currents in high temperature ceramic superconductors
[DE89-636232] N90-14973
MAGNETIC FLUX
Testing and performance of a high-gain flux-compression generator
[DE90-002808] N90-14492
MAGNETIC LEVITATION VEHICLES
California air transportation study: A transportation system for the California Corridor of the year 2010
[NASA-CR-186219] N90-14212
Markets for high-speed intercity Maglev technology: A systems analysis approach
[DE89-017683] N90-14623
Applications of superconductor technologies to transportation
[DE90-000856] N90-14961
MAGNETIC MATERIALS
Magnetic excitations in thulium metal
[DE90-002475] N90-14970
MAGNETIC MEASUREMENT
On-line system to measure magnetic characteristics of steel samples
[DE89-633443] N90-14861
MAGNETIC PERMEABILITY
Multiple martensitic transformations, incommensurate/commensurate phases, and charge-density-wave states in plutonium metal: Their consequences
[DE90-001235] N90-14350
MAGNETIC PROBES
Measuring the thickness of austenitic weld deposits on carbon steel walls using a magnetic method
[DE89-635446] N90-14628
MAGNETIC PROPERTIES
On-line system to measure magnetic characteristics of steel samples
[DE89-633443] N90-14861
Solid State Division
[DE90-000979] N90-14945
Muon SR investigation of magnetism and superconductivity in (Y(1-x)Pr(x))Ba2Cu3O7
[DE90-000689] N90-14956
Magnetic excitations in thulium metal
[DE90-002475] N90-14970
Magnetotransport studies of epitaxial Cr thin films
[DE90-001930] N90-14975
Magnetic and electrical properties
[DE90-002183] N90-14977
Surface magneto-optical studies of ultrathin ferromagnetic films
[DE90-002199] N90-14980
MAGNETIC SUSPENSION
Techniques for extreme attitude suspension of a wind tunnel model in a magnetic suspension and balance system
[NASA-CR-181895] N90-14245
Opportunities and prospects for Maglev in North America
[DE90-002190] N90-14627
MAGNETIZATION
Static and dynamic magnetization properties of Y1Ba2Cu3O(sub z) thin films
[DE89-017584] N90-14940
MAGNETO-OPTICS
Surface magneto-optical studies of ultrathin ferromagnetic films
[DE90-002199] N90-14980
MAGNETOHYDRODYNAMIC FLOW
Unsteady hydromagnetic flow of a radiating gas in a vertical channel with axial temperature variation
[DE90-600934] N90-14525
Ion collection by probing objects in flowing magnetized plasmas
[DE90-001711] N90-14916
On the thermal stability of flow of a radiating two-component plasma in a porous medium between two rotating cylinders
[DE89-636426] N90-14928
MAGNETOHYDRODYNAMIC STABILITY
Experimental study on the filamentary instability in laser-matter interactions at short wave lengths
N90-14547
Effects of temporal and induced spatial incoherence on parametric instabilities in laser plasma interactions
N90-14549
Limitations in the growing of a plasma wave produced by heterodyning two lasers due to modulations and decay instabilities N90-14552
Use of plasmas for the acceleration of particles to very high energy N90-14553
High-frequency instability of the sheath-plasma resonance
[NASA-CR-186127] N90-14910
Two-dimensional behavior of Megagauss-field-confined solid fiber Z-pinches
[DE90-000684] N90-14918
Stability of the Global Alfven Eigenmode in the presence of fusion alpha particles in an ignited tokamak plasma
[DE89-016618] N90-14930
MAGNETOHYDRODYNAMIC WAVES
Stability of the Global Alfven Eigenmode in the presence of fusion alpha particles in an ignited tokamak plasma
[DE89-016618] N90-14930
MAGNETOHYDRODYNAMICS
Modelling of the effects of the equatorial electrojet on its environment
[DE89-636298] N90-14720
MAGNETORESISTIVITY
Magnetotransport studies of epitaxial Cr thin films
[DE90-001930] N90-14975
MAGNETOSTRICTION
Method and apparatus to enhance the sensitivity of cylindrical magnetostrictive transducer to magnetic fields
[AD-D014218] N90-14459
MAGNETS
Further studies of transverse stress effects in cable-in-conduit conductors
[DE90-001517] N90-14484
MAN ENVIRONMENT INTERACTIONS
A model for the simulation of the ozone budget in the atmosphere under anthropogenic perturbation
[DE89-636294] N90-14719
MAN-COMPUTER INTERFACE
MIPs and BIPs are megaflops: Limits of unidimensional assessments
[DE89-015707] N90-14770
MANAGEMENT INFORMATION SYSTEMS
GRAFIN: GRAFIX interactive manual
[PB89-232136] N90-14809
A dynamic systems engineering methodology research study. Phase 2: Evaluating methodologies, tools, and techniques for applicability to NASA's systems projects
[NASA-CR-181319] N90-14985
MANAGEMENT METHODS
How far can the world get on energy efficiency alone
[DE90-001349] N90-14886
MANAGEMENT SYSTEMS
Level 2 software reuse study N90-14800
An SSE approach to reusability N90-14801
MANATEES
Summary of 1987 and 1988 manatee aerial surveys at Kennedy Space Center
[NASA-TM-102783] N90-14869
MANEUVERABLE SPACECRAFT
Project Argo: The design and analysis of an all-propulsive and an aeroassisted version of a manned space transportation vehicle
[NASA-CR-186047] N90-14266
MANIPULATORS
Manipulation strategies for massive space payloads
[NASA-CR-186081] N90-14247
Controller design for a robotic manipulator
N90-14615
Results of the manipulator test test stand study: Comparison of manipulators and evaluation of equipment items
[DE90-000977] N90-14625
French technological progress in the field of robotics and teleoperation
[DE90-001590] N90-14626
MANNED MARS MISSIONS
Aerobraking characteristics for several potential manned Mars entry vehicles
[NASA-TM-101669] N90-14272
MANNED SPACECRAFT
Risk-based fire safety experiment definition for manned spacecraft
[NASA-CR-183835] N90-14262
Project Argo: The design and analysis of an all-propulsive and an aeroassisted version of a manned space transportation vehicle
[NASA-CR-186047] N90-14266
MANUFACTURING
Superplasticity
[AGARD-LS-168] N90-14325
Superplasticity: An overview N90-14326
The manufacture of superplastic alloys N90-14333
MAPPING
Low level range coverage performance prediction for VHF radar N90-14439
NORDA's pattern analysis laboratory: Current contributions to naval mapping, charting, and geodesy
[AD-A212731] N90-14665
Evaluation of the airborne visible-infrared imaging spectrometer for mapping subtle lithological variation
[NASA-CR-186213] N90-14670
Nomenclature for physical mapping of complex genomes
[DE89-015173] N90-14994
MARINE ENVIRONMENTS
Weather satellite and computer modeling approaches to assessing propagation over marine environments
N90-14443
Managing marine protected areas: An action plan
[PB89-158778] N90-14701
MARINE METEOROLOGY
Physical models for aerosol in the marine mixed-layer
N90-14438
MARINE TECHNOLOGY
NORDA's pattern analysis laboratory: Current contributions to naval mapping, charting, and geodesy
[AD-A212731] N90-14665
MARKET RESEARCH
California air transportation study: A transportation system for the California Corridor of the year 2010
[NASA-CR-186219] N90-14212
Markets for high-speed intercity Maglev technology: A systems analysis approach
[DE89-017683] N90-14623
MARKETING
Consumer Ozone Protection Act of 1989
[S-HRG-101-377] N90-14708
MARS ATMOSPHERE
Saltation thresholds and entrainment of fine particles at Earth and Martian pressures
[NASA-TM-102193] N90-14997
MARS ENVIRONMENT
M.I.N.G., Mars Investment for a New Generation: Robotic construction of a permanently manned Mars base
[NASA-CR-186224] N90-15028
MARTENSITE
Martensite transformation in NiTi alloys induced by tensile stress pulses
[DE90-001832] N90-14346
MARTENSITIC TRANSFORMATION
Martensite transformation in NiTi alloys induced by tensile stress pulses
[DE90-001832] N90-14346

Multiple martensitic transformations, incommensurate/commensurate phases, and charge-density-wave states in plutonium metal: Their consequences
[DE90-001235] N90-14350
Theory of the energetics and nonclassical nucleation for martensitic transformations from partially soft lattice modes
[DE90-002182] N90-14964

MASERS
Nonlinear quantum effects in the Maser model: A large N scaling behaviour
[DE89-631631] N90-14584

MASS
Black-hole decay and topological stability in quantum gravity
[DE89-618785] N90-15017

MASS DISTRIBUTION
Biomodal spontaneous fission
[DE90-001516] N90-14886

MASS SPECTROSCOPY
Combined capillary electrophoresis and electrospray ionization mass spectrometry
[DE90-001903] N90-14322

MASS TRANSFER
Heat and mass transfer design issues in PEM fuel cell hardware
[DE89-016779] N90-14677

MASSIVELY PARALLEL PROCESSORS
Krylov methods preconditioned with incompletely factored matrices on the CM-2
[NASA-CR-181961] N90-14779
High performance parallel architectures
[DE90-001055] N90-14782

MATHEMATICAL MODELS
Efficient real gas Navier-Stokes computations of high speed flows using an LU scheme
[NASA-TM-102429] N90-14203
Risk-based fire safety experiment definition for manned spacecraft
[NASA-CR-183835] N90-14262
Slush Hydrogen (SLH2) technology development for application to the National Aerospace Plane (NASP)
[NASA-TM-102315] N90-14268
Optimal stochastic modeling and control of flexible structures
[AD-A212347] N90-14269
A generalized thermomechanical constitutive model for metal matrix composites with plastic strain and damage N90-14293
Investigation of combustion instability in ramjet combustors N90-14303
Kinetics and mechanism of soot formation in hydrocarbon combustion
[NASA-CR-186162] N90-14305
A numerical study of thin flame representations
[DE89-017889] N90-14313
The thermally induced gas-phase reactions of methane and oxygen: A comparison of experimental and computational results
[DE90-000785] N90-14317
RPE: A parabolic equation radio assessment model N90-14419
A forecasting system using the parabolic equation: Application to surface-to-air propagation in the presence of elevated layers N90-14420
Propagation modeling for some horizontally varying tropospheric ducts N90-14422
Propagation prediction for the North Sea environment N90-14423
Forward scatter propagation path loss testing using surrogate terrain in the 100 to 1500 MHz region N90-14425
Improved reliability prediction for HF digital voice transmission N90-14429
The thermal behavior of natural backgrounds and its prediction by means of numerical models N90-14436
Low level range coverage performance prediction for VHF radar N90-14439
Weather satellite and computer modeling approaches to assessing propagation over marine environments N90-14443
The FTZ HF propagation model for use on small computers and its accuracy N90-14447
Electron heating and static sheath enhancement in front of energized RF antennas
[DE90-001334] N90-14456
Modeling of sodium/metal chloride batteries
[DE89-017685] N90-14478
The fluid mechanics of filters N90-14499
Granular flow: Numerical simulation of dry granular flows and calculation of hydrodynamic interactions in suspensions
[DE89-017544] N90-14518
Pipe and bend erosion by pneumatic transport of solids at high temperature
[DE89-015741] N90-14524
Course A: Numerical modeling of two-phase flows for presentation at Ecole d'Ete d'Analyse Numerique
[DE90-002074] N90-14526
Electrothermal response testing more than a quality assurance tool
[DE90-001449] N90-14536
Theoretical studies of solar lasers and converters
[NASA-CR-186194] N90-14583
The current status of x ray conversion efficiency modeling
[DE90-000931] N90-14591
Theory of harmonic radiation using a single-electron source model
[DE90-002412] N90-14606
Tire modeling by finite elements N90-14614
BES welding science contractors summary report, 1988 to 1989
[DE90-001004] N90-14619
Thermal fatigue durability for advanced propulsion materials
[NASA-TM-102348] N90-14641
Comparison of shock severity measures
[DE90-000790] N90-14654
Implications and origins of shock structure in solids
[DE90-000846] N90-14658
Critical time step estimation for three-dimensional explicit impact analysis
[DE90-002187] N90-14662
Earth Sciences Division annual report 1988
[DE90-002617] N90-14663
Heat transfer of buried pipe for heat pump application
[DE90-000580] N90-14697
Turbulent wind at the equatorial segment of an operating Darrieus wind turbine blade
[DE90-002672] N90-14698
A model for the simulation of the ozone budget in the atmosphere under anthropogenic perturbation
[DE89-636294] N90-14719
Quantifying the link between change in radiative balance and atmospheric temperature
[DE90-000819] N90-14721
Extraterrestrial halogen and sulfur content of the stratosphere
[DE89-017623] N90-14738
Meteorological monitoring for environmental/dose assessment and emergency response modeling: How much is enough
[DE90-002726] N90-14757
Factors affecting electron spin polarization in photosynthetic systems
[DE90-000196] N90-14764
The development of a model of the human responses to load carriage N90-14775
Program CICC flow and heat transfer in Cable-in-Conduit Conductors
[DE90-001519] N90-14818
Symmetry breaking bifurcations of a current sheet
[DE90-601005] N90-14864
Wide-angle propagation in inhomogeneous fluids and elastic solids using perturbation methods N90-14868
Particle simulations in magnetospheric plasmas
[NASA-CR-186238] N90-14934
REFLECT: A computer program for the x ray reflectivity of bent perfect crystals
[DE90-001266] N90-14946
Developing integrated parametric planning models for budgeting and managing complex projects
[NASA-CR-186006] N90-14986
A model of the thermal and electrical properties of cosmic dust particles N90-15014
Dark matter and the solar neutrino problem: Can particle physics provide a single solution
[DE90-001827] N90-15024

MATRICES (CIRCUITS)
Characterization of two MMIC GaAs switch matrices at microwave frequencies
[NASA-TM-102449] N90-14273

MATRICES (MATHEMATICS)
Parallel eigenanalysis of finite element models in a completely connected architecture
[NASA-CR-185166] N90-14652
Krylov methods preconditioned with incompletely factored matrices on the CM-2
[NASA-CR-181961] N90-14779

MATRIX MATERIALS
Elasto-plastic analysis of unidirectional fiber-reinforced composites subjected to transverse normal loading using the finite element method N90-14292

MATTER (PHYSICS)
The ultimate structure of matter: The US High Energy Physics Program from the 1950s through the 1980s
[DE90-001784] N90-14887

MAXIMUM ENTROPY METHOD
Power spectral estimation algorithms
[NASA-CR-186189] N90-14812

MAXIMUM LIKELIHOOD ESTIMATES
Estimating methods for counting process intensities: Non-parametric methods
[IMAG-RR-774-M] N90-14846

MAXWELL EQUATION
Assessment of anomalous propagation predictions using minisonde refractivity data and the parabolic equation method N90-14424

MAXWELL-BOLTZMANN DENSITY FUNCTION
Modification of ionic population by non-Maxwellian effects N90-14565

MEASURING INSTRUMENTS
Measuring the thickness of austenitic weld deposits on carbon steel walls using a magnetic method
[DE89-635446] N90-14628
Rocket studies of the lower ionosphere
[NASA-CR-186187] N90-14735
X ray microprobe for the microcharacterization of materials
[DE89-006038] N90-14863
Effective utilization of acoustic wave sensor responses: Simultaneous measurement of velocity and attenuation
[DE90-002580] N90-14872

MECHANICAL DRIVES
Performance and modification of the MEA RF drive system N90-14895

MECHANICAL ENGINEERING
Superplastic sheet forming N90-14327

MECHANICAL PROPERTIES
Elastomeric impulse energy storage and transfer system
[AD-D014223] N90-14255
Superplasticity: An overview N90-14326
The mechanical properties of superplastically formed titanium and aluminium alloys N90-14331
The 4.2 K fracture toughness of 304 stainless steel in a magnetic field
[DE90-002083] N90-14347
Mechanical properties and morphology of oriented polymer blends N90-14361
Bulk and shear moduli of epoxy encapsulants
[DE90-000899] N90-14371
Numerical and empirical verification of the stress state in a ceramic, button-head, tensile specimen
[DE90-001645] N90-14375
Practical superconductor development for electrical power applications
[DE90-001804] N90-14487
Engineering approaches to the application of fracture toughness data in the nuclear industry
[DE90-001586] N90-14659
Process monitoring using optical ultrasonic wave detection
[DE90-002021] N90-14870
Dynamical simulation of dislocation microstructure
[DE90-003192] N90-14982

MEDITERRANEAN SEA
Analysis of propagation in an inhomogeneous atmosphere in the horizontal and vertical direction using the parabolic equation method N90-14421

MELTING
Noncontacting laser ultrasonic generation and detection at the surface of molten metal
[DE90-002020] N90-14605

MELTING POINTS
Thermophysical properties of isopropyl alcohol. Part 2: Thermodynamic properties at elevated pressures
[ESDU-89020-PT-2] N90-14300

MEMBRANES
Asymptotic analysis of performance of membrane modules for gas separations
[DE90-000699] N90-14316
Test and evaluation of polymeric membranes for oxygen enrichment of air
[DE90-000555] N90-14321
Ordered ceramic membranes
[DE89-017426] N90-14364
Comparison of structural subunits of the core light-harvesting complexes of photosynthetic bacteria
[DE90-001412] N90-14765

MEMORY
Advanced Software Development Workstation Project N90-14807

MEMORY (COMPUTERS)
Concurrent processing adaptation of aeroplastic analysis of propfans
[NASA-TM-102455] N90-14658

MERCURY TELLURIDES
Thin film cadmium telluride, zinc telluride, and mercury zinc telluride solar cells
[DE89-009499] N90-14681

MESH
Method for fabricating thin film metallic meshes for use as Fabry-Perot interferometer elements, filters and other devices
[AD-D014236] N90-14529
MESOMETEOROLOGY
Weather satellite and computer modeling approaches to assessing propagation over marine environments N90-14443
MESOSCALE PHENOMENA
The identification of terrain-induced circulations using principal components
[DE90-001991] N90-14739
MESOSPHERE
Remote sensing of atmospheric water vapour by pressure modulation radiometry N90-14667
A measurement of hydroxyl in the daytime mesosphere N90-14732
METABOLISM
Decomposition in Arctic terrestrial environments
[DE90-001198] N90-14706
METAL BONDING
Superplastic sheet forming N90-14327
Diffusion bonding of metals N90-14330
Designing for superplastic alloys N90-14332
METAL COATINGS
Laser Raman spectroscopy in studies of corrosion and electrocatalysis
[DE90-001414] N90-14311
METAL CRYSTALS
Spectral properties of one dimensional quasi-crystals
[PREPRINT-659] N90-14936
METAL FATIGUE
A nonlinear high temperature fracture mechanics basis for strainrange partitioning
[NASA-TM-4133] N90-14642
Fatigue fracture in the presence of shot peening residual stresses: Initiation, propagation, and relaxation phenomena N90-14644
METAL FILMS
Improved performance of low-T(sub c) superconductors for detection of minimum-ionizing particles
[DE90-001985] N90-14978
METAL FLUORIDES
Investigation of the phase stabilizing effect of potassium fluoride on ammonium nitrate
[AD-A213042] N90-14381
METAL FOILS
Electric-gun studies of conductors in high magnetic fields and experiments in dynamic flux compression
[DE90-000815] N90-14470
Experimental investigation of a fast-acting exploding metallic foil opening switch
[DE90-001051] N90-14479
METAL JOINTS
Influence of hole surface finish, cyclic frequency and spectrum severity on the fatigue behavior of thick section aluminum alloy pin joints
[ARL-STRUC-R-430] N90-14336
METAL MATRIX COMPOSITES
Carbon fiber reinforced metal matrix composites
[AD-D014245] N90-14289
Analysis of metal matrix composite structures using a microchemical constitutive theory N90-14290
A generalized thermomechanical constitutive model for metal matrix composites with plastic strain and damage N90-14293
Parametric studies to determine the effect of compliant layers on metal matrix composite systems
[NASA-TM-102465] N90-14294
Advances and future directions in superplastic materials N90-14328
METAL OXIDES
Micro-scale simulation of dynamic compaction of oxide and metal powder mixture
[DE90-002220] N90-14978
METAL PLATES
Perturbations in high-velocity gas flow
[DE90-000539] N90-14520
METAL POWDER
Micro-scale simulation of dynamic compaction of oxide and metal powder mixture
[DE90-002220] N90-14978
METAL SURFACES
Noncontacting laser ultrasonic generation and detection at the surface of molten metal
[DE90-002020] N90-14505
A method of soldering aluminum
[AD-D014226] N90-14611
METAL-GAS SYSTEMS
The formation of metal-oxygen species at low temperatures
[DE90-002296] N90-14323
METALLOGRAPHY
Performance characteristics of a three-stage railgun
[DE90-002533] N90-14254
METALS
Interaction of hydrogen isotopes with metals: Deuterium trapped at lattice defects in palladium
[DE90-000811] N90-14344
Acoustic emission during intergranular stress corrosion cracking
[DE90-002894] N90-14355
METEORITES
Abstracts for the 52nd Annual Meeting of the Meteoritical Society
[NASA-CR-186160] N90-14998
METEORITIC COMPOSITION
Meteoritic basalts
[NASA-CR-185949] N90-15004
METEOROID PROTECTION
On protection of Freedom's solar dynamic radiator from the orbital debris environment. Part 1: Preliminary analyses and testing
[NASA-TM-102458] N90-14285
METEOROLOGICAL CHARTS
The development of a spatial synoptic climatological index for environmental analysis N90-14744
Use of operational 0-6 and 3-9 h quantitative precipitation forecasts for predicting heavy rain events
[PB90-103946] N90-14750
METEOROLOGICAL FLIGHT
Global stratospheric change: Requirements for a Very-High-Altitude Aircraft for Atmospheric Research
[NASA-CP-10041] N90-14220
METEOROLOGICAL INSTRUMENTS
The Tactical Environmental Support System (TESS(3)) N90-14409
Meteorological monitoring for environmental/dose assessment and emergency response modeling: How much is enough
[DE90-002726] N90-14757
METEOROLOGICAL PARAMETERS
A forecasting system using the parabolic equation: Application to surface-to-air propagation in the presence of elevated layers N90-14420
Propagation prediction for the North Sea environment N90-14423
The thermal behavior of natural backgrounds and its prediction by means of numerical models N90-14436
Climatology of Lawrence Livermore National Laboratory
[DE90-000905] N90-14756
Meteorological monitoring for environmental/dose assessment and emergency response modeling: How much is enough
[DE90-002726] N90-14757
METEOROLOGICAL RADAR
Adaptive clutter rejection filters for airborne Doppler weather radar applied to the detection of low altitude windshear
[NASA-CR-186211] N90-14453
METEOROLOGICAL SATELLITES
Weather satellite and computer modeling approaches to assessing propagation over marine environments N90-14443
METEOROLOGICAL SERVICES
Summary of papers, studies, conference presentations: 1987-1988 (from the National Weather Service, southern region)
[PB90-103896] N90-14749
METEOROLOGY
Analysis of propagation in an inhomogeneous atmosphere in the horizontal and vertical direction using the parabolic equation method N90-14421
Application of surface analysis methods to studies of atmospheric deposition in forests
[DE90-000582] N90-14714
Summary of papers, studies, conference presentations: 1987-1988 (from the National Weather Service, southern region)
[PB90-103896] N90-14749
METEOSAT SATELLITE
Rainfall estimation over Africa using satellite data N90-14742
METHANE
The thermally induced gas-phase reactions of methane and oxygen: A comparison of experimental and computational results
[DE90-000785] N90-14317
METHYL ALCOHOL
Assessment of costs and benefits of flexible and alternative fuel use in the US transportation sector. Technical report three: Methanol production and transportation costs
[DE90-002625] N90-14396
Cold starting a neat methanol (M100) vehicle with long duration spark ignition
[PB89-230692] N90-14613
METRICATION
Metric handbook for Federal officials: Recommendations of the Interagency Committee on Metric Policy
[PB89-226922] N90-14400
METROLOGY
Metric handbook for Federal officials: Recommendations of the Interagency Committee on Metric Policy
[PB89-226922] N90-14400
MICROANALYSIS
Calibration approach to electron probe microanalysis: A study with PWA-1480, a nickel base superalloy
[NASA-TM-102393] N90-14335
X ray microprobe for the microcharacterization of materials
[DE89-006038] N90-14863
Practical limitations of ALCHEMI measurements on ordered intermetallic alloys
[DE90-000700] N90-14957
MICROBURSTS (METEOROLOGY)
A candidate concept for display of forward-looking wind shear information
[NASA-TM-101585] N90-14232
The effects of clutter-rejection filtering on estimating weather spectrum parameters
[NASA-CR-186212] N90-14754
MICROCRACKS
Mechanics of interaction of a crack with microcracks N90-14650
MICROCRYSTALS
Study of microcrystalline, silicon-carbon p-layers prepared by photo-CVD and glow discharge
[DE89-009438] N90-14939
MICROELECTRONICS
Integrating and enhancing tools for ASIC (Application-Specific Integrated Circuits) design using MOSIS (Metal Oxide Semiconductor Implementation Service) fabrication
[DE90-001601] N90-14475
Monolithic laser diode structure for microwave generation
[AD-D014210] N90-14543
MICROMECHANICS
Analysis of metal matrix composite structures using a microchemical constitutive theory N90-14290
Parametric studies to determine the effect of compliant layers on metal matrix composite systems
[NASA-TM-102465] N90-14294
MICROMETEOROIDS
On protection of Freedom's solar dynamic radiator from the orbital debris environment. Part 1: Preliminary analyses and testing
[NASA-TM-102458] N90-14285
MICROMETEOROLOGY
An initial look at the dynamics of the microscale flow field within a large wind farm in response to variations in the natural inflow
[DE89-009501] N90-14682
MICROORGANISMS
Decomposition in Arctic terrestrial environments
[DE90-001198] N90-14706
MICROPROCESSORS
Automated glass fiber drawing
[DE90-000894] N90-14367
Coordination of processing elements in a multiprocessor computer
[WO-PATENT-88/04075] N90-14830
MICROSCOPES
Soft x ray microscope using Fourier transform holography
[DE90-002291] N90-14539
MICROSTRUCTURE
Superplastic sheet forming N90-14327
Advances and future directions in superplastic materials N90-14328
Cavitation and superplasticity N90-14329
The mechanical properties of superplastically formed titanium and aluminium alloys N90-14331
Phases in lanthanum-nickel-aluminum intermetallic alloys
[DE90-000651] N90-14343
Embrittlement of laboratory- and reactor-aged CF-3, CF-8, and CF-8M duplex stainless steels
[DE90-002777] N90-14354
Mechanical properties and morphology of oriented polymer blends N90-14361
The 7th International Conference on Ceramics
[DE90-002144] N90-14374
Characterization of nanophase materials by x ray diffraction and computer simulation
[DE90-002270] N90-14378
Primary arm spacing in directionally solidified Pb-10 wt percent Sn alloys
[NASA-CR-185190] N90-14398

Practical superconductor development for electrical power applications
[DE90-001804] N90-14487
Microstructure induced by laser shock in an austenitic steel N90-14558
BES welding science contractors summary report, 1988 to 1989
[DE90-001004] N90-14619
The feasibility of welding of irradiated materials
[DE90-002200] N90-14631
Engineering approaches to the application of fracture toughness data in the nuclear industry
[DE90-001596] N90-14659
Electrode development in monolithic solid oxide fuel cells
[DE90-001910] N90-14684
Process monitoring using optical ultrasonic wave detection
[DE90-002021] N90-14870
Atomic matching across internal interfaces
[DE90-002266] N90-14889
X ray studies of strain, interface, and impurity in semiconductors
[DE90-001525] N90-14947
Flux pinning and microstructure in YBa2Cu3O7
[DE90-001562] N90-14948
Superconducting and microstructural properties of shock-compacted high-T sub c oxide powders
[DE90-000823] N90-14958
The effect of composition and processing on high T(sub c) superconductors containing bismuth
[DE90-002203] N90-14965
Microstructure and electrical properties of bulk high-T(sub c) superconductors
[DE90-001762] N90-14974

MICROWAVE AMPLIFIERS
Recent developments of gigatron technology
[DE90-001067] N90-14474
Gigatron: A new technology for microwave power devices
[DE90-001066] N90-14483

MICROWAVE EQUIPMENT
Microwave Tokamak Experiment: An overview of the construction and checkout phase
[DE90-000834] N90-14924

MICROWAVE SWITCHING
Characterization of two MMIC GaAs switch matrices at microwave frequencies
[NASA-TM-102449] N90-14273

MICROWAVE TRANSMISSION
Microwave Transport Systems for the MTX (Microwave Tokamak Experiment)
[DE90-000821] N90-14921

MICROWAVES
SEM (Scanning Electron Microscope) image analysis of grain growth in microwave-annealed alumina
[DE90-001606] N90-14339
Symmetric waveguide junction combiner
[AD-D014243] N90-14466
Monolithic laser diode structure for microwave generation
[AD-D014210] N90-14543
Microwave Tokamak Experiment (MTX) first year of operation and future plans
[DE90-000817] N90-14920
MTX (Microwave Tokamak Experiment)/ELF (Electron Laser Facility) 2 microwave power measurements and calibration for the 2-GW, 140-GHz, ELF 2 Free Electron Laser (FEL)
[DE90-000825] N90-14922
Microwave characterization of high-temperature superconductors
[DE90-002408] N90-14968
Laboratory evaluation and application of microwave absorption properties under simulated conditions for planetary atmospheres
[NASA-CR-185916] N90-15025

MIE SCATTERING
The effect of oblate spheroidal drops on rain attenuation at 94 GHz: Comparison between theory and experiment N90-14440

MILITARY OPERATIONS
Concerning advanced architectures for strategic defense
[DE90-001894] N90-14857

MILITARY TECHNOLOGY
Configuration development for ROMENET
[AD-A213367] N90-14450

MILLIMETER WAVES
Laboratory evaluation and application of microwave absorption properties under simulated conditions for planetary atmospheres
[NASA-CR-185916] N90-15025

MINERALOGY
Abstracts for the 52nd Annual Meeting of the Meteoritical Society
[NASA-CR-186160] N90-14998

MINES (EXCAVATIONS)
Verification of the NIKE3D structural analysis code by comparison against the analytic solution for a spherical cavity under a far-field uniaxial stress
[DE90-000929] N90-14653

MINIATURIZATION
A portable ionosonde in support of reliable communications N90-14431

MINIMA
A computational analysis of the transonic flow field of two-dimensional minimum length nozzles N90-14194

MIRRORS
Optical design and performance of an XUV FEL (Free-Electron Laser) oscillator
[DE90-002381] N90-14599
Deferred electronic heterodyne moire deflectometry: A method for transient density fields measurement
[NASA-CR-182982] N90-14907

MISSILE DEFENSE
A review of gas-cooled reactor concepts for SDI (Strategic Defense Initiative)
[DE89-016962] N90-14898

MISSION PLANNING
Project Argo: The design and analysis of an all-propulsive and an aeroassisted version of a manned space transportation vehicle
[NASA-CR-186047] N90-14266
Communication Overview Program (COP) N90-14435

MIXERS
Cavitation-controlled ultrasonic agitator
[DE90-002773] N90-14871

MIXING
Development of a titanium/boron blending process
[DE90-001450] N90-14386
Physical models for aerosol in the marine mixed-layer N90-14438

MIXING LAYERS (FLUIDS)
An experimental investigation of shear layer mixing in supersonic flows N90-14508
Comparative study of the vorticity field in turbulent flows: Theory, experiments, and computations
[DE90-001399] N90-14516

MIXING LENGTH FLOW THEORY
Navier-Stokes analysis of airfoils with leading edge ice accretions N90-14196

MIXTURES
The generalized van der Waals theory of pure fluids and mixtures
[DE90-000504] N90-14307

MOBILE COMMUNICATION SYSTEMS
Improving the quality of a spread-spectrum radiomobile link N90-14426

MODELS
Steady state model to determine lake resources at risk to acid deposition in the Sierra Nevada, California
[PB89-103995] N90-14705

MODULATION
Remote sensing of atmospheric water vapour by pressure modulation radiometry N90-14667

MODULATORS
Modification of MEA modulator-klystron units enabling short pulse injection into a pulse-stretcher ring N90-14894
Performance and modification of the MEA RF drive system N90-14895

MODULES
Fast serial communication module
[DE89-633753] N90-14454
Performance of the 10-kV, 100-kA pulsed-power modules for the FRX-C magnetic compression experiment
[DE89-014027] N90-14917

MODULUS OF ELASTICITY
Parametric studies to determine the effect of compliant layers on metal matrix composite systems
[NASA-TM-102465] N90-14294

MOIRE FRINGES
A sampled-grating model of moire patterns from digital imaging
[AD-A213364] N90-14902
Deferred electronic heterodyne moire deflectometry: A method for transient density fields measurement
[NASA-CR-182982] N90-14907

MOIRE INTERFEROMETRY
Interferometric surface distortion detector
[AD-D014211] N90-14901

MOISTURE
Development of a titanium/boron blending process
[DE90-001450] N90-14386
Low-temperature conversion of high-moisture biomass: Continuous reactor system results
[DE90-000984] N90-14683

MOLECULAR CHAINS
The structure and properties of liquid crystal polymers N90-14356

MOLECULAR CLOUDS
Very high resolution radio observations of molecular cloud cores N90-15013

MOLECULAR DIFFUSION
Non-linear optical studies of adsorbates: Spectroscopy and dynamics
[DE90-001543] N90-14312

MOLECULAR IONS
Structural peculiarities and molecular properties of charge complexes formed on positive ion injection into dense inert gas media
[DE89-633953] N90-14877

MOLECULAR ORBITALS
A diagnostic for determining the quality of single-reference electron correlation methods
[NASA-TM-101929] N90-14874

MOLECULAR STRUCTURE
Laser Raman spectroscopy in studies of corrosion and electrocatalysis
[DE90-001414] N90-14311
The structure and properties of liquid crystal polymers N90-14356
Chemistry of large molecules
[DE90-000813] N90-14366
Comparison of structural subunits of the core light-harvesting complexes of photosynthetic bacteria
[DE90-001412] N90-14765

MOMENTS
Effect of unshielded and shielded horn balances on hinge moment coefficients for controls at low speeds
[ESDU-89003-A] N90-14238
Hinge moment coefficient derivatives for trailing-edge controls on wings at subsonic speeds
[ESDU-89009] N90-14239
Example of procedure in calculation of control hinge moments
[ESDU-89010] N90-14240

MOMENTUM TRANSFER
A low-order model of the equatorial ocean-atmosphere system N90-14730

MONITORS
Biological effects of hyperthermia and potential risk associated with ultrasonic exposure
[PB89-100702] N90-14768
Human factors survey of advanced instrumentation and controls
[DE90-002477] N90-14776
Development of a real time monitor for superconductive thin film preparation
[DE89-017772] N90-14952

MONOCHROMATORS
REFLECT: A computer program for the x ray reflectivity of bent perfect crystals
[DE90-001266] N90-14946

MONTE CARLO METHOD
Electron heating and static sheath enhancement in front of energized RF antennas
[DE90-001334] N90-14456
A new simulation method for the efficient calculation of benchmarks for detonation products equations of state
[DE90-001837] N90-14522
Derivation of synthetic mission profiles from electric vehicle field data
[DE89-011125] N90-14620
An observational study of intramonthly quasi-periodicities in the Northern Hemisphere, extratropical geopotential height field N90-14729
Path integral simulations of liquid helium
[DE90-001171] N90-14862

MOON
CIS-lunar space infrastructure lunar technologies: Executive summary
[NASA-CR-186220] N90-15029

MORPHOLOGY
Mechanical properties and morphology of oriented polymer blends N90-14361
A study of the infrared emission of galactic supernova remnants N90-15006

MOTOR VEHICLES
Cold starting a neat methanol (M100) vehicle with long duration spark ignition
[PB89-230692] N90-14613

MSAT
Vehicle antenna for the mobile satellite experiment
[NASA-CR-186109] N90-14271

MULTICHANNEL COMMUNICATION
Frequency independent constant beamwidth directional lens antenna for very wideband and multi-channel electromagnetic communications
[AD-D014214] N90-14449

MULTILAYER INSULATION
Fabrication of NBN based electronic devices with silicon barriers
[AD-D014230] N90-14463
MULTIPATH TRANSMISSION
Improving the quality of a spread-spectrum radiomobile link N90-14426
Improved reliability prediction for HF digital voice transmission N90-14429
Mitigating Doppler shift effect in HF multitone data modem N90-14441
TROPO: A technique for predicting propagation and modem performance of digital troposcatter systems N90-14444
Modelling UHF propagation for frequency assignment in radio relay networks N90-14445
The characteristics of the HF radio channel and its influence on modern HF data communication system design N90-14448
MULTIPHASE FLOW
Heat transfer in convective boundary layer and channel flows N90-14505
The laminar to slug flow transition in Hele-Shaw flow
[DE90-000636] N90-14521
MULTIPROCESSING (COMPUTERS)
The Aerospace Energy Systems Laboratory: A BITBUS networking application
[NASA-TM-4149] N90-14829
NETRA: A parallel architecture for integrated vision systems. 1: Architecture and organization
[NASA-CR-185955] N90-14839
MULTISPECTRAL BAND SCANNERS
Image processing of LANDSAT MSS data for buried valley detection in northern Indiana N90-14668
MULTIVARIATE STATISTICAL ANALYSIS
Optimal stochastic modeling and control of flexible structures
[AD-A212347] N90-14269
MUONS
Cold fusion: Alchemist's dream
[DE90-000865] N90-14925
MUSCLES
The development of a model of the human responses to load carriage N90-14775

N

NARROWBAND
Narrow band and wide angle hemispherical interference optical filter
[AD-D014238] N90-14904
NASA PROGRAMS
Review of the Aerospace Safety Advisory Panel report for NASA fiscal year 1990 authorization
[GPO-24-234] N90-14213
An international discussion on research in solar and space physics N90-14996
NASA SPACE PROGRAMS
Space station attached payload program support
[NASA-CR-183838] N90-14274
NATIONAL AEROSPACE PLANE PROGRAM
Design and demonstration of heat pipe cooling for NASP and evaluation of heating methods at high heating rates
[DE89-016995] N90-14227
Slush Hydrogen (SLH2) technology development for application to the National Aerospace Plane (NASP)
[NASA-TM-102315] N90-14268
NATIONAL AIRSPACE SYSTEM
National airspace system monitoring operational concept
[NAS-SR-1330] N90-14214
NATURAL GAS
The thermally induced gas-phase reactions of methane and oxygen: A comparison of experimental and computational results
[DE90-000785] N90-14317
NAVIER-STOKES EQUATION
An investigation of the bursting of trailing vortices using numerical simulation N90-14191
Navier-Stokes solutions of 2-D transonic flow over unconventional airfoils N90-14195
Navier-Stokes analysis of airfoils with leading edge ice accretions N90-14196
Efficient real gas Navier-Stokes computations of high speed flows using an LU scheme
[NASA-TM-102429] N90-14203
Surface flow and heating distributions on a cylinder in near wake of Aeroassist Flight Experiment (AFE) configuration at incidence in Mach 10 Air
[NASA-TP-2954] N90-14493
Numerical solution of the incompressible Navier-Stokes equations N90-14501
Applications of a new exact solution of the Navier-Stokes equations to flow in pipes of varying width N90-14504
The analysis and modeling of dilatational terms in compressible turbulence
[NASA-CR-181959] N90-14513
NAVIGATION
Programmable near-infrared ranging system
[AD-D014237] N90-14903
NEAR WAKES
Surface flow and heating distributions on a cylinder in near wake of Aeroassist Flight Experiment (AFE) configuration at incidence in Mach 10 Air
[NASA-TP-2954] N90-14493
NEBULAE
Studies of elementary particles: Proposal
[DE90-001120] N90-14879
NEODYMIUM LASERS
Fast electrons in a laser generated plasma N90-14545
Production of homogeneous plasmas for laser-plasma interaction experiments N90-14546
Experimental study on the filamentary instability in laser-matter interactions at short wave lengths N90-14547
Interaction of a low flux laser beam with a solid target N90-14554
Ultrahigh-brightness lasers and their applications
[DE90-000877] N90-14596
NETWORK CONTROL
Configuration development for ROMENET
[AD-A213367] N90-14450
JPL reuse program N90-14795
NEUTRINOS
A theoretical perspective on neutrino physics
[DE90-000759] N90-14878
Supernovae, compact stars, and nuclear physics
[DE90-002682] N90-15022
NEUTRON DIFFRACTION
Application of neutron diffraction NDE to high-temperature superconducting composites
[DE90-002184] N90-14295
Charge transfer and bond lengths in YBa2Cu(sub 3-x)M(sub x)O(sub 6+y)
[DE90-002241] N90-14966
Powder neutron diffraction study of the structural phase diagram of the Ba(sub 1-x)K(sub x)BiO3 system
[DE90-002264] N90-14967
Magnetic excitations in thulium metal
[DE90-002475] N90-14970
NEUTRON SCATTERING
Solid State Division
[DE90-000979] N90-14945
NICKEL
An electroformed nickel-sulfur alloy for a nose cone
[DE90-000866] N90-14337
Silver-nickel composite cathodes for alkaline secondary batteries
[AD-D014231] N90-14464
NICKEL ALLOYS
Phases in lanthanum-nickel-aluminum intermetallic alloys
[DE90-000651] N90-14343
Martensite transformation in NiTi alloys induced by tensile stress pulses
[DE90-001832] N90-14346
NICKEL HYDROGEN BATTERIES
Terrestrial nickel/hydrogen battery development at Johnson Controls, Inc.
[DE89-015843] N90-14471
NIOBIUM COMPOUNDS
Fabrication of NBN based electronic devices with silicon barriers
[AD-D014230] N90-14463
NIOBIUM STANNIDES
Further studies of transverse stress effects in cable-in-conduit conductors
[DE90-001517] N90-14484
NITRIC ACID
Profile measurements of sulfur dioxide, nitrogen oxides, and nitric acid deposition velocities in California's south coast air basin
[PB90-104001] N90-14703
NITRIC OXIDE
The retrieval of the concentrations of nitric oxide and nitrogen dioxide from satellite solar occultation measurements at sunset and sunrise N90-14733
NITROGEN
Phase changes in carbon and nitrogen systems: Their effects on the detonation properties of high explosives
[DE90-000829] N90-14392
Nitrogen deposition to forest trees
[DE90-003285] N90-14726
NITROGEN COMPOUNDS
Pentafluorothio polynitroaliphatic explosives
[AD-D014221] N90-14383
Nitrogen deposition to forest trees
[DE90-003285] N90-14726
NITROGEN DIOXIDE
The retrieval of the concentrations of nitric oxide and nitrogen dioxide from satellite solar occultation measurements at sunset and sunrise N90-14733
NITROGEN OXIDES
Profile measurements of sulfur dioxide, nitrogen oxides, and nitric acid deposition velocities in California's south coast air basin
[PB90-104001] N90-14703
NOISE (SOUND)
Control of an experiment to measure acoustic noise in the space shuttle
[NPS62-89-022] N90-14869
NOISE INTENSITY
Cavitation-controlled ultrasonic agitator
[DE90-002773] N90-14871
NOISE PREDICTION (AIRCRAFT)
Evaluation of analysis techniques for low frequency interior noise and vibration of commercial aircraft
[NASA-CR-181851] N90-14866
NOISE REDUCTION
A communications system with an adaptive multi-functional architecture N90-14415
NOMENCLATURES
Nomenclature for physical mapping of complex genomes
[DE89-015173] N90-14994
NONDESTRUCTIVE TESTS
Application of neutron diffraction NDE to high-temperature superconducting composites
[DE90-002184] N90-14295
Diffusion bonding of metals N90-14330
Nondestructive evaluation of flaw clusters and thin layer interfaces N90-14633
Assessment of the efficiency of nondestructive techniques in materials testing studies based on the information criterion
[DE89-635444] N90-14634
NONEQUILIBRIUM CONDITIONS
Non-equilibrium effects of slow diffusion controlled reactions on the properties of explosives
[DE90-000822] N90-14391
NONLINEAR EQUATIONS
The stability of Taylor-Couette flow with radial heating N90-14502
Local error estimates for discontinuous solutions of nonlinear hyperbolic equations
[NASA-CR-181960] N90-14847
NONLINEAR SYSTEMS
A helicopter flight path controller design via a nonlinear transformation technique N90-14242
Dynamics and control of flexible spacecraft during and after slewing maneuvers
[NASA-CR-186123] N90-14270
Box experiments. Nonlinear effects at plasma resonance N90-14555
Non-linear vibrations, stability, and dynamics of structures and mechanisms
[AD-A212152] N90-14639
NONLINEARITY
Non-linear optical studies of adsorbates: Spectroscopy and dynamics
[DE90-001543] N90-14312
Nonlinear quantum effects in the Maser model: A large N scaling behaviour
[DE89-631631] N90-14584
Chaotic behavior in nonlinear polarization dynamics
[DE89-013453] N90-14589
A study of incremental-iterative strategies for nonlinear analyses
[PB89-226005] N90-14646
NORMAL SHOCK WAVES
Measured and predicted aerodynamic coefficients and shock shapes for Aeroassist Flight Experiment (AFE) configuration
[NASA-TP-2956] N90-14185
NORTH SEA
Propagation prediction for the North Sea environment N90-14423
NORTHERN HEMISPHERE
An observational study of intramonthly quasi-periodicities in the Northern Hemisphere, extratropical geopotential height field N90-14729
NOSE CONES
An electroformed nickel-sulfur alloy for a nose cone
[DE90-000866] N90-14337
NOZZLE DESIGN
A numerical technique for analysis of resistojet nozzle flow N90-14506
NOZZLE FLOW
A computational analysis of the transonic flow field of two-dimensional minimum length nozzles N90-14194
A numerical technique for analysis of resistojet nozzle flow N90-14506

NOZZLE GEOMETRY
A computational analysis of the transonic flow field of two-dimensional minimum length nozzles N90-14194
NUCLEAR ENGINE FOR ROCKET VEHICLES
A review of gas-cooled reactor concepts for SDI (Strategic Defense Initiative)
[DE89-016962] N90-14898
NUCLEAR FUEL REPROCESSING
Results of the manipulator test test stand study: Comparison of manipulators and evaluation of equipment items
[DE90-000977] N90-14625
NUCLEAR FUELS
Starlight: A stationary inertial-confinement-fusion reactor with nonvaporizing walls
[DE90-002315] N90-14927
NUCLEAR FUSION
Quality assurance and quality control for the Compact Physics Research Facility (CPRF) and ZTH experiment
[DE90-002352] N90-14636
Lawrence Livermore National Laboratory (LLNL) research on cold fusion
[DE90-000930] N90-14915
Cold fusion: Alchemist's dream
[DE90-000865] N90-14925
Stability of the Global Alfven Eigenmode in the presence of fusion alpha particles in an ignited tokamak plasma
[DE89-016618] N90-14930
NUCLEAR INTERACTIONS
A study of recoil protons in ultra-relativistic nucleus-nucleus collisions
[LUIP-8907] N90-14873
The creation of high energy densities with antimatter beams
[DE90-002383] N90-14899
NUCLEAR MAGNETIC RESONANCE
Perturbed angular correlations in zirconia ceramics
[DE89-017272] N90-14369
Use of superconducting plates and shells to deflect magnetic noise fields: Application to MEG
[DE89-012592] N90-14676
NUCLEAR PHYSICS
Supernovae, compact stars, and nuclear physics
[DE90-002682] N90-15022
NUCLEAR REACTIONS
Cold fusion: Alchemist's dream
[DE90-000865] N90-14925
NUCLEAR REACTORS
Energy ratings for metal oxide varistors under repetitively pulsed operation
[DE90-002353] N90-14480
A cost effective battery bank for I(sup 2)T testing and evaluation of electrical switchgear
[DE90-002350] N90-14490
Failure probability estimate of Type 304 stainless steel piping
[DE90-000659] N90-14635
Human factors survey of advanced instrumentation and controls
[DE90-002477] N90-14776
NUCLEAR SPIN
Proceedings of the Conference on High-Spin Nuclear Structure and Novel Nuclear Shapes
[DE88-013968] N90-14875
NUCLEAR STRUCTURE
Proceedings of the Conference on High-Spin Nuclear Structure and Novel Nuclear Shapes
[DE88-013968] N90-14875
Heavy ion interactions
[DE90-001410] N90-14884
NUCLEATION
Cavitation and superplasticity N90-14329
Theory of the energetics and nonclassical nucleation for martensitic transformations from partially soft lattice modes
[DE90-002182] N90-14964
The influence of the substrate surface on the nucleation and growth of superconducting thin films
[DE90-003649] N90-14983
NUCLEI (NUCLEAR PHYSICS)
Proceedings of the Conference on High-Spin Nuclear Structure and Novel Nuclear Shapes
[DE88-013968] N90-14875
NUMERICAL ANALYSIS
Research in mathematics and computer science at Argonne, July 1, 1986 to January 6, 1988
[DE88-010343] N90-14781
NUMERICAL CONTROL
A computer-controlled automated test system for fatigue and fracture testing
[DE90-002931] N90-14661
NUMERICAL INTEGRATION
Symplectic numerical integration of Hamiltonian systems
[DE90-002380] N90-14855
NUMERICAL STABILITY
Group implicit concurrent algorithms in nonlinear structural dynamics
[NASA-CR-185950] N90-14638
Numerical methodologies for solving partial differential equations
[DE90-001842] N90-14849

O

O STARS
A source of observational constraints on the structure of Wolf-Rayet winds
[DE90-001236] N90-15023
OCCULTATION
The retrieval of the concentrations of nitric oxide and nitrogen dioxide from satellite solar occultation measurements at sunset and sunrise N90-14733
OCEAN BOTTOM
Mid-Oceanic Ridge: A Dynamic Global System
[PB89-198691] N90-14758
OCEAN MODELS
A low-order model of the equatorial ocean-atmosphere system N90-14730
Tuning of the OSCURS (Ocean Surface Current Simulations) numerical model to ocean surface measurements in the Gulf of Alaska
[PB89-103979] N90-14759
OCEAN SURFACE
A global ocean wind stress climatology based on ECMWF (European Centre for Medium Range Weather Forecasts) analyses
[PB90-109968] N90-14752
Tuning of the OSCURS (Ocean Surface Current Simulations) numerical model to ocean surface measurements in the Gulf of Alaska
[PB89-103979] N90-14759
OCEANOGRAPHY
Tuning of the OSCURS (Ocean Surface Current Simulations) numerical model to ocean surface measurements in the Gulf of Alaska
[PB89-103979] N90-14759
OGIVES
Subsonic sting interference on the aerodynamic characteristics of a family of slanted-base ogive-cylinders
[NASA-CR-186193] N90-14204
OIL EXPLORATION
Devices and methods for in-situ combustion ignition
[DE89-000766] N90-14309
OILS
Thermocapillary migration of liquid droplets in a temperature gradient in a density matched system
[NASA-CR-185178] N90-14512
ON-LINE SYSTEMS
Survey of adaptive control theory and its applications
[DE89-901270] N90-14840
On-line system to measure magnetic characteristics of steel samples
[DE89-633443] N90-14861
OPACITY
Equation of state and opacity of dense plasmas
[DE90-002223] N90-14926
OPERATING SYSTEMS (COMPUTERS)
The role of order in distributed programs
[NASA-CR-186252] N90-14826
The Aerospace Energy Systems Laboratory: A BITBUS networking application
[NASA-TM-4149] N90-14829
How robust are distributed systems
[NASA-CR-186242] N90-14837
OPERATORS (MATHEMATICS)
Numerical methodologies for solving partial differential equations
[DE90-001842] N90-14849
OPERATORS (PERSONNEL)
Human factors survey of advanced instrumentation and controls
[DE90-002477] N90-14776
OPTICAL COMMUNICATION
Shuttle Laser Technology Experiment Facility (LTEF)-to-airplane lasercom experiment: Airplane considerations
[NASA-TM-100749] N90-14260
OPTICAL DISKS
Document preservation by electronic imaging. Volume 1: Synopsis
[PB89-226526] N90-14987
Document preservation by electronic imaging. Volume 2: System and experiment description
[PB89-226534] N90-14988
Document preservation by electronic imaging. Volume 3: Appendices
[PB89-226542] N90-14989
OPTICAL EQUIPMENT
Method and apparatus to enhance the sensitivity of cylindrical magnetostrictive transducer to magnetic fields
[AD-D014218] N90-14459
Interferometric surface distortion detector
[AD-D014211] N90-14901
OPTICAL FIBERS
Simulated Brillouin backscattering in optical fibers: A ring resonator N90-14556
OPTICAL FILTERS
Narrow band and wide angle hemispherical interference optical filter
[AD-D014238] N90-14904
OPTICAL MEASUREMENT
Process monitoring using optical ultrasonic wave detection
[DE90-002021] N90-14870
OPTICAL MEASURING INSTRUMENTS
Spectral contents readout of birefringent sensor
[NASA-CR-179444] N90-14905
OPTICAL PROPERTIES
Optical design and performance of an XUV FEL (Free-Electron Laser) oscillator
[DE90-002381] N90-14599
OPTICAL RADAR
Field evaluation of a Nissan laser collision avoidance system
[PB90-105602] N90-14215
Remote sensing of the aerosol scattering coefficient with a multi-field-of view lidar N90-14437
High resolution Doppler lidar
[NASA-CR-183288] N90-14542
OPTICAL RESONATORS
Simulated Brillouin backscattering in optical fibers: A ring resonator N90-14556
OPTICAL SCANNERS
Proceedings of the Conference on Application of Scanning Methodologies in Libraries
[PB89-233415] N90-14990
OPTICS
Optics of the Amsterdam pulse stretcher (AmPS) N90-14893
OPTIMAL CONTROL
Optimal control of aero-assisted orbit transfer vehicles N90-14241
Guidance and Control strategies for aerospace vehicles
[NASA-CR-186195] N90-14243
OPTIMIZATION
Introduction to data items on flight path optimisation
[ESDU-89015] N90-14221
New heating and cooling technology: Regenerative heat pump according to the Vuilleumier principle
[DE90-002701] N90-14699
Parallel projected variable metric algorithms for unconstrained optimization
[NASA-CR-181930] N90-14842
Application of heuristic satellite plan synthesis algorithms to requirements of the WARC-88 allotment plan
[NASA-TM-102479] N90-14856
ORBIT CALCULATION
Correction of ionospheric effects for the precise orbit determination of satellites N90-14432
ORBIT SPECTRUM UTILIZATION
Application of heuristic satellite plan synthesis algorithms to requirements of the WARC-88 allotment plan
[NASA-TM-102479] N90-14856
ORBIT TRANSFER VEHICLES
Optimal control of aero-assisted orbit transfer vehicles N90-14241
Guidance and Control strategies for aerospace vehicles
[NASA-CR-186195] N90-14243
Optimal trajectories for the aeroassisted flight experiment
[NASA-CR-186133] N90-14250
ORGANIC COMPOUNDS
Energies of organic compounds
[DE90-003174] N90-14324
ORTHOGONALITY
Symmetric waveguide junction combiner
[AD-D014243] N90-14466
OSCILLATORS
Symmetric waveguide junction combiner
[AD-D014243] N90-14466
Numerical simulations of free-electron laser oscillators
[DE89-003488] N90-14588
Optical design and performance of an XUV FEL (Free-Electron Laser) oscillator
[DE90-002381] N90-14599

INEX (Integrated Numerical Experiment) simulations of the Los Alamos HIBAF (High-Brightness Accelerator Free-Electron Laser) free-electron laser MOPA (Master Oscillator Power Amplifier) experiment
[DE90-002387] N90-14601

OXIDASE
Amperometric biosensors for glucose, lactate, and glycolate based on oxidases and redox-modified siloxane polymers
[DE90-002301] N90-14541

OXIDATION
Predictive aging of elastomers in air: The importance of understanding diffusion-limited oxidation effects
[DE90-001385] N90-14372

OXIDATION RESISTANCE
Oxidation effects on the mechanical properties of SiC fiber-reinforced reaction-bonded silicon nitride matrix composites
[NASA-TM-102360] N90-14287

OXIDE FILMS
Glancing angle x ray studies of oxide films
[DE89-017828] N90-14953

OXIDES
A model of the isotope effect of the oxide superconductor
[DE89-635907] N90-14971

OXYGEN
The thermally induced gas-phase reactions of methane and oxygen: A comparison of experimental and computational results
[DE90-000785] N90-14317
Test and evaluation of polymeric membranes for oxygen enrichment of air
[DE90-000555] N90-14321
The formation of metal-oxygen species at low temperatures
[DE90-002298] N90-14323
Oxygen stoichiometry, structural transitions, and thermodynamic behavior of the YBa2Cu3O(x) system
[DE89-017694] N90-14951
Anisotropy of oxygen tracer diffusion in YBa2Cu3O7-delta single crystals
[DE90-001931] N90-14979

OXYGEN SUPPLY EQUIPMENT
Comparison of protective breathing equipment performance at ground level and 8,000 feet altitude using parameters prescribed by portions of FAA action notice A-8150.2
[AD-A212852] N90-14773

OZONE
Discussions of global environmental problems
[DE90-002747] N90-14718
A model for the simulation of the ozone budget in the atmosphere under anthropogenic perturbation
[DE89-636294] N90-14719
The retrieval of the concentrations of nitric oxide and nitrogen dioxide from satellite solar occultation measurements at sunset and sunrise N90-14733

OZONE DEPLETION
Consumer Ozone Protection Act of 1989
[S-HRG-101-377] N90-14708

P

P-I-N JUNCTIONS
Preparation and properties of high deposition a-Si:H films and solar cells using disilane
[DE89-009467] N90-14679

PACIFIC OCEAN
Tuning of the OSCURS (Ocean Surface Current Simulations) numerical model to ocean surface measurements in the Gulf of Alaska
[PB89-103979] N90-14759

PACKET SWITCHING
Multiple crossbar network: A switched high-speed local network
[DE90-001839] N90-14833

PACKETS (COMMUNICATION)
Configuration development for ROMENET
[AD-A213367] N90-14450

PALEOCLIMATOLOGY
Evaluation of climatic models: Comparison of simulated and observed patterns for past climates
[DE90-001228] N90-14755

PALLADIUM
Interaction of hydrogen isotopes with metals: Deuterium trapped at lattice defects in palladium
[DE90-000611] N90-14344
Characterization of nanophase materials by x ray diffraction and computer simulation
[DE90-002270] N90-14378
Atomic matching across internal interfaces
[DE90-002266] N90-14889

PALLADIUM ALLOYS
Effects of composition and age hardening on precious metal electrical contacts
[DE88-008791] N90-14476

PANEL METHOD (FLUID DYNAMICS)
Program VSAERO theory document: A computer program for calculating nonlinear aerodynamic characteristics of arbitrary configurations
[NASA-CR-4023] N90-14200

PARABOLIC ANTENNAS
Frequency independent constant beamwidth directional lens antenna for very wideband and multi-channel electromagnetic communications
[AD-D014214] N90-14449

PARABOLIC DIFFERENTIAL EQUATIONS
A forecasting system using the parabolic equation: Application to surface-to-air propagation in the presence of elevated layers N90-14420
Analysis of propagation in an inhomogeneous atmosphere in the horizontal and vertical direction using the parabolic equation method N90-14421
Propagation modeling for some horizontally varying tropospheric ducts N90-14422
Assessment of anomalous propagation predictions using minisonde refractivity data and the parabolic equation method N90-14424

PARALLEL COMPUTERS
Block predictor (low order) corrector methods to solve ordinary differential equations on parallel computers
[IMAG-RR-757-M] N90-14845

PARALLEL PROCESSING (COMPUTERS)
Group implicit concurrent algorithms in nonlinear structural dynamics
[NASA-CR-185950] N90-14638
Parallel eigenanalysis of finite element models in a completely connected architecture
[NASA-CR-185166] N90-14652
Krylov methods preconditioned with incompletely factored matrices on the CM-2
[NASA-CR-181961] N90-14779
Research in mathematics and computer science at Argonne, July 1, 1986 to January 6, 1988
[DE88-010343] N90-14781
High performance parallel architectures
[DE90-001055] N90-14782
Force user's manual: A portable, parallel FORTRAN
[NASA-CR-4265] N90-14785
Parallel mathematical software
[DE90-002694] N90-14822
Strand: A practical parallel programming language
[DE90-002861] N90-14825
PCP (Parallel C Preprocessor): A parallel extension of C that is 99 percent fat free
[DE90-002813] N90-14834
Generalization in backpropagation networks: An empirical study using image data
[DE89-012658] N90-14835
Architectures for reasoning in parallel
[NASA-CR-186237] N90-14836
NETRA: A parallel architecture for integrated vision systems. 1: Architecture and organization
[NASA-CR-185955] N90-14839
Block predictor (low order) corrector methods to solve ordinary differential equations on parallel computers
[IMAG-RR-757-M] N90-14845

PARTIAL DIFFERENTIAL EQUATIONS
Aspects of field theory related to the Zakharov problem N90-14551
Research in mathematics and computer science at Argonne, July 1, 1986 to January 6, 1988
[DE88-010343] N90-14781
User's guide to PMESH: A grid-generation program for single-rotation and counterrotation advanced turboprops
[NASA-CR-185156] N90-14783
Numerical methodologies for solving partial differential equations
[DE90-001842] N90-14849
Two-dimensional behavior of Megagauss-field-confined solid fiber Z-pinches
[DE90-000684] N90-14918

PARTIAL PRESSURE
Comparison of protective breathing equipment performance at ground level and 8,000 feet altitude using parameters prescribed by portions of FAA action notice A-8150.2
[AD-A212852] N90-14773

PARTICLE ACCELERATION
Use of plasmas for the acceleration of particles to very high energy N90-14553

PARTICLE ACCELERATORS
NIKHEF-K contributions to the 1989 Particle Accelerator Conference
[NIKHEF/AMPS/89/03] N90-14891
The Amsterdam pulse stretcher project (AmPS)
N90-14892
Optics of the Amsterdam pulse stretcher (AmPS)
N90-14893

PARTICLE COLLISIONS
A study of recoil protons in ultra-relativistic nucleus-nucleus collisions
[LUIP-8907] N90-14873
Calculation of two-neutron multiplicity in photonuclear reactions
[NASA-TP-2968] N90-14890

PARTICLE EMISSION
Calculation of two-neutron multiplicity in photonuclear reactions
[NASA-TP-2968] N90-14890

PARTICLE INTERACTIONS
Supersymmetric dark matter above the W mass
[NASA-CR-186168] N90-15016

PARTICLE MOTION
Self-field-induced chaotic electron motion in free electron lasers
[DE90-001710] N90-14598

PARTICLE SIZE DISTRIBUTION
Ordered ceramic membranes
[DE89-017426] N90-14364
Particle size effects in the initiation of explosives containing reactive and nonreactive continuous phases
[DE90-000786] N90-14390
Comparison of two droplet sizing systems in an icing wind tunnel
[NASA-TM-102456] N90-14617

PARTICLES
The fluid mechanics of filters N90-14499

PARTITIONS (MATHEMATICS)
Classification of modular invariant partition functions for the twisted N=2 superconformal algebra, twisted SU(2) Kac-Moody algebra and D(sub 2K) parafermions
[DE90-600767] N90-14853

PASSIVITY
Laser Raman spectroscopy in studies of corrosion and electrocatalysis
[DE90-001414] N90-14311

PATTERN RECOGNITION
Weather satellite and computer modeling approaches to assessing propagation over marine environments
N90-14443
Pattern recognition techniques applied to the NASA-ACTS order-wire problem N90-14446
NORDA's pattern analysis laboratory: Current contributions to naval mapping, charting, and geodesy
[AD-A212731] N90-14665
A rough transform technique for extracting lead features from sea ice imagery
[AD-A212758] N90-14666
Generalization in backpropagation networks: An empirical study using image data
[DE89-012658] N90-14835
NETRA: A parallel architecture for integrated vision systems. 1: Architecture and organization
[NASA-CR-185955] N90-14839

PAYLOAD INTEGRATION
Payload crew utilization for spacelab missions
[NASA-TP-2976] N90-14256

PAYLOADS
Unsteady aerodynamic simulation of multiple bodies in relative motion: A prototype method
[NASA-TM-102181] N90-14188
Manipulation strategies for massive space payloads
[NASA-CR-186081] N90-14247

PEAT
Decomposition in Arctic terrestrial environments
[DE90-001198] N90-14706

PELLETS
Characteristics of an electron-beam rocket pellet accelerator
[DE90-001595] N90-14252
Starlight: A stationary inertial-confinement-fusion reactor with nonvaporizing walls
[DE90-002315] N90-14927
Microstructure and electrical properties of bulk high-T(sub c) superconductors
[DE90-001762] N90-14974

PEPTIDES
Combined capillary electrophoresis and electrospray ionization mass spectrometry
[DE90-001903] N90-14322

PERFORMANCE PREDICTION
Normal force, pitching moment, and side force of forebody-cylinder combinations for angles of attack up to 90 degrees and Mach numbers up to 5
[ESDU-89014] N90-14192
Effect of unshielded and shielded horn balances on hinge moment coefficients for controls at low speeds
[ESDU-89003-A] N90-14238
Hinge moment coefficient derivatives for trailing-edge controls on wings at subsonic speeds
[ESDU-89009] N90-14239

SRB thermal environments
[NASA-CR-183801] N90-14276
Investigation of combustion instability in ramjet combustors N90-14303
Numerical and empirical verification of the stress state in a ceramic, button-head, tensile specimen
[DE90-001645] N90-14375
The Tactical Environmental Support System (TESS(3)) N90-14409
Decision-aid design factors in connection with HF communication and emitter location disciplines N90-14413
RPE: A parabolic equation radio assessment model N90-14419
Improved reliability prediction for HF digital voice transmission N90-14429
Low level range coverage performance prediction for VHF radar N90-14439
Weather satellite and computer modeling approaches to assessing propagation over marine environments N90-14443
TROPO: A technique for predicting propagation and modem performance of digital troposcatter systems N90-14444
Transient response of flexible rotor-bearing systems subjected to combined unbalance and ground excitations N90-14616
System design and performance prediction of a free-piston Stirling engine/magnetic coupling/compressor assembly in a gas residential heat pump
[DE89-016070] N90-14696

PERFORMANCE TESTS
Effect of blade planform variation on a small-scale hovering rotor
[NASA-TM-4146] N90-14186
Arcjet thruster research and technology. Phase 1: Executive summary
[NASA-CR-182106] N90-14278
Flight set 360T004 (STS-30) field joint protection system, volume 7
[NASA-CR-183829] N90-14280
Study of new materials for gun propellant formulations
[DE89-015285] N90-14388
Zinc/bromine battery evaluation at SNL (Sandia National Laboratory)
[DE89-015847] N90-14473
Laboratory testing of Sonnenschein DF6V180 6 volt traction battery
[DE90-002080] N90-14486
Testing and performance of a high-gain flux-compression generator
[DE90-002808] N90-14492
Field testing of a ceramic heat exchanger for heat recovery application
[DE90-002082] N90-14523
A laboratory test for fuel injector deposit studies
[DE90-000802] N90-14629
Performance evaluation of the Puritan-Bennett crew-member portable protective breathing device as prescribed by portions of FAA action notice A-8150.2
[AD-A211113] N90-14772
Performance of the 10-kV, 100-kA pulsed-power modules for the FRX-C magnetic compression experiment
[DE89-014027] N90-14917

PERIODIC VARIATIONS
Localized vibrations of nearly periodic structures with irregularities N90-14648
An observational study of intramonthly quasi-periodicities in the Northern Hemisphere, extratropical geopotential height field N90-14729

PERMEABILITY
Asymptotic analysis of performance of membrane modules for gas separations
[DE90-000699] N90-14316
Test and evaluation of polymeric membranes for oxygen enrichment of air
[DE90-000555] N90-14321
Ordered ceramic membranes
[DE89-017426] N90-14364

PERMUTATIONS
Frequency agile synthetic aperture radar
[AD-D014235] N90-14451

PERSONAL COMPUTERS
Personal computer process data acquisition
[DE89-017877] N90-14816

PERSONNEL
Rocket studies of the lower ionosphere
[NASA-CR-186187] N90-14735

PERSONNEL DEVELOPMENT
Cognitive and Neural Sciences Division 1989 programs
[AD-A212634] N90-14769

PERSONNEL SELECTION
Cognitive and Neural Sciences Division 1989 programs
[AD-A212634] N90-14769

PERTURBATION
The stability of Taylor-Couette flow with radial heating N90-14502
Atomic structure and spectral perturbations in hot dense plasmas N90-14567
Perturbation methods for the calculation of gravitational waves from slightly non-spherical spacetimes with applications to stellar core collapse N90-15015

PERTURBATION THEORY
Optimal control of aero-assisted orbit transfer vehicles N90-14241
Localized vibrations of nearly periodic structures with irregularities N90-14648
Wide-angle propagation in inhomogeneous fluids and elastic solids using perturbation methods N90-14868

PETN
Fast transit gas- and condensed-phase chemistry of energetic materials
[DE90-001656] N90-14395

PETROLOGY
Workshop on the Archean Mantle
[NASA-CR-186156] N90-14736
Workshop on Moon in Transition: Apollo 14, KREEP, and Evolved Lunar Rocks
[NASA-CR-186153] N90-15026
The Apollo 15 coarse fines (4-10 mm)
[NASA-TM-101934] N90-15027

PH
Characterization of cloud chemistry and frequency of canopy exposure to clouds in the Sierra Nevada
[PB89-104035] N90-14753

PHASE DIAGRAMS
Solid oxide fuel cells electrodes based on In(sub 2)O(sub 3)-PrO(sub 1.83)-ZrO(sub 2)
[DE90-002666] N90-14691
Powder neutron diffraction study of the structural phase diagram of the Ba(sub 1-x)K(sub x)BiO3 system
[DE90-002264] N90-14967

PHASE ERROR
An Energy Spectrum Compressor system (ESC) for the Amsterdam pulse stretcher (AmPS) N90-14896

PHASE SHIFT
The phase gradient autofocus algorithm: An optimal estimator of the phase derivative
[DE90-000895] N90-14814

PHASE SHIFT KEYING
Mitigating Doppler shift effect in HF multitone data modem N90-14441

PHASE TRANSFORMATIONS
Shock-induced solid state reactions and phase transitions: X ray profile studies on shock-modified Fe3O4 and ZrO2 powders
[DE90-000669] N90-14315
The metallurgical determinants of toughness as cryogenic temperature
[DE90-002331] N90-14351
First-principles interatomic potentials in transition metals: Multi-ion interactions and their analytic representation
[DE90-001990] N90-14353
Investigation of the phase stabilizing effect of potassium fluoride on ammonium nitrate
[AD-A213042] N90-14381
Phase changes in carbon and nitrogen systems: Their effects on the detonation properties of high explosives
[DE90-000829] N90-14392
Oxygen stoichiometry, structural transitions, and thermodynamic behavior of the YBa2Cu3O(x) system
[DE89-017694] N90-14951
Muon SR investigation of magnetism and superconductivity in (Y(1-x)Pr(x))Ba2Cu3O7
[DE90-000689] N90-14956
Theory of the energetics and nonclassical nucleation for martensitic transformations from partially soft lattice modes
[DE90-002182] N90-14964

PHASED ARRAYS
Vehicle antenna for the mobile satellite experiment
[NASA-CR-186109] N90-14271

PHOSPHORESCENCE
Mapping of upper electronic reaction surfaces by tuned laser photolysis and by absorption and emission spectroscopies
[DE90-000125] N90-14314

PHOTOCHEMICAL REACTIONS
The retrieval of the concentrations of nitric oxide and nitrogen dioxide from satellite solar occultation measurements at sunset and sunrise N90-14733

PHOTOCONDUCTIVITY
Multiband photoconductive detector based on layered semiconductor quantum wells
[AD-D014232] N90-14936

PHOTODIODES
High-efficiency large-area CdTe modules
[DE89-009498] N90-14689
Method of sensitizing PB-Salt epitaxial films for Schottky diodes
[AD-D014244] N90-14937

PHOTOELASTIC ANALYSIS
The stress analysis of thin-walled screwed tubular joints N90-14637

PHOTOELECTRIC EMISSION
High resolution-angle resolved photoemission studies of high temperature superconductors
[DE89-017691] N90-14950

PHOTOELECTRONS
A Scanning Photoelectron Microscope (SPEM) at the National Synchrotron Light Source (NSLS)
[DE90-001551] N90-14537

PHOTOGRAPHIC FILM
Development of X diagnostics around the pulse 1 laser N90-14580

PHOTOLYSIS
Corrections for non-ideal effects in reflected shock waves at low Mach numbers
[DE90-002192] N90-14208
Mapping of upper electronic reaction surfaces by tuned laser photolysis and by absorption and emission spectroscopies
[DE90-000125] N90-14314

PHOTOMETERS
Multiband photoconductive detector based on layered semiconductor quantum wells
[AD-D014232] N90-14936

PHOTONS
Nonresonant and resonant multiphoton ionization of (NO)(sub n) and Ar(sub n)NO clusters with picosecond laser pulses
[DE89-016853] N90-14607
Is the number of photons conserved in an expanding universe
[DE89-618836] N90-15018

PHOTONUCLEAR REACTIONS
Calculation of two-neutron multiplicity in photonuclear reactions
[NASA-TP-2968] N90-14890

PHOTOSYNTHESIS
Factors affecting electron spin polarization in photosynthetic systems
[DE90-000196] N90-14764
Comparison of structural subunits of the core light-harvesting complexes of photosynthetic bacteria
[DE90-001412] N90-14765

PHOTOVOLTAIC CONVERSION
Photovoltaic Measurements and Performance Branch
[DE89-009500] N90-14695

PHYSIOLOGICAL EFFECTS
Exploring the living universe: A strategy for space life sciences
[NASA-TM-101891] N90-14778

PHYSIOLOGICAL RESPONSES
The development of a model of the human responses to load carriage N90-14775

PICOSECOND PULSES
Nonresonant and resonant multiphoton ionization of (NO)(sub n) and Ar(sub n)NO clusters with picosecond laser pulses
[DE89-016853] N90-14607

PIEZORESISTIVE TRANSDUCERS
Evaluation of shock isolation techniques for a piezoresistive accelerometer
[DE89-014496] N90-14535

PILOT PERFORMANCE
A candidate concept for display of forward-looking wind shear information
[NASA-TM-101585] N90-14232
Workload induced spatio-temporal distortions and safety of flight
[DE89-016613] N90-14771

PINCH EFFECT
Laser probing non-cylindrical Z-pinch in near-isolator region of a discharged chamber
[DE89-632018] N90-14912

PINS
Influence of hole surface finish, cyclic frequency and spectrum severity on the fatigue behavior of thick section aluminum alloy pin joints
[ARL-STRUC-R-430] N90-14336

PIONS
Heavy ion interactions
[DE90-001410] N90-14884

PIPE FLOW
An investigation of the bursting of trailing vortices using numerical simulation N90-14191
Selection of the energy-efficient enhancement geometry for single-phase turbulent flow inside tubes
[DE89-017690] N90-14519

Pipe and bend erosion by pneumatic transport of solids at high temperature
[DE89-015741] N90-14524
PIPES (TUBES)
Applications of a new exact solution of the Navier-Stokes equations to flow in pipes of varying width N90-14504
Failure probability estimate of Type 304 stainless steel piping
[DE90-000659] N90-14635
Heat transfer of buried pipe for heat pump application
[DE90-000580] N90-14697
PISTON ENGINES
System design and performance prediction of a free-piston Stirling engine/magnetic coupling/compressor assembly in a gas residential heat pump
[DE89-016070] N90-14696
PITCH (INCLINATION)
Development of a three-axis trim program
[AD-A212883] N90-14237
PITCHING MOMENTS
Normal force, pitching moment, and side force of forebody-cylinder combinations for angles of attack up to 90 degrees and Mach numbers up to 5
[ESDU-89014] N90-14192
PIXELS
SAS graphics in DCF
[PNR90563] N90-14399
PLANETARY ATMOSPHERES
Laboratory evaluation and application of microwave absorption properties under simulated conditions for planetary atmospheres
[NASA-CR-185916] N90-15025
PLANETARY BOUNDARY LAYER
A one-dimensional shipboard model for forecasting refractive effects in the planetary boundary layer N90-14442
PLANETARY EVOLUTION
Workshop on the Archean Mantle
[NASA-CR-186156] N90-14736
PLANETARY MAGNETOSPHERES
Particle simulations in magnetospheric plasmas
[NASA-CR-186238] N90-14934
PLANETARY WAVES
Long wave propagation assessment N90-14414
PLANNING
Battery technology assessment and R and D plan
[DE90-002007] N90-14489
PLASMA CONTROL
Computation of electromagnetic effects in a tokamak due to a plasma disruption
[DE90-001764] N90-14931
PLASMA CYLINDERS
On the thermal stability of flow of a radiating two-component plasma in a porous medium between two rotating cylinders
[DE89-636426] N90-14928
PLASMA DECAY
Limitations in the growing of a plasma wave produced by heterodyning two lasers due to modulations and decay instabilities N90-14552
PLASMA DIAGNOSTICS
Laser probing non-cylindrical Z-pinch in near-isolator region of a discharged chamber
[DE89-632018] N90-14912
Ion collection by probing objects in flowing magnetized plasmas
[DE90-001711] N90-14916
Microwave Tokamak Experiment (MTX) first year of operation and future plans
[DE90-000817] N90-14920
Precision timing and interlocks systems for FEL (Free-Electron Laser) heating experiments on MTX (Microwave Tokamak Experiment)
[DE90-000833] N90-14923
Microwave Tokamak Experiment: An overview of the construction and checkout phase
[DE90-000834] N90-14924
PLASMA DRIFT
Ion collection by probing objects in flowing magnetized plasmas
[DE90-001711] N90-14916
PLASMA ENGINES
Energy deposition in low power coaxial plasma thrusters N90-14911
PLASMA EQUILIBRIUM
Stability of the Global Alfven Eigenmode in the presence of fusion alpha particles in an ignited tokamak plasma
[DE89-016618] N90-14930
PLASMA GENERATORS
Activities report in laser matter interactions
[ETN-90-95515] N90-14544
PLASMA HEATING
Electron heating and static sheath enhancement in front of energized RF antennas
[DE90-001334] N90-14456
PLASMA JETS
Microwave Tokamak Experiment (MTX) first year of operation and future plans
[DE90-000817] N90-14920
PLASMA OSCILLATIONS
High-frequency instability of the sheath-plasma resonance
[NASA-CR-186127] N90-14910
PLASMA PHYSICS
Fundamental studies of fusion plasmas
[DE90-002343] N90-14933
Particle simulations in magnetospheric plasmas
[NASA-CR-186238] N90-14934
PLASMA POTENTIALS
Electron heating and static sheath enhancement in front of energized RF antennas
[DE90-001334] N90-14456
PLASMA RADIATION
Study of lithium-like ions for amplifying radiation below 100 angstroms. Experiment at the Rutherford Appleton Laboratory N90-14572
PLASMA RESONANCE
Box experiments. Nonlinear effects at plasma resonance N90-14555
Simulated Brillouin backscattering in optical fibers: A ring resonator N90-14556
High-frequency instability of the sheath-plasma resonance
[NASA-CR-186127] N90-14910
PLASMA SHEATHS
High-frequency instability of the sheath-plasma resonance
[NASA-CR-186127] N90-14910
PLASMA SPECTRA
Transversal inhomogeneity and radiative transfer in plasmas obtained by laser impact N90-14568
PLASMA TURBULENCE
Strong Langmuir turbulence and second harmonics in laser-matter interactions N90-14548
PLASMA WAVES
The supersonic anisotropic collapse of Langmuir waves N90-14550
Limitations in the growing of a plasma wave produced by heterodyning two lasers due to modulations and decay instabilities N90-14552
Use of plasmas for the acceleration of particles to very high energy N90-14553
Box experiments. Nonlinear effects at plasma resonance N90-14555
Toroidal rotation retardation and ion anomalous transport by drift waves in a tokamak
[DE89 934427] N90-14913
Particle simulations in magnetospheric plasmas
[NASA-CR-186238] N90-14934
PLASMAS (PHYSICS)
Energy deposition in low power coaxial plasma thrusters N90-14911
Two-dimensional behavior of Megagauss-field-confined solid fiber Z-pinches
[DE90-000684] N90-14918
Fundamental studies of fusion plasmas
[DE90-002343] N90-14933
PLASTIC DEFORMATION
Approximate methods for dynamic plastic deformation of structures
[DE90-002214] N90-14660
PLASTIC PROPERTIES
A generalized thermomechanical constitutive model for metal matrix composites with plastic strain and damage N90-14293
Superplasticity
[AGARD-LS-168] N90-14325
A theoretical investigation of the column behavior of cold-formed square hollow sections
[PB89-225981] N90-14645
PLATE THEORY
Analysis of metal matrix composite structures using a microchemical constitutive theory N90-14290
PLUMES
Convective boundary layer and modeling of dispersion N90-14731
PLUTONIUM
Multiple martensitic transformations, incommensurate/commensurate phases, and charge-density-wave states in plutonium metal: Their consequences
[DE90-001235] N90-14350
PLUTONIUM OXIDES
Draft Environmental Impact Statement for the Ulysses Mission (Tier 2)
[NASA-TM-102903] N90-14727
PNEUMATIC EQUIPMENT
Flight evaluation of a pneumatic system for unsteady pressure measurements using conventional sensors
[NASA-TM-4131] N90-14225
PNEUMATICS
Pipe and bend erosion by pneumatic transport of solids at high temperature
[DE89-015741] N90-14524
POLARIZATION (CHARGE SEPARATION)
Polarization of Li/SOCl2 cells
[DE90-000883] N90-14680
POLARIZATION (SPIN ALIGNMENT)
Factors affecting electron spin polarization in photosynthetic systems
[DE90-000196] N90-14764
POLARIZATION (WAVES)
Anisotropy of electron distributions related to the anisotropy and polarization of the continuous emitted x rays N90-14566
Chaotic behavior in nonlinear polarization dynamics
[DE89-013453] N90-14589
POLICIES
Metric handbook for Federal officials: Recommendations of the Interagency Committee on Metric Policy
[PB89-226922] N90-14400
A dynamic systems engineering methodology research study. Phase 2: Evaluating methodologies, tools, and techniques for applicability to NASA's systems projects
[NASA-CR-181319] N90-14985
DOD (Department of Defense) Freedom of Information Act Program (incorporating changes 1 and 2)
[PB90-104753] N90-14993
POLLUTION CONTROL
Consumer Ozone Protection Act of 1989
[S-HRG-101-377] N90-14708
POLLUTION MONITORING
Nitrogen deposition to forest trees
[DE90-003285] N90-14726
POLLUTION TRANSPORT
Meteorological monitoring for environmental/dose assessment and emergency response modeling: How much is enough
[DE90-002726] N90-14757
POLYACRYLONITRILE
Method for stabilization of pan-based carbon fibers
[AD-D014228] N90-14288
POLYIMIDES
The 3F condensation polyimides: Review and update
[NASA-TM-102353] N90-14363
POLYMER BLENDS
Mechanical properties and morphology of oriented polymer blends N90-14361
POLYMER CHEMISTRY
The 3F condensation polyimides: Review and update
[NASA-TM-102353] N90-14363
Synthesis and properties of new preceramic materials
[DE90-002562] N90-14373
POLYMERIC FILMS
The 3F condensation polyimides: Review and update
[NASA-TM-102353] N90-14363
Heat and mass transfer design issues in PEM fuel cell hardware
[DE89-016779] N90-14677
POLYMERIZATION
Method for stabilization of pan-based carbon fibers
[AD-D014228] N90-14288
The 3F condensation polyimides: Review and update
[NASA-TM-102353] N90-14363
Challenges in processing for polymer composites
[DE90-002224] N90-14376
POLYMERS
The structure and properties of liquid crystal polymers N90-14356
POLYNOMIALS
On some integral relations involving a generalized hypergeometric polynomial
[DE90-600729] N90-14852
POLYPEPTIDES
Comparison of structural subunits of the core light-harvesting complexes of photosynthetic bacteria
[DE90-001412] N90-14765
PONDS
Environmental Projects. Volume 8: Modifications of wastewater evaporation ponds
[NASA-CR-186099] N90-14700
POPULATION INVERSION
Activities report in laser matter interactions
[ETN-90-95515] N90-14544
Population inversions calculated for lithium-like ions in a plasma N90-14571
POPULATIONS
Summary of 1987 and 1988 manatee aerial surveys at Kennedy Space Center
[NASA-TM-102783] N90-14669
POROUS MATERIALS
Fracture mechanics of porous materials
[DE90-000023] N90-14657

On the thermal stability of flow of a radiating two-component plasma in a porous medium between two rotating cylinders
[DE89-636426] N90-14926

POSITION (LOCATION)
Decision-aid design factors in connection with HF communication and emitter location disciplines N90-14413
Adaptive clutter rejection filters for airborne Doppler weather radar applied to the detection of low altitude windshear
[NASA-CR-186211] N90-14453
Robotic vision system
[AD-D014246] N90-14838

POSITION SENSING
Techniques for extreme attitude suspension of a wind tunnel model in a magnetic suspension and balance system
[NASA-CR-181895] N90-14245

POSITIONING
Correction of ionospheric effects for the precise orbit determination of satellites N90-14432

POSITIONING DEVICES (MACHINERY)
New tool-holding concept
[DE90-000880] N90-14624

POSITIVE IONS
Structural peculiarities and molecular properties of charge complexes formed on positive ion injection into dense inert gas media
[DE89-633953] N90-14877

POSITRON ANNIHILATION
The AMY Experiment
[DE90-001153] N90-14880

POSITRONS
Interaction of low-energy electrons and positrons with condensed matter: Stopping powers and inelastic mean free paths from optical data
[DE90-001001] N90-14882

POTASSIUM COMPOUNDS
Investigation of the phase stabilizing effect of potassium fluoride on ammonium nitrate
[AD-A213042] N90-14381

POTENTIAL ENERGY
Elastomeric impulse energy storage and transfer system
[AD-D014223] N90-14255

POTENTIAL FLOW
Program VSAERO theory document: A computer program for calculating nonlinear aerodynamic characteristics of arbitrary configurations
[NASA-CR-4023] N90-14200

POWDER (PARTICLES)
Shock-induced solid state reactions and phase transitions: X ray profile studies on shock-modified Fe3O4 and ZrO2 powders
[DE90-000669] N90-14315
Superconducting and microstructural properties of shock-compacted high-T sub c oxide powders
[DE90-000823] N90-14958
Powder neutron diffraction study of the structural phase diagram of the Ba(sub 1-x)K(sub x)BiO3 system
[DE90-002264] N90-14967

POWDER METALLURGY
Dynamic sintering of metallic powders by laser shock N90-14559
Micro-scale simulation of dynamic compaction of oxide and metal powder mixture
[DE90-002220] N90-14978

POWER AMPLIFIERS
Proof-of-principle experiment for a hot electron pumped XUV amplifier
[DE90-000820] N90-14586

POWER FACTOR CONTROLLERS
Power factor controller study
[DE89-017655] N90-14458

POWER SPECTRA
Power spectral estimation algorithms
[NASA-CR-186189] N90-14812
A two dimensional power spectral estimate for some nonstationary processes
[NASA-CR-186100] N90-14843

PRASEODYMIUM
Muon SR investigation of magnetism and superconductivity in (Y(1-x)Pr(x))Ba2Cu3O7
[DE90-000689] N90-14956

PRECIPITATES
Effects of precipitate distribution on 293 K and 77 K properties of 2090-T81 weldments
[DE90-002332] N90-14349

PRECIPITATION (METEOROLOGY)
Climate system research studies of global and regional instrumental data
[DE90-001205] N90-14707

PRECIPITATION HARDENING
Effects of composition and age hardening on precious metal electrical contacts
[DE88-008791] N90-14476

PRECIPITATION PARTICLE MEASUREMENT
Comparison of two droplet sizing systems in an icing wind tunnel
[NASA-TM-102456] N90-14617

PREDICTION ANALYSIS TECHNIQUES
Orthobaric densities and molar volumes of liquids. Introduction to data items issued after July 1989
[ESDU-89018] N90-14298
Propagation-based decision aids in the U.S. Navy N90-14410
Engineer's Refractive Effects Prediction System (EREPS) N90-14411
The FTZ HF propagation model for use on small computers and its accuracy N90-14447

PREDICTIONS
Orthobaric densities and molar volumes of liquids. Aromatic hydrocarbons
[ESDU-89019] N90-14299
Predictive aging of elastomers in air: The importance of understanding diffusion-limited oxidation effects
[DE90-001385] N90-14372
The parabolic equation approach to predicting tropospheric propagation effects in operational environments N90-14418
Assessment of anomalous propagation predictions using minisonde refractivity data and the parabolic equation method N90-14424
Boundary element analysis of single and multidomain problems in acoustics N90-14867
Gamma ray lines from dark matter annihilation
[DE90-000779] N90-15021

PREDICTOR-CORRECTOR METHODS
Block predictor (low order) corrector methods to solve ordinary differential equations on parallel computers
[IMAG-RR-757-M] N90-14845

PREFORMS
Computer synthesis of ceramic preforms for molten-metal infiltration
[DE90-000826] N90-14370

PREMIXED FLAMES
Kinetics and mechanism of soot formation in hydrocarbon combustion
[NASA-CR-186162] N90-14305

PREPARATION
Electrochemical preparation of silver oxide electrodes having high thermal stability
[AD-D014224] N90-14460

PREPREGS
A capacitive technique for real-time monitoring polymer coating thickness on carbon filaments during prepregging process
[NASA-TM-101682] N90-14533

PREPROCESSING
PCP (Parallel C Preprocessor): A parallel extension of C that is 99 percent fat free
[DE90-002813] N90-14834

PRESSURE
Pressure sensitive release device
[AD-D014220] N90-14610

PRESSURE EFFECTS
Projectile impact Hugoniot parameters for selected materials
[DE90-000891] N90-14618

PRESSURE MEASUREMENT
Flight evaluation of a pneumatic system for unsteady pressure measurements using conventional sensors
[NASA-TM-4131] N90-14225
Laser velocimeter and total pressure measurements in circular-to-rectangular transition ducts
[NASA-CR-182286] N90-14494

PRESSURE SENSORS
Flight evaluation of a pneumatic system for unsteady pressure measurements using conventional sensors
[NASA-TM-4131] N90-14225

PRESSURE SUITS
Integrated G-suit/immersion suit
[AD-A212989] N90-14774

PRESSURE VESSELS
Measuring the thickness of austenitic weld deposits on carbon steel walls using a magnetic method
[DE89-635446] N90-14628

PRINTED CIRCUITS
Vehicle antenna for the mobile satellite experiment
[NASA-CR-186109] N90-14271

PRINTERS (DATA PROCESSING)
SAS graphics in DCF
[PNR90563] N90-14399

PROBABILITY DENSITY FUNCTIONS
Probability density function of optical scintillations (scintillation distribution)
[PB89-103912] N90-14906

PROBABILITY THEORY
Failure probability estimate of Type 304 stainless steel piping
[DE90-000659] N90-14635

PROBLEM SOLVING
Introduction to data items on flight path optimisation
[ESDU-89015] N90-14221
Human factors aspects of decision support systems N90-14408
Numerical methodologies for solving partial differential equations
[DE90-001842] N90-14849

PROCESS CONTROL (INDUSTRY)
Automated glass fiber drawing
[DE90-000894] N90-14367
Ion beam analysis and modification of thin-film, high-temperature superconductors
[DE90-000918] N90-14941
The effect of composition and processing on high T(sub c) superconductors containing bismuth
[DE90-002203] N90-14965

PRODUCTION ENGINEERING
Challenges in processing for polymer composites
[DE90-002224] N90-14376

PROGRAM VERIFICATION (COMPUTERS)
Validation of a computer code for analysis of subsonic aerodynamic performance of wings with flaps in combination with a canard or horizontal tail and an application to optimization
[NASA-TP-2961] N90-14187
Development of a three-axis trim program
[AD-A212883] N90-14237
Verification of the NIKE3D structural analysis code by comparison against the analytic solution for a spherical cavity under a far-field uniaxial stress
[DE90-000929] N90-14653
QUEST/Ada: Query utility environment for software testing of Ada
[NASA-CR-186121] N90-14787
Initial Ada components evaluation N90-14803

PROGRAMMING LANGUAGES
Research in mathematics and computer science at Argonne, July 1, 1986 to January 6, 1988
[DE88-010343] N90-14781
Continuation of research in software for space operations support
[NASA-CR-186092] N90-14808
Using object-oriented development to support prototyping
[DE90-000547] N90-14821
Strand: A practical parallel programming language
[DE90-002861] N90-14825

PROJECT MANAGEMENT
Sandia Satellite Program summary of operational procedures
[DE90-000892] N90-14249
Space station attached payload program support
[NASA-CR-183838] N90-14274
Exploring the living universe: A strategy for space life sciences
[NASA-TM-101891] N90-14778
A dynamic systems engineering methodology research study. Phase 2: Evaluating methodologies, tools, and techniques for applicability to NASA's systems projects
[NASA-CR-181319] N90-14985
Developing integrated parametric planning models for budgeting and managing complex projects
[NASA-CR-186006] N90-14986

PROJECT PLANNING
Developing integrated parametric planning models for budgeting and managing complex projects
[NASA-CR-186006] N90-14986

PROJECTILES
Solving the blow-by problem in a two-stage gun
[DE90-000842] N90-14246
Acceleration of small, light projectiles (including hydrogen isotopes) to high speeds using a two-stage light gas gun
[DE90-002479] N90-14253
Performance characteristics of a three-stage railgun
[DE90-002533] N90-14254
Elastomeric impulse energy storage and transfer system
[AD-D014223] N90-14255
An electroformed nickel-sulfur alloy for a nose cone
[DE90-000866] N90-14337
Electric-gun studies of conductors in high magnetic fields and experiments in dynamic flux compression
[DE90-000815] N90-14470
Projectile impact Hugoniot parameters for selected materials
[DE90-000891] N90-14618

PROPAGATION MODES
Wide-angle propagation in inhomogeneous fluids and elastic solids using perturbation methods N90-14868

PROPAGATION VELOCITY
A numerical study of thin flame representations
[DE89-017889] N90-14313
PROPELLANT BINDERS
A surface coupled flamelet approach to dynamic response in heterogeneous propellant combustion
N90-14302
PROPELLANT COMBUSTION
A surface coupled flamelet approach to dynamic response in heterogeneous propellant combustion
N90-14302
PROPELLANT STORAGE
Atomic hydrogen as a launch vehicle propellant
[NASA-TM-102459] N90-14284
Investigation of the phase stabilizing effect of potassium fluoride on ammonium nitrate
[AD-A213042] N90-14381
PROPELLANTS
Stick propellant x ray inspection
[AD-A212601] N90-14380
PROPELLER FANS
Concurrent processing adaptation of aeroplastic analysis of propfans
[NASA-TM-102455] N90-14656
PROPELLER NOISE
Evaluation of analysis techniques for low frequency interior noise and vibration of commercial aircraft
[NASA-CR-181851] N90-14866
PROPORTIONAL COUNTERS
The softest Einstein AGN (Active Galactic Nuclei)
[DE89-009389] N90-15020
PROPULSION
AGARD Highlights 89/2 N90-14184
CIS-lunar space infrastructure lunar technologies: Executive summary
[NASA-CR-186220] N90-15029
PROPULSION SYSTEM CONFIGURATIONS
Main propulsion system test requirements for the two-engine Shuttle-C
[NASA-TM-100382] N90-14282
PROPULSION SYSTEM PERFORMANCE
Main propulsion system test requirements for the two-engine Shuttle-C
[NASA-TM-100382] N90-14282
PROPULSIVE EFFICIENCY
Energy deposition in low power coaxial plasma thrusters N90-14911
PROTECTION
Flight set 360T004 (STS-30) field joint protection system, volume 7
[NASA-CR-183829] N90-14280
Means for protecting electroexplosive devices which are subject to a wide variety of radio frequency
[AD-D014219] N90-14382
Performance evaluation of the Puritan-Bennett crew-member portable protective breathing device as prescribed by portions of FAA action notice A-8150.2
[AD-A211113] N90-14772
PROTECTIVE CLOTHING
Integrated G-suit/immersion suit
[AD-A212989] N90-14774
PROTEINS
Combined capillary electrophoresis and electrospray ionization mass spectrometry
[DE90-001903] N90-14322
PROTOCOL (COMPUTERS)
The characteristics of the HF radio channel and its influence on modern HF data communication system design N90-14448
The Delta-t transport protocol: Features and experience useful for high performance networks
[DE89-016542] N90-14832
Multiple crossbar network: A switched high-speed local network
[DE90-001839] N90-14833
PROTON BEAMS
Direction-dependent stopping power and beam deflection in anisotropic solids
[DE90-001076] N90-14883
PROTONS
Narrow one-channel resonances and their manifestation in the pure elastic scattering of unpolarized particles
[DE89-632177] N90-14876
PROTOTYPES
Manipulation strategies for massive space payloads
[NASA-CR-186081] N90-14247
Integrated G-suit/immersion suit
[AD-A212989] N90-14774
QUEST/Ada: Query utility environment for software testing of Ada
[NASA-CR-186121] N90-14787
Using object-oriented development to support prototyping
[DE90-000547] N90-14821
PSEUDOPOTENTIALS
First-principles interatomic potentials in transition metals: Multi-ion interactions and their analytic representation
[DE90-001990] N90-14353
PULSARS
Supernovae, compact stars, and nuclear physics
[DE90-002682] N90-15022
PULSE AMPLITUDE MODULATION
Means for protecting electroexplosive devices which are subject to a wide variety of radio frequency
[AD-D014219] N90-14382
PULSE COMMUNICATION
Mitigating Doppler shift effect in HF multitone data modem N90-14441
PULSE GENERATORS
A software-based controller for generation of synchronized pulses for use with rotating machinery
[DE89-016672] N90-14477
Laser activities N90-14576
Performance of the 10-kV, 100-kA pulsed-power modules for the FRX-C magnetic compression experiment
[DE89-014027] N90-14917
PULSED LASERS
Experimental study of the shock waves generated by high energy laser pulses N90-14557
Development of X diagnostics with 1 Gw laser pulses N90-14578
Development of X diagnostics around the pulse 1 laser N90-14580
Ultrahigh-brightness lasers and their applications
[DE90-000877] N90-14596
Nonresonant and resonant multiphoton ionization of (NO)(sub n) and Ar(sub n)NO clusters with picosecond laser pulses
[DE89-016853] N90-14607
PULSES
Martensite transformation in NiTi alloys induced by tensile stress pulses
[DE90-001832] N90-14346
Frequency agile synthetic aperture radar
[AD-D014235] N90-14451
NIKHEF-K contributions to the 1989 Particle Accelerator Conference
[NIKHEF/AMPS/89/03] N90-14891
The Amsterdam pulse stretcher project (AmPS) N90-14892
Optics of the Amsterdam pulse stretcher (AmPS) N90-14893
Modification of MEA modulator-klystron units enabling short pulse injection into a pulse-stretcher ring N90-14894
An Energy Spectrum Compressor system (ESC) for the Amsterdam pulse stretcher (AmPS) N90-14896
PUMPS
Eurolaser CO2 laser
[ETN-90-95907] N90-14582
PYLONS
Effect of pylon wake with and without pylon blowing on propeller thrust
[NASA-TM-4162] N90-14190
PYROLYSIS
The conversion of carbonaceous materials to clean carbon and co-product gaseous fuel
[DE90-001561] N90-14387
PYROTECHNICS
Development of a titanium/boron blending process
[DE90-001450] N90-14386

Q

QUADRATURES
Mitigating Doppler shift effect in HF multitone data modem N90-14441
QUALIFICATIONS
Qualification of diode foil materials for excimer lasers
[DE90-000602] N90-14593
QUALITY CONTROL
Review of the Aerospace Safety Advisory Panel report for NASA fiscal year 1990 authorization
[GPO-24-234] N90-14213
Electrothermal response testing more than a quality assurance tool
[DE90-001449] N90-14536
Quality assurance and quality control for the Compact Physics Research Facility (CPRF) and ZTH experiment
[DE90-002352] N90-14636
QUANTUM ELECTRONICS
Multiband photoconductive detector based on layered semiconductor quantum wells
[AD-D014232] N90-14936
QUANTUM MECHANICS
Nonlinear quantum effects in the Maser model: A large N scaling behaviour
[DE89-631631] N90-14584
QUANTUM WELLS
Multiband photoconductive detector based on layered semiconductor quantum wells
[AD-D014232] N90-14936
QUASARS
VLA and VLBI observations of core dominated quasars N90-15002
The softest Einstein AGN (Active Galactic Nuclei)
[DE89-009389] N90-15020

R

RADAR
A radar simulation program for a 1024-processor hypercube
[DE89-014494] N90-14455
High resolution, wide band Chirp-Z signal analyzer
[AD-D014240] N90-14465
RADAR DETECTION
Adaptive clutter rejection filters for airborne Doppler weather radar applied to the detection of low altitude windshear
[NASA-CR-186211] N90-14453
RADAR ECHOES
Propagation-based decision aids in the U.S. Navy N90-14410
RADAR IMAGERY
Analysis of propagation in an inhomogeneous atmosphere in the horizontal and vertical direction using the parabolic equation method N90-14421
RADAR MEASUREMENT
The effects of clutter-rejection filtering on estimating weather spectrum parameters
[NASA-CR-186212] N90-14754
RADAR RANGE
Low level range coverage performance prediction for VHF radar N90-14439
RADAR TRANSMITTERS
Frequency agile synthetic aperture radar
[AD-D014235] N90-14451
RADIAL VELOCITY
Kilometric type III radio bursts and interplanetary transients N90-15038
RADIANCE
Synoptic scale tropical waves in multichannel satellite radiance data N90-14745
RADIATION ABSORPTION
Atlas of albedo and absorbed solar radiation derived from Nimbus 6 earth radiation budget data set, July 1975 to May 1978
[NASA-RP-1230] N90-14741
RADIATION BELTS
JPRS Report: Science and technology. USSR: Space. Soviet space program to the year 2000
[JPRS-USP-89-008] N90-14248
RADIATION COUNTERS
Superconducting magnets in space
[DE90-002671] N90-14865
RADIATION DAMAGE
Radiation damage and its influence on source requirements for high resolution x ray holography
[DE90-002508] N90-14540
RADIATION DETECTORS
A fiber-fed imaging spectrometer
[DE90-001008] N90-14538
RADIATION DOSAGE
Radiation damage and its influence on source requirements for high resolution x ray holography
[DE90-002508] N90-14540
RADIATION EFFECTS
Operational Decision Aids for Exploiting or Mitigating Electromagnetic Propagation Effects
[AGARD-CP-453] N90-14405
The effects of heavy particle radiation on semiconductor devices
[DE90-001679] N90-14962
RADIATION HAZARDS
Draft Environmental Impact Statement for the Ulysses Mission (Tier 2)
[NASA-TM-102903] N90-14727
RADIATION MEASURING INSTRUMENTS
Beyond the IDMY (International Daylighting Measurements Year): A network instrument for low-cost data acquisition
[DE90-002722] N90-14740
RADIATION SHIELDING
Starlight: A stationary inertial-confinement-fusion reactor with nonvaporizing walls
[DE90-002315] N90-14927

RADIATIVE HEAT TRANSFER
On the thermal stability of flow of a radiating two-component plasma in a porous medium between two rotating cylinders
[DE89-636426] N90-14928
RADIATIVE TRANSFER
Activities report in laser matter interactions
[ETN-90-95515] N90-14544
Atomic structure and spectral perturbations in hot dense plasmas N90-14567
Transversal inhomogeneity and radiative transfer in plasmas obtained by laser impact N90-14568
XRAD: A one dimensional Lagrangian code with radiative transport N90-14570
RADICALS
Pentafluorothio polynitroaliphatic explosives
[AD-D014221] N90-14383
Hydrogen radical enhanced growth of solar cells
[DE89-009497] N90-14694
RADIO ANTENNAS
Electron heating and static sheath enhancement in front of energized RF antennas
[DE90-001334] N90-14456
RADIO ASTRONOMY
Laboratory evaluation and application of microwave absorption properties under simulated conditions for planetary atmospheres
[NASA-CR-185916] N90-15025
RADIO COMMUNICATION
PROPHET and future signal warfare decision aids N90-14412
A communications system with an adaptive multi-functional architecture N90-14415
RADIO FREQUENCIES
Means for protecting electroexplosive devices which are subject to a wide variety of radio frequency
[AD-D014219] N90-14382
The characteristics of the HF radio channel and its influence on modern HF data communication system design N90-14448
High-frequency instability of the sheath-plasma resonance
[NASA-CR-186127] N90-14910
Fundamental studies of fusion plasmas
[DE90-002343] N90-14933
RF superconductivity research and development at Los Alamos National Laboratory
[DE90-002440] N90-14969
RADIO GALAXIES
Radio and optical observations of nearby active galaxies N90-15000
MERLIN and VLBI observations of the radio galaxy Virgo A N90-15001
RADIO INTERFEROMETERS
MERLIN and VLBI observations of the radio galaxy Virgo A N90-15001
RADIO OBSERVATION
Radio and optical observations of nearby active galaxies N90-15000
Very high resolution radio observations of molecular cloud cores N90-15013
RADIO OCCULTATION
Laboratory evaluation and application of microwave absorption properties under simulated conditions for planetary atmospheres
[NASA-CR-185916] N90-15025
RADIO RELAY SYSTEMS
Modelling UHF propagation for frequency assignment in radio relay networks N90-14445
RADIO SIGNALS
A modern trans-ionospheric propagation sensing system N90-14430
RADIO TRANSMISSION
Long wave propagation assessment N90-14414
RPE: A parabolic equation radio assessment model N90-14419
New perspectives for the inversion of backscatter ionograms N90-14427
RADIO WAVES
The importance of environmental data N90-14406
RADIOACTIVE CONTAMINANTS
Draft Environmental Impact Statement for the Ulysses Mission (Tier 2)
[NASA-TM-102903] N90-14727
RADIOACTIVE DECAY
Mapping of upper electronic reaction surfaces by tuned laser photolysis and by absorption and emission spectroscopies
[DE90-000125] N90-14314
RADIOISOTOPE BATTERIES
Draft Environmental Impact Statement for the Ulysses Mission (Tier 2)
[NASA-TM-102903] N90-14727
RADIOMETERS
Remote sensing of atmospheric water vapour by pressure modulation radiometry N90-14687
RAILGUN ACCELERATORS
Performance characteristics of a three-stage railgun
[DE90-002533] N90-14254
RAIN
Rainfall estimation over Africa using satellite data N90-14742
Frequency distributions of heavy rainstorms in Illinois
[PB90-100215] N90-14748
Use of operational 0-6 and 3-9 h quantitative precipitation forecasts for predicting heavy rain events
[PB90-103946] N90-14750
RAINDROPS
The effect of oblate spheroidal drops on rain attenuation at 94 GHz: Comparison between theory and experiment N90-14440
RAINSTORMS
Frequency distributions of heavy rainstorms in Illinois
[PB90-100215] N90-14748
RAMAN SPECTROSCOPY
Laser Raman spectroscopy in studies of corrosion and electrocatalysis
[DE90-001414] N90-14311
RAMJET ENGINES
Acoustic-vortical-combustion interaction in a solid fuel ramjet simulator N90-14234
Investigation of combustion instability in ramjet combustors N90-14303
RANDOM PROCESSES
Algorithmic randomness, physical entropy, measurements, and the second law
[DE90-002413] N90-14823
RANGEFINDING
A modern trans-ionospheric propagation sensing system N90-14430
Programmable near-infrared ranging system
[AD-D014237] N90-14903
RANKINE-HUGONIOT RELATION
Projectile impact Hugoniot parameters for selected materials
[DE90-000891] N90-14618
RAPID TRANSIT SYSTEMS
California air transportation study: A transportation system for the California Corridor of the year 2010
[NASA-CR-186219] N90-14212
Markets for high-speed intercity Maglev technology: A systems analysis approach
[DE89-017683] N90-14623
RARE EARTH ALLOYS
High power transducers
[AD-D014225] N90-14461
RARE GASES
Structural peculiarities and molecular properties of charge complexes formed on positive ion injection into dense inert gas media
[DE89-633953] N90-14877
REACTION BONDING
Oxidation effects on the mechanical properties of SiC fiber-reinforced reaction-bonded silicon nitride matrix composites
[NASA-TM-102360] N90-14287
REACTION KINETICS
Numerical modeling of supersonic turbulent reacting free shear layers N90-14197
The thermally induced gas-phase reactions of methane and oxygen: A comparison of experimental and computational results
[DE90-000785] N90-14317
Reactive flow measurements and calculations for ZrH2-based composite explosives
[DE90-000831] N90-14393
Fast transit gas- and condensed-phase chemistry of energetic materials
[DE90-001656] N90-14395
REACTIVITY
Chemistry of large molecules
[DE90-000813] N90-14366
Particle size effects in the initiation of explosives containing reactive and nonreactive continuous phases
[DE90-000786] N90-14390
Reactive flow measurements and calculations for ZrH2-based composite explosives
[DE90-000831] N90-14393
A measurement of hydroxyl in the daytime mesosphere N90-14732
REACTOR DESIGN
Introductory testimony: Hearing on nuclear power in space
[DE90-001137] N90-14897
Starlight: A stationary inertial-confinement-fusion reactor with nonvaporizing walls
[DE90-002315] N90-14927
REACTOR SAFETY
Course A: Numerical modeling of two-phase flows for presentation at Ecole d'Ete d'Analyse Numerique
[DE90-002074] N90-14526
Results of the manipulator test test stand study: Comparison of manipulators and evaluation of equipment items
[DE90-000977] N90-14625
Critical time step estimation for three-dimensional explicit impact analysis
[DE90-002187] N90-14662
REACTOR TECHNOLOGY
Human factors survey of advanced instrumentation and controls
[DE90-002477] N90-14776
Starlight: A stationary inertial-confinement-fusion reactor with nonvaporizing walls
[DE90-002315] N90-14927
Fundamental studies of fusion plasmas
[DE90-002343] N90-14933
READOUT
Spectral contents readout of birefringent sensor
[NASA-CR-179444] N90-14905
REAL GASES
Efficient real gas Navier-Stokes computations of high speed flows using an LU scheme
[NASA-TM-102429] N90-14203
REAL TIME OPERATION
The biocorrosion of copper by biopolymers as examined in situ, in real time FT-IR/CIR/ATR in conjunction with pre and post XPS/AES
[DE90-002086] N90-14348
Propagation assessment and tactical decision aids N90-14407
PROPHET and future signal warfare decision aids N90-14412
A communications system with an adaptive multi-functional architecture N90-14415
Assessment of anomalous propagation predictions using minisonde refractivity data and the parabolic equation method N90-14424
New perspectives for the inversion of backscatter ionograms N90-14427
A modern trans-ionospheric propagation sensing system N90-14430
A portable ionosonde in support of reliable communications N90-14431
The use of broadcast signals for passive sensing in automated HF communication systems N90-14433
An image compression algorithm for a high-resolution digital still camera
[NASA-CR-185079] N90-14532
Application of reusable software components at the SEI N90-14804
Continuation of research in software for space operations support
[NASA-CR-186092] N90-14808
Robotic vision system
[AD-D014246] N90-14838
Realtime tracking system for wide-field-of-view telescope
[DE90-001147] N90-14908
Development of a real time monitor for superconductive thin film preparation
[DE89-017772] N90-14952
RECEIVERS
A heat receiver design for solar dynamic space power systems
[NASA-TM-102473] N90-14283
RECOIL PROTONS
A study of recoil protons in ultra-relativistic nucleus-nucleus collisions
[LUIP-8907] N90-14873
RECOMBINATION REACTIONS
Calorimetric measurements on electrochemical cells with Pd-D cathodes
[DE90-002198] N90-14685
RECONSTRUCTION
Fatigue analysis and reconstruction of helicopter load spectra N90-14304
RECOVERY VEHICLES
Preliminary design of the Shuttle-C avionics recovery system
[NASA-CR-186230] N90-14258
RECTANGULAR PLANFORMS
Effect of blade planform variation on a small-scale hovering rotor
[NASA-TM-4146] N90-14186
RECTANGULAR PLATES
Finite element analysis of laminated composite plates N90-14291
REDUCED GRAVITY
Partial gravity habitat study: With application to lunar base design
[NASA-CR-186048] N90-14267
Materials processing in low gravity
[NASA-CR-183733] N90-14397
Thermocapillary migration of liquid droplets in a temperature gradient in a density matched system
[NASA-CR-185178] N90-14512

Engineering sciences design. Design and implementation of components for a bioregenerative system for growing higher order plants in space [NASA-CR-186056] N90-14761
REDUCTION (CHEMISTRY)
Pentafluorothio polynitroaliphatic explosives [AD-D014221] N90-14383
REENTRY VEHICLES
Preliminary design of the Shuttle-C avionics recovery system [NASA-CR-186230] N90-14258
REFLECTANCE
Frequency agile synthetic aperture radar [AD-D014235] N90-14451
X ray reflectivity study of SiO2 on Si [DE90-001326] N90-14943
REFLECT: A computer program for the x ray reflectivity of bent perfect crystals [DE90-001266] N90-14946
REFLECTED WAVES
Corrections for non-ideal effects in reflected shock waves at low Mach numbers [DE90-002192] N90-14208
REFRACTIVITY
Engineer's Refractive Effects Prediction System (EREPS) N90-14411
Analysis of propagation in an inhomogeneous atmosphere in the horizontal and vertical direction using the parabolic equation method N90-14421
Propagation modeling for some horizontally varying tropospheric ducts N90-14422
Assessment of anomalous propagation predictions using minisonde refractivity data and the parabolic equation method N90-14424
A one-dimensional shipboard model for forecasting refractive effects in the planetary boundary layer N90-14442
REFRACTORY MATERIALS
High-temperature corrosion of heat exchanger materials [DE90-001963] N90-14352
REFRACTORY METALS
Spall strength measurements on shockloaded refractory metals [DE90-000839] N90-14345
REFRIGERATORS
Thermal design of a 10-kW helium refrigerator [DE90-701785] N90-14403
REGENERATION (ENGINEERING)
New heating and cooling technology: Regenerative heat pump according to the Vuilleumier principle [DE90-002701] N90-14699
REGULATIONS
Consumer Ozone Protection Act of 1989 [S-HRG-101-377] N90-14708
REINFORCING FIBERS
Method for stabilization of pan-based carbon fibers [AD-D014228] N90-14286
REINFORCING MATERIALS
Carbon fiber reinforced metal matrix composites [AD-D014245] N90-14289
RELATIVISTIC EFFECTS
String models for ultrarelativistic heavy ion collisions: Lund model versus color exchange models [DE88-015856] N90-14881
RELATIVITY
Black-hole decay and topological stability in quantum gravity [DE89-616785] N90-15017
Classical approach to higher-derivative gravity [DE89-631649] N90-15019
RELAXATION METHOD (MATHEMATICS)
Group-kinetic theory and modeling of atmospheric turbulence [NASA-CR-183776] N90-14728
RELEASING
Pressure sensitive release device [AD-D014220] N90-14610
RELIABILITY
AGARD Highlights 89/2 N90-14184
Review of the Aerospace Safety Advisory Panel report for NASA fiscal year 1990 authorization [GPO-24-234] N90-14213
RELIABILITY ENGINEERING
A tutorial on software reliability engineering [DE89-012368] N90-14828
How robust are distributed systems [NASA-CR-186242] N90-14837
REMOTE SENSING
Global stratospheric change: Requirements for a Very-High-Altitude Aircraft for Atmospheric Research [NASA-CP-10041] N90-14220
The importance of environmental data N90-14406
The use of broadcast signals for passive sensing in automated HF communication systems N90-14433
Remote sensing of the aerosol scattering coefficient with a multi-field-of view lidar N90-14437
An investigation of satellite sounding products for the remote sensing of the surface energy balance and soil moisture [NASA-CR-188073] N90-14664
Remote sensing of atmospheric water vapour by pressure modulation radiometry N90-14667
A measurement of hydroxyl in the daytime mesosphere N90-14732
REMOTE SENSORS
A rough transform technique for extracting lead features from sea ice imagery [AD-A212758] N90-14666
REQUIREMENTS
Integrated G-suit/immersion suit [AD-A212989] N90-14774
RESEARCH
Chronology of KSC and KSC related events for 1988 [NASA-TM-101915] N90-15040
RESEARCH AND DEVELOPMENT
AGARD Highlights 89/2 N90-14184
Challenges in processing for polymer composites [DE90-002224] N90-14376
Science and technology resources in US industry: Surveys of science resources series, 1975-1986 [PB90-107194] N90-14401
Eurolaser CO2 laser [ETN-90-95907] N90-14582
NORDA's pattern analysis laboratory: Current contributions to naval mapping, charting, and geodesy [AD-A212731] N90-14665
RESEARCH FACILITIES
Johnson Space Center software reuse activity N90-14796
Chronology of KSC and KSC related events for 1988 [NASA-TM-101915] N90-15040
RESIDUAL STRESS
Fatigue fracture in the presence of shot peening residual stresses: Initiation, propagation, and relaxation phenomena N90-14644
A theoretical investigation of the column behavior of cold-formed square hollow sections [PB89-225981] N90-14645
RESISTOJET ENGINES
A numerical technique for analysis of resistojet nozzle flow N90-14506
RESISTORS
Energy ratings for metal oxide varistors under repetitively pulsed operation [DE90-002353] N90-14480
RESOLUTION
Power spectral estimation algorithms [NASA-CR-186189] N90-14812
RESONANCE FLUORESCENCE
A measurement of hydroxyl in the daytime mesosphere N90-14732
RESONANCE SCATTERING
Narrow one-channel resonances and their manifestation in the pure elastic scattering of unpolarized particles [DE89-632177] N90-14876
RESOURCES MANAGEMENT
Decision-aid design factors in connection with HF communication and emitter location disciplines N90-14413
Global natural resource monitoring and assessment [DE90-001294] N90-14671
The role of order in distributed programs [NASA-CR-186252] N90-14826
RESPONSE TIME (COMPUTERS)
Multiple crossbar network: Integrated supercomputing framework [DE89-012614] N90-14831
REUSABLE SPACECRAFT
Aerospace vehicle design, spacecraft section. Volume 1: Project Groups 3 through 5 [NASA-CR-186053] N90-14263
Aerospace vehicle design, spacecraft section. Volume 2: Project Groups 6 through 8 [NASA-CR-186054] N90-14264
REVERSE FIELD PINCH
Quality assurance and quality control for the Compact Physics Research Facility (CPRF) and ZTH experiment [DE90-002352] N90-14636
Theoretical reversed field pinch studies [DE90-002114] N90-14929
REYNOLDS EQUATION
Numerical modeling of supersonic turbulent reacting free shear layers N90-14197
RISK
Review of the Aerospace Safety Advisory Panel report for NASA fiscal year 1990 authorization [GPO-24-234] N90-14213
Battery technology assessment and R and D plan [DE90-002007] N90-14489
Biological effects of hyperthermia and potential risk associated with ultrasonic exposure [PB89-100702] N90-14768
RIVERS
Summary of 1987 and 1988 manatee aerial surveys at Kennedy Space Center [NASA-TM-102783] N90-14669
ROBOT ARMS
Manipulation strategies for massive space payloads [NASA-CR-186081] N90-14247
Controller design for a robotic manipulator N90-14615
ROBOTICS
The space station tethered elevator system [NASA-CR-186051] N90-14265
Results of the manipulator test test stand study: Comparison of manipulators and evaluation of equipment items [DE90-000977] N90-14625
French technological progress in the field of robotics and teleoperation [DE90-001590] N90-14626
Robotic vision system [AD-D014246] N90-14838
Programmable near-infrared ranging system [AD-D014237] N90-14903
M.I.N.G., Mars Investment for a New Generation: Robotic construction of a permanently manned Mars base [NASA-CR-186224] N90-15028
CIS-lunar space infrastructure lunar technologies: Executive summary [NASA-CR-186220] N90-15029
ROBOTS
French technological progress in the field of robotics and teleoperation [DE90-001590] N90-14626
Non-linear vibrations, stability, and dynamics of structures and mechanisms [AD-A212152] N90-14639
Robotic vision system [AD-D014246] N90-14838
ROCKET ENGINE CASES
JPS heater and sensor lightning qualification [NASA-CR-183830] N90-14530
ROCKET ENGINES
AGARD Highlights 89/2 N90-14184
ROCKET OXIDIZERS
A surface coupled flamelet approach to dynamic response in heterogeneous propellant combustion N90-14302
ROCKET PROPELLANTS
Atomic hydrogen as a launch vehicle propellant [NASA-TM-102459] N90-14284
ROCKET-BORNE INSTRUMENTS
Rocket studies of the lower ionosphere [NASA-CR-186187] N90-14735
ROCKY MOUNTAINS (NORTH AMERICA)
Inverted surface troughs accompanying Rocky Mountain lee-side cyclogenesis N90-14746
RODS
Effects of dislocation substructure and prestrain on fracture behavior in aluminum and steel alloys N90-14334
ROLLING CONTACT LOADS
Tire modeling by finite elements N90-14614
ROTARY WINGS
An experimental investigation of the interaction between a model rotor and airframe in forward flight N90-14219
ROTATING CYLINDERS
On the thermal stability of flow of a radiating two-component plasma in a porous medium between two rotating cylinders [DE89-636426] N90-14928
ROTATING GENERATORS
A software-based controller for generation of synchronized pulses for use with rotating machinery [DE89-016672] N90-14477
ROTATING PLASMAS
Toroidal rotation retardation and ion anomalous transport by drift waves in a tokamak [DE89-634427] N90-14913
ROTATION
Expert system for fault diagnostics of rotating machines [DE89-766980] N90-14621
The dynamics of simulated convective storms in hurricane environments N90-14747
ROTOR BLADES
Effect of blade planform variation on a small-scale hovering rotor [NASA-TM-4146] N90-14186
ROTOR BLADES (TURBOMACHINERY)
An analysis of the viscous flow through a compact radial turbine by the average passage approach [NASA-TM-102471] N90-14206

ROTORS
Effect of blade planform variation on a small-scale hovering rotor
[NASA-TM-4146] N90-14186
Transient response of flexible rotor-bearing systems subjected to combined unbalance and ground excitations N90-14616
RUBY LASERS
Laser probing non-cylindrical Z-pinch in near-isolator region of a discharged chamber
[DE89-632018] N90-14912
RUDDERS
Hinge moment coefficient derivatives for trailing-edge controls on wings at subsonic speeds
[ESDU-89009] N90-14239
RUNGE-KUTTA METHOD
A one equation turbulence model for transonic airfoils N90-14199

S

S MATRIX THEORY
Narrow one-channel resonances and their manifestation in the pure elastic scattering of unpolarized particles
[DE89-632177] N90-14876
SAFETY
Battery technology assessment and R and D plan
[DE90-002007] N90-14489
Biological effects of hyperthermia and potential risk associated with ultrasonic exposure
[PB89-100702] N90-14768
SAFETY MANAGEMENT
Review of the Aerospace Safety Advisory Panel report for NASA fiscal year 1990 authorization
[GPO-24-234] N90-14213
Risk-based fire safety experiment definition for manned spacecraft
[NASA-CR-183835] N90-14262
SAMPLING
The fluid mechanics of filters N90-14499
SATELLITE IMAGERY
Image processing of LANDSAT MSS data for buried valley detection in northern Indiana N90-14668
Synoptic scale tropical waves in multichannel satellite radiance data N90-14745
SATELLITE OBSERVATION
Rainfall estimation over Africa using satellite data N90-14742
SATELLITE ORBITS
Application of heuristic satellite plan synthesis algorithms to requirements of the WARC-88 allotment plan
[NASA-TM-102479] N90-14856
SATELLITE SOUNDING
An investigation of satellite sounding products for the remote sensing of the surface energy balance and soil moisture
[NASA-CR-186073] N90-14664
Synoptic scale tropical waves in multichannel satellite radiance data N90-14745
SATELLITE TRACKING
Application of heuristic satellite plan synthesis algorithms to requirements of the WARC-88 allotment plan
[NASA-TM-102479] N90-14856
SATELLITE-BORNE INSTRUMENTS
The solar activity measurements experiments (SAMEX) for improved scientific understanding of solar activity
[NASA-TM-100372] N90-15036
SATURATION
Thermophysical properties of isopropyl alcohol. Part 1: The ideal gas and the saturated liquid and vapour
[ESDU-89017-PT-1] N90-14297
Thermophysical properties of isopropyl alcohol. Part 2: Thermodynamic properties at elevated pressures
[ESDU-89020-PT-2] N90-14300
SCALARS
On the application of subcell resolution to conservation laws with stiff source terms
[NASA-TM-102384] N90-14844
SCANNERS
Vehicle antenna for the mobile satellite experiment
[NASA-CR-186109] N90-14271
SCANNING
Programmable near-infrared ranging system
[AD-D014237] N90-14903
SCATTER PROPAGATION
Forward scatter propagation path loss testing using surrogate terrain in the 100 to 1500 MHz region N90-14425
SCATTERING
TROPO: A technique for predicting propagation and modem performance of digital troposcatter systems N90-14444
SCATTERING COEFFICIENTS
Remote sensing of the aerosol scattering coefficient with a multi-field-of view lidar N90-14437
SCHEDULES
QUEST/Ada: Query utility environment for software testing of Ada
[NASA-CR-186121] N90-14767
SCHEDULING
Payload crew utilization for spacelab missions
[NASA-TP-2976] N90-14256
SCHOTTKY DIODES
Method of sensitizing PB-Salt epitaxial films for Schottky diodes
[AD-D014244] N90-14937
SCHROEDINGER EQUATION
The supersonic anisotropic collapse of Langmuir waves N90-14550
Spectral properties of one dimensional quasi-crystals
[PREPRINT-659] N90-14938
SCIENTISTS
Science and technology resources in US industry: Surveys of science resources series, 1975-1986
[PB90-107194] N90-14401
SCINTILLATION
Probability density function of optical scintillations (scintillation distribution)
[PB89-103912] N90-14906
SCINTILLATION COUNTERS
A large detector for cosmic ray abundance and energy measurements N90-15037
SEA ICE
A rough transform technique for extracting lead features from sea ice imagery
[AD-A212758] N90-14666
SEA LAUNCHING
Kestrel 3 Program
[DE90-001796] N90-14209
Elastomeric impulse energy storage and transfer system
[AD-D014223] N90-14255
SEA SURFACE TEMPERATURE
Airborne FLIR detection of surface targets N90-14416
SEA WATER
The biocorrosion of copper by biopolymers as examined in situ, in real time FT-IR/CIR/ATR in conjunction with pre and post XPS/AES
[DE90-002086] N90-14348
SEALS (STOPPERS)
Sodium/sulfur post-test analysis at ANL
[DE90-001911] N90-14488
SEASONS
Summary of 1989 Atlantic tropical cyclone activity and seasonal forecast verification N90-14743
SEDIMENT TRANSPORT
Saltation thresholds and entrainment of fine particles at Earth and Martian pressures
[NASA-TM-102193] N90-14997
SELECTIVE DISSEMINATION OF INFORMATION
DOD (Department of Defense) Freedom of Information Act Program (incorporating changes 1 and 2)
[PB90-104753] N90-14993
SELF ALIGNMENT
Method of making self-aligned GaAs/AlGaAs FET's
[AD-D014229] N90-14935
SELF CONSISTENT FIELDS
A diagnostic for determining the quality of single-reference electron correlation methods
[NASA-TM-101929] N90-14874
SELF LUBRICATING MATERIALS
Friction and wear of glassy carbon in sliding contact, revision 1
[DE90-000743] N90-14365
SEMICONDUCTOR DEVICES
The effects of heavy particle radiation on semiconductor devices
[DE90-001679] N90-14962
SEMICONDUCTOR JUNCTIONS
Research on high-efficiency, multiple-gap, multijunction, amorphous-silicon-based alloy thin-film solar cells
[DE89-009444] N90-14673
SEMICONDUCTOR LASERS
Monolithic laser diode structure for microwave generation
[AD-D014210] N90-14543
Qualification of diode foil materials for excimer lasers
[DE90-000602] N90-14593
SEMICONDUCTORS (MATERIALS)
Electrical properties of materials for high temperature strain gage applications
[NASA-CR-186192] N90-14534
Photovoltaic Measurements and Performance Branch
[DE89-009500] N90-14695
Method of making self-aligned GaAs/AlGaAs FET's
[AD-D014229] N90-14935
Multiband photoconductive detector based on layered semiconductor quantum wells
[AD-D014232] N90-14936
Ion beam processing of advanced electronic materials
[DE89-017342] N90-14944
X ray studies of strain, interface, and impurity in semiconductors
[DE90-001525] N90-14947
SENSITIZING
Method of sensitizing PB-Salt epitaxial films for Schottky diodes
[AD-D014244] N90-14937
SEPARATED FLOW
A one equation turbulence model for transonic airfoils N90-14199
Asymptotic analysis of performance of membrane modules for gas separations
[DE90-000699] N90-14316
SEQUENCING
Nomenclature for physical mapping of complex genomes
[DE89-015173] N90-14994
SERVICE LIFE
Crazing and degradation of flexure strength in acrylic plates as a function of time
[AD-A212835] N90-14357
A nonlinear high temperature fracture mechanics basis for strainrange partitioning
[NASA-TM-4133] N90-14642
SERVOCONTROL
Results of the manipulator test test stand study: Comparison of manipulators and evaluation of equipment items
[DE90-000977] N90-14625
SERVOMECHANISMS
Results of the manipulator test test stand study: Comparison of manipulators and evaluation of equipment items
[DE90-000977] N90-14625
SEYFERT GALAXIES
Radio and optical observations of nearby active galaxies N90-15000
SHADOWGRAPH PHOTOGRAPHY
X ray shadowscopy in implosion experiments N90-14563
SHALES
Organic geochemical and tectonic evolution of the midcontinent rift system: Organic geochemistry and micropaleontology
[DE89-017561] N90-14760
SHEAR LAYERS
Numerical modeling of supersonic turbulent reacting free shear layers N90-14197
An experimental investigation of shear layer mixing in supersonic flows N90-14508
SHEAR PROPERTIES
The structure and properties of liquid crystal polymers N90-14356
SHEAR STRAIN
Shear strain localization phenomenon in viscoplastic materials N90-14649
SHEAR STRESS
Visualization of boundary layer transition zone movement on oscillating airfoils with shear-sensitive liquid-crystal coatings
[DE89-009570] N90-14210
Shear strain localization phenomenon in viscoplastic materials N90-14649
SHIELDING
Effect of unshielded and shielded horn balances on hinge moment coefficients for controls at low speeds
[ESDU-89003-A] N90-14238
On protection of Freedom's solar dynamic radiator from the orbital debris environment. Part 1: Preliminary analyses and testing
[NASA-TM-102458] N90-14285
SHIVERING
The effects of nonselective and selective beta blockade upon nonshivering thermogenesis during an acute cold exposure in cold acclimated men N90-14767
SHOCK ABSORBERS
Evaluation of shock isolation techniques for a piezoresistive accelerometer
[DE89-014496] N90-14535
SHOCK FRONTS
Thermodynamic properties and hydrodynamic response of high-density high-temperature C H N O mixtures
[DE90-000836] N90-14318
The instability and fragmentation of the envelope of supernova 1987A N90-15011
SHOCK HEATING
Thermal/structural analyses of several hydrogen-cooled leading-edge concepts for hypersonic flight vehicles
[NASA-TM-102391] N90-14511

SHOCK LOADS
Shock-induced solid state reactions and phase transitions: X ray profile studies on shock-modified Fe3O4 and ZrO2 powders
[DE90-000669] N90-14315
Shock-induced defects and flux pinning in YBa2Cu3O sub 7-delta + Ag composites
[DE90-000827] N90-14960
SHOCK TUBES
Corrections for non-ideal effects in reflected shock waves at low Mach numbers
[DE90-002192] N90-14208
SHOCK WAVE PROPAGATION
Propagation of detonation waves from an impact region
[DE90-001184] N90-14515
SHOCK WAVES
Corrections for non-ideal effects in reflected shock waves at low Mach numbers
[DE90-002192] N90-14208
Solving the blow-by problem in a two-stage gun
[DE90-000842] N90-14246
Particle size effects in the initiation of explosives containing reactive and nonreactive continuous phases
[DE90-000786] N90-14390
CTH: A three-dimensional shock wave physics code
[DE89-016529] N90-14528
Experimental study of the shock waves generated by high energy laser pulses N90-14557
Microstructure induced by laser shock in an austenitic steel N90-14558
Dynamic sintering of metallic powders by laser shock N90-14559
Time integrated study of spectral emission in the X-UV domain at the outlet of a laser shock, at the back of single or double foil targets N90-14561
Pressure sensitive release device
[AD-D014220] N90-14610
Projectile impact Hugoniot parameters for selected materials
[DE90-000891] N90-14618
Comparison of shock severity measures
[DE90-000790] N90-14654
Implications and origins of shock structure in solids
[DE90-000846] N90-14658
Superconducting and microstructural properties of shock-compacted high-T sub c oxide powders
[DE90-000823] N90-14958
Effects of shock-induced defects on flux pinning in YBa2Cu3O(7-delta)
[DE90-000824] N90-14959
SHORT CIRCUITS
JPS heater and sensor lightning qualification
[NASA-CR-183830] N90-14530
SHOT PEENING
Fatigue fracture in the presence of shot peening residual stresses: Initiation, propagation, and relaxation phenomena N90-14644
SHUTTLE DERIVED VEHICLES
Main propulsion system test requirements for the two-engine Shuttle-C
[NASA-TM-100382] N90-14282
SIERRA NEVADA MOUNTAINS (CA)
Steady state model to determine lake resources at risk to acid deposition in the Sierra Nevada, California
[PB89-103995] N90-14705
Characterization of cloud chemistry and frequency of canopy exposure to clouds in the Sierra Nevada
[PB89-104035] N90-14753
SIGNAL ANALYZERS
The use of broadcast signals for passive sensing in automated HF communication systems N90-14433
High resolution, wide band Chirp-Z signal analyzer
[AD-D014240] N90-14465
SIGNAL DETECTION
A portable ionosonde in support of reliable communications N90-14431
Detection of a chirping electromagnetic signal
[DE90-002105] N90-14457
High resolution Doppler lidar
[NASA-CR-183288] N90-14542
Effective utilization of acoustic wave sensor responses: Simultaneous measurement of velocity and attenuation
[DE90-002580] N90-14872
SIGNAL DETECTORS
Effective utilization of acoustic wave sensor responses: Simultaneous measurement of velocity and attenuation
[DE90-002580] N90-14872
Narrow band and wide angle hemispherical interference optical filter
[AD-D014238] N90-14904
SIGNAL PROCESSING
PROPHET and future signal warfare decision aids N90-14412
Hybrid PE-ray-mode formulation of high frequency propagation in a bilinear tropospheric surface duct N90-14417
Design of a compensation filter for a quadratic phase communication channel N90-14428
Improved reliability prediction for HF digital voice transmission N90-14429
A modern trans-ionospheric propagation sensing system N90-14430
A portable ionosonde in support of reliable communications N90-14431
The use of broadcast signals for passive sensing in automated HF communication systems N90-14433
Pattern recognition techniques applied to the NASA-ACTS order-wire problem N90-14446
The characteristics of the HF radio channel and its influence on modern HF data communication system design N90-14448
Frequency agile synthetic aperture radar
[AD-D014235] N90-14451
Symmetric waveguide junction combiner
[AD-D014243] N90-14466
Nondestructive evaluation of flaw clusters and thin layer interfaces N90-14633
Synoptic scale tropical waves in multichannel satellite radiance data N90-14745
The effects of clutter-rejection filtering on estimating weather spectrum parameters
[NASA-CR-186212] N90-14754
JPL reuse program N90-14795
SILICON
Elastic softening in nanocrystalline silicon
[DE90-002268] N90-14377
Fabrication of NBN based electronic devices with silicon barriers
[AD-D014230] N90-14463
SILICON CARBIDES
Oxidation effects on the mechanical properties of SiC fiber-reinforced reaction-bonded silicon nitride matrix composites
[NASA-TM-102360] N90-14287
Friction and wear of glassy carbon in sliding contact, revision 1
[DE90-000743] N90-14365
The 7th International Conference on Ceramics
[DE90-002144] N90-14374
Study of microcrystalline, silicon-carbon p-layers prepared by photo-CVD and glow discharge
[DE89-009438] N90-14939
SILICON DIOXIDE
X ray reflectivity study of SiO2 on Si
[DE90-001326] N90-14843
SILICON NITRIDES
Oxidation effects on the mechanical properties of SiC fiber-reinforced reaction-bonded silicon nitride matrix composites
[NASA-TM-102360] N90-14287
Strength and toughness of monolithic and composite silicon nitrides
[NASA-TM-102423] N90-14368
Process monitoring using optical ultrasonic wave detection
[DE90-002021] N90-14870
SILICON OXIDES
Ordered ceramic membranes
[DE89-017426] N90-14364
SILOXANES
Amperometric biosensors for glucose, lactate, and glycolate based on oxidases and redox-modified siloxane polymers
[DE90-002301] N90-14541
SILVER
Silver composite cathodes for alkaline secondary batteries
[AD-D014227] N90-14462
Silver-nickel composite cathodes for alkaline secondary batteries
[AD-D014231] N90-14464
Shock-induced defects and flux pinning in YBa2Cu3O sub 7-delta + Ag composites
[DE90-000827] N90-14960
SILVER NITRATES
Silver-nickel composite cathodes for alkaline secondary batteries
[AD-D014231] N90-14464
SILVER OXIDES
Electrochemical preparation of silver oxide electrodes having high thermal stability
[AD-D014224] N90-14460
SIMULATION
Evaluation of the indirect effects of lightning on a system: Double transfer function method
[RAE-TRANS-2172] N90-14211
Design of a compensation filter for a quadratic phase communication channel N90-14428
Thermocapillary migration of liquid droplets in a temperature gradient in a density matched system
[NASA-CR-185178] N90-14512
Granular flow: Numerical simulation of dry granular flows and calculation of hydrodynamic interactions in suspensions
[DE89-017544] N90-14518
Technology development program for an advanced microsheet glass concentrator
[NASA-TM-102406] N90-14678
A model for the simulation of the ozone budget in the atmosphere under anthropogenic perturbation
[DE89-636294] N90-14719
The dynamics of simulated convective storms in hurricane environments N90-14747
Tuning of the OSCURS (Ocean Surface Current Simulations) numerical model to ocean surface measurements in the Gulf of Alaska
[PB89-103979] N90-14759
Engineering sciences design. Design and implementation of components for a bioregenerative system for growing higher order plants in space
[NASA-CR-186056] N90-14761
Path integral simulations of liquid helium
[DE90-001171] N90-14862
SIMULATORS
Acoustic-vortical-combustion interaction in a solid fuel ramjet simulator N90-14234
SINGLE CRYSTALS
Magnetic excitations in thulium metal
[DE90-002475] N90-14970
The influence of the substrate surface on the nucleation and growth of superconducting thin films
[DE90-003649] N90-14983
SINGLE-PHASE FLOW
Selection of the energy-efficient enhancement geometry for single-phase turbulent flow inside tubes
[DE89-017690] N90-14519
SINGULARITY (MATHEMATICS)
Vector fields and gravity on the lattice
[DE89-633885] N90-14860
SINTERING
Dynamic sintering of metallic powders by laser shock N90-14559
Process monitoring using optical ultrasonic wave detection
[DE90-002021] N90-14870
SKIN FRICTION
A one equation turbulence model for transonic airfoils N90-14199
SKIN TEMPERATURE (BIOLOGY)
The effects of nonselective and selective beta blockade upon nonshivering thermogenesis during an acute cold exposure in cold acclimated men N90-14767
SKY SURVEYS (ASTRONOMY)
Realtime tracking system for wide-field-of-view telescope
[DE90-001147] N90-14908
SLEWING
Dynamics and control of flexible spacecraft during and after slewing maneuvers
[NASA-CR-186123] N90-14270
SLIDING FRICTION
Friction and wear of glassy carbon in sliding contact, revision 1
[DE90-000743] N90-14365
SLURRIES
The secondary slurry-zinc/air battery
[DE90-002600] N90-14491
SLUSH
Slush Hydrogen (SLH2) technology development for application to the National Aerospace Plane (NASP)
[NASA-TM-102315] N90-14268
SMOOTHING
Estimating methods for counting process intensities: Non-parametric methods
[IMAG-RR-774-M] N90-14846
SODIUM
Modeling of sodium/metal chloride batteries
[DE89-017685] N90-14478
SODIUM SULFUR BATTERIES
Sodium/sulfur evaluation at SNL
[DE89-015846] N90-14472
Sodium/sulfur post-test analysis at ANL
[DE90-001911] N90-14488
SOFTENING
Elastic softening in nanocrystalline silicon
[DE90-002268] N90-14377
SOFTWARE ENGINEERING
QUEST/Ada: Query utility environment for software testing of Ada
[NASA-CR-186121] N90-14787
Software Reuse Issues
[NASA-CP-3057] N90-14789
Knowledge-based reusable software synthesis system N90-14791

Impact of domain analysis on reuse methods N90-14792
Prototype software reuse environment at Goddard Space Flight Center N90-14794
JPL reuse program N90-14795
Johnson Space Center software reuse activity N90-14796
Reuse research plans at Langley Research Center N90-14797
Reuse at the Software Productivity Consortium N90-14798
SSFP approach to software reuse N90-14799
Level 2 software reuse study N90-14800
An SSE approach to reusability N90-14801
Support for life-cycle product reuse in NASA's SSE N90-14802
Application of reusable software components at the SEI N90-14804
Technology transfer in software engineering N90-14805
AdaNET services N90-14806
Advanced Software Development Workstation Project N90-14807
Continuation of research in software for space operations support
[NASA-CR-186092] N90-14808
Using object-oriented development to support prototyping
[DE90-000547] N90-14821
A tutorial on software reliability engineering
[DE89-012368] N90-14828

SOFTWARE TOOLS

Integrated computer-based tools to facilitate environmental monitoring, assessment, and restoration
[DE90-002732] N90-14717
The effects of clutter-rejection filtering on estimating weather spectrum parameters
[NASA-CR-186212] N90-14754
Software Reuse Issues
[NASA-CP-3057] N90-14789
Classic-Ada(TM) N90-14793
Prototype software reuse environment at Goddard Space Flight Center N90-14794
Reuse research plans at Langley Research Center N90-14797
SSFP approach to software reuse N90-14799
Application of reusable software components at the SEI N90-14804
Technology transfer in software engineering N90-14805
Selecting and effectively using a computer aided software engineering tool
[DE89-017876] N90-14815

SOIL MOISTURE

An investigation of satellite sounding products for the remote sensing of the surface energy balance and soil moisture
[NASA-CR-186073] N90-14664

SOILS

Image processing of LANDSAT MSS data for buried valley detection in northern Indiana N90-14668

SOLAR ACTIVITY

Solar-geophysical data number 538, June 1989. Part 1: (Prompt reports). Data for May, April 1989, and late data
[PB89-223838] N90-15031
Solar-geophysical data number 540, August 1989. Part 1: (Prompt reports). Data for July, June 1989, and late data
[PB90-108572] N90-15035
The solar activity measurements experiments (SAMEX) for improved scientific understanding of solar activity
[NASA-TM-100372] N90-15036

SOLAR ACTIVITY EFFECTS

Solar-geophysical data number 538, June 1989. Part 1: (Prompt reports). Data for May, April 1989, and late data
[PB89-223838] N90-15031

SOLAR ARRAYS

Results of the 1989 NASA/JPL balloon flight solar cell calibration program
[NASA-CR-186114] N90-14672

SOLAR CELLS

Results of the 1989 NASA/JPL balloon flight solar cell calibration program
[NASA-CR-186114] N90-14672
Research on high-efficiency, multiple-gap, multijunction, amorphous-silicon-based alloy thin-film solar cells
[DE89-009444] N90-14673
Preparation and properties of high deposition a-Si:H films and solar cells using disilane
[DE89-009467] N90-14679
Thin film cadmium telluride, zinc telluride, and mercury zinc telluride solar cells
[DE89-009499] N90-14681
Research on high-efficiency, single-junction, monolithic, thin-film amorphous silicon solar cells
[DE89-000846] N90-14687
High-efficiency large-area CdTe modules
[DE89-009498] N90-14689
Hydrogen radical enhanced growth of solar cells
[DE89-009497] N90-14694
Photovoltaic Measurements and Performance Branch
[DE89-009500] N90-14695
Study of microcrystalline, silicon-carbon p-layers prepared by photo-CVD and glow discharge
[DE89-009438] N90-14939

SOLAR COLLECTORS

Conceptual design study of a 5 kilowatt solar dynamic Brayton power system using a dome Fresnel lens solar concentrator
[NASA-CR-185134] N90-14281
Technology development program for an advanced microsheet glass concentrator
[NASA-TM-102406] N90-14678

SOLAR DYNAMIC POWER SYSTEMS

Conceptual design study of a 5 kilowatt solar dynamic Brayton power system using a dome Fresnel lens solar concentrator
[NASA-CR-185134] N90-14281
A heat receiver design for solar dynamic space power systems
[NASA-TM-102473] N90-14283
On protection of Freedom's solar dynamic radiator from the orbital debris environment. Part 1: Preliminary analyses and testing
[NASA-TM-102458] N90-14285
Technology development program for an advanced microsheet glass concentrator
[NASA-TM-102406] N90-14678

SOLAR FLARES

Solar-geophysical data number 538, June 1989. Part 1: (Prompt reports). Data for May, April 1989, and late data
[PB89-223838] N90-15031
Solar-geophysical data number 538, June 1989. Part 2: (Comprehensive reports). Data for December 1988 and miscellaneous
[PB89-223846] N90-15032
Solar-geophysical data number 539, July 1989. Part 1: (Prompt reports). Data for June, May 1989, and late data
[PB89-235451] N90-15033
Solar-geophysical data number 539, July 1989. Part 2: (Comprehensive reports). Data for January 1989, and miscellaneous
[PB89-235469] N90-15034
Solar-geophysical data number 540, August 1989. Part 1: (Prompt reports). Data for July, June 1989, and late data
[PB90-108572] N90-15035
Solar-geophysical data number 540, August 1989. Part 2: (Comprehensive reports). Data for February 1989
[PB89-108598] N90-15039

SOLAR INSTRUMENTS

The solar activity measurements experiments (SAMEX) for improved scientific understanding of solar activity
[NASA-TM-100372] N90-15036

SOLAR MAGNETIC FIELD

Solar-geophysical data number 538, June 1989. Part 1: (Prompt reports). Data for May, April 1989, and late data
[PB89-223838] N90-15031
Solar-geophysical data number 539, July 1989. Part 1: (Prompt reports). Data for June, May 1989, and late data
[PB89-235451] N90-15033
Solar-geophysical data number 540, August 1989. Part 1: (Prompt reports). Data for July, June 1989, and late data
[PB90-108572] N90-15035
The solar activity measurements experiments (SAMEX) for improved scientific understanding of solar activity
[NASA-TM-100372] N90-15036

SOLAR NEUTRINOS

Dark matter and the solar neutrino problem: Can particle physics provide a single solution
[DE90-001827] N90-15024

SOLAR OBSERVATORIES

The solar activity measurements experiments (SAMEX) for improved scientific understanding of solar activity
[NASA-TM-100372] N90-15036

SOLAR PHYSICS

An international discussion on research in solar and space physics N90-14996
Solar-geophysical data number 539, July 1989. Part 2: (Comprehensive reports). Data for January 1989, and miscellaneous
[PB89-235469] N90-15034

SOLAR PROMINENCES

Solar-geophysical data number 538, June 1989. Part 2: (Comprehensive reports). Data for December 1988 and miscellaneous
[PB89-223846] N90-15032
Solar-geophysical data number 540, August 1989. Part 2: (Comprehensive reports). Data for February 1989
[PB89-108598] N90-15039

SOLAR RADIATION

Beyond the IDMY (International Daylighting Measurements Year): A network instrument for low-cost data acquisition
[DE90-002722] N90-14740
Atlas of albedo and absorbed solar radiation derived from Nimbus 6 earth radiation budget data set, July 1975 to May 1978
[NASA-RP-1230] N90-14741

SOLAR RADIO BURSTS

Solar-geophysical data number 538, June 1989. Part 2: (Comprehensive reports). Data for December 1988 and miscellaneous
[PB89-223846] N90-15032
Solar-geophysical data number 539, July 1989. Part 2: (Comprehensive reports). Data for January 1989, and miscellaneous
[PB89-235469] N90-15034
Solar-geophysical data number 540, August 1989. Part 2: (Comprehensive reports). Data for February 1989
[PB89-108598] N90-15039

SOLAR RADIO EMISSION

Solar-geophysical data number 538, June 1989. Part 1: (Prompt reports). Data for May, April 1989, and late data
[PB89-223838] N90-15031
Solar-geophysical data number 539, July 1989. Part 1: (Prompt reports). Data for June, May 1989, and late data
[PB89-235451] N90-15033
Solar-geophysical data number 540, August 1989. Part 1: (Prompt reports). Data for July, June 1989, and late data
[PB90-108572] N90-15035

SOLAR SPECTRA

Solar-geophysical data number 538, June 1989. Part 1: (Prompt reports). Data for May, April 1989, and late data
[PB89-223838] N90-15031
Solar-geophysical data number 540, August 1989. Part 1: (Prompt reports). Data for July, June 1989, and late data
[PB90-108572] N90-15035

SOLAR SYSTEM

JPRS Report: Science and technology. USSR: Space. Soviet space program to the year 2000
[JPRS-USP-89-008] N90-14248

SOLAR WIND

Solar-geophysical data number 538, June 1989. Part 2: (Comprehensive reports). Data for December 1988 and miscellaneous
[PB89-223846] N90-15032
Solar-geophysical data number 540, August 1989. Part 2: (Comprehensive reports). Data for February 1989
[PB89-108598] N90-15039

SOLAR X-RAYS

Solar-geophysical data number 538, June 1989. Part 2: (Comprehensive reports). Data for December 1988 and miscellaneous
[PB89-223846] N90-15032
Solar-geophysical data number 539, July 1989. Part 2: (Comprehensive reports). Data for January 1989, and miscellaneous
[PB89-235469] N90-15034
Solar-geophysical data number 540, August 1989. Part 2: (Comprehensive reports). Data for February 1989
[PB89-108598] N90-15039

SOLDERING

A method of soldering aluminum
[AD-D014226] N90-14611

SOLID ELECTRODES

Electrode development in monolithic solid oxide fuel cells
[DE90-001910] N90-14684
Solid oxide fuel cells electrodes based on In(sub 2)O(sub 3)-PrO(sub 1.83)-ZrO(sub 2)
[DE90-002666] N90-14691

SOLID ELECTROLYTES

Modeling of sodium/metal chloride batteries
[DE89-017685] N90-14478
Proceedings of the First Annual Fuel Cells Contractors Review Meeting
[DE89-011699] N90-14675
Interfacial effects in monolithic solid oxide fuel cells
[DE90-001914] N90-14690
Solid State Division
[DE90-000979] N90-14945

SOLID PROPELLANT COMBUSTION
A surface coupled flamelet approach to dynamic response in heterogeneous propellant combustion
N90-14302
SOLID PROPELLANT ROCKET ENGINES
Review of the Aerospace Safety Advisory Panel report for NASA fiscal year 1990 authorization
[GPO-24-234] N90-14213
Flight set 360T004 (STS-30) field joint protection system, volume 7
[NASA-CR-183829] N90-14280
A surface coupled flamelet approach to dynamic response in heterogeneous propellant combustion
N90-14302
SOLID STATE
Shock-induced solid state reactions and phase transitions: X ray profile studies on shock-modified Fe3O4 and ZrO2 powders
[DE90-000669] N90-14315
Solid-state fluorescence above 1000 C: Application to high-temperature laser thermometry
[DE90-000728] N90-14594
Solid State Division
[DE90-000979] N90-14945
SOLID STATE PHYSICS
Spectral properties of one dimensional quasi-crystals
[PREPRINT-659] N90-14938
SOLID SUSPENSIONS
Fluid-particle interaction in solid-liquid two-phase grid turbulence N90-14496
SOLIDS
Granular flow: Numerical simulation of dry granular flows and calculation of hydrodynamic interactions in suspensions
[DE89-017544] N90-14518
Implications and origins of shock structure in solids
[DE90-000846] N90-14658
Wide-angle propagation in inhomogeneous fluids and elastic solids using perturbation methods N90-14868
Direction-dependent stopping power and beam deflection in anisotropic solids
[DE90-001076] N90-14883
SOLUTIONS
The generalized van der Waals theory of pure fluids and mixtures
[DE90-000504] N90-14307
SOOT
Kinetics and mechanism of soot formation in hydrocarbon combustion
[NASA-CR-186162] N90-14305
SOUND TRANSMISSION
Boundary element analysis of single and multidomain problems in acoustics N90-14867
SOUND WAVES
Effective utilization of acoustic wave sensor responses: Simultaneous measurement of velocity and attenuation
[DE90-002580] N90-14872
SOUNDING ROCKETS
A measurement of hydroxyl in the daytime mesosphere N90-14732
SPACE BASES
M.I.N.G., Mars Investment for a New Generation: Robotic construction of a permanently manned Mars base
[NASA-CR-186224] N90-15028
SPACE DEBRIS
On protection of Freedom's solar dynamic radiator from the orbital debris environment. Part 1: Preliminary analyses and testing
[NASA-TM-102458] N90-14285
SPACE FLIGHT
Sandia Satellite Program summary of operational procedures
[DE90-000892] N90-14249
Design considerations for space flight hardware
[NASA-TM-102300] N90-14275
SPACE HABITATS
M.I.N.G., Mars Investment for a New Generation: Robotic construction of a permanently manned Mars base
[NASA-CR-186224] N90-15028
SPACE INFRARED TELESCOPE FACILITY
Long-lived space observatories for astronomy and astrophysics
[NASA-CR-185373] N90-14261
CCD TV focal plane guider development and comparison to SIRTF applications
[NASA-CR-185977] N90-14900
SPACE LOGISTICS
Superconducting magnets in space
[DE90-002671] N90-14865
SPACE MANUFACTURING
Materials processing in low gravity
[NASA-CR-183733] N90-14397
SPACE MISSIONS
Continuation of research in software for space operations support
[NASA-CR-186092] N90-14808
SPACE PLASMAS
Particle simulations in magnetospheric plasmas
[NASA-CR-186238] N90-14934
Solar-geophysical data number 539, July 1989. Part 2: (Comprehensive reports). Data for January 1989, and miscellaneous
[PB89-235469] N90-15034
SPACE POWER REACTORS
Electrical performance characteristics of high power converters for space power applications
[NASA-CR-185947] N90-14279
Introductory testimony: Hearing on nuclear power in space
[DE90-001137] N90-14897
A review of gas-cooled reactor concepts for SDI (Strategic Defense Initiative)
[DE89-016962] N90-14898
SPACE POWER UNIT REACTORS
SP-100 power system conceptual design for lunar base applications
[NASA-TM-102090] N90-15030
SPACE PROCESSING
Materials processing in low gravity
[NASA-CR-183733] N90-14397
Extravehicular activity welding experiment
[NASA-CR-183848] N90-14608
SPACE PROGRAMS
An international discussion on research in solar and space physics N90-14996
SPACE SHUTTLE BOOSTERS
SRB thermal environments
[NASA-CR-183801] N90-14276
SPACE SHUTTLE ORBITERS
Control of an experiment to measure acoustic noise in the space shuttle
[NPS62-89-022] N90-14869
SPACE SHUTTLE PAYLOADS
Main propulsion system test requirements for the two-engine Shuttle-C
[NASA-TM-100382] N90-14282
SPACE SHUTTLES
Preliminary design of the Shuttle-C avionics recovery system
[NASA-CR-186230] N90-14258
Chronology of KSC and KSC related events for 1988
[NASA-TM-101915] N90-15040
SPACE SIMULATORS
Thermal environmental tests on space simulation chamber
[DE90-000927] N90-14251
SPACE STATION PAYLOADS
Space station attached payload program support
[NASA-CR-183838] N90-14274
SPACE STATIONS
Review of the Aerospace Safety Advisory Panel report for NASA fiscal year 1990 authorization
[GPO-24-234] N90-14213
Aerospace vehicle design, spacecraft section. Volume 1: Project Groups 3 through 5
[NASA-CR-186053] N90-14263
Aerospace vehicle design, spacecraft section. Volume 2: Project Groups 6 through 8
[NASA-CR-186054] N90-14264
An image compression algorithm for a high-resolution digital still camera
[NASA-CR-185079] N90-14532
Software Reuse Issues
[NASA-CP-3057] N90-14789
SSFP approach to software reuse N90-14799
Level 2 software reuse study N90-14800
Support for life-cycle product reuse in NASA's SSE
N90-14802
SPACE TRANSPORTATION SYSTEM
Review of the Aerospace Safety Advisory Panel report for NASA fiscal year 1990 authorization
[GPO-24-234] N90-14213
Flight set 360T004 (STS-30) field joint protection system, volume 7
[NASA-CR-183829] N90-14280
SPACE WEAPONS
A review of gas-cooled reactor concepts for SDI (Strategic Defense Initiative)
[DE89-016962] N90-14898
SPACEBORNE ASTRONOMY
Long-lived space observatories for astronomy and astrophysics
[NASA-CR-185373] N90-14261
SPACEBORNE EXPERIMENTS
Shuttle Laser Technology Experiment Facility (LTEF)-to-airplane lasercom experiment: Airplane considerations
[NASA-TM-100749] N90-14260
Design considerations for space flight hardware
[NASA-TM-102300] N90-14275
Extravehicular activity welding experiment
[NASA-CR-183848] N90-14608
SPACECRAFT ANTENNAS
Dynamics and control of flexible spacecraft during and after slewing maneuvers
[NASA-CR-186123] N90-14270
SPACECRAFT COMMUNICATION
Aerospace vehicle design, spacecraft section. Volume 2: Project Groups 6 through 8
[NASA-CR-186054] N90-14264
SPACECRAFT CONFIGURATIONS
Aerospace vehicle design, spacecraft section. Volume 1: Project Groups 3 through 5
[NASA-CR-186053] N90-14263
Aerospace vehicle design, spacecraft section. Volume 2: Project Groups 6 through 8
[NASA-CR-186054] N90-14264
SPACECRAFT CONTROL
Dynamics and control of flexible spacecraft during and after slewing maneuvers
[NASA-CR-186123] N90-14270
SPACECRAFT DESIGN
Preliminary design document: Ground based testbed for avionics systems
[NASA-CR-183821] N90-14231
Aerospace vehicle design, spacecraft section. Volume 1: Project Groups 3 through 5
[NASA-CR-186053] N90-14263
Aerospace vehicle design, spacecraft section. Volume 2: Project Groups 6 through 8
[NASA-CR-186054] N90-14264
The space station tethered elevator system
[NASA-CR-186051] N90-14265
Project Argo: The design and analysis of an all-propulsive and an aeroassisted version of a manned space transportation vehicle
[NASA-CR-186047] N90-14266
Design considerations for space flight hardware
[NASA-TM-102300] N90-14275
Main propulsion system test requirements for the two-engine Shuttle-C
[NASA-TM-100382] N90-14282
SPACECRAFT ENVIRONMENTS
Partial gravity habitat study: With application to lunar base design
[NASA-CR-186048] N90-14267
Exploring the living universe: A strategy for space life sciences
[NASA-TM-101891] N90-14778
SPACECRAFT LAUNCHING
An in-flight technique for wind measurement in support of the space shuttle program
[NASA-TM-4154] N90-14224
Draft Environmental Impact Statement for the Ulysses Mission (Tier 2)
[NASA-TM-102903] N90-14727
SPACECRAFT POWER SUPPLIES
Electrical performance characteristics of high power converters for space power applications
[NASA-CR-185947] N90-14279
A heat receiver design for solar dynamic space power systems
[NASA-TM-102473] N90-14283
Draft Environmental Impact Statement for the Ulysses Mission (Tier 2)
[NASA-TM-102903] N90-14727
Introductory testimony: Hearing on nuclear power in space
[DE90-001137] N90-14897
SPACECRAFT PROPULSION
Project Argo: The design and analysis of an all-propulsive and an aeroassisted version of a manned space transportation vehicle
[NASA-CR-186047] N90-14266
SPACECRAFT RADIATORS
On protection of Freedom's solar dynamic radiator from the orbital debris environment. Part 1: Preliminary analyses and testing
[NASA-TM-102458] N90-14285
SPACECRAFT RECOVERY
Preliminary design of the Shuttle-C avionics recovery system
[NASA-CR-186230] N90-14258
SPACECRAFT TRACKING
Shuttle Laser Technology Experiment Facility (LTEF)-to-airplane lasercom experiment: Airplane considerations
[NASA-TM-100749] N90-14260
SPACECREWS
Payload crew utilization for spacelab missions
[NASA-TP-2976] N90-14256

SPACING
Primary arm spacing in directionally solidified Pb-10 wt percent Sn alloys
[NASA-CR-185190] N90-14398
SPALLING
Spall strength measurements on shockloaded refractory metals
[DE90-000839] N90-14345
SPANLOADER AIRCRAFT
Design of a spanloader cargo aircraft
[NASA-CR-186046] N90-14216
SPARK IGNITION
Cold starting a neat methanol (M100) vehicle with long duration spark ignition
[PB89-230692] N90-14613
SPATIAL DISTRIBUTION
Spatial evolution of nonlinear acoustic mode instabilities on hypersonic boundary layers
[NASA-TM-102431] N90-14517
Frequency distributions of heavy rainstorms in Illinois
[PB90-100215] N90-14748
SPATIAL RESOLUTION
Temporally and spatially resolved flow in a two-stage axial compressor. Part 2: Computational assessment
[NASA-TM-102273] N90-14236
X ray microimaging for the life sciences
[DE90-002613] N90-14766
SPECIFIC IMPULSE
Energy deposition in low power coaxial plasma thrusters N90-14911
SPECIFICATIONS
Markets for high-speed intercity Maglev technology: A systems analysis approach
[DE89-017683] N90-14623
A graphically oriented specification language for automatic code generation. GRASP/Ada: A Graphical Representation of Algorithms, Structure, and Processes for Ada, phase 1
[NASA-CR-183212] N90-14813
SPECTRA
Fatigue analysis and reconstruction of helicopter load spectra N90-14304
SPECTRAL CORRELATION
Statistics of two-color laser beam propagation in the turbulent atmosphere (spectral correlation)
[PB89-236699] N90-14581
SPECTRAL METHODS
Modified Chebyshev pseudospectral method with O(N exp -1) time step restriction
[NASA-CR-181958] N90-14848
SPECTRAL RESOLUTION
As observational and theoretical investigation of stellar flares N90-15012
SPECTRAL THEORY
Proceedings of the Focused Research Program on Spectral Theory and Boundary Value Problems. Volume 4: Nonlinear Differential Equations
[DE90-000920] N90-14780
SPECTROGRAPHS
Assessment of research needs for laser technologies applied to advanced spectrographic methods
[DE90-001154] N90-14587
SPECTROSCOPIC ANALYSIS
Combined capillary electrophoresis and electrospray ionization mass spectrometry
[DE90-001903] N90-14322
Photovoltaic Measurements and Performance Branch
[DE89-009500] N90-14695
SPECTROSCOPY
Supercritical fluid chromatography/supersonic jet spectroscopy
[DE90-001378] N90-14308
Non-linear optical studies of adsorbates: Spectroscopy and dynamics
[DE90-001543] N90-14312
Spectral properties of one dimensional quasi-crystals
[PREPRINT-659] N90-14938
SPECTRUM ANALYSIS
Spectral contents readout of birefringent sensor
[NASA-CR-179444] N90-14905
SPHERES
Single particle friction tests with cellulose acetate sphere samples
[DE89-017537] N90-14622
SPHERICAL PLASMAS
Numerical simulation of the preheating by x rays in spherical plasmas N90-14564
SPLINE FUNCTIONS
A tensor product b-spline method for 3D multi-block elliptic grid generation
[DE89-017440] N90-14859
SPONTANEOUS COMBUSTION
Devices and methods for in-situ combustion ignition
[DE89-000766] N90-14309
SPREAD SPECTRUM TRANSMISSION
Improving the quality of a spread-spectrum radiomobile link N90-14426
SQUARE WELLS
The generalized van der Waals theory of pure fluids and mixtures
[DE90-000504] N90-14307
STABILITY
Superplasticity: An overview N90-14326
Stability and dynamics of constrained flexible multibody systems N90-14609
Block predictor (low order) corrector methods to solve ordinary differential equations on parallel computers
[IMAG-RR-757-M] N90-14845
STABILIZATION
Investigation of the phase stabilizing effect of potassium fluoride on ammonium nitrate
[AD-A213042] N90-14381
STAINLESS STEELS
Advances and future directions in superplastic materials N90-14328
An evaluation of electrochemical potentiokinetic reactivation techniques for in-service measurements on Type 304 stainless steel
[DE89-017859] N90-14340
Rapid heating tensile tests of hydrogen-charged high-energy-rate-forged 316L stainless steel
[DE90-000591] N90-14342
The 4.2 K fracture toughness of 304 stainless steel in a magnetic field
[DE90-002083] N90-14347
Embrittlement of laboratory- and reactor-aged CF-3, CF-8, and CF-8M duplex stainless steels
[DE90-002777] N90-14354
The feasibility of welding of irradiated materials
[DE90-002200] N90-14631
Failure probability estimate of Type 304 stainless steel piping
[DE90-000659] N90-14635
STANDARDIZATION
Transferring data objects: A focused Ada investigation
[NASA-CR-186065] N90-14786
STANDARDS
Calibration curves for some standard Gap Tests
[DE89-016599] N90-14389
Results of the 1989 NASA/JPL balloon flight solar cell calibration program
[NASA-CR-186114] N90-14672
Nomenclature for physical mapping of complex genomes
[DE89-015173] N90-14994
STAR CLUSTERS
Equation of state and opacity of dense plasmas
[DE90-002223] N90-14926
STAR FORMATION
Very high resolution radio observations of molecular cloud cores N90-15013
STATE ESTIMATION
Viscoplasticity: A thermodynamic formulation
[NASA-TM-102388] N90-14640
STATISTICAL ANALYSIS
Modelling UHF propagation for frequency assignment in radio relay networks N90-14445
Statistics of two-color laser beam propagation in the turbulent atmosphere (spectral correlation)
[PB89-236699] N90-14581
An initial look at the dynamics of the microscale flow field within a large wind farm in response to variations in the natural inflow
[DE89-009501] N90-14682
Frequency distributions of heavy rainstorms in Illinois
[PB90-100215] N90-14748
STATISTICAL DISTRIBUTIONS
Frequency distributions of heavy rainstorms in Illinois
[PB90-100215] N90-14748
STATISTICAL TESTS
An evaluation of trend detection techniques for use in water quality monitoring programs
[PB89-100058] N90-14702
STEADY FLOW
Computational investigation of incompressible airfoil flows at high angles of attack
[AD-A205885] N90-14201
STEELS
A finite strip method for the elastic-plastic large displacement analysis of thin-walled and cold-formed steel sections
[PB89-226021] N90-14647
On-line system to measure magnetic characteristics of steel samples
[DE89-633443] N90-14861
STEERING
Guidance, steering, load relief and control of an asymmetric launch vehicle
[NASA-CR-185598] N90-14257
Vehicle antenna for the mobile satellite experiment
[NASA-CR-186109] N90-14271
STELLAR ATMOSPHERES
Ultraviolet properties of hot stars in globular clusters N90-15007
STELLAR ENVELOPES
Properties of evolved star circumstellar grains N90-15003
STELLAR EVOLUTION
Properties of evolved star circumstellar grains N90-15003
Meteoritic basalts
[NASA-CR-185949] N90-15004
Ultraviolet properties of hot stars in globular clusters N90-15007
The instability and fragmentation of the envelope of supernova 1987A N90-15011
STELLAR FLARES
As observational and theoretical investigation of stellar flares N90-15012
STELLAR LUMINOSITY
Studies of elementary particles: Proposal
[DE90-001120] N90-14879
Theory of wide-angle photometry from standard stars
[NASA-CR-185964] N90-14999
STELLAR MODELS
The instability and fragmentation of the envelope of supernova 1987A N90-15011
As observational and theoretical investigation of stellar flares N90-15012
Perturbation methods for the calculation of gravitational waves from slightly non-spherical spacetimes with applications to stellar core collapse N90-15015
STELLAR RADIATION
Theory of wide-angle photometry from standard stars
[NASA-CR-185964] N90-14999
The instability and fragmentation of the envelope of supernova 1987A N90-15011
Perturbation methods for the calculation of gravitational waves from slightly non-spherical spacetimes with applications to stellar core collapse N90-15015
STELLAR SPECTRA
The softest Einstein AGN (Active Galactic Nuclei)
[DE89-009389] N90-15020
STELLAR SPECTROPHOTOMETRY
Theory of wide-angle photometry from standard stars
[NASA-CR-185964] N90-14999
STELLAR WINDS
Very high resolution radio observations of molecular cloud cores N90-15013
A source of observational constraints on the structure of Wolf-Rayet winds
[DE90-001236] N90-15023
STIFFNESS
Finite element analysis of frictional contact problems N90-14612
STIFFNESS MATRIX
A study of incremental-iterative strategies for nonlinear analyses
[PB89-226005] N90-14646
STIRLING CYCLE
System design and performance prediction of a free-piston Stirling engine/magnetic coupling/compressor assembly in a gas residential heat pump
[DE89-016070] N90-14696
SP-100 power system conceptual design for lunar base applications
[NASA-TM-102090] N90-15030
STIRLING ENGINES
SP-100 power system conceptual design for lunar base applications
[NASA-TM-102090] N90-15030
STOCHASTIC PROCESSES
Optimal stochastic modeling and control of flexible structures
[AD-A212347] N90-14269
A two dimensional power spectral estimate for some nonstationary processes
[NASA-CR-186100] N90-14843
STOICHIOMETRY
Application of neutron diffraction NDE to high-temperature superconducting composites
[DE90-002184] N90-14295
Oxygen stoichiometry, structural transitions, and thermodynamic behavior of the YBa2Cu3O(x) system
[DE89-017694] N90-14951
STOPPING POWER
Interaction of low-energy electrons and positrons with condensed matter: Stopping powers and inelastic mean free paths from optical data
[DE90-001001] N90-14882
Direction-dependent stopping power and beam deflection in anisotropic solids
[DE90-001076] N90-14883

STORAGE BATTERIES
Silver composite cathodes for alkaline secondary batteries
[AD-D014227] N90-14462
Silver-nickel composite cathodes for alkaline secondary batteries
[AD-D014231] N90-14464
The secondary slurry-zinc/air battery
[DE90-002600] N90-14491
STORAGE RINGS (PARTICLE ACCELERATORS)
NIKHEF-K contributions to the 1989 Particle Accelerator Conference
[NIKHEF/AMPS/89/03] N90-14891
The Amsterdam pulse stretcher project (AmPS) N90-14892
Optics of the Amsterdam pulse stretcher (AmPS) N90-14893
Modification of MEA modulator-klystron units enabling short pulse injection into a pulse-stretcher ring N90-14894
Performance and modification of the MEA RF drive system N90-14895
STORAGE TANKS
The strength-toughness combination of the aluminum-lithium alloys 2090 and 2091 at cryogenic temperatures
[DE90-001425] N90-14338
STRAIN GAGES
Electrical properties of materials for high temperature strain gage applications
[NASA-CR-186192] N90-14534
STRAIN HARDENING
The 4.2 K fracture toughness of 304 stainless steel in a magnetic field
[DE90-002083] N90-14347
Viscoplasticity: A thermodynamic formulation
[NASA-TM-102388] N90-14640
Shear strain localization phenomenon in viscoplastic materials N90-14649
Approximate methods for dynamic plastic deformation of structures
[DE90-002214] N90-14660
STRAIN MEASUREMENT
Spectral contents readout of birefringent sensor
[NASA-CR-179444] N90-14905
STRAIN RATE
Shear strain localization phenomenon in viscoplastic materials N90-14649
STRATEGY
The processes of scientific research: The strategy of experimentation N90-14788
Concerning advanced architectures for strategic defense
[DE90-001894] N90-14857
STRATIGRAPHY
Organic geochemical and tectonic evolution of the midcontinent rift system: Organic geochemistry and micropaleontology
[DE89-017561] N90-14760
STRATOPAUSE
Remote sensing of atmospheric water vapour by pressure modulation radiometry N90-14667
STRATOSPHERE
Global stratospheric change: Requirements for a Very-High-Altitude Aircraft for Atmospheric Research
[NASA-CP-10041] N90-14220
Remote sensing of atmospheric water vapour by pressure modulation radiometry N90-14667
The retrieval of the concentrations of nitric oxide and nitrogen dioxide from satellite solar occultation measurements at sunset and sunrise N90-14733
Extraterrestrial halogen and sulfur content of the stratosphere
[DE89-017623] N90-14738
STRESS ANALYSIS
Parametric studies to determine the effect of compliant layers on metal matrix composite systems
[NASA-TM-102465] N90-14294
Numerical and empirical verification of the stress state in a ceramic, button-head, tensile specimen
[DE90-001645] N90-14375
Further studies of transverse stress effects in cable-in-conduit conductors
[DE90-001517] N90-14484
The stress analysis of thin-walled screwed tubular joints N90-14637
Flexural and torsional-flexural buckling of thin-walled open section struts
[ESDU-89007] N90-14643
Magnetotransport studies of epitaxial Cr thin films
[DE90-001930] N90-14975
STRESS CORROSION CRACKING
An evaluation of electrochemical potentiokinetic reactivation techniques for in-service measurements on Type 304 stainless steel
[DE89-017859] N90-14340
Acoustic emission during intergranular stress corrosion cracking
[DE90-002894] N90-14355
Failure probability estimate of Type 304 stainless steel piping
[DE90-000659] N90-14635
STRESS DISTRIBUTION
The effect of hydrogen charging on the mechanical properties of aluminum alloy 2090
[DE90-000129] N90-14341
A global ocean wind stress climatology based on ECMWF (European Centre for Medium Range Weather Forecasts) analyses
[PB90-109968] N90-14752
STRESS MEASUREMENT
Spectral contents readout of birefringent sensor
[NASA-CR-179444] N90-14905
STRESS RELAXATION
Fatigue fracture in the presence of shot peening residual stresses: Initiation, propagation, and relaxation phenomena N90-14644
STRESS-STRAIN RELATIONSHIPS
A theoretical investigation of the column behavior of cold-formed square hollow sections
[PB89-225981] N90-14645
A finite strip method for the elastic-plastic large displacement analysis of thin-walled and cold-formed steel sections
[PB89-226021] N90-14647
STRESSES
A generalized thermomechanical constitutive model for metal matrix composites with plastic strain and damage N90-14293
High speed transfer switch with 50 kA and 50 kV ratings
[DE90-002448] N90-14481
STRETCHING
Effects of flame stretch on the propagation, extinction, and stability of premixed flames N90-14301
NIKHEF-K contributions to the 1989 Particle Accelerator Conference
[NIKHEF/AMPS/89/03] N90-14891
The Amsterdam pulse stretcher project (AmPS) N90-14892
Optics of the Amsterdam pulse stretcher (AmPS) N90-14893
Modification of MEA modulator-klystron units enabling short pulse injection into a pulse-stretcher ring N90-14894
STRING THEORY
Hamiltonian flows, SU(infinity), SO(infinity), USp(infinity), and strings
[DE90-001987] N90-14851
String models for ultrarelativistic heavy ion collisions: Lund model versus color exchange models
[DE88-015856] N90-14881
STRONTIUM COMPOUNDS
Bi-Sr-Ca-Cu-O superconducting ceramics
[DE89-636225] N90-14972
The influence of the substrate surface on the nucleation and growth of superconducting thin films
[DE90-003649] N90-14983
STRUCTURAL ANALYSIS
A theoretical investigation of the column behavior of cold-formed square hollow sections
[PB89-225981] N90-14645
A study of incremental-iterative strategies for nonlinear analyses
[PB89-226005] N90-14646
Verification of the NIKE3D structural analysis code by comparison against the analytic solution for a spherical cavity under a far-field uniaxial stress
[DE90-000929] N90-14653
Control of the variable speed generator on the Sandia 34-metre vertical axis wind turbine
[DE90-000803] N90-14674
STRUCTURAL DESIGN
Design and demonstration of heat pipe cooling for NASP and evaluation of heating methods at high heating rates
[DE89-016995] N90-14227
Preliminary design document: Ground based testbed for avionics systems
[NASA-CR-183821] N90-14231
Sandia Satellite Program summary of operational procedures
[DE90-000892] N90-14249
Mechanisms of wear in structural ceramic materials N90-14360
Technology development program for an advanced microsheet glass concentrator
[NASA-TM-102406] N90-14678
STRUCTURAL VIBRATION
Measurement of damping of graphite epoxy composite materials and structural joints
[NASA-CR-183802] N90-14286
Non-linear vibrations, stability, and dynamics of structures and mechanisms
[AD-A212152] N90-14639
Evaluation of analysis techniques for low frequency interior noise and vibration of commercial aircraft
[NASA-CR-181851] N90-14866
STRUTS
Flexural and torsional-flexural buckling of thin-walled open section struts
[ESDU-89007] N90-14643
SUBMARINES
Elastomeric impulse energy storage and transfer system
[AD-D014223] N90-14255
SUBMERGED BODIES
Heat transfer to a stationary and moving sphere immersed in a fluidized bed N90-14503
SUBSONIC SPEED
Hinge moment coefficient derivatives for trailing-edge controls on wings at subsonic speeds
[ESDU-89009] N90-14239
SUBSTRATES
Method for fabricating thin film metallic meshes for use as Fabry-Perot interferometer elements, filters and other devices
[AD-D014236] N90-14529
The influence of the substrate surface on the nucleation and growth of superconducting thin films
[DE90-003649] N90-14983
SUBSTRUCTURES
Effects of dislocation substructure and prestrain on fracture behavior in aluminum and steel alloys N90-14334
SUDDEN IONOSPHERIC DISTURBANCES
Solar-geophysical data number 538, June 1989. Part 1: (Prompt reports). Data for May, April 1989, and late data
[PB89-223838] N90-15031
Solar-geophysical data number 539, July 1989. Part 1: (Prompt reports). Data for June, May 1989, and late data
[PB89-235451] N90-15033
Solar-geophysical data number 540, August 1989. Part 1: (Prompt reports). Data for July, June 1989, and late data
[PB90-108572] N90-15035
SUDDEN STORM COMMENCEMENTS
Solar-geophysical data number 538, June 1989. Part 1: (Prompt reports). Data for May, April 1989, and late data
[PB89-223838] N90-15031
SULFATES
High temperature chemistry of complex vaporization/decomposition processes
[DE89-016559] N90-14306
SULFUR
An electroformed nickel-sulfur alloy for a nose cone
[DE90-000866] N90-14337
Extraterrestrial halogen and sulfur content of the stratosphere
[DE89-017623] N90-14738
Mobility of sulfur in thermally altered meteorites N90-15010
SULFUR DIOXIDES
Profile measurements of sulfur dioxide, nitrogen oxides, and nitric acid deposition velocities in California's south coast air basin
[PB90-104001] N90-14703
SULFURIC ACID
Steady state model to determine lake resources at risk to acid deposition in the Sierra Nevada, California
[PB89-103995] N90-14705
SUNLIGHT
A measurement of hydroxyl in the daytime mesosphere N90-14732
SUNRISE
The retrieval of the concentrations of nitric oxide and nitrogen dioxide from satellite solar occultation measurements at sunset and sunrise N90-14733
SUNSET
The retrieval of the concentrations of nitric oxide and nitrogen dioxide from satellite solar occultation measurements at sunset and sunrise N90-14733
SUPERCONDUCTING FILMS
Ion beam analysis and modification of thin-film, high-temperature superconductors
[DE90-000918] N90-14941
The influence of the substrate surface on the nucleation and growth of superconducting thin films
[DE90-003649] N90-14983
SUPERCONDUCTING MAGNETS
Superconducting magnets in space
[DE90-002671] N90-14885
Applications of superconductor technologies to transportation
[DE90-000856] N90-14961

SUPERCONDUCTING SUPER COLLIDER
Recent developments of gigatron technology
[DE90-001067] N90-14474
SUPERCONDUCTIVITY
Theory of strongly fluctuating superconductivity
[DE90-001073] N90-14942
Solid State Division
[DE90-000979] N90-14945
X ray studies of strain, interface, and impurity in semiconductors
[DE90-001525] N90-14947
Development of a real time monitor for superconductive thin film preparation
[DE89-017772] N90-14952
Superconductivity from finite-U valence fluctuations
[DE90-000603] N90-14954
A simple figure of merit for high temperature superconducting switches
[DE90-000610] N90-14955
Muon SR investigation of magnetism and superconductivity in (Y(1-x)Pr(x))Ba2Cu3O7
[DE90-000689] N90-14956
Superconducting and microstructural properties of shock-compacted high-T sub c oxide powders
[DE90-000823] N90-14958
Applications of superconductor technologies to transportation
[DE90-000856] N90-14961
Charge transfer and bond lengths in YBa2Cu(sub 3-x)M(sub x)O(sub 6+y)
[DE90-002241] N90-14966
Powder neutron diffraction study of the structural phase diagram of the Ba(sub 1-x)K(sub x)BiO3 system
[DE90-002264] N90-14967
RF superconductivity research and development at Los Alamos National Laboratory
[DE90-002440] N90-14969
A model of the isotope effect of the oxide superconductor
[DE89-635907] N90-14971
Macroscopic persistent currents in high temperature ceramic superconductors
[DE89-636232] N90-14973
Anisotropy of oxygen tracer diffusion in YBa2Cu3O7-delta single crystals
[DE90-001931] N90-14979
SUPERCONDUCTORS
The formation of metal-oxygen species at low temperatures
[DE90-002298] N90-14323
The 7th International Conference on Ceramics
[DE90-002144] N90-14374
Studies of neutral and ion transport during laser ablation of 1:2:3 superconductors by optical absorption spectroscopy
[DE90-001968] N90-14604
Use of superconducting plates and shells to deflect magnetic noise fields: Application to MEG
[DE89-012592] N90-14676
Photovoltaic Measurements and Performance Branch
[DE89-009500] N90-14695
Program CICC flow and heat transfer in Cable-In-Conduit Conductors
[DE90-001519] N90-14818
Solid State Division
[DE90-000979] N90-14945
Superconductivity from finite-U valence fluctuations
[DE90-000603] N90-14954
Muon SR investigation of magnetism and superconductivity in (Y(1-x)Pr(x))Ba2Cu3O7
[DE90-000689] N90-14956
Superconducting and microstructural properties of shock-compacted high-T sub c oxide powders
[DE90-000823] N90-14958
Shock-induced defects and flux pinning in YBa2Cu3O sub 7-delta + Ag composites
[DE90-000827] N90-14960
Applications of superconductor technologies to transportation
[DE90-000856] N90-14961
Dissipation measurement in high T(sub c) superconductors with electromagnetic probes
[DE90-002058] N90-14963
The effect of composition and processing on high T(sub c) superconductors containing bismuth
[DE90-002203] N90-14965
A model of the isotope effect of the oxide superconductor
[DE89-635907] N90-14971
Bi-Sr-Ca-Cu-O superconducting ceramics
[DE89-636225] N90-14972
Microstructure and electrical properties of bulk high-T(sub c) superconductors
[DE90-001762] N90-14974
Improved performance of low-T(sub c) superconductors for detection of minimum-ionizing particles
[DE90-001985] N90-14976
SUPERCRITICAL FLUIDS
Supercritical fluid chromatography/supersonic jet spectroscopy
[DE90-001378] N90-14308
SUPERFLUIDITY
Path integral simulations of liquid helium
[DE90-001171] N90-14862
SUPERGIANT STARS
Properties of evolved star circumstellar grains
N90-15003
SUPERGRAVITY
Physics with ultra-low energy antiprotons
[DE90-002397] N90-14888
SUPERLATTICES
Elastic softening in nanocrystalline silicon
[DE90-002268] N90-14377
Magnetic and electrical properties
[DE90-002183] N90-14977
SUPERNOVA REMNANTS
A study of the infrared emission of galactic supernova remnants N90-15006
SUPERNOVA 1987A
The instability and fragmentation of the envelope of supernova 1987A N90-15011
SUPERNOVAE
Perturbation methods for the calculation of gravitational waves from slightly non-spherical spacetimes with applications to stellar core collapse N90-15015
Supernovae, compact stars, and nuclear physics
[DE90-002682] N90-15022
SUPERPLASTICITY
Superplasticity
[AGARD-LS-168] N90-14325
Superplasticity: An overview N90-14326
Superplastic sheet forming N90-14327
Advances and future directions in superplastic materials N90-14328
Cavitation and superplasticity N90-14329
Diffusion bonding of metals N90-14330
The mechanical properties of superplastically formed titanium and aluminium alloys N90-14331
Designing for superplastic alloys N90-14332
The manufacture of superplastic alloys N90-14333
SUPERSONIC BOUNDARY LAYERS
Stability of a supersonic boundary layer on a sharp cone at a small angle of attack N90-14510
SUPERSONIC COMBUSTION
Numerical modeling of supersonic turbulent reacting free shear layers N90-14197
SUPERSONIC COMBUSTION RAMJET ENGINES
Numerical modeling of supersonic turbulent reacting free shear layers N90-14197
RAMSCRAM: A flexible ramjet/scramjet engine simulation program
[NASA-TM-102451] N90-14235
SUPERSONIC FLIGHT
RAMSCRAM: A flexible ramjet/scramjet engine simulation program
[NASA-TM-102451] N90-14235
SUPERSONIC FLOW
A computational analysis of the transonic flow field of two-dimensional minimum length nozzles N90-14194
Supercritical fluid chromatography/supersonic jet spectroscopy
[DE90-001378] N90-14308
An experimental investigation of shear layer mixing in supersonic flows N90-14508
The supersonic anisotropic collapse of Langmuir waves N90-14550
SUPERSYMMETRY
Supersymmetric dark matter above the W mass
[NASA-CR-186168] N90-15016
SUPPLYING
Aerospace vehicle design, spacecraft section. Volume 1: Project Groups 3 through 5
[NASA-CR-186053] N90-14263
Aerospace vehicle design, spacecraft section. Volume 2: Project Groups 6 through 8
[NASA-CR-186054] N90-14264
SUPPORT INTERFERENCE
Subsonic sting interference on the aerodynamic characteristics of a family of slanted-base ogive-cylinders
[NASA-CR-186193] N90-14204
SUPPORT SYSTEMS
Human factors aspects of decision support systems
N90-14408
The Tactical Environmental Support System (TESS(3))
N90-14409
SURFACE ACOUSTIC WAVE DEVICES
Improving the quality of a spread-spectrum radiomobile link N90-14426
SURFACE CRACKS
Crazing and degradation of flexure strength in acrylic plates as a function of time
[AD-A212835] N90-14357
SURFACE DEFECTS
Structure-property relationships in surface-modified ceramics. NATO Advanced Science Institutes, series E: Applied Sciences, volume 170
[AD-A212939] N90-14359
SURFACE DISTORTION
Interferometric surface distortion detector
[AD-D014211] N90-14901
SURFACE ENERGY
An investigation of satellite sounding products for the remote sensing of the surface energy balance and soil moisture
[NASA-CR-186073] N90-14664
SURFACE FINISHING
Influence of hole surface finish, cyclic frequency and spectrum severity on the fatigue behavior of thick section aluminum alloy pin joints
[ARL-STRUC-R-430] N90-14336
The influence of the substrate surface on the nucleation and growth of superconducting thin films
[DE90-003649] N90-14983
SURFACE PROPERTIES
Non-linear optical studies of adsorbates: Spectroscopy and dynamics
[DE90-001543] N90-14312
Superplasticity: An overview N90-14326
Solid State Division
[DE90-000979] N90-14945
Surface magneto-optical studies of ultrathin ferromagnetic films
[DE90-002199] N90-14980
SURFACE ROUGHNESS
X ray reflectivity study of SiO2 on Si
[DE90-001326] N90-14943
SURFACE TEMPERATURE
The thermal behavior of natural backgrounds and its prediction by means of numerical models N90-14436
SURVEYS
Summary of 1987 and 1988 manatee aerial surveys at Kennedy Space Center
[NASA-TM-102783] N90-14669
SWEPT FORWARD WINGS
An in-flight investigation of ground effect on a forward-swept wing airplane
[NASA-TM-101708] N90-14202
SWEPT WINGS
Experimental transonic flutter characteristics of two 72 deg-sweep delta-wing models
[NASA-TM-101659] N90-14205
SWITCHES
Experimental investigation of a fast-acting exploding metallic foil opening switch
[DE90-001051] N90-14479
High speed transfer switch with 50 kA and 50 kV ratings
[DE90-002448] N90-14481
A simple figure of merit for high temperature superconducting switches
[DE90-000610] N90-14955
SWITCHING CIRCUITS
Characterization of two MMIC GaAs switch matrices at microwave frequencies
[NASA-TM-102449] N90-14273
High power density dc/dc converter: Selection of converter topology
[NASA-CR-186129] N90-14467
Inductive store opening switch and tests for energy transfer to a load
[DE90-002818] N90-14482
A cost effective battery bank for I(sup 2)T testing and evaluation of electrical switchgear
[DE90-002350] N90-14490
SYNCHRONIZED OSCILLATORS
Laser activities N90-14576
SYNCHROTRONS
A Scanning Photoelectron Microscope (SPEM) at the National Synchrotron Light Source (NSLS)
[DE90-001551] N90-14537
SYNOPTIC METEOROLOGY
The identification of terrain-induced circulations using principal components
[DE90-001991] N90-14739
The development of a spatial synoptic climatological index for environmental analysis N90-14744
Synoptic scale tropical waves in multichannel satellite radiance data N90-14745
Workshop on synoptic meteorology instruction
[PB90-109950] N90-14751
SYNTHESIS (CHEMISTRY)
Computer synthesis of ceramic preforms for molten-metal infiltration
[DE90-000826] N90-14370

Pentafluorothio polynitroaliphatic explosives
[AD-D014221] N90-14383
SYNTHETIC APERTURE RADAR
Frequency agile synthetic aperture radar
[AD-D014235] N90-14451
SYNTHETIC APERTURES
MERLIN and VLBI observations of the radio galaxy Virgo A N90-15001
SYNTHETIC FUELS
Environmental quality and the shift to alternative fuels: Progress and interim findings of a Department of Energy study of transition in vehicular power systems
[DE90-002178] N90-14716
SYSTEM FAILURES
Electrical breakdown in vacuum
[DE90-001623] N90-14485
A tutorial on software reliability engineering
[DE89-012368] N90-14828
SYSTEMS ANALYSIS
Review of the Aerospace Safety Advisory Panel report for NASA fiscal year 1990 authorization
[GPO-24-234] N90-14213
Preliminary design document: Ground based testbed for avionics systems
[NASA-CR-183821] N90-14231
Mathematical techniques for system realization and identification
[AD-A212088] N90-14841
Solution bias in complex systems modeling
[DE90-002001] N90-14858
SYSTEMS ENGINEERING
Preliminary design document: Ground based testbed for avionics systems
[NASA-CR-183821] N90-14231
Sandia Satellite Program summary of operational procedures
[DE90-000892] N90-14249
The space station tethered elevator system
[NASA-CR-186051] N90-14265
Propagation assessment and tactical decision aids N90-14407
A communications system with an adaptive multi-functional architecture N90-14415
Controller design for a robotic manipulator N90-14615
Exploring the living universe: A strategy for space life sciences
[NASA-TM-101891] N90-14778
Reuse research plans at Langley Research Center N90-14797
Application of reusable software components at the SEI N90-14804
A dynamic systems engineering methodology research study. Phase 2: Evaluating methodologies, tools, and techniques for applicability to NASA's systems projects
[NASA-CR-181319] N90-14985
SYSTEMS INTEGRATION
Engineering sciences design. Design and implementation of components for a bioregenerative system for growing higher order plants in space
[NASA-CR-186056] N90-14761
SSFP approach to software reuse N90-14799
Developing integrated parametric planning models for budgeting and managing complex projects
[NASA-CR-186006] N90-14986
SYSTEMS MANAGEMENT
Impact of domain analysis on reuse methods N90-14792
A dynamic systems engineering methodology research study. Phase 2: Evaluating methodologies, tools, and techniques for applicability to NASA's systems projects
[NASA-CR-181319] N90-14985
SYSTEMS SIMULATION
Definition of avionics concepts for a heavy lift cargo vehicle. Volume 1: Executive summary
[NASA-CR-183818] N90-14229
Definition of avionics concepts for a heavy lift cargo vehicle, volume 2
[NASA-CR-183819] N90-14230

T

TABLES (DATA)
Thermophysical properties of isopropyl alcohol. Part 2: Thermodynamic properties at elevated pressures
[ESDU-89020-PT-2] N90-14300
TACTICS
Propagation-based decision aids in the U.S. Navy N90-14410
Engineer's Refractive Effects Prediction System (EREPS) N90-14411
TARGET ACQUISITION
Airborne FLIR detection of surface targets N90-14416
TASK COMPLEXITY
Payload crew utilization for spacelab missions
[NASA-TP-2976] N90-14256
TASKS
Human factors aspects of decision support systems N90-14408
TECHNOLOGY ASSESSMENT
Propagation assessment and tactical decision aids N90-14407
Battery technology assessment and R and D plan
[DE90-002007] N90-14489
Assessment of research needs for laser technologies applied to advanced spectrographic methods
[DE90-001154] N90-14587
French technological progress in the field of robotics and teleoperation
[DE90-001590] N90-14626
Applications of superconductor technologies to transportation
[DE90-000856] N90-14961
Accessing Japanese technical information: A group of essays extracted from the NTIS (National Technical Information Service) Directory of Japanese Technical Resources in the United States for 1987 and 1988
[PB90-100165] N90-14992
TECHNOLOGY TRANSFER
Technology transfer in software engineering N90-14805
Accessing Japanese technical information: A group of essays extracted from the NTIS (National Technical Information Service) Directory of Japanese Technical Resources in the United States for 1987 and 1988
[PB90-100165] N90-14992
DOD (Department of Defense) Freedom of Information Act Program (incorporating changes 1 and 2)
[PB90-104753] N90-14993
TECTONICS
Organic geochemical and tectonic evolution of the midcontinent rift system: Organic geochemistry and micropaleontology
[DE89-017561] N90-14760
TELECOMMUNICATION
A communications system with an adaptive multi-functional architecture N90-14415
A portable ionosonde in support of reliable communications N90-14431
The use of broadcast signals for passive sensing in automated HF communication systems N90-14433
Communication Overview Program (COP) N90-14435
AdaNET services N90-14806
Publications of the Jet Propulsion Laboratory, 1988
[NASA-CR-185956] N90-14995
TELEMETRY
SAND DEVIL: A digital video link for telemetry applications
[DE90-001879] N90-14259
A rough transform technique for extracting lead features from sea ice imagery
[AD-A212758] N90-14666
TELEOPERATORS
French technological progress in the field of robotics and teleoperation
[DE90-001590] N90-14626
TELESCOPES
Realtime tracking system for wide-field-of-view telescope
[DE90-001147] N90-14908
Design of incoherent imaging arrays
[DE90-000861] N90-14909
Evidence for anomalous cosmic ray hydrogen N90-15005
TELEVISION CAMERAS
CCD TV focal plane guider development and comparison to SIRTF applications
[NASA-CR-185977] N90-14900
TELEVISION SYSTEMS
Theoretical and material studies of thin-film electroluminescent devices
[NASA-CR-186104] N90-14468
TEMPERATURE
Comparison of protective breathing equipment performance at ground level and 8,000 feet altitude using parameters prescribed by portions of FAA action notice A-8150.2
[AD-A212852] N90-14773
TEMPERATURE DEPENDENCE
Flux pinning and microstructure in YBa2Cu3O7
[DE90-001562] N90-14948
TEMPERATURE DISTRIBUTION
Modelling of the effects of the equatorial electrojet on its environment
[DE89-636298] N90-14720
Inverted surface troughs accompanying Rocky Mountain lee-side cyclogenesis N90-14746
TEMPERATURE EFFECTS
Cryogenic temperature effects on sting-balance deflections in the National Transonic Facility
[NASA-TM-4157] N90-14244
Thermophysical properties of isopropyl alcohol. Part 1: The ideal gas and the saturated liquid and vapour
[ESDU-89017-PT-1] N90-14297
The thermally induced gas-phase reactions of methane and oxygen: A comparison of experimental and computational results
[DE90-000785] N90-14317
Superplastic sheet forming N90-14327
The metallurgical determinants of toughness as cryogenic temperature
[DE90-002331] N90-14351
Strength and toughness of monolithic and composite silicon nitrides
[NASA-TM-102423] N90-14368
Airborne FLIR detection of surface targets N90-14416
The thermal behavior of natural backgrounds and its prediction by means of numerical models N90-14436
Effects of composition and age hardening on precious metal electrical contacts
[DE88-008791] N90-14476
Pipe and bend erosion by pneumatic transport of solids at high temperature
[DE89-015741] N90-14524
Shear strain localization phenomenon in viscoplastic materials N90-14649
Low-temperature conversion of high-moisture biomass: Continuous reactor system results
[DE90-000984] N90-14683
Calorimetric measurements on electrochemical cells with Pd-D cathodes
[DE90-002198] N90-14685
TEMPERATURE GRADIENTS
Thermocapillary migration of liquid droplets in a temperature gradient in a density matched system
[NASA-CR-185178] N90-14512
TEMPORAL RESOLUTION
Temporally and spatially resolved flow in a two-stage axial compressor. Part 2: Computational assessment
[NASA-TM-102273] N90-14236
TENSILE PROPERTIES
Spall strength measurements on shockloaded refractory metals
[DE90-000839] N90-14345
Effects of precipitate distribution on 293 K and 77 K properties of 2090-T81 weldments
[DE90-002332] N90-14349
The structure and properties of liquid crystal polymers N90-14356
Predictive aging of elastomers in air: The importance of understanding diffusion-limited oxidation effects
[DE90-001385] N90-14372
Qualification of diode foil materials for excimer lasers
[DE90-000602] N90-14593
TENSILE STRENGTH
The strength-toughness combination of the aluminum-lithium alloys 2090 and 2091 at cryogenic temperatures
[DE90-001425] N90-14338
The effect of hydrogen charging on the mechanical properties of aluminum alloy 2090
[DE90-000129] N90-14341
TENSILE STRESS
Martensite transformation in NiTi alloys induced by tensile stress pulses
[DE90-001832] N90-14346
TENSORS
A tensor product b-spline method for 3D multi-block elliptic grid generation
[DE89-017440] N90-14859
TERRAIN
Forward scatter propagation path loss testing using surrogate terrain in the 100 to 1500 MHz region N90-14425
Low level range coverage performance prediction for VHF radar N90-14439
The identification of terrain-induced circulations using principal components
[DE90-001991] N90-14739
TEST CHAMBERS
Performance evaluation of the Puritan-Bennett crew-member portable protective breathing device as prescribed by portions of FAA action notice A-8150.2
[AD-A211113] N90-14772
TEST FACILITIES
Definition of avionics concepts for a heavy lift cargo vehicle. Volume 1: Executive summary
[NASA-CR-183818] N90-14229
Definition of avionics concepts for a heavy lift cargo vehicle, volume 2
[NASA-CR-183819] N90-14230

Thermal environmental tests on space simulation chamber
[DE90-000927] N90-14251
Flame acceleration studies in the MINIFLAME facility
[DE90-000041] N90-14310
TETHERING
The space station tethered elevator system
[NASA-CR-186051] N90-14265
TEXTS
The design and implementation of an intelligent interface for information retrieval N90-14991
THEOREM PROVING
A comparison result and elliptic equations involving subcritical exponents
[DE90-001772] N90-14850
THEORETICAL PHYSICS
A theoretical perspective on neutrino physics
[DE90-000759] N90-14878
THERAPY
Biological effects of hyperthermia and potential risk associated with ultrasonic exposure
[PB89-100702] N90-14768
THERMAL ANALYSIS
Thermal design of a 10-kW helium refrigerator
[DE90-701785] N90-14403
THERMAL CONDUCTIVITY
Thermal/structural analyses of several hydrogen-cooled leading-edge concepts for hypersonic flight vehicles
[NASA-TM-102391] N90-14511
THERMAL ENERGY
A heat receiver design for solar dynamic space power systems
[NASA-TM-102473] N90-14283
THERMAL ENVIRONMENTS
SRB thermal environments
[NASA-CR-183801] N90-14276
Arcjet thruster research and technology. Phase 1: Executive summary
[NASA-CR-182106] N90-14278
THERMAL FATIGUE
Thermal fatigue durability for advanced propulsion materials
[NASA-TM-102348] N90-14641
THERMAL PLASMAS
Thermal loads on tokamak plasma facing components during normal operation and disruptions
[DE90-000794] N90-14919
THERMAL RADIATION
The thermal behavior of natural backgrounds and its prediction by means of numerical models N90-14436
THERMAL SIMULATION
Thermal environmental tests on space simulation chamber
[DE90-000927] N90-14251
THERMAL STABILITY
Method for stabilization of pan-based carbon fibers
[AD-D014228] N90-14288
Temperature stable ceramic dielectric compositions
[AD-D014209] N90-14358
The 3F condensation polyimides: Review and update
[NASA-TM-102353] N90-14363
Pentafluorothio polynitroaliphatic explosives
[AD-D014221] N90-14383
Thermal stability of jet fuel
[DE90-001160] N90-14385
Study of new materials for gun propellant formulations
[DE89-015285] N90-14388
Electrochemical preparation of silver oxide electrodes having high thermal stability
[AD-D014224] N90-14460
Practical superconductor development for electrical power applications
[DE90-001804] N90-14487
On the thermal stability of flow of a radiating two-component plasma in a porous medium between two rotating cylinders
[DE89-636426] N90-14928
THERMAL STRESSES
Thermal/structural analyses of several hydrogen-cooled leading-edge concepts for hypersonic flight vehicles
[NASA-TM-102391] N90-14511
THERMOCHEMISTRY
Method for fabricating thin film metallic meshes for use as Fabry-Perot interferometer elements, filters and other devices
[AD-D014236] N90-14529
THERMODYNAMIC COUPLING
A model of the isotope effect of the oxide superconductor
[DE89-635907] N90-14971
THERMODYNAMIC EQUILIBRIUM
RAMSCRAM: A flexible ramjet/scramjet engine simulation program
[NASA-TM-102451] N90-14235
THERMODYNAMIC PROPERTIES
Efficient real gas Navier-Stokes computations of high speed flows using an LU scheme
[NASA-TM-102429] N90-14203
High temperature chemistry of complex vaporization/decomposition processes
[DE89-016559] N90-14306
Thermodynamic properties and hydrodynamic response of high-density high-temperature C H N O mixtures
[DE90-000836] N90-14318
Earth Sciences Division annual report 1988
[DE90-002617] N90-14863
Oxygen stoichiometry, structural transitions, and thermodynamic behavior of the YBa2Cu3O(x) system
[DE89-017694] N90-14951
A model of the thermal and electrical properties of cosmic dust particles N90-15014
THERMODYNAMICS
A generalized thermomechanical constitutive model for metal matrix composites with plastic strain and damage N90-14293
Structure-property relationships in surface-modified ceramics. NATO Advanced Science Institutes, series E: Applied Sciences, volume 170
[AD-A212939] N90-14359
Hypervelocity impact calculations using CTH: Case studies
[DE90-002891] N90-14632
Viscoplasticity: A thermodynamic formulation
[NASA-TM-102388] N90-14640
Thermal fatigue durability for advanced propulsion materials
[NASA-TM-102348] N90-14641
New heating and cooling technology: Regenerative heat pump according to the Vuilleumier principle
[DE90-002701] N90-14699
Algorithmic randomness, physical entropy, measurements, and the second law
[DE90-002413] N90-14823
THERMOELECTRIC GENERATORS
Draft Environmental Impact Statement for the Ulysses Mission (Tier 2)
[NASA-TM-102903] N90-14727
THERMOMETERS
Solid-state fluorescence above 1000 C: Application to high-temperature laser thermometry
[DE90-000728] N90-14594
THERMOPLASTIC FILMS
A capacitive technique for real-time monitoring polymer coating thickness on carbon filaments during prepregging process
[NASA-TM-101682] N90-14533
THERMOREGULATION
The effects of nonselective and selective beta blockade upon nonshivering thermogenesis during an acute cold exposure in cold acclimated men N90-14767
THICK PLATES
Finite element analysis of laminated composite plates N90-14291
Crazing and degradation of flexure strength in acrylic plates as a function of time
[AD-A212835] N90-14357
THICKNESS
Measuring the thickness of austenitic weld deposits on carbon steel walls using a magnetic method
[DE89-635446] N90-14628
THIN FILMS
The biocorrosion of copper by biopolymers as examined in situ, in real time FT-IR/CIR/ATR in conjunction with pre and post XPS/AES
[DE90-002086] N90-14348
Fast transit gas- and condensed-phase chemistry of energetic materials
[DE90-001656] N90-14395
Theoretical and material studies of thin-film electroluminescent devices
[NASA-CR-186104] N90-14468
Practical superconductor development for electrical power applications
[DE90-001804] N90-14487
Method for fabricating thin film metallic meshes for use as Fabry-Perot interferometer elements, filters and other devices
[AD-D014236] N90-14529
Research on high-efficiency, multiple-gap, multijunction, amorphous-silicon-based alloy thin-film solar cells
[DE89-009444] N90-14673
Preparation and properties of high deposition a-Si:H films and solar cells using disilane
[DE89-009467] N90-14679
Thin film cadmium telluride, zinc telluride, and mercury zinc telluride solar cells
[DE89-009499] N90-14681
Research on high-efficiency, single-junction, monolithic, thin-film amorphous silicon solar cells
[DE89-000846] N90-14687
Photovoltaic Measurements and Performance Branch
[DE89-009500] N90-14695
Static and dynamic magnetization properties of Y1Ba2Cu3O(sub z) thin films
[DE89-017584] N90-14940
Ion beam analysis and modification of thin-film, high-temperature superconductors
[DE90-000918] N90-14941
X ray reflectivity study of SiO2 on Si
[DE90-001326] N90-14943
Solid State Division
[DE90-000979] N90-14945
Development of a real time monitor for superconductive thin film preparation
[DE89-017772] N90-14952
Magnetotransport studies of epitaxial Cr thin films
[DE90-001930] N90-14975
Magnetic and electrical properties
[DE90-002183] N90-14977
The influence of the substrate surface on the nucleation and growth of superconducting thin films
[DE90-003649] N90-14983
THIN WALLS
The stress analysis of thin-walled screwed tubular joints N90-14637
A finite strip method for the elastic-plastic large displacement analysis of thin-walled and cold-formed steel sections
[PB89-226021] N90-14647
THREADS
The stress analysis of thin-walled screwed tubular joints N90-14637
THREE DIMENSIONAL BODIES
Tire modeling by finite elements N90-14614
THREE DIMENSIONAL FLOW
Numerical investigations in three-dimensional internal flows
[NASA-CR-186068] N90-14189
A note concerning the onset of three dimensionality and time dependence in Goertler vortices
[NASA-CR-181956] N90-14193
Advanced 3-D CFD algorithm for turbomachinery N90-14233
A dynamic multiblock approach to solving the unsteady Euler equations about complex configurations N90-14497
Comparative study of the vorticity field in turbulent flows: Theory, experiments, and computations
[DE90-001399] N90-14516
THREE DIMENSIONAL MODELS
An analysis of the viscous flow through a compact radial turbine by the average passage approach
[NASA-TM-102471] N90-14206
Mechanical properties and morphology of oriented polymer blends N90-14361
THRUST
Effect of pylon wake with and without pylon blowing on propeller thrust
[NASA-TM-4162] N90-14190
Energy deposition in low power coaxial plasma thrusters N90-14911
THULIUM
Magnetic excitations in thulium metal
[DE90-002475] N90-14970
TILT ROTOR AIRCRAFT
Preliminary design of four aircraft to service the California Corridor in the year 2010: The California Condor, California Sky-Hopper, high capacity short range transport tilt rotor aircraft needed to simplify intercity transportation
[NASA-CR-186232] N90-14226
TIME DEPENDENCE
A note concerning the onset of three dimensionality and time dependence in Goertler vortices
[NASA-CR-181956] N90-14193
Crazing and degradation of flexure strength in acrylic plates as a function of time
[AD-A212835] N90-14357
General exact solution for homogeneous time-dependent self-gravitating perfect fluids
[DE89-618425] N90-14514
Nonlinear quantum effects in the Maser model: A large N scaling behaviour
[DE89-631631] N90-14584
TIME DIVISION MULTIPLE ACCESS
Characterization of two MMIC GaAs switch matrices at microwave frequencies
[NASA-TM-102449] N90-14273
TIME LAG
Frequency agile synthetic aperture radar
[AD-D014235] N90-14451
TIME MARCHING
Derivation of synthetic mission profiles from electric vehicle field data
[DE89-011125] N90-14620

Group implicit concurrent algorithms in nonlinear structural dynamics
[NASA-CR-185950] N90-14838
Modified Chebyshev pseudospectral method with O(N exp -1) time step restriction
[NASA-CR-181958] N90-14848
TIME OPTIMAL CONTROL
Optimal control of aero-assisted orbit transfer vehicles N90-14241
TIME SERIES ANALYSIS
Turbulent wind at the equatorial segment of an operating Darrieus wind turbine blade
[DE90-002672] N90-14698
TIMING DEVICES
Precision timing and interlocks systems for FEL (Free-Electron Laser) heating experiments on MTX (Microwave Tokamak Experiment)
[DE90-000833] N90-14923
TIN
Noncontacting laser ultrasonic generation and detection at the surface of molten metal
[DE90-002020] N90-14605
TIN ALLOYS
Primary arm spacing in directionally solidified Pb-10 wt percent Sn alloys
[NASA-CR-185190] N90-14398
TIN OXIDES
Research on high-efficiency, single-junction, monolithic, thin-film amorphous silicon solar cells
[DE89-000846] N90-14687
TIRES
Tire modeling by finite elements N90-14614
TITANIUM
Development of a titanium/boron blending process
[DE90-001450] N90-14386
TITANIUM ALLOYS
The mechanical properties of superplastically formed titanium and aluminium alloys N90-14331
The manufacture of superplastic alloys N90-14333
Martensite transformation in NiTi alloys induced by tensile stress pulses
[DE90-001832] N90-14346
TITANIUM OXIDES
Ordered ceramic membranes
[DE89-017426] N90-14364
TOKAMAK DEVICES
Acceleration of small, light projectiles (including hydrogen isotopes) to high speeds using a two-stage light gas gun
[DE90-002479] N90-14253
Modeling of runaway electron damage for the design of tokamak plasma facing components
[DE90-000847] N90-14914
Thermal loads on tokamak plasma facing components during normal operation and disruptions
[DE90-000794] N90-14919
Microwave Tokamak Experiment (MTX) first year of operation and future plans
[DE90-000817] N90-14920
Microwave Transport Systems for the MTX (Microwave Tokamak Experiment)
[DE90-000821] N90-14921
MTX (Microwave Tokamak Experiment)/ELF (Electron Laser Facility) 2 microwave power measurements and calibration for the 2-GW, 140-GHz, ELF 2 Free Electron Laser (FEL)
[DE90-000825] N90-14922
Precision timing and interlocks systems for FEL (Free-Electron Laser) heating experiments on MTX (Microwave Tokamak Experiment)
[DE90-000833] N90-14923
Microwave Tokamak Experiment: An overview of the construction and checkout phase
[DE90-000834] N90-14924
Stability of the Global Alfven Eigenmode in the presence of fusion alpha particles in an ignited tokamak plasma
[DE89-016618] N90-14930
Computation of electromagnetic effects in a tokamak due to a plasma disruption
[DE90-001764] N90-14931
Practical aspects of a 2-D edge-plasma model
[DE90-002995] N90-14932
Fundamental studies of fusion plasmas
[DE90-002343] N90-14933
TOMOGRAPHY
Tomographic imagery by multislot coding applied to x ray diagnostics of laser plasmas: Implementation of a direct electronic detection camera N90-14579
TOPOGRAPHY
Climatology of Lawrence Livermore National Laboratory
[DE90-000905] N90-14756
TOROIDAL PLASMAS
Anisotropy of electron distributions related to the anisotropy and polarization of the continuous emitted x rays N90-14566
Toroidal rotation retardation and ion anomalous transport by drift waves in a tokamak
[DE89-634427] N90-14913
Thermal loads on tokamak plasma facing components during normal operation and disruptions
[DE90-000794] N90-14919
Computation of electromagnetic effects in a tokamak due to a plasma disruption
[DE90-001764] N90-14931
Practical aspects of a 2-D edge-plasma model
[DE90-002995] N90-14932
TORSION
Flexural and torsional-flexural buckling of thin-walled open section struts
[ESDU-89007] N90-14643
TOUGHNESS
The metallurgical determinants of toughness as cryogenic temperature
[DE90-002331] N90-14351
TRACE ELEMENTS
Mobility of sulfur in thermally altered meteorites N90-15010
TRACKING (POSITION)
Realtime tracking system for wide-field-of-view telescope
[DE90-001147] N90-14908
TRAILING EDGES
Hinge moment coefficient derivatives for trailing-edge controls on wings at subsonic speeds
[ESDU-89009] N90-14239
TRAJECTORIES
Optimal trajectories for the aeroassisted flight experiment
[NASA-CR-186133] N90-14250
Guidance, steering, load relief and control of an asymmetric launch vehicle
[NASA-CR-185598] N90-14257
Aerobraking characteristics for several potential manned Mars entry vehicles
[NASA-TM-101669] N90-14272
TRAJECTORY CONTROL
Manipulation strategies for massive space payloads
[NASA-CR-186081] N90-14247
TRAJECTORY OPTIMIZATION
Guidance and Control strategies for aerospace vehicles
[NASA-CR-186195] N90-14243
Optimal trajectories for the aeroassisted flight experiment
[NASA-CR-186133] N90-14250
TRANSDUCERS
Method and apparatus to enhance the sensitivity of cylindrical magnetostrictive transducer to magnetic fields
[AD-D014218] N90-14459
High power transducers
[AD-D014225] N90-14461
TRANSFER FUNCTIONS
Evaluation of the indirect effects of lightning on a system: Double transfer function method
[RAE-TRANS-2172] N90-14211
AcSim: Aircraft simulation program with application to flight profile generation
[AD-A212466] N90-14217
Design of a compensation filter for a quadratic phase communication channel N90-14428
Applications of a new exact solution of the Navier-Stokes equations to flow in pipes of varying width N90-14504
TRANSFER ORBITS
Optimal trajectories for the aeroassisted flight experiment
[NASA-CR-186133] N90-14250
TRANSFERRING
High speed transfer switch with 50 kA and 50 kV ratings
[DE90-002448] N90-14481
TRANSFORMATIONS (MATHEMATICS)
A helicopter flight path controller design via a nonlinear transformation technique N90-14242
TRANSFORMERS
High power density dc/dc converter: Selection of converter topology
[NASA-CR-186129] N90-14467
TRANSIENT RESPONSE
Transient response of flexible rotor-bearing systems subjected to combined unbalance and ground excitations N90-14616
TRANSITION FLOW
The laminar to slug flow transition in Hele-Shaw flow
[DE90-000636] N90-14521
TRANSITION METALS
First-principles interatomic potentials in transition metals: Multi-ion interactions and their analytic representation
[DE90-001990] N90-14353
Electrical properties of materials for high temperature strain gage applications
[NASA-CR-186192] N90-14534
TRANSITION TEMPERATURE
The effect of composition and processing on high T(sub c) superconductors containing bismuth
[DE90-002203] N90-14965
Improved performance of low-T(sub c) superconductors for detection of minimum-ionizing particles
[DE90-001985] N90-14976
TRANSMISSION LINES
JPS heater and sensor lightning qualification
[NASA-CR-183830] N90-14530
Program CICC flow and heat transfer in Cable-In-Conduit Conductors
[DE90-001519] N90-14818
TRANSMISSIVITY
Probability density function of optical scintillations (scintillation distribution)
[PB89-103912] N90-14906
TRANSONIC FLOW
A computational analysis of the transonic flow field of two-dimensional minimum length nozzles N90-14194
Navier-Stokes solutions of 2-D transonic flow over unconventional airfoils N90-14195
Computation of unsteady transonic flow about airfoils in frequency domain using the full-potential equation N90-14198
Three-dimensional solution-adaptive grid generation of composite configurations N90-14509
TRANSONIC FLUTTER
Experimental transonic flutter characteristics of two 72 deg-sweep delta-wing models
[NASA-TM-101659] N90-14205
TRANSONIC WIND TUNNELS
Cryogenic temperature effects on sting-balance deflections in the National Transonic Facility
[NASA-TM-4157] N90-14244
TRANSPORT AIRCRAFT
Preliminary design of four aircraft to service the California Corridor in the year 2010: The California Condor, California Sky-Hopper, high capacity short range transport tilt rotor aircraft needed to simplify intercity transportation
[NASA-CR-186232] N90-14226
TRANSPORT PROPERTIES
Local error estimates for discontinuous solutions of nonlinear hyperbolic equations
[NASA-CR-181960] N90-14847
TRANSPORT THEORY
Efficient real gas Navier-Stokes computations of high speed flows using an LU scheme
[NASA-TM-102429] N90-14203
The Delta-t transport protocol: Features and experience useful for high performance networks
[DE89-016542] N90-14832
Fundamental studies of fusion plasmas
[DE90-002343] N90-14933
TRANSPORTATION
Opportunities and prospects for Maglev in North America
[DE90-002190] N90-14627
Applications of superconductor technologies to transportation
[DE90-000856] N90-14961
TRANSPORTATION ENERGY
Opportunities and prospects for Maglev in North America
[DE90-002190] N90-14627
TRAPEZOIDS
Trapezoidal crystal in the six beam implosion N90-14577
TRAVELING WAVE AMPLIFIERS
Theoretical studies of solar lasers and converters
[NASA-CR-186194] N90-14583
TRAVELING WAVE TUBES
Gigatron: A new technology for microwave power devices
[DE90-001086] N90-14483
TREES (PLANTS)
Nitrogen deposition to forest trees
[DE90-003285] N90-14726
TRENDS
Diffusion bonding of metals N90-14330
TRIBOLOGY
Mechanisms of wear in structural ceramic materials N90-14360
TRIGGER CIRCUITS
Pressure sensitive release device
[AD-D014220] N90-14610
TRITIUM
Rapid heating tensile tests of hydrogen-charged high-energy-rate-forged 316L stainless steel
[DE90-000591] N90-14342
Phases in lanthanum-nickel-aluminum intermetallic alloys
[DE90-000651] N90-14343

Lawrence Livermore National Laboratory (LLNL) research on cold fusion
[DE90-000930] N90-14915
Cold fusion: Alchemist's dream
[DE90-000865] N90-14925

TROPICAL REGIONS
Synoptic scale tropical waves in multichannel satellite radiance data N90-14745

TROPOSPHERE
Hybrid PE-ray-mode formulation of high frequency propagation in a bilinear tropospheric surface duct N90-14417
The parabolic equation approach to predicting tropospheric propagation effects in operational environments N90-14418
RPE: A parabolic equation radio assessment model N90-14419
Propagation modeling for some horizontally varying tropospheric ducts N90-14422
Assessment of anomalous propagation predictions using minisonde refractivity data and the parabolic equation method N90-14424
An observational study of intramonthly quasi-periodicities in the Northern Hemisphere, extratropical geopotential height field N90-14729

TROUGHS
Inverted surface troughs accompanying Rocky Mountain lee-side cyclogenesis N90-14746

TUNABLE LASERS
Prospects for wavelength tunable lasers based on vacancy defects in alkaline-earth oxides
[DE90-001078] N90-14592

TUNING
The use of broadcast signals for passive sensing in automated HF communication systems N90-14433

TURBINE BLADES
Turbulent wind at the equatorial segment of an operating Darrieus wind turbine blade
[DE90-002672] N90-14698

TURBINE ENGINES
Fluid flow analysis of the SSME high pressure fuel and oxidizer turbine coolant systems
[NASA-CR-183736] N90-14277

TURBINES
An analysis of the viscous flow through a compact radial turbine by the average passage approach
[NASA-TM-102471] N90-14206

TURBOCOMPRESSORS
Temporally and spatially resolved flow in a two-stage axial compressor. Part 2: Computational assessment
[NASA-TM-102273] N90-14236

TURBOGENERATORS
Expert system for fault diagnostics of rotating machines
[DE89-766980] N90-14621

TURBOMACHINERY
Advanced 3-D CFD algorithm for turbomachinery N90-14233

TURBOPROP ENGINES
User's guide to PMESH: A grid-generation program for single-rotation and counterrotation advanced turboprops
[NASA-CR-185156] N90-14783

TURBULENCE
Numerical modeling of supersonic turbulent reacting free shear layers N90-14197
A one equation turbulence model for transonic airfoils N90-14199
Fluid-particle interaction in solid-liquid two-phase grid turbulence N90-14496
The analysis and modeling of dilatational terms in compressible turbulence
[NASA-CR-181959] N90-14513
Aspects of field theory related to the Zakharov problem N90-14551
Statistics of two-color laser beam propagation in the turbulent atmosphere (spectral correlation)
[PB89-236699] N90-14581
An initial look at the dynamics of the microscale flow field within a large wind farm in response to variations in the natural inflow
[DE89-009501] N90-14682
Convective boundary layer and modeling of dispersion N90-14731

TURBULENCE MODELS
A one equation turbulence model for transonic airfoils N90-14199
A one-dimensional shipboard model for forecasting refractive effects in the planetary boundary layer N90-14442
Group-kinetic theory and modeling of atmospheric turbulence
[NASA-CR-183776] N90-14728

TURBULENT BOUNDARY LAYER
Numerical investigations in three-dimensional internal flows
[NASA-CR-186068] N90-14189

TURBULENT FLOW
A one equation turbulence model for transonic airfoils N90-14199
Acoustic-vortical-combustion interaction in a solid fuel ramjet simulator N90-14234
Embedded function methods for compressible high speed turbulent flow
[NASA-CR-186131] N90-14498
Comparative study of the vorticity field in turbulent flows: Theory, experiments, and computations
[DE90-001399] N90-14516
Selection of the energy-efficient enhancement geometry for single-phase turbulent flow inside tubes
[DE89-017690] N90-14519

TURBULENT JETS
Numerical modeling of supersonic turbulent reacting free shear layers N90-14197

TURBULENT MIXING
Numerical modeling of supersonic turbulent reacting free shear layers N90-14197
An experimental and theoretical study of the aeroacoustics of external-Coanda gas flares N90-14495

TURBULENT WAKES
Effect of pylon wake with and without pylon blowing on propeller thrust
[NASA-TM-4162] N90-14190

TVD SCHEMES
An entropy based approach to nonlinear stability N90-14500

TWO DIMENSIONAL FLOW
Navier-Stokes solutions of 2-D transonic flow over unconventional airfoils N90-14195
Computational investigation of incompressible airfoil flows at high angles of attack
[AD-A205885] N90-14201
Multigrid solutions of elliptic fluid flow problems N90-14507

TWO DIMENSIONAL MODELS
Perturbations in high-velocity gas flow
[DE90-000539] N90-14520
Some edge-enhancing operators and their applications to image enhancement and edge detection N90-14810
A two dimensional power spectral estimate for some nonstationary processes
[NASA-CR-186100] N90-14843
Two-dimensional behavior of Megagauss-field-confined solid fiber Z-pinches
[DE90-000684] N90-14918
Practical aspects of a 2-D edge-plasma model
[DE90-002995] N90-14932

TWO PHASE FLOW
Fluid-particle interaction in solid-liquid two-phase grid turbulence N90-14496
Course A: Numerical modeling of two-phase flows for presentation at Ecole d'Ete d'Analyse Numerique
[DE90-002074] N90-14526
Interfacial area in two-phase flow
[DE90-002210] N90-14527

TYPE 3 BURSTS
Kilometric type III radio bursts and interplanetary transients N90-15038

U

U.S.S.R.
USSR Space Life Sciences Digest. Index to issues 21-25
[NASA-CR-3922(30)] N90-14763

U.S.S.R. SPACE PROGRAM
JPRS Report: Science and technology. USSR: Space. Soviet space program to the year 2000
[JPRS-USP-89-008] N90-14248

U-2 AIRCRAFT
Global stratospheric change: Requirements for a Very-High-Altitude Aircraft for Atmospheric Research
[NASA-CP-10041] N90-14220

ULTRAHIGH FREQUENCIES
Modelling UHF propagation for frequency assignment in radio relay networks N90-14445

ULTRASONIC AGITATION
Cavitation-controlled ultrasonic agitator
[DE90-002773] N90-14871

ULTRASONIC FLAW DETECTION
Nondestructive evaluation of flaw clusters and thin layer interfaces N90-14633

ULTRASONIC RADIATION
Process monitoring using optical ultrasonic wave detection
[DE90-002021] N90-14870
Cavitation-controlled ultrasonic agitator
[DE90-002773] N90-14871

ULTRASONICS
Noncontacting laser ultrasonic generation and detection at the surface of molten metal
[DE90-002020] N90-14805
Biological effects of hyperthermia and potential risk associated with ultrasonic exposure
[PB89-100702] N90-14768

ULTRAVIOLET ASTRONOMY
Ultraviolet properties of hot stars in globular clusters N90-15007

ULTRAVIOLET RADIATION
Measurement of the X-UV emission from the back face of thin foils illuminated by an A4 omega laser N90-14562
X-UV amplification in a plasma column of five centimeters. Five beams experiment N90-14574

ULTRAVIOLET SPECTRA
A source of observational constraints on the structure of Wolf-Rayet winds
[DE90-001236] N90-15023

ULYSSES MISSION
Draft Environmental Impact Statement for the Ulysses Mission (Tier 2)
[NASA-TM-102903] N90-14727

UNDERGROUND TRANSMISSION LINES
Heat transfer of buried pipe for heat pump application
[DE90-000580] N90-14697

UNITED STATES
Science and technology resources in US industry: Surveys of science resources series, 1975-1986
[PB90-107194] N90-14401

UNIVERSE
Is the number of photons conserved in an expanding universe
[DE89-618836] N90-15018

UNSTEADY AERODYNAMICS
Unsteady aerodynamic simulation of multiple bodies in relative motion: A prototype method
[NASA-TM-102181] N90-14188
Computation of unsteady transonic flow about airfoils in frequency domain using the full-potential equation N90-14198
An analytical method for the prediction of unsteady rotor/airframe interactions in forward flight N90-14223
Flight evaluation of a pneumatic system for unsteady pressure measurements using conventional sensors
[NASA-TM-4131] N90-14225
Temporally and spatially resolved flow in a two-stage axial compressor. Part 2: Computational assessment
[NASA-TM-102273] N90-14236
Concurrent processing adaptation of aeroplastic analysis of propfans
[NASA-TM-102455] N90-14656

UNSTEADY FLOW
Unsteady hydromagnetic flow of a radiating gas in a vertical channel with axial temperature variation
[DE90-600934] N90-14525

USER MANUALS (COMPUTER PROGRAMS)
User's guide to PMESH: A grid-generation program for single-rotation and counterrotation advanced turboprops
[NASA-CR-185156] N90-14783
Force user's manual: A portable, parallel FORTRAN
[NASA-CR-4265] N90-14785
GRAFIN: GRAFIX interactive manual
[PB89-232136] N90-14809
The development of an Ada programming support environment database: SEAD (Software Engineering and Ada Database), user's manual
[NASA-CR-181219] N90-14811

V

VACANCIES (CRYSTAL DEFECTS)
Prospects for wavelength tunable lasers based on vacancy defects in alkaline-earth oxides
[DE90-001078] N90-14592

VACUUM
Electrical breakdown in vacuum
[DE90-001623] N90-14485

VACUUM DEPOSITION
Method of sensitizing PB-Salt epitaxial films for Schottky diodes
[AD-D014244] N90-14937

VALLEYS
Image processing of LANDSAT MSS data for buried valley detection in northern Indiana N90-14668

VAPOR DEPOSITION
Study of microcrystalline, silicon-carbon p-layers prepared by photo-CVD and glow discharge
[DE89-009438] N90-14939

VARIABILITY
Tuning of the OSCURS (Ocean Surface Current Simulations) numerical model to ocean surface measurements in the Gulf of Alaska
[PB89-103979] N90-14759

VARIABLE STARS
Equation of state and opacity of dense plasmas
[DE90-002223] N90-14926
VARIANCE
Power spectral estimation algorithms
[NASA-CR-186189] N90-14812
VARISTORS
Energy ratings for metal oxide varistors under repetitively pulsed operation
[DE90-002353] N90-14480
VAX-11 SERIES COMPUTERS
NORDA's pattern analysis laboratory: Current contributions to naval mapping, charting, and geodesy
[AD-A212731] N90-14665
VECTOR ANALYSIS
AcSim: Aircraft simulation program with application to flight profile generation
[AD-A212466] N90-14217
VECTOR CURRENTS
Tuning of the OSCURS (Ocean Surface Current Simulations) numerical model to ocean surface measurements in the Gulf of Alaska
[PB89-103979] N90-14759
VECTORS (MATHEMATICS)
Krylov methods preconditioned with incompletely factored matrices on the CM-2
[NASA-CR-181961] N90-14779
Parallel projected variable metric algorithms for unconstrained optimization
[NASA-CR-181930] N90-14842
Vector fields and gravity on the lattice
[DE89-633865] N90-14860
VEGETATION GROWTH
Carbon dioxide and climate: Summaries of research in FY 1989
[DE90-001791] N90-14723
VELOCITY
Profile measurements of sulfur dioxide, nitrogen oxides, and nitric acid deposition velocities in California's south coast air basin
[PB90-104001] N90-14703
VELOCITY DISTRIBUTION
Fluid-particle interaction in solid-liquid two-phase grid turbulence N90-14496
Characterization of electric vehicle velocity and power profiles using road test data
[DE90-002085] N90-14630
VELOCITY MEASUREMENT
Effective utilization of acoustic wave sensor responses: Simultaneous measurement of velocity and attenuation
[DE90-002580] N90-14872
VENTILATION
High-frequency ventilation in dogs with three gases of different densities
[AD-A212862] N90-14762
VERTICAL AIR CURRENTS
Convective boundary layer and modeling of dispersion N90-14731
The dynamics of simulated convective storms in hurricane environments N90-14747
VERY HIGH FREQUENCIES
Low level range coverage performance prediction for VHF radar N90-14439
VERY LARGE ARRAY (VLA)
VLA and VLBI observations of core dominated quasars N90-15002
VERY LONG BASE INTERFEROMETRY
MERLIN and VLBI observations of the radio galaxy Virgo A N90-15001
VLA and VLBI observations of core dominated quasars N90-15002
VIBRATION
Manipulation strategies for massive space payloads
[NASA-CR-186081] N90-14247
Localized vibrations of nearly periodic structures with irregularities N90-14648
Control of an experiment to measure acoustic noise in the space shuttle
[NPS62-89-022] N90-14869
VIBRATION DAMPING
Dynamics and control of flexible spacecraft during and after slewing maneuvers
[NASA-CR-186123] N90-14270
Measurement of damping of graphite epoxy composite materials and structural joints
[NASA-CR-183802] N90-14286
VIBRATION EFFECTS
Localized vibrations of nearly periodic structures with irregularities N90-14648
VIBRATION TESTS
Measurement of damping of graphite epoxy composite materials and structural joints
[NASA-CR-183802] N90-14286
VIDEO DATA
Data compression techniques applied to high resolution high frame rate video technology
[NASA-CR-4263] N90-14452
VIDEO SIGNALS
SAND DEVIL: A digital video link for telemetry applications
[DE90-001879] N90-14259
VISCOPLASTICITY
Viscoplasticity: A thermodynamic formulation
[NASA-TM-102388] N90-14640
Shear strain localization phenomenon in viscoplastic materials N90-14649
A new uniformly valid asymptotic integration algorithm for elasto-plastic-creep and unified viscoplastic theories including continuum damage
[NASA-TM-102344] N90-14655
VISCOUS FLOW
Unsteady aerodynamic simulation of multiple bodies in relative motion: A prototype method
[NASA-TM-102181] N90-14188
Numerical investigations in three-dimensional internal flows
[NASA-CR-186068] N90-14189
Program VSAERO theory document: A computer program for calculating nonlinear aerodynamic characteristics of arbitrary configurations
[NASA-CR-4023] N90-14200
An analysis of the viscous flow through a compact radial turbine by the average passage approach
[NASA-TM-102471] N90-14206
VISUAL OBSERVATION
Radio and optical observations of nearby active galaxies N90-15000
VISUAL PERCEPTION
Workload induced spatio-temporal distortions and safety of flight
[DE89-016613] N90-14771
VOICE COMMUNICATION
Improved reliability prediction for HF digital voice transmission N90-14429
VOLTAGE CONTROLLED OSCILLATORS
High resolution, wide band Chirp-Z signal analyzer
[AD-D014240] N90-14465
VOLTAGE CONVERTERS (DC TO DC)
High power density dc/dc converter: Selection of converter topology
[NASA-CR-186129] N90-14467
VOLTAGE REGULATORS
Electrical performance characteristics of high power converters for space power applications
[NASA-CR-185947] N90-14279
VOLTMETERS
Personal computer process data acquisition
[DE89-017877] N90-14816
VORTEX FILAMENTS
A composite numerical procedure for calculating the motion of vortex filaments N90-14207
VORTEX RINGS
A composite numerical procedure for calculating the motion of vortex filaments N90-14207
VORTEX SHEETS
An experimental investigation of the interaction between a model rotor and airframe in forward flight N90-14219
VORTICES
An investigation of the bursting of trailing vortices using numerical simulation N90-14191
A note concerning the onset of three dimensionality and time dependence in Goertler vortices
[NASA-CR-181956] N90-14193
A composite numerical procedure for calculating the motion of vortex filaments N90-14207
An experimental investigation of the interaction between a model rotor and airframe in forward flight N90-14219
Acoustic-vortical-combustion interaction in a solid fuel ramjet simulator N90-14234
Comparative study of the vorticity field in turbulent flows: Theory, experiments, and computations
[DE90-001399] N90-14516
VORTICITY
A composite numerical procedure for calculating the motion of vortex filaments N90-14207
Comparative study of the vorticity field in turbulent flows: Theory, experiments, and computations
[DE90-001399] N90-14516
VOYAGER 1 SPACECRAFT
Evidence for anomalous cosmic ray hydrogen N90-15005
VOYAGER 2 SPACECRAFT
Evidence for anomalous cosmic ray hydrogen N90-15005

W

WAKES
An experimental investigation of the interaction between a model rotor and airframe in forward flight N90-14219
An analytical method for the prediction of unsteady rotor/airframe interactions in forward flight N90-14223
Detailed analysis of the wake and free-flow characteristics at the Goodnoe Hills MOD-2 site
[DE90-002725] N90-14692
WALL JETS
An experimental and theoretical study of the aeroacoustics of external-Coanda gas flares N90-14495
Heat transfer in convective boundary layer and channel flows N90-14505
WALLS
Heat transfer in convective boundary layer and channel flows N90-14505
Measuring the thickness of austenitic weld deposits on carbon steel walls using a magnetic method
[DE89-635446] N90-14628
Starlight: A stationary inertial-confinement-fusion reactor with nonvaporizing walls
[DE90-002315] N90-14927
WARFARE
The importance of environmental data N90-14406
Propagation-based decision aids in the U.S. Navy N90-14410
PROPHET and future signal warfare decision aids N90-14412
WARNING SYSTEMS
Field evaluation of a Nissan laser collision avoidance system
[PB90-105602] N90-14215
WASTE ENERGY UTILIZATION
Field testing of a ceramic heat exchanger for heat recovery application
[DE90-002082] N90-14523
WASTE TREATMENT
Environmental Projects. Volume 8: Modifications of wastewater evaporation ponds
[NASA-CR-186099] N90-14700
WASTE WATER
Environmental Projects. Volume 8: Modifications of wastewater evaporation ponds
[NASA-CR-186099] N90-14700
WATER IMMERSION
Integrated G-suit/immersion suit
[AD-A212989] N90-14774
WATER POLLUTION
Steady state model to determine lake resources at risk to acid deposition in the Sierra Nevada, California
[PB89-103995] N90-14705
WATER PRESSURE
Remote sensing of atmospheric water vapour by pressure modulation radiometry N90-14667
WATER QUALITY
Environmental Projects. Volume 8: Modifications of wastewater evaporation ponds
[NASA-CR-186099] N90-14700
An evaluation of trend detection techniques for use in water quality monitoring programs
[PB89-100058] N90-14702
WATER RESOURCES
Steady state model to determine lake resources at risk to acid deposition in the Sierra Nevada, California
[PB89-103995] N90-14705
WATER VAPOR
Remote sensing of atmospheric water vapour by pressure modulation radiometry N90-14667
WAVE EQUATIONS
RPE: A parabolic equation radio assessment model N90-14419
WAVE FUNCTIONS
A diagnostic for determining the quality of single-reference electron correlation methods
[NASA-TM-101929] N90-14874
WAVE PROPAGATION
Operational Decision Aids for Exploiting or Mitigating Electromagnetic Propagation Effects
[AGARD-CP-453] N90-14405
The importance of environmental data N90-14406
Propagation assessment and tactical decision aids N90-14407
Propagation-based decision aids in the U.S. Navy N90-14410
PROPHET and future signal warfare decision aids N90-14412
Long wave propagation assessment N90-14414
Hybrid PE-ray-mode formulation of high frequency propagation in a bilinear tropospheric surface duct N90-14417

Analysis of propagation in an inhomogeneous atmosphere in the horizontal and vertical direction using the parabolic equation method N90-14421
Propagation modeling for some horizontally varying tropospheric ducts N90-14422
Propagation prediction for the North Sea environment N90-14423
Low level range coverage performance prediction for VHF radar N90-14439
Detection of a chirping electromagnetic signal [DE90-002105] N90-14457
Propagation of detonation waves from an impact region [DE90-001184] N90-14515
Nondestructive evaluation of flaw clusters and thin layer interfaces N90-14633
Effective utilization of acoustic wave sensor responses: Simultaneous measurement of velocity and attenuation [DE90-002580] N90-14872

WAVEGUIDES
Long wave propagation assessment N90-14414
Symmetric waveguide junction combiner [AD-D014243] N90-14466

WEAPON SYSTEMS
Operational Decision Aids for Exploiting or Mitigating Electromagnetic Propagation Effects [AGARD-CP-453] N90-14405
The importance of environmental data N90-14406
The parabolic equation approach to predicting tropospheric propagation effects in operational environments N90-14418

WEAR
Mechanisms of wear in structural ceramic materials N90-14360
Friction and wear of glassy carbon in sliding contact, revision 1 [DE90-000743] N90-14365
Pipe and bend erosion by pneumatic transport of solids at high temperature [DE89-015741] N90-14524

WEAR TESTS
Effects of composition and age hardening on precious metal electrical contacts [DE88-008791] N90-14476

WEATHER
Flight in adverse environmental conditions [AGARD-AR-277] N90-14218
Airborne FLIR detection of surface targets N90-14416
The thermal behavior of natural backgrounds and its prediction by means of numerical models N90-14436
Summary of papers, studies, conference presentations: 1987-1988 (from the National Weather Service, southern region) [PB90-103896] N90-14749
Climatology of Lawrence Livermore National Laboratory [DE90-000905] N90-14756

WEATHER FORECASTING
An in-flight technique for wind measurement in support of the space shuttle program [NASA-TM-4154] N90-14224
Summary of 1989 Atlantic tropical cyclone activity and seasonal forecast verification N90-14743
Use of operational 0-6 and 3-9 h quantitative precipitation forecasts for predicting heavy rain events [PB90-103946] N90-14750
A global ocean wind stress climatology based on ECMWF (European Centre for Medium Range Weather Forecasts) analyses [PB90-109968] N90-14752

WEBS (SHEETS)
Stick propellant x ray inspection [AD-A212601] N90-14380

WEIGHT REDUCTION
Aerobraking characteristics for several potential manned Mars entry vehicles [NASA-TM-101669] N90-14272

WELDABILITY
Effects of precipitate distribution on 293 K and 77 K properties of 2090-T81 weldments [DE90-002332] N90-14349
The feasibility of welding of irradiated materials [DE90-002200] N90-14631

WELDED JOINTS
Effects of precipitate distribution on 293 K and 77 K properties of 2090-T81 weldments [DE90-002332] N90-14349
BES welding science contractors summary report, 1988 to 1989 [DE90-001004] N90-14619
Measuring the thickness of austenitic weld deposits on carbon steel walls using a magnetic method [DE89-635446] N90-14628

WHISKER COMPOSITES
Advances and future directions in superplastic materials N90-14328
The 7th International Conference on Ceramics [DE90-002144] N90-14374

WIDE ANGLE LENSES
Theory of wide-angle photometry from standard stars [NASA-CR-185964] N90-14999

WIDEBAND COMMUNICATION
Frequency independent constant beamwidth directional lens antenna for very wideband and multi-channel electromagnetic communications [AD-D014214] N90-14449

WIGGLER MAGNETS
Compact RF-linac free-electron lasers [DE90-002386] N90-14600
INEX (Integrated Numerical Experiment) simulations of the Los Alamos HIBAF (High-Brightness Accelerator Free-Electron Laser) free-electron laser MOPA (Master Oscillator Power Amplifier) experiment [DE90-002387] N90-14601
Microwave Transport Systems for the MTX (Microwave Tokamak Experiment) [DE90-000821] N90-14921

WIND (METEOROLOGY)
Airdata calibration of a high-performance aircraft for measuring atmospheric wind profiles [NASA-TM-101714] N90-14228
The identification of terrain-induced circulations using principal components [DE90-001991] N90-14739
Summary of 1989 Atlantic tropical cyclone activity and seasonal forecast verification N90-14743
Climatology of Lawrence Livermore National Laboratory [DE90-000905] N90-14756

WIND EFFECTS
Airborne FLIR detection of surface targets N90-14416
A global ocean wind stress climatology based on ECMWF (European Centre for Medium Range Weather Forecasts) analyses [PB90-109968] N90-14752

WIND MEASUREMENT
An in-flight technique for wind measurement in support of the space shuttle program [NASA-TM-4154] N90-14224
Airdata calibration of a high-performance aircraft for measuring atmospheric wind profiles [NASA-TM-101714] N90-14228
High resolution Doppler lidar [NASA-CR-183288] N90-14542

WIND PRESSURE
Computer simulation of wind/diesel system operation [DE89-009445] N90-14688

WIND PROFILES
An in-flight technique for wind measurement in support of the space shuttle program [NASA-TM-4154] N90-14224
Airdata calibration of a high-performance aircraft for measuring atmospheric wind profiles [NASA-TM-101714] N90-14228

WIND SHEAR
A candidate concept for display of forward-looking wind shear information [NASA-TM-101585] N90-14232
Adaptive clutter rejection filters for airborne Doppler weather radar applied to the detection of low altitude windshear [NASA-CR-186211] N90-14453

WIND TUNNEL CALIBRATION
Cryogenic temperature effects on sting-balance deflections in the National Transonic Facility [NASA-TM-4157] N90-14244

WIND TUNNEL MODELS
Techniques for extreme attitude suspension of a wind tunnel model in a magnetic suspension and balance system [NASA-CR-181895] N90-14245

WIND TUNNEL TESTS
Measured and predicted aerodynamic coefficients and shock shapes for Aeroassist Flight Experiment (AFE) configuration [NASA-TP-2956] N90-14185
Subsonic sting interference on the aerodynamic characteristics of a family of slanted-base ogive-cylinders [NASA-CR-186193] N90-14204
Cryogenic temperature effects on sting-balance deflections in the National Transonic Facility [NASA-TM-4157] N90-14244
Techniques for extreme attitude suspension of a wind tunnel model in a magnetic suspension and balance system [NASA-CR-181895] N90-14245
Saltation thresholds and entrainment of fine particles at Earth and Martian pressures [NASA-TM-102193] N90-14997

WIND TUNNELS
Comparison of two droplet sizing systems in an icing wind tunnel [NASA-TM-102456] N90-14617

WIND TURBINES
Control of the variable speed generator on the Sandia 34-metre vertical axis wind turbine [DE90-000803] N90-14674
An initial look at the dynamics of the microscale flow field within a large wind farm in response to variations in the natural inflow [DE89-009501] N90-14682
Detailed analysis of the wake and free-flow characteristics at the Goodnoe Hills MOD-2 site [DE90-002725] N90-14692
Turbulent wind at the equatorial segment of an operating Darrieus wind turbine blade [DE90-002672] N90-14698

WIND VELOCITY
High resolution Doppler lidar [NASA-CR-183288] N90-14542
Detailed analysis of the wake and free-flow characteristics at the Goodnoe Hills MOD-2 site [DE90-002725] N90-14692
A global ocean wind stress climatology based on ECMWF (European Centre for Medium Range Weather Forecasts) analyses [PB90-109968] N90-14752

WINDPOWER UTILIZATION
Detailed analysis of the wake and free-flow characteristics at the Goodnoe Hills MOD-2 site [DE90-002725] N90-14692

WINDPOWERED GENERATORS
Computer simulation of wind/diesel system operation [DE89-009445] N90-14688

WINDS ALOFT
Airdata calibration of a high-performance aircraft for measuring atmospheric wind profiles [NASA-TM-101714] N90-14228

WIRE BRIDGE CIRCUITS
Electrothermal response testing more than a quality assurance tool [DE90-001449] N90-14536

WIRE CLOTH
Method for fabricating thin film metallic meshes for use as Fabry-Perot interferometer elements, filters and other devices [AD-D014236] N90-14529

WOLF-RAYET STARS
A source of observational constraints on the structure of Wolf-Rayet winds [DE90-001236] N90-15023

WORKING FLUIDS
Superconducting magnets in space [DE90-002671] N90-14865

WORKLOADS (PSYCHOPHYSIOLOGY)
A candidate concept for display of forward-looking wind shear information [NASA-TM-101585] N90-14232
Workload induced spatio-temporal distortions and safety of flight [DE89-016613] N90-14771

WORKSTATIONS
Advanced Software Development Workstation Project N90-14807
Continuation of research in software for space operations support [NASA-CR-186092] N90-14808

X

X RAY ABSORPTION
Glancing angle x ray studies of oxide films [DE89-017828] N90-14953

X RAY ANALYSIS
Soft x ray microscope using Fourier transform holography [DE90-002291] N90-14539
X ray microprobe for the microcharacterization of materials [DE89-006038] N90-14863
X ray studies of strain, interface, and impurity in semiconductors [DE90-001525] N90-14947

X RAY ASTRONOMY
JPRS Report: Science and technology. USSR: Space. Soviet space program to the year 2000 [JPRS-USP-89-008] N90-14248

X RAY ASTROPHYSICS FACILITY
Long-lived space observatories for astronomy and astrophysics [NASA-CR-185373] N90-14261

X RAY DIFFRACTION
Shock-induced solid state reactions and phase transitions: X ray profile studies on shock-modified Fe3O4 and ZrO2 powders
[DE90-000669] N90-14315
Characterization of nanophase materials by x ray diffraction and computer simulation
[DE90-002270] N90-14378
X ray reflectivity study of SiO2 on Si
[DE90-001326] N90-14943
High-temperature/high-pressure x ray diffraction: Recent developments
[DE89-015255] N90-14949
X RAY IMAGERY
Measurement of the X-UV emission from the back face of thin foils illuminated by an A4 omega laser N90-14562
Tomographic imagery by multislot coding applied to x ray diagnostics of laser plasmas: Implementation of a direct electronic detection camera N90-14579
X ray microimaging for the life sciences
[DE90-002613] N90-14766
Versatility of the CFR algorithm for limited angle reconstruction
[DE90-001421] N90-14817
X RAY INSPECTION
Stick propellant x ray inspection
[AD-A212601] N90-14380
X RAY IRRADIATION
As observational and theoretical investigation of stellar flares N90-15012
X RAY LASERS
Activities report in laser matter interactions
[ETN-90-95515] N90-14544
Study of lithium-like ions for amplifying radiation below 100 angstroms. Experiment at the Rutherford Appleton Laboratory N90-14572
Single beam interactions for the study of x ray lasers N90-14573
X-UV amplification in a plasma column of five centimeters. Five beams experiment N90-14574
Proof-of-principle experiment for a hot electron pumped XUV amplifier
[DE90-000820] N90-14586
Laboratory x ray lasers
[DE90-000879] N90-14590
The development of coherent x ray lasers for x ray holography
[DE90-000784] N90-14595
Ultrahigh-brightness lasers and their applications
[DE90-000877] N90-14596
X RAY SOURCES
The current status of x ray conversion efficiency modeling
[DE90-000931] N90-14591
X RAY SPECTRA
Activities report in laser matter interactions
[ETN-90-95515] N90-14544
Anisotropy of electron distributions related to the anisotropy and polarization of the continuous emitted x rays N90-14566
Study of lithium-like ions for amplifying radiation below 100 angstroms. Experiment at the Rutherford Appleton Laboratory N90-14572
Single beam interactions for the study of x ray lasers N90-14573
Characteristics of an x ray source created by a laser plasma N90-14575
X RAY SPECTROSCOPY
Time integrated study of spectral emission in the X-UV domain at the outlet of a laser shock, at the back of single or double foil targets N90-14561
Measurement of the X-UV emission from the back face of thin foils illuminated by an A4 omega laser N90-14562
Development of X diagnostics with 1 Gw laser pulses N90-14578
Development of X diagnostics around the pulse 1 laser N90-14580
X RAYS
Radiation damage and its influence on source requirements for high resolution x ray holography
[DE90-002508] N90-14540
The current status of x ray conversion efficiency modeling
[DE90-000931] N90-14591
X ray microprobe for the microcharacterization of materials
[DE89-006038] N90-14863
Glancing angle x ray studies of oxide films
[DE89-017828] N90-14953

Y

YAW
Development of a three-axis trim program
[AD-A212883] N90-14237
YIELD STRENGTH
Elasto-plastic analysis of unidirectional fiber-reinforced composites subjected to transverse normal loading using the finite element method N90-14292
Spall strength measurements on shockloaded refractory metals
[DE90-000839] N90-14345
The metallurgical determinants of toughness as cryogenic temperature
[DE90-002331] N90-14351
YTTRIUM COMPOUNDS
Muon SR investigation of magnetism and superconductivity in (Y(1-x)Pr(x))Ba2Cu3O7
[DE90-000689] N90-14956
YTTRIUM OXIDES
High resolution-angle resolved photoemission studies of high temperature superconductors
[DE89-017691] N90-14950
Superconducting and microstructural properties of shock-compacted high-T sub c oxide powders
[DE90-000823] N90-14958
Effects of shock-induced defects on flux pinning in YBa2Cu3O(7-delta)
[DE90-000824] N90-14959
Shock-induced defects and flux pinning in YBa2Cu3O sub 7-delta + Ag composites
[DE90-000827] N90-14960
Anisotropy of oxygen tracer diffusion in YBa2Cu3O7-delta single crystals
[DE90-001931] N90-14979

Z

ZETA PINCH
Two-dimensional behavior of Megagauss-field-confined solid fiber Z-pinches
[DE90-000684] N90-14918
ZINC
The secondary slurry-zinc/air battery
[DE90-002600] N90-14491
ZINC OXIDES
Energy ratings for metal oxide varistors under repetitively pulsed operation
[DE90-002353] N90-14480
ZINC TELLURIDES
Thin film cadmium telluride, zinc telluride, and mercury zinc telluride solar cells
[DE89-009499] N90-14681
ZINC-BROMIDE BATTERIES
Zinc/bromine battery evaluation at SNL (Sandia National Laboratory)
[DE89-015847] N90-14473
ZIRCONIUM HYDRIDES
Reactive flow measurements and calculations for ZrH2-based composite explosives
[DE90-000831] N90-14393
ZIRCONIUM OXIDES
Perturbed angular correlations in zirconia ceramics
[DE89-017272] N90-14369
Solid oxide fuel cells electrodes based on In(sub 2)O(sub 3)-PrO(sub 1.83)-ZrO(sub 2)
[DE90-002666] N90-14691

PERSONAL AUTHOR INDEX

Typical Personal Author Index Listing

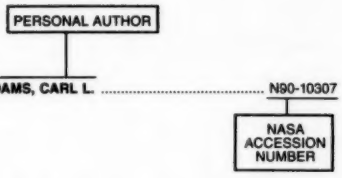

Listings in this index are arranged alphabetically by personal author. The NASA accession number denotes the number by which the citation is identified.

A

AAMODT, R. E. N90-14933
ABOU-ELFOTOUH, F. A. N90-14695
ABREU, VINCENT J. N90-14542
ACCIOLY, A. J. N90-15019
ACKERMAN, B. N90-14689
ADAMOVICH, M. I. N90-14873
ADAMS, T. R. N90-14956
ADCOCK, JERRY B. N90-14244
ADE, HAROLD N90-14537
ADOLF, DOUGLAS N90-14371
AFANASEV, O. V. N90-14861
AGGARWAL, M. M. N90-14873
AHMED, NIZAM UDDIN N90-14731
AHUJA, NARENDRA N90-14839
AJAYI, OYELAYO OLADIMEJI N90-14360
AKAU, RONALD L. N90-14251
AKHIDIME, EVAL N90-14267
AKL, F. A. N90-14652
AKRE, RON N90-14380
ALBRIGHT, S. P. N90-14689
ALCORN, CHARLES W. N90-14204
ALDRIDGE, F. T. N90-14915
ALEXANDER, D. J. N90-14661
ALEXANDROV, Y. A. N90-14873
ALEXOVICH, ROBERT E. N90-14452
ALI, MOHAMED EL-SAYED N90-14502
ALLEN, GARRY N90-14485
ALLEN, KENNETH C. N90-14446
ALLEY, G. T. N90-14475
ALLISON, S. W. N90-14594
ALSOP, C. N90-15037
ALSTON, WILLIAM B. N90-14363
ALTHOFF, SUSAN L. N90-14186
ALTNER, BRUCE M. N90-15007
AMIRANOFF, FRANCOIS N90-14545
N90-14546
AMOS, JEFF N90-15028
ANDERSON, ERIK N90-14537
N90-14539
ANDERSON, LOREN A. N90-14265
ANDERSON, MARC A. N90-14364
ANDERSON, R. A. N90-14469
N90-14479
ANDERSON, R. G. N90-14593
ANDERSON, ROBERT N90-14485
ANDERSON, ROGER E. N90-14782
ANDREW, J. F. N90-14350
ANGEL, JAMES R. N90-14748
ANGIBAULT, FRANCOISE N90-14544
ANSPAUGH, B. E. N90-14672
ANTONIADIS, A. N90-14846
ANTONICHEV, G. M. N90-14861
ANZ-MEADOR, PHILLIP DELBERT N90-15014
APOSTOLAKIS, G. E. N90-14262
ARABSHAHI, ABDOLLAH N90-14497
ARENBURG, ROBERT THOMAS N90-14290
ARENDT, P. N. N90-14968
ARENDT, RICHARD GILES N90-15006
ARENSTORF, NORBERT S. N90-14785
ARGROW, BRIAN MAURICE N90-14194
ARKO, A. J. N90-14950
ARMENGAUD, MICHEL N90-14547
N90-14554
ARNAS, CECILE N90-14547
N90-14548
N90-14564
ARORA, R. N90-14873
ARTERBURY, R. L. N90-14237
ASAY, J. R. N90-14254
ASAY, JAMES R. N90-14345
ASHLEY, J. C. N90-14882
ASHWAL, L. D. N90-14736
ATTOCKNIE, P. A. N90-14773
ATTWOOD, DAVID N90-14766
AUER, LARRY H. N90-15023
AUFLICK, JACK L. N90-14777
AWADALLA, N. G. N90-14635
AYRA, R. R. N90-14687
AZEVEDO, S. G. N90-14824

B

BACA, THOMAS J. N90-14654
BADAL, DAVID L. N90-14801
BADER, S. D. N90-14980
BAE, GYOUNG HYUN N90-14241
BAKER, E. G. N90-14683
BAKER, J. E. N90-14979
BAKER, KARL W. N90-14283
BALACHANDRAN, UTHAMALINGAM N90-14487
N90-14684
N90-14690
N90-14974
BALASUBRAMANIAM, R. N90-14512
BALDOCCHI, DENNIS D. N90-14711
BALKE, B. N90-14915
BALLARD, PATRICK N90-14557
BANKS, WILLIAM W. N90-14770
BANON, JOSE N90-14567
BARBOUX, P. N90-14966
BARINAGA, CHARLES J. N90-14322
BARKER, LYNN M. N90-14246
N90-14345
BARNARD, J. C. N90-14692
BARNES, JOHN E. N90-14542
BARRETT, CHRISTOPHER L. N90-14771
BARTON, BOB N90-14766
BASARAN, OSMAN A. N90-14316
BASOVA, E. N90-14873
BASSOM, ANDREW P. N90-14193
BASU, S. N90-14809
BASU, SOUMENDRA NATH N90-14983
BATCHELOR, D. B. N90-14456
BATEMAN, VESTA I. N90-14535
BATES, J. LAMBERT N90-14691
BEACH, TIMOTHY A. N90-14206
BEALE, W. T. N90-14696
BEAUCHAMP, R. L. N90-14471
BECHER, P. F. N90-14374
BECKLIN, ERIC E. N90-14261
BECKWITH, STEVEN V. W. N90-14261
BEDARD, M. G. N90-14430
BEEMAN, RANDY N90-15028
BEERY, J. G. N90-14968
BELL, H. H. N90-14924
BELL, LARRY N90-14267
BELL, R. GLENN N90-14535
BELL, R. MICHAEL N90-14259
BELLEMAIN, A. N90-14579
BELLISSARD, J. N90-14938
BENATTAR, RENE N90-14562
N90-14563
N90-14580
BENEDICK, W. B. N90-14310
BENNER, ROBERT E. N90-14455
BENNETT, B. L. N90-14968
BENNETT, M. S. N90-14687
BENOLIEL, I. N90-14435
BENTEN, MUHAMMAD S. N90-14785
BENTLEY, J. N90-14957
BERAN, PHILIP STEWART N90-14191
BERGE, LUC N90-14548
N90-14550
N90-14551
N90-14564
BERKNER, K. H. N90-14885
BERNSTEIN, E. M. N90-14885
BERRYMAN, HARRY N90-14779
BERTEL, L. N90-14427
BESENBACHER, F. N90-14344
BESHEARS, D. L. N90-14296
BESS, T. DALE N90-14741
BESTMAN, A. R. N90-14525
N90-14719
N90-14720
N90-14928
BHALLA, K. B. N90-14873
BHASIN, A. N90-14873
BHAT, P. K. N90-14679
BHATIA, MANJIT S. N90-14812
BHATIA, V. S. N90-14873
BHATT, RAMAKRISHNA T. N90-14287
BIJLEVELD, J. H. M. N90-14892
BIRMAN, KENNETH P. N90-14826
N90-14837
BISHOP, G. J. N90-14430
BISHOP, PETER C. N90-14805
BISHOP, STEPHEN G. N90-14936
BISSONNETTE, LAURENT C. N90-14255
BISSONNETTE, LUC R. N90-14437
BJARKE, LISA J. N90-14224
BLACK, KEN U. N90-14986
BLACKMAN, HAROLD N90-14858
BLAMBERG, DONALD L. N90-14990
BLANDER, M. N90-14951
BLOOM, I. D. N90-14487
BLOOMFIELD, HARVEY S. N90-15030
BLOYD, C. N. N90-14724
BOEKEMA, C. N90-14956
BOELITZ, FREDERICK W. N90-14257
BOHN, M. P. N90-14402
BOLSHOV, L. A. N90-14585
BOLT, H. H. N90-14914
BONDARENKO, R. A. N90-14873
BONIVERT, W. D. N90-14337
BOOK, WAYNE J. N90-14247
BOOTH, EARL R., JR. N90-14190
BORDES, NICOLE N90-14983
BORGMANN, DETLEV N90-14448
BORREGO, J. M. N90-14694
BORZONE, LUIS A. N90-14524
BOTINEAU, JEAN N90-14556
BOTTOMLEY, I. N90-14331
BOUDENE, JEAN-MICHEL N90-14563
BOULDIN, D. W. N90-14475
BOUSQUET, CLAIRE N90-14568
BOWERS, J. N90-14915
BOWHILL, SIDNEY A. N90-14735
BOWLING, DONALD R. N90-14466
BOWMAN, ALLEN L. N90-14389
BRAAMS, B. J. N90-14932
BRADLEY, RAYMOND S. N90-14707
BRAND, ALBERT GERARD N90-14219
BRANDOW, B. H. N90-14954
BRASE, J. N90-14824
BRASHEAR, H. R. N90-14475
BREITHAUPT, R. DON N90-14384
N90-14393
BRESSIANI, JOSE CARLOS N90-14972
BREWER, J. A. N90-14687
BRIAND, JACQUES N90-14547
N90-14548
N90-14554
N90-14564
BRIGHT, A. A. N90-14943
BRITCHER, COLIN P. N90-14204
BRITTAIN, JOHN O. N90-14534
BRITTON, C. L., JR. N90-14475
BROADBENT, T. P. N90-14637
BRODSKY, M. B. N90-14975
N90-14977
BROOKFIELD, MORGAN N90-14258
BROOKS, EUGENE D., III N90-14834
BROWN, BARDLE D. N90-14274
BROWN, D. R. N90-14968

BROWN, DAVID B. N90-14787
BROWN, H. C. N90-14294
BROWN, JAMES C. N90-14717
BROWN, JAMES W. N90-14795
BROWN, SUSAN N90-15028
BRUETSCH, ROBERT I. N90-14613
BRUINSMA, P. J. T. N90-14892
BRUMAGE, WILLIAM H. N90-14838
BRUMITT, B. N90-14975
BRUNEAU, DIDIER N90-14576
BRYAN, SHERYL KAY N90-14293
BRYAN, W. L. N90-14475
BUCHANAN, RELVA C. N90-14358
BUGOS, A. R. N90-14594
BULLEN, D. B. N90-14915
BUNCH, MICHAEL N90-14267
BURKARDT, LEO A. N90-14235
BURKE, A. F. N90-14630
BURKHARD, N. R. N90-14737
BURNETT, T. H. N90-14873
BURNS, THOMAS J. N90-14827
BURSA, MICHAL N90-14364
BURTON, R. GAINES N90-14365
BURTON, RALPH A. N90-14365
BUSH, RALPH W. N90-14334
BUSS, RICHARD H., JR. N90-15003
BUSTAMANTE, PEGGY L. N90-14765
BUTLER, P. C. N90-14473
BUTNER, R. S. N90-14683
BUTTERFIELD, C. P. N90-14210
BUTTRAM, MALCOLM N90-14485

C

CABLE, M. D. N90-14915
CAFFEE, M. N90-14915
CAGEAO, RICHARD PHILIP N90-14732
CALHOUN, JOHN N90-15028
CAMERON, CHARLES B. N90-14869
CAMPBELL, R. B. N90-14915
CANN, GERALD N90-14406
CAPPS, G. J. N90-14296
CAPPS, STEPHEN N90-14267
CARATORI, J. N90-14434
CARILLON, ANTOINE N90-14572
N90-14573
N90-14574
CARLSON, D. E. N90-14687
CARLSON, G. A. N90-14366
CARLSON, HARRY W. N90-14187
CARLSON, N. M. N90-14605
CARLSTEN, BRUCE E. N90-14600
N90-14601
CARTALIS, CONSTANTINOS IOANNIS N90-14733
CARTER, M. D. N90-14456
CARTER, RICHARD J. N90-14776
CARTER, WILLIAM N90-14463
CARUSO, J. J. N90-14294
CATALANO, A. W. N90-14687
CATES, M. R. N90-14296
N90-14594
CATTO, P. J. N90-14933
CERJAN, C. N90-14586
CHA, PHILIP DAO N90-14648
CHABOCHE, J. L. N90-14640
CHAKER, M. N90-14575
CHAMBERT, G. N90-14211
CHAMIS, C. C. N90-14294
CHAN, J. W. N90-14347
N90-14351
CHAN, S.-K. N90-14964
CHANG, MARY C. N90-14765
CHANG, SHIH-HUNG N90-14844
CHANG, Y. C. N90-14950
CHAPMAN, JOHN J. N90-14533
CHAPMAN, K. RENEE N90-14756
CHARALAMBOUS, C. D. N90-14243
CHARBA, JEROME P. N90-14750
CHASE, J. B. N90-14482
N90-14492
CHATHAM, H. N90-14679
CHAU, H. H. N90-14470
CHEN, C. H. N90-14952
CHEN, CHIPING N90-14598
CHEN, G. N90-14696
CHEN, JIE N90-14323
CHEN, Y. N90-14592
CHENAIS-POPOVICS, CLAUDE N90-14560
N90-14561
CHENG, CHUNYUEN RAYMOND N90-14867
CHEUNG, J. O. N90-14616
CHEUNG, N. W. N90-14944
CHHABILDAS, LALIT C. N90-14345
CHIAO, LEROY N90-14378
CHIAO, T. T. N90-14376
CHILDRESS, CAROLYN N90-14371
CHIN, B. A. N90-14631
CHOCOL, C. N90-14209
CHOMKWAY, VIRAT N90-14291
CHOPRA, M. A. N90-14398
CHOUDHARY, ALOK N. N90-14839
CHRISTIAN, ERIC RICHARD N90-15005
CHRISTIANSEN, ERIC L. N90-14285
CHRISTOU, A. N90-14935
CHU, D. N90-14341
CHU, HARRY N90-14380
CHU, T. L. N90-14681
CHU, TAK-KIN N90-14937
CHULYA, A. N90-14655
CHUNG, H. H. N90-14271
CHUNG, H. M. N90-14354
CHUNG, KYU-SUN N90-14916
CHURNSIDE, JAMES H. N90-14581
N90-14906
CITERNE, J. N90-14426
CLANCY, SEAN PATRICK N90-15011
CLARK, A. N90-14586
CLARK, ARTHUR E. N90-14461
CLARK, M. W. N90-14885
CLARKE, M. J. N90-14646
CLAYTON, E. D. N90-14925
CLOUGH, ROGER L. N90-14372
COFFEY, HELEN E. N90-15031
N90-15032
N90-15033
N90-15034
N90-15035
N90-15039
COFFEY, HOWARD T. N90-14623
N90-14627
COHEN, MICHAEL R. N90-14983
COIRIER, WILLIAM J. N90-14203
COLGAN, TRACY N90-14504
COLLETT, JEFFREY L., JR. N90-14753
COLLIER, MARK D. N90-14808
COLMENARES, C. N90-14915
COLTMAN, MICHAEL N90-14531
COMBS, S. K. N90-14253
COMMON, D. N90-14331
CONNELL, J. R. N90-14698
COOK, M. N90-14530
COOKE, D. W. N90-14956
N90-14968
N90-14969
COPELAND, ROBERT J. N90-14379
COPENHAVER, R. M. N90-14385
CORDOVA, F. A. N90-15020
COTTET, FRANCIS N90-14558
N90-14559
COULAUD, GERARD N90-14567
COUSY, MICHEL N90-14574
COWIE, LENNOX L. N90-14261
COWLEY, PAULA J. N90-14717
COWLING, DAVID H. N90-14838
COX, H. A. N90-14195
CRAIG, K. H. N90-14420
N90-14424
CRAIN, W. K. N90-14276
CRANE, ROGER N90-14283
CRAWFORD, OAKLEY H. N90-14883
CRAWFORD, P. C. N90-14390
CROCKER, MALCOLM J. N90-14286
CROESSMANN, C. D. N90-14914
CROMARTY, ANDREW DAVID N90-14830
CROS, BRIGITTE N90-14555
CROSS, JAMES H., II N90-14813
CROUCH, L. D. N90-14515
CROW, J. E. N90-14956
CUKAUSKAS, EDWARD N90-14463
CURRY, ROBERT E. N90-14202
N90-14225
CURTISS, L. A. N90-14951
CUTTING, J. L. N90-14482
N90-14492
CZECH, B. N90-14951

D

DABROWSKI, B. D. N90-14967
DAIELLO, R. V. N90-14687
DAJEH, DEIFALLAH ALI N90-14510
DALE, VIRGINIA H. N90-14671
N90-14722
DALLEK, STEVEN N90-14460
DAMBOLDT, TH. N90-14447
DANIEL, A. N90-14426
DANYLUK, S. N90-14974
DARDEN, CHRISTINE M. N90-14187
DARQUEY, PATRICK N90-14558
N90-14559
DAUBE, BRUCE C., JR. N90-14753
DAUGHERTY, W. L. N90-14635
DAVENPORT, A. J. N90-14953
DAVEY, JOHN E. N90-14935
DAVID, DANIEL N90-14589
DAVID, S. A. N90-14619
DAVIDSON, KENNETH L. N90-14438
DAVIDSON, RONALD C. N90-14598
DAVIE, NEIL T. N90-14535
DAVIES, PHIL N90-14399
DAVIS, G. R. N90-14667
DAVIS, JAMES ARTHUR N90-14234
DAVIS, ROBERT EUGENE N90-14744
DAVIS, W. T. N90-14754
DAWSON, W. K. N90-14956
DEBEAUCOUDREY, N. N90-14579
DEBROY, T. N90-14619
DECKER, DERON N90-14258
DEES, DENNIS W. N90-14684
N90-14685
N90-14690
DELEEUW, GERRIT N90-14438
DELNICK, FRANK M. N90-14680
DESAI, CHETAN JITENDRA N90-14503
DETAT, BRIGITTE N90-14567
DEUR, JOHN MARK N90-14302
DEWAR, R. L. N90-14864
DEWITT, RICHARD L. N90-14268
DHEZ, P. N90-14574
DIAK, GEORGE R. N90-14664
DIAZ, HENRY F. N90-14707
DICKSON, C. R. N90-14687
DIGMAN, MICHAEL N90-14806
DINGUIRARD, J.-P. N90-14547
N90-14548
N90-14554
N90-14564
DIPPO, P. N90-14695
DIPPOLITO, D. A. N90-14933
DIVAN, DEEPAKRAJ M. N90-14467
DIVECHA, A. P. N90-14611
DOBREV, VLADIMIR K. N90-14853
DOCKERY, G. DANIEL N90-14418
DOGGETT, ROBERT V., JR. N90-14205
DONALDSON, CAMMIE N90-14791
DORRIS, STEPHEN E. N90-14487
N90-14684
N90-14690
DOUCETT, NOEL A. N90-14404
DOW, ROBERT L. N90-14382
DOWGIALLO, E. J. N90-14630
DOWLING, CAROL N90-14990
DOWNEY, J. W. N90-14979
DRAPER, J. V. N90-14625
DRING, ROBERT P. N90-14236
DROEGE, MICHAEL W. N90-14317
DSOUZA, GILES N90-14742
DUBASOV, YU. B. N90-14861
DUBOIS, R. D. N90-14885
DUNN, J. E. N90-14658
DUPREE, ANDREA K. N90-14261
DUSEK, J. T. N90-14487
DUSTIN, MILES O. N90-14283
DWORJANYN, L. O. N90-14816

E

EARLY, E. A. N90-14958
N90-14959
N90-14960
EASTHAM, TONY R. N90-14627
EASTMAN, J. A. N90-14378
EDDINGTON, LEE N90-14443
EDER, FRANZ X. N90-14699
EDMONDS, CHARLES G. N90-14322
EDMONDS, JAMES A. N90-14709
EDWARDS, J. N90-14572
EFTEKHARI, ABE N90-14533
EGUCHI, MASAYOSHI N90-14840
EHERNBERGER, L. J. N90-14224
EICHEL, P. H. N90-14814
EKLUND, DEAN ROBERT N90-14197
ELLIOT, JAMES L. N90-14261
ELLIOTT, C. JAMES N90-14588
N90-14603
N90-14606
ELLIOTT, D. C. N90-14683
ELLIOTT, D. L. N90-14692
ELLIOTT, STEPHEN M. N90-14474
N90-14483
ELRICK, M. G. N90-14528
ELZEIN, G. N90-14426
EMERSON, J. E. N90-14487
EMERY, M. S. N90-14475
ENGEL, C. D. N90-14276

ENGEL, WALTER N90-14381
ENGLAND, H. M. N90-14773
ENLOE, LON N90-14485
ERICKSON, GEORGE N90-14485
ERICKSON, K. L. N90-14395
ERICSON, M. N. N90-14475
ERLEBACHER, G. N90-14513
ERSKINE, DAVID J. N90-14394
ESER, S. N90-14385
ESTES, MAURICE G., JR. N90-14274
ETELAENIEMI, V. N90-14946
ETNYRE, VANCE A. N90-14986
EVANS, SUZANNE THERESA N90-15008
EVERETT, HOBART R., JR. N90-14903
EVERETT, RICHARD K. N90-14289
EVESSON, DONNA N90-14811
EVRENOGLOU, KYRIAKOS M. N90-14767

F

FABBRO, REMY N90-14557
N90-14561
N90-14575
FABRE, EDOUARD N90-14557
N90-14563
FALLER, H. L. N90-14271
FALLER, W. N90-15029
FANG, D. J. N90-14435
FANG, Y. N90-14979
FARAL, BERNARD N90-14561
FARIA, LUIS OLIVEIRA N90-14614
FEDERER, J. I. N90-14352
FEEZEL, L. L. N90-14764
FEINBERG, DANIEL N90-14379
FELDMAN, D. W. N90-14602
FELKER, B. N90-14921
N90-14922
FELSEN, L. B. N90-14417
FERBER, M. K. N90-14375
FERGUSON, JERRY A. N90-14414
FERGUSON, S. W. N90-14921
N90-14922
FERNANDEZ-BACA, J. A. N90-14970
FERRANDO, WILLIAM A. N90-14462
N90-14464
N90-14611
FETTERER, FLORENCE M. N90-14666
FIELDS, D. N90-14586
FIEVET, CHRISTIAN N90-14560
FINK, R. K. N90-14630
FINK, RAYMOND K. N90-14620
FIRTH, JAMES A. N90-14774
FISCHER, JACQUELINE N90-14529
FISCHER, PIERRE N90-14555
FISHER, BENJAMIN R. N90-14768
FISHER, J. R. N90-14208
FITCH, J. P. N90-14824
N90-14909
FLEMING, MICHAEL L. N90-14285
FLEURY, R. N90-14432
FLYNN, EDWARD R. N90-14676
FLYNN, G. J. N90-14738
FOGLER, R. JOSEPH N90-14835
FORTMANN, C. M. N90-14687
FOSTER, C. A. N90-14252
FOSTER, IAN N90-14825
FOSTER, NANCY N90-14701
FOUCHER, F. N90-14432
FOURNET, P. N90-14579
FOURNIER, JEAN N90-14557
FOURNIER, MICHEL N90-14421
FOUST, C. R. N90-14253
FOX, ALAN D. N90-14443
FOY, W. N90-14271
FRANCISCUS, LEO C. N90-14235
FRANKLIN, R. N90-14922
FREED, A. D. N90-14640
FREEMAN, T. L. N90-14842
FREEMAN, WILLIE B. N90-14610
FREESE, J. M. N90-14472
N90-14473
FREISEL, MARK A. N90-14355
FRENKLACH, MICHAEL N90-14305
FRESHOUR, J. PAUL N90-14251
FROST, C. L. N90-14276
FU, G. Y. N90-14930
FUJIEDA, I. N90-14817
FUJIKAWA, GENE N90-14273
FUJITA, V. N90-14625
FULKERSON, WILLIAM N90-14712
FUNKHOUSER, G. E. N90-14772

G

GABUTTI, ALBERTO N90-14976
GADI, FOUARD N90-14573
N90-14574
GAETANO, ARMANDO J. N90-14901
GAETE, PATRICIO N90-14514
GAIER, JAMES R. N90-14362
GALL, ROBERT N90-14751
GALLAGHER, GABRIEL ALOYSIUS N90-14361
GALLAGHER, JOHN S. N90-14261
GANCHEV, ALEXANDER H. N90-14853
GARCIA, G. V. N90-14605
N90-14870
GARNERO, L. N90-14579
GATHMAN, STUART G. N90-14438
GAUTHE, BERNARD N90-14573
N90-14574
GAUTHIER, JEAN-CLAUDE N90-14560
N90-14561
N90-14569
N90-14570
GEESEY, GILL G. N90-14348
GEINDRE, JEAN-PAUL N90-14560
N90-14561
N90-14569
N90-14570
GENTRY, GARL L., JR. N90-14190
GEOHEGAN, D. B. N90-14604
GERLAND, M. N90-14558
GERTLER, ALAN W. N90-14703
GHANDHI, S. K. N90-14694
GHOSH, A. K. N90-14948
GIANOTTO, ANITA K. N90-14348
GIBBS, W. R. N90-14899
GIESELMANN, MARY N90-14364
GILBERT, HAROLD N90-14258
GILL, MICHAEL J. N90-14987
N90-14988
N90-14989
GILL, TEPPER L. N90-14985
GILLEN, KENNETH T. N90-14372
GILLIGAN, J. G. N90-14914
GILLIGAN, WILLIAM H. N90-14383
GILROY, KATHY N90-14790
N90-14792
GILYARD, GLENN B. N90-14225
GINSBERG, D. M. N90-14979
GITOMER, S. J. N90-14588
N90-14602
GIUDICE, G. F. N90-15021
GLADDEN, HERBERT J. N90-14511
GLANTZ, CLIFFORD S. N90-14757
GLAZER, JUDITH N90-14338
N90-14347
N90-14351
GLEN, DANIEL R. N90-14460
GLENDENNING, NORMAN K. N90-15022
GLIMM, JAMES N90-14521
GLOVER, DANIEL N90-14275
GLOVER, RICHARD D. N90-14829
GOATES, STEVEN R. N90-14308
GODART, J. L. N90-14562
GODIOT, JACQUES N90-14555
GOERZ, D. A. N90-14479
GOLDBERG, LEW N90-14543
GOLDSTEIN, JOHN C. N90-14588
N90-14599
N90-14600
N90-14601
GOLDSTEIN, M. E. N90-14517
GOLDSTEIN, W. N90-14586
GOMES, ALAIN N90-14547
N90-14548
N90-14554
N90-14564
GOMES, LAERCIO N90-14972
GONZALEZ, R. N90-14592
GOODMAN, JOHN M. N90-14413
GORETTA, K. C. N90-14487
N90-14965
N90-14974
GORMAN, F. J. N90-14431
GORMAN, STEVE N90-14796
GOTSIS, PASCALIS K. N90-14292
GOUGE, M. J. N90-14253
GOUTELARD, C. N90-14434
GOUVEIA, FRANK J. N90-14756
GOVER, JAMES E. N90-14962
GRAHAM, R. A. N90-14315
GRAHAM, W. G. N90-14885
GRANDE, M. N90-14572
N90-14574
GRANT, C. N90-14824
GRATZ, ROY F. N90-14363
GRAY, E. R. N90-14968
N90-14969
GRAY, HENRY N90-14474
N90-14483
GRAY, K. E. N90-14487
N90-14976
GRAY, L. J. N90-14657
GRAY, WILLIAM M. N90-14743
GREELEY, RONALD N90-14997
GREEN, LEROY G. N90-14394
GREEN, MICHAEL A. N90-14865
GREEN, P. H. N90-14945
GREENE, L. H. N90-14966
GREGOIRE, G. N90-14846
GRIBBIN, JEFF N90-14399
GRIEST, KIM N90-15016
GRIFFIN, CURTIS W. N90-14691
GRIMES, R. N90-14333
GROPP, WILLIAM N90-14779
GROSSMAN, JULIUS N90-14529
GRUMBERG, JEANNE N90-14567
N90-14568
GUENNOU, HELENE N90-14571
GUENTHER, ART N90-14485
GUHA, S. N90-14673
GUILINGER, TERRY R. N90-14680
GUILLEMOT, Y. N90-14211
GULLUGLO, A. N90-14982
GUNDY-BURLET, KAREN L. N90-14236
GUO, WEI N90-14521
GUSTAFSON, JOHN L. N90-14455
GUTSEV, G. L. N90-14877

H

HACHMAN, J. T. N90-14337
HAERING, EDWARD A., JR. N90-14228
HAGHIGHI, A. N90-14809
HAILEY, C. J. N90-14538
HAINES, D. MARK N90-14431
HAINLEY, DONALD C. N90-15030
HAIR, LUCY M. N90-14317
HALE, ELGIE N90-14280
HALE, PAUL D. N90-14541
HALFORD, GARY R. N90-14641
N90-14642
HALL, LAWRENCE O. N90-14836
HALLOUIN, MARTINE N90-14558
N90-14559
HALVERSON, DANNY C. N90-14370
HAMILTON, C. H. N90-14327
HAMMEN, JOHN LEO, III N90-14668
HAMMOND, D. W. N90-14644
HANCOCK, G. J. N90-14645
N90-14646
N90-14647
HANKINS, MICHAEL R. N90-14348
HANNUM, DAVID N90-14371
HANSON, PAUL J. N90-14726
HARDIN, J. E. N90-14486
HARDY, TERRY L. N90-14268
HARRIS, MICHAEL T. N90-14316
HARRISON, BRIAN A. N90-15000
HARRISON, JOHN NORMAN N90-14830
HARRISON, L. N90-14740
HARTMANN, MICHEL N90-14576
HARTZ, WILLIAM G. N90-14452
HARVEY, W. B. N90-14520
HATFIELD, JERRY L. N90-14711
HATFIELD, LYNN N90-14485
HAUSER, SUSAN E. N90-14987
N90-14988
N90-14989
HAWKE, R. S. N90-14254
N90-14482
HAWLEY, SUZANNE LOUISE N90-15012
HAYASHI, S. N90-14625
HAYES, J. M. N90-14760
HAYNES, L. C. N90-14602
HAYS, PAUL B. N90-14542
HEALD, S. M. N90-14943
HEARST, J. R. N90-14737
HEATON, B. D. N90-15013
HEDSTROM, JAMES C. N90-14677
HEIBERGER, JOHN J. N90-14684
N90-14690
HEIDMANN, JAMES D. N90-14206
HEIGES, MICHAEL WILLIAM N90-14242
HEINBOCKEL, JOHN H. N90-14583
HEINE, E. N90-14894
HEISKANEN, K. N90-14817
HELFAND, DAVID J. N90-14261
HELLER, BARBARA A. N90-14765
HELM, F. H. N90-14390
HELVEY, ROGER A. N90-14443

HENDRICKS, J. N90-14209
HENRIKSEN, GARY L. N90-14489
HENSHAW, WILLIAM F. N90-14289
HERITSCH, R. R. N90-14479
HERMAN, SCOTT E. N90-14800
HERRING, J. S. N90-14961
HERTEL, GERARD N90-14704
HESSE, P. N90-14611
HEUTENIK, B. N90-14895
HEYWARD, ANN O. N90-14856
HIBEY, J. L. N90-14243
HIGGINS, E. A. N90-14772
N90-14773
HILDENBRAND, D. L. N90-14306
HILDYARD, MICHAEL LEWIS N90-14499
HILL, CHARLES G., JR. N90-14364
HILL, D. N. N90-14932
HILL, G. V. N90-14624
HILL, JOHN N90-15028
HINKS, D. G. N90-14967
HINTON, DAVID A. N90-14232
HITNEY, HERBERT V. N90-14411
HITTERMAN, R. L. N90-14295
HIYAMA, TADAO N90-14403
HO, V. S. N90-14262
HOARD, R. N90-14209
HOEBELHEINRICH, RANDY L. N90-14831
N90-14833
HOEHN, A. N90-15029
HOFER, WOLFGANG O. N90-14359
HOFFMANN, MICHAEL R. N90-14753
HOJMAN, ROBERTO N90-14514
HOLIBAUGH, ROBERT N90-14804
HOLM, D. D. N90-14589
HOLT, J. B. N90-14958
HOLTKAMP, D. B. N90-14888
HOLYER, RONALD J. N90-14666
HOLZRICHTER, J. F. N90-14915
HOLZSCHEITER, M. H. N90-14888
HONIG, E. M. N90-14955
HOOKE, LYDIA RAZRAN N90-14763
HORII, S. N90-14625
HOSTETLER, LARRY D. N90-14835
HOULTON, R. J. N90-14968
N90-14969
HOWELLS, M. R. N90-14539
HOWORTH, LARK N90-15028
HSU, I-MIN N90-14651
HUANG, SHIH L. N90-14901
HUBBARD, C. R. N90-14315
HUBER, W. J. N90-14675
HUFF, FLOYD A. N90-14748
HUFFMAN, GEORGE N90-14751
HUGHES, HERBERT G. N90-14416
HUGHES, R. J. N90-14888
HUGONIN, J. P. N90-14579
HULBERT, STEVE N90-14537
HULET, E. K. N90-14886
HULL, J. R. N90-14487
HUSSAIN, FAZLE N90-14516
HUSSAINI, M. Y. N90-14513
HUTT, DANIEL L. N90-14437
HUTTON, J. T. N90-14661
HWANG, HORNG-REN N90-14198
HYMAN, JAMES M. N90-14849

I

IBRAHIM, K. Y. N90-14256
ICE, G. E. N90-14863
IDE, R. F. N90-14617
IDER, SITKI KEMAL N90-14609
IGLESIAS, C. A. N90-14926
IM, MOON HYUK N90-14612
INAGAKI, TORU N90-14541
INGRAHAM, W. JAMES, JR. N90-14759
ISAACS, H. S. N90-14953
ISHIHARA, Y. N90-14417
ISHII, M. N90-14527
IVANOV, V. B. N90-14634

J

JACKSON, M. C. N90-14920
JACOBSEN, C. N90-14539
JACOBSON, A. J. N90-14967
JAEGER, E. F. N90-14456
JAEGER, MARC L. N90-14762
JAEGLE, PIERRE N90-14572
N90-14573
N90-14574
JAHAN, M. S. N90-14956
N90-14968
JAMELOT, GERARD N90-14572
N90-14573
N90-14574
JANETZKE, DAVID C. N90-14656
JANNEY, MARK A. N90-14339
JANUS, J. MARK N90-14233
JAYANETTI, J. K. D. N90-14943
JENKINS, EDWARD F. N90-14261
JENKINS, M. G. N90-14375
JENSEN, JACK J. N90-14409
JESINGER, RICHARD N90-14582
JIANG, P. Z. N90-14950
JOCHUM, B. N90-14938
JOHNSEN, H. A. N90-14337
JOHNSON, ERIK N90-14537
JOHNSON, J. A. N90-14605
JOHNSON, J. L. N90-14864
JOHNSON, LARRY R. N90-14623
JOHNSON, S. N90-15029
JOHNSON, S. W. N90-14949
JOHNSTON, KENNETH J. N90-14261
JOLLEY, JOHN G. N90-14348
JONES, PHILIP D. N90-14707
JONES, RUSSEL H. N90-14355
JORDAN, HARRY F. N90-14785
JORGENSEN, J. D. N90-14966
N90-14967
JUNOR, WILLIAM N90-15001

K

KAAN, A. P. N90-14892
KAKAD, YOGENDRA P. N90-14270
KALIL, FORD N90-14260
KALMAN, RODOLT EMIL N90-14841
KAMEGAI, M. N90-14958
N90-14978
KAMIONKOWSKI, MARC N90-15016
KAMPWIRTH, R. T. N90-14487
KANEVSKIJ, M. F. N90-14585
KANSA, EDWARD J. N90-14653
KANYUKOVA, V. D. N90-14585
KAO, YI-HAN N90-14947
KAPLAN, BRUCE N90-14858
KARAN, HIROKO I. N90-14541
KARMARKAR, S. N90-14611
KARPUK, MICHAEL N90-14379
KARTJE, J. N90-15020
KASIK, R. J. N90-14481
KATO, TAKASHI N90-14403
KATZMAN, MARTIN T. N90-14686
KAWAKAMI, H. N90-14625
KAWANO, KATSUMI N90-14403
KEBEDE, A. N90-14956
KECHTER, GEORGE EDWARD N90-14633
KEEL, BYRON M. N90-14453
KEIZER, W. P. M. N. N90-14440
KELLEY, N. D. N90-14682
KELLOGG, MARK A. N90-14709
KEMP, A. H. N90-14415
KENSKI, D. M. N90-14724
KERN, DIETER N90-14537
KESHISHIAN, LEN GEORGE N90-14746
KETTERSON, J. B. N90-14975
KEWISH, R. W., JR. N90-14636
KEY, M. H. N90-14572
KEY, P. W. N90-14645
N90-14647
KHAN, I. A. N90-14852
KHATSYMOVSKY, V. M. N90-14860
KHOROMSKY, B. N. N90-14854
KHOSROVANEH, ABOLHASSAN KHOSROW N90-14304
KIEFFER, JEAN-CLAUDE N90-14547
N90-14548
N90-14554
N90-14564
KIEHN, G. N90-14572
KILAAS, ROAR N90-14820
KILGORE, W. ALLEN N90-14204
KIM, CHANG-HO N90-14649
KIM, YEONGDAE N90-14301
KING, GEORGE A. N90-14734
KING, ROGER J. N90-14279
KINOSHITA, KIM N90-14693
KIRZ, JANOS N90-14537
N90-14539
KITAMURA, TAKAYUKI N90-14642
KITROSSER, D. F. N90-14431
KLAPETZKY, A. J. N90-14968
KLINZING, GEORGE E. N90-14524
KLISNICK, ANNIE N90-14571
N90-14572
N90-14573
N90-14574
KLOBUCHAR, J. A. N90-14430
KNOLL, ANDREW H. N90-14760
KNOX, E. C. N90-14276
KOENIG, MICHEL N90-14567
KOENIGSBERGER, GLORIA N90-15023
KOLLGAARD, RONALD IVAN N90-15002
KONIG, CHARLES E. N90-14485
KORTENIEMI, A. N90-14621
KOSLOFF, DAN N90-14848
KOSSOWSKY, RAM N90-14359
KRAHL-URBAN, BERNHARD N90-14718
KRAISS, K. F. N90-14408
KRAMER, M. J. N90-14960
KREISS, H. O. N90-14513
KRESSE, JOHN N90-14202
KRING, C. T. N90-14625
KROES, F. B. N90-14892
N90-14894
N90-14895
KRUK, J. W. N90-14899
KRUMM, JOHN N90-14902
KRUMPELT, M. N90-14685
KRUSE, FRED A. N90-14670
KUHN, D. L. N90-14815
KUHN, RODNEY N90-14214
KUHNE, CRAIG MILLER N90-14207
KUIJER, L. H. N90-14892
KULAK, R. F. N90-14662
KULKARNI, DEEPAK N90-14788
KUNERTH, D. C. N90-14870
KUPPERMAN, D. S. N90-14295
KURY, JOHN W. N90-14384
N90-14390
KUSCHEL, H. N90-14439
KUTZBACH, JOHN E. N90-14755
KWOK, R. S. N90-14956
KWONG, MAN KAM N90-14850

L

LABAUNE, CHRISTINE N90-14544
N90-14545
N90-14546
LACY, DOVIE E. N90-14678
LADD, ANTHONY J. C. N90-14518
LAGRON, J. C. N90-14574
LAMBRIGHT, JOHN A. N90-14402
LAMOUREUX, MICHELE N90-14565
N90-14566
LANDMANN, A. E. N90-14866
LANG, L. L. N90-14924
LANGER, STEVEN N90-14591
LANZANTE, JOHN ROBERT N90-14729
LARGE, WILLIAM G. N90-14752
LARRICK, BENJAMIN F. N90-14460
LASSUDRIE-DUCHESNE, P. N90-14432
LATAITIS, RICHARD J. N90-14581
N90-14906
LATHAM, ROD N90-14485
LAURSEN, GARY A. N90-14706
LAVAL, G. N90-14552
LAWRENCE, G. P. N90-14969
LAWRENCE, J. DENNIS N90-14828
LAWRENCE, W. P. N90-14871
LEACH, RODMAN N90-14997
LEAX, T. R. N90-14354
LEBARON, B. A. N90-14740
LEBEDEV, A. A. N90-14454
LEBOUCHER, ELISABETH N90-14567
N90-14568
LEE, BO N90-14474
N90-14483
LEE, DANIEL N90-14807
LEE, HARVEY N90-14531
LEE, HUNG SUI N90-14541
LEE, KIEN-YIN N90-14388
LEE, MILTON L. N90-14308
LEE, R. S. N90-14470
N90-14515
LEE, TIMOTHY J. N90-14874
LEE, W. Y. N90-14250
LEE, YIM N90-14565
LEE, YIN-NAN N90-14713
LEGGIERE, D. N90-14271
LEGNANI, ROBERTO N90-14730
LEGRAND, OLIVIER N90-14556
LEGRAND, SUE N90-14786
LEMAY, MICHELE H. N90-14701
LESAOUT, J. Y. N90-14427
LESAR, R. N90-14982
LEVY, M. F. N90-14420
N90-14424
LEWIS, C. L. S. N90-14572
LEYCURAS, CLAUDE N90-14556
LIAW, MORRIS N90-14811
LICHTI, R. L. N90-14956
LIM, DONG-JIN N90-14615
LIN, C. L. N90-14323

LIN, H. T. N90-14631
LINDBERG, S. E. N90-14714
LINDEMUTH, IRVIN R. N90-14918
LINDNER, JUEGEN N90-14448
LINNARTZ, JEAN-PAUL M. G. N90-14445
LIST, R. S. N90-14950
LIU, C. N90-14980
LIU, J. Z. N90-14950
LIU, J.-Z. N90-14979
LIU, R. N90-14950
LIU, S. H. N90-14942
LOACH, PAUL A. N90-14765
LOFTIS, JIM C. N90-14702
LOHRENZ, MAURA C. N90-14665
LOMDAHL, P. S. N90-14982
LONDON, RICHARD A. N90-14540
N90-14595
LOO, JOSEPH A. N90-14322
LORANDOS, JASON N90-14267
LOTT, S. L. N90-14473
LOUARN, PHILIPPE N90-14555
LOVE, C. M. N90-14386
LUIJCKX, G. N90-14892
LUM, BEVERLY Y. N90-14370
LUND, DENISE N90-14267
LUTSKO, J. F. N90-14377
LUXMOORE, ROBERT J. N90-14711
LYNCH, D. W. N90-14950
LYNE, P. J. N90-14772
N90-14773
LYNN, E. E. N90-14282
LYONS, STEVEN W. N90-14443
LYUBOSHITS, V. L. N90-14876

M

MAAS, R. N90-14892
N90-14893
N90-14896
MABILLE, BERTRAND N90-14545
MACCRACKEN, MICHAEL C. N90-14715
MACDOWALL, ROBERT JOHN N90-15038
MACK, GREGORY N90-14821
MACLIN, ARLENE P. N90-14985
MAEZ, M. A. N90-14968
MAHMOOD, TAHIR N90-14505
MAJUMDAR, S. N90-14295
MAKI, J. N. N90-14584
MALAGA, ALFONSO N90-14429
MALIK, JAMES M. N90-14784
MALKA, VICTOR N90-14562
N90-14563
MALNOULT, PHILIPPE N90-14567
MANKE, JOSEPH W. N90-14859
MANN, J. Y. N90-14336
MANN, MICHAEL J. N90-14187
MANSFIELD, CHARLES N90-14485
MANSOUR, AZZAM N. N90-14460
MAPLE, M. B. N90-14958
N90-14959
N90-14960
MARCIANO, WILLIAM J. N90-14878
MARCUS, E. N90-14262
MARSHALL, A. C. N90-14898
MARSHALL, S. E. N90-14866
MARTIN, R. L. N90-14375
MARTIN, S. J. N90-14872
MARWICK, A. D. N90-14944
MARZULLO, KEITH N90-14826
MASHBURN, D. N. N90-14604
MASKEW, BRIAN N90-14200
MASON, G. E. N90-14491
MASON, K. O. N90-15020
MASON, LEE S. N90-15030
MASSEY, W. N90-14209
MATA, FERNANDO N90-14856
MATHRE, JOHN MARK N90-14201
MATLOCK, D. K. N90-14619
MATTHEWS, D. L. N90-14590
N90-14595
MATTHIEUSSENT, GILLES N90-14545
N90-14546
N90-14555
MATTSON, J. E. N90-14975
N90-14977
MAURICE, ALENA K. N90-14358
MAVRIS, DIMITRIS N. N90-14223
MAY, CHARLES H., JR. N90-14813
MAYOTTE, JACKIE R. N90-14339
MAZURKEVICH, G. E. N90-14854
MCALICE, A. J. N90-14482
MCCAUL, EUGENE WILLIAMSON, JR. N90-14747
MCCORMICK, DUANE C. N90-14494
MCCRACKEN, MICHAEL C. N90-14721
MCDANAL, A. J. N90-14281
MCDARMAID, D. S. N90-14331
MCFADEN, CLAY N90-15028
MCGILL, J. A. N90-14969
MCGLAUN, J. MICHAEL N90-14528
N90-14632
MCGRATH, ROBERT T. N90-14919
MCGUIRE, M. J. N90-14974
MCHALE, G. N90-14809
MCHARGUE, CARL J. N90-14359
MCINTYRE, PETER M. N90-14474
N90-14483
MCLEAN, G. A. N90-14772
N90-14773
MCNULTY, I. N90-14539
MCPHEETERS, CHARLES C. N90-14684
N90-14690
MCQUEEN, R. G. N90-14520
MCVEY, BRIAN D. N90-14588
N90-14599
N90-14601
MEACHAM, JAMES A. N90-14259
MEAKIN, ROBERT L. N90-14188
MECHERIKOFF, MIKE N90-14858
MEDVED, S. A. N90-14454
MEHTA, H. S. N90-14635
MEI, VIUNG C. N90-14697
MEI, Z. N90-14347
MEIKSIN, AVERY ABRAHAM N90-15009
MELENDRES, C. A. N90-14311
MELIS, MATTHEW E. N90-14511
MELTON, J. G. N90-14480
MERKLE, J. G. N90-14659
MERKLE, KARL L. N90-14889
MERRIAM, MARSHAL LOCKHART N90-14500
MERRIGAN, MICHAEL A. N90-14227
MESSER, L. N90-14271
MEYER, E. N90-14969
MICELI, P. F. N90-14966
MICHAEL, J. V. N90-14208
MICHALSKI, TOMASZ N90-14765
MICHALSKY, J. J. N90-14740
MICHARD, ALAIN N90-14563
MICKELSON, R. L. N90-14428
MIELE, A. N90-14250
MIKHAJLOV, V. I. N90-14912
MIKHAJLOV, YU. V. N90-14454
MILLER, J. R. N90-14484
MILLER, JOHN C. N90-14607
MILLER, M. N90-14824
MILORA, S. L. N90-14253
MIRCHANDANEY, RAVI N90-14779
MITCHELL, A. W. N90-14967
MITCHELTREE, ROBERT ALAN N90-14199
MITTAZ, J. P. D. N90-15020
MIYAHARA, ROBERT K. N90-14759
MIYASATO, S. N90-14349
MOCKLER, THEODORE T. N90-14511
MOEBES, TRAVIS N90-14803
MOELLER, CLARY N90-14571
MOELLER, JOEL T. N90-14750
MOLAU, N. E. N90-14479
MONTAGUT, ERIC LOUIS N90-14650
MONTES, CARLOS N90-14556
MOODENBAUGH, A. R. N90-14948
MOOK, D. T. N90-14639
MOORE, DAVID N90-14258
MOORE, NATHAN N90-14267
MOOS, P. N90-15029
MORA, PATRICK N90-14553
MORATO, SPERO PENHA N90-14972
MOREL, M. R. N90-14652
MORGAN, MEREDITH ANN N90-14314
MORGAN, T. J. N90-14885
MORIARTY, JOHN A. N90-14353
MOROSIN, B. N90-14315
MORRIS, A. L. N90-14764
MORRIS, C. N90-14969
MORRIS, J. W. N90-14619
MORRIS, J. W., JR. N90-14341
N90-14347
N90-14349
N90-14351
MORRIS, V. R. N90-14698
MORRISON, KELLY I. N90-14813
MOSLEY, W. C. N90-14342
N90-14343
MOSTACCI, DOMINIAZIANO N90-14564
MOULTON, BRYAN J. N90-14202
MOYA, MARY M. N90-14835
MUCCILLO, ELIANA N. S. N90-14972
MUCCILLO, REGINALDO N90-14972
MUELLER, D. W. N90-14885
MUHS, J. D. N90-14296
MUNGER, A. C. N90-14536
MUNIR, ZUHAIR A. N90-14370
MURAKAWA, KIO N90-14267
MURPHY, MICHAEL J. N90-14393
MURTHY, DURBHA V. N90-14656
MYERS, ROGER METCALF N90-14911
MYERS, S. M. N90-14344
MYLES, K. M. N90-14685
MYRA, J. R. N90-14933

N

NAIDU, D. S. N90-14243
NAIL, KEN, JR. N90-15040
NANSTAD, R. K. N90-14661
NASH, A. S. N90-14965
NASTASI, MICHAEL N90-14941
N90-14983
NAYFEH, A. H. N90-14639
NELLIS, W. J. N90-14958
N90-14959
N90-14960
NELSON, J. N90-14271
NELSON, P. A. N90-14478
NEMES, M. C. N90-14584
NERHEIM, ROSALEE N90-14532
NEUBEK, DEB N90-14267
NEUENSCHWANDER, G. G. N90-14683
NEUMANN, D. A. N90-14966
NEUSTADTER, MARC S. N90-14452
NEVILL, GALE E., JR. N90-14761
NEWMAN, M. N90-14209
NEWNAM, BRIAN E. N90-14599
NEWPORT, D. F. N90-14475
NEWSAM, J. M. N90-14967
NEWTON, J. L. N90-14687
NGUYEN, HOE N90-14567
N90-14568
NGUYEN, P. D. N90-14491
NGUYEN, PAUL N90-15028
NGUYEN, TRUNG N90-14677
NICKLOW, R. M. N90-14970
NICOLETTE, VERNON F. N90-14402
NIELSEN, B. BECH N90-14344
NIEMER, K. A. N90-14914
NISHIDA, ANDREW I. N90-14705
NISHIKAWA, KEN-ICHI N90-14934
NOERSKOV, J. K. N90-14344
NOLAN, JOHN N90-14897
NOOMEN, J. G. N90-14892
N90-14896
NOONAN, KEVIN W. N90-14186
NOONKESTER, R. V. N90-14438
NORBURY, JOHN W. N90-14890
NORDLANDER, P. N90-14344
NORRIS, J. R. N90-14764
NOVELLO, M. N90-15018
NOWLEN, STEVEN P. N90-14402

O

OBRIEN, T. K. N90-14963
ODOWD, J. G. N90-14687
OKAMOTO, YOSHI N90-14541
OKEEFE, M. A. N90-14820
OLDENBURG, J. R. N90-14617
OLEN, CARL N90-14856
OLIVEIRA, L. A. R. N90-15018
OLSON, C. G. N90-14950
OLSON, D. L. N90-14619
OLSON, JERRY G. N90-14752
OMORI, E. N90-14625
ONEILL-ROOD, NORA N90-14829
ONEILL, KATHLEEN M. N90-14460
ONEILL, MARK J. N90-14281
ORERA, V. M. N90-14592
ORLOV, M. M. N90-14912
ORTIZ, M. N90-14638
OSHER, J. E. N90-14470
OSIPENKO, M. V. N90-14913
OTTESEN, CORY W. N90-14259
OVERTON, WILLIAM CALVIN, JR. N90-14676

P

PAGE, A. G. N90-14217
PAGELS, W. N90-14271
PAIRE, JEAN-BAPTISTE N90-14546
PALASZEWSKI, BRYAN A. N90-14284
PANG, YAOQI N90-14474
N90-14483
PANOSSIAN, HAGOP V. N90-14269
PAPPERT, RICHARD A. N90-14422
PARIS, BERTRAND N90-14580
PARK, HYE-SOOK N90-14908
PARK, SOON YOUNG N90-14810
PARKER, DAVID HUW N90-14245

PARKER, ELLEN C. N90-14205
PARKER, R. D. N90-14864
PARKES-LOACH, PAMELA S. N90-14765
PARL, STEEN A. N90-14444
PARSEGHIAN, ZAREH N90-14215
PARSONS, CAROLINE N90-14495
PARTRIDGE, P. G. N90-14330
N90-14331
PATEL, JANAK H. N90-14839
PATLAK, JONATHAN N90-14364
PATO, M. P. N90-14584
PATRICK, WILLIAM P. N90-14494
PAUL, ARTHUR S. N90-14985
PAULIKAS, A. P. N90-14950
PAULUS, RICHARD A. N90-14410
PEARCE, ROGER N90-14326
PECKERAR, MARTIN C. N90-14529
PEEBLES, D. E. N90-14476
PEEBLES, LEIGHTON H. N90-14288
PEI, S. Y. N90-14967
PELL, R. A. N90-14336
PELLETIER, G. N90-14550
PENG, SHENG Y. N90-14271
PENKO, PAUL FRANK N90-14506
PEPIN, H. N90-14561
N90-14575
PEREZ-MENDEZ, V. N90-14817
PEREZ, R. N90-14740
PERISON, J. N90-14385
PERRY, A. T. N90-14262
PERRY, M. D. N90-14596
PESME, DENIS N90-14548
N90-14549
N90-14550
N90-14552
PETERSEN, D. E. N90-14923
PETERSON, REID N90-14364
PHALIPPOU, D. N90-14579
PHILLIPS, RONALD D. N90-14702
PHILLPOT, S. R. N90-14377
PICCIOLO, JOHN J. N90-14684
N90-14690
PICHOLLE, ERIC N90-14556
PICKERELL, THOMAS N90-14214
PIEPER, GAIL W. N90-14780
N90-14781
PIHLMAN, MICHAEL N90-14770
PINCOSY, P. A. N90-14482
N90-14492
PINDERA, M. Z. N90-14313
PINOLI, A. A. N90-14491
PITTS, JOHN H. N90-14927
PITZ, WILLIAM J. N90-14317
PLANK, GORDON N90-14531
PLATT, G. K. N90-14282
POEPPEL, ROGER B. N90-14487
N90-14965
N90-14974
POGATSHNIK, G. J. N90-14594
POGUTSE, O. P. N90-14913
POLLACK, JAMES N90-14997
POLLOCK, ROY N90-14862
POPE, L. E. N90-14476
POPERNACK, THOMAS G., JR. N90-14244
POPOVIC, MILORAD B. N90-14474
N90-14483
POQUERUSSE, ALAIN N90-14568
N90-14577
N90-14578
PORTER, G. D. N90-14932
PORTER, ROBERT P. N90-14406
POST, J. C. N90-14892
POTAPCZUK, MARK GREGORY N90-14196
POTAPOV, S. G. N90-14877
POTEAT, R. M. N90-14375
POULSEN, P. N90-14482
PRASAD, R. N90-14852
PRATT, L. M. N90-14760
PRELL, WARREN L. N90-14755
PRICE, D. N90-14586
PRIMUS, THOMAS MICHAEL N90-15010
PROCTOR, PAUL W. N90-14382
PROVANCHA, JANE A. N90-14669
PROVANCHA, MARK J. N90-14669
PROWELL, GROVER N90-14703

Q

QIU, S. L. N90-14323
QUEMENER, YVES N90-14547
N90-14548
N90-14554
N90-14564
QUIMBY, D. C. N90-14603

R

RABAS, T. J. N90-14519
RAGLAND, KENNETH W. N90-14321
RAI, MAN MOHAN N90-14236
RAJAN, JOHN B. N90-14716
RAJU, P. K. N90-14286
RALPH, MARK E. N90-14674
RAMANAN, ARUNA V. N90-14785
RANDLE, IAN P. M. N90-14775
RANGANATH, S. N90-14635
RANK, DAVID M. N90-14900
RANSOM, VICTOR N90-14526
RAO, MOHAN D. N90-14286
RAO, P. S. N90-14845
RAPTIS, A. C. N90-14295
N90-14871
RARBACK, H. N90-14539
RASHIDNIA, N. N90-14512
REASS, W. A. N90-14481
N90-14490
REDA, DANIEL N90-14210
REDEY, L. N90-14685
REDNER, ALEX S. N90-14905
REE, FRANCIS H. N90-14391
N90-14392
REID, PHILIP N90-15028
REILLY, CHARLES H. N90-14856
REINISCH, B. W. N90-14431
REJ, D. J. N90-14917
RENAUDIE, J. F. N90-14218
RENLUND, A. M. N90-14395
RENSINK, M. E. N90-14932
REUTER, DIERK MARTIN N90-14303
REVILL, G. W. N90-14336
REXRODE, STUART N90-15028
RHATIGAN, JENNIFER L. N90-14285
RHUE, LAWRENCE N90-14450
RHYNE, J. J. N90-14966
N90-14970
RIBBENS, C. J. N90-14822
RICCO, A. J. N90-14872
RICE, J. P. N90-14979
RICHARDS, D. R. N90-14967
RICHARDSON, B. S. N90-14626
RICHARDSON, R. A. N90-14630
RICHTER, G. PAUL N90-14268
RICHTER, JUERGEN H. N90-14407
RICHTER, SCOTT W. N90-14678
RIDLEY, NORMAN N90-14329
RIEGER, HARRY N90-14904
RILEY, N. G. N90-14433
RIST, MARK N90-14258
RIVIER, N. N90-14981
ROBERTO, J. B. N90-14944
ROBINSON, NORMAN F. N90-14703
RODRIGUES, LIGIA M. C. S. N90-15017
ROGERS, DAVID N90-14703
ROGERS, F. J. N90-14926
ROGERS, FRED N90-14703
ROGERS, STUART EAMES N90-14501
ROLLETT, ANTHONY D. N90-14983
ROMAIN, JEAN-PIERRE N90-14558
N90-14559
ROMIG, JAMES C. N90-14402
RONN, A. E. N90-14430
ROOKHUIZEN, H. BOER N90-14892
ROSE, E. A. N90-14593
ROSE, ROBERT B. N90-14412
ROSE, WILLIAM C. N90-14189
ROSEN, M. N90-14586
N90-14595
ROSENTHAL, JAY S. N90-14443
ROTE, D. M. N90-14961
ROTHMAN, S. J. N90-14979
ROTMAN, D. A. N90-14313
ROUSSEAUX, CHRISTOPHE N90-14545
N90-14546
ROUTBORT, J. L. N90-14979
RUBLOFF, G. W. N90-14943
RUELLE, N. N90-14427
RUSNAK, B. N90-14969
RUTAN, DAVID N90-14741
RYAN, F. J. N90-14419
RYDER, GRAHAM N90-15027

S

SAIF, A. G. N90-14973
SALEHUDIN, M. N90-14426
SALEM, JONATHAN A. N90-14368
SALIM, J. M. N90-15018
SALTZ, JOEL N90-14779
SANDENAW, T. A. N90-14350
SANDLER, STANLEY I. N90-14307
SANTIAGO, FRANCISCO N90-14937
SAPANKEVICH, A. P. N90-14984
SARICKS, CHRISTOPHER L. N90-14716
SARKAR, S. N90-14513
SATO, MASAHIKO N90-14403
SAVAGE, BLAIR D. N90-14261
SCHADE, H. N90-14939
SCHAEFER, JAMES ROYAL N90-14745
SCHAFFNER, G. N90-14271
SCHECHTER, D. E. N90-14252
SCHIFERL, D. N90-14949
SCHIFFER, JOHN P. N90-14884
SCHLACHTER, A. S. N90-14885
SCHLEGEL, T. T. N90-14773
SCHMIDT, MONICA A. N90-14339
SCHMITT, MARK J. N90-14588
N90-14606
SCHNOOR, JERALD L. N90-14705
SCHOBERT, H. H. N90-14385
SCHRECK, STEFAN GEORG N90-14496
SCHROCK, S. L. N90-14625
SCHULTZ, ROBERT W. N90-14709
SCHWARTZ, M. N. N90-14739
SCHWARZ, R. B. N90-14346
SCHWEGLER, J. N90-14956
SCOPPOLA, E. N90-14938
SCOTESE, ARTHUR E. N90-14901
SCOTT, MICHAEL J. N90-14709
SCOVEL, CLINT N90-14855
SEALOCK, L. J., JR. N90-14683
SEAMAN, C. L. N90-14958
N90-14959
N90-14960
SEARS, MARK P. N90-14455
SEDDOUGUI, SHARON O. N90-14193
SEIDEL, H. EDWARD N90-15015
SEKULA, S. T. N90-14940
SENA, J. TOM N90-14227
SHAFER, STEVEN A. N90-14902
SHALLCROSS, DAVID C. N90-14309
SHANABROOK, BENJAMIN V. N90-14936
SHAW, M. S. N90-14522
SHEAHEN, T. P. N90-14961
SHEEN, S. H. N90-14871
SHEFFIELD, RICHARD L. N90-14600
SHERBY, OLEG D. N90-14328
SHERMAN, M. P. N90-14310
SHERMAN, SARAH BEAN N90-15027
SHI, DONGLU N90-14974
N90-14979
SHIMAMOTO, SUSUMU N90-14403
SHOTTON, CHARLES N90-14802
SHURTER, R. P. N90-14593
SHURYGIN, R. V. N90-14913
SIERRAALCAZAR, H. B. N90-14491
SILVA, WALTER A. N90-14205
SIMPSON, RANDALL L. N90-14390
N90-14393
SINDELAR, R. L. N90-14635
SINGH, J. P. N90-14295
SINGH, MARGARET K. N90-14716
SINHA, S. K. N90-14967
SITZMANN, MICHAEL E. N90-14383
SKOCYPEC, R. D. N90-14395
SKOTHEIM, TERJE A. N90-14541
SKUDERA, WILLIAM J., JR. N90-14465
SKYLLINGSTAD, E. D. N90-14739
SLABE, MELISSA E. N90-14362
SLIVINSKY, V. N90-14586
SLUYK, T. G. B. W. N90-14895
SMADJA, DANIELLE N90-14544
SMAGA, JOHN A. N90-14488
SMITH, CHARLES F. N90-14486
SMITH, D. BARTON N90-14607
SMITH, G. LOUIS N90-14741
SMITH, G. S. N90-14958
SMITH, GREGORY L. N90-14843
SMITH, HOWARD A. N90-14529
SMITH, KATHRYN A. N90-14789
SMITH, RICHARD D. N90-14322
SMITH, U. N90-14764
SMITH, WILLIAM L. N90-14367
SNEDDON, LARRY G. N90-14373
SNYDER, F. PERRY N90-14414
SNYDER, MELVIN H. N90-14222
SNYDER, PEG N90-14799
SOARES, IVANO DAMIAO N90-15017
SOHAL, M. S. N90-14523
SOICHER, H. N90-14435
SOISTMANN, DAVID L. N90-14205
SOMMER, STANLEY C. N90-14389
SONLU, YASAR N90-14441
SOTELINO, E. D. N90-14638
SPAIN, CHARLES V. N90-14205
SPARKS, C. J. N90-14863

SPEARS, DON H. N90-14281
SROLOVITZ, D. J. N90-14982
STACHIW, J. D. N90-14357
STACHIW, J. L. N90-14357
STARKE, T. P. N90-14969
STAUTER, R. CHARLES N90-14236
STEARNS, J. W. N90-14885
STEARNS, SAMUEL D. N90-14457
STEFFES, PAUL G. N90-15025
STEFFLER, JEAN C. N90-14774
STEIN, ANTHONY C. N90-14215
STEIN, W. E. N90-14602
STEINBERG, MEYER N90-14387
STENZEL, R. L. N90-14910
STEPHEN, D. N90-14332
STERNBERG, ROBERT L. N90-14449
STEVENSON, JOEL O. N90-14680
STEVER, R. N90-14922
STEWART, J. M. N90-14315
STINECIPHER, MARY M. N90-14388
STOCKLI, M. P. N90-14885
STONER, KAREN J. N90-14340
STREETS, D. G. N90-14724
STRICKER, JOSEF N90-14907
STRONGIN, MYRON N90-14323
STUART, THOMAS A. N90-14279
SUCHANOV, L. P. N90-14877
SUENAGA, M. N90-14948
SUESSMANN, P. N90-14447
SUIT, WILLIAM T. N90-14272
SULLINS, GARY ALAN N90-14508
SULLIVAN, THOMAS D. N90-14455
SUMMERS, C. J. N90-14468
SUMMERS, L. T. N90-14484
SUNWOO, A. J. N90-14349
N90-14619
SUORTTI, P. N90-14946
SUREAU, ALAIN N90-14571
SUTTON, S. R. N90-14738
SWAIN, R. L. N90-14661
SYLVESTRE, NICOLAS N90-14552
SZEKELY, J. N90-14619
SZYMBER, RICHARD N90-14443

T

TADA, EISUKE N90-14403
TADMOR, EITAN N90-14847
TAG, PAUL M. N90-14442
TAKALLU, M. A. N90-14190
TAL-EZER, HILLEL N90-14848
TALBOTT, C. N90-14993
TAN, M. J. N90-14527
TANI, B. N90-14951
TAO, W. C. N90-14515
TARASCON, J. M. N90-14966
TARTABINI, PAUL V. N90-14272
TARVER, CRAIG M. N90-14393
N90-14394
TAYLOR, A. G. N90-14978
TAYLOR, CHARLES H. N90-14702
TAYLOR, CHARLES J. N90-14529
TAYLOR, G. J. N90-15026
TAYLOR, GEORGE E., JR. N90-14726
TAYLOR, LOUIS L. N90-14425
TAYLOR, PETER R. N90-14874
TAYLOR, STEPHEN N90-14825
TCHEN, C. M. N90-14728
TEAL, G. A. N90-14277
TELSCHOW, K. L. N90-14605
N90-14870
N90-14963
TENNERY, V. J. N90-14375
TEREPKA, F. M. N90-14335
TERRAY, LAURENT N90-14567
TESTARD, D. N90-14938
TETENBAUM, M. N90-14951
TEWARI, S. N. N90-14335
N90-14398
THADHANI, N. N. N90-14346
THAKUR, A. M. N90-14346
THEWS, ERIC R. N90-14418
THODE, L. E. N90-14588
THOMA, GEORGE R. N90-14987
N90-14988
N90-14989
THOMAS, D. L. N90-14661
THOMASSEN, K. I. N90-14915
THOMLINSON, W. N90-14946
THOMPSON, L. J. N90-14378
N90-14979
THOMPSON, ROGER HOWARD N90-14991
THOMPSON, S. L. N90-14262
N90-14528
THOMSEN, RICHARD G. N90-14833
THROOP, A. N90-14922
THURNAUER, M. C. N90-14764
TIESZEN, S. R. N90-14310
TILLEMA, H. F. N90-14866
TIMSIT, HENRI N90-14563
TIPTON, R. E. N90-14470
TOBIN, K. W. N90-14296
TOKAR, R. L. N90-14588
TOLMIE, DON E. N90-14819
TONG, MIKE N90-14511
TOUBHANS, ISABELLE N90-14575
TOURNADE, ANNE-MARIE N90-14563
N90-14576
TOWNSEND, LAWRENCE W. N90-14890
TRAGIN, NATHALIE N90-14560
TRATNIK, MICHAEL V. N90-14589
TREBES, J. N90-14595
TREIMAN, ALLAN H. N90-15004
TRENBERTH, KEVIN E. N90-14752
TRENT, WILLIAM N90-14214
TROTT, W. M. N90-14395
TROTTI, GUILLERMO N90-14267
TROUGHTON, MICHAEL JOHN N90-14356
TRUCANO, TIMOTHY G. N90-14345
N90-14632
TRUSZKOWSKI, WALT N90-14794
TRYSTRAM, D. N90-14845
TSAI, C. C. N90-14252
TU, YEN N90-14509
TURNER, LARRY R. N90-14931
TURNER, MICHAEL S. N90-15016
TUZUN, U. N90-14622

U

UDSETH, HAROLD R. N90-14322
USHER, PETER D. N90-14999

V

VAKNIN, D. N90-14967
VALLEY, LOIS N90-14793
VANDAM, J. W. N90-14930
VANDERBORGH, NICHOLAS E. N90-14677
VANHULSTEYN, DAVID B. N90-14676
VANTHIEL, MATHIAS N90-14318
N90-14391
N90-14392
VAUGHAN, WILLARD S. N90-14769
VAYNER, M. N90-14271
VEAL, B. W. N90-14950
VERDIELL, JEAN-MARC N90-14546
VERNAZZA, J. E. N90-14479
VIETH, R. N90-14423
VIGIL, MANUEL G. N90-14618
VIJAYAKUMAR, M. N90-14335
VISSERS, D. R. N90-14685
VITEK, J. M. N90-14619
VOGTLIN, GEORGE N90-14485
VOIGT, SUSAN J. N90-14789
N90-14797
VOROBEV, V. A. N90-14585

W

WADDEL, KATHRYN C. N90-14813
WADSWORTH, JEFFREY N90-14328
WAGANAAR, W. J. N90-14917
WAGNER, K. N90-14628
WAGNER, R. G. N90-14976
WALES, STEPHEN CHARLES N90-14868
WALKER, CARRIE N90-14797
WALKER, F. L. N90-14987
N90-14988
N90-14989
WALKER, J. D. A. N90-14498
WALKER, K. P. N90-14655
WALTER, J. B. N90-14870
WALTON, ERIC K. N90-14856
WALTON, OTIS R. N90-14518
N90-14978
WANG, T. N90-14250
WARD, ROBERT C. N90-14702
WARREN, P. H. N90-15026
WARREN, ROGER W. N90-14600
N90-14602
WARSI, SAIF A. N90-14783
WASH, CARLYLE N90-14751
WATSON, D. M. N90-14945
WATSON, J. KEVIN N90-14608
WATSON, JOHN G. N90-14703
WATSON, L. T. N90-14822
WATSON, RICHARD W. N90-14832
WATTS, NORMAN W. N90-14404
WEBB, THOMPSON, III N90-14755
WEBER, WILLIAM J. N90-14891
WEHNER, DONALD R. N90-14451
WEILER, J. D. N90-14256
WEINGART, R. C. N90-14470
WEINSTOCK, HERBERT N90-14531
WEIR, S. T. N90-14959
N90-14960
WEISGERBER, SCOTT A. N90-14771
WEISS, DAVID M. N90-14798
WEISS, R. S. N90-14672
WEISSHAAR, TERRENCE A. N90-14216
WELCH, D. O. N90-14948
WELLER, JOSEPH F. N90-14543
WELLMAN, G. W. N90-14246
WELLS, WILLIAM L. N90-14185
N90-14493
WERNER, K. N90-14881
WEST, GEOFFREY B. N90-15024
WESTBROOK, CHARLES K. N90-14317
WESTON, CLAUDIA V. N90-14990
WHALEN, MARGARET V. N90-14268
WHIPPLE, JOHN G. N90-14321
WIBERG, K. B. N90-14324
WICHLACZ, PAUL L. N90-14348
WILDE, STEVE L. N90-14251
WILDS, W. A. N90-14481
WILLI, O. N90-14572
WILLIAMS, LLOYD G. N90-14821
WILTBERGER, N. N90-15029
WINEFORDNER, J. D. N90-14320
WITRIOL, NORMAN M. N90-14838
WOLF, D. N90-14377
WOLLENWEBER, FRITZ G. N90-14436
WONG, ROBERT L. N90-14818
WOOD, LOWELL N90-14857
WORKMAN, GARY L. N90-14397
WRIGHT, JOHN N90-14379
WRIGHT, NIGEL GEORGE N90-14507
WRIGHT, RANDY B. N90-14348
WU, Y. Y. N90-14893
WUEBBLES, DONALD J. N90-14710
WUNDROW, D. W. N90-14517

X

XU, QUNYIN N90-14364
XU, YOUWEN N90-14948

Y

YAMAMURA, HIDEMASA N90-14403
YAN, XINCHE N90-14286
YANG, WEN-CHING N90-14524
YEH, K. C. N90-14428
YOUNG, DAVID A. N90-14319
YOUNG, J. W. N90-14772
YOUNGDAHL, C. A. N90-14974
YOUNGDAHL, CARL K. N90-14860
YUDIN, A. I. N90-14585
YUREK, AILEEN M. N90-14459

Z

ZACHARIA, T. N90-14619
ZACHOS, COSMAS N90-14851
ZAGRODNIK, J. P. N90-14471
ZANELLI, JORGE N90-15017
ZAYTSEV, YURIY IVANOVICH N90-14248
ZEITOUN, P. N90-14546
ZELTNER, WALTER Z. N90-14364
ZHANG, LI-YUAN N90-14971
ZHANG, QIANG N90-14521
ZHANG, Y. N90-14315
ZHAO, Z. G. N90-14250
ZHIDKOV, E. P. N90-14854
ZHU, XIANGDONG N90-14312
ZHU, Y. N90-14948
ZIEDMAN, DAVID N90-14215
ZINN, A. S. N90-14949
ZIOCK, K. P. N90-14538
ZUCCONI, LIN N90-14821
ZUREK, WOJCIECH H. N90-14823
ZURLOYE, AXEL O. N90-14477

Typical Corporate Source Index Listing

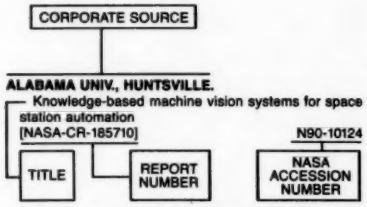

Listings in this index are arranged alphabetically by corporate source. The title of the document provides the user with a brief description of the subject matter. The report number helps to indicate the type of document cited (e.g., NASA report, translation, NASA contractor report). The NASA accession number denotes the number by which the citation is identified. The titles are arranged under each corporate source in ascending accession number order.

A

ADVISORY GROUP FOR AEROSPACE RESEARCH AND DEVELOPMENT, NEUILLY-SUR-SEINE (FRANCE).
AGARD Highlights 89/2 N90-14184
Flight in adverse environmental conditions
[AGARD-AR-277] N90-14218
Superplasticity
[AGARD-LS-168] N90-14325
Operational Decision Aids for Exploiting or Mitigating Electromagnetic Propagation Effects
[AGARD-CP-453] N90-14405

AERONAUTICAL RESEARCH LABS., MELBOURNE (AUSTRALIA).
AcSim: Aircraft simulation program with application to flight profile generation
[AD-A212466] N90-14217
Influence of hole surface finish, cyclic frequency and spectrum severity on the fatigue behavior of thick section aluminum alloy pin joints
[ARL-STRUC-R-430] N90-14336

AEROVIRONMENT, INC., MONROVIA, CA.
Computer simulation of wind/diesel system operation
[DE89-009445] N90-14688

AIR FORCE SYSTEMS COMMAND, HANSCOM AFB, MA.
A modern trans-ionospheric propagation sensing system N90-14430

AKRON UNIV., OH.
Navier-Stokes analysis of airfoils with leading edge ice accretions N90-14196

ALABAMA UNIV., HUNTSVILLE.
Materials processing in low gravity
[NASA-CR-183733] N90-14397
A graphically oriented specification language for automatic code generation. GRASP/Ada: A Graphical Representation of Algorithms, Structure, and Processes for Ada, phase 1
[NASA-CR-183212] N90-14813

ALASKA UNIV., FAIRBANKS.
Decomposition in Arctic terrestrial environments
[DE90-001198] N90-14706

ALCAN INTERNATIONAL LTD., BANBURY (ENGLAND).
The manufacture of superplastic alloys N90-14333

ALLGEMEINE ELEKTRIZITAETS-GESELLSCHAFT, ULM (GERMANY, F.R.).
The characteristics of the HF radio channel and its influence on modern HF data communication system design N90-14448

ALLIED-SIGNAL AEROSPACE CO. KANSAS CITY, MO.
New tool-holding concept
[DE90-000880] N90-14624

ANALEX CORP., CLEVELAND, OH.
Data compression techniques applied to high resolution high frame rate video technology
[NASA-CR-4263] N90-14452

ANALYTICAL METHODS, INC., REDMOND, WA.
Program VSAERO theory document: A computer program for calculating nonlinear aerodynamic characteristics of arbitrary configurations
[NASA-CR-4023] N90-14200

ARGONNE NATIONAL LAB., IL.
Corrections for non-ideal effects in reflected shock waves at low Mach numbers
[DE90-002192] N90-14208
Application of neutron diffraction NDE to high-temperature superconducting composites
[DE90-002184] N90-14295
Laser Raman spectroscopy in studies of corrosion and electrocatalysis
[DE90-001414] N90-14311
Embrittlement of laboratory- and reactor-aged CF-3, CF-8, and CF-8M duplex stainless steels
[DE90-002777] N90-14354
Elastic softening in nanocrystalline silicon
[DE90-002268] N90-14377
Characterization of nanophase materials by x ray diffraction and computer simulation
[DE90-002270] N90-14378
Modeling of sodium/metal chloride batteries
[DE89-017685] N90-14478
Practical superconductor development for electrical power applications
[DE90-001804] N90-14487
Sodium/sulfur post-test analysis at ANL
[DE90-001911] N90-14488
Selection of the energy-efficient enhancement geometry for single-phase turbulent flow inside tubes
[DE89-017690] N90-14519
Markets for high-speed intercity Maglev technology: A systems analysis approach
[DE89-017683] N90-14623
Opportunities and prospects for Maglev in North America
[DE90-002190] N90-14627
Approximate methods for dynamic plastic deformation of structures
[DE90-002214] N90-14660
Critical time step estimation for three-dimensional explicit impact analysis
[DE90-002187] N90-14662
Electrode development in monolithic solid oxide fuel cells
[DE90-001910] N90-14684
Calorimetric measurements on electrochemical cells with Pd-D cathodes
[DE90-002198] N90-14685
Interfacial effects in monolithic solid oxide fuel cells
[DE90-001914] N90-14690
Environmental quality and the shift to alternative fuels: Progress and interim findings of a Department of Energy study of transition in vehicular power systems
[DE90-002178] N90-14716
US energy use: New technologies and policies in response to global warming
[DE90-002170] N90-14724
Factors affecting electron spin polarization in photosynthetic systems
[DE90-000196] N90-14764
Proceedings of the Focused Research Program on Spectral Theory and Boundary Value Problems. Volume 4: Nonlinear Differential Equations
[DE90-000920] N90-14780
Research in mathematics and computer science at Argonne, July 1, 1986 to January 6, 1988
[DE88-010343] N90-14781
Strand: A practical parallel programming language
[DE90-002861] N90-14825
A comparison result and elliptic equations involving subcritical exponents
[DE90-001772] N90-14850
Hamiltonian flows, SU(infinity), SO(infinity), USp(infinity), and strings
[DE90-001987] N90-14851
Cavitation-controlled ultrasonic agitator
[DE90-002773] N90-14871
Proceedings of the Conference on High-Spin Nuclear Structure and Novel Nuclear Shapes
[DE88-013968] N90-14875
Heavy ion interactions
[DE90-001410] N90-14884
Atomic matching across internal interfaces
[DE90-002266] N90-14889
Computation of electromagnetic effects in a tokamak due to a plasma disruption
[DE90-001764] N90-14931
High resolution-angle resolved photoemission studies of high temperature superconductors
[DE89-017691] N90-14950
Oxygen stoichiometry, structural transitions, and thermodynamic behavior of the YBa2Cu3O(x) system
[DE89-017694] N90-14951
Applications of superconductor technologies to transportation
[DE90-000856] N90-14961
Theory of the energetics and nonclassical nucleation for martensitic transformations from partially soft lattice modes
[DE90-002182] N90-14964
The effect of composition and processing on high T(sub c) superconductors containing bismuth
[DE90-002203] N90-14965
Charge transfer and bond lengths in YBa2Cu(sub 3-x)M(sub x)O(sub 6+y)
[DE90-002241] N90-14966
Powder neutron diffraction study of the structural phase diagram of the Ba(sub 1-x)K(sub x)BiO3 system
[DE90-002264] N90-14967
Microstructure and electrical properties of bulk high-T(sub c) superconductors
[DE90-001762] N90-14974
Magnetotransport studies of epitaxial Cr thin films
[DE90-001930] N90-14975
Improved performance of low-T(sub c) superconductors for detection of minimum-ionizing particles
[DE90-001985] N90-14976
Magnetic and electrical properties
[DE90-002183] N90-14977
Anisotropy of oxygen tracer diffusion in YBa2Cu3O7-delta single crystals
[DE90-001931] N90-14979
Surface magneto-optical studies of ultrathin ferromagnetic films
[DE90-002199] N90-14980
Quasicrystals and grain boundaries
[DE90-002213] N90-14981

ARIZONA STATE UNIV., TEMPE.
Mobility of sulfur in thermally altered meteorites N90-15010

ARMY AEROSTRUCTURES DIRECTORATE, HAMPTON, VA.
Effect of blade planform variation on a small-scale hovering rotor
[NASA-TM-4146] N90-14186

ARMY AVIATION SYSTEMS COMMAND, CLEVELAND, OH.
The 3F condensation polyimides: Review and update
[NASA-TM-102353] N90-14363

ARMY PROPULSION LAB., CLEVELAND, OH.
Oxidation effects on the mechanical properties of SiC fiber-reinforced reaction-bonded silicon nitride matrix composites
[NASA-TM-102360] N90-14287

ARNOLD ENGINEERING DEVELOPMENT CENTER, ARNOLD AIR FORCE STATION, TN.
Development of a three-axis trim program
[AD-A212883] N90-14237

ASSISTANT SECRETARY OF DEFENSE (PUBLIC AFFAIRS), WASHINGTON, DC.
DOD (Department of Defense) Freedom of Information Act Program (incorporating changes 1 and 2)
[PB90-104753] N90-14993

AUBURN UNIV., AL.
Preliminary design of the Shuttle-C avionics recovery system
[NASA-CR-186230] N90-14258

Measurement of damping of graphite epoxy composite materials and structural joints
[NASA-CR-183802] N90-14286
QUEST/Ada: Query utility environment for software testing of Ada
[NASA-CR-186121] N90-14787
A graphically oriented specification language for automatic code generation. GRASP/Ada: A Graphical Representation of Algorithms, Structure, and Processes for Ada, phase 1
[NASA-CR-183212] N90-14813

AUSTRALIAN NATIONAL UNIV., CANBERRA.
Symmetry breaking bifurcations of a current sheet
[DE90-601005] N90-14864

B

BAYLOR UNIV., WACO, TX.
A model of the thermal and electrical properties of cosmic dust particles N90-15014

BIONETICS CORP., COCOA BEACH, FL.
Summary of 1987 and 1988 manatee aerial surveys at Kennedy Space Center
[NASA-TM-102783] N90-14689

BOEING COMMERCIAL AIRPLANE CO., SEATTLE, WA.
Evaluation of analysis techniques for low frequency interior noise and vibration of commercial aircraft
[NASA-CR-181851] N90-14866

BONNEVILLE POWER ADMINISTRATION, PORTLAND, OR.
Power factor controller study
[DE89-017655] N90-14458

BOSTON UNIV., MA.
Meteoritic basalts
[NASA-CR-185949] N90-15004

BOWIE STATE COLL., MD.
Power spectral estimation algorithms
[NASA-CR-186189] N90-14812

BRANDEIS UNIV., WALTHAM, MA.
VLA and VLBI observations of core dominated quasars N90-15002

BRIGHAM YOUNG UNIV., PROVO, UT.
Supercritical fluid chromatography/supersonic jet spectroscopy
[DE90-001378] N90-14308

BRISTOL UNIV. (ENGLAND).
Rainfall estimation over Africa using satellite data N90-14742
A large detector for cosmic ray abundance and energy measurements N90-15037

BRITISH AEROSPACE PUBLIC LTD. CO., BRISTOL (ENGLAND).
Designing for superplastic alloys N90-14332

BRITISH PETROLEUM CO. LTD., LONDON (ENGLAND).
Coordination of processing elements in a multiprocessor computer
[WO-PATENT-88/04075] N90-14830

BROOKHAVEN NATIONAL LAB., UPTON, NY.
The formation of metal-oxygen species at low temperatures
[DE90-002298] N90-14323
The conversion of carbonaceous materials to clean carbon and co-product gaseous fuel
[DE90-001561] N90-14367
Soft x ray microscope using Fourier transform holography
[DE90-002291] N90-14539
Amperometric biosensors for glucose, lactate, and glycolate based on oxidases and redox-modified siloxane polymers
[DE90-002301] N90-14541
International Conference on Global and Regional Atmospheric Environmental Chemistry and visit to Hangzhou, China, foreign trip report
[DE90-000099] N90-14713
Extraterrestrial halogen and sulfur content of the stratosphere
[DE89-017623] N90-14738
A theoretical perspective on neutrino physics
[DE90-000759] N90-14878
String models for ultrarelativistic heavy ion collisions: Lund model versus color exchange models
[DE88-015856] N90-14881
X ray reflectivity study of SiO2 on Si
[DE90-001326] N90-14943
REFLECT: A computer program for the x ray reflectivity of bent perfect crystals
[DE90-001266] N90-14946
Flux pinning and microstructure in YBa2Cu3O7
[DE90-001562] N90-14948
Glancing angle x ray studies of oxide films
[DE89-017828] N90-14953

BROWN UNIV., PROVIDENCE, RI.
Group implicit concurrent algorithms in nonlinear structural dynamics
[NASA-CR-185950] N90-14638
Evaluation of climatic models: Comparison of simulated and observed patterns for past climates
[DE90-001228] N90-14755

BURTON TECHNOLOGIES, INC., RALEIGH, NC.
Friction and wear of glassy carbon in sliding contact, revision 1
[DE90-000743] N90-14365

C

CALIFORNIA INST. OF TECH., PASADENA.
An investigation of the bursting of trailing vortices using numerical simulation N90-14191
Characterization of cloud chemistry and frequency of canopy exposure to clouds in the Sierra Nevada
[PB89-104035] N90-14753
Evidence for anomalous cosmic ray hydrogen N90-15005

CALIFORNIA POLYTECHNIC STATE UNIV., SAN LUIS OBISPO.
California air transportation study: A transportation system for the California Corridor of the year 2010
[NASA-CR-186219] N90-14212
Preliminary design of four aircraft to service the California Corridor in the year 2010: The California Condor, California Sky-Hopper, high capacity short range transport tilt rotor aircraft needed to simplify intercity transportation
[NASA-CR-186232] N90-14226

CALIFORNIA UNIV., BERKELEY.
Non-linear optical studies of adsorbates: Spectroscopy and dynamics
[DE90-001543] N90-14312
The strength-toughness combination of the aluminum-lithium alloys 2090 and 2091 at cryogenic temperatures
[DE90-001425] N90-14338
The 4.2 K fracture toughness of 304 stainless steel in a magnetic field
[DE90-002083] N90-14347
Effects of precipitate distribution on 293 K and 77 K properties of 2090-T81 weldments
[DE90-002332] N90-14349
The metallurgical determinants of toughness as cryogenic temperature
[DE90-002331] N90-14351
Cooling flows in clusters of galaxies N90-15009
Supersymmetric dark matter above the W mass
[NASA-CR-186168] N90-15016

CALIFORNIA UNIV., BERKELEY. LAWRENCE BERKELEY LAB.
Mapping of upper electronic reaction surfaces by tuned laser photolysis and by absorption and emission spectroscopies
[DE90-000125] N90-14314
The effect of hydrogen charging on the mechanical properties of aluminum alloy 2090
[DE90-000129] N90-14341
The 4.2 K fracture toughness of 304 stainless steel in a magnetic field
[DE90-002083] N90-14347
Effects of precipitate distribution on 293 K and 77 K properties of 2090-T81 weldments
[DE90-002332] N90-14349
The metallurgical determinants of toughness as cryogenic temperature
[DE90-002331] N90-14351
The secondary slurry-zinc/air battery
[DE90-002600] N90-14491
Earth Sciences Division annual report 1988
[DE90-002617] N90-14663
Technology Base Research Project for electrochemical energy storage
[DE90-002604] N90-14693
X ray microimaging for the life sciences
[DE90-002613] N90-14766
Versatility of the CFR algorithm for limited angle reconstruction
[DE90-001421] N90-14817
The design of a computer system for image simulation and image processing of high resolution electron micrographs
[DE90-000179] N90-14820
Superconducting magnets in space
[DE90-002671] N90-14865
Multiple electron capture in close ion-atom collisions
[DE90-001541] N90-14885
Realtime tracking system for wide-field-of-view telescope
[DE90-001147] N90-14908
Supernovae, compact stars, and nuclear physics
[DE90-002682] N90-15022

CALIFORNIA UNIV., LOS ANGELES.
Risk-based fire safety experiment definition for manned spacecraft
[NASA-CR-183835] N90-14262
Elasto-plastic analysis of unidirectional fiber-reinforced composites subjected to transverse normal loading using the finite element method N90-14292
High-frequency instability of the sheath-plasma resonance
[NASA-CR-186127] N90-14910

CALIFORNIA UNIV., SAN FRANCISCO.
Nomenclature for physical mapping of complex genomes
[DE89-015173] N90-14994

CALSPAN CORP., ARNOLD AFS, TN.
Development of a three-axis trim program
[AD-A212883] N90-14237

CAMBRIDGE COLLABORATIVE, INC., MA.
Evaluation of analysis techniques for low frequency interior noise and vibration of commercial aircraft
[NASA-CR-181851] N90-14866

CARNEGIE-MELLON UNIV., PITTSBURGH, PA.
The processes of scientific research: The strategy of experimentation N90-14788
Application of reusable software components at the SEI N90-14804
A sampled-grating model of moire patterns from digital imaging
[AD-A213364] N90-14902

CATHOLIC UNIV. OF AMERICA, WASHINGTON, DC.
Wide-angle propagation in inhomogeneous fluids and elastic solids using perturbation methods N90-14868

CENTRAL RESEARCH INST. OF ELECTRIC POWER INDUSTRY, TOKYO (JAPAN).
Survey of adaptive control theory and its applications
[DE89-901270] N90-14840

CENTRE NATIONAL D'ETUDES DES TELECOMMUNICATIONS, LANNION (FRANCE).
New perspectives for the inversion of backscatter ionograms N90-14427
Correction of ionospheric effects for the precise orbit determination of satellites N90-14432

CENTRO BRASILEIRO DE PESQUISAS FISICAS, RIO DE JANEIRO.
General exact solution for homogeneous time-dependent self-gravitating perfect fluids
[DE89-618425] N90-14514
Black-hole decay and topological stability in quantum gravity
[DE89-618785] N90-15017
Is the number of photons conserved in an expanding universe
[DE89-618836] N90-15018

CHICAGO UNIV., IL.
Extraterrestrial halogen and sulfur content of the stratosphere
[DE89-017623] N90-14738

CHRONAR CORP., PRINCETON, NJ.
Study of microcrystalline, silicon-carbon p-layers prepared by photo-CVD and glow discharge
[DE89-009438] N90-14939

CITROEN INDUSTRIE, PARIS (FRANCE).
Experimental study of the shock waves generated by high energy laser pulses N90-14557

CIVIL AEROMEDICAL INST., OKLAHOMA CITY, OK.
Performance evaluation of the Puritan-Bennett crew-member portable protective breathing device as prescribed by portions of FAA action notice A-8150.2
[AD-A211113] N90-14772

CLEMSON UNIV., SC.
Adaptive clutter rejection filters for airborne Doppler weather radar applied to the detection of low altitude windshear
[NASA-CR-186211] N90-14453
The effects of clutter-rejection filtering on estimating weather spectrum parameters
[NASA-CR-186212] N90-14754

CLEVELAND STATE UNIV., OH.
Primary arm spacing in directionally solidified Pb-10 wt percent Sn alloys
[NASA-CR-185190] N90-14398

COLORADO STATE UNIV., FORT COLLINS.
An evaluation of trend detection techniques for use in water quality monitoring programs
[PB89-100058] N90-14702
Summary of 1989 Atlantic tropical cyclone activity and seasonal forecast verification N90-14743

COLORADO UNIV., BOULDER.
The stability of Taylor-Couette flow with radial heating N90-14502
Evaluation of the airborne visible-infrared imaging spectrometer for mapping subtle lithological variation
[NASA-CR-186213] N90-14670
Force user's manual: A portable, parallel FORTRAN
[NASA-CR-4265] N90-14785

Properties of evolved star circumstellar grains
N90-15003
CIS-lunar space infrastructure lunar technologies: Executive summary
[NASA-CR-186220] N90-15029

COMMERCE DEPT., WASHINGTON, DC.
Metric handbook for Federal officials: Recommendations of the Interagency Committee on Metric Policy
[PB89-226922] N90-14400

COMMITTEE ON COMMERCE, SCIENCE, AND TRANSPORTATION (U.S. SENATE).
Consumer Ozone Protection Act of 1989
[S-HRG-101-377] N90-14708

COMMITTEE ON SCIENCE, SPACE AND TECHNOLOGY (U.S. HOUSE).
Review of the Aerospace Safety Advisory Panel report for NASA fiscal year 1990 authorization
[GPO-24-234] N90-14213

COMPUTER RESOURCE MANAGEMENT, INC., VIENNA, VA.
National airspace system monitoring operational concept
[NAS-SR-1330] N90-14214

CONNECTICUT COLL., NEW LONDON.
A compact, high-powered far-infrared (FIR) laser
[DE89-016786] N90-14597

CONSULTEC SCIENTIFIC, INC., KNOXVILLE, TN.
Assessment of research needs for laser technologies applied to advanced spectrographic methods
[DE90-001154] N90-14587

CORNELL UNIV., ITHACA, NY.
The role of order in distributed programs
[NASA-CR-186252] N90-14826

CORNELL UNIV., NEW YORK, NY.
How robust are distributed systems
[NASA-CR-186242] N90-14837

COUNCIL FOR NATIONAL ACADEMIC AWARDS (ENGLAND).
Transient response of flexible rotor-bearing systems subjected to combined unbalance and ground excitations N90-14616
Fatigue fracture in the presence of shot peening residual stresses: Initiation, propagation, and relaxation phenomena N90-14644

CRANFIELD INST. OF TECH., BEDFORD (ENGLAND).
Superplasticity: An overview N90-14326

D

DEFENCE AND CIVIL INST. OF ENVIRONMENTAL MEDICINE, DOWNSVIEW (ONTARIO).
Integrated G-suit/immersion suit
[AD-A212989] N90-14774

DEFENCE RESEARCH ESTABLISHMENT VALCARTIER (QUEBEC).
Remote sensing of the aerosol scattering coefficient with a multi-field-of view lidar N90-14437

DELAWARE UNIV., NEWARK.
The generalized van der Waals theory of pure fluids and mixtures
[DE90-000504] N90-14307
The development of a spatial synoptic climatological index for environmental analysis N90-14744

DEPARTMENT OF ENERGY, WASHINGTON, DC.
Assessment of costs and benefits of flexible and alternative fuel use in the US transportation sector. Technical report three: Methanol production and transportation costs
[DE90-002625] N90-14396
New heating and cooling technology: Regenerative heat pump according to the Vuilleumier principle
[DE90-002701] N90-14699
Carbon dioxide and climate: Summaries of research in FY 1989
[DE90-001791] N90-14723
The ultimate structure of matter: The US High Energy Physics Program from the 1950s through the 1980s
[DE90-001784] N90-14887
Nomenclature for physical mapping of complex genomes
[DE89-015173] N90-14994

DEPARTMENT OF THE ARMY, WASHINGTON, DC.
High resolution, wide band Chirp-Z signal analyzer
[AD-D014240] N90-14465

DEPARTMENT OF THE NAVY, WASHINGTON, DC.
Elastomeric impulse energy storage and transfer system
[AD-D014223] N90-14255
Method for stabilization of pan-based carbon fibers
[AD-D014228] N90-14288
Carbon fiber reinforced metal matrix composites
[AD-D014245] N90-14289
Temperature stable ceramic dielectric compositions
[AD-D014209] N90-14358
Means for protecting electroexplosive devices which are subject to a wide variety of radio frequency
[AD-D014219] N90-14382
Pentafluorothio polynitroaliphatic explosives
[AD-D014221] N90-14383
Frequency independent constant beamwidth directional lens antenna for very wideband and multi-channel electromagnetic communications
[AD-D014214] N90-14449
Frequency agile synthetic aperture radar
[AD-D014235] N90-14451
Method and apparatus to enhance the sensitivity of cylindrical magnetostrictive transducer to magnetic fields
[AD-D014218] N90-14459
Electrochemical preparation of silver oxide electrodes having high thermal stability
[AD-D014224] N90-14460
High power transducers
[AD-D014225] N90-14461
Silver composite cathodes for alkaline secondary batteries
[AD-D014227] N90-14462
Fabrication of NBN based electronic devices with silicon barriers
[AD-D014230] N90-14463
Silver-nickel composite cathodes for alkaline secondary batteries
[AD-D014231] N90-14464
Symmetric waveguide junction combiner
[AD-D014243] N90-14466
Method for fabricating thin film metallic meshes for use as Fabry-Perot interferometer elements, filters and other devices
[AD-D014236] N90-14529
Monolithic laser diode structure for microwave generation
[AD-D014210] N90-14543
Pressure sensitive release device
[AD-D014220] N90-14610
A method of soldering aluminum
[AD-D014226] N90-14611
Robotic vision system
[AD-D014246] N90-14838
Interferometric surface distortion detector
[AD-D014211] N90-14901
Programmable near-infrared ranging system
[AD-D014237] N90-14903
Narrow band and wide angle hemispherical interference optical filter
[AD-D014238] N90-14904
Method of making self-aligned GaAs/AlGaAs FET's
[AD-D014229] N90-14935
Multiband photoconductive detector based on layered semiconductor quantum wells
[AD-D014232] N90-14936
Method of sensitizing PB-Salt epitaxial films for Schottky diodes
[AD-D014244] N90-14937

DEPAUL UNIV., CHICAGO, IL.
An image compression algorithm for a high-resolution digital still camera
[NASA-CR-185079] N90-14532

DORNIER SYSTEM G.M.B.H., FRIEDRICHSHAFEN (GERMANY, F.R.).
Propagation prediction for the North Sea environment
N90-14423

DRAPER (CHARLES STARK) LAB., INC., CAMBRIDGE, MA.
Guidance, steering, load relief and control of an asymmetric launch vehicle
[NASA-CR-185598] N90-14257

E

ECOLE NATIONALE SUPERIEURE DE MECANIQUE ET D'AEROTECHNIQUE, POITIERS (FRANCE).
Microstructure induced by laser shock in an austenitic steel N90-14558
Dynamic sintering of metallic powders by laser shock
N90-14559

ECOLE POLYTECHNIQUE, PALAISEAU (FRANCE).
Fast electrons in a laser generated plasma
N90-14545
Production of homogeneous plasmas for laser-plasma interaction experiments N90-14546
Effects of temporal and induced spatial incoherence on parametric instabilities in laser plasma interactions
N90-14549
Limitations in the growing of a plasma wave produced by heterodyning two lasers due to modulations and decay instabilities N90-14552
Use of plasmas for the acceleration of particles to very high energy N90-14553
Measurement of the high density zone of a plasma target by absorption spectroscopy N90-14560
Time integrated study of spectral emission in the X-UV domain at the outlet of a laser shock, at the back of single or double foil targets N90-14561
Measurement of the X-UV emission from the back face of thin foils illuminated by an A4 omega laser
N90-14562
X ray shadowscopy in implosion experiments
N90-14563
The average ion model. Computation of the absorption and emission coefficients in hot plasmas N90-14569
XRAD: A one dimensional Lagrangian code with radiative transport N90-14570
Characteristics of an x ray source created by a laser plasma N90-14575
Laser activities N90-14576
Development of X diagnostics around the pulse 1 laser N90-14580

EDGERTON, GERMESHAUSEN AND GRIER, INC., IDAHO FALLS, ID.
The biocorrosion of copper by biopolymers as examined in situ, in real time FT-IR/CIR/ATR in conjunction with pre and post XPS/AES
[DE90-002086] N90-14348
Laboratory testing of Sonnenschein DF6V180 6 volt traction battery
[DE90-002080] N90-14486
Field testing of a ceramic heat exchanger for heat recovery application
[DE90-002082] N90-14523
Derivation of synthetic mission profiles from electric vehicle field data
[DE89-011125] N90-14620
Human factors evaluation of electroluminescent display Number 1
[DE90-002231] N90-14777
Dissipation measurement in high T(sub c) superconductors with electromagnetic probes
[DE90-002058] N90-14963

EG AND G MOUND APPLIED TECHNOLOGIES, MIAMISBURG, OH.
Development of a titanium/boron blending process
[DE90-001450] N90-14386
Electrothermal response testing more than a quality assurance tool
[DE90-001449] N90-14536

ENERGY CONVERSION DEVICES, INC., TROY, MI.
Research on high-efficiency, multiple-gap, multijunction, amorphous-silicon-based alloy thin-film solar cells
[DE89-009444] N90-14673

ENTECH CORP., DALLAS-FORT WORTH AIRPORT, TX.
Conceptual design study of a 5 kilowatt solar dynamic Brayton power system using a dome Fresnel lens solar concentrator
[NASA-CR-185134] N90-14281

ENVIRONMENTAL PROTECTION AGENCY, ANN ARBOR, MI.
Cold starting a neat methanol (M100) vehicle with long duration spark ignition
[PB89-230692] N90-14613

ESDU INTERNATIONAL LTD., LONDON (ENGLAND).
Normal force, pitching moment, and side force of forebody-cylinder combinations for angles of attack up to 90 degrees and Mach numbers up to 5
[ESDU-89014] N90-14192
Introduction to data items on flight path optimisation
[ESDU-89015] N90-14221
Effect of unshielded and shielded horn balances on hinge moment coefficients for controls at low speeds
[ESDU-89003-A] N90-14238
Hinge moment coefficient derivatives for trailing-edge controls on wings at subsonic speeds
[ESDU-89009] N90-14239
Example of procedure in calculation of control hinge moments
[ESDU-89010] N90-14240
Thermophysical properties of isopropyl alcohol. Part 1: The ideal gas and the saturated liquid and vapour
[ESDU-89017-PT-1] N90-14297
Orthobaric densities and molar volumes of liquids. Introduction to data items issued after July 1989
[ESDU-89018] N90-14298
Orthobaric densities and molar volumes of liquids. Aromatic hydrocarbons
[ESDU-89019] N90-14299
Thermophysical properties of isopropyl alcohol. Part 2: Thermodynamic properties at elevated pressures
[ESDU-89020-PT-2] N90-14300
Flexural and torsional-flexural buckling of thin-walled open section struts
[ESDU-89007] N90-14643

EXETER UNIV. (ENGLAND).
An experimental and theoretical study of the aeroacoustics of external-Coanda gas flares
N90-14495

F

FEDERAL AVIATION ADMINISTRATION, ATLANTIC CITY, NJ.
Data Link Processor (DLP) operational test and evaluation/integration test plan
[DOT/FAA/CT-TN89/32] N90-14404
FEDERAL AVIATION ADMINISTRATION, OKLAHOMA CITY, OK.
Comparison of protective breathing equipment performance at ground level and 8,000 feet altitude using parameters prescribed by portions of FAA action notice A-8150.2
[AD-A212852] N90-14773
FERMI NATIONAL ACCELERATOR LAB., BATAVIA, IL.
Gamma ray lines from dark matter annihilation
[DE90-000779] N90-15021
FLORIDA UNIV., GAINESVILLE.
Development of laser excited atomic fluorescence and ionization spectrometric methods
[DE90-001567] N90-14320
Engineering sciences design. Design and implementation of components for a bioregenerative system for growing higher order plants in space
[NASA-CR-185056] N90-14761
High-frequency ventilation in dogs with three gases of different densities
[AD-A212862] N90-14762
Mathematical techniques for system realization and identification
[AD-A212088] N90-14841
FOOD AND DRUG ADMINISTRATION, ROCKVILLE, MD.
Biological effects of hyperthermia and potential risk associated with ultrasonic exposure
[PB89-100702] N90-14768
FORSCHUNGSINSTITUT DER DEUTSCHEN BUNDESPOST, DARMSTADT (GERMANY, F.R.).
The FTZ HF propagation model for use on small computers and its accuracy N90-14447
FORSCHUNGSINSTITUT FUER ANTHROPOTECHNIK, WACHTBERG (GERMANY, F.R.).
Human factors aspects of decision support systems N90-14408
FORSCHUNGSINSTITUT FUER HOCHFREQUENZPHYSIK, WERTHHOVEN (GERMANY, F.R.).
Low level range coverage performance prediction for VHF rader N90-14439
FORTUNA-WERKE, STUTTGART (GERMANY, F.R.).
Euriaser CO2 laser
[ETN-90-95907] N90-14582
FRAUNHOFER-INST. FUER CHEMISCHE TECHNOLOGIE, BERGHAUSEN (GERMANY, F.R.).
Investigation of the phase stabilizing effect of potassium fluoride on ammonium nitrate
[AD-A213042] N90-14381

G

GENERAL DYNAMICS CORP., SAN DIEGO, CA.
Definition of avionics concepts for a heavy lift cargo vehicle. Volume 1: Executive summary
[NASA-CR-183818] N90-14229
Definition of avionics concepts for a heavy lift cargo vehicle, volume 2
[NASA-CR-183819] N90-14230
Preliminary design document: Ground based testbed for avionics systems
[NASA-CR-183821] N90-14231
GENERAL SCIENCES CORP., LAUREL, MD.
Analysis of acid rain and associated phenomena
[DE90-002555] N90-14725
GEORGE WASHINGTON UNIV., WASHINGTON, DC.
A composite numerical procedure for calculating the motion of vortex filaments N90-14207
GEORGIA INST. OF TECH., ATLANTA.
An experimental investigation of the interaction between a model rotor and airframe in forward flight N90-14219
An analytical method for the prediction of unsteady rotor/airframe interactions in forward flight N90-14223
Acoustic-vortical-combustion interaction in a solid fuel ramjet simulator N90-14234
Optimal control of aero-assisted orbit transfer vehicles N90-14241
A helicopter flight path controller design via a nonlinear transformation technique N90-14242
Manipulation strategies for massive space payloads
[NASA-CR-186081] N90-14247
A surface coupled flamelet approach to dynamic response in heterogeneous propellant combustion N90-14302
Investigation of combustion instability in ramjet combustors N90-14303
Laboratory evaluation and application of microwave absorption properties under simulated conditions for planetary atmospheres
[NASA-CR-185916] N90-15025
GEORGIA TECH RESEARCH INST., ATLANTA.
Theoretical and material studies of thin-film electroluminescent devices
[NASA-CR-186104] N90-14468
GERMAN MILITARY GEOPHYSICAL OFFICE, TRABEN-TRARBACH (GERMANY, F.R.).
The thermal behavior of natural backgrounds and its prediction by means of numerical models N90-14436
GLASSTECH SOLAR, INC., WHEATRIDGE, CO.
Preparation and properties of high deposition a-Si:H films and solar cells using disilane
[DE89-009467] N90-14679
GOSUDARSTVENNYI KOMITET PO ISPOLZOVANIYU ATOMNOI ENERGII, MOSCOW (USSR).
Numerical simulation of laser radiation propagation in non-uniform absorbing medium. Geometrical optics approximation
[DE89-632014] N90-14585
Structural peculiarities and molecular properties of charge complexes formed on positive ion injection into dense inert gas media
[DE89-633953] N90-14877
Laser probing non-cylindrical Z-pinch in near-isolator region of a discharged chamber
[DE89-632018] N90-14912
Toroidal rotation retardation and ion anomalous transport by drift waves in a tokamak
[DE89-634427] N90-14913
GOSUDARSTVENNYI KOMITET PO ISPOLZOVANIYU ATOMNOI ENERGII, OBNINSK (USSR).
Semi-empirical theory of heat-transfer when boiling
[DE89-635418] N90-14984
GOSUDARSTVENNYI KOMITET PO ISPOLZOVANIYU ATOMNOI ENERGII, SERPUKHOV (USSR).
Fast serial communication module
[DE89-633753] N90-14454
On-line system to measure magnetic characteristics of steel samples
[DE89-633443] N90-14861
GRENOBLE-1 UNIV. (FRANCE).
Block predictor (low order) corrector methods to solve ordinary differential equations on parallel computers
[IMAG-RR-757-M] N90-14845
Estimating methods for counting process intensities: Non-parametric methods
[IMAG-RR-774-M] N90-14846
GROUPEMENT DE RECHERCHES COORDONNEES INTERACTION LASER MATIERE, PALAISEAU (FRANCE).
Activities report in laser matter interactions
[ETN-90-95515] N90-14544
Trapezoidal crystal in the six beam implosion N90-14577
Development of X diagnostics with 1 Gw laser pulses N90-14578
GRUMMAN TECHNICAL SERVICES, INC., RESTON, VA.
Level 2 software reuse study N90-14800

H

HAMPTON UNIV., VA.
A two dimensional power spectral estimate for some nonstationary processes
[NASA-CR-186100] N90-14843
HARVARD UNIV., CAMBRIDGE, MA.
A low-order model of the equatorial ocean-atmosphere system N90-14730
HAVA IKMAL BAKIM MERKEZI KOMUTANLIGI, ANKARA (TURKEY).
Mitigating Doppler shift effect in HF multitone data modem N90-14441
HOUSTON UNIV., CLEAR LAKE, TX.
Transferring data objects: A focused Ada investigation
[NASA-CR-186065] N90-14786
Technology transfer in software engineering N90-14805
The development of an Ada programming support environment database: SEAD (Software Engineering and Ada Database), user's manual
[NASA-CR-181219] N90-14811
Developing integrated parametric planning models for budgeting and managing complex projects
[NASA-CR-186006] N90-14986
HOUSTON UNIV., TX.
Partial gravity habitat study: With application to lunar base design
[NASA-CR-186048] N90-14267
Fluid-particle interaction in solid-liquid two-phase grid turbulence N90-14496
Comparative study of the vorticity field in turbulent flows: Theory, experiments, and computations
[DE90-001399] N90-14516
HOWARD UNIV., WASHINGTON, DC.
A dynamic systems engineering methodology research study. Phase 2: Evaluating methodologies, tools, and techniques for applicability to NASA's systems projects
[NASA-CR-181319] N90-14985
HULL UNIV. (ENGLAND).
A communications system with an adaptive multi-functional architecture N90-14415
The use of broadcast signals for passive sensing in automated HF communication systems N90-14433
HYDRAULIC RESEARCH TEXTRON, VALENCIA, CA.
Optimal stochastic modeling and control of flexible structures
[AD-A212347] N90-14269

I

IDAHO NATIONAL ENGINEERING LAB., IDAHO FALLS.
Battery technology assessment and R and D plan
[DE90-002007] N90-14489
Course A: Numerical modeling of two-phase flows for presentation at Ecole d'Ete d'Analyse Numerique
[DE90-002074] N90-14526
Noncontacting laser ultrasonic generation and detection at the surface of molten metal
[DE90-002020] N90-14605
Characterization of electric vehicle velocity and power profiles using road test data
[DE90-002085] N90-14630
Solution bias in complex systems modeling
[DE90-002001] N90-14858
Process monitoring using optical ultrasonic wave detection
[DE90-002021] N90-14870
ILLINOIS STATE WATER SURVEY, CHAMPAIGN.
Frequency distributions of heavy rainstorms in Illinois
[PB90-100215] N90-14748
ILLINOIS UNIV., CHICAGO.
Stability and dynamics of constrained flexible multibody systems N90-14609
ILLINOIS UNIV., URBANA-CHAMPAIGN.
Aerospace vehicle design, spacecraft section. Volume 1: Project Groups 3 through 5
[NASA-CR-186053] N90-14263
Aerospace vehicle design, spacecraft section. Volume 2: Project Groups 6 through 8
[NASA-CR-186054] N90-14264
Design of a compensation filter for a quadratic phase communication channel N90-14428
Rocket studies of the lower ionosphere
[NASA-CR-186187] N90-14735
NETRA: A parallel architecture for integrated vision systems. 1: Architecture and organization
[NASA-CR-185955] N90-14839
A study of the infrared emission of galactic supernova remnants N90-15006
IMATRAN VOIMA OY, HELSINKI (FINLAND).
Expert system for fault diagnostics of rotating machines
[DE89-766980] N90-14621
INDIANA STATE UNIV., TERRE HAUTE.
Image processing of LANDSAT MSS data for buried valley detection in northern Indiana N90-14868
INDIANA UNIV., BLOOMINGTON.
Organic geochemical and tectonic evolution of the midcontinent rift system: Organic geochemistry and micropaleontology
[DE89-017561] N90-14760
INFERENCE CORP., LOS ANGELES, CA.
Advanced Software Development Workstation Project N90-14807
INSTITUT D'OPTIQUE THEORIQUE ET APPLIQUEE, PARIS (FRANCE).
Tomographic imagery by multislot coding applied to x ray diagnostics of laser plasmas: Implementation of a direct electronic detection camera N90-14579
INSTITUT NATIONAL DES SCIENCES APPLIQUEES, RENNES (FRANCE).
Improving the quality of a spread-spectrum radiomobile link N90-14426
INSTITUTE FOR COMPUTER APPLICATIONS IN SCIENCE AND ENGINEERING, HAMPTON, VA.
A note concerning the onset of three dimensionality and time dependence in Goertler vortices
[NASA-CR-181956] N90-14193
The analysis and modeling of dilatational terms in compressible turbulence
[NASA-CR-181959] N90-14513
Krylov methods preconditioned with incompletely factored matrices on the CM-2
[NASA-CR-181961] N90-14779

Parallel projected variable metric algorithms for unconstrained optimization
[NASA-CR-181930] N90-14842
Local error estimates for discontinuous solutions of nonlinear hyperbolic equations
[NASA-CR-181960] N90-14847
Modified Chebyshev pseudospectral method with O(N exp -1) time step restriction
[NASA-CR-181958] N90-14848

INSTITUTE OF NUCLEAR PHYSICS, NOVOSIBIRSK (USSR).
Vector fields and gravity on the lattice
[DE89-633885] N90-14860

INSTITUTO DE PESQUISAS ENERGETICAS E NUCLEARES, SAO PAULO (BRAZIL).
Bi-Sr-Ca-Cu-O superconducting ceramics
[DE89-636225] N90-14972

INTEGRAL TECHNOLOGIES, INC., WESTMONT, IL.
Computer simulation of wind/diesel system operation
[DE89-009445] N90-14688

INTERNATIONAL CENTRE FOR THEORETICAL PHYSICS, TRIESTE (ITALY).
Unsteady hydromagnetic flow of a radiating gas in a vertical channel with axial temperature variation
[DE90-600934] N90-14525
A model for the simulation of the ozone budget in the atmosphere under anthropogenic perturbation
[DE89-636294] N90-14719
Modelling of the effects of the equatorial electrojet on its environment
[DE89-636298] N90-14720
On some integral relations involving a generalized hypergeometric polynomial
[DE90-600729] N90-14852
Classification of modular invariant partition functions for the twisted N=2 superconformal algebra, twisted SU(2) Kac-Moody algebra and D(sub 2K) parafermions
[DE90-600767] N90-14853
On the thermal stability of flow of a radiating two-component plasma in a porous medium between two rotating cylinders
[DE89-636426] N90-14928
A model of the isotope effect of the oxide superconductor
[DE89-635907] N90-14971
Macroscopic persistent currents in high temperature ceramic superconductors
[DE89-636232] N90-14973

IOWA STATE UNIV. OF SCIENCE AND TECHNOLOGY, AMES.
Navier-Stokes solutions of 2-D transonic flow over unconventional airfoils N90-14195
Heat transfer to a stationary and moving sphere immersed in a fluidized bed N90-14503

IOWA UNIV., IOWA CITY.
Controller design for a robotic manipulator N90-14615
Steady state model to determine lake resources at risk to acid deposition in the Sierra Nevada, California
[PB89-103995] N90-14705
Particle simulations in magnetospheric plasmas
[NASA-CR-186238] N90-14934

IRT CORP., SAN DIEGO, CA.
Stick propellant x ray inspection
[AD-A212601] N90-14380

J

JAPAN ATOMIC ENERGY RESEARCH INST., TOKAI.
Thermal design of a 10-kW helium refrigerator
[DE90-701785] N90-14403

JET PROPULSION LAB., CALIFORNIA INST. OF TECH., PASADENA.
Results of the 1989 NASA/JPL balloon flight solar cell calibration program
[NASA-CR-186114] N90-14672
Environmental Projects. Volume 8: Modifications of wastewater evaporation ponds
[NASA-CR-186099] N90-14700
JPL reuse program N90-14795
Publications of the Jet Propulsion Laboratory, 1988
[NASA-CR-185956] N90-14995

JOHNS HOPKINS UNIV., LAUREL, MD.
The parabolic equation approach to predicting tropospheric propagation effects in operational environments N90-14418

JOINT INST. FOR NUCLEAR RESEARCH, DUBNA (USSR).
Iterative methods of domain decomposition with cross-points for the solution of discrete elliptic problems
[DE90-000719] N90-14854
Narrow one-channel resonances and their manifestation in the pure elastic scattering of unpolarized particles
[DE89-632177] N90-14876

JOINT PUBLICATIONS RESEARCH SERVICE, ARLINGTON, VA.
JPRS Report: Science and technology. USSR: Space. Soviet space program to the year 2000
[JPRS-USP-89-008] N90-14248

K

KANSAS UNIV., LAWRENCE.
Computation of unsteady transonic flow about airfoils in frequency domain using the full-potential equation N90-14198

KENT UNIV., CANTERBURY (ENGLAND).
Hypervelocity impact studies on the Giotto comet Halley mission N90-15008
Very high resolution radio observations of molecular cloud cores N90-15013

KENTUCKY UNIV., LEXINGTON.
Boundary element analysis of single and multidomain problems in acoustics N90-14867

KNUDSON ENGINEERING, INC., PORTLAND, OR.
Power factor controller study
[DE89-017655] N90-14458

L

LAWRENCE LIVERMORE NATIONAL LAB., CA.
Kestrel 3 Program
[DE90-001796] N90-14209
Performance characteristics of a three-stage railgun
[DE90-002533] N90-14254
A numerical study of thin flame representations
[DE89-017889] N90-14313
The thermally induced gas-phase reactions of methane and oxygen: A comparison of experimental and computational results
[DE90-000785] N90-14317
Thermodynamic properties and hydrodynamic response of high-density high-temperature C H N O mixtures
[DE90-000836] N90-14318
The Periodic Law at high pressures
[DE90-000837] N90-14319
First-principles interatomic potentials in transition metals: Multi-ion interactions and their analytic representation
[DE90-001990] N90-14353
Computer synthesis of ceramic preforms for molten-metal infiltration
[DE90-000826] N90-14370
Challenges in processing for polymer composites
[DE90-002224] N90-14376
Detonation product equation of state for Baratol
[DE90-001050] N90-14384
Particle size effects in the initiation of explosives containing reactive and nonreactive continuous phases
[DE90-000786] N90-14390
Non-equilibrium effects of slow diffusion controlled reactions on the properties of explosives
[DE90-000822] N90-14391
Phase changes in carbon and nitrogen systems: Their effects on the detonation properties of high explosives
[DE90-000829] N90-14392
Reactive flow measurements and calculations for ZrH2-based composite explosives
[DE90-000831] N90-14393
Reaction zone structure in supracompressed detonating explosives
[DE90-000832] N90-14394
Electric-gun studies of conductors in high magnetic fields and experiments in dynamic flux compression
[DE90-000815] N90-14470
Experimental investigation of a fast-acting exploding metallic foil opening switch
[DE90-001051] N90-14479
Inductive store opening switch and tests for energy transfer to a load
[DE90-002818] N90-14482
Further studies of transverse stress effects in cable-in-conduit conductors
[DE90-001517] N90-14484
Testing and performance of a high-gain flux-compression generator
[DE90-002808] N90-14492
Propagation of detonation waves from an impact region
[DE90-001184] N90-14515
Granular flow: Numerical simulation of dry granular flows and calculation of hydrodynamic interactions in suspensions
[DE89-017544] N90-14518
A fiber-fed imaging spectrometer
[DE90-001008] N90-14538
Radiation damage and its influence on source requirements for high resolution x ray holography
[DE90-002508] N90-14540
Modification of ionic population by non-Maxwellian effects N90-14565
Proof-of-principle experiment for a hot electron pumped XUV amplifier
[DE90-000820] N90-14586
Laboratory x ray lasers
[DE90-000879] N90-14590
The current status of x ray conversion efficiency modeling
[DE90-000931] N90-14591
The development of coherent x ray lasers for x ray holography
[DE90-000784] N90-14595
Ultrahigh-brightness lasers and their applications
[DE90-000877] N90-14596
Single particle friction tests with cellulose acetate sphere samples
[DE89-017537] N90-14622
Verification of the NIKE3D structural analysis code by comparison against the analytic solution for a spherical cavity under a far-field uniaxial stress
[DE90-000929] N90-14653
On the mitigation of non-CO2 greenhouse gases
[DE89-016659] N90-14710
Climate projections with regional resolution
[DE90-000858] N90-14715
Quantifying the link between change in radiative balance and atmospheric temperature
[DE90-000819] N90-14721
A study of the difference between gravimetric and gamma-gamma density near the surface in northern Yucca Flat
[DE89-017886] N90-14737
Climatology of Lawrence Livermore National Laboratory
[DE90-000905] N90-14756
MIPs and BIPs are megaflops: Limits of unidimensional assessments
[DE89-015707] N90-14770
High performance parallel architectures
[DE90-001055] N90-14782
Program CICC flow and heat transfer in Cable-In-Conduit Conductors
[DE90-001519] N90-14818
Using object-oriented development to support prototyping
[DE90-000547] N90-14821
Interactive multidimensional data analysis and understanding
[DE90-001794] N90-14824
A tutorial on software reliability engineering
[DE89-012368] N90-14828
The Delta-t transport protocol: Features and experience useful for high performance networks
[DE89-016542] N90-14832
PCP (Parallel C Preprocessor): A parallel extension of C that is 99 percent fat free
[DE90-002813] N90-14834
Concerning advanced architectures for strategic defense
[DE90-001894] N90-14857
Path integral simulations of liquid helium
[DE90-001171] N90-14862
Biomodal spontaneous fission
[DE90-001516] N90-14886
Design of incoherent imaging arrays
[DE90-000861] N90-14909
Lawrence Livermore National Laboratory (LLNL) research on cold fusion
[DE90-000930] N90-14915
Microwave Tokamak Experiment (MTX) first year of operation and future plans
[DE90-000817] N90-14920
Microwave Transport Systems for the MTX (Microwave Tokamak Experiment)
[DE90-000821] N90-14921
MTX (Microwave Tokamak Experiment)/ELF (Electron Laser Facility) 2 microwave power measurements and calibration for the 2-GW, 140-GHz, ELF 2 Free Electron Laser (FEL)
[DE90-000825] N90-14922
Precision timing and interlocks systems for FEL (Free-Electron Laser) heating experiments on MTX (Microwave Tokamak Experiment)
[DE90-000833] N90-14923
Microwave Tokamak Experiment: An overview of the construction and checkout phase
[DE90-000834] N90-14924
Equation of state and opacity of dense plasmas
[DE90-002223] N90-14926
Starlight: A stationary inertial-confinement-fusion reactor with nonvaporizing walls
[DE90-002315] N90-14927

Practical aspects of a 2-D edge-plasma model
[DE90-002995] N90-14932
Superconducting and microstructural properties of shock-compacted high-T sub c oxide powders
[DE90-000823] N90-14958
Effects of shock-induced defects on flux pinning in YBa2Cu3O(7-delta)
[DE90-000824] N90-14959
Shock-induced defects and flux pinning in YBa2Cu3O sub 7-delta + Ag composites
[DE90-000827] N90-14960
Micro-scale simulation of dynamic compaction of oxide and metal powder mixture
[DE90-002220] N90-14978

LEEDS UNIV. (ENGLAND).
The structure and properties of liquid crystal polymers N90-14356
Mechanical properties and morphology of oriented polymer blends N90-14361
The fluid mechanics of filters N90-14499
Heat transfer in convective boundary layer and channel flows N90-14505
Multigrid solutions of elliptic fluid flow problems N90-14507

LEHIGH UNIV., BETHLEHEM, PA.
Embedded function methods for compressible high speed turbulent flow
[NASA-CR-186131] N90-14498

LICK OBSERVATORY, SANTA CRUZ, CA.
CCD TV focal plane guider development and comparison to SIRTF applications
[NASA-CR-185977] N90-14900

LISTER HILL NATIONAL CENTER FOR BIOMEDICAL COMMUNICATIONS, BETHESDA, MD.
Document preservation by electronic imaging. Volume 1: Synopsis
[PB89-226526] N90-14987
Document preservation by electronic imaging. Volume 2: System and experiment descriptions
[PB89-226534] N90-14988
Document preservation by electronic imaging. Volume 3: Appendices
[PB89-226542] N90-14989

LIVERPOOL UNIV. (ENGLAND).
Applications of a new exact solution of the Navier-Stokes equations to flow in pipes of varying width N90-14504

LOCKHEED ENGINEERING AND SCIENCES CO., WASHINGTON, DC.
USSR Space Life Sciences Digest. Index to issues 21-25
[NASA-CR-3922(30)] N90-14763

LOCKHEED MISSILES AND SPACE CO., HOUSTON, TX.
An SSE approach to reusability N90-14801

LOCKHEED MISSILES AND SPACE CO., HUNTSVILLE, AL.
Fluid flow analysis of the SSME high pressure fuel and oxidizer turbine coolant systems
[NASA-CR-183736] N90-14277

LODESTAR RESEARCH CORP., BOULDER, CO.
Fundamental studies of fusion plasmas
[DE90-002343] N90-14933

LOS ALAMOS NATIONAL LAB., NM.
Design and demonstration of heat pipe cooling for NASP and evaluation of heating methods at high heating rates
[DE89-016995] N90-14227
Martensite transformation in NiTi alloys induced by tensile stress pulses
[DE90-001832] N90-14346
Multiple martensitic transformations, incommensurate/commensurate phases, and charge-density-wave states in plutonium metal: Their consequences
[DE90-001235] N90-14350
Study of new materials for gun propellant formulations
[DE89-015285] N90-14388
Calibration curves for some standard Gap Tests
[DE89-016599] N90-14389
Energy ratings for metal oxide varistors under repetitively pulsed operation
[DE90-002353] N90-14480
High speed transfer switch with 50 kA and 50 kV ratings
[DE90-002448] N90-14481
A cost effective battery bank for I(sup 2)T testing and evaluation of electrical switchgear
[DE90-002350] N90-14490
Perturbations in high-velocity gas flow
[DE90-000539] N90-14520
A new simulation method for the efficient calculation of benchmarks for detonation products equations of state
[DE90-001837] N90-14522
Numerical simulations of free-electron laser oscillators
[DE89-003486] N90-14588
Chaotic behavior in nonlinear polarization dynamics
[DE89-013453] N90-14589
Qualification of diode foil materials for excimer lasers
[DE90-000602] N90-14593
Optical design and performance of an XUV FEL (Free-Electron Laser) oscillator
[DE90-002381] N90-14599
Compact RF-linac free-electron lasers
[DE90-002386] N90-14600
INEX (Integrated Numerical Experiment) simulations of the Los Alamos HIBAF (High-Brightness Accelerator Free-Electron Laser) free-electron laser MOPA (Master Oscillator Power Amplifier) experiment
[DE90-002387] N90-14601
Lasing on the third harmonic
[DE90-002389] N90-14602
Analytical treatment of electron trajectory straightener issues in free-electron lasers
[DE90-002405] N90-14603
Theory of harmonic radiation using a single-electron source model
[DE90-002412] N90-14606
Quality assurance and quality control for the Compact Physics Research Facility (CPRF) and ZTH experiment
[DE90-002352] N90-14636
Use of superconducting plates and shells to deflect magnetic noise fields: Application to MEG
[DE89-012592] N90-14676
Heat and mass transfer design issues in PEM fuel cell hardware
[DE89-016779] N90-14677
Workload induced spatio-temporal distortions and safety of flight
[DE89-016613] N90-14771
The High-Speed Channel (HSC) and ultra-speed networks
[DE89-015283] N90-14819
Algorithmic randomness, physical entropy, measurements, and the second law
[DE90-002413] N90-14823
Multiple crossbar network: Integrated supercomputing framework
[DE89-012614] N90-14831
Multiple crossbar network: A switched high-speed local network
[DE90-001839] N90-14833
Numerical methodologies for solving partial differential equations
[DE90-001842] N90-14849
Symplectic numerical integration of Hamiltonian systems
[DE90-002380] N90-14855
Physics with ultra-low energy antiprotons
[DE90-002397] N90-14888
The creation of high energy densities with antimatter beams
[DE90-002383] N90-14899
Performance of the 10-kV, 100-kA pulsed-power modules for the FRX-C magnetic compression experiment
[DE89-014027] N90-14917
Two-dimensional behavior of Megagauss-field-confined solid fiber Z-pinches
[DE90-000684] N90-14918
Ion beam analysis and modification of thin-film, high-temperature superconductors
[DE90-000918] N90-14941
High-temperature/high-pressure x ray diffraction: Recent developments
[DE89-015255] N90-14949
Superconductivity from finite-U valence fluctuations
[DE90-000603] N90-14954
A simple figure of merit for high temperature superconducting switches
[DE90-000610] N90-14955
Muon SR investigation of magnetism and superconductivity in (Y(1-x)Pr(x))Ba2Cu3O7
[DE90-000689] N90-14956
Microwave characterization of high-temperature superconductors
[DE90-002408] N90-14968
RF superconductivity research and development at Los Alamos National Laboratory
[DE90-002440] N90-14969
Dynamical simulation of dislocation microstructure
[DE90-003192] N90-14982
The influence of the substrate surface on the nucleation and growth of superconducting thin films
[DE90-003649] N90-14983
The softest Einstein AGN (Active Galactic Nuclei)
[DE89-009389] N90-15020
A source of observational constraints on the structure of Wolf-Rayet winds
[DE90-001236] N90-15023
Dark matter and the solar neutrino problem: Can particle physics provide a single solution
[DE90-001827] N90-15024

LOWELL UNIV., MA.
A portable ionosonde in support of reliable communications N90-14431

LUNAR AND PLANETARY INST., HOUSTON, TX.
Workshop on the Archean Mantle
[NASA-CR-186156] N90-14736
Abstracts for the 52nd Annual Meeting of the Meteoritical Society
[NASA-CR-186160] N90-14998
Workshop on Moon in Transition: Apollo 14, KREEP, and Evolved Lunar Rocks
[NASA-CR-186153] N90-15026

LUND UNIV. (SWEDEN).
A study of recoil protons in ultra-relativistic nucleus-nucleus collisions
[LUIP-8907] N90-14873

M

MANCHESTER UNIV. (ENGLAND).
Cavitation and superplasticity N90-14329
Radio and optical observations of nearby active galaxies N90-15000
MERLIN and VLBI observations of the radio galaxy Virgo A N90-15001

MARYLAND UNIV., COLLEGE PARK.
An experimental investigation of shear layer mixing in supersonic flows N90-14508
An observational study of intramonthly quasi-periodicities in the Northern Hemisphere, extratropical geopotential height field N90-14729
Kilometric type III radio bursts and interplanetary transients N90-15038

MASSACHUSETTS INST. OF TECH., CAMBRIDGE.
Self-field-induced chaotic electron motion in free electron lasers
[DE90-001710] N90-14598
Ion collection by probing objects in flowing magnetized plasmas
[DE90-001711] N90-14916

MASSACHUSETTS TECHNOLOGICAL LAB., INC., BETHESDA, MD.
Communication Overview Program (COP) N90-14435

MASSACHUSETTS UNIV., AMHERST.
Climate system research studies of global and regional instrumental data
[DE90-001205] N90-14707
The design and implementation of an intelligent interface for information retrieval N90-14991

MICHIGAN UNIV., ANN ARBOR.
Project Argo: The design and analysis of an all-propulsive and an aeroassisted version of a manned space transportation vehicle
[NASA-CR-186047] N90-14266
Mechanisms of wear in structural ceramic materials N90-14360
High resolution Doppler lidar
[NASA-CR-183288] N90-14542
Localized vibrations of nearly periodic structures with irregularities N90-14648
A measurement of hydroxyl in the daytime mesosphere N90-14732
The retrieval of the concentrations of nitric oxide and nitrogen dioxide from satellite solar occultation measurements at sunset and sunrise N90-14733
Studies of elementary particles: Proposal
[DE90-001120] N90-14879

MIDWEST RESEARCH INST., GOLDEN, CO.
Preparation and properties of high deposition a-Si:H films and solar cells using disilane
[DE89-009467] N90-14679
Thin film cadmium telluride, zinc telluride, and mercury zinc telluride solar cells
[DE89-009499] N90-14681
An initial look at the dynamics of the microscale flow field within a large wind farm in response to variations in the natural inflow
[DE89-009501] N90-14682
Research on high-efficiency, single-junction, monolithic, thin-film amorphous silicon solar cells
[DE89-000846] N90-14687
Computer simulation of wind/diesel system operation
[DE89-009445] N90-14688
High-efficiency large-area CdTe modules
[DE89-009498] N90-14689
Hydrogen radical enhanced growth of solar cells
[DE89-009497] N90-14694
Photovoltaic Measurements and Performance Branch
[DE89-009500] N90-14695

MISSISSIPPI STATE UNIV., STATE COLLEGE.
Advanced 3-D CFD algorithm for turbomachinery N90-14233
A dynamic multiblock approach to solving the unsteady Euler equations about complex configurations N90-14497

Three-dimensional solution-adaptive grid generation of composite configurations N90-14509

MISSOURI UNIV., ROLLA.

Finite element analysis of laminated composite plates N90-14291

Shear strain localization phenomenon in viscoplastic materials N90-14649

MITRE CORP., EATONTOWN, NJ.

Forward scatter propagation path loss testing using surrogate terrain in the 100 to 1500 MHz region N90-14425

MORGANTOWN TECHNOLOGY CENTER, WV.

Proceedings of the First Annual Fuel Cells Contractors Review Meeting [DE89-011699] N90-14675

MOUNTAINNET, DELLSLOW, WV.

AdaNET services N90-14806

N

NATIONAAL INST. VOOR KERNFYSICA EN HOGE ENERGIEFYSICA, AMSTERDAM (NETHERLANDS).

NIKHEF-K contributions to the 1989 Particle Accelerator Conference [NIKHEF/AMPS/89/03] N90-14891

The Amsterdam pulse stretcher project (AmPS) N90-14892

Optics of the Amsterdam pulse stretcher (AmPS) N90-14893

Modification of MEA modulator-klystron units enabling short pulse injection into a pulse-stretcher ring N90-14894

Performance and modification of the MEA RF drive system N90-14895

An Energy Spectrum Compressor system (ESC) for the Amsterdam pulse stretcher (AmPS) N90-14896

NATIONAL ACADEMY OF SCIENCES - NATIONAL RESEARCH COUNCIL, WASHINGTON, DC.

Long-lived space observatories for astronomy and astrophysics [NASA-CR-185373] N90-14261

Mid-Oceanic Ridge: A Dynamic Global System [PB89-198691] N90-14758

An international discussion on research in solar and space physics N90-14996

NATIONAL AERONAUTICS AND SPACE ADMINISTRATION, WASHINGTON, DC.

Draft Environmental Impact Statement for the Ulysses Mission (Tier 2) [NASA-TM-102903] N90-14727

Exploring the living universe: A strategy for space life sciences [NASA-TM-101891] N90-14778

SSFP approach to software reuse N90-14799

NATIONAL AERONAUTICS AND SPACE ADMINISTRATION. AMES RESEARCH CENTER, MOFFETT FIELD, CA.

Unsteady aerodynamic simulation of multiple bodies in relative motion: A prototype method [NASA-TM-102181] N90-14188

Global stratospheric change: Requirements for a Very-High-Altitude Aircraft for Atmospheric Research [NASA-CP-10041] N90-14220

Airdata calibration of a high-performance aircraft for measuring atmospheric wind profiles [NASA-TM-101714] N90-14228

Temporally and spatially resolved flow in a two-stage axial compressor. Part 2: Computational assessment [NASA-TM-102273] N90-14236

A diagnostic for determining the quality of single-reference electron correlation methods [NASA-TM-101929] N90-14874

Saltation thresholds and entrainment of fine particles at Earth and Martian pressures [NASA-TM-102193] N90-14997

NATIONAL AERONAUTICS AND SPACE ADMINISTRATION. GODDARD SPACE FLIGHT CENTER, GREENBELT, MD.

Shuttle Laser Technology Experiment Facility (LTEF)-to-airplane lasercom experiment: Airplane considerations [NASA-TM-100749] N90-14260

Prototype software reuse environment at Goddard Space Flight Center N90-14794

NATIONAL AERONAUTICS AND SPACE ADMINISTRATION. HUGH L. DRYDEN FLIGHT RESEARCH FACILITY, EDWARDS, CA.

An in-flight investigation of ground effect on a forward-swept wing airplane [NASA-TM-101708] N90-14202

An in-flight technique for wind measurement in support of the space shuttle program [NASA-TM-4154] N90-14224

Flight evaluation of a pneumatic system for unsteady pressure measurements using conventional sensors [NASA-TM-4131] N90-14225

The Aerospace Energy Systems Laboratory: A BITBUS networking application [NASA-TM-4149] N90-14829

NATIONAL AERONAUTICS AND SPACE ADMINISTRATION. LYNDON B. JOHNSON SPACE CENTER, HOUSTON, TX.

Johnson Space Center software reuse activity N90-14796

The Apollo 15 coarse fines (4-10 mm) [NASA-TM-101934] N90-15027

NATIONAL AERONAUTICS AND SPACE ADMINISTRATION. LANGLEY RESEARCH CENTER, HAMPTON, VA.

Measured and predicted aerodynamic coefficients and shock shapes for Aeroassist Flight Experiment (AFE) configuration [NASA-TP-2956] N90-14185

Effect of blade planform variation on a small-scale hovering rotor [NASA-TM-4148] N90-14186

Validation of a computer code for analysis of subsonic aerodynamic performance of wings with flaps in combination with a canard or horizontal tail and an application to optimization [NASA-TP-2961] N90-14187

Effect of pylon wake with and without pylon blowing on propeller thrust [NASA-TM-4162] N90-14190

Experimental transonic flutter characteristics of two 72 deg-sweep delta-wing models [NASA-TM-101659] N90-14205

A candidate concept for display of forward-looking wind shear information [NASA-TM-101585] N90-14232

Cryogenic temperature effects on sting-balance deflections in the National Transonic Facility [NASA-TM-4157] N90-14244

Aerobraking characteristics for several potential manned Mars entry vehicles [NASA-TM-101669] N90-14272

Surface flow and heating distributions on a cylinder in near wake of Aeroassist Flight Experiment (AFE) configuration at incidence in Mach 10 Air [NASA-TP-2954] N90-14493

A capacitive technique for real-time monitoring polymer coating thickness on carbon filaments during prepregging process [NASA-TM-101682] N90-14533

Atlas of albedo and absorbed solar radiation derived from Nimbus 6 earth radiation budget data set, July 1975 to May 1978 [NASA-RP-1230] N90-14741

Software Reuse Issues [NASA-CP-3057] N90-14789

Reuse research plans at Langley Research Center N90-14797

Calculation of two-neutron multiplicity in photonuclear reactions [NASA-TP-2968] N90-14890

NATIONAL AERONAUTICS AND SPACE ADMINISTRATION. LEWIS RESEARCH CENTER, CLEVELAND, OH.

Efficient real gas Navier-Stokes computations of high speed flows using an LU scheme [NASA-TM-102429] N90-14203

An analysis of the viscous flow through a compact radial turbine by the average passage approach [NASA-TM-102471] N90-14206

RAMSCRAM: A flexible ramjet/scramjet engine simulation program [NASA-TM-102451] N90-14235

Slush Hydrogen (SLH2) technology development for application to the National Aerospace Plane (NASP) [NASA-TM-102315] N90-14268

Characterization of two MMIC GaAs switch matrices at microwave frequencies [NASA-TM-102449] N90-14273

Design considerations for space flight hardware [NASA-TM-102300] N90-14275

A heat receiver design for solar dynamic space power systems [NASA-TM-102473] N90-14283

Atomic hydrogen as a launch vehicle propellant [NASA-TM-102459] N90-14284

On protection of Freedom's solar dynamic radiator from the orbital debris environment. Part 1: Preliminary analyses and testing [NASA-TM-102458] N90-14285

Oxidation effects on the mechanical properties of SiC fiber-reinforced reaction-bonded silicon nitride matrix composites [NASA-TM-102360] N90-14287

Parametric studies to determine the effect of compliant layers on metal matrix composite systems [NASA-TM-102465] N90-14294

Calibration approach to electron probe microanalysis: A study with PWA-1480, a nickel base superalloy [NASA-TM-102393] N90-14335

Density of intercalated graphite fibers [NASA-TM-102411] N90-14362

The 3F condensation polyimides: Review and update [NASA-TM-102353] N90-14363

Strength and toughness of monolithic and composite silicon nitrides [NASA-TM-102423] N90-14368

Thermal/structural analyses of several hydrogen-cooled leading-edge concepts for hypersonic flight vehicles [NASA-TM-102391] N90-14511

Spatial evolution of nonlinear acoustic mode instabilities on hypersonic boundary layers [NASA-TM-102431] N90-14517

Comparison of two droplet sizing systems in an icing wind tunnel [NASA-TM-102456] N90-14617

Viscoplasticity: A thermodynamic formulation [NASA-TM-102388] N90-14640

Thermal fatigue durability for advanced propulsion materials [NASA-TM-102348] N90-14641

A nonlinear high temperature fracture mechanics basis for strainrange partitioning [NASA-TM-4133] N90-14642

A new uniformly valid asymptotic integration algorithm for elasto-plastic-creep and unified viscoplastic theories including continuum damage [NASA-TM-102344] N90-14655

Concurrent processing adaptation of aeroplastic analysis of propfans [NASA-TM-102455] N90-14656

Technology development program for an advanced microsheet glass concentrator [NASA-TM-102406] N90-14678

On the application of subcell resolution to conservation laws with stiff source terms [NASA-TM-102384] N90-14844

Application of heuristic satellite plan synthesis algorithms to requirements of the WARC-88 allotment plan [NASA-TM-102479] N90-14856

SP-100 power system conceptual design for lunar base applications [NASA-TM-102090] N90-15030

NATIONAL AERONAUTICS AND SPACE ADMINISTRATION. MARSHALL SPACE FLIGHT CENTER, HUNTSVILLE, AL.

Payload crew utilization for spacelab missions [NASA-TP-2976] N90-14256

Main propulsion system test requirements for the two-engine Shuttle-C [NASA-TM-100382] N90-14282

The solar activity measurements experiments (SAMEX) for improved scientific understanding of solar activity [NASA-TM-100372] N90-15036

NATIONAL AGRICULTURAL LIBRARY, BELTSVILLE, MD.

Proceedings of the Conference on Application of Scanning Methodologies in Libraries [PB89-233415] N90-14990

NATIONAL CENTER FOR ATMOSPHERIC RESEARCH, BOULDER, CO.

Workshop on synoptic meteorology instruction [PB90-109950] N90-14751

A global ocean wind stress climatology based on ECMWF (European Centre for Medium Range Weather Forecasts) analyses [PB90-109968] N90-14752

NATIONAL DEFENCE ACADEMY, YOKOSUKA (JAPAN).

Hybrid PE-ray-mode formulation of high frequency propagation in a bilinear tropospheric surface duct N90-14417

NATIONAL GEOPHYSICAL DATA CENTER, BOULDER, CO.

Solar-geophysical data number 536, June 1989. Part 1: (Prompt reports). Data for May, April 1989, and late data [PB89-223838] N90-15031

Solar-geophysical data number 538, June 1989. Part 2: (Comprehensive reports). Data for December 1988 and miscellaneous [PB89-223846] N90-15032

Solar-geophysical data number 539, July 1989. Part 1: (Prompt reports). Data for June, May 1989, and late data [PB89-235451] N90-15033

Solar-geophysical data number 539, July 1989. Part 2: (Comprehensive reports). Data for January 1989, and miscellaneous [PB89-235469] N90-15034

Solar-geophysical data number 540, August 1989. Part 1: (Prompt reports). Data for July, June 1989, and late data
[PB90-106572] N90-15035
Solar-geophysical data number 540, August 1989. Part 2: (Comprehensive reports). Data for February 1989
[PB89-108598] N90-15039

NATIONAL INST. OF GENERAL MEDICAL SCIENCES, BETHESDA, MD.
Nomenclature for physical mapping of complex genomes
[DE89-015173] N90-14994

NATIONAL MARINE FISHERIES SERVICE, SEATTLE, WA.
Tuning of the OSCURS (Ocean Surface Current Simulations) numerical model to ocean surface measurements in the Gulf of Alaska
[PB89-103979] N90-14759

NATIONAL OCEANIC AND ATMOSPHERIC ADMINISTRATION, BOULDER, CO.
Statistics of two-color laser beam propagation in the turbulent atmosphere (spectral correlation)
[PB89-236699] N90-14581
Probability density function of optical scintillations (scintillation distribution)
[PB89-103912] N90-14906

NATIONAL SCIENCE FOUNDATION, WASHINGTON, DC.
Science and technology resources in US industry: Surveys of science resources series, 1975-1986
[PB90-107194] N90-14401

NATIONAL TECHNICAL INFORMATION SERVICE, SPRINGFIELD, VA.
Accessing Japanese technical information: A group of essays extracted from the NTIS (National Technical Information Service) Directory of Japanese Technical Resources in the United States for 1987 and 1988
[PB90-100165] N90-14992

NATIONAL TELECOMMUNICATIONS AND INFORMATION ADMINISTRATION, BOULDER, CO.
Pattern recognition techniques applied to the NASA-ACTS order-wire problem N90-14446

NATIONAL WEATHER SERVICE, FORT WORTH, TX.
Summary of papers, studies, conference presentations: 1987-1988 (from the National Weather Service, southern region)
[PB90-103896] N90-14749

NATIONAL WEATHER SERVICE, SILVER SPRING, MD.
Use of operational 0-6 and 3-9 h quantitative precipitation forecasts for predicting heavy rain events
[PB90-103946] N90-14750

NATO ADVANCED STUDY INST., LUCCA (ITALY).
Structure-property relationships in surface-modified ceramics. NATO Advanced Science Institutes, series E: Applied Sciences, volume 170
[AD-A212939] N90-14359

NAUCHNO-ISSLEDOVATELSKII INST. ATOMNYKH REAKTOROROV, DIMITROVGRAD (USSR).
Assessment of the efficiency of nondestructive techniques in materials testing studies based on the information criterion
[DE89-635444] N90-14634

NAVAL ENVIRONMENTAL PREDICTION RESEARCH FACILITY, MONTEREY, CA.
A one-dimensional shipboard model for forecasting refractive effects in the planetary boundary layer N90-14442

NAVAL OCEAN RESEARCH AND DEVELOPMENT ACTIVITY, BAY SAINT LOUIS, MS.
NORDA's pattern analysis laboratory: Current contributions to naval mapping, charting, and geodesy
[AD-A212731] N90-14665
A rough transform technique for extracting lead features from sea ice imagery
[AD-A212758] N90-14666

NAVAL OCEAN SYSTEMS CENTER, SAN DIEGO, CA.
Crazing and degradation of flexure strength in acrylic plates as a function of time
[AD-A212835] N90-14357
Propagation assessment and tactical decision aids N90-14407
Propagation-based decision aids in the U.S. Navy N90-14410
Engineer's Refractive Effects Prediction System (EREPS) N90-14411
PROPHET and future signal warfare decision aids N90-14412
Long wave propagation assessment N90-14414
Airborne FLIR detection of surface targets N90-14416
RPE: A parabolic equation radio assessment model N90-14419
Propagation modeling for some horizontally varying tropospheric ducts N90-14422

NAVAL POSTGRADUATE SCHOOL, MONTEREY, CA.
Computational investigation of incompressible airfoil flows at high angles of attack
[AD-A205885] N90-14201
Physical models for aerosol in the marine mixed-layer N90-14438
Control of an experiment to measure acoustic noise in the space shuttle
[NPS62-89-022] N90-14869

NAVAL RESEARCH ADVISORY COMMITTEE, WASHINGTON, DC.
The importance of environmental data N90-14406

NAVAL RESEARCH LAB., WASHINGTON, DC.
Decision-aid design factors in connection with HF communication and emitter location disciplines N90-14413

NEVADA UNIV., RENO.
Numerical investigations in three-dimensional internal flows
[NASA-CR-186068] N90-14189
Convective boundary layer and modeling of dispersion N90-14731

NEVADA UNIV. SYSTEM, RENO.
Profile measurements of sulfur dioxide, nitrogen oxides, and nitric acid deposition velocities in California's south coast air basin
[PB90-104001] N90-14703

NEW WORLD SERVICES, INC., FL.
Chronology of KSC and KSC related events for 1988
[NASA-TM-101915] N90-15040

NEW YORK UNIV., NEW YORK.
The laminar to slug flow transition in Hele-Shaw flow
[DE90-000636] N90-14521

NORTH CAROLINA STATE UNIV., RALEIGH.
Numerical modeling of supersonic turbulent reacting free shear layers N90-14197
A one equation turbulence model for transonic airfoils N90-14199

NORTH CAROLINA UNIV., CHARLOTTE.
Dynamics and control of flexible spacecraft during and after slewing maneuvers
[NASA-CR-186123] N90-14270

NORTHEASTERN FOREST EXPERIMENT STATION, BROOMALL, PA.
Proceedings of the US/FRG (Fed. Republic of Germany) research symposium: Effects of Atmospheric Pollutants on the Spruce-Fir Forests of the Eastern United States and the Fed. Republic of Germany
[PB90-107160] N90-14704

NORTHWESTERN UNIV., EVANSTON, IL.
Effects of flame stretch on the propagation, extinction, and stability of premixed flames N90-14301
Electrical properties of materials for high temperature strain gage applications
[NASA-CR-186192] N90-14534
Nondestructive evaluation of flaw clusters and thin layer interfaces N90-14633
Comparison of structural subunits of the core light-harvesting complexes of photosynthetic bacteria
[DE90-001412] N90-14765

NOTTINGHAM UNIV. (ENGLAND).
The stress analysis of thin-walled screwed tubular joints N90-14637

NSI TECHNOLOGY SERVICES CORP., CORVALLIS, OR.
Climate-biosphere interactions scope of work
[PB90-106444] N90-14734

O

OAK RIDGE NATIONAL LAB., TN.
Characteristics of an electron-beam rocket pellet accelerator
[DE90-001595] N90-14252
Acceleration of small, light projectiles (including hydrogen isotopes) to high speeds using a two-stage light gas gun
[DE90-002479] N90-14253
Fiber-optic sensors for composite cure analysis and lifetime nondestructive evaluation
[DE90-001739] N90-14296
Asymptotic analysis of performance of membrane modules for gas separations
[DE90-000699] N90-14316
SEM (Scanning Electron Microscope) image analysis of grain growth in microwave-annealed alumina
[DE90-001606] N90-14339
High-temperature corrosion of heat exchanger materials
[DE90-001963] N90-14352
The 7th International Conference on Ceramics
[DE90-002144] N90-14374
Numerical and empirical verification of the stress state in a ceramic, button-head, tensile specimen
[DE90-001645] N90-14375
Electron heating and static sheath enhancement in front of energized RF antennas
[DE90-001334] N90-14456
Integrating and enhancing tools for ASIC (Application-Specific Integrated Circuits) design using MOSIS (Metal Oxide Semiconductor Implementation Service) fabrication
[DE90-001601] N90-14475
Prospects for wavelength tunable lasers based on vacancy defects in alkaline-earth oxides
[DE90-001078] N90-14592
Solid-state fluorescence above 1000 C: Application to high-temperature laser thermometry
[DE90-000728] N90-14594
Studies of neutral and ion transport during laser ablation of 1:2:3 superconductors by optical absorption spectroscopy
[DE90-001968] N90-14604
Nonresonant and resonant multiphoton ionization of (NO)(sub n) and Ar(sub n)NO clusters with picosecond laser pulses
[DE89-016853] N90-14607
BES welding science contractors summary report, 1988 to 1989
[DE90-001004] N90-14619
Results of the manipulator test test stand study: Comparison of manipulators and evaluation of equipment items
[DE90-000977] N90-14625
French technological progress in the field of robotics and teleoperation
[DE90-001590] N90-14626
The feasibility of welding of irradiated materials
[DE90-002200] N90-14631
Fracture mechanics of porous materials
[DE90-000023] N90-14657
Engineering approaches to the application of fracture toughness data in the nuclear industry
[DE90-001596] N90-14659
A computer-controlled automated test system for fatigue and fracture testing
[DE90-002931] N90-14661
Global natural resource monitoring and assessment
[DE90-001294] N90-14671
How far can the world get on energy efficiency alone
[DE90-001349] N90-14686
Heat transfer of buried pipe for heat pump application
[DE90-000580] N90-14697
Canopy stomatal conductance
[DE89-016860] N90-14711
The impact of global warming on the energy system
[DE89-017775] N90-14712
Application of surface analysis methods to studies of atmospheric deposition in forests
[DE90-000582] N90-14714
Discussions of global environmental problems
[DE90-002747] N90-14718
Strategy for monitoring the effects of land use change on atmospheric CO2 concentrations
[DE90-001635] N90-14722
Nitrogen deposition to forest trees
[DE90-003285] N90-14726
Human factors survey of advanced instrumentation and controls
[DE90-002477] N90-14776
Some numerical experiments concerning the equation of state algorithm for multi-material cells in HULL
[DE89-006240] N90-14827
X ray microprobe for the microcharacterization of materials
[DE89-006036] N90-14883
Interaction of low-energy electrons and positrons with condensed matter: Stopping powers and inelastic mean free paths from optical data
[DE90-001001] N90-14882
Direction-dependent stopping power and beam deflection in anisotropic solids
[DE90-001076] N90-14883
Static and dynamic magnetization properties of Y1Ba2Cu3O(sub z) thin films
[DE89-017584] N90-14940
Theory of strongly fluctuating superconductivity
[DE90-001073] N90-14942
Ion beam processing of advanced electronic materials
[DE89-017342] N90-14944
Solid State Division
[DE90-000979] N90-14945
Development of a real time monitor for superconductive thin film preparation
[DE89-017772] N90-14952
Practical limitations of ALCHEMI measurements on ordered intermetallic alloys
[DE90-000700] N90-14957
Magnetic excitations in thulium metal
[DE90-002475] N90-14970

OBSERVATOIRE DU MONT-GROS, NICE (FRANCE).
Simulated Brillouin backscattering in optical fibers: A ring resonator N90-14556
OFFICE OF NAVAL RESEARCH, ARLINGTON, VA.
Cognitive and Neural Sciences Division 1989 programs
[AD-A212634] N90-14769
OHIO STATE UNIV., COLUMBUS.
Finite element analysis of frictional contact problems N90-14612
Crack problems for elastic-plastic materials under antiplane shear loadings N90-14651
OHIO UNIV., ATHENS.
Parallel eigenanalysis of finite element models in a completely connected architecture
[NASA-CR-185166] N90-14652
OKLAHOMA UNIV., NORMAN.
A computational analysis of the transonic flow field of two-dimensional minimum length nozzles N90-14194
Stability of a supersonic boundary layer on a sharp cone at a small angle of attack N90-14510
The dynamics of simulated convective storms in hurricane environments N90-14747
OLD DOMINION UNIV., NORFOLK, VA.
Subsonic sting interference on the aerodynamic characteristics of a family of slanted-base ogive-cylinders
[NASA-CR-186193] N90-14204
Guidance and Control strategies for aerospace vehicles
[NASA-CR-186195] N90-14243
Theoretical studies of solar lasers and converters
[NASA-CR-186194] N90-14583
OREGON STATE UNIV., CORVALLIS.
Perturbed angular correlations in zirconia ceramics
[DE89-017272] N90-14369
ORGANISATIE VOOR TOEGEPAST NATUURWETENSCHAPPELIJK ONDERZOEK, THE HAGUE (NETHERLANDS).
The effect of oblate spheroidal drops on rain attenuation at 94 GHz: Comparison between theory and experiment N90-14440
Modelling UHF propagation for frequency assignment in radio relay networks N90-14445
OXFORD UNIV. (ENGLAND).
Remote sensing of atmospheric water vapour by pressure modulation radiometry N90-14667

P

PACIFIC MISSILE TEST CENTER, POINT MUGU, CA.
Weather satellite and computer modeling approaches to assessing propagation over marine environments N90-14443
PACIFIC NORTHWEST LAB., RICHLAND, WA.
Combined capillary electrophoresis and electrospray ionization mass spectrometry
[DE90-001903] N90-14322
Acoustic emission during intergranular stress corrosion cracking
[DE90-002894] N90-14355
Low-temperature conversion of high-moisture biomass: Continuous reactor system results
[DE90-000984] N90-14683
Solid oxide fuel cells electrodes based on In(sub 2)O(sub 3)-PrO(sub 1.83)-ZrO(sub 2)
[DE90-002666] N90-14691
Detailed analysis of the wake and free-flow characteristics at the Goodnoe Hills MOD-2 site
[DE90-002725] N90-14692
Turbulent wind at the equatorial segment of an operating Darrieus wind turbine blade
[DE90-002672] N90-14698
Global energy and the greenhouse issue
[DE90-001394] N90-14709
Integrated computer-based tools to facilitate environmental monitoring, assessment, and restoration
[DE90-002732] N90-14717
The identification of terrain-induced circulations using principal components
[DE90-001991] N90-14739
Beyond the IDMY (International Daylighting Measurements Year): A network instrument for low-cost data acquisition
[DE90-002722] N90-14740
Meteorological monitoring for environmental/dose assessment and emergency response modeling: How much is enough
[DE90-002726] N90-14757
Cold fusion: Alchemist's dream
[DE90-000865] N90-14925
PARIS-SUD UNIV., CACHAN (FRANCE).
The use of backscatter for modelling ionosphere and jamming in very short term forecasts N90-14434
PARIS-SUD UNIV., ORSAY (FRANCE).
Anisotropy of electron distributions related to the anisotropy and polarization of the continuous emitted x rays N90-14566
Population inversions calculated for lithium-like ions in a plasma N90-14571
Study of lithium-like ions for amplifying radiation below 100 angstroms. Experiment at the Rutherford Appleton Laboratory N90-14572
Single beam interactions for the study of x ray lasers N90-14573
X-UV amplification in a plasma column of five centimeters. Five beams experiment N90-14574
PARIS VI UNIV. (FRANCE).
Atomic structure and spectral perturbations in hot dense plasmas N90-14567
Transversal inhomogeneity and radiative transfer in plasmas obtained by laser impact N90-14568
PARIS XI UNIV., ORSAY (FRANCE).
Box experiments. Nonlinear effects at plasma resonance N90-14555
PENNSYLVANIA STATE UNIV., UNIVERSITY PARK.
Kinetics and mechanism of soot formation in hydrocarbon combustion
[NASA-CR-186162] N90-14305
Thermal stability of jet fuel
[DE90-001160] N90-14385
Theory of wide-angle photometry from standard stars
[NASA-CR-185964] N90-14999
PENNSYLVANIA UNIV., PHILADELPHIA.
Synthesis and properties of new preceramic materials
[DE90-002562] N90-14373
PINNACLE RESEARCH INST., CUPERTINO, CA.
The secondary slurry-zinc/air battery
[DE90-002600] N90-14491
PITTSBURGH UNIV., PA.
Pipe and bend erosion by pneumatic transport of solids at high temperature
[DE89-015741] N90-14524
PLANNING RESEARCH CORP., HOUSTON, TX.
Support for life-cycle product reuse in NASA's SSE N90-14802
PRINCETON UNIV., NJ.
Energy deposition in low power coaxial plasma thrusters N90-14911
PURDUE UNIV., WEST LAFAYETTE, IN.
Design of a spanloader cargo aircraft
[NASA-CR-186046] N90-14216
Interfacial area in two-phase flow
[DE90-002210] N90-14527

R

REMTECH, INC., HUNTSVILLE, AL.
SRB thermal environments
[NASA-CR-183801] N90-14276
RICE UNIV., HOUSTON, TX.
Optimal trajectories for the aeroassisted flight experiment
[NASA-CR-186133] N90-14250
RJO ENTERPRISES, INC., LEXINGTON, MA.
Configuration development for ROMENET
[AD-A213367] N90-14450
ROCHESTER UNIV., NY.
Effects of dislocation substructure and prestrain on fracture behavior in aluminum and steel alloys N90-14334
ROCKET RESEARCH CORP., REDMOND, WA.
Arcjet thruster research and technology. Phase 1: Executive summary
[NASA-CR-182106] N90-14278
ROCKWELL INTERNATIONAL CORP., CANOGA PARK, CA.
Extravehicular activity welding experiment
[NASA-CR-183848] N90-14608
ROLLS-ROYCE LTD., DERBY (ENGLAND).
SAS graphics in DCF
[PNR90563] N90-14399
ROME UNIV. (ITALY).
Spectral properties of one dimensional quasi-crystals
[PREPRINT-659] N90-14938
ROYAL AIRCRAFT ESTABLISHMENT, FARNBOROUGH (ENGLAND).
Evaluation of the indirect effects of lightning on a system: Double transfer function method
[RAE-TRANS-2172] N90-14211
Diffusion bonding of metals N90-14330
The mechanical properties of superplastically formed titanium and aluminium alloys N90-14331
RUTGERS - THE STATE UNIV., NEW BRUNSWICK, NJ.
Ultraviolet properties of hot stars in globular clusters N90-15007

S

SANDIA NATIONAL LABS., ALBUQUERQUE, NM.
Visualization of boundary layer transition zone movement on oscillating airfoils with shear-sensitive liquid-crystal coatings
[DE89-009570] N90-14210
Solving the blow-by problem in a two-stage gun
[DE90-000842] N90-14246
Sandia Satellite Program summary of operational procedures
[DE90-000892] N90-14249
Thermal environmental tests on space simulation chamber
[DE90-000927] N90-14251
Performance characteristics of a three-stage railgun
[DE90-002533] N90-14254
Flame acceleration studies in the MINIFLAME facility
[DE90-000041] N90-14310
Shock-induced solid state reactions and phase transitions: X ray profile studies on shock-modified Fe3O4 and ZrO2 powders
[DE90-000669] N90-14315
Interaction of hydrogen isotopes with metals: Deuterium trapped at lattice defects in palladium
[DE90-000811] N90-14344
Spall strength measurements on shockloaded refractory metals
[DE90-000839] N90-14345
Chemistry of large molecules
[DE90-000813] N90-14366
Automated glass fiber drawing
[DE90-000894] N90-14367
Bulk and shear moduli of epoxy encapsulants
[DE90-000899] N90-14371
Predictive aging of elastomers in air: The importance of understanding diffusion-limited oxidation effects
[DE90-001385] N90-14372
Fast transit gas- and condensed-phase chemistry of energetic materials
[DE90-001656] N90-14395
A discussion of fire suppression induced equipment damage and systems impact through an examination of spurious fire suppression actuation incidents
[DE90-000792] N90-14402
A radar simulation program for a 1024-processor hypercube
[DE89-014494] N90-14455
Detection of a chirping electromagnetic signal
[DE90-002105] N90-14457
Review of surface flashover theory
[DE90-000806] N90-14469
Terrestrial nickel/hydrogen battery development at Johnson Controls, Inc.
[DE89-015843] N90-14471
Sodium/sulfur evaluation at SNL
[DE89-015846] N90-14472
Zinc/bromine battery evaluation at SNL (Sandia National Laboratory)
[DE89-015847] N90-14473
Effects of composition and age hardening on precious metal electrical contacts
[DE88-008791] N90-14476
A software-based controller for generation of synchronized pulses for use with rotating machinery
[DE89-016672] N90-14477
Electrical breakdown in vacuum
[DE90-001623] N90-14485
CTH: A three-dimensional shock wave physics code
[DE89-016529] N90-14526
Evaluation of shock isolation techniques for a piezoresistive accelerometer
[DE89-014496] N90-14535
Projectile impact Hugoniot parameters for selected materials
[DE90-000891] N90-14618
A laboratory test for fuel injector deposit studies
[DE90-000802] N90-14629
Hypervelocity impact calculations using CTH: Case studies
[DE90-002891] N90-14632
Comparison of shock severity measures
[DE90-000790] N90-14654
Implications and origins of shock structure in solids
[DE90-000846] N90-14658
Control of the variable speed generator on the Sandia 34-metre vertical axis wind turbine
[DE90-000803] N90-14674
Polarization of Li/SOCl2 cells
[DE90-000883] N90-14680
The phase gradient autofocus algorithm: An optimal estimator of the phase derivative
[DE90-000895] N90-14814

SANDIA NATIONAL LABS.

Generalization in backpropagation networks: An empirical study using image data
[DE89-012658] N90-14835
Effective utilization of acoustic wave sensor responses: Simultaneous measurement of velocity and attenuation
[DE90-002580] N90-14872
A review of gas-cooled reactor concepts for SDI (Strategic Defense Initiative)
[DE89-016962] N90-14898
Modeling of runaway electron damage for the design of tokamak plasma facing components
[DE90-000847] N90-14914
Thermal loads on tokamak plasma facing components during normal operation and disruptions
[DE90-000794] N90-14919
The effects of heavy particle radiation on semiconductor devices
[DE90-001679] N90-14962

SANDIA NATIONAL LABS., LIVERMORE, CA.
SAND DEVIL: A digital video link for telemetry applications
[DE90-001879] N90-14259
An electroformed nickel-sulfur alloy for a nose cone
[DE90-000866] N90-14337

SAO PAULO UNIV. (BRAZIL).
Nonlinear quantum effects in the Maser model: A large N scaling behaviour
[DE89-631631] N90-14584

SCIENCE APPLICATIONS INTERNATIONAL CORP., HOUSTON, TX.
Initial Ada components evaluation N90-14803

SCIENCE RESEARCH COUNCIL, CHILTON (ENGLAND).
A forecasting system using the parabolic equation: Application to surface-to-air propagation in the presence of elevated layers N90-14420
Assessment of anomalous propagation predictions using minisonde refractivity data and the parabolic equation method N90-14424

SCIENTEX CORP., ROCKVILLE, MD.
GRAFIN: GRAFIX interactive manual
[PB89-232136] N90-14809

SIGNATRON, INC., LEXINGTON, MA.
Improved reliability prediction for HF digital voice transmission N90-14429
TROPO: A technique for predicting propagation and modem performance of digital troposcatter systems N90-14444

SKODA WORKS, PILSEN (CZECHOSLOVAKIA).
Measuring the thickness of austenitic weld deposits on carbon steel walls using a magnetic method
[DE89-635446] N90-14628

SOFTWARE PRODUCTIVITY CONSORTIUM, HERNDON, VA.
Reuse at the Software Productivity Consortium N90-14798

SOFTWARE PRODUCTIVITY SOLUTIONS, INC., MELBOURNE, FL.
Automated reuseable components system study results N90-14790
Knowledge-based reusable software synthesis system N90-14791
Impact of domain analysis on reuse methods N90-14792
Classic-Ada(TM) N90-14793

SOLAREX CORP., NEWTOWN, PA.
Research on high-efficiency, single-junction, monolithic, thin-film amorphous silicon solar cells
[DE89-000846] N90-14687

SOUTHAMPTON UNIV. (ENGLAND).
Techniques for extreme attitude suspension of a wind tunnel model in a magnetic suspension and balance system
[NASA-CR-181895] N90-14245

SOUTHWEST RESEARCH INST., SAN ANTONIO, TX.
High volume data storage architecture analysis
[NASA-CR-186239] N90-14784
Continuation of research in software for space operations support
[NASA-CR-186092] N90-14808

SPACE AND NAVAL WARFARE SYSTEM, WASHINGTON, DC.
The Tactical Environmental Support System (TESS(3)) N90-14409

SRI INTERNATIONAL CORP., MENLO PARK, CA.
High temperature chemistry of complex vaporization/decomposition processes
[DE89-016559] N90-14306

STANFORD UNIV., CA.
Devices and methods for in-situ combustion ignition
[DE89-000766] N90-14309
Advances and future directions in superplastic materials N90-14328
An entropy based approach to nonlinear stability N90-14500
Numerical solution of the incompressible Navier-Stokes equations N90-14501

STATE UNIV. OF NEW YORK, ALBANY.
Inverted surface troughs accompanying Rocky Mountain lee-side cyclogenesis N90-14746

STATE UNIV. OF NEW YORK, BUFFALO.
X ray studies of strain, interface, and impurity in semiconductors
[DE90-001525] N90-14947

STATE UNIV. OF NEW YORK, STONY BROOK.
A Scanning Photoelectron Microscope (SPEM) at the National Synchrotron Light Source (NSLS)
[DE90-001551] N90-14537

STATE UNIV. OF NEW YORK AT BUFFALO, AMHERST.
Some edge-enhancing operators and their applications to image enhancement and edge detection N90-14810

STRAINOPTIC TECHNOLOGIES, INC., NORTH WALES, PA.
Spectral contents readout of birefringent sensor
[NASA-CR-179444] N90-14905

SUNPOWER, INC., ATHENS, OH.
System design and performance prediction of a free-piston Stirling engine/magnetic coupling/compressor assembly in a gas residential heat pump
[DE89-016070] N90-14696

SURREY UNIV., GUILDFORD (ENGLAND).
Single particle friction tests with cellulose acetate sphere samples
[DE89-017537] N90-14622

SURREY UNIV., LONDON (ENGLAND).
The development of a model of the human responses to load carriage N90-14775

SVERDRUP TECHNOLOGY, INC., CLEVELAND, OH.
Thermocapillary migration of liquid droplets in a temperature gradient in a density matched system
[NASA-CR-185178] N90-14512
User's guide to PMESH: A grid-generation program for single-rotation and counterrotation advanced turboprops
[NASA-CR-185156] N90-14783

SYDNEY UNIV. (AUSTRALIA).
A theoretical investigation of the column behavior of cold-formed square hollow sections
[PB89-225981] N90-14645
A study of incremental-iterative strategies for nonlinear analyses
[PB89-226005] N90-14646
A finite strip method for the elastic-plastic large displacement analysis of thin-walled and cold-formed steel sections
[PB89-226021] N90-14647

SYSTEMS TECHNOLOGY, INC., HAWTHORNE, CA.
Field evaluation of a Nissan laser collision avoidance system
[PB90-105602] N90-14215

T

TDA RESEARCH, INC., WHEAT RIDGE, CO.
Photoconversion of inorganics to methane
[PB89-230643] N90-14379

TECHNION - ISRAEL INST. OF TECH., HAIFA.
Deferred electronic heterodyne moire deflectometry: A method for transient density fields measurement
[NASA-CR-182982] N90-14907

TELEDYNE RYAN ELECTRONICS, SAN DIEGO, CA.
Vehicle antenna for the mobile satellite experiment
[NASA-CR-186109] N90-14271

TEMPLE UNIV., PHILADELPHIA, PA.
The effects of nonselective and selective beta blockade upon nonshivering thermogenesis during an acute cold exposure in cold acclimated men N90-14767

TEXAS A&M UNIV., COLLEGE STATION.
A generalized thermomechanical constitutive model for metal matrix composites with plastic strain and damage N90-14293
Recent developments of gigatron technology
[DE90-001067] N90-14474
Gigatron: A new technology for microwave power devices
[DE90-001066] N90-14483
Synoptic scale tropical waves in multichannel satellite radiance data N90-14745

TEXAS UNIV., AUSTIN.
Tire modeling by finite elements N90-14614
Stability of the Global Alfven Eigenmode in the presence of fusion alpha particles in an ignited tokamak plasma
[DE89-016618] N90-14930
The instability and fragmentation of the envelope of supernova 1987A N90-15011
As observational and theoretical investigation of stellar flares N90-15012
M.I.N.G., Mars Investment for a New Generation: Robotic construction of a permanently manned Mars base
[NASA-CR-186224] N90-15028

THIOKOL CORP., BRIGHAM CITY, UT.
Flight set 360T004 (STS-30) field joint protection system, volume 7
[NASA-CR-183829] N90-14280
JPS heater and sensor lightning qualification
[NASA-CR-183830] N90-14530

THOMSON-CSF, VELIZY (FRANCE).
Analysis of propagation in an inhomogeneous atmosphere in the horizontal and vertical direction using the parabolic equation method N90-14421

TOLEDO UNIV., OH.
Electrical performance characteristics of high power converters for space power applications
[NASA-CR-185947] N90-14279
A numerical technique for analysis of resistojet nozzle flow N90-14506

TOULOUSE UNIV. (FRANCE).
Experimental study on the filamentary instability in laser-matter interactions at short wave lengths N90-14547
Strong Langmuir turbulence and second harmonics in laser-matter interactions N90-14548
The supersonic anisotropic collapse of Langmuir waves N90-14550
Aspects of field theory related to the Zakharov problem N90-14551
Interaction of a low flux laser beam with a solid target N90-14554
Numerical simulation of the preheating by x rays in spherical plasmas N90-14564

TRANSPORTATION SYSTEMS CENTER, CAMBRIDGE, MA.
Methodology for the calibration of and data acquisition with a six-degree-of-freedom acceleration measurement device
[PB89-233597] N90-14531

TUFTS UNIV., MEDFORD, MA.
Mechanics of interaction of a crack with microcracks N90-14650

U

UNITED STATES MAN AND THE BIOSPHERE PROGRAM, WASHINGTON, DC.
Managing marine protected areas: An action plan
[PB89-158778] N90-14701

UNITED TECHNOLOGIES RESEARCH CENTER, EAST HARTFORD, CT.
Laser velocimeter and total pressure measurements in circular-to-rectangular transition ducts
[NASA-CR-182286] N90-14494

UNIVERSIDADE FEDERAL DO RIO DE JANEIRO (BRAZIL).
Classical approach to higher-derivative gravity
[DE89-631649] N90-15019

UNIVERSITIES SPACE RESEARCH ASSOCIATION, BOULDER, CO.
Group-kinetic theory and modeling of atmospheric turbulence
[NASA-CR-183776] N90-14728

UNIVERSITIES SPACE RESEARCH ASSOCIATION, HUNTSVILLE, AL.
Space station attached payload program support
[NASA-CR-183838] N90-14274

UNIVERSITY OF CENTRAL FLORIDA, ORLANDO.
The space station tethered elevator system
[NASA-CR-186051] N90-14265

UNIVERSITY OF SOUTH FLORIDA, TAMPA.
Architectures for reasoning in parallel
[NASA-CR-186237] N90-14836

V

VIRGINIA POLYTECHNIC INST. AND STATE UNIV., BLACKSBURG.
Analysis of metal matrix composite structures using a microchemical constitutive theory N90-14290
Fatigue analysis and reconstruction of helicopter load spectra N90-14304
Non-linear vibrations, stability, and dynamics of structures and mechanisms
[AD-A212152] N90-14639
Parallel mathematical software
[DE90-002694] N90-14822
The AMY Experiment
[DE90-001153] N90-14880

W

WASHINGTON STATE UNIV., PULLMAN.
Superplastic sheet forming N90-14327

WASHINGTON UNIV., SEATTLE.
A tensor product b-spline method for 3D multi-block elliptic grid generation
[DE89-017440] N90-14859
WESTINGHOUSE HANFORD CO., RICHLAND, WA.
Introductory testimony: Hearing on nuclear power in space
[DE90-001137] N90-14897
WESTINGHOUSE SAVANNAH RIVER CO., AIKEN, SC.
An evaluation of electrochemical potentiokinetic reactivation techniques for in-service measurements on Type 304 stainless steel
[DE89-017859] N90-14340
Rapid heating tensile tests of hydrogen-charged high-energy-rate-forged 316L stainless steel
[DE90-000591] N90-14342
Phases in lanthanum-nickel-aluminum intermetallic alloys
[DE90-000651] N90-14343
Failure probability estimate of Type 304 stainless steel piping
[DE90-000659] N90-14635
Selecting and effectively using a computer aided software engineering tool
[DE89-017876] N90-14815
Personal computer process data acquisition
[DE89-017877] N90-14816
WICHITA STATE UNIV., KS.
Stall/spin aerodynamic data project
[DOT/FAA/CT-88/29] N90-14222
WISCONSIN UNIV., MADISON.
Test and evaluation of polymeric membranes for oxygen enrichment of air
[DE90-000555] N90-14321
Ordered ceramic membranes
[DE89-017426] N90-14364
High power density dc/dc converter: Selection of converter topology
[NASA-CR-186129] N90-14467
An investigation of satellite sounding products for the remote sensing of the surface energy balance and soil moisture
[NASA-CR-186073] N90-14664
Theoretical reversed field pinch studies
[DE90-002114] N90-14929

Y

YALE UNIV., NEW HAVEN, CT.
Energies of organic compounds
[DE90-003174] N90-14324
Perturbation methods for the calculation of gravitational waves from slightly non-spherical spacetimes with applications to stellar core collapse N90-15015

Typical Contract Number Index Listing

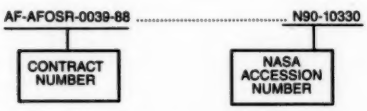

Listings in this index are arranged alphanumerically by contract number. Under each contract number the NASA accession numbers denoting documents that have been produced as a result of research done under that contract are arranged in ascending order. The NASA accession number denotes the number by which the citation is identified.

AF PROJ. 2304 ..... N90-14841
AF-AFOSR-0154-86 ..... N90-14859
AF-AFOSR-0249-87 ..... N90-14841
ARB-A4-145-32 ..... N90-14703
ARB-A6-185-32 ..... N90-14753
ARB-A7-320-36 ..... N90-14705
ARPA ORDER 4850 ..... N90-14690
ARPA ORDER 4976 ..... N90-14902
ARPA ORDER 6037 ..... N90-14826
N90-14837
ASL-87-8013 ..... N90-14906
BMFT-13-EU-0035 ..... N90-14582
DA PROJ. 1L1-61102-AH-45-A N90-14186
DA PROJ. 1L1-62209-A4-7A N90-14617
DAAA21-86-C-0336 ..... N90-14380
DAAB07-87-K-A0006 ..... N90-14428
DAAL03-88-G-0013 ..... N90-14639
DAJA45-88-M-0051 ..... N90-14381
DE-AC01-85FE-60850 ..... N90-14725
DE-AC01-88ER-30131 ..... N90-14587
DE-AC02-76CH-00016 ..... N90-14323
N90-14387
N90-14537
N90-14539
N90-14541
N90-14713
N90-14738
N90-14878
N90-14881
N90-14943
N90-14946
N90-14948
N90-14953
DE-AC02-76CH-03000 ..... N90-15021
DE-AC02-76ER-01112 ..... N90-14879
DE-AC02-76ER-01198 ..... N90-14979
DE-AC02-78ET-51013 ..... N90-14598
N90-14916
DE-AC02-83CH-10093 ..... N90-14673
N90-14679
N90-14681
N90-14682
N90-14687
N90-14688
N90-14689
N90-14694
N90-14695
N90-14939
DE-AC02-85ER-40236 ..... N90-14474
N90-14483
DE-AC02-88CE-90027 ..... N90-14365
DE-AC03-76SF-00078 ..... N90-14537
DE-AC03-76SF-00098 ..... N90-14312
N90-14314
N90-14338
N90-14341
N90-14347
N90-14349
N90-14351
N90-14491
N90-14663
N90-14693
N90-14766
N90-14817
N90-14820
N90-14865
N90-14885
N90-15022
DE-AC03-87SF-17128 ..... N90-14597
DE-AC04-76DP-00613 ..... N90-14624
DE-AC04-76DP-00789 ..... N90-14210
N90-14246
N90-14249
N90-14251
N90-14254
N90-14310
N90-14315
N90-14344
N90-14345
N90-14366
N90-14367
N90-14371
N90-14372
N90-14395
N90-14402
N90-14455
N90-14457
N90-14469
N90-14471
N90-14472
N90-14473
N90-14476
N90-14485
N90-14528
N90-14535
N90-14618
N90-14629
N90-14632
N90-14654
N90-14658
N90-14674
N90-14680
N90-14814
N90-14835
N90-14872
N90-14898
N90-14914
N90-14919
N90-14962
DE-AC04-76DR-00789 ..... N90-14259
N90-14337
N90-14477
DE-AC04-88DP-43495 ..... N90-14386
N90-14536
DE-AC05-84OR-21400 ..... N90-14252
N90-14253
N90-14296
N90-14316
N90-14339
N90-14352
N90-14374
N90-14375
N90-14456
N90-14475
N90-14592
N90-14594
N90-14604
N90-14607
N90-14619
N90-14625
N90-14626
N90-14631
N90-14657
N90-14659
N90-14661
N90-14671
N90-14686
N90-14696
N90-14697
N90-14711
N90-14712
N90-14714
N90-14718
N90-14722
N90-14726
N90-14776
N90-14827
N90-14863
N90-14882
N90-14883
N90-14940
N90-14942
N90-14944
N90-14945
N90-14952
N90-14957
N90-14970
DE-AC06-76RL-01830 ..... N90-14322
N90-14355
N90-14683
N90-14691
N90-14692
N90-14698
N90-14709
N90-14717
N90-14739
N90-14740
N90-14757
N90-14885
N90-14925
DE-AC06-87RL-10930 ..... N90-14897
DE-AC07-76ID-01570 ..... N90-14348
N90-14486
N90-14489
N90-14523
N90-14526
N90-14605
N90-14620
N90-14630
N90-14777
N90-14858
N90-14870
N90-14963
DE-AC09-89SR-18035 ..... N90-14340
N90-14342
N90-14343
N90-14635
N90-14815
N90-14816
DE-AC22-88PC-88827 ..... N90-14385
DE-AI05-87OR-21749 ..... N90-14368
DE-AM79-86BP-64849 ..... N90-14458
DE-AS05-80ER-10713 ..... N90-14880
DE-AS05-80ER-10742 ..... N90-14943
N90-14953
DE-AS07-86ID-12626 ..... N90-14364
DE-FC07-81ID-12170 ..... N90-14523
DE-FG02-85ER-13436 ..... N90-14307
DE-FG02-85ER-53212 ..... N90-14929
DE-FG02-85ER-60304 ..... N90-14755
DE-FG02-86ER-13460 ..... N90-14324
DE-FG02-87ER-13732 ..... N90-14373
DE-FG02-87ER-45283 ..... N90-14947
DE-FG02-88ER-13978 ..... N90-14760
DE-FG02-88ER-25053 ..... N90-14521
DE-FG02-88ER-53263 ..... N90-14933
DE-FG02-89ER-69017 ..... N90-14707
DE-FG03-86ER-13541 ..... N90-14306
DE-FG05-80ET-53088 ..... N90-14930
DE-FG05-88ER-13839 ..... N90-14516
DE-FG05-88ER-13881 ..... N90-14320
DE-FG05-88ER-25068 ..... N90-14822
DE-FG06-84ER-60248 ..... N90-14706
DE-FG06-85ER-45191 ..... N90-14369
DE-FG06-88ER-25061 ..... N90-14859
DE-FG07-88ID-12701 ..... N90-14321
DE-FG22-85PC-80524 ..... N90-14524
DE-FG22-86PC-90534 ..... N90-14308
DE-FG22-87BC-14126 ..... N90-14309
DTFA01-88-Y-01073 ..... N90-14214
DTFH61-87-Z-00116 ..... N90-14809
DTNH22-87-D-07174 ..... N90-14215
EY-76-C-03-0115 ..... N90-14306
F09603-87-G-0659 ..... N90-14450
F33615-85-C-3220 ..... N90-14269
F33615-87-C-1499 ..... N90-14902
GM-11741 ..... N90-14765

GRI-5087-260-1543 ..... N90-14379
N-020/87 ..... N90-14514
N-0622/88 ..... N90-14514
NAGW-533 ..... N90-15025
NAGW-933 ..... N90-14907
NAGW-1143 ..... N90-14670
NAGW-1239 ..... N90-14934
NAGW-1340 ..... N90-15016
NAGW-1570 ..... N90-14910
NAG1-535 ..... N90-14270
NAG1-586 ..... N90-14468
NAG1-613 ..... N90-14839
NAG1-623 ..... N90-14247
NAG1-634 ..... N90-14638
NAG1-640 ..... N90-14785
NAG1-716 ..... N90-14204
NAG1-736 ..... N90-14243
NAG1-757 ..... N90-14583
NAG1-768 ..... N90-14843
NAG1-817 ..... N90-14542
NAG1-928 ..... N90-14453
N90-14754
NAG1-8321 ..... N90-14498
NAG2-487 ..... N90-14836
NAG2-593 ..... N90-14826
N90-14837
NAG3-159 ..... N90-14856
NAG3-501 ..... N90-14534
NAG3-668 ..... N90-14305
NAG3-708 ..... N90-14279
NAG3-742 ..... N90-14656
NAG3-762 ..... N90-14652
NAG3-804 ..... N90-14467
NAG5-361 ..... N90-14999
NAG5-499 ..... N90-14812
NAG5-854 ..... N90-14654
NAG5-995 ..... N90-14985
NAG8-091 ..... N90-14335
NAG8-755 ..... N90-14250
NAG9-168 ..... N90-15004
NAG9-313 ..... N90-14532
NAG9-388 ..... N90-14808
NASA ORDER C-99066-G N90-14517
N90-14655
N90-14844
NASW-3482 ..... N90-14261
NASW-4066 ..... N90-14736
N90-14998
N90-15026
N90-15027
NASW-4292 ..... N90-14763
NASW-4435 ..... N90-14212
N90-14216
N90-14226
N90-14258
N90-14263
N90-14264
N90-14265
N90-14266
N90-14267
N90-14761
N90-15028
N90-15029
NAS1-18027 ..... N90-14866
NAS1-18605 ..... N90-14193
N90-14513
N90-14779
N90-14842
N90-14847
N90-14848
NAS2-11945 ..... N90-14200
NAS2-12666 ..... N90-14905
NAS3-24105 ..... N90-14783
NAS3-24564 ..... N90-14452
NAS3-24616 ..... N90-14494
NAS3-24631 ..... N90-14278
NAS3-24677 ..... N90-14281
NAS3-25266 ..... N90-14512
N90-14517
NAS7-918 ..... N90-14700
NAS8-30490 ..... N90-14280
N90-14530
NAS8-36146 ..... N90-14286
NAS8-36153 ..... N90-14728
NAS8-36284 ..... N90-14277
NAS8-36476 ..... N90-14276
NAS8-36620 ..... N90-14397
NAS8-37578 ..... N90-14229
N90-14230
N90-14231
NAS8-37583 ..... N90-14274
NAS8-37750 ..... N90-14262
NAS8-37753 ..... N90-14608
NAS9-17766 ..... N90-14807
NAS9-18147 ..... N90-14257
NAS10-10285 ..... N90-14669
NAS10-10600 ..... N90-15040
NA86AA-N-RG0100 ..... N90-14752
NCC2-346 ..... N90-14997
NCC2-371 ..... N90-14874
NCC2-485 ..... N90-14900
NCC2-507 ..... N90-14189
NCC2-552 ..... N90-14874
NCC3-95 ..... N90-14398
NCC3-140 ..... N90-14512
NCC8-13 ..... N90-14813
NCC8-14 ..... N90-14787
NCC9-16 ..... N90-14784
N90-14786
N90-14811
N90-14986
NGR-14-005-181 ..... N90-14735
NGT-50085 ..... N90-14517
NGT-70055 ..... N90-14754
NSF ATM-87-09659 ..... N90-14751
N90-14752
NSF DMB-87-17997 ..... N90-14765
NSF DMR-88-15043 ..... N90-14537
NSF DMS-88-19856 ..... N90-14521
NSG-7523 ..... N90-14245
N00014-85-K-0123 ..... N90-14762
N00014-88-F-0019 ..... N90-14377
N00140-87-C-8904 ..... N90-14826
N90-14837
PA-129 ..... N90-14306
PROJ. A-4168 ..... N90-14468
SWRI PROJ. 05-2984 ..... N90-14808
SWRI PROJ. 05-3269 ..... N90-14784
W-31-109-ENG-38 ..... N90-14208
N90-14295
N90-14311
N90-14354
N90-14377
N90-14378
N90-14478
N90-14487
N90-14488
N90-14519
N90-14527
N90-14623
N90-14627
N90-14660
N90-14662
N90-14684
N90-14685
N90-14690
N90-14716
N90-14724
N90-14764
N90-14765
N90-14780
N90-14781
N90-14825
N90-14850
N90-14851
N90-14871
N90-14875
N90-14884
N90-14889
N90-14931
N90-14950
N90-14951
N90-14961
N90-14964
N90-14965
N90-14966
N90-14967
N90-14974
N90-14975
N90-14976
N90-14977
N90-14979
N90-14980
N90-14981
W-7405-ENG-36 ..... N90-14227
N90-14346
N90-14350
N90-14388
N90-14389
N90-14480
N90-14481
N90-14490
N90-14520
N90-14522
N90-14588
N90-14589
N90-14593
N90-14599
N90-14600
N90-14601
N90-14602
N90-14603
N90-14606
N90-14636
N90-14676
N90-14677
N90-14771
N90-14819
N90-14823
N90-14831
N90-14833
N90-14849
N90-14855
N90-14888
N90-14899
N90-14917
N90-14918
N90-14941
N90-14949
N90-14954
N90-14955
N90-14956
N90-14968
N90-14969
N90-14982
N90-14983
N90-15020
N90-15023
N90-15024
W-7405-ENG-48 ..... N90-14209
N90-14313
N90-14317
N90-14318
N90-14319
N90-14353
N90-14370
N90-14376
N90-14384
N90-14390
N90-14391
N90-14392
N90-14393
N90-14394
N90-14470
N90-14479
N90-14482
N90-14484
N90-14492
N90-14515
N90-14518
N90-14538
N90-14540
N90-14549
N90-14586
N90-14590
N90-14591
N90-14595
N90-14596
N90-14622
N90-14653
N90-14710
N90-14715
N90-14721
N90-14737
N90-14756
N90-14770
N90-14782
N90-14818
N90-14821
N90-14824
N90-14828
N90-14832
N90-14834
N90-14857
N90-14862
N90-14886
N90-14908
N90-14909
N90-14915
N90-14920
N90-14921
N90-14922
N90-14923
N90-14924
N90-14926
N90-14927
N90-14932
N90-14958
N90-14959
N90-14960
N90-14978
XB-5-04092-1 ..... N90-14939
ZB-7-06003-4 ..... N90-14673
147-14-12 ..... N90-14220
199-04-16-11 ..... N90-14890
314-40-32-10-23 ..... N90-14700
326-31-31 ..... N90-15030
474-10-52 ..... N90-14285

505-05-01	N90-14206
505-60-00	N90-14188
	N90-14238
505-60-21	N90-14202
505-61-01-02	N90-14245
505-61-51-10	N90-14186
505-61-85-01	N90-14244
505-62-21	N90-14517
	N90-14844
505-62-51	N90-14203
505-62-91	N90-14494
505-63-1A	N90-14335
505-63-1B	N90-14294
	N90-14640
	N90-14652
	N90-14656
505-63-1M	N90-14368
505-63-00	N90-14905
505-63-01-10	N90-14785
505-65-11-02	N90-14789
505-66-41-42	N90-14232
505-68-00	N90-14829
505-68-11	N90-14617
505-68-31	N90-14224
	N90-14228
505-68-91-02	N90-14187
505-69-31	N90-14235
505-80-31	N90-14511
505-90-21-01	N90-14193
	N90-14513
	N90-14779
	N90-14842
	N90-14847
	N90-14848
506-40-41-01	N90-14185
	N90-14493
506-41-31	N90-14281
	N90-14283
	N90-14678
506-41-41	N90-14362
506-42-00	N90-14284
506-43-21-05	N90-14533
506-46-21-01	N90-14272
506-48-21	N90-14275
506-80-31-03	N90-14205
510-01-0A	N90-14287
	N90-14363
533-02-91	N90-14225
535-03-01-02	N90-14190
535-03-11-03	N90-14866
535-05-01	N90-14783
535-07-01	N90-14655
553-13-00	N90-14641
	N90-14642
643-10-01	N90-14856
650-60-23	N90-14273
672-40-05-70	N90-14741
674-24-05	N90-14512
674-25-05	N90-14398
694-03-03	N90-14452
763-01-21	N90-14268

Typical Report Number Index Listing

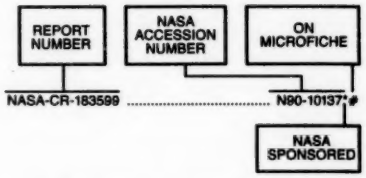

Listings in this index are arranged alphanumerically by report number. The NASA accession number denotes the number by which the citation is identified. An asterisk (*) indicates that the item is a NASA report. A pound sign (#) indicates that the item is available on microfiche.

A-89095 ..... N90-14188* #
A-89136 ..... N90-14997* #
A-89243 ..... N90-14220* #
A-90048 ..... N90-14236* #

AAE-241-VOL-1 ..... N90-14263* #
AAE-241-VOL-2 ..... N90-14264* #

AD-A205885 ..... N90-14201 #
AD-A211113 ..... N90-14772 #
AD-A212088 ..... N90-14841 #
AD-A212152 ..... N90-14639 #
AD-A212347 ..... N90-14269 #
AD-A212466 ..... N90-14217 #
AD-A212601 ..... N90-14380 #
AD-A212634 ..... N90-14769 #
AD-A212731 ..... N90-14685 #
AD-A212758 ..... N90-14666 #
AD-A212835 ..... N90-14357 #
AD-A212852 ..... N90-14773 #
AD-A212862 ..... N90-14762 #
AD-A212883 ..... N90-14237 #
AD-A212939 ..... N90-14359 #
AD-A212989 ..... N90-14774 #
AD-A213042 ..... N90-14381 #
AD-A213364 ..... N90-14902 #
AD-A213367 ..... N90-14450 #

AD-D014209 ..... N90-14358 #
AD-D014210 ..... N90-14543 #
AD-D014211 ..... N90-14901 #
AD-D014214 ..... N90-14449 #
AD-D014218 ..... N90-14459
AD-D014219 ..... N90-14382
AD-D014220 ..... N90-14810
AD-D014221 ..... N90-14383
AD-D014223 ..... N90-14255
AD-D014224 ..... N90-14460 #
AD-D014225 ..... N90-14461 #
AD-D014226 ..... N90-14611 #
AD-D014227 ..... N90-14462 #
AD-D014228 ..... N90-14288 #
AD-D014229 ..... N90-14935 #
AD-D014230 ..... N90-14463 #
AD-D014231 ..... N90-14464 #
AD-D014232 ..... N90-14936 #
AD-D014235 ..... N90-14451
AD-D014236 ..... N90-14529
AD-D014237 ..... N90-14903
AD-D014238 ..... N90-14904
AD-D014240 ..... N90-14465 #
AD-D014243 ..... N90-14466
AD-D014244 ..... N90-14937
AD-D014245 ..... N90-14289
AD-D014246 ..... N90-14838

AEDC-TR-89-10 ..... N90-14237 #

AERO-483 ..... N90-14266* #

AFOSR-89-1201TR ..... N90-14841 #

AFWAL-TR-88-3066 ..... N90-14269 #

AGARD-AR-277 ..... N90-14218 #

AGARD-CP-453 ..... N90-14405 #

AGARD-LS-154-REV ..... N90-14325 #
AGARD-LS-168 ..... N90-14325 #

AIAA-90-0053 ..... N90-14511* #
AIAA-90-0320 ..... N90-14228* #
AIAA-90-0391 ..... N90-14203* #
AIAA-90-0668 ..... N90-14617* #
AIAA-90-0715 ..... N90-14284* #
AIAA-90-0740 ..... N90-14398* #
AIAA-90-0815 ..... N90-14856* #

AMI-8416 ..... N90-14200* #

ANL-HEP-CP-89-55 ..... N90-14851 #

ANL-PHY-88-2 ..... N90-14875 #

ANL-87-26-VOL-4 ..... N90-14780 #
ANL-88-18 ..... N90-14781 #
ANL-88-37 ..... N90-14487 #

ANL/CNSV-68 ..... N90-14961 #

ANU/TPP-88/01 ..... N90-14864 #

AR-004-570 ..... N90-14336 #

ARB-R-89/407 ..... N90-14705 #
ARB-R-89/408 ..... N90-14753 #

ARL-STRUC-R-430 ..... N90-14336 #

ARL-SYS-TM-106 ..... N90-14217 #

ARO-25614.1-EG-CF ..... N90-14639 #

ARPAD-CR-89002 ..... N90-14380 #

AVSCOM-TM-88-B-009 ..... N90-14186* #
AVSCOM-TM-89-C-015 ..... N90-14617* #

AVSCOM-TR-89-C-017 ..... N90-14383* #
AVSCOM-TR-89-C-018 ..... N90-14287* #

BNL-41502 ..... N90-14881 #
BNL-42124 ..... N90-14387 #
BNL-42550 ..... N90-14953 #
BNL-42928 ..... N90-14943 #
BNL-43096 ..... N90-14738 #
BNL-43112 ..... N90-14541 #
BNL-43247 ..... N90-14948 #
BNL-43292 ..... N90-14878 #
BNL-43312 ..... N90-14948 #
BNL-43327 ..... N90-14537 #
BNL-43372 ..... N90-14323 #
BNL-43374 ..... N90-14539 #

BR111413 ..... N90-14211 #

CBPF-NF-058/88 ..... N90-15018 #
CBPF-NF-060/88 ..... N90-15017 #
CBPF-NF-063/88 ..... N90-14514 #

CFPA-TH-89-016 ..... N90-15016* #

CMU-RI-TR-89-19 ..... N90-14902 #

CONF-880496 ..... N90-14875 #
CONF-880724-29 ..... N90-14523 #
CONF-880732-3 ..... N90-14311 #
CONF-880946-1 ..... N90-14478 #
CONF-881058-6 ..... N90-14858 #
CONF-881155-44 ..... N90-14863 #
CONF-890238-5 ..... N90-14348 #
CONF-890335-269 ..... N90-14966 #
CONF-890430-6 ..... N90-14317 #
CONF-890480-3 ..... N90-14967 #

CONF-890572 ..... N90-14675 #
CONF-890665-31 ..... N90-14917 #
CONF-890665-49 ..... N90-14955 #
CONF-890665-51 ..... N90-14479 #
CONF-890701-8 ..... N90-14341 #
CONF-890701-11 ..... N90-14484 #
CONF-890701-14 ..... N90-14347 #
CONF-890701-15 ..... N90-14351 #
CONF-890701-16 ..... N90-14349 #
CONF-890708-9 ..... N90-14885 #
CONF-890710-19 ..... N90-14918 #
CONF-890710-20 ..... N90-14470 #
CONF-890710-23 ..... N90-14492 #
CONF-890710-24 ..... N90-14482 #
CONF-890718-29 ..... N90-14950 #
CONF-890718-30 ..... N90-14959 #
CONF-890739-5 ..... N90-14313 #
CONF-890756-3 ..... N90-14208 #
CONF-890770-2 ..... N90-14870 #
CONF-890770-3 ..... N90-14295 #
CONF-890770-4 ..... N90-14805 #
CONF-890770-5 ..... N90-14963 #
CONF-890770-6 ..... N90-14355 #
CONF-890771-5 ..... N90-14977 #
CONF-890790-3 ..... N90-14627 #
CONF-890796-6 ..... N90-14949 #
CONF-890802-14 ..... N90-14539 #
CONF-890803-28 ..... N90-14474 #
CONF-890806-2 ..... N90-14951 #
CONF-890809-2 ..... N90-14537 #
CONF-890811-32 ..... N90-14522 #
CONF-890811-33 ..... N90-14390 #
CONF-890811-34 ..... N90-14394 #
CONF-890811-35 ..... N90-14393 #
CONF-890811-36 ..... N90-14392 #
CONF-890811-37 ..... N90-14391 #
CONF-890811-38 ..... N90-14384 #
CONF-890811-40 ..... N90-14515 #
CONF-890812-48 ..... N90-14520 #
CONF-890812-50 ..... N90-14315 #
CONF-890812-51 ..... N90-14346 #
CONF-890812-52 ..... N90-14658 #
CONF-890812-53 ..... N90-14345 #
CONF-890812-54 ..... N90-14319 #
CONF-890812-56 ..... N90-14318 #
CONF-890812-57 ..... N90-14958 #
CONF-890812-58 ..... N90-14960 #
CONF-890812-60 ..... N90-14978 #
CONF-890814-9 ..... N90-14716 #
CONF-890815-29 ..... N90-14478 #
CONF-890819-25 ..... N90-14519 #
CONF-890826-4 ..... N90-14884 #
CONF-890826-6 ..... N90-15022 #
CONF-890836-16 ..... N90-14538 #
CONF-890872-2 ..... N90-14888 #
CONF-890875-3 ..... N90-14823 #
CONF-890901-1 ..... N90-14709 #
CONF-890906-4 ..... N90-14919 #
CONF-890931-9 ..... N90-14932 #
CONF-890939-1 ..... N90-14940 #
CONF-890953-4 ..... N90-14956 #
CONF-890953-6 ..... N90-14954 #
CONF-890960-1 ..... N90-14953 #
CONF-890971-1 ..... N90-14942 #
CONF-890971-2 ..... N90-14948 #
CONF-890971-3 ..... N90-14974 #
CONF-890971-5 ..... N90-14604 #
CONF-890981-2 ..... N90-14674 #
CONF-890981-3 ..... N90-14682 #
CONF-890981-4 ..... N90-14692 #
CONF-891002-2 ..... N90-14710 #
CONF-891007-3 ..... N90-14914 #
CONF-891007-4 ..... N90-14923 #
CONF-891007-5 ..... N90-14924 #
CONF-891007-7 ..... N90-14920 #
CONF-891007-8 ..... N90-14922 #
CONF-891007-9 ..... N90-14921 #
CONF-891007-14 ..... N90-14818 #
CONF-891007-17 ..... N90-14252 #
CONF-891007-49 ..... N90-14927 #
CONF-891007-54 ..... N90-14480 #
CONF-891007-58 ..... N90-14636 #
CONF-891007-58 ..... N90-14490 #

CONF-891007-61 ..... N90-14481 #
CONF-891013-1 ..... N90-14316 #
CONF-891034-1 ..... N90-14387 #
CONF-891044-1 ..... N90-14851 #
CONF-891053-8 ..... N90-14717 #
CONF-891053-9 ..... N90-14757 #
CONF-891081-3 ..... N90-14366 #
CONF-891087-2 ..... N90-14817 #
CONF-891087-4 ..... N90-14475 #
CONF-891090-1 ..... N90-14968 #
CONF-891091-1 ..... N90-14594 #
CONF-891091-2 ..... N90-14296 #
CONF-891093-4 ..... N90-14943 #
CONF-891093-7 ..... N90-14323 #
CONF-891093-9 ..... N90-14253 #
CONF-891113-1 ..... N90-14677 #
CONF-891113-5 ..... N90-14684 #
CONF-891117-5 ..... N90-14975 #
CONF-891117-9 ..... N90-14970 #
CONF-891119-14 ..... N90-14983 #
CONF-891127-1 ..... N90-15020 #
CONF-891132-1 ..... N90-14473 #
CONF-891132-2 ..... N90-14471 #
CONF-891132-3 ..... N90-14472 #
CONF-891132-7 ..... N90-14488 #
CONF-891133-1 ..... N90-14620 #
CONF-891148-1 ..... N90-14676 #
CONF-891149-2 ..... N90-14831 #
CONF-891149-3 ..... N90-14455 #
CONF-891149-7 ..... N90-14782 #
CONF-891149-10-REV-1 ..... N90-14834 #
CONF-891150-1 ..... N90-14835 #
CONF-891151-1 ..... N90-14589 #
CONF-891152-1 ..... N90-14535 #
CONF-891152-3 ..... N90-14654 #
CONF-891192-6 ..... N90-14816 #
CONF-891192-7 ..... N90-14815 #
CONF-891204-4 ..... N90-14631 #
CONF-891206-2 ..... N90-14210 #
CONF-891208-14 ..... N90-14696 #
CONF-891208-19 ..... N90-14697 #
CONF-891208-23 ..... N90-14865 #
CONF-891214-1 ..... N90-14827 #
CONF-891214-6 ..... N90-14528 #
CONF-891214-9 ..... N90-14632 #
CONF-891222-1 ..... N90-14828 #
CONF-891252-1 ..... N90-14607 #
CONF-8707219-1 ..... N90-14659 #
CONF-8803244-1 ..... N90-14857 #
CONF-8805142-24 ..... N90-14881 #
CONF-8808146-6 ..... N90-14588 #
CONF-8810203-3 ..... N90-14370 #
CONF-8810432-1 ..... N90-14483 #
CONF-8901170-1 ..... N90-14698 #
CONF-8902135-1 ..... N90-14820 #
CONF-8903111-5 ..... N90-14738 #
CONF-8903121-2 ..... N90-14849 #
CONF-8904252-SUMM ..... N90-14994 #
CONF-8904269-1 ..... N90-14711 #
CONF-8904275 ..... N90-14944 #
CONF-8904276-1 ..... N90-14721 #
CONF-8904290-1 ..... N90-14377 #
CONF-8904290-2 ..... N90-14378 #
CONF-8904290-3 ..... N90-14889 #
CONF-8905112-3 ..... N90-14661 #
CONF-8905126-5 ..... N90-14344 #
CONF-8905126-7 ..... N90-14685 #
CONF-8905183-4 ..... N90-14878 #
CONF-8905188-2 ..... N90-14960 #
CONF-8905192 ..... N90-14766 #
CONF-8905192-1 ..... N90-14555 #
CONF-8905192-2 ..... N90-14540 #
CONF-8905209-1 ..... N90-14518 #
CONF-8905222-1 ..... N90-15021 #
CONF-8905239-1 ..... N90-14981 #
CONF-8906112-2 ..... N90-14527 #
CONF-8906112-3 ..... N90-14660 #
CONF-8906119-4 ..... N90-14965 #
CONF-8906194-3 ..... N90-14899 #
CONF-8906200-2 ..... N90-14469 #
CONF-8906200-3 ..... N90-14485 #
CONF-8906218-1 ..... N90-14593 #
CONF-8906230-1 ..... N90-14353 #
CONF-8906244-1 ..... N90-14724 #
CONF-8906248-1 ..... N90-14855 #
CONF-8906249-1 ..... N90-14526 #
CONF-8907114-3 ..... N90-14964 #
CONF-8907116-4 ..... N90-14340 #
CONF-8907116-5 ..... N90-14339 #
CONF-8907130-4 ..... N90-14586 #
CONF-8907161-1 ..... N90-14662 #
CONF-8908106-4 ..... N90-14862 #
CONF-8908117-6 ..... N90-14764 #
CONF-8908125-6 ..... N90-14402 #
CONF-8908133-5 ..... N90-14926 #
CONF-8908134-8 ..... N90-14599 #
CONF-8908134-9 ..... N90-14600 #
CONF-8908134-10 ..... N90-14601 #
CONF-8908134-12 ..... N90-14602 #
CONF-8908134-13 ..... N90-14603 #
CONF-8908134-14 ..... N90-14598 #
CONF-8908134-16 ..... N90-14606 #
CONF-8908139-1 ..... N90-14389 #
CONF-8908144-2 ..... N90-14623 #
CONF-8908144-3 ..... N90-14630 #
CONF-8908145-4 ..... N90-14969 #
CONF-8908164-1 ..... N90-14765 #
CONF-8908167-1 ..... N90-15023 #
CONF-8908175-1 ..... N90-14354 #
CONF-8908178-1 ..... N90-14850 #
CONF-8909113-5 ..... N90-14536 #
CONF-8909113-6 ..... N90-14386 #
CONF-8909163-2 ..... N90-14737 #
CONF-8909181-6 ..... N90-14489 #
CONF-8909192-1 ..... N90-14712 #
CONF-8909207-2 ..... N90-14957 #
CONF-8909210-1 ..... N90-14883 #
CONF-8909210-2 ..... N90-14882 #
CONF-8909211-1 ..... N90-14592 #
CONF-8909218-1 ..... N90-14976 #
CONF-8909219-1 ..... N90-14629 #
CONF-8909225-2 ..... N90-14350 #
CONF-8909229-1 ..... N90-14246 #
CONF-8909229-2 ..... N90-14254 #
CONF-8909240-1 ..... N90-14821 #
CONF-8909243-1 ..... N90-14722 #
CONF-8909252-1 ..... N90-14322 #
CONF-8909256-1 ..... N90-14541 #
CONF-8909257-1 ..... N90-14931 #
CONF-8910107-2 ..... N90-14690 #
CONF-8910107-3 ..... N90-14691 #
CONF-8910120-1 ..... N90-14352 #
CONF-8910122-1 ..... N90-14714 #
CONF-8910155-2-REV-1 ..... N90-14770 #
CONF-8910157-1 ..... N90-14388 #
CONF-8910158-1 ..... N90-14819 #
CONF-8910162-4 ..... N90-14686 #
CONF-8910192-8 ..... N90-14835 #
CONF-8910196-2 ..... N90-14908 #
CONF-8910197-2 ..... N90-14952 #
CONF-8910203-1 ..... N90-14227 #
CONF-8910208-1 ..... N90-14771 #
CONF-8910209-1 ..... N90-14832 #
CONF-8910209-2 ..... N90-14833 #
CONF-8910215-1 ..... N90-14343 #
CONF-8910216-2 ..... N90-14872 #
CONF-8910216-3 ..... N90-14871 #
CONF-8910222-5 ..... N90-14776 #
CONF-8910225-5 ..... N90-14456 #
CONF-8910227-1 ..... N90-14886 #
CONF-8910248-1 ..... N90-14375 #
CONF-8910263-1 ..... N90-14395 #
CONF-8910264-1 ..... N90-14457 #
CONF-8910267-1 ..... N90-14372 #
CONF-8910273-1 ..... N90-14979 #
CONF-8910277-1 ..... N90-14739 #
CONF-8910285-1 ..... N90-14740 #
CONF-8910288-1 ..... N90-14825 #
CONF-8910290-1 ..... N90-14376 #
CONF-8910304-1 ..... N90-14982 #
CONF-8911103-1 ..... N90-14962 #

CRIE-T-87116 ..... N90-14840 #

CSDL-T-1036 ..... N90-14257* #

CSG-117 ..... N90-14839* #

DCIEM-89-TR-22 ..... N90-14774 #

DE88-008791 ..... N90-14476 #
DE88-010343 ..... N90-14781 #
DE88-013968 ..... N90-14875 #
DE88-015856 ..... N90-14881 #
DE89-000766 ..... N90-14309 #
DE89-000846 ..... N90-14687 #
DE89-003488 ..... N90-14588 #
DE89-006038 ..... N90-14863 #
DE89-008240 ..... N90-14827 #
DE89-009389 ..... N90-15020 #
DE89-009438 ..... N90-14939 #
DE89-009444 ..... N90-14673 #
DE89-009445 ..... N90-14688 #
DE89-009467 ..... N90-14679 #
DE89-009497 ..... N90-14694 #
DE89-009498 ..... N90-14689 #
DE89-009499 ..... N90-14681 #
DE89-009500 ..... N90-14695 #
DE89-009501 ..... N90-14682 #
DE89-009570 ..... N90-14210 #
DE89-011125 ..... N90-14620 #
DE89-011699 ..... N90-14675 #
DE89-012368 ..... N90-14828 #
DE89-012592 ..... N90-14676 #
DE89-012614 ..... N90-14831 #
DE89-012658 ..... N90-14835 #
DE89-013453 ..... N90-14589 #
DE89-014027 ..... N90-14917 #
DE89-014494 ..... N90-14455 #
DE89-014496 ..... N90-14535 #
DE89-015173 ..... N90-14994 #
DE89-015255 ..... N90-14949 #
DE89-015283 ..... N90-14819 #
DE89-015285 ..... N90-14388 #
DE89-015707 ..... N90-14770 #
DE89-015741 ..... N90-14524 #
DE89-015843 ..... N90-14471 #
DE89-015846 ..... N90-14472 #
DE89-015847 ..... N90-14473 #
DE89-016070 ..... N90-14696 #
DE89-016529 ..... N90-14528 #
DE89-016542 ..... N90-14832 #
DE89-016559 ..... N90-14306 #
DE89-016599 ..... N90-14389 #
DE89-016613 ..... N90-14771 #
DE89-016618 ..... N90-14930 #
DE89-016659 ..... N90-14710 #
DE89-016672 ..... N90-14477 #
DE89-016779 ..... N90-14677 #
DE89-016786 ..... N90-14597 #
DE89-016853 ..... N90-14607 #
DE89-016860 ..... N90-14711 #
DE89-016962 ..... N90-14898 #
DE89-016995 ..... N90-14227 #
DE89-017272 ..... N90-14369 #
DE89-017342 ..... N90-14944 #
DE89-017426 ..... N90-14364 #
DE89-017440 ..... N90-14859 #
DE89-017537 ..... N90-14622 #
DE89-017544 ..... N90-14518 #
DE89-017561 ..... N90-14760 #
DE89-017584 ..... N90-14940 #
DE89-017623 ..... N90-14738 #
DE89-017655 ..... N90-14458 #
DE89-017683 ..... N90-14623 #
DE89-017685 ..... N90-14478 #
DE89-017690 ..... N90-14519 #
DE89-017691 ..... N90-14950 #
DE89-017694 ..... N90-14951 #
DE89-017772 ..... N90-14952 #
DE89-017775 ..... N90-14712 #
DE89-017828 ..... N90-14953 #
DE89-017859 ..... N90-14340 #
DE89-017876 ..... N90-14815 #
DE89-017877 ..... N90-14816 #
DE89-017886 ..... N90-14737 #
DE89-017889 ..... N90-14313 #
DE89-618425 ..... N90-14514 #
DE89-618785 ..... N90-15017 #
DE89-618836 ..... N90-15018 #
DE89-631631 ..... N90-14584 #
DE89-631649 ..... N90-15019 #
DE89-632014 ..... N90-14585 #
DE89-632018 ..... N90-14912 #
DE89-632177 ..... N90-14876 #
DE89-633443 ..... N90-14861 #
DE89-633753 ..... N90-14454 #
DE89-633885 ..... N90-14880 #
DE89-633953 ..... N90-14877 #
DE89-634427 ..... N90-14913 #
DE89-635416 ..... N90-14984 #
DE89-635444 ..... N90-14634 #
DE89-635446 ..... N90-14628 #
DE89-635907 ..... N90-14971 #
DE89-636225 ..... N90-14972 #
DE89-636232 ..... N90-14973 #
DE89-636294 ..... N90-14719 #
DE89-636298 ..... N90-14720 #
DE89-636426 ..... N90-14928 #
DE89-766980 ..... N90-14621 #
DE89-901270 ..... N90-14840 #
DE90-000023 ..... N90-14657 #
DE90-000041 ..... N90-14310 #
DE90-000099 ..... N90-14713 #
DE90-000125 ..... N90-14314 #
DE90-000129 ..... N90-14341 #
DE90-000179 ..... N90-14820 #
DE90-000196 ..... N90-14764 #
DE90-000504 ..... N90-14307 #
DE90-000539 ..... N90-14520 #
DE90-000547 ..... N90-14821 #
DE90-000555 ..... N90-14321 #
DE90-000562 ..... N90-14714 #
DE90-000580 ..... N90-14697 #
DE90-000591 ..... N91-14342 #
DE90-000602 ..... N90-14593 #
DE90-000603 ..... N90-14954 #
DE90-000610 ..... N90-14955 #

DE90-000636 N90-14521 #
DE90-000651 N90-14343 #
DE90-000659 N90-14635 #
DE90-000669 N90-14315 #
DE90-000684 N90-14918 #
DE90-000689 N90-14956 #
DE90-000699 N90-14316 #
DE90-000700 N90-14957 #
DE90-000719 N90-14854 #
DE90-000728 N90-14594 #
DE90-000743 N90-14365 #
DE90-000759 N90-14878 #
DE90-000779 N90-15021 #
DE90-000784 N90-14595 #
DE90-000785 N90-14317 #
DE90-000786 N90-14390 #
DE90-000790 N90-14654 #
DE90-000792 N90-14402 #
DE90-000794 N90-14919 #
DE90-000802 N90-14629 #
DE90-000803 N90-14674 #
DE90-000806 N90-14469 #
DE90-000811 N90-14344 #
DE90-000813 N90-14366 #
DE90-000815 N90-14470 #
DE90-000817 N90-14920 #
DE90-000819 N90-14721 #
DE90-000820 N90-14586 #
DE90-000821 N90-14921 #
DE90-000822 N90-14391 #
DE90-000823 N90-14958 #
DE90-000824 N90-14959 #
DE90-000825 N90-14922 #
DE90-000826 N90-14370 #
DE90-000827 N90-14960 #
DE90-000829 N90-14392 #
DE90-000831 N90-14393 #
DE90-000832 N90-14394 #
DE90-000833 N90-14923 #
DE90-000834 N90-14924 #
DE90-000836 N90-14318 #
DE90-000837 N90-14319 #
DE90-000839 N90-14345 #
DE90-000842 N90-14246 #
DE90-000846 N90-14658 #
DE90-000847 N90-14914 #
DE90-000856 N90-14961 #
DE90-000858 N90-14715 #
DE90-000861 N90-14909 #
DE90-000865 N90-14925 #
DE90-000866 N90-14337 #
DE90-000877 N90-14596 #
DE90-000879 N90-14590 #
DE90-000880 N90-14624 #
DE90-000883 N90-14680 #
DE90-000891 N90-14618 #
DE90-000892 N90-14249 #
DE90-000894 N90-14367 #
DE90-000895 N90-14814 #
DE90-000899 N90-14371 #
DE90-000905 N90-14756 #
DE90-000918 N90-14941 #
DE90-000920 N90-14780 #
DE90-000927 N90-14251 #
DE90-000929 N90-14653 #
DE90-000930 N90-14915 #
DE90-000931 N90-14591 #
DE90-000977 N90-14625 #
DE90-000979 N90-14945 #
DE90-000984 N90-14683 #
DE90-001001 N90-14882 #
DE90-001004 N90-14619 #
DE90-001008 N90-14538 #
DE90-001050 N90-14384 #
DE90-001051 N90-14479 #
DE90-001055 N90-14782 #
DE90-001066 N90-14483 #
DE90-001067 N90-14474 #
DE90-001073 N90-14942 #
DE90-001076 N90-14883 #
DE90-001078 N90-14592 #
DE90-001120 N90-14879 #
DE90-001137 N90-14897 #
DE90-001147 N90-14908 #
DE90-001153 N90-14880 #
DE90-001154 N90-14587 #
DE90-001160 N90-14385 #
DE90-001171 N90-14862 #
DE90-001184 N90-14515 #
DE90-001198 N90-14706 #
DE90-001205 N90-14707 #
DE90-001228 N90-14755 #
DE90-001235 N90-14350 #
DE90-001236 N90-15023 #
DE90-001266 N90-14946 #
DE90-001294 N90-14671 #
DE90-001326 N90-14943 #
DE90-001334 N90-14456 #
DE90-001349 N90-14686 #
DE90-001378 N90-14308 #
DE90-001385 N90-14372 #
DE90-001394 N90-14709 #
DE90-001399 N90-14516 #
DE90-001410 N90-14884 #
DE90-001412 N90-14765 #
DE90-001414 N90-14311 #
DE90-001421 N90-14817 #
DE90-001425 N90-14338 #
DE90-001449 N90-14536 #
DE90-001450 N90-14386 #
DE90-001516 N90-14886 #
DE90-001517 N90-14484 #
DE90-001519 N90-14818 #
DE90-001525 N90-14947 #
DE90-001541 N90-14885 #
DE90-001543 N90-14312 #
DE90-001551 N90-14537 #
DE90-001561 N90-14387 #
DE90-001562 N90-14948 #
DE90-001567 N90-14320 #
DE90-001590 N90-14626 #
DE90-001595 N90-14252 #
DE90-001596 N90-14659 #
DE90-001601 N90-14475 #
DE90-001606 N90-14339 #
DE90-001623 N90-14485 #
DE90-001635 N90-14722 #
DE90-001645 N90-14375 #
DE90-001656 N90-14395 #
DE90-001679 N90-14962 #
DE90-001710 N90-14598 #
DE90-001711 N90-14916 #
DE90-001739 N90-14296 #
DE90-001762 N90-14974 #
DE90-001764 N90-14931 #
DE90-001772 N90-14850 #
DE90-001784 N90-14887 #
DE90-001791 N90-14723 #
DE90-001794 N90-14824 #
DE90-001796 N90-14209 #
DE90-001804 N90-14487 #
DE90-001827 N90-15024 #
DE90-001832 N90-14346 #
DE90-001837 N90-14522 #
DE90-001839 N90-14833 #
DE90-001842 N90-14849 #
DE90-001879 N90-14259 #
DE90-001894 N90-14857 #
DE90-001903 N90-14322 #
DE90-001910 N90-14684 #
DE90-001911 N90-14488 #
DE90-001914 N90-14690 #
DE90-001930 N90-14975 #
DE90-001931 N90-14979 #
DE90-001963 N90-14352 #
DE90-001968 N90-14604 #
DE90-001985 N90-14976 #
DE90-001987 N90-14851 #
DE90-001990 N90-14353 #
DE90-001991 N90-14739 #
DE90-002001 N90-14858 #
DE90-002007 N90-14489 #
DE90-002020 N90-14605 #
DE90-002021 N90-14870 #
DE90-002058 N90-14963 #
DE90-002074 N90-14526 #
DE90-002080 N90-14486 #
DE90-002082 N90-14523 #
DE90-002083 N90-14347 #
DE90-002085 N90-14630 #
DE90-002086 N90-14348 #
DE90-002105 N90-14457 #
DE90-002114 N90-14929 #
DE90-002144 N90-14374 #
DE90-002170 N90-14724 #
DE90-002178 N90-14716 #
DE90-002182 N90-14964 #
DE90-002183 N90-14977 #
DE90-002184 N90-14295 #
DE90-002187 N90-14662 #
DE90-002190 N90-14627 #
DE90-002192 N90-14208 #
DE90-002198 N90-14685 #
DE90-002199 N90-14980 #
DE90-002200 N90-14631 #
DE90-002203 N90-14965 #
DE90-002210 N90-14527 #
DE90-002213 N90-14981 #
DE90-002214 N90-14660 #
DE90-002220 N90-14978 #
DE90-002223 N90-14926 #
DE90-002224 N90-14376 #
DE90-002231 N90-14777 #
DE90-002241 N90-14966 #
DE90-002264 N90-14967 #
DE90-002266 N90-14889 #
DE90-002268 N90-14377 #
DE90-002270 N90-14378 #
DE90-002291 N90-14539 #
DE90-002298 N90-14323 #
DE90-002301 N90-14541 #
DE90-002315 N90-14927 #
DE90-002331 N90-14351 #
DE90-002332 N90-14349 #
DE90-002343 N90-14933 #
DE90-002350 N90-14490 #
DE90-002352 N90-14636 #
DE90-002353 N90-14480 #
DE90-002380 N90-14855 #
DE90-002381 N90-14599 #
DE90-002383 N90-14899 #
DE90-002386 N90-14600 #
DE90-002387 N90-14601 #
DE90-002389 N90-14602 #
DE90-002397 N90-14888 #
DE90-002405 N90-14603 #
DE90-002408 N90-14968 #
DE90-002412 N90-14606 #
DE90-002413 N90-14823 #
DE90-002440 N90-14969 #
DE90-002448 N90-14481 #
DE90-002475 N90-14970 #
DE90-002477 N90-14776 #
DE90-002479 N90-14253 #
DE90-002508 N90-14540 #
DE90-002533 N90-14254 #
DE90-002555 N90-14725 #
DE90-002562 N90-14373 #
DE90-002580 N90-14872 #
DE90-002600 N90-14491 #
DE90-002604 N90-14693 #
DE90-002613 N90-14766 #
DE90-002617 N90-14663 #
DE90-002625 N90-14396 #
DE90-002666 N90-14691 #
DE90-002671 N90-14865 #
DE90-002672 N90-14698 #
DE90-002682 N90-15022 #
DE90-002694 N90-14822 #
DE90-002701 N90-14699 #
DE90-002722 N90-14740 #
DE90-002725 N90-14692 #
DE90-002726 N90-14757 #
DE90-002732 N90-14717 #
DE90-002747 N90-14718 #
DE90-002773 N90-14871 #
DE90-002777 N90-14354 #
DE90-002808 N90-14492 #
DE90-002813 N90-14834 #
DE90-002818 N90-14482 #
DE90-002861 N90-14825 #
DE90-002891 N90-14632 #
DE90-002894 N90-14355 #
DE90-002931 N90-14661 #
DE90-002995 N90-14932 #
DE90-003174 N90-14324 #
DE90-003192 N90-14982 #
DE90-003285 N90-14726 #
DE90-003649 N90-14983 #
DE90-600729 N90-14852 #
DE90-600767 N90-14853 #
DE90-600934 N90-14525 #
DE90-601005 N90-14864 #
DE90-701785 N90-14403 #

DOD-5400.7-R N90-14993 #

DODA-AR-005-512 N90-14217 #

DOE-TR-89-13 N90-14699 #

DOE/BC-14126/12 N90-14309 #

DOE/BP-64849/1 N90-14458 #

DOE/CE-90027/1-REV-1 N90-14365 #

DOE/ER-0412 N90-14887 #
DOE/ER-0425 N90-14723 #
DOE/ER-01112/1989 N90-14879 #
DOE/ER-10713/T2 N90-14880 #
DOE/ER-13436/4 N90-14307 #
DOE/ER-13460/T2 N90-14324 #
DOE/ER-13541/T1 N90-14306 #
DOE/ER-13732/2 N90-14373 #
DOE/ER-13839/2 N90-14516 #
DOE/ER-13881/2 N90-14320 #
DOE/ER-13978/1 N90-14760 #

DOE/ER-25053/2 ..... N90-14521 #
DOE/ER-25061/2 ..... N90-14859 #
DOE/ER-25068/1 ..... N90-14822 #
DOE/ER-30131/T8 ..... N90-14587 #
DOE/ER-45191/6 ..... N90-14369 #
DOE/ER-45263/4 ..... N90-14947 #
DOE/ER-53212/144 ..... N90-14929 #
DOE/ER-53263/7 ..... N90-14933 #
DOE/ER-60248/T1 ..... N90-14706 #
DOE/ER-60304/5 ..... N90-14755 #
DOE/ER-69017/1 ..... N90-14707 #

DOE/ET-51013/275 ..... N90-14916 #
DOE/ET-53068/370 ..... N90-14930 #

DOE/FE-60850/T1 ..... N90-14725 #

DOE/FTR-90000099 ..... N90-14713 #

DOE/ID-12626/4 ..... N90-14364 #
DOE/ID-12701/1 ..... N90-14321 #

DOE/METC-89/6105 ..... N90-14675 #

DOE/PC-80524/T15 ..... N90-14524 #
DOE/PC-88827/T3 ..... N90-14385 #
DOE/PC-90534/13 ..... N90-14308 #

DOE/PE-0093 ..... N90-14396 #

DOE/SF-17128/T1 ..... N90-14597 #

DOT-HS-807-370 ..... N90-14531 #
DOT-HS-807-417 ..... N90-14215 #

DOT-TSC-NHTSA-88-3 ..... N90-14531 #

DOT/FAA/AM-89-8 ..... N90-14772 #
DOT/FAA/AM-89-10 ..... N90-14773 #

DOT/FAA/CT-TN89/32 ..... N90-14404 #

DOT/FAA/CT-88/29 ..... N90-14222 #

DOT/FAA/DS-89/23 ..... N90-14232* #
DOT/FAA/DS-89/31 ..... N90-14214 #

DP-MS-89-83 ..... N90-14635 #

DRI-8067.1F1 ..... N90-14703 #

DTS-74 ..... N90-14531 #

E-4733 ..... N90-14642* #
E-4788 ..... N90-14511* #
E-4979 ..... N90-14275* #
E-5001 ..... N90-14268* #
E-5052 ..... N90-14655* #
E-5057 ..... N90-14641* #
E-5062 ..... N90-14363* #
E-5074 ..... N90-14287* #
E-5075-1 ..... N90-14517* #
E-5083 ..... N90-15030* #
E-5105 ..... N90-14656* #
E-5123 ..... N90-14844* #
E-5126 ..... N90-14452* #
E-5129 ..... N90-14640* #
E-5138 ..... N90-14335* #
E-5141 ..... N90-14398* #
E-5152 ..... N90-14783* #
E-5158 ..... N90-14678* #
E-5167 ..... N90-14362* #
E-5188 ..... N90-14368* #
E-5192 ..... N90-14512* #
E-5197 ..... N90-14203* #
E-5234 ..... N90-14273* #
E-5236 ..... N90-14235* #
E-5240 ..... N90-14617* #
E-5245 ..... N90-14285* #
E-5246 ..... N90-14284* #
E-5252 ..... N90-14294* #
E-5253 ..... N90-14283* #
E-5258 ..... N90-14206* #
E-5266 ..... N90-14856* #

ECS-1012-VOL-7 ..... N90-14280* #

EGG-EAST-8548 ..... N90-14526 #

EGG-EP-8656 ..... N90-14486 #

EGG-HFRU-8654 ..... N90-14777 #

EGG-M-36387 ..... N90-14523 #
EGG-M-88114 ..... N90-14620 #
EGG-M-88277 ..... N90-14858 #
EGG-M-88357 ..... N90-14348 #
EGG-M-89119 ..... N90-14870 #
EGG-M-89153 ..... N90-14963 #
EGG-M-89209 ..... N90-14605 #
EGG-M-89258 ..... N90-14630 #
EGG-M-89361 ..... N90-14489 #

EGM-4001 ..... N90-14761* #

EPA/AA/CTAB-89/05 ..... N90-14613 #

EPA/600/3-89/037 ..... N90-14702 #
EPA/600/3-89/054 ..... N90-14734 #

ESDU-AERO-C.04.01.00 ..... N90-14239
ESDU-AERO-C.04.01.05 ..... N90-14239
ESDU-AERO-C.04.01.07 ..... N90-14238
ESDU-AERO-C.04.01.09 ..... N90-14240

ESDU-STRUCT-01.01.22 ..... N90-14643

ESDU-76012 ..... N90-14300
ESDU-83039 ..... N90-14192
ESDU-85025 ..... N90-14192
ESDU-86009 ..... N90-14192
ESDU-87032 ..... N90-14238
ESDU-89003-A N90-14238
ESDU-89007 ..... N90-14643
ESDU-89009 ..... N90-14239
ESDU-89010 ..... N90-14240
ESDU-89014 ..... N90-14192
ESDU-89015 ..... N90-14221
ESDU-89017-PT-1 ..... N90-14297
ESDU-89018 ..... N90-14298
ESDU-89019 ..... N90-14299
ESDU-89020-PT-2 ..... N90-14300

ETN-89-95550 ..... N90-14399 #
ETN-90-95242 ..... N90-14830
ETN-90-95515 ..... N90-14544 #
ETN-90-95692 ..... N90-14845 #
ETN-90-95703 ..... N90-14846 #
ETN-90-95791 ..... N90-14938 #
ETN-90-95907 ..... N90-14582 #
ETN-90-95976 ..... N90-14891 #

FDA/CDRH-89/106 ..... N90-14768 #

FEI-1956 ..... N90-14984 #

FERMILAB-PUB-89/239-A ..... N90-15016* #

FHWA/RD-89/176 ..... N90-14809 #

FNAL/C-89/188-T ..... N90-15021 #

FSGTR-NE-120 ..... N90-14704 #

GPO-24-159 ..... N90-14708 #
GPO-24-234 ..... N90-14213 #

GRI-89/0145 ..... N90-14379 #

H-1508 ..... N90-14225* #
H-1566 ..... N90-14224* #
H-1569 ..... N90-14829* #
H-1573 ..... N90-14202* #
H-1580 ..... N90-14228* #
H-1581 ..... N90-14905* #

IAE-4623/12 ..... N90-14877 #
IAE-4663/6 ..... N90-14913 #
IAE-4672/7 ..... N90-14912 #
IAE-4732/16 ..... N90-14585 #

IAF-89-361 ..... N90-14250* #

IC-89/21 ..... N90-14971 #
IC-89/30 ..... N90-14928 #
IC-89/33 ..... N90-14720 #
IC-89/34 ..... N90-14719 #
IC-89/49 ..... N90-14973 #
IC-89/93 ..... N90-14852 #
IC-89/94 ..... N90-14525 #
IC-89/98 ..... N90-14853 #

ICASE-89-54 ..... N90-14779* #
ICASE-89-71 ..... N90-14848* #
ICASE-89-73 ..... N90-14842* #
ICASE-89-77 ..... N90-14193* #
ICASE-89-79 ..... N90-14513* #
ICASE-89-80 ..... N90-14847* #

ICOMP-89-22 ..... N90-14655* #
ICOMP-89-27 ..... N90-14844* #
ICOMP-89-30 ..... N90-14517* #
IFSR-370 ..... N90-14930 #

IFT-P-31/88 ..... N90-15019 #

IFUSP-P-763 ..... N90-14584 #

IFVE-ONF-88-28 ..... N90-14454 #

IFVE-OUNK-88-132 ..... N90-14861 #

IMAG-RR-757-M ..... N90-14845 #
IMAG-RR-774-M ..... N90-14846 #

INT-PATENT-CLASS-G06F-15/06 ..... N90-14830

IPEN-PUB-247 ..... N90-14972 #

ISBN-0-85679-635-2 ..... N90-14238
ISBN-0-85679-678-6 ..... N90-14643
ISBN-0-85679-680-8 ..... N90-14239
ISBN-0-85679-681-6 ..... N90-14240
ISBN-0-85679-686-7 ..... N90-14192
ISBN-0-85679-687-5 ..... N90-14221
ISBN-0-85679-689-1 ..... N90-14297
ISBN-0-85679-690-5 ..... N90-14298
ISBN-0-85679-691-3 ..... N90-14299
ISBN-0-85679-692-3 ..... N90-14300
ISBN-92-835-0524-7 ..... N90-14405 #
ISBN-92-835-0525-5 ..... N90-14325 #
ISBN-92-835-0531-X ..... N90-14218 #

ISSN-0029-3865 ..... N90-14514 #
ISSN-0029-3865 ..... N90-15017 #
ISSN-0029-3865 ..... N90-15018 #
ISSN-0038-0911 ..... N90-15031 #
ISSN-0038-0911 ..... N90-15032 #
ISSN-0038-0911 ..... N90-15033 #
ISSN-0038-0911 ..... N90-15034 #
ISSN-0038-0911 ..... N90-15035 #
ISSN-0038-0911 ..... N90-15039 #
ISSN-0101-3084 ..... N90-14972 #
ISSN-0141-397X N90-14192
ISSN-0141-397X N90-14238
ISSN-0141-397X N90-14239
ISSN-0141-397X N90-14240
ISSN-0141-4054 ..... N90-14221
ISSN-0141-4062 ..... N90-14297
ISSN-0141-4062 ..... N90-14298
ISSN-0141-4062 ..... N90-14299
ISSN-0141-4062 ..... N90-14300
ISSN-0141-4097 ..... N90-14643
ISSN-0348-9329 ..... N90-14873 #

ISWS/CIR-172/89 ..... N90-14748 #

IVO-A-06/88 ..... N90-14621 #

IYF-88-105 ..... N90-14860 #

JAERI-M-89-040 ..... N90-14403 #

JINR-E-11-89-174 ..... N90-14854 #

JINR-R-2-88-507 ..... N90-14876 #

JPL-BIBL-39-30 ..... N90-14995* #

JPL-PUBL-87-4-VOL-8 ..... N90-14700* #
JPL-PUBL-89-47 ..... N90-14672* #

JPRS-USP-89-008 ..... N90-14248 #

JSC-24035 ..... N90-15027* #

KCP-613-4126 ..... N90-14624 #

KSC-KHR-13 ..... N90-15040* #

L-16601 ..... N90-14741* #
L-16608 ..... N90-14186* #
L-16610 ..... N90-14890* #
L-16611 ..... N90-14187* #
L-16623 ..... N90-14493* #
L-16626 ..... N90-14244* #
L-16644 ..... N90-14185* #
L-16645 ..... N90-14190* #
L-16667 ..... N90-14789* #

LA-UR-88-3758 ..... N90-14588 #
LA-UR-89-863 ..... N90-15020 #
LA-UR-89-1520 ..... N90-14676 #
LA-UR-89-1627 ..... N90-14831 #
LA-UR-89-1664 ..... N90-14589 #
LA-UR-89-1909 ..... N90-14917 #
LA-UR-89-2419 ..... N90-14949 #
LA-UR-89-2550 ..... N90-14388 #

LA-UR-89-2560 ..... N90-14819 #
LA-UR-89-2622 ..... N90-14389 #
LA-UR-89-2876 ..... N90-14227 #
LA-UR-89-2895 ..... N90-14771 #
LA-UR-89-2946 ..... N90-14955 #
LA-UR-89-2947 ..... N90-14677 #
LA-UR-89-3017 ..... N90-14520 #
LA-UR-89-3037 ..... N90-14954 #
LA-UR-89-3041 ..... N90-14593 #
LA-UR-89-3060 ..... N90-14522 #
LA-UR-89-3105 ..... N90-14346 #
LA-UR-89-3124 ..... N90-15024 #
LA-UR-89-3135 ..... N90-14350 #
LA-UR-89-3136 ..... N90-14849 #
LA-UR-89-3155 ..... N90-14833 #
LA-UR-89-3221 ..... N90-14956 #
LA-UR-89-3250 ..... N90-14918 #
LA-UR-89-3271 ..... N90-14480 #
LA-UR-89-3275 ..... N90-14636 #
LA-UR-89-3277 ..... N90-14490 #
LA-UR-89-3291 ..... N90-14481 #
LA-UR-89-3310 ..... N90-15023 #
LA-UR-89-3331 ..... N90-14969 #
LA-UR-89-3394 ..... N90-14602 #
LA-UR-89-3397 ..... N90-14601 #
LA-UR-89-3406 ..... N90-14600 #
LA-UR-89-3426 ..... N90-14899 #
LA-UR-89-3438 ..... N90-14599 #
LA-UR-89-3465 ..... N90-14855 #
LA-UR-89-3486 ..... N90-14603 #
LA-UR-89-3537 ..... N90-14888 #
LA-UR-89-3576 ..... N90-14823 #
LA-UR-89-3581 ..... N90-14606 #
LA-UR-89-3616 ..... N90-14968 #
LA-UR-89-3721 ..... N90-14982 #
LA-UR-89-4010 ..... N90-14983 #

LA-11499-MS ..... N90-14941 #

LBL-26362 ..... N90-14663 #
LBL-27037 ..... N90-14693 #
LBL-27377 ..... N90-14351 #
LBL-27378 ..... N90-14347 #
LBL-27379 ..... N90-14341 #
LBL-27380 ..... N90-14349 #
LBL-27444 ..... N90-14820 #
LBL-27466 ..... N90-14491 #
LBL-27553 ..... N90-14885 #
LBL-27607 ..... N90-14338 #
LBL-27632 ..... N90-14314 #
LBL-27660 ..... N90-14766 #
LBL-27694 ..... N90-14312 #
LBL-27696 ..... N90-14817 #
LBL-27745 ..... N90-14865 #
LBL-27747 ..... N90-15022 #

LC-79-640375 ..... N90-15031 #
LC-79-640375 ..... N90-15032 #
LC-79-640375 ..... N90-15033 #
LC-79-640375 ..... N90-15034 #
LC-79-640375 ..... N90-15035 #
LC-79-640375 ..... N90-15039 #

LMSC-HEC-TR-F268780 ..... N90-14277* #

LPI-CONTRIB-712 ..... N90-14998* #

LPI-TR-89-03 ..... N90-15026* #
LPI-TR-89-05 ..... N90-14736* #

LRC-89-7 ..... N90-14933 #

LUIP-8907 ..... N90-14873 #

LUNFD6/(NFFK-7104)1-13(1989) ..... N90-14873 #

MLM-3606(OP) ..... N90-14386 #
MLM-3607(OP) ..... N90-14536 #

NAS 1.15:4131 ..... N90-14225* #
NAS 1.15:4133 ..... N90-14642* #
NAS 1.15:4146 ..... N90-14186* #
NAS 1.15:4149 ..... N90-14829* #
NAS 1.15:4154 ..... N90-14224* #
NAS 1.15:4157 ..... N90-14244* #
NAS 1.15:4162 ..... N90-14190* #
NAS 1.15:100372 ..... N90-15036* #
NAS 1.15:100382 ..... N90-14282* #
NAS 1.15:100749 ..... N90-14260* #
NAS 1.15:101585 ..... N90-14232* #
NAS 1.15:101659 ..... N90-14205* #
NAS 1.15:101669 ..... N90-14272* #
NAS 1.15:101682 ..... N90-14533* #
NAS 1.15:101708 ..... N90-14202* #
NAS 1.15:101714 ..... N90-14228* #
NAS 1.15:101891 ..... N90-14778* #
NAS 1.15:101915 ..... N90-15040* #
NAS 1.15:101929 ..... N90-14874* #
NAS 1.15:101934 ..... N90-15027* #
NAS 1.15:102090 ..... N90-15030* #
NAS 1.15:102181 ..... N90-14188* #
NAS 1.15:102193 ..... N90-14997* #
NAS 1.15:102273 ..... N90-14236* #
NAS 1.15:102300 ..... N90-14275* #
NAS 1.15:102315 ..... N90-14268* #
NAS 1.15:102344 ..... N90-14655* #
NAS 1.15:102348 ..... N90-14641* #
NAS 1.15:102353 ..... N90-14363* #
NAS 1.15:102360 ..... N90-14267* #
NAS 1.15:102384 ..... N90-14844* #
NAS 1.15:102388 ..... N90-14640* #
NAS 1.15:102391 ..... N90-14511* #
NAS 1.15:102393 ..... N90-14335* #
NAS 1.15:102406 ..... N90-14678* #
NAS 1.15:102411 ..... N90-14362* #
NAS 1.15:102423 ..... N90-14368* #
NAS 1.15:102429 ..... N90-14203* #
NAS 1.15:102431 ..... N90-14517* #
NAS 1.15:102449 ..... N90-14273* #
NAS 1.15:102451 ..... N90-14235* #
NAS 1.15:102455 ..... N90-14656* #
NAS 1.15:102456 ..... N90-14617* #
NAS 1.15:102458 ..... N90-14285* #
NAS 1.15:102459 ..... N90-14284* #
NAS 1.15:102465 ..... N90-14294* #
NAS 1.15:102471 ..... N90-14206* #
NAS 1.15:102473 ..... N90-14283* #
NAS 1.15:102479 ..... N90-14856* #
NAS 1.15:102783 ..... N90-14669* #
NAS 1.15:102903 ..... N90-14727* #
NAS 1.26:3922(30) ..... N90-14763* #
NAS 1.26:4023 ..... N90-14200* #
NAS 1.26:4263 ..... N90-14452* #
NAS 1.26:4265 ..... N90-14785* #
NAS 1.26:179444 ..... N90-14905* #
NAS 1.26:181219 ..... N90-14811* #
NAS 1.26:181319 ..... N90-14985* #
NAS 1.26:181851 ..... N90-14866* #
NAS 1.26:181895 ..... N90-14245* #
NAS 1.26:181930 ..... N90-14842* #
NAS 1.26:181956 ..... N90-14193* #
NAS 1.26:181958 ..... N90-14848* #
NAS 1.26:181959 ..... N90-14513* #
NAS 1.26:181960 ..... N90-14847* #
NAS 1.26:181961 ..... N90-14779* #
NAS 1.26:182106 ..... N90-14278*
NAS 1.26:182286 ..... N90-14494* #
NAS 1.26:182982 ..... N90-14907* #
NAS 1.26:183212 ..... N90-14813* #
NAS 1.26:183288 ..... N90-14542* #
NAS 1.26:183733 ..... N90-14397* #
NAS 1.26:183736 ..... N90-14277* #
NAS 1.26:183776 ..... N90-14728* #
NAS 1.26:183801 ..... N90-14276* #
NAS 1.26:183802 ..... N90-14286* #
NAS 1.26:183818 ..... N90-14229* #
NAS 1.26:183819 ..... N90-14230* #
NAS 1.26:183821 ..... N90-14231* #
NAS 1.26:183829 ..... N90-14280* #
NAS 1.26:183830 ..... N90-14530* #
NAS 1.26:183835 ..... N90-14262* #
NAS 1.26:183838 ..... N90-14274* #
NAS 1.26:183848 ..... N90-14608* #
NAS 1.26:185079 ..... N90-14532* #
NAS 1.26:185134 ..... N90-14281* #
NAS 1.26:185156 ..... N90-14783* #
NAS 1.26:185166 ..... N90-14652* #
NAS 1.26:185178 ..... N90-14512* #
NAS 1.26:185190 ..... N90-14398* #
NAS 1.26:185373 ..... N90-14261* #
NAS 1.26:185598 ..... N90-14257* #
NAS 1.26:185916 ..... N90-15025* #
NAS 1.26:185947 ..... N90-14279* #
NAS 1.26:185949 ..... N90-15004* #
NAS 1.26:185950 ..... N90-14638* #
NAS 1.26:185955 ..... N90-14839* #
NAS 1.26:185956 ..... N90-14995* #
NAS 1.26:185964 ..... N90-14999* #
NAS 1.26:185977 ..... N90-14900* #
NAS 1.26:186006 ..... N90-14986* #
NAS 1.26:186046 ..... N90-14216* #
NAS 1.26:186047 ..... N90-14266* #
NAS 1.26:186048 ..... N90-14267* #
NAS 1.26:186051 ..... N90-14265* #
NAS 1.26:186053 ..... N90-14263* #
NAS 1.26:186054 ..... N90-14264* #
NAS 1.26:186056 ..... N90-14761* #
NAS 1.26:186065 ..... N90-14786* #
NAS 1.26:186068 ..... N90-14189* #
NAS 1.26:186073 ..... N90-14664* #
NAS 1.26:186081 ..... N90-14247* #
NAS 1.26:186092 ..... N90-14808* #
NAS 1.26:186099 ..... N90-14700* #
NAS 1.26:186100 ..... N90-14843* #
NAS 1.26:186104 ..... N90-14468* #
NAS 1.26:186109 ..... N90-14271* #
NAS 1.26:186114 ..... N90-14672* #
NAS 1.26:186121 ..... N90-14787* #
NAS 1.26:186123 ..... N90-14270* #
NAS 1.26:186127 ..... N90-14910* #
NAS 1.26:186129 ..... N90-14467* #
NAS 1.26:186131 ..... N90-14498* #
NAS 1.26:186133 ..... N90-14250* #
NAS 1.26:186153 ..... N90-15026* #
NAS 1.26:186156 ..... N90-14736* #
NAS 1.26:186160 ..... N90-14998* #
NAS 1.26:186162 ..... N90-14205* #
NAS 1.26:186168 ..... N90-15016* #
NAS 1.26:186187 ..... N90-14735* #
NAS 1.26:186189 ..... N90-14812* #
NAS 1.26:186192 ..... N90-14534* #
NAS 1.26:186193 ..... N90-14204* #
NAS 1.26:186194 ..... N90-14583* #
NAS 1.26:186195 ..... N90-14243* #
NAS 1.26:186211 ..... N90-14453* #
NAS 1.26:186212 ..... N90-14754* #
NAS 1.26:186213 ..... N90-14670* #
NAS 1.26:186219 ..... N90-14212* #
NAS 1.26:186220 ..... N90-15029* #
NAS 1.26:186224 ..... N90-15028* #
NAS 1.26:186230 ..... N90-14258* #
NAS 1.26:186232 ..... N90-14226* #
NAS 1.26:186237 ..... N90-14836* #
NAS 1.26:186238 ..... N90-14934* #
NAS 1.26:186239 ..... N90-14784* #
NAS 1.26:186242 ..... N90-14837* #
NAS 1.26:186252 ..... N90-14826* #
NAS 1.55:3057 ..... N90-14789* #
NAS 1.55:10041 ..... N90-14220* #
NAS 1.60:2954 ..... N90-14493* #
NAS 1.60:2956 ..... N90-14185* #
NAS 1.60:2961 ..... N90-14187* #
NAS 1.60:2968 ..... N90-14890* #
NAS 1.60:2976 ..... N90-14256* #
NAS 1.61:1230 ..... N90-14741* #

NAS-SR-1330 ..... N90-14214 #

NASA-CP-3057 ..... N90-14789* #
NASA-CP-10041 ..... N90-14220* #

NASA-CR-3922(30) ..... N90-14763* #
NASA-CR-4023 ..... N90-14200* #
NASA-CR-4263 ..... N90-14452* #
NASA-CR-4265 ..... N90-14785* #
NASA-CR-179444 ..... N90-14905* #
NASA-CR-181219 ..... N90-14811* #
NASA-CR-181319 ..... N90-14985* #
NASA-CR-181851 ..... N90-14866* #
NASA-CR-181895 ..... N90-14245* #
NASA-CR-181930 ..... N90-14842* #
NASA-CR-181956 ..... N90-14193* #
NASA-CR-181958 ..... N90-14848* #
NASA-CR-181959 ..... N90-14513* #
NASA-CR-181960 ..... N90-14847* #
NASA-CR-181961 ..... N90-14779* #
NASA-CR-182106 ..... N90-14278*
NASA-CR-182286 ..... N90-14494* #
NASA-CR-182982 ..... N90-14907* #
NASA-CR-183212 ..... N90-14813* #
NASA-CR-183288 ..... N90-14542* #
NASA-CR-183733 ..... N90-14397* #
NASA-CR-183736 ..... N90-14277* #
NASA-CR-183776 ..... N90-14728* #
NASA-CR-183801 ..... N90-14276* #
NASA-CR-183802 ..... N90-14286* #
NASA-CR-183818 ..... N90-14229* #
NASA-CR-183819 ..... N90-14230* #
NASA-CR-183821 ..... N90-14231* #
NASA-CR-183829 ..... N90-14280* #
NASA-CR-183830 ..... N90-14530* #
NASA-CR-183835 ..... N90-14262* #
NASA-CR-183838 ..... N90-14274* #
NASA-CR-183848 ..... N90-14608* #
NASA-CR-185079 ..... N90-14532* #
NASA-CR-185134 ..... N90-14281* #
NASA-CR-185156 ..... N90-14783* #
NASA-CR-185166 ..... N90-14652* #
NASA-CR-185178 ..... N90-14512* #
NASA-CR-185190 ..... N90-14398* #
NASA-CR-185373 ..... N90-14261* #
NASA-CR-185598 ..... N90-14257* #
NASA-CR-185916 ..... N90-15025* #
NASA-CR-185947 ..... N90-14279* #
NASA-CR-185949 ..... N90-15004* #
NASA-CR-185950 ..... N90-14638* #
NASA-CR-185955 ..... N90-14839* #
NASA-CR-185956 ..... N90-14995* #

NASA-CR-185964 ..... N90-14999* #
NASA-CR-185977 ..... N90-14900* #
NASA-CR-186006 ..... N90-14986* #
NASA-CR-186046 ..... N90-14216* #
NASA-CR-186047 ..... N90-14266* #
NASA-CR-186048 ..... N90-14267* #
NASA-CR-186051 ..... N90-14265* #
NASA-CR-186053 ..... N90-14263* #
NASA-CR-186054 ..... N90-14264* #
NASA-CR-186056 ..... N90-14761* #
NASA-CR-186065 ..... N90-14786* #
NASA-CR-186068 ..... N90-14189* #
NASA-CR-186073 ..... N90-14664* #
NASA-CR-186081 ..... N90-14247* #
NASA-CR-186092 ..... N90-14808* #
NASA-CR-186099 ..... N90-14700* #
NASA-CR-186100 ..... N90-14843* #
NASA-CR-186104 ..... N90-14468* #
NASA-CR-186109 ..... N90-14271* #
NASA-CR-186114 ..... N90-14672* #
NASA-CR-186121 ..... N90-14787* #
NASA-CR-186123 ..... N90-14270* #
NASA-CR-186127 ..... N90-14910* #
NASA-CR-186129 ..... N90-14467* #
NASA-CR-186131 ..... N90-14498* #
NASA-CR-186133 ..... N90-14250* #
NASA-CR-186153 ..... N90-15026* #
NASA-CR-186156 ..... N90-14736* #
NASA-CR-186160 ..... N90-14998* #
NASA-CR-186162 ..... N90-14305* #
NASA-CR-186168 ..... N90-15016* #
NASA-CR-186187 ..... N90-14735* #
NASA-CR-186189 ..... N90-14812* #
NASA-CR-186192 ..... N90-14534* #
NASA-CR-186193 ..... N90-14204* #
NASA-CR-186194 ..... N90-14583* #
NASA-CR-186195 ..... N90-14243* #
NASA-CR-186211 ..... N90-14453* #
NASA-CR-186212 ..... N90-14754* #
NASA-CR-186213 ..... N90-14670* #
NASA-CR-186219 ..... N90-14212* #
NASA-CR-186220 ..... N90-15029* #
NASA-CR-186224 ..... N90-15028* #
NASA-CR-186230 ..... N90-14258* #
NASA-CR-186232 ..... N90-14226* #
NASA-CR-186237 ..... N90-14836* #
NASA-CR-186238 ..... N90-14934* #
NASA-CR-186239 ..... N90-14784* #
NASA-CR-186242 ..... N90-14837* #
NASA-CR-186252 ..... N90-14826* #

NASA-RP-1230 ..... N90-14741* #

NASA-TM-4131 ..... N90-14225* #
NASA-TM-4133 ..... N90-14642* #
NASA-TM-4146 ..... N90-14186* #
NASA-TM-4149 ..... N90-14829* #
NASA-TM-4154 ..... N90-14224* #
NASA-TM-4157 ..... N90-14244* #
NASA-TM-4162 ..... N90-14190* #
NASA-TM-100372 ..... N90-15036* #
NASA-TM-100382 ..... N90-14282* #
NASA-TM-100749 ..... N90-14260* #
NASA-TM-101585 ..... N90-14232* #
NASA-TM-101659 ..... N90-14205* #
NASA-TM-101669 ..... N90-14272* #
NASA-TM-101682 ..... N90-14533* #
NASA-TM-101708 ..... N90-14202* #
NASA-TM-101714 ..... N90-14228* #
NASA-TM-101891 ..... N90-14778* #
NASA-TM-101915 ..... N90-15040* #
NASA-TM-101929 ..... N90-14874* #
NASA-TM-101934 ..... N90-15027* #
NASA-TM-102090 ..... N90-15030* #
NASA-TM-102181 ..... N90-14188* #
NASA-TM-102193 ..... N90-14997* #
NASA-TM-102273 ..... N90-14236* #
NASA-TM-102300 ..... N90-14275* #
NASA-TM-102315 ..... N90-14268* #
NASA-TM-102344 ..... N90-14655* #
NASA-TM-102348 ..... N90-14641* #
NASA-TM-102353 ..... N90-14363* #
NASA-TM-102360 ..... N90-14287* #
NASA-TM-102384 ..... N90-14844* #
NASA-TM-102388 ..... N90-14640* #
NASA-TM-102391 ..... N90-14511* #
NASA-TM-102393 ..... N90-14335* #
NASA-TM-102406 ..... N90-14678* #
NASA-TM-102411 ..... N90-14362* #
NASA-TM-102423 ..... N90-14368* #
NASA-TM-102429 ..... N90-14203* #
NASA-TM-102431 ..... N90-14517* #
NASA-TM-102449 ..... N90-14273* #
NASA-TM-102451 ..... N90-14235* #
NASA-TM-102455 ..... N90-14656* #
NASA-TM-102456 ..... N90-14617* #

NASA-TM-102458 ..... N90-14285* #
NASA-TM-102459 ..... N90-14284* #
NASA-TM-102465 ..... N90-14294* #
NASA-TM-102471 ..... N90-14206* #
NASA-TM-102473 ..... N90-14283* #
NASA-TM-102479 ..... N90-14858* #
NASA-TM-102783 ..... N90-14669* #
NASA-TM-102903 ..... N90-14727* #

NASA-TP-2954 ..... N90-14493* #
NASA-TP-2956 ..... N90-14185* #
NASA-TP-2961 ..... N90-14187* #
NASA-TP-2968 ..... N90-14890* #
NASA-TP-2976 ..... N90-14256* #

NCAR/TN-338+STR ..... N90-14752 #

NEFES/89-17 ..... N90-14704 #

NIIAR-10(721) ..... N90-14634 #

NIKHEF/AMPS/89/03 ..... N90-14891 #

NOAA-TM-ERL-WPL-167 ..... N90-14581 #
NOAA-TM-ERL-WPL-169 ..... N90-14906 #

NOAA-TM-NMFS-F/NWC-168 ..... N90-14759 #

NOAA-TM-NWS-SR-126 ..... N90-14749 #

NOAA-TM-NWS-TDL-80 ..... N90-14750 #

NORDA-PR-89-034-321 ..... N90-14666 #

NORDA-221 ..... N90-14665 #

NOSC/TR-1303 ..... N90-14357 #

NPS62-89-022 ..... N90-14889 #

NSF-88-321 ..... N90-14401 #

OCNR-114289-22 ..... N90-14769 #

ORNL-6571 ..... N90-14945 #

ORNL/FTR-3156 ..... N90-14374 #
ORNL/FTR-3377 ..... N90-14657 #
ORNL/FTR-3406 ..... N90-14626 #
ORNL/FTR-3411 ..... N90-14671 #
ORNL/FTR-3432 ..... N90-14726 #
ORNL/FTR-3452 ..... N90-14718 #

ORNL/M-939 ..... N90-14619 #

ORNL/TM-11023 ..... N90-14625 #

PB89-100058 ..... N90-14702 #
PB89-100702 ..... N90-14768 #
PB89-103912 ..... N90-14906 #
PB89-103979 ..... N90-14759 #
PB89-103995 ..... N90-14705 #
PB89-104035 ..... N90-14753 #
PB89-108598 ..... N90-15039 #
PB89-158778 ..... N90-14701 #
PB89-196691 ..... N90-14758 #
PB89-223838 ..... N90-15031 #
PB89-223846 ..... N90-15032 #
PB89-225981 ..... N90-14645 #
PB89-226005 ..... N90-14646 #
PB89-226021 ..... N90-14647 #
PB89-226526 ..... N90-14987 #
PB89-226534 ..... N90-14988 #
PB89-226542 ..... N90-14989 #
PB89-226922 ..... N90-14400 #
PB89-230643 ..... N90-14379 #
PB89-230692 ..... N90-14613 #
PB89-232136 ..... N90-14809 #
PB89-233415 ..... N90-14990 #
PB89-233597 ..... N90-14531 #
PB89-235451 ..... N90-15033 #
PB89-235469 ..... N90-15034 #
PB89-236699 ..... N90-14581 #
PB90-100165 ..... N90-14992 #
PB90-100215 ..... N90-14748 #
PB90-103896 ..... N90-14749 #
PB90-103946 ..... N90-14750 #
PB90-104001 ..... N90-14703 #
PB90-104753 ..... N90-14993 #
PB90-105602 ..... N90-14215 #
PB90-106444 ..... N90-14734 #
PB90-107160 ..... N90-14704 #
PB90-107194 ..... N90-14401 #
PB90-108572 ..... N90-15035 #
PB90-109950 ..... N90-14751 #
PB90-109968 ..... N90-14752 #

PFC/JA-89-43 ..... N90-14598 #

PFC/RR-89-13 ..... N90-14916 #

PNL-SA-16496-1 ..... N90-14709 #
PNL-SA-16875 ..... N90-14717 #
PNL-SA-17036 ..... N90-14691 #
PNL-SA-17164-HEDR ..... N90-14739 #
PNL-SA-17250 ..... N90-14692 #
PNL-SA-17257 ..... N90-14322 #
PNL-SA-17311 ..... N90-14740 #
PNL-SA-17367 ..... N90-14757 #
PNL-SA-17443 ..... N90-14355 #
PNL-SA-17459 ..... N90-14698 #

PNL-6993 ..... N90-14925 #
PNL-7126 ..... N90-14683 #

PNR90563 ..... N90-14399 #

PREPRINT-659 ..... N90-14938 #

PSB-PUBL-81 ..... N90-15027* #

PUB-9673 ..... N90-14701 #

R-583 ..... N90-14647 #
R-584 ..... N90-14645 #
R-587 ..... N90-14646 #

R/D-5955-CH-01 ..... N90-14381 #

RADC-TR-89-170 ..... N90-14450 #

RAE-TRANS-2172 ..... N90-14211 #

REPT-4 ..... N90-14274* #
REPT-87-955 ..... N90-14905* #
REPT-90B00014 ..... N90-14260* #
REPT-9100 ..... N90-14809 #

RI/RD89-216 ..... N90-14608* #

RICIS-IM-7 ..... N90-14986* #

RTR-142-03 ..... N90-14276* #

S-HRG-101-377 ..... N90-14708 #

SA-SR-12 ..... N90-15025* #

SAND-87-0558 ..... N90-14898 #
SAND-88-1004C ..... N90-14476 #
SAND-88-3231C ..... N90-14210 #
SAND-89-0397 ..... N90-14249 #
SAND-89-0598C ..... N90-14632 #
SAND-89-0607C ..... N90-14528 #
SAND-89-0640 ..... N90-14251 #
SAND-89-0748 ..... N90-14371 #
SAND-89-0761 ..... N90-14814 #
SAND-89-0836C ..... N90-14345 #
SAND-89-0859 ..... N90-14310 #
SAND-89-0875 ..... N90-14680 #
SAND-89-0986C ..... N90-14674 #
SAND-89-0991C ..... N90-14315 #
SAND-89-1011C ..... N90-14658 #
SAND-89-1278C ..... N90-14469 #
SAND-89-1423C ..... N90-14455 #
SAND-89-1437C ..... N90-14395 #
SAND-89-1442C ..... N90-14835 #
SAND-89-1472C ..... N90-14872 #
SAND-89-1571 ..... N90-14818 #
SAND-89-1641C ..... N90-14535 #
SAND-89-1674 ..... N90-14367 #
SAND-89-1678C ..... N90-14654 #
SAND-89-1852C ..... N90-14473 #
SAND-89-1886C ..... N90-14472 #
SAND-89-1956C ..... N90-14402 #
SAND-89-2034C ..... N90-14246 #
SAND-89-2064C ..... N90-14919 #
SAND-89-2198C ..... N90-14254 #
SAND-89-2216C ..... N90-14485 #
SAND-89-2222C ..... N90-14629 #
SAND-89-2232C ..... N90-14344 #
SAND-89-2401C ..... N90-14366 #
SAND-89-2405C ..... N90-14914 #
SAND-89-2441C ..... N90-14372 #
SAND-89-2525C ..... N90-14457 #
SAND-89-2539C ..... N90-14962 #
SAND-89-7103C ..... N90-14471 #
SAND-89-8247 ..... N90-14477 #
SAND-89-8251 ..... N90-14259 #
SAND-89-8648 ..... N90-14337 #

SERI/PR-213-3590 ..... N90-14695 #

SERI/STR-211-3410 ..... N90-14687 #
SERI/STR-211-3526 ..... N90-14673 #
SERI/STR-211-3527 ..... N90-14939 #
SERI/STR-211-3562 ..... N90-14679 #
SERI/STR-211-3584 ..... N90-14694 #
SERI/STR-211-3585 ..... N90-14689 #
SERI/STR-211-3586 ..... N90-14681 #
SERI/STR-257-3479 ..... N90-14688 #

SERI/TP-257-3591 ..... N90-14682 #

SGD-538-PT-1 ..... N90-15031 #
SGD-538-PT-2 ..... N90-15032 #
SGD-539-PT-1 ..... N90-15033 #
SGD-539-PT-2 ..... N90-15034 #
SGD-540-PT-1 ..... N90-15035 #
SGD-540-PT-2 ..... N90-15039 #

SRL-HTS-89-0022 ..... N90-14342 #

STI-TR-1256-1-1 ..... N90-14215 #

SUPRI-TR-69 ..... N90-14309 #

TDA-89-GRI-002 ..... N90-14379 #

TR-10 ..... N90-14754* #
TR-11 ..... N90-14453* #
TR-89-1001 ..... N90-14826* #
TR-89-1014 ..... N90-14837* #

TRE/SD105665-3B ..... N90-14271* #

TWR-16389A-REV-A ..... N90-14530* #
TWR-17543-VOL-7 ..... N90-14280* #

UCID-21674 ..... N90-14209 #
UCID-21686 ..... N90-14756 #
UCID-21751 ..... N90-14909 #
UCID-21769 ..... N90-14715 #
UCID-21796 ..... N90-14824 #
UCID-21801 ..... N90-14591 #
UCID-21803 ..... N90-14590 #
UCID-21805 ..... N90-14596 #
UCID-21809 ..... N90-14915 #
UCID-21811 ..... N90-14653 #

UCLA-ENG-90-11 ..... N90-14262* #

UCRL-21228 ..... N90-14622 #
UCRL-98434 ..... N90-14857 #
UCRL-98854 ..... N90-14370 #
UCRL-99559 ..... N90-14515 #
UCRL-99565 ..... N90-14391 #
UCRL-99673-REV-1 ..... N90-14834 #
UCRL-99801 ..... N90-14908 #
UCRL-100261 ..... N90-14313 #
UCRL-100272 ..... N90-14484 #
UCRL-100323 ..... N90-14470 #
UCRL-100362 ..... N90-14479 #
UCRL-100568 ..... N90-14317 #
UCRL-100585 ..... N90-14492 #
UCRL-100641 ..... N90-14482 #
UCRL-100671 ..... N90-14828 #
UCRL-100702 ..... N90-14540 #
UCRL-100752 ..... N90-14353 #
UCRL-100792 ..... N90-14978 #
UCRL-100832 ..... N90-14316 #
UCRL-100906 ..... N90-14586 #
UCRL-100920 ..... N90-14595 #
UCRL-100927 ..... N90-14319 #
UCRL-101061-REV-1 ..... N90-14770 #
UCRL-101104 ..... N90-14922 #
UCRL-101115 ..... N90-14926 #
UCRL-101130 ..... N90-14923 #
UCRL-101132 ..... N90-14920 #
UCRL-101174 ..... N90-14886 #
UCRL-101184 ..... N90-14921 #
UCRL-101186 ..... N90-14924 #
UCRL-101241 ..... N90-14818 #
UCRL-101437 ..... N90-14821 #
UCRL-101481 ..... N90-14932 #
UCRL-101523 ..... N90-14710 #
UCRL-101605 ..... N90-14518 #
UCRL-101652 ..... N90-14832 #
UCRL-101689 ..... N90-14390 #
UCRL-101709 ..... N90-14737 #
UCRL-101736 ..... N90-14721 #
UCRL-101761 ..... N90-14384 #
UCRL-101800 ..... N90-14538 #
UCRL-101861 ..... N90-14393 #
UCRL-101862 ..... N90-14394 #
UCRL-101900 ..... N90-14959 #
UCRL-101901 ..... N90-14958 #
UCRL-101902 ..... N90-14392 #
UCRL-101904 ..... N90-14960 #
UCRL-101905 ..... N90-14862 #
UCRL-101911 ..... N90-14782 #
UCRL-102028 ..... N90-14376 #
UCRL-102100 ..... N90-14927 #

UILU-ENG-89-2241 ..... N90-14839* #

US-PATENT-APPL-SN-070841 ..... N90-14255
US-PATENT-APPL-SN-079962 ..... N90-14529
US-PATENT-APPL-SN-151042 ..... N90-14451
US-PATENT-APPL-SN-160944 ..... N90-14903
US-PATENT-APPL-SN-179327 ..... N90-14838
US-PATENT-APPL-SN-181996 ..... N90-14459
US-PATENT-APPL-SN-212553 ..... N90-14289
US-PATENT-APPL-SN-213034 ..... N90-14904
US-PATENT-APPL-SN-213039 ..... N90-14383
US-PATENT-APPL-SN-216056 ..... N90-14449 #
US-PATENT-APPL-SN-236696 ..... N90-14610
US-PATENT-APPL-SN-244962 ..... N90-14937
US-PATENT-APPL-SN-254554 ..... N90-14466
US-PATENT-APPL-SN-342919 ..... N90-14901 #
US-PATENT-APPL-SN-347132 ..... N90-14543 #
US-PATENT-APPL-SN-364416 ..... N90-14358 #
US-PATENT-APPL-SN-371778 ..... N90-14935 #
US-PATENT-APPL-SN-372961 ..... N90-14936 #
US-PATENT-APPL-SN-373980 ..... N90-14288 #
US-PATENT-APPL-SN-374035 ..... N90-14463 #
US-PATENT-APPL-SN-374119 ..... N90-14461 #
US-PATENT-APPL-SN-389218 ..... N90-14462 #
US-PATENT-APPL-SN-395547 ..... N90-14464 #
US-PATENT-APPL-SN-401197 ..... N90-14611 #
US-PATENT-APPL-SN-411752 ..... N90-14465 #
US-PATENT-APPL-SN-674254 ..... N90-14460 #
US-PATENT-APPL-SN-782325 ..... N90-14382

US-PATENT-CLASS-29-527.2 ..... N90-14459
US-PATENT-CLASS-89-1.810 ..... N90-14255
US-PATENT-CLASS-428-614 ..... N90-14289
US-PATENT-CLASS-560-156 ..... N90-14383

US-PATENT-4,818,661 ..... N90-14529
US-PATENT-4,847,628 ..... N90-14449 #
US-PATENT-4,848,210 ..... N90-14255
US-PATENT-4,848,233 ..... N90-14382
US-PATENT-4,848,262 ..... N90-14610
US-PATENT-4,849,540 ..... N90-14383
US-PATENT-4,850,098 ..... N90-14459
US-PATENT-4,851,661 ..... N90-14903
US-PATENT-4,851,664 ..... N90-14904
US-PATENT-4,851,848 ..... N90-14451
US-PATENT-4,853,294 ..... N90-14289
US-PATENT-4,853,339 ..... N90-14937
US-PATENT-4,853,650 ..... N90-14466
US-PATENT-4,853,771 ..... N90-14838

UTRC-87-41 ..... N90-14494* #

WHC-SA-0727 ..... N90-14897 #

WO-PATENT-APPL-SN-PCT/GB87/000 ... N90-14830

WO-PATENT-88/04075 ..... N90-14830

WSRC-RP-89-268 ..... N90-14342 #
WSRC-RP-89-333 ..... N90-14340 #
WSRC-RP-89-461 ..... N90-14816 #
WSRC-RP-89-483 ..... N90-14815 #
WSRC-RP-89-517 ..... N90-14343 #

ZJE-280 ..... N90-14628 #

Appendix—About STAR

Scientific and Technical Aerospace Reports (STAR) is a major component of a comprehensive National Aeronautics and Space Administration information system covering aeronautics, space, and supporting disciplines. *STAR* is issued on the 8th and 23rd of each month and announces current publications of the following types:

- NASA, NASA contractor, and NASA grantee reports
- Reports issued by other U.S. Government agencies, domestic and foreign institutions, universities, and private firms
- Translations in report form
- NASA-owned patents and patent applications
- Other U.S. Government agency and foreign patents and patent applications
- Domestic and foreign dissertations and theses

Journal, book, and conference literature, cover-to-cover journal translations, and certain foreign dissertations are announced in a companion journal, *International Aerospace Abstracts (IAA),* available on subscription from the American Institute of Aeronautics and Astronautics, Technical Information Service, 555 West 57th Street, 12th Floor, New York, NY 10019.

SUBJECT SCOPE

The subject scope of *STAR* and *IAA* includes all aspects of aeronautics and space research and development, supporting basic and applied research, and applications. Aerospace aspects of earth resources, energy development, conservation, oceanography, environmental protection, urban transportation, and other topics of high national priority are also covered.

OTHER NASA PUBLICATIONS

Other NASA publications and information services are described in the publication, *The NASA Scientific and Technical Information System ... and How to Use It,* available without charge from the NASA Scientific and Technical Information Facility, P.O. Box 8757, BWI Airport, MD 21240.

HOW TO USE *STAR* SUBJECT CATEGORIES

STAR is categorized by 10 major subject divisions broken down further into 76 specific subject categories and one general division/category. The major subject divisions are listed on page ii in the Table of Contents, together with a note for each that defines its scope and provides any cross-references. For example:

AERONAUTICS

Includes aeronautics (general); aerodynamics; air transportation and safety; aircraft communications and navigation; aircraft design, testing and performance; aircraft instrumentation; aircraft propulsion and power; aircraft stability and control; and research and support facilities (air).

For related information see also *Astronautics.*

Each major division is further divided into as many as nine specific categories, which are identified by category numbers.

Abstracts in *STAR* are grouped by subject category, the categories appearing in sequential order. Category breaks in the abstract section are identified by the category number and title, and a scope note. Cross-references to other categories are provided as appropriate. For example:

02 AERODYNAMICS

Includes aerodynamics of bodies, combinations, wings, rotors, and control surfaces; and internal flow in ducts and turbomachinery.

For related information see also *34 Fluid Mechanics and Heat Transfer.*

CROSS-REFERENCES

Individual *STAR* abstracts are not ordinarily cross-referenced, except for certain conference reports or book translations that have had separate abstracts written for their component papers or chapters. Citations and abstracts of the components follow immediately after those of the parent document. When the subject content of a component differs sufficiently from the general content of the parent, a cross-reference citation also is printed at the end of the category to which it normally would have been assigned if it were independent.

DOCUMENTS ON MICROFICHE

Documents on microfiche[1] are designated by a pound sign (#) following the accession number. The pound sign is used without regard to the source or quality of the microfiche.

LIMITED REPRODUCIBILITY

A Note of Limited Reproducibility appears in the citation, if one or a combination of the following factors affect the reproducibility of more than 20% of the document. These factors include: faint or broken type, color photographs, black and white photographs, foldouts, dot matrix print, charts/graphs with script notation, non-Roman alphabet, or some other factor that limits the reproducibility of that document. This notation also appears on the microfiche header, with the specific causing factor checked off on a list visible in the second frame.

AVAILABILITIES

One or more sources from which a document announced in *STAR* is available to the public is given in each citation. The most commonly indicated sources and their acronyms or abbreviations are listed below. If the publication is available from a source other than those listed, the publisher and his address will be displayed on the availability line or in combination with the corporate source line.

Avail: NTIS. Sold by the National Technical Information Service. Prices for hard copy (HC) and microfiche (MF) are indicated by a price code following the letters HC or MF in the *STAR* citation. Current values for the price codes are given in the tables on page A-7.

Initially distributed microfiche under the NTIS SRIM (Selected Research in Microfiche) is available at greatly reduced unit prices. For this service and for information concerning subscription to NASA printed reports, consult the NTIS Subscription Section, Springfield, VA 22161.

NOTE ON ORDERING DOCUMENTS: When ordering NASA publications (those followed by the * symbol), use the N accession number. NASA patent applications (only the specifications are offered) should be ordered by the US-Patent-Appl-SN number. Non-NASA publications (no asterisk) should be ordered by the AD, PB, or other *report number* shown on the last line of the citation, not by the N accession number. It is also advisable to cite the title and other bibliographic identification.

(1) A microfiche is a transparent sheet of film, 105 by 148 mm in size, containing as many as 60 to 98 pages of information reduced to micro images (not to exceed 26:1 reduction).

Avail: SOD (or GPO). Sold by the Superintendent of Documents, U.S. Government Printing Office, in hard copy. The current price and order number are given following the availability line. (NTIS will fill microfiche requests, as indicated above, for those documents identified by a # symbol.)

Avail: BLL (formerly NLL): British Library Lending Division, Boston Spa, Wetherby, Yorkshire, England. Photocopies available from this organization at the price shown. (If none is given, inquiry should be addressed to the BLL.)

Avail: DOE Depository Libraries. Organizations in U.S. cities and abroad that maintain collections of Department of Energy reports, usually in microfiche form, are listed in *Energy Research Abstracts*. Services available from the DOE and its depositories are described in a booklet, *DOE Technical Information Center - Its Functions and Services* (TID-4660), which may be obtained without charge from the DOE Technical Information Center.

Avail: ESDU. Pricing information on specific data, computer programs, and details on Engineering Sciences Data Unit (ESDU) topic categories can be obtained from ESDU International Ltd. Requesters in North America should use the Virginia address while all other requesters should use the London address, both of which are on page A-6.

Avail: Fachinformationszentrum, Karlsruhe. Sold by the Fachinformationszentrum Energie, Physik, Mathematik GMBH, Eggenstein Leopoldshafen, Federal Republic of Germany, at the price shown in deutschmarks (DM).

Avail: HMSO. Publications of Her Majesty's Stationery Office are sold in the U.S. by Pendragon House, Inc. (PHI), Redwood City, CA. The U.S. price (including a service and mailing charge) is given, or a conversion table may be obtained from PHI.

Avail: NASA Public Document Rooms. Documents so indicated may be examined at or purchased from the National Aeronautics and Space Administration, Public Documents Room (Room 126), 600 Independence Ave., S.W., Washington, DC 20546, or public document rooms located at NASA installations, and the NASA Pasadena Office at the Jet Propulsion Laboratory.

Avail: Univ. Microfilms. Documents so indicated are dissertations selected from *Dissertation Abstracts* and are sold by University Microfilms as xerographic copy (HC) and microfilm. All requests should cite the author and the Order Number as they appear in the citation.

Avail: US Patent and Trademark Office. Sold by Commissioner of Patents and Trademarks, U.S. Patent and Trademark Office, at the standard price of $1.50 each, postage free. (See discussion of NASA patents and patent applications below.)

Avail: (US Sales Only). These foreign documents are available to users within the United States from the National Technical Information Service (NTIS). They are available to users outside the United States through the International Nuclear Information Service (INIS) representative in their country, or by applying directly to the issuing organization.

Avail: USGS. Originals of many reports from the U.S. Geological Survey, which may contain color illustrations, or otherwise may not have the quality of illustrations preserved in the microfiche or facsimile reproduction may be examined by the public at the libraries of the USGS field offices whose addresses are listed in this Introduction. The libraries may be queried

concerning the availability of specific documents and the possible utilization of local copying services, such as color reproduction.

Avail: Issuing Activity, or Corporate Author, or no indication of availability. Inquiries as to the availability of these documents should be addressed to the organization shown in the citation as the corporate author of the document.

NASA PATENTS AND PATENT APPLICATIONS

Patents and patent applications owned by NASA are announced in *STAR* under appropriate subject categories and are referenced in the *STAR* indexes. In the Report/Accession Number Index, patents are indexed by the NASA Case Number (which appears in lieu of the report number in other indexes), the U.S. Patent Number, the U.S. Patent Application Serial Number, and the U.S. Patent Class. Patent applications for which patents have not yet been issued are indexed by the NASA Case Number and the U.S. Patent Application Serial Number.

NASA *patent application specifications* are sold in paper copy and microfiche by the National Technical Information Service (NTIS). The US-Patent-Appl-SN- number should be used in ordering either paper copy or microfiche from NTIS. Printed copies of *patents* (which are not microfiched) are available for purchase from:

Commissioner of Patents and Trademarks
U.S. Patent and Trademark Office
Washington, DC 20231

When ordering patents, the U.S. Patent Number should be used, and payment must be remitted in advance, by money order or check payable to the Commissioner of Patents and Trademarks. Prepaid purchase coupons for ordering are also available from the Patent and Trademark Office. The patents and patent applications announced in *STAR* are owned by NASA and are available for royalty-free licensing. Requests for licensing terms and further information should be addressed to:

Associate General Counsel for Intellectual Property/Code GP
National Aeronautics and Space Administration
Washington, DC 20546

ELIGIBILITY AND REGISTRATION FOR NASA INFORMATION PRODUCTS AND SERVICES

A variety of services is available to organizations of the following types that have registered with NASA to receive specific services or products:

1. NASA offices and installations, contractors, subcontractors, grantees, and consultants;
2. Other U.S. Government agencies and their contractors;
3. Libraries in the United States that have arrangements with NASA to maintain collections of NASA documents for public reference;
4. Other organizations in the United States having a need for NASA documents in work related to aeronautics and space research;
5. Organizations abroad that have established reciprocal document exchange arrangements with NASA.

Only the central service points or central points of document acquisition and control within qualified organizations are eligible to register for NASA products and services. Domestic organizations that may be eligible to receive various classes of NASA publications and services should address their requests for registration or for further information to:

NASA Scientific and Technical Information Facility
ATTN: Registration Services
P.O. Box 8757
BWI Airport, MD 21240
301-621-0153

Organizations abroad should direct requests to Manager, International STI Activities, NTT, NASA Headquarters, Washington, DC 20546.

AVAILABILITY OF *STAR* ABSTRACTS ON MICROFICHE

Microfiche of the abstract sections of this issue and other issues of *STAR* are available on annual subscription from NTIS as PB90-911300, Attn: Subscriptions, 5285 Port Royal Road, Springfield, VA 22161. Annual subscription rates are $75.50 North America; $151.00 foreign. Abstract sections for previous years retroactive to 1964 are available at the current rates. Microfiche for individual *STAR* issue abstract sections are not available.

PUBLIC COLLECTIONS OF NASA DOCUMENTS

DOMESTIC: NASA and NASA-sponsored documents and a large number of aerospace publications are available to the public for reference purposes at the library maintained by the American Institute of Aeronautics and Astronautics, Technical Information Service, 555 West 57th Street, 12th Floor, New York, NY 10019

EUROPEAN: An extensive collection of NASA and NASA-sponsored publications is maintained by the British Library Lending Division, Boston Spa, Wetherby, Yorkshire, England, for public access. The British Library Lending Division also has available many of the non-NASA publications cited in *STAR*. European requesters may purchase facsimile copy or microfiche of NASA and NASA-sponsored documents, those identified by both the symbols # and * from ESA - Information Retrieval Service, European Space Agency, 8-10 rue Mario-Nikis, 75738 Paris CEDEX 15, France.

FEDERAL DEPOSITORY LIBRARY PROGRAM

In order to provide the general public with greater access to U.S. Government publications, Congress established the Federal Depository Library Program under the Government Printing Office (GPO), with 51 regional depositories responsible for permanent retention of material, inter-library loan, and reference services. At least one copy of nearly every NASA and NASA-sponsored publication, either in printed or microfiche format, is received and retained by the 51 regional depositories. A list of the regional GPO libraries, arranged alphabetically by state, appears on the inside back cover. These libraries are *not* sales outlets. A local library can contact a Regional Depository to help locate specific reports, or direct contact may be made by an individual.

ADDRESSES OF ORGANIZATIONS

American Institute of Aeronautics and Astronautics
Technical Information Service
555 West 57th Street, 12th Floor
New York, New York 10019

British Library Lending Division,
Boston Spa, Wetherby, Yorkshire,
England

Commissioner of Patents and Trademarks
U.S. Patent and Trademark Office
Washington, DC 20231

Department of Energy
Technical Information Center
P.O. Box 62
Oak Ridge, Tennessee 37830

European Space Agency-Information Retrieval Service
ESRIN
Via Galileo Galilei
00044 Frascati (Rome) Italy

Engineering Sciences Data Unit International
P.O. Box 1633
Manassas, Virginia 22110

Engineering Sciences Data Unit International, Ltd.
251-259 Regent Street
London, W1R 7AD, England

Fachinformationszentrum Energie, Physik, Mathematik
GMBH
7514 Eggenstein Leopoldshafen
Federal Republic of Germany

Her Majesty's Stationery Office
P.O. Box 569, S.E. 1
London, England

NASA Scientific and Technical Information Facility
P.O. Box 8757
BWI Airport, Maryland 21240

National Aeronautics and Space Administration
Scientific and Technical Information Division (NTT)
Washington, DC 20546

National Technical Information Service
5285 Port Royal Road
Springfield, Virginia 22161

Pendragon House, Inc.
899 Broadway Avenue
Redwood City, California 94063

Superintendent of Documents
U.S. Government Printing Office
Washington, DC 20402

University Microfilms
A Xerox Company
300 North Zeeb Road
Ann Arbor, Michigan 48106

University Microfilms, Ltd.
Tylers Green
London, England

U.S. Geological Survey Library National Center
MS 950
12201 Sunrise Valley Drive
Reston, Virginia 22092

U.S. Geological Survey Library
2255 North Gemini Drive
Flagstaff, Arizona 86001

U.S. Geological Survey
345 Middlefield Road
Menlo Park, California 94025

U.S. Geological Survey Library
Box 25046
Denver Federal Center, MS914
Denver, Colorado 80225

NTIS PRICE SCHEDULES

(Effective January 1, 1990)

Schedule A
STANDARD PRICE DOCUMENTS AND MICROFICHE

PRICE CODE	NORTH AMERICAN PRICE	FOREIGN PRICE
A01	$ 8.00	$ 16.00
A02	11.00	22.00
A03	15.00	30.00
A04-A05	17.00	34.00
A06-A09	23.00	46.00
A10-A13	31.00	52.00
A14-A17	39.00	78.00
A18-A21	45.00	90.00
A22-A25	53.00	106.00
A99	*	*
N01	60.00	120.00
N02	59.00	118.00
N03	20.00	40.00

Schedule E
EXCEPTION PRICE DOCUMENTS AND MICROFICHE

PRICE CODE	NORTH AMERICAN PRICE	FOREIGN PRICE
E01	$10.00	$ 20.00
E02	12.00	24.00
E03	14.00	28.00
E04	16.50	33.00
E05	18.50	37.00
E06	21.50	43.00
E07	24.00	48.00
E08	27.00	54.00
E09	29.50	59.00
E10	32.50	65.00
E11	35.00	70.00
E12	38.50	77.00
E13	41.00	82.00
E14	45.00	90.00
E15	48.50	97.00
E16	53.00	106.00
E17	57.50	115.00
E18	62.00	124.00
E19	69.00	138.00
E20	80.00	160.00
E99	*	*

* Contact NTIS for price quote.

IMPORTANT NOTICE

NTIS Shipping and Handling Charges

U.S., Canada, Mexico — ADD $3.00 per TOTAL ORDER

All Other Countries — ADD $4.00 per TOTAL ORDER

Exceptions — Does NOT apply to:

ORDERS REQUESTING NTIS RUSH HANDLING
ORDERS FOR SUBSCRIPTION OR STANDING ORDER PRODUCTS *ONLY*

NOTE: Each additional delivery address on an order requires a separate shipping and handling charge.

FEDERAL REGIONAL DEPOSITORY LIBRARIES

ALABAMA

AUBURN UNIV. AT MONTGOMERY LIBRARY
Documents Department
Montgomery, AL 36193
(205) 279-9110 ext.253

UNIV. OF ALABAMA LIBRARY
Reference Department/Documents
Box S
Tuscaloosa, AL 35486
(205) 348-6046

ARIZONA

DEPT. OF LIBRARY, ARCHIVES, AND PUBLIC RECORDS
Third Floor State Capitol
1700 West Washington
Phoenix, AZ 85007
(602) 255-4121

ARKANSAS

ARKANSAS STATE LIBRARY
Documents Service Section
One Capitol Mall
Little Rock, AR 72201
(501) 371-2090

CALIFORNIA

CALIFORNIA STATE LIBRARY
Govt. Publications Section
914 Capitol Mall
Sacramento, CA 95814
(916) 322-4572

COLORADO

UNIV. OF COLORADO
Norlin Library
Government Publications Division
Campus Box 184
Boulder, CO 80309
(303) 492-8834

DENVER PUBLIC LIBRARY
Govt. Pub. Department
1357 Broadway
Denver, CO 80203
(303) 571-2346

CONNECTICUT

CONNECTICUT STATE LIBRARY
231 Capitol Avenue
Hartford, CT 06106
(203) 566-4971

FLORIDA

UNIV. OF FLORIDA LIBRARIES
Documents Department
Library West
Gainesville, FL 32611
(904) 392-0367

GEORGIA

UNIV. OF GEORGIA LIBRARIES
Government Documents Dept.
Athens, GA 30602
(404) 542-8949

HAWAII

UNIV. OF HAWAII
Hamilton Library
Government Documents Collection
2550 The Mall
Honolulu, HI 96822
(808) 948-8230

IDAHO

UNIV. OF IDAHO LIBRARY
Documents Section
Moscow, ID 83843
(208) 885-6344

ILLINOIS

ILLINOIS STATE LIBRARY
Federal Documents
Centennial Building
Springfield, IL 62756
(217) 782-5012

INDIANA

INDIANA STATE LIBRARY
Serials Section
140 North Senate Avenue
Indianapolis, IN 46204
(317) 232-3686

IOWA

UNIV. OF IOWA LIBRARIES
Government Publications Dept.
Iowa City, IA 52242
(319) 335-5926

KANSAS

UNIVERSITY OF KANSAS
Spencer Research Library
Government Documents
Lawrence, KS 66045
(913) 864-4662

KENTUCKY

UNIV. OF KENTUCKY LIBRARIES
Government Publications/Maps Dept.
Lexington, KY 40506
(606) 257-8400

LOUISIANA

LOUISIANA STATE UNIVERSITY
Middleton Library
Government Documents Dept.
Baton Rouge, LA 70803
(504) 388-2570

LOUISIANA TECHNICAL UNIV.
Prescott Memorial Library
Government Documents Dept.
Ruston, LA 71272
(318) 257-4962

MAINE

UNIVERSITY OF MAINE
Raymond H. Fogler Library
Govt. Documents & Microforms Dept.
Orono, ME 04469
(207) 581-1680

MARYLAND

UNIVERSITY OF MARYLAND
McKeldin Library
Documents/Maps Room
College Park, MD 20742
(301) 454-3034

MASSACHUSETTS

BOSTON PUBLIC LIBRARY
Government Documents Dept.
666 Boylston Street
Boston, MA 02117
(617) 536-5400 ext.226

MICHIGAN

DETROIT PUBLIC LIBRARY
5201 Woodward Avenue
Detroit, MI 48202
(313) 833-1409

LIBRARY OF MICHIGAN
Government Documents
P.O. Box 30007
735 E. Michigan Avenue
Lansing, MI 48909
(517) 373-1593

MINNESOTA

UNIVERSITY OF MINNESOTA
Wilson Library
Government Publications
309 Nineteenth Avenue South
Minneapolis, MN 55455
(612) 373-7813

MISSISSIPPI

UNIV. OF MISSISSIPPI LIB.
Government Documents Dept.
106 Old Gym Bldg.
University, MS 38677
(601) 232-5857

MISSOURI

University of Missouri at Columbia Library
Government Documents
Columbia, MO 65201
(314) 882-6733

MONTANA

UNIV. OF MONTANA
Mansfield Library
Documents Division
Missoula, MT 59812
(406) 243-6700

NEBRASKA

UNIVERSITY OF NEBRASKA - LINCOLN
Love Memorial Library
Documents Department
Lincoln, NE 68588
(402) 472-2562

NEVADA

UNIV. OF NEVADA-RENO LIB.
Govt. Pub. Department
Reno, NV 89557
(702) 784-6579

NEW JERSEY

NEWARK PUBLIC LIBRARY
U.S. Documents Division
5 Washington Street
P.O. Box 630
Newark, NJ 07101
(201) 733-7812

NEW MEXICO

UNIVERSITY OF NEW MEXICO
General Library
Government Publications/Maps Dept.
Albuquerque, NM 87131
(505) 277-5441

NEW MEXICO STATE LIBRARY
325 Don Gaspar Avenue
Santa Fe, NM 87501
(505) 827-3826

NEW YORK

NEW YORK STATE LIBRARY
Documents Sect. Cultural Educ. Ctr.
Empire State Plaza
Albany, NY 12230
(518) 474-5563

NORTH CAROLINA

UNIVERSITY OF NORTH CAROLINA AT CHAPEL HILL
Davis Library 080A
BA/SS Department Documents
Chapel Hill, NC 27514
(919) 962-1151

NORTH DAKOTA

NORTH DAKOTA STATE UNIVERSITY LIBRARY
Government Documents Dept.
Fargo, ND 58105
(701) 237-8352
In cooperation with Univ. of North Dakota, Chester Fritz Library Grand Forks

OHIO

STATE LIBRARY OF OHIO
Documents Section
65 South Front Street
Columbus, OH 43266
(614) 644-7051

OKLAHOMA

OKLAHOMA DEPT. OF LIBRARIES
Government Documents
200 NE 18th Street
Oklahoma City, OK 73105
(405) 521-2502, ext. 252

OKLAHOMA STATE UNIV. LIB.
Documents Department
Stillwater, OK 74078
(405) 624-0489

OREGON

PORTLAND STATE UNIV.
Millar Library
934 SW Harrison - P.O. Box 1151
Portland, OR 97207
(503) 229-3673

PENNSYLVANIA

STATE LIBRARY OF PENN.
Government Publications Section
Box 1601
Walnut St. & Commonwealth Ave.
Harrisburg, PA 17105
(717) 787-3752

SOUTH CAROLINA

CLEMSON UNIV. COOPER LIB.
Documents Department
Clemson, SC 29634
(803) 656-5174
In cooperation with Univ. of South Carolina, Thomas Cooper Library, Columbia

TEXAS

TEXAS STATE LIBRARY
Public Services Department
P.O. Box 12927 - 1201 Brazos
Austin, TX 78711
(512) 463-5455

TEXAS TECH. UNIV. LIBRARY
Documents Department
Lubbock, TX 79409
(806) 742-2268

UTAH

UTAH STATE UNIVERSITY
Merrill Library & Learning Resources Center, UMC-30
Documents Department
Logan, UT 84322
(801) 750-2682

VIRGINIA

UNIVERSITY OF VIRGINIA
Alderman Library
Government Documents
Charlottesville, VA 22903
(804) 924-3133

WASHINGTON

WASHINGTON STATE LIBRARY
Document Section
Olympia, WA 98504
(206) 753-4027

WEST VIRGINIA

WEST VIRGINIA UNIV. LIB.
Government Documents Section
P.O. Box 6069
Morgantown, WV 26506
(304) 293-3640

WISCONSIN

ST. HIST SOC. OF WISCONSIN LIB.
Government Pub. Section
816 State Street
Madison, WI 53706
(608) 262-2781
In cooperation with Univ. of Wisconsin-Madison, Memorial Library

MILWAUKEE PUBLIC LIBRARY
Documents Division
814 West Wisconsin Avenue
Milwaukee, WI 53233
(414) 278-3065

WYOMING

WYOMING STATE LIBRARY
Supreme Court & Library Bldg.
Cheyenne, WY 82002
(307) 777-5919

National Aeronautics and
Space Administration
Code NTT
Washington, D.C.
20546
Official Business
Penalty for Private Use, $300

SPECIAL FOURTH-CLASS RATE
POSTAGE & FEES PAID
NASA
PERMIT No. G27

NASA

POSTMASTER: If Undeliverable (Section 158
Postal Manual) Do Not Return